

**Ongoing Face Recognition
Vendor Test (FRVT)**
Part 1: Verification

Patrick Grother
Mei Ngan
Kayee Hanaoka
*Information Access Division
Information Technology Laboratory*

This publication is available free of charge from:
<https://www.nist.gov/programs-projects/face-recognition-vendor-test-frvt-ongoing>

2019/09/11

ACKNOWLEDGMENTS

The authors are grateful to Wayne Salamon and Greg Fiumara at NIST for robust software infrastructure, particularly that which leverages [Berkeley DB Btrees](#) for storage of images and templates, and [Open MPI](#) for parallel execution of algorithms across our computers. Thanks also to Brian Cochran at NIST for providing highly available computers and network-attached storage.

DISCLAIMER

Specific hardware and software products identified in this report were used in order to perform the evaluations described in this document. In no case does identification of any commercial product, trade name, or vendor, imply recommendation or endorsement by the National Institute of Standards and Technology, nor does it imply that the products and equipment identified are necessarily the best available for the purpose.

FRVT STATUS

This report is a draft NIST Interagency Report, and is open for comment. It is the sixteenth edition of the report since the first was published in June 2017. Prior editions of this report are maintained on the FRVT website, and may contain useful information about older algorithms and datasets no longer used in FRVT.

FRVT remains open: All [four tracks](#) of the FRVT remain open to new algorithm submissions indefinitely. This report will be updated as new algorithms are evaluated, as new datasets are added, and as new analyses are included. Comments and suggestions should be directed to frvt@nist.gov.

Changes since July 31 2019:

- ▷ The [FRVT 1:1 homepage](#) has been updated to include a column for cross-domain Visa-Border verification. Results for this new dataset appeared in the July 29 report under the name "CrossEV" - these are now renamed "Visa-Border".
- ▷ The [FRVT 1:1 homepage](#) lists algorithms according to lowest mean rank accuracy:

$$\begin{aligned} & \text{Rank(FNMR}_{\text{VISA}} \text{ at FMR = 0.000001}) + \\ & \text{Rank(FNMR}_{\text{VISA-BORDER}} \text{ at FMR = 0.000001}) + \\ & \text{Rank(FNMR}_{\text{MUGSHOT}} \text{ at FMR = 0.00001 after 14 years}) + \\ & \text{Rank(FNMR}_{\text{WILD}} \text{ at FMR = 0.00001}) \end{aligned}$$

This ordering rewards high accuracy across all datasets.

- ▷ The main results in Table 8 is now in landscape format to accomodate extra columns for the Visa-Border set, and mugshot comparisons after at least 12 years.
- ▷ The report adds results for nine new participants: Alpha SSTG, Intel Research, ULSee, Chungwa Telecon, iSAP Solution, Rokid, Shenzhen EI Networks, CSA Intellicloud, Shenzhen Intellifusion Technologies.
- ▷ The reports adds results for six new algorithms from returning developers: Innovatrics, Dahua Technology, Tech5 SA, Intellivision, Nodeflux and Imperial College, London. One algorithm, from Imperial has been retired, per policy to list results for two algorithms per developer.
- ▷ The cross-country false match rate heatmaps starting from Figure 279 have been replotted to reveal more structure by listing countries by region instead of alphabetically.
- ▷ The next version of this report will be posted around October 18, 2019.

Changes since July 3 2019:

- ▷ The HTML table on the [FRVT 1:1 homepage](#) has been updated to list the 20 most accurate developers rather than algorithms, choosing the most accurate algorithm from each developer based on visa and mugshot results. Also, the algorithms are ordered in terms of lowest mean rank across mugshot, visa and wild datasets, rewarding broad accuracy over a good result on one particular dataset.
- ▷ This report includes results for a new dataset - see the column labelled "crossEV" in Table 5. It compares a new set of high quality visa portraits with a set webcam photos that exhibit moderately poor pose variations and background illumination. The two new sets are described in sections 2.3 and 2.5. The comparisons are "cross-domain" in that the algorithm must compare "visa" and "wild" images. Results for other algorithms will be added in future reports as they become available.
- ▷ This report adds results for algorithms from 9 developers submitted in early July 2019. These are from 3DiVi, Camvi, EverAI-Paravision, Facesoft, Farbar (F8), Institute of Information Technologies, Shanghai U. Film Academy, Via Technologies, and Ulucu Electronics Tech. Six of these are new participants.
- ▷ Several other algorithms have been submitted and are being evaluated. Results will be released in the next report, scheduled for September 5. That report will include results for new datasets.

- ▷ Older algorithms from Everai, Camvi and 3DiVi, have been retired, per the policy to list only two algorithms per developer.

Changes since June 2019:

- ▷ This report adds results for algorithms from 18 developers submitted in early June 2019. These are from CTBC Bank, Deep Glint, Thales Cogent, Ever AI Paravision, Gorilla Technology, Imagus, Incode, Kneron, N-Tech Lab, Neurotechnology, Notiontag Technologies, Star Hybrid, Videonetics, Vigilant Solutions, Winsense, Anke Investments, CEIEC, and DSK. Nine of these are new participants.
- ▷ Several other algorithms have been submitted and are being evaluated. Results will be released in the next report, scheduled for August 1.
- ▷ Older algorithms from Everai, Thales Cogent, Gorilla Technology, Incode, Neurotechnology, N-Tech Lab and Vigilant Solutions have been retired, per the policy to list only two algorithms per developer.

Changes since April 2019:

- ▷ This report adds results for nine algorithms from nine developers submitted in early June 2019. These are from Tencent Deepsea, Hengrui, Kedacom, Moontime, Guangzhou Pixel, Rank One Computing, Synesis, Sensetime and Vocord.
- ▷ Another 23 algorithms have been submitted and are being evaluated. Results will be released in the next report, scheduled for July 3.
- ▷ Older algorithms for Rank One, Synesis, and Vocord have been retired, per the policy to list only two algorithms per developer.

Changes since February 2019:

- ▷ This report adds results for 49 algorithms from 42 developers submitted in early March 2019.
- ▷ This report omits results for algorithms that we retired. We retired for three reasons: 1. The developer submitted a new algorithm, and we only list two. 2. The algorithm needs a GPU, and we no longer allow GPU-based algorithms. 3. Inoperable algorithms.
- ▷ Previous results for retired algorithms are available in older editions of this report linked [here](#).
- ▷ The mugshot database used from February 2017 to January 2019 has been replaced with an extract of the mugshot database documented in NIST Interagency Report 8238, November 2018. The new mugshot set is described in section [2.4](#) and is adopted because:
 - ▷ It has much better identity label integrity, so that false non-match rates are substantially lower than those reported in FRVT 1:1 reports to date - see Figure [27](#).
 - ▷ It includes images collected over a 17 year period such that ageing can be much better characterized - - see Figure [116](#).
- ▷ Using the new mugshot database, Figure [116](#) shows accuracy for four demographic groups identified in the biographic metadata that accompanies the data: black females, black males, white females and white males.
- ▷ The report adds Figure [10](#) with results for the twenty human-difficult pairs used in the May 2018 paper *Face recognition accuracy of forensic examiners, superrecognizers, and face recognition algorithms* by Phillips et al. [\[1\]](#).
- ▷ The report uses an update to the wild image database that corrects some ground truth labels.
- ▷ Some results for the child exploitation database are not complete. They are typically updated less frequently than for other image sets.

Contents

ACKNOWLEDGMENTS	1
DISCLAIMER	1
1 METRICS	26
1.1 CORE ACCURACY	26
2 DATASETS	27
2.1 CHILD EXPLOITATION IMAGES	27
2.2 VISA IMAGES	27
2.3 VISA IMAGES II	27
2.4 MUGSHOT IMAGES	28
2.5 WEBCAM IMAGES	28
2.6 WILD IMAGES	29
3 RESULTS	29
3.1 TEST GOALS	29
3.2 TEST DESIGN	29
3.3 FAILURE TO ENROLL	32
3.4 RECOGNITION ACCURACY	36
3.5 GENUINE DISTRIBUTION STABILITY	128
3.5.1 EFFECT OF BIRTH PLACE ON THE GENUINE DISTRIBUTION	128
3.5.2 EFFECT OF AGEING	142
3.5.3 EFFECT OF AGE ON GENUINE SUBJECTS	152
3.6 IMPOSTOR DISTRIBUTION STABILITY	167
3.6.1 EFFECT OF BIRTH PLACE ON THE IMPOSTOR DISTRIBUTION	167
3.6.2 EFFECT OF AGE ON IMPOSTORS	466

List of Tables

1 ALGORITHM SUMMARY	16
2 ALGORITHM SUMMARY	17
3 ALGORITHM SUMMARY	18
4 ALGORITHM SUMMARY	19
5 FALSE NON-MATCH RATE	20
6 FALSE NON-MATCH RATE	21
7 FALSE NON-MATCH RATE	22
8 FALSE NON-MATCH RATE	23
9 FAILURE TO ENROL RATES	33
10 FAILURE TO ENROL RATES	34
11 FAILURE TO ENROL RATES	35

List of Figures

1 PERFORMANCE SUMMARY: FNMR VS. TEMPLATE SIZE TRADEOFF	24
2 PERFORMANCE SUMMARY: FNMR VS. TEMPLATE TIME TRADEOFF	25
3 EXAMPLE IMAGES	29
(A) VISA	29
(B) MUGSHOT	29
(C) WILD	29

4	PERFORMANCE ON 20 HUMAN-DIFFICULT PAIRS	37
5	PERFORMANCE ON 20 HUMAN-DIFFICULT PAIRS	38
6	PERFORMANCE ON 20 HUMAN-DIFFICULT PAIRS	39
7	PERFORMANCE ON 20 HUMAN-DIFFICULT PAIRS	40
8	PERFORMANCE ON 20 HUMAN-DIFFICULT PAIRS	41
9	PERFORMANCE ON 20 HUMAN-DIFFICULT PAIRS	42
10	PERFORMANCE ON 20 HUMAN-DIFFICULT PAIRS	43
11	ERROR TRADEOFF CHARACTERISTIC: VISA IMAGES	44
12	ERROR TRADEOFF CHARACTERISTIC: VISA IMAGES	45
13	ERROR TRADEOFF CHARACTERISTIC: VISA IMAGES	46
14	ERROR TRADEOFF CHARACTERISTIC: VISA IMAGES	47
15	ERROR TRADEOFF CHARACTERISTIC: VISA IMAGES	48
16	ERROR TRADEOFF CHARACTERISTIC: VISA IMAGES	49
17	ERROR TRADEOFF CHARACTERISTIC: VISA IMAGES	50
18	ERROR TRADEOFF CHARACTERISTIC: VISA IMAGES	51
19	ERROR TRADEOFF CHARACTERISTIC: VISA IMAGES	52
20	ERROR TRADEOFF CHARACTERISTIC: VISA IMAGES	53
21	ERROR TRADEOFF CHARACTERISTIC: VISA IMAGES	54
22	ERROR TRADEOFF CHARACTERISTIC: VISA IMAGES	55
23	ERROR TRADEOFF CHARACTERISTIC: VISA IMAGES	56
24	ERROR TRADEOFF CHARACTERISTIC: VISA IMAGES	57
25	ERROR TRADEOFF CHARACTERISTIC: VISA IMAGES	58
26	ERROR TRADEOFF CHARACTERISTIC: MUGSHOT IMAGES	59
27	ERROR TRADEOFF CHARACTERISTIC: MUGSHOT IMAGES	60
28	ERROR TRADEOFF CHARACTERISTIC: WILD IMAGES	61
29	ERROR TRADEOFF CHARACTERISTIC: WILD IMAGES	62
30	ERROR TRADEOFF CHARACTERISTIC: WILD IMAGES	63
31	ERROR TRADEOFF CHARACTERISTIC: WILD IMAGES	64
32	ERROR TRADEOFF CHARACTERISTIC: WILD IMAGES	65
33	ERROR TRADEOFF CHARACTERISTIC: WILD IMAGES	66
34	ERROR TRADEOFF CHARACTERISTICS: CHILD EXPLOITATION IMAGES	67
35	ERROR TRADEOFF CHARACTERISTICS: CHILD EXPLOITATION IMAGES	68
36	ERROR TRADEOFF CHARACTERISTICS: CHILD EXPLOITATION IMAGES	69
37	ERROR TRADEOFF CHARACTERISTICS: CHILD EXPLOITATION IMAGES	70
38	CMC CHARACTERISTICS: CHILD EXPLOITATION IMAGES	71
39	CMC CHARACTERISTICS: CHILD EXPLOITATION IMAGES	72
40	CMC CHARACTERISTICS: CHILD EXPLOITATION IMAGES	73
41	CMC CHARACTERISTICS: CHILD EXPLOITATION IMAGES	74
42	FALSE MATCH RATES WITHIN AND ACROSS DEMOGRAPHIC GROUPS	75
43	FALSE MATCH RATES WITHIN AND ACROSS DEMOGRAPHIC GROUPS	76
44	FALSE MATCH RATES WITHIN AND ACROSS DEMOGRAPHIC GROUPS	77
45	FALSE MATCH RATES WITHIN AND ACROSS DEMOGRAPHIC GROUPS	78
46	FALSE MATCH RATES WITHIN AND ACROSS DEMOGRAPHIC GROUPS	79
47	FALSE MATCH RATES WITHIN AND ACROSS DEMOGRAPHIC GROUPS	80
48	FALSE MATCH RATES WITHIN AND ACROSS DEMOGRAPHIC GROUPS	81
49	FALSE MATCH RATES WITHIN AND ACROSS DEMOGRAPHIC GROUPS	82
50	SEX AND RACE EFFECTS: MUGSHOT IMAGES	83
51	SEX AND RACE EFFECTS: MUGSHOT IMAGES	84
52	SEX AND RACE EFFECTS: MUGSHOT IMAGES	85
53	SEX AND RACE EFFECTS: MUGSHOT IMAGES	86
54	SEX AND RACE EFFECTS: MUGSHOT IMAGES	87
55	SEX AND RACE EFFECTS: MUGSHOT IMAGES	88
56	SEX AND RACE EFFECTS: MUGSHOT IMAGES	89
57	SEX AND RACE EFFECTS: MUGSHOT IMAGES	90
58	SEX EFFECTS: VISA IMAGES	91
59	SEX EFFECTS: VISA IMAGES	92
60	SEX EFFECTS: VISA IMAGES	93

61	SEX EFFECTS: VISA IMAGES	94
62	SEX EFFECTS: VISA IMAGES	95
63	SEX EFFECTS: VISA IMAGES	96
64	SEX EFFECTS: VISA IMAGES	97
65	SEX EFFECTS: VISA IMAGES	98
66	SEX EFFECTS: VISA IMAGES	99
67	SEX EFFECTS: VISA IMAGES	100
68	SEX EFFECTS: VISA IMAGES	101
69	SEX EFFECTS: VISA IMAGES	102
70	SEX EFFECTS: VISA IMAGES	103
71	FALSE MATCH RATE CALIBRATION: MUGSHOT IMAGES	104
72	FALSE MATCH RATE CALIBRATION: MUGSHOT IMAGES	105
73	FALSE MATCH RATE CALIBRATION: MUGSHOT IMAGES	106
74	FALSE MATCH RATE CALIBRATION: MUGSHOT IMAGES	107
75	FALSE MATCH RATE CALIBRATION: MUGSHOT IMAGES	108
76	FALSE MATCH RATE CALIBRATION: MUGSHOT IMAGES	109
77	FALSE MATCH RATE CALIBRATION: MUGSHOT IMAGES	110
78	FALSE MATCH RATE CALIBRATION: MUGSHOT IMAGES	111
79	FALSE MATCH RATE CALIBRATION: VISA IMAGES	112
80	FALSE MATCH RATE CALIBRATION: VISA IMAGES	113
81	FALSE MATCH RATE CALIBRATION: VISA IMAGES	114
82	FALSE MATCH RATE CALIBRATION: VISA IMAGES	115
83	FALSE MATCH RATE CALIBRATION: VISA IMAGES	116
84	FALSE MATCH RATE CALIBRATION: VISA IMAGES	117
85	FALSE MATCH RATE CALIBRATION: VISA IMAGES	118
86	FALSE MATCH RATE CALIBRATION: VISA IMAGES	119
87	FALSE MATCH RATE CALIBRATION: VISA IMAGES	120
88	FALSE MATCH RATE CALIBRATION: VISA IMAGES	121
89	FALSE MATCH RATE CALIBRATION: VISA IMAGES	122
90	FALSE MATCH RATE CALIBRATION: VISA IMAGES	123
91	FALSE MATCH RATE CALIBRATION: VISA IMAGES	124
92	FALSE MATCH RATE CALIBRATION: VISA IMAGES	125
93	FALSE MATCH RATE CALIBRATION: VISA IMAGES	126
94	FALSE MATCH RATE CONCENTRATION: VISA IMAGES	127
95	EFFECT OF COUNTRY OF BIRTH ON FNMR	129
96	EFFECT OF COUNTRY OF BIRTH ON FNMR	130
97	EFFECT OF COUNTRY OF BIRTH ON FNMR	131
98	EFFECT OF COUNTRY OF BIRTH ON FNMR	132
99	EFFECT OF COUNTRY OF BIRTH ON FNMR	133
100	EFFECT OF COUNTRY OF BIRTH ON FNMR	134
101	EFFECT OF COUNTRY OF BIRTH ON FNMR	135
102	EFFECT OF COUNTRY OF BIRTH ON FNMR	136
103	EFFECT OF COUNTRY OF BIRTH ON FNMR	137
104	EFFECT OF COUNTRY OF BIRTH ON FNMR	138
105	EFFECT OF COUNTRY OF BIRTH ON FNMR	139
106	EFFECT OF COUNTRY OF BIRTH ON FNMR	140
107	EFFECT OF COUNTRY OF BIRTH ON FNMR	141
108	ERROR TRADEOFF CHARACTERISTIC: MUGSHOT IMAGES	143
109	ERROR TRADEOFF CHARACTERISTIC: MUGSHOT IMAGES	144
110	ERROR TRADEOFF CHARACTERISTIC: MUGSHOT IMAGES	145
111	ERROR TRADEOFF CHARACTERISTIC: MUGSHOT IMAGES	146
112	ERROR TRADEOFF CHARACTERISTIC: MUGSHOT IMAGES	147
113	ERROR TRADEOFF CHARACTERISTIC: MUGSHOT IMAGES	148
114	ERROR TRADEOFF CHARACTERISTIC: MUGSHOT IMAGES	149
115	ERROR TRADEOFF CHARACTERISTIC: MUGSHOT IMAGES	150
116	ERROR TRADEOFF CHARACTERISTIC: MUGSHOT IMAGES	151
117	EFFECT OF SUBJECT AGE ON FNMR	153

118	EFFECT OF SUBJECT AGE ON FNMR	154
119	EFFECT OF SUBJECT AGE ON FNMR	155
120	EFFECT OF SUBJECT AGE ON FNMR	156
121	EFFECT OF SUBJECT AGE ON FNMR	157
122	EFFECT OF SUBJECT AGE ON FNMR	158
123	EFFECT OF SUBJECT AGE ON FNMR	159
124	EFFECT OF SUBJECT AGE ON FNMR	160
125	EFFECT OF SUBJECT AGE ON FNMR	161
126	EFFECT OF SUBJECT AGE ON FNMR	162
127	EFFECT OF SUBJECT AGE ON FNMR	163
128	EFFECT OF SUBJECT AGE ON FNMR	164
129	EFFECT OF SUBJECT AGE ON FNMR	165
130	WORST CASE REGIONAL EFFECT FNMR	168
131	IMPOSTOR DISTRIBUTION SHIFTS FOR SELECT COUNTRY PAIRS	170
132	ALGORITHM 3DIVI-003 CROSS REGION FMR	171
133	ALGORITHM 3DIVI-004 CROSS REGION FMR	172
134	ALGORITHM ADERA-001 CROSS REGION FMR	173
135	ALGORITHM ALCHERA-000 CROSS REGION FMR	174
136	ALGORITHM ALCHERA-001 CROSS REGION FMR	175
137	ALGORITHM ALLGOVISION-000 CROSS REGION FMR	176
138	ALGORITHM ALPHAFACE-001 CROSS REGION FMR	177
139	ALGORITHM AMPLIFIEDGROUP-001 CROSS REGION FMR	178
140	ALGORITHM ANKE-003 CROSS REGION FMR	179
141	ALGORITHM ANKE-004 CROSS REGION FMR	180
142	ALGORITHM ANYVISION-002 CROSS REGION FMR	181
143	ALGORITHM ANYVISION-004 CROSS REGION FMR	182
144	ALGORITHM AWARE-003 CROSS REGION FMR	183
145	ALGORITHM AWARE-004 CROSS REGION FMR	184
146	ALGORITHM AYONIX-000 CROSS REGION FMR	185
147	ALGORITHM BM-001 CROSS REGION FMR	186
148	ALGORITHM CAMVI-002 CROSS REGION FMR	187
149	ALGORITHM CAMVI-004 CROSS REGION FMR	188
150	ALGORITHM CEIEC-001 CROSS REGION FMR	189
151	ALGORITHM CEIEC-002 CROSS REGION FMR	190
152	ALGORITHM CHTFACE-001 CROSS REGION FMR	191
153	ALGORITHM COGENT-003 CROSS REGION FMR	192
154	ALGORITHM COGENT-004 CROSS REGION FMR	193
155	ALGORITHM COGNITEC-000 CROSS REGION FMR	194
156	ALGORITHM COGNITEC-001 CROSS REGION FMR	195
157	ALGORITHM CTBCBANK-000 CROSS REGION FMR	196
158	ALGORITHM CYBEREXTRUDER-001 CROSS REGION FMR	197
159	ALGORITHM CYBEREXTRUDER-002 CROSS REGION FMR	198
160	ALGORITHM CYBERLINK-001 CROSS REGION FMR	199
161	ALGORITHM CYBERLINK-002 CROSS REGION FMR	200
162	ALGORITHM DAHUA-002 CROSS REGION FMR	201
163	ALGORITHM DAHUA-003 CROSS REGION FMR	202
164	ALGORITHM DEEGLINT-001 CROSS REGION FMR	203
165	ALGORITHM DEEPSEA-001 CROSS REGION FMR	204
166	ALGORITHM DERMALOG-005 CROSS REGION FMR	205
167	ALGORITHM DERMALOG-006 CROSS REGION FMR	206
168	ALGORITHM DIGITALBARRIERS-002 CROSS REGION FMR	207
169	ALGORITHM DSK-000 CROSS REGION FMR	208
170	ALGORITHM EINetworks-000 CROSS REGION FMR	209
171	ALGORITHM EVERAI-002 CROSS REGION FMR	210
172	ALGORITHM F8-001 CROSS REGION FMR	211

173 ALGORITHM FACESOFT-000 CROSS REGION FMR	212
174 ALGORITHM GLORY-000 CROSS REGION FMR	213
175 ALGORITHM GLORY-001 CROSS REGION FMR	214
176 ALGORITHM GORILLA-002 CROSS REGION FMR	215
177 ALGORITHM GORILLA-003 CROSS REGION FMR	216
178 ALGORITHM HIK-001 CROSS REGION FMR	217
179 ALGORITHM HR-001 CROSS REGION FMR	218
180 ALGORITHM ID3-003 CROSS REGION FMR	219
181 ALGORITHM ID3-004 CROSS REGION FMR	220
182 ALGORITHM IDEMIA-003 CROSS REGION FMR	221
183 ALGORITHM IDEMIA-004 CROSS REGION FMR	222
184 ALGORITHM IIT-000 CROSS REGION FMR	223
185 ALGORITHM IIT-001 CROSS REGION FMR	224
186 ALGORITHM IMAGUS-000 CROSS REGION FMR	225
187 ALGORITHM IMPERIAL-000 CROSS REGION FMR	226
188 ALGORITHM IMPERIAL-002 CROSS REGION FMR	227
189 ALGORITHM INCODE-003 CROSS REGION FMR	228
190 ALGORITHM INCODE-004 CROSS REGION FMR	229
191 ALGORITHM INNOVATRICS-004 CROSS REGION FMR	230
192 ALGORITHM INNOVATRICS-006 CROSS REGION FMR	231
193 ALGORITHM INTELLICLOUDAI-001 CROSS REGION FMR	232
194 ALGORITHM INTELLIFUSION-001 CROSS REGION FMR	233
195 ALGORITHM INTELLIVISION-001 CROSS REGION FMR	234
196 ALGORITHM INTELLIVISION-002 CROSS REGION FMR	235
197 ALGORITHM INTELRESEARCH-000 CROSS REGION FMR	236
198 ALGORITHM INTSYSMSU-000 CROSS REGION FMR	237
199 ALGORITHM IQFACE-000 CROSS REGION FMR	238
200 ALGORITHM ISAP-001 CROSS REGION FMR	239
201 ALGORITHM ISITYOU-000 CROSS REGION FMR	240
202 ALGORITHM ISYSTEMS-001 CROSS REGION FMR	241
203 ALGORITHM ISYSTEMS-002 CROSS REGION FMR	242
204 ALGORITHM ITMO-005 CROSS REGION FMR	243
205 ALGORITHM ITMO-006 CROSS REGION FMR	244
206 ALGORITHM KAKAO-001 CROSS REGION FMR	245
207 ALGORITHM KAKAO-002 CROSS REGION FMR	246
208 ALGORITHM KEDACOM-000 CROSS REGION FMR	247
209 ALGORITHM KNERON-003 CROSS REGION FMR	248
210 ALGORITHM LOOKMAN-002 CROSS REGION FMR	249
211 ALGORITHM LOOKMAN-004 CROSS REGION FMR	250
212 ALGORITHM MEGVII-001 CROSS REGION FMR	251
213 ALGORITHM MEGVII-002 CROSS REGION FMR	252
214 ALGORITHM MEIYA-001 CROSS REGION FMR	253
215 ALGORITHM MICROFOCUS-001 CROSS REGION FMR	254
216 ALGORITHM MICROFOCUS-002 CROSS REGION FMR	255
217 ALGORITHM MT-000 CROSS REGION FMR	256
218 ALGORITHM NEUROTECHNOLOGY-005 CROSS REGION FMR	257
219 ALGORITHM NEUROTECHNOLOGY-006 CROSS REGION FMR	258
220 ALGORITHM NODEFLUX-001 CROSS REGION FMR	259
221 ALGORITHM NODEFLUX-002 CROSS REGION FMR	260
222 ALGORITHM NOTIONTAG-000 CROSS REGION FMR	261
223 ALGORITHM NTECHLAB-006 CROSS REGION FMR	262
224 ALGORITHM NTECHLAB-007 CROSS REGION FMR	263
225 ALGORITHM PIXELALL-002 CROSS REGION FMR	264
226 ALGORITHM PSL-001 CROSS REGION FMR	265
227 ALGORITHM PSL-002 CROSS REGION FMR	266
228 ALGORITHM RANKONE-006 CROSS REGION FMR	267
229 ALGORITHM RANKONE-007 CROSS REGION FMR	268

230 ALGORITHM REALNETWORKS-002 CROSS REGION FMR	269
231 ALGORITHM REALNETWORKS-003 CROSS REGION FMR	270
232 ALGORITHM REMARKAI-000 CROSS REGION FMR	271
233 ALGORITHM REMARKAI-001 CROSS REGION FMR	272
234 ALGORITHM ROKID-000 CROSS REGION FMR	273
235 ALGORITHM SAFFE-001 CROSS REGION FMR	274
236 ALGORITHM SAFFE-002 CROSS REGION FMR	275
237 ALGORITHM SENSETIME-001 CROSS REGION FMR	276
238 ALGORITHM SENSETIME-002 CROSS REGION FMR	277
239 ALGORITHM SHAMAN-000 CROSS REGION FMR	278
240 ALGORITHM SHAMAN-001 CROSS REGION FMR	279
241 ALGORITHM SHU-001 CROSS REGION FMR	280
242 ALGORITHM SIAT-002 CROSS REGION FMR	281
243 ALGORITHM SIAT-004 CROSS REGION FMR	282
244 ALGORITHM SMILART-002 CROSS REGION FMR	283
245 ALGORITHM SMILART-003 CROSS REGION FMR	284
246 ALGORITHM STARHYBRID-001 CROSS REGION FMR	285
247 ALGORITHM SYNESIS-004 CROSS REGION FMR	286
248 ALGORITHM SYNESIS-005 CROSS REGION FMR	287
249 ALGORITHM TECH5-002 CROSS REGION FMR	288
250 ALGORITHM TECH5-003 CROSS REGION FMR	289
251 ALGORITHM TEVIAN-003 CROSS REGION FMR	290
252 ALGORITHM TEVIAN-004 CROSS REGION FMR	291
253 ALGORITHM TIGER-002 CROSS REGION FMR	292
254 ALGORITHM TIGER-003 CROSS REGION FMR	293
255 ALGORITHM TONGYI-005 CROSS REGION FMR	294
256 ALGORITHM TOSHIBA-002 CROSS REGION FMR	295
257 ALGORITHM TOSHIBA-003 CROSS REGION FMR	296
258 ALGORITHM ULSEE-001 CROSS REGION FMR	297
259 ALGORITHM ULUFACE-002 CROSS REGION FMR	298
260 ALGORITHM UPC-001 CROSS REGION FMR	299
261 ALGORITHM VCOG-002 CROSS REGION FMR	300
262 ALGORITHM VD-001 CROSS REGION FMR	301
263 ALGORITHM VERIDAS-001 CROSS REGION FMR	302
264 ALGORITHM VERIDAS-002 CROSS REGION FMR	303
265 ALGORITHM VIA-000 CROSS REGION FMR	304
266 ALGORITHM VIDEONETICS-001 CROSS REGION FMR	305
267 ALGORITHM VIGILANTSOLUTIONS-006 CROSS REGION FMR	306
268 ALGORITHM VIGILANTSOLUTIONS-007 CROSS REGION FMR	307
269 ALGORITHM VION-000 CROSS REGION FMR	308
270 ALGORITHM VISIONBOX-000 CROSS REGION FMR	309
271 ALGORITHM VISIONBOX-001 CROSS REGION FMR	310
272 ALGORITHM VISIONLABS-006 CROSS REGION FMR	311
273 ALGORITHM VISIONLABS-007 CROSS REGION FMR	312
274 ALGORITHM VOCORD-006 CROSS REGION FMR	313
275 ALGORITHM VOCORD-007 CROSS REGION FMR	314
276 ALGORITHM WINSENSE-000 CROSS REGION FMR	315
277 ALGORITHM YISHENG-004 CROSS REGION FMR	316
278 ALGORITHM YITU-003 CROSS REGION FMR	317
279 ALGORITHM 3DIVI-003 CROSS COUNTRY FMR	318
280 ALGORITHM 3DIVI-004 CROSS COUNTRY FMR	319
281 ALGORITHM ADERA-001 CROSS COUNTRY FMR	320
282 ALGORITHM ALCHERA-000 CROSS COUNTRY FMR	321
283 ALGORITHM ALCHERA-001 CROSS COUNTRY FMR	322
284 ALGORITHM ALLGOVISION-000 CROSS COUNTRY FMR	323
285 ALGORITHM ALPHAFACE-001 CROSS COUNTRY FMR	324
286 ALGORITHM AMPLIFIEDGROUP-001 CROSS COUNTRY FMR	325

287 ALGORITHM ANKE-003 CROSS COUNTRY FMR	326
288 ALGORITHM ANKE-004 CROSS COUNTRY FMR	327
289 ALGORITHM ANYVISION-002 CROSS COUNTRY FMR	328
290 ALGORITHM ANYVISION-004 CROSS COUNTRY FMR	329
291 ALGORITHM AWARE-003 CROSS COUNTRY FMR	330
292 ALGORITHM AWARE-004 CROSS COUNTRY FMR	331
293 ALGORITHM AYONIX-000 CROSS COUNTRY FMR	332
294 ALGORITHM BM-001 CROSS COUNTRY FMR	333
295 ALGORITHM CAMVI-002 CROSS COUNTRY FMR	334
296 ALGORITHM CAMVI-004 CROSS COUNTRY FMR	335
297 ALGORITHM CEIEC-001 CROSS COUNTRY FMR	336
298 ALGORITHM CEIEC-002 CROSS COUNTRY FMR	337
299 ALGORITHM CHTFACE-001 CROSS COUNTRY FMR	338
300 ALGORITHM COGENT-003 CROSS COUNTRY FMR	339
301 ALGORITHM COGENT-004 CROSS COUNTRY FMR	340
302 ALGORITHM COGNITEC-000 CROSS COUNTRY FMR	341
303 ALGORITHM COGNITEC-001 CROSS COUNTRY FMR	342
304 ALGORITHM CTBCBANK-000 CROSS COUNTRY FMR	343
305 ALGORITHM CYBEREXTRUDER-001 CROSS COUNTRY FMR	344
306 ALGORITHM CYBEREXTRUDER-002 CROSS COUNTRY FMR	345
307 ALGORITHM CYBERLINK-001 CROSS COUNTRY FMR	346
308 ALGORITHM CYBERLINK-002 CROSS COUNTRY FMR	347
309 ALGORITHM DAHUA-002 CROSS COUNTRY FMR	348
310 ALGORITHM DAHUA-003 CROSS COUNTRY FMR	349
311 ALGORITHM DEEPLINT-001 CROSS COUNTRY FMR	350
312 ALGORITHM DEEPSEA-001 CROSS COUNTRY FMR	351
313 ALGORITHM DERMALOG-005 CROSS COUNTRY FMR	352
314 ALGORITHM DERMALOG-006 CROSS COUNTRY FMR	353
315 ALGORITHM DIGITALBARIERS-002 CROSS COUNTRY FMR	354
316 ALGORITHM DSK-000 CROSS COUNTRY FMR	355
317 ALGORITHM EINETWORKS-000 CROSS COUNTRY FMR	356
318 ALGORITHM EVERAI-002 CROSS COUNTRY FMR	357
319 ALGORITHM F8-001 CROSS COUNTRY FMR	358
320 ALGORITHM FACESOFT-000 CROSS COUNTRY FMR	359
321 ALGORITHM GLORY-000 CROSS COUNTRY FMR	360
322 ALGORITHM GLORY-001 CROSS COUNTRY FMR	361
323 ALGORITHM GORILLA-002 CROSS COUNTRY FMR	362
324 ALGORITHM GORILLA-003 CROSS COUNTRY FMR	363
325 ALGORITHM HIK-001 CROSS COUNTRY FMR	364
326 ALGORITHM HR-001 CROSS COUNTRY FMR	365
327 ALGORITHM ID3-003 CROSS COUNTRY FMR	366
328 ALGORITHM ID3-004 CROSS COUNTRY FMR	367
329 ALGORITHM IDEMIA-003 CROSS COUNTRY FMR	368
330 ALGORITHM IDEMIA-004 CROSS COUNTRY FMR	369
331 ALGORITHM IIT-000 CROSS COUNTRY FMR	370
332 ALGORITHM IIT-001 CROSS COUNTRY FMR	371
333 ALGORITHM IMAGUS-000 CROSS COUNTRY FMR	372
334 ALGORITHM IMPERIAL-000 CROSS COUNTRY FMR	373
335 ALGORITHM IMPERIAL-002 CROSS COUNTRY FMR	374
336 ALGORITHM INCODE-003 CROSS COUNTRY FMR	375
337 ALGORITHM INCODE-004 CROSS COUNTRY FMR	376
338 ALGORITHM INNOVATRICS-004 CROSS COUNTRY FMR	377
339 ALGORITHM INNOVATRICS-006 CROSS COUNTRY FMR	378
340 ALGORITHM INTELICLOUDAI-001 CROSS COUNTRY FMR	379
341 ALGORITHM INTELLIFUSION-001 CROSS COUNTRY FMR	380
342 ALGORITHM INTELLIVISION-001 CROSS COUNTRY FMR	381
343 ALGORITHM INTELLIVISION-002 CROSS COUNTRY FMR	382

344 ALGORITHM INTELRESEARCH-000 CROSS COUNTRY FMR	383
345 ALGORITHM INTSYSMSU-000 CROSS COUNTRY FMR	384
346 ALGORITHM IQFACE-000 CROSS COUNTRY FMR	385
347 ALGORITHM ISAP-001 CROSS COUNTRY FMR	386
348 ALGORITHM ISITYOU-000 CROSS COUNTRY FMR	387
349 ALGORITHM ISYSTEMS-001 CROSS COUNTRY FMR	388
350 ALGORITHM ISYSTEMS-002 CROSS COUNTRY FMR	389
351 ALGORITHM ITMO-005 CROSS COUNTRY FMR	390
352 ALGORITHM ITMO-006 CROSS COUNTRY FMR	391
353 ALGORITHM KAKAO-001 CROSS COUNTRY FMR	392
354 ALGORITHM KAKAO-002 CROSS COUNTRY FMR	393
355 ALGORITHM KEDACOM-000 CROSS COUNTRY FMR	394
356 ALGORITHM KNERON-003 CROSS COUNTRY FMR	395
357 ALGORITHM LOOKMAN-002 CROSS COUNTRY FMR	396
358 ALGORITHM LOOKMAN-004 CROSS COUNTRY FMR	397
359 ALGORITHM MEGVII-001 CROSS COUNTRY FMR	398
360 ALGORITHM MEGVII-002 CROSS COUNTRY FMR	399
361 ALGORITHM MEIYA-001 CROSS COUNTRY FMR	400
362 ALGORITHM MICROFOCUS-001 CROSS COUNTRY FMR	401
363 ALGORITHM MICROFOCUS-002 CROSS COUNTRY FMR	402
364 ALGORITHM MT-000 CROSS COUNTRY FMR	403
365 ALGORITHM NEUROTECHNOLOGY-005 CROSS COUNTRY FMR	404
366 ALGORITHM NEUROTECHNOLOGY-006 CROSS COUNTRY FMR	405
367 ALGORITHM NODEFLUX-001 CROSS COUNTRY FMR	406
368 ALGORITHM NODEFLUX-002 CROSS COUNTRY FMR	407
369 ALGORITHM NOTIONTAG-000 CROSS COUNTRY FMR	408
370 ALGORITHM NTECHLAB-006 CROSS COUNTRY FMR	409
371 ALGORITHM NTECHLAB-007 CROSS COUNTRY FMR	410
372 ALGORITHM PIXELALL-002 CROSS COUNTRY FMR	411
373 ALGORITHM PSL-001 CROSS COUNTRY FMR	412
374 ALGORITHM PSL-002 CROSS COUNTRY FMR	413
375 ALGORITHM RANKONE-006 CROSS COUNTRY FMR	414
376 ALGORITHM RANKONE-007 CROSS COUNTRY FMR	415
377 ALGORITHM REALNETWORKS-002 CROSS COUNTRY FMR	416
378 ALGORITHM REALNETWORKS-003 CROSS COUNTRY FMR	417
379 ALGORITHM REMARKAI-000 CROSS COUNTRY FMR	418
380 ALGORITHM REMARKAI-001 CROSS COUNTRY FMR	419
381 ALGORITHM ROKID-000 CROSS COUNTRY FMR	420
382 ALGORITHM SAFFE-001 CROSS COUNTRY FMR	421
383 ALGORITHM SAFFE-002 CROSS COUNTRY FMR	422
384 ALGORITHM SENSETIME-001 CROSS COUNTRY FMR	423
385 ALGORITHM SENSETIME-002 CROSS COUNTRY FMR	424
386 ALGORITHM SHAMAN-000 CROSS COUNTRY FMR	425
387 ALGORITHM SHAMAN-001 CROSS COUNTRY FMR	426
388 ALGORITHM SHU-001 CROSS COUNTRY FMR	427
389 ALGORITHM SIAT-002 CROSS COUNTRY FMR	428
390 ALGORITHM SIAT-004 CROSS COUNTRY FMR	429
391 ALGORITHM SMILART-002 CROSS COUNTRY FMR	430
392 ALGORITHM SMILART-003 CROSS COUNTRY FMR	431
393 ALGORITHM STARHYBRID-001 CROSS COUNTRY FMR	432
394 ALGORITHM SYNESIS-004 CROSS COUNTRY FMR	433
395 ALGORITHM SYNESIS-005 CROSS COUNTRY FMR	434
396 ALGORITHM TECH5-002 CROSS COUNTRY FMR	435
397 ALGORITHM TECH5-003 CROSS COUNTRY FMR	436
398 ALGORITHM TEVIAN-003 CROSS COUNTRY FMR	437
399 ALGORITHM TEVIAN-004 CROSS COUNTRY FMR	438

400 ALGORITHM TIGER-002 CROSS COUNTRY FMR	439
401 ALGORITHM TIGER-003 CROSS COUNTRY FMR	440
402 ALGORITHM TONGYI-005 CROSS COUNTRY FMR	441
403 ALGORITHM TOSHIBA-002 CROSS COUNTRY FMR	442
404 ALGORITHM TOSHIBA-003 CROSS COUNTRY FMR	443
405 ALGORITHM ULSEE-001 CROSS COUNTRY FMR	444
406 ALGORITHM ULUFACE-002 CROSS COUNTRY FMR	445
407 ALGORITHM UPC-001 CROSS COUNTRY FMR	446
408 ALGORITHM VCOG-002 CROSS COUNTRY FMR	447
409 ALGORITHM VD-001 CROSS COUNTRY FMR	448
410 ALGORITHM VERIDAS-001 CROSS COUNTRY FMR	449
411 ALGORITHM VERIDAS-002 CROSS COUNTRY FMR	450
412 ALGORITHM VIA-000 CROSS COUNTRY FMR	451
413 ALGORITHM VIDEONETICS-001 CROSS COUNTRY FMR	452
414 ALGORITHM VIGILANTSOLUTIONS-006 CROSS COUNTRY FMR	453
415 ALGORITHM VIGILANTSOLUTIONS-007 CROSS COUNTRY FMR	454
416 ALGORITHM VION-000 CROSS COUNTRY FMR	455
417 ALGORITHM VISIONBOX-000 CROSS COUNTRY FMR	456
418 ALGORITHM VISIONBOX-001 CROSS COUNTRY FMR	457
419 ALGORITHM VISIONLABS-006 CROSS COUNTRY FMR	458
420 ALGORITHM VISIONLABS-007 CROSS COUNTRY FMR	459
421 ALGORITHM VOCORD-006 CROSS COUNTRY FMR	460
422 ALGORITHM VOCORD-007 CROSS COUNTRY FMR	461
423 ALGORITHM WINSENSE-000 CROSS COUNTRY FMR	462
424 ALGORITHM YISHENG-004 CROSS COUNTRY FMR	463
425 ALGORITHM YITU-003 CROSS COUNTRY FMR	464
426 IMPOSTOR COUNTS FOR CROSS COUNTRY FMR CALCULATIONS	465
427 ALGORITHM 3DIVI-003 CROSS AGE FMR	467
428 ALGORITHM 3DIVI-004 CROSS AGE FMR	468
429 ALGORITHM ADERA-001 CROSS AGE FMR	469
430 ALGORITHM ALCHERA-000 CROSS AGE FMR	470
431 ALGORITHM ALCHERA-001 CROSS AGE FMR	471
432 ALGORITHM ALLGOVISION-000 CROSS AGE FMR	472
433 ALGORITHM ALPHAFACE-001 CROSS AGE FMR	473
434 ALGORITHM AMPLIFIEDGROUP-001 CROSS AGE FMR	474
435 ALGORITHM ANKE-003 CROSS AGE FMR	475
436 ALGORITHM ANKE-004 CROSS AGE FMR	476
437 ALGORITHM ANYVISION-002 CROSS AGE FMR	477
438 ALGORITHM ANYVISION-004 CROSS AGE FMR	478
439 ALGORITHM AWARE-003 CROSS AGE FMR	479
440 ALGORITHM AWARE-004 CROSS AGE FMR	480
441 ALGORITHM AYONIX-000 CROSS AGE FMR	481
442 ALGORITHM BM-001 CROSS AGE FMR	482
443 ALGORITHM CAMVI-002 CROSS AGE FMR	483
444 ALGORITHM CAMVI-004 CROSS AGE FMR	484
445 ALGORITHM CEIEC-001 CROSS AGE FMR	485
446 ALGORITHM CEIEC-002 CROSS AGE FMR	486
447 ALGORITHM CHTFACE-001 CROSS AGE FMR	487
448 ALGORITHM COGENT-003 CROSS AGE FMR	488
449 ALGORITHM COGENT-004 CROSS AGE FMR	489
450 ALGORITHM COGNITEC-000 CROSS AGE FMR	490
451 ALGORITHM COGNITEC-001 CROSS AGE FMR	491
452 ALGORITHM CTBCBANK-000 CROSS AGE FMR	492
453 ALGORITHM CYBEREXTRUDER-001 CROSS AGE FMR	493
454 ALGORITHM CYBEREXTRUDER-002 CROSS AGE FMR	494
455 ALGORITHM CYBERLINK-001 CROSS AGE FMR	495

456 ALGORITHM CYBERLINK-002 CROSS AGE FMR	496
457 ALGORITHM DAHUA-002 CROSS AGE FMR	497
458 ALGORITHM DAHUA-003 CROSS AGE FMR	498
459 ALGORITHM DEEPLINT-001 CROSS AGE FMR	499
460 ALGORITHM DEEPSEA-001 CROSS AGE FMR	500
461 ALGORITHM DERMALOG-005 CROSS AGE FMR	501
462 ALGORITHM DERMALOG-006 CROSS AGE FMR	502
463 ALGORITHM DIGITALBARRIERS-002 CROSS AGE FMR	503
464 ALGORITHM DSK-000 CROSS AGE FMR	504
465 ALGORITHM EINETWORKS-000 CROSS AGE FMR	505
466 ALGORITHM EVERAI-002 CROSS AGE FMR	506
467 ALGORITHM F8-001 CROSS AGE FMR	507
468 ALGORITHM FACESOFT-000 CROSS AGE FMR	508
469 ALGORITHM GLORY-000 CROSS AGE FMR	509
470 ALGORITHM GLORY-001 CROSS AGE FMR	510
471 ALGORITHM GORILLA-002 CROSS AGE FMR	511
472 ALGORITHM GORILLA-003 CROSS AGE FMR	512
473 ALGORITHM HIK-001 CROSS AGE FMR	513
474 ALGORITHM HR-001 CROSS AGE FMR	514
475 ALGORITHM ID3-003 CROSS AGE FMR	515
476 ALGORITHM ID3-004 CROSS AGE FMR	516
477 ALGORITHM IDEMIA-003 CROSS AGE FMR	517
478 ALGORITHM IDEMIA-004 CROSS AGE FMR	518
479 ALGORITHM IIT-000 CROSS AGE FMR	519
480 ALGORITHM IIT-001 CROSS AGE FMR	520
481 ALGORITHM IMAGUS-000 CROSS AGE FMR	521
482 ALGORITHM IMPERIAL-000 CROSS AGE FMR	522
483 ALGORITHM IMPERIAL-002 CROSS AGE FMR	523
484 ALGORITHM INCODE-003 CROSS AGE FMR	524
485 ALGORITHM INCODE-004 CROSS AGE FMR	525
486 ALGORITHM INNOVATRICS-004 CROSS AGE FMR	526
487 ALGORITHM INNOVATRICS-006 CROSS AGE FMR	527
488 ALGORITHM INTELLICLOUDAI-001 CROSS AGE FMR	528
489 ALGORITHM INTELLIFUSION-001 CROSS AGE FMR	529
490 ALGORITHM INTELLIVISION-001 CROSS AGE FMR	530
491 ALGORITHM INTELLIVISION-002 CROSS AGE FMR	531
492 ALGORITHM INTELRESEARCH-000 CROSS AGE FMR	532
493 ALGORITHM INTSYSMSU-000 CROSS AGE FMR	533
494 ALGORITHM IQFACE-000 CROSS AGE FMR	534
495 ALGORITHM ISAP-001 CROSS AGE FMR	535
496 ALGORITHM ISITYOU-000 CROSS AGE FMR	536
497 ALGORITHM ISYSTEMS-001 CROSS AGE FMR	537
498 ALGORITHM ISYSTEMS-002 CROSS AGE FMR	538
499 ALGORITHM ITMO-005 CROSS AGE FMR	539
500 ALGORITHM ITMO-006 CROSS AGE FMR	540
501 ALGORITHM KAKAO-001 CROSS AGE FMR	541
502 ALGORITHM KAKAO-002 CROSS AGE FMR	542
503 ALGORITHM KEDACOM-000 CROSS AGE FMR	543
504 ALGORITHM KNERON-003 CROSS AGE FMR	544
505 ALGORITHM LOOKMAN-002 CROSS AGE FMR	545
506 ALGORITHM LOOKMAN-004 CROSS AGE FMR	546
507 ALGORITHM MEGVII-001 CROSS AGE FMR	547
508 ALGORITHM MEGVII-002 CROSS AGE FMR	548
509 ALGORITHM MEIYA-001 CROSS AGE FMR	549
510 ALGORITHM MICROFOCUS-001 CROSS AGE FMR	550
511 ALGORITHM MICROFOCUS-002 CROSS AGE FMR	551
512 ALGORITHM MT-000 CROSS AGE FMR	552

513 ALGORITHM NEUROTECHNOLOGY-005 CROSS AGE FMR	553
514 ALGORITHM NEUROTECHNOLOGY-006 CROSS AGE FMR	554
515 ALGORITHM NODEFLUX-001 CROSS AGE FMR	555
516 ALGORITHM NODEFLUX-002 CROSS AGE FMR	556
517 ALGORITHM NOTIONTAG-000 CROSS AGE FMR	557
518 ALGORITHM NTECHLAB-006 CROSS AGE FMR	558
519 ALGORITHM NTECHLAB-007 CROSS AGE FMR	559
520 ALGORITHM PIXELALL-002 CROSS AGE FMR	560
521 ALGORITHM PSL-001 CROSS AGE FMR	561
522 ALGORITHM PSL-002 CROSS AGE FMR	562
523 ALGORITHM RANKONE-006 CROSS AGE FMR	563
524 ALGORITHM RANKONE-007 CROSS AGE FMR	564
525 ALGORITHM REALNETWORKS-002 CROSS AGE FMR	565
526 ALGORITHM REALNETWORKS-003 CROSS AGE FMR	566
527 ALGORITHM REMARKAI-000 CROSS AGE FMR	567
528 ALGORITHM REMARKAI-001 CROSS AGE FMR	568
529 ALGORITHM ROKID-000 CROSS AGE FMR	569
530 ALGORITHM SAFFE-001 CROSS AGE FMR	570
531 ALGORITHM SAFFE-002 CROSS AGE FMR	571
532 ALGORITHM SENSETIME-001 CROSS AGE FMR	572
533 ALGORITHM SENSETIME-002 CROSS AGE FMR	573
534 ALGORITHM SHAMAN-000 CROSS AGE FMR	574
535 ALGORITHM SHAMAN-001 CROSS AGE FMR	575
536 ALGORITHM SHU-001 CROSS AGE FMR	576
537 ALGORITHM SIAT-002 CROSS AGE FMR	577
538 ALGORITHM SIAT-004 CROSS AGE FMR	578
539 ALGORITHM SMILART-002 CROSS AGE FMR	579
540 ALGORITHM SMILART-003 CROSS AGE FMR	580
541 ALGORITHM STARHYBRID-001 CROSS AGE FMR	581
542 ALGORITHM SYNESIS-004 CROSS AGE FMR	582
543 ALGORITHM SYNESIS-005 CROSS AGE FMR	583
544 ALGORITHM TECH5-002 CROSS AGE FMR	584
545 ALGORITHM TECH5-003 CROSS AGE FMR	585
546 ALGORITHM TEVIAN-003 CROSS AGE FMR	586
547 ALGORITHM TEVIAN-004 CROSS AGE FMR	587
548 ALGORITHM TIGER-002 CROSS AGE FMR	588
549 ALGORITHM TIGER-003 CROSS AGE FMR	589
550 ALGORITHM TONGYI-005 CROSS AGE FMR	590
551 ALGORITHM TOSHIBA-002 CROSS AGE FMR	591
552 ALGORITHM TOSHIBA-003 CROSS AGE FMR	592
553 ALGORITHM ULSEE-001 CROSS AGE FMR	593
554 ALGORITHM ULUFACE-002 CROSS AGE FMR	594
555 ALGORITHM UPC-001 CROSS AGE FMR	595
556 ALGORITHM VCOG-002 CROSS AGE FMR	596
557 ALGORITHM VD-001 CROSS AGE FMR	597
558 ALGORITHM VERIDAS-001 CROSS AGE FMR	598
559 ALGORITHM VERIDAS-002 CROSS AGE FMR	599
560 ALGORITHM VIA-000 CROSS AGE FMR	600
561 ALGORITHM VIDEONETICS-001 CROSS AGE FMR	601
562 ALGORITHM VIGILANTSOLUTIONS-006 CROSS AGE FMR	602
563 ALGORITHM VIGILANTSOLUTIONS-007 CROSS AGE FMR	603
564 ALGORITHM VION-000 CROSS AGE FMR	604
565 ALGORITHM VISIONBOX-000 CROSS AGE FMR	605
566 ALGORITHM VISIONBOX-001 CROSS AGE FMR	606
567 ALGORITHM VISIONLABS-006 CROSS AGE FMR	607
568 ALGORITHM VISIONLABS-007 CROSS AGE FMR	608
569 ALGORITHM VOCORD-006 CROSS AGE FMR	609

570 ALGORITHM VOCORD-007 CROSS AGE FMR	610
571 ALGORITHM WINSENSE-000 CROSS AGE FMR	611
572 ALGORITHM YISHENG-004 CROSS AGE FMR	612
573 ALGORITHM YITU-003 CROSS AGE FMR	613

	Developer	Short	Seq.	Validation	Config ¹	Template		GPU	Comparison Time (ns) ³
	Name	Name	Num.	Date	Data (KB)	Size (B)	Time (ms) ²	Genuine	Impostor
1	3DiVi	3divi	003	2018-10-09	191636	¹⁴⁰ 4096 ± 0	⁹⁵ 650 ± 90	No	²² 627 ± 11 ²⁶ 623 ± 32
2	3DiVi	3divi	004	2019-07-22	263670	⁷⁷ 2048 ± 0	¹⁴⁸ 984 ± 131	No	³⁵ 794 ± 35 ³⁷ 801 ± 40
3	Adera Global PTE Ltd	aderा	001	2019-06-17	0	¹²⁹ 2560 ± 0	⁴⁹⁷ ± 0	No	⁷⁰ 1604 ± 71 ⁷¹ 1649 ± 56
4	Alchera	alchera	000	2019-03-01	258450	⁶⁹ 2048 ± 0	⁸⁴ 587 ± 13	No	⁹⁸ 3189 ± 32 ⁹⁸ 3031 ± 142
5	Alchera	alchera	000	2019-03-01	174013	⁶⁷ 2048 ± 0	⁹⁰ 627 ± 11	No	¹⁰⁰ 3342 ± 81 ¹⁰⁰ 3243 ± 47
6	AllGoVision	allgovision	000	2019-03-01	172509	⁸⁸ 2048 ± 0	⁵³ 384 ± 8	No	¹⁴⁰ 29903 ± 406 ¹⁴¹ 29735 ± 194
7	AlphaSSTG	alphaface	001	2019-09-03	259849	⁷³ 2048 ± 0	⁸⁷ 613 ± 3	No	¹⁰¹ 3482 ± 41 ¹⁰² 3279 ± 91
8	Amplified Group	amplifiedgroup	001	2019-03-01	0	²⁸ 866 ± 2	³⁹³ ± 0	No	¹⁴⁴ 57803 ± 4210 ¹⁴⁴ 56365 ± 1196
9	Anke Investments	anke	003	2019-02-27	340160	¹¹⁷ 2056 ± 0	¹²⁸ 811 ± 23	No	⁸ 425 ± 28 ¹⁰ 437 ± 32
10	Anke Investments	anke	004	2019-06-27	349388	¹¹⁵ 2056 ± 0	⁸⁹ 625 ± 1	No	²³ 633 ± 22 ²⁸ 632 ± 34
11	AnyVision	anyvision	002	2018-01-31	662659	³⁷ 1024 ± 0	²³ 248 ± 0	No	¹⁴⁵ 74069 ± 188 ¹⁴⁵ 74019 ± 198
12	AnyVision	anyvision	004	2018-06-15	401001	³³ 1024 ± 0	⁴⁶ 355 ± 1	No	⁷⁷ 1891 ± 51 ⁷⁵ 1829 ± 85
13	Aware	aware	003	2018-10-19	377729	¹³² 3108 ± 0	¹²⁴ 783 ± 10	No	⁶² 1392 ± 42 ⁶⁴ 1334 ± 80
14	Aware	aware	004	2019-03-01	427829	¹²⁶ 2084 ± 0	¹⁴² 900 ± 10	No	⁵⁸ 1279 ± 50 ⁶³ 1287 ± 100
15	Ayonix	ayonix	000	2017-06-22	58505	³⁸ 1036 ± 0	¹⁸ ± 2	No	²¹ 621 ± 23 ²⁵ 620 ± 26
16	Bitmain	bitmain	001	2018-10-17	287734	¹ 64 ± 0	⁶¹ 444 ± 88	No	⁷⁶ 1887 ± 31 ⁷⁷ 1877 ± 26
17	Camvi Technologies	camvitech	002	2018-10-19	236278	³⁵ 1024 ± 0	¹⁰⁷ 677 ± 7	No	²⁰ 612 ± 26 ²¹ 603 ± 20
18	Camvi Technologies	camvitech	004	2019-07-12	280733	⁸³ 2048 ± 0	¹²⁰ 759 ± 10	No	⁴¹ 948 ± 40 ⁴³ 963 ± 31
19	China Electronics Import-Export Corp	ceiec	001	2019-03-01	159618	³⁶ 1024 ± 0	³⁹ 314 ± 3	No	¹³⁸ 22831 ± 108 ¹³⁸ 22813 ± 120
20	China Electronics Import-Export Corp	ceiec	002	2019-06-12	269063	⁶⁶ 2048 ± 0	⁸⁶ 612 ± 17	No	⁸⁶ 2188 ± 57 ⁸⁶ 2301 ± 56
21	Chunghwa Telecom Co. Ltd	chtface	001	2019-08-06	94088	⁸⁵ 2048 ± 0	¹⁹ 218 ± 12	No	⁸³ 2089 ± 45 ⁸³ 2087 ± 23
22	Gemalto Cogent	cogent	003	2019-03-01	698290	²⁹ 973 ± 0	¹⁴⁰ 952 ± 0	No	¹²⁷ 12496 ± 75 ¹²⁶ 11822 ± 163
23	Gemalto Cogent	cogent	004	2019-06-14	722919	⁵⁶ 1983 ± 0	¹⁴³ 941 ± 28	No	¹³⁰ 14448 ± 56 ¹³² 15882 ± 81
24	Cognitec Systems GmbH	cognitec	000	2018-10-19	474759	¹⁰⁴ 2052 ± 0	²⁰ 224 ± 1	No	¹⁰⁷ 3835 ± 108 ¹⁰⁵ 3782 ± 83
25	Cognitec Systems GmbH	cognitec	001	2019-03-01	476809	¹¹⁰ 2052 ± 0	³⁵ 297 ± 17	No	¹⁰⁹ 4253 ± 59 ¹⁰⁸ 4102 ± 167
26	CTBC Bank Co. Ltd	ctbcbank	000	2019-06-28	257208	⁷⁰ 2048 ± 0	⁸¹ 568 ± 43	No	¹⁰³ 3551 ± 87 ¹¹¹ 4805 ± 209
27	Cyberextruder	cyberex	001	2017-08-02	121211	⁹ 256 ± 0	¹⁴¹ 893 ± 25	No	⁴⁸ 1083 ± 16 ⁵¹ 1079 ± 19
28	Cyberextruder	cyberex	002	2018-01-30	168909	⁵⁹ 2048 ± 0	⁷⁰ 532 ± 6	No	⁷⁵ 1803 ± 14 ⁷⁴ 1779 ± 22
29	Cyberlink Corp	cyberlink	001	2019-03-01	222009	¹¹³ 2052 ± 0	⁵⁹ 425 ± 29	No	⁸² 2051 ± 32 ⁸² 2060 ± 31
30	Cyberlink Corp	cyberlink	002	2019-06-12	222311	¹⁰⁶ 2052 ± 0	⁹⁹ 656 ± 22	No	⁸⁸ 2264 ± 71 ⁹⁵ 2649 ± 195
31	Dahua Technology Co. Ltd	dahua	002	2019-03-01	526452	⁶⁸ 2048 ± 0	⁹¹ 628 ± 7	No	¹⁰ 461 ± 23 ¹² 454 ± 20
32	Dahua Technology Co. Ltd	dahua	003	2019-08-14	605337	⁸⁴ 2048 ± 0	⁷² 537 ± 4	No	²⁶ 653 ± 28 ²² 606 ± 38
33	Deepglint	deepglint	001	2019-06-21	569802	¹³⁷ 4096 ± 0	¹¹² 721 ± 4	No	¹⁰⁴ 3680 ± 35 ¹⁰³ 3517 ± 182
34	Tencent Deepsea Lab	deepsea	001	2019-06-03	147497	³⁰ 1024 ± 0	⁹² 630 ± 7	No	⁶⁴ 1401 ± 37 ⁶⁷ 1467 ± 50
35	Dermalog	dermalog	005	2018-02-02	0	² 128 ± 0	⁶ 130 ± 11	No	¹³ 499 ± 22 ¹⁵ 500 ± 22
36	Dermalog	dermalog	006	2018-10-18	0	³ 128 ± 0	⁶⁹ 532 ± 12	No	¹⁴ 506 ± 23 ¹³ 459 ± 23
37	Digital Barriers	barriers	002	2019-03-01	83002	¹¹⁸ 2056 ± 0	¹⁶ 209 ± 11	No	¹²⁹ 13409 ± 228 ¹²⁹ 13267 ± 206
38	DSK	dsk	000	2019-06-28	11967	¹⁸ 512 ± 0	³⁷ 304 ± 47	No	¹²² 7152 ± 115 ¹²¹ 7134 ± 111
39	Shenzhen EI Networks Limited	einetworks	000	2019-08-13	372608	¹²² 2056 ± 0	⁹⁴ 645 ± 3	No	¹¹² 4876 ± 66 ¹¹³ 5156 ± 77
40	Ever AI	everai	002	2019-03-01	561727	¹⁴² 4096 ± 0	¹¹⁸ 758 ± 0	No	²⁵ 644 ± 14 ²⁷ 624 ± 35
41	Ever AI Paravision	everai paravision	003	2019-07-01	539802	¹³⁶ 4096 ± 0	¹⁰⁵ 674 ± 4	No	³¹ 699 ± 20 ³² 713 ± 47
42	FarBar Inc.	f8	001	2019-07-11	272977	⁶⁵ 2048 ± 0	¹³² 822 ± 39	No	¹³¹ 15262 ± 139 ¹³¹ 15277 ± 212
43	FaceSoft Ltd.	facesoft	000	2019-07-10	370120	⁹⁸ 2048 ± 0	¹⁰⁶ 675 ± 18	No	⁸⁷ 2239 ± 28 ⁸⁵ 2277 ± 96
44	Glory Ltd	glory	000	2018-06-06	0	¹⁵ 418 ± 0	⁸ 165 ± 2	No	¹²¹ 7003 ± 84 ¹¹⁹ 6978 ± 71

Notes

- 1 The configuration size does not capture static data included in libraries. We do not count these because some algorithms include common ancillary libraries for image processing (e.g. openCV) or numerical computation (e.g. blas).
- 2 The median template creation times are measured on Intel®Xeon®CPU E5-2630 v4 @ 2.20GHz processors or, for GPU-enabled implementations, NVidia Tesla K40.
- 3 The comparison durations, in nanoseconds, are estimated using std::chrono::high_resolution_clock which on the machine in (2) counts 1ns clock ticks. Precision is somewhat worse than that however. The ± value is the median absolute deviation times 1.48 for Normal consistency.

Table 1: Summary of algorithms and properties included in this report. The red superscripts give ranking for the quantity in that column.

	Developer	Short	Seq.	Validation	Config ¹	Template		GPU	Comparison Time (ns) ³			
						Name	Date		Size (B)	Time (ms) ²	Genuine	Impostor
45	Glory Ltd	glory	001	2018-06-08	0	53	1726 ± 0	55	393 ± 2	No	1259607 ± 128	1269539 ± 182
46	Gorilla Technology	gorilla	002	2018-10-17	93869	42	1132 ± 0	42	322 ± 14	No	952715 ± 68	942585 ± 84
47	Gorilla Technology	gorilla	003	2019-06-19	94409	41	1132 ± 0	44	334 ± 25	No	962840 ± 42	962865 ± 87
48	Hikvision	hik	001	2019-03-01	667866	46	1408 ± 0	96	651 ± 0	No	12488 ± 19	14477 ± 22
49	Hengrui AI Technology Ltd	hr	001	2019-06-04	346156	124	2057 ± 0	100	665 ± 3	No	13317816 ± 260	13317878 ± 464
50	ID3 Technology	id3	003	2018-10-05	265951	11	264 ± 0	40	316 ± 19	No	611330 ± 25	651354 ± 28
51	ID3 Technology	id3	004	2019-03-01	171526	10	264 ± 0	76	541 ± 11	No	491135 ± 23	561156 ± 32
52	Idemia	Idemia	003	2018-10-19	427244	14	352 ± 0	49	368 ± 6	No	1206654 ± 75	1124835 ± 90
53	Idemia	Idemia	004	2019-03-01	406924	13	352 ± 0	38	306 ± 5	No	1155592 ± 518	1165533 ± 426
54	Institute of Information Technologies	iitvision	000	2019-03-01	237317	34	1024 ± 0	15	197 ± 8	No	671537 ± 81	621282 ± 20
55	Institute of Information Technologies	iitvision	001	2019-07-05	269176	79	2048 ± 0	109	699 ± 4	No	461060 ± 48	491074 ± 54
56	Imagus Technology Pty Ltd	imagus	000	2019-06-19	183453	91	2048 ± 0	60	425 ± 24	No	501145 ± 25	731718 ± 63
57	Imperial College London	imperial	000	2019-03-01	370120	76	2048 ± 0	102	669 ± 1	No	842130 ± 32	812052 ± 100
58	Imperial College London	imperial	002	2019-08-28	472327	60	2048 ± 0	82	570 ± 2	No	1114827 ± 69	1094557 ± 160
59	Incode Technologies Inc	incode	003	2019-03-01	170632	139	4096 ± 0	52	384 ± 11	No	791928 ± 44	761876 ± 81
60	Incode Technologies Inc	incode	004	2019-06-12	260224	64	2048 ± 0	63	479 ± 23	No	781913 ± 60	902443 ± 114
61	Innovatrics	innovatrics	004	2018-10-19	0	40	1076 ± 0	54	391 ± 0	No	1248573 ± 274	1237929 ± 244
62	Innovatrics	innovatrics	006	2019-08-13	0	23	538 ± 0	133	824 ± 10	No	1175763 ± 217	1175631 ± 824
63	CSA IntelliCloud Technology	intellicloudai	001	2019-08-13	220831	98	2048 ± 0	64	479 ± 18	No	441010 ± 16	461024 ± 31
64	Shenzhen Intellifusion Technologies Co. Ltd	intellifusion	001	2019-08-22	271872	63	2048 ± 0	121	778 ± 61	No	1063756 ± 59	1073953 ± 126
65	Intellivision	intellivision	001	2017-10-10	43692	120	2056 ± 0	26	62 ± 2	No	912573 ± 91	932544 ± 38
66	Intellivision	intellivision	002	2019-08-23	43692	116	2056 ± 0	45	342 ± 30	No	13216049 ± 195	13015136 ± 389
67	Intel Research Group	intelresearch	000	2019-07-08	388229	61	2048 ± 0	143	902 ± 6	No	1104800 ± 152	1104561 ± 97
68	Lomonosov Moscow State University	intsymsu	000	2019-06-18	650193	62	2048 ± 0	71	535 ± 20	No	18610 ± 22	24613 ± 31
69	iQIYI Inc	iqface	000	2019-06-04	268819	146	4750 ± 32	73	538 ± 26	No	148636433 ± 38446	148632654 ± 85615
70	iSAP Solution Corporation	isap	001	2019-08-07	99049	141	4096 ± 0	9171	1 ± 12	No	12612413 ± 154	12712251 ± 382
71	Is It You	isityou	000	2017-06-26	48010	147	19200 ± 0	511	113 ± 5	No	146237517 ± 1318	146237374 ± 1279
72	Innovation Systems	isystems	001	2018-06-12	274621	57	2048 ± 0	33	291 ± 9	No	16557 ± 16	18564 ± 22
73	Innovation Systems	isystems	002	2018-10-18	358984	82	2048 ± 0	131	822 ± 8	No	33749 ± 31	29632 ± 28
74	ITMO University	itmo	005	2018-10-19	482155	145	4173 ± 0	119	759 ± 1	No	12813214 ± 164	12812576 ± 257
75	ITMO University	itmo	006	2019-03-01	599187	128	2121 ± 0	129	814 ± 1	No	13926154 ± 148	13926217 ± 260
76	Kakao Corp	kakao	001	2019-03-01	107616	32	1024 ± 0	51	379 ± 1	No	39930 ± 22	42948 ± 38
77	Kakao Corp	kakao	002	2019-06-19	479406	99	2048 ± 0	116	747 ± 6	No	731720 ± 62	721715 ± 83
78	Kedacom International Pte	kedacom	000	2019-06-03	245292	12	292 ± 0	67	506 ± 3	No	27684 ± 14	30682 ± 16
79	Kneron Inc	kenron	003	2019-07-01	58366	74	2048 ± 0	31	281 ± 3	No	1145237 ± 63	1152747 ± 99
80	Lookman Electroplast Industries	lookman	002	2018-06-13	138200	25	548 ± 0	10	173 ± 1	No	19610 ± 19	23612 ± 22
81	Lookman Electroplast Industries	lookman	004	2019-06-03	244775	24	548 ± 0	68	507 ± 5	No	37871 ± 29	41878 ± 29
82	Megvii/Face++	megvii	001	2018-06-15	1361523	95	2048 ± 0	77	543 ± 0	No	1135228 ± 32	1145252 ± 60
83	Megvii/Face++	megvii	002	2018-10-19	1809564	144	4100 ± 0	93	644 ± 0	No	14350630 ± 183	14347591 ± 716
84	Xiamen Meiya Pico Information Co. Ltd	meiya	001	2019-03-01	280055	102	2049 ± 0	88	622 ± 12	No	1238356 ± 615	1248134 ± 97
85	MicroFocus	microfocus	001	2018-06-13	104524	8	256 ± 0	27	264 ± 18	No	1215 ± 8	1217 ± 10
86	MicroFocus	microfocus	002	2018-10-17	96288	6	256 ± 0	25	259 ± 18	No	4337 ± 34	2230 ± 25
87	Moontime Smart Technology	mt	000	2019-06-03	372169	100	2049 ± 0	113	724 ± 12	No	721678 ± 47	701614 ± 85
88	Neurotechnology	neurotech	005	2019-03-01	270450	7	256 ± 0	57	399 ± 0	No	2238 ± 10	3237 ± 7

Notes

1 The configuration size does not capture static data included in libraries. We do not count these because some algorithms include common ancillary libraries for image processing (e.g. openCV) or numerical computation (e.g. blas).

2 The median template creation times are measured on Intel®Xeon®CPU E5-2630 v4 @ 2.20GHz processors or, for GPU-enabled implementations, NVidia Tesla K40.

3 The comparison durations, in nanoseconds, are estimated using std::chrono::high_resolution_clock which on the machine in (2) counts 1ns clock ticks. Precision is somewhat worse than that however. The ± value is the median absolute deviation times 1.48 for Normal consistency.

Table 2: Summary of algorithms and properties included in this report. The red superscripts give ranking for the quantity in that column.

	Developer	Short	Seq.	Validation	Config ¹	Template		GPU	Comparison Time (ns) ³	
						Name	Num.		Date	Data (KB)
89	Neurotechnology	neurotech	006	2019-06-26	525541	¹⁹ 512 ± 0	¹⁰⁸ 678 ± 56	No	¹⁵ 513 ± 14	¹⁷ 535 ± 26
90	Nodeflux	nodeflux	001	2019-03-01	262553	⁸¹ 2048 ± 0	²² 247 ± 1	No	⁹⁹ 3242 ± 81	¹⁰¹ 3255 ± 93
91	Nodeflux	nodeflux	002	2019-08-13	774668	⁹⁷ 2048 ± 0	¹¹¹ 717 ± 16	No	¹¹⁸ 5922 ± 170	¹²² 7911 ± 367
92	NotionTag Technologies Private Limited	notiontag	000	2019-06-12	92753	²⁰ 584 ± 0	⁷⁹ 548 ± 64	No	¹⁴² 44672 ± 269	¹⁴² 44593 ± 358
93	N-Tech Lab	ntech	006	2019-03-01	7901590	¹³¹ 2600 ± 0	¹¹⁷ 749 ± 1	No	⁴⁵ 1055 ± 93	⁴⁰ 844 ± 48
94	N-Tech Lab	ntech	007	2019-06-25	2509686	¹³³ 3348 ± 0	¹²⁶ 792 ± 3	No	⁵³ 1209 ± 59	⁶⁰ 1267 ± 65
95	Guangzhou Pixel Solutions Co. Ltd	pixelall	002	2019-06-06	0	¹³⁰ 2560 ± 0	¹⁴ 191 ± 1	No	⁵⁴ 1223 ± 56	⁵⁸ 1230 ± 47
96	Panasonic R+D Center Singapore	psl	001	2018-10-12	382035	¹²³ 2056 ± 0	¹²⁵ 785 ± 16	No	³ 298 ± 13	⁴ 292 ± 14
97	Panasonic R+D Center Singapore	psl	002	2019-02-28	804934	¹⁰⁷ 2052 ± 0	¹⁴⁰ 888 ± 9	No	⁶⁹ 1590 ± 48	⁵² 1133 ± 78
98	Rank One Computing	rankone	006	2019-02-27	0	⁵ 165 ± 0	¹⁷ 210 ± 1	No	⁹ 443 ± 26	⁸ 395 ± 22
99	Rank One Computing	rankone	007	2019-06-03	0	⁴ 165 ± 0	²¹ 245 ± 5	No	²⁸ 688 ± 20	²⁰ 601 ± 16
100	Realnetworks Inc	realnetworks	002	2019-02-28	95328	⁵⁵ 1848 ± 0	²⁴ 250 ± 2	No	⁵⁹ 1285 ± 17	⁵⁹ 1247 ± 42
101	Realnetworks Inc	realnetworks	003	2019-06-12	95334	⁵⁴ 1848 ± 0	¹² 177 ± 10	No	⁶⁶ 1516 ± 29	⁶⁸ 1522 ± 60
102	KanKan Ai	remarkai	000	2019-03-01	240152	⁵⁸ 2048 ± 0	¹³⁴ 829 ± 7	No	³⁸ 873 ± 4	³⁹ 835 ± 35
103	KanKan Ai	remarkai	001	2019-03-01	241857	¹⁰⁹ 2052 ± 0	¹³⁵ 831 ± 6	No	⁵⁵ 1229 ± 20	³⁸ 805 ± 56
104	Rokid Corporation Ltd	rokid	000	2019-08-01	258612	¹²¹ 2056 ± 0	⁷⁸ 547 ± 2	No	¹⁰⁵ 3711 ± 88	¹⁰⁴ 3746 ± 209
105	Saffe Ltd	saffe	001	2018-10-19	85973	⁴⁴ 1280 ± 0	³⁰ 281 ± 1	No	⁵⁷ 1274 ± 19	⁶¹ 1277 ± 26
106	Saffe Ltd	saffe	002	2019-03-01	260622	⁹⁰ 2048 ± 0	¹³⁰ 817 ± 11	No	³² 717 ± 7	³³ 714 ± 29
107	Sensetime Group Ltd	sensetime	002	2018-10-19	531783	¹⁰³ 2052 ± 0	¹¹⁴ 725 ± 3	No	⁹⁰ 2546 ± 102	⁸⁸ 2371 ± 45
108	Sensetime Group Ltd	sensetime	002	2018-10-19	531783	¹¹¹ 2052 ± 0	¹²⁷ 797 ± 3	No	⁹⁴ 2713 ± 90	⁸⁷ 2301 ± 25
109	Shaman Software	shaman	000	2017-12-05	0	¹³⁸ 4096 ± 0	⁹⁷ 653 ± 16	No	⁶ 380 ± 25	⁷ 379 ± 31
110	Shaman Software	shaman	001	2018-01-13	0	¹³⁵ 4096 ± 0	³⁴ 294 ± 2	No	²⁴ 635 ± 19	¹¹ 441 ± 25
111	Shanghai Universiy - Shanghai Film Academy	shu	001	2019-06-17	329513	⁹⁴ 2048 ± 0	⁸⁵ 612 ± 5	No	⁹³ 2619 ± 19	⁹⁷ 2987 ± 143
112	Shenzhen Inst. Adv. Integrated Tech. CAS	SIAT	002	2018-06-13	486842	¹¹² 2052 ± 0	⁸³ 579 ± 0	No	³⁴ 769 ± 13	³⁵ 750 ± 13
113	Shenzhen Inst. Adv. Integrated Tech. CAS	SIAT	004	2019-03-01	940063	¹⁴³ 4100 ± 0	¹⁰³ 670 ± 0	No	¹⁰⁸ 4013 ± 45	¹⁰⁶ 3782 ± 173
114	Smilart	smilart	002	2018-02-06	111826	³¹ 1024 ± 0	¹¹ 176 ± 16	No	¹³⁵ 18784 ± 136	¹³⁶ 18795 ± 151
115	Smilart	smilart	003	2018-06-18	67339	¹⁷ 512 ± 0	¹³ 180 ± 12	No	⁶³ 1395 ± 74	⁴⁷ 1027 ± 66
116	Star Hybrid Limited	starhybrid	001	2019-06-19	100509	⁷⁷ 2048 ± 0	⁴⁸ 358 ± 82	No	⁴⁷ 1075 ± 51	⁵⁰ 1078 ± 53
117	Synesis	synesis	004	2019-03-01	270628	⁹³ 2048 ± 0	¹¹⁵ 735 ± 15	No	⁷⁴ 424 ± 14	⁹ 430 ± 22
118	Synesis	synesis	005	2019-06-06	146509	⁸⁰ 2048 ± 0	¹⁸ 211 ± 9	No	¹⁷ 599 ± 23	¹⁹ 581 ± 32
119	Tech5 SA	tech5	002	2019-03-01	1150887	⁴⁵ 1280 ± 0	¹²² 780 ± 10	No	⁶⁵ 1406 ± 120	⁴⁸ 1048 ± 57
120	Tech5 SA	tech5	003	2019-08-19	1427464	⁴⁷ 1536 ± 0	¹⁴⁴ 937 ± 39	No	⁶⁰ 1313 ± 35	⁶⁶ 1360 ± 41
121	Tevian	tevian	003	2018-10-19	791725	¹⁰¹ 2049 ± 0	⁵⁸ 404 ± 15	No	⁵ 350 ± 11	⁶ 338 ± 25
122	Tevian	tevian	004	2019-03-01	863474	⁷² 2048 ± 0	⁶⁶ 506 ± 30	No	¹¹ 474 ± 31	⁵ 326 ± 20
123	TigerIT Americas LLC	tiger	002	2018-06-13	341638	¹¹⁹ 2056 ± 0	⁵⁰ 393 ± 20	No	⁸⁵ 2135 ± 29	⁸⁴ 2137 ± 38
124	TigerIT Americas LLC	tiger	003	2018-10-16	426164	¹¹⁴ 2056 ± 0	⁶² 458 ± 21	No	⁸¹ 2031 ± 35	⁸⁰ 2029 ± 38
125	TongYi Transportation Technology	tongyi	005	2019-06-12	1140701	¹²⁷ 2089 ± 0	⁷ 165 ± 1	No	¹³⁶ 18924 ± 65	¹³⁷ 20158 ± 103
126	Toshiba	toshiba	002	2018-10-19	813606	⁵⁰ 1560 ± 0	⁷⁵ 541 ± 0	No	¹⁰² 3521 ± 369	⁹¹ 2449 ± 124
127	Toshiba	toshiba	003	2019-03-01	984125	⁵¹ 1560 ± 0	⁷⁴ 540 ± 0	No	⁸⁹ 2390 ± 41	⁸⁹ 2407 ± 81
128	ULSee Inc	ulsee	001	2019-07-31	370519	⁸⁹ 2048 ± 0	⁹⁸ 654 ± 2	No	¹¹⁹ 6065 ± 94	¹¹⁸ 6228 ± 77
129	Shanghai Ulucu Electronics Technology Co. Ltd	uluface	002	2019-07-10	0	⁷⁸ 2048 ± 0	¹³⁸ 873 ± 42	No	¹³⁷ 19207 ± 1114	¹³⁵ 18501 ± 274
130	China University of Petroleum	upc	001	2019-06-05	0	³⁹ 1052 ± 0	⁸⁰ 551 ± 15	No	⁹⁷ 3114 ± 44	⁹⁹ 3165 ± 97
131	VCognition	vcog	002	2017-06-12	3229434	¹⁴⁸ 61504 ± 5	⁴⁷ 357 ± 25	No	¹⁴⁷ 296154 ± 3077	¹⁴⁷ 296436 ± 4183
132	Visidon	visidon	001	2019-02-26	170262	¹⁰⁵ 2052 ± 0	⁴¹ 316 ± 6	No	⁵⁶ 1258 ± 38	⁵⁴ 1148 ± 109

Notes	
1	The configuration size does not capture static data included in libraries. We do not count these because some algorithms include common ancillary libraries for image processing (e.g. openCV) or numerical computation (e.g. blas).
2	The median template creation times are measured on Intel®Xeon®CPU E5-2630 v4 @ 2.20GHz processors or, for GPU-enabled implementations, NVidia Tesla K40.
3	The comparison durations, in nanoseconds, are estimated using std::chrono::high_resolution_clock which on the machine in (2) counts 1ns clock ticks. Precision is somewhat worse than that however. The ± value is the median absolute deviation times 1.48 for Normal consistency.

Table 3: Summary of algorithms and properties included in this report. The red superscripts give ranking for the quantity in that column.

	Developer	Short	Seq.	Validation	Config ¹	Template		GPU	Comparison Time (ns) ³					
						Name	Num.		Date	Data (KB)	Size (B)	Time (ms) ²	Genuine	Impostor
133	Veridas Digital Authentication Solutions S.L.	veridas	001	2019-03-01	196540	75	2048 ± 0	104	671 ± 21	No	116	5748 ± 20	120	7111 ± 148
134	Veridas Digital Authentication Solutions S.L.	veridas	000	2019-03-01	193466	22	512 ± 0	101	669 ± 20	No	74	1733 ± 81	78	1934 ± 44
135	Via Technologies Inc.	via	000	2019-07-08	124422	86	2048 ± 0	110	707 ± 8	No	43	966 ± 28	45	1021 ± 44
136	Videonetics Technology Pvt Ltd	videonetics	001	2019-06-19	30875	16	512 ± 0	26	262 ± 3	No	51	1153 ± 38	53	1142 ± 65
137	Vigilant Solutions	vigilant	006	2019-03-01	343048	49	1548 ± 0	136	841 ± 8	No	40	939 ± 32	31	711 ± 37
138	Vigilant Solutions	vigilant	007	2019-06-27	255600	48	1548 ± 0	65	493 ± 6	No	36	803 ± 35	36	800 ± 40
139	Beijing Vion Technology Inc	vion	000	2018-10-19	228219	108	2052 ± 0	43	333 ± 1	No	141	39839 ± 3561	140	26830 ± 2241
140	Vision-Box	visionbox	000	2019-02-26	176501	92	2048 ± 0	36	304 ± 7	No	71	1648 ± 57	57	1192 ± 42
141	Vision-Box	visionbox	001	2019-03-01	256869	87	2048 ± 0	147	983 ± 7	No	52	1161 ± 22	58	1154 ± 20
142	VisionLabs	visionlabs	006	2019-03-01	353044	21	512 ± 0	28	270 ± 0	No	30	698 ± 19	34	734 ± 28
143	VisionLabs	visionlabs	007	2019-06-12	357204	20	512 ± 0	29	272 ± 0	No	42	965 ± 41	44	972 ± 31
144	Vocord	vocord	006	2019-03-01	559457	27	768 ± 0	139	886 ± 1	No	80	2020 ± 72	79	1969 ± 62
145	Vocord	vocord	007	2019-06-06	587489	52	1664 ± 0	123	780 ± 2	No	92	2593 ± 83	92	2526 ± 59
146	Winsense Co. Ltd	winsense	000	2019-06-17	270819	43	1280 ± 0	32	283 ± 1	No	68	1551 ± 31	69	1532 ± 42
147	Zhuhai Yisheng Electronics Technology	yisheng	004	2018-06-12	486351	134	3704 ± 0	50	378 ± 12	No	29	693 ± 137	16	526 ± 34
148	Shanghai Yitu Technology	yitu	003	2019-03-01	1525719	125	2082 ± 0	137	860 ± 0	No	134	18305 ± 71	134	18286 ± 62

Notes

- 1 The configuration size does not capture static data included in libraries. We do not count these because some algorithms include common ancillary libraries for image processing (e.g. openCV) or numerical computation (e.g. blas).
- 2 The median template creation times are measured on Intel®Xeon®CPU E5-2630 v4 @ 2.20GHz processors or, for GPU-enabled implementations, NVidia Tesla K40.
- 3 The comparison durations, in nanoseconds, are estimated using std::chrono::high_resolution_clock which on the machine in (2) counts 1ns clock ticks. Precision is somewhat worse than that however. The ± value is the median absolute deviation times 1.48 for Normal consistency.

Table 4: Summary of algorithms and properties included in this report. The red superscripts give ranking for the quantity in that column.

	Algorithm	FALSE NON-MATCH RATE (FNMR)											
		CONSTRAINED, COOPERATIVE						LESS CONSTRAINED, NON-COOP.					
		Name	VISAMC	VISA	VISA	MUGSHOT	MUGSHOT12+YRS	VISABORDER	WILD	CHILDEXP			
	FMR	0.0001	1E-06	0.0001	1E-05	0.0001	1E-05	0.0001	1E-06	0.0001	0.01		
1	3divi-003	0.0318	103	0.0588	104	0.0097	95	0.0389	102	0.0639	100	0.0619	92
2	3divi-004	0.0095	34	0.0153	37	0.0049	51	0.0097	35	0.0145	31	0.0175	42
3	adera-001	0.1021	119	0.1757	118	0.0368	118	0.1823	125	0.2967	123	0.1714	105
4	alchera-000	0.0165	73	0.0243	63	0.0086	89	0.0125	61	0.0186	57	0.0204	48
5	alchera-001	0.0183	78	0.0299	77	0.0078	84	0.0142	67	0.0234	70	0.0239	55
6	allgovision-000	0.0346	105	0.0527	100	0.0210	109	0.0232	89	0.0339	78	-	0.0607
7	alphaface-001	0.0065	18	0.0097	17	0.0025	18	0.0039	3	0.0063	6	0.0083	6
8	amplifiedgroup-001	0.5034	138	0.5848	138	0.2999	140	0.6973	138	0.8316	135	0.7807	116
9	anke-003	0.0131	55	0.0213	54	0.0056	58	0.0094	31	0.0175	51	0.0134	25
10	anke-004	0.0080	27	0.0154	38	0.0031	24	0.0073	16	0.0112	18	0.0102	14
11	anyvision-002	0.0660	113	0.0898	110	0.0387	119	0.0928	118	0.1512	114	-	0.2227
12	anyvision-004	0.0267	97	0.0385	93	0.0081	86	0.0258	91	0.0487	94	-	0.0470
13	aware-003	0.0793	115	0.1161	115	0.0288	116	0.1028	119	0.1708	117	-	0.3180
14	aware-004	0.0690	114	0.0949	113	0.0257	112	0.0837	116	0.1436	112	0.1171	103
15	ayonix-000	0.4351	135	0.4872	133	0.2299	136	0.6150	135	0.7510	132	-	0.3635
16	bm-001	0.7431	144	0.9494	145	0.6188	145	0.9586	142	0.9843	139	-	0.9935
17	camvi-002	0.0125	51	0.0221	58	0.0049	52	0.0089	28	0.0145	33	0.0142	26
18	camvi-004	0.0171	76	0.0316	82	0.0049	50	0.0042	5	0.0049	2	0.0097	13
19	ceiec-001	0.0328	104	0.0475	97	0.0163	103	0.0295	97	0.0478	92	0.0621	93
20	ceiec-002	0.0161	71	0.0193	49	0.0124	101	0.0122	59	0.0164	47	0.0270	60
21	chtface-001	0.9993	147	0.9994	147	0.9993	147	0.9999	144	-	1.0000	121	0.9980
22	cogent-003	0.0091	30	0.0188	48	0.0032	25	0.0098	37	0.0132	26	0.0187	44
23	cogent-004	0.0064	17	0.0116	25	0.0024	17	0.0096	33	0.0134	27	0.0157	29
24	cognitec-000	0.0116	46	0.0177	42	0.0036	30	0.0118	56	0.0167	48	0.0285	64
25	cognitec-001	0.0126	52	0.0185	47	0.0047	46	0.0120	58	0.0168	49	0.0270	59
26	ctcbank-000	0.0168	74	0.0250	69	0.0064	64	0.0146	70	0.0224	65	0.0211	49
27	cyberextruder-001	0.1972	127	0.2547	126	0.0755	128	0.4686	133	0.6387	130	-	0.1747
28	cyberextruder-002	0.0811	116	0.1336	117	0.0265	113	0.1465	123	0.2266	121	-	0.1000
29	cyberlink-001	0.0131	54	0.0210	53	0.0050	53	0.0439	105	0.0517	96	0.0173	41
30	cyberlink-002	0.0114	45	0.0195	50	0.0044	39	0.0101	40	0.0163	44	0.0160	30
31	dahua-002	0.0129	53	0.0157	39	0.0090	92	0.0116	55	0.0153	37	0.0134	24
32	dahua-003	0.0052	9	0.0068	8	0.0023	16	0.0056	8	0.0062	5	0.0113	19
33	deepglint-001	0.0040	6	0.0062	5	0.0014	8	0.0047	6	0.0067	7	0.0069	4
34	deepsea-001	0.0136	58	0.0215	56	0.0071	80	0.0142	68	0.0214	62	0.0163	34
35	dermalog-005	0.1526	125	0.1823	121	0.0658	126	0.2580	128	0.4018	125	-	0.0855
36	dermalog-006	0.0253	94	0.0369	91	0.0172	106	0.0171	76	0.0283	74	-	0.0623
37	digitalbarriers-002	0.3360	132	0.3690	131	0.0968	131	0.0877	117	0.1557	115	0.0971	102
38	dsk-000	0.1526	124	0.2169	123	0.0765	129	0.3787	132	0.5426	129	0.3115	110
39	einetworks-000	0.0099	37	0.0180	44	0.0047	45	0.0088	26	0.0140	29	0.0130	23
40	everai-002	0.0104	42	0.0159	40	0.0041	37	0.0063	12	0.0112	19	0.0182	43
41	everai-paravision-003	0.0034	2	0.0050	3	0.0011	3	0.0036	2	0.0052	3	0.0092	10
42	f8-001	0.0249	93	0.0336	83	0.0182	107	0.0178	78	0.0232	69	0.0303	70
43	facesoft-000	0.0085	29	0.0112	24	0.0032	26	0.0064	13	0.0107	15	0.0091	9
44	glory-000	0.1094	120	0.1286	116	0.0514	123	0.2179	126	0.2656	122	-	0.4762

Table 5: FNMR is the proportion of mated comparisons below a threshold set to achieve the FMR given in the header on the fourth row. FMR is the proportion of impostor comparisons at or above that threshold. The light grey values give rank over all algorithms in that column. The pink column uses only same-sex impostors; others are selected regardless of demographics. The exception, in the green column, uses “matched-covariates” i.e. impostors of the same sex, age group, and country of birth. The pink column includes effects of extended ageing. Missing entries for border, visa, mugshot and wild images generally mean the algorithm did not run to completion. For child exploitation, missing entries arise because NIST executes those runs only infrequently.

Algorithm	FALSE NON-MATCH RATE (FNMR)									
	CONSTRAINED, COOPERATIVE						LESS CONSTRAINED, NON-COOP.			
	Name	VISAMC	VISA	VISA	MUGSHOT	MUGSHOT12+YRS	VISABORDER	WILD	CHILDEXP	
FMR	0.0001	1E-06	0.0001	1E-05		1E-05	1E-06	0.0001	0.01	
45 glory-001	0.0902	117	0.1082	114	0.0410	120	0.1642	124	0.2065	120
46 gorilla-002	0.0256	95	0.0413	94	0.0076	83	0.0478	108	0.0912	106
47 gorilla-003	0.0165	72	0.0291	74	0.0053	55	0.0205	85	0.0437	86
48 hik-001	0.0096	35	0.0125	27	0.0036	32	0.0093	30	0.0164	46
49 hr-001	0.0044	7	0.0072	10	0.0019	11	0.0073	18	0.0108	16
50 id3-003	0.0361	106	0.0757	107	0.0104	99	0.0292	95	0.0476	89
51 id3-004	0.0198	83	0.0344	86	0.0084	88	0.0238	90	0.0423	85
52 idemria-003	0.0222	87	0.0316	81	0.0082	87	0.0188	81	0.0325	76
53 idemria-004	0.0160	70	0.0244	65	0.0065	66	0.0199	84	0.0354	81
54 iit-000	0.1516	123	0.1981	122	0.0620	125	0.0828	115	0.1442	113
55 iit-001	0.0104	40	0.0179	43	0.0048	49	0.0099	39	0.0142	30
56 imagus-000	0.0642	111	0.0882	108	0.0330	117	0.0497	109	0.0905	105
57 imperial-000	0.0067	20	0.0108	22	0.0022	15	0.0080	22	0.0134	28
58 imperial-002	0.0058	13	0.0081	12	0.0027	19	0.0055	7	0.0085	9
59 incode-003	0.0142	61	0.0249	68	0.0054	56	0.0448	106	0.0869	104
60 incode-004	0.0077	25	0.0132	29	0.0034	28	0.0096	34	0.0160	41
61 innovatrics-004	0.0194	81	0.0292	75	0.0068	73	0.0344	99	0.0617	99
62 innovatrics-006	0.0058	14	0.0089	14	0.0021	13	0.0061	11	0.0096	13
63 intellicloudai-001	0.0142	62	0.0234	62	0.0064	65	0.0092	29	0.0145	32
64 intelligfusion-001	0.0072	22	0.0094	16	0.0028	22	0.0056	9	0.0085	10
65 intelligfusion-001	0.1335	122	0.2205	124	0.0417	121	0.1090	121	0.1670	116
66 intelligfusion-002	0.1000	118	0.1775	119	0.0265	114	0.0610	112	0.1009	107
67 intelresearch-000	0.0307	100	0.0578	103	0.0093	93	0.0385	101	0.0751	103
68 intsysmsu-000	0.0135	57	0.0204	51	0.0069	75	0.0112	50	0.0161	42
69 iqface-000	0.0091	31	0.0143	33	0.0043	38	0.0075	21	0.0110	17
70 isap-001	0.5092	139	0.6588	140	0.2338	138	0.6899	137	0.7978	133
71 isityou-000	0.5682	141	0.7033	141	0.4145	143	1.0000	145	-	-
72 isystems-001	0.0149	66	0.0245	66	0.0067	71	0.0138	66	0.0210	61
73 isystems-002	0.0118	47	0.0182	46	0.0066	67	0.0111	47	0.0162	43
74 itmo-005	0.0182	77	0.0345	87	0.0067	72	0.0181	79	0.0348	80
75 itmo-006	0.0125	50	0.0220	57	0.0046	42	0.0149	71	0.0266	73
76 kakao-001	0.4553	137	0.5532	137	0.2034	135	0.6580	136	0.8150	134
77 kakao-002	0.0625	110	0.1779	120	0.0168	105	0.0791	114	0.1381	111
78 kedacom-000	0.0055	11	0.0081	13	0.0027	20	0.0111	49	0.0120	22
79 kneron-003	0.0542	108	0.0902	111	0.0218	110	0.0346	100	0.0562	98
80 lookman-002	0.0297	99	0.0547	102	0.0102	98	0.0339	98	0.0562	97
81 lookman-004	0.0074	24	0.0099	19	0.0037	33	0.0124	60	0.0149	34
82 megvii-001	0.0157	68	0.0244	64	0.0045	41	0.0392	103	0.0671	101
83 megvii-002	0.0104	41	0.0145	35	0.0036	31	0.0225	86	0.0345	79
84 meiya-001	0.0171	75	0.0275	73	0.0066	69	0.0159	75	0.0261	72
85 microfocus-001	0.4482	136	0.5524	136	0.2309	137	0.7256	139	0.8416	136
86 microfocus-002	0.3605	133	0.5057	134	0.1566	134	0.5783	134	0.7223	131
87 mt-000	0.0100	38	0.0170	41	0.0047	44	0.0074	20	0.0118	21
88 neurotechnology-005	0.0141	60	0.0300	78	0.0051	54	0.0108	45	0.0163	45

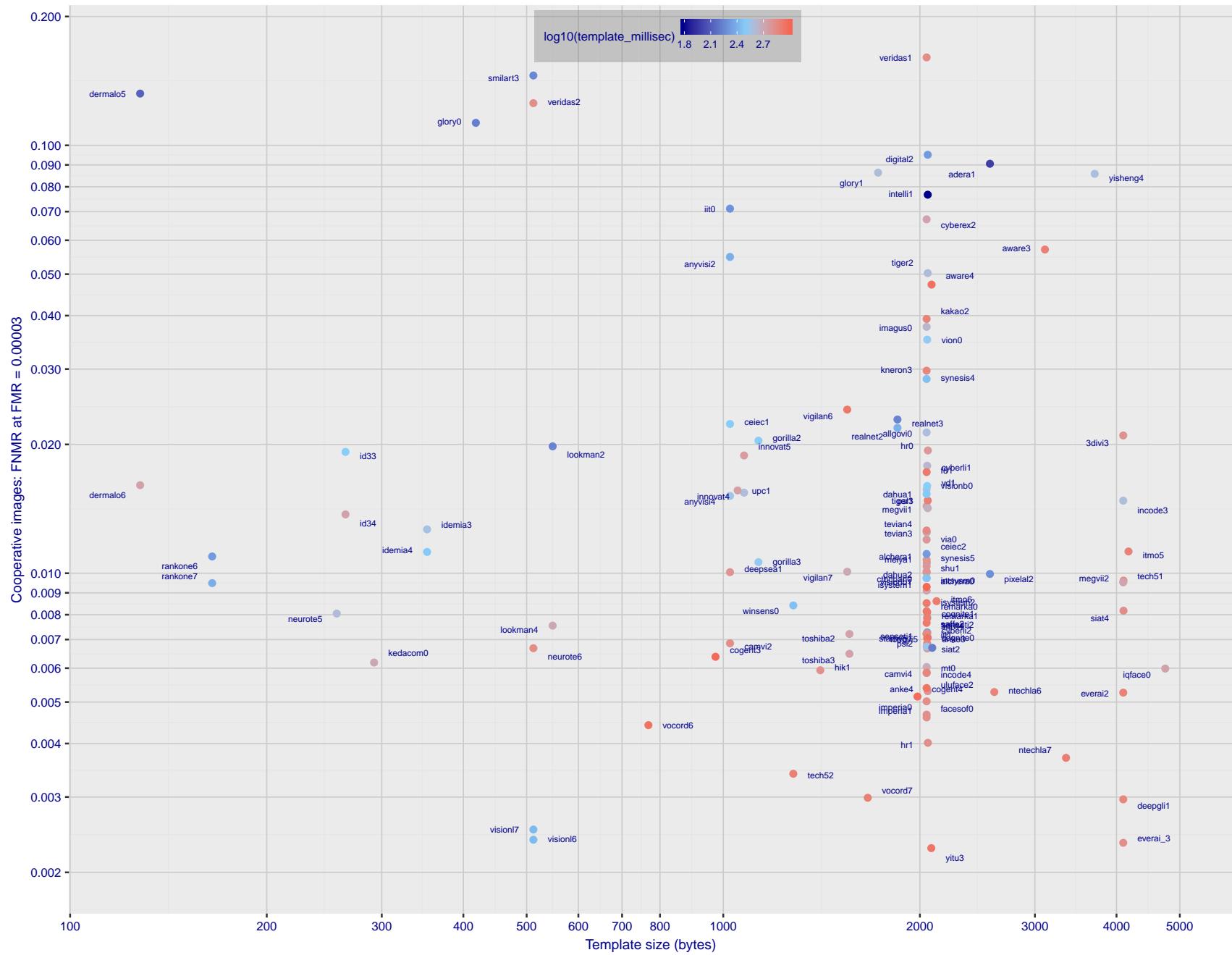
Table 6: FNMR is the proportion of mated comparisons below a threshold set to achieve the FMR given in the header on the fourth row. FMR is the proportion of impostor comparisons at or above that threshold. The light grey values give rank over all algorithms in that column. The pink column uses only same-sex impostors; others are selected regardless of demographics. The exception, in the green column, uses “matched-covariates” i.e. impostors of the same sex, age group, and country of birth. The pink column includes effects of extended ageing. Missing entries for border, visa, mugshot and wild images generally mean the algorithm did not run to completion. For child exploitation, missing entries arise because NIST executes those runs only infrequently.

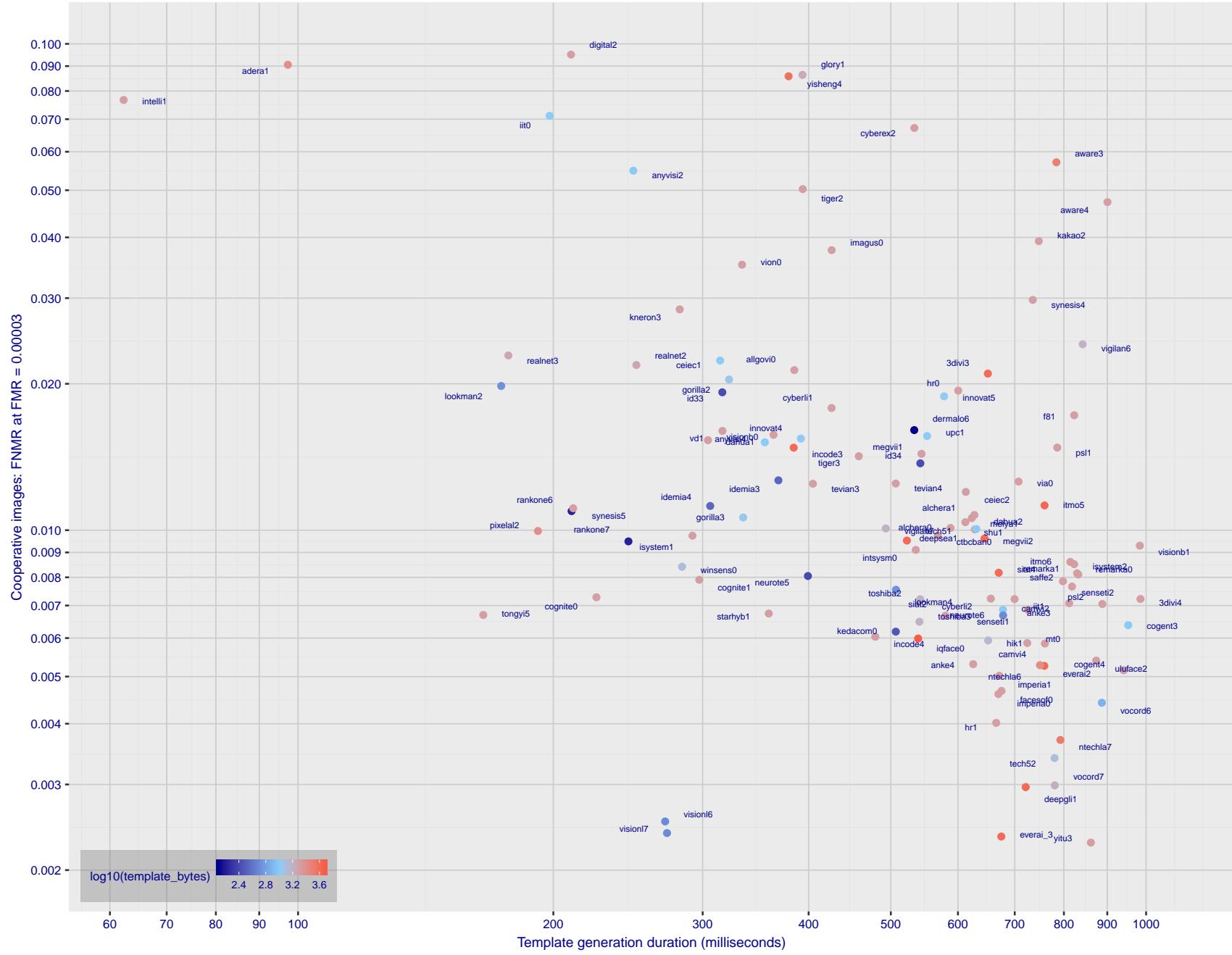
Algorithm	FALSE NON-MATCH RATE (FNMR)									
	CONSTRAINED, COOPERATIVE								LESS CONSTRAINED, NON-COOP.	
	Name	VISAMC	VISA	VISA	MUGSHOT	MUGSHOT12+YRS	VISABORDER	WILD	CHILDEXP	
FMR	0.0001	1E-06	0.0001	1E-05	1E-05	1E-06	0.0001	0.01		
89	neurotechnology-006	0.0098	36	0.0136	30	0.0040	36	0.0105	43	0.0182
90	nodeflux-001	1.0000	148	1.0000	148	1.0000	148	-	0.5169	114
91	nodeflux-002	0.0186	79	0.0340	84	0.0070	77	0.0261	92	0.0451
92	notiontag-000	0.6669	142	0.7885	142	0.3222	142	0.3715	131	0.4978
93	ntechlab-006	0.0078	26	0.0111	23	0.0021	14	0.0112	51	0.0227
94	ntechlab-007	0.0056	12	0.0076	11	0.0018	10	0.0073	19	0.0128
95	pixelall-002	0.0193	80	0.0340	85	0.0066	68	0.0127	63	0.0209
96	psl-001	0.0549	109	0.0927	112	0.0198	108	0.0096	32	0.0149
97	psl-002	0.0107	43	0.0180	45	0.0048	48	0.0089	27	0.0120
98	rankone-006	0.0242	90	0.0460	96	0.0070	76	0.0119	57	0.0188
99	rankone-007	0.0197	82	0.0366	90	0.0057	60	0.0113	53	0.0177
100	realnetworks-002	0.0248	92	0.0358	88	0.0099	96	0.0153	110	0.1127
101	realnetworks-003	0.0259	96	0.0372	92	0.0100	97	0.0541	111	0.1208
102	remarkai-000	0.0147	65	0.0257	71	0.0062	63	0.0102	41	0.0158
103	remarkai-001	0.0144	63	0.0256	70	0.0061	62	0.0102	42	0.0159
104	rokid-000	0.0093	33	0.0145	34	0.0038	34	0.0073	17	0.0102
105	saffe-001	0.4339	134	0.5261	135	0.2340	139	0.7539	141	0.8736
106	saffe-002	0.0119	48	0.0206	52	0.0054	57	0.0107	44	0.0177
107	sensetime-001	0.0063	16	0.0092	15	0.0030	23	0.0130	64	-
108	sensetime-002	0.0068	21	0.0098	18	0.0035	29	0.0143	69	-
109	shaman-000	0.9297	146	0.9774	146	0.9128	146	0.9990	143	-
110	shaman-001	0.3346	131	0.4616	132	0.1360	133	0.2368	127	0.3723
111	shu-001	0.0103	39	0.0140	32	0.0044	40	0.0293	96	0.0688
112	siat-002	0.0091	32	0.0126	28	0.0039	35	0.0109	46	0.0190
113	siat-004	0.0067	19	0.0099	20	0.0028	21	0.0152	73	-
114	smilart-002	0.2440	130	0.3532	130	0.0821	130	-	-	0.3785
115	smilart-003	0.6944	143	0.8836	143	0.1088	132	0.0695	113	0.1193
116	starhybrid-001	0.0108	44	0.0138	31	0.0058	61	0.0081	23	0.0113
117	synesis-004	0.0310	101	0.0480	98	0.0166	104	0.0476	107	0.0443
118	synesis-005	0.0147	64	0.0226	60	0.0073	82	0.0153	74	0.0226
119	tech5-002	0.0046	8	0.0063	6	0.0009	2	0.0113	54	0.0216
120	tech5-003	0.0053	10	0.0070	9	0.0014	7	0.0099	38	0.0185
121	tevian-003	0.0217	86	0.0298	76	0.0067	70	0.0230	88	0.0484
122	tevian-004	0.0228	88	0.0304	79	0.0069	74	0.0226	87	0.0478
123	tiger-002	0.0658	112	0.0889	109	0.0227	111	0.1083	120	0.1766
124	tiger-003	0.0313	102	0.0602	106	0.0087	90	0.0188	82	0.0359
125	tongyi-005	0.0073	23	0.0146	36	0.0019	12	0.0187	80	0.0421
126	toshiba-002	0.0134	56	0.0222	59	0.0048	47	0.0097	36	0.0154
127	toshiba-003	0.0125	49	0.0214	55	0.0047	43	0.0085	25	0.0131
128	ulsee-001	0.0151	67	0.0246	67	0.0080	85	0.0113	52	0.0185
129	uluface-002	0.0081	28	0.0123	26	0.0033	27	0.0071	15	0.0095
130	upc-001	0.0234	89	0.0519	99	0.0071	79	0.0291	94	0.0490
131	vcoq-002	0.7522	145	0.9033	144	0.5040	144	-	-	-
132	vd-001	0.0243	91	0.0452	95	0.0093	94	0.0271	93	0.0402

Table 7: FNMR is the proportion of mated comparisons below a threshold set to achieve the FMR given in the header on the fourth row. FMR is the proportion of impostor comparisons at or above that threshold. The light grey values give rank over all algorithms in that column. The pink column uses only same-sex impostors; others are selected regardless of demographics. The exception, in the green column, uses “matched-covariates” i.e. impostors of the same sex, age group, and country of birth. The pink column includes effects of extended ageing. Missing entries for border, visa, mugshot and wild images generally mean the algorithm did not run to completion. For child exploitation, missing entries arise because NIST executes those runs only infrequently.

	Algorithm	FALSE NON-MATCH RATE (FNMR)															
		CONSTRAINED, COOPERATIVE						LESS CONSTRAINED, NON-COOP.									
		Name	VISAMC	VISA	VISA	MUGSHOT	MUGSHOT12+YRS	VISABORDER	WILD	CHILDEXP							
	FMR	0.0001	1E-06	0.0001	1E-05	1E-05	1E-05	1E-06	0.0001	0.01							
133	veridas-001	0.1998	129	0.2724	127	0.0742	127	0.2987	130	0.4587	127	0.2599	109	0.0501	81	-	
134	veridas-002	0.1733	126	0.2257	125	0.0528	124	0.2617	129	0.4147	126	0.2073	107	0.0450	73	-	
135	via-000	0.0216	85	0.0365	89	0.0088	91	0.0177	77	0.0287	75	0.0296	68	0.0349	53	0.7638	60
136	videonetics-001	0.5483	140	0.6446	139	0.3063	141	0.7517	140	0.8607	137	0.8664	119	0.2986	125	0.7297	57
137	vigilantsolutions-006	0.1264	121	0.3221	128	0.0136	102	0.0150	72	0.0254	71	0.0493	85	0.0321	41	-	
138	vigilantsolutions-007	0.0202	84	0.0307	80	0.0070	78	0.0136	65	0.0227	67	0.0356	76	0.0306	31	1.0000	140
139	vion-000	0.0419	107	0.0590	105	0.0288	115	0.0422	104	0.0478	91	0.0581	90	0.2479	120	0.8765	71
140	visionbox-000	0.0293	98	0.0541	101	0.0110	100	0.0197	83	0.0339	77	0.0349	74	0.0476	79	-	
141	visionbox-001	0.0159	69	0.0270	72	0.0072	81	0.0111	48	0.0173	50	0.0190	46	0.0389	62	-	
142	visionlabs-006	0.0037	3	0.0066	7	0.0012	4	0.0041	4	0.0060	4	0.0061	2	0.0285	16	-	
143	visionlabs-007	0.0038	4	0.0048	2	0.0012	6	0.0036	1	0.0048	1	0.0057	1	0.0286	17	0.3708	5
144	vocord-006	0.0062	15	0.0102	21	0.0016	9	0.0082	24	0.0151	36	0.0475	84	0.0282	13	-	
145	vocord-007	0.0039	5	0.0053	4	0.0012	5	0.0061	10	0.0094	11	0.0520	86	0.0280	8	0.8468	68
146	winsense-000	0.0140	59	0.0228	61	0.0056	59	0.0125	62	0.0215	63	0.0226	51	0.0352	55	0.8600	70
147	yisheng-004	0.1988	128	0.3329	129	0.0475	122	0.1147	122	0.1849	119	0.2044	106	0.0908	101	0.7152	54
148	yitu-003	0.0015	1	0.0026	1	0.0003	1	0.0066	14	0.0085	8	0.0064	3	0.0325	44	-	

Table 8: FNMR is the proportion of mated comparisons below a threshold set to achieve the FMR given in the header on the fourth row. FMR is the proportion of impostor comparisons at or above that threshold. The light grey values give rank over all algorithms in that column. The pink column uses only same-sex impostors; others are selected regardless of demographics. The exception, in the green column, uses “matched-covariates” i.e. impostors of the same sex, age group, and country of birth. The pink column includes effects of extended ageing. Missing entries for border, visa, mugshot and wild images generally mean the algorithm did not run to completion. For child exploitation, missing entries arise because NIST executes those runs only infrequently.





1 Metrics

1.1 Core accuracy

Given a vector of N genuine scores, u , the false non-match rate (FNMR) is computed as the proportion below some threshold, T:

$$\text{FNMR}(T) = 1 - \frac{1}{N} \sum_{i=1}^N H(u_i - T) \quad (1)$$

where $H(x)$ is the unit step function, and $H(0)$ taken to be 1.

Similarly, given a vector of N impostor scores, v , the false match rate (FMR) is computed as the proportion above T:

$$\text{FMR}(T) = \frac{1}{N} \sum_{i=1}^N H(v_i - T) \quad (2)$$

The threshold, T, can take on any value. We typically generate a set of thresholds from quantiles of the observed impostor scores, v , as follows. Given some interesting false match rate range, $[\text{FMR}_L, \text{FMR}_U]$, we form a vector of K thresholds corresponding to FMR measurements evenly spaced on a logarithmic scale

$$T_k = Q_v(1 - \text{FMR}_k) \quad (3)$$

where Q is the quantile function, and FMR_k comes from

$$\log_{10} \text{FMR}_k = \log_{10} \text{FMR}_L + \frac{k}{K} [\log_{10} \text{FMR}_U - \log_{10} \text{FMR}_L] \quad (4)$$

Error tradeoff characteristics are plots of FNMR(T) vs. FMR(T). These are plotted with $\text{FMR}_U \rightarrow 1$ and FMR_L as low as is sustained by the number of impostor comparisons, N. This is somewhat higher than the “rule of three” limit $3/N$ because samples are not independent, due to re-use of images.

2 Datasets

2.1 Child exploitation images

- ▷ The number of images is on the order of 10^4 .
- ▷ The number of subjects is on the order of 10^3 .
- ▷ The number of subjects with two images on the order of 10^3 .
- ▷ The images are operational. They are taken from ongoing investigations of child exploitation crimes. The images are arbitrarily unconstrained. Pose varies considerably around all three axes, including subject lying down. Resolution varies very widely. Faces can be occluded by other objects, including hair and hands. Lighting varies, although the images are intended for human viewing. Mis-focus is rare. Images are given to the algorithm without any cropping; faces may occupy widely varying areas.
- ▷ The images are usually large from contemporary cameras. The mean interocular distance (IOD) is 70 pixels.
- ▷ The images are of subjects from several countries, due to the global production of this imagery.
- ▷ The images are of children, from infancy to late adolescence.
- ▷ All of the images are live capture, none are scanned. Many have been cropped.
- ▷ When these images are input to the algorithm, they are labelled as being of type "EXPLOITATION" - see Table 4 of the FRVT API.

2.2 Visa images

- ▷ The number of images is on the order of 10^5 .
- ▷ The number of subjects is on the order of 10^5 .
- ▷ The number of subjects with two images on the order of 10^4 .
- ▷ The images have geometry in reasonable conformance with the ISO/IEC 19794-5 Full Frontal image type. Pose is generally excellent.
- ▷ The images are of size 252x300 pixels. The mean interocular distance (IOD) is 69 pixels.
- ▷ The images are of subjects from greater than 100 countries, with significant imbalance due to visa issuance patterns.
- ▷ The images are of subjects of all ages, including children, again with imbalance due to visa issuance demand.
- ▷ Many of the images are live capture. A substantial number of the images are photographs of paper photographs.
- ▷ When these images are input to the algorithm, they are labelled as being of type "ISO" - see Table 4 of the FRVT API.

2.3 Visa images II

- ▷ The number of images is on the order of 10^6 .
- ▷ The number of subjects is on the order of 10^6 .
- ▷ The number of subjects with two images on the order of 10^6 .

- ▷ The images have geometry in good conformance with the ISO/IEC 19794-5 Full Frontal image type. Pose is generally excellent.
- ▷ The images are of size 300x300 pixels. The mean interocular distance (IOD) is 61 pixels.
- ▷ The images are of subjects from greater than 100 countries, with significant imbalance due to visa issuance patterns.
- ▷ The images are of subjects of all ages, including children, again with imbalance due to visa issuance demand.
- ▷ All of the images are live capture.
- ▷ When these images are input to the algorithm, they are labelled as being of type "ISO" - see Table 4 of the FRVT API.

2.4 Mugshot images

- ▷ The number of images is on the order of 10^6 .
- ▷ The number of subjects is on the order of 10^6 .
- ▷ The number of subjects with two images on the order of 10^6 .
- ▷ The images have geometry in reasonable conformance with the ISO/IEC 19794-5 Full Frontal image type.
- ▷ The images are of variable sizes. The median IOD is 105 pixels. The mean IOD is 113 pixels. The 1-st, 5-th, 10-th, 25-th, 75-th, 90-th and 99-th percentiles are 34, 58, 70, 87, 121, 161 and 297 pixels.
- ▷ The images are of subjects from the United States.
- ▷ The images are of adults.
- ▷ The images are all live capture.
- ▷ When these images are input to the algorithm, they are labelled as being of type "mugshot" - see Table 4 of the FRVT API.

2.5 Webcam images

- ▷ The number of images is on the order of 10^6 .
- ▷ The number of subjects is on the order of 10^6 .
- ▷ All subjects have a webcam image, and a portrait image.
- ▷ The portrait images are in poor conformance with the ISO/IEC 19794-5 Full Frontal image type.
- ▷ The webcam images are taken with a camera oriented by an attendant toward a cooperating subject. This is done under time constraints so there are roll, pitch and yaw angle variation. Also background illumination is sometimes strong, so the face is under exposed. There is sometimes perspective distortion due to close range images.
- ▷ The images have mean IOD of 38 pixels.
- ▷ The images are all live capture.
- ▷ When these images are input to the algorithm, they are labelled as being of type "WILD" - see Table 4 of the FRVT API.

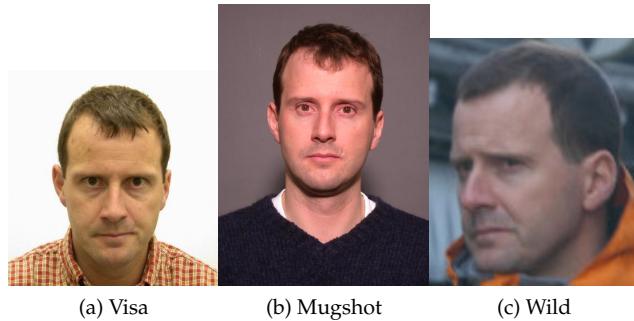


Figure 3: The figure gives simulated samples of image types used in this report.

2.6 Wild images

- ▷ The number of images is on the order of 10^5 .
 - ▷ The number of subjects is on the order of 10^3 .
 - ▷ The number of subjects with two images on the order of 10^3 .
 - ▷ The images include many photojournalism-style images. Images are given to the algorithm using a variable but generally tight crop of the head. Resolution varies very widely. The images are very unconstrained, with wide yaw and pitch pose variation. Faces can be occluded, including hair and hands.
 - ▷ The images are of adults.
 - ▷ All of the images are live capture, none are scanned.
 - ▷ When these images are input to the algorithm, they are labelled as being of type "WILD" - see Table 4 of the FRVT API.

3 Results

3.1 Test goals

- ▷ To state overall accuracy.
 - ▷ To compare algorithms.

3.2 Test design

Method: For visa images:

- ▷ The comparisons are of visa photos against visa photos.
 - ▷ The number of genuine comparisons is on the order of 10^4 .
 - ▷ The number of impostor comparisons is on the order of 10^{10} .
 - ▷ The comparisons are fully zero-effort, meaning impostors are paired without attention to sex, age or other covariates. However, later analysis is conducted on subsets.

- ▷ The number of persons is on the order of 10^5 .
- ▷ The number of images used to make 1 template is 1.
- ▷ The number of templates used to make each comparison score is two corresponding to simple one-to-one verification.

For mugshot images:

- ▷ The comparisons are of mugshot photos against mugshot photos.
- ▷ The number of genuine comparisons is on the order of 10^6 .
- ▷ The number of impostor comparisons is on the order of 10^8 .
- ▷ The impostors are paired by sex, but not by age or other covariates.
- ▷ The number of persons is on the order of 10^6 .
- ▷ The number of images used to make 1 template is 1.
- ▷ The number of templates used to make each comparison score is two corresponding to simple one-to-one verification.

Method: For wild images:

- ▷ The comparisons are of wild photos against wild photos.
- ▷ The number of genuine comparisons is on the order of 10^6 .
- ▷ The number of impostor comparisons is on the order of 10^7 .
- ▷ The comparisons are fully zero-effort, meaning impostors are paired without attention to sex, age or other covariates.
- ▷ The number of persons is on the order of 10^4 .
- ▷ The number of images used to make 1 template is 1.
- ▷ The number of templates used to make each comparison score is two corresponding to simple one-to-one verification.

For child exploitation images:

- ▷ The comparisons are of unconstrained child exploitation photos against others of the same type.
- ▷ The number of genuine comparisons is on the order of 10^4 .
- ▷ The number of impostor comparisons is on the order of 10^7 .
- ▷ The comparisons are fully zero-effort, meaning impostors are paired without attention to sex, age or other covariates.
- ▷ The number of persons is on the order of 10^3 .
- ▷ The number of images used to make 1 template is 1.
- ▷ The number of templates used to make each comparison score is two corresponding to simple one-to-one verification.

▷ We produce two performance statements. First, is a DET as used for visa and mugshot images. The second is a cumulative match characteristic (CMC) summarizing a simulated one-to-many search process. This is done as follows.

- We regard M enrollment templates as items in a gallery.
- These M templates come from $M > N$ individuals, because multiple images of a subject are present in the gallery under separate identifiers.
- We regard the verification templates as search templates.
- For each search we compute the rank of the highest scoring mate.
- This process should properly be conducted with a 1:N algorithm, such as those tested in NIST IR 8009. We use the 1:1 algorithms in a simulated 1:N mode here to a) better reflect what a child exploitation analyst does, and b) to show algorithm efficacy is better than that revealed in the verification DETs.

3.3 Failure to enroll

	Algorithm Name	Failure to Enrol Rate ¹							
		CHILD-EXPLOIT	MUGSHOT	VISA	WILD				
1	3divi-003	0.1806	60	0.0007	104	0.0006	101	0.0294	120
2	3divi-004	-	148	0.0008	107	0.0006	103	0.0222	119
3	adera-001	0.1928	63	0.0003	79	0.0005	96	0.0505	131
4	alchera-000	-	148	0.0004	94	0.0014	128	0.0038	87
5	alchera-001	-	148	0.0004	93	0.0014	127	0.0038	86
6	allgovision-000	-	148	0.0026	132	0.0052	146	0.0131	110
7	alphaface-001	-	148	0.0000	46	0.0004	76	0.0004	49
8	amplifiedgroup-001	-	148	0.0189	148	0.0279	152	0.1390	143
9	anke-003	-	148	0.0001	57	0.0004	68	0.0006	59
10	anke-004	0.0944	45	0.0001	58	0.0004	77	0.0006	63
11	anyvision-002	0.4866	84	0.0070	143	0.0090	148	0.1146	139
12	anyvision-004	0.1660	57	0.0001	65	0.0004	73	0.0080	99
13	aware-003	0.3314	78	0.0016	127	0.0013	124	0.0745	136
14	aware-004	-	148	0.0002	69	0.0005	83	0.0014	77
15	ayonix-000	0.0000	3	0.0113	145	0.0137	150	0.1194	140
16	bm-001	0.0000	18	0.0000	35	0.0000	14	0.0000	11
17	camvi-002	0.0000	4	0.0000	20	0.0000	22	0.0000	18
18	camvi-004	-	148	0.0000	24	0.0000	26	0.0000	22
19	ceiec-001	-	148	0.0029	135	0.0023	135	0.0068	95
20	ceiec-002	0.2482	72	0.0036	137	0.0031	141	0.0081	100
21	chtface-001	-	148	0.0000	27	0.0000	29	0.0000	25
22	cogent-003	-	148	0.0001	54	0.0004	71	0.0009	73
23	cogent-004	0.0000	6	0.0000	3	0.0000	4	0.0000	2
24	cognitec-000	0.6342	88	0.0007	105	0.0007	108	0.0388	128
25	cognitec-001	-	148	0.0008	111	0.0010	110	0.0185	115
26	ctcbcbank-000	0.3285	77	0.0011	118	0.0019	132	0.0868	138
27	cyberextruder-001	0.5338	86	0.0024	130	0.0029	139	0.0597	134
28	cyberextruder-002	0.2672	75	0.0027	133	0.0028	138	0.0335	125
29	cyberlink-001	-	148	0.0073	144	0.0005	85	0.0008	65
30	cyberlink-002	0.1463	56	0.0004	87	0.0004	81	0.0007	64
31	dahua-002	-	148	0.0024	131	0.0022	134	0.0009	70
32	dahua-003	-	148	0.0002	73	0.0003	42	0.0002	40
33	deepglint-001	0.0000	19	0.0000	13	0.0000	15	0.0000	12
34	deepsea-001	0.0000	8	0.0000	6	0.0000	7	0.0000	5
35	dermalog-005	0.1796	58	0.0013	123	0.0041	143	0.0163	113
36	dermalog-006	0.1797	59	0.0013	122	0.0041	144	0.0163	114
37	digitalbarriers-002	-	148	0.0028	134	0.0027	137	0.0071	96
38	dsk-000	0.0000	14	0.0000	10	0.0000	11	0.0000	8
39	einetworks-000	-	148	0.0002	71	0.0005	94	0.0008	66
40	everai-002	-	148	0.0002	74	0.0004	54	0.0004	54
41	everai-paravision-003	0.0705	41	0.0002	68	0.0004	61	0.0004	52
42	f8-001	0.2026	65	0.0035	136	0.0030	140	0.0087	103
43	facesoft-000	0.0000	24	0.0000	34	0.0000	36	0.0000	29
44	glory-000	0.0000	16	0.0053	141	0.0013	125	0.1565	144
45	glory-001	0.0000	11	0.0051	140	0.0010	111	0.1651	145
46	gorilla-002	0.1347	52	0.0003	86	0.0004	82	0.0117	106
47	gorilla-003	0.1347	51	0.0003	85	0.0004	80	0.0043	90
48	hik-001	-	148	0.0000	28	0.0000	28	0.0000	24
49	hr-001	0.1198	50	0.0001	47	0.0004	62	0.0003	46
50	id3-003	0.3032	76	0.0016	128	0.0011	121	0.0317	123
51	id3-004	-	148	0.0015	126	0.0011	120	-	148
52	idemia-003	0.0481	31	0.0000	37	0.0004	55	0.0042	89
53	idemia-004	-	148	0.0000	40	0.0004	58	0.0003	47
54	iit-000	-	148	0.0007	103	0.0011	115	0.0836	137
55	iit-001	0.0843	44	0.0001	67	0.0004	74	0.0104	104
56	imagus-000	0.1107	48	0.0010	117	0.0012	123	0.0347	126
57	imperial-000	-	148	0.0000	15	0.0000	17	0.0000	14
58	imperial-002	-	148	0.0000	5	0.0000	6	0.0000	4
59	incode-003	-	148	0.0004	98	0.0007	105	0.0014	76
60	incode-004	0.2202	66	0.0004	97	0.0007	104	0.0014	75

Table 9: FTE is the proportion of failed template generation attempts. Failures can occur because the software throws an exception, or because the software electively refuses to process the input image. This would typically occur if a face is not detected. FTE is measured as the number of function calls that give EITHER a non-zero error code OR that give a “small” template. This is defined as one whose size is less than 0.3 times the median template size for that algorithm. This second rule is needed because some algorithms incorrectly fail to return a non-zero error code when template generation fails.

¹The effects of FTE are included in the accuracy results of this report by regarding any template comparison involving a failed template to produce a low similarity score. Thus higher FTE results in higher FNMR and lower FMR.

	Algorithm Name	Failure to Enrol Rate ¹							
		CHILD-EXPLOIT	MUGSHOT	VISA	WILD				
61	innovatrics-004	0.1170	49	0.0000	45	0.0004	75	0.0041	88
62	innovatrics-006	-	148	0.0000	42	0.0004	53	0.0003	48
63	intellicloudai-001	-	148	0.0000	33	0.0000	35	0.0001	37
64	intellifusion-001	-	148	0.0001	51	0.0003	49	0.0005	58
65	intellivision-001	0.5495	87	0.0048	139	0.0042	145	0.1358	141
66	intellivision-002	-	148	0.0012	120	0.0005	99	0.0146	111
67	intelresearch-000	-	148	0.0000	44	0.0003	48	0.0001	38
68	intsysmsu-000	-	148	0.0004	92	0.0012	122	0.0031	85
69	iqface-000	0.0000	9	0.0000	25	0.0000	27	0.0000	23
70	isap-001	-	148	0.0000	23	0.0000	25	0.0000	21
71	isityou-000	0.4714	82	0.0023	129	0.0010	113	0.0663	135
72	isystems-001	0.1421	54	0.0010	115	0.0007	106	0.0128	108
73	isystems-002	0.1421	55	0.0010	116	0.0007	107	0.0128	109
74	itmo-005	0.1353	53	0.0005	100	0.0002	38	0.0075	97
75	itmo-006	-	148	0.0004	96	0.0004	72	0.0006	62
76	kakao-001	-	148	0.0002	75	0.0005	87	0.0310	121
77	kakao-002	0.2494	73	0.0002	76	0.0005	91	0.0310	122
78	kedacom-000	0.0000	17	0.0000	12	0.0000	13	0.0000	10
79	kneron-003	0.4883	85	0.0044	138	0.0016	131	0.1823	146
80	lookman-002	-	148	0.0000	22	0.0000	24	0.0000	20
81	lookman-004	0.0000	1	0.0000	19	0.0000	21	0.0000	17
82	megvii-001	0.0274	29	0.0007	106	0.0004	60	0.0152	112
83	megvii-002	0.0274	28	0.0054	142	0.0004	59	0.0126	107
84	meiya-001	-	148	0.0004	99	0.0010	114	0.0025	82
85	microfocus-001	0.0791	43	0.0008	110	0.0016	130	0.0220	118
86	microfocus-002	0.0791	42	0.0008	109	0.0016	129	0.0220	117
87	mt-000	0.1043	46	0.0002	72	0.0004	78	0.0004	50
88	neurotechnology-005	-	148	0.0004	90	0.0004	64	0.0018	78
89	neurotechnology-006	0.1068	47	0.0004	91	0.0004	65	0.0018	79
90	nodeflux-001	-	148	0.0001	59	0.0002	39	0.0003	43
91	nodeflux-002	-	148	0.0008	108	0.0005	93	0.0008	69
92	notiontag-000	0.0000	22	0.0000	16	0.0000	18	0.0000	15
93	ntechlab-006	-	148	0.0000	36	0.0004	51	0.0003	42
94	ntechlab-007	0.0682	40	0.0001	48	0.0004	56	0.0005	57
95	pixelall-002	0.0001	25	0.0000	9	0.0000	10	0.0001	34
96	psl-001	0.0000	20	0.0000	32	0.0000	34	0.0000	28
97	psl-002	-	148	0.0000	11	0.0000	12	0.0000	9
98	rankone-006	-	148	0.0000	31	0.0000	33	0.0000	27
99	rankone-007	0.3518	80	0.0003	81	0.0004	79	0.0043	91
100	realnetworks-002	-	148	0.0004	89	0.0003	44	0.0004	51
101	realnetworks-003	0.0076	26	0.0004	88	0.0003	43	0.0004	53
102	remarkai-000	-	148	0.0000	2	0.0000	2	0.0000	32
103	remarkai-001	-	148	0.0000	18	0.0000	20	0.0000	33
104	rokid-000	-	148	0.0001	56	0.0005	92	0.0354	127
105	saffe-001	0.0000	21	0.0000	14	0.0000	16	0.0000	13
106	saffe-002	-	148	0.0000	30	0.0000	32	0.0000	26
107	sensetime-001	0.0631	39	0.0000	39	0.0004	67	0.0003	44
108	sensetime-002	0.3345	79	0.0011	119	0.0005	97	0.0218	116
109	shaman-000	0.0000	5	0.0000	21	0.0000	23	0.0000	19
110	shaman-001	0.0000	2	0.0000	1	0.0000	1	0.0000	30
111	shu-001	0.1822	61	0.0010	114	0.0006	100	0.0499	130
112	siat-002	0.0616	36	0.0000	43	0.0004	70	0.0048	93
113	siat-004	-	148	0.0000	41	0.0004	69	0.0003	45
114	smilart-002	0.2422	69	0.0003	84	0.0011	117	0.0575	133
115	smilart-003	-	148	0.0014	124	0.0013	126	0.0555	132
116	starhybrid-001	0.2340	68	0.0009	113	0.0023	136	0.0044	92
117	synesis-004	-	148	0.0164	147	0.0035	142	0.0485	129
118	synesis-005	0.1862	62	0.0001	55	0.0005	84	0.0021	80
119	tech5-002	-	148	0.0001	53	0.0003	40	0.0000	31
120	tech5-003	-	148	0.0001	52	0.0003	41	0.0002	39

Table 10: FTE is the proportion of failed template generation attempts. Failures can occur because the software throws an exception, or because the software electively refuses to process the input image. This would typically occur if a face is not detected. FTE is measured as the number of function calls that give EITHER a non-zero error code OR that give a “small” template. This is defined as one whose size is less than 0.3 times the median template size for that algorithm. This second rule is needed because some algorithms incorrectly fail to return a non-zero error code when template generation fails.

¹The effects of FTE are included in the accuracy results of this report by regarding any template comparison involving a failed template to produce a low similarity score. Thus higher FTE results in higher FNMR and lower FMR.

	Algorithm	Failure to Enrol Rate ¹					
		Name	CHILD-EXPLOIT	MUGSHOT	VISA	WILD	
121	tevian-003	0.2430	71	0.0003	78	0.0005	98
122	tevian-004	-	148	0.0002	70	0.0005	95
123	tiger-002	0.0619	37	0.0001	62	0.0004	66
124	tiger-003	0.0619	38	0.0001	60	0.0004	63
125	tongyi-005	0.0000	7	0.0000	4	0.0000	5
126	toshiba-002	0.0000	13	0.0000	8	0.0000	9
127	toshiba-003	-	148	0.0001	63	0.0001	37
128	ulsee-001	-	148	0.0000	29	0.0000	31
129	uluface-002	0.0000	23	0.0000	17	0.0000	19
130	upc-001	0.0450	30	0.0003	77	0.0003	47
131	vd-001	-	148	0.0004	95	0.0009	109
132	veridas-001	-	148	0.0001	61	0.0005	88
133	veridas-002	-	148	0.0001	64	0.0005	90
134	via-000	0.0000	10	0.0000	26	0.0000	30
135	videonetics-001	0.4799	83	0.0015	125	0.0010	112
136	vigilantsolutions-006	-	148	0.0001	50	0.0004	57
137	vigilantsolutions-007	0.2538	74	0.0001	49	0.0004	52
138	vion-000	0.6388	89	0.0130	146	0.0078	147
139	visionbox-000	-	148	0.0005	102	0.0011	119
140	visionbox-001	-	148	0.0005	101	0.0011	118
141	visionlabs-006	-	148	0.0003	83	0.0005	89
142	visionlabs-007	0.1939	64	0.0003	82	0.0005	86
143	vocord-006	-	148	0.0003	80	0.0003	46
144	vocord-007	0.0000	15	0.0001	66	0.0004	50
145	winsense-000	0.0000	12	0.0000	7	0.0000	8
146	yisheng-004	0.4279	81	0.0013	121	0.0006	102
147	yitu-003	-	148	0.0009	112	0.0000	3

Table 11: FTE is the proportion of failed template generation attempts. Failures can occur because the software throws an exception, or because the software electively refuses to process the input image. This would typically occur if a face is not detected. FTE is measured as the number of function calls that give EITHER a non-zero error code OR that give a “small” template. This is defined as one whose size is less than 0.3 times the median template size for that algorithm. This second rule is needed because some algorithms incorrectly fail to return a non-zero error code when template generation fails.

¹The effects of FTE are included in the accuracy results of this report by regarding any template comparison involving a failed template to produce a low similarity score. Thus higher FTE results in higher FNMR and lower FMR.

3.4 Recognition accuracy

Core algorithm accuracy is stated via:

▷ **Cooperative subjects**

- The summary table of Figure 8;
- The visa image DETs of Figure 25;
- The mugshot DETs of Figure 27;
- The mugshot ageing profiles of Figure 116;
- The human-difficult pairs of Figure 10

▷ **Non-cooperative subjects**

- The photojournalism DET of Figure 33
- The child-exploitation DET of Figure 37;
- The child-exploitation CMC of Figure 40.

Figure 93 shows dependence of false match rate on algorithm score threshold. This allows a deployer to set a threshold to target a particular false match rate appropriate to the security objectives of the application.

Figure 78 likewise shows FMR(T) but for mugshots, and specially four subsets of the population.

Note that in both the mugshot and visa sets false match rates vary with the ethnicity, age, and sex, of the enrollee and impostor - see section 3.6. For example figure 49 summarizes FMR for impostors paired from four groups black females, black males, white females, white males.

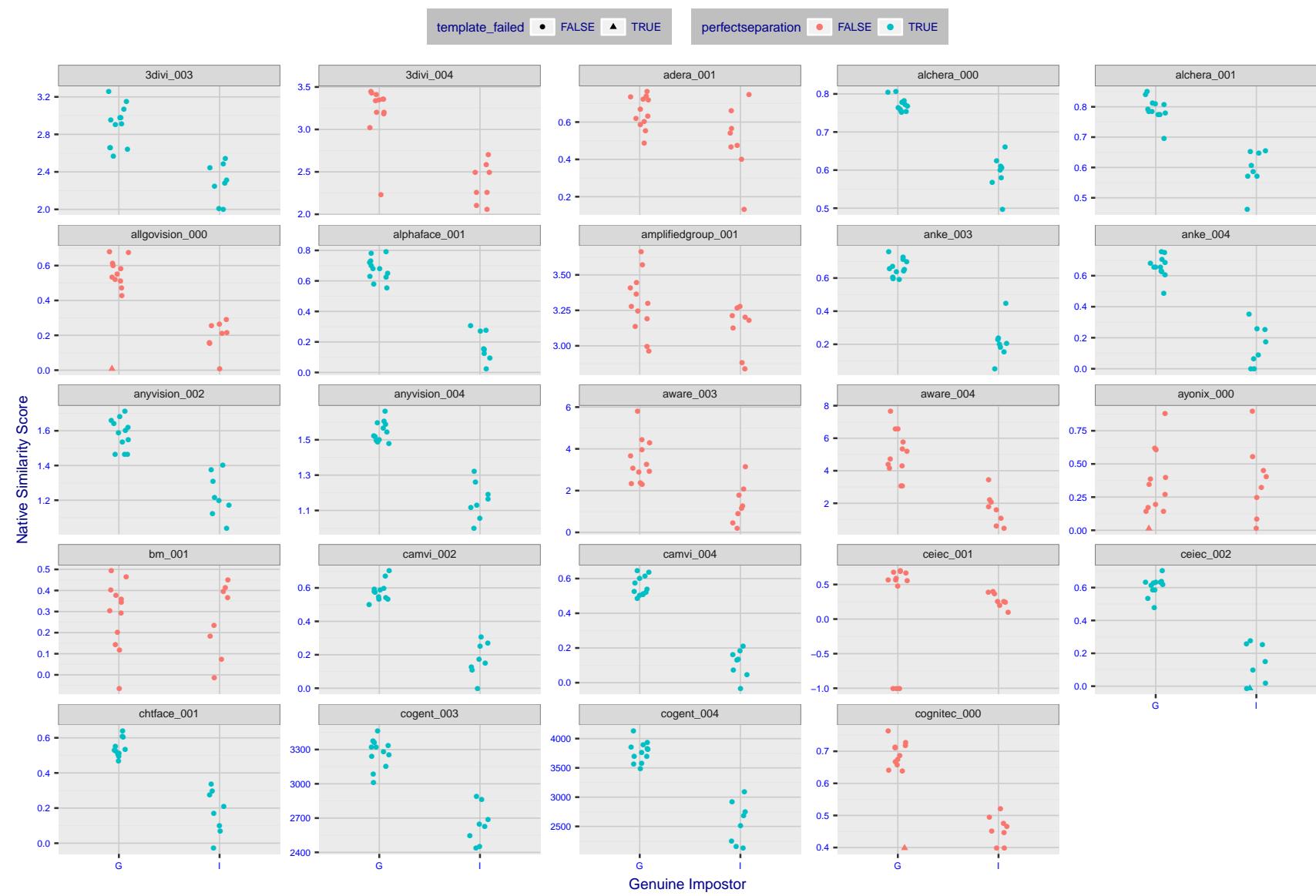


Figure 4: The Figure shows, in blue, algorithms that correctly separate the 12 genuine and 8 impostor pairs used in the May 2018 paper [Face recognition accuracy of forensic examiners, superrecognizers, and face recognition algorithms](#) (Phillips et al. [1]). In red are algorithms that are imperfect. Some algorithms fail only because they failed to make a template e.g. due to face detection failure (shown as a triangle). Others fail because the pairs were selected for that study because they had been difficult for three leading algorithms used in FRVT 2006. Caution: Given the small sample size ($n=20$) the figure may change substantially if larger or different sets were used. The images can be downloaded from the [Supplemental Information](#) page provided with that publication.

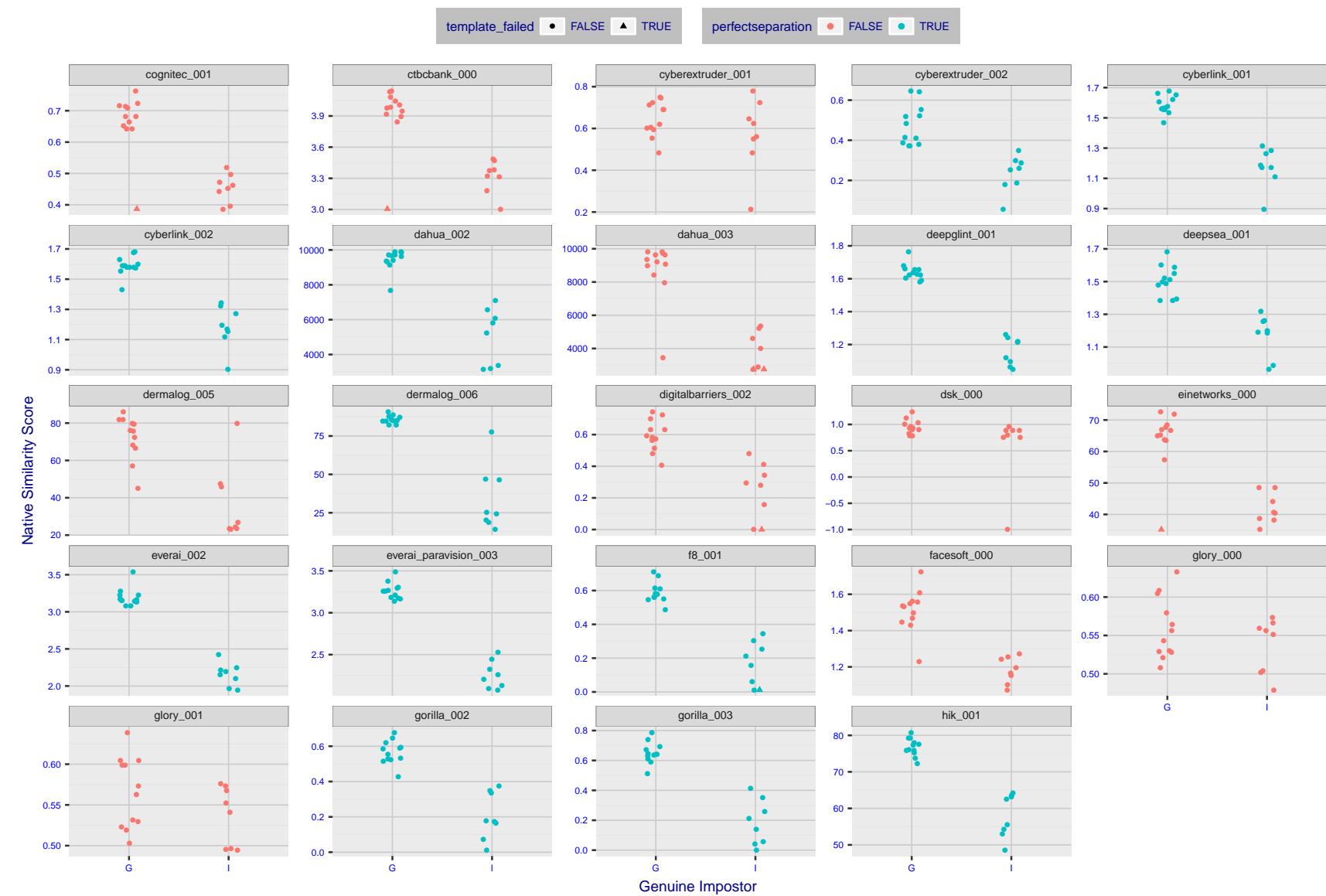


Figure 5: The Figure shows, in blue, algorithms that correctly separate the 12 genuine and 8 impostor pairs used in the May 2018 paper [Face recognition accuracy of forensic examiners, superrecognizers, and face recognition algorithms](#) (Phillips et al. [1]). In red are algorithms that are imperfect. Some algorithms fail only because they failed to make a template e.g. due to face detection failure (shown as a triangle). Others fail because the pairs were selected for that study because they had been difficult for three leading algorithms used in FRVT 2006. Caution: Given the small sample size ($n=20$) the figure may change substantially if larger or different sets were used. The images can be downloaded from the [Supplemental Information](#) page provided with that publication.

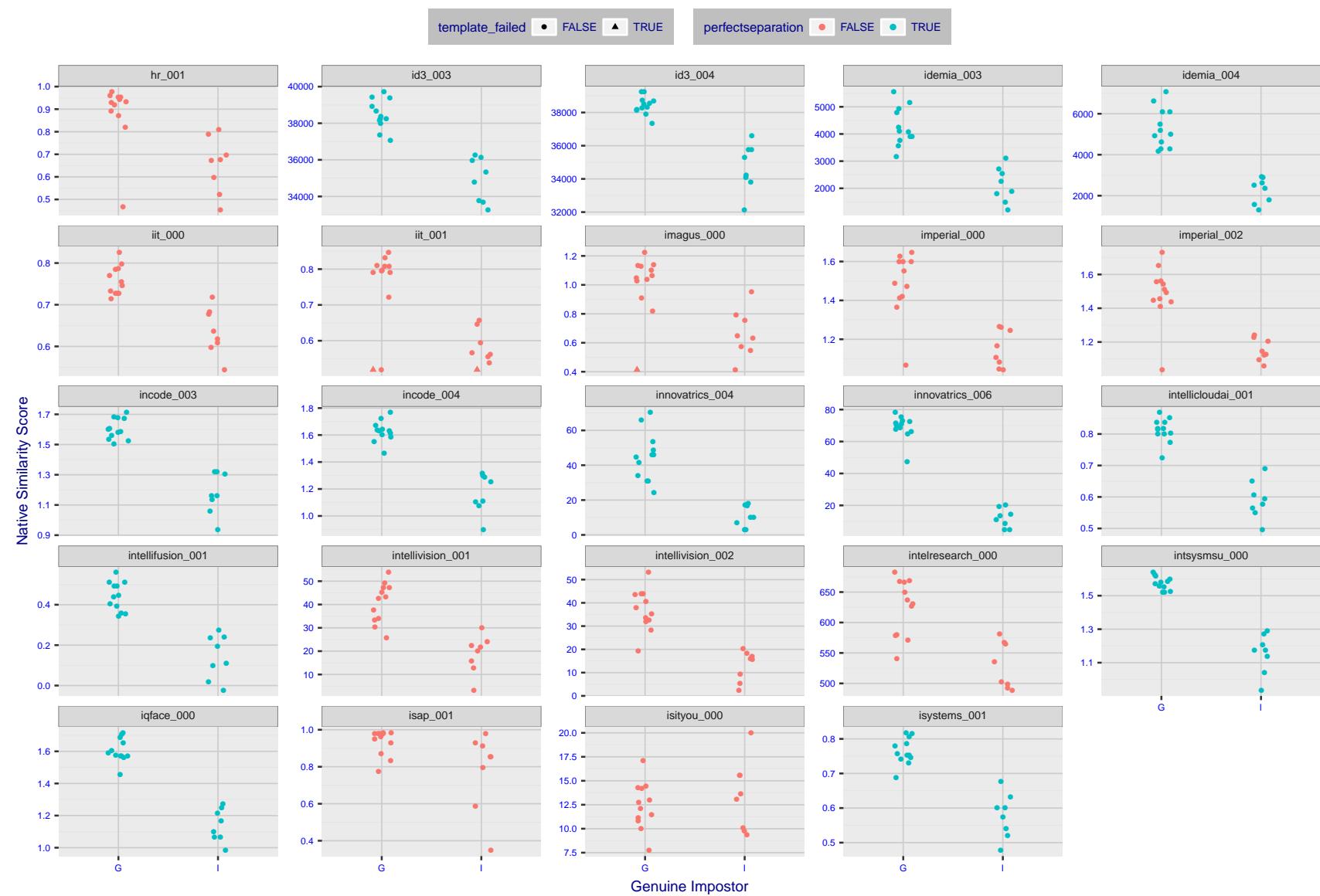


Figure 6: The Figure shows, in blue, algorithms that correctly separate the 12 genuine and 8 impostor pairs used in the May 2018 paper [Face recognition accuracy of forensic examiners, superrecognizers, and face recognition algorithms](#) (Phillips et al. [1]). In red are algorithms that are imperfect. Some algorithms fail only because they failed to make a template e.g. due to face detection failure (shown as a triangle). Others fail because the pairs were selected for that study because they had been difficult for three leading algorithms used in FRVT 2006. Caution: Given the small sample size ($n=20$) the figure may change substantially if larger or different sets were used. The images can be downloaded from the [Supplemental Information](#) page provided with that publication.

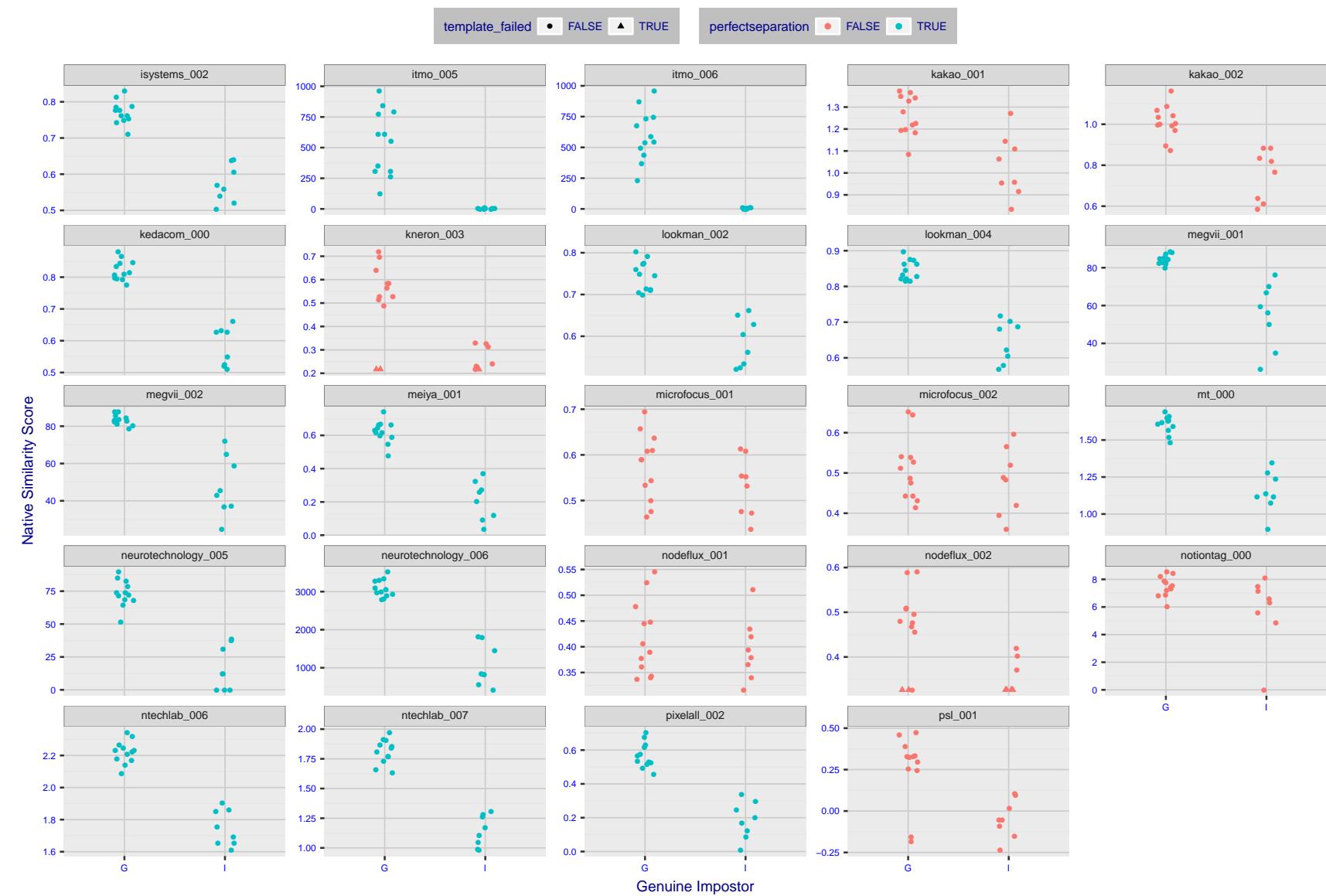


Figure 7: The Figure shows, in blue, algorithms that correctly separate the 12 genuine and 8 impostor pairs used in the May 2018 paper [Face recognition accuracy of forensic examiners, superrecognizers, and face recognition algorithms](#) (Phillips et al. [1]). In red are algorithms that imperfect. Some algorithms fail only because they failed to make a template e.g. due to face detection failure (shown as a triangle). Others fail because the pairs were selected for that study because they had been difficult for three leading algorithms used in FRVT 2006. Caution: Given the small sample size ($n=20$) the figure may change substantially if larger or different sets were used. The images can be downloaded from the [Supplemental Information](#) page provided with that publication.

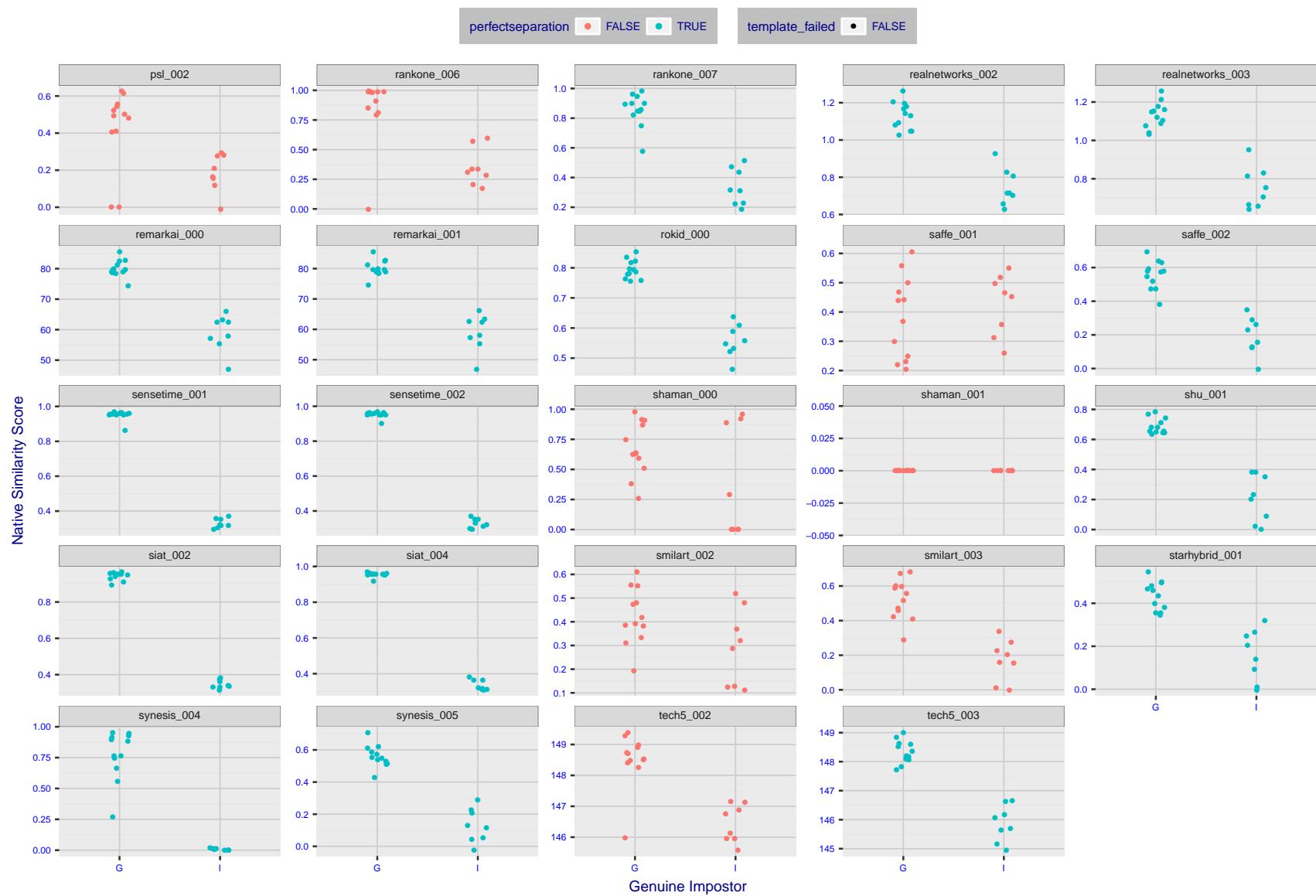


Figure 8: The Figure shows, in blue, algorithms that correctly separate the 12 genuine and 8 impostor pairs used in the May 2018 paper Face recognition accuracy of forensic examiners, superrecognizers, and face recognition algorithms (Phillips et al. [1]). In red are algorithms that are imperfect. Some algorithms fail only because they failed to make a template e.g. due to face detection failure (shown as a triangle). Others fail because the pairs were selected for that study because they had been difficult for three leading algorithms used in FRVT 2006. Caution: Given the small sample size ($n=20$) the figure may change substantially if larger or different sets were used. The images can be downloaded from the [Supplemental Information](#) page provided with that publication.

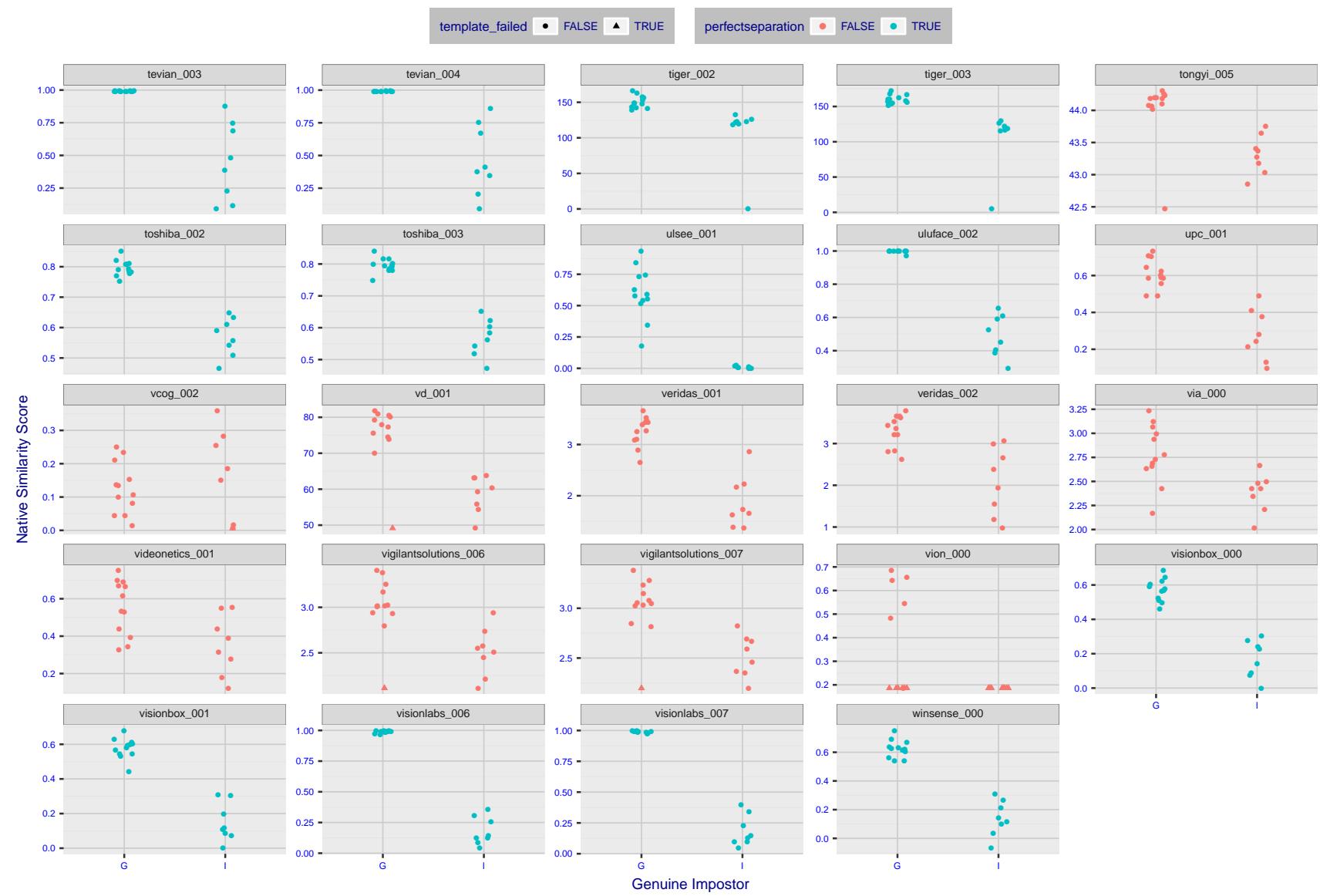


Figure 9: The Figure shows, in blue, algorithms that correctly separate the 12 genuine and 8 impostor pairs used in the May 2018 paper [Face recognition accuracy of forensic examiners, superrecognizers, and face recognition algorithms](#) (Phillips et al. [1]). In red are algorithms that are imperfect. Some algorithms fail only because they failed to make a template e.g. due to face detection failure (shown as a triangle). Others fail because the pairs were selected for that study because they had been difficult for three leading algorithms used in FRVT 2006. Caution: Given the small sample size ($n=20$) the figure may change substantially if larger or different sets were used. The images can be downloaded from the [Supplemental Information](#) page provided with that publication.

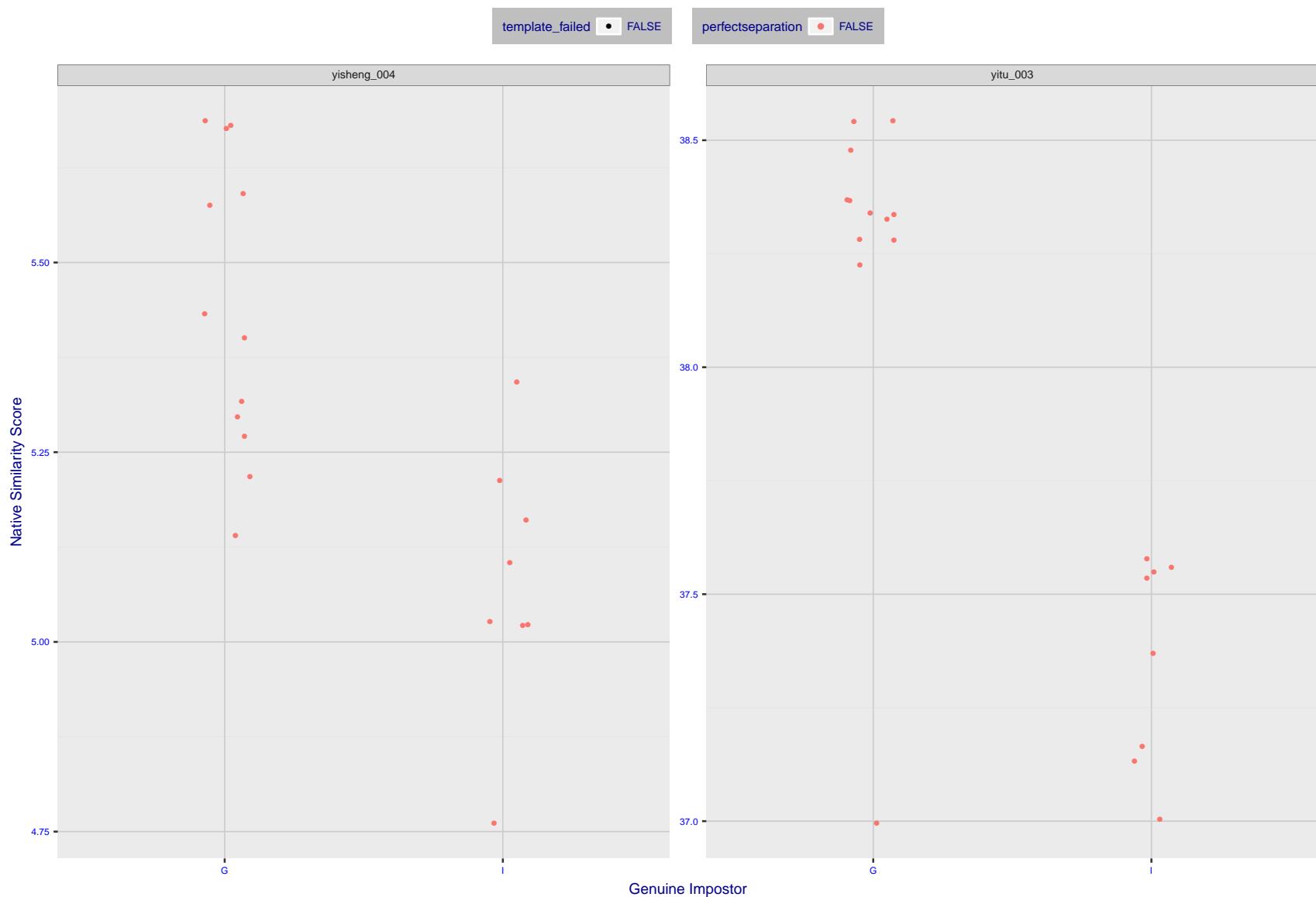


Figure 10: The Figure shows, in blue, algorithms that correctly separate the 12 genuine and 8 impostor pairs used in the May 2018 paper [Face recognition accuracy of forensic examiners, superrecognizers, and face recognition algorithms](#) (Phillips et al. [1]). In red are algorithms that are imperfect. Some algorithms fail only because they failed to make a template e.g. due to face detection failure (shown as a triangle). Others fail because the pairs were selected for that study because they had been difficult for three leading algorithms used in FRVT 2006. Caution: Given the small sample size ($n=20$) the figure may change substantially if larger or different sets were used. The images can be downloaded from the [Supplemental Information](#) page provided with that publication.

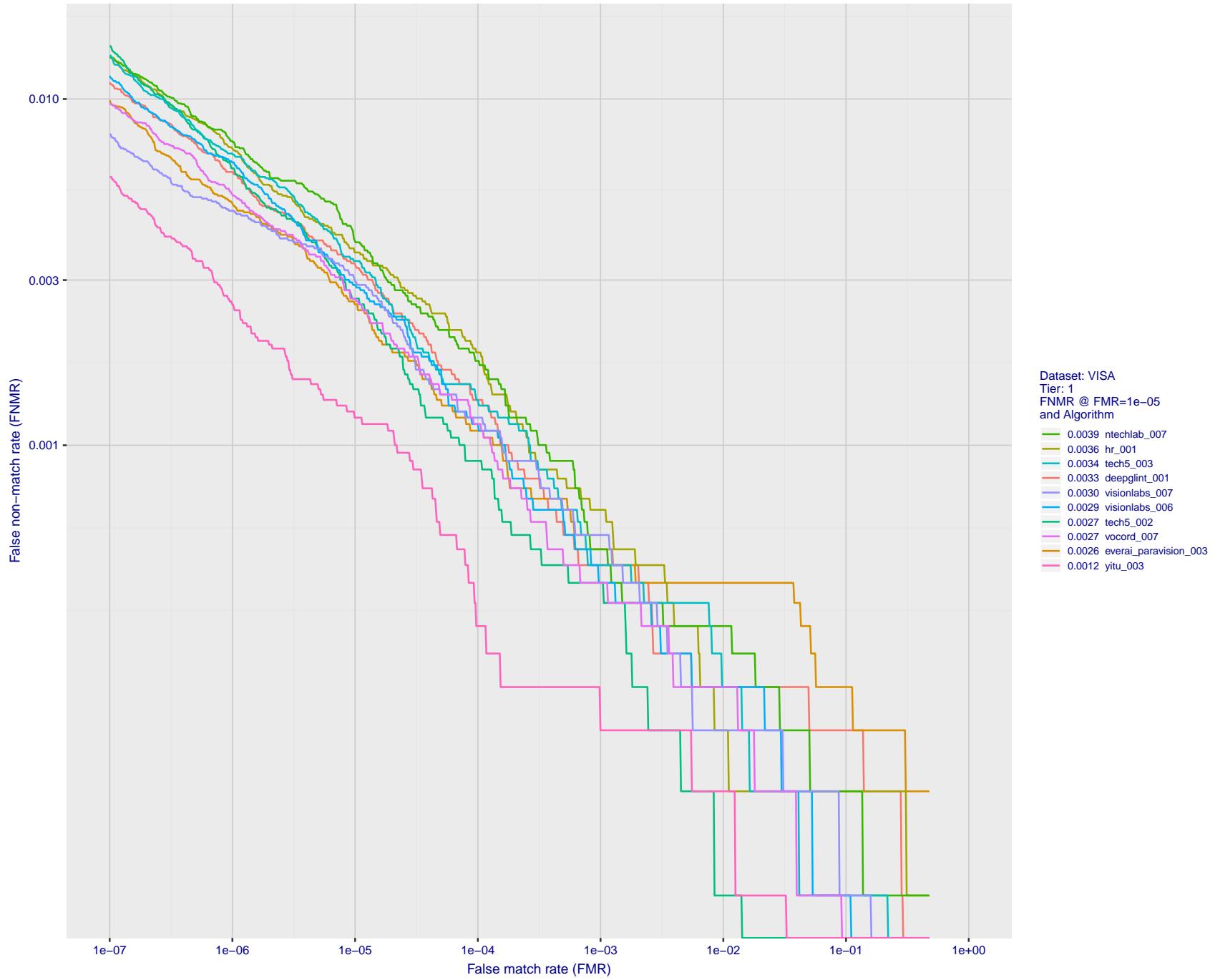


Figure 11: For the visa images, detection error tradeoff (DET) characteristics showing false non-match rate vs. false match rate plotted parametrically on threshold, T . The scales are logarithmic in order to show many decades of FMR.

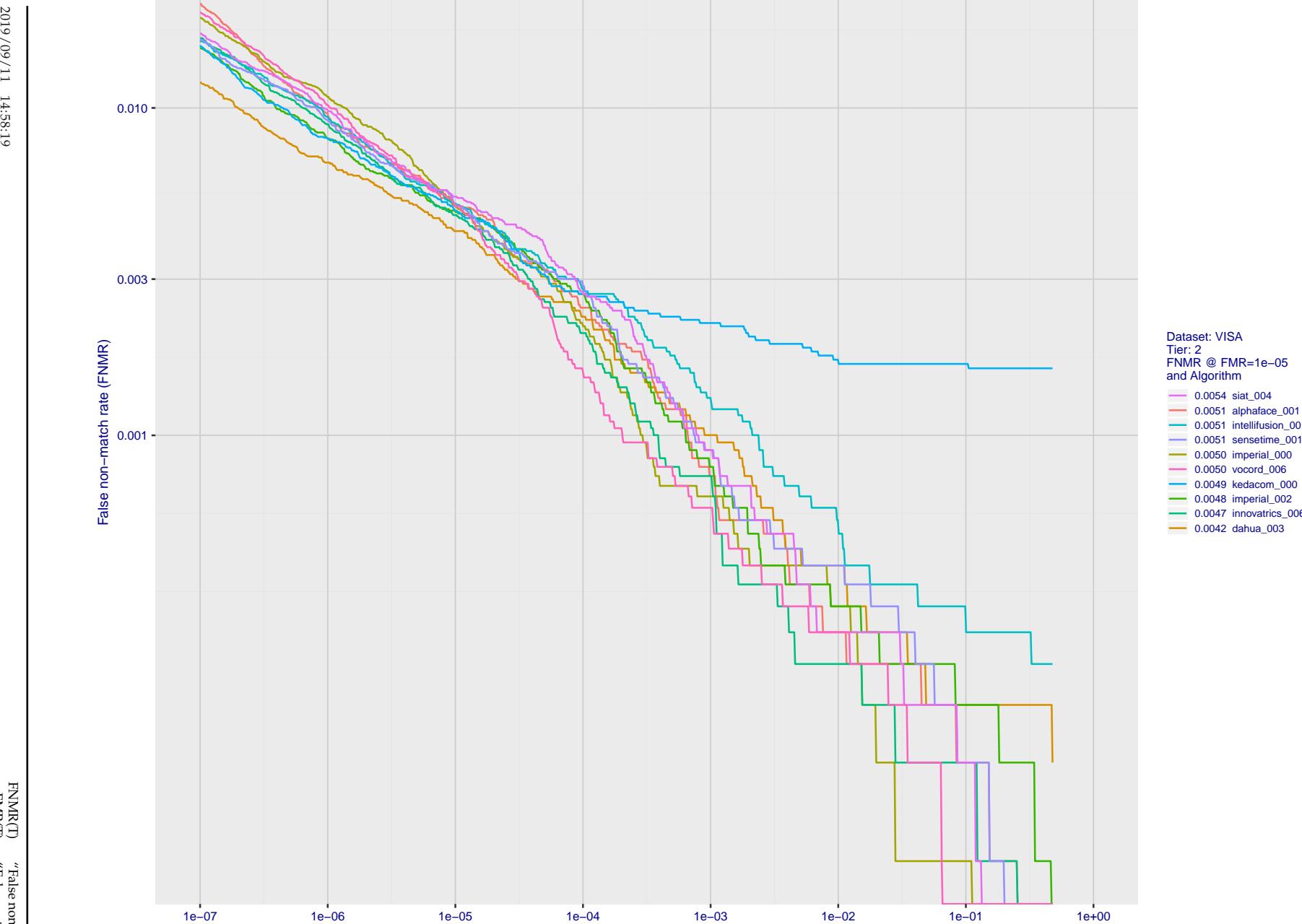


Figure 12: For the visa images, detection error tradeoff (DET) characteristics showing false non-match rate vs. false match rate plotted parametrically on threshold, T . The scales are logarithmic in order to show many decades of FMR.

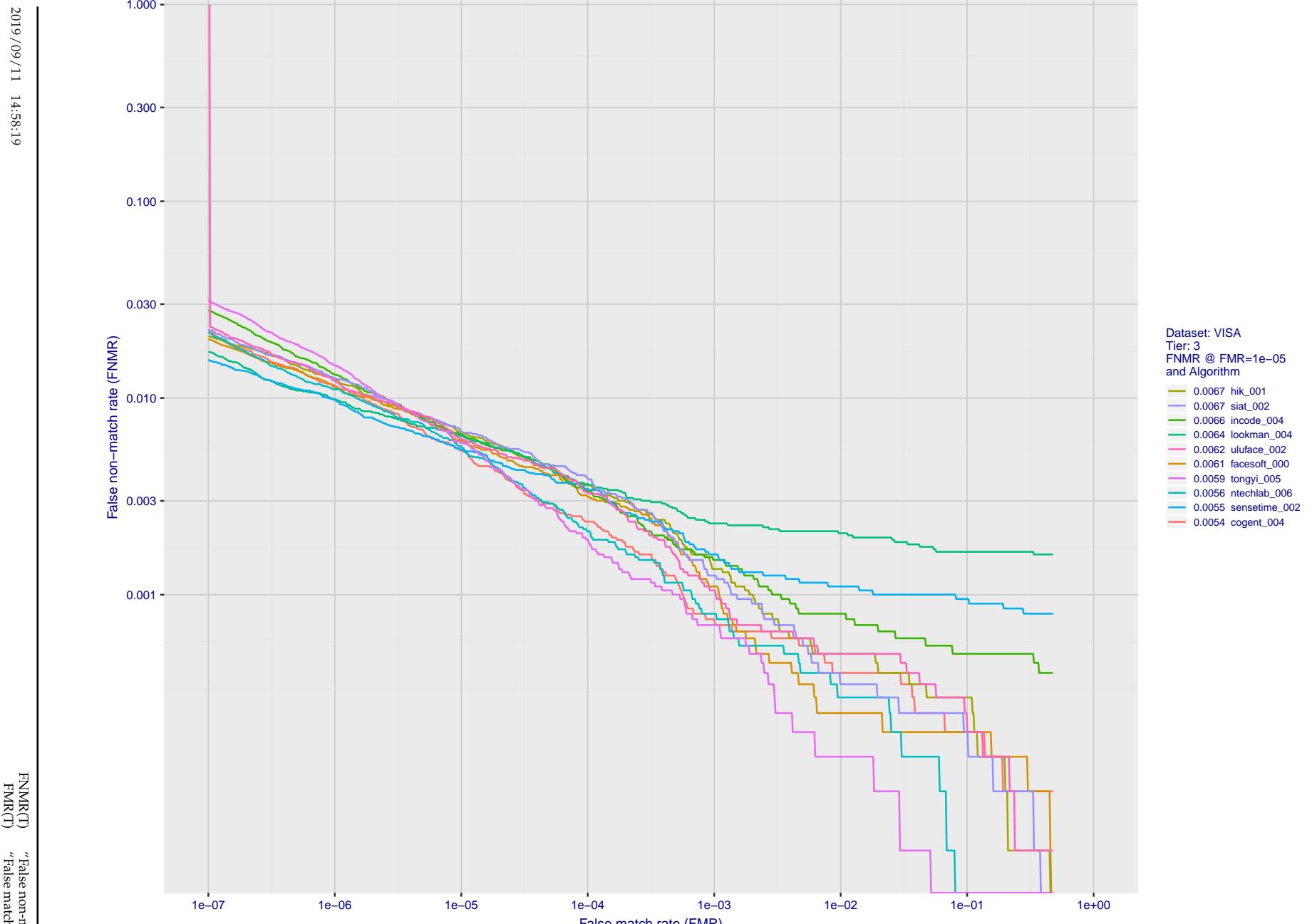


Figure 13: For the visa images, detection error tradeoff (DET) characteristics showing false non-match rate vs. false match rate plotted parametrically on threshold, T . The scales are logarithmic in order to show many decades of FMR.

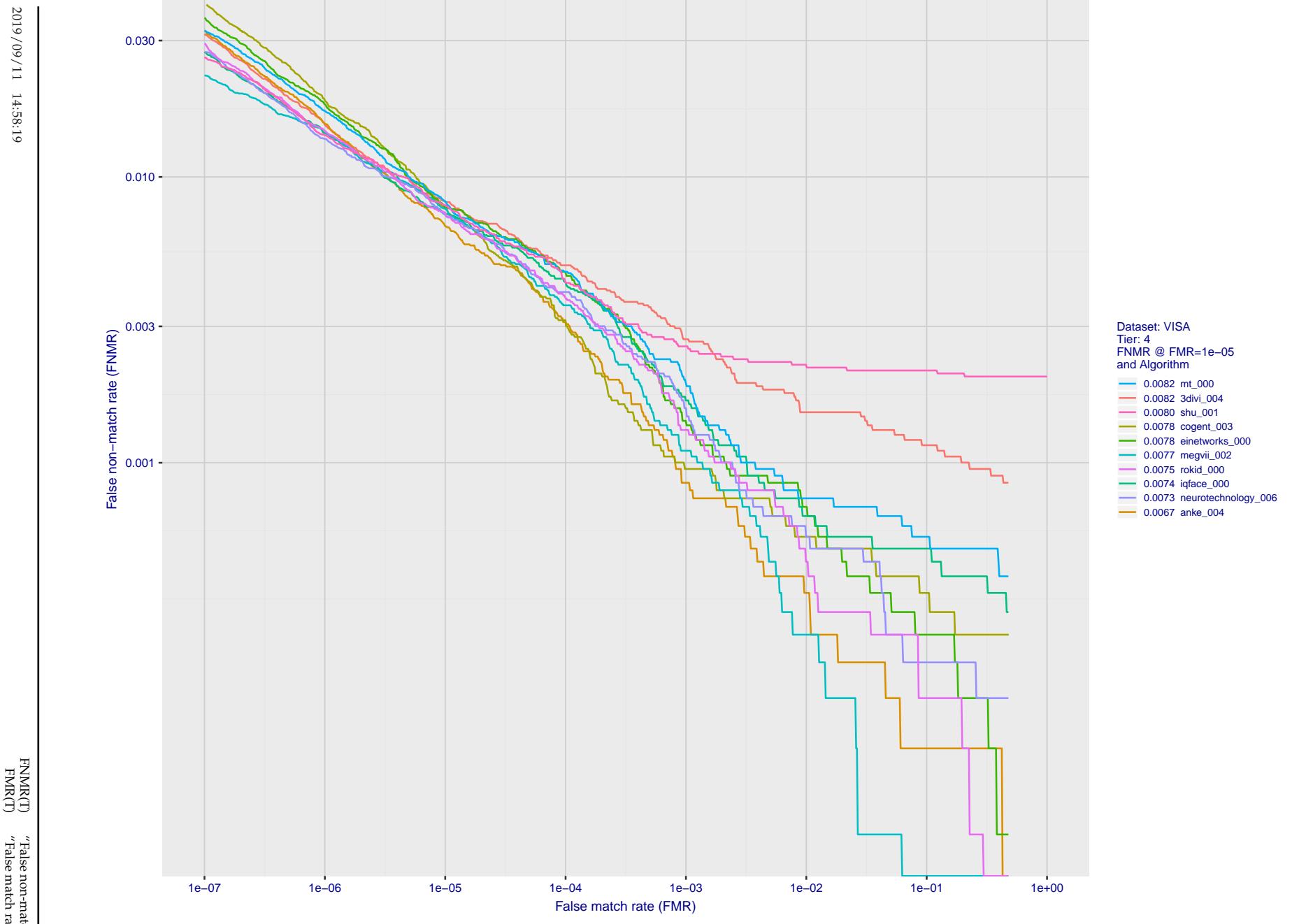


Figure 14: For the visa images, detection error tradeoff (DET) characteristics showing false non-match rate vs. false match rate plotted parametrically on threshold, T . The scales are logarithmic in order to show many decades of FMR.

2019/09/11 14:58:19

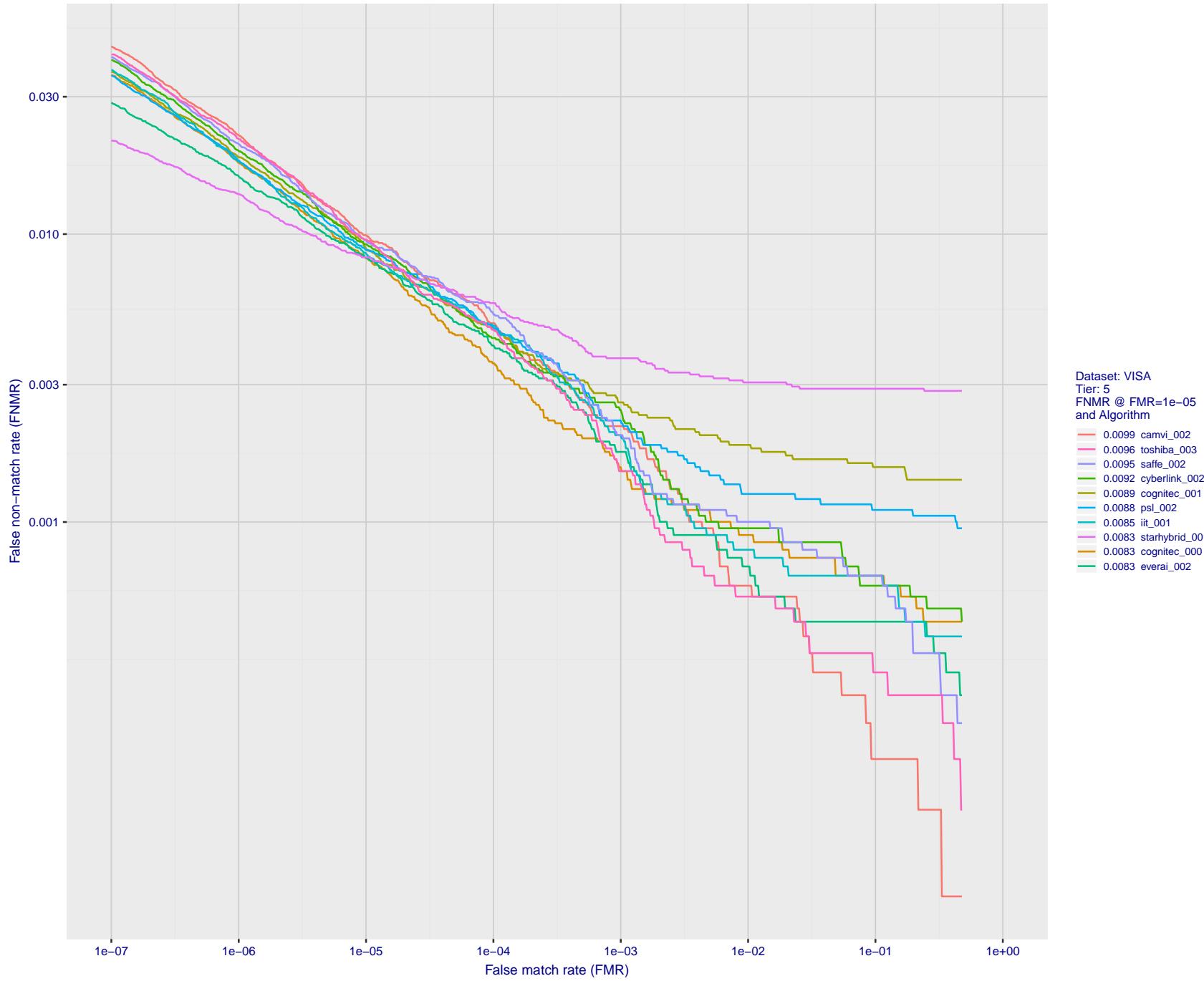


Figure 15: For the visa images, detection error tradeoff (DET) characteristics showing false non-match rate vs. false match rate plotted parametrically on threshold, T . The scales are logarithmic in order to show many decades of FMR.

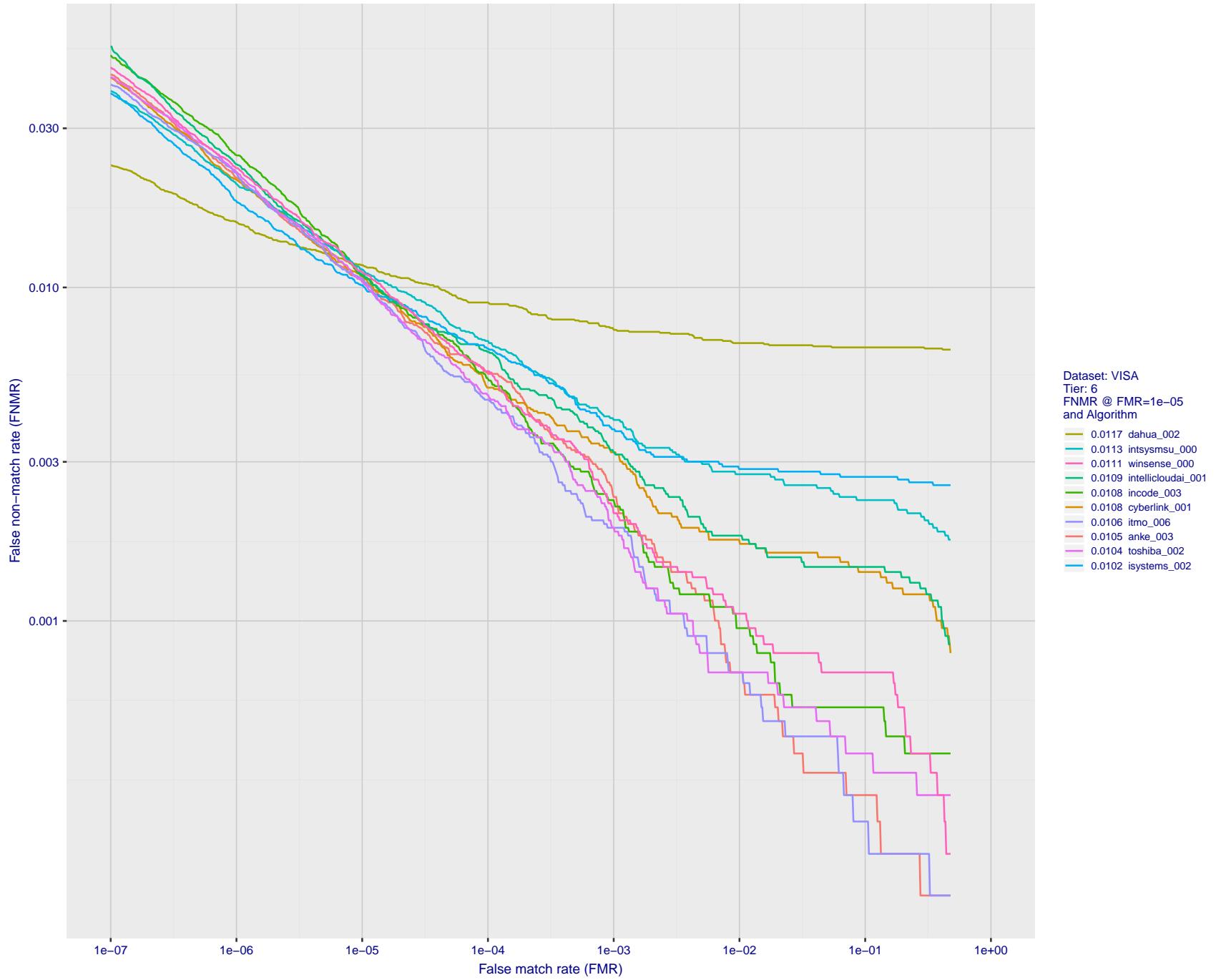


Figure 16: For the visa images, detection error tradeoff (DET) characteristics showing false non-match rate vs. false match rate plotted parametrically on threshold, T . The scales are logarithmic in order to show many decades of FMR.

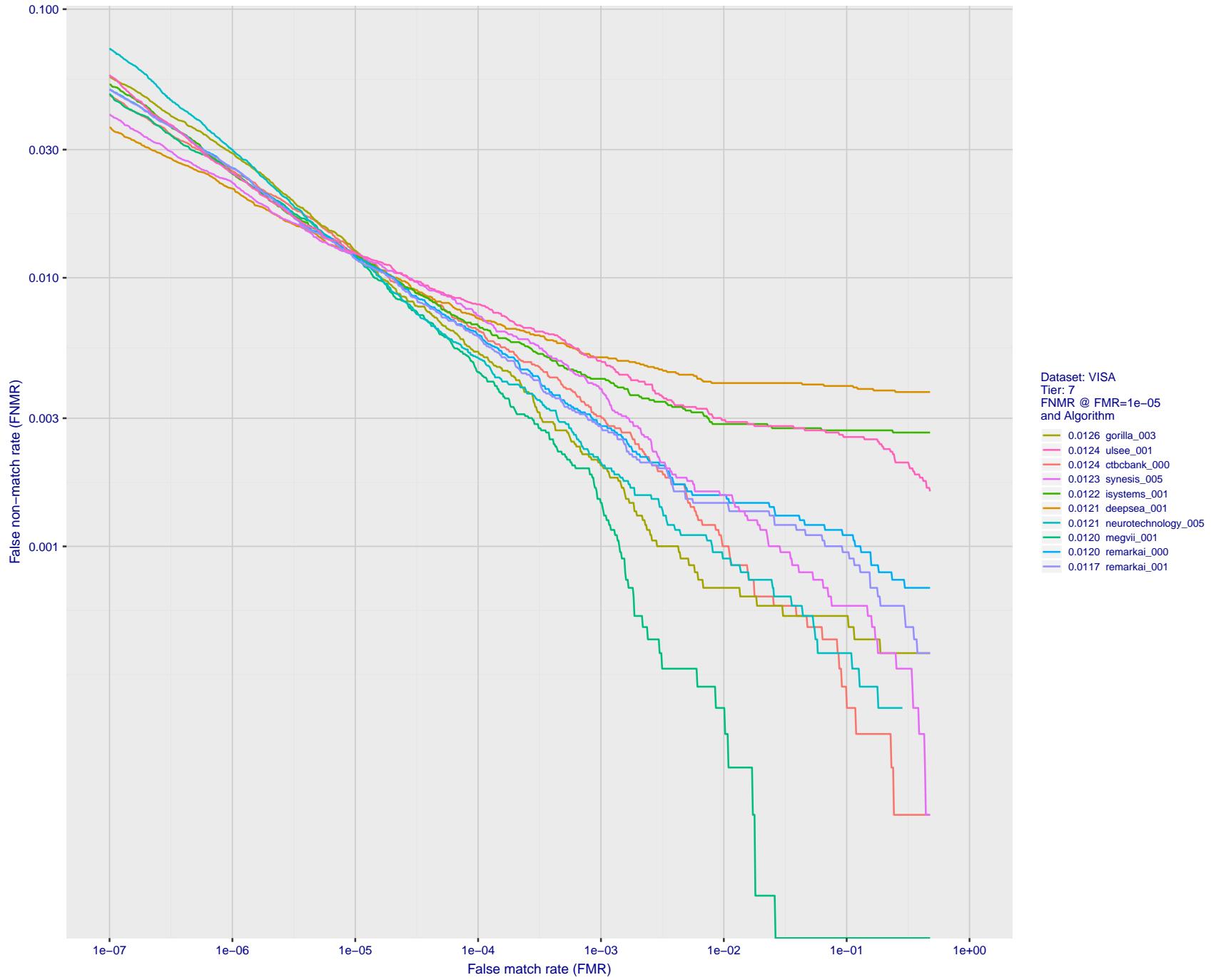


Figure 17: For the visa images, detection error tradeoff (DET) characteristics showing false non-match rate vs. false match rate plotted parametrically on threshold, T . The scales are logarithmic in order to show many decades of FMR.

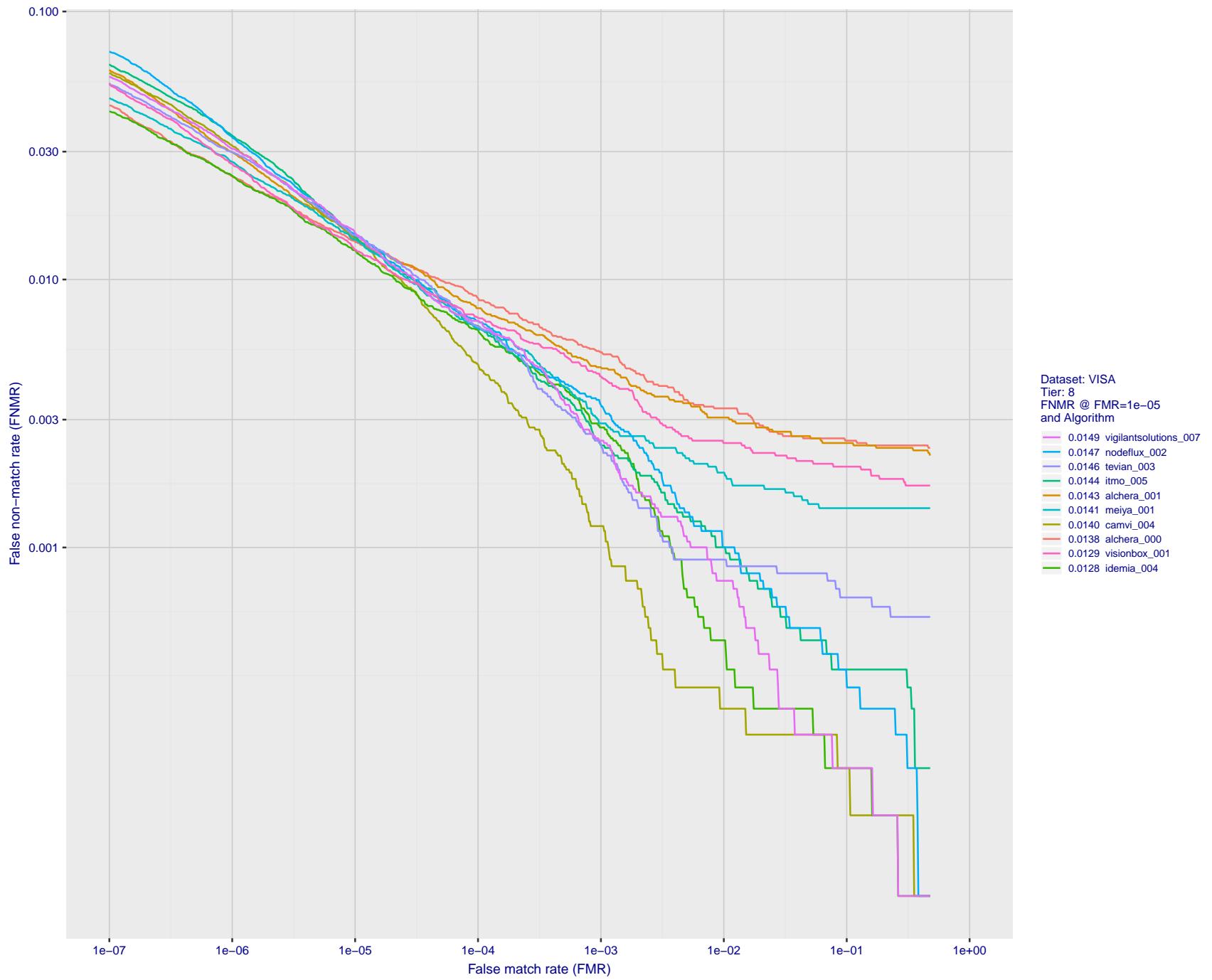


Figure 18: For the visa images, detection error tradeoff (DET) characteristics showing false non-match rate vs. false match rate plotted parametrically on threshold, T . The scales are logarithmic in order to show many decades of FMR.

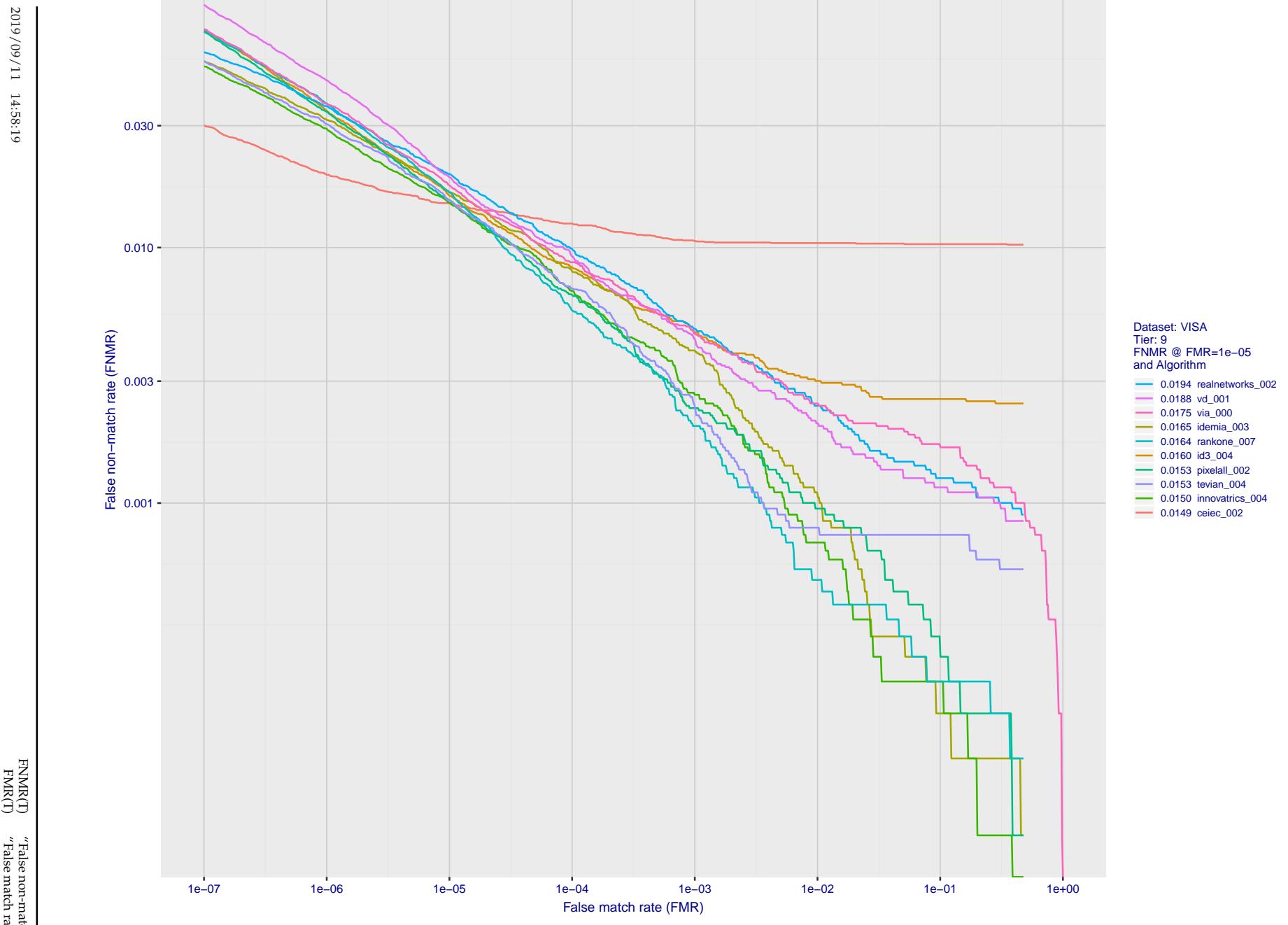


Figure 19: For the visa images, detection error tradeoff (DET) characteristics showing false non-match rate vs. false match rate plotted parametrically on threshold, T . The scales are logarithmic in order to show many decades of FMR.

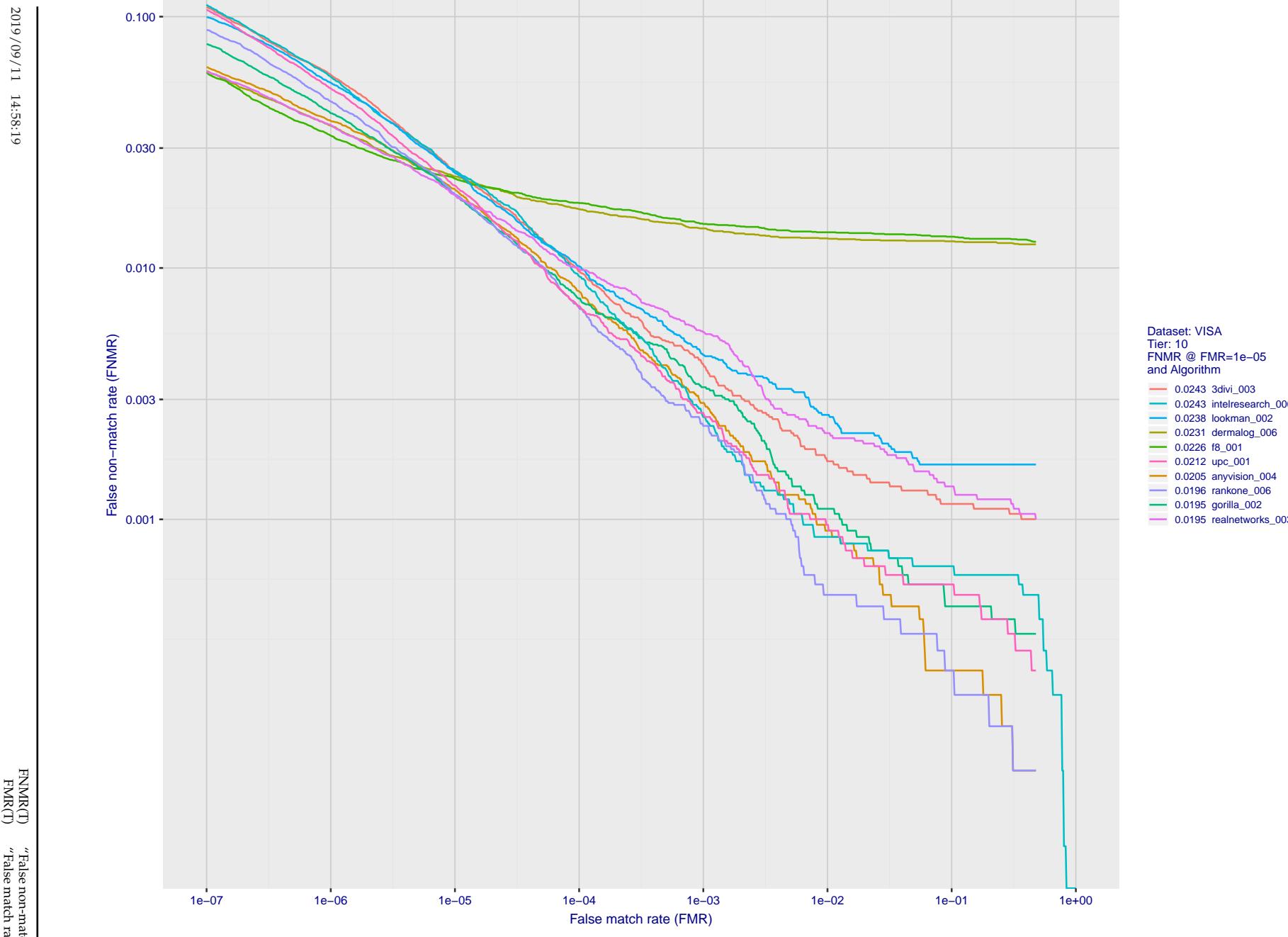


Figure 20: For the visa images, detection error tradeoff (DET) characteristics showing false non-match rate vs. false match rate plotted parametrically on threshold, T . The scales are logarithmic in order to show many decades of FMR.

2019/09/11 14:58:19

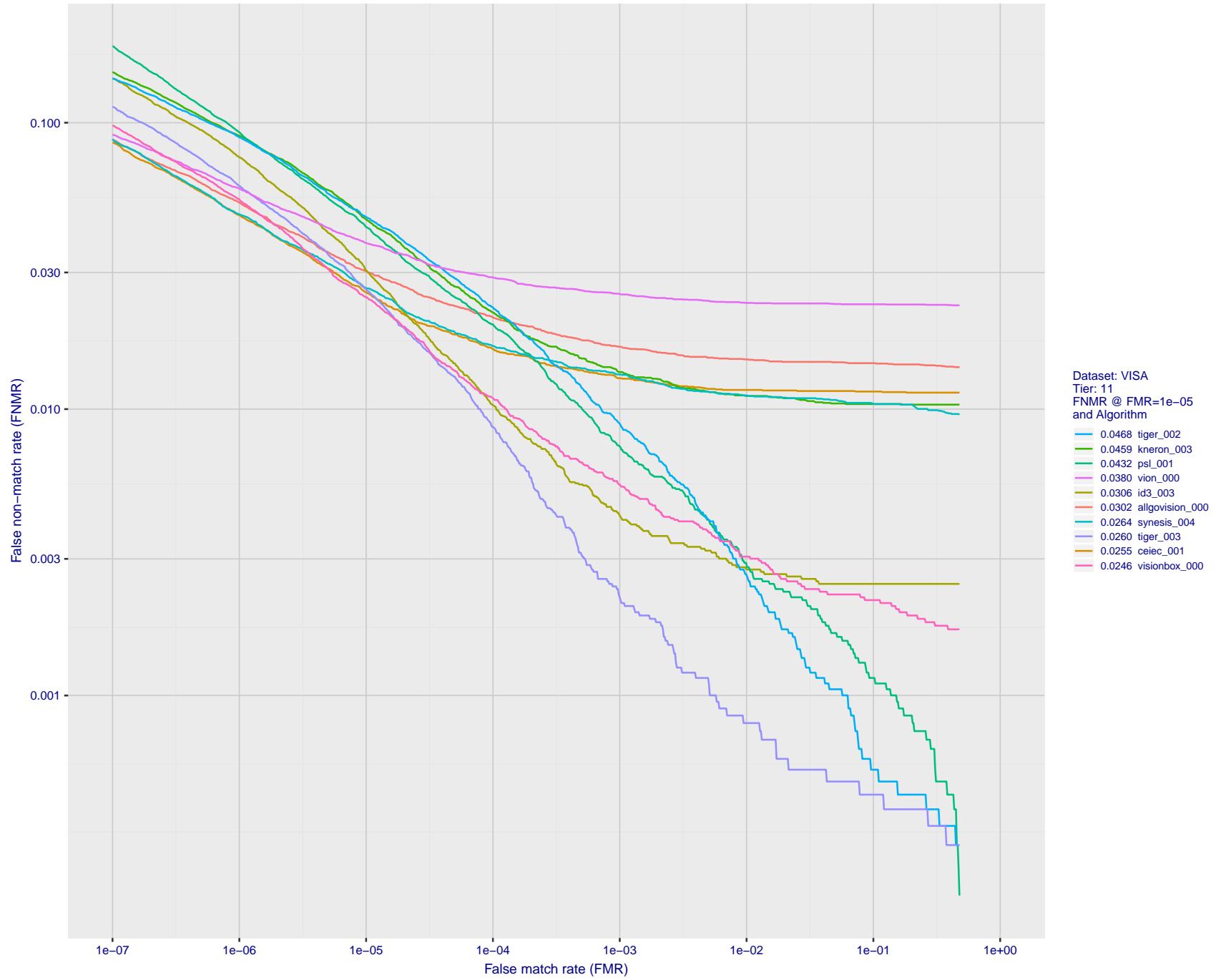


Figure 21: For the visa images, detection error tradeoff (DET) characteristics showing false non-match rate vs. false match rate plotted parametrically on threshold, T . The scales are logarithmic in order to show many decades of FMR.

2019/09/11 14:58:19

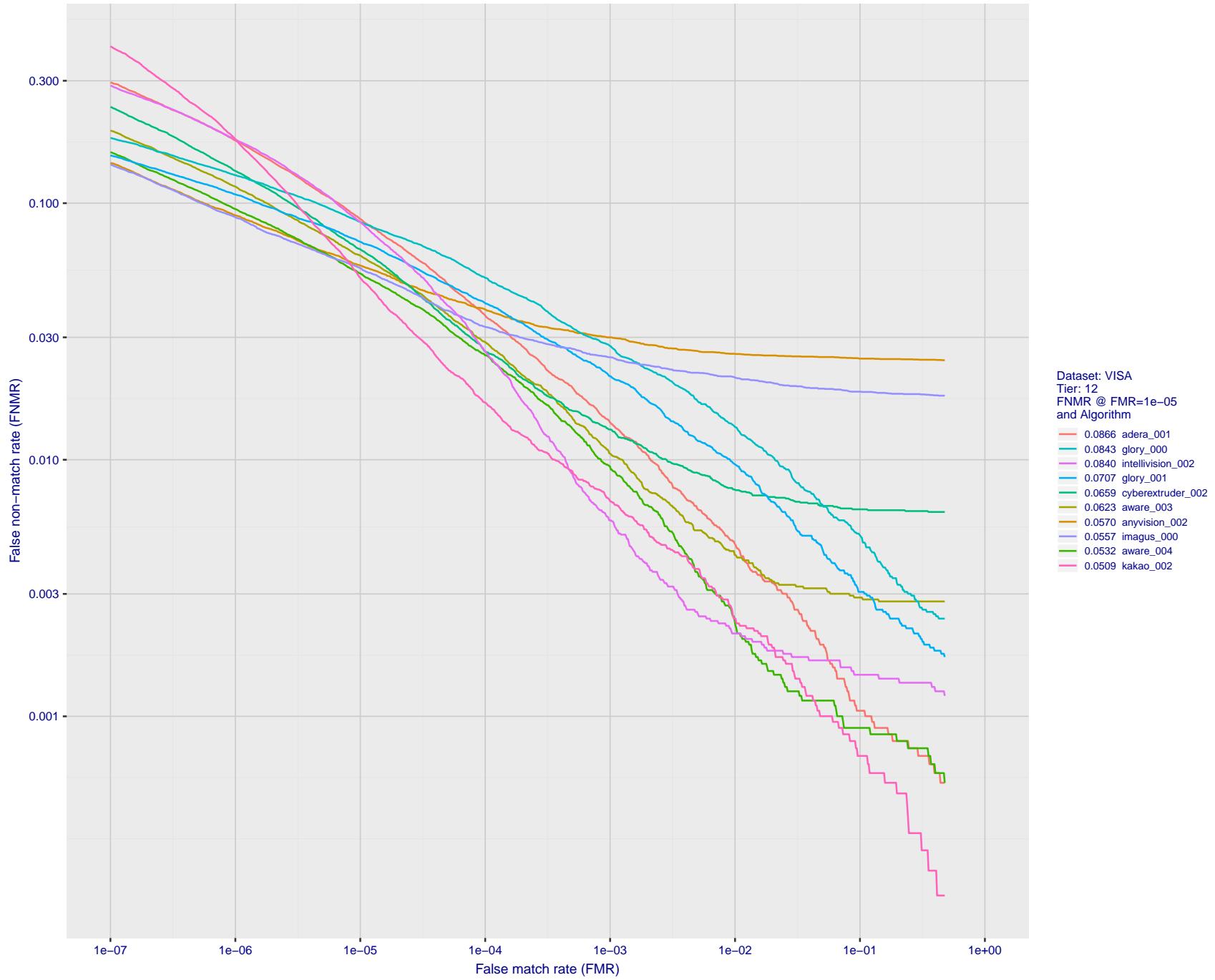


Figure 22: For the visa images, detection error tradeoff (DET) characteristics showing false non-match rate vs. false match rate plotted parametrically on threshold, T . The scales are logarithmic in order to show many decades of FMR.

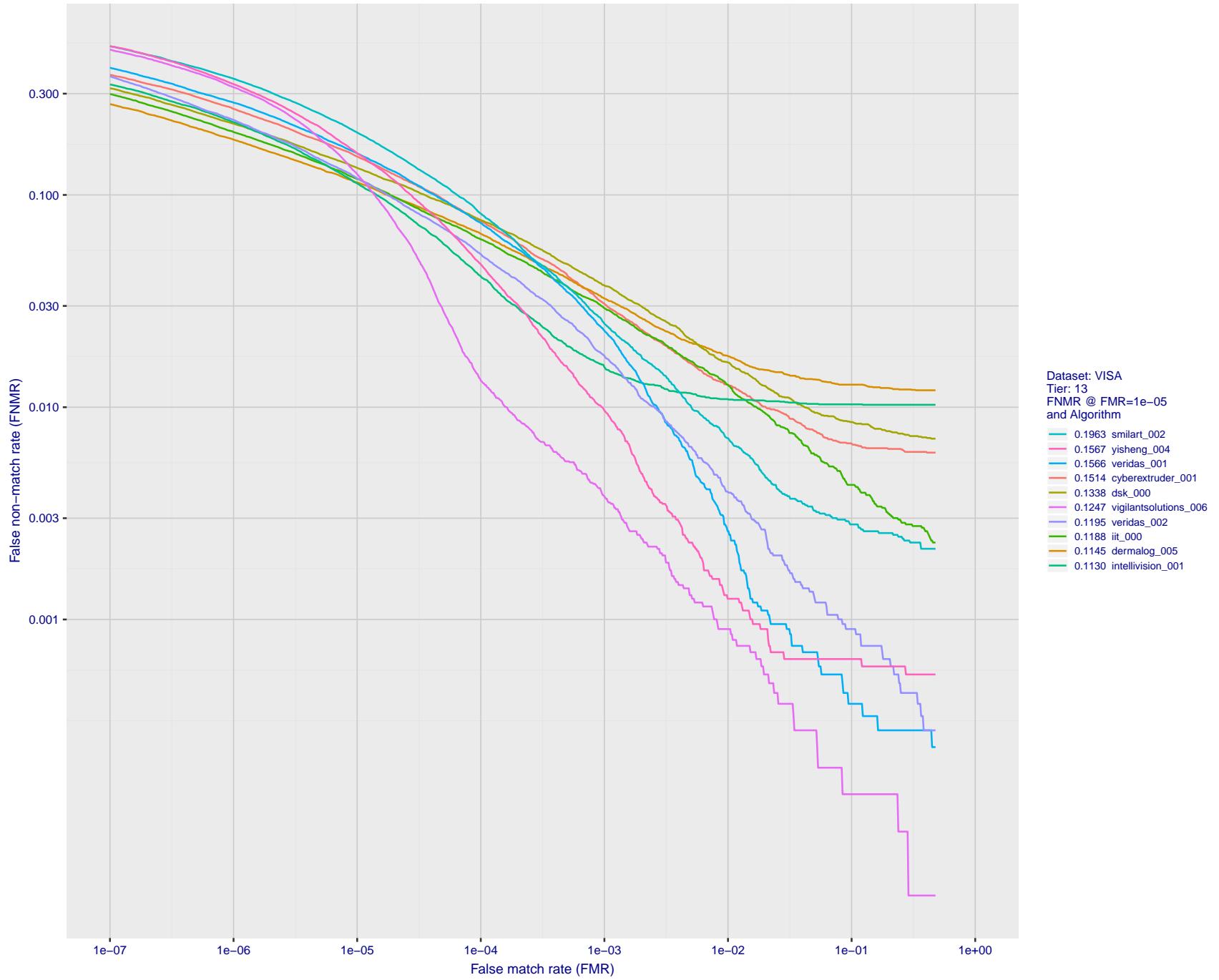


Figure 23: For the visa images, detection error tradeoff (DET) characteristics showing false non-match rate vs. false match rate plotted parametrically on threshold, T . The scales are logarithmic in order to show many decades of FMR.

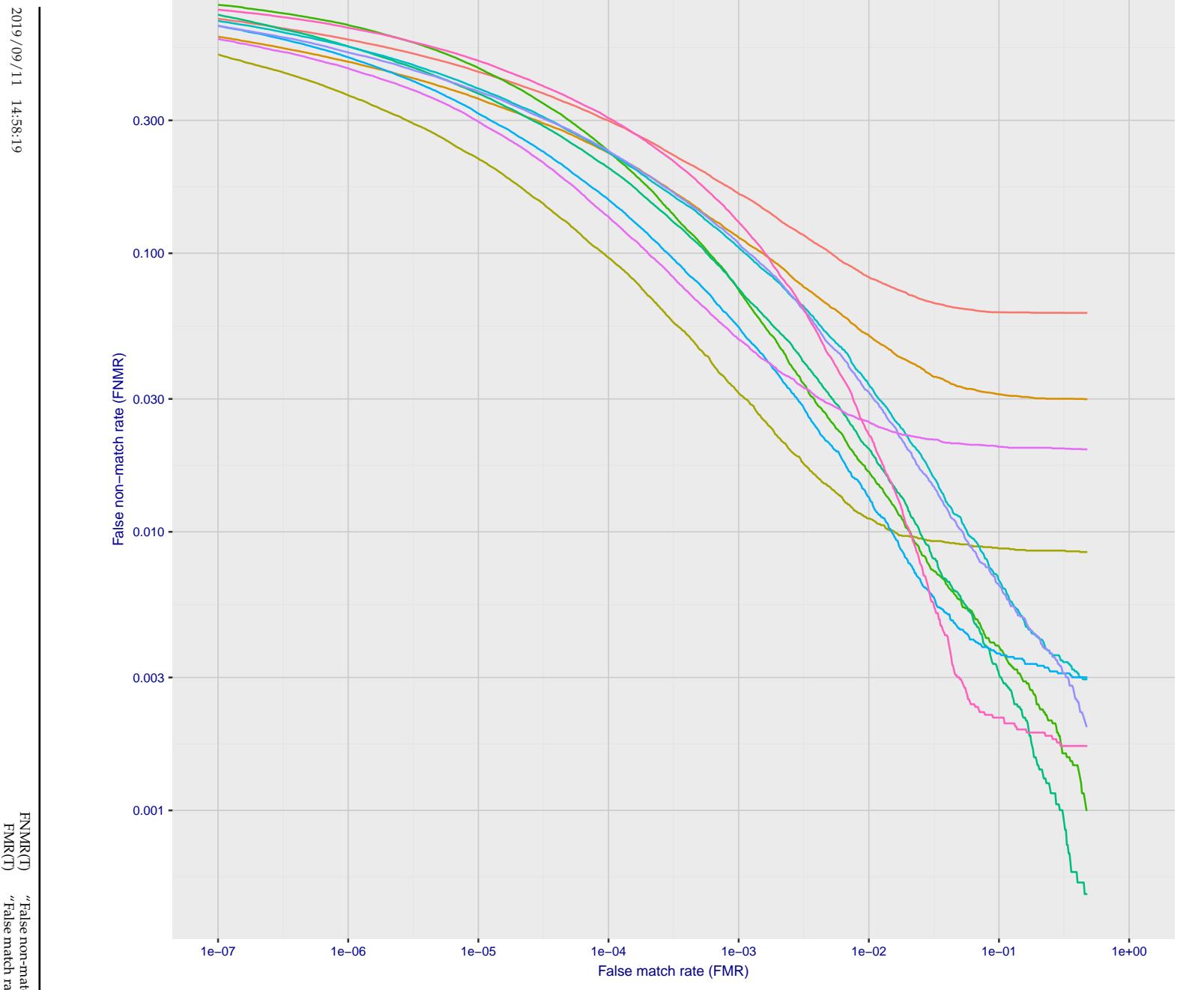


Figure 24: For the visa images, detection error tradeoff (DET) characteristics showing false non-match rate vs. false match rate plotted parametrically on threshold, T . The scales are logarithmic in order to show many decades of FMR.

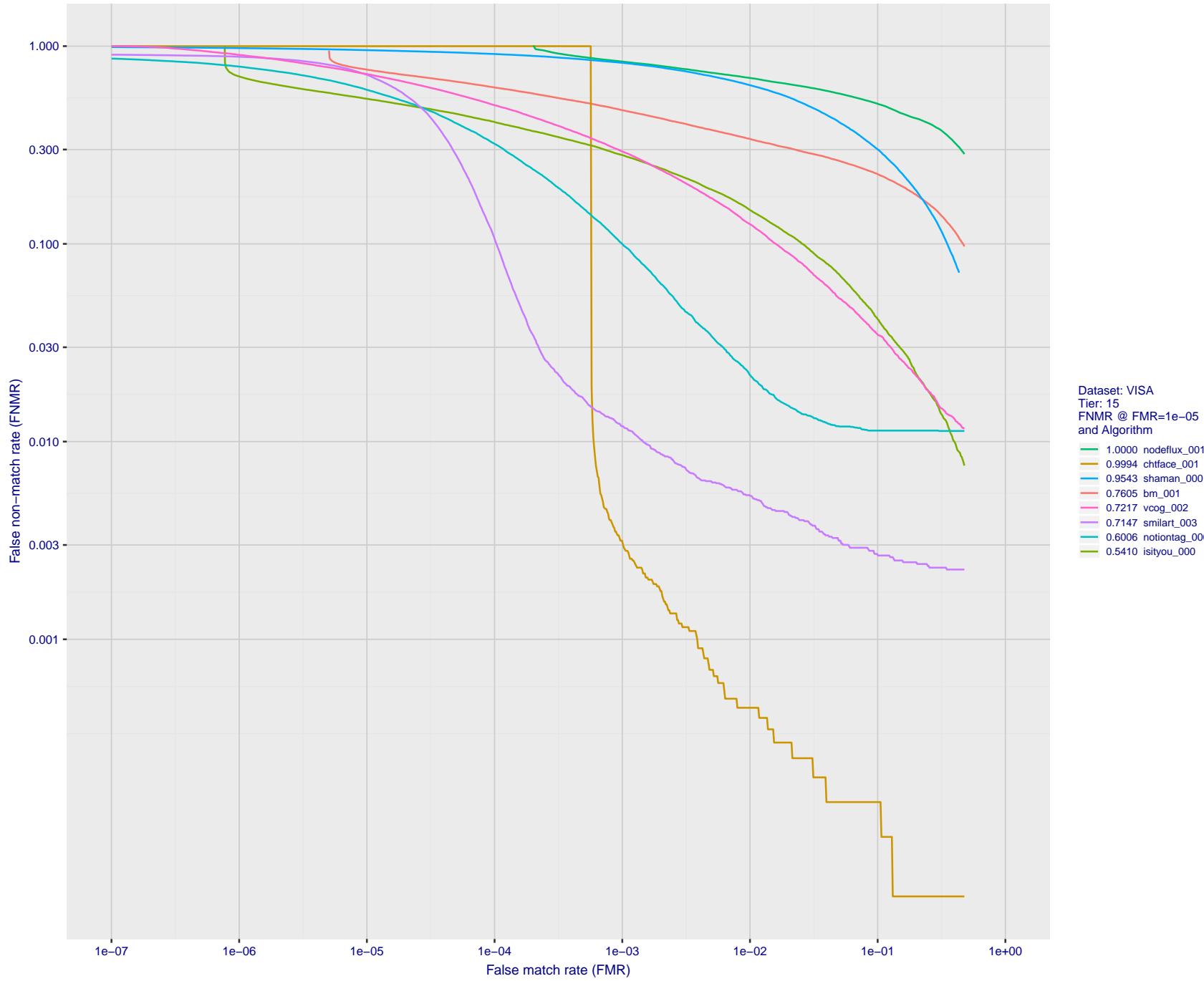


Figure 25: For the visa images, detection error tradeoff (DET) characteristics showing false non-match rate vs. false match rate plotted parametrically on threshold, T . The scales are logarithmic in order to show many decades of FMR.

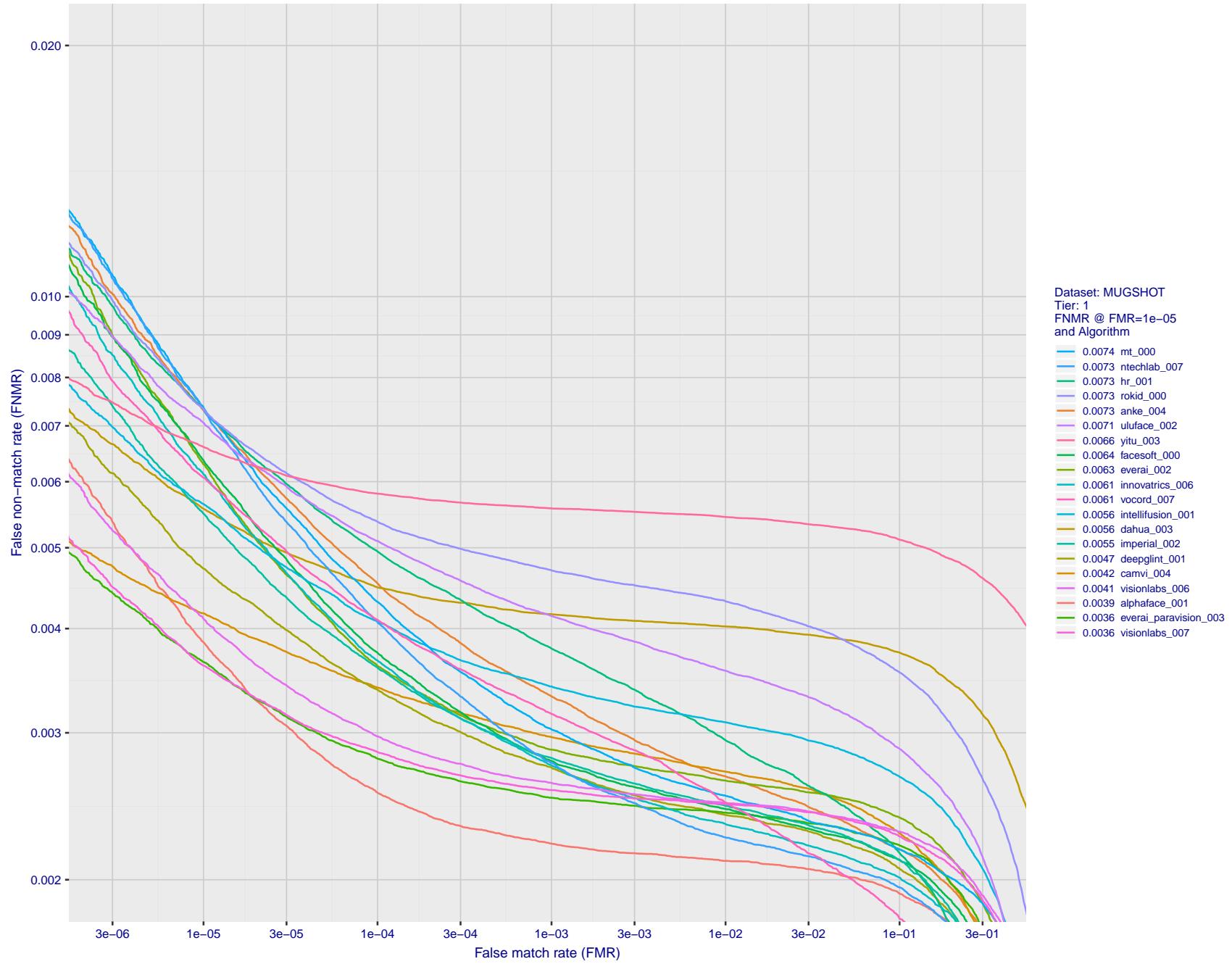


Figure 26: For the mugshot images, detection error tradeoff (DET) characteristics showing false non-match rate vs. false match rate plotted parametrically on threshold, T . The scales are logarithmic in order to show decades of FMR.

Figure 27: For the mugshot images, detection error tradeoff (DET) characteristics showing false non-match rate vs. false match rate plotted parametrically on threshold, T . The scales are logarithmic in order to show decades of FMR.

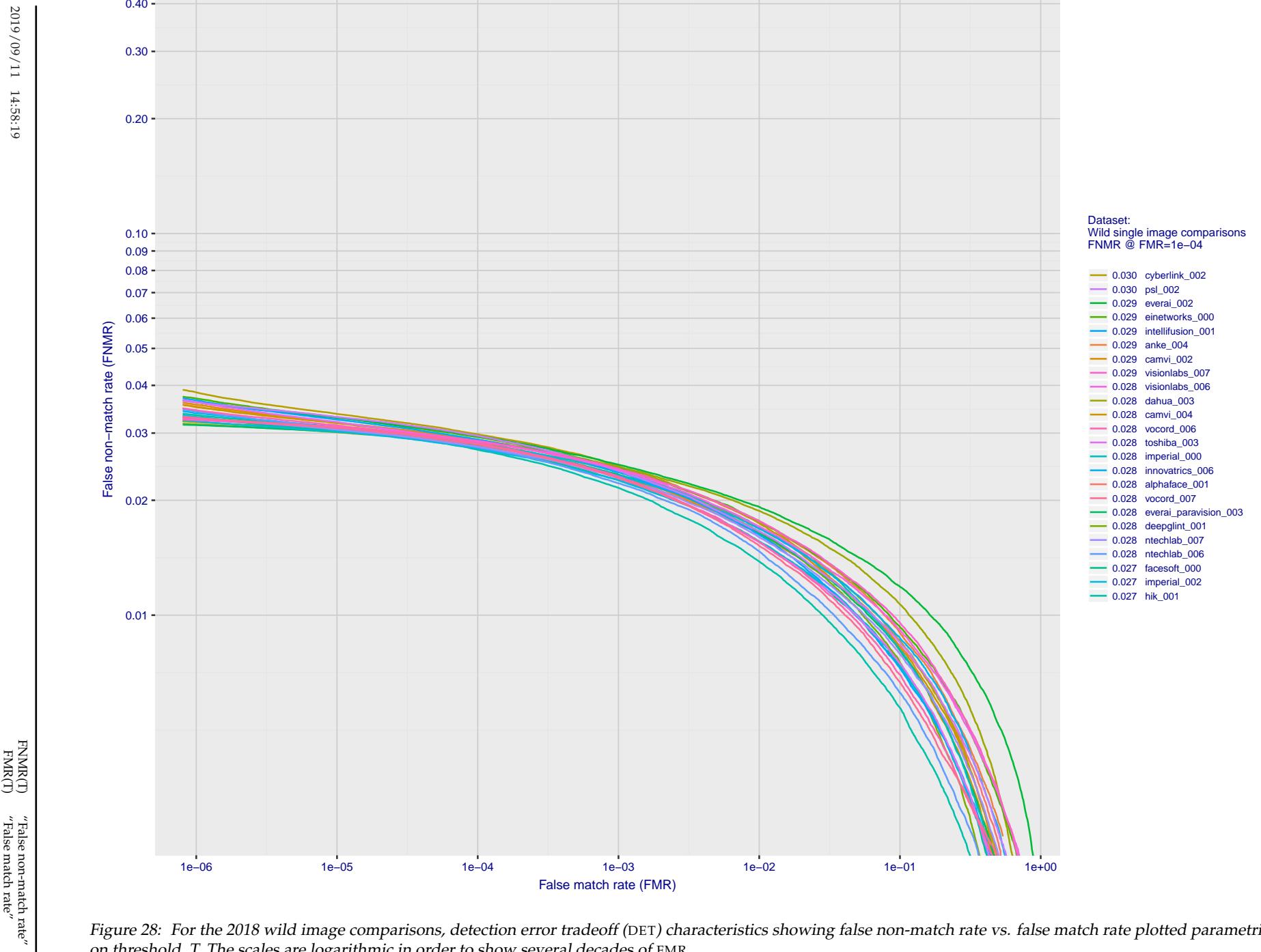


Figure 28: For the 2018 wild image comparisons, detection error tradeoff (DET) characteristics showing false non-match rate vs. false match rate plotted parametrically on threshold, T . The scales are logarithmic in order to show several decades of FMR.

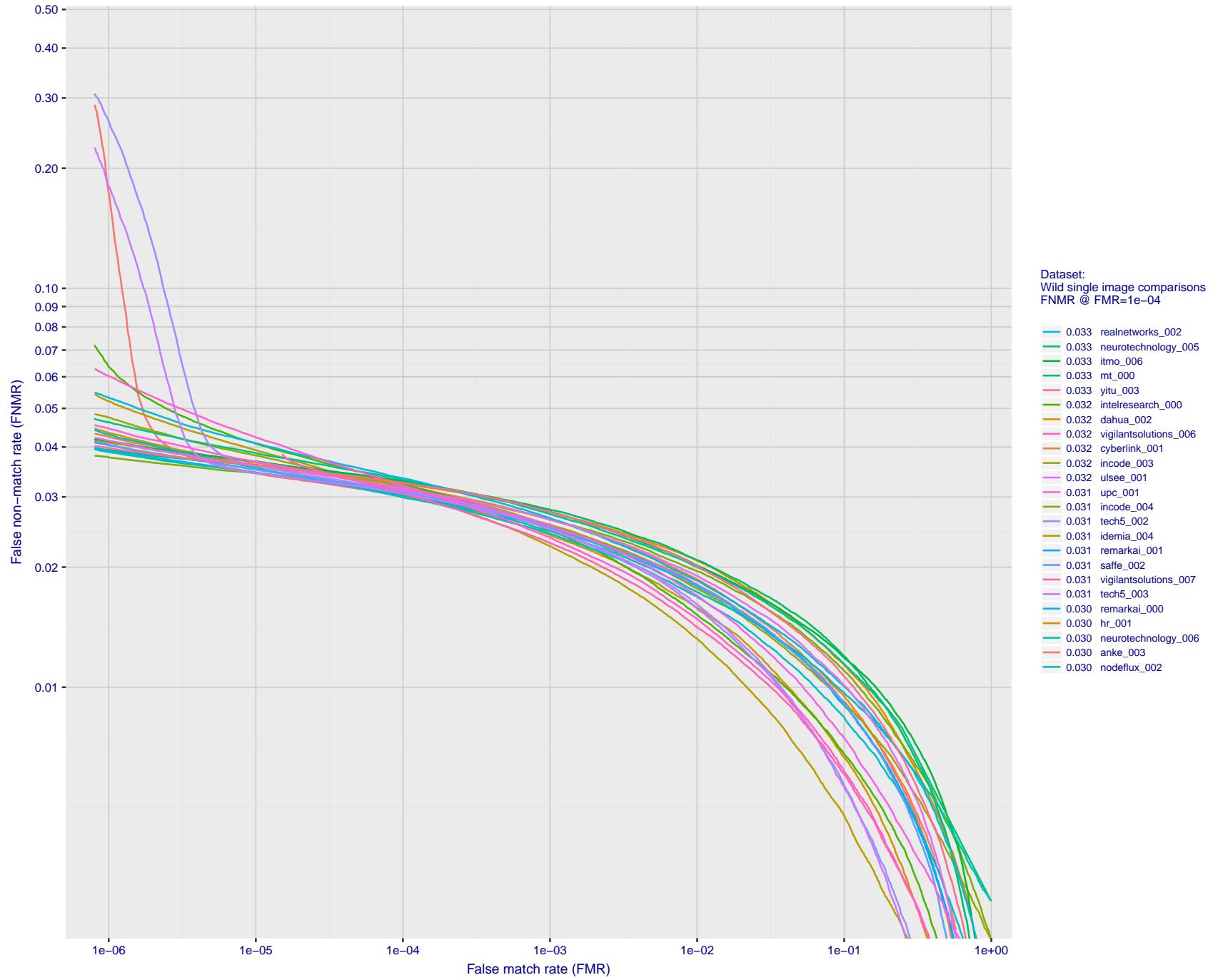


Figure 29: For the 2018 wild image comparisons, detection error tradeoff (DET) characteristics showing false non-match rate vs. false match rate plotted parametrically on threshold, T . The scales are logarithmic in order to show several decades of FMR.

2019/09/11 14:58:19

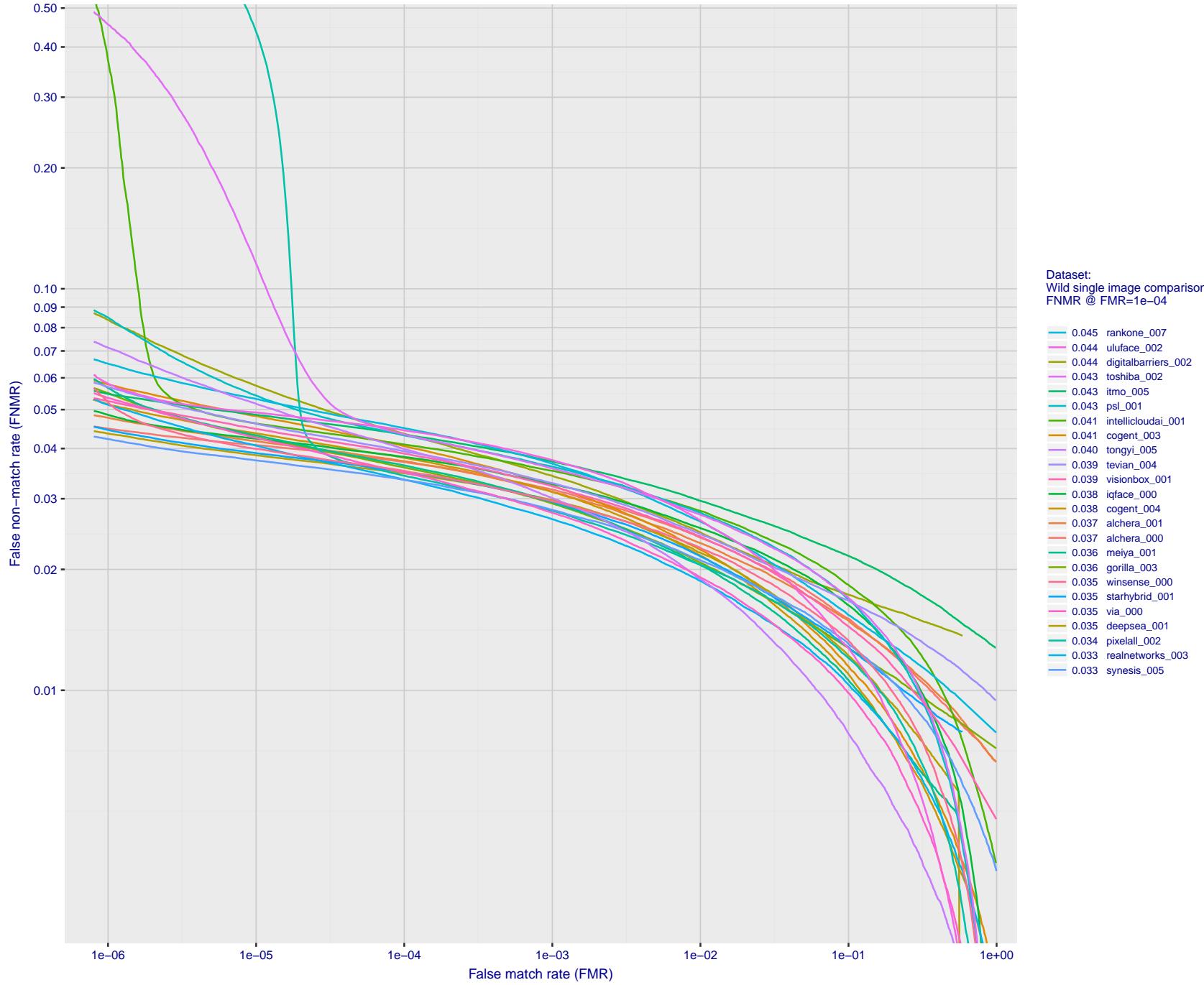


Figure 30: For the 2018 wild image comparisons, detection error tradeoff (DET) characteristics showing false non-match rate vs. false match rate plotted parametrically on threshold, T . The scales are logarithmic in order to show several decades of FMR.

2019/09/11 14:58:19

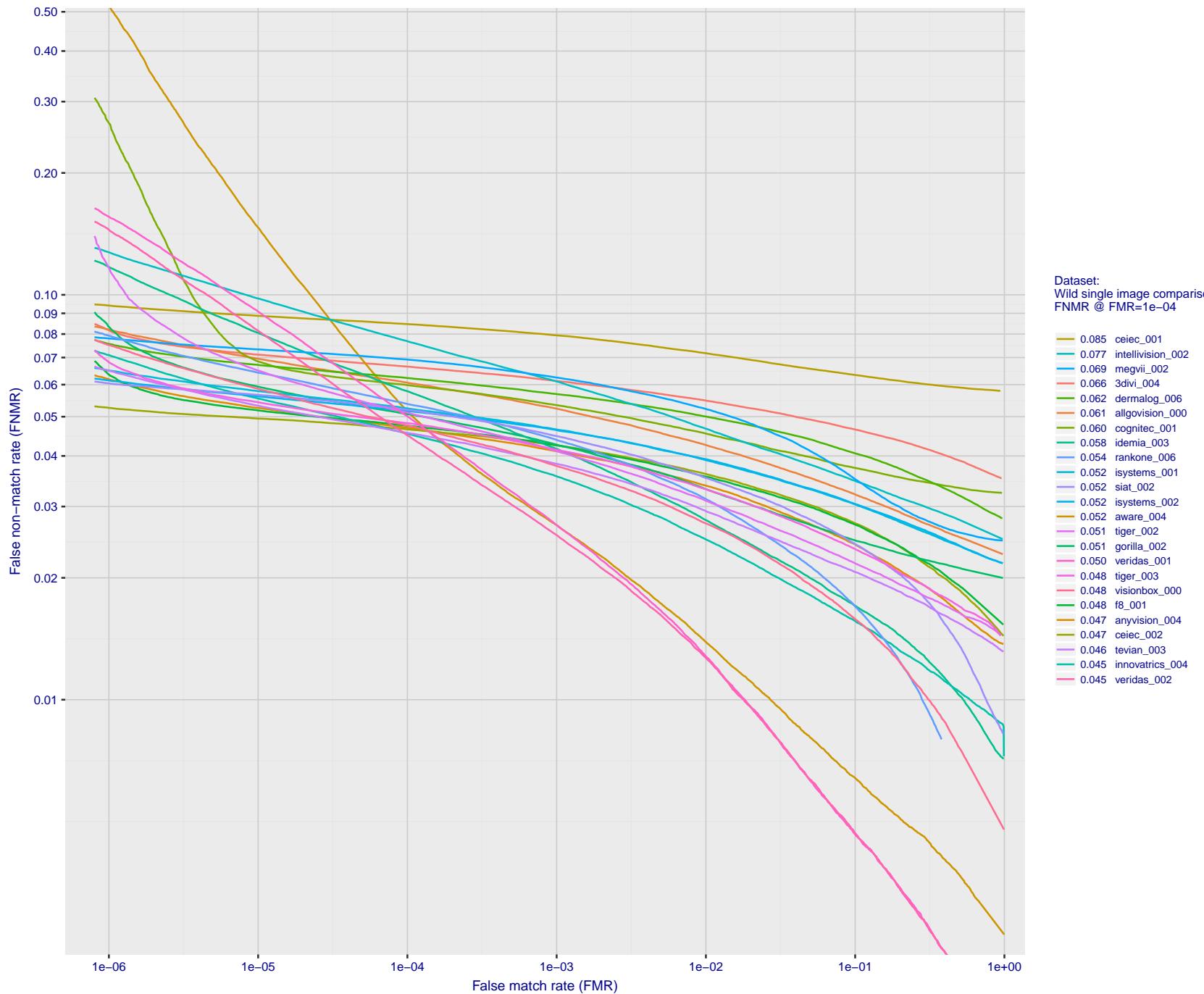


Figure 31: For the 2018 wild image comparisons, detection error tradeoff (DET) characteristics showing false non-match rate vs. false match rate plotted parametrically on threshold, T . The scales are logarithmic in order to show several decades of FMR.

FNMR(T)"False non-match rate"
"False match rate"

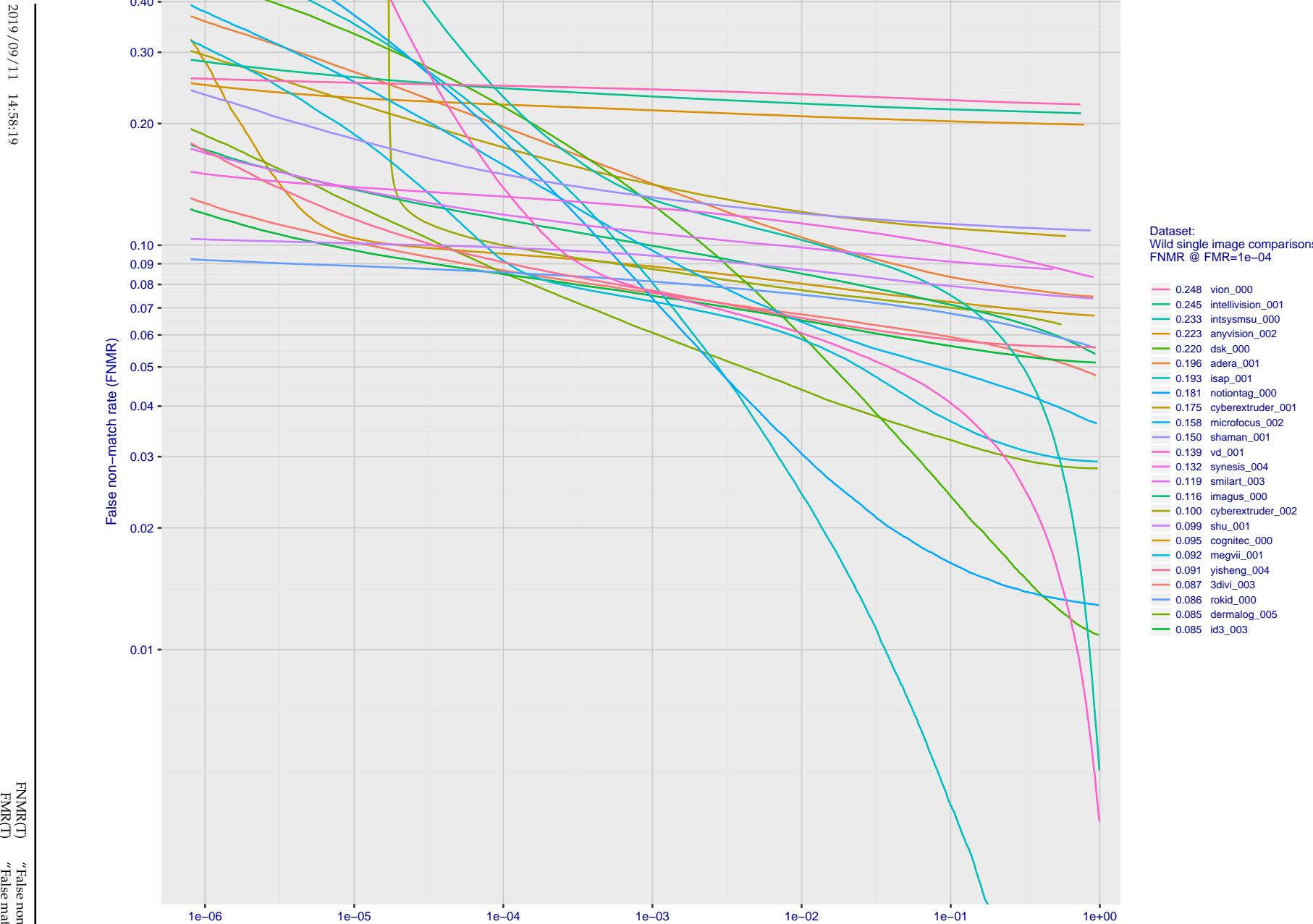


Figure 32: For the 2018 wild image comparisons, detection error tradeoff (DET) characteristics showing false non-match rate vs. false match rate plotted parametrically on threshold, T. The scales are logarithmic in order to show several decades of FMR.

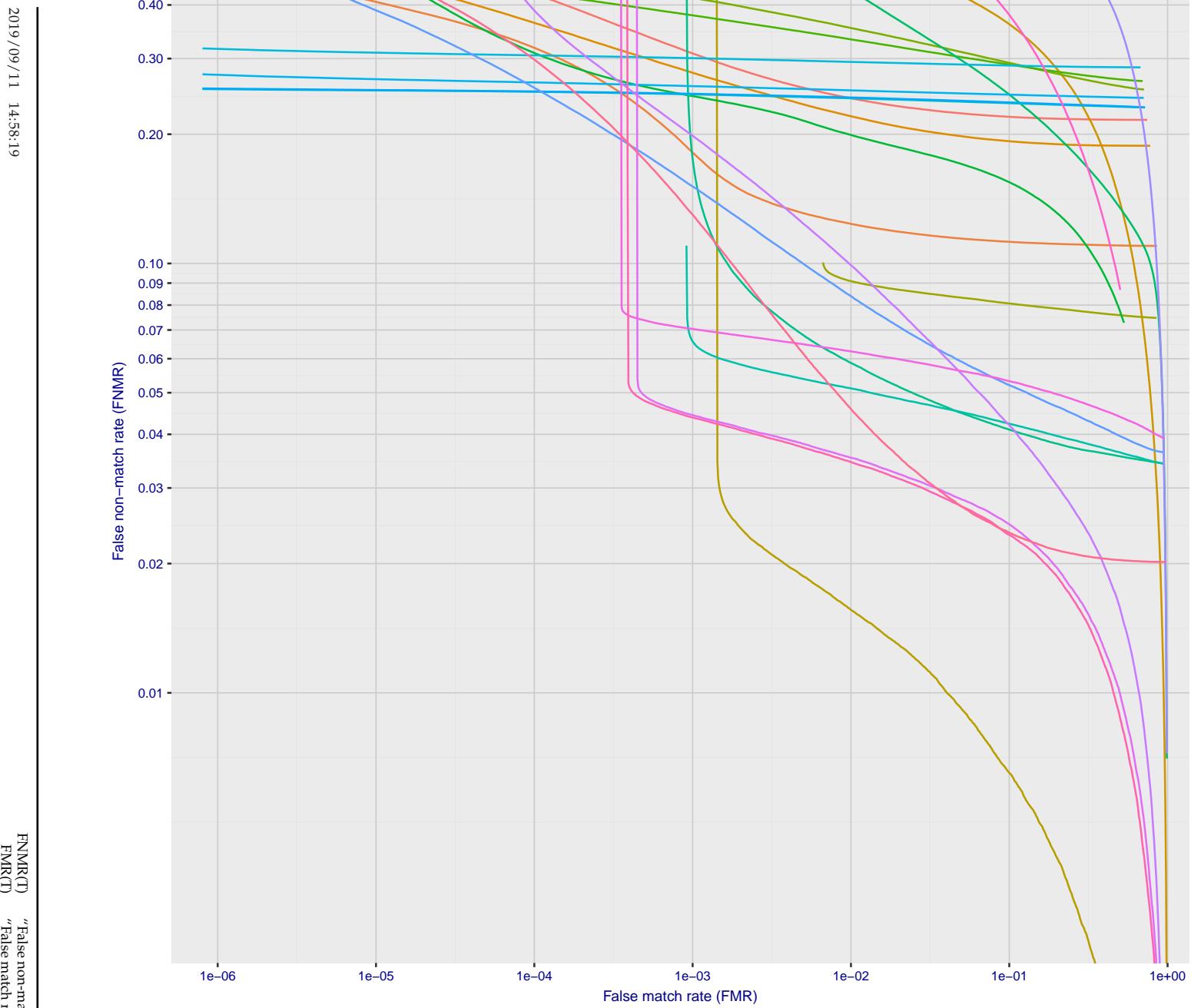


Figure 33: For the 2018 wild image comparisons, detection error tradeoff (DET) characteristics showing false non-match rate vs. false match rate plotted parametrically on threshold, T . The scales are logarithmic in order to show several decades of FMR.

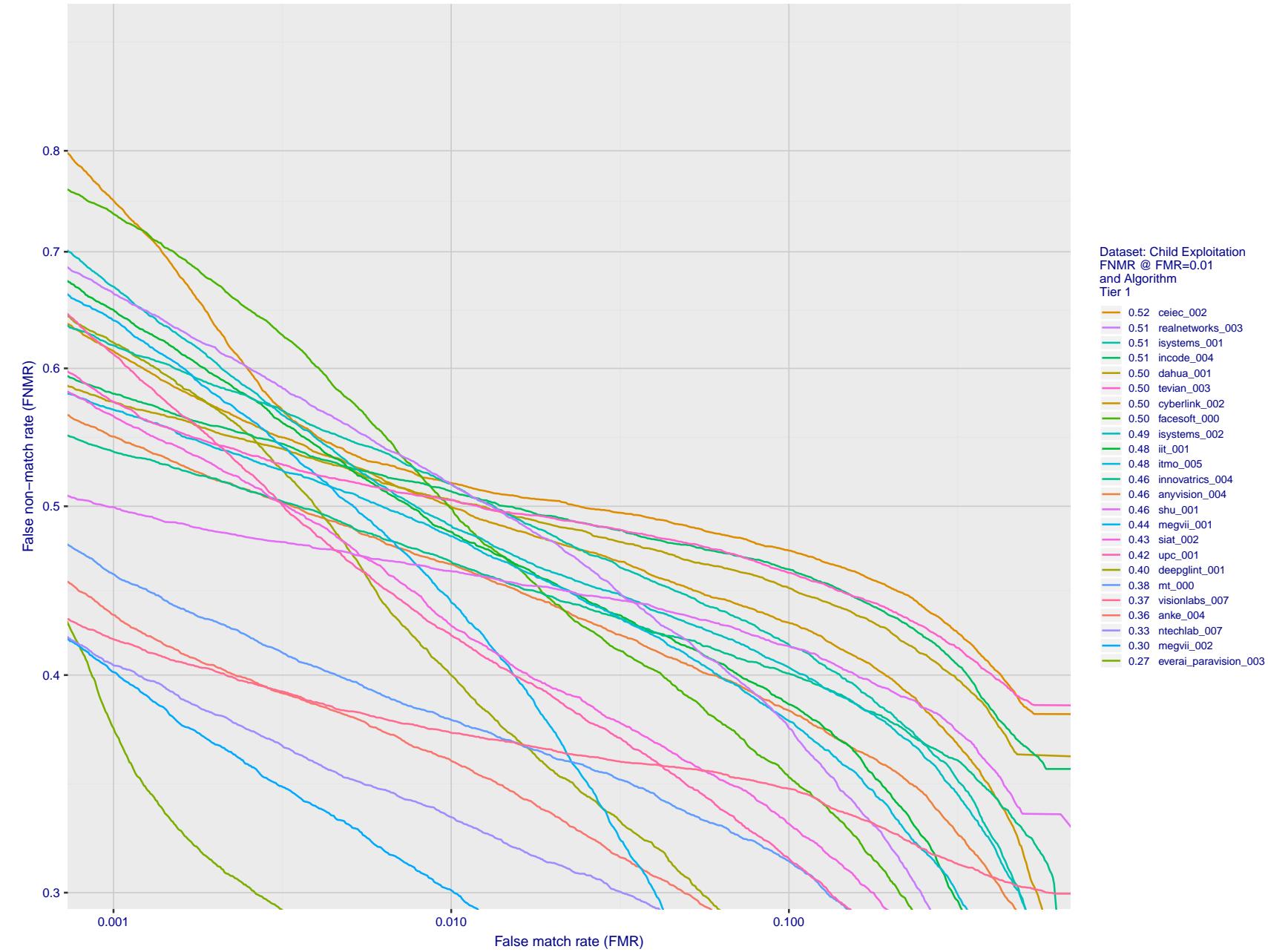


Figure 34: For child exploitation images, detection error tradeoff (DET) characteristics showing false non-match rate vs. false match rate plotted parametrically on threshold, T. The scales are logarithmic in order to show many decades of FMR. Accuracy is poor because many images have adverse quality characteristics, and because detection and enrollment fails.

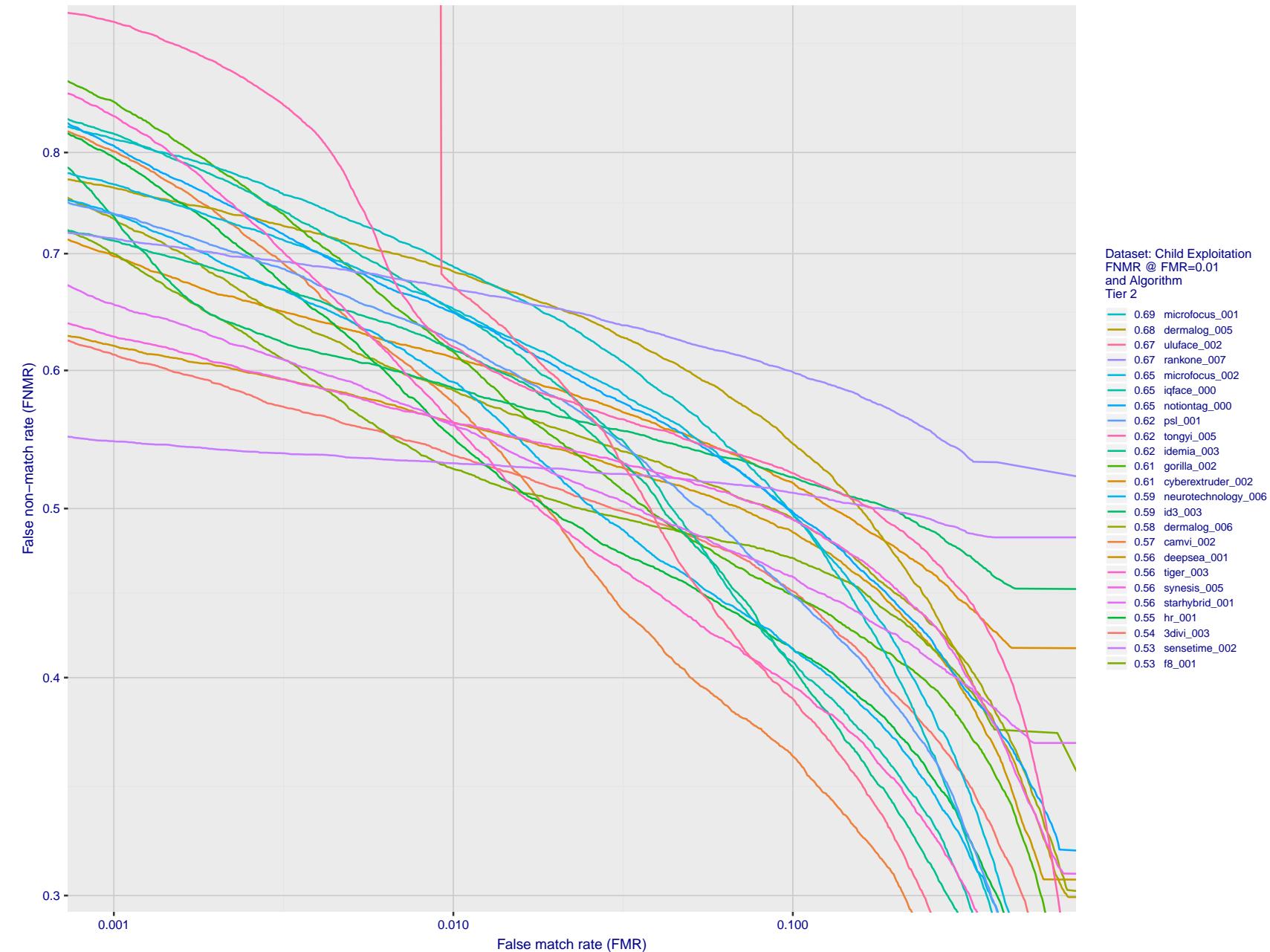


Figure 35: For child exploitation images, detection error tradeoff (DET) characteristics showing false non-match rate vs. false match rate plotted parametrically on threshold, T. The scales are logarithmic in order to show many decades of FMR. Accuracy is poor because many images have adverse quality characteristics, and because detection and enrollment fails.

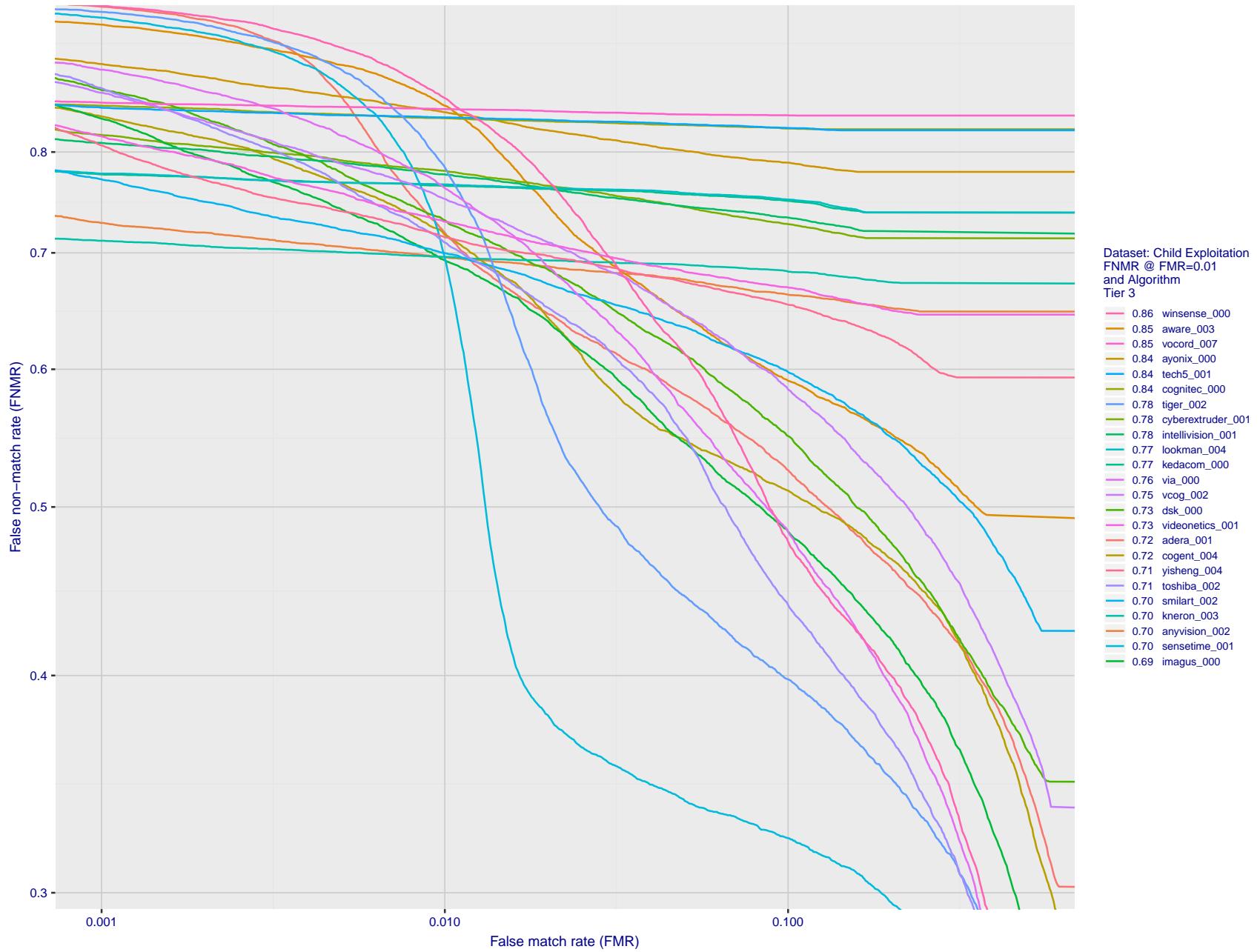


Figure 36: For child exploitation images, detection error tradeoff (DET) characteristics showing false non-match rate vs. false match rate plotted parametrically on threshold, T . The scales are logarithmic in order to show many decades of FMR. Accuracy is poor because many images have adverse quality characteristics, and because detection and enrollment fails.

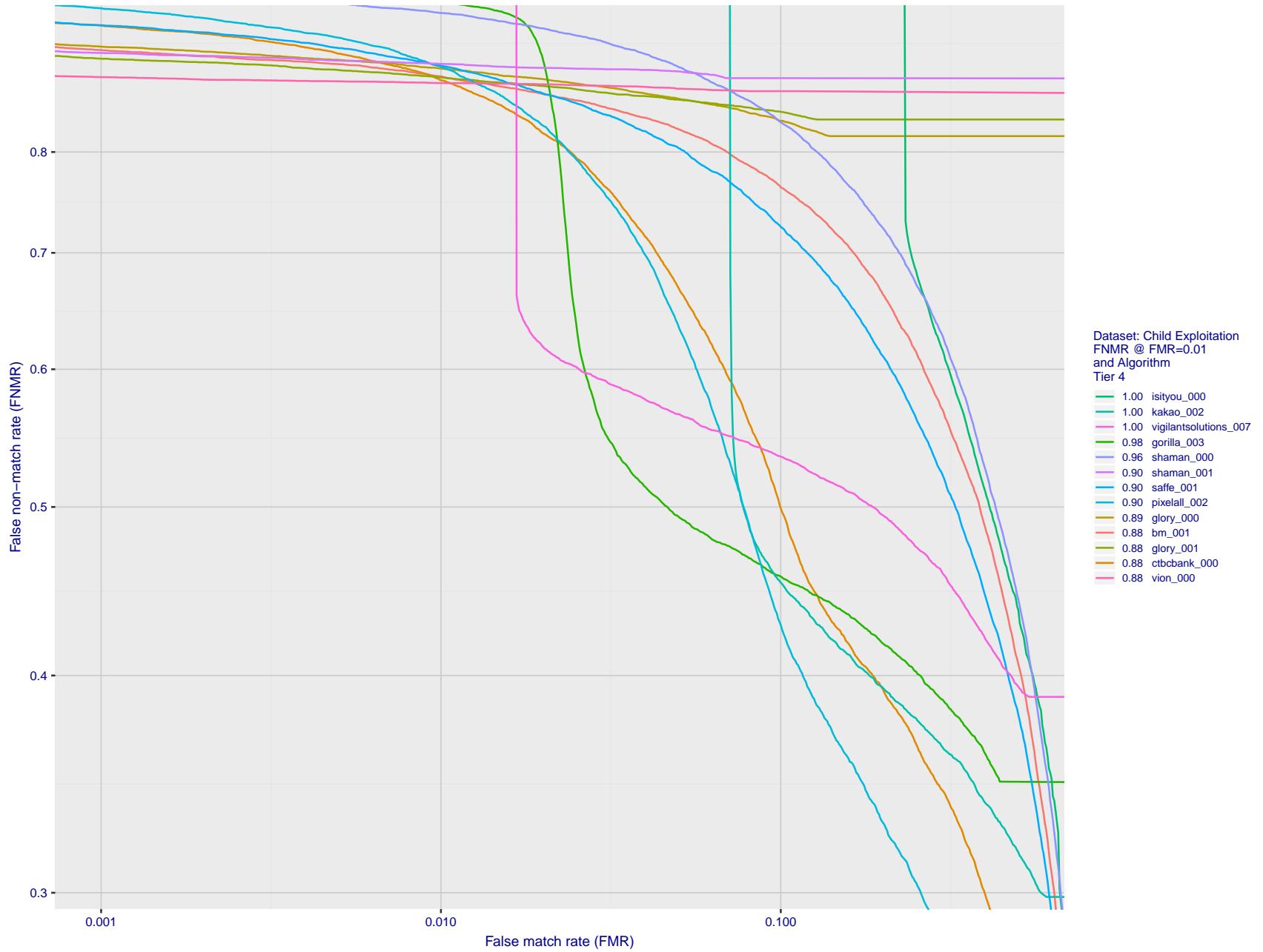


Figure 37: For child exploitation images, detection error tradeoff (DET) characteristics showing false non-match rate vs. false match rate plotted parametrically on threshold, T . The scales are logarithmic in order to show many decades of FMR. Accuracy is poor because many images have adverse quality characteristics, and because detection and enrollment fails.

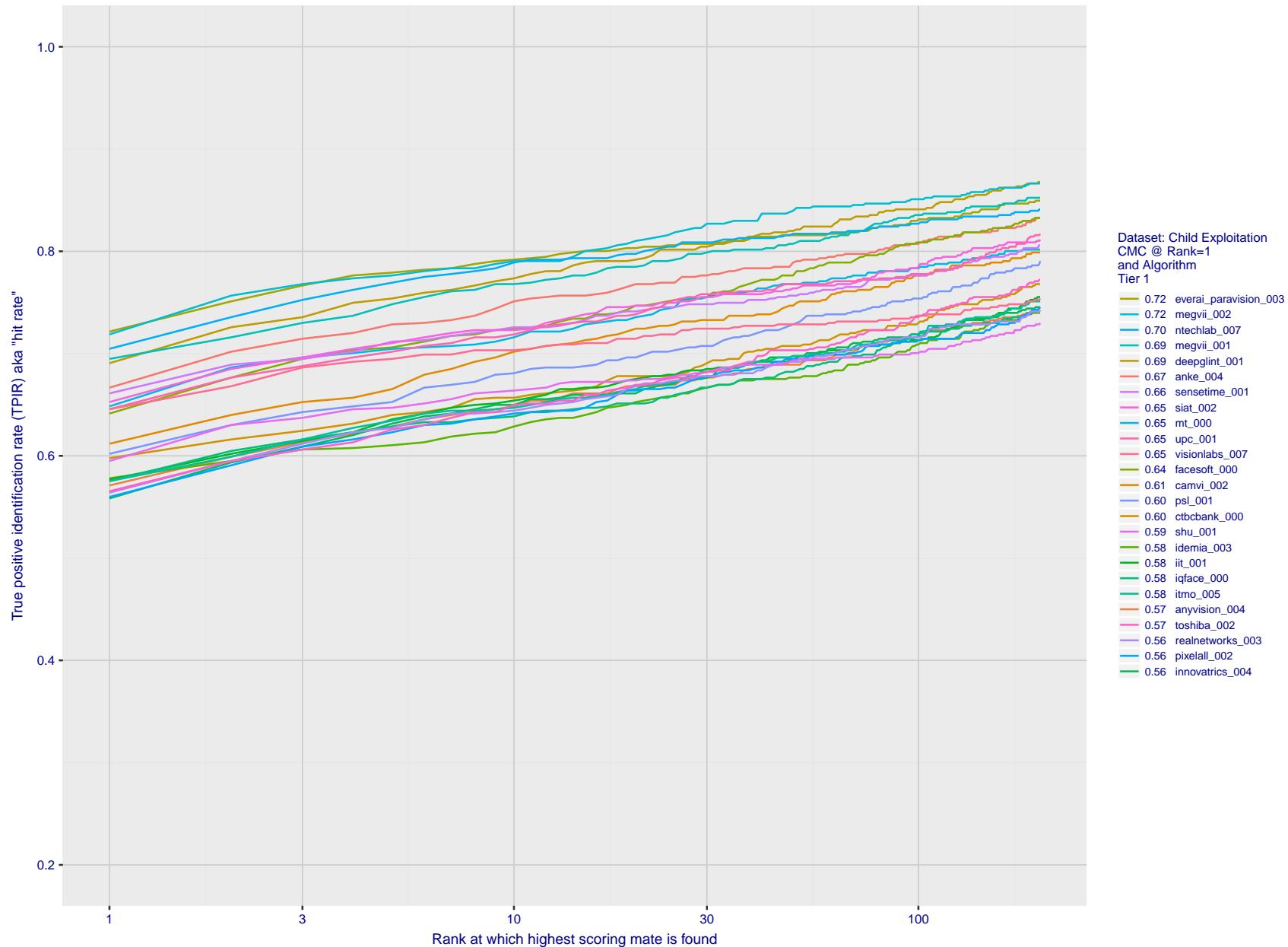


Figure 38: For child exploitation images, cumulative match characteristics (CMC) showing true positive identification rate vs. rank. This is simulation of a one-to-many search experiment - see discussion in section 3.2. The scales are logarithmic in order to show the effect of long candidate lists. Accuracy is poor but much improved relative to the 1:1 DETs of Fig. 37 because a search can succeed if any of a subject's several enrolled images matches the search image with a high score.

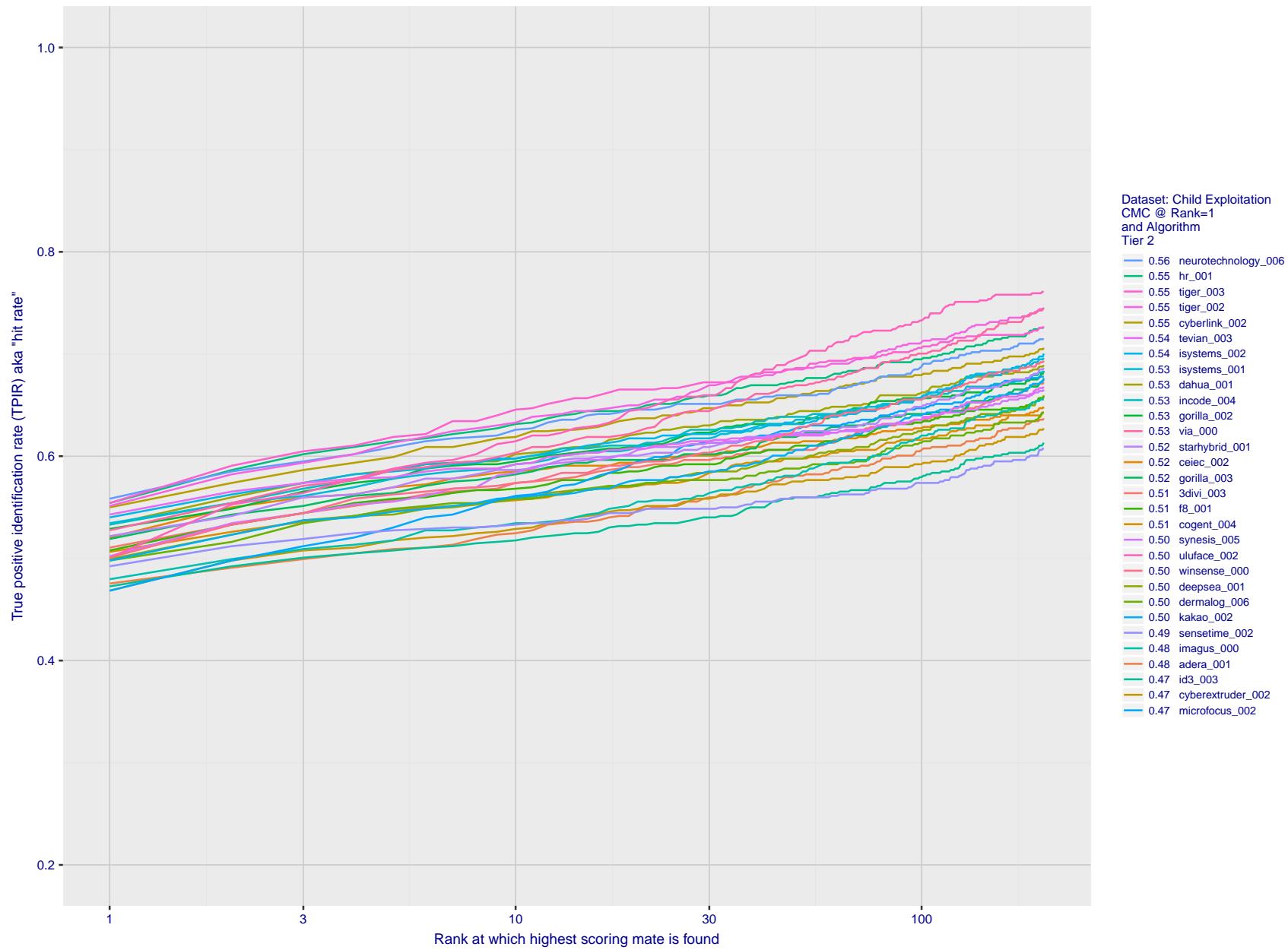


Figure 39: For child exploitation images, cumulative match characteristics (CMC) showing true positive identification rate vs. rank. This is simulation of a one-to-many search experiment - see discussion in section 3.2. The scales are logarithmic in order to show the effect of long candidate lists. Accuracy is poor but much improved relative to the 1:1 DETs of Fig. 37 because a search can succeed if any of a subject's several enrolled images matches the search image with a high score.

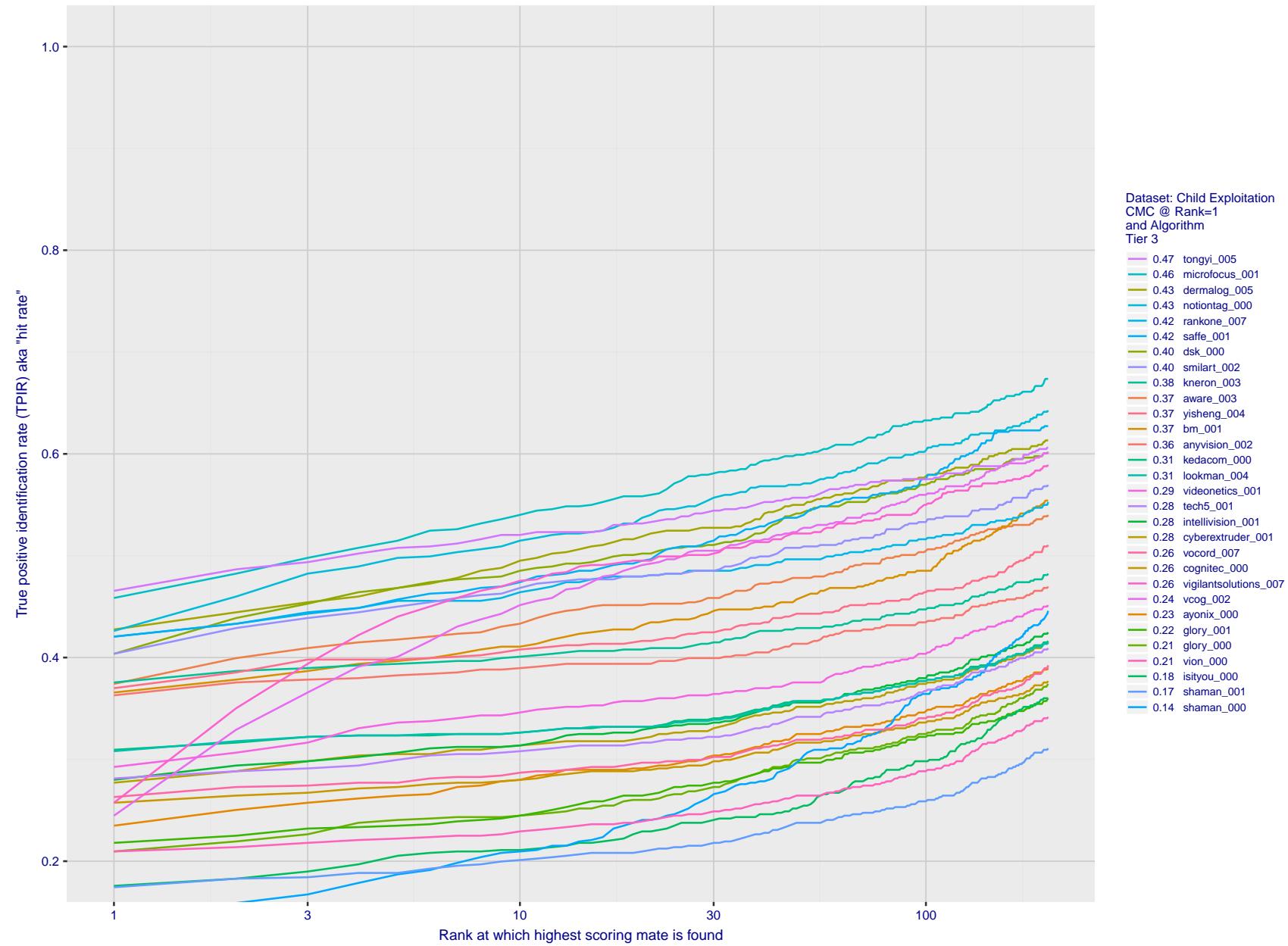


Figure 40: For child exploitation images, cumulative match characteristics (CMC) showing true positive identification rate vs. rank. This is simulation of a one-to-many search experiment - see discussion in section 3.2. The scales are logarithmic in order to show the effect of long candidate lists. Accuracy is poor but much improved relative to the 1:1 DETs of Fig. 37 because a search can succeed if any of a subject's several enrolled images matches the search image with a high score.

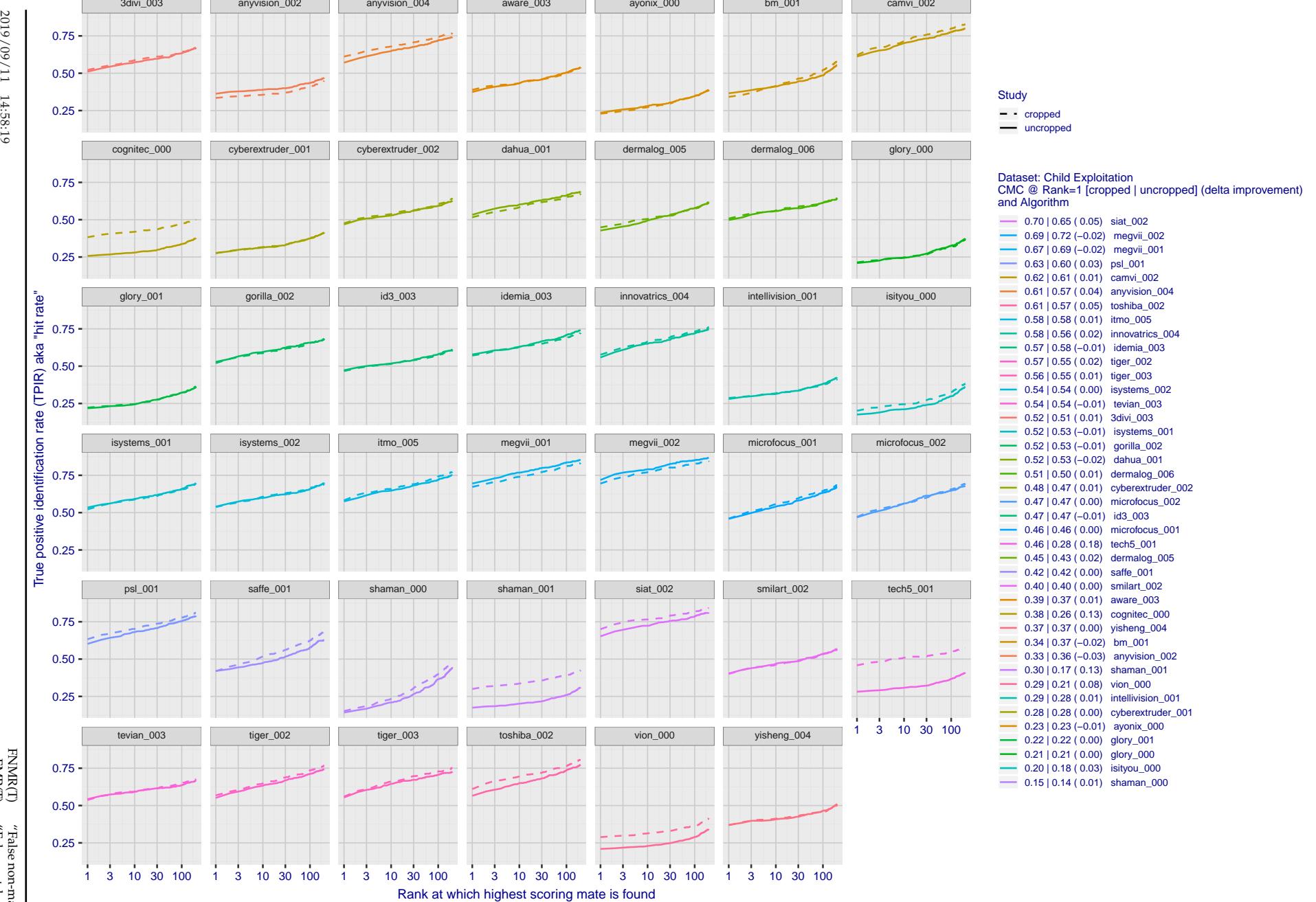


Figure 41: For child exploitation images, cumulative match characteristics (CMC) showing true positive identification rate vs. rank for two cases: 1. Whole image provided to the algorithm; 2. Human annotated rectangular region, cropped and provided to the algorithm. The difference between the traces is associated with detection of difficult faces, and fine localization.

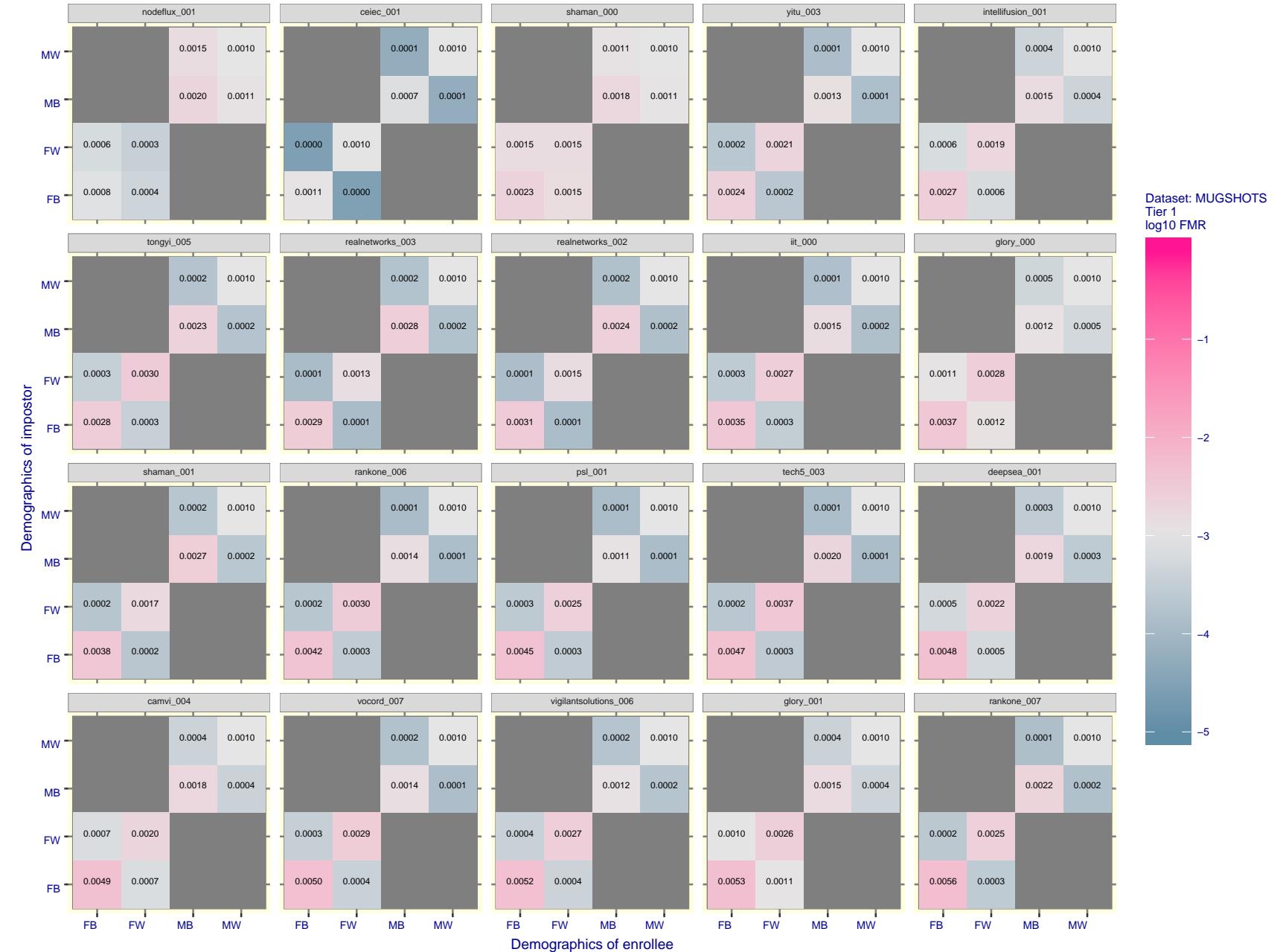


Figure 42: For the mugshot images, FMR for same-sex impostor pairs of images annotated with codes for black female, black male, white female, white male. The threshold is set for each algorithm to give $FMR = 0.001$ for white males which is the demographic that usually gives the lowest FMR. This means the top right box is the same color in all panels. The panels are sorted over multiple pages in order of FMR on black females, which is the demographic that usually gives the highest FMR.

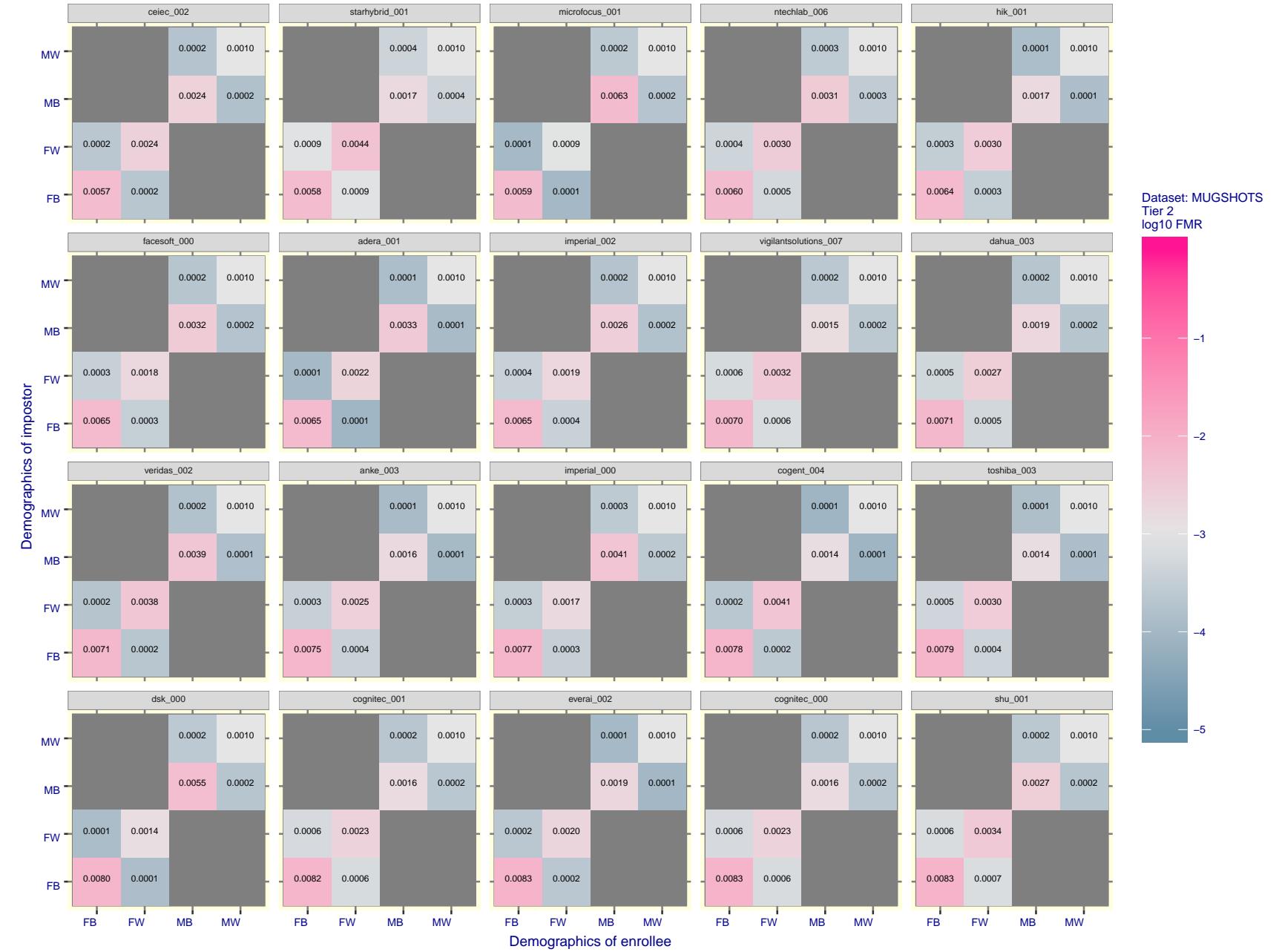


Figure 43: For the mugshot images, FMR for same-sex impostor pairs of images annotated with codes for black female, black male, white female, white male. The threshold is set for each algorithm to give FMR = 0.001 for white males which is the demographic that usually gives the lowest FMR. This means the top right box is the same color in all panels. The panels are sorted over multiple pages in order of FMR on black females, which is the demographic that usually gives the highest FMR.

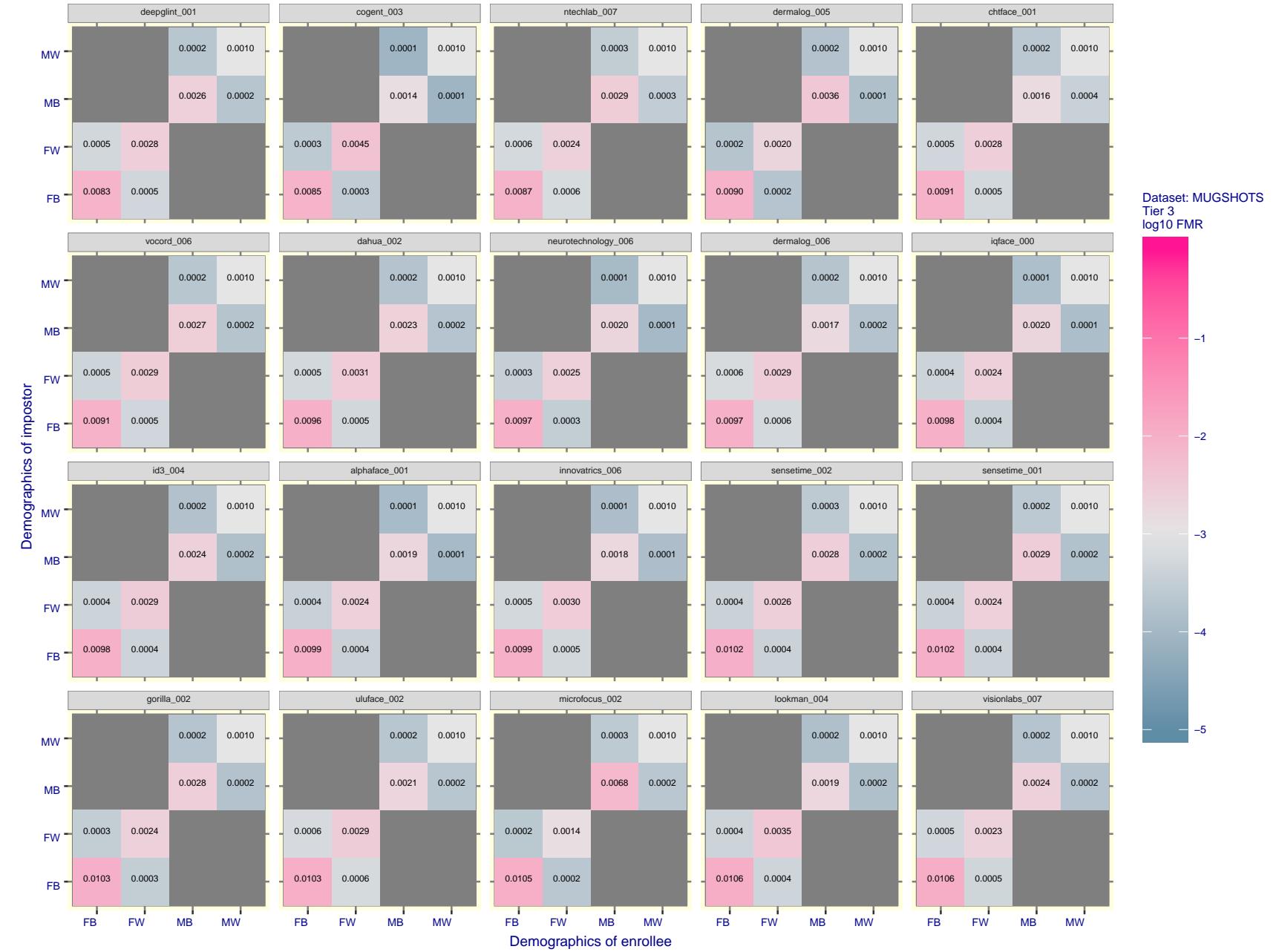


Figure 44: For the mugshot images, FMR for same-sex impostor pairs of images annotated with codes for black female, black male, white female, white male. The threshold is set for each algorithm to give $FMR = 0.001$ for white males which is the demographic that usually gives the lowest FMR. This means the top right box is the same color in all panels. The panels are sorted over multiple pages in order of FMR on black females, which is the demographic that usually gives the highest FMR.

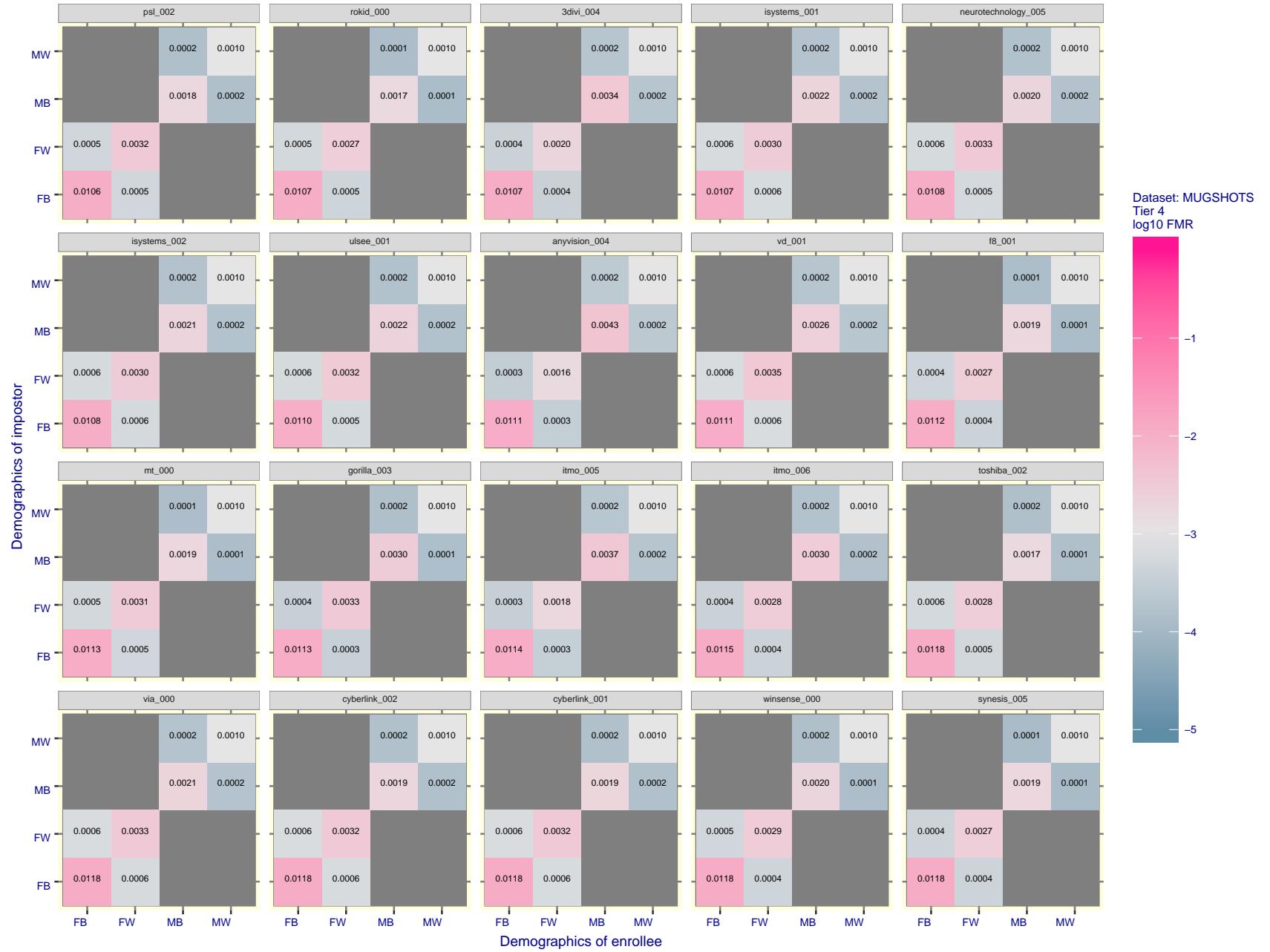


Figure 45: For the mugshot images, FMR for same-sex impostor pairs of images annotated with codes for black female, black male, white female, white male. The threshold is set for each algorithm to give $FMR = 0.001$ for white males which is the demographic that usually gives the lowest FMR. This means the top right box is the same color in all panels. The panels are sorted over multiple pages in order of FMR on black females, which is the demographic that usually gives the highest FMR.

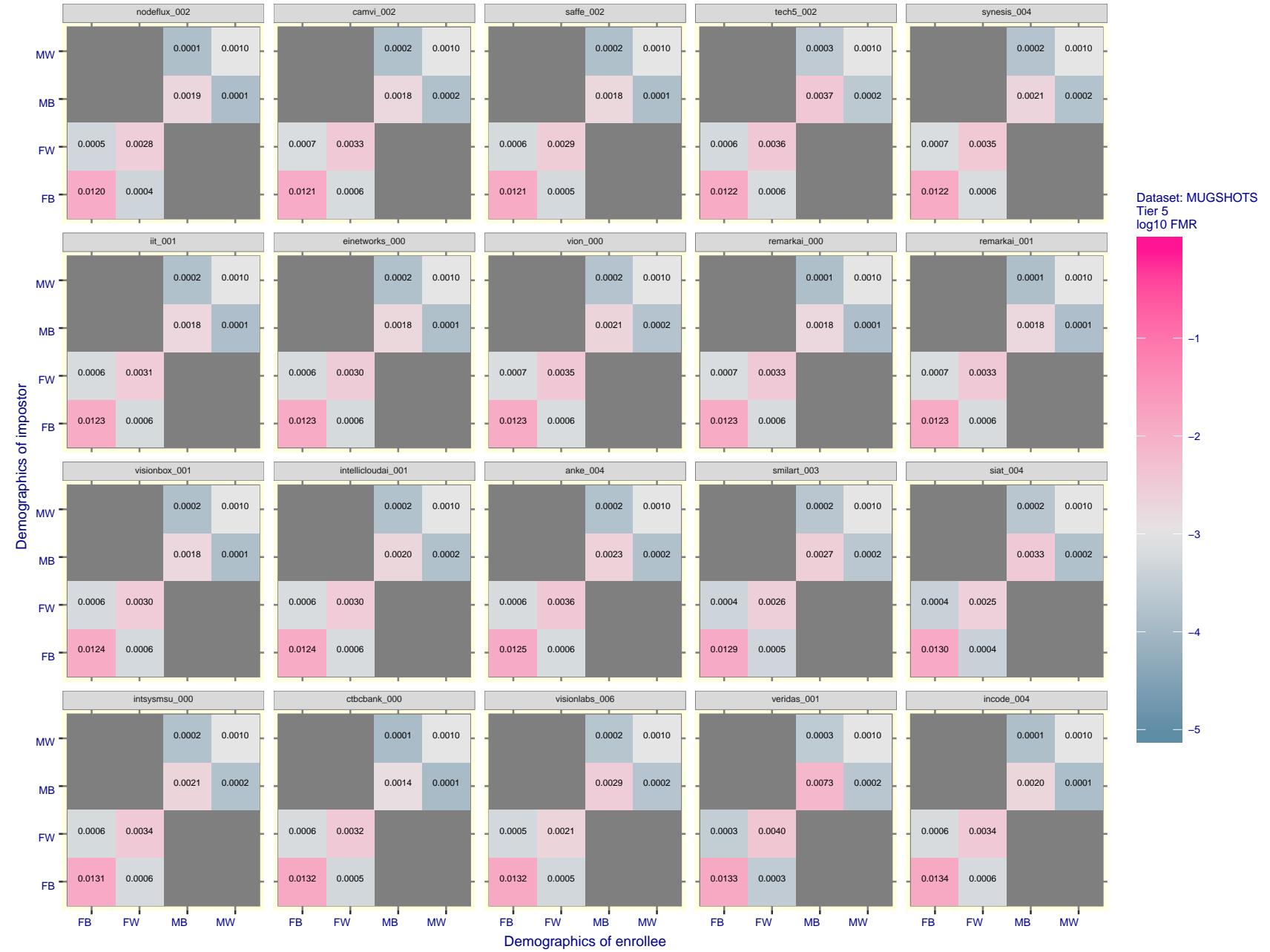


Figure 46: For the mugshot images, FMR for same-sex impostor pairs of images annotated with codes for black female, black male, white female, white male. The threshold is set for each algorithm to give $FMR = 0.001$ for white males which is the demographic that usually gives the lowest FMR. This means the top right box is the same color in all panels. The panels are sorted over multiple pages in order of FMR on black females, which is the demographic that usually gives the highest FMR.

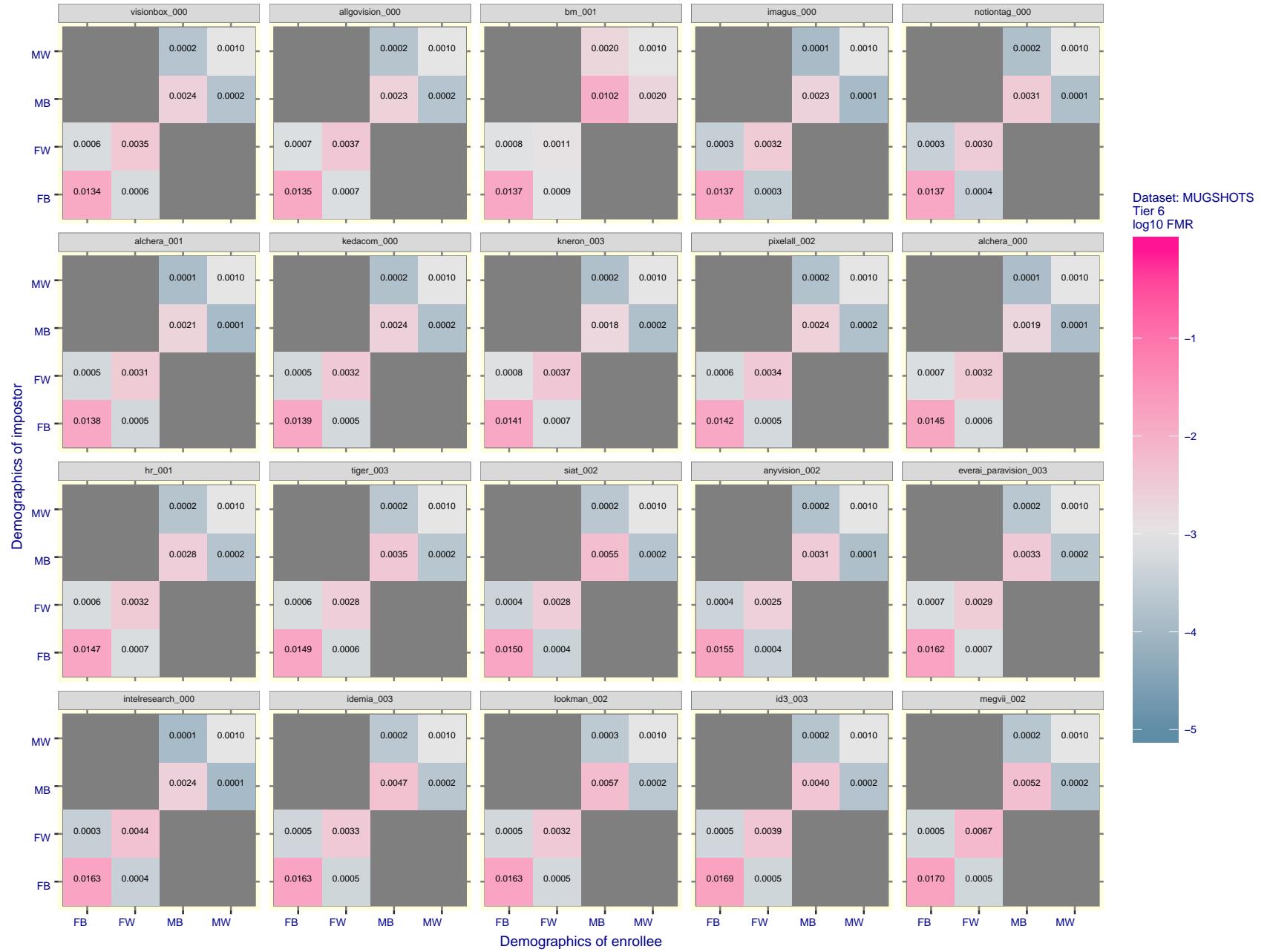


Figure 47: For the mugshot images, FMR for same-sex impostor pairs of images annotated with codes for black female, black male, white female, white male. The threshold is set for each algorithm to give $FMR = 0.001$ for white males which is the demographic that usually gives the lowest FMR. This means the top right box is the same color in all panels. The panels are sorted over multiple pages in order of FMR on black females, which is the demographic that usually gives the highest FMR.

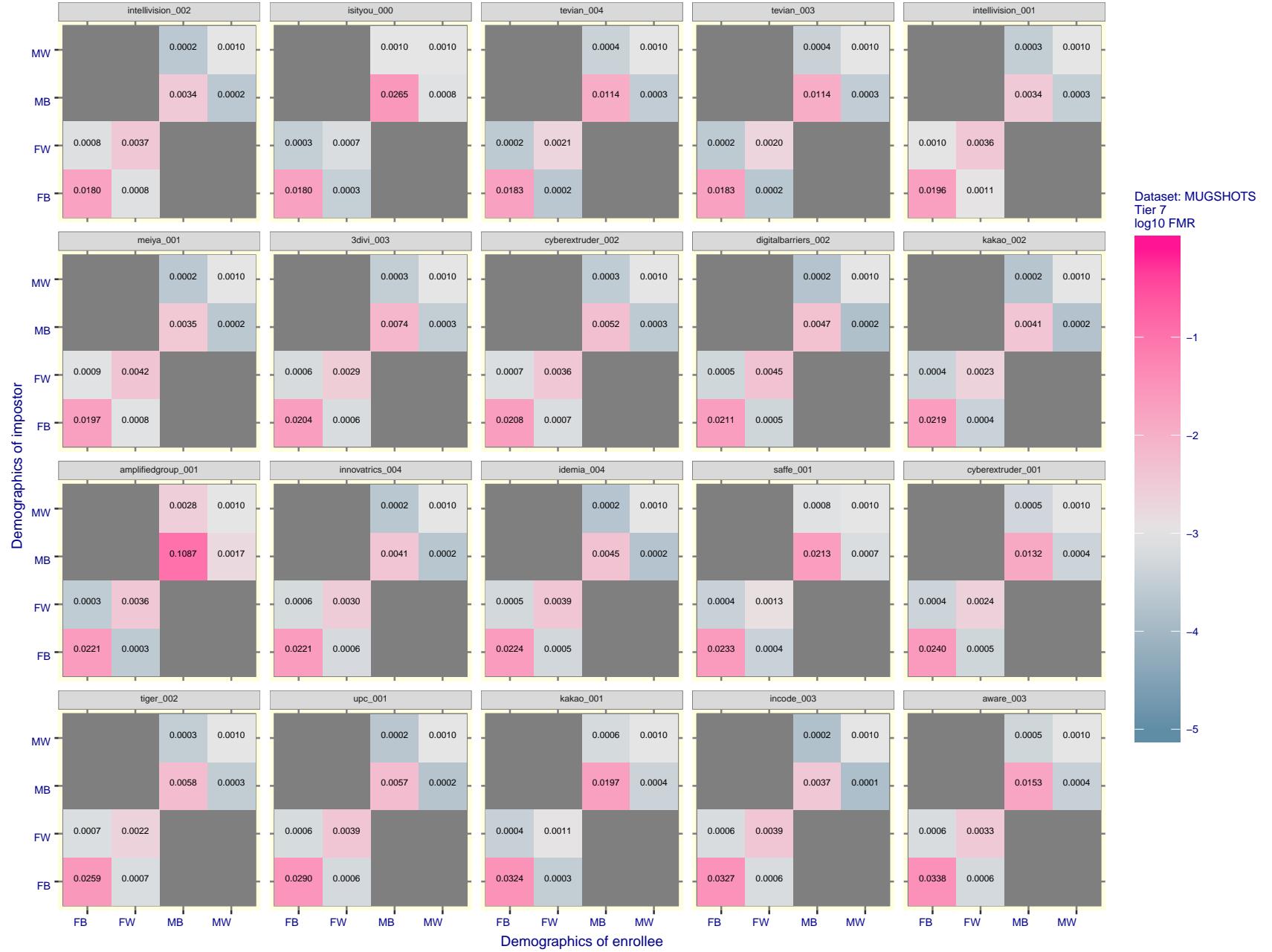


Figure 48: For the mugshot images, FMR for same-sex impostor pairs of images annotated with codes for black female, black male, white female, white male. The threshold is set for each algorithm to give $FMR = 0.001$ for white males which is the demographic that usually gives the lowest FMR. This means the top right box is the same color in all panels. The panels are sorted over multiple pages in order of FMR on black females, which is the demographic that usually gives the highest FMR.

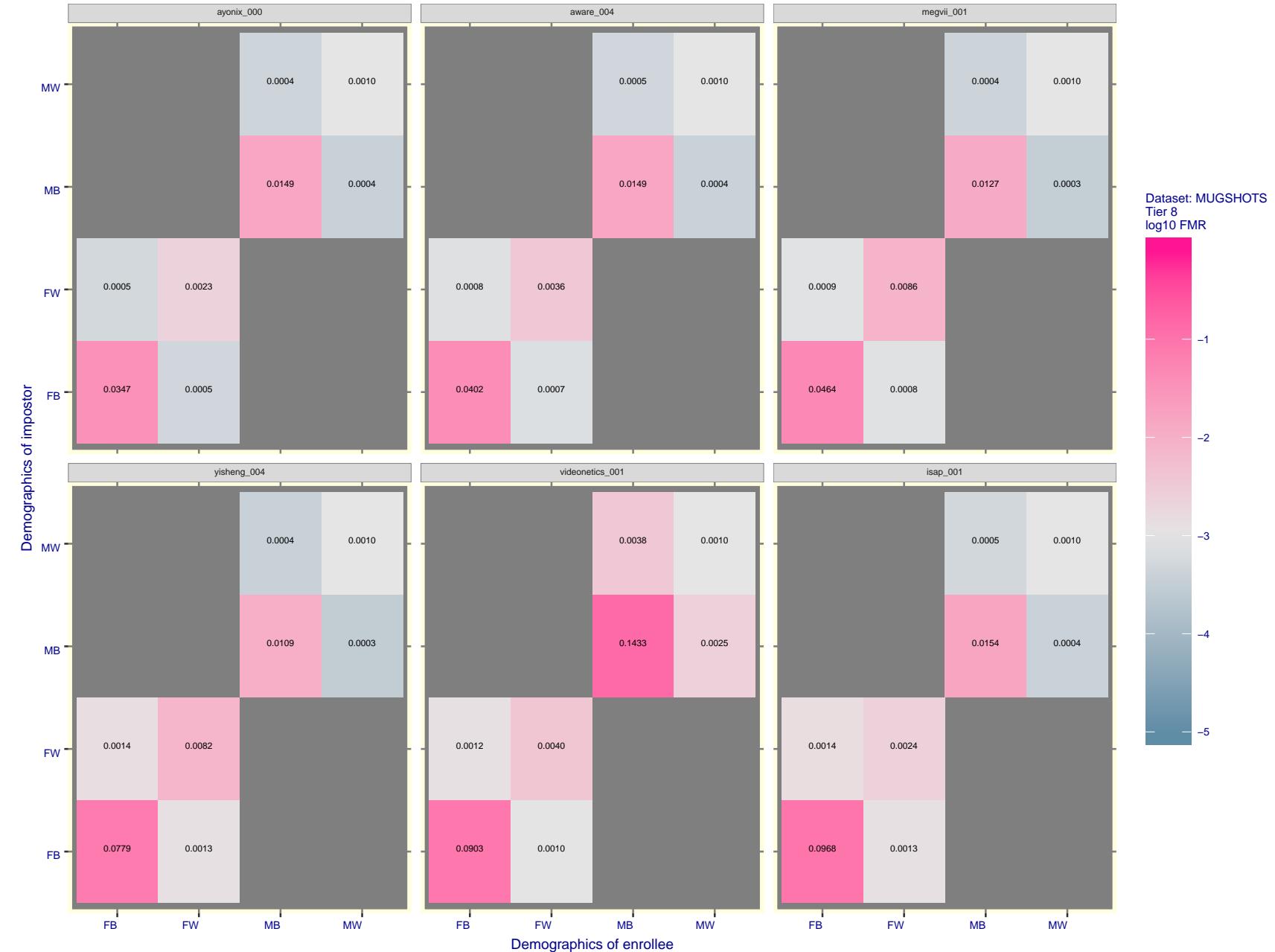


Figure 49: For the mugshot images, FMR for same-sex impostor pairs of images annotated with codes for black female, black male, white female, white male. The threshold is set for each algorithm to give $\text{FMR} = 0.001$ for white males which is the demographic that usually gives the lowest FMR. This means the top right box is the same color in all panels. The panels are sorted over multiple pages in order of FMR on black females, which is the demographic that usually gives the highest FMR.

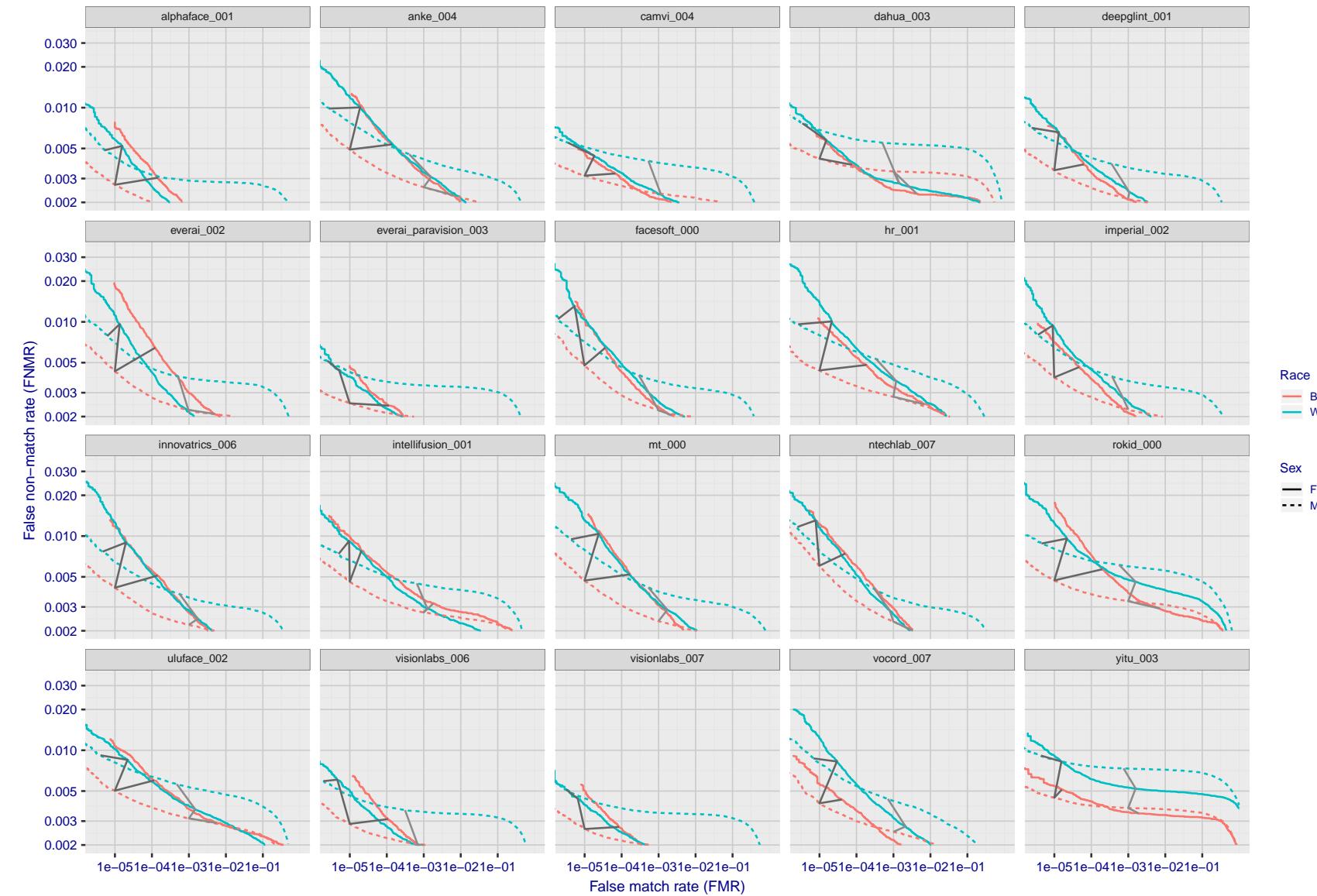


Figure 50: For the mugshot images, error tradeoff characteristics for white females, black females, black males and white males. The Z-shaped grey lines correspond to fixed thresholds, showing both FNMR and FMR vary at one T value. Note: Many of the plots will naively be read as saying women gives worse error rates than men because the solid traces lie above the dotted ones. However, this is misleading and incomplete: The grey lines show the traces reveal horizontal shifts. Thus for the cogent-003 algorithm FNMR for men is higher than for women at a fixed threshold but, at the same time, FMR is higher for women - see Figure 78. As access control systems almost always operate at a fixed threshold, the naive interpretation is incorrect.

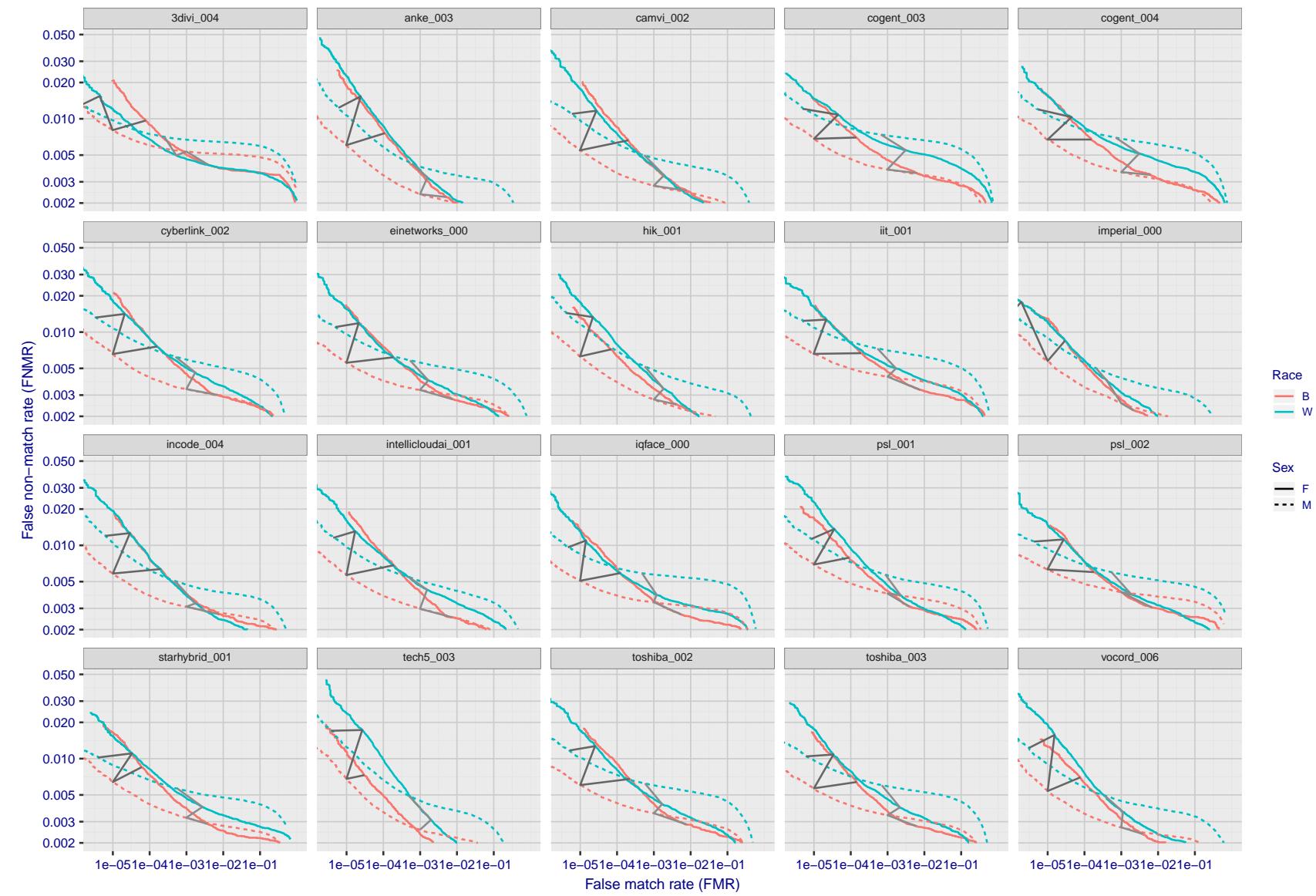


Figure 51: For the mugshot images, error tradeoff characteristics for white females, black females, black males and white males. The Z-shaped grey lines correspond to fixed thresholds, showing both FNMR and FMR vary at one T value. Note: Many of the plots will naively be read as saying women gives worse error rates than men because the solid traces lie above the dotted ones. However, this is misleading and incomplete: The grey lines show the traces reveal horizontal shifts. Thus for the cogen-003 algorithm FNMR for men is higher than for women at a fixed threshold but, at the same time, FMR is higher for women - see Figure 78. As access control systems almost always operate at a fixed threshold, the naive interpretation is incorrect.

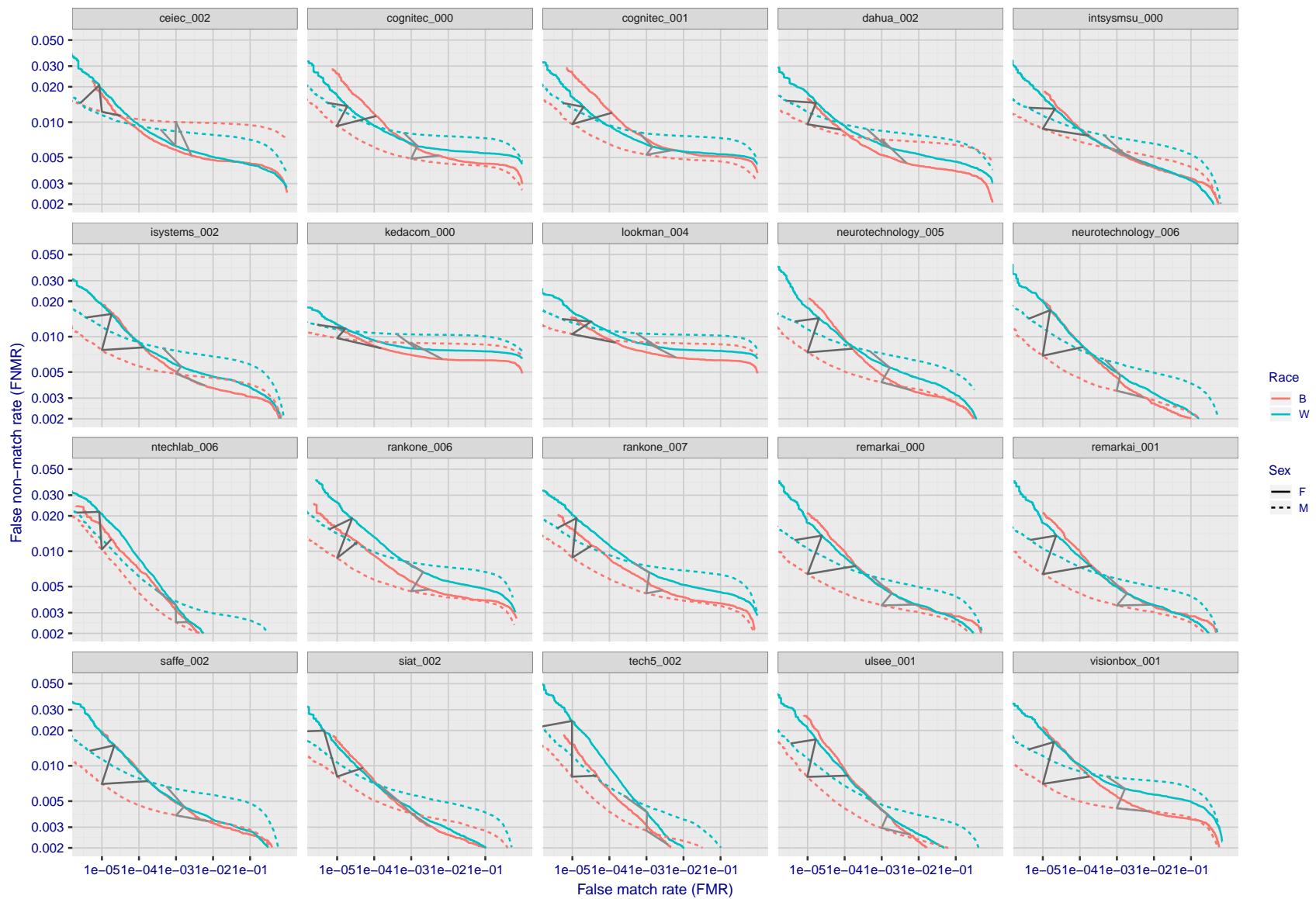


Figure 52: For the mugshot images, error tradeoff characteristics for white females, black females, black males and white males. The Z-shaped grey lines correspond to fixed thresholds, showing both FNMR and FMR vary at one T value. Note: Many of the plots will naively be read as saying women gives worse error rates than men because the solid traces lie above the dotted ones. However, this is misleading and incomplete: The grey lines show the traces reveal horizontal shifts. Thus for the cogent-003 algorithm FNMR for men is higher than for women at a fixed threshold but, at the same time, FMR is higher for women - see Figure 78. As access control systems almost always operate at a fixed threshold, the naive interpretation is incorrect.

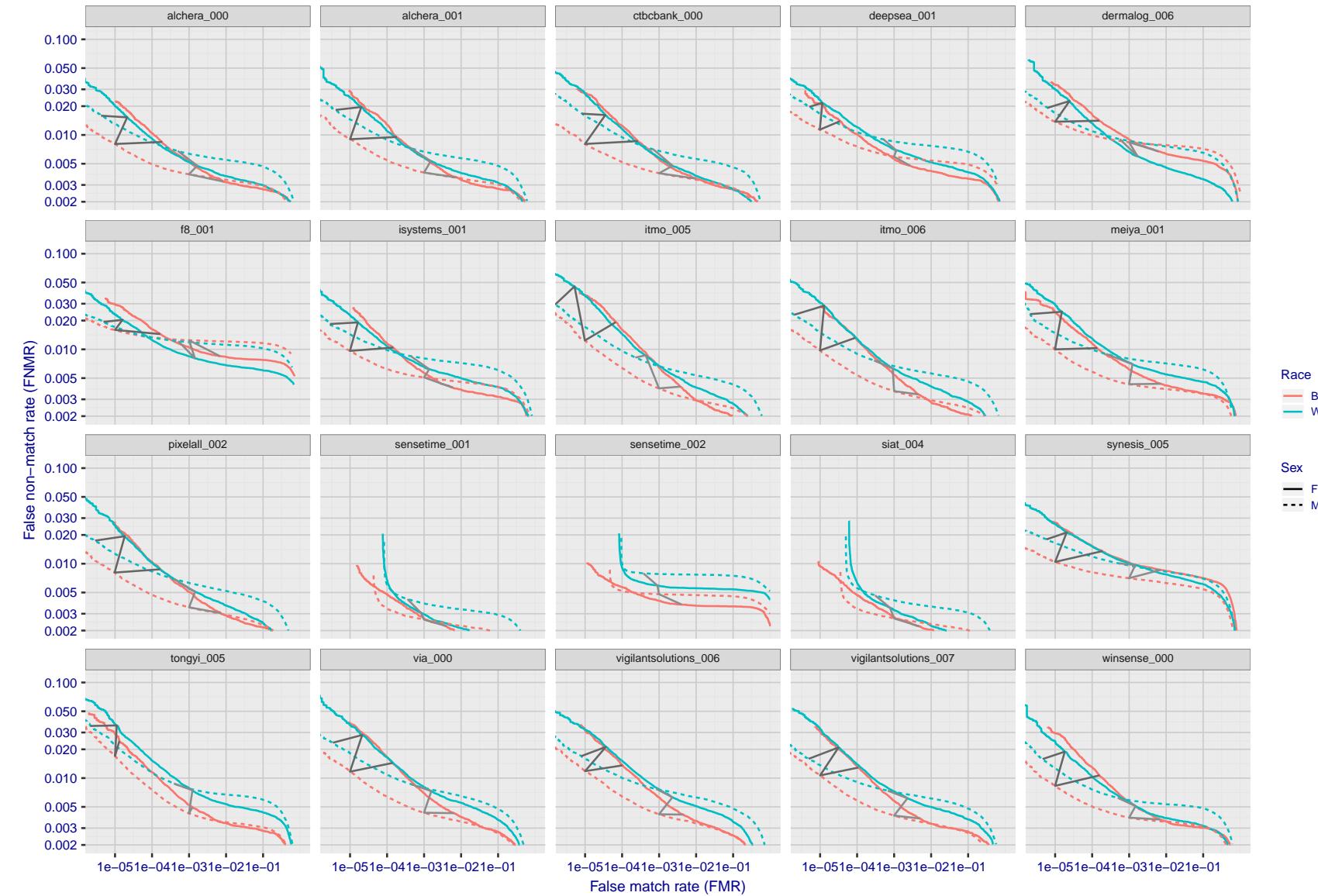


Figure 53: For the mugshot images, error tradeoff characteristics for white females, black females, black males and white males. The Z-shaped grey lines correspond to fixed thresholds, showing both FNMR and FMR vary at one T value. Note: Many of the plots will naively be read as saying women gives worse error rates than men because the solid traces lie above the dotted ones. However, this is misleading and incomplete: The grey lines show the traces reveal horizontal shifts. Thus for the cogent-003 algorithm FNMR for men is higher than for women at a fixed threshold but, at the same time, FMR is higher for women - see Figure 78. As access control systems almost always operate at a fixed threshold, the naive interpretation is incorrect.

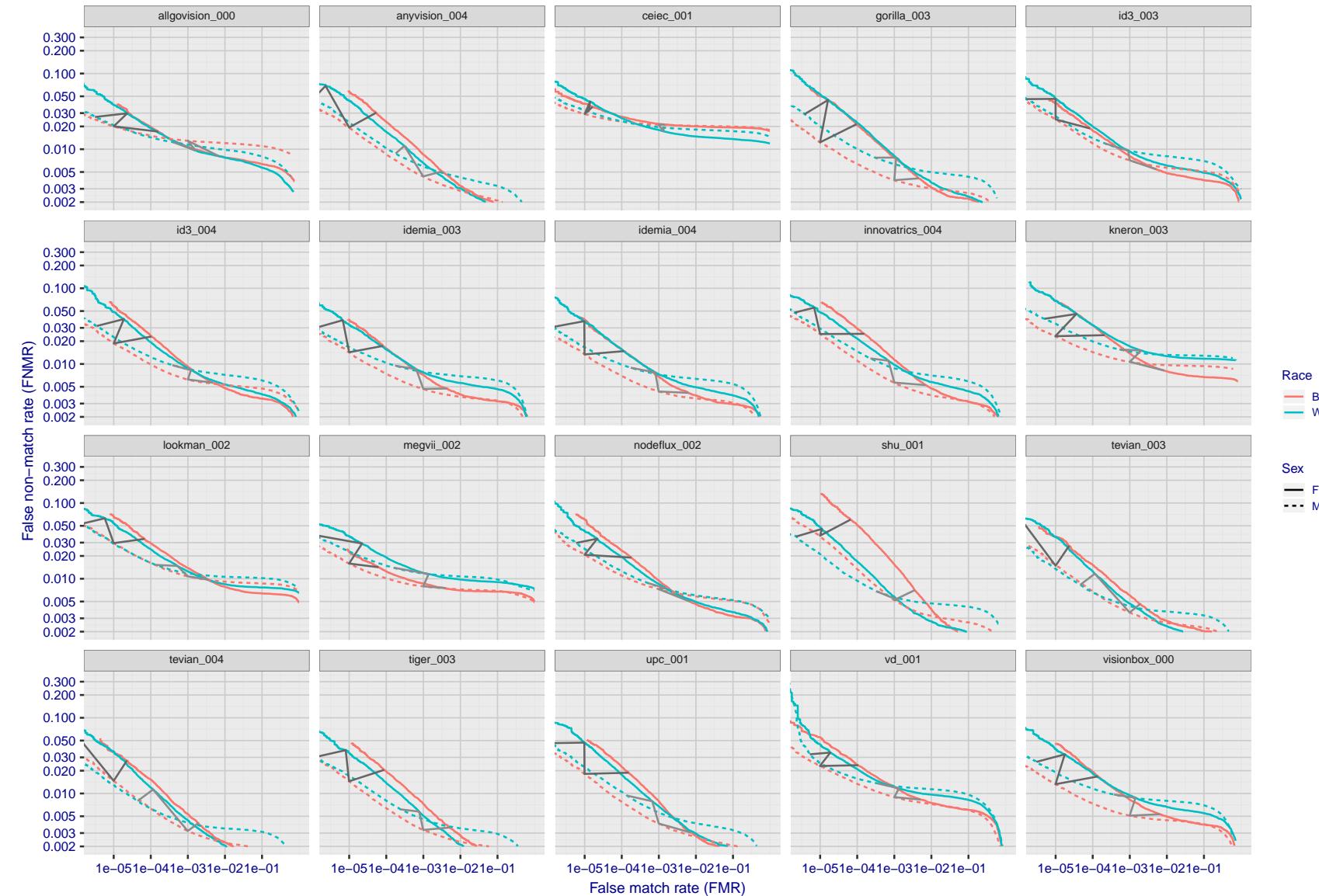


Figure 54: For the mugshot images, error tradeoff characteristics for white females, black females, black males and white males. The Z-shaped grey lines correspond to fixed thresholds, showing both FNMR and FMR vary at one T value. Note: Many of the plots will naively be read as saying women gives worse error rates than men because the solid traces lie above the dotted ones. However, this is misleading and incomplete: The grey lines show the traces reveal horizontal shifts. Thus for the cogent-003 algorithm FNMR for men is higher than for women at a fixed threshold but, at the same time, FMR is higher for women - see Figure 78. As access control systems almost always operate at a fixed threshold, the naive interpretation is incorrect.

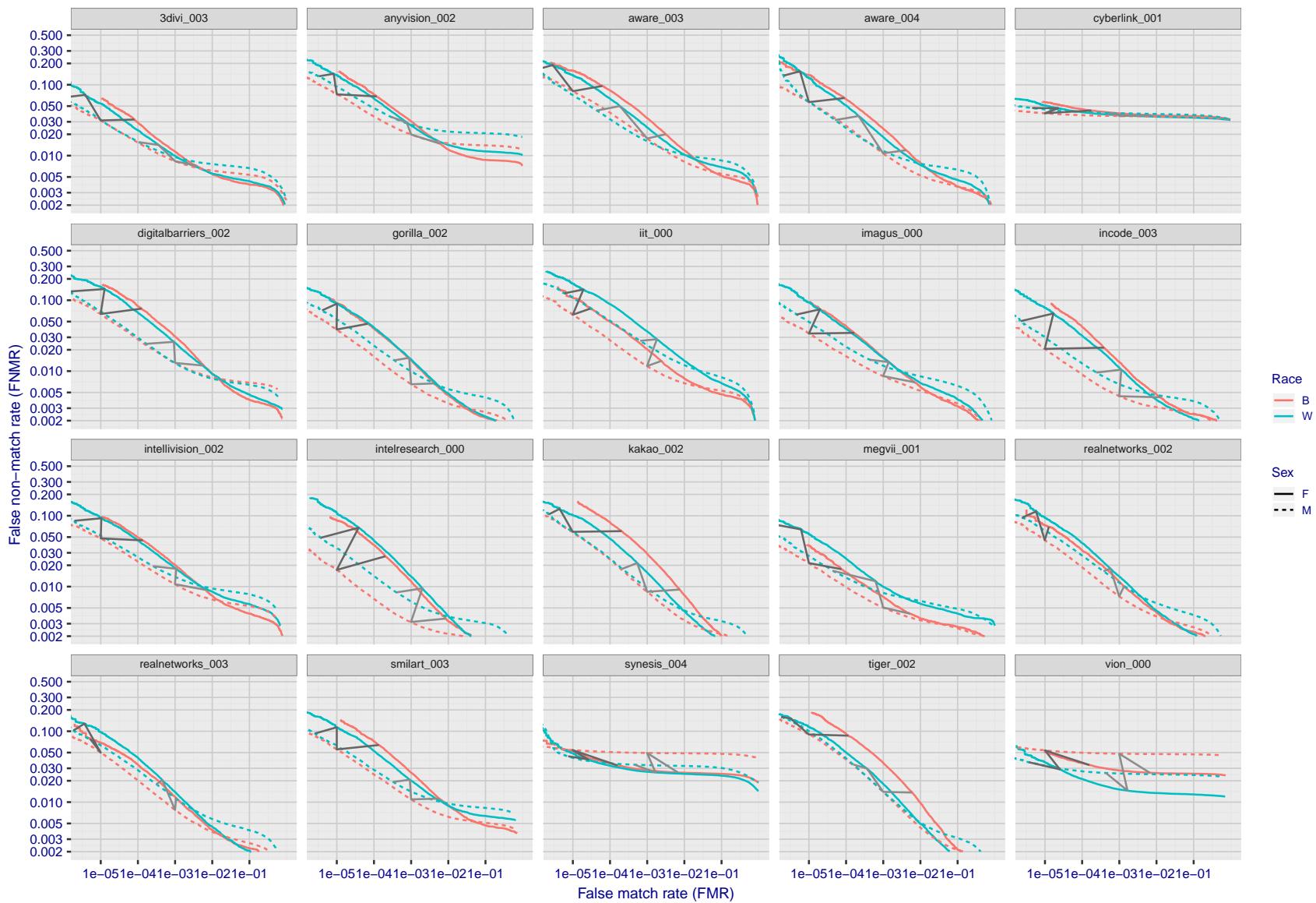


Figure 55: For the mugshot images, error tradeoff characteristics for white females, black females, black males and white males. The Z-shaped grey lines correspond to fixed thresholds, showing both FNMR and FMR vary at one T value. Note: Many of the plots will naively be read as saying women gives worse error rates than men because the solid traces lie above the dotted ones. However, this is misleading and incomplete: The grey lines show the traces reveal horizontal shifts. Thus for the cogent-003 algorithm FNMR for men is higher than for women at a fixed threshold but, at the same time, FMR is higher for women - see Figure 78. As access control systems almost always operate at a fixed threshold, the naive interpretation is incorrect.

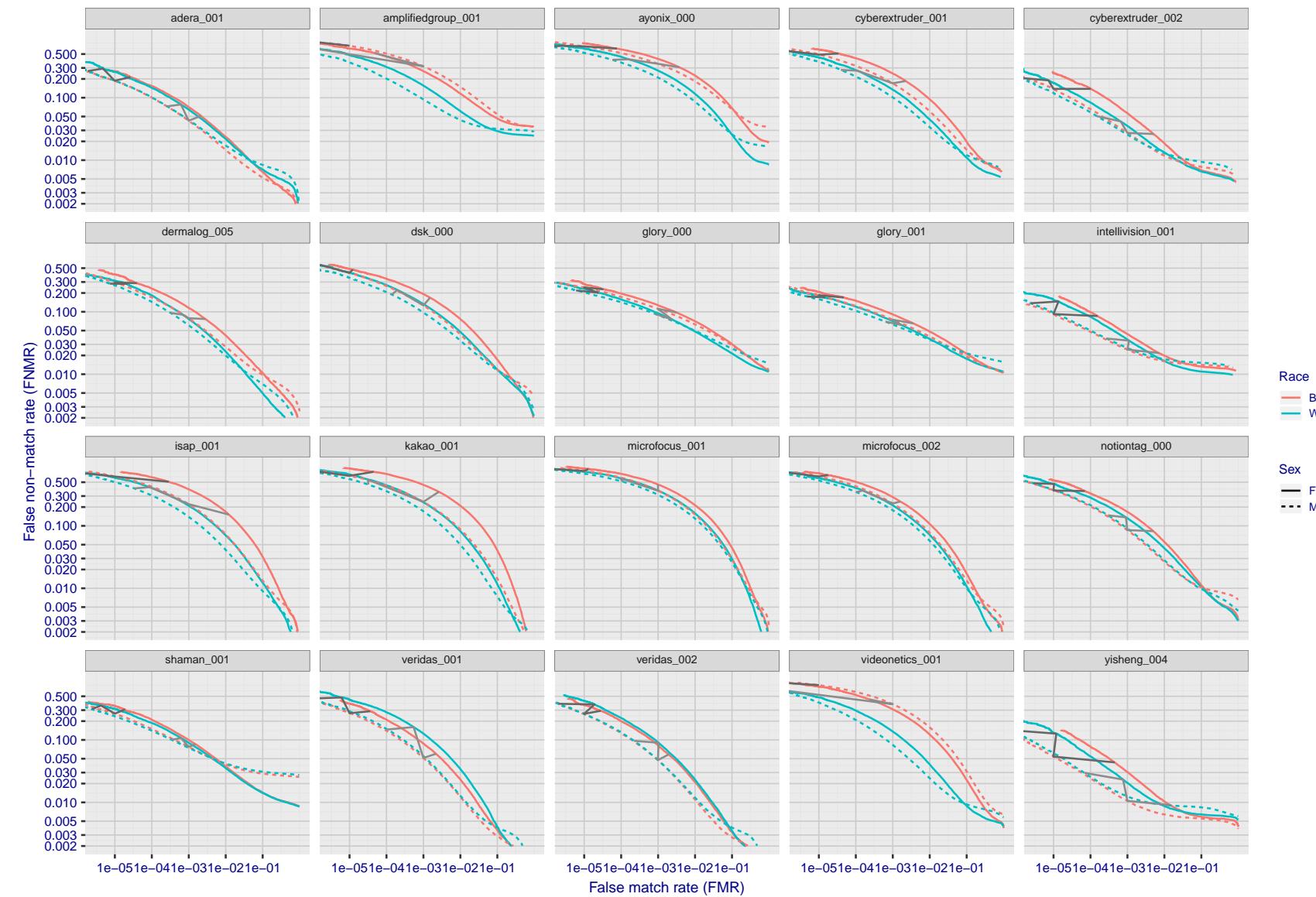


Figure 56: For the mugshot images, error tradeoff characteristics for white females, black females, black males and white males. The Z-shaped grey lines correspond to fixed thresholds, showing both FNMR and FMR vary at one T value. Note: Many of the plots will naively be read as saying women gives worse error rates than men because the solid traces lie above the dotted ones. However, this is misleading and incomplete: The grey lines show the traces reveal horizontal shifts. Thus for the cogent-003 algorithm FNMR for men is higher than for women at a fixed threshold but, at the same time, FMR is higher for women - see Figure 78. As access control systems almost always operate at a fixed threshold, the naive interpretation is incorrect.

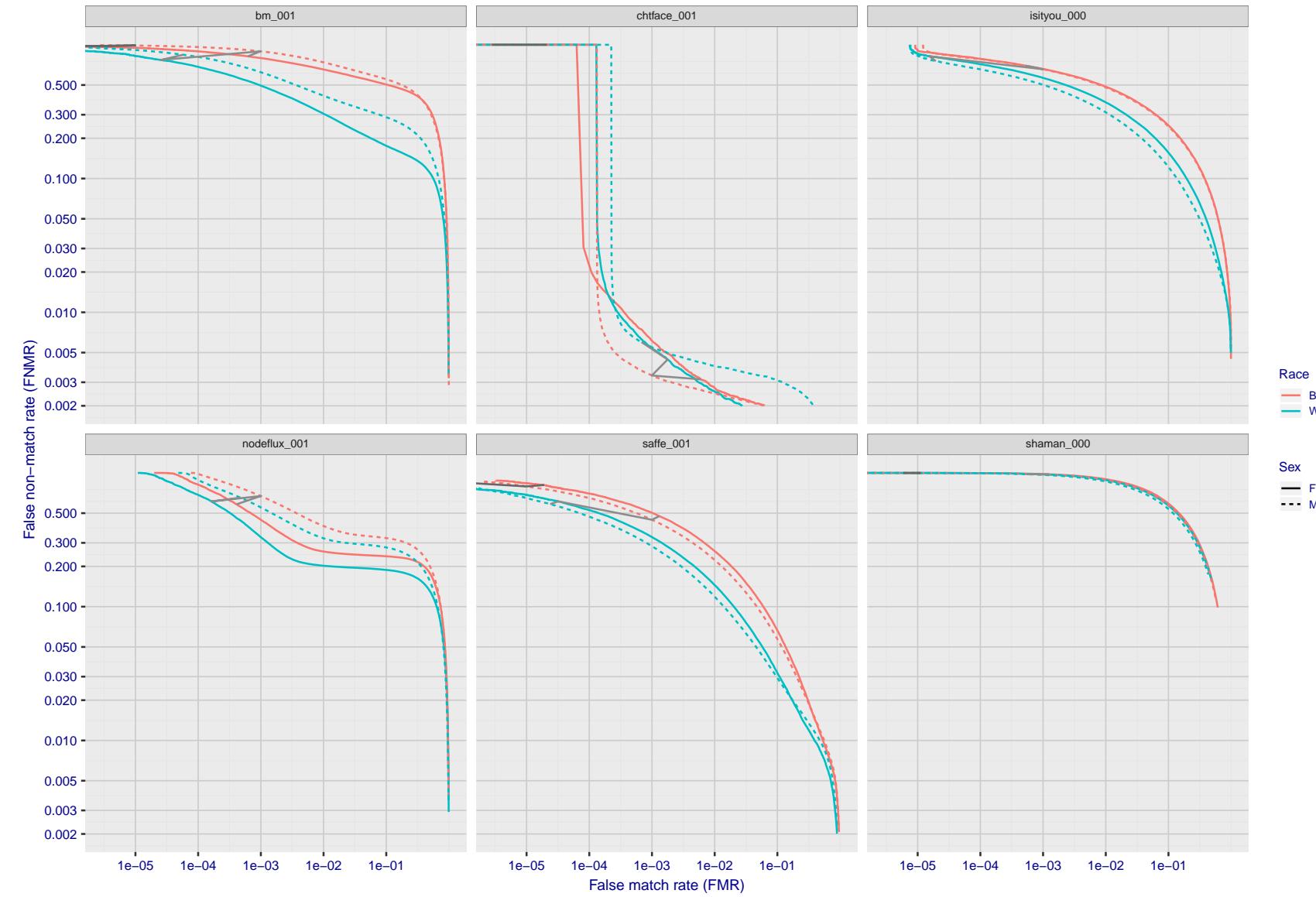


Figure 57: For the mugshot images, error tradeoff characteristics for white females, black females, black males and white males. The Z-shaped grey lines correspond to fixed thresholds, showing both FNMR and FMR vary at one T value. Note: Many of the plots will naively be read as saying women gives worse error rates than men because the solid traces lie above the dotted ones. However, this is misleading and incomplete: The grey lines show the traces reveal horizontal shifts. Thus for the cogent-003 algorithm FNMR for men is higher than for women at a fixed threshold but, at the same time, FMR is higher for women - see Figure 78. As access control systems almost always operate at a fixed threshold, the naive interpretation is incorrect.

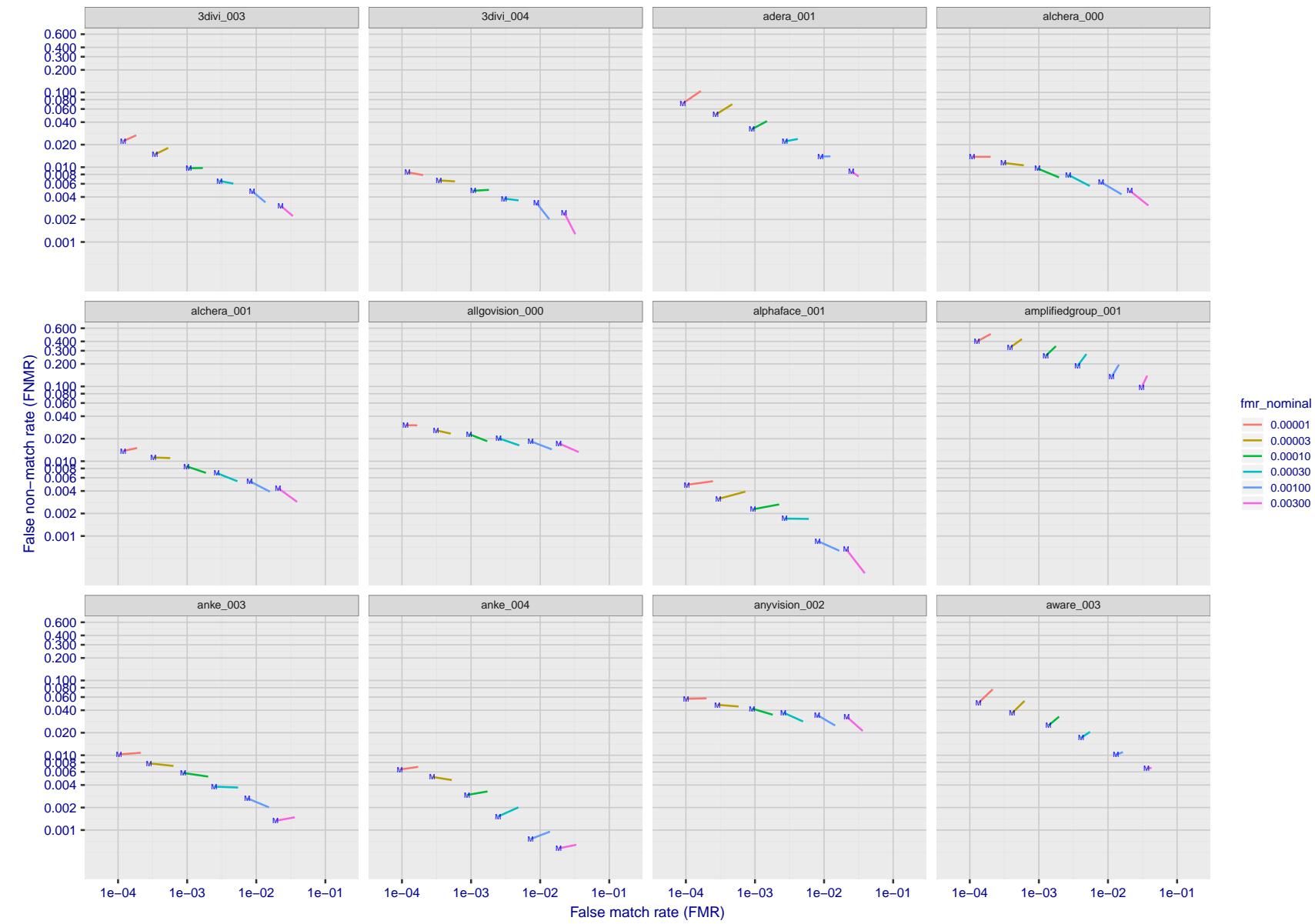


Figure 58: For the visa images, FNMR and FMR at six operating points along the DET characteristic. At each point a line is drawn between $(FMR, FNMR)_{MALE}$ and $(FMR, FNMR)_{FEMALE}$ showing how which sex has lower FMR and/or FNMR. The "M" label denotes male, the other end of the line corresponds to female. The six operating thresholds are selected to give the nominal false match rates given in the legend, and are computed over all impostor pairs regardless of age, sex, and place of birth. The plotted FMR values are broadly an order of magnitude larger than the nominal rates because FMR is computed over demographically-matched impostor pairs i.e individuals of the same sex, from the same geographic region (see section 3.6.1), and the same age group (see section 3.6.2).

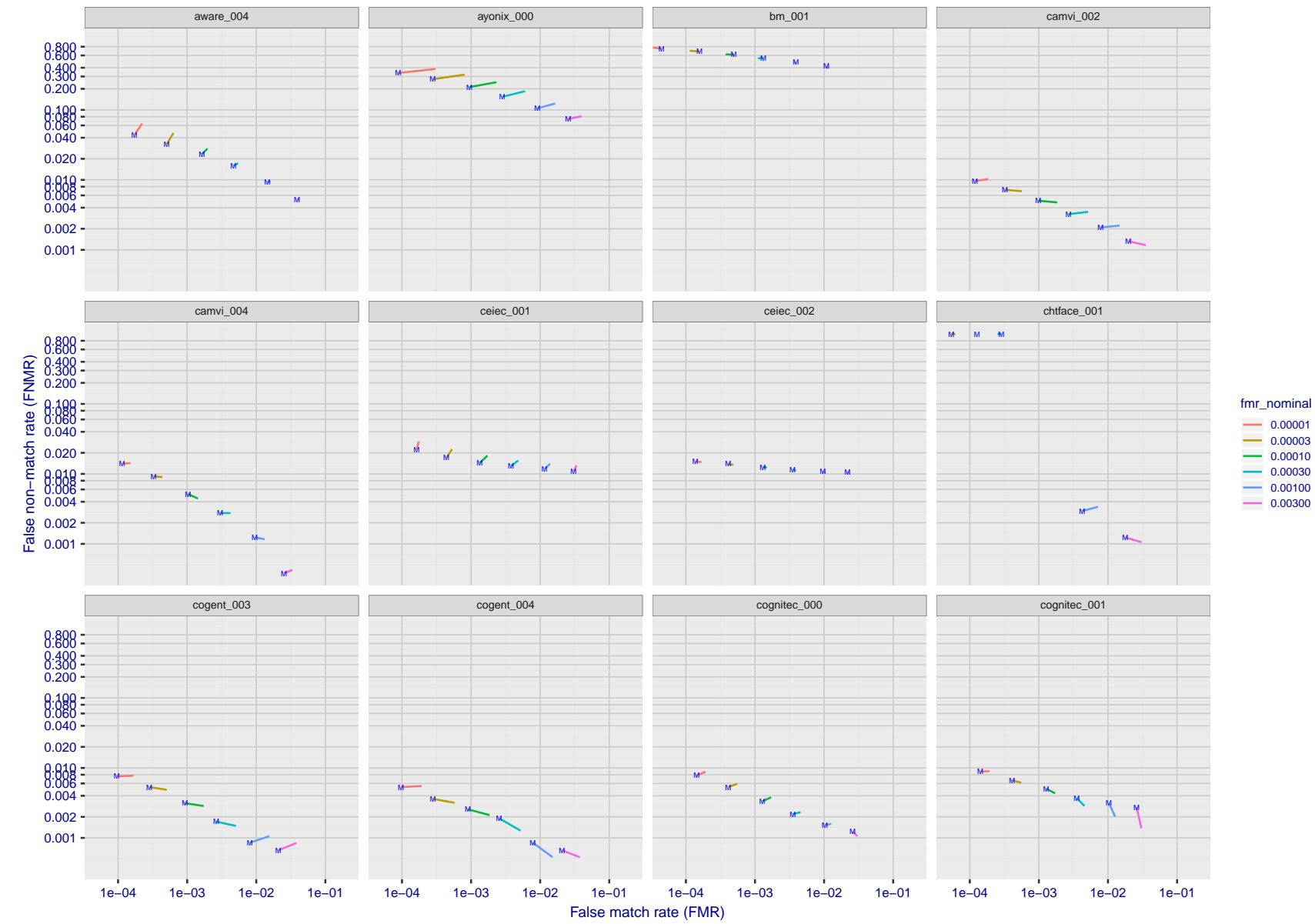


Figure 59: For the visa images, FNMR and FMR at six operating points along the DET characteristic. At each point a line is drawn between $(FMR, FNMR)_{MALE}$ and $(FMR, FNMR)_{FEMALE}$ showing how which sex has lower FMR and/or FNMR. The "M" label denotes male, the other end of the line corresponds to female. The six operating thresholds are selected to give the nominal false match rates given in the legend, and are computed over all impostor pairs regardless of age, sex, and place of birth. The plotted FMR values are broadly an order of magnitude larger than the nominal rates because FMR is computed over demographically-matched impostor pairs i.e individuals of the same sex, from the same geographic region (see section 3.6.1), and the same age group (see section 3.6.2).

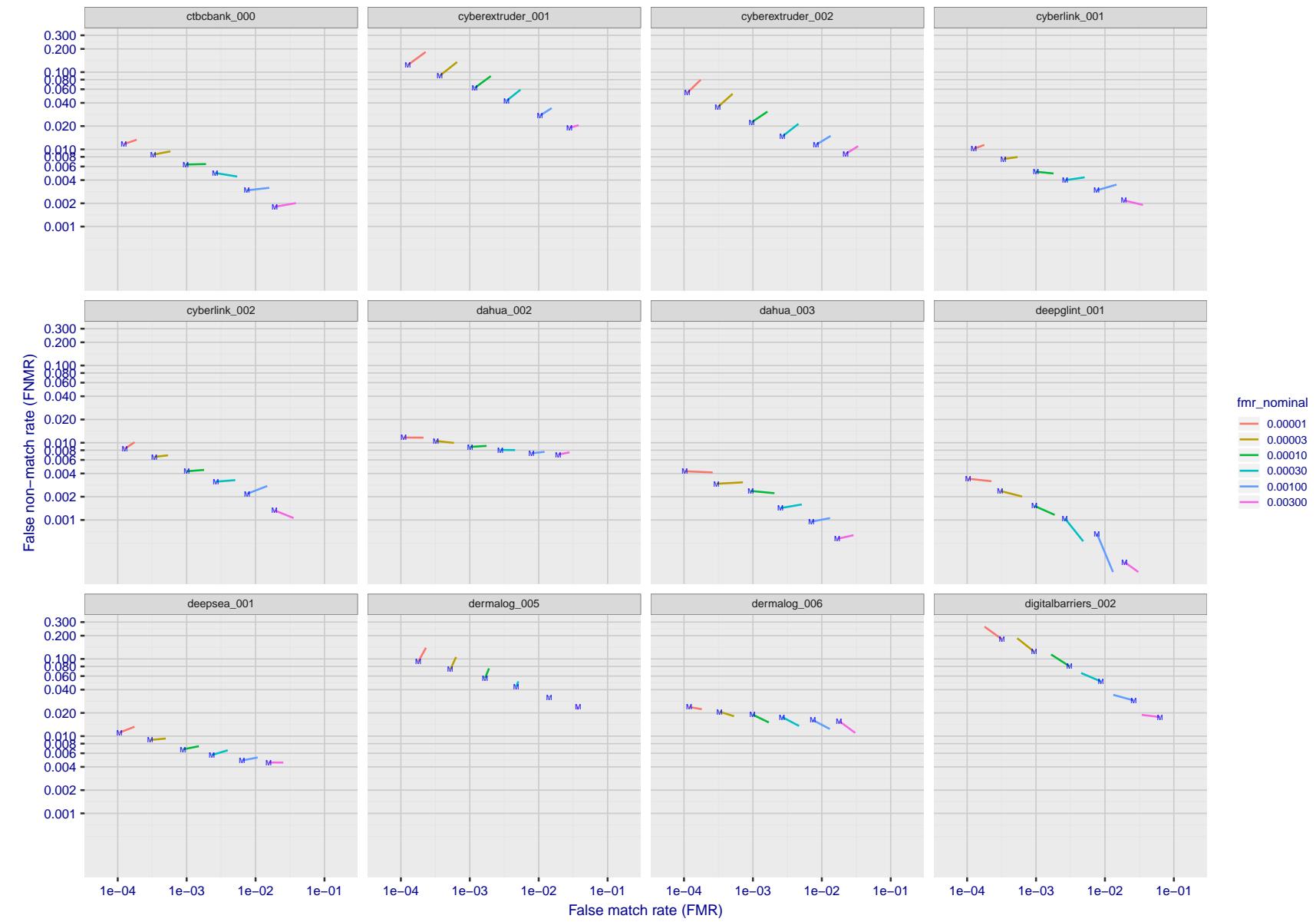


Figure 60: For the visa images, FNMR and FMR at six operating points along the DET characteristic. At each point a line is drawn between $(FMR, FNMR)_{MALE}$ and $(FMR, FNMR)_{FEMALE}$ showing how which sex has lower FMR and/or FNMR. The "M" label denotes male, the other end of the line corresponds to female. The six operating thresholds are selected to give the nominal false match rates given in the legend, and are computed over all impostor pairs regardless of age, sex, and place of birth. The plotted FMR values are broadly an order of magnitude larger than the nominal rates because FMR is computed over demographically-matched impostor pairs i.e individuals of the same sex, from the same geographic region (see section 3.6.1), and the same age group (see section 3.6.2).

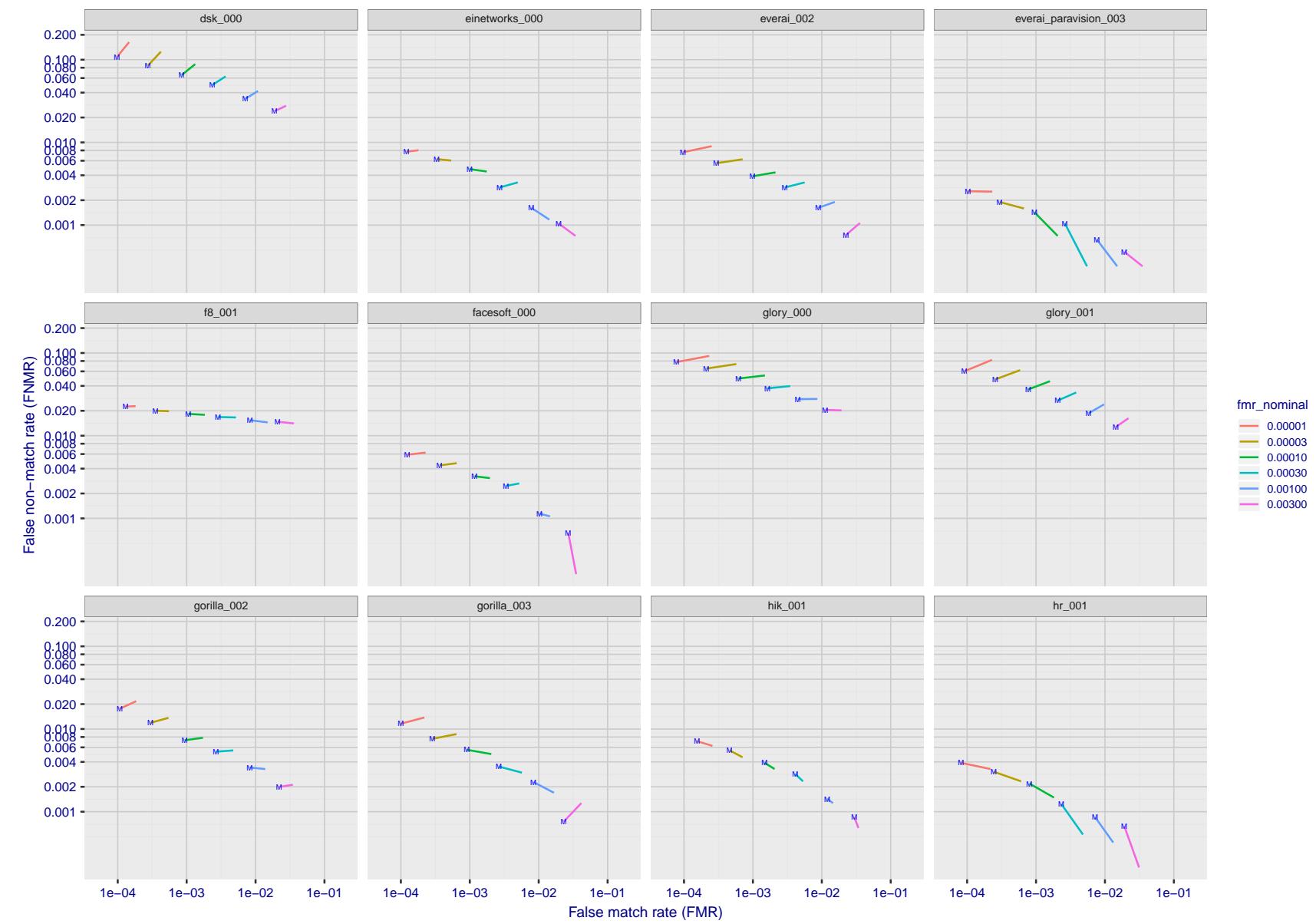


Figure 61: For the visa images, FNMR and FMR at six operating points along the DET characteristic. At each point a line is drawn between $(FMR, FNMR)_{MALE}$ and $(FMR, FNMR)_{FEMALE}$ showing how which sex has lower FMR and/or FNMR. The "M" label denotes male, the other end of the line corresponds to female. The six operating thresholds are selected to give the nominal false match rates given in the legend, and are computed over all impostor pairs regardless of age, sex, and place of birth. The plotted FMR values are broadly an order of magnitude larger than the nominal rates because FMR is computed over demographically-matched impostor pairs i.e individuals of the same sex, from the same geographic region (see section 3.6.1), and the same age group (see section 3.6.2).

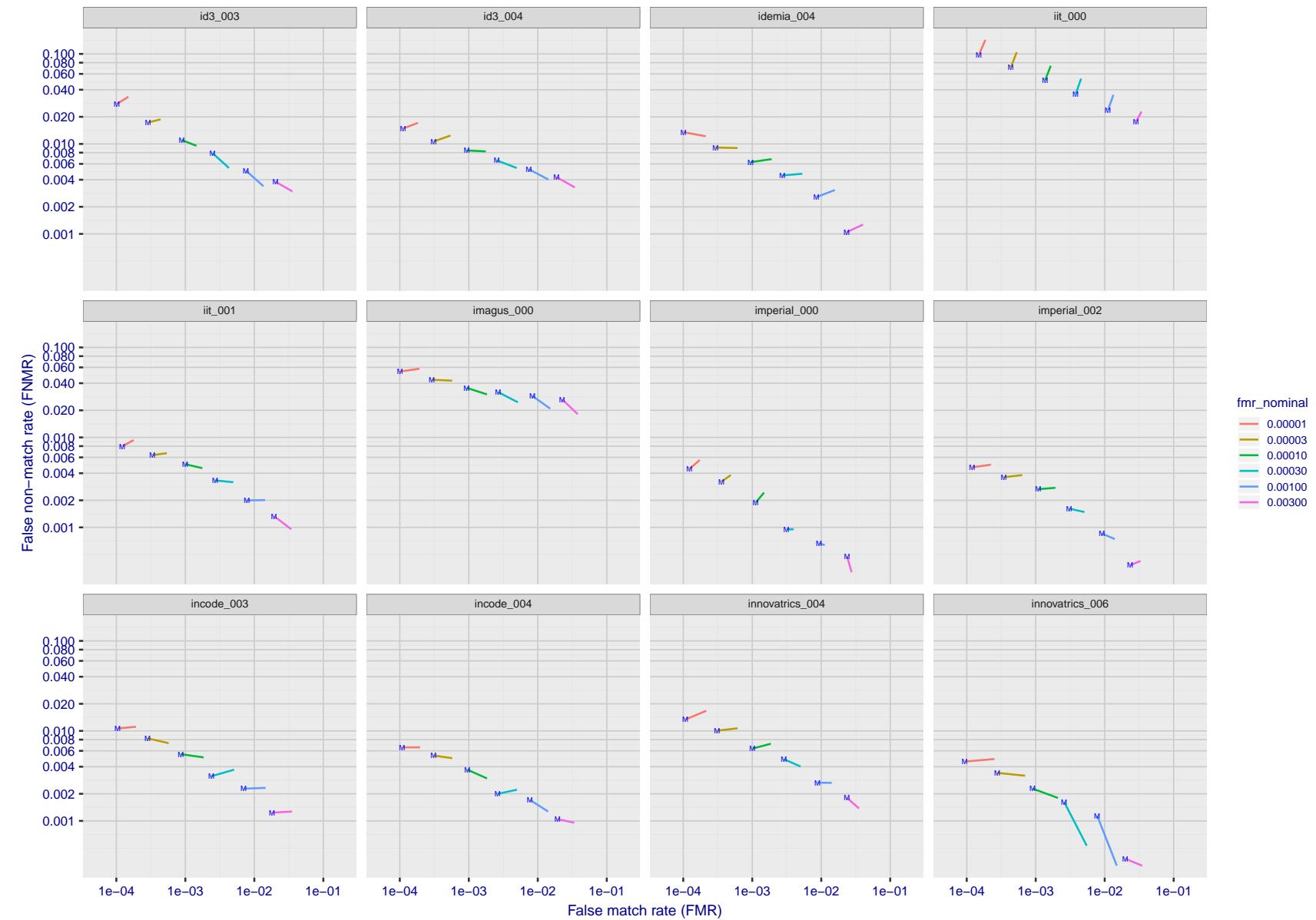


Figure 62: For the visa images, FNMR and FMR at six operating points along the DET characteristic. At each point a line is drawn between $(FMR, FNMR)_{MALE}$ and $(FMR, FNMR)_{FEMALE}$ showing how which sex has lower FMR and/or FNMR. The "M" label denotes male, the other end of the line corresponds to female. The six operating thresholds are selected to give the nominal false match rates given in the legend, and are computed over all impostor pairs regardless of age, sex, and place of birth. The plotted FMR values are broadly an order of magnitude larger than the nominal rates because FMR is computed over demographically-matched impostor pairs i.e individuals of the same sex, from the same geographic region (see section 3.6.1), and the same age group (see section 3.6.2).

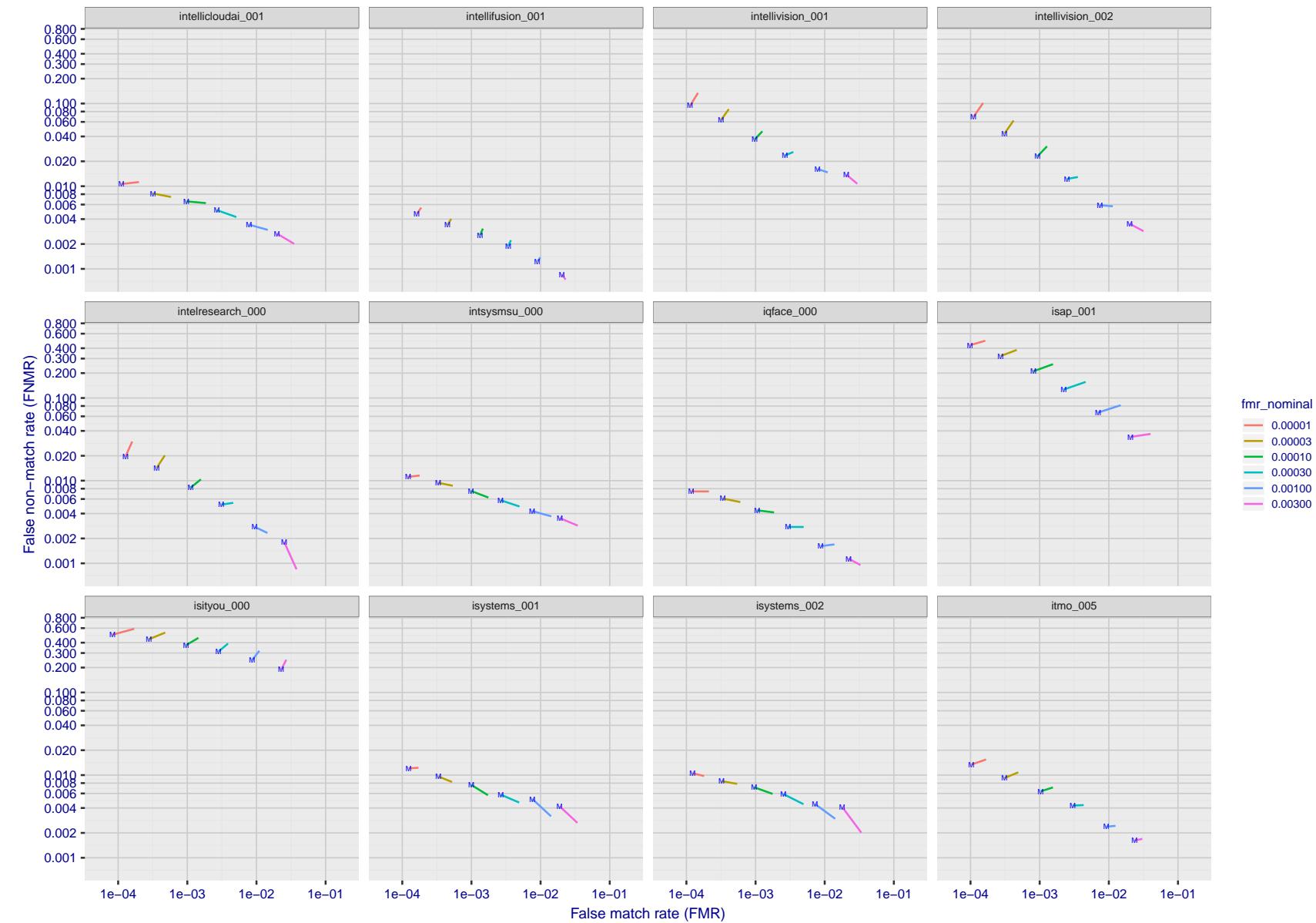


Figure 63: For the visa images, FNMR and FMR at six operating points along the DET characteristic. At each point a line is drawn between $(FMR, FNMR)_{MALE}$ and $(FMR, FNMR)_{FEMALE}$ showing how which sex has lower FMR and/or FNMR. The "M" label denotes male, the other end of the line corresponds to female. The six operating thresholds are selected to give the nominal false match rates given in the legend, and are computed over all impostor pairs regardless of age, sex, and place of birth. The plotted FMR values are broadly an order of magnitude larger than the nominal rates because FMR is computed over demographically-matched impostor pairs i.e individuals of the same sex, from the same geographic region (see section 3.6.1), and the same age group (see section 3.6.2).

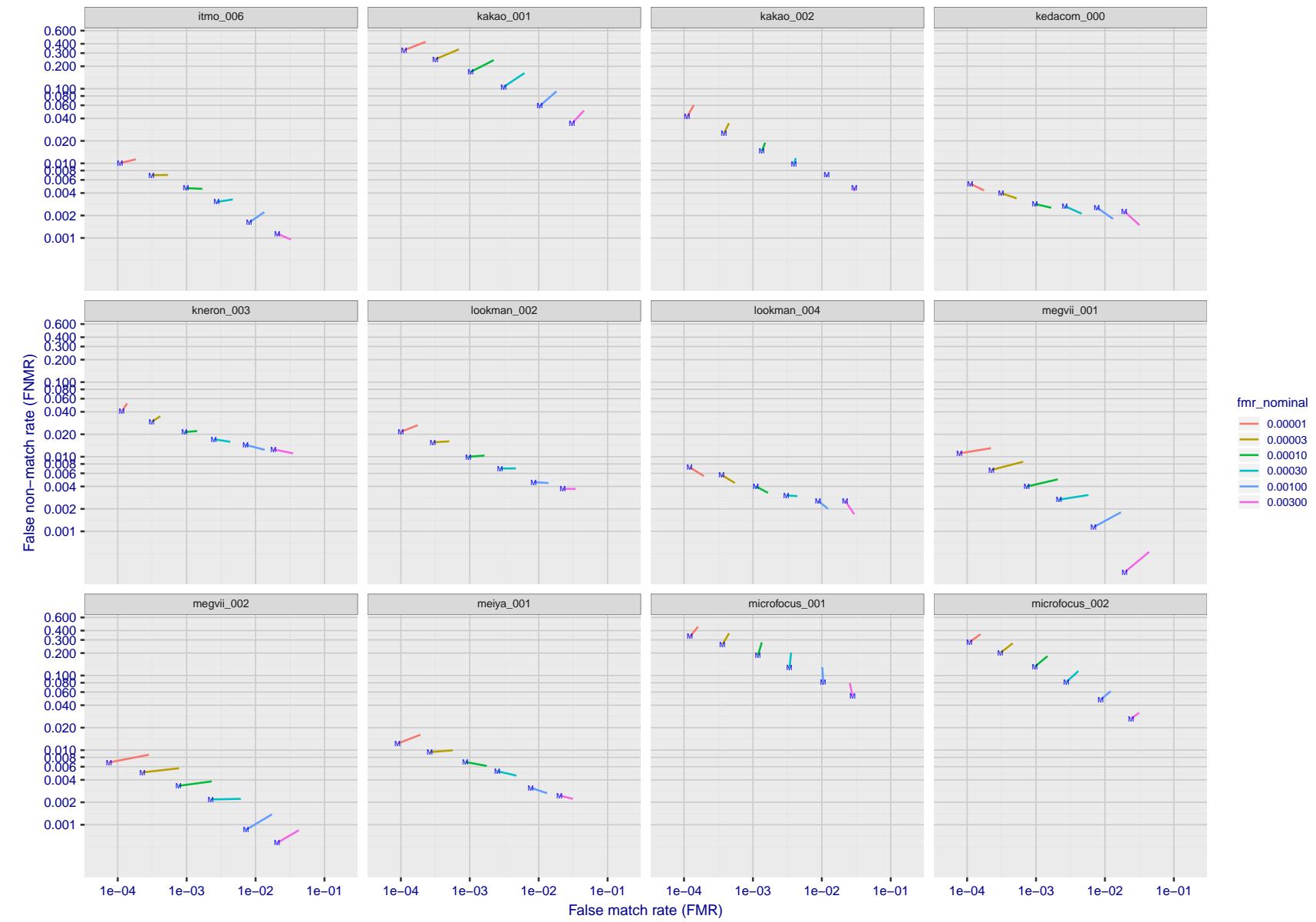


Figure 64: For the visa images, FNMR and FMR at six operating points along the DET characteristic. At each point a line is drawn between $(FMR, FNMR)_{MALE}$ and $(FMR, FNMR)_{FEMALE}$ showing how which sex has lower FMR and/or FNMR. The "M" label denotes male, the other end of the line corresponds to female. The six operating thresholds are selected to give the nominal false match rates given in the legend, and are computed over all impostor pairs regardless of age, sex, and place of birth. The plotted FMR values are broadly an order of magnitude larger than the nominal rates because FMR is computed over demographically-matched impostor pairs i.e individuals of the same sex, from the same geographic region (see section 3.6.1), and the same age group (see section 3.6.2).

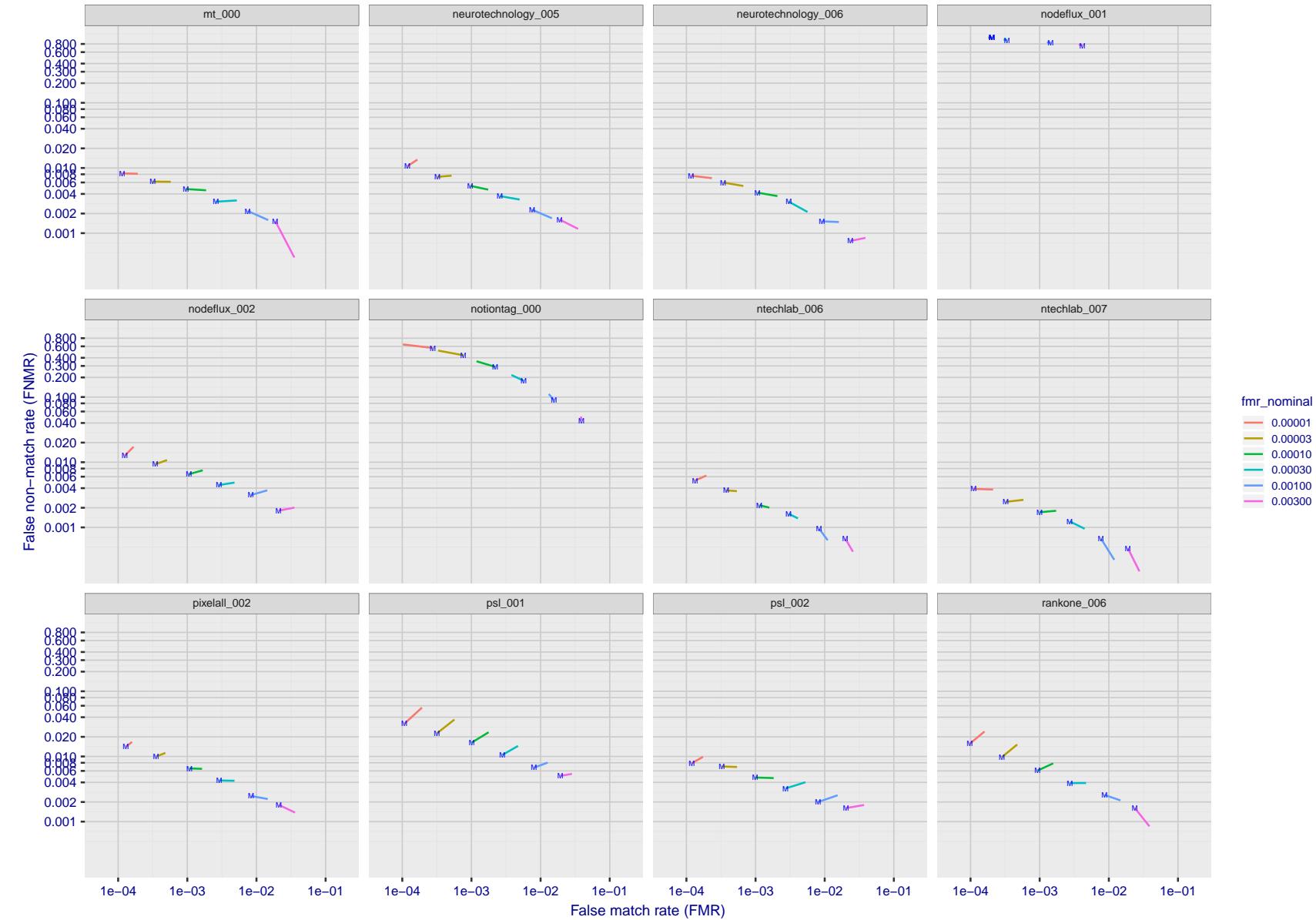


Figure 65: For the visa images, FNMR and FMR at six operating points along the DET characteristic. At each point a line is drawn between $(FMR, FNMR)_{MALE}$ and $(FMR, FNMR)_{FEMALE}$ showing how which sex has lower FMR and/or FNMR. The "M" label denotes male, the other end of the line corresponds to female. The six operating thresholds are selected to give the nominal false match rates given in the legend, and are computed over all impostor pairs regardless of age, sex, and place of birth. The plotted FMR values are broadly an order of magnitude larger than the nominal rates because FMR is computed over demographically-matched impostor pairs i.e individuals of the same sex, from the same geographic region (see section 3.6.1), and the same age group (see section 3.6.2).

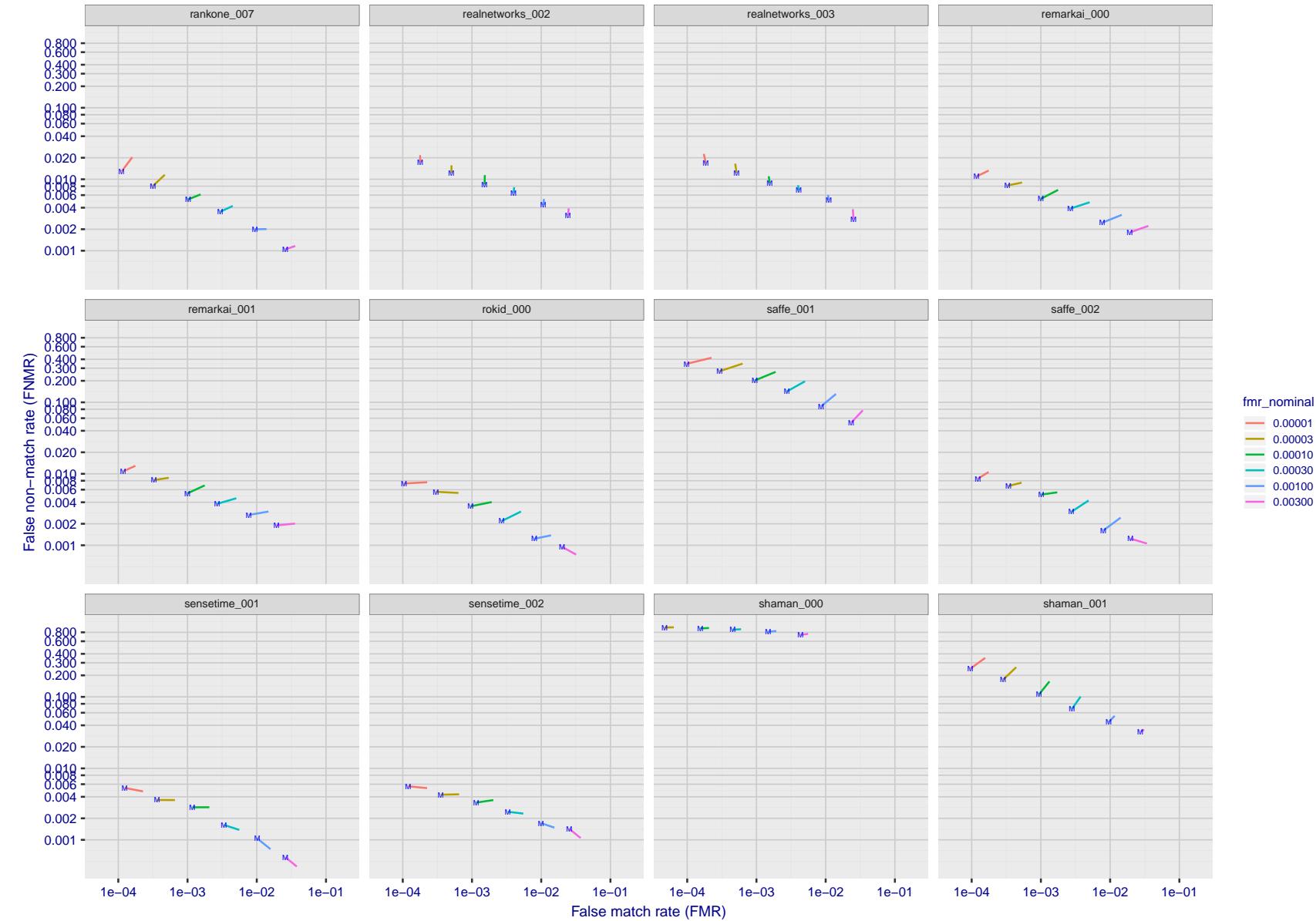


Figure 66: For the visa images, FNMR and FMR at six operating points along the DET characteristic. At each point a line is drawn between $(FMR, FNMR)_{MALE}$ and $(FMR, FNMR)_{FEMALE}$ showing how which sex has lower FMR and/or FNMR. The "M" label denotes male, the other end of the line corresponds to female. The six operating thresholds are selected to give the nominal false match rates given in the legend, and are computed over all impostor pairs regardless of age, sex, and place of birth. The plotted FMR values are broadly an order of magnitude larger than the nominal rates because FMR is computed over demographically-matched impostor pairs i.e individuals of the same sex, from the same geographic region (see section 3.6.1), and the same age group (see section 3.6.2).

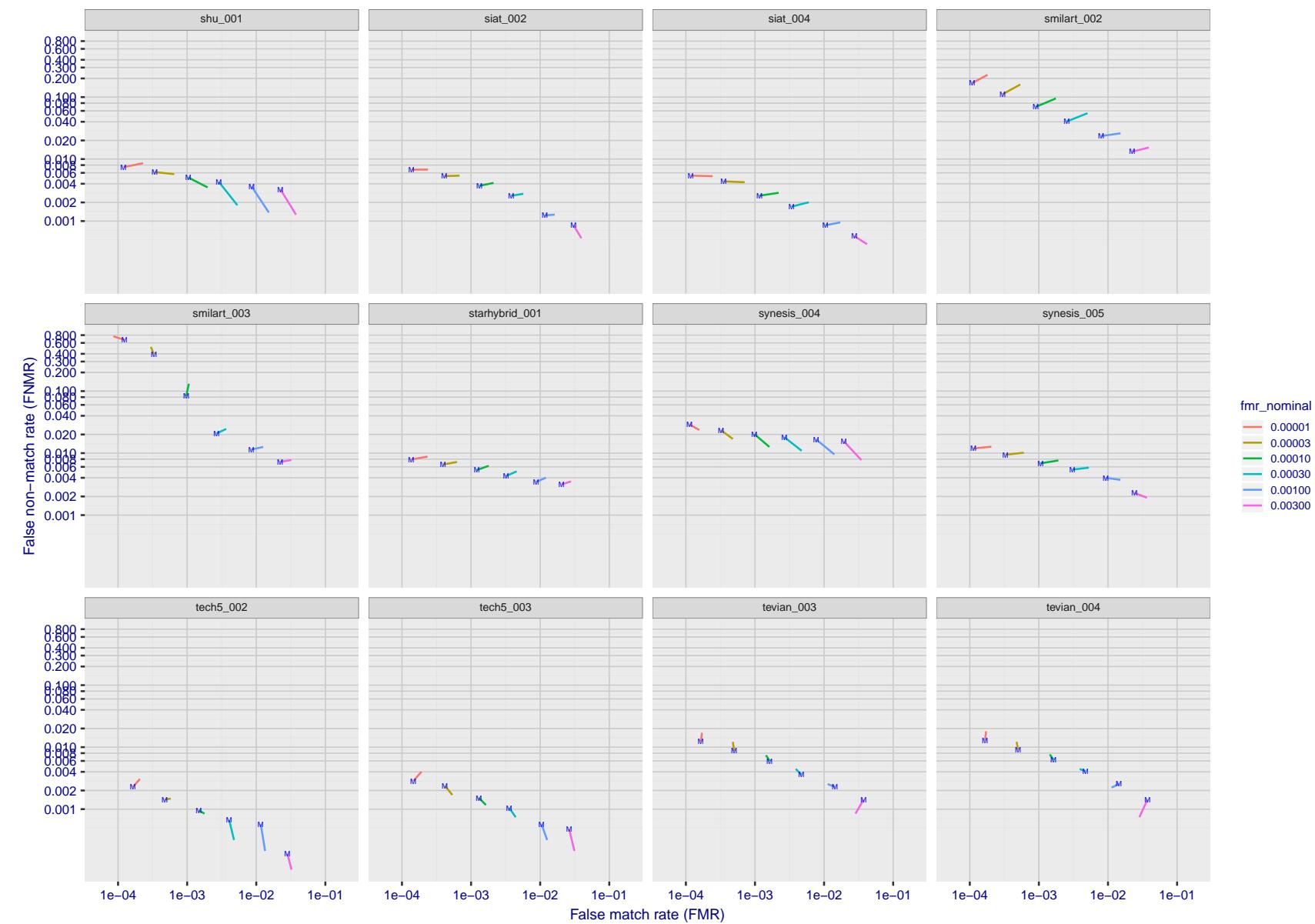


Figure 67: For the visa images, FNMR and FMR at six operating points along the DET characteristic. At each point a line is drawn between $(FMR, FNMR)_{MALE}$ and $(FMR, FNMR)_{FEMALE}$ showing how which sex has lower FMR and/or FNMR. The "M" label denotes male, the other end of the line corresponds to female. The six operating thresholds are selected to give the nominal false match rates given in the legend, and are computed over all impostor pairs regardless of age, sex, and place of birth. The plotted FMR values are broadly an order of magnitude larger than the nominal rates because FMR is computed over demographically-matched impostor pairs i.e individuals of the same sex, from the same geographic region (see section 3.6.1), and the same age group (see section 3.6.2).

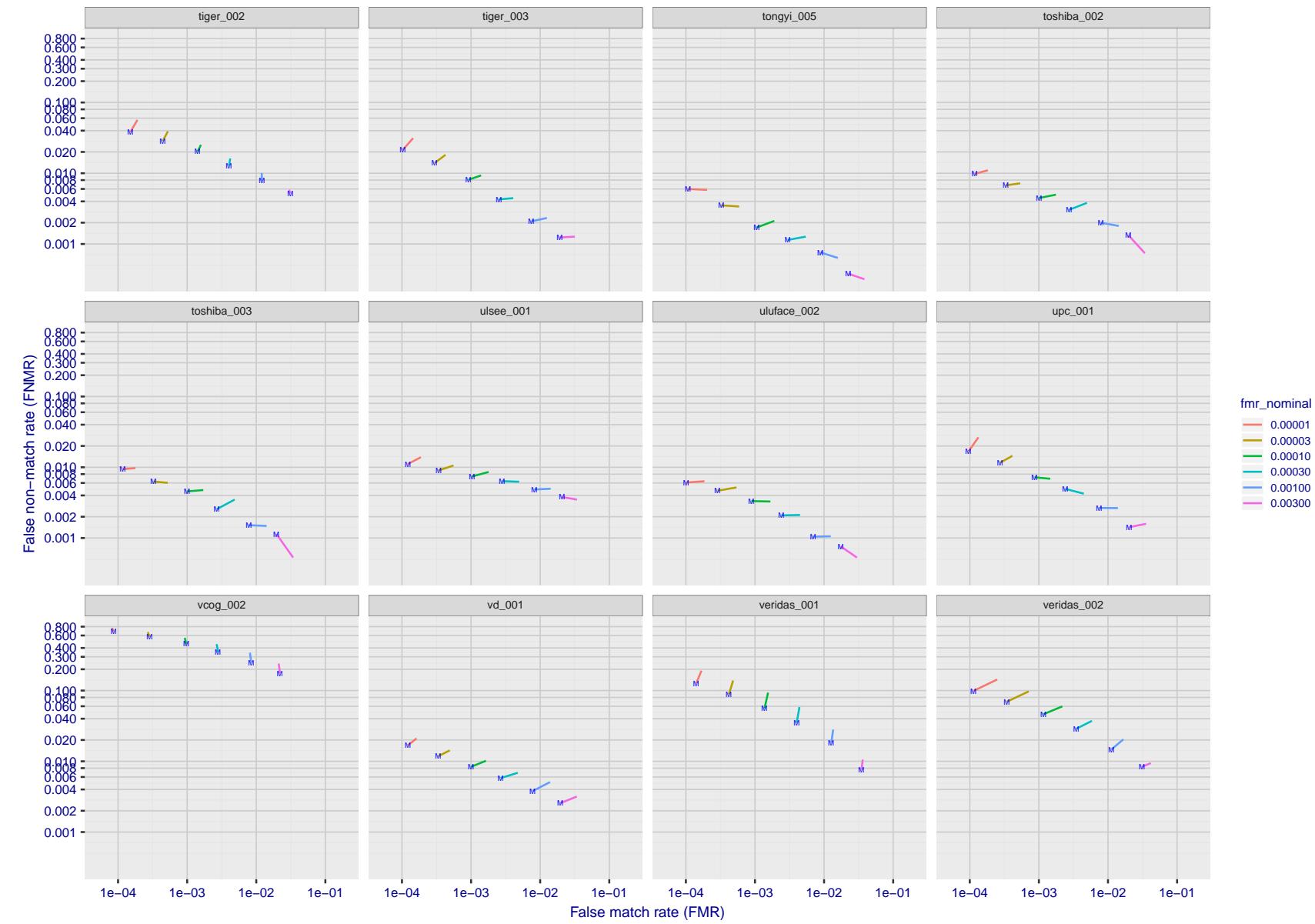


Figure 68: For the visa images, FNMR and FMR at six operating points along the DET characteristic. At each point a line is drawn between $(FMR, FNMR)_{MALE}$ and $(FMR, FNMR)_{FEMALE}$ showing how which sex has lower FMR and/or FNMR. The "M" label denotes male, the other end of the line corresponds to female. The six operating thresholds are selected to give the nominal false match rates given in the legend, and are computed over all impostor pairs regardless of age, sex, and place of birth. The plotted FMR values are broadly an order of magnitude larger than the nominal rates because FMR is computed over demographically-matched impostor pairs i.e individuals of the same sex, from the same geographic region (see section 3.6.1), and the same age group (see section 3.6.2).

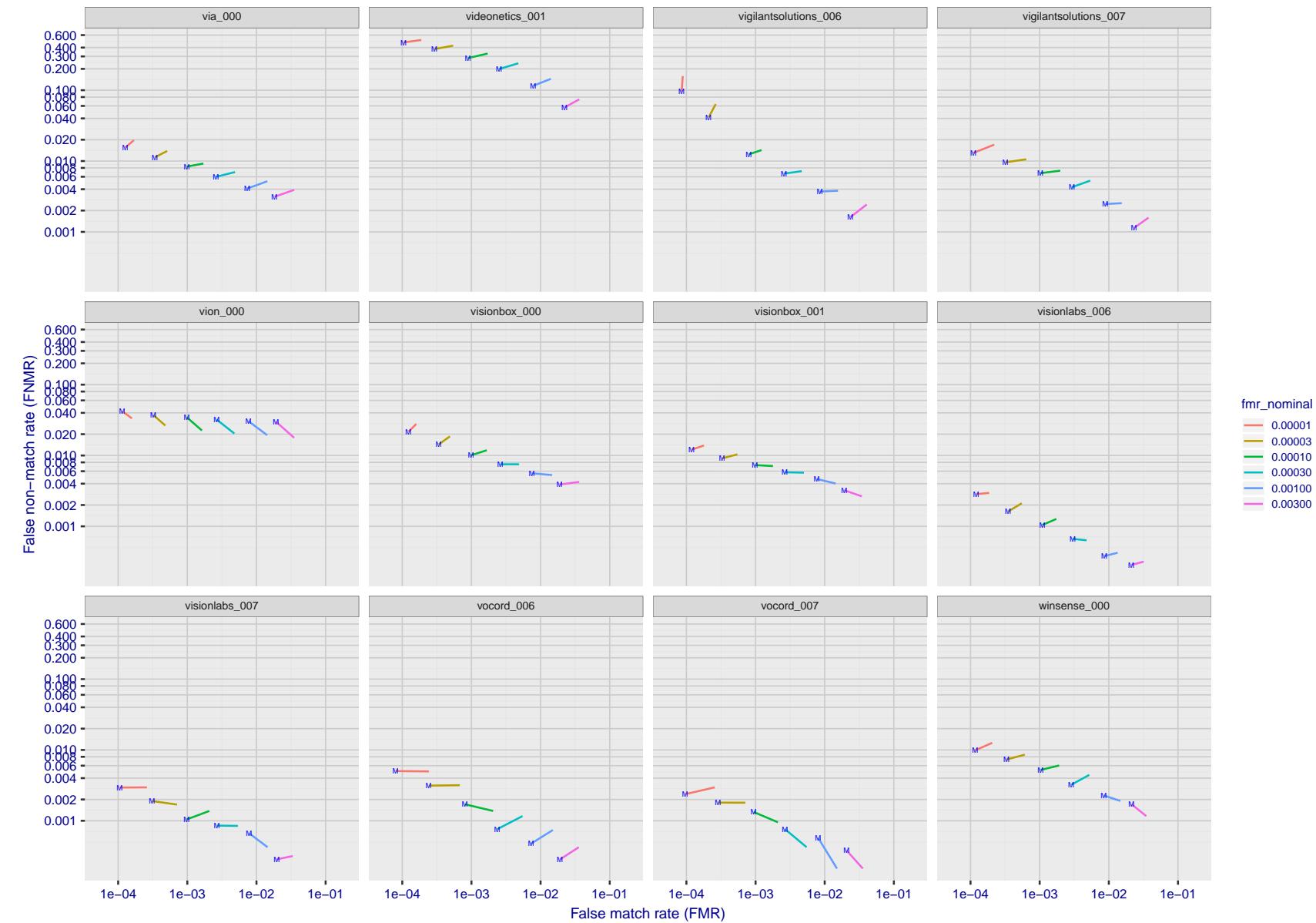


Figure 69: For the visa images, FNMR and FMR at six operating points along the DET characteristic. At each point a line is drawn between $(FMR, FNMR)_{MALE}$ and $(FMR, FNMR)_{FEMALE}$ showing how which sex has lower FMR and/or FNMR. The "M" label denotes male, the other end of the line corresponds to female. The six operating thresholds are selected to give the nominal false match rates given in the legend, and are computed over all impostor pairs regardless of age, sex, and place of birth. The plotted FMR values are broadly an order of magnitude larger than the nominal rates because FMR is computed over demographically-matched impostor pairs i.e individuals of the same sex, from the same geographic region (see section 3.6.1), and the same age group (see section 3.6.2).

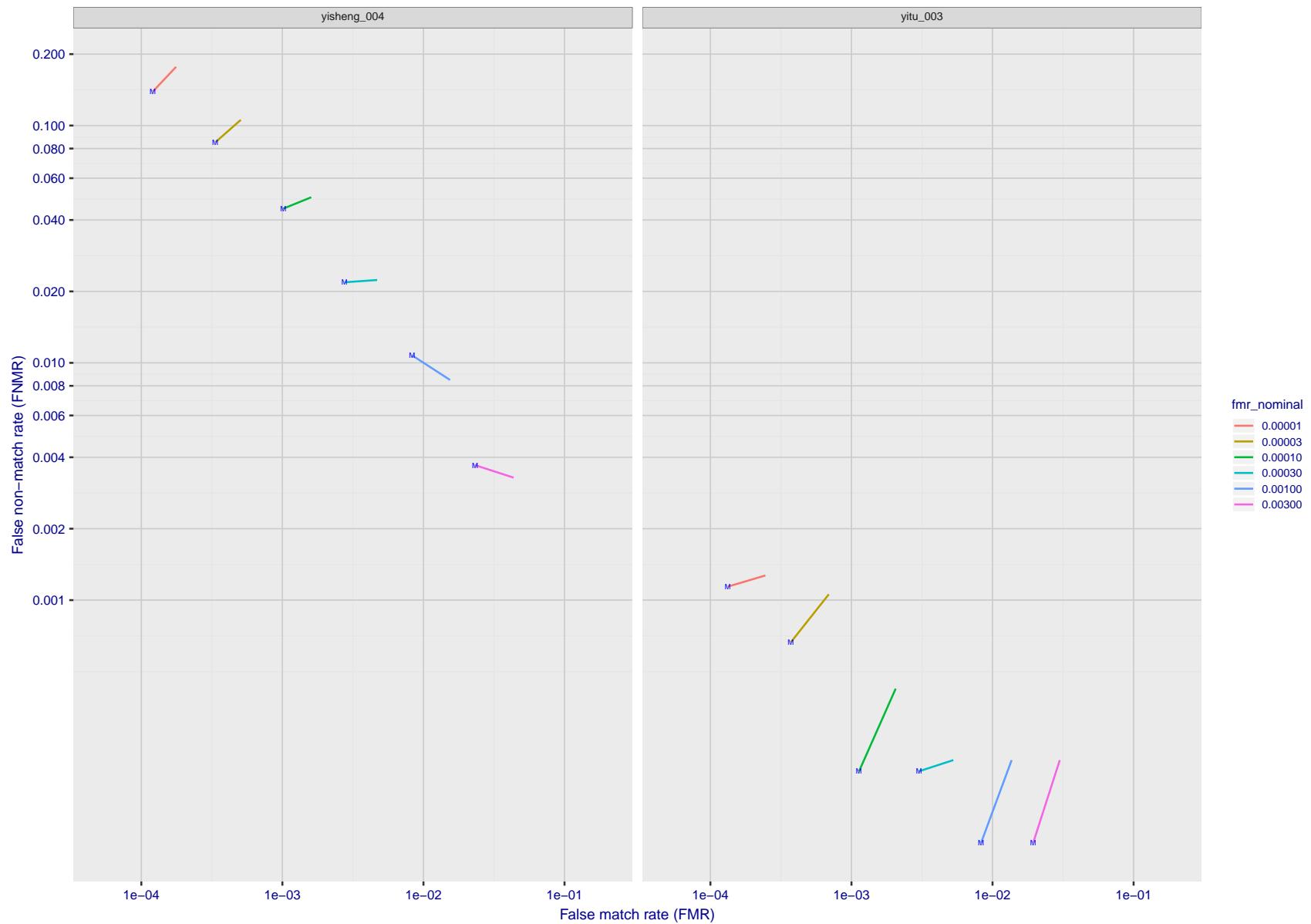


Figure 70: For the visa images, FNMR and FMR at six operating points along the DET characteristic. At each point a line is drawn between $(FMR, FNMR)_{MALE}$ and $(FMR, FNMR)_{FEMALE}$ showing how which sex has lower FMR and/or FNMR. The "M" label denotes male, the other end of the line corresponds to female. The six operating thresholds are selected to give the nominal false match rates given in the legend, and are computed over all impostor pairs regardless of age, sex, and place of birth. The plotted FMR values are broadly an order of magnitude larger than the nominal rates because FMR is computed over demographically-matched impostor pairs i.e individuals of the same sex, from the same geographic region (see section 3.6.1), and the same age group (see section 3.6.2).

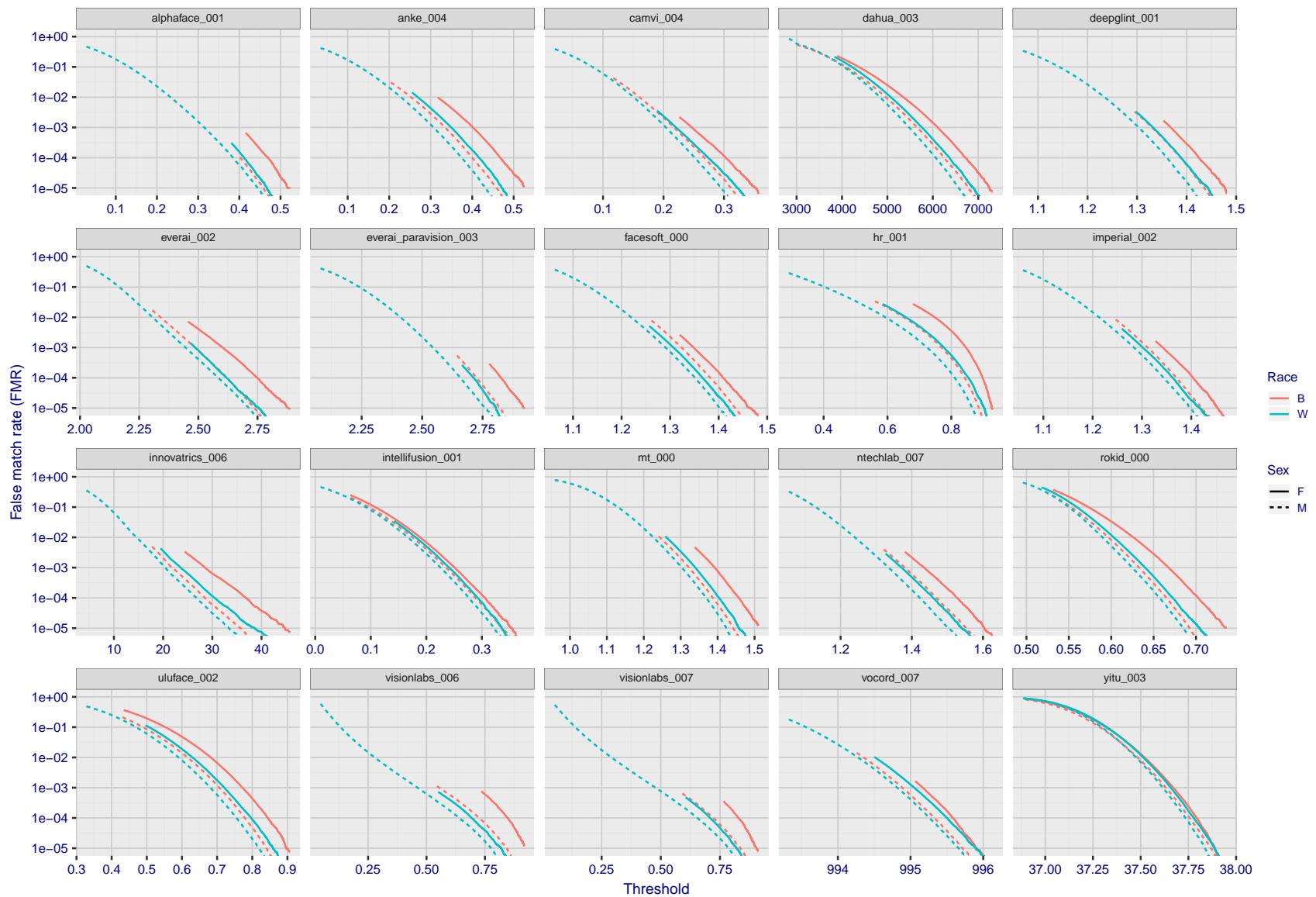


Figure 71: For the mugshot images, the false match calibration curves show false match rate vs. threshold. Separate curves appear for white females, black females, black males and white males.

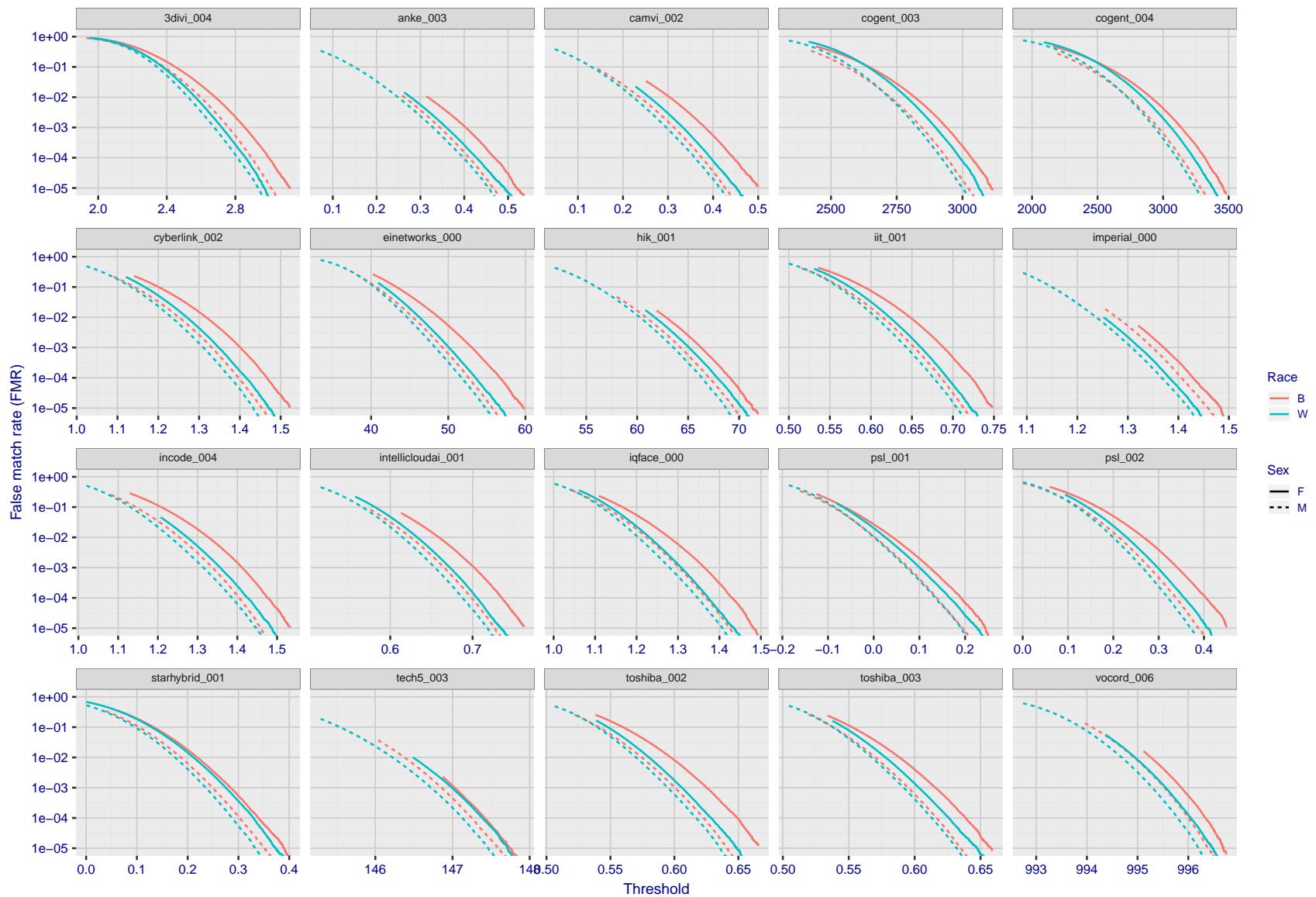


Figure 72: For the mugshot images, the false match calibration curves show false match rate vs. threshold. Separate curves appear for white females, black females, black males and white males.

2019/09/11 14:58:19

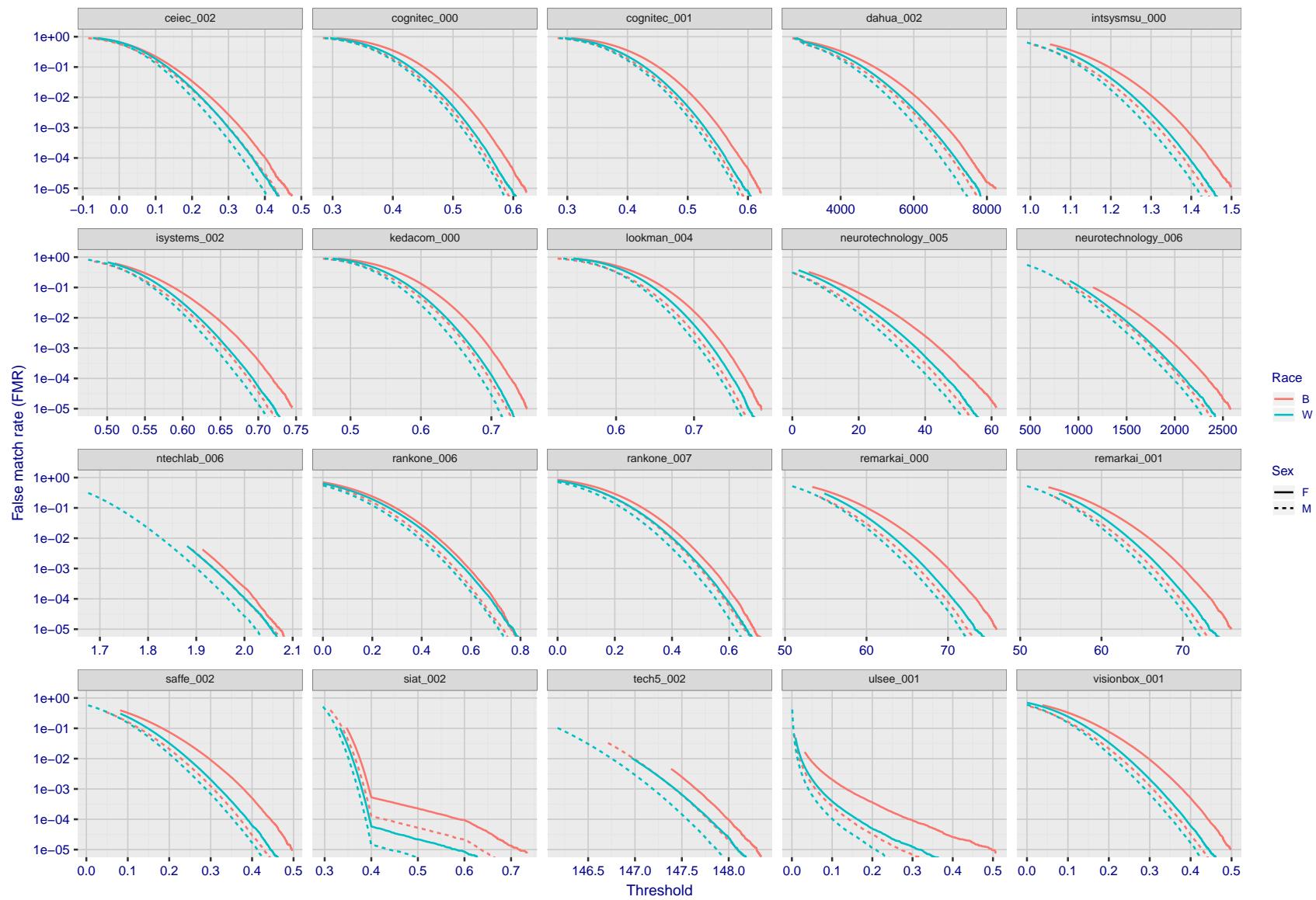


Figure 73: For the mugshot images, the false match calibration curves show false match rate vs. threshold. Separate curves appear for white females, black females, black males and white males.

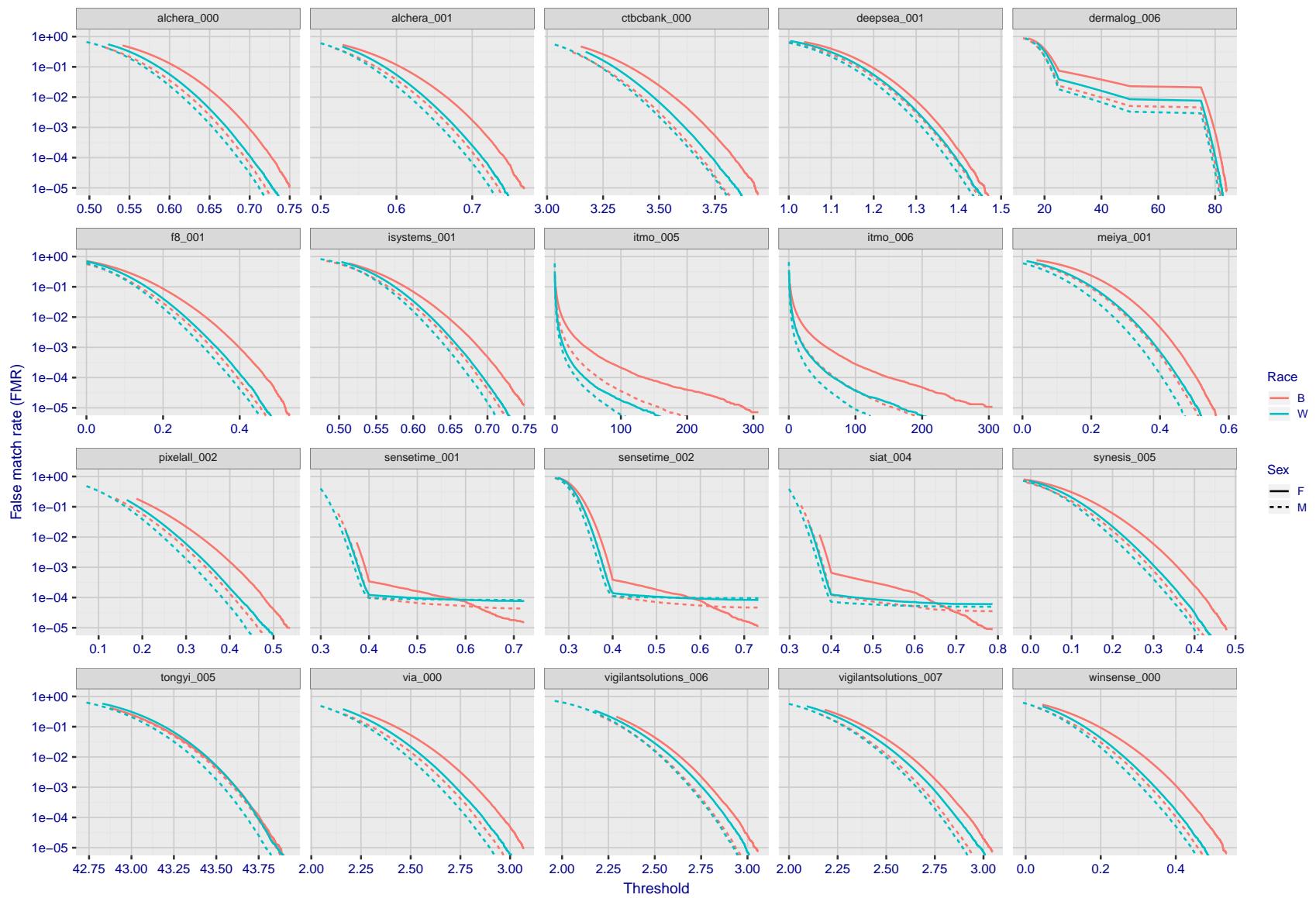


Figure 74: For the mugshot images, the false match calibration curves show false match rate vs. threshold. Separate curves appear for white females, black females, black males and white males.

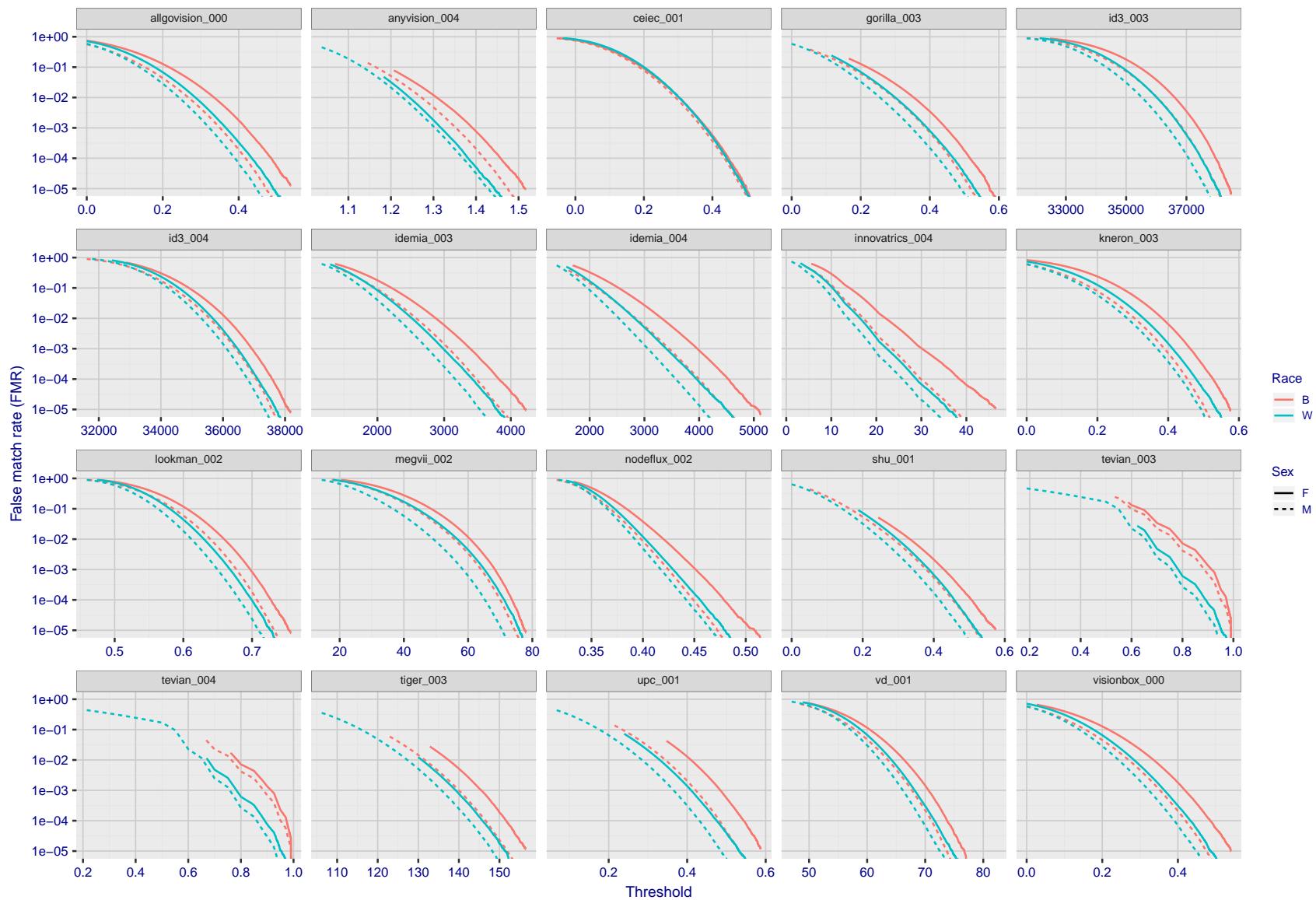


Figure 75: For the mugshot images, the false match calibration curves show false match rate vs. threshold. Separate curves appear for white females, black females, black males and white males.

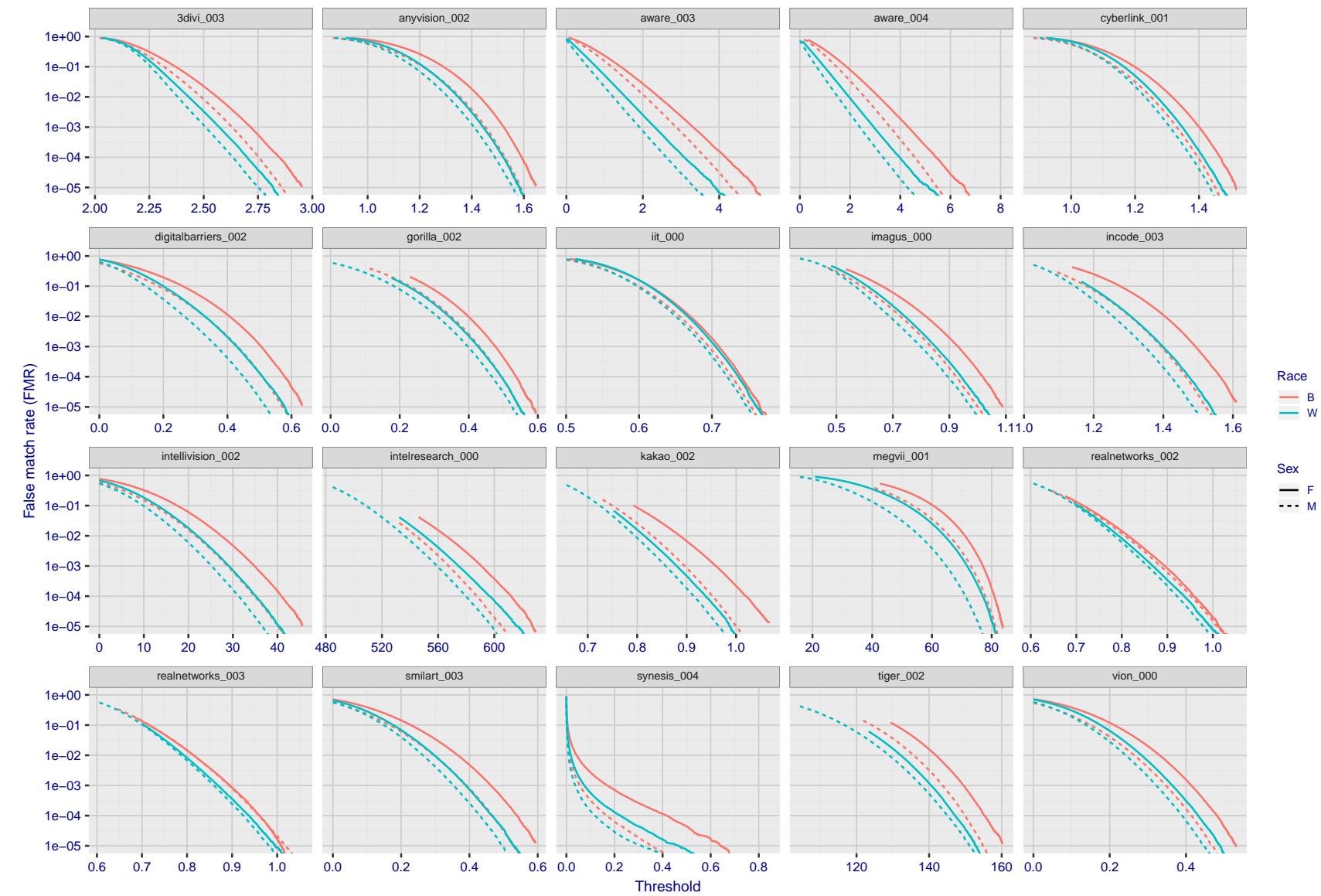


Figure 76: For the mugshot images, the false match calibration curves show false match rate vs. threshold. Separate curves appear for white females, black females, black males and white males.

2019/09/11 14:58:19

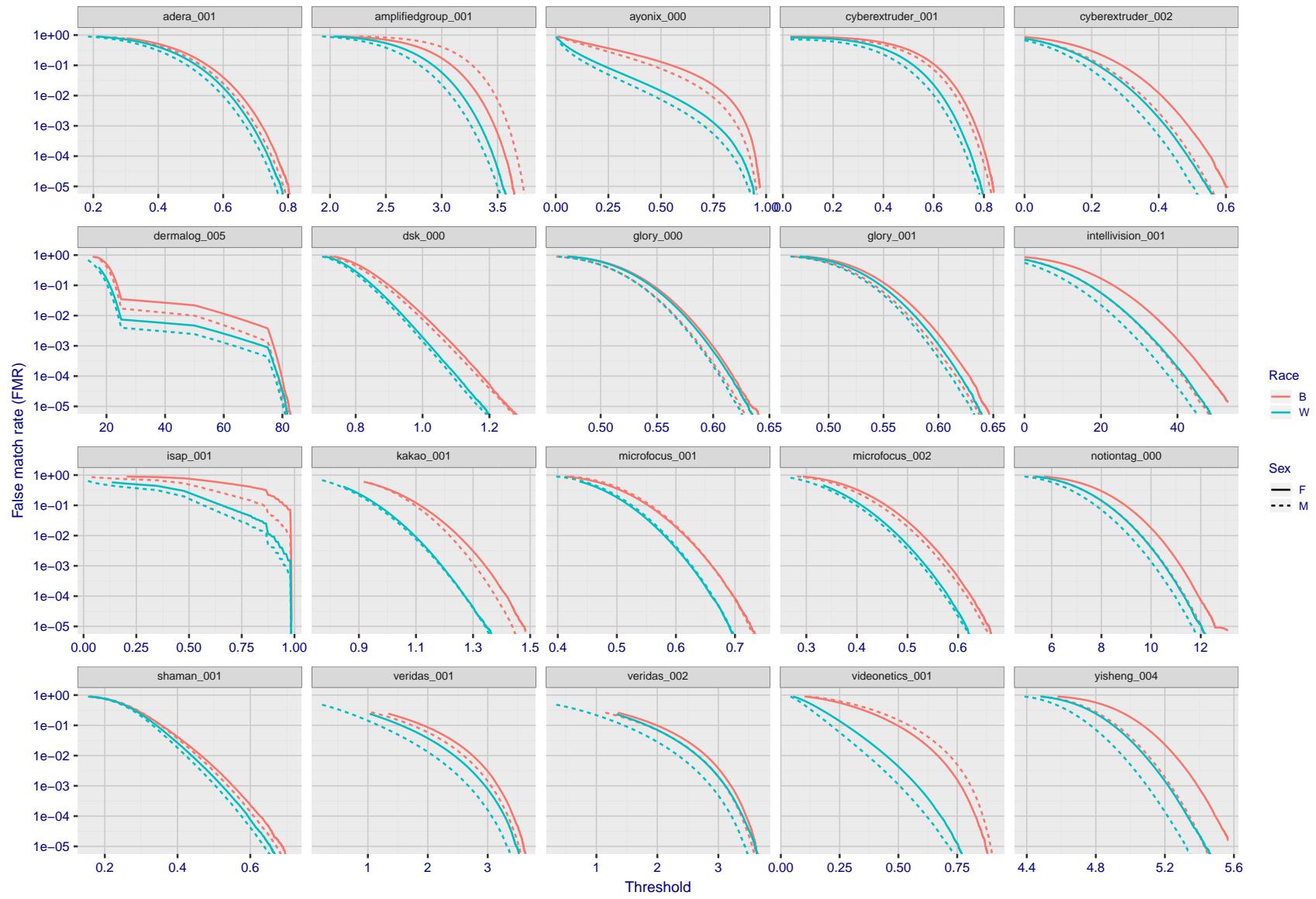


Figure 77: For the mugshot images, the false match calibration curves show false match rate vs. threshold. Separate curves appear for white females, black females, black males and white males.

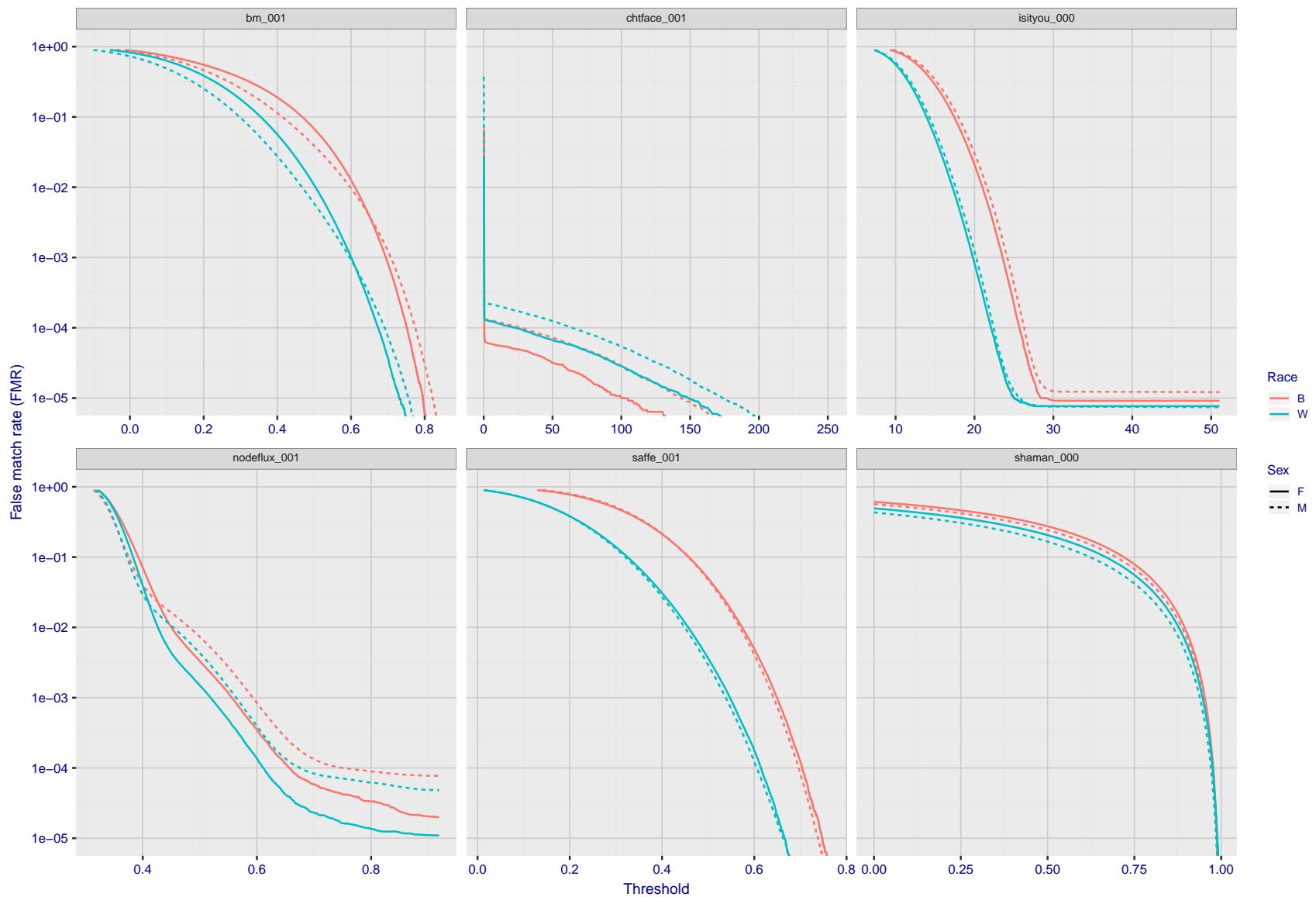


Figure 78: For the mugshot images, the false match calibration curves show false match rate vs. threshold. Separate curves appear for white females, black females, black males and white males.

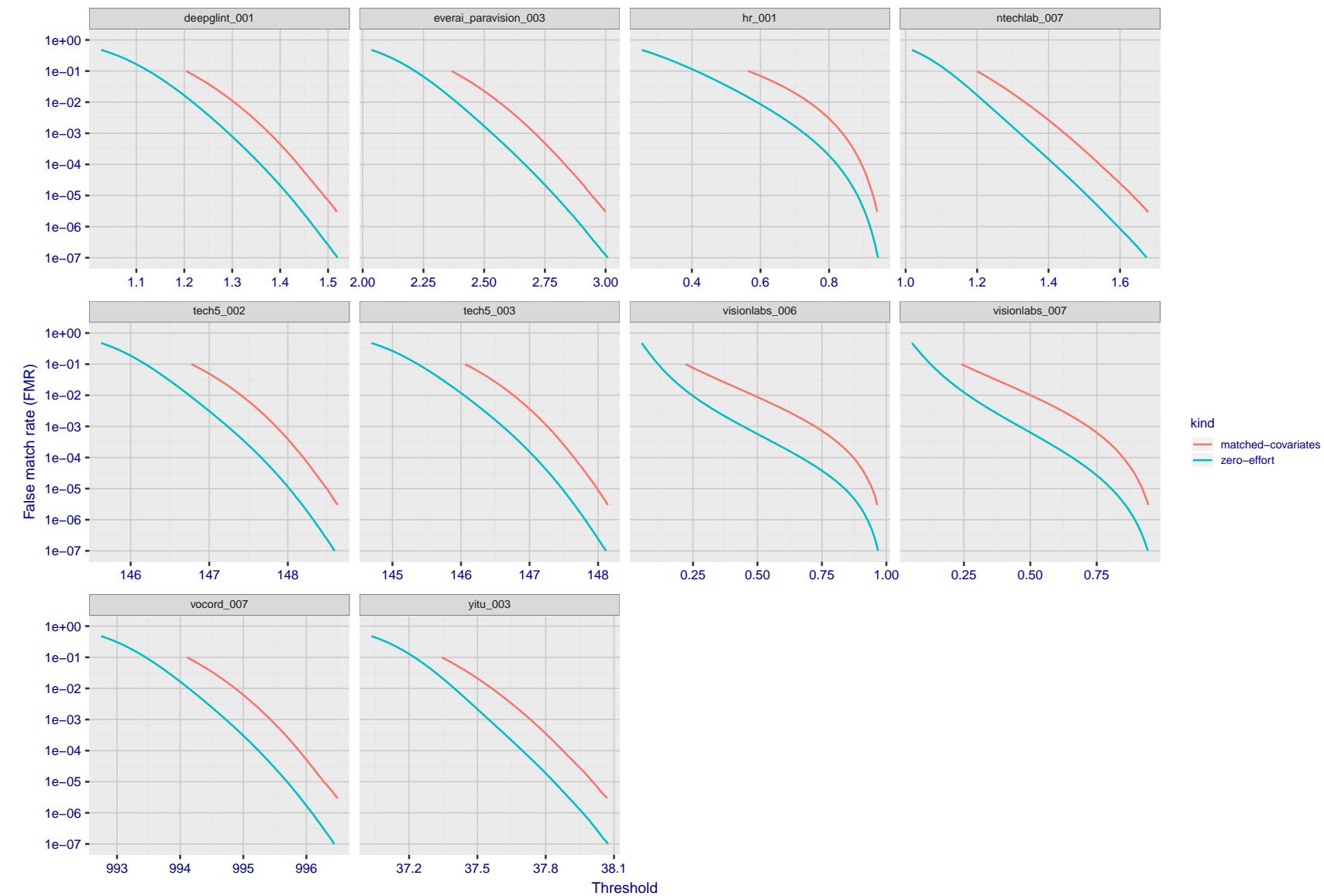


Figure 79: For the visa images, the false match calibration curves show FMR vs. threshold, T . The blue (lower) curves are for zero-effort impostors (i.e. comparing all images against all). The red (upper) curves are for persons of the same-sex, same-age, and same national-origin. This shows that FMR is underestimated (by a factor of 10 or more) by using a zero-effort impostor calculation to calibrate T . As shown later (sec. 3.6), FMR is higher for demographic-matched impostors.

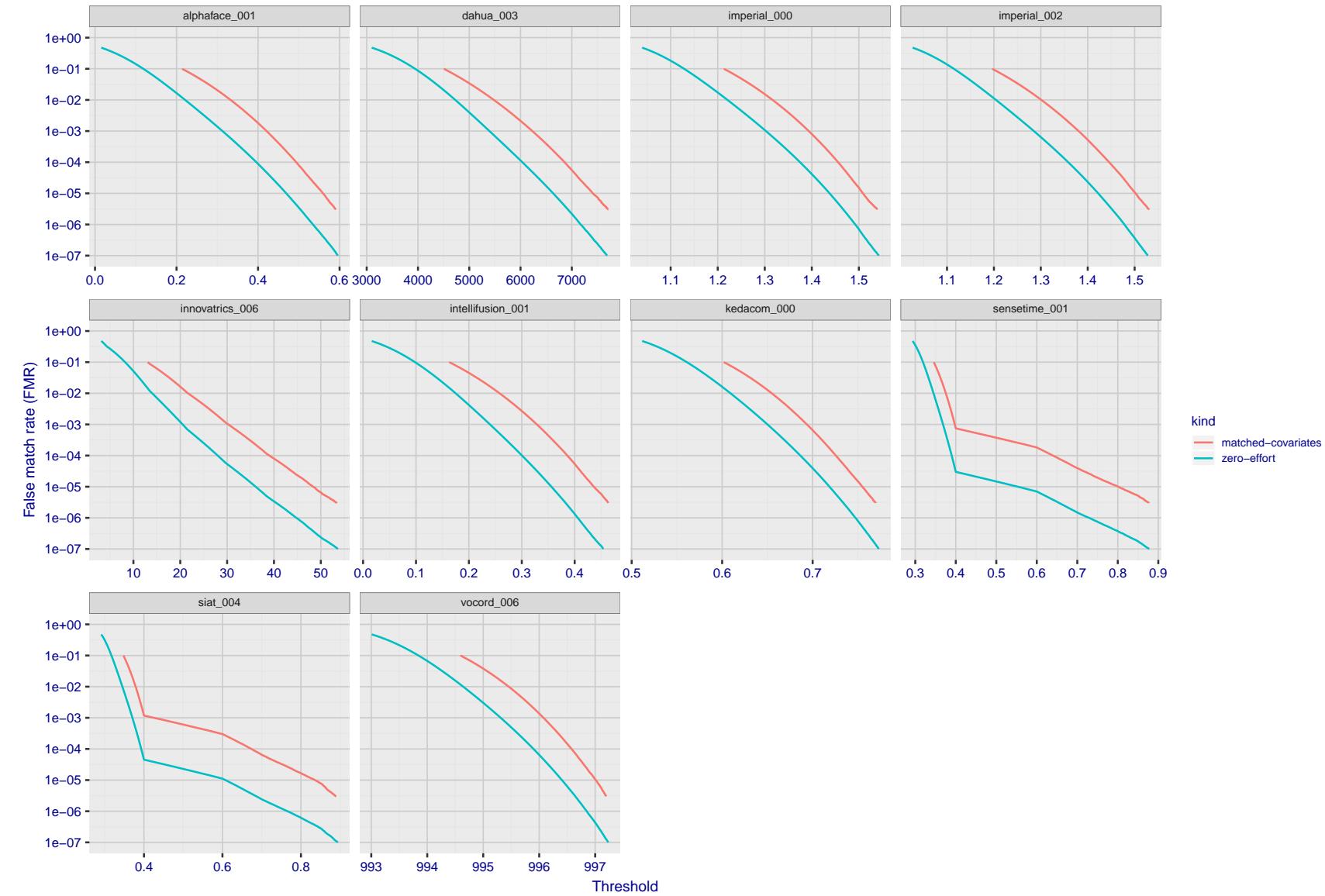


Figure 80: For the visa images, the false match calibration curves show FMR vs. threshold, T . The blue (lower) curves are for zero-effort impostors (i.e. comparing all images against all). The red (upper) curves are for persons of the same-sex, same-age, and same national-origin. This shows that FMR is underestimated (by a factor of 10 or more) by using a zero-effort impostor calculation to calibrate T . As shown later (sec. 3.6), FMR is higher for demographic-matched impostors.

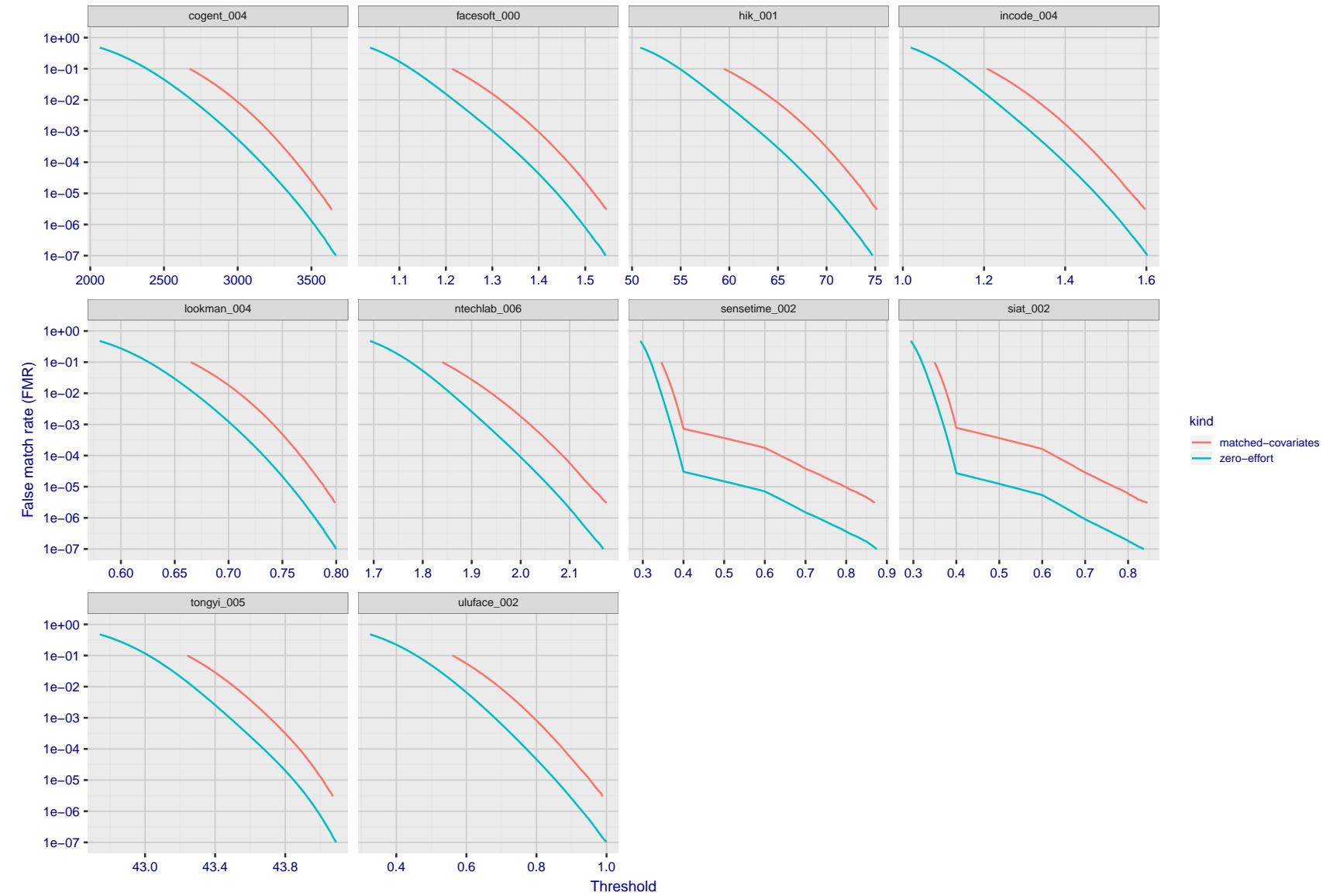


Figure 81: For the visa images, the false match calibration curves show FMR vs. threshold, T . The blue (lower) curves are for zero-effort impostors (i.e. comparing all images against all). The red (upper) curves are for persons of the same-sex, same-age, and same national-origin. This shows that FMR is underestimated (by a factor of 10 or more) by using a zero-effort impostor calculation to calibrate T . As shown later (sec. 3.6), FMR is higher for demographic-matched impostors.

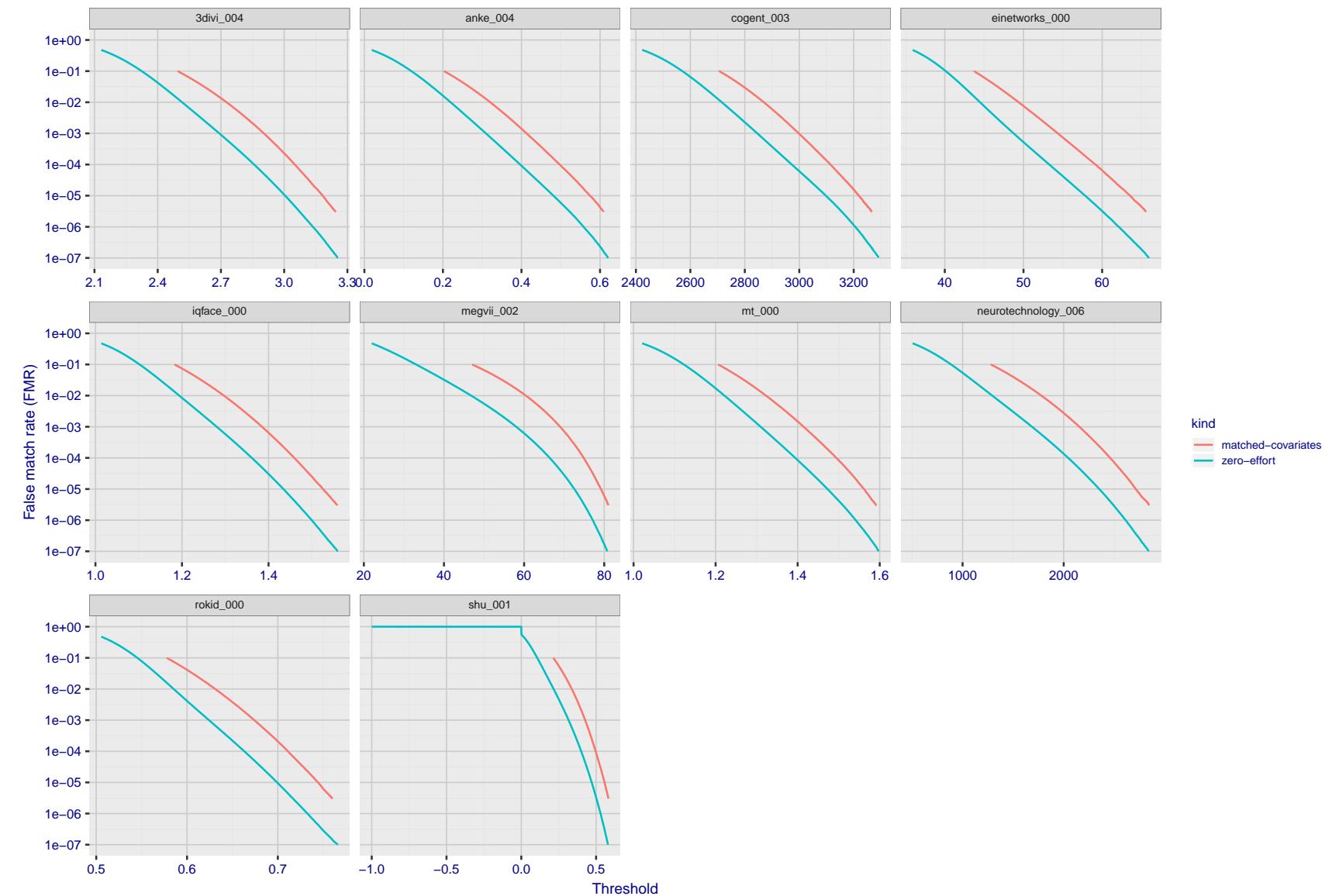


Figure 82: For the visa images, the false match calibration curves show FMR vs. threshold, T . The blue (lower) curves are for zero-effort impostors (i.e. comparing all images against all). The red (upper) curves are for persons of the same-sex, same-age, and same national-origin. This shows that FMR is underestimated (by a factor of 10 or more) by using a zero-effort impostor calculation to calibrate T . As shown later (sec. 3.6), FMR is higher for demographic-matched impostors.

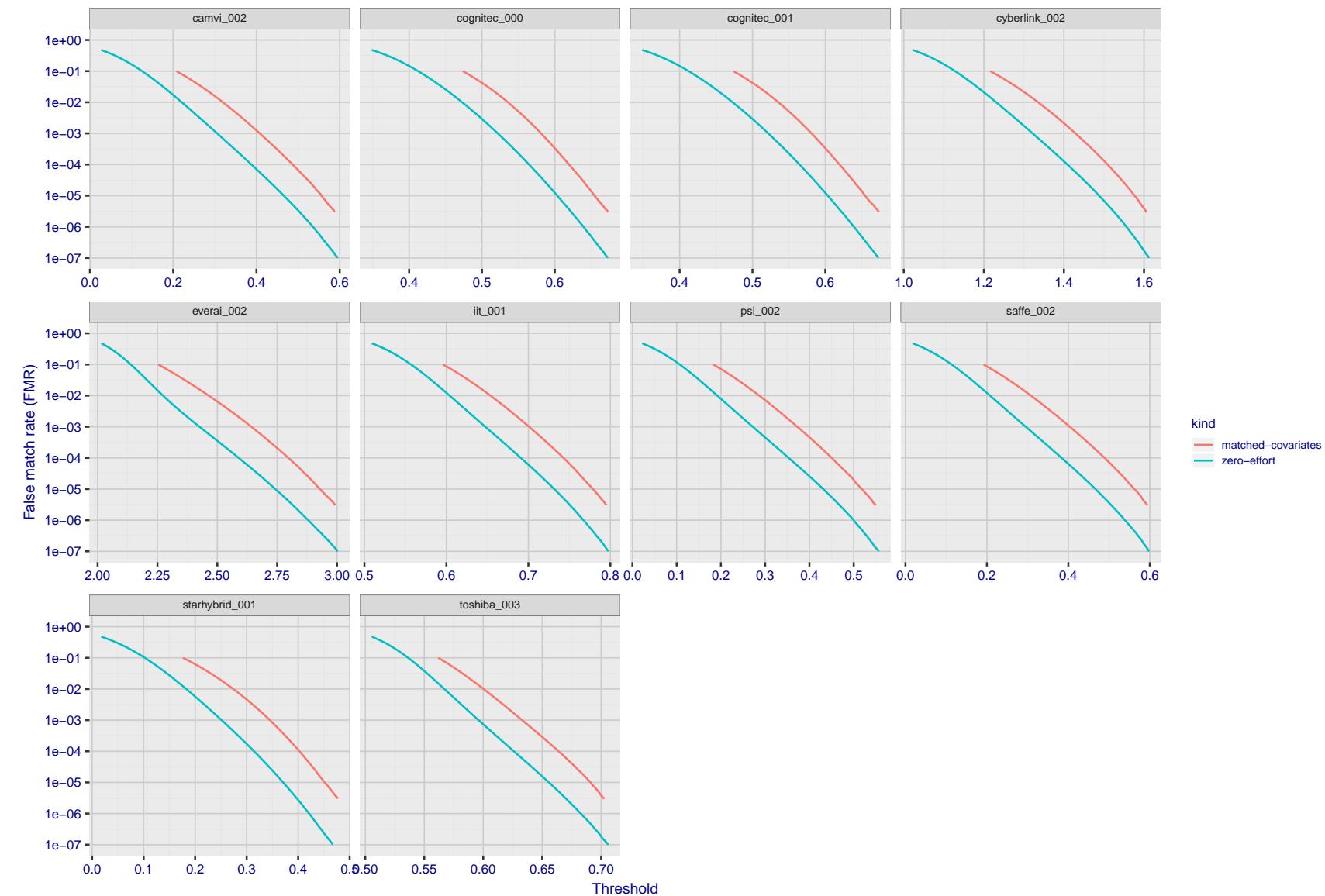


Figure 83: For the visa images, the false match calibration curves show FMR vs. threshold, T . The blue (lower) curves are for zero-effort impostors (i.e. comparing all images against all). The red (upper) curves are for persons of the same-sex, same-age, and same national-origin. This shows that FMR is underestimated (by a factor of 10 or more) by using a zero-effort impostor calculation to calibrate T . As shown later (sec. 3.6), FMR is higher for demographic-matched impostors.

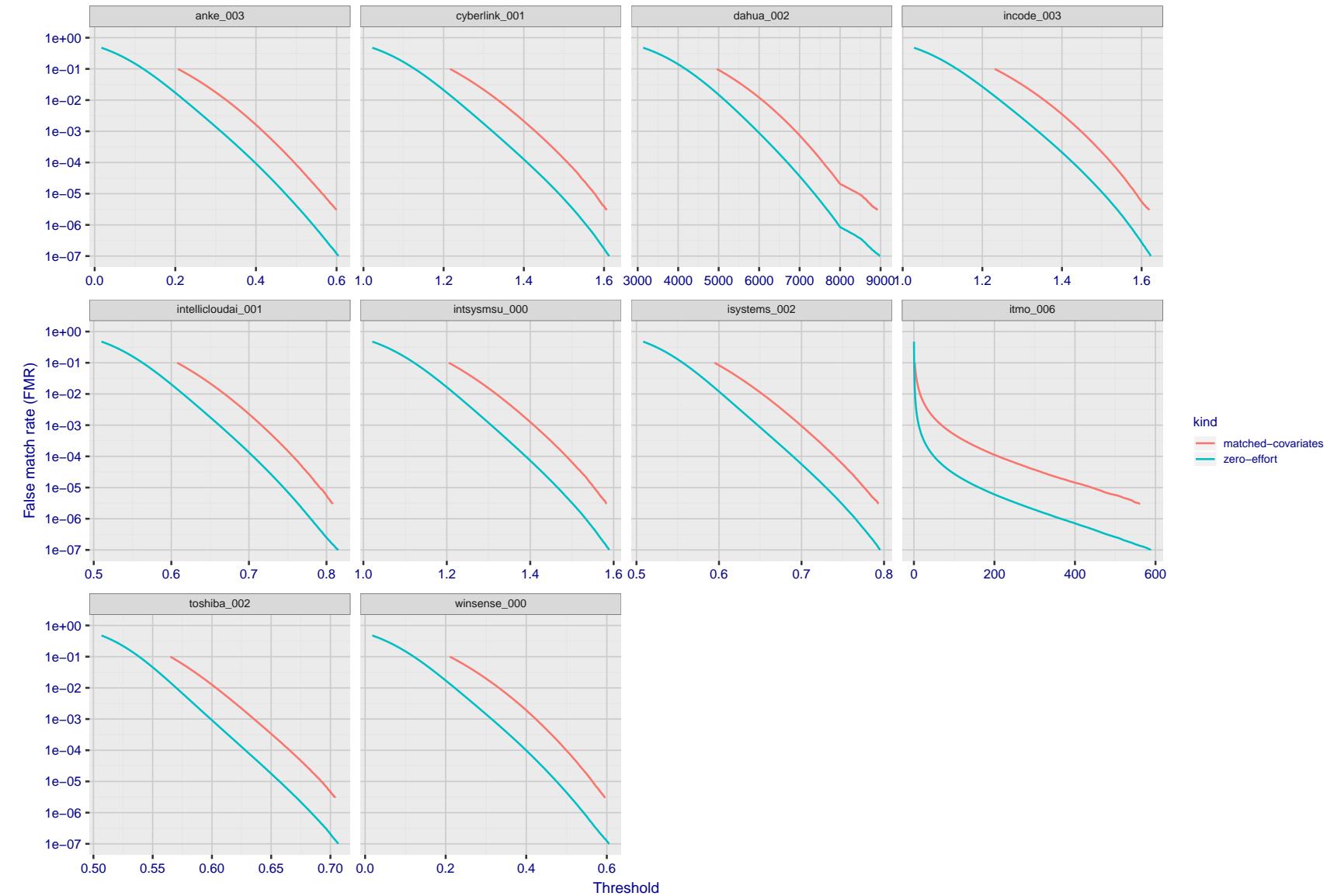


Figure 84: For the visa images, the false match calibration curves show FMR vs. threshold, T . The blue (lower) curves are for zero-effort impostors (i.e. comparing all images against all). The red (upper) curves are for persons of the same-sex, same-age, and same national-origin. This shows that FMR is underestimated (by a factor of 10 or more) by using a zero-effort impostor calculation to calibrate T . As shown later (sec. 3.6), FMR is higher for demographic-matched impostors.

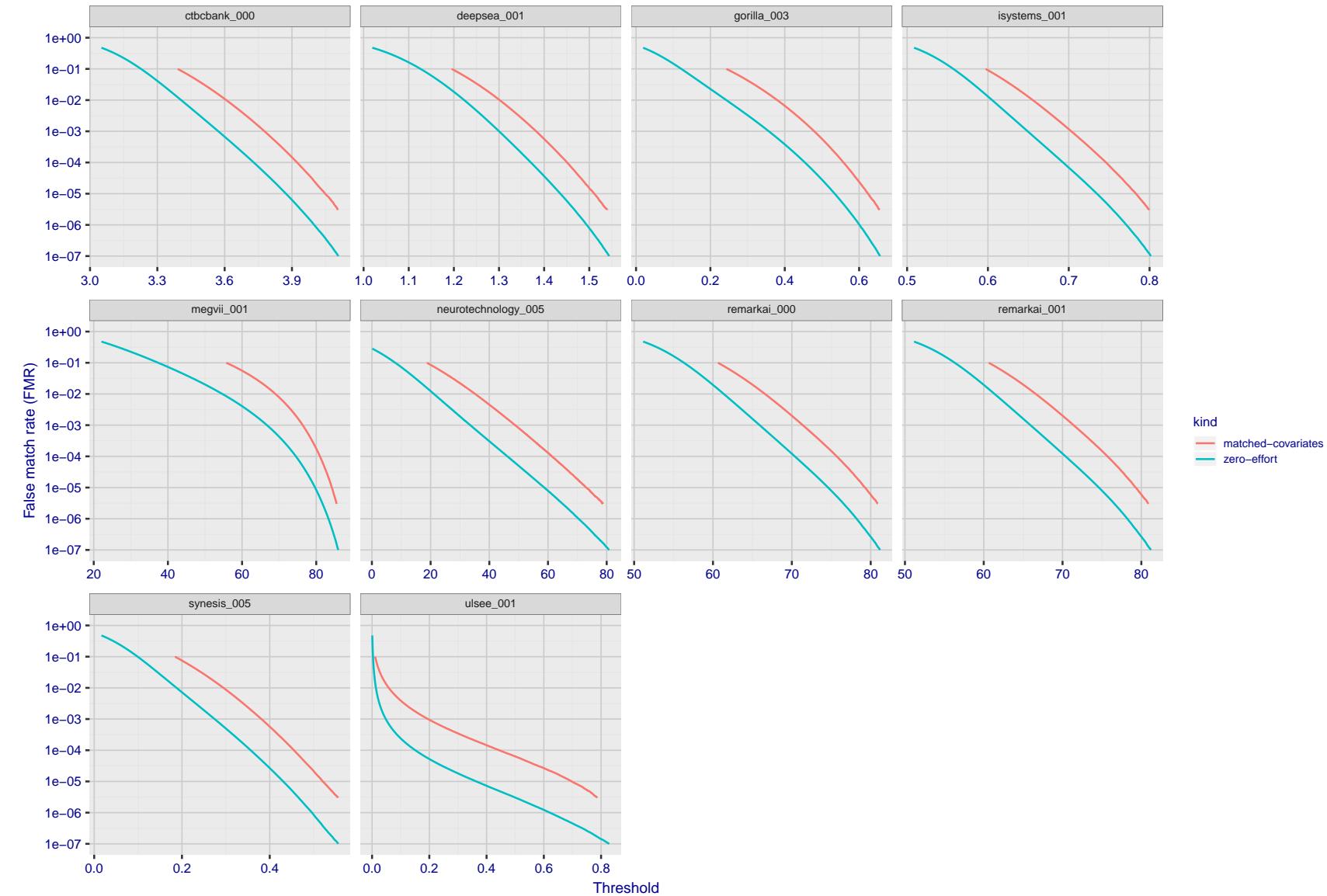


Figure 85: For the visa images, the false match calibration curves show FMR vs. threshold, T . The blue (lower) curves are for zero-effort impostors (i.e. comparing all images against all). The red (upper) curves are for persons of the same-sex, same-age, and same national-origin. This shows that FMR is underestimated (by a factor of 10 or more) by using a zero-effort impostor calculation to calibrate T . As shown later (sec. 3.6), FMR is higher for demographic-matched impostors.

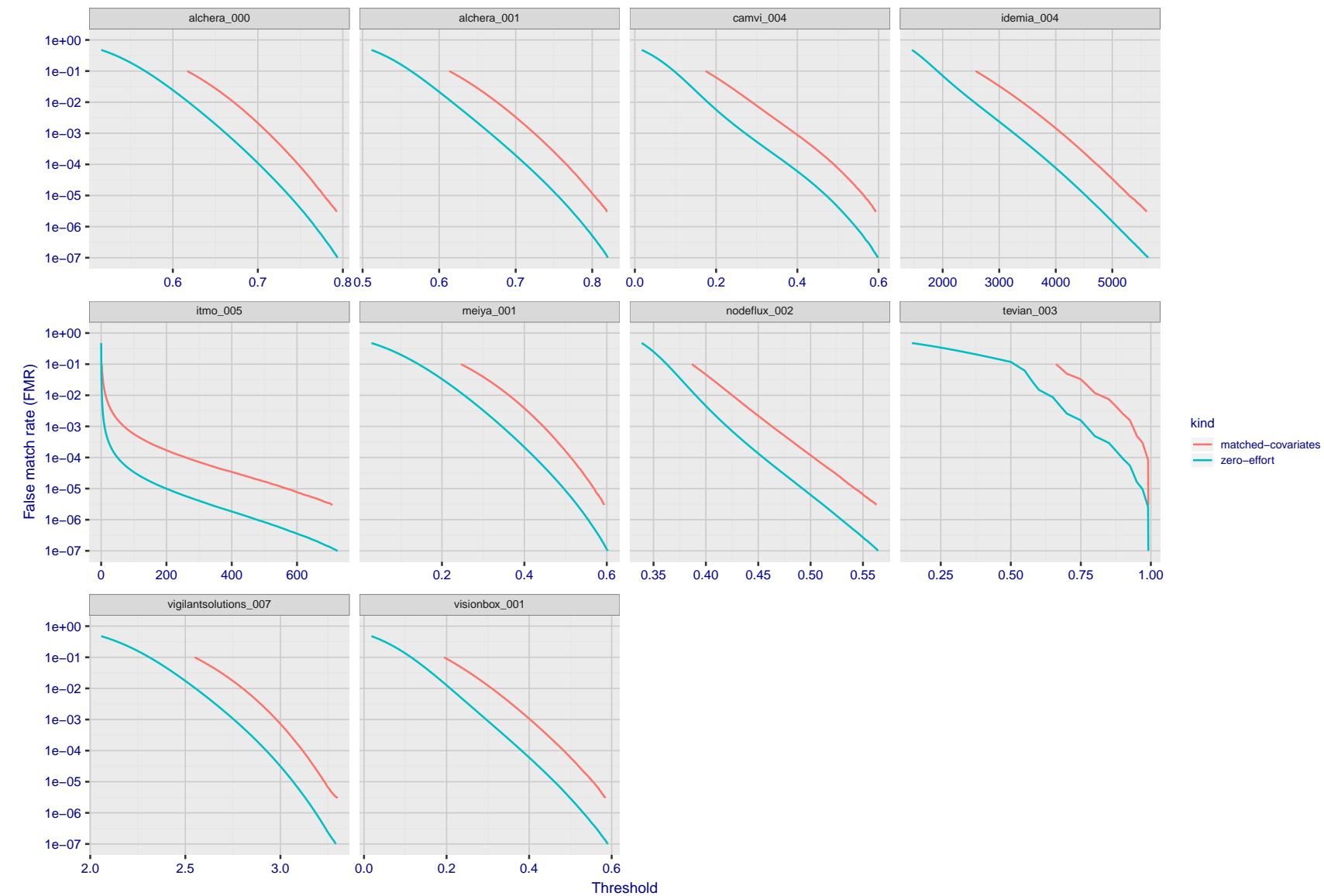


Figure 86: For the visa images, the false match calibration curves show FMR vs. threshold, T . The blue (lower) curves are for zero-effort impostors (i.e. comparing all images against all). The red (upper) curves are for persons of the same-sex, same-age, and same national-origin. This shows that FMR is underestimated (by a factor of 10 or more) by using a zero-effort impostor calculation to calibrate T . As shown later (sec. 3.6), FMR is higher for demographic-matched impostors.

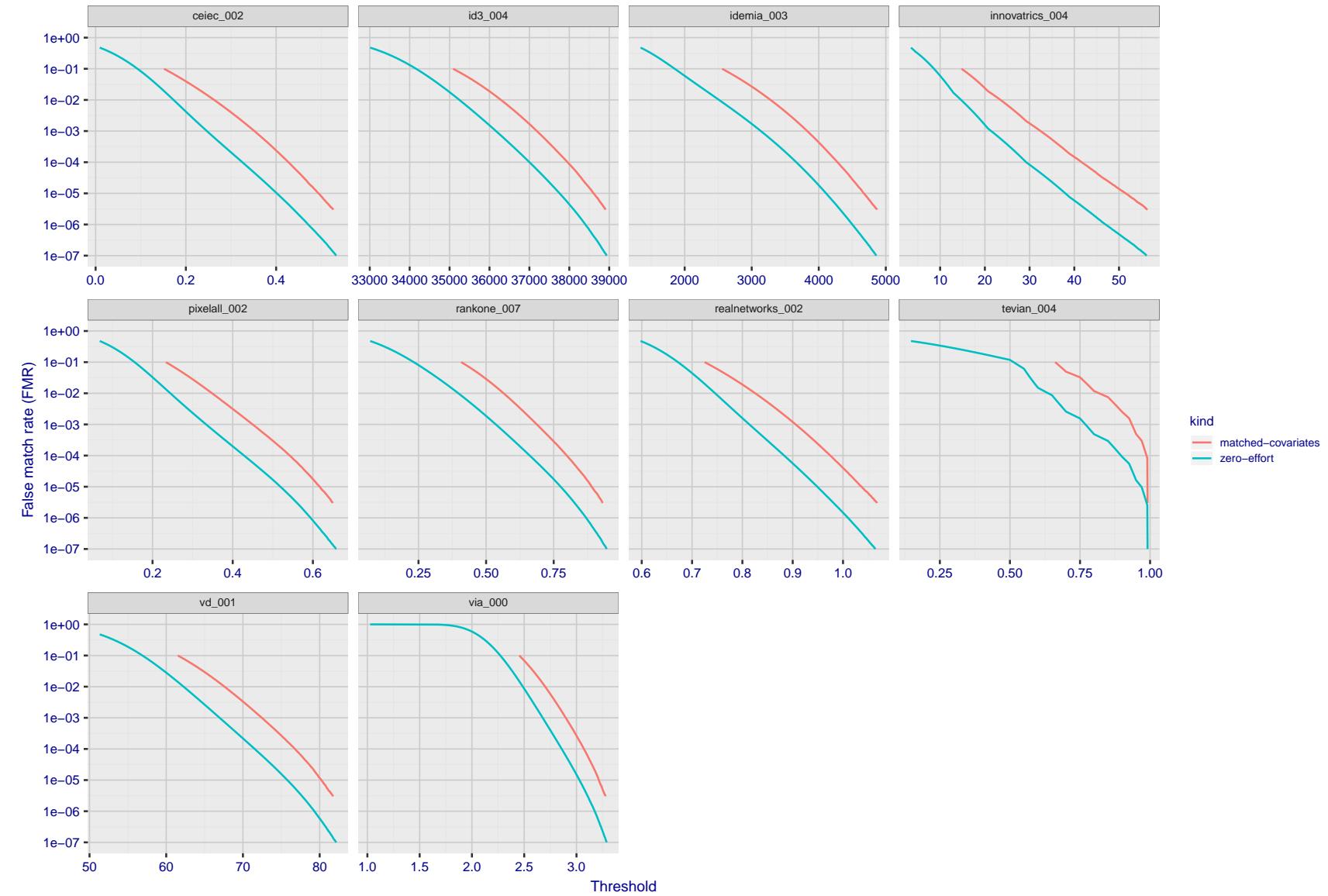


Figure 87: For the visa images, the false match calibration curves show FMR vs. threshold, T . The blue (lower) curves are for zero-effort impostors (i.e. comparing all images against all). The red (upper) curves are for persons of the same-sex, same-age, and same national-origin. This shows that FMR is underestimated (by a factor of 10 or more) by using a zero-effort impostor calculation to calibrate T . As shown later (sec. 3.6), FMR is higher for demographic-matched impostors.

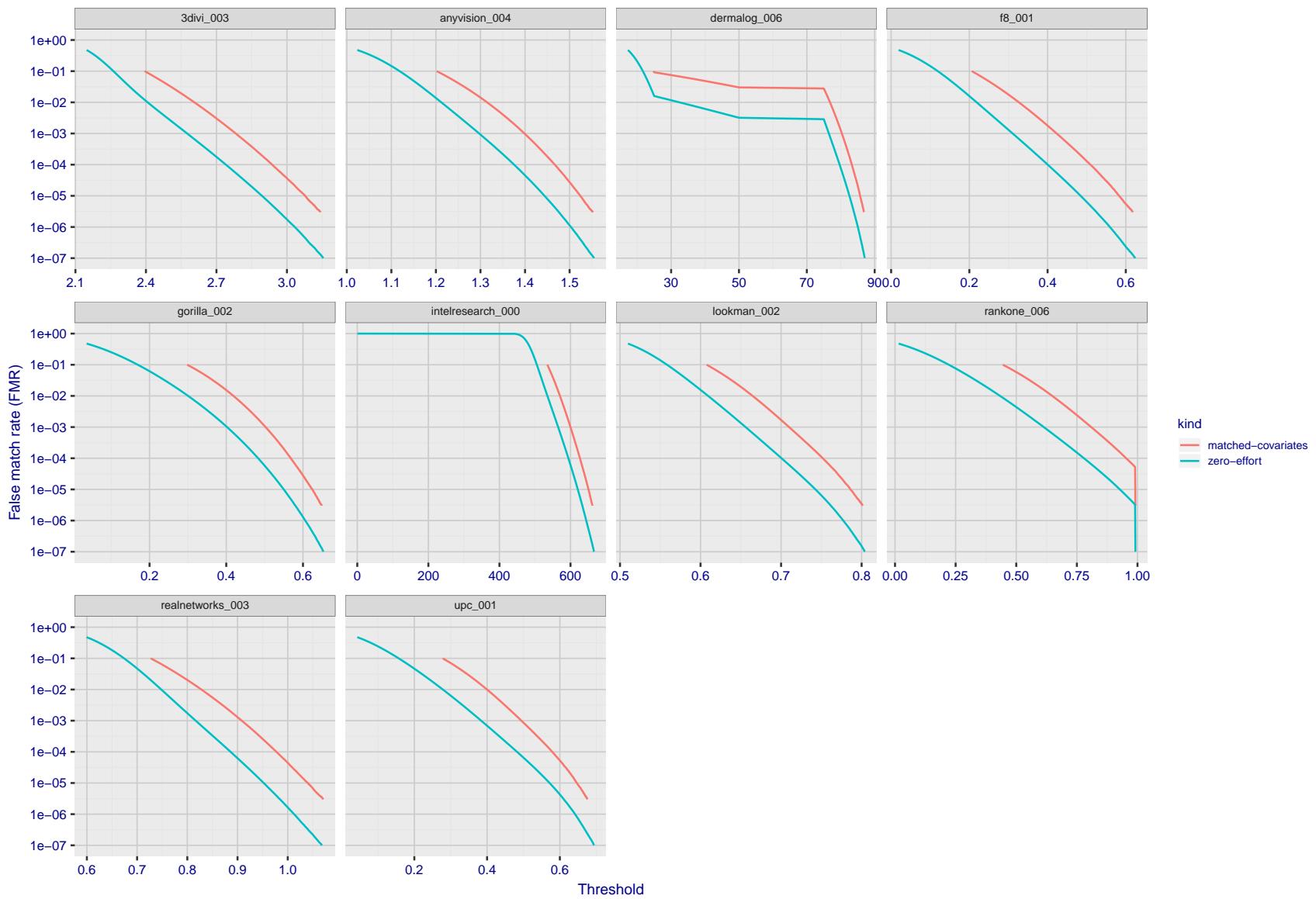


Figure 88: For the visa images, the false match calibration curves show FMR vs. threshold, T . The blue (lower) curves are for zero-effort impostors (i.e. comparing all images against all). The red (upper) curves are for persons of the same-sex, same-age, and same national-origin. This shows that FMR is underestimated (by a factor of 10 or more) by using a zero-effort impostor calculation to calibrate T . As shown later (sec. 3.6), FMR is higher for demographic-matched impostors.

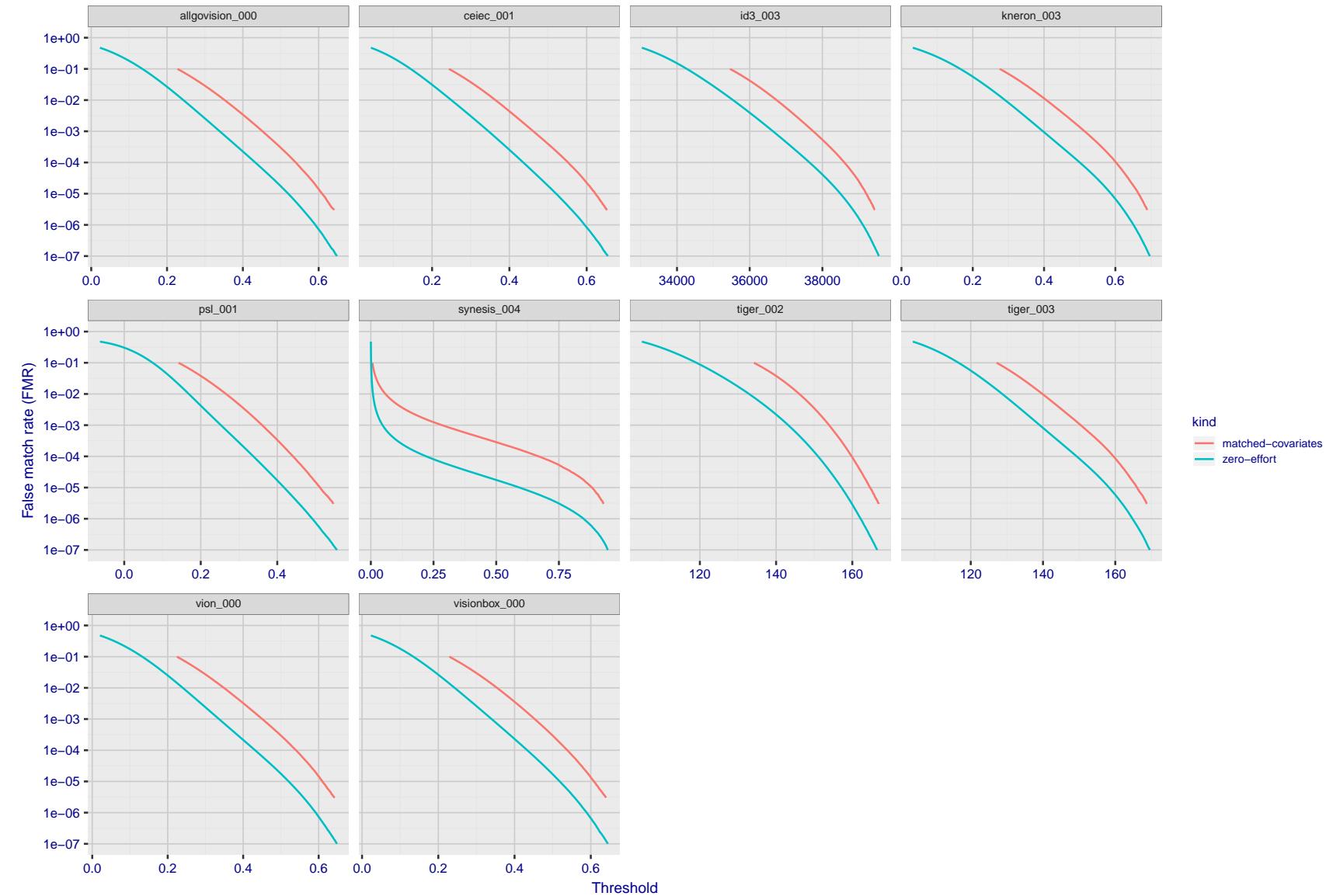


Figure 89: For the visa images, the false match calibration curves show FMR vs. threshold, T . The blue (lower) curves are for zero-effort impostors (i.e. comparing all images against all). The red (upper) curves are for persons of the same-sex, same-age, and same national-origin. This shows that FMR is underestimated (by a factor of 10 or more) by using a zero-effort impostor calculation to calibrate T . As shown later (sec. 3.6), FMR is higher for demographic-matched impostors.

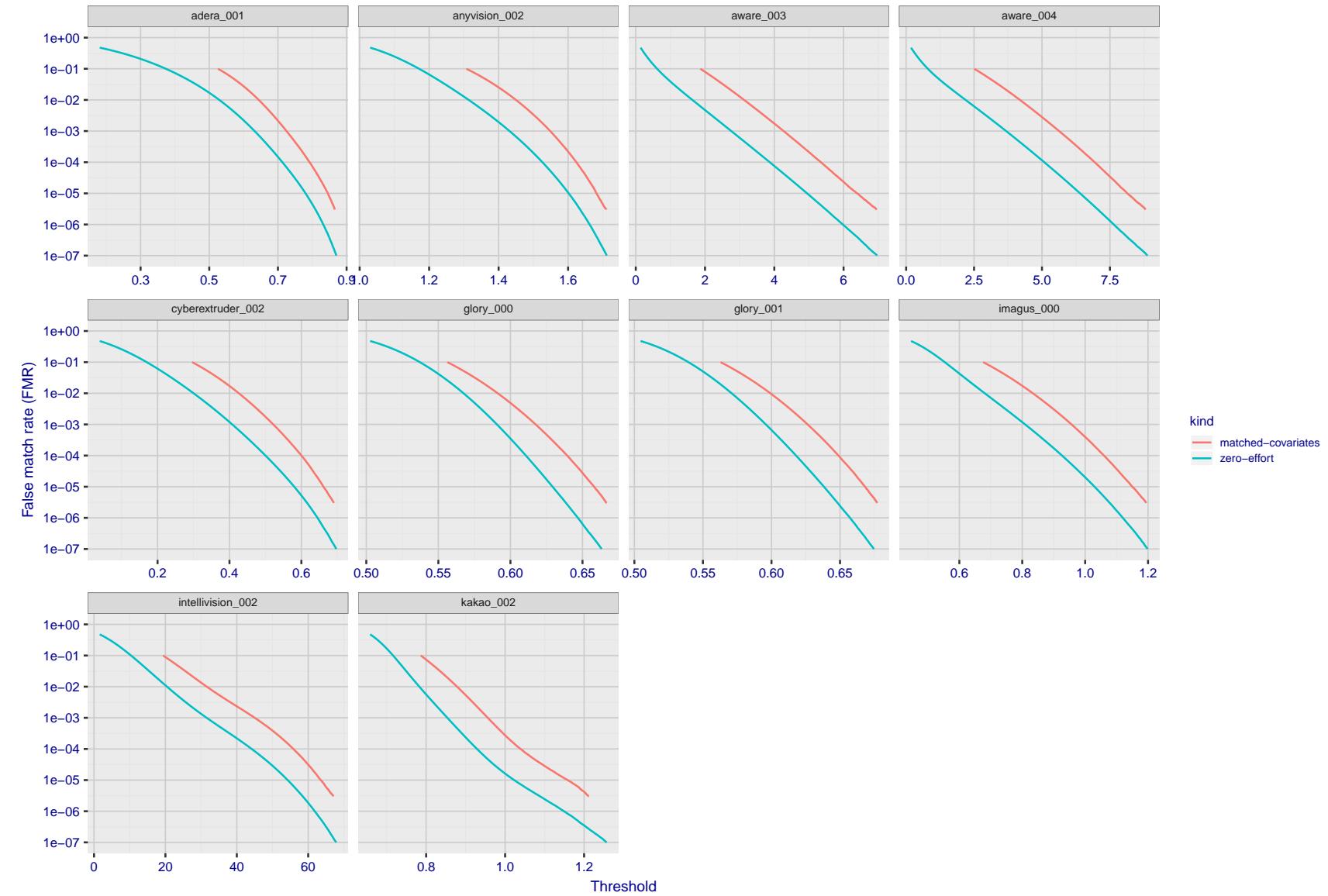


Figure 90: For the visa images, the false match calibration curves show FMR vs. threshold, T . The blue (lower) curves are for zero-effort impostors (i.e. comparing all images against all). The red (upper) curves are for persons of the same-sex, same-age, and same national-origin. This shows that FMR is underestimated (by a factor of 10 or more) by using a zero-effort impostor calculation to calibrate T . As shown later (sec. 3.6), FMR is higher for demographic-matched impostors.

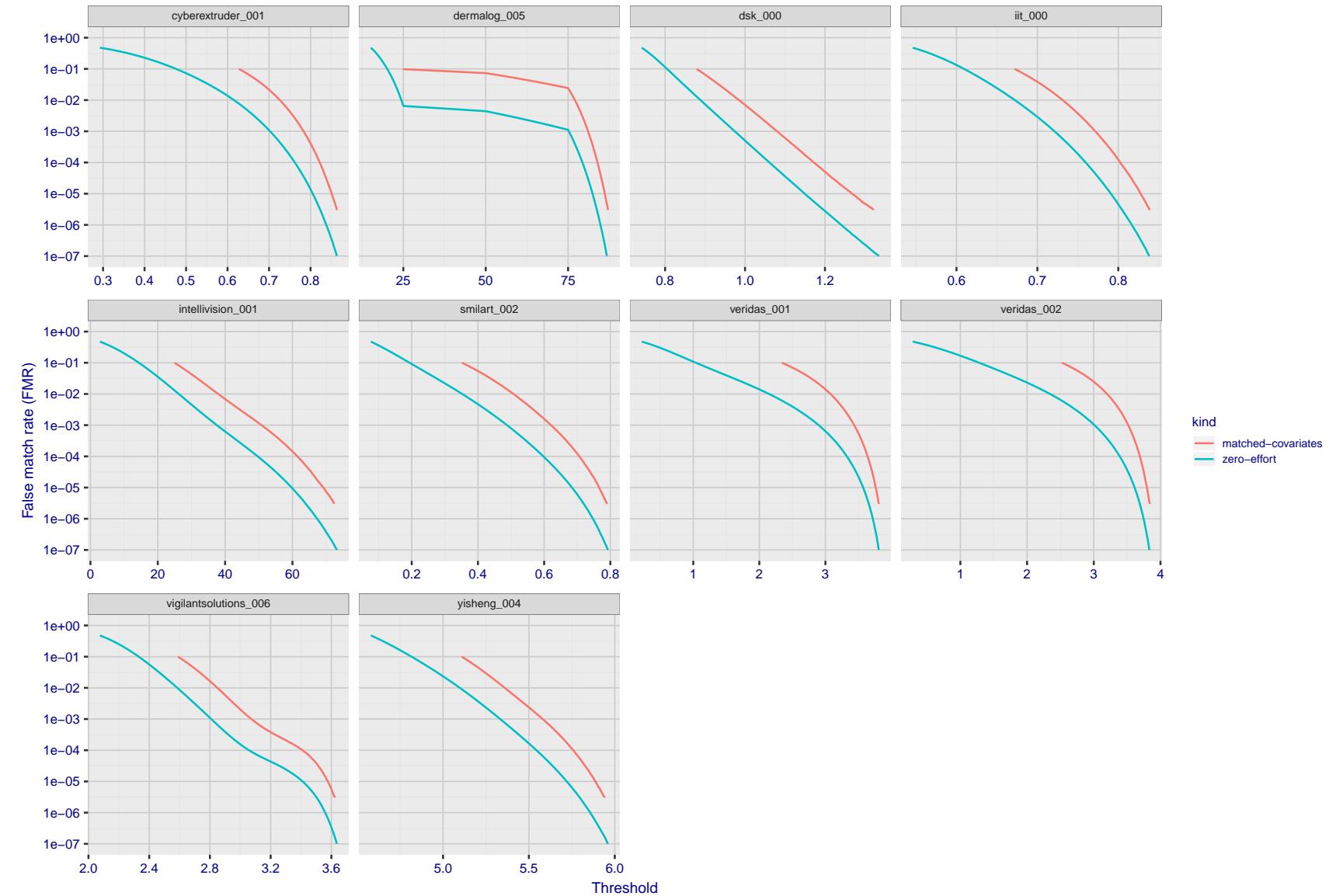


Figure 91: For the visa images, the false match calibration curves show FMR vs. threshold, T . The blue (lower) curves are for zero-effort impostors (i.e. comparing all images against all). The red (upper) curves are for persons of the same-sex, same-age, and same national-origin. This shows that FMR is underestimated (by a factor of 10 or more) by using a zero-effort impostor calculation to calibrate T . As shown later (sec. 3.6), FMR is higher for demographic-matched impostors.

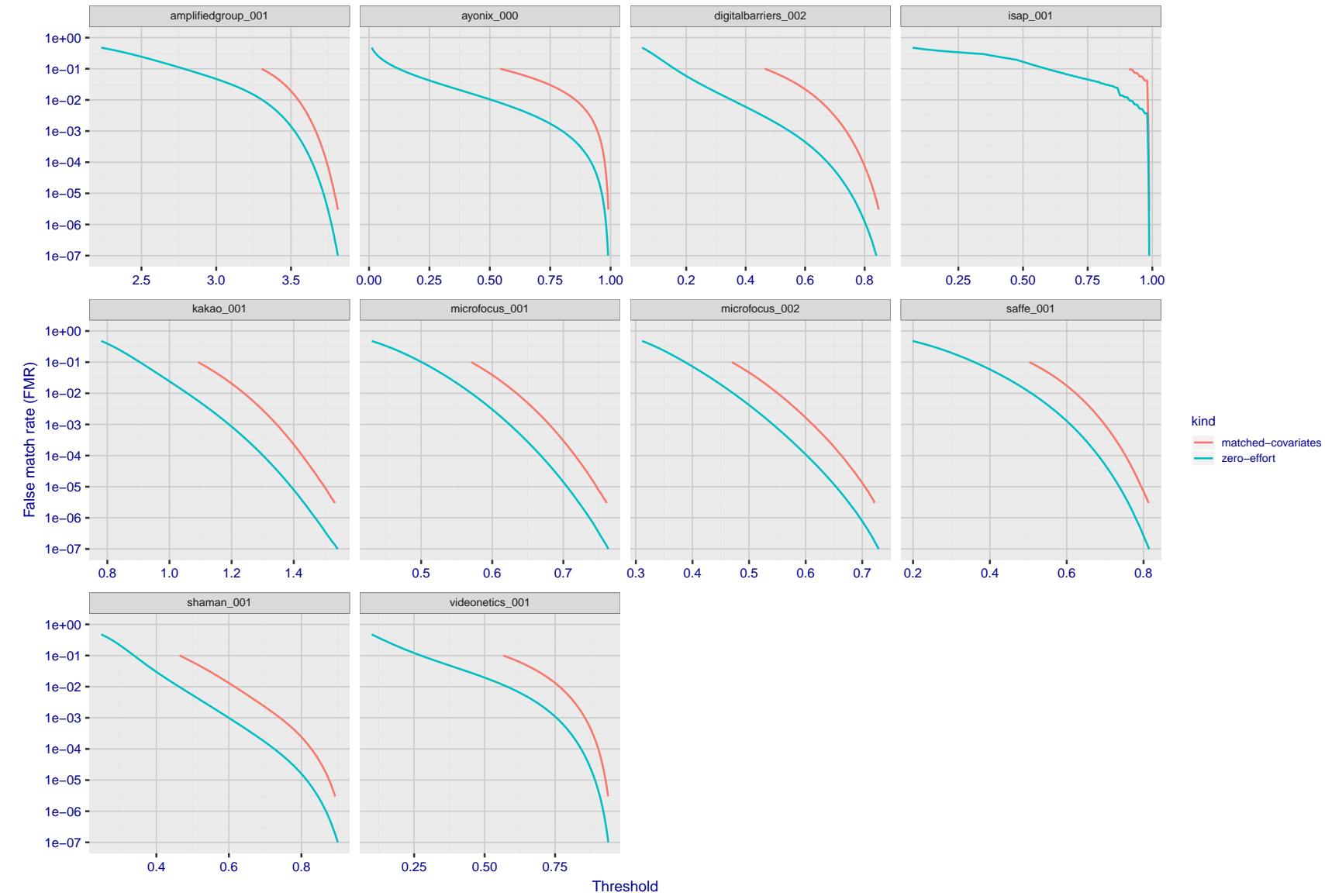


Figure 92: For the visa images, the false match calibration curves show FMR vs. threshold, T . The blue (lower) curves are for zero-effort impostors (i.e. comparing all images against all). The red (upper) curves are for persons of the same-sex, same-age, and same national-origin. This shows that FMR is underestimated (by a factor of 10 or more) by using a zero-effort impostor calculation to calibrate T . As shown later (sec. 3.6), FMR is higher for demographic-matched impostors.

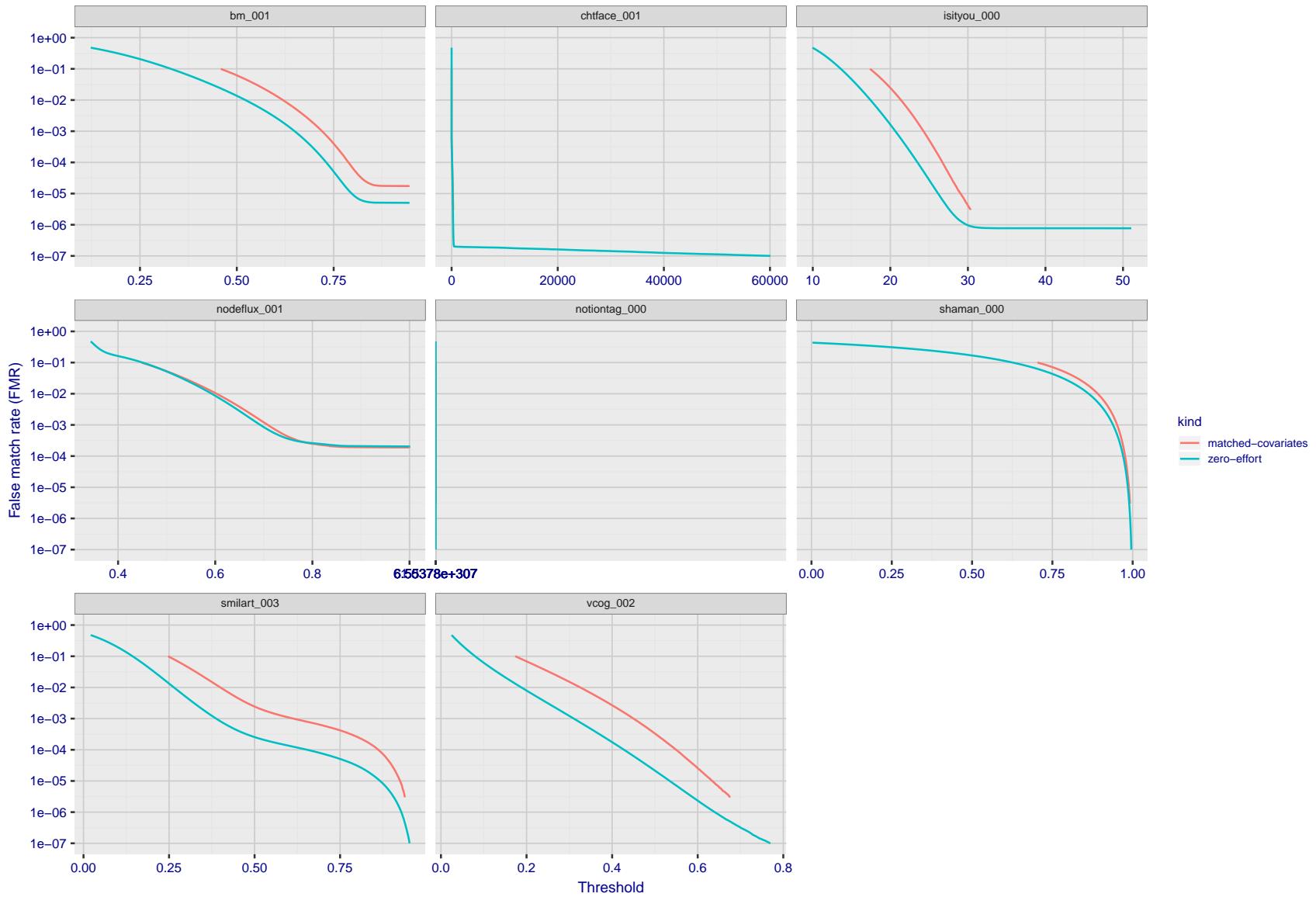


Figure 93: For the visa images, the false match calibration curves show FMR vs. threshold, T . The blue (lower) curves are for zero-effort impostors (i.e. comparing all images against all). The red (upper) curves are for persons of the same-sex, same-age, and same national-origin. This shows that FMR is underestimated (by a factor of 10 or more) by using a zero-effort impostor calculation to calibrate T . As shown later (sec. 3.6), FMR is higher for demographic-matched impostors.

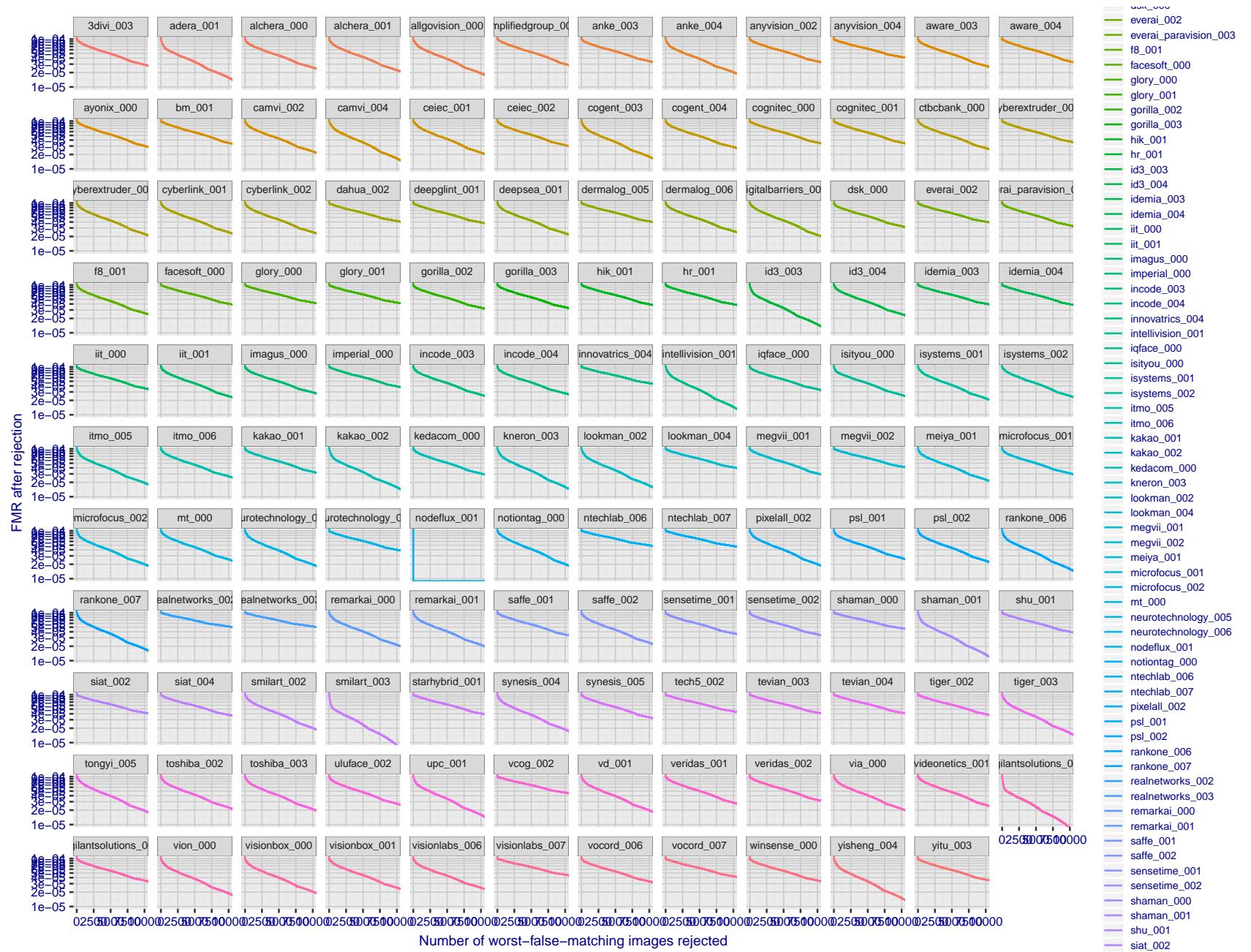


Figure 94: For the visa images, the curves show how false matches are concentrated in certain images. Specifically each line plots $FMR(k)$ with k the number of images rejected in decreasing order of how many false matches that image was involved in. $FMR(0) = 10^{-4}$. In terms of the biometric zoo, the most “wolf-ish” images are rejected first i.e. those enrollment or verification images most often involved in false matches. A flatter response is considered superior. A steeply descending response indicates that certain kinds of images false match against others, e.g. if hypothetically images of men with particular mustaches would falsely match others.

3.5 Genuine distribution stability

3.5.1 Effect of birth place on the genuine distribution

Background: Both skin tone and bone structure vary geographically. Prior studies have reported variations in FNMR and FMR.

Goal: To measure false non-match rate (FNMR) variation with country of birth.

Methods: Thresholds are determined that give $FMR = \{0.001, 0.0001\}$ over the entire impostor set. Then FNMR is measured over 1000 bootstrap replications of the genuine scores. Only those countries with at least 140 individuals are included in the analysis.

Results: Figure 107 shows FNMR by country of birth for the two thresholds.

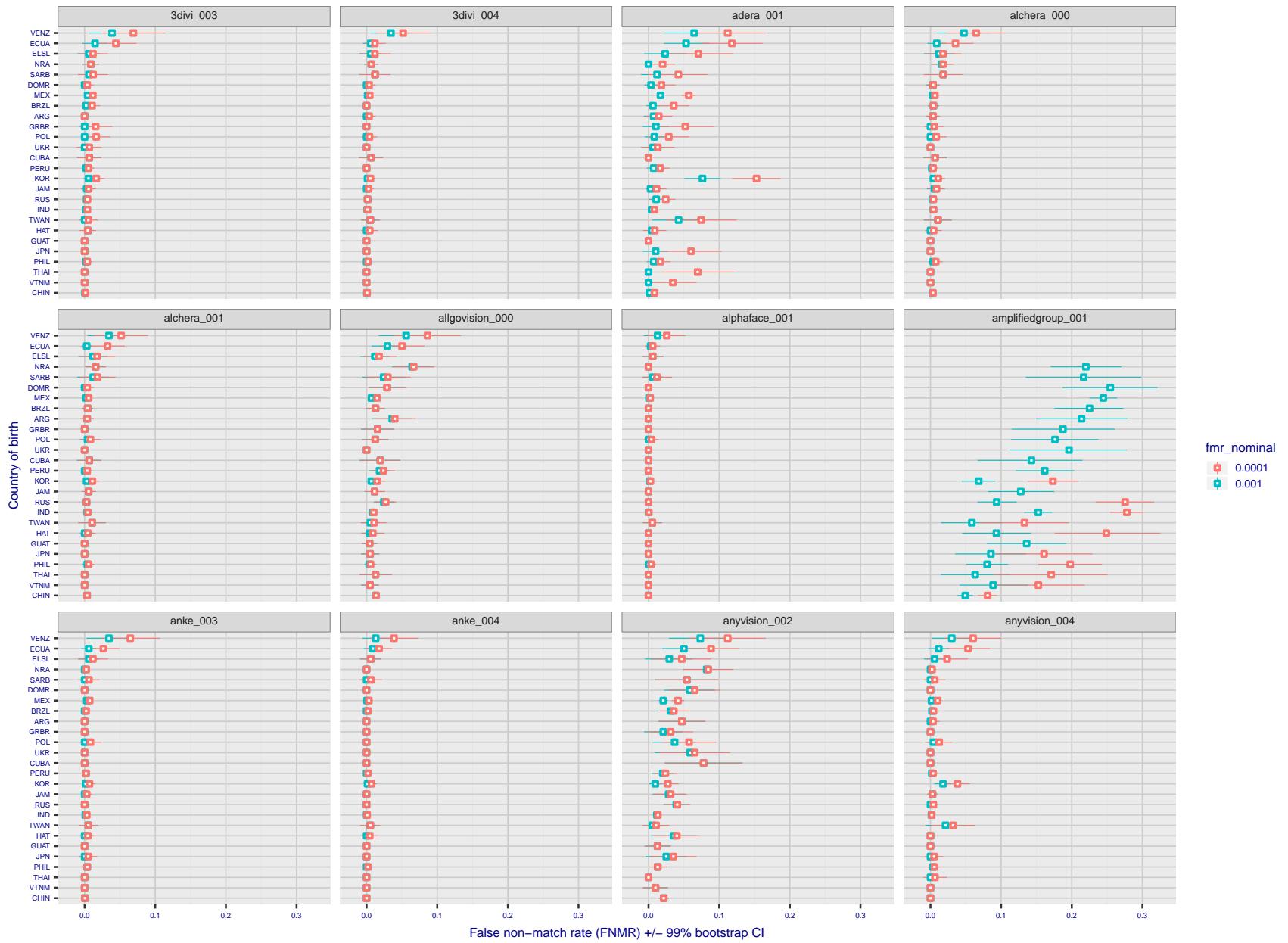


Figure 95: For the visa images, the dots show FNMR by country of birth for two globally set operating thresholds corresponding to $FMR = \{0.001, 0.0001\}$ computed over all on the order of 10^{10} impostor scores. The FMR in each bin will vary also - see subsequent impostor heatmaps in sec. 3.6.1. The figures shows an order of magnitude variation in FNMR across country of birth; these effects are likely due quality variations, then demographics like age and race. The error rates in some cases are zero, and in others the DET is flat so the error rates at the two thresholds are identical. The lines span 1% and 99% of bootstrap replicated FNMR estimates.

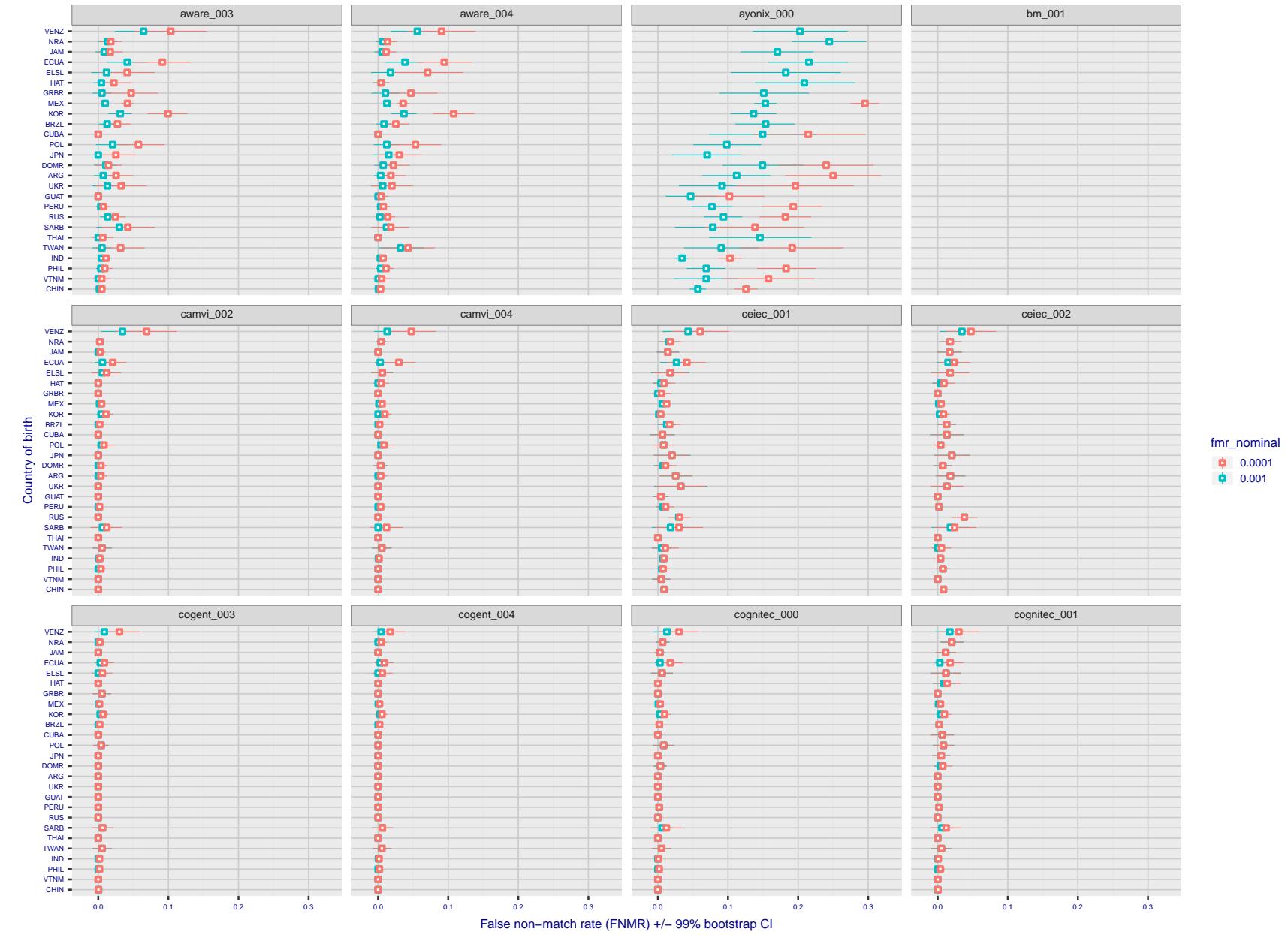


Figure 96: For the visa images, the dots show FNMR by country of birth for two globally set operating thresholds corresponding to $FMR = \{0.001, 0.0001\}$ computed over all on the order of 10^{10} impostor scores. The FMR in each bin will vary also - see subsequent impostor heatmaps in sec. 3.6.1. The figures shows an order of magnitude variation in FNMR across country of birth; these effects are likely due quality variations, then demographics like age and race. The error rates in some cases are zero, and in others the DET is flat so the error rates at the two thresholds are identical. The lines span 1% and 99% of bootstrap replicated FNMR estimates.

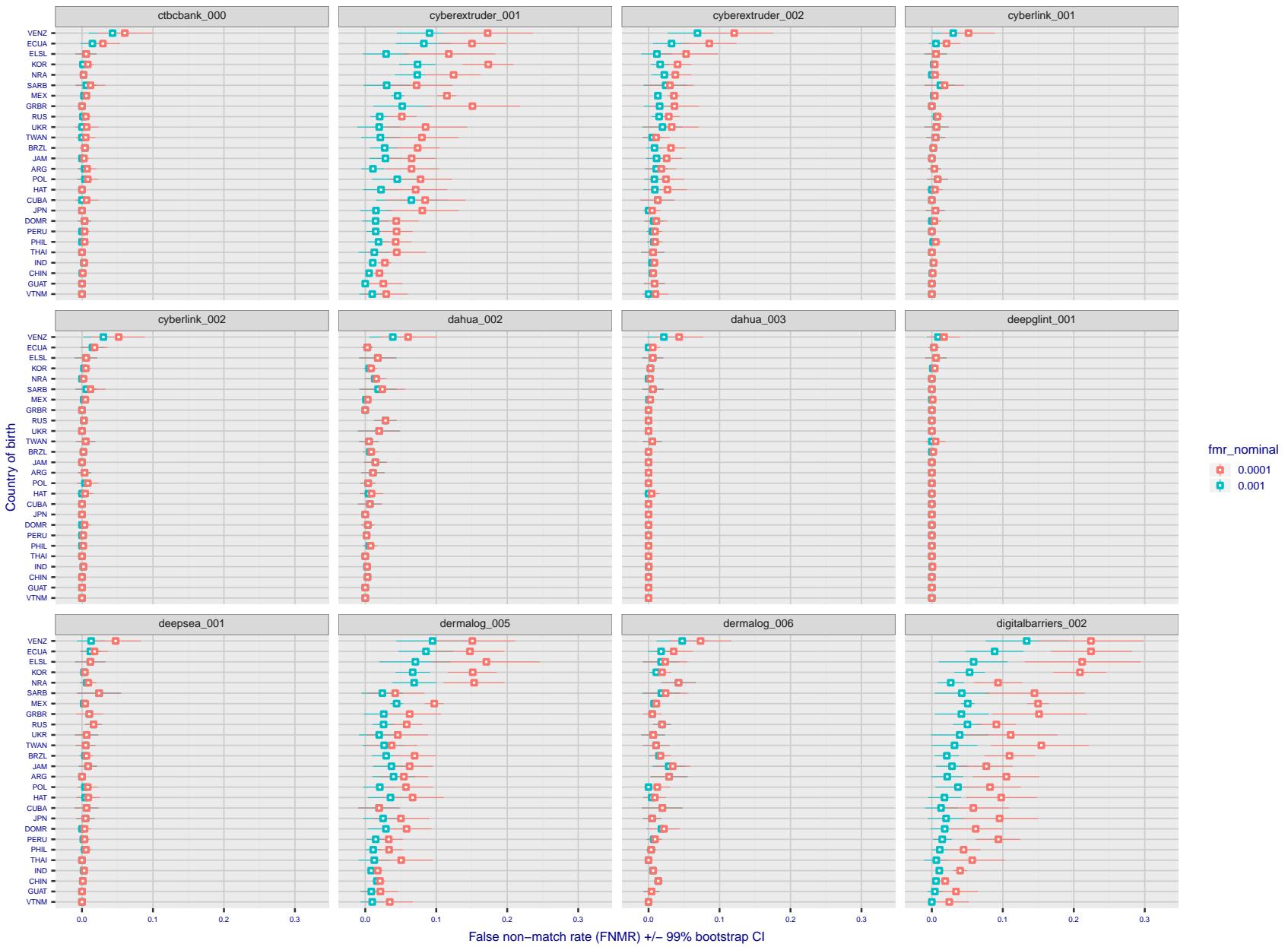


Figure 97: For the visa images, the dots show FNMR by country of birth for two globally set operating thresholds corresponding to $FMR = \{0.001, 0.0001\}$ computed over all on the order of 10^{10} impostor scores. The FMR in each bin will vary also - see subsequent impostor heatmaps in sec. 3.6.1. The figures shows an order of magnitude variation in FNMR across country of birth; these effects are likely due quality variations, then demographics like age and race. The error rates in some cases are zero, and in others the DET is flat so the error rates at the two thresholds are identical. The lines span 1% and 99% of bootstrap replicated FNMR estimates.

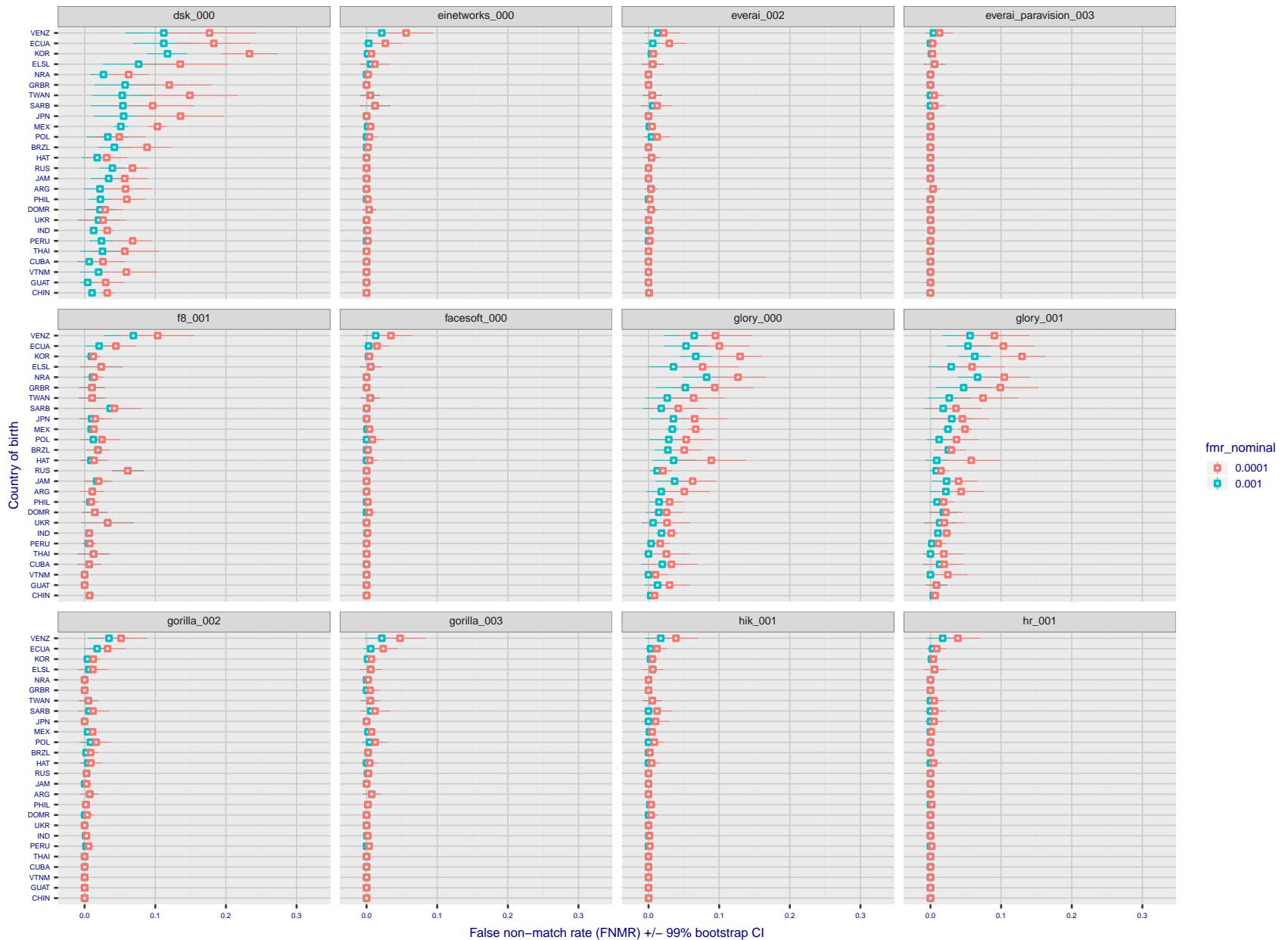


Figure 98: For the visa images, the dots show FNMR by country of birth for two globally set operating thresholds corresponding to $FMR = \{0.001, 0.0001\}$ computed over all on the order of 10^{10} impostor scores. The FMR in each bin will vary also - see subsequent impostor heatmaps in sec. 3.6.1. The figures shows an order of magnitude variation in FNMR across country of birth; these effects are likely due quality variations, then demographics like age and race. The error rates in some cases are zero, and in others the DET is flat so the error rates at the two thresholds are identical. The lines span 1% and 99% of bootstrap replicated FNMR estimates.

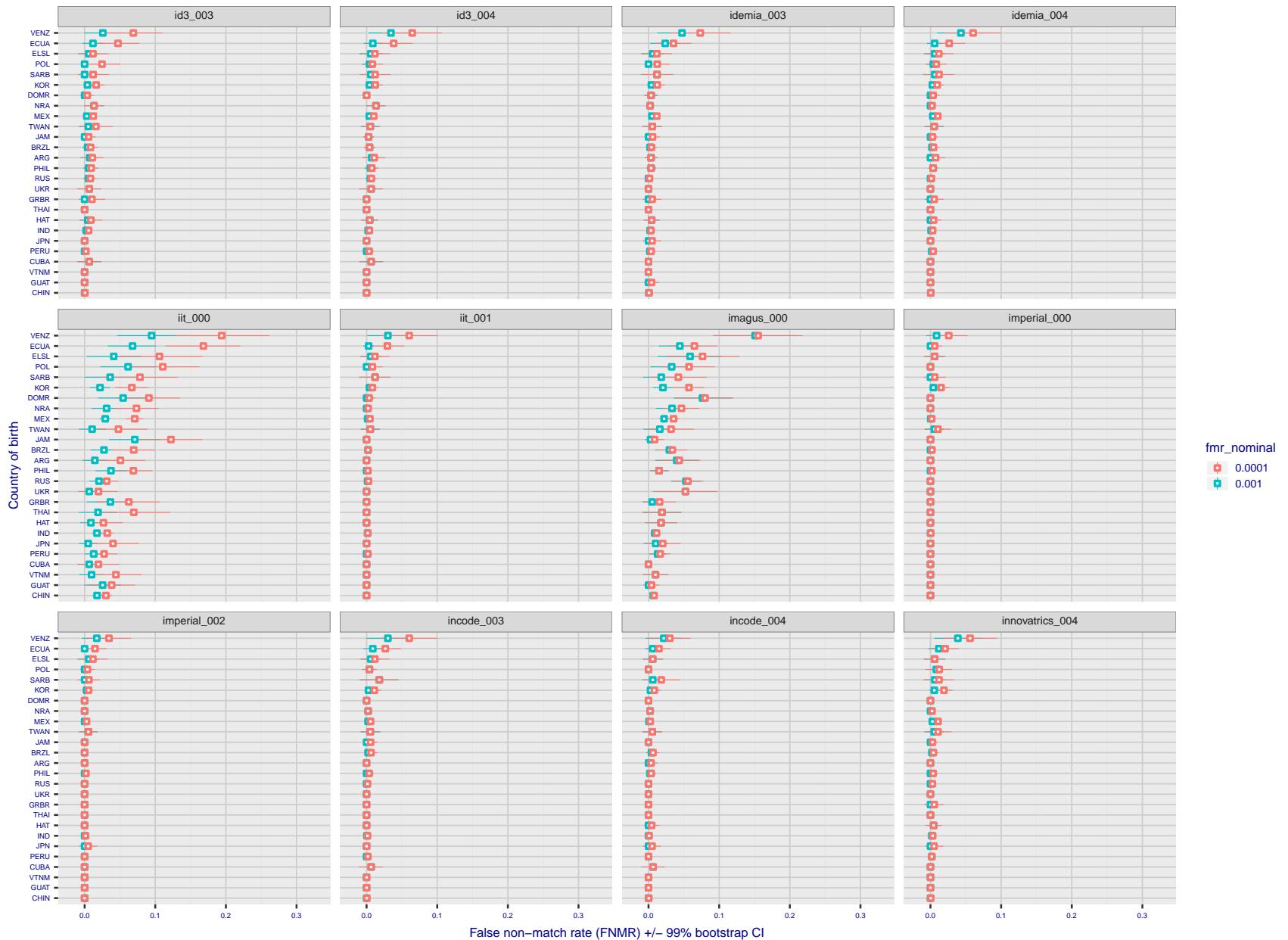


Figure 99: For the visa images, the dots show FNMR by country of birth for two globally set operating thresholds corresponding to $FMR = \{0.001, 0.0001\}$ computed over all on the order of 10^{10} impostor scores. The FMR in each bin will vary also - see subsequent impostor heatmaps in sec. 3.6.1. The figures shows an order of magnitude variation in FNMR across country of birth; these effects are likely due quality variations, then demographics like age and race. The error rates in some cases are zero, and in others the DET is flat so the error rates at the two thresholds are identical. The lines span 1% and 99% of bootstrap replicated FNMR estimates.

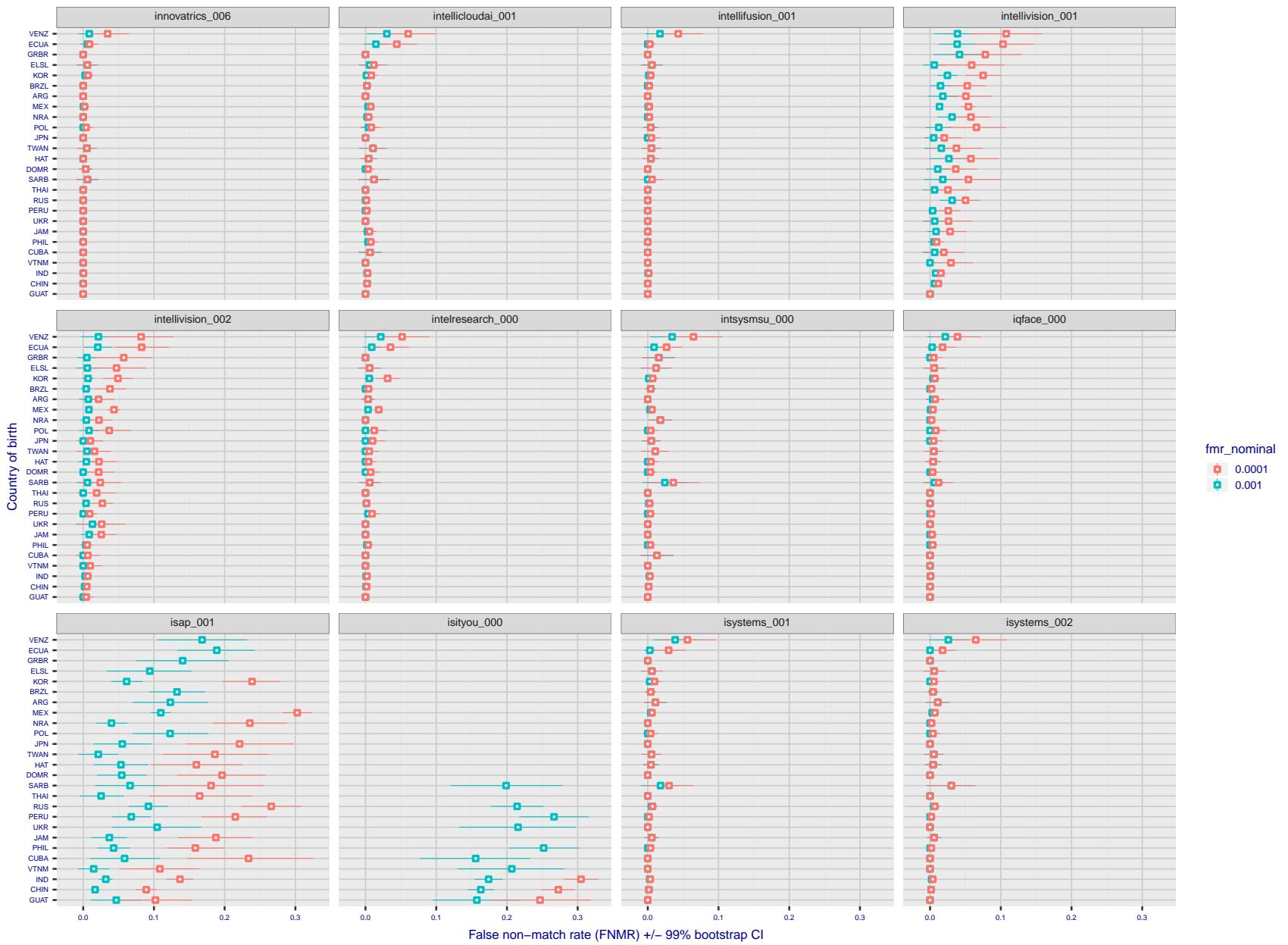


Figure 100: For the visa images, the dots show FNMR by country of birth for two globally set operating thresholds corresponding to $FMR = \{0.001, 0.0001\}$ computed over all on the order of 10^{10} impostor scores. The FMR in each bin will vary also - see subsequent impostor heatmaps in sec. 3.6.1. The figures shows an order of magnitude variation in FNMR across country of birth; these effects are likely due quality variations, then demographics like age and race. The error rates in some cases are zero, and in others the DET is flat so the error rates at the two thresholds are identical. The lines span 1% and 99% of bootstrap replicated FNMR estimates.

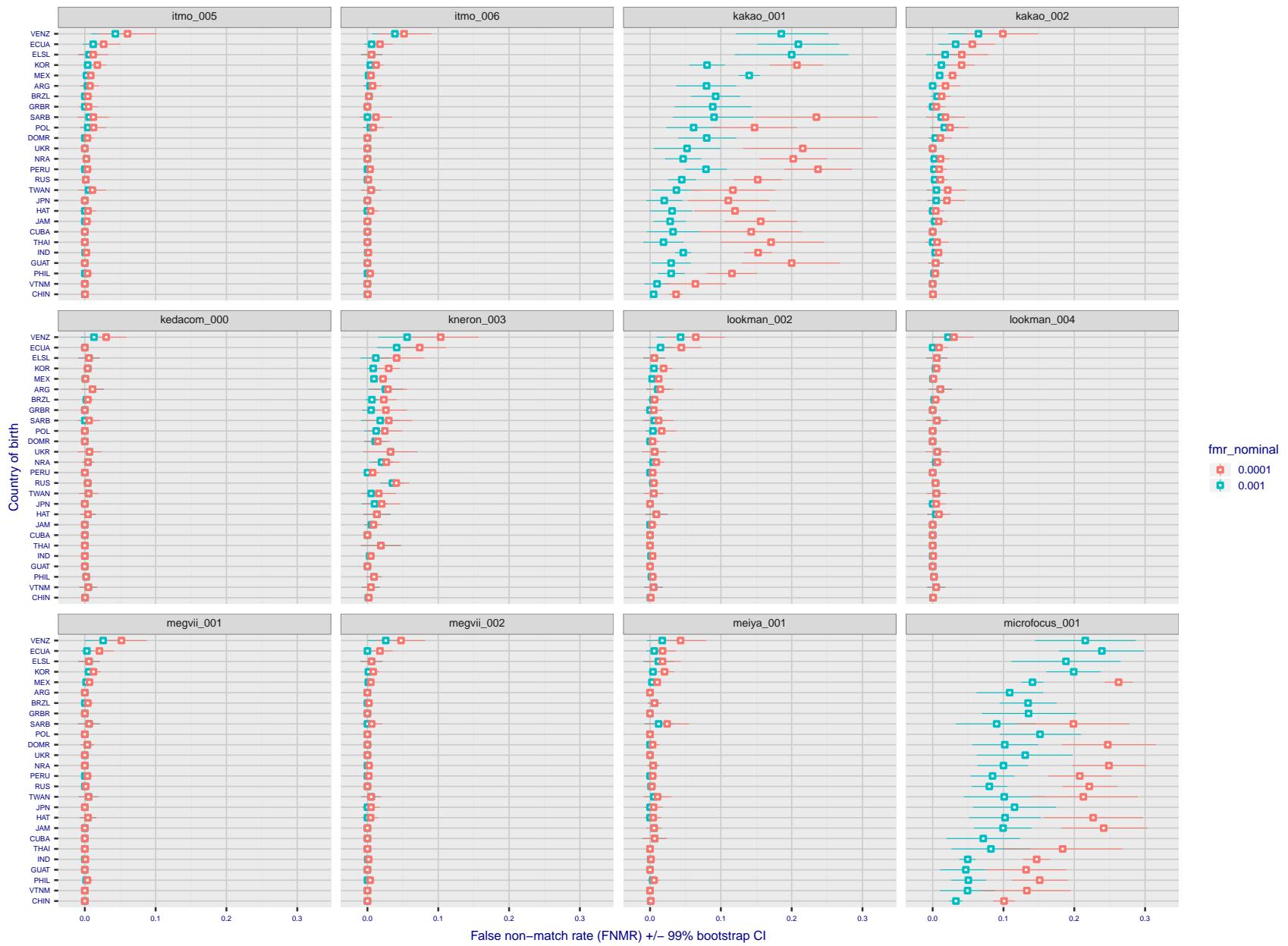


Figure 101: For the visa images, the dots show FNMR by country of birth for two globally set operating thresholds corresponding to $FMR = \{0.001, 0.0001\}$ computed over all on the order of 10^{10} impostor scores. The FMR in each bin will vary also - see subsequent impostor heatmaps in sec. 3.6.1. The figures shows an order of magnitude variation in FNMR across country of birth; these effects are likely due quality variations, then demographics like age and race. The error rates in some cases are zero, and in others the DET is flat so the error rates at the two thresholds are identical. The lines span 1% and 99% of bootstrap replicated FNMR estimates.

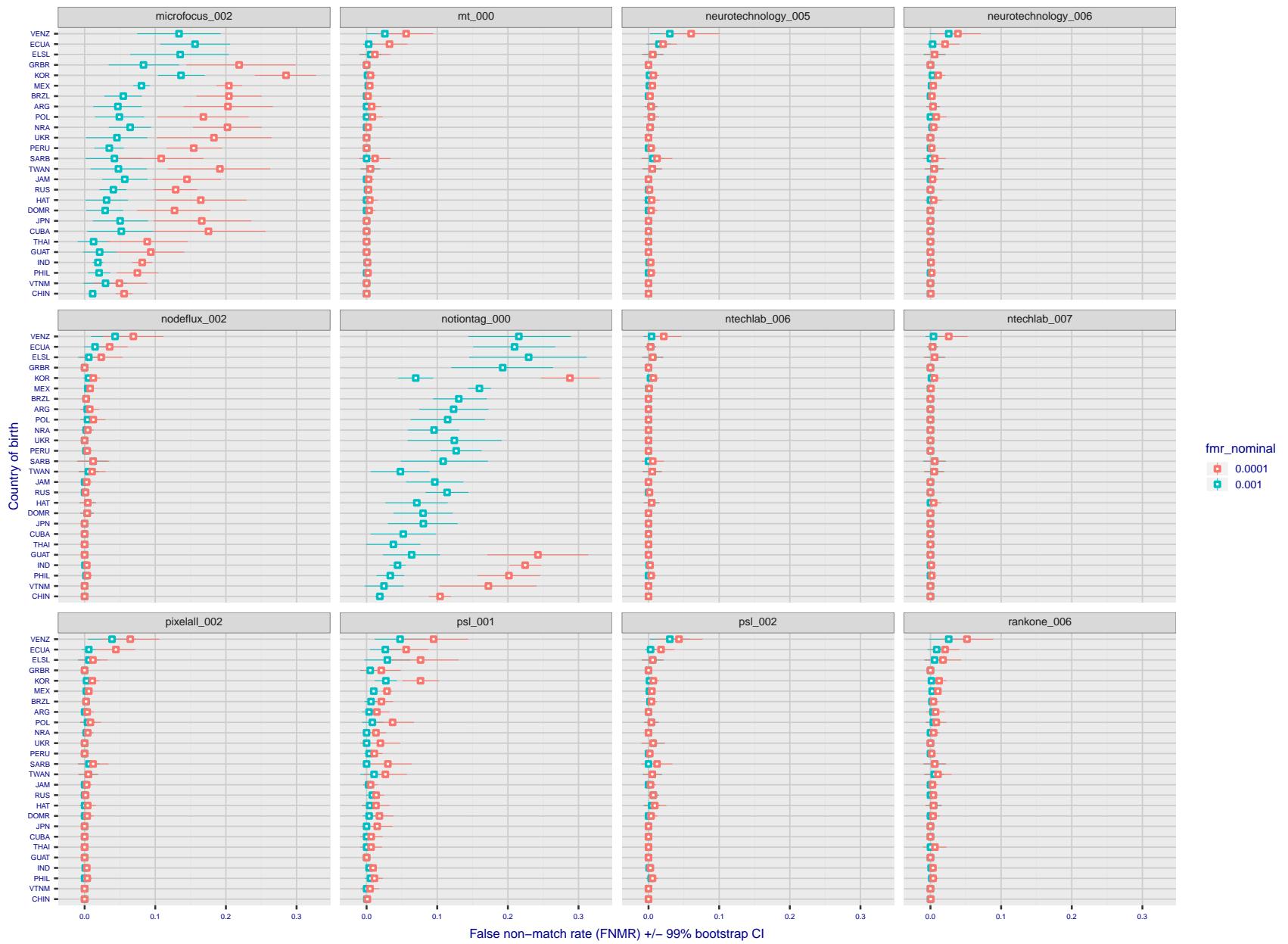


Figure 102: For the visa images, the dots show FNMR by country of birth for two globally set operating thresholds corresponding to $FMR = \{0.001, 0.0001\}$ computed over all on the order of 10^{10} impostor scores. The FMR in each bin will vary also - see subsequent impostor heatmaps in sec. 3.6.1. The figures shows an order of magnitude variation in FNMR across country of birth; these effects are likely due quality variations, then demographics like age and race. The error rates in some cases are zero, and in others the DET is flat so the error rates at the two thresholds are identical. The lines span 1% and 99% of bootstrap replicated FNMR estimates.

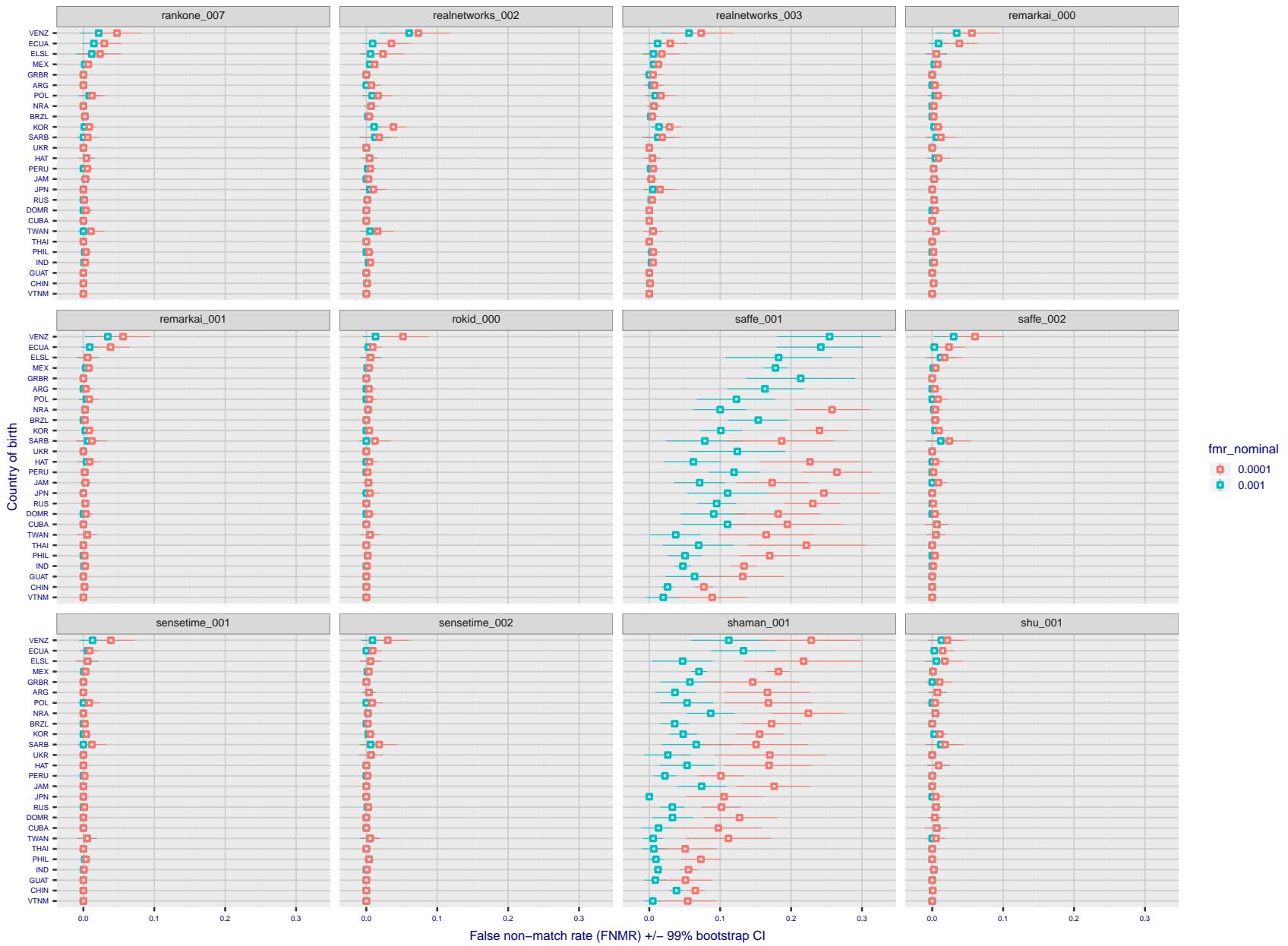


Figure 103: For the visa images, the dots show FNMR by country of birth for two globally set operating thresholds corresponding to $FMR = \{0.001, 0.0001\}$ computed over all on the order of 10^{10} impostor scores. The FMR in each bin will vary also - see subsequent impostor heatmaps in sec. 3.6.1. The figures shows an order of magnitude variation in FNMR across country of birth; these effects are likely due quality variations, then demographics like age and race. The error rates in some cases are zero, and in others the DET is flat so the error rates at the two thresholds are identical. The lines span 1% and 99% of bootstrap replicated FNMR estimates.

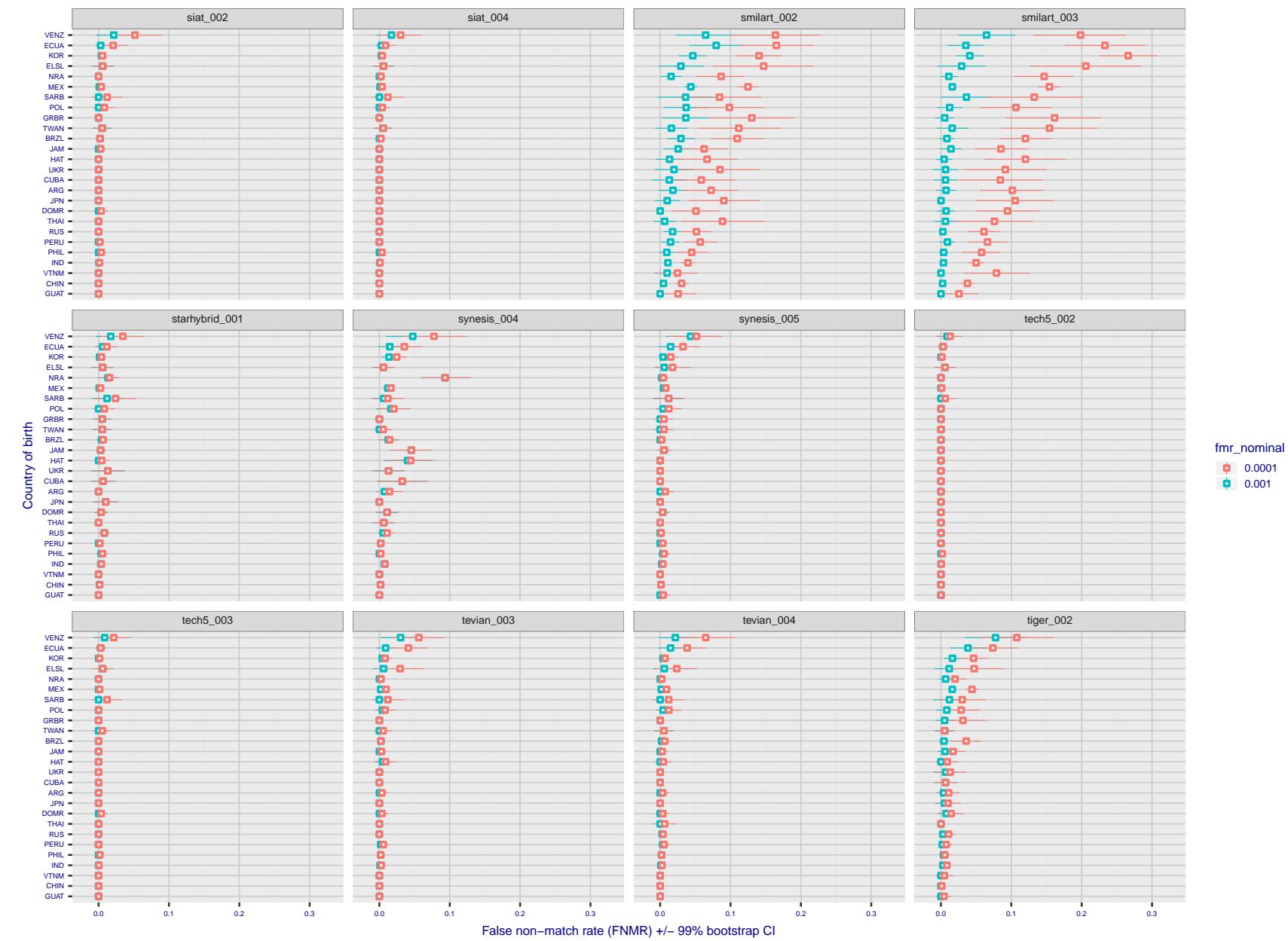


Figure 104: For the visa images, the dots show FNMR by country of birth for two globally set operating thresholds corresponding to $FMR = \{0.001, 0.0001\}$ computed over all on the order of 10^{10} impostor scores. The FMR in each bin will vary also - see subsequent impostor heatmaps in sec. 3.6.1. The figures shows an order of magnitude variation in FNMR across country of birth; these effects are likely due quality variations, then demographics like age and race. The error rates in some cases are zero, and in others the DET is flat so the error rates at the two thresholds are identical. The lines span 1% and 99% of bootstrap replicated FNMR estimates.

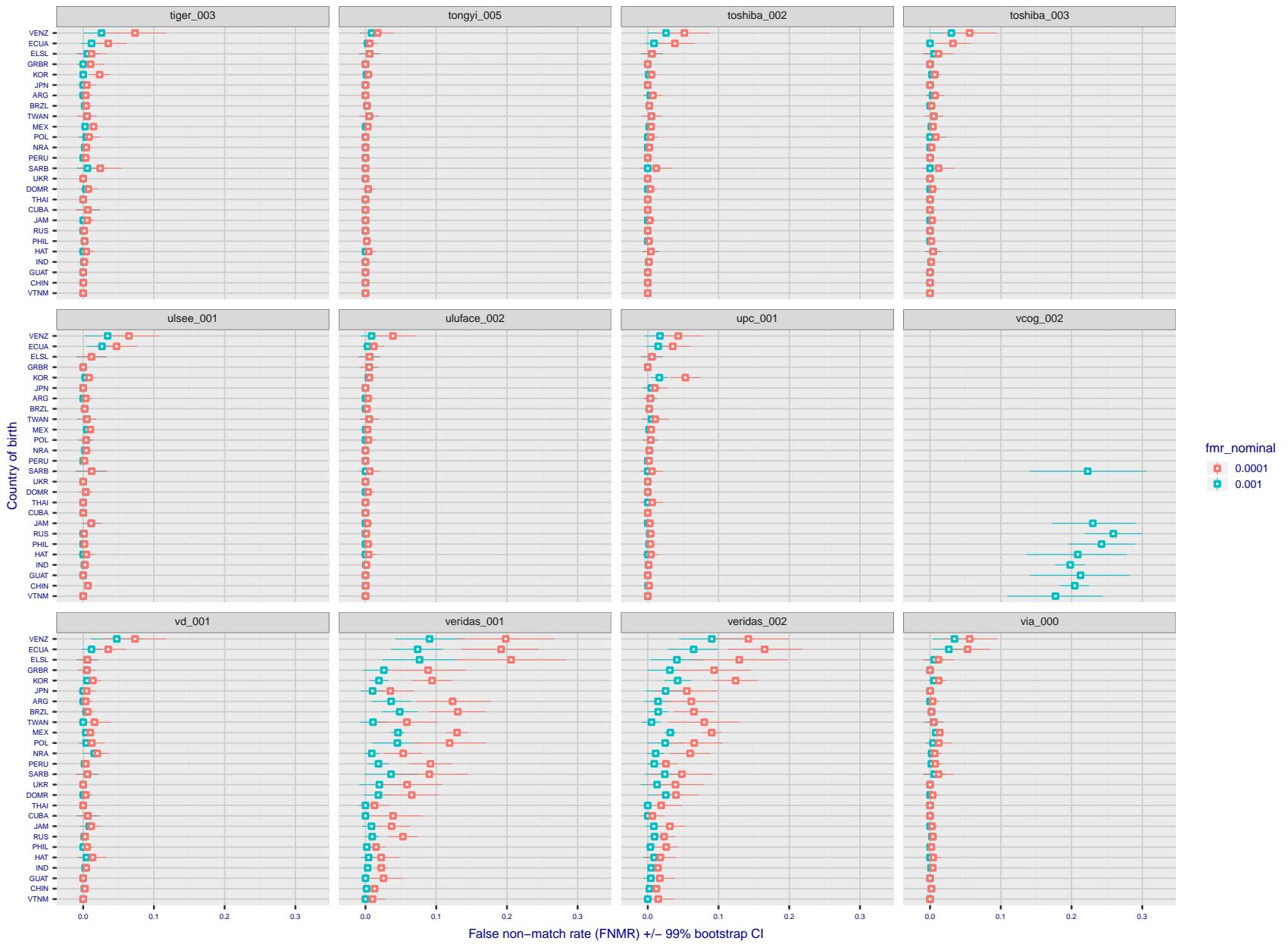


Figure 105: For the visa images, the dots show FNMR by country of birth for two globally set operating thresholds corresponding to $FMR = \{0.001, 0.0001\}$ computed over all on the order of 10^{10} impostor scores. The FMR in each bin will vary also - see subsequent impostor heatmaps in sec. 3.6.1. The figures shows an order of magnitude variation in FNMR across country of birth; these effects are likely due quality variations, then demographics like age and race. The error rates in some cases are zero, and in others the DET is flat so the error rates at the two thresholds are identical. The lines span 1% and 99% of bootstrap replicated FNMR estimates.

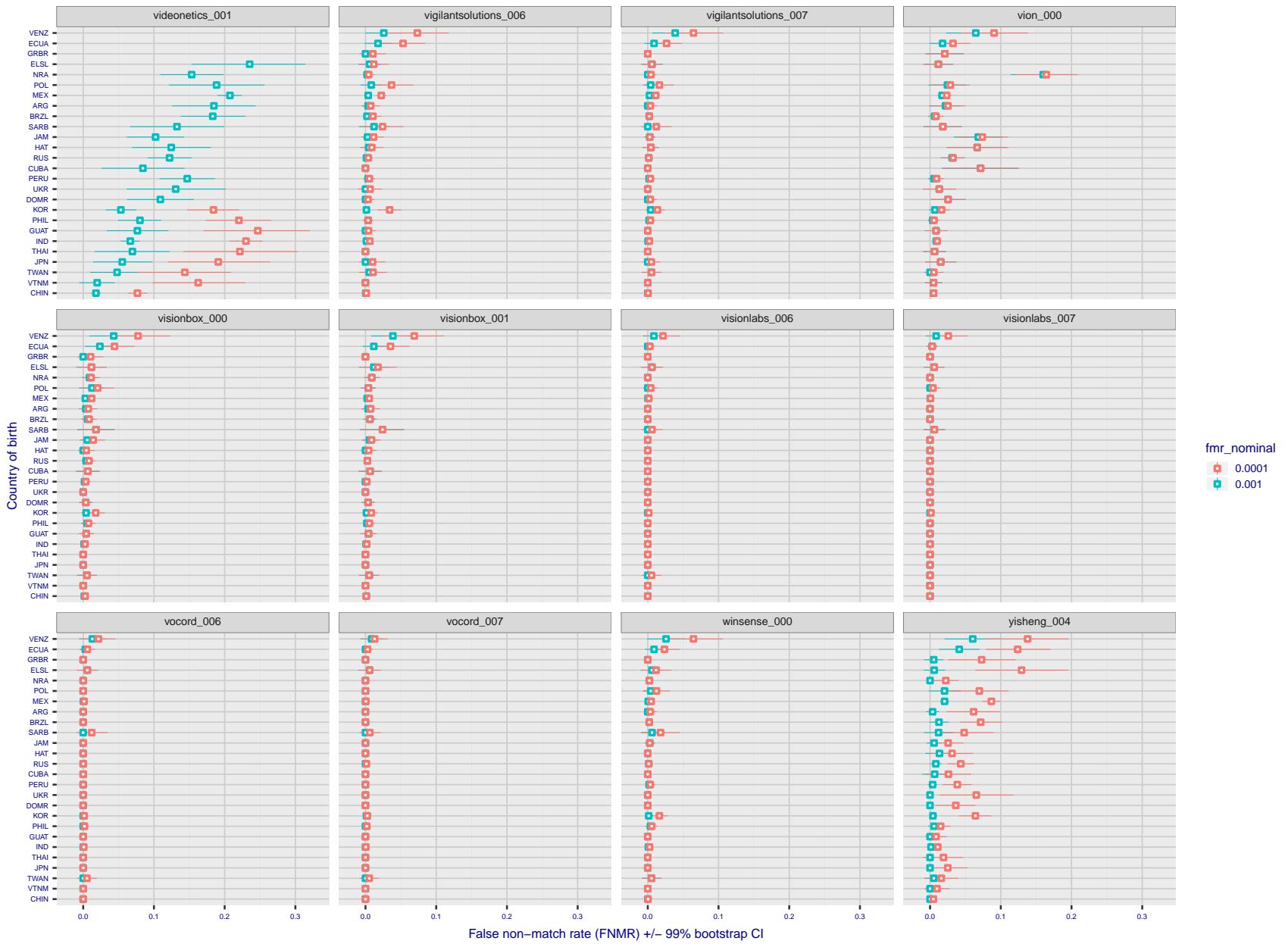


Figure 106: For the visa images, the dots show FNMR by country of birth for two globally set operating thresholds corresponding to $FMR = \{0.001, 0.0001\}$ computed over all on the order of 10^{10} impostor scores. The FMR in each bin will vary also - see subsequent impostor heatmaps in sec. 3.6.1. The figures shows an order of magnitude variation in FNMR across country of birth; these effects are likely due quality variations, then demographics like age and race. The error rates in some cases are zero, and in others the DET is flat so the error rates at the two thresholds are identical. The lines span 1% and 99% of bootstrap replicated FNMR estimates.



Figure 107: For the visa images, the dots show FNMR by country of birth for two globally set operating thresholds corresponding to $FMR = \{0.001, 0.0001\}$ computed over all on the order of 10^{10} impostor scores. The FMR in each bin will vary also - see subsequent impostor heatmaps in sec. 3.6.1. The figures shows an order of magnitude variation in FNMR across country of birth; these effects are likely due quality variations, then demographics like age and race. The error rates in some cases are zero, and in others the DET is flat so the error rates at the two thresholds are identical. The lines span 1% and 99% of bootstrap replicated FNMR estimates.

Caveats: The results may not relate to subject-specific properties. Instead they could reflect image-specific quality differences, which could occur due to collection protocol or software processing variations.

3.5.2 Effect of ageing

Background: Faces change appearance throughout life. This change gradually reduces similarity of a new image to an earlier image. Face recognition algorithms give reduced similarity scores and more frequent false rejections.

Goal: To quantify false non-match rates (FNMR) as a function of elapsed time in an adult population.

Methods: Using the mugshot images, a threshold is set to give FMR = 0.00001 over the entire impostor set. Then FNMR is measured over 1000 bootstrap replications of the genuine scores.

Results: For the visa images, Figure 116 shows how false non-match rates for genuine users, as a function of age group.

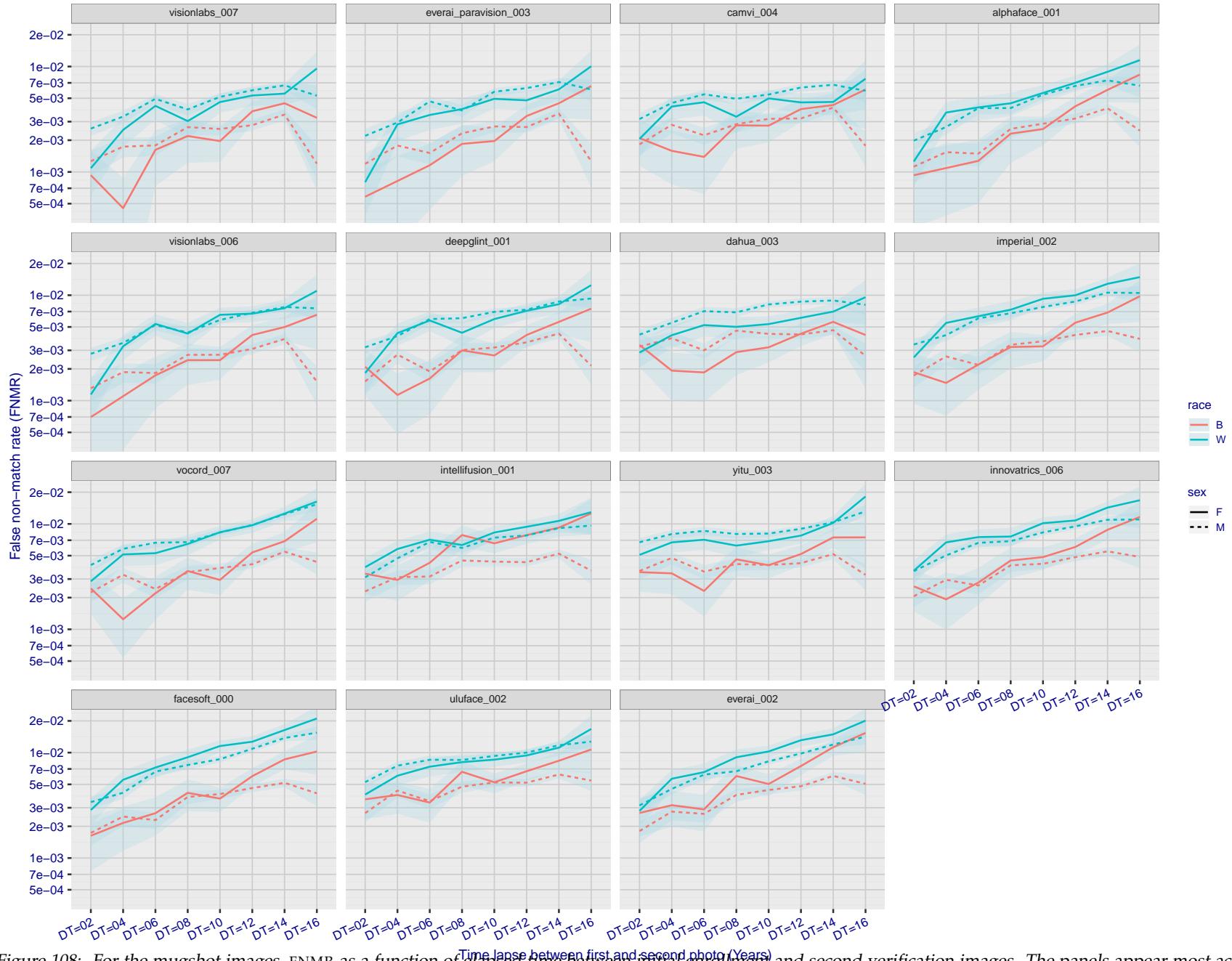


Figure 108: For the mugshot images, FNMR as a function of elapsed time between initial enrollment and second verification images. The panels appear most accurate first, and vertical scale changes on each page. The four traces correspond to images annotated with codes for black female, black male, white female, white male. The threshold is fixed for each algorithm to give FMR = 0.00001 over all (10^8) impostor comparisons. For short time-lapses, the most accurate algorithms give very few errors (FNMR < 0.001) so that the uncertainty estimates are high.

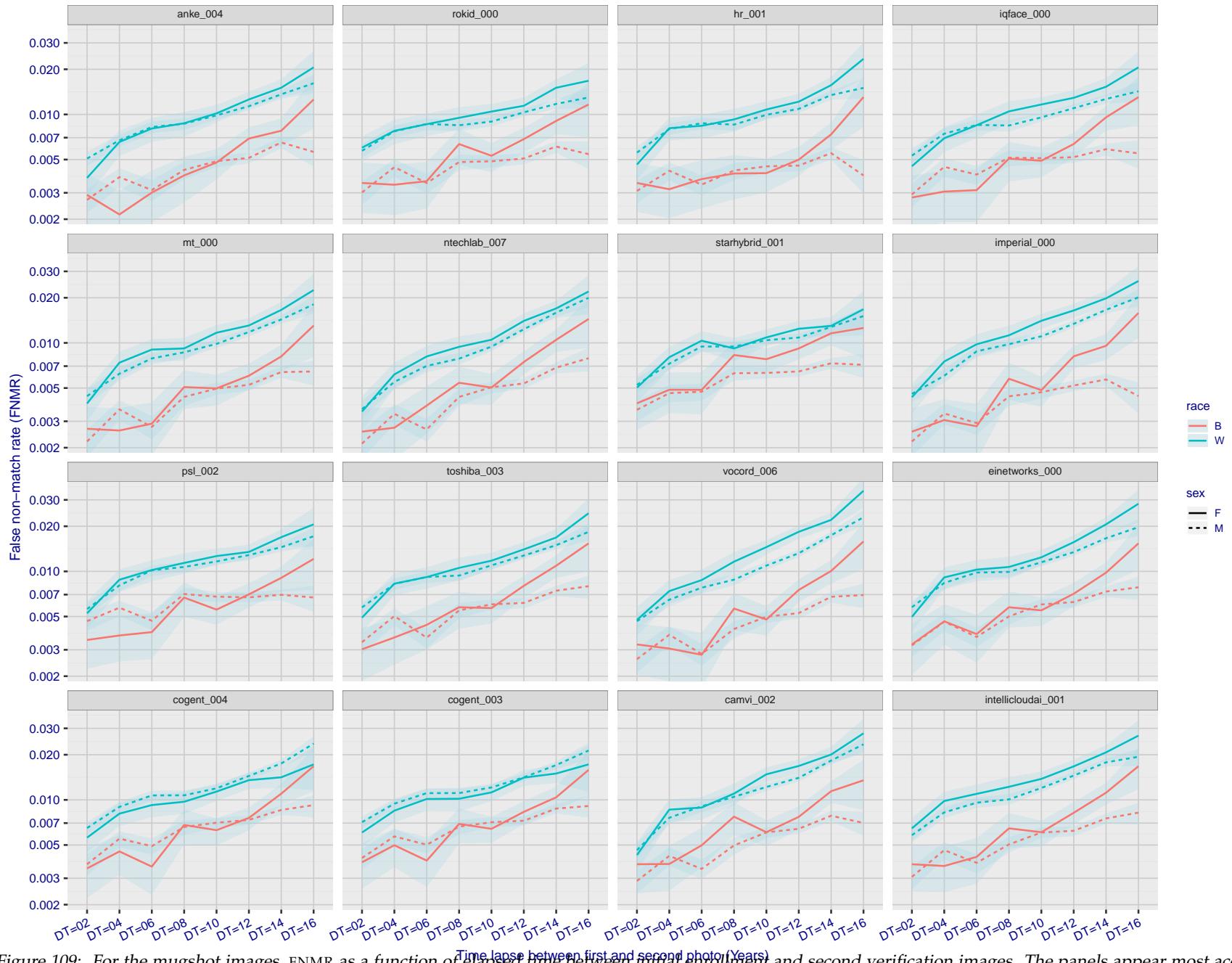


Figure 109: For the mugshot images, FNMR as a function of elapsed time between initial enrollment and second verification images. The panels appear most accurate first, and vertical scale changes on each page. The four traces correspond to images annotated with codes for black female, black male, white female, white male. The threshold is fixed for each algorithm to give FMR = 0.00001 over all (10^8) impostor comparisons. For short time-lapses, the most accurate algorithms give very few errors (FNMR < 0.001) so that the uncertainty estimates are high.

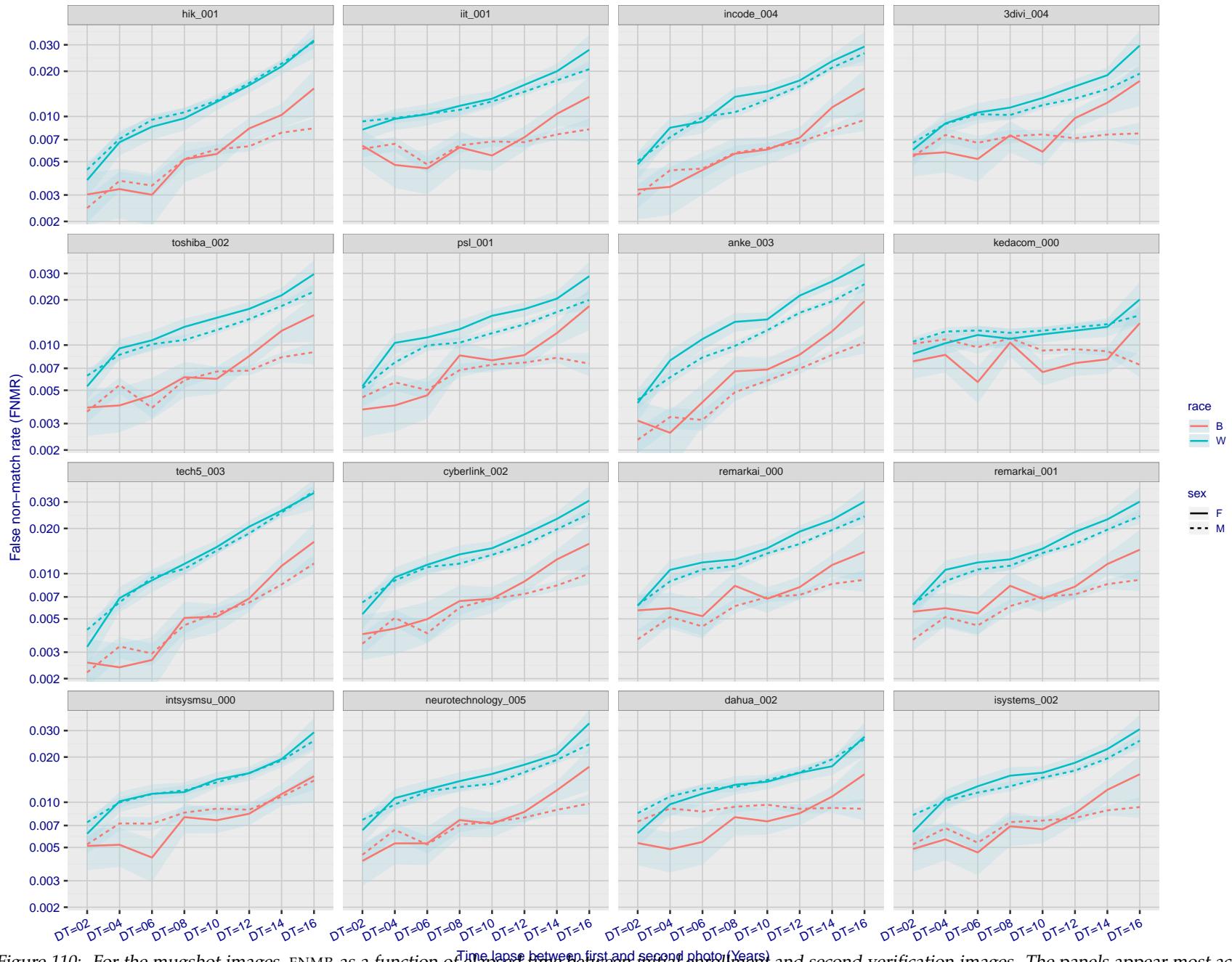


Figure 110: For the mugshot images, FNMR as a function of elapsed time between initial enrollment and second verification images. The panels appear most accurate first, and vertical scale changes on each page. The four traces correspond to images annotated with codes for black female, black male, white female, white male. The threshold is fixed for each algorithm to give FMR = 0.00001 over all (10^8) impostor comparisons. For short time-lapses, the most accurate algorithms give very few errors (FNMR < 0.001) so that the uncertainty estimates are high.

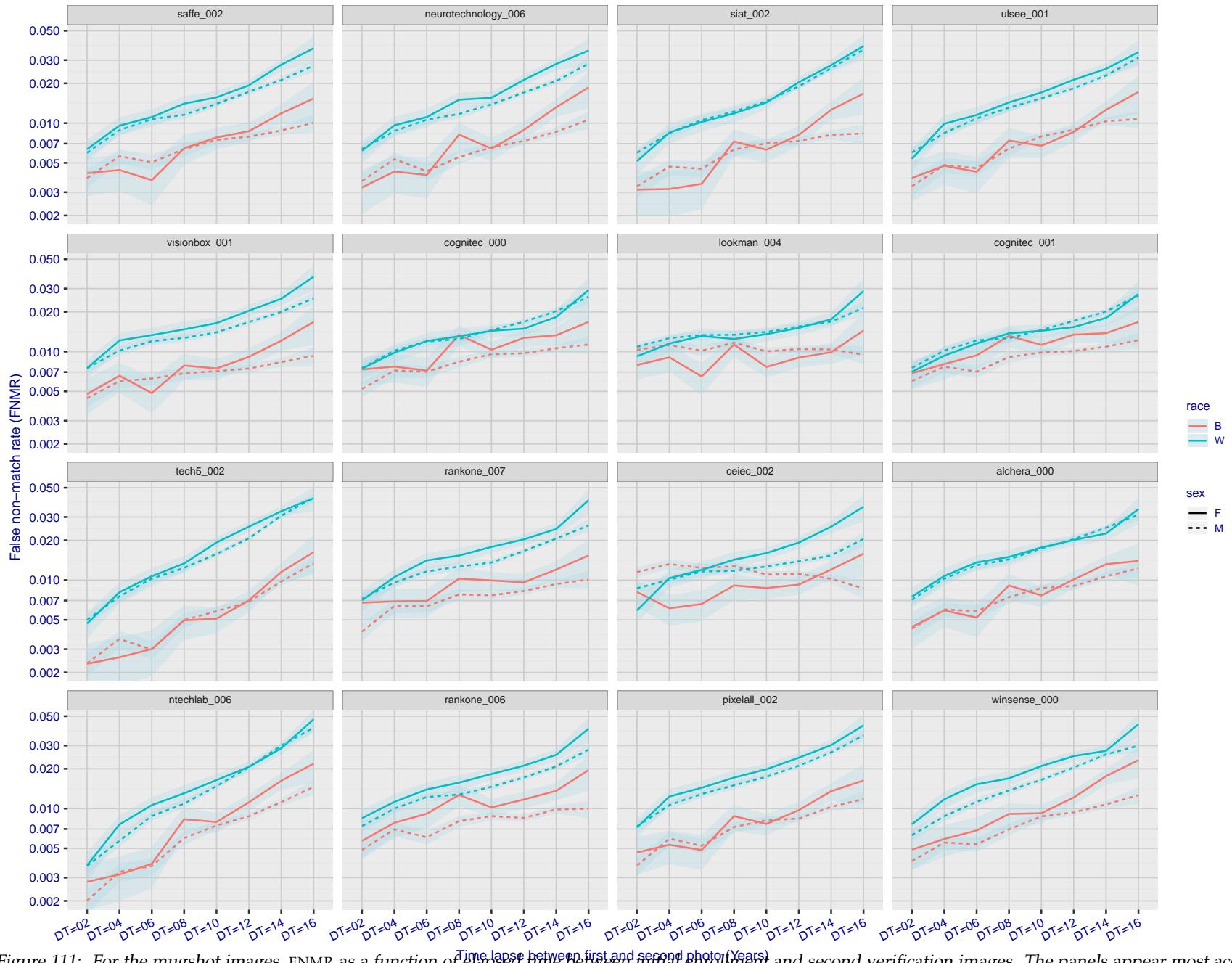


Figure 111: For the mugshot images, FNMR as a function of elapsed time between initial enrollment and second verification images. The panels appear most accurate first, and vertical scale changes on each page. The four traces correspond to images annotated with codes for black female, black male, white female, white male. The threshold is fixed for each algorithm to give FMR = 0.00001 over all (10^8) impostor comparisons. For short time-lapses, the most accurate algorithms give very few errors (FNMR < 0.001) so that the uncertainty estimates are high.

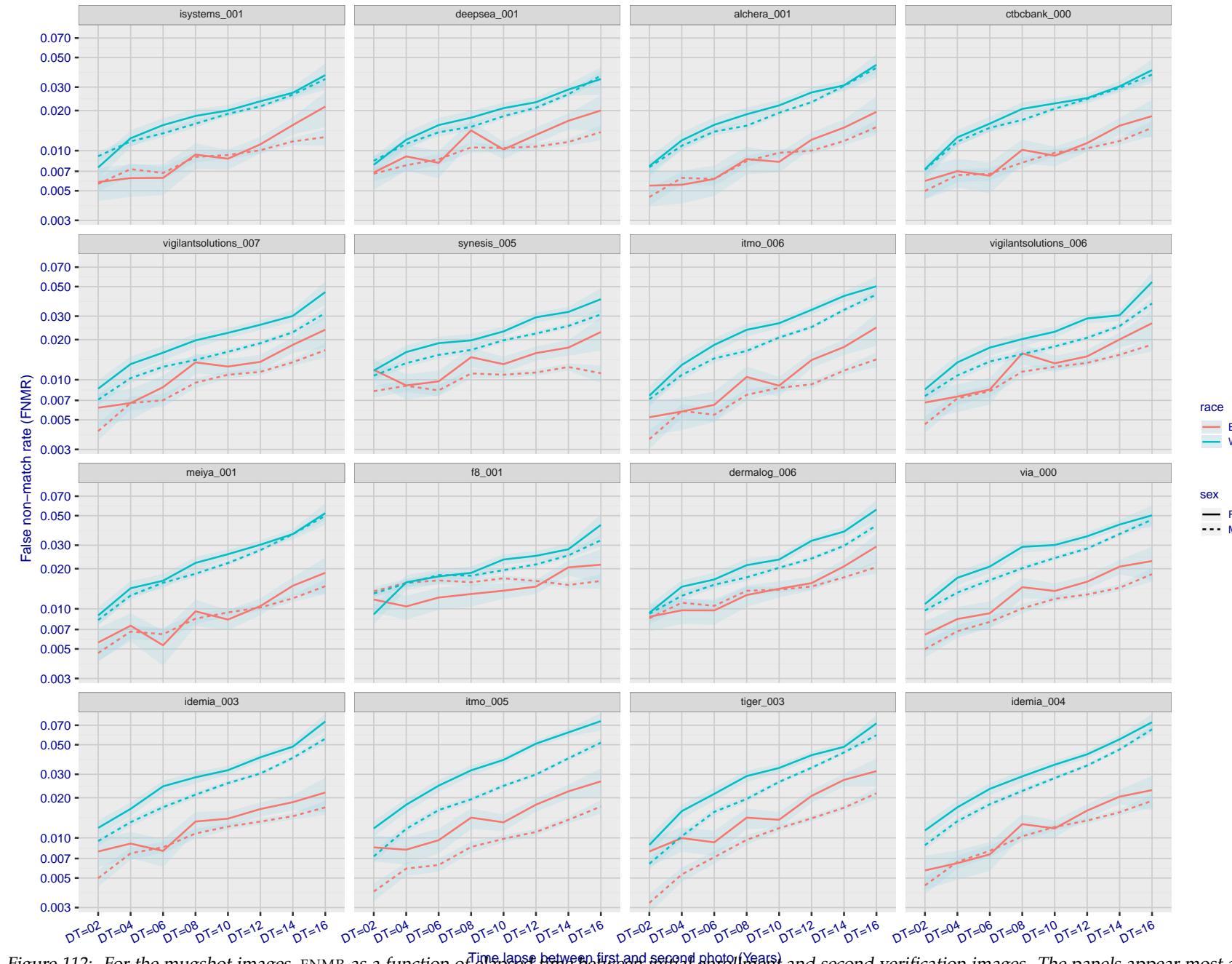


Figure 112: For the mugshot images, FNMR as a function of elapsed time between initial enrollment and second verification images. The panels appear most accurate first, and vertical scale changes on each page. The four traces correspond to images annotated with codes for black female, black male, white female, white male. The threshold is fixed for each algorithm to give FMR = 0.00001 over all (10^8) impostor comparisons. For short time-lapses, the most accurate algorithms give very few errors (FNMR < 0.001) so that the uncertainty estimates are high.

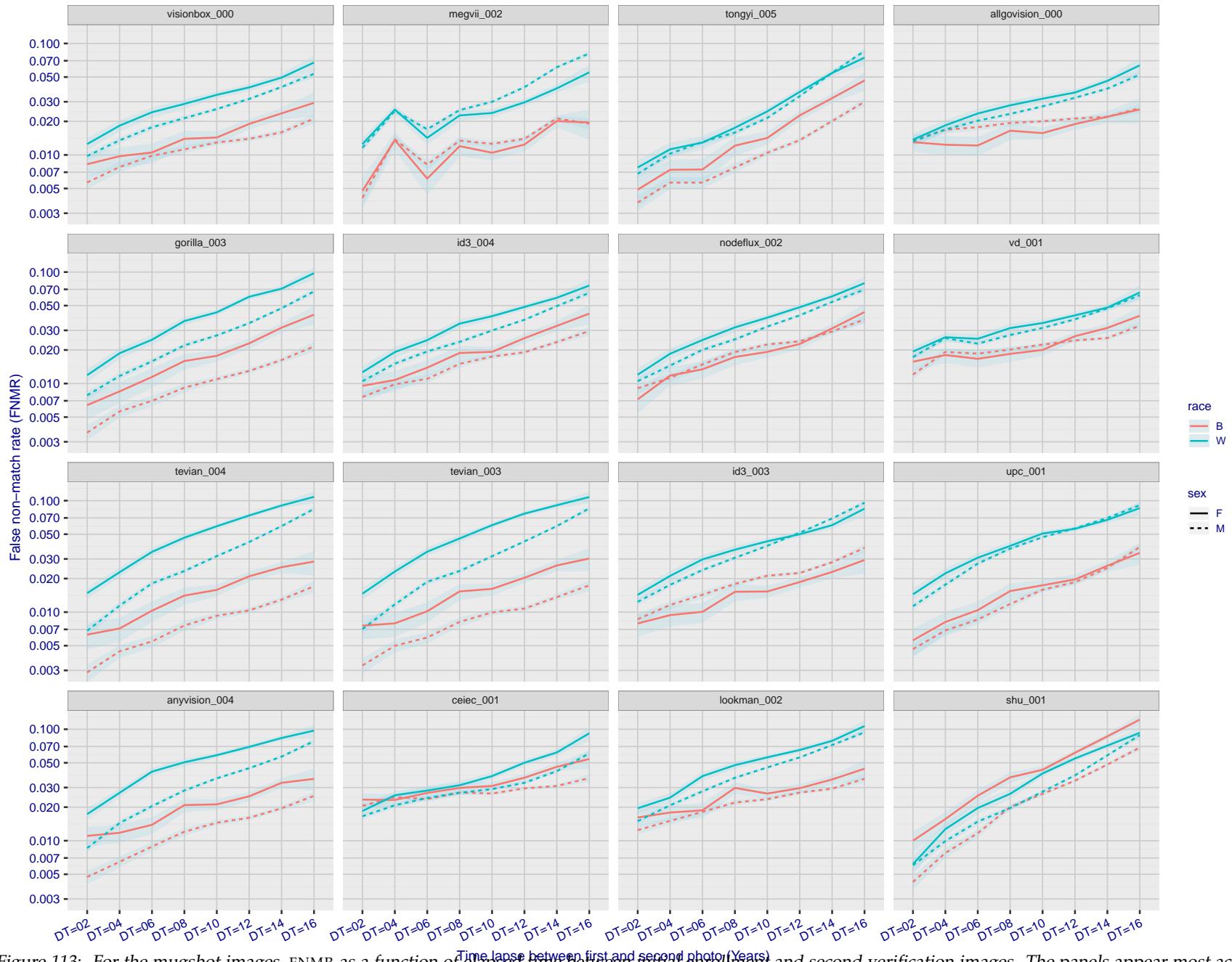


Figure 113: For the mugshot images, FNMR as a function of elapsed time between initial enrollment and second verification images. The panels appear most accurate first, and vertical scale changes on each page. The four traces correspond to images annotated with codes for black female, black male, white female, white male. The threshold is fixed for each algorithm to give FMR = 0.00001 over all (10^8) impostor comparisons. For short time-lapses, the most accurate algorithms give very few errors (FNMR < 0.001) so that the uncertainty estimates are high.

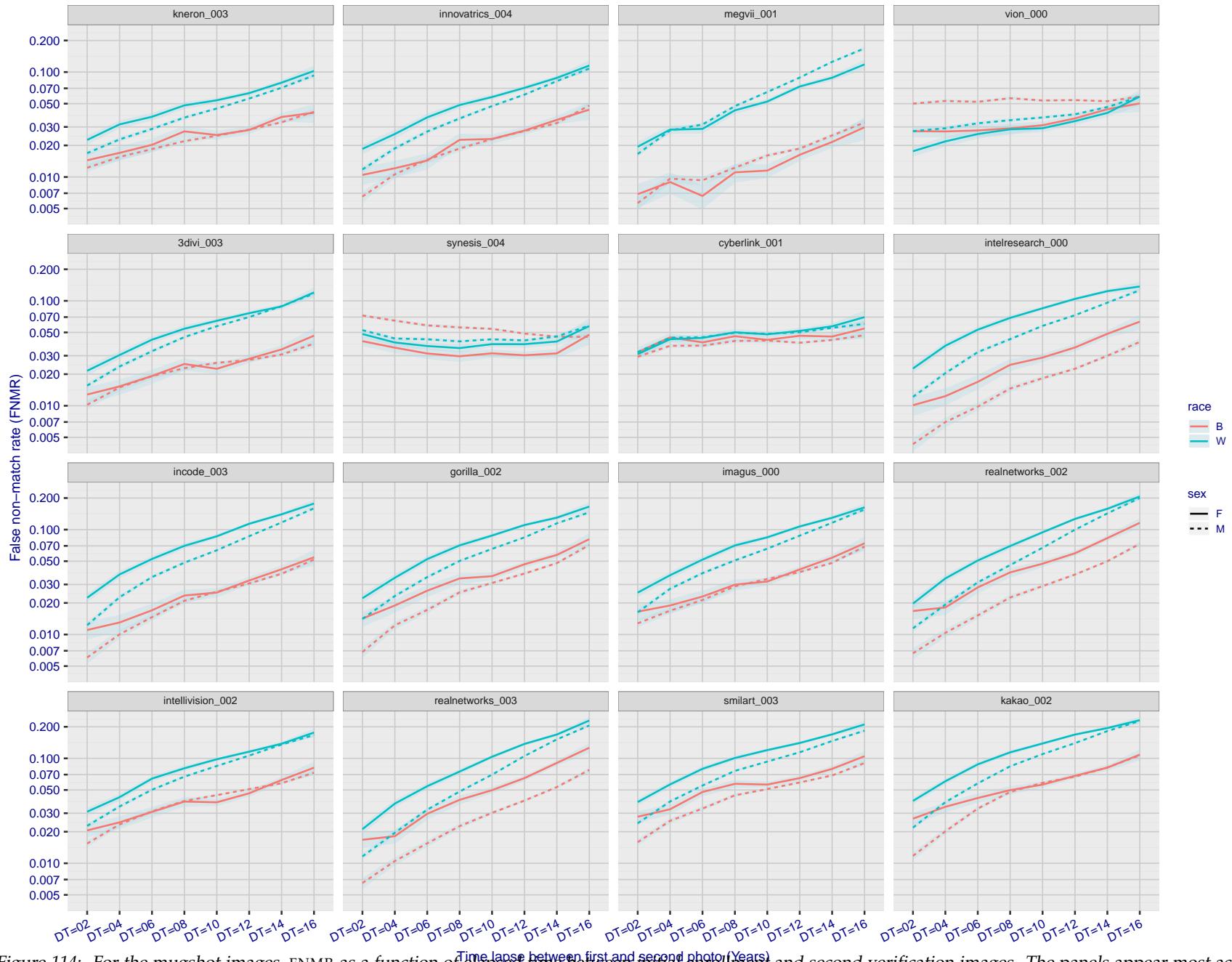


Figure 114: For the mugshot images, FNMR as a function of elapsed time between initial enrollment and second verification images. The panels appear most accurate first, and vertical scale changes on each page. The four traces correspond to images annotated with codes for black female, black male, white female, white male. The threshold is fixed for each algorithm to give $FMR = 0.00001$ over all (10^8) impostor comparisons. For short time-lapses, the most accurate algorithms give very few errors ($FNMR < 0.001$) so that the uncertainty estimates are high.

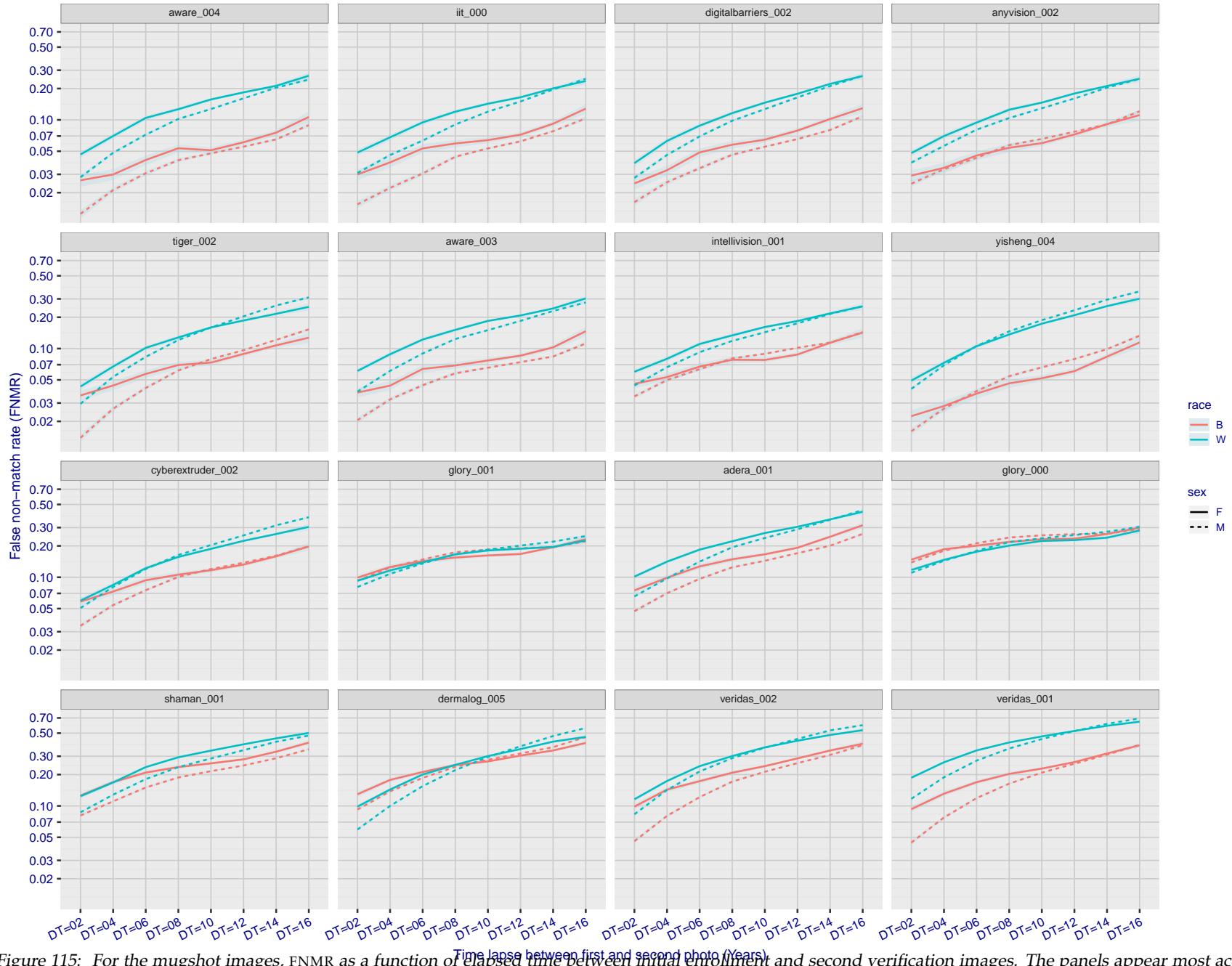


Figure 115: For the mugshot images, FNMR as a function of elapsed time between initial enrollment and second verification images. The panels appear most accurate first, and vertical scale changes on each page. The four traces correspond to images annotated with codes for black female, black male, white female, white male. The threshold is fixed for each algorithm to give FMR = 0.00001 over all (10^8) impostor comparisons. For short time-lapses, the most accurate algorithms give very few errors (FNMR < 0.001) so that the uncertainty estimates are high.

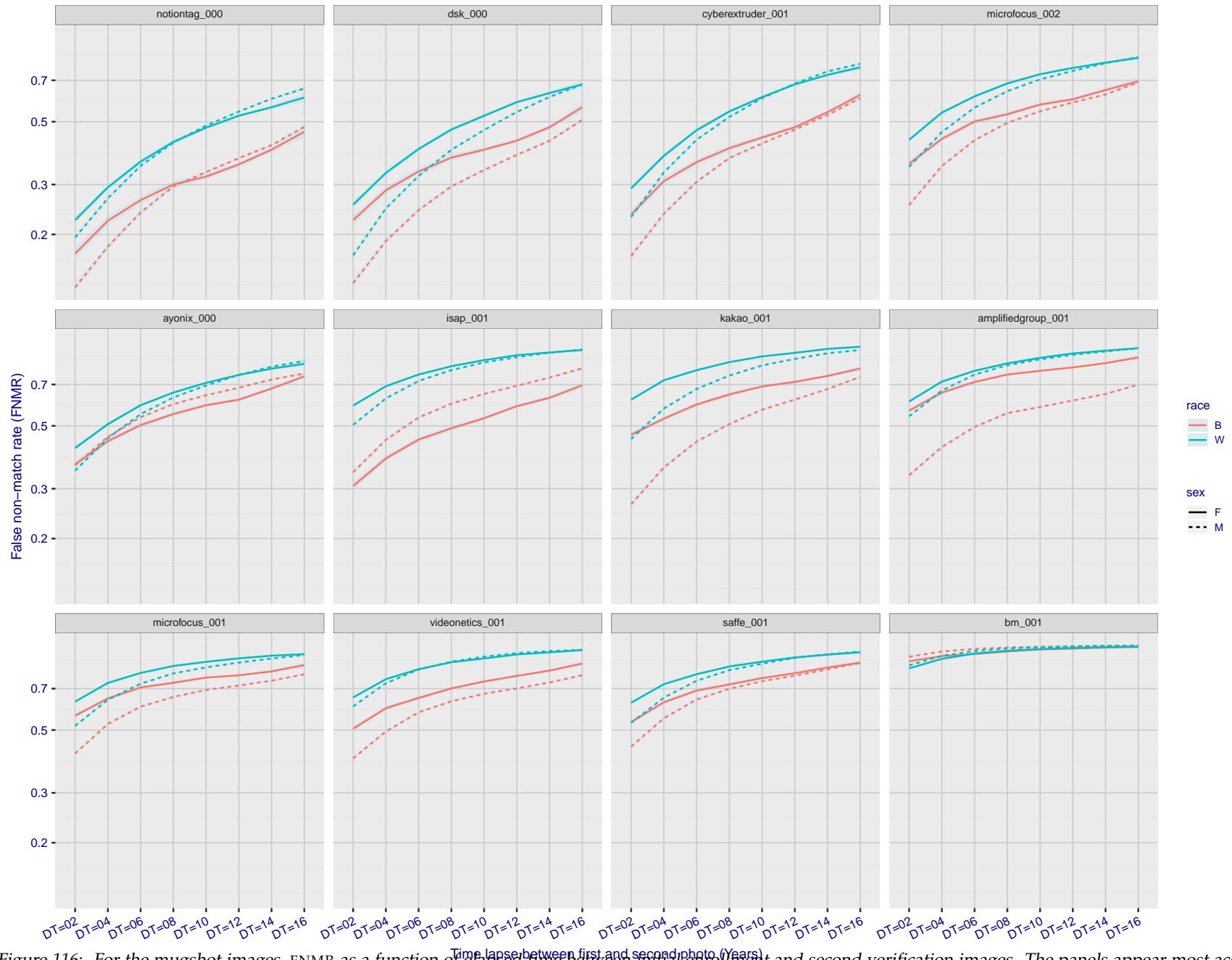


Figure 116: For the mugshot images, FNMR as a function of elapsed time between initial enrollment and second verification images. The panels appear most accurate first, and vertical scale changes on each page. The four traces correspond to images annotated with codes for black female, black male, white female, white male. The threshold is fixed for each algorithm to give FMR = 0.00001 over all (10^8) impostor comparisons. For short time-lapses, the most accurate algorithms give very few errors (FNMR < 0.001) so that the uncertainty estimates are high.

3.5.3 Effect of age on genuine subjects

Background: Faces change appearance throughout life. Face recognition algorithms have previously been reported to give better accuracy on older individuals (See NIST IR 8009).

Goal: To quantify false non-match rates (FNMR) as a function of age, without an ageing component.

Methods: Using the visa images, which span fewer than five years, thresholds are determined that give FMR = 0.001 and 0.0001 over the entire impostor set. Then FNMR is measured over 1000 bootstrap replications of the genuine scores.

Results: For the visa images, Figure 129 shows how false non-match rates for genuine users, as a function of age group.

The notable aspects are:

- ▷ Younger subjects give considerably higher FNMR. This is likely due to rapid growth and change in facial appearance.
- ▷ FNMR trends down throughout life. The last bin, AGE > 72, contains fewer than 140 mated pairs, and may be affected by small sample size.

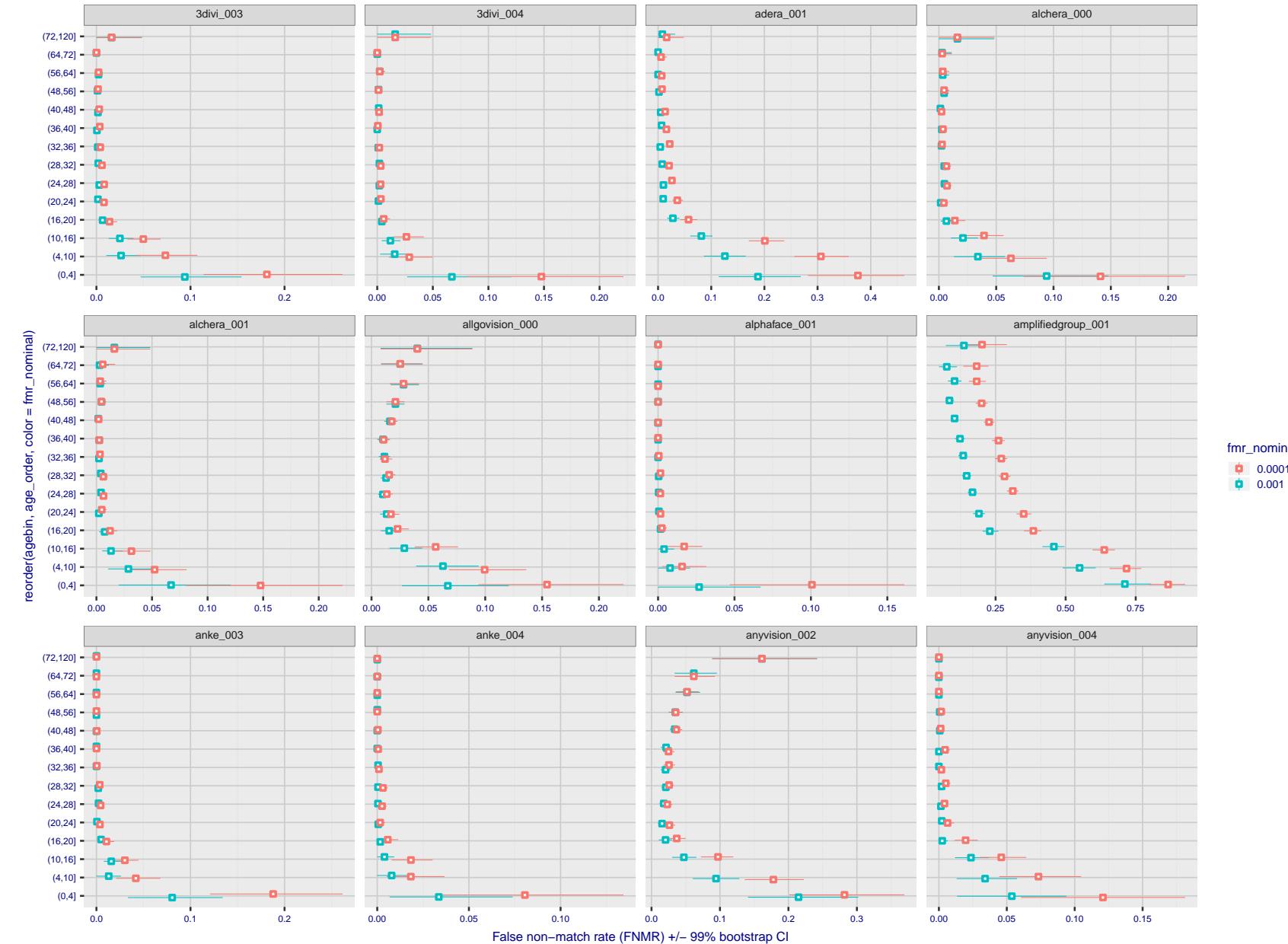


Figure 117: For the visa images, the dots show FNMR by age group for two operating thresholds corresponding to $FMR = \{0.001, 0.0001\}$ computed over all on the order of 10^{10} impostor scores. The FMR in each bin will vary also - see subsequent impostor heatmaps in sec. 3.6.2. Given a pair of face images taken at different times, we assign the comparison to the bin that is the arithmetic average of the subject's ages. This plot shows only the effect of age, not ageing. The number of comparisons in each bin is generally in the thousands, however the first and last bins are computed over 149 and 124 respectively. The error rates in some (adult) cases are zero, and in others the DET is flat so the error rates at the two thresholds are identical. The lines span 1% and 99% of bootstrap replicated FNMR estimates.

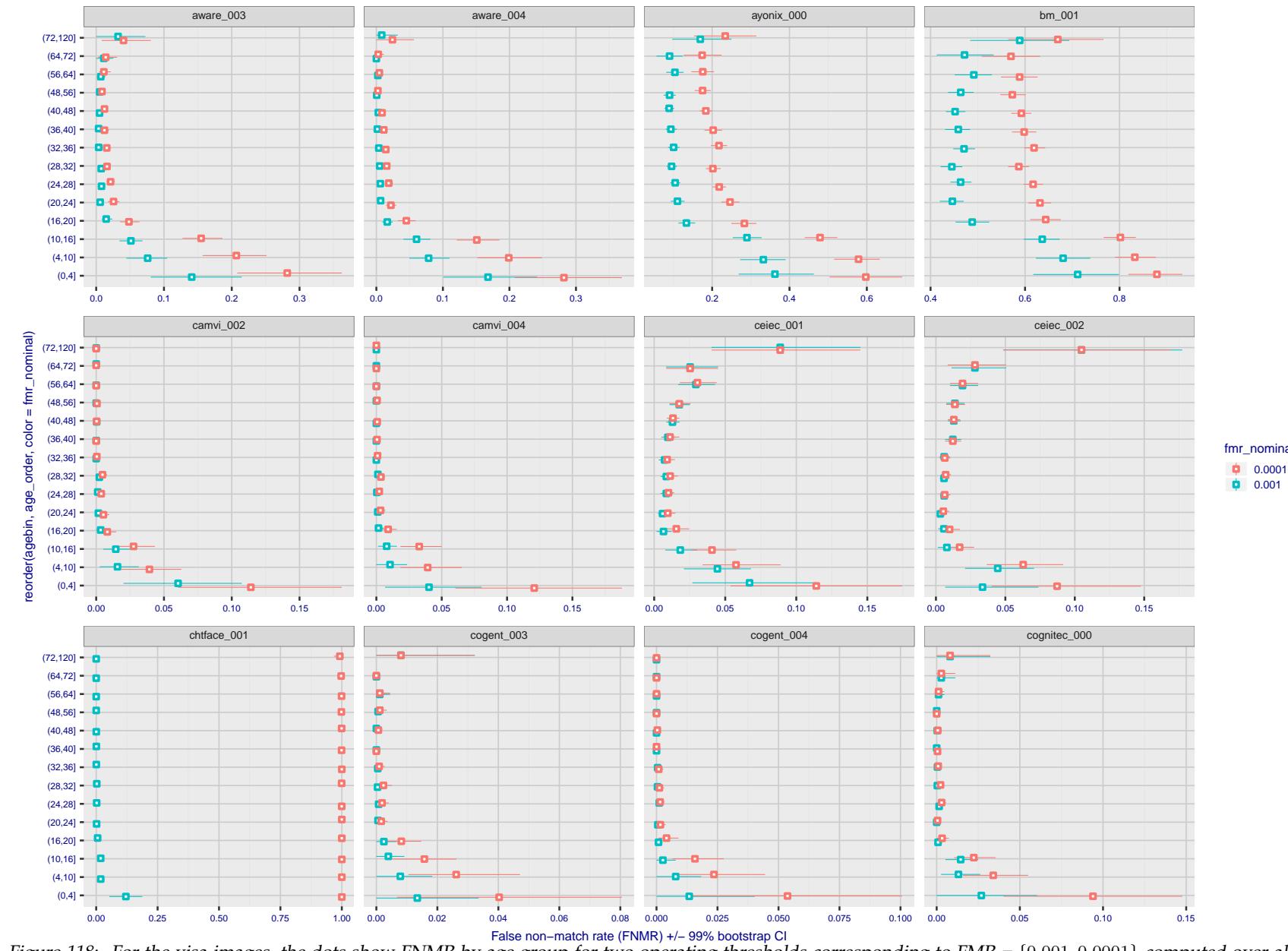


Figure 118: For the visa images, the dots show FNMR by age group for two operating thresholds corresponding to $FMR = \{0.001, 0.0001\}$ computed over all on the order of 10^{10} impostor scores. The FMR in each bin will vary also - see subsequent impostor heatmaps in sec. 3.6.2. Given a pair of face images taken at different times, we assign the comparison to the bin that is the arithmetic average of the subject's ages. This plot shows only the effect of age, not ageing. The number of comparisons in each bin is generally in the thousands, however the first and last bins are computed over 149 and 124 respectively. The error rates in some (adult) cases are zero, and in others the DET is flat so the error rates at the two thresholds are identical. The lines span 1% and 99% of bootstrap replicated FNMR estimates.



Figure 119: For the visa images, the dots show FNMR by age group for two operating thresholds corresponding to $FMR = \{0.001, 0.0001\}$ computed over all on the order of 10^{10} impostor scores. The FMR in each bin will vary also - see subsequent impostor heatmaps in sec. 3.6.2. Given a pair of face images taken at different times, we assign the comparison to the bin that is the arithmetic average of the subject's ages. This plot shows only the effect of age, not ageing. The number of comparisons in each bin is generally in the thousands, however the first and last bins are computed over 149 and 124 respectively. The error rates in some (adult) cases are zero, and in others the DET is flat so the error rates at the two thresholds are identical. The lines span 1% and 99% of bootstrap replicated FNMR estimates.

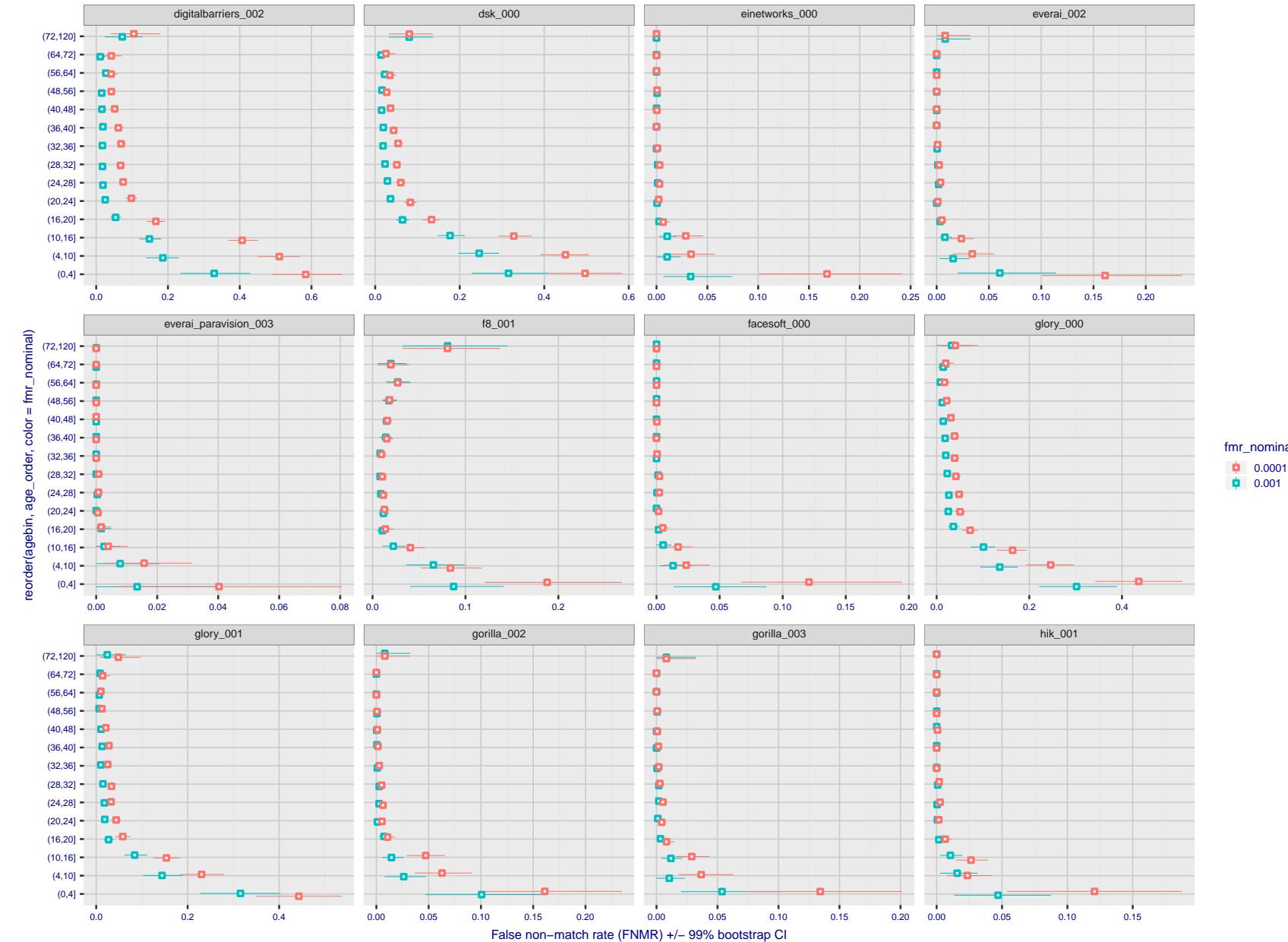


Figure 120: For the visa images, the dots show FNMR by age group for two operating thresholds corresponding to $FMR = \{0.001, 0.0001\}$ computed over all on the order of 10^{10} impostor scores. The FMR in each bin will vary also - see subsequent impostor heatmaps in sec. 3.6.2. Given a pair of face images taken at different times, we assign the comparison to the bin that is the arithmetic average of the subject's ages. This plot shows only the effect of age, not ageing. The number of comparisons in each bin is generally in the thousands, however the first and last bins are computed over 149 and 124 respectively. The error rates in some (adult) cases are zero, and in others the DET is flat so the error rates at the two thresholds are identical. The lines span 1% and 99% of bootstrap replicated FNMR estimates.

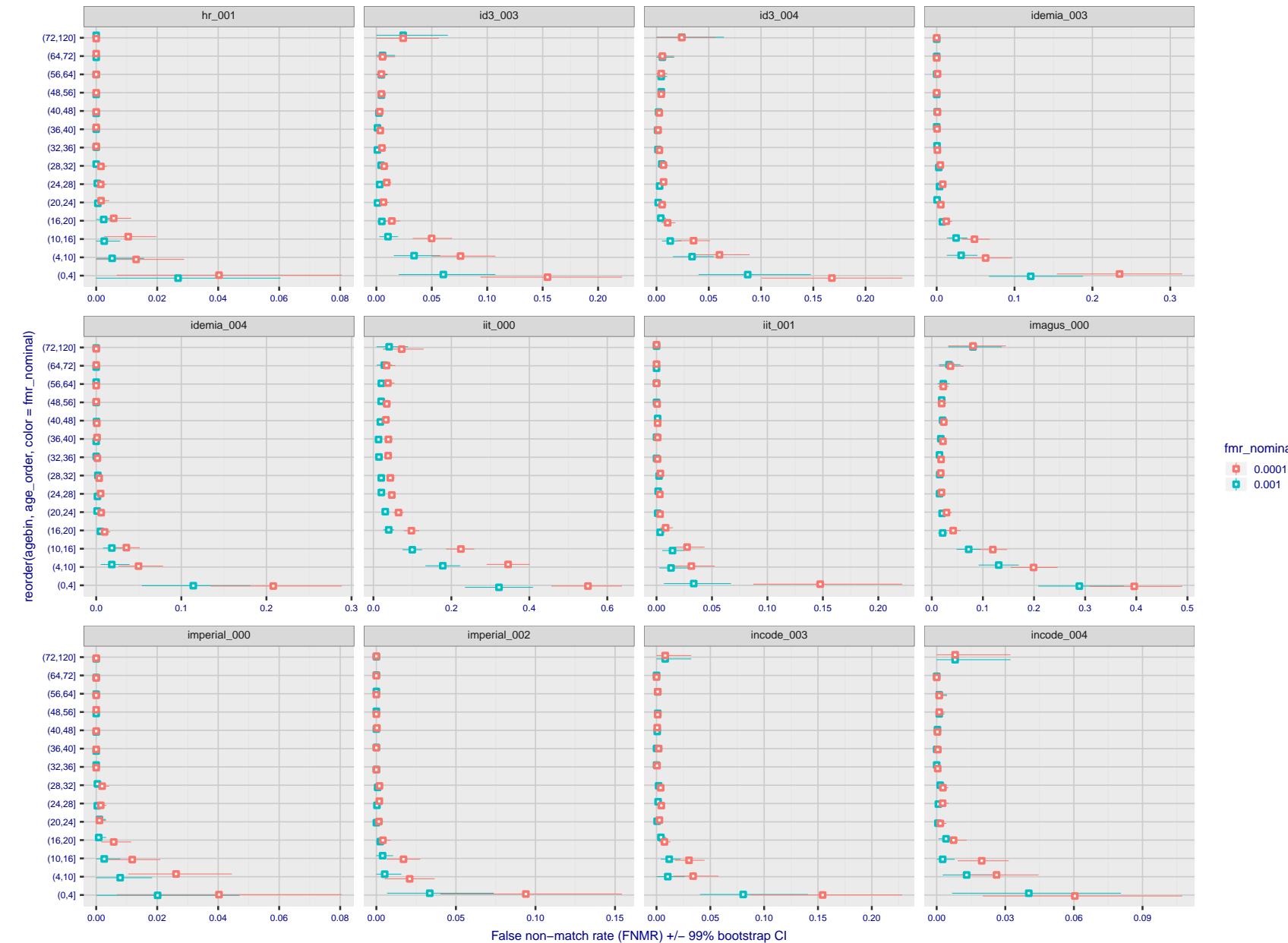


Figure 121: For the visa images, the dots show FNMR by age group for two operating thresholds corresponding to $FMR = \{0.001, 0.0001\}$ computed over all on the order of 10^{10} impostor scores. The FMR in each bin will vary also - see subsequent impostor heatmaps in sec. 3.6.2. Given a pair of face images taken at different times, we assign the comparison to the bin that is the arithmetic average of the subject's ages. This plot shows only the effect of age, not ageing. The number of comparisons in each bin is generally in the thousands, however the first and last bins are computed over 149 and 124 respectively. The error rates in some (adult) cases are zero, and in others the DET is flat so the error rates at the two thresholds are identical. The lines span 1% and 99% of bootstrap replicated FNMR estimates.

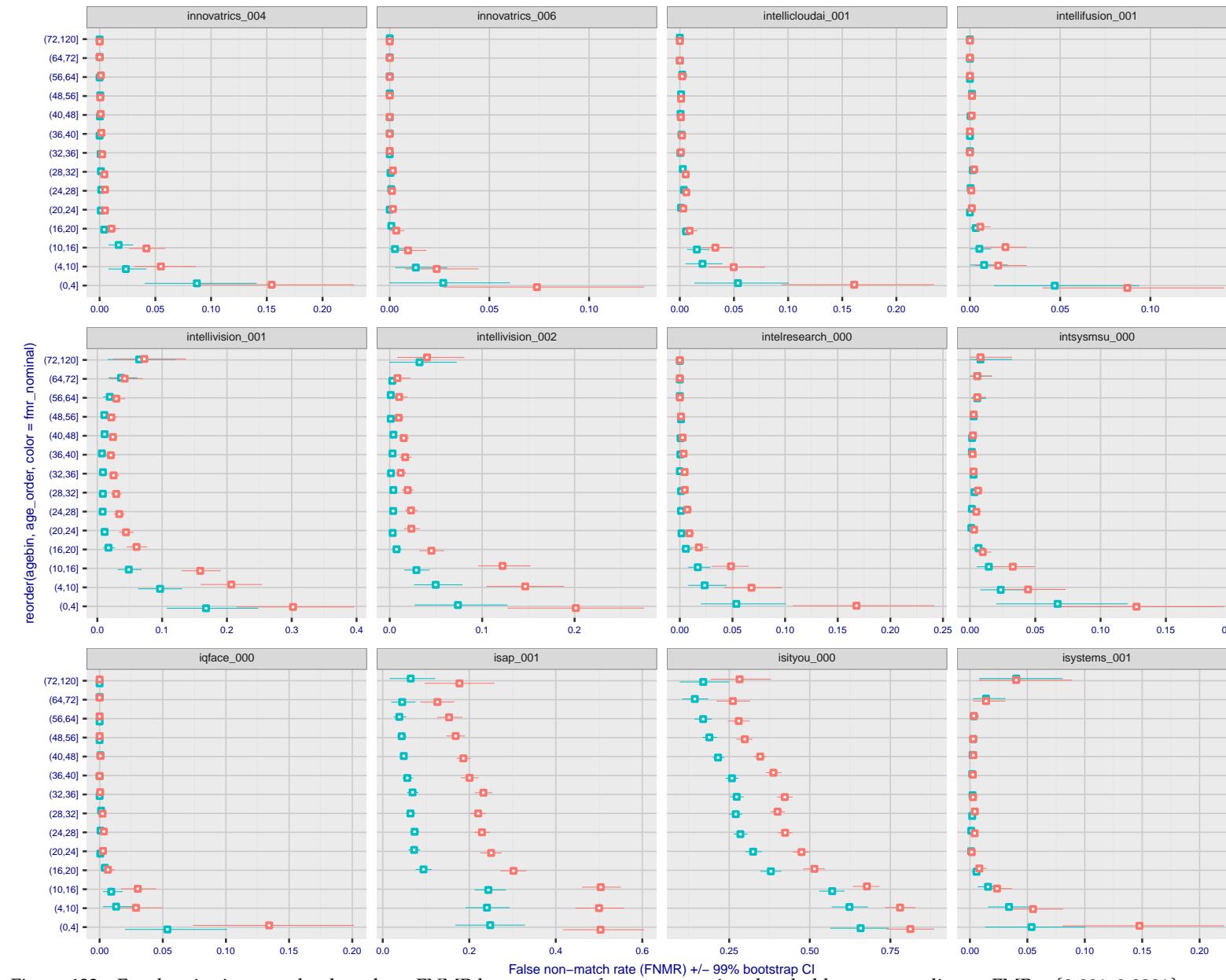


Figure 122: For the visa images, the dots show FNMR by age group for two operating thresholds corresponding to $FMR = \{0.001, 0.0001\}$ computed over all on the order of 10^{10} impostor scores. The FMR in each bin will vary also - see subsequent impostor heatmaps in sec. 3.6.2. Given a pair of face images taken at different times, we assign the comparison to the bin that is the arithmetic average of the subject's ages. This plot shows only the effect of age, not ageing. The number of comparisons in each bin is generally in the thousands, however the first and last bins are computed over 149 and 124 respectively. The error rates in some (adult) cases are zero, and in others the DET is flat so the error rates at the two thresholds are identical. The lines span 1% and 99% of bootstrap replicated FNMR estimates.

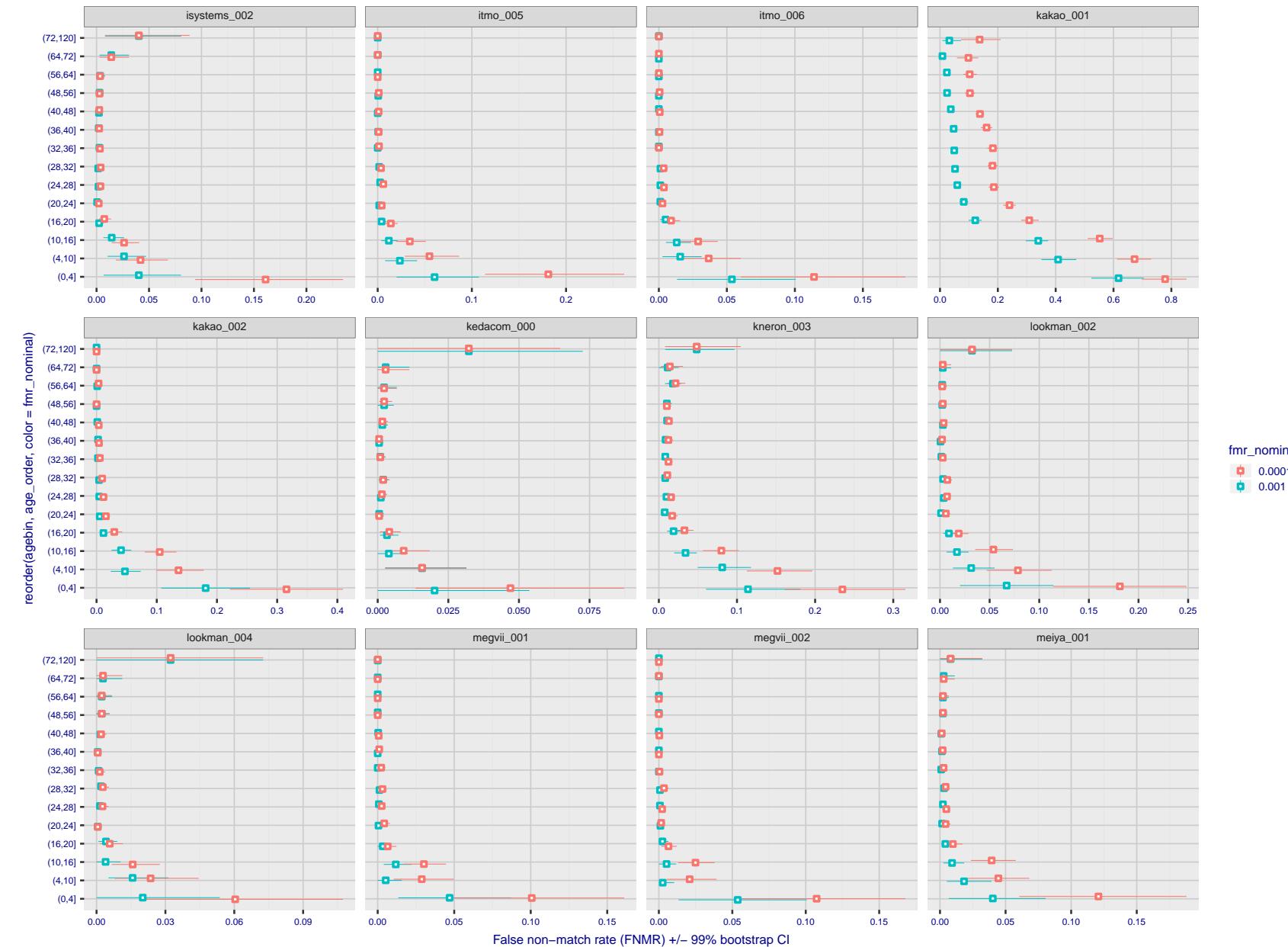


Figure 123: For the visa images, the dots show FNMR by age group for two operating thresholds corresponding to $FMR = \{0.001, 0.0001\}$ computed over all on the order of 10^{10} impostor scores. The FMR in each bin will vary also - see subsequent impostor heatmaps in sec. 3.6.2. Given a pair of face images taken at different times, we assign the comparison to the bin that is the arithmetic average of the subject's ages. This plot shows only the effect of age, not ageing. The number of comparisons in each bin is generally in the thousands, however the first and last bins are computed over 149 and 124 respectively. The error rates in some (adult) cases are zero, and in others the DET is flat so the error rates at the two thresholds are identical. The lines span 1% and 99% of bootstrap replicated FNMR estimates.

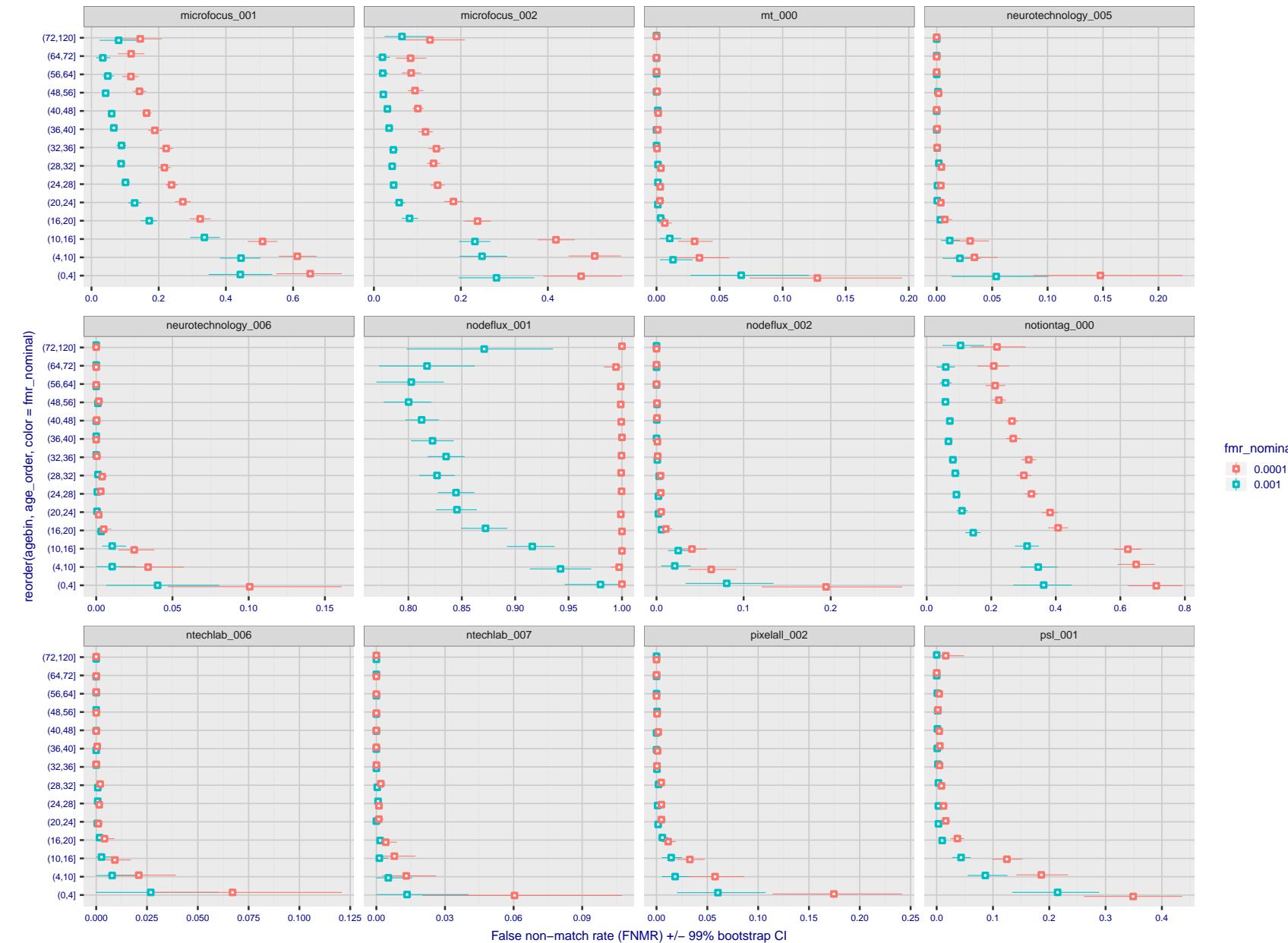


Figure 124: For the visa images, the dots show FNMR by age group for two operating thresholds corresponding to $FMR = \{0.001, 0.0001\}$ computed over all on the order of 10^{10} impostor scores. The FMR in each bin will vary also - see subsequent impostor heatmaps in sec. 3.6.2. Given a pair of face images taken at different times, we assign the comparison to the bin that is the arithmetic average of the subject's ages. This plot shows only the effect of age, not ageing. The number of comparisons in each bin is generally in the thousands, however the first and last bins are computed over 149 and 124 respectively. The error rates in some (adult) cases are zero, and in others the DET is flat so the error rates at the two thresholds are identical. The lines span 1% and 99% of bootstrap replicated FNMR estimates.



Figure 125: For the visa images, the dots show FNMR by age group for two operating thresholds corresponding to $FMR = \{0.001, 0.0001\}$ computed over all on the order of 10^{10} impostor scores. The FMR in each bin will vary also - see subsequent impostor heatmaps in sec. 3.6.2. Given a pair of face images taken at different times, we assign the comparison to the bin that is the arithmetic average of the subject's ages. This plot shows only the effect of age, not ageing. The number of comparisons in each bin is generally in the thousands, however the first and last bins are computed over 149 and 124 respectively. The error rates in some (adult) cases are zero, and in others the DET is flat so the error rates at the two thresholds are identical. The lines span 1% and 99% of bootstrap replicated FNMR estimates.



Figure 126: For the visa images, the dots show FNMR by age group for two operating thresholds corresponding to $FMR = \{0.001, 0.0001\}$ computed over all on the order of 10^{10} impostor scores. The FMR in each bin will vary also - see subsequent impostor heatmaps in sec. 3.6.2. Given a pair of face images taken at different times, we assign the comparison to the bin that is the arithmetic average of the subject's ages. This plot shows only the effect of age, not ageing. The number of comparisons in each bin is generally in the thousands, however the first and last bins are computed over 149 and 124 respectively. The error rates in some (adult) cases are zero, and in others the DET is flat so the error rates at the two thresholds are identical. The lines span 1% and 99% of bootstrap replicated FNMR estimates.



Figure 127: For the visa images, the dots show FNMR by age group for two operating thresholds corresponding to $FMR = \{0.001, 0.0001\}$ computed over all on the order of 10^{10} impostor scores. The FMR in each bin will vary also - see subsequent impostor heatmaps in sec. 3.6.2. Given a pair of face images taken at different times, we assign the comparison to the bin that is the arithmetic average of the subject's ages. This plot shows only the effect of age, not ageing. The number of comparisons in each bin is generally in the thousands, however the first and last bins are computed over 149 and 124 respectively. The error rates in some (adult) cases are zero, and in others the DET is flat so the error rates at the two thresholds are identical. The lines span 1% and 99% of bootstrap replicated FNMR estimates.

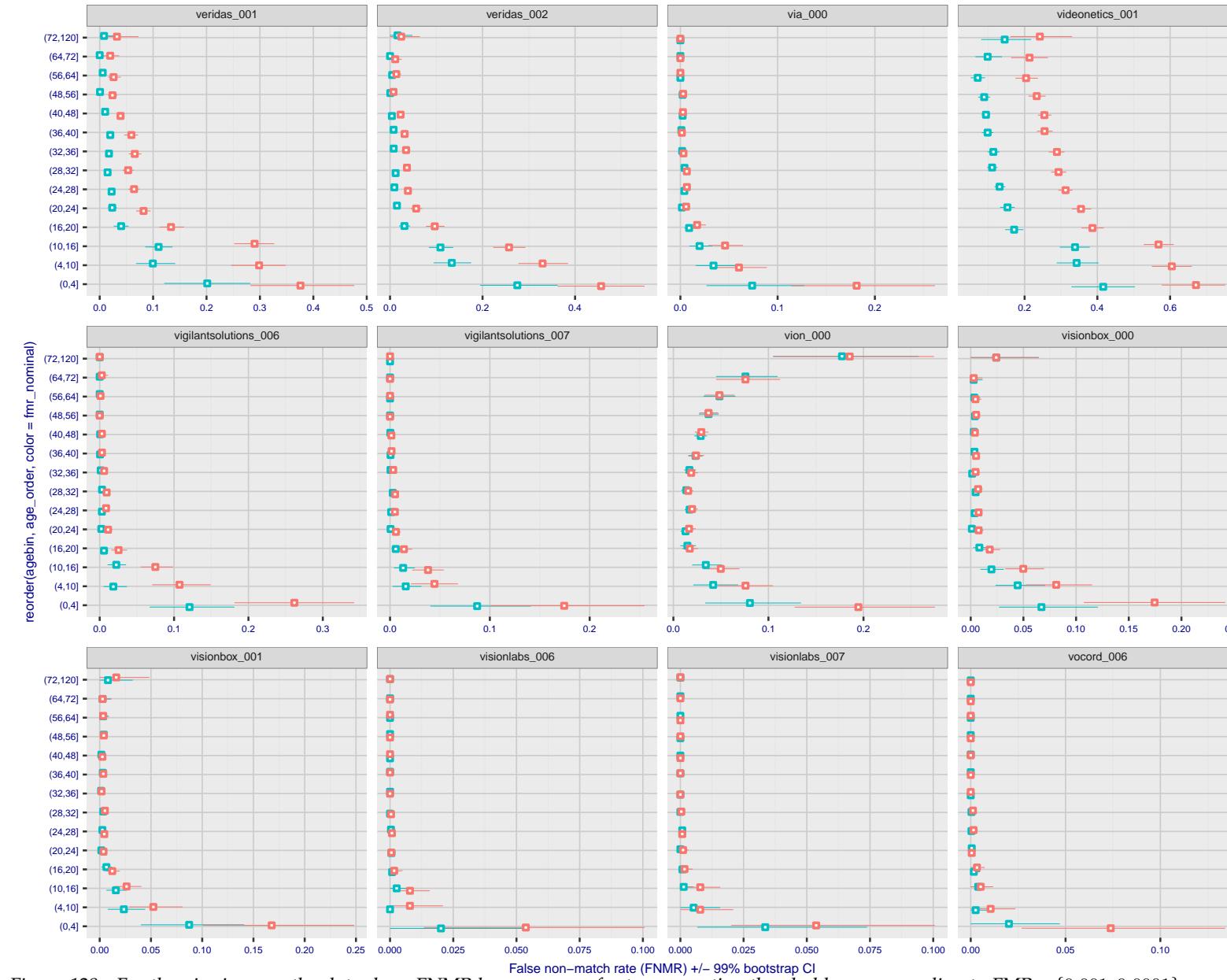


Figure 128: For the visa images, the dots show FNMR by age group for two operating thresholds corresponding to $FMR = \{0.001, 0.0001\}$ computed over all on the order of 10^{10} impostor scores. The FMR in each bin will vary also - see subsequent impostor heatmaps in sec. 3.6.2. Given a pair of face images taken at different times, we assign the comparison to the bin that is the arithmetic average of the subject's ages. This plot shows only the effect of age, not ageing. The number of comparisons in each bin is generally in the thousands, however the first and last bins are computed over 149 and 124 respectively. The error rates in some (adult) cases are zero, and in others the DET is flat so the error rates at the two thresholds are identical. The lines span 1% and 99% of bootstrap replicated FNMR estimates.

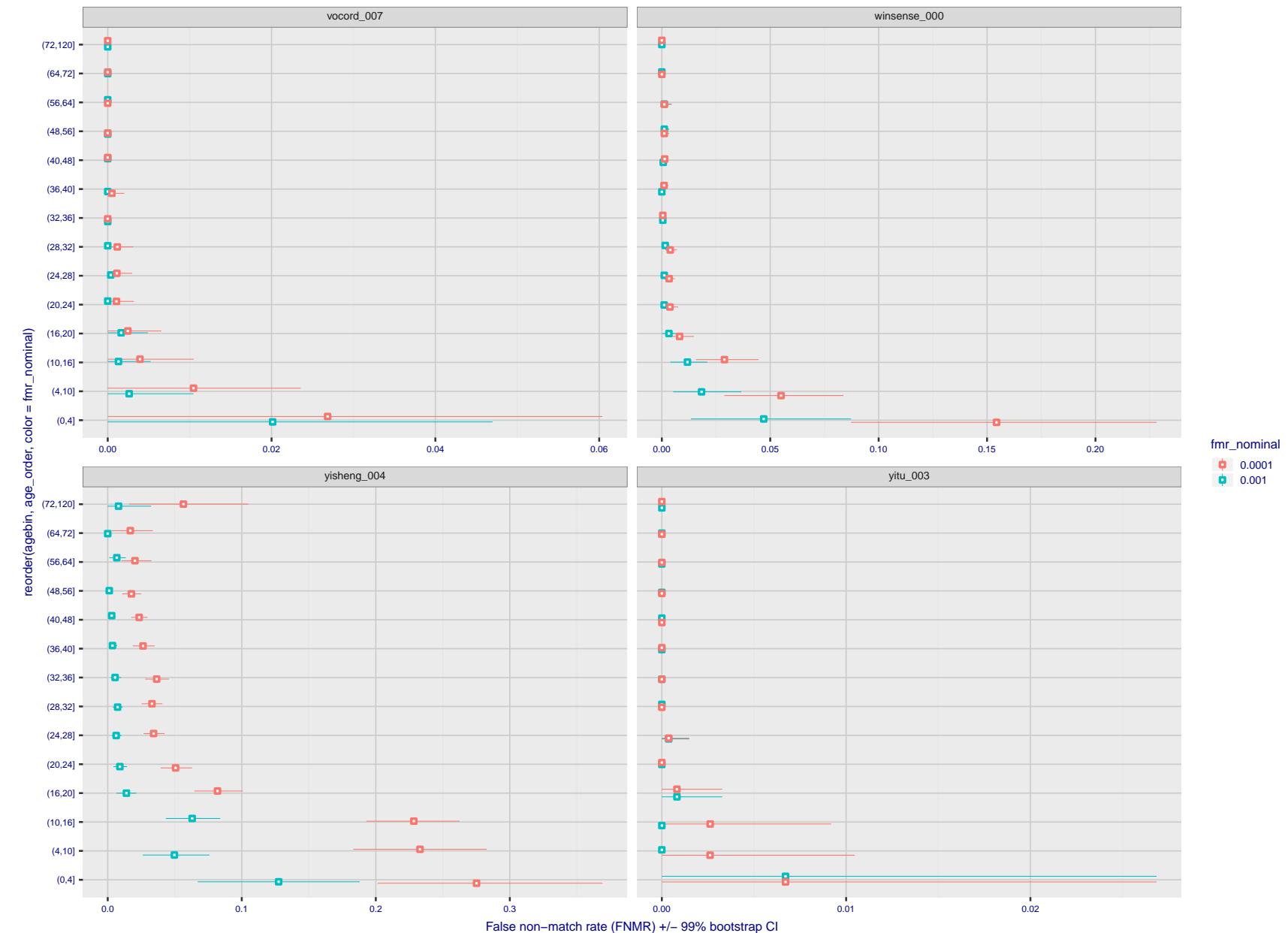


Figure 129: For the visa images, the dots show FNMR by age group for two operating thresholds corresponding to $FMR = \{0.001, 0.0001\}$ computed over all on the order of 10^{10} impostor scores. The FMR in each bin will vary also - see subsequent impostor heatmaps in sec. 3.6.2. Given a pair of face images taken at different times, we assign the comparison to the bin that is the arithmetic average of the subject's ages. This plot shows only the effect of age, not ageing. The number of comparisons in each bin is generally in the thousands, however the first and last bins are computed over 149 and 124 respectively. The error rates in some (adult) cases are zero, and in others the DET is flat so the error rates at the two thresholds are identical. The lines span 1% and 99% of bootstrap replicated FNMR estimates.

Caveats: None.

3.6 Impostor distribution stability

3.6.1 Effect of birth place on the impostor distribution

Background: Facial appearance varies geographically, both in terms of skin tone, cranio-facial structure and size. This section addresses whether false match rates vary intra- and inter-regionally.

Goals:

- ▷ To show the effect of birth region of the impostor and enrollee on false match rates.
- ▷ To determine whether some algorithms give better impostor distribution stability.

Methods:

- ▷ For the visa images, NIST defined 10 regions: Sub-Saharan Africa, South Asia, Polynesia, North Africa, Middle East, Europe, East Asia, Central and South America, Central Asia, and the Caribbean.
- ▷ For the visa images, NIST mapped each country of birth to a region. There is some arbitrariness to this. For example, Egypt could reasonably be assigned to the Middle East instead of North Africa. An alternative methodology could, for example, assign the Philippines to *both* Polynesia and East Asia.
- ▷ FMR is computed for cases where all face images of impostors born in region r_2 are compared with enrolled face images of persons born in region r_1 .

$$\text{FMR}(r_1, r_2, T) = \frac{\sum_{i=1}^{N_{r_1, r_2}} H(s_i - T)}{N_{r_1, r_2}} \quad (5)$$

where the same threshold, T , is used in all cells, and H is the unit step function. The threshold is set to give $\text{FMR}(T) = 0.001$ over the entire set of visa image impostor comparisons.

- ▷ This analysis is then repeated by country-pair, but only for those country pairs where both have at least 1000 images available. The countries¹ appear in the axes of graphs that follow.
- ▷ The mean number of impostor scores in any cross-region bin is 33 million. The smallest number of impostor scores in any bin is 135000, for Central Asia - North Africa. While these counts are large enough to support reasonable significance, the number of individual faces is much smaller, on the order of $N^{0.5}$.
- ▷ The numbers of impostor scores in any cross-country bin is shown in Figure 426.

Results: Subsequent figures show heatmaps that use color to represent the base-10 logarithm of the false match rate. Red colors indicate high (bad) false match rates. Dark colors indicate benign false match rates. There are two series of graphs corresponding to aggregated geographical regions, and to countries. The notable observations are:

- ▷ The on-diagonal elements correspond to within-region impostors. FMR is generally above the nominal value of $\text{FMR} = 0.001$. Particularly there is usually higher FMR in, Sub-Saharan Africa, South Asia, and the Caribbean. Europe and Central Asia, on the other hand, usually give FMR closer to the nominal value.
- ▷ The off-diagonal elements correspond to across-region impostors. The highest FMR is produced between the Caribbean and Sub-Saharan Africa.
- ▷ Algorithms vary.

¹These are Argentina, Australia, Brazil, Chile, China, Costa Rica, Cuba, Czech Republic, Dominican Republic, Ecuador, Egypt, El Salvador, Germany, Ghana, Great Britain, Greece, Guatemala, Haiti, Hong Kong, Honduras, Indonesia, India, Israel, Jamaica, Japan, Kenya, Korea, Lebanon, Mexico, Malaysia, Nepal, Nigeria, Peru, Philippines, Pakistan, Poland, Romania, Russia, South Africa, Saudi Arabia, Thailand, Trinidad, Turkey, Taiwan, Ukraine, Venezuela, and Vietnam.

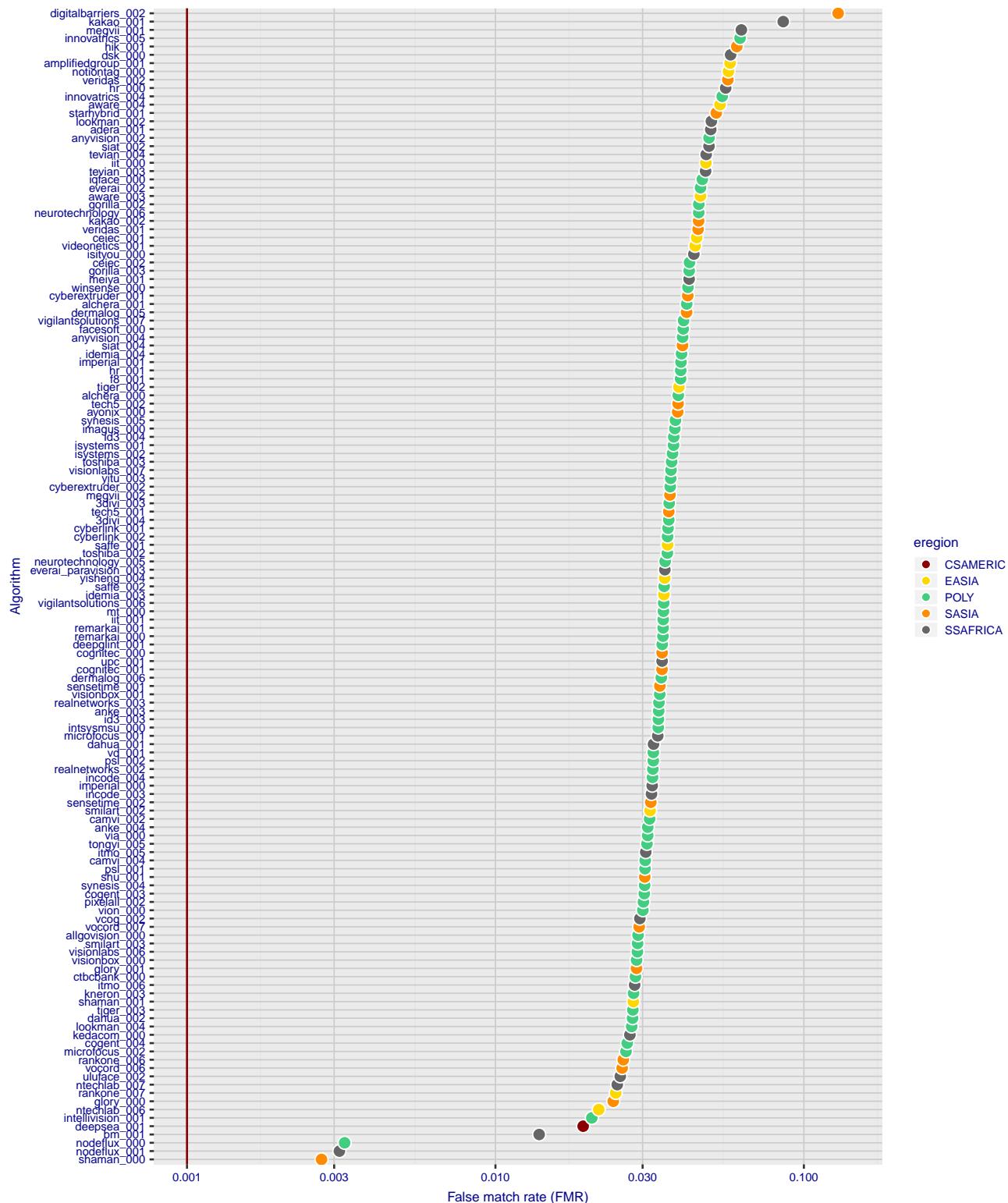


Figure 130: For the visa images, the dots show FMR for impostor comparisons of individuals of the same sex and same age group for the region of the world that gives the worst (highest) FMR when the threshold is set to give $FMR = 0.001$ (red vertical line) over all on the order of 10^{10} impostor scores i.e. zero-effort. The shift of the dots to right shows massive increases in FMR when impostors have the same sex, age, and region of birth. The color code indicates which region gives the worst case FMR. If the observed variation is due to the prevalence of one kind of images in the training imagery, then algorithms developed on one kind of data might be expected to give higher FMR on other kinds.

- ▷ We computed the same quantities for a global FMR = 0.0001. The effects are similar.

Caveats:

- ▷ The effects of variable impostor rates on one-to-many identification systems may well differ from what's implied by these one-to-one verification results. Two reasons for this are a) the enrollment galleries are usually imbalanced across countries of birth, age and sex; b) one-to-many identification algorithms often implement techniques aimed at stabilizing the impostor distribution. Further research is necessary.
- ▷ In principle, the effects seen in this subsection could be due to differences in the image capture process. We consider this unlikely since the effects are maintained across geography - e.g. Caribbean vs. Africa, or Japan vs. China.

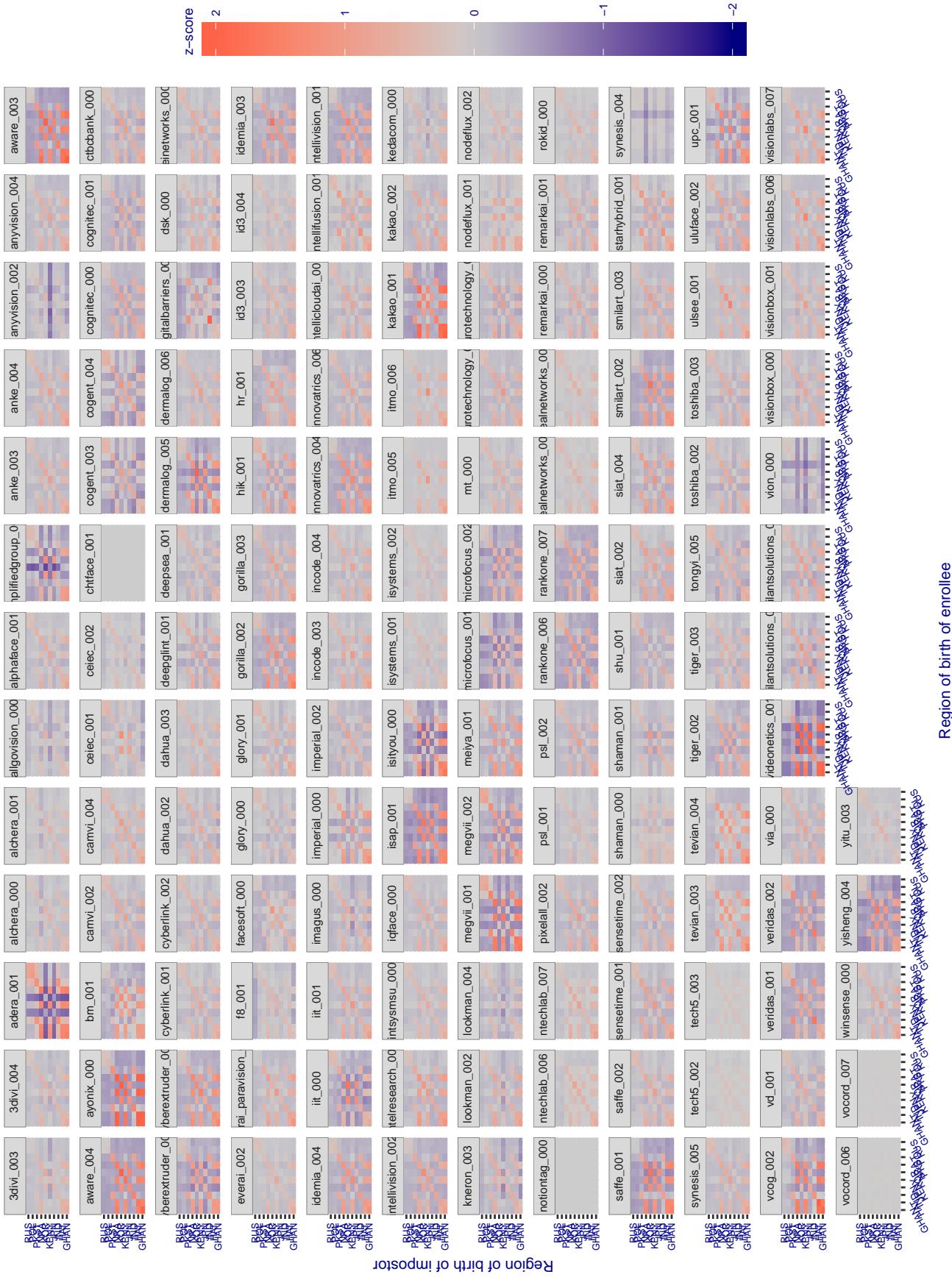


Figure 131: For visa images, the heatmap shows how the mean of the impostor distribution for the country pair (a,b) is shifted relative to the mean of the global impostor distribution, expressed as a number of standard deviations of the global impostor distribution. This statistic is designed to show shifts in the entire impostor distribution, not just tail effects that manifest as the anomalously high (or low) false match rates that appear in the subsequent figures. The countries are chosen to show that skin tone alone does not explain impostor distribution shifts. The reduced shift in Asian populations with the Yitu and TongYiTrans algorithms, is accompanied by positive shifts in the European populations. This reversal relative to most other algorithms, may derive from use of nationally weighted training sets. The Visionlabs algorithm appears most insensitive to country effects. The figure is computed from same-sex and same-age impostor pairs.

Cross region FMR at threshold T = 2.740 for algorithm 3divi_003, giving FMR(T) = 0.0001 globally.

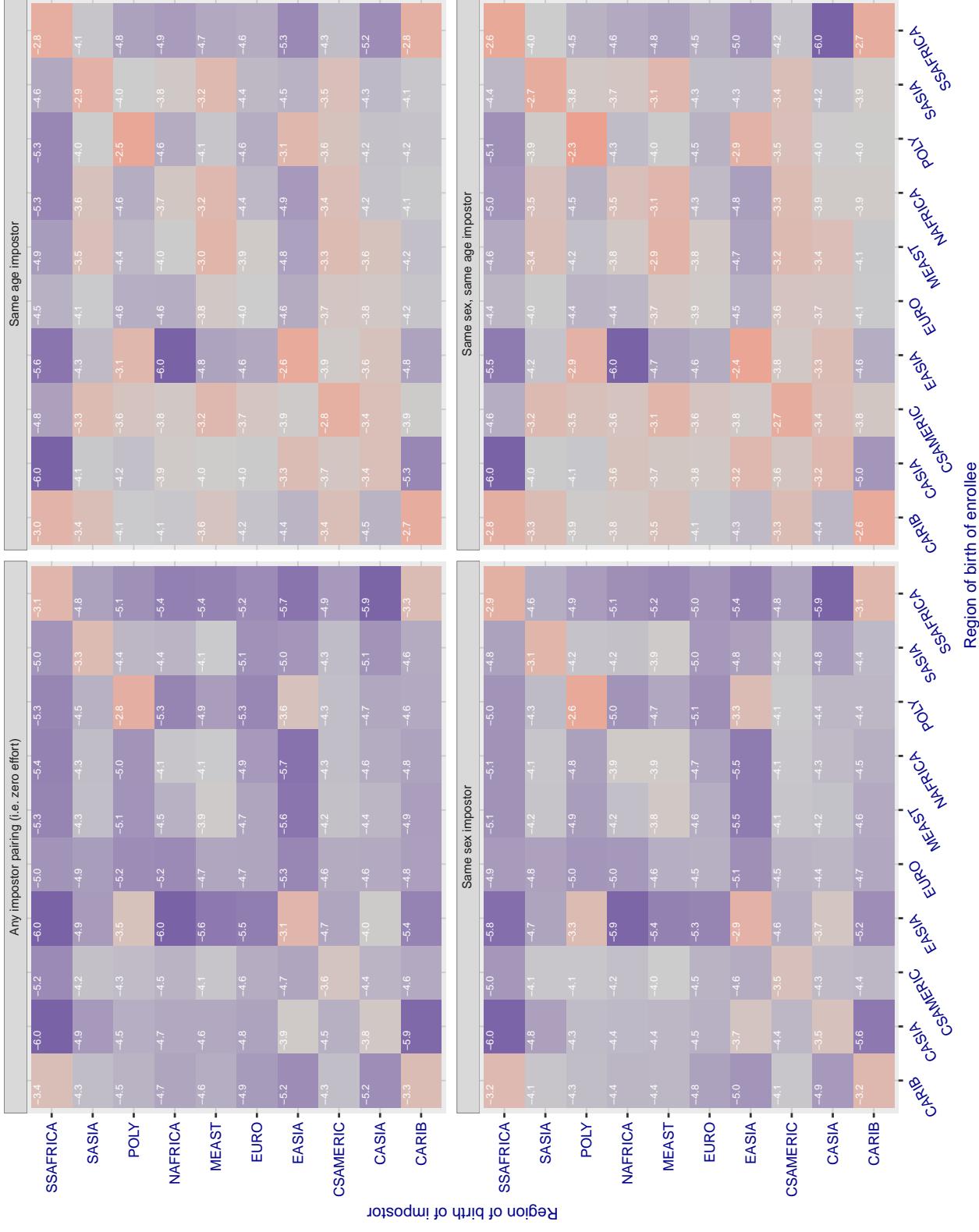


Figure 132: For algorithm 3divi_003 operating on visa images, the heatmap shows false match rates observed over impostor comparisons of faces from different individuals who were born in the given region pair. False matches are counted against a recognition threshold fixed globally to give the target FMR in the plot title, computed over all on the order of 10^{10} impostor comparisons. If text appears in each box it give the same quantity as that coded by the color. Grey indicates FMR is at the intended FMR target level. Light red colors present a security vulnerability to, for example, a passport gate. Each +1 increase in \log_{10} FMR corresponds to a factor of 10 increase in FMR. The matrix is not quite symmetric because images in the enrollment and verification sets are different.

Cross region FMR at threshold T = 2.857 for algorithm 3divi_004, giving FMR(T) = 0.0001 globally.

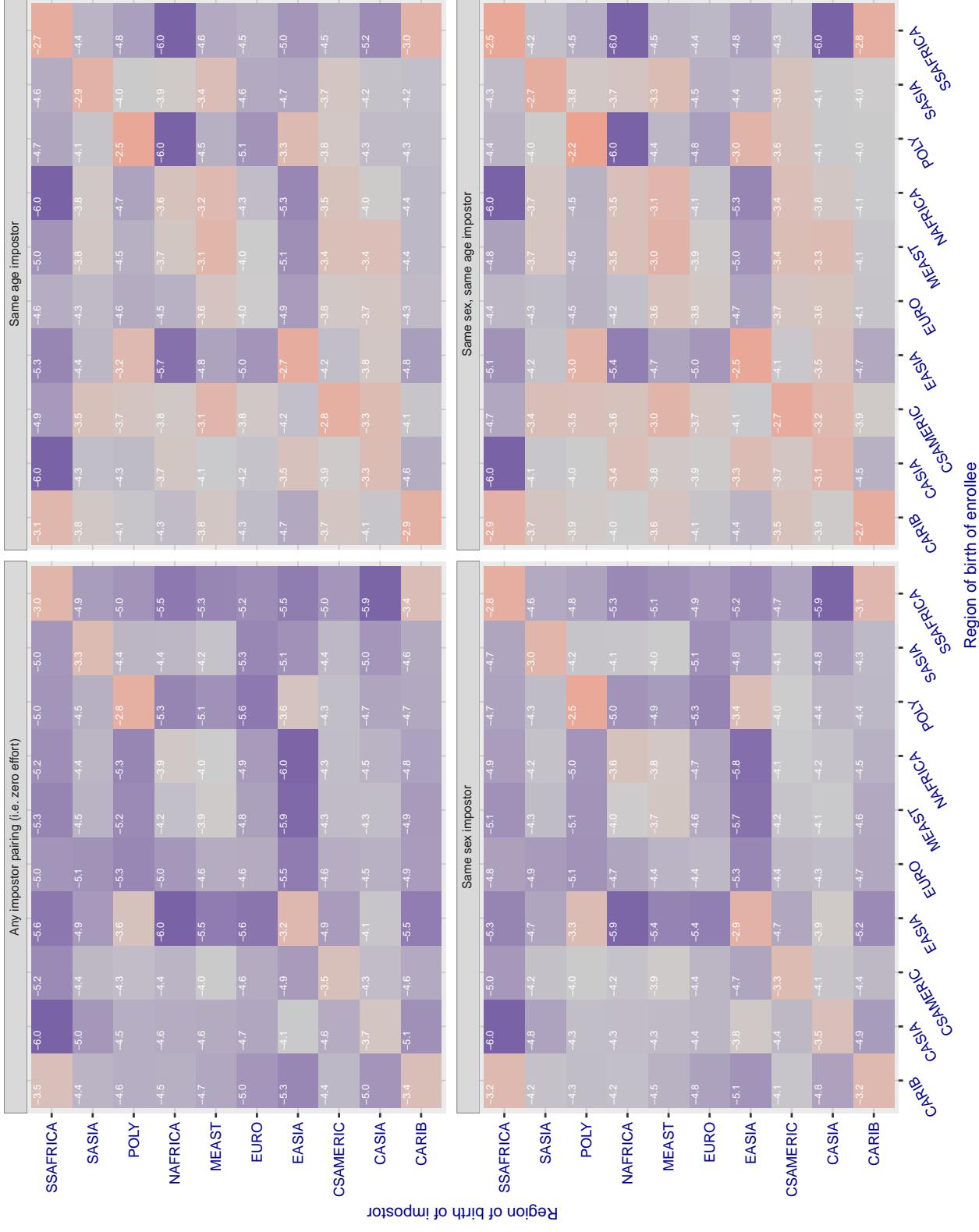


Figure 133: For algorithm 3divi-004 operating on visa images, the heatmap shows false match rates observed over impostor comparisons of faces from different individuals who were born in the given region pair. False matches are counted against a recognition threshold fixed globally to give the target FMR in the plot title, computed over all on the order of 10^{10} impostor comparisons. If text appears in each box it give the same quantity as that coded by the color. Grey indicates FMR is at the intended FMR target level. Light red colors present a security vulnerability to, for example, a passport gate. Each +1 increase in $\log_{10} \text{FMR}$ corresponds to a factor of 10 increase in FMR. The matrix is not quite symmetric because images in the enrollment and verification sets are different.

Cross region FMR at threshold T = 0.713 for algorithm adera_001, giving FMR(T) = 0.0001 globally.

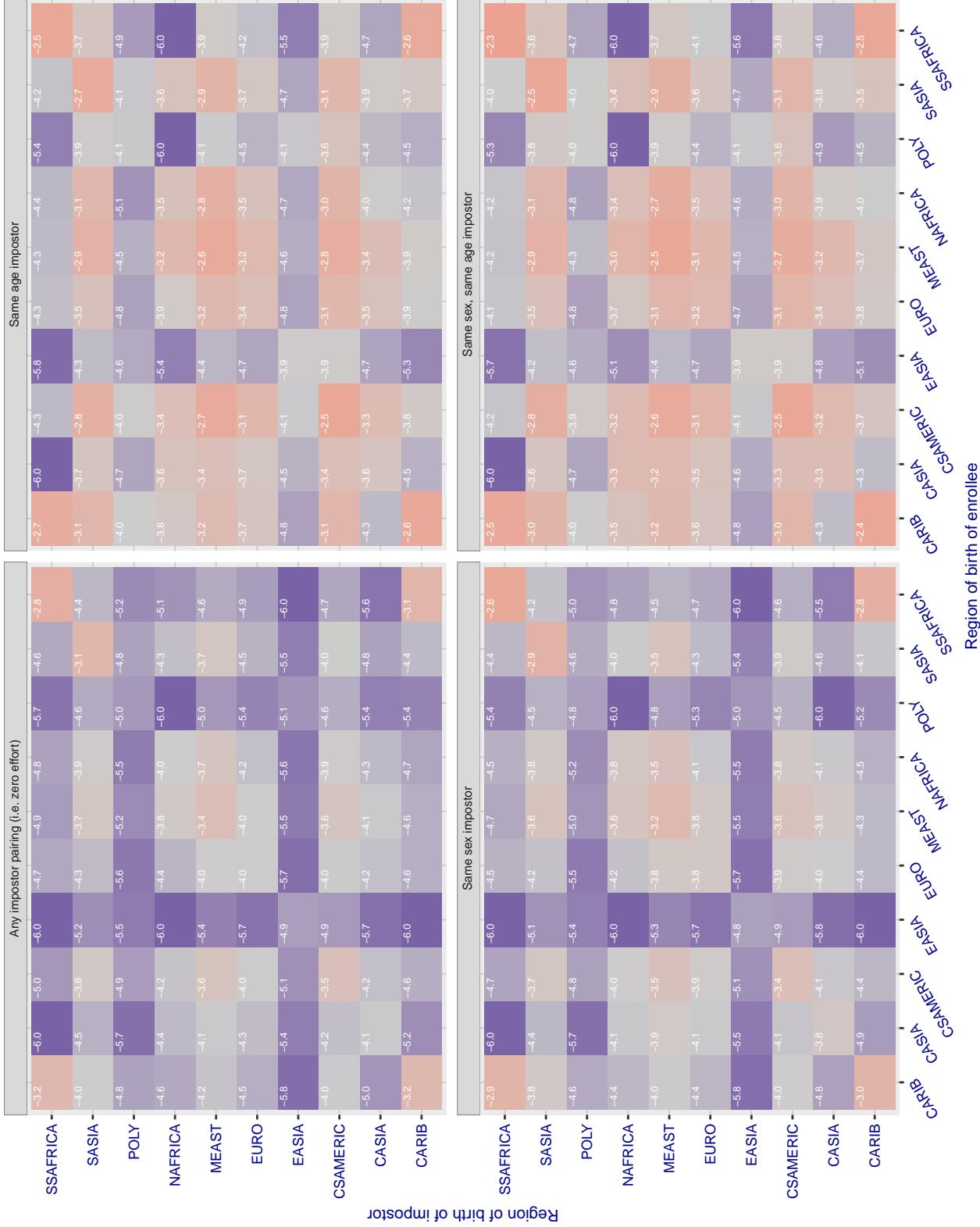


Figure 134: For algorithm adera-001 operating on visa images, the heatmap shows false match rates observed over impostor comparisons of faces from different individuals who were born in the given region pair. False matches are counted against a recognition threshold fixed globally to give the target FMR in the plot title, computed over all on the order of 10^{10} impostor comparisons. If text appears in each box it give the same quantity as that coded by the color. Grey indicates FMR is at the intended FMR target level. Light red colors present a security vulnerability to, for example, a passport gate. Each +1 increase in $\log_{10} FMR$ corresponds to a factor of 10 increase in FMR. The matrix is not quite symmetric because images in the enrollment and verification sets are different.

Cross region FMR at threshold T = 0.702 for algorithm alchera_000, giving FMR(T) = 0.0001 globally.

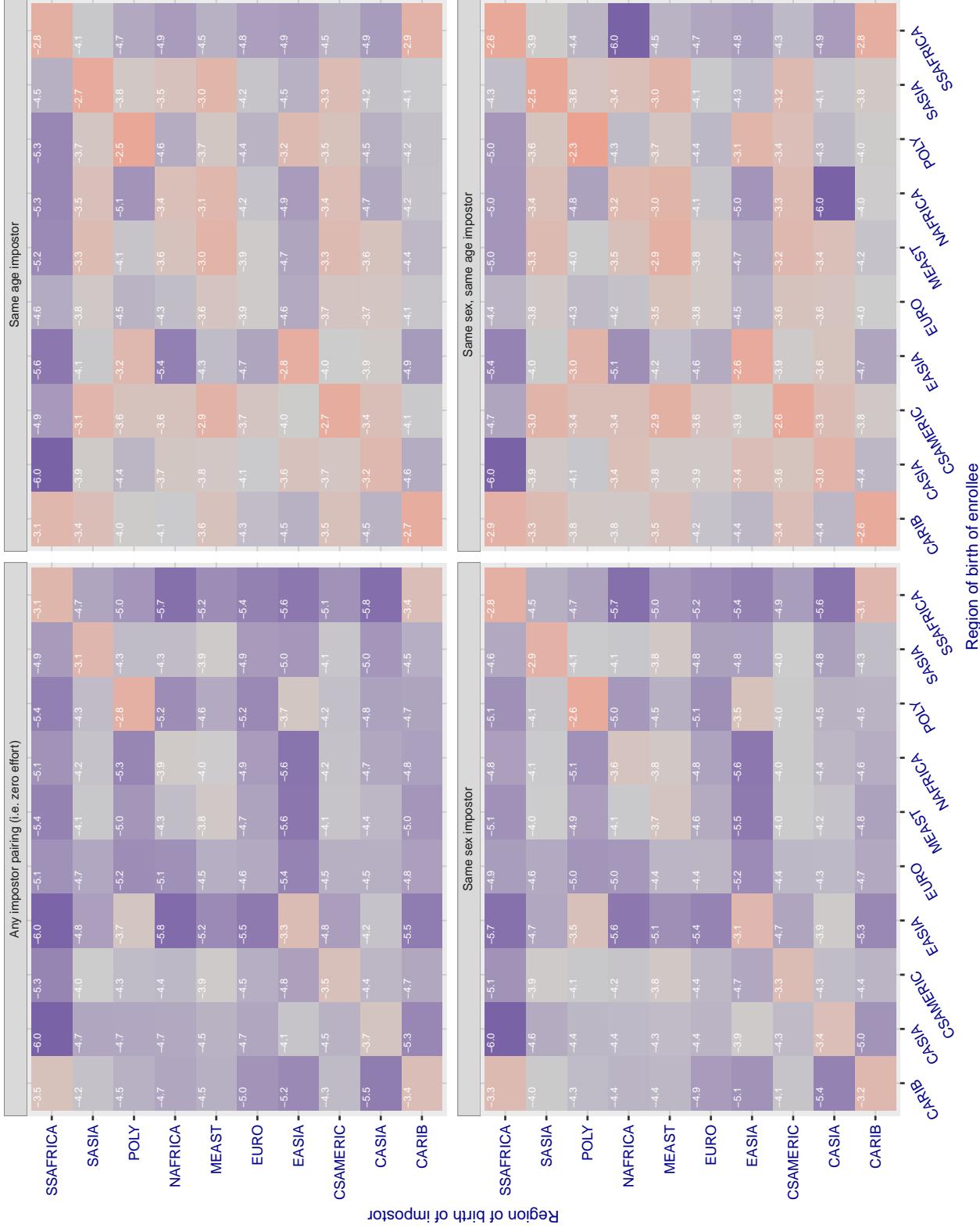


Figure 135: For algorithm alchera-000 operating on visa images, the heatmap shows false match rates observed over impostor comparisons of faces from different individuals who were born in the given region pair. False matches are counted against a recognition threshold fixed globally to give the target FMR in the plot title, computed over all on the order of 10^{10} impostor comparisons. If text appears in each box it give the same quantity as that coded by the color. Grey indicates FMR is at the intended FMR target level. Light red colors present a security vulnerability to, for example, a passport gate. Each +1 increase in $\log_{10} FMR$ corresponds to a factor of 10 increase in FMR. The matrix is not quite symmetric because images in the enrollment and verification sets are different.

Cross region FMR at threshold T = 0.713 for algorithm alchera_001, giving FMR(T) = 0.0001 globally.

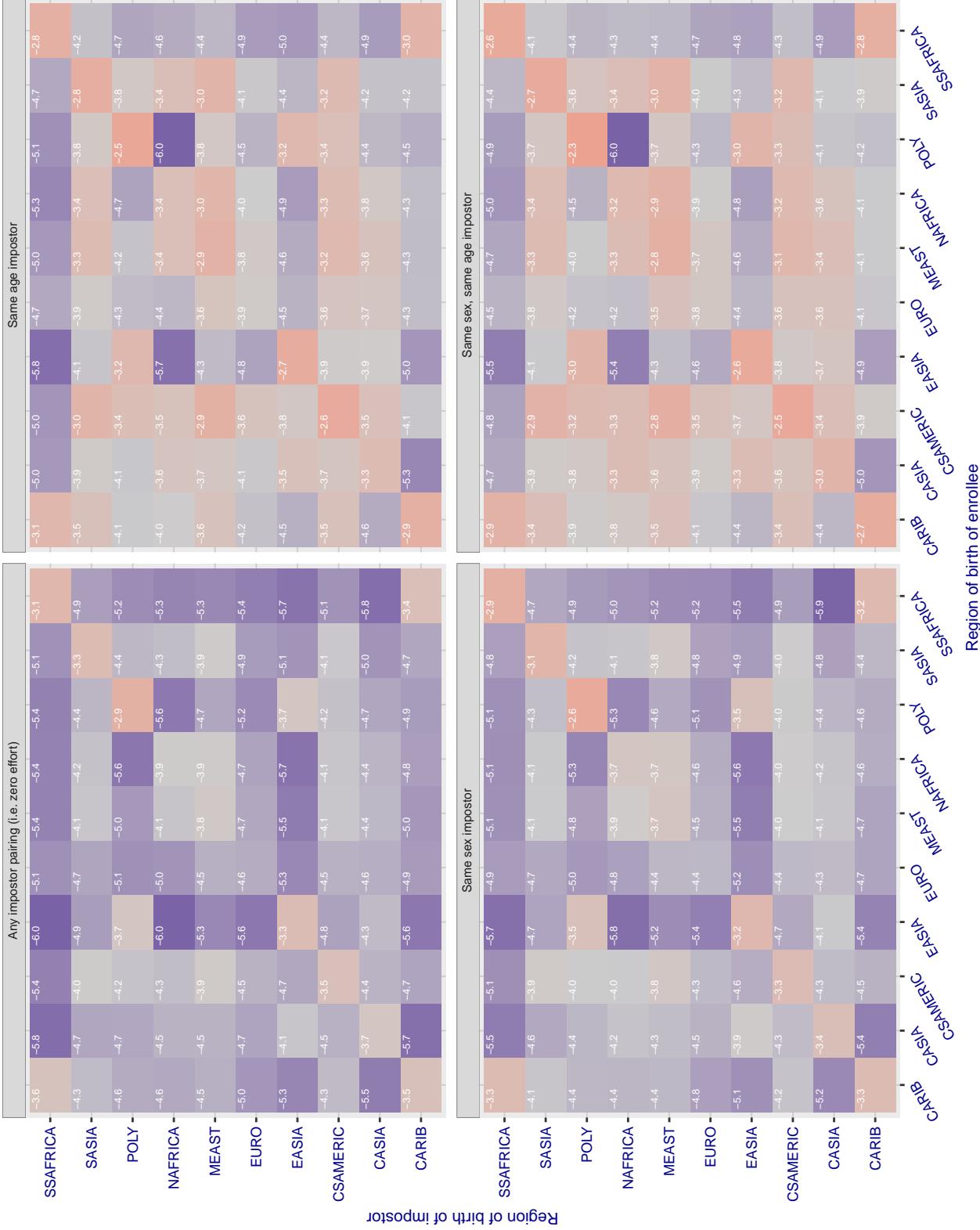


Figure 136: For algorithm alchera-001 operating on visa images, the heatmap shows false match rates observed over impostor comparisons of faces from different individuals who were born in the given region pair. False matches are counted against a recognition threshold fixed globally to give the target FMR in the plot title, computed over all on the order of 10^{10} impostor comparisons. If text appears in each box it give the same quantity as that coded by the color. Grey indicates FMR is at the intended FMR target level. Light red colors present a security vulnerability to, for example, a passport gate. Each +1 increase in $\log_{10} FMR$ corresponds to a factor of 10 increase in FMR. The matrix is not quite symmetric because images in the enrollment and verification sets are different.

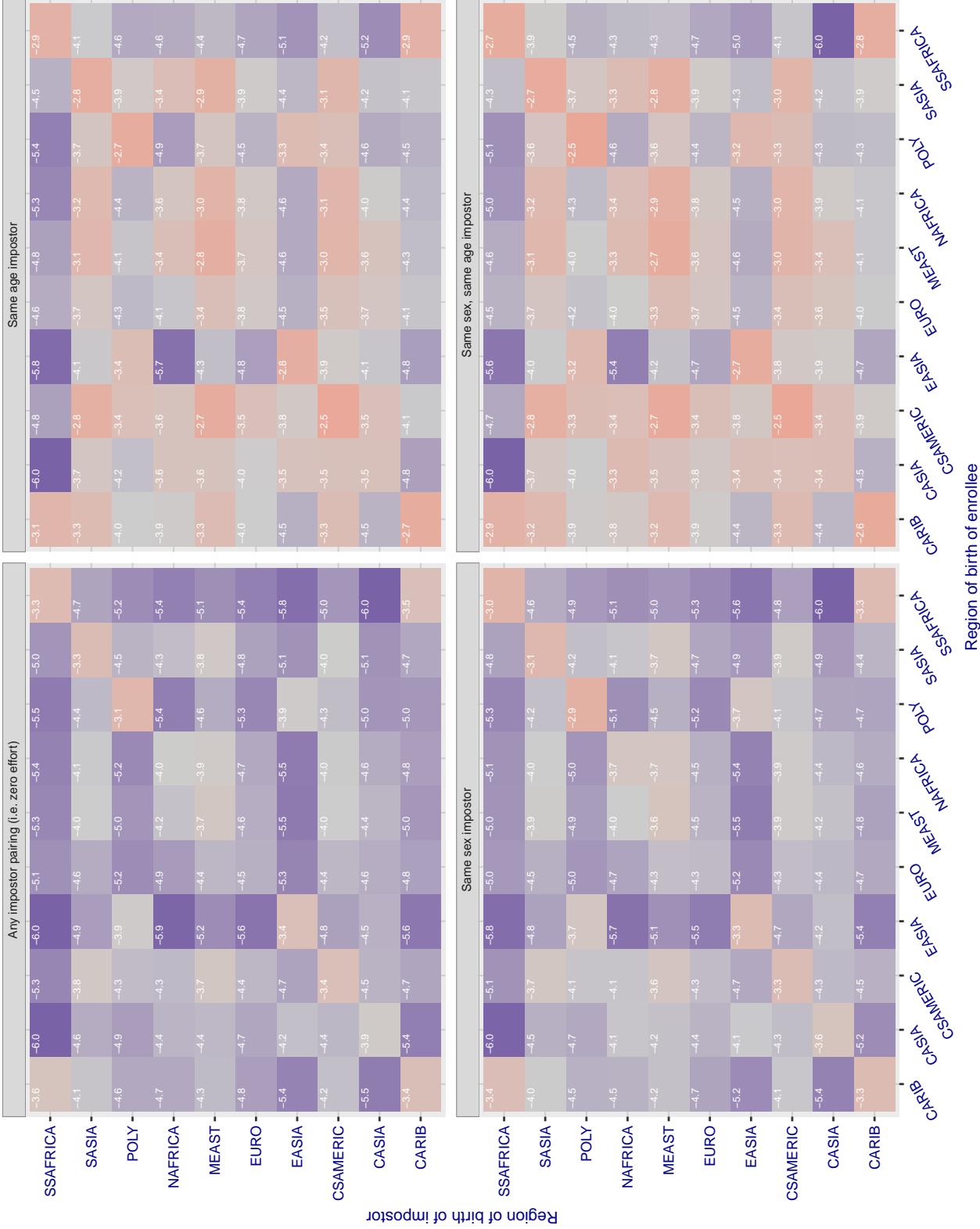
Cross region FMR at threshold T = 0.433 for algorithm allgovision_000, giving FMR(T) = 0.0001 globally.

Figure 137: For algorithm allgovision-000 operating on visa images, the heatmap shows false match rates observed over impostor comparisons of faces from different individuals who were born in the given region pair. False matches are counted against a recognition threshold fixed globally to give the target FMR in the plot title, computed over all on the order of 10^{10} impostor comparisons. If text appears in each box it give the same quantity as that coded by the color. Grey indicates FMR is at the intended FMR target level. Light red colors present a security vulnerability to, for example, a passport gate. Each +1 increase in $\log_{10} FMR$ corresponds to a factor of 10 increase in FMR. The matrix is not quite symmetric because images in the enrollment and verification sets are different.

Cross region FMR at threshold T = 0.396 for algorithm alphaface_001, giving FMR(T) = 0.00001 globally.

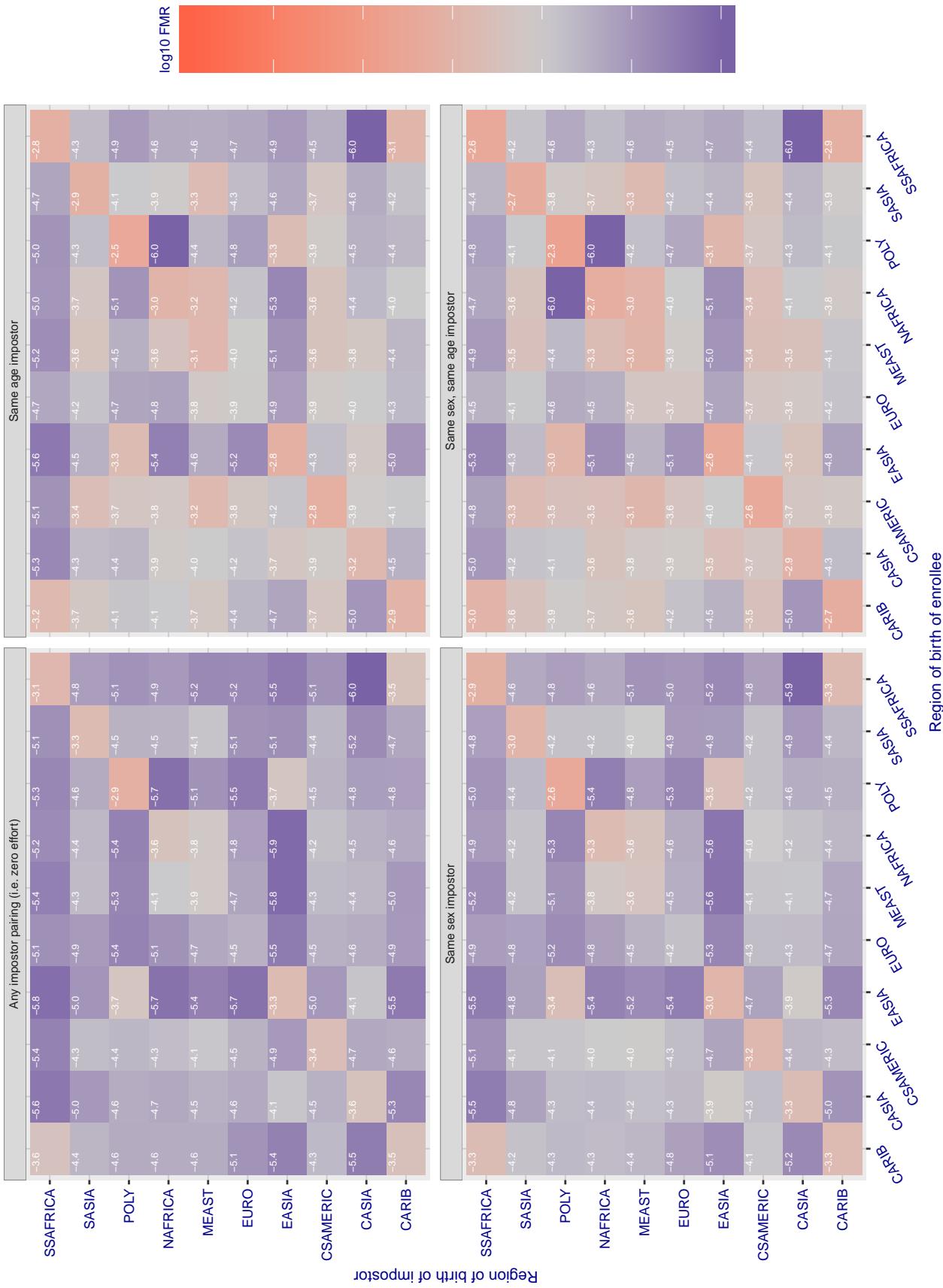


Figure 138: For algorithm alphaface-001 operating on visa images, the heatmap shows false match rates observed over impostor comparisons of faces from different individuals who were born in the given region pair. False matches are counted against a recognition threshold fixed globally to give the target FMR in the plot title, computed over all on the order of 10^{10} impostor comparisons. If text appears in each box it give the same quantity as that coded by the color. Grey indicates FMR is at the intended FMR target level. Light red colors present a security vulnerability to, for example, a passport gate. Each +1 increase in $\log_{10} FMR$ corresponds to a factor of 10 increase in FMR. The matrix is not quite symmetric because images in the enrollment and verification sets are different.

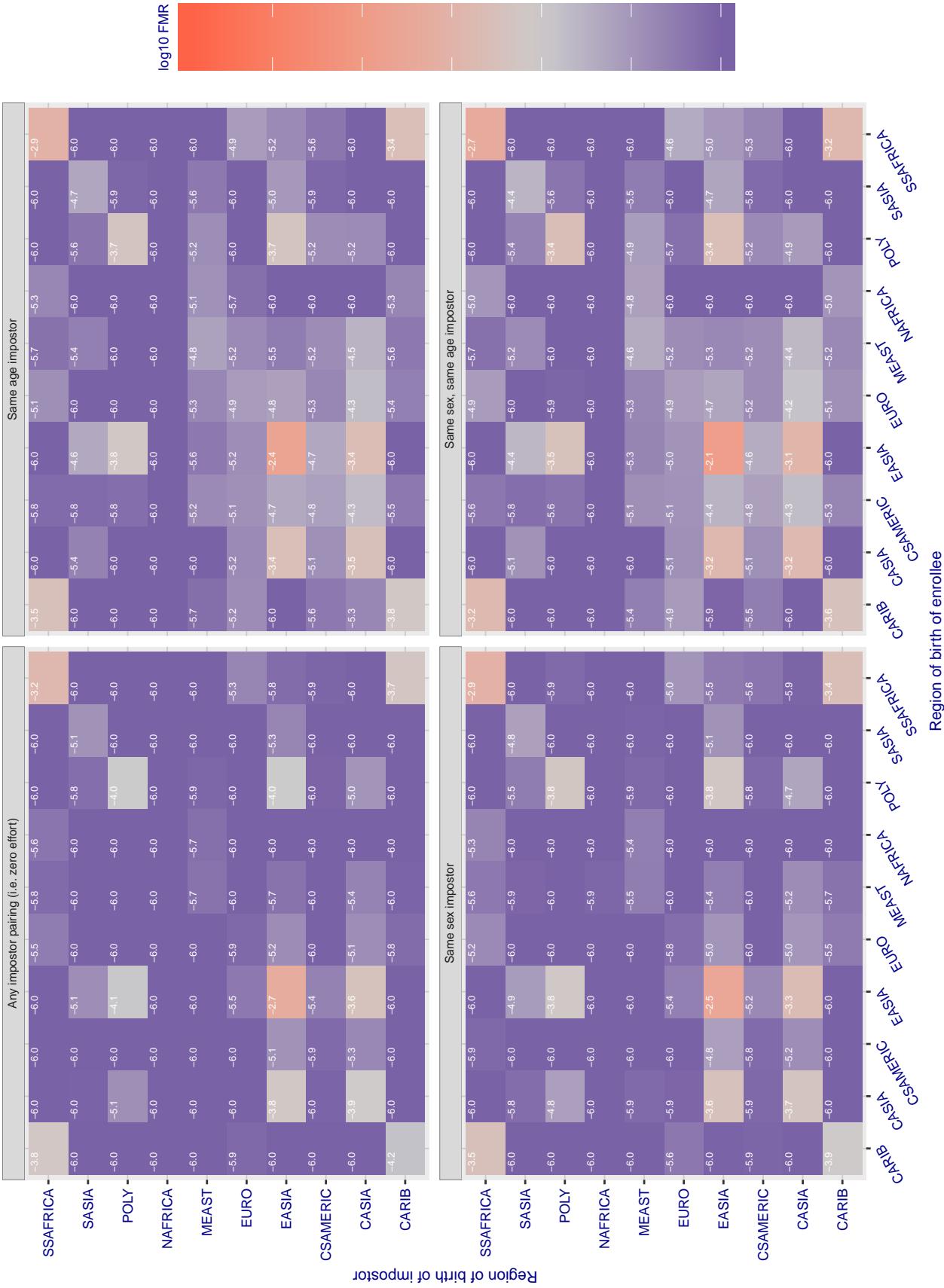
Cross region FMR at threshold T = 3.640 for algorithm amplifiedgroup_001, giving FMR(T) = 0.0001 globally.

Figure 139: For algorithm amplifiedgroup-001 operating on visa images, the heatmap shows false match rates observed over impostor comparisons of faces from different individuals who were born in the given region pair. False matches are counted against a recognition threshold fixed globally to give the target FMR in the plot title, computed over all on the order of 10^{10} impostor comparisons. If text appears in each box it give the same quantity as that coded by the color. Grey indicates FMR is at the intended FMR target level. Light red colors present a security vulnerability to, for example, a passport gate. Each +1 increase in $\log_{10} \text{FMR}$ corresponds to a factor of 10 increase in FMR. The matrix is not quite symmetric because images in the enrollment and verification sets are different.

Cross region FMR at threshold T = 0.397 for algorithm anke_003, giving FMR(T) = 0.0001 globally.

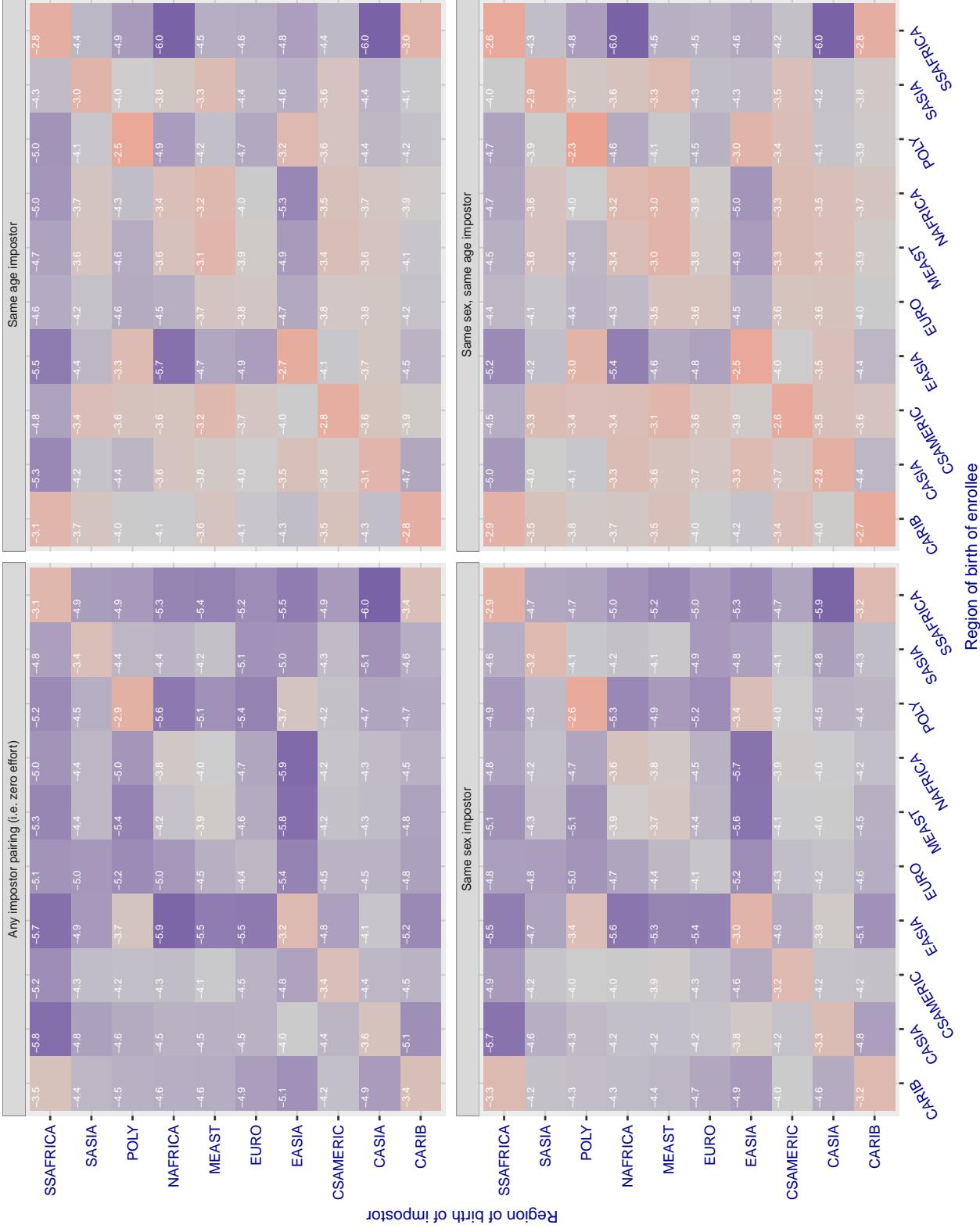


Figure 140: For algorithm anke-003 operating on visa images, the heatmap shows false match rates observed over impostor comparisons of faces from different individuals who were born in the given region pair. False matches are counted against a recognition threshold fixed globally to give the target FMR in the plot title, computed over all on the order of 10^{10} impostor comparisons. If text appears in each box it give the same quantity as that coded by the color. Grey indicates FMR is at the intended FMR target level. Light red colors present a security vulnerability to, for example, a passport gate. Each +1 increase in $\log_{10} \text{FMR}$ corresponds to a factor of 10 increase in FMR. The matrix is not quite symmetric because images in the enrollment and verification sets are different.

Cross region FMR at threshold T = 0.397 for algorithm anke_004, giving FMR(T) = 0.0001 globally.

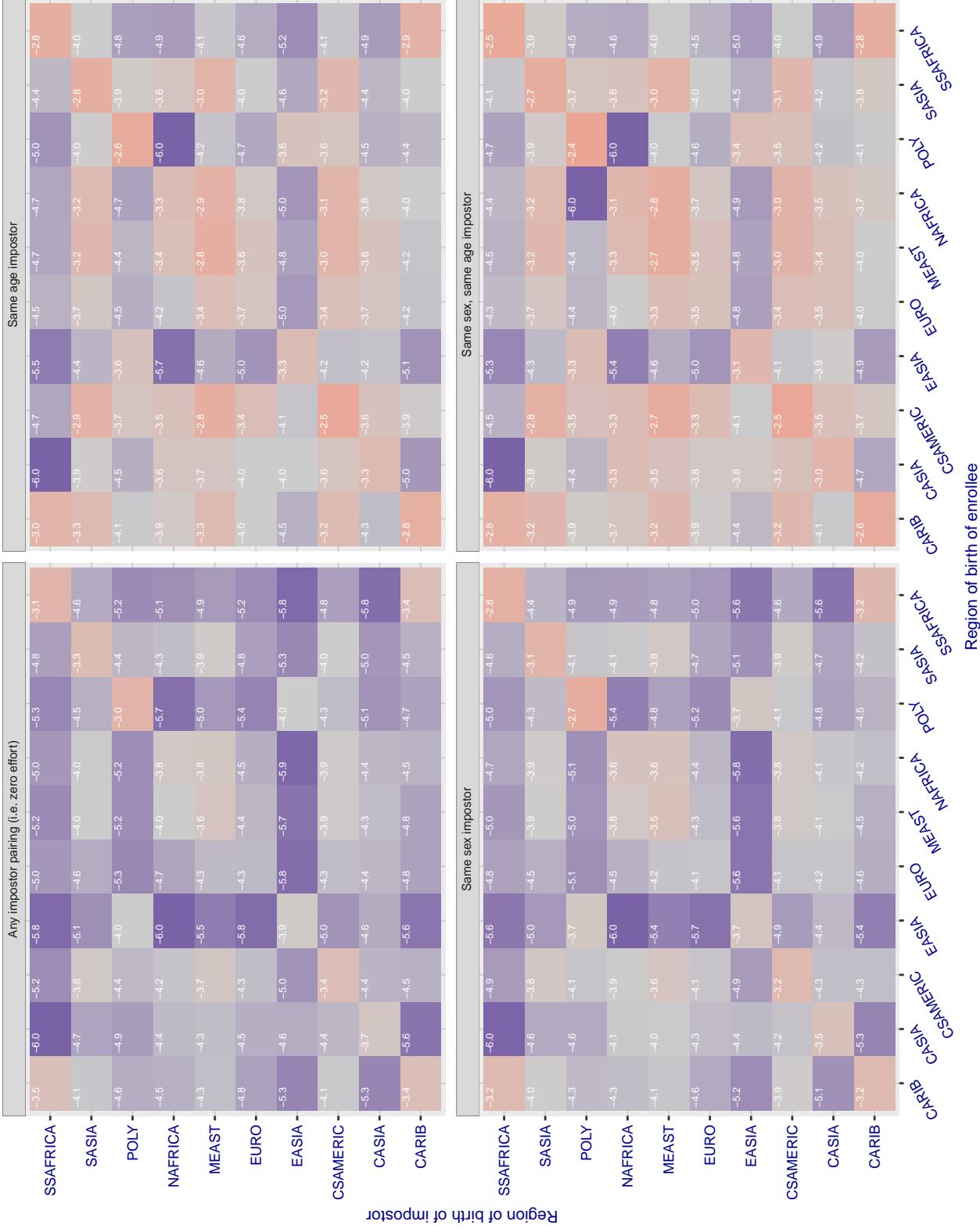


Figure 141: For algorithm anke-004 operating on visa images, the heatmap shows false match rates observed over impostor comparisons of faces from different individuals who were born in the given region pair. False matches are counted against a recognition threshold fixed globally to give the target FMR in the plot title, computed over all on the order of 10^{10} impostor comparisons. If text appears in each box it give the same quantity as that coded by the color. Grey indicates FMR is at the intended FMR target level. Light red colors present a security vulnerability to, for example, a passport gate. Each +1 increase in $\log_{10} \text{FMR}$ corresponds to a factor of 10 increase in FMR. The matrix is not quite symmetric because images in the enrollment and verification sets are different.

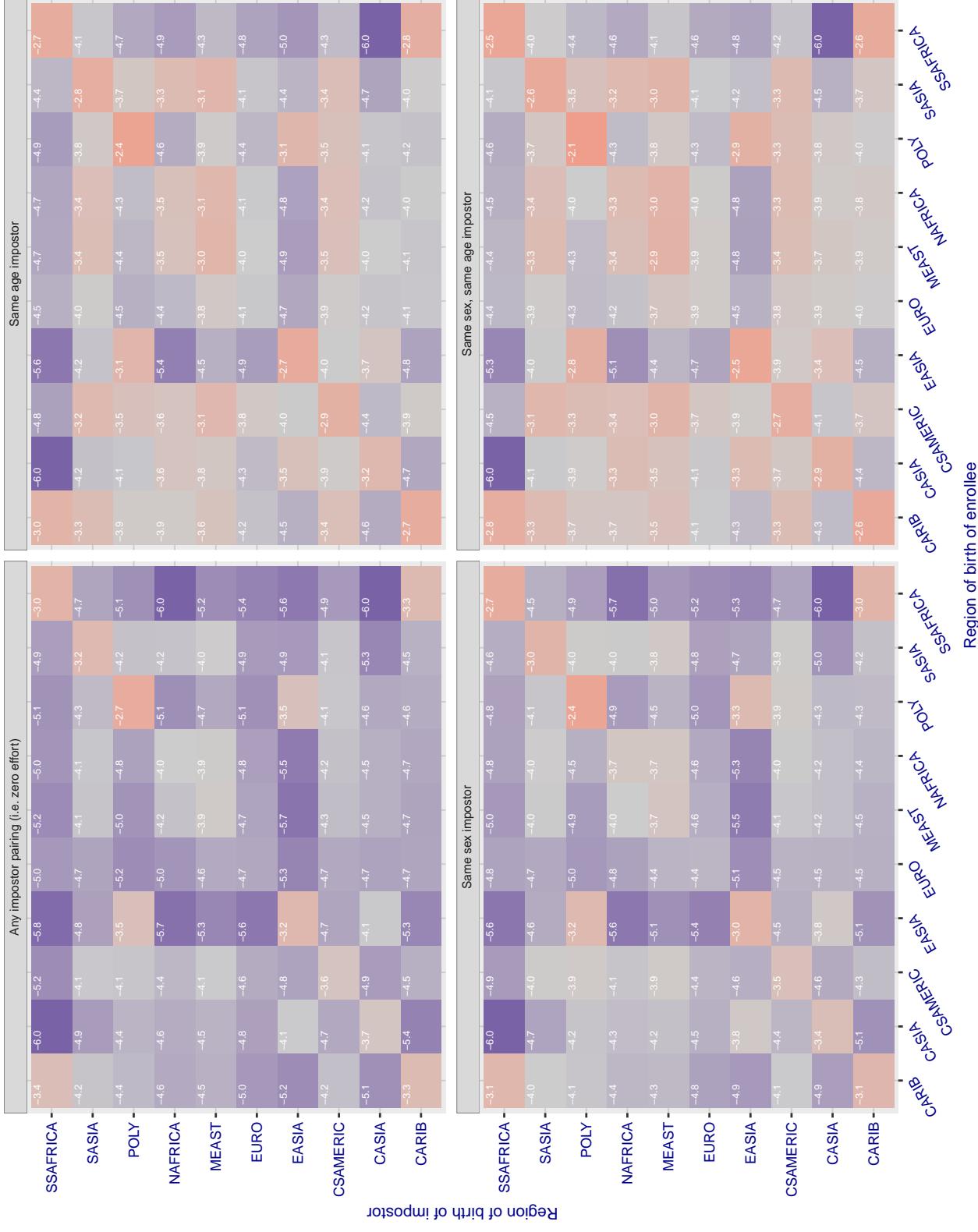
Cross region FMR at threshold T = 1.526 for algorithm anyvision_002, giving FMR(T) = 0.00001 globally.

Figure 142: For algorithm anyvision-002 operating on visa images, the heatmap shows false match rates observed over impostor comparisons of faces from different individuals who were born in the given region pair. False matches are counted against a recognition threshold fixed globally to give the target FMR in the plot title, computed over all on the order of 10^{10} impostor comparisons. If text appears in each box it give the same quantity as that coded by the color. Grey indicates FMR is at the intended FMR target level. Light red colors present a security vulnerability to, for example, a passport gate. Each +1 increase in $\log_{10} \text{FMR}$ corresponds to a factor of 10 increase in FMR. The matrix is not quite symmetric because images in the enrollment and verification sets are different.

Cross region FMR at threshold T = 1.375 for algorithm anyvision_004, giving FMR(T) = 0.00001 globally.

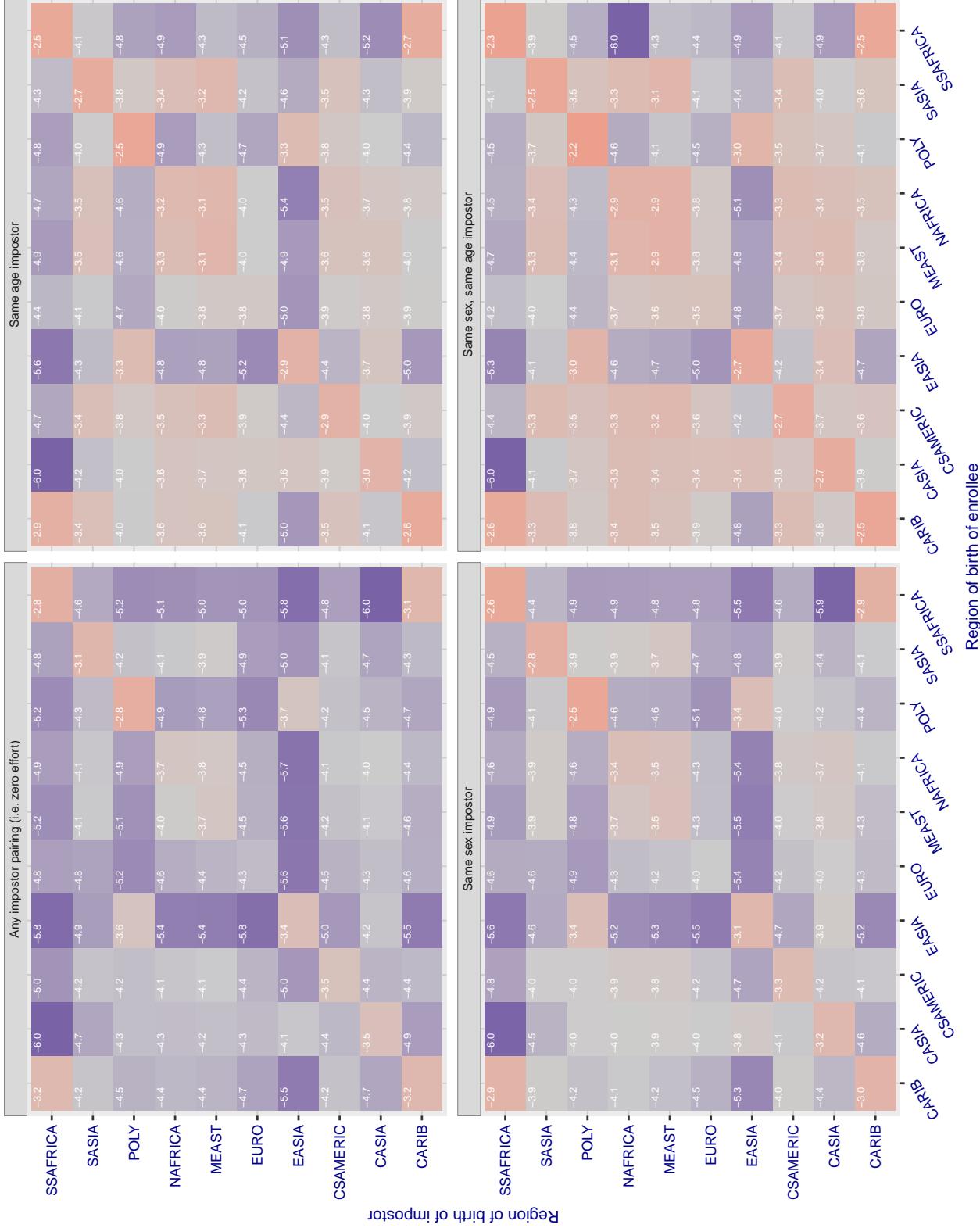
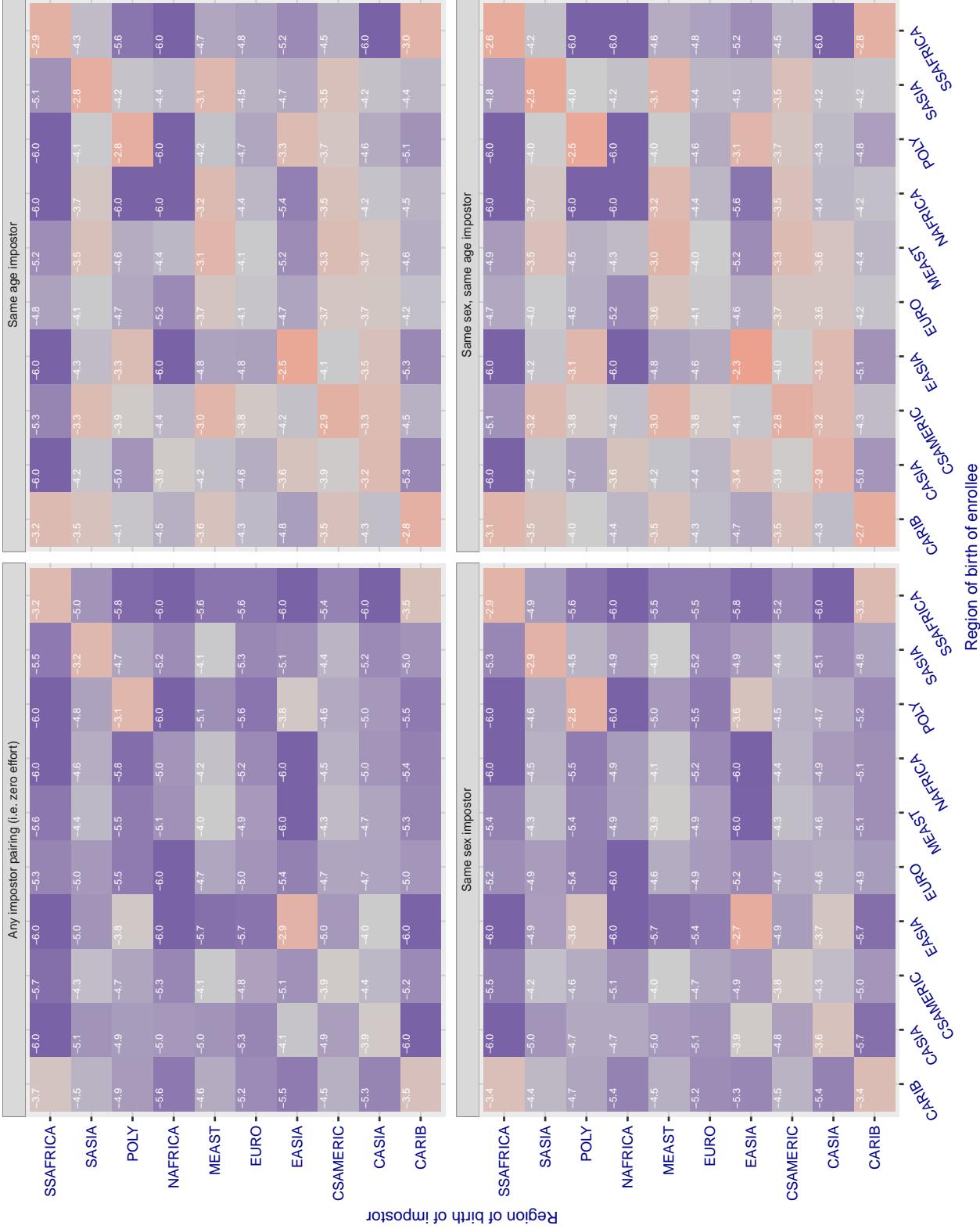


Figure 143: For algorithm anyvision-004 operating on visa images, the heatmap shows false match rates observed over impostor comparisons of faces from different individuals who were born in the given region pair. False matches are counted against a recognition threshold fixed globally to give the target FMR in the plot title, computed over all on the order of 10^{10} impostor comparisons. If text appears in each box it give the same quantity as that coded by the color. Grey indicates FMR is at the intended FMR target level. Light red colors present a security vulnerability to, for example, a passport gate. Each +1 increase in $\log_{10} \text{FMR}$ corresponds to a factor of 10 increase in FMR. The matrix is not quite symmetric because images in the enrollment and verification sets are different.

Cross region FMR at threshold T = 3.868 for algorithm aware_003, giving FMR(T) = 0.0001 globally.



2019/09/11 14:58:19

$\text{FNMR}(T)$ "False non-match rate"
 $\text{FMR}(T)$ "False match rate"

Figure 144: For algorithm aware-003 operating on visa images, the heatmap shows false match rates observed over impostor comparisons of faces from different individuals who were born in the given region pair. False matches are counted against a recognition threshold fixed globally to give the target FMR in the plot title, computed over all on the order of 10^{10} impostor comparisons. If text appears in each box it give the same quantity as that coded by the color. Grey indicates FMR is at the intended FMR target level. Light red colors present a security vulnerability to, for example, a passport gate. Each +1 increase in $\log_{10} \text{FMR}$ corresponds to a factor of 10 increase in FMR. The matrix is not quite symmetric because images in the enrollment and verification sets are different.

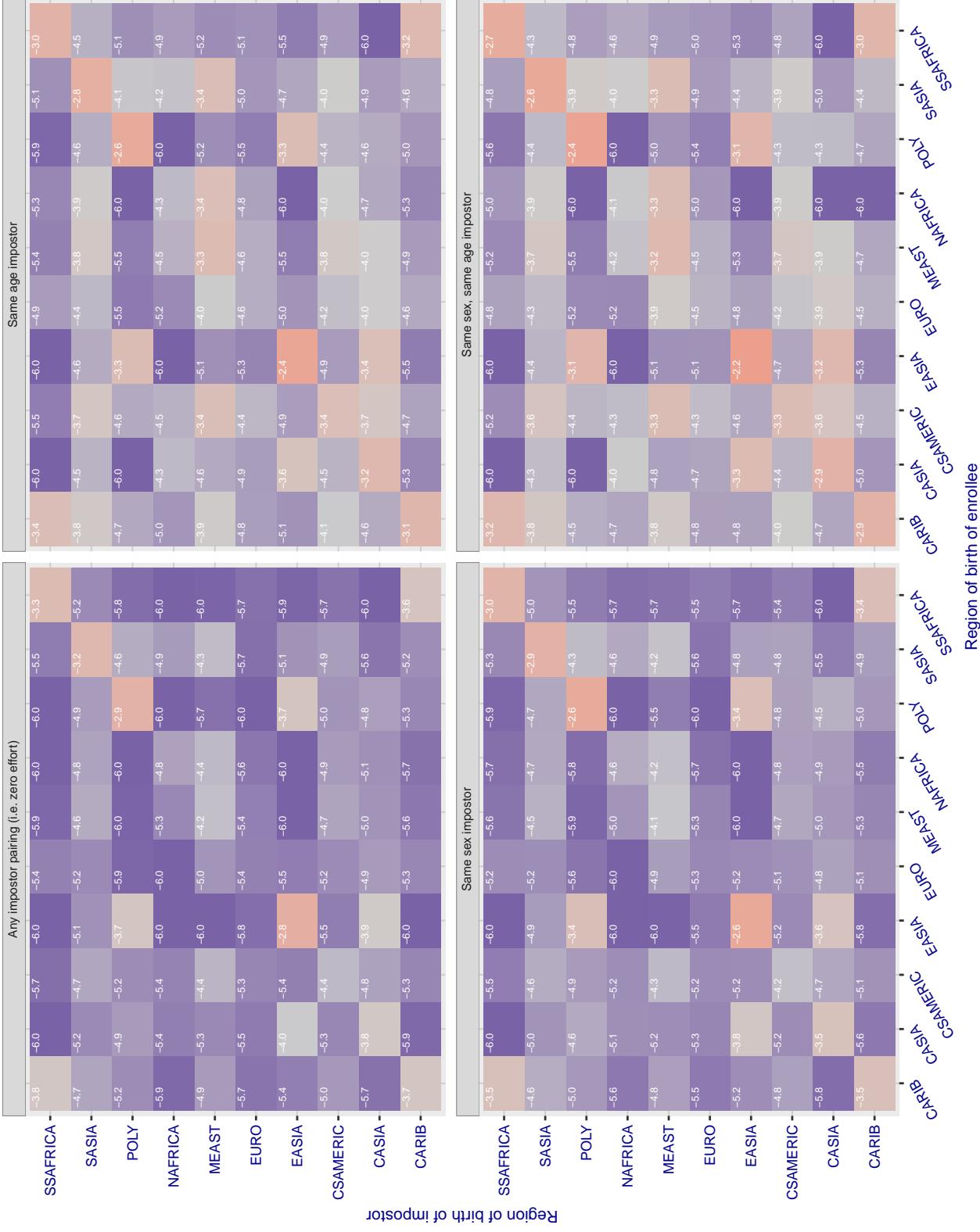
Cross region FMR at threshold T = 5.084 for algorithm aware_004, giving FMR(T) = 0.0001 globally.

Figure 145: For algorithm aware-004 operating on visa images, the heatmap shows false match rates observed over impostor comparisons of faces from different individuals who were born in the given region pair. False matches are counted against a recognition threshold fixed globally to give the target FMR in the plot title, computed over all on the order of 10^{10} impostor comparisons. If text appears in each box it give the same quantity as that coded by the color. Grey indicates FMR is at the intended FMR target level. Light red colors present a security vulnerability to, for example, a passport gate. Each +1 increase in $\log_{10} FMR$ corresponds to a factor of 10 increase in FMR. The matrix is not quite symmetric because images in the enrollment and verification sets are different.

Cross region FMR at threshold T = 0.919 for algorithm ayonix_000, giving $FMR(T) = 0.0001$ globally.

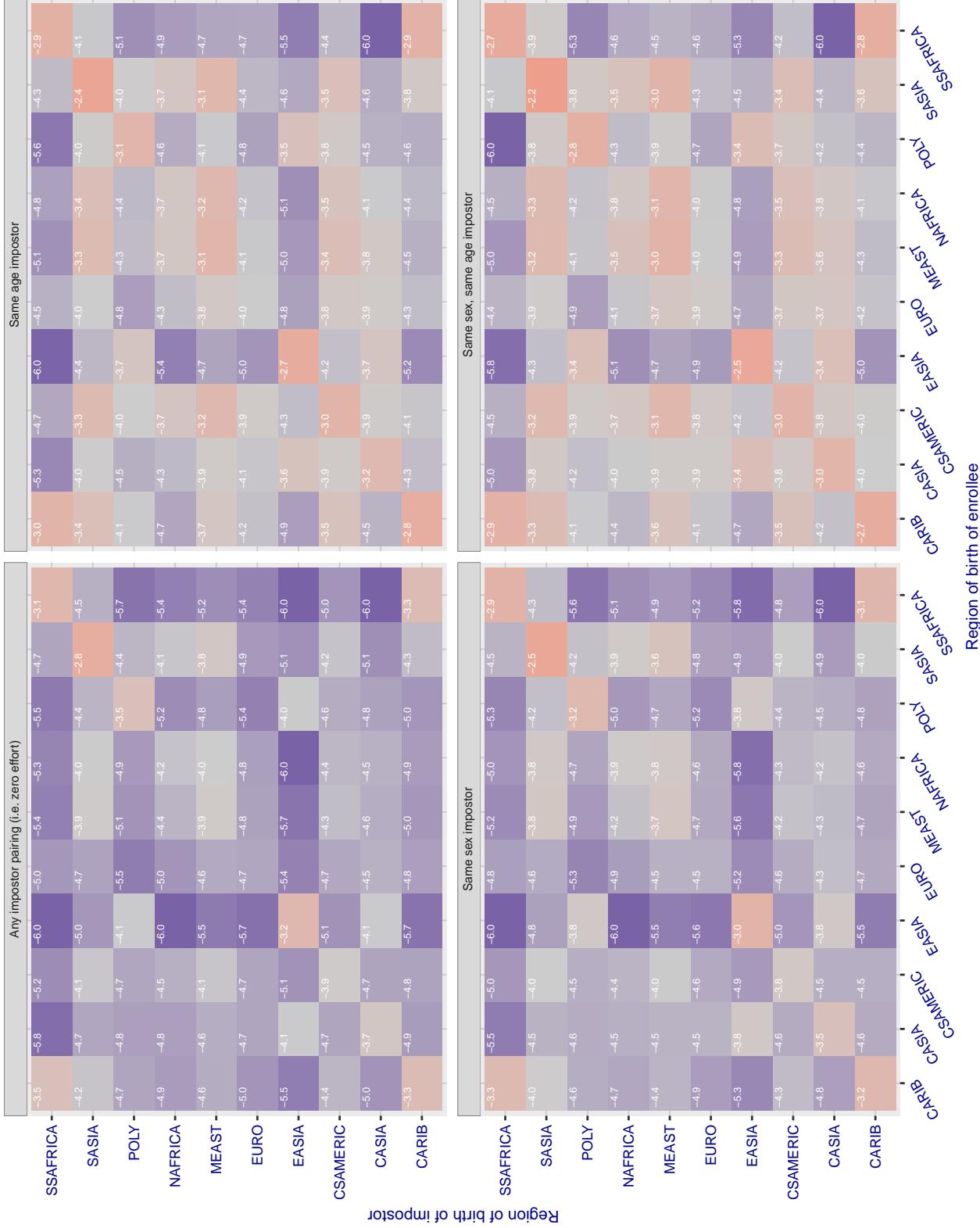


Figure 146: For algorithm ayonix-000 operating on visa images, the heatmap shows false match rates observed over impostor comparisons of faces from different individuals who were born in the given region pair. False matches are counted against a recognition threshold fixed globally to give the target FMR in the plot title, computed over all on the order of 10^{10} impostor comparisons. If text appears in each box it give the same quantity as that coded by the color. Grey indicates FMR is at the intended FMR target level. Light red colors present a security vulnerability to, for example, a passport gate. Each +1 increase in $\log_{10} FMR$ corresponds to a factor of 10 increase in FMR. The matrix is not quite symmetric because images in the enrollment and verification sets are different.

Cross region FMR at threshold T = 0.731 for algorithm bm_001, giving FMR(T) = 0.0001 globally.

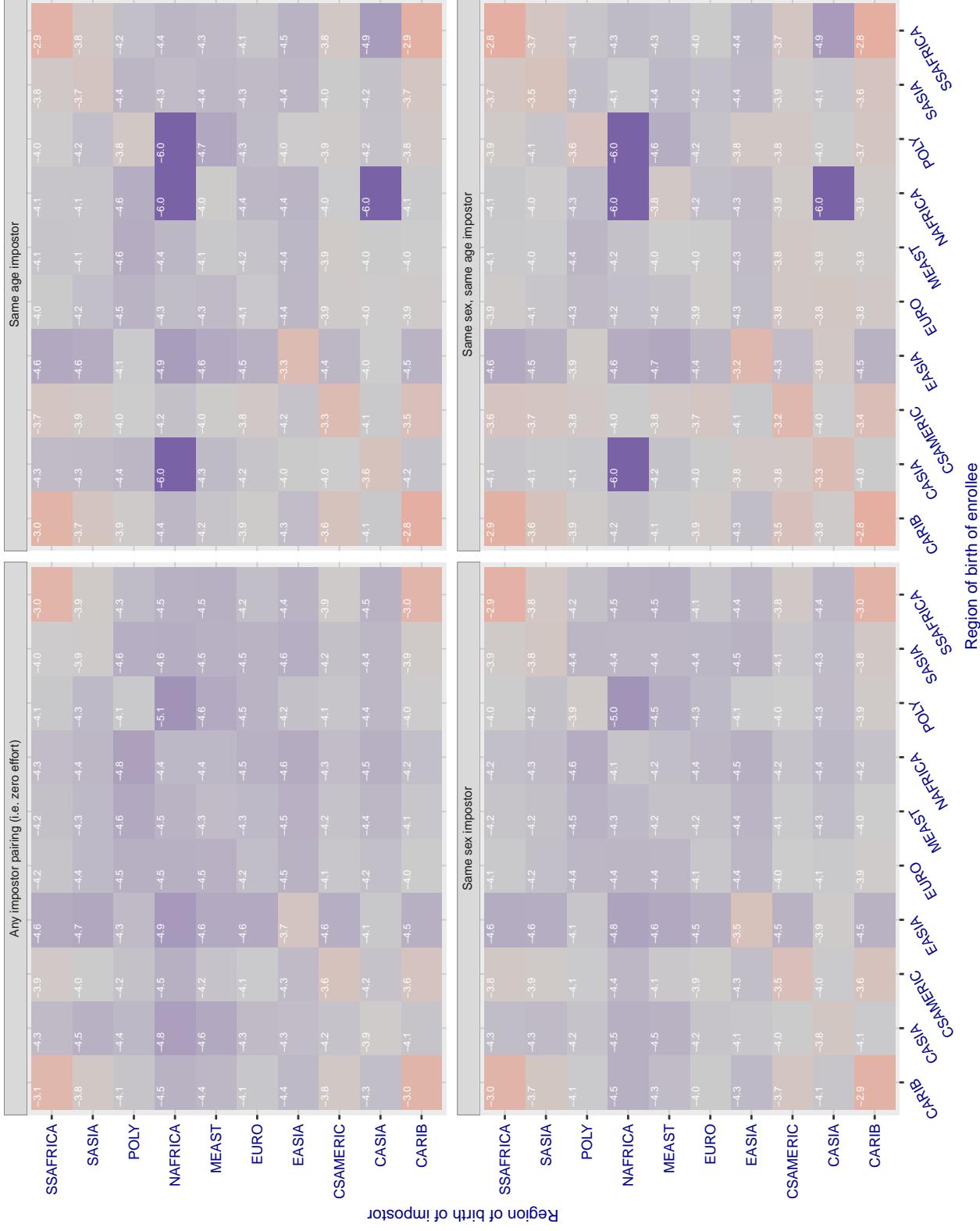


Figure 147: For algorithm bm-001 operating on visa images, the heatmap shows false match rates observed over impostor comparisons of faces from different individuals who were born in the given region pair. False matches are counted against a recognition threshold fixed globally to give the target FMR in the plot title, computed over all on the order of 10^{10} impostor comparisons. If text appears in each box it give the same quantity as that coded by the color. Grey indicates FMR is at the intended FMR target level. Light red colors present a security vulnerability to, for example, a passport gate. Each +1 increase in \log_{10} FMR corresponds to a factor of 10 increase in FMR. The matrix is not quite symmetric because images in the enrollment and verification sets are different.

Cross region FMR at threshold T = 0.388 for algorithm camvi_002, giving FMR(T) = 0.0001 globally.

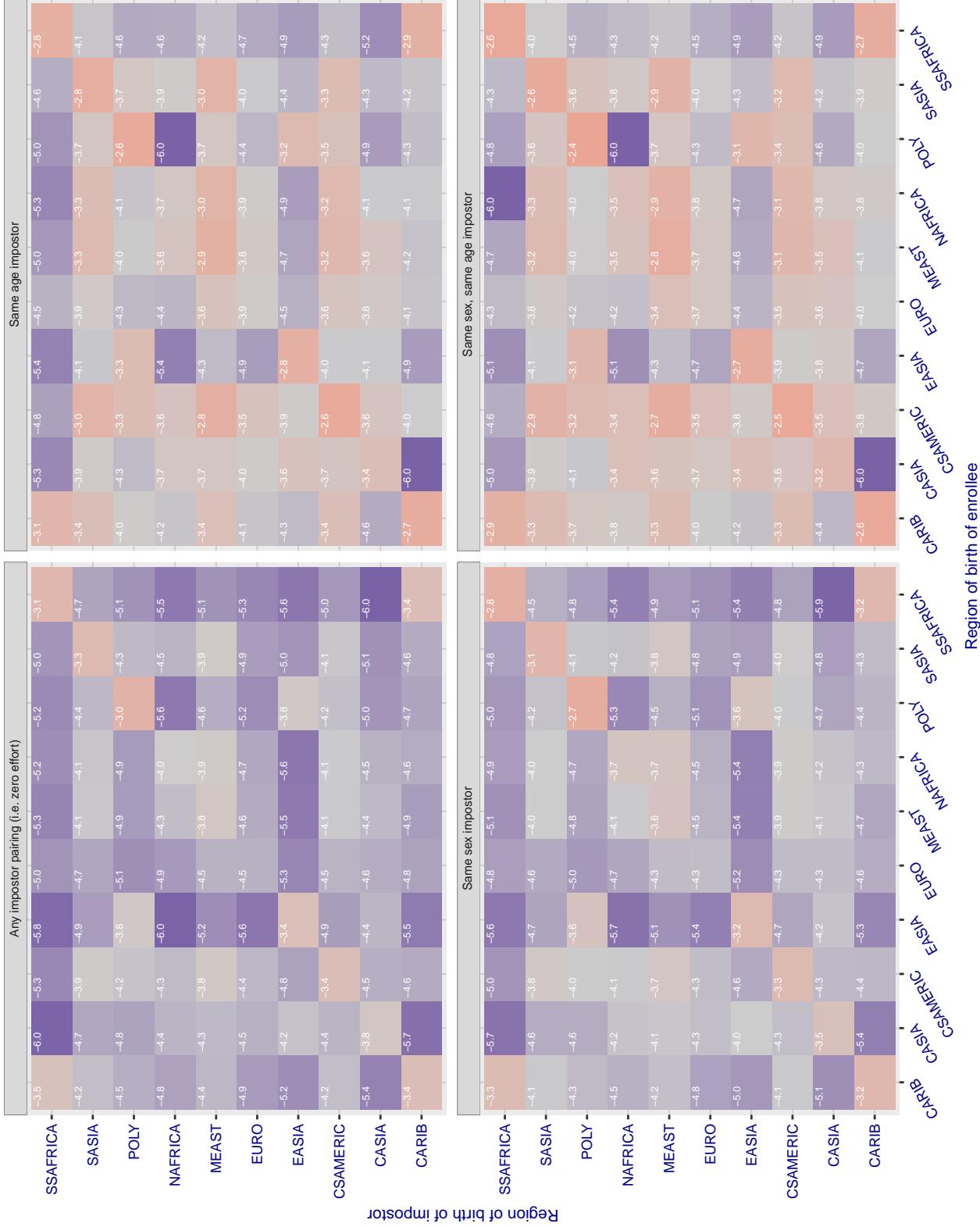


Figure 148: For algorithm camvi-002 operating on visa images, the heatmap shows false match rates observed over impostor comparisons of faces from different individuals who were born in the given region pair. False matches are counted against a recognition threshold fixed globally to give the target FMR in the plot title, computed over all on the order of 10^{10} impostor comparisons. If text appears in each box it give the same quantity as that coded by the color. Grey indicates FMR is at the intended FMR target level. Light red colors present a security vulnerability to, for example, a passport gate. Each +1 increase in $\log_{10} \text{FMR}$ corresponds to a factor of 10 increase in FMR. The matrix is not quite symmetric because images in the enrollment and verification sets are different.

Cross region FMR at threshold T = 0.377 for algorithm camvi_004, giving FMR(T) = 0.0001 globally.

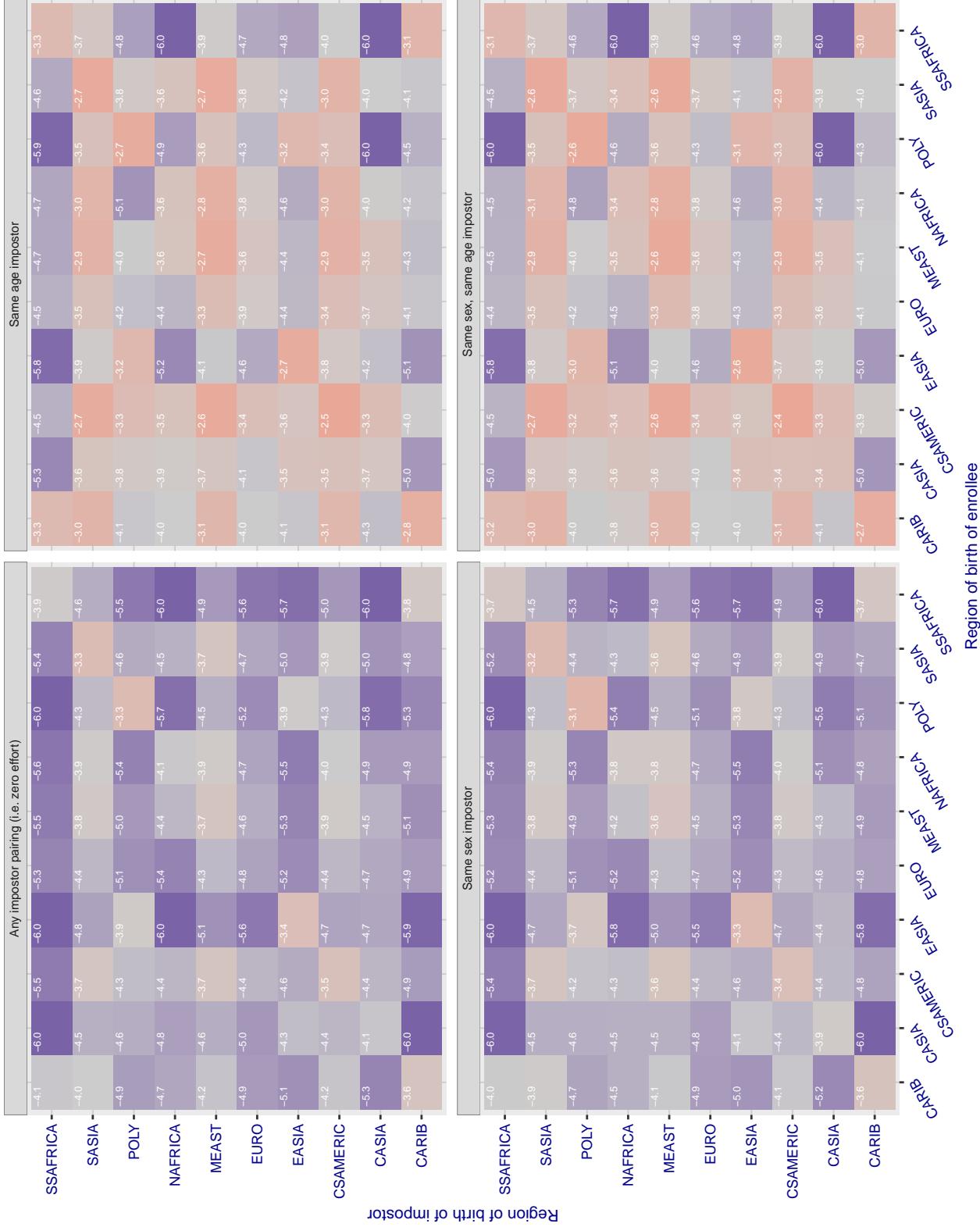


Figure 149: For algorithm camvi-004 operating on visa images, the heatmap shows false match rates observed over impostor comparisons of faces from different individuals who were born in the given region pair. False matches are counted against a recognition threshold fixed globally to give the target FMR in the plot title, computed over all on the order of 10^{10} impostor comparisons. If text appears in each box it give the same quantity as that coded by the color. Grey indicates FMR is at the intended FMR target level. Light red colors present a security vulnerability to, for example, a passport gate. Each +1 increase in $\log_{10} FMR$ corresponds to a factor of 10 increase in FMR. The matrix is not quite symmetric because images in the enrollment and verification sets are different.

Cross region FMR at threshold T = 0.436 for algorithm ceiec_001, giving FMR(Γ) = 0.0001 globally.

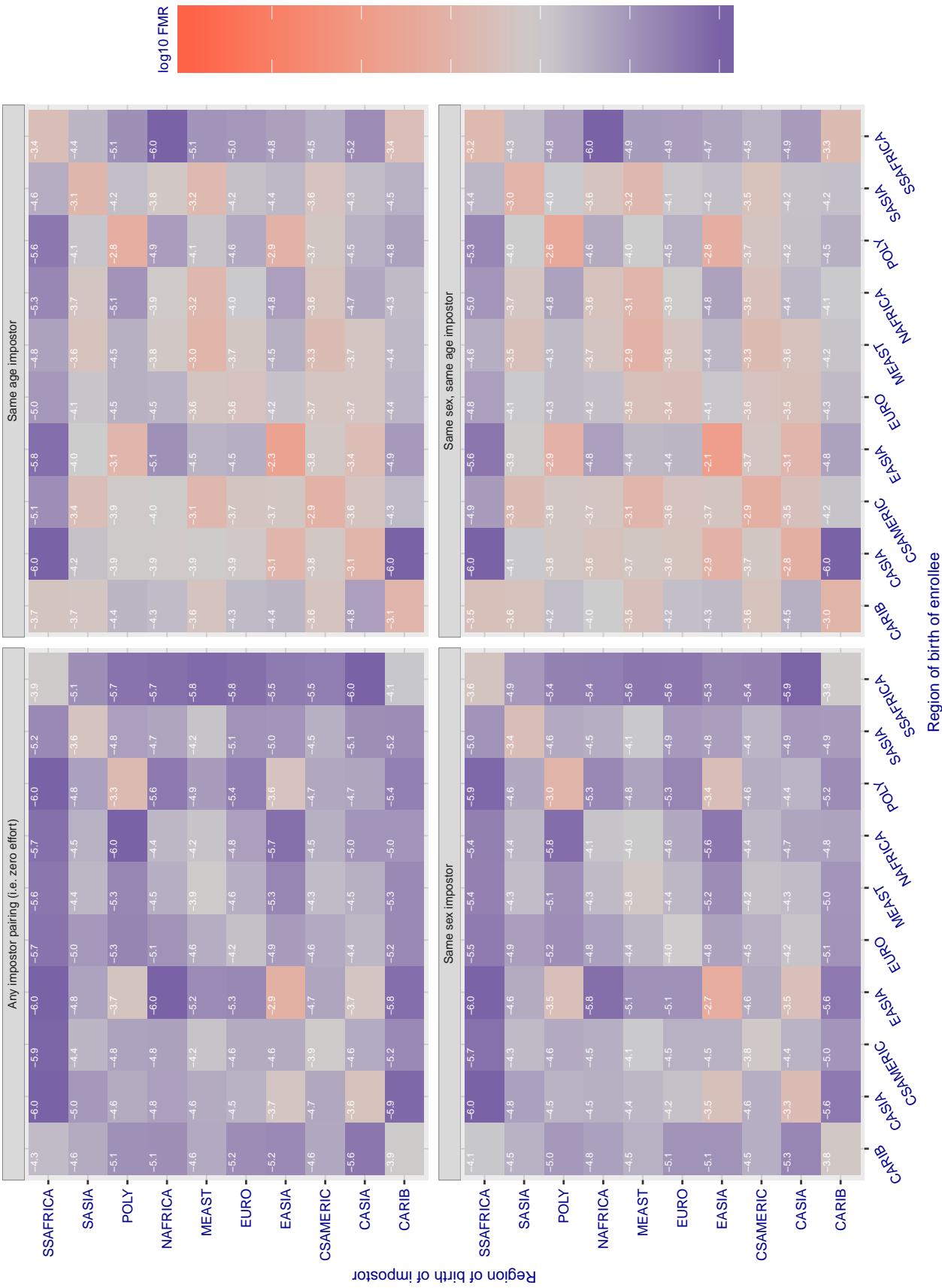


Figure 150: For algorithm ceiec_001 operating on visa images, the heatmap shows false match rates observed over impostor comparisons of faces from different individuals who were born in the given region pair. False matches are counted against a recognition threshold fixed globally to give the target FMR in the plot title, computed over all on the order of 10^{10} impostor comparisons. If text appears in each box it give the same quantity as that coded by the color. Grey indicates FMR is at the intended FMR target level. Light red colors present a security vulnerability to, for example, a passport gate. Each +1 increase in $\log 10$ FMR corresponds to a factor of 10 increase in FMR. The matrix is not quite symmetric because images in the enrollment and verification sets are different.

Cross region FMR at threshold T = 0.325 for algorithm ceiec_002, giving FMR(Γ) = 0.0001 globally.

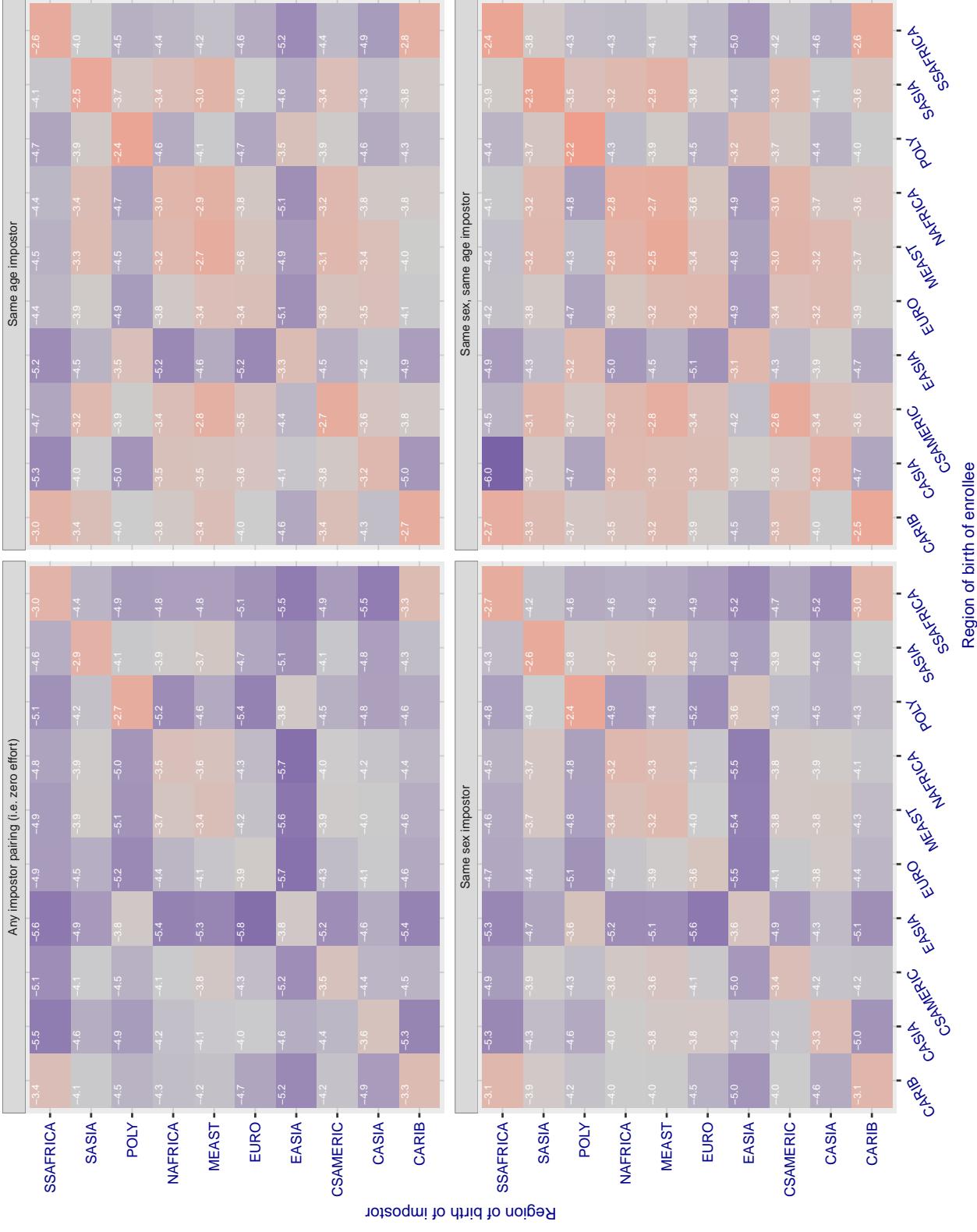


Figure 151: For algorithm ceiec-002 operating on visa images, the heatmap shows false match rates observed over impostor comparisons of faces from different individuals who were born in the given region pair. False matches are counted against a recognition threshold fixed globally to give the target FMR in the plot title, computed over all on the order of 10^{10} impostor comparisons. If text appears in each box it give the same quantity as that coded by the color. Grey indicates FMR is at the intended FMR target level. Light red colors present a security vulnerability to, for example, a passport gate. Each +1 increase in $\log 10$ FMR corresponds to a factor of 10 increase in FMR. The matrix is not quite symmetric because images in the enrollment and verification sets are different.

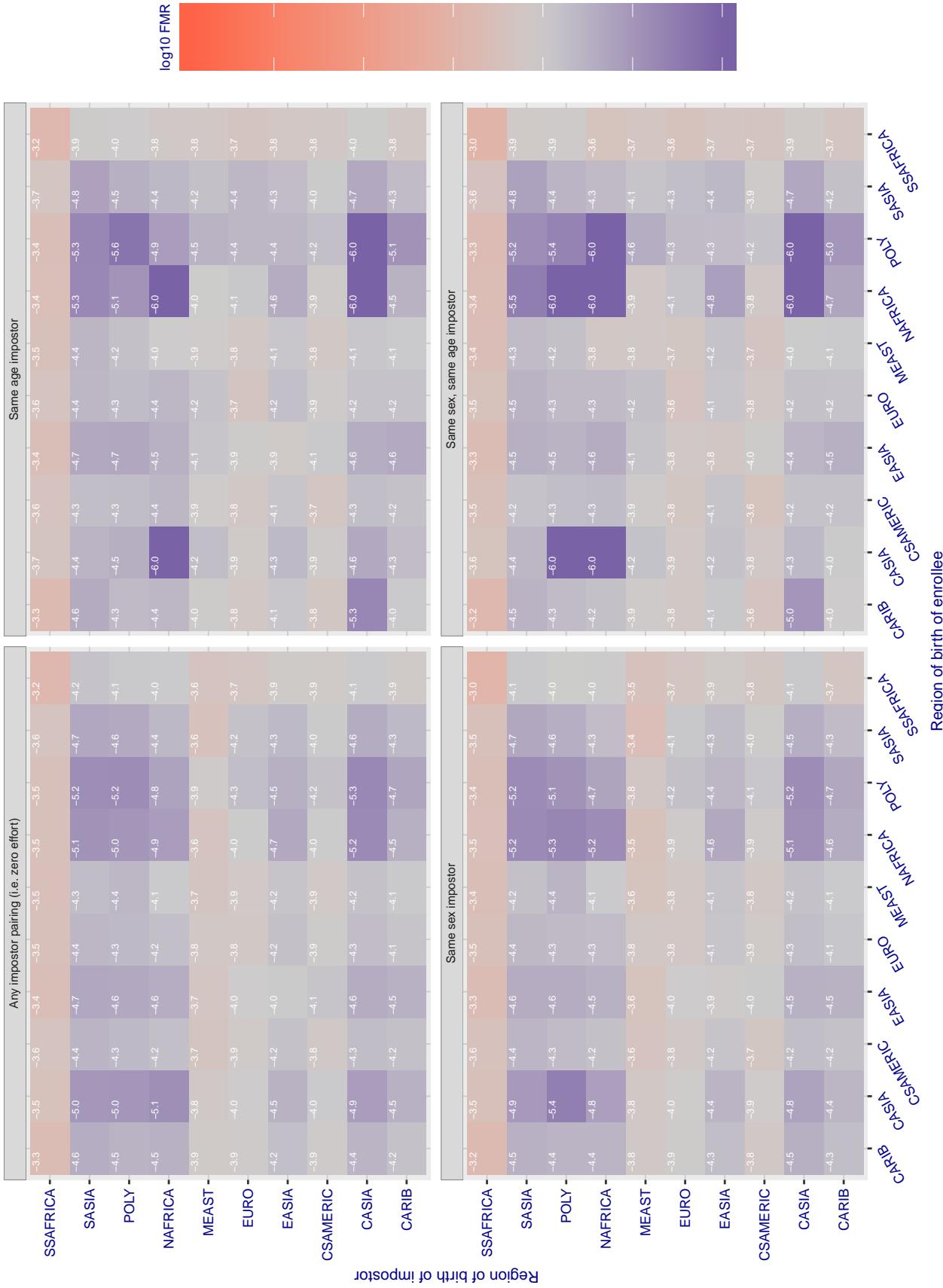
Cross region FMR at threshold T = 106.748 for algorithm chtface_001, giving FMR(T) = 0.00001 globally.

Figure 152: For algorithm chtface-001 operating on visa images, the heatmap shows false match rates observed over impostor comparisons of faces from different individuals who were born in the given region pair. False matches are counted against a recognition threshold fixed globally to give the target FMR in the plot title, computed over all on the order of 10^{10} impostor comparisons. If text appears in each box it give the same quantity as that coded by the color. Grey indicates FMR is at the intended FMR target level. Light red colors present a security vulnerability to, for example, a passport gate. Each +1 increase in $\log_{10} FMR$ corresponds to a factor of 10 increase in FMR. The matrix is not quite symmetric because images in the enrollment and verification sets are different.

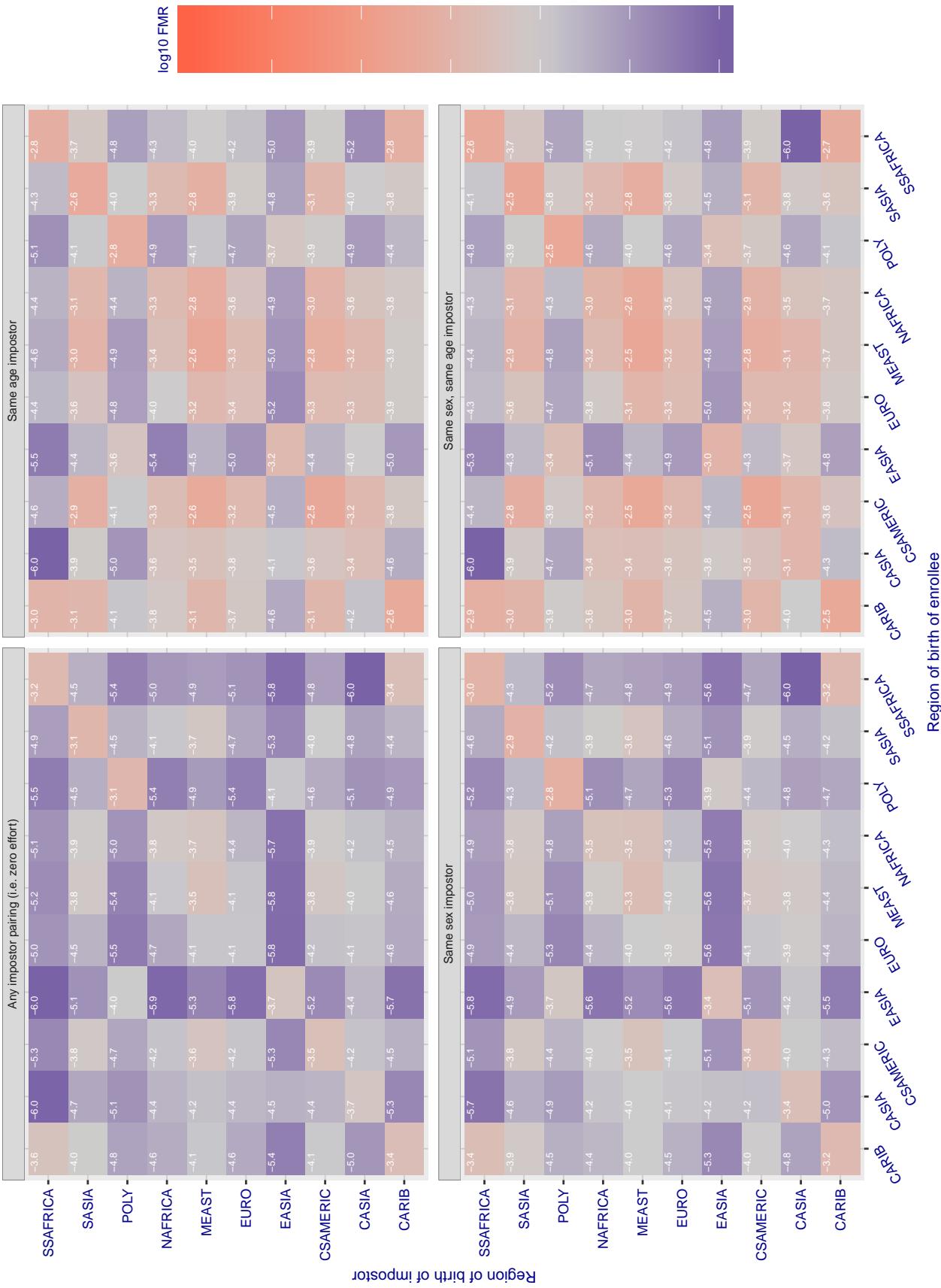
Cross region FMR at threshold T = 2972.000 for algorithm cogent_003, giving FMR(T) = 0.0001 globally.

Figure 153: For algorithm cogent-003 operating on visa images, the heatmap shows false match rates observed over impostor comparisons of faces from different individuals who were born in the given region pair. False matches are counted against a recognition threshold fixed globally to give the target FMR in the plot title, computed over all on the order of 10^{10} impostor comparisons. If text appears in each box it give the same quantity as that coded by the color. Grey indicates FMR is at the intended FMR target level. Light red colors present a security vulnerability to, for example, a passport gate. Each +1 increase in $\log_{10} FMR$ corresponds to a factor of 10 increase in FMR. The matrix is not quite symmetric because images in the enrollment and verification sets are different.

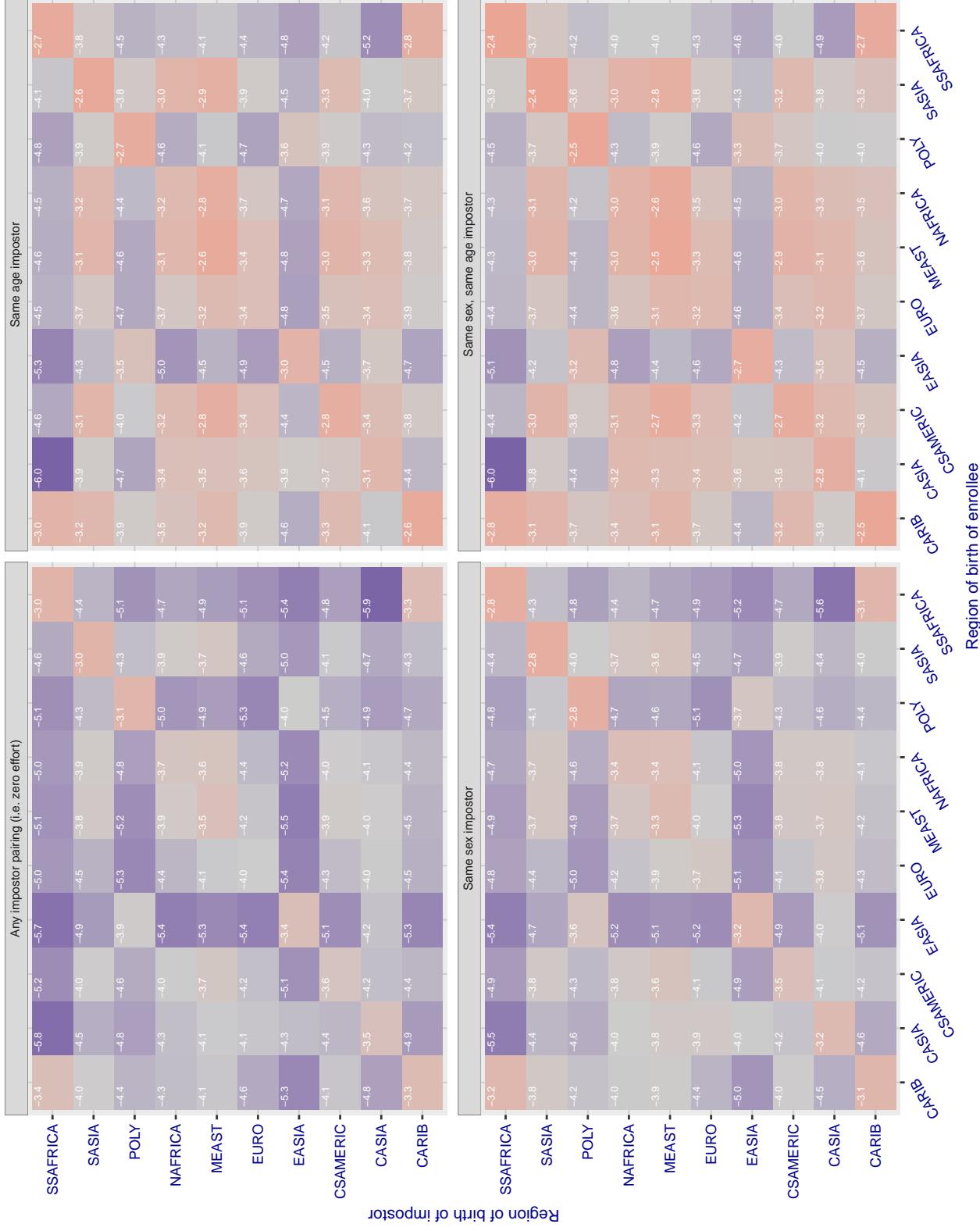
Cross region FMR at threshold T = 3156.000 for algorithm cogent_004, giving FMR(T) = 0.0001 globally.

Figure 154: For algorithm cogent-004 operating on visa images, the heatmap shows false match rates observed over impostor comparisons of faces from different individuals who were born in the given region pair. False matches are counted against a recognition threshold fixed globally to give the target FMR in the plot title, computed over all on the order of 10^{10} impostor comparisons. If text appears in each box it give the same quantity as that coded by the color. Grey indicates FMR is at the intended FMR target level. Light red colors present a security vulnerability to, for example, a passport gate. Each +1 increase in $\log_{10} FMR$ corresponds to a factor of 10 increase in FMR. The matrix is not quite symmetric because images in the enrollment and verification sets are different.

Cross region FMR at threshold T = 0.565 for algorithm cognitec_000, giving FMR(T) = 0.0001 globally.

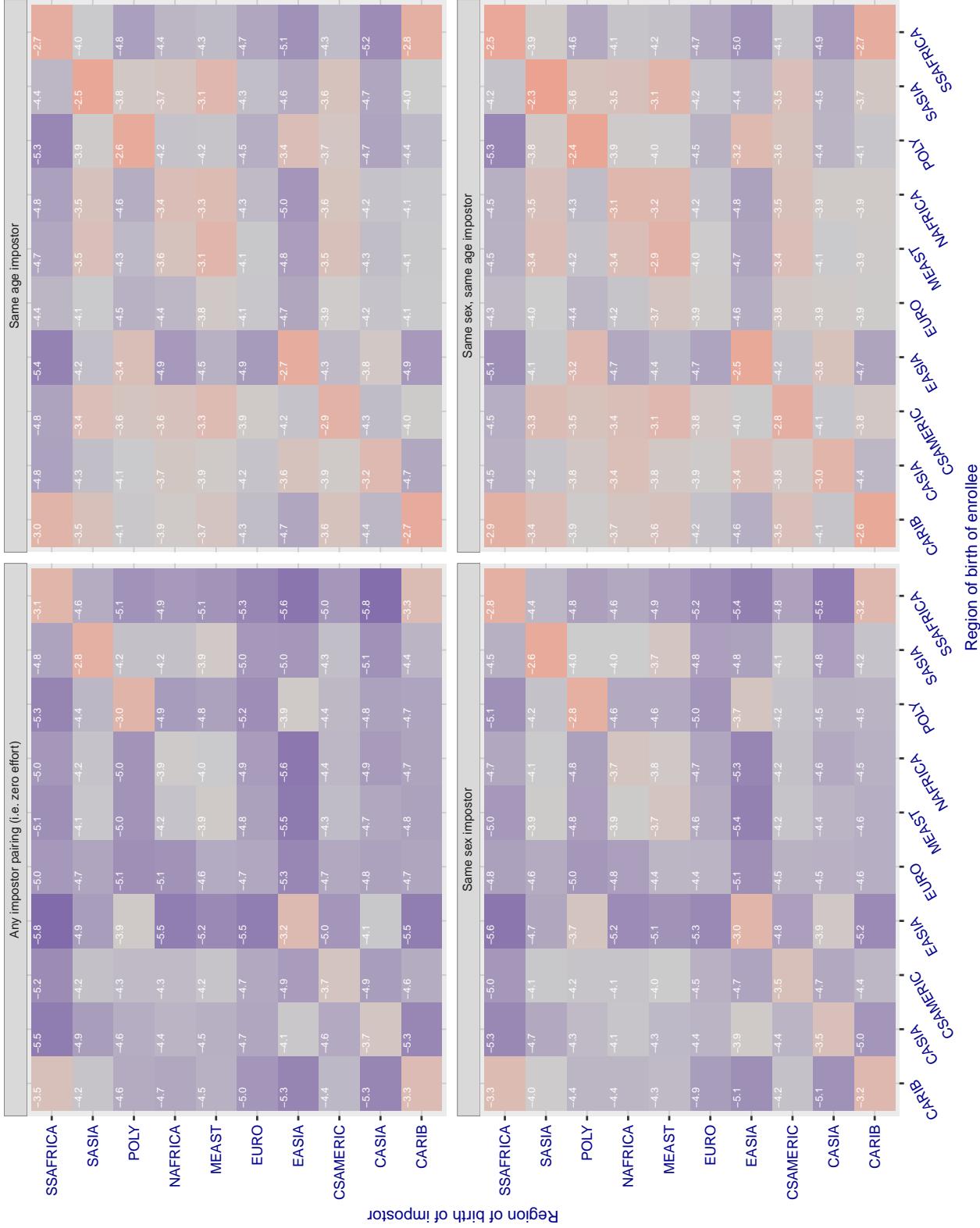


Figure 155: For algorithm cognitec-000 operating on visa images, the heatmap shows false match rates observed over impostor comparisons of faces from different individuals who were born in the given region pair. False matches are counted against a recognition threshold fixed globally to give the target FMR in the plot title, computed over all on the order of 10^{10} impostor comparisons. If text appears in each box it give the same quantity as that coded by the color. Grey indicates FMR is at the intended FMR target level. Light red colors present a security vulnerability to, for example, a passport gate. Each +1 increase in $\log_{10} FMR$ corresponds to a factor of 10 increase in FMR. The matrix is not quite symmetric because images in the enrollment and verification sets are different.

Cross region FMR at threshold T = 0.565 for algorithm cognitec_001, giving FMR(T) = 0.0001 globally.

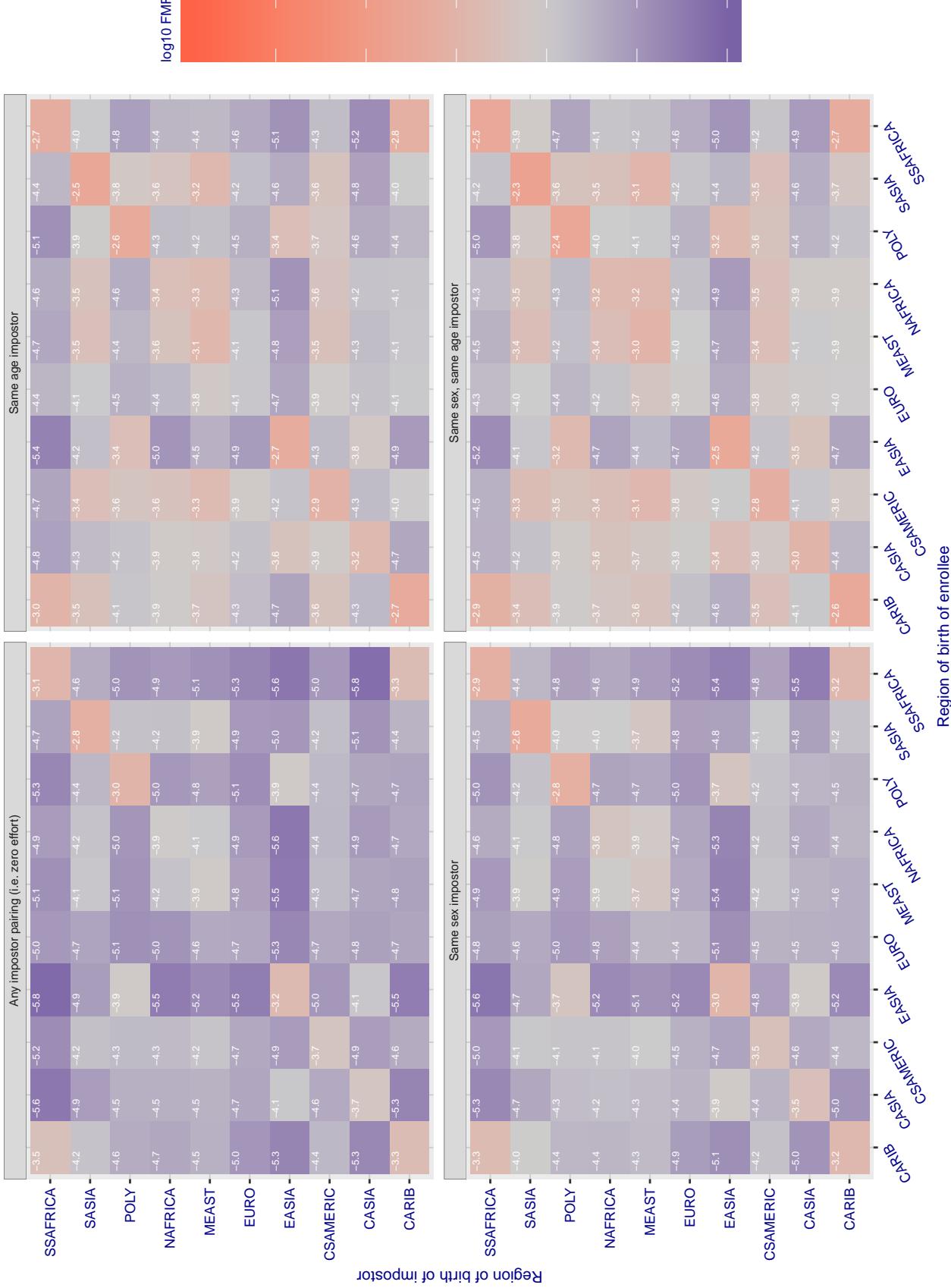


Figure 156: For algorithm cognitec-001 operating on visa images, the heatmap shows false match rates observed over impostor comparisons of faces from different individuals who were born in the given region pair. False matches are counted against a recognition threshold fixed globally to give the target FMR in the plot title, computed over all on the order of 10^{10} impostor comparisons. If text appears in each box it give the same quantity as that coded by the color. Grey indicates FMR is at the intended FMR target level. Light red colors present a security vulnerability to, for example, a passport gate. Each +1 increase in $\log_{10} \text{FMR}$ corresponds to a factor of 10 increase in FMR. The matrix is not quite symmetric because images in the enrollment and verification sets are different.

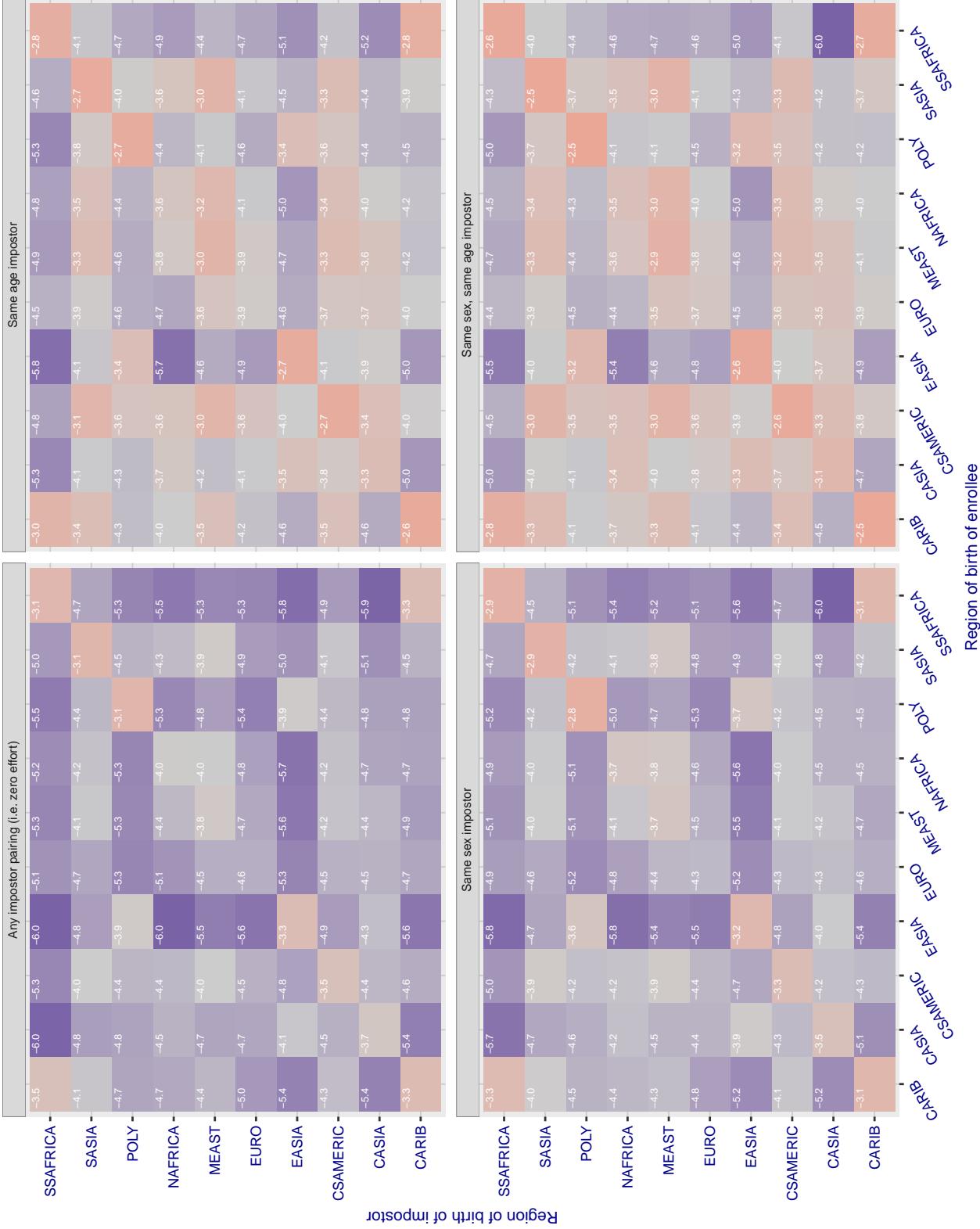
Cross region FMR at threshold T = 3.730 for algorithm ct tcbcbank_000, giving FMR(T) = 0.0001 globally.

Figure 157: For algorithm ct tcbcbank-000 operating on visa images, the heatmap shows false match rates observed over impostor comparisons of faces from different individuals who were born in the given region pair. False matches are counted against a recognition threshold fixed globally to give the target FMR in the plot title, computed over all on the order of 10^{10} impostor comparisons. If text appears in each box it give the same quantity as that coded by the color. Grey indicates FMR is at the intended FMR target level. Light red colors present a security vulnerability to, for example, a passport gate. Each +1 increase in log10 FMR corresponds to a factor of 10 increase in FMR. The matrix is not quite symmetric because images in the enrollment and verification sets are different.

Cross region FMR at threshold T = 0.762 for algorithm cyberextruder_001, giving FMR(T) = 0.00001 globally.

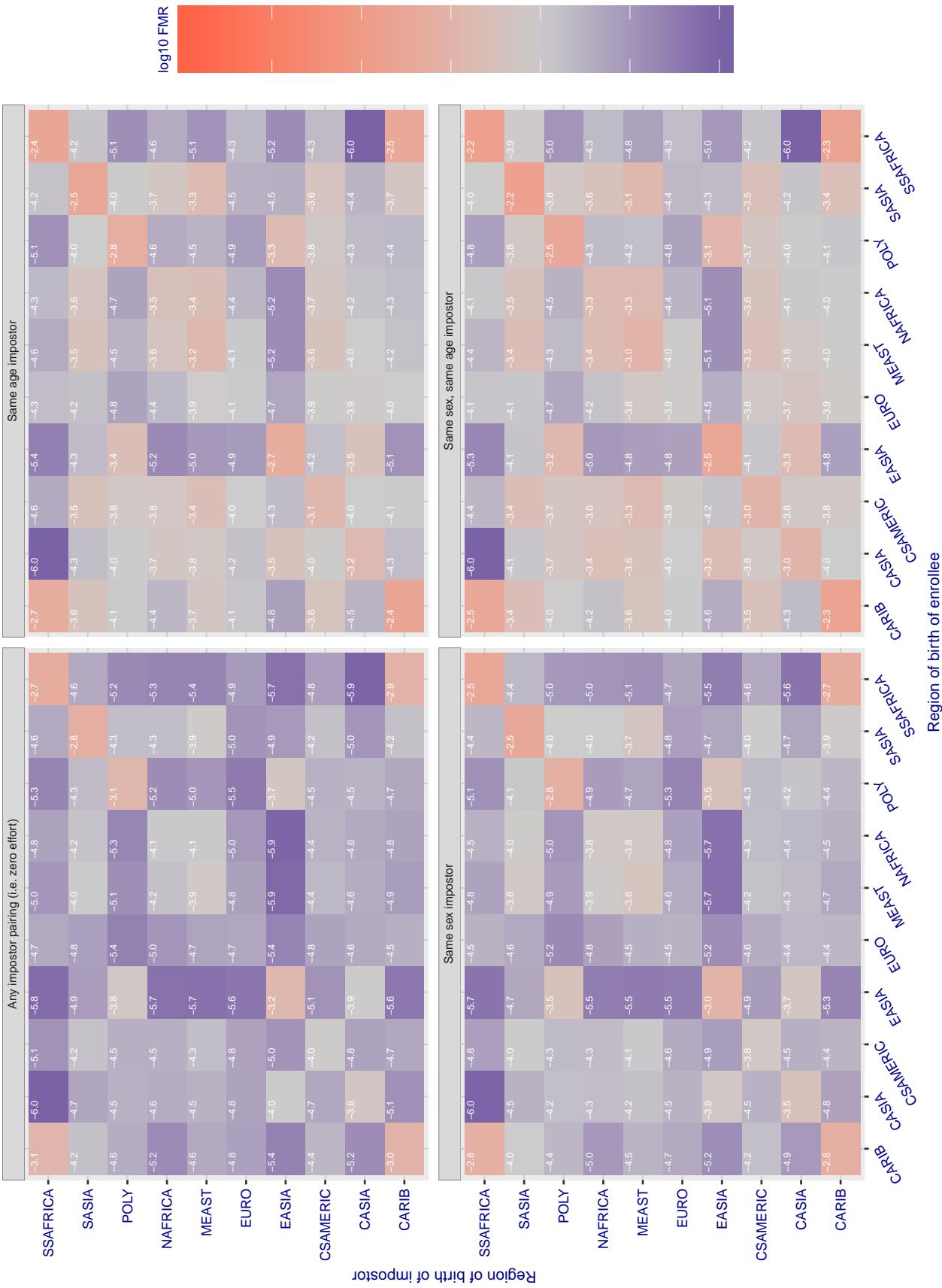


Figure 158: For algorithm cyberextruder-001 operating on visa images, the heatmap shows false match rates observed over impostor comparisons of faces from different individuals who were born in the given region pair. False matches are counted against a recognition threshold fixed globally to give the target FMR in the plot title, computed over all on the order of 10^{10} impostor comparisons. If text appears in each box it give the same quantity as that coded by the color. Grey indicates FMR is at the intended FMR target level. Light red colors present a security vulnerability to, for example, a passport gate. Each +1 increase in $\log_{10} FMR$ corresponds to a factor of 10 increase in FMR. The matrix is not quite symmetric because images in the enrollment and verification sets are different.

Cross region FMR at threshold T = 0.500 for algorithm cyberextruder_002, giving FMR(T) = 0.0001 globally.

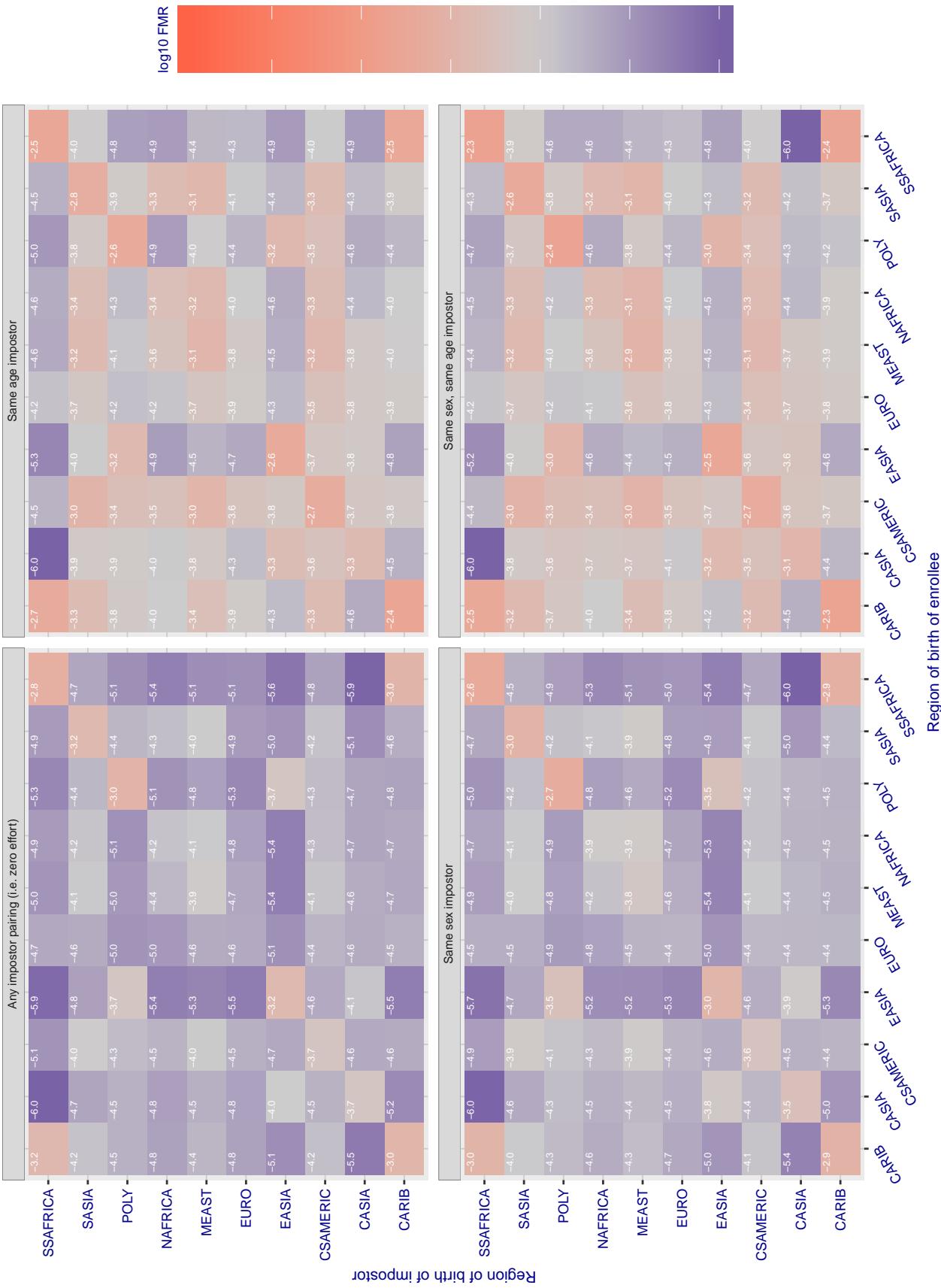


Figure 159: For algorithm cyberextruder-002 operating on visa images, the heatmap shows false match rates observed over impostor comparisons of faces from different individuals who were born in the given region pair. False matches are counted against a recognition threshold fixed globally to give the target FMR in the plot title, computed over all on the order of 10^{10} impostor comparisons. If text appears in each box it give the same quantity as that coded by the color. Grey indicates FMR is at the intended FMR target level. Light red colors present a security vulnerability to, for example, a passport gate. Each +1 increase in $\log_{10} FMR$ corresponds to a factor of 10 increase in FMR. The matrix is not quite symmetric because images in the enrollment and verification sets are different.

Cross region FMR at threshold T = 1.408 for algorithm cyberlink_001, giving $\text{FMR}(\text{T}) = 0.0001$ globally.

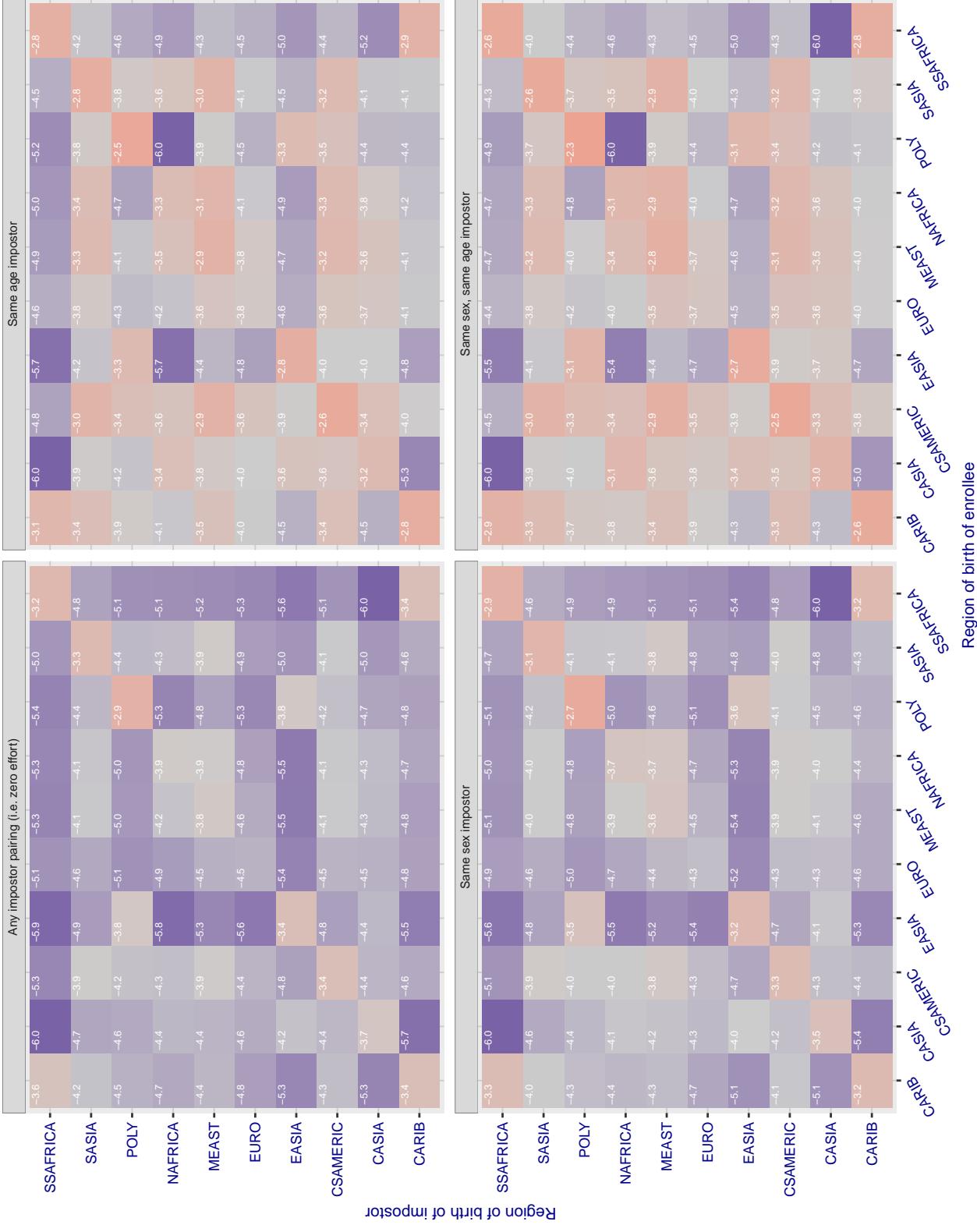


Figure 160: For algorithm cyberlink-001 operating on visa images, the heatmap shows false match rates observed over impostor comparisons of faces from different individuals who were born in the given region pair. False matches are counted against a recognition threshold fixed globally to give the target FMR in the plot title, computed over all on the order of 10^{10} impostor comparisons. If text appears in each box it give the same quantity as that coded by the color. Grey indicates FMR is at the intended FMR target level. Light red colors present a security vulnerability to, for example, a passport gate. Each +1 increase in $\log_{10} \text{FMR}$ corresponds to a factor of 10 increase in FMR. The matrix is not quite symmetric because images in the enrollment and verification sets are different.

Cross region FMR at threshold T = 1.409 for algorithm cyberlink_002, giving $\text{FMR}(\text{T}) = 0.0001$ globally.

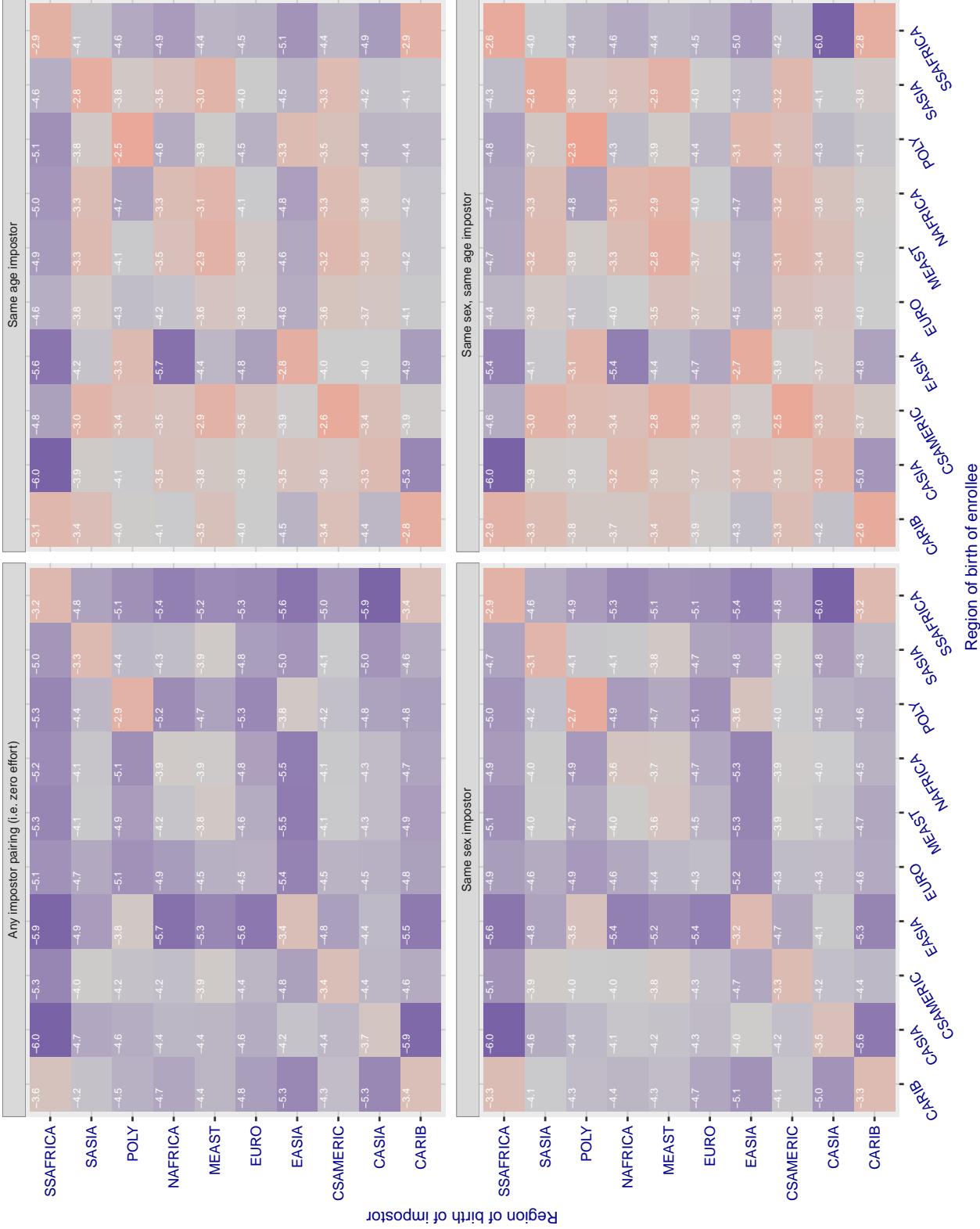


Figure 161: For algorithm cyberlink-002 operating on visa images, the heatmap shows false match rates observed over impostor comparisons of faces from different individuals who were born in the given region pair. False matches are counted against a recognition threshold fixed globally to give the target FMR in the plot title, computed over all on the order of 10^{10} impostor comparisons. If text appears in each box it give the same quantity as that coded by the color. Grey indicates FMR is at the intended FMR target level. Light red colors present a security vulnerability to, for example, a passport gate. Each +1 increase in $\log_{10} \text{FMR}$ corresponds to a factor of 10 increase in FMR. The matrix is not quite symmetric because images in the enrollment and verification sets are different.

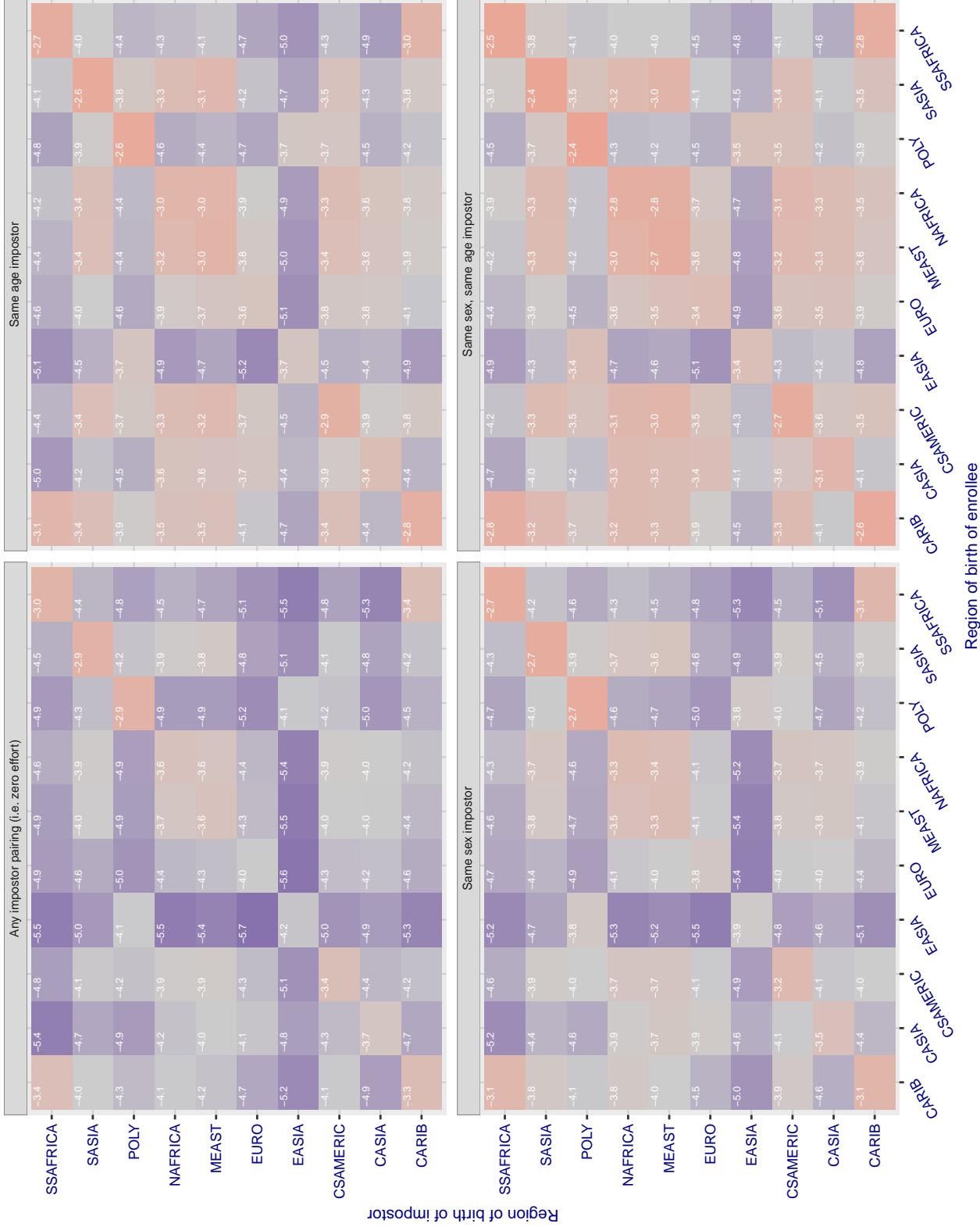
Cross region FMR at threshold T = 6696.000 for algorithm dahua_002, giving FMR(T) = 0.00001 globally.

Figure 162: For algorithm dahua-002 operating on visa images, the heatmap shows false match rates observed over impostor comparisons of faces from different individuals who were born in the given region pair. False matches are counted against a recognition threshold fixed globally to give the target FMR in the plot title, computed over all on the order of 10^{10} impostor comparisons. If text appears in each box it give the same quantity as that coded by the color. Grey indicates FMR is at the intended FMR target level. Light red colors present a security vulnerability to, for example, a passport gate. Each +1 increase in $\log_{10} \text{FMR}$ corresponds to a factor of 10 increase in FMR. The matrix is not quite symmetric because images in the enrollment and verification sets are different.

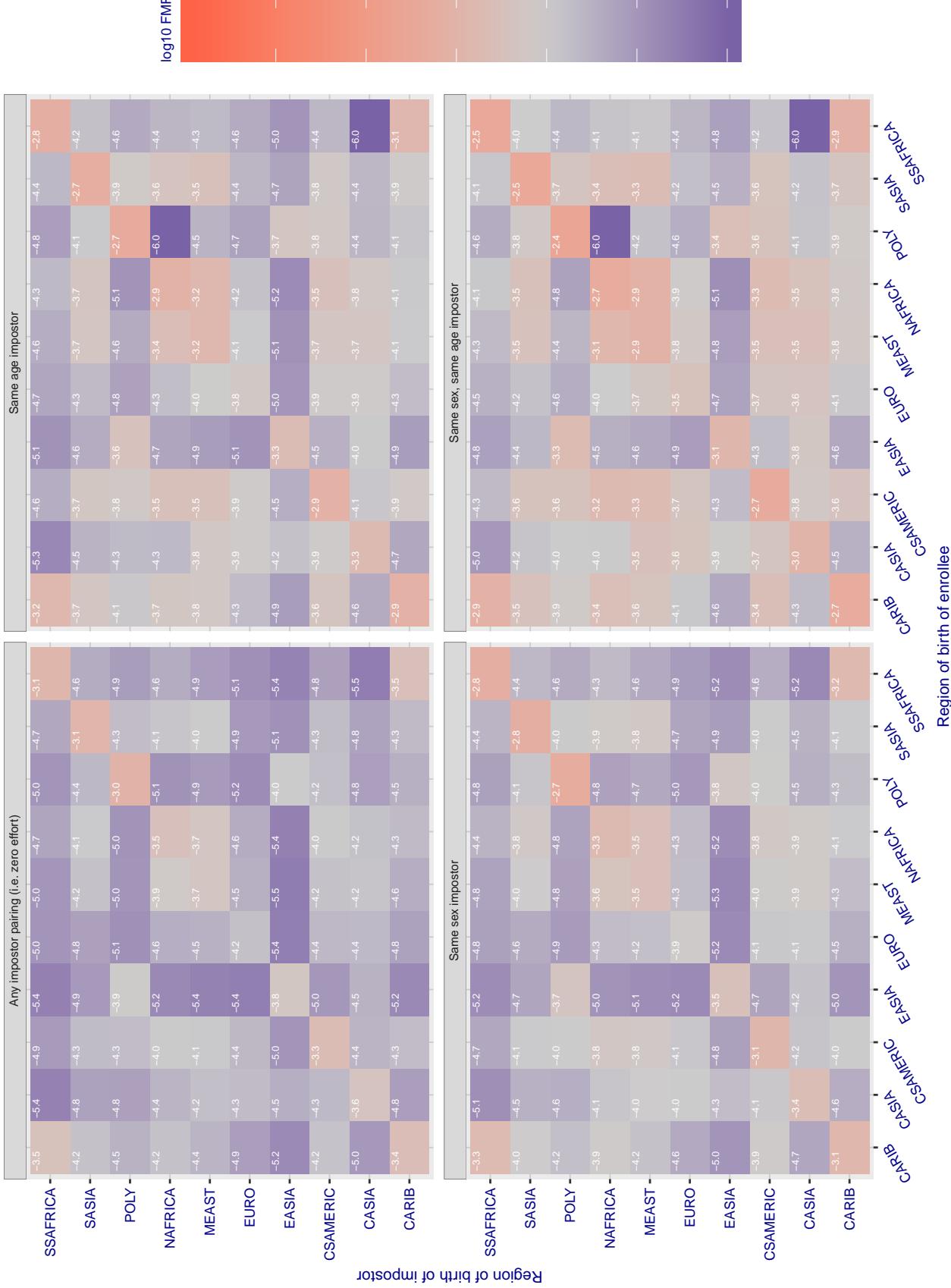
Cross region FMR at threshold T = 6034.000 for algorithm dahua_003, giving FMR(T) = 0.00001 globally.

Figure 163: For algorithm dahua-003 operating on visa images, the heatmap shows false match rates observed over impostor comparisons of faces from different individuals who were born in the given region pair. False matches are counted against a recognition threshold fixed globally to give the target FMR in the plot title, computed over all on the order of 10^{10} impostor comparisons. If text appears in each box it give the same quantity as that coded by the color. Grey indicates FMR is at the intended FMR target level. Light red colors present a security vulnerability to, for example, a passport gate. Each +1 increase in $\log_{10} FMR$ corresponds to a factor of 10 increase in FMR. The matrix is not quite symmetric because images in the enrollment and verification sets are different.

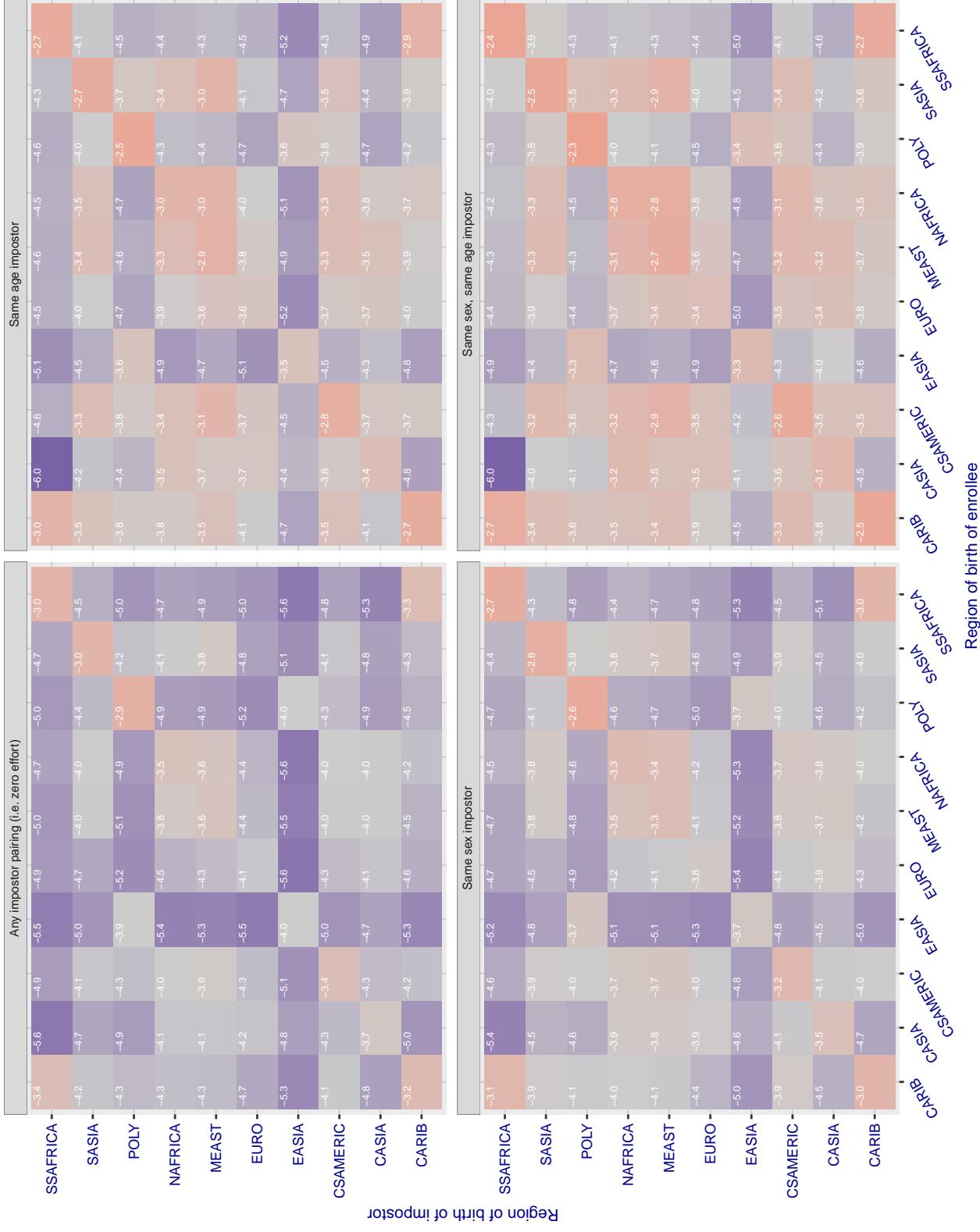
Cross region FMR at threshold T = 1.359 for algorithm deepglint_001, giving FMR(T) = 0.0001 globally.

Figure 164: For algorithm deepglint-001 operating on visa images, the heatmap shows false match rates observed over impostor comparisons of faces from different individuals who were born in the given region pair. False matches are counted against a recognition threshold fixed globally to give the target FMR in the plot title, computed over all on the order of 10^{10} impostor comparisons. If text appears in each box it give the same quantity as that coded by the color. Grey indicates FMR is at the intended FMR target level. Light red colors present a security vulnerability to, for example, a passport gate. Each +1 increase in $\log_{10} FMR$ corresponds to a factor of 10 increase in FMR. The matrix is not quite symmetric because images in the enrollment and verification sets are different.

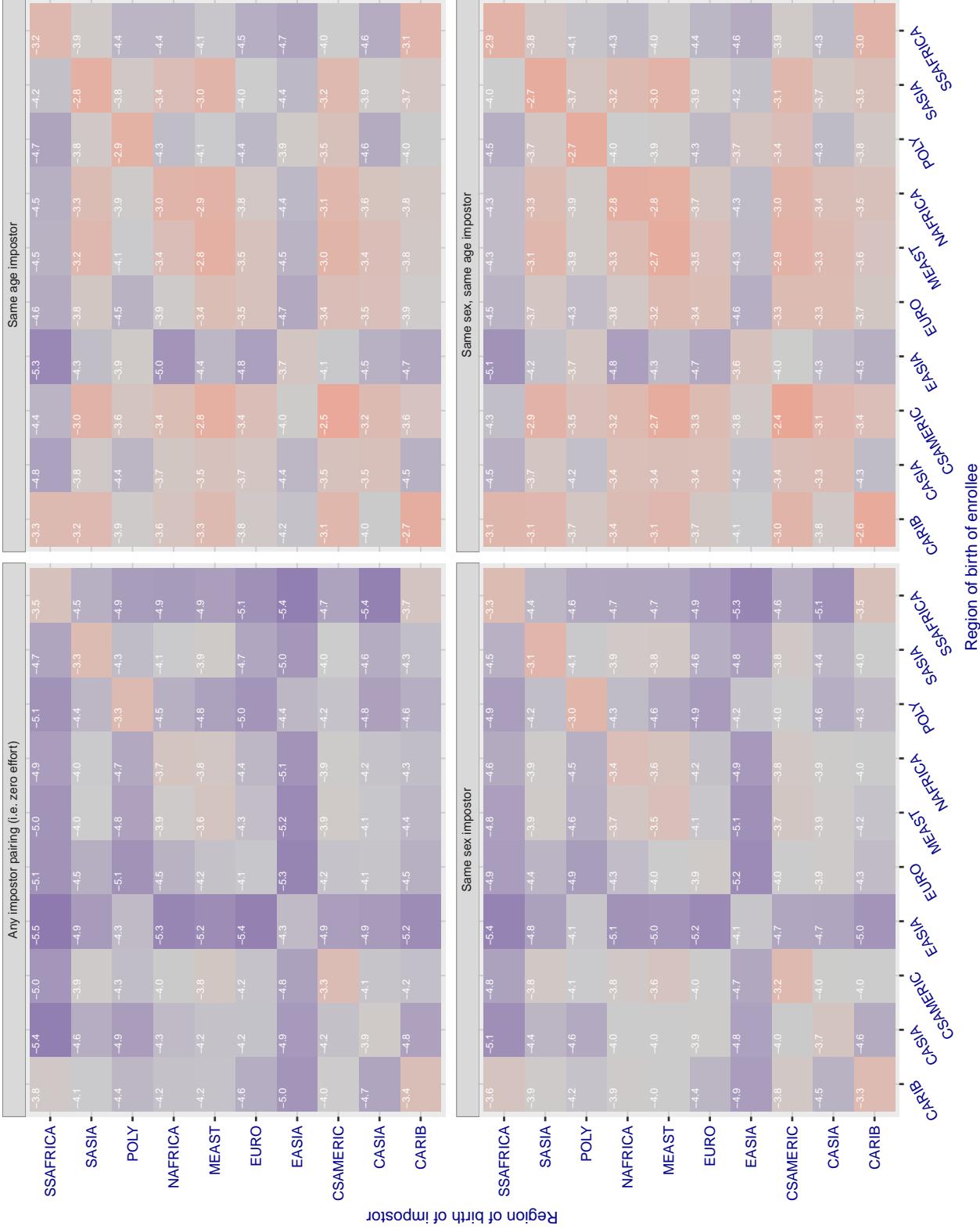
Cross region FMR at threshold T = 1.371 for algorithm deepsea_001, giving FMR(T) = 0.0001 globally.

Figure 165: For algorithm deepsea-001 operating on visa images, the heatmap shows false match rates observed over impostor comparisons of faces from different individuals who were born in the given region pair. False matches are counted against a recognition threshold fixed globally to give the target FMR in the plot title, computed over all on the order of 10^{10} impostor comparisons. If text appears in each box it give the same quantity as that coded by the color. Grey indicates FMR is at the intended FMR target level. Light red colors present a security vulnerability to, for example, a passport gate. Each +1 increase in $\log_{10} \text{FMR}$ corresponds to a factor of 10 increase in FMR. The matrix is not quite symmetric because images in the enrollment and verification sets are different.

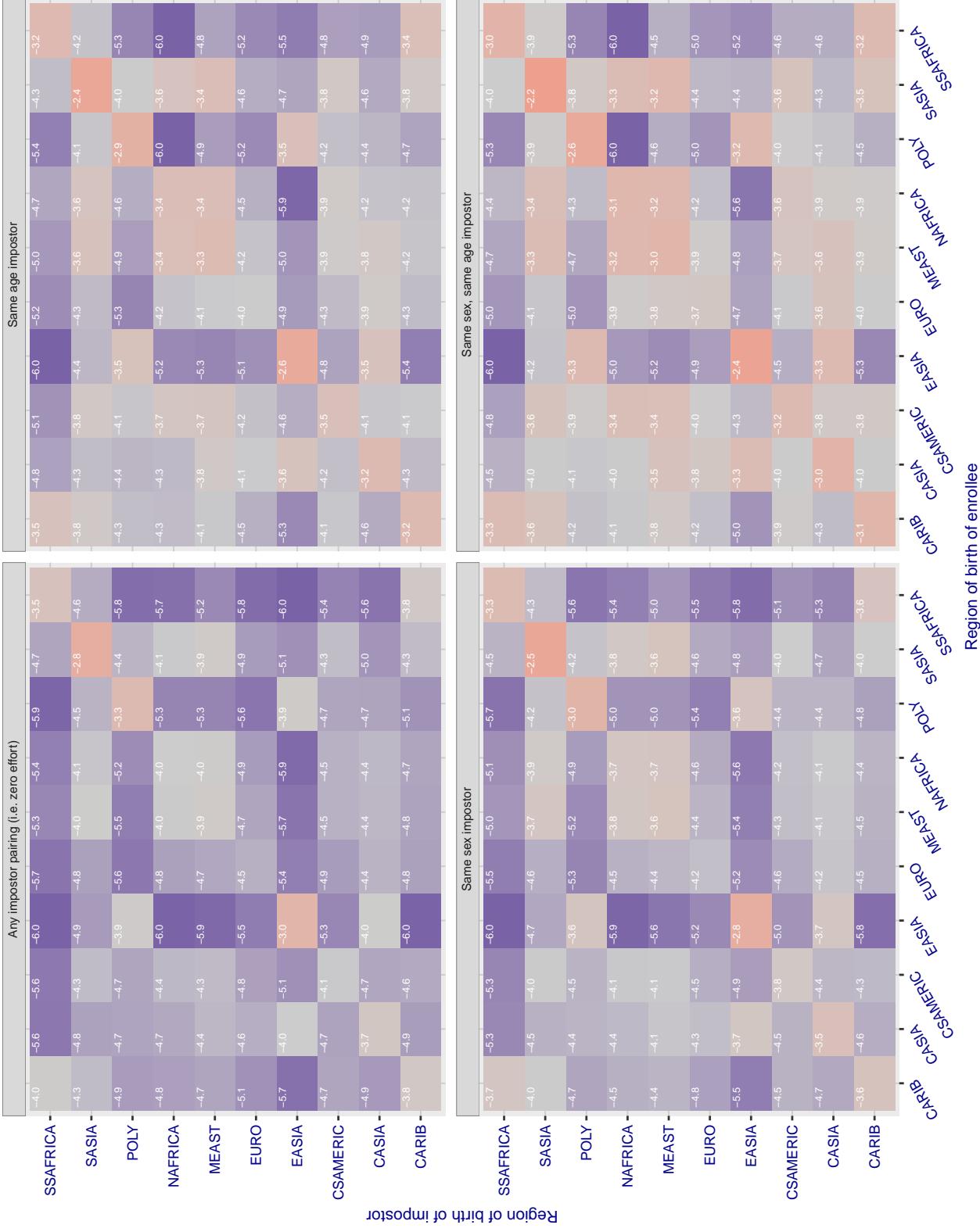
Cross region FMR at threshold T = 79.344 for algorithm dermalog_005, giving FMR(T) = 0.0001 globally.

Figure 166: For algorithm dermalog-005 operating on visa images, the heatmap shows false match rates observed over impostor comparisons of faces from different individuals who were born in the given region pair. False matches are counted against a recognition threshold fixed globally to give the target FMR in the plot title, computed over all on the order of 10^{10} impostor comparisons. If text appears in each box it give the same quantity as that coded by the color. Grey indicates FMR is at the intended FMR target level. Light red colors present a security vulnerability to, for example, a passport gate. Each +1 increase in $\log_{10} \text{FMR}$ corresponds to a factor of 10 increase in FMR. The matrix is not quite symmetric because images in the enrollment and verification sets are different.

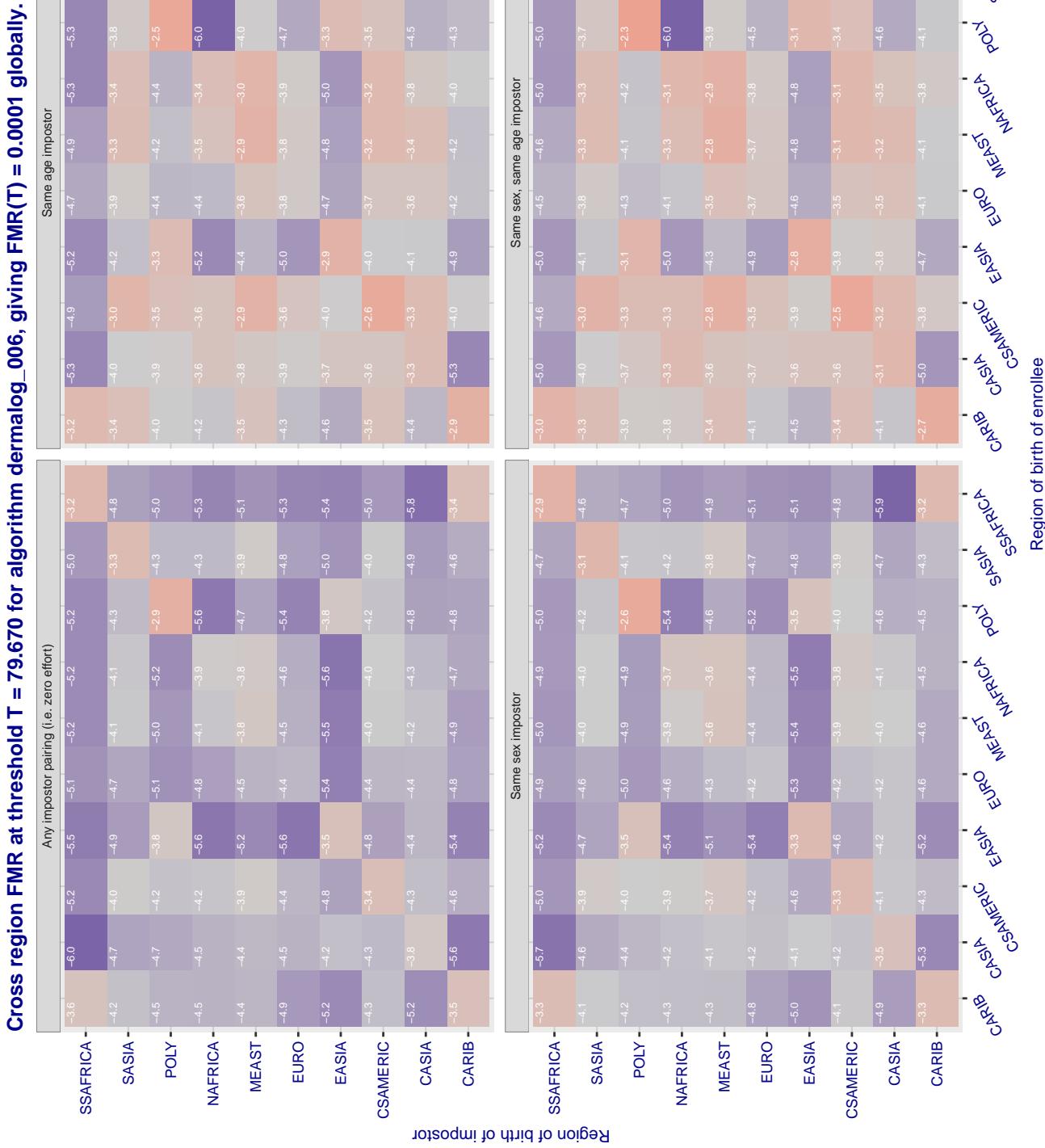


Figure 167: For algorithm dermalog-006 operating on visa images, the heatmap shows false match rates observed over impostor comparisons of faces from different individuals who were born in the given region pair. False matches are counted against a recognition threshold fixed globally to give the target FMR in the plot title, computed over all on the order of 10^{10} impostor comparisons. If text appears in each box it give the same quantity as that coded by the color. Grey indicates FMR is at the intended FMR target level. Light red colors present a security vulnerability to, for example, a passport gate. Each +1 increase in \log_{10} FMR corresponds to a factor of 10 increase in FMR. The matrix is not quite symmetric because images in the enrollment and verification sets are different.

Cross region FMR at threshold T = 0.675 for algorithm digitalbarriers_002, giving FMR(T) = 0.00001 globally.

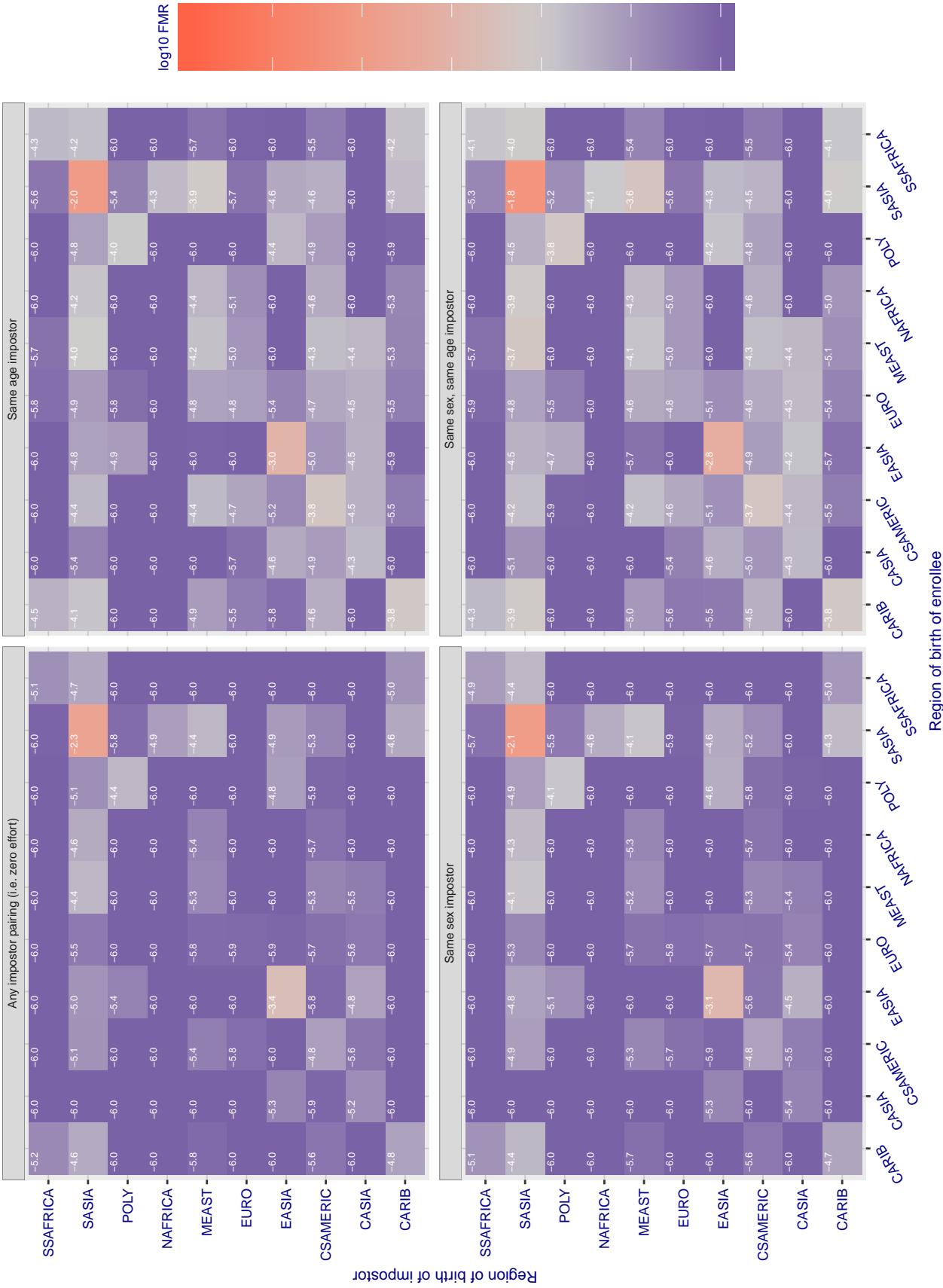


Figure 168: For algorithm digitalbarriers-002 operating on visa images, the heatmap shows false match rates observed over impostor comparisons of faces from different individuals who were born in the given region pair. False matches are counted against a recognition threshold fixed globally to give the target FMR in the plot title, computed over all on the order of 10^{10} impostor comparisons. If text appears in each box it give the same quantity as that coded by the color. Grey indicates FMR is at the intended FMR target level. Light red colors present a security vulnerability to, for example, a passport gate. Each +1 increase in $\log_{10} FMR$ corresponds to a factor of 10 increase in FMR. The matrix is not quite symmetric because images in the enrollment and verification sets are different.

Cross region FMR at threshold T = 1.061 for algorithm dsk_000, giving FMR(T) = 0.0001 globally.

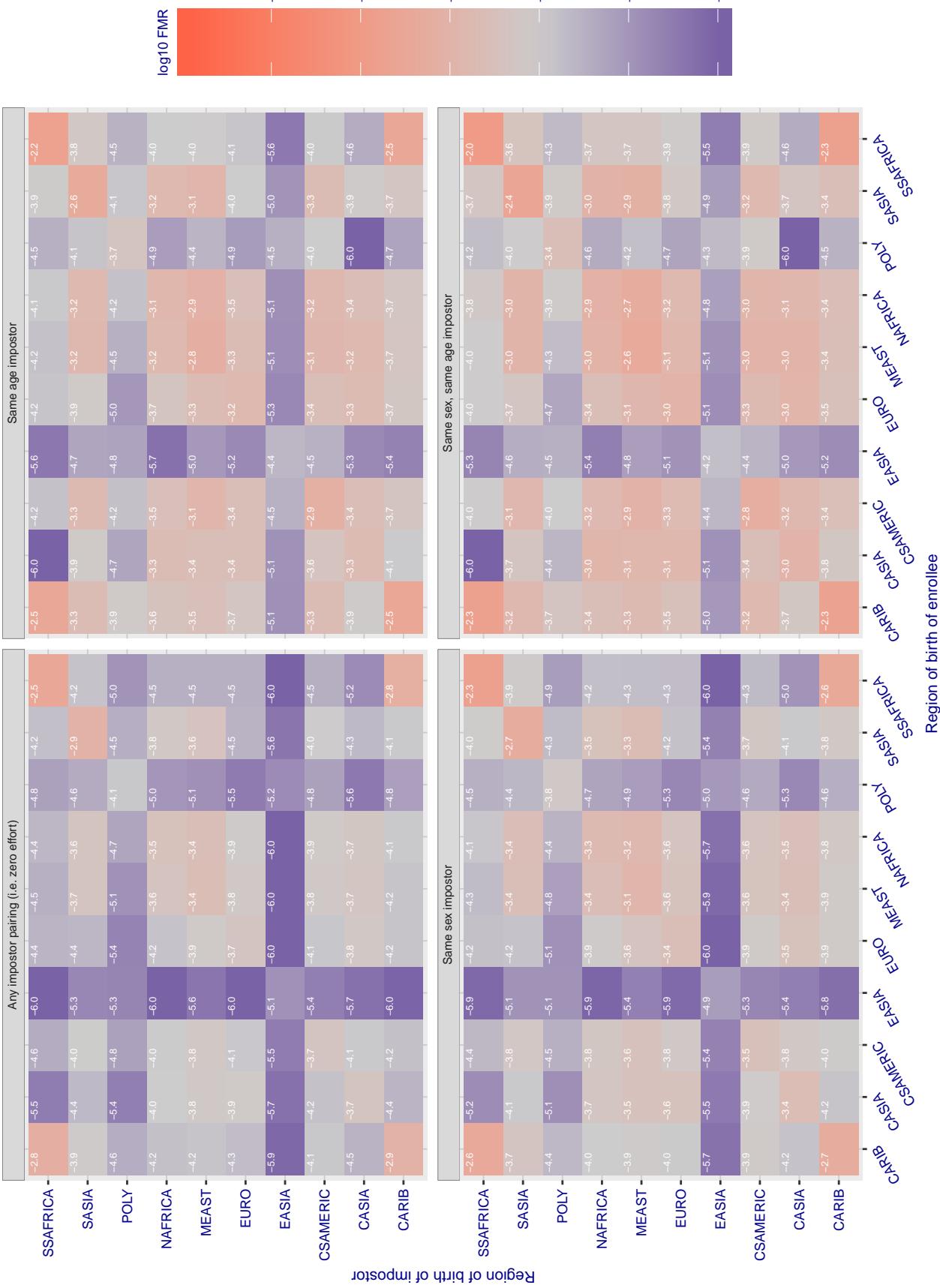


Figure 169: For algorithm dsk-000 operating on visa images, the heatmap shows false match rates observed over impostor comparisons of faces from different individuals who were born in the given region pair. False matches are counted against a recognition threshold fixed globally to give the target FMR in the plot title, computed over all on the order of 10^{10} impostor comparisons. If text appears in each box it give the same quantity as that coded by the color. Grey indicates FMR is at the intended FMR target level. Light red colors present a security vulnerability to, for example, a passport gate. Each +1 increase in \log_{10} FMR corresponds to a factor of 10 increase in FMR. The matrix is not quite symmetric because images in the enrollment and verification sets are different.

Cross region FMR at threshold T = 53.280 for algorithm einetworks_000, giving FMR(T) = 0.0001 globally.

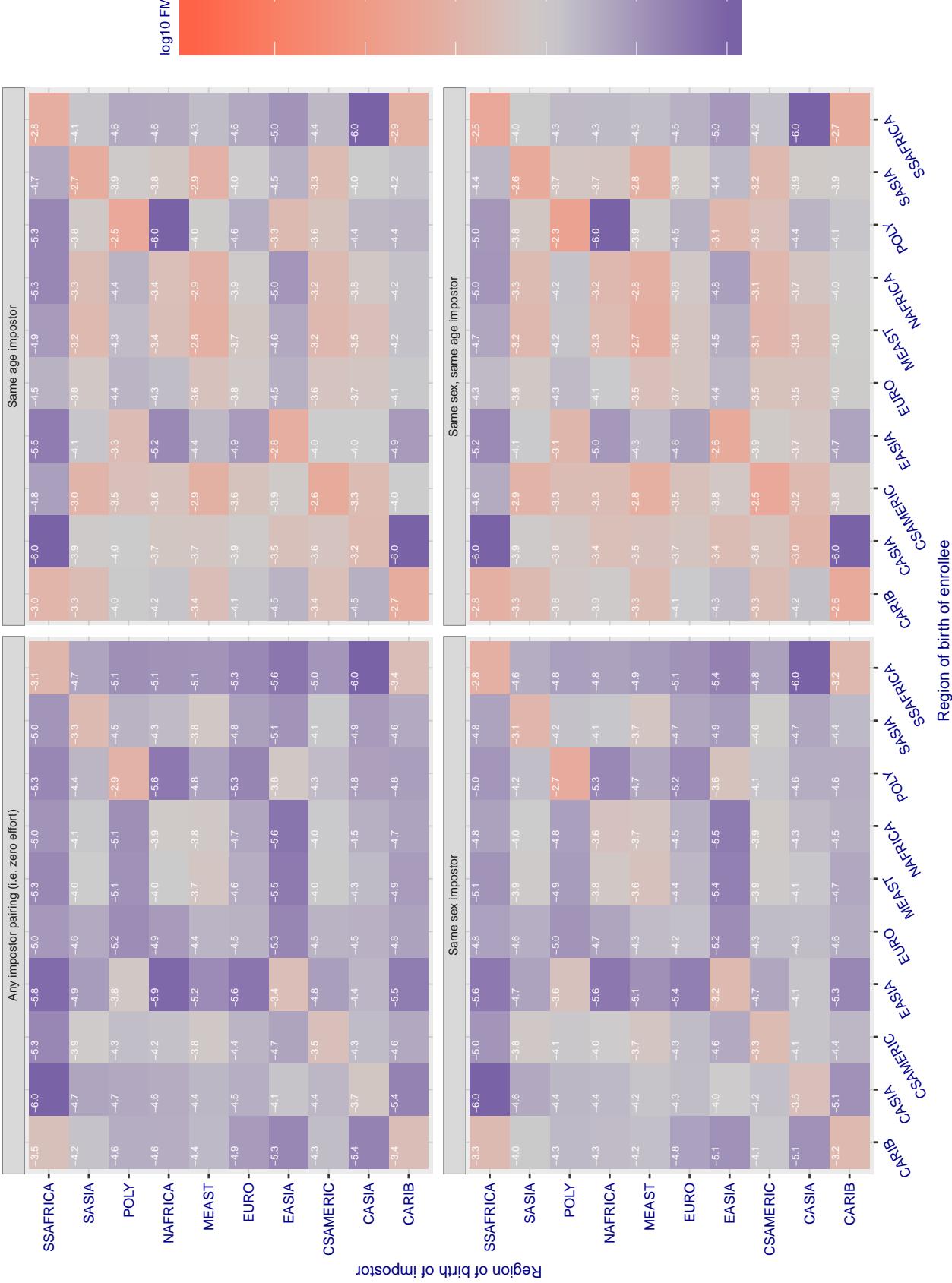


Figure 170: For algorithm einetworks-000 operating on visa images, the heatmap shows false match rates observed over impostor comparisons of faces from different individuals who were born in the given region pair. False matches are counted against a recognition threshold fixed globally to give the target FMR in the plot title, computed over all on the order of 10^{10} impostor comparisons. If text appears in each box it give the same quantity as that coded by the color. Grey indicates FMR is at the intended FMR target level. Light red colors present a security vulnerability to, for example, a passport gate. Each +1 increase in $\log_{10} FMR$ corresponds to a factor of 10 increase in FMR. The matrix is not quite symmetric because images in the enrollment and verification sets are different.

Cross region FMR at threshold T = 2.589 for algorithm everai_002, giving FMR(T) = 0.0001 globally.

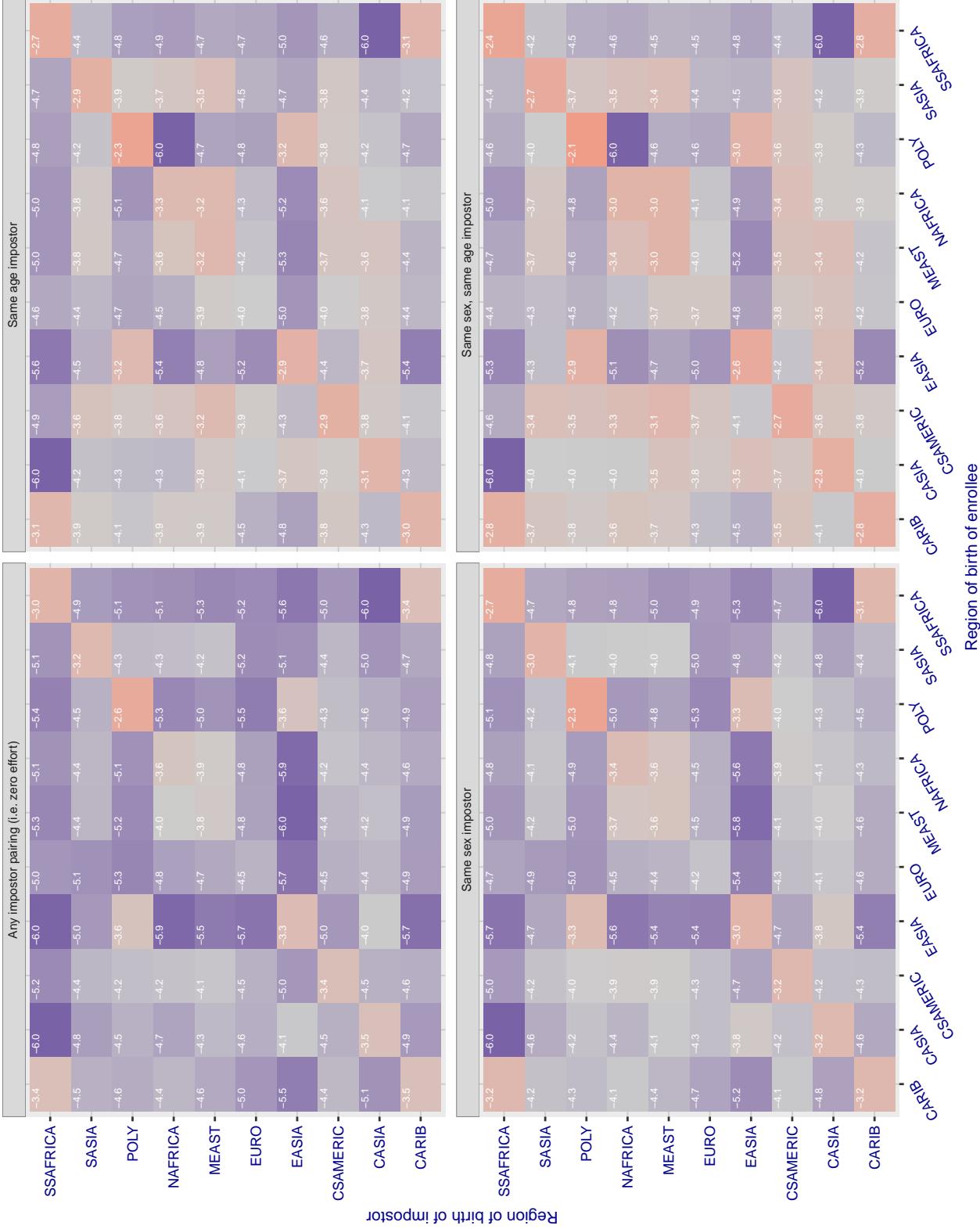


Figure 171: For algorithm everai-002 operating on visa images, the heatmap shows false match rates observed over impostor comparisons of faces from different individuals who were born in the given region pair. False matches are counted against a recognition threshold fixed globally to give the target FMR in the plot title, computed over all on the order of 10^{10} impostor comparisons. If text appears in each box it give the same quantity as that coded by the color. Grey indicates FMR is at the intended FMR target level. Light red colors present a security vulnerability to, for example, a passport gate. Each +1 increase in $\log_{10} FMR$ corresponds to a factor of 10 increase in FMR. The matrix is not quite symmetric because images in the enrollment and verification sets are different.

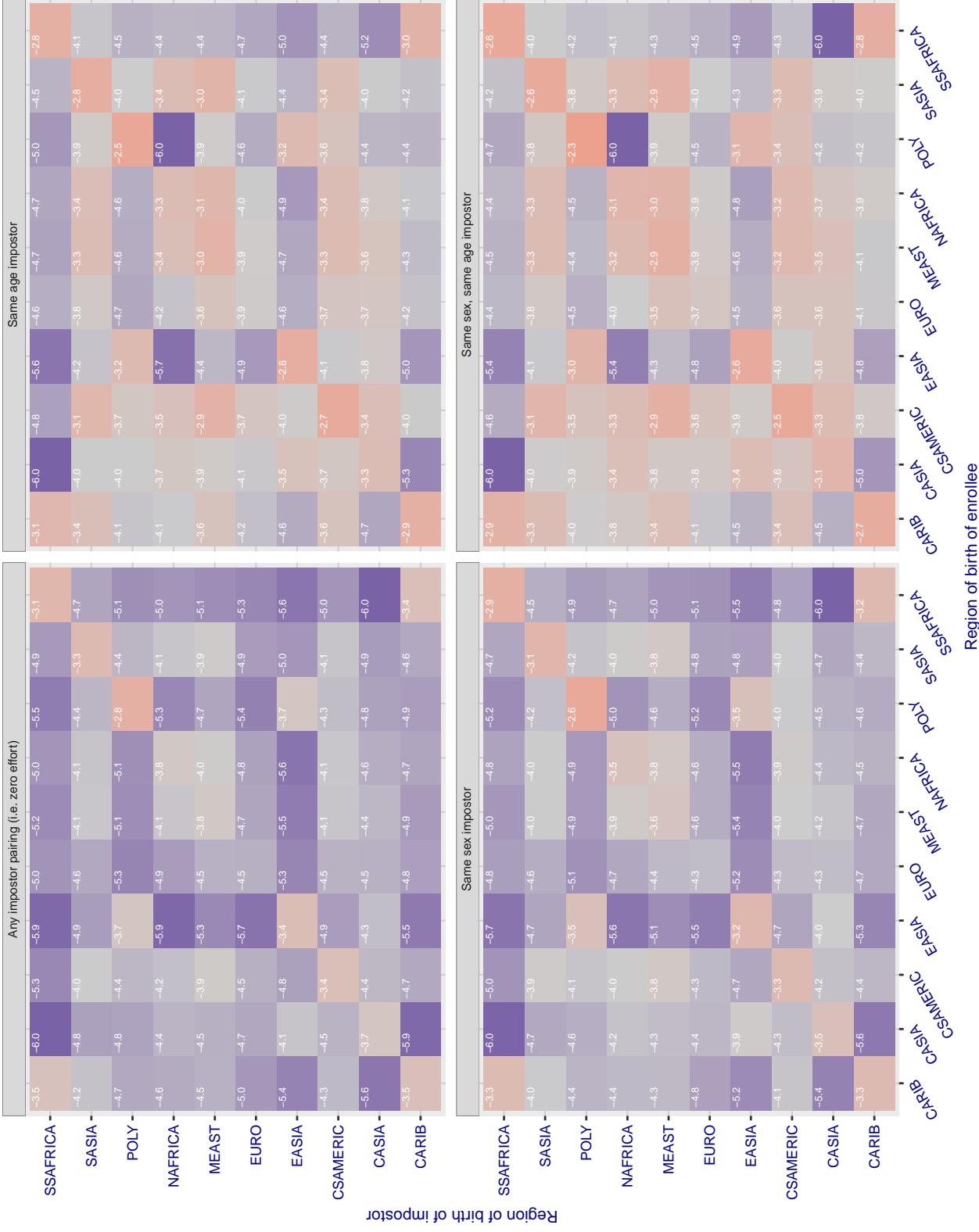
Cross region FMR at threshold T = 0.400 for algorithm f8_001, giving FMR(T) = 0.0001 globally.

Figure 172: For algorithm f8_001 operating on visa images, the heatmap shows false match rates observed over impostor comparisons of faces from different individuals who were born in the given region pair. False matches are counted against a recognition threshold fixed globally to give the target FMR in the plot title, computed over all on the order of 10^{10} impostor comparisons. If text appears in each box it give the same quantity as that coded by the color. Grey indicates FMR is at the intended FMR target level. Light red colors present a security vulnerability to, for example, a passport gate. Each +1 increase in $\log 10 \text{ FMR}$ corresponds to a factor of 10 increase in FMR. The matrix is not quite symmetric because images in the enrollment and verification sets are different.

Cross region FMR at threshold T = 1.375 for algorithm facesoft_000, giving FMR(T) = 0.0001 globally.

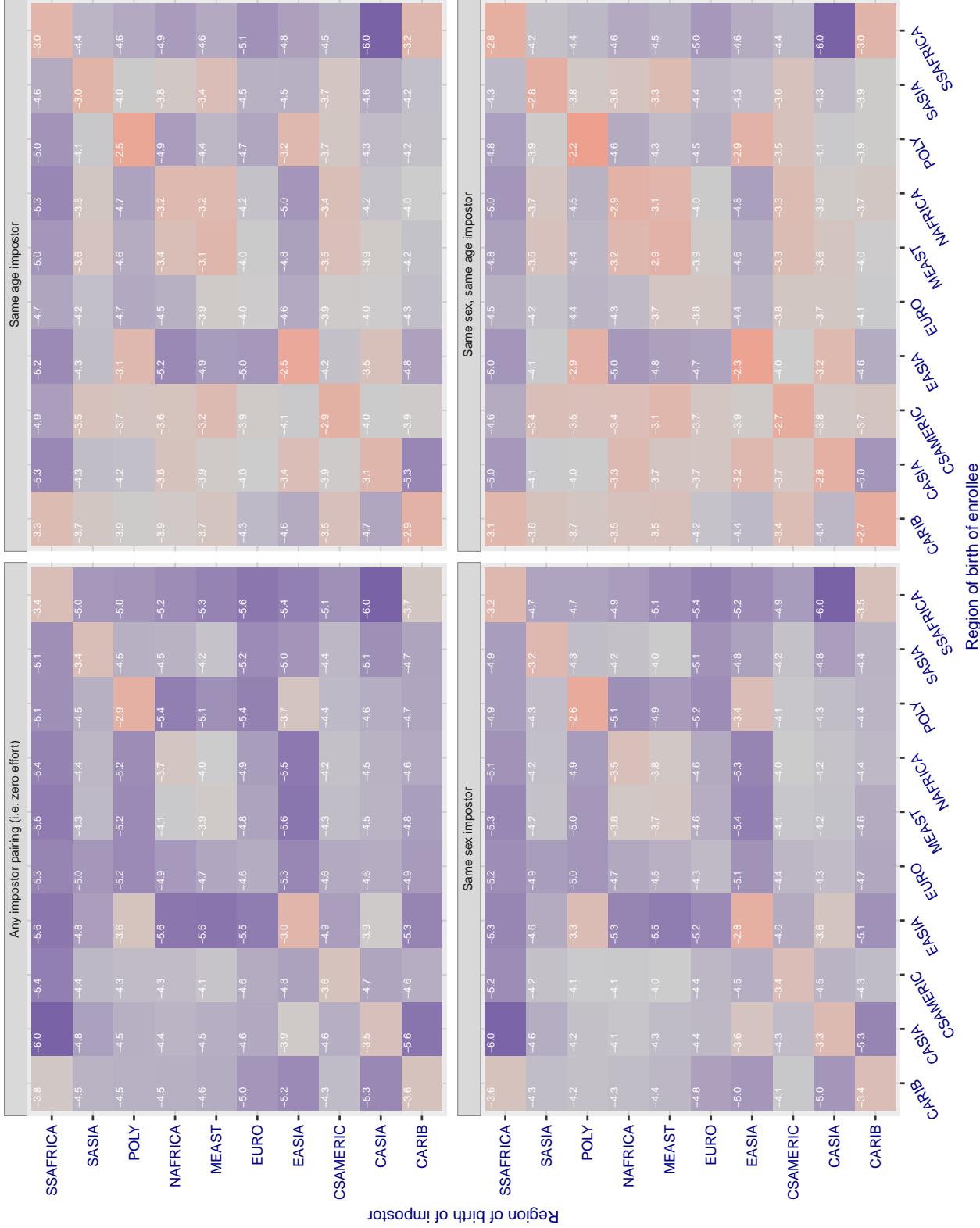


Figure 173: For algorithm facesoft-000 operating on visa images, the heatmap shows false match rates observed over impostor comparisons of faces from different individuals who were born in the given region pair. False matches are counted against a recognition threshold fixed globally to give the target FMR in the plot title, computed over all on the order of 10^{10} impostor comparisons. If text appears in each box it give the same quantity as that coded by the color. Grey indicates FMR is at the intended FMR target level. Light red colors present a security vulnerability to, for example, a passport gate. Each +1 increase in $\log_{10} FMR$ corresponds to a factor of 10 increase in FMR. The matrix is not quite symmetric because images in the enrollment and verification sets are different.

Cross region FMR at threshold T = 0.611 for algorithm glory_000, giving FMR(T) = 0.0001 globally.

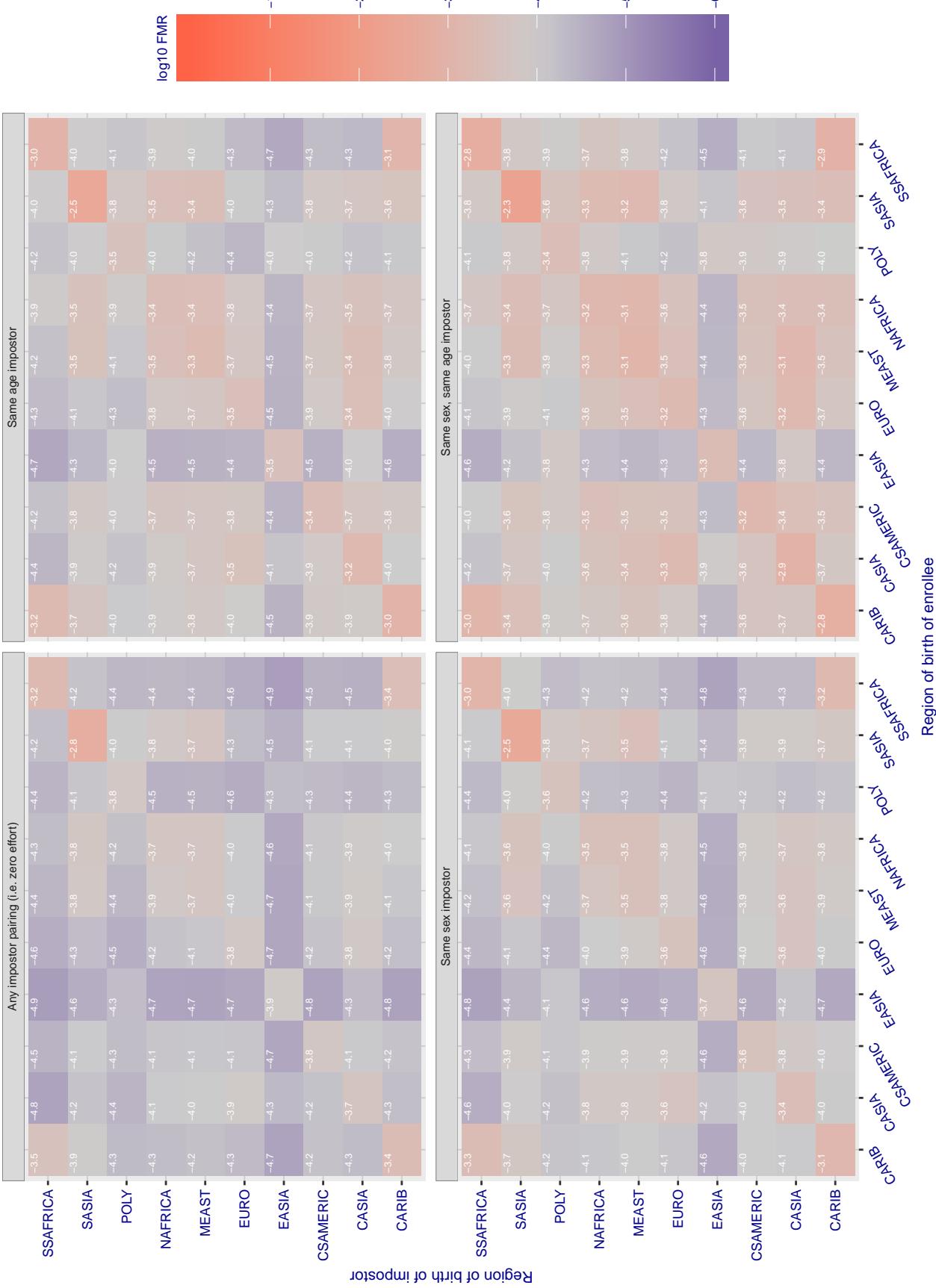


Figure 174: For algorithm *glory-000* operating on visa images, the heatmap shows false match rates observed over impostor comparisons of faces from different individuals who were born in the given region pair. False matches are counted against a recognition threshold fixed globally to give the target FMR in the plot title, computed over all on the order of 10^{10} impostor comparisons. If text appears in each box it give the same quantity as that coded by the color. Grey indicates FMR is at the intended FMR target level. Light red colors present a security vulnerability to, for example, a passport gate. Each +1 increase in $\log_{10} FMR$ corresponds to a factor of 10 increase in FMR. The matrix is not quite symmetric because images in the enrollment and verification sets are different.

Cross region FMR at threshold T = 0.618 for algorithm glory_001, giving FMR(T) = 0.0001 globally.

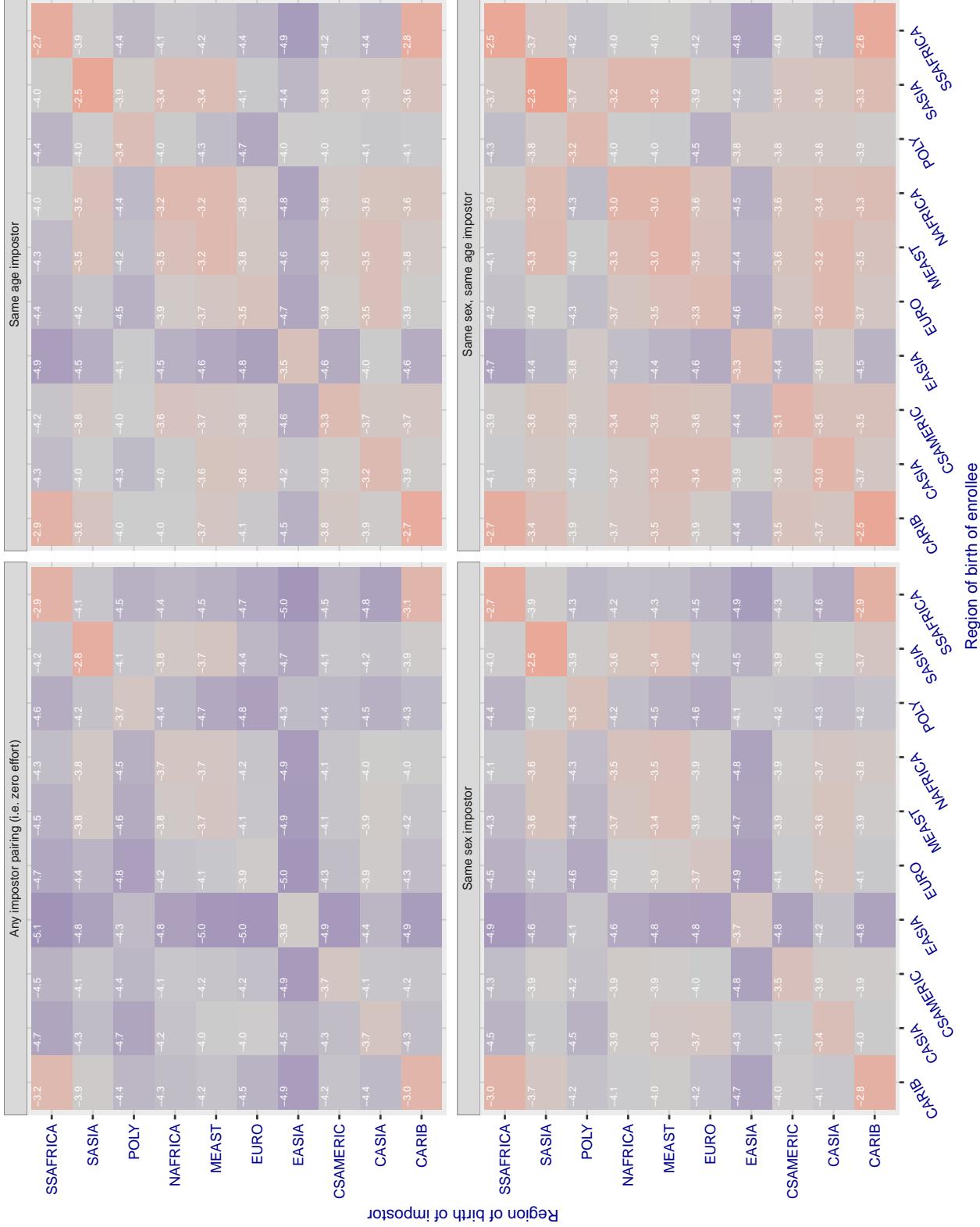
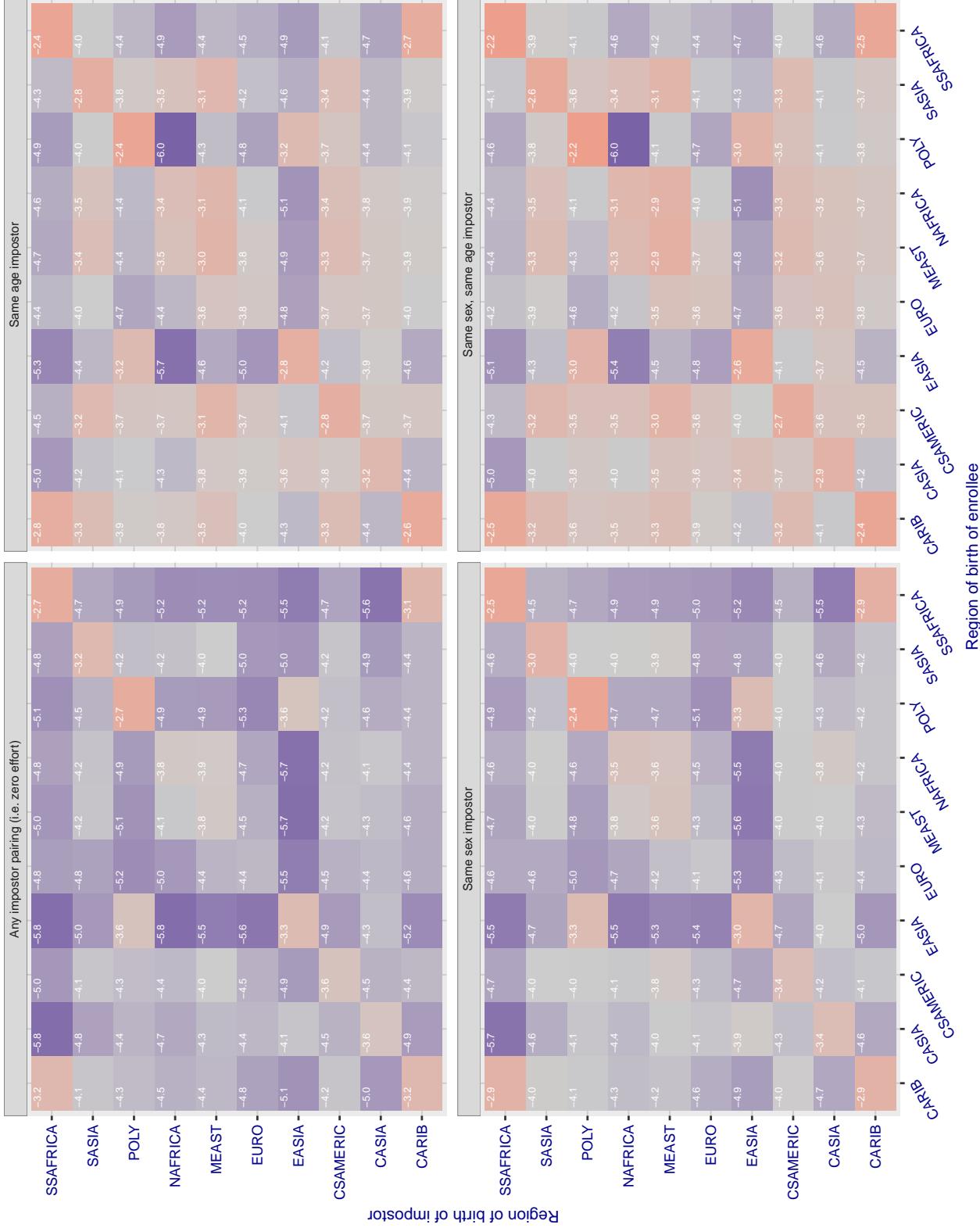


Figure 175: For algorithm glory-001 operating on visa images, the heatmap shows false match rates observed over impostor comparisons of faces from different individuals who were born in the given region pair. False matches are counted against a recognition threshold fixed globally to give the target FMR in the plot title, computed over all on the order of 10^{10} impostor comparisons. If text appears in each box it give the same quantity as that coded by the color. Grey indicates FMR is at the intended FMR target level. Light red colors present a security vulnerability to, for example, a passport gate. Each +1 increase in $\log_{10} \text{FMR}$ corresponds to a factor of 10 increase in FMR. The matrix is not quite symmetric because images in the enrollment and verification sets are different.

Cross region FMR at threshold T = 0.483 for algorithm gorilla_002, giving FMR(T) = 0.0001 globally.



2019/09/11 14:58:19

$\text{FNMR}(T)$ "False non-match rate"
 $\text{FMR}(T)$ "False match rate"

Figure 176: For algorithm gorilla-002 operating on visa images, the heatmap shows false match rates observed over impostor comparisons of faces from different individuals who were born in the given region pair. False matches are counted against a recognition threshold fixed globally to give the target FMR in the plot title, computed over all on the order of 10^{10} impostor comparisons. If text appears in each box it give the same quantity as that coded by the color. Grey indicates FMR is at the intended FMR target level. Light red colors present a security vulnerability to, for example, a passport gate. Each +1 increase in $\log_{10} \text{FMR}$ corresponds to a factor of 10 increase in FMR. The matrix is not quite symmetric because images in the enrollment and verification sets are different.

Cross region FMR at threshold T = 0.454 for algorithm gorilla_003, giving FMR(T) = 0.0001 globally.

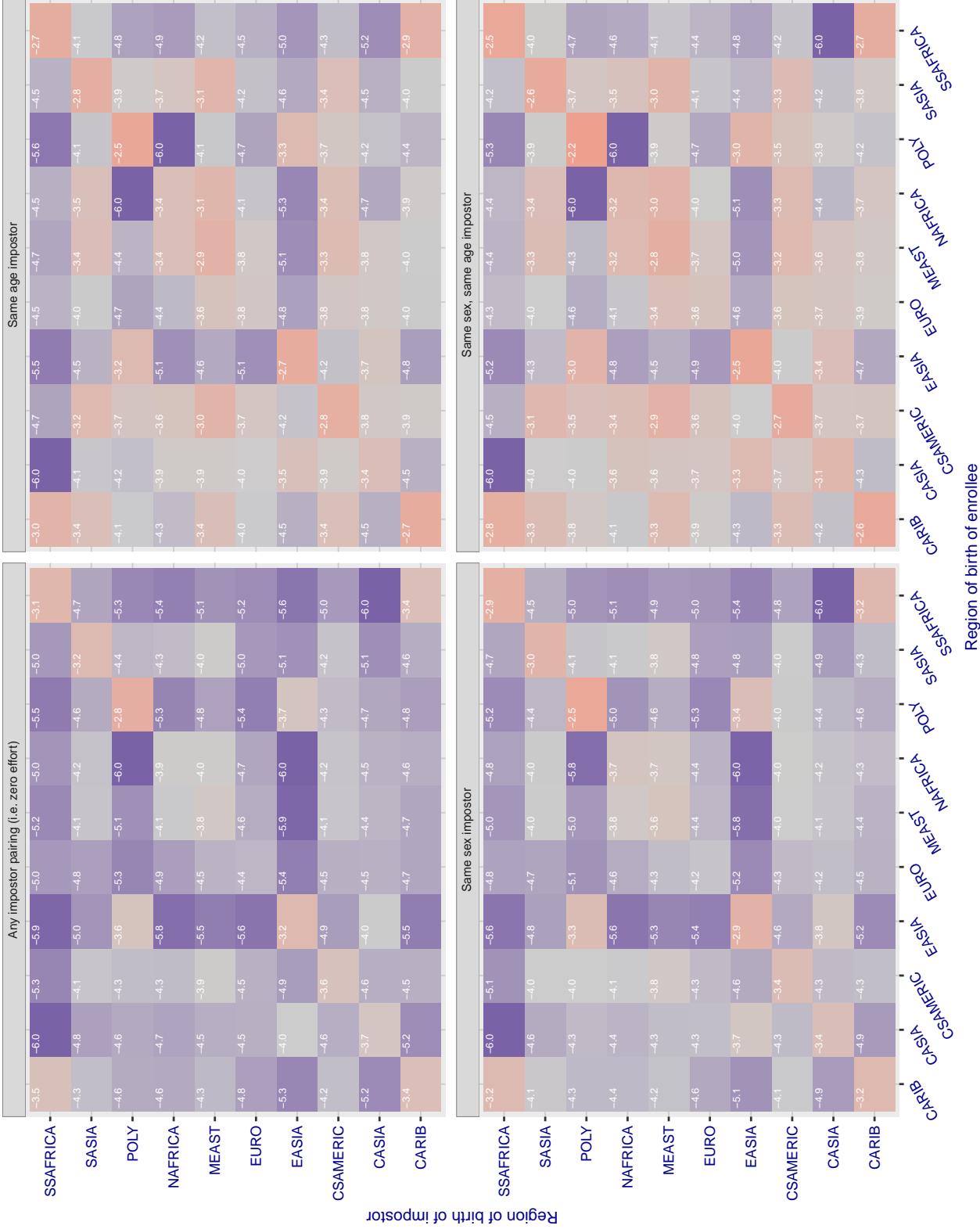


Figure 177: For algorithm gorilla-003 operating on visa images, the heatmap shows false match rates observed over impostor comparisons of faces from different individuals who were born in the given region pair. False matches are counted against a recognition threshold fixed globally to give the target FMR in the plot title, computed over all on the order of 10^{10} impostor comparisons. If text appears in each box it give the same quantity as that coded by the color. Grey indicates FMR is at the intended FMR target level. Light red colors present a security vulnerability to, for example, a passport gate. Each +1 increase in $\log_{10} \text{FMR}$ corresponds to a factor of 10 increase in FMR. The matrix is not quite symmetric because images in the enrollment and verification sets are different.

Cross region FMR at threshold T = 66.565 for algorithm hik_001, giving FMR(T) = 0.0001 globally.

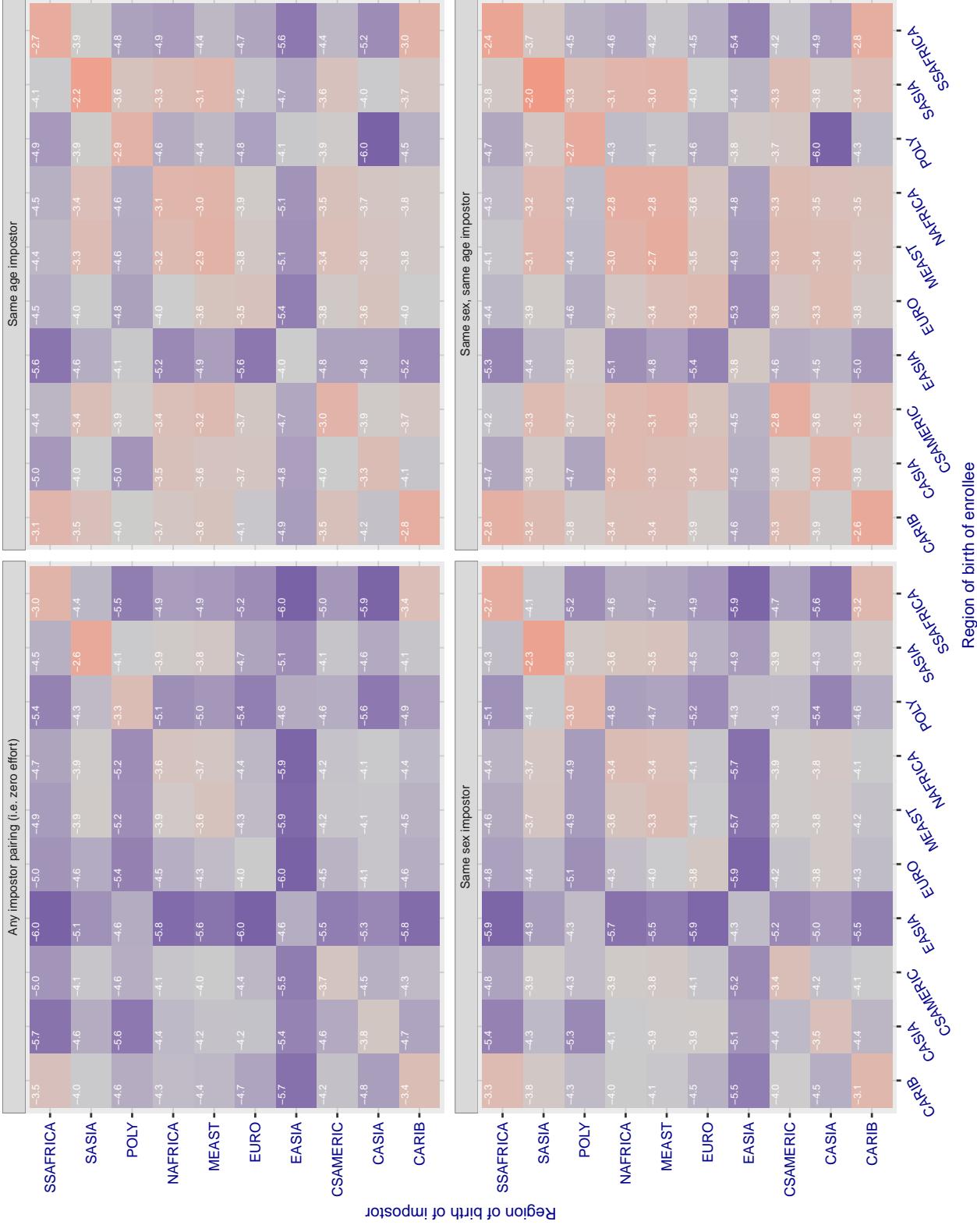


Figure 178: For algorithm hik-001 operating on visa images, the heatmap shows false match rates observed over impostor comparisons of faces from different individuals who were born in the given region pair. False matches are counted against a recognition threshold fixed globally to give the target FMR in the plot title, computed over all on the order of 10^{10} impostor comparisons. If text appears in each box it give the same quantity as that coded by the color. Grey indicates FMR is at the intended FMR target level. Light red colors present a security vulnerability to, for example, a passport gate. Each +1 increase in $\log_{10} \text{FMR}$ corresponds to a factor of 10 increase in FMR. The matrix is not quite symmetric because images in the enrollment and verification sets are different.

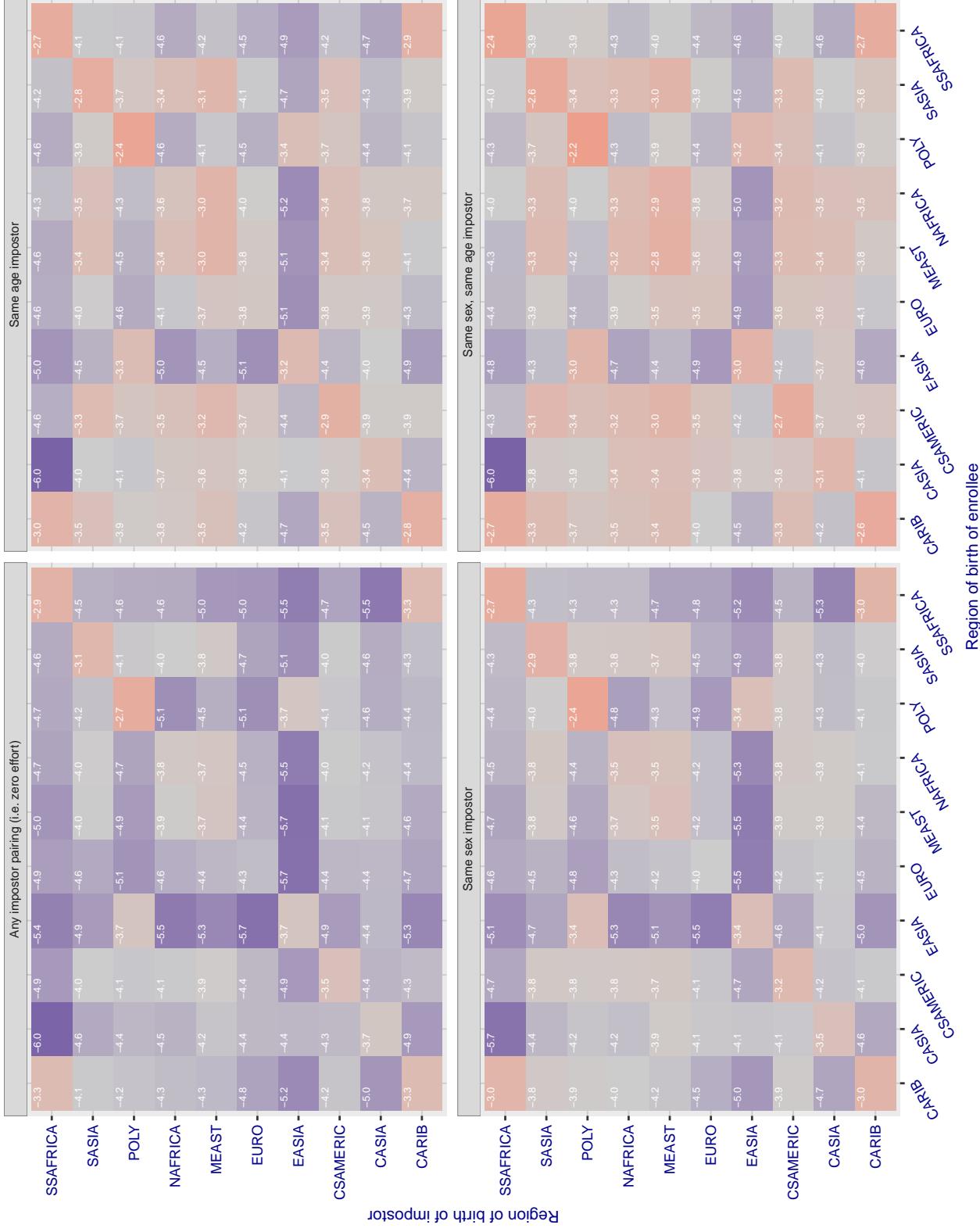
Cross region FMR at threshold T = 0.823 for algorithm hr_001, giving FMR(T) = 0.0001 globally.

Figure 179: For algorithm hr-001 operating on visa images, the heatmap shows false match rates observed over impostor comparisons of faces from different individuals who were born in the given region pair. False matches are counted against a recognition threshold fixed globally to give the target FMR in the plot title, computed over all on the order of 10^{10} impostor comparisons. If text appears in each box it give the same quantity as that coded by the color. Grey indicates FMR is at the intended FMR target level. Light red colors present a security vulnerability to, for example, a passport gate. Each +1 increase in $\log 10$ FMR corresponds to a factor of 10 increase in FMR. The matrix is not quite symmetric because images in the enrollment and verification sets are different.

Cross region FMR at threshold T = 37645.000 for algorithm id3_003, giving FMR(T) = 0.0001 globally.

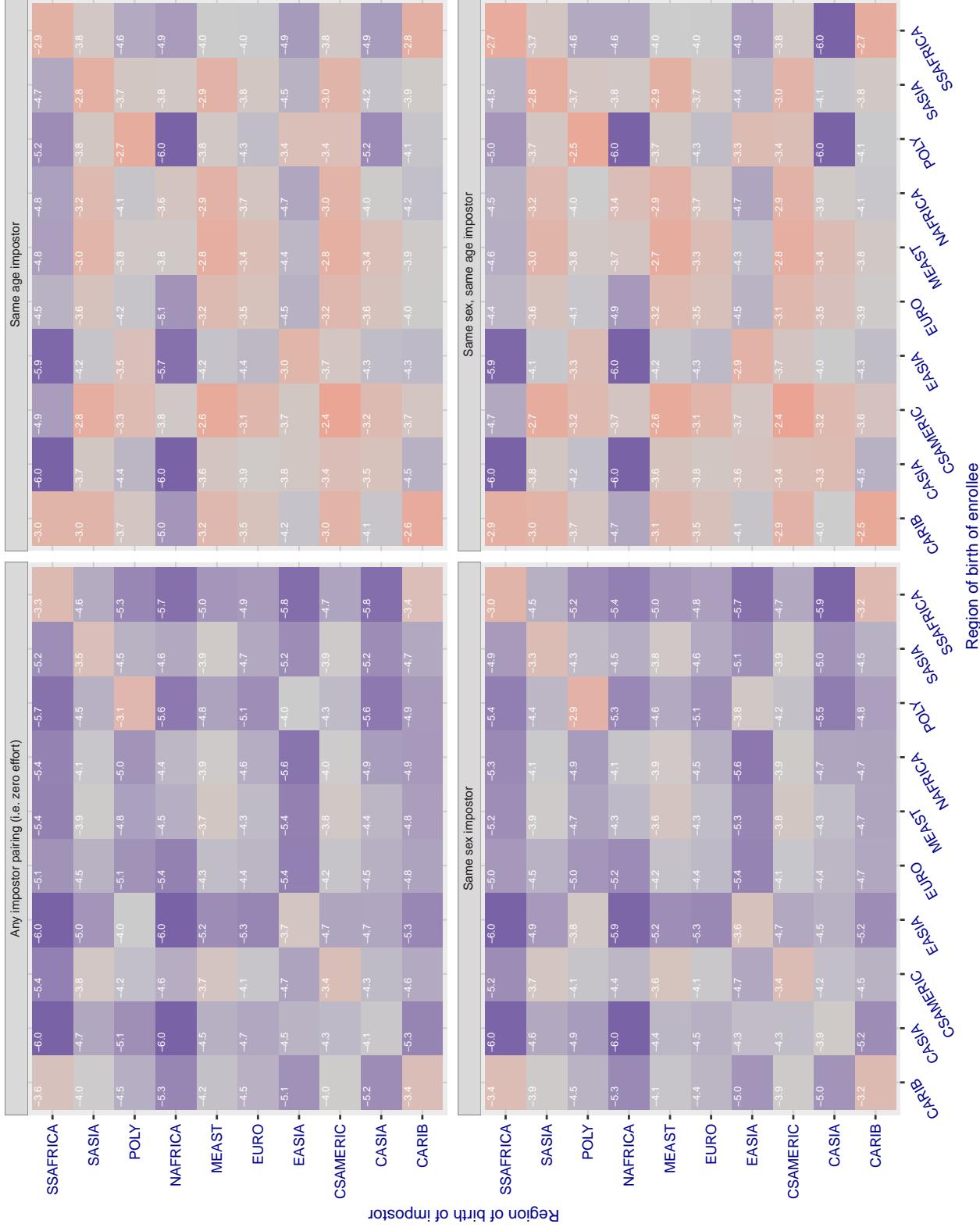


Figure 180: For algorithm id3_003 operating on visa images, the heatmap shows false match rates observed over impostor comparisons of faces from different individuals who were born in the given region pair. False matches are counted against a recognition threshold fixed globally to give the target FMR in the plot title, computed over all on the order of 10^{10} impostor comparisons. If text appears in each box it give the same quantity as that coded by the color. Grey indicates FMR is at the intended FMR target level. Light red colors present a security vulnerability to, for example, a passport gate. Each +1 increase in $\log 10 \text{ FMR}$ corresponds to a factor of 10 increase in FMR. The matrix is not quite symmetric because images in the enrollment and verification sets are different.

Cross region FMR at threshold T = 37001.000 for algorithm id3_004, giving FMR(T) = 0.0001 globally.

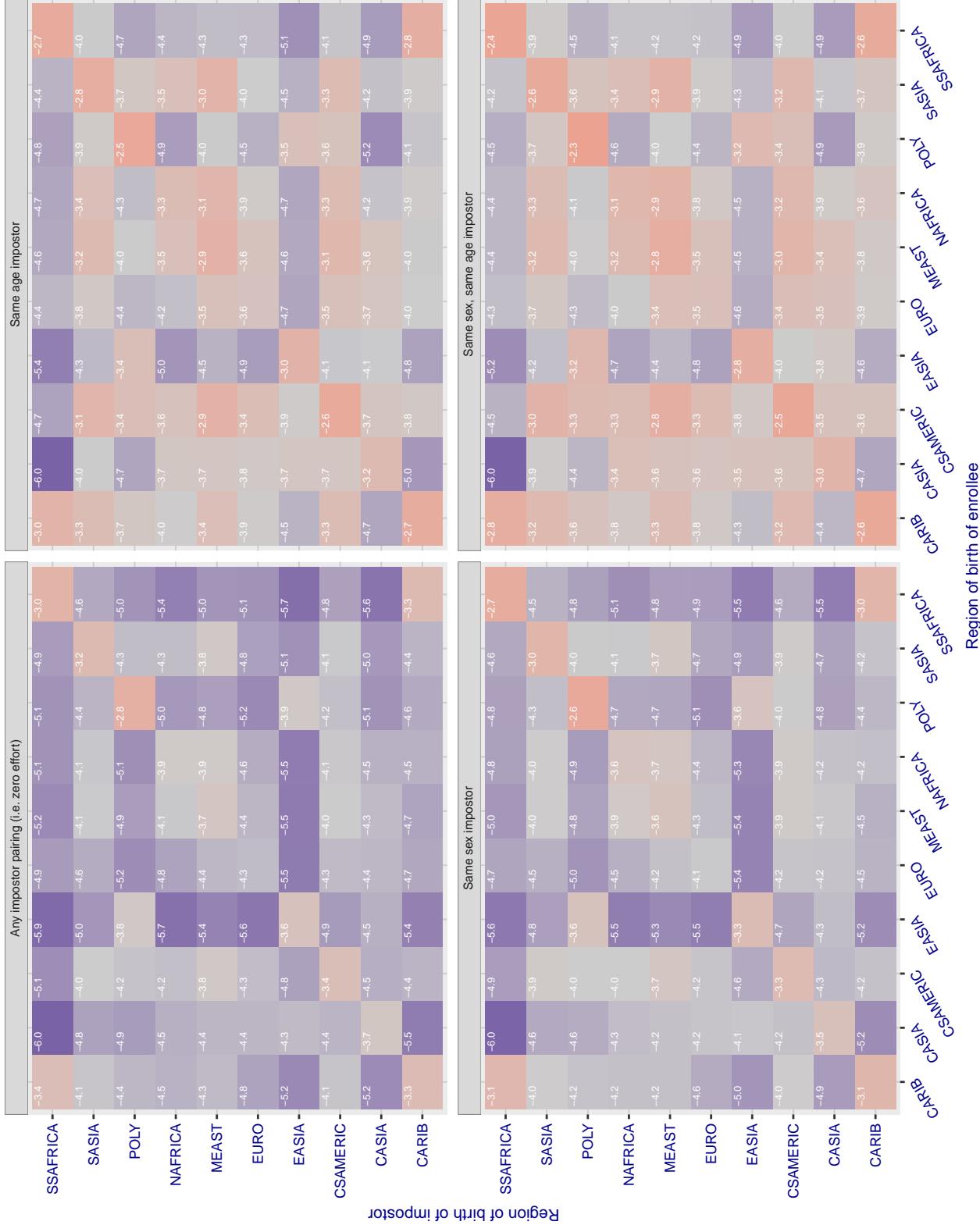
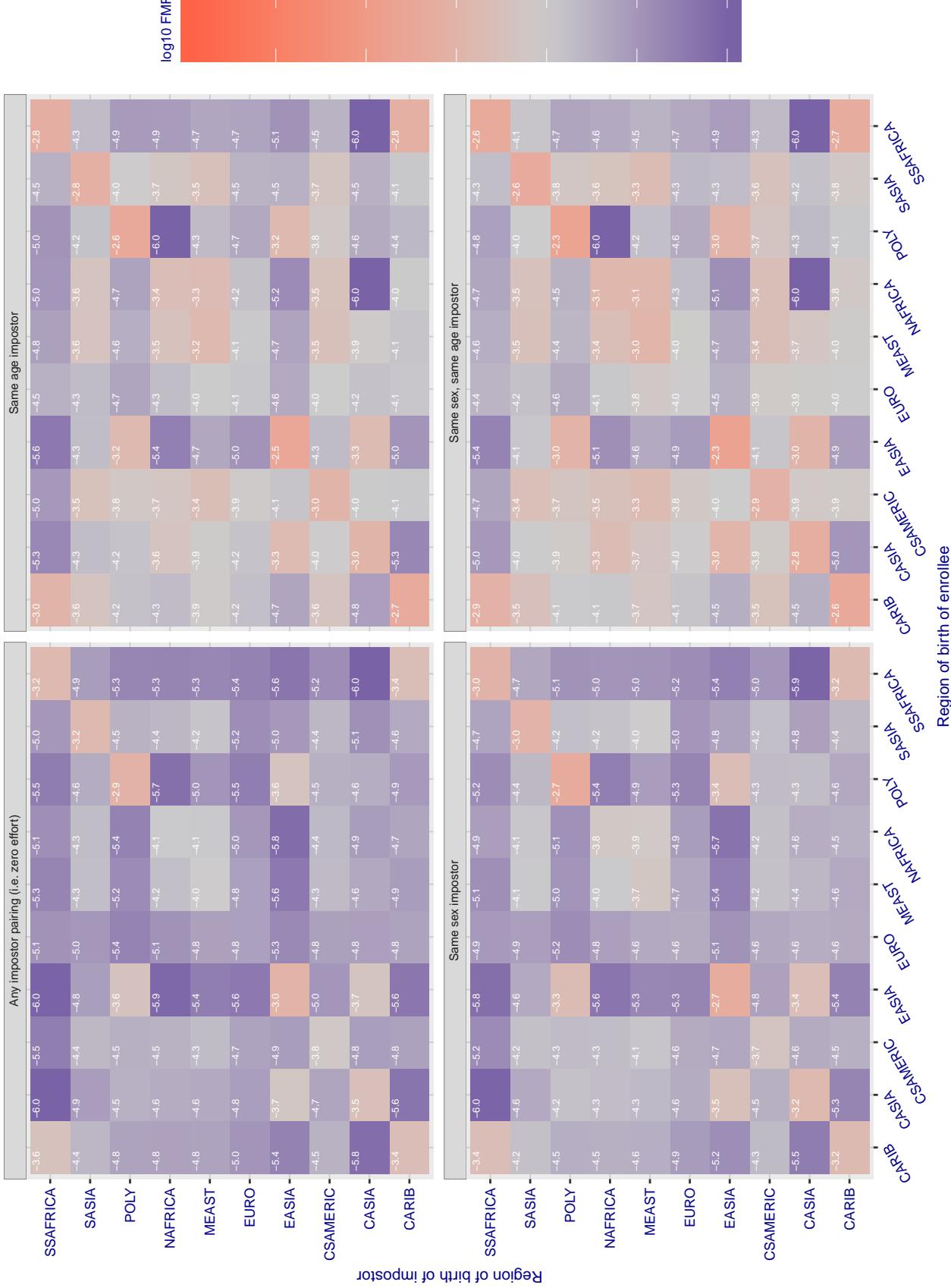


Figure 181: For algorithm id3_004 operating on visa images, the heatmap shows false match rates observed over impostor comparisons of faces from different individuals who were born in the given region pair. False matches are counted against a recognition threshold fixed globally to give the target FMR in the plot title, computed over all on the order of 10^{10} impostor comparisons. If text appears in each box it give the same quantity as that coded by the color. Grey indicates FMR is at the intended FMR target level. Light red colors present a security vulnerability to, for example, a passport gate. Each +1 increase in $\log_{10} \text{FMR}$ corresponds to a factor of 10 increase in FMR. The matrix is not quite symmetric because images in the enrollment and verification sets are different.

Cross region FMR at threshold T = 3664.380 for algorithm idemia_003, giving FMR(T) = 0.0001 globally.

2019/09/11 14:58:19

FNMR(T)
FMR(T) "False non-match rate"
"False match rate"

Figure 182: For algorithm idemia-003 operating on visa images, the heatmap shows false match rates observed over impostor comparisons of faces from different individuals who were born in the given region pair. False matches are counted against a recognition threshold fixed globally to give the target FMR in the plot title, computed over all on the order of 10^{10} impostor comparisons. If text appears in each box it give the same quantity as that coded by the color. Grey indicates FMR is at the intended FMR target level. Light red colors present a security vulnerability to, for example, a passport gate. Each +1 increase in $\log_{10} FMR$ corresponds to a factor of 10 increase in FMR. The matrix is not quite symmetric because images in the enrollment and verification sets are different.

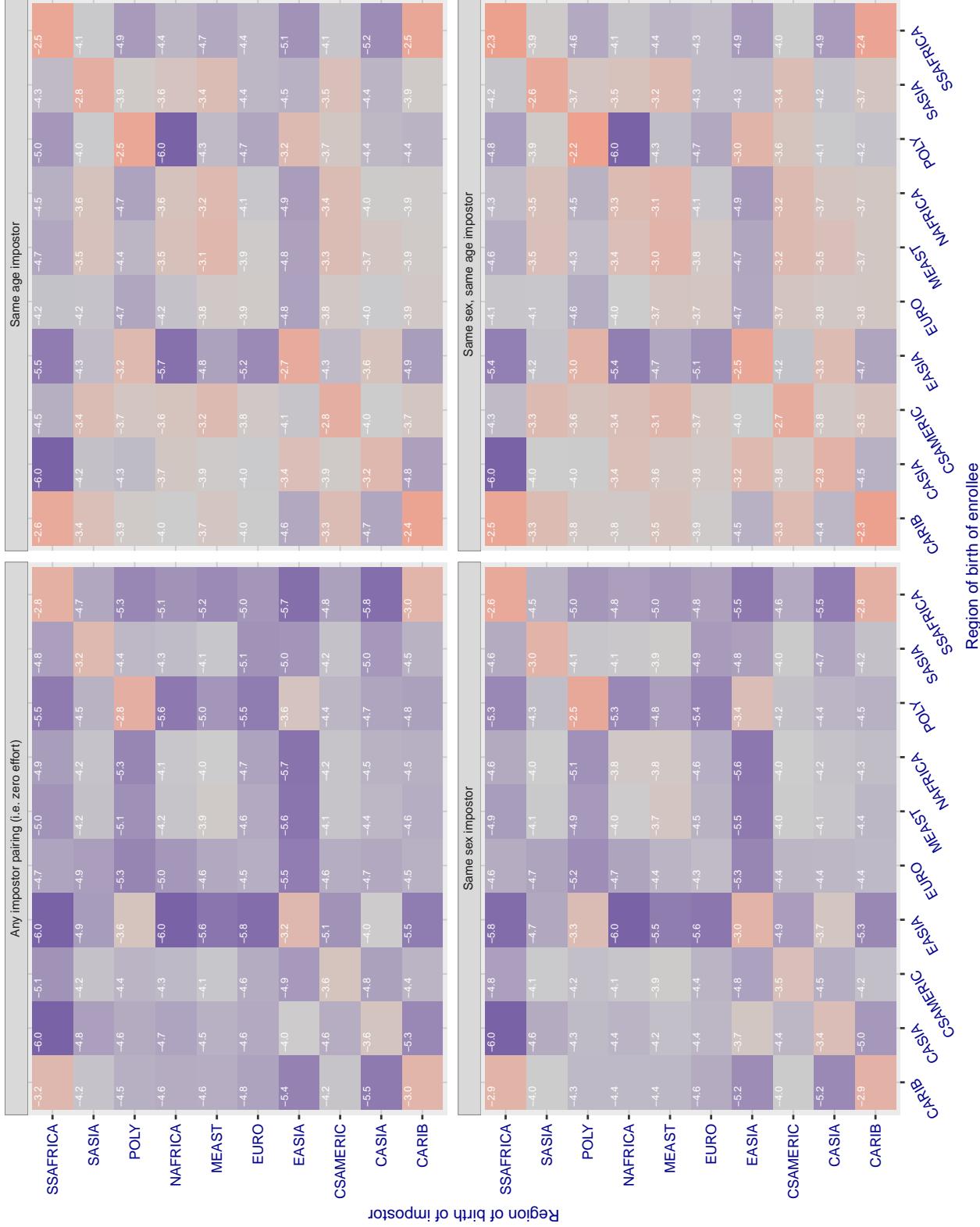
Cross region FMR at threshold T = 3925.463 for algorithm idemia_004, giving FMR(T) = 0.0001 globally.

Figure 183: For algorithm idemia-004 operating on visa images, the heatmap shows false match rates observed over impostor comparisons of faces from different individuals who were born in the given region pair. False matches are counted against a recognition threshold fixed globally to give the target FMR in the plot title, computed over all on the order of 10^{10} impostor comparisons. If text appears in each box it give the same quantity as that coded by the color. Grey indicates FMR is at the intended FMR target level. Light red colors present a security vulnerability to, for example, a passport gate. Each +1 increase in $\log_{10} \text{FMR}$ corresponds to a factor of 10 increase in FMR. The matrix is not quite symmetric because images in the enrollment and verification sets are different.

Cross region FMR at threshold T = 0.760 for algorithm iit_000, giving FMR(T) = 0.0001 globally.

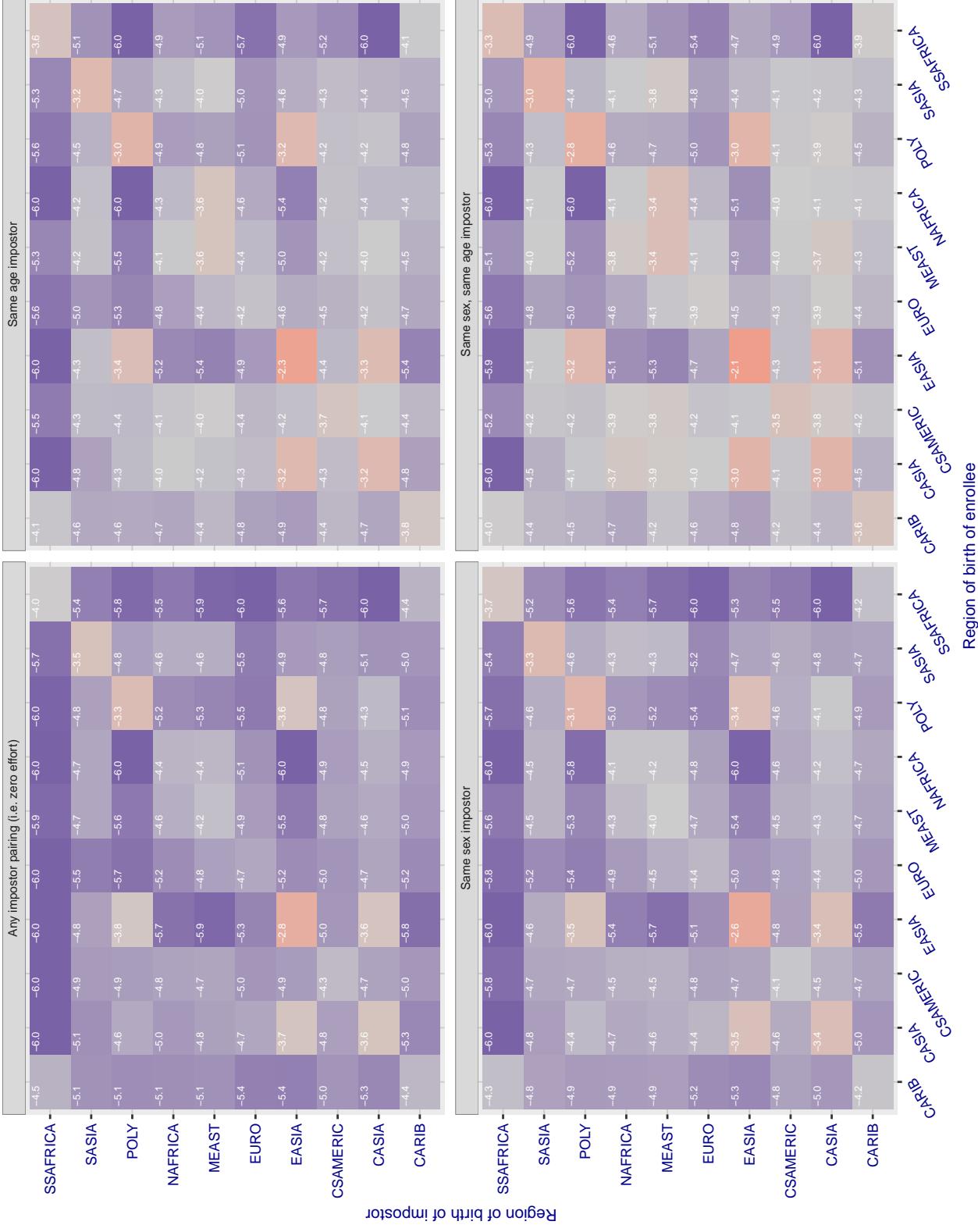


Figure 184: For algorithm iit-000 operating on visa images, the heatmap shows false match rates observed over impostor comparisons of faces from different individuals who were born in the given region pair. False matches are counted against a recognition threshold fixed globally to give the target FMR in the plot title, computed over all on the order of 10^{10} impostor comparisons. If text appears in each box it give the same quantity as that coded by the color. Grey indicates FMR is at the intended FMR target level. Light red colors present a security vulnerability to, for example, a passport gate. Each +1 increase in $\log 10$ FMR corresponds to a factor of 10 increase in FMR. The matrix is not quite symmetric because images in the enrollment and verification sets are different.

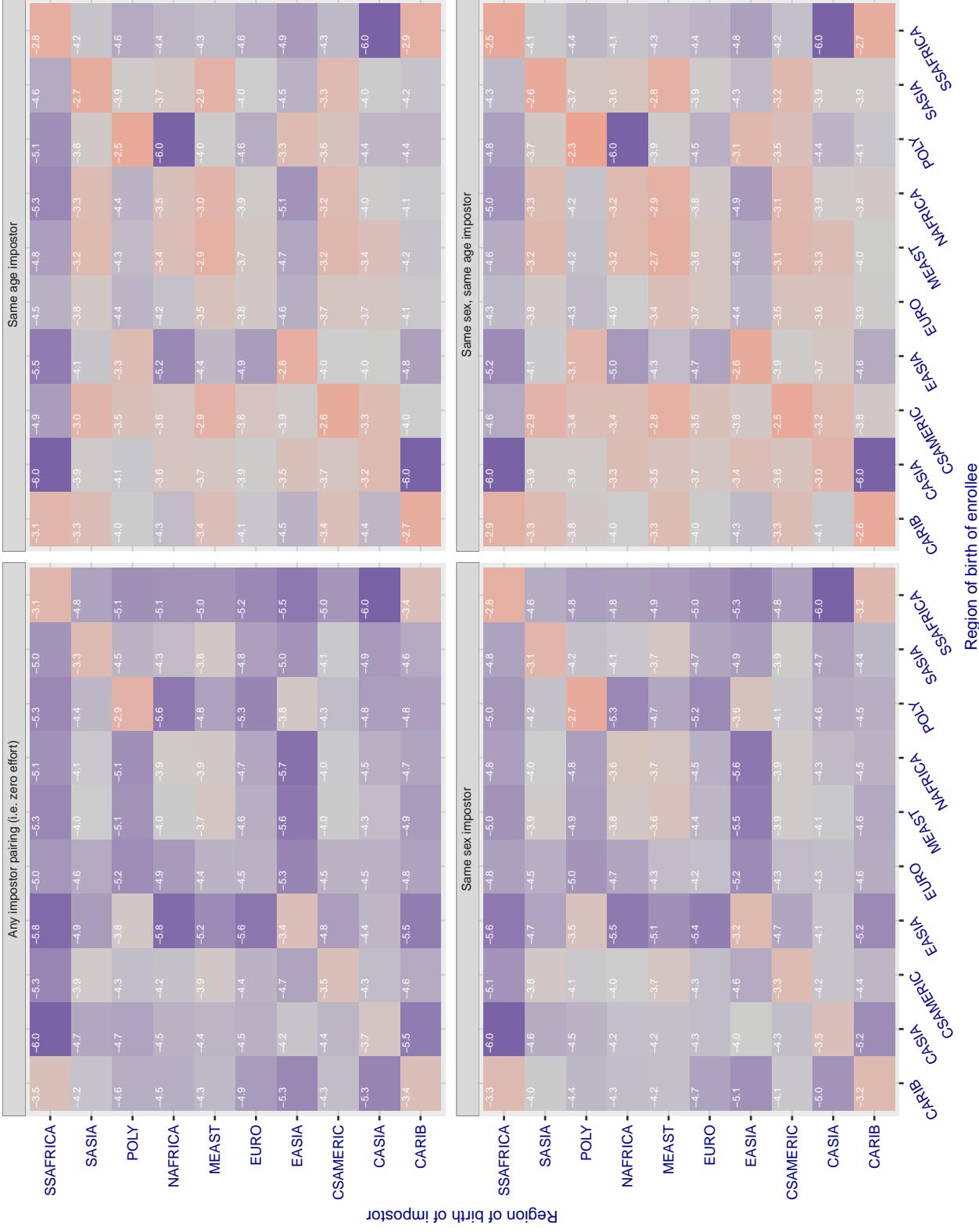
Cross region FMR at threshold T = 0.691 for algorithm iit_001, giving FMR(T) = 0.0001 globally.

Figure 185: For algorithm iit-001 operating on visa images, the heatmap shows false match rates observed over impostor comparisons of faces from different individuals who were born in the given region pair. False matches are counted against a recognition threshold fixed globally to give the target FMR in the plot title, computed over all on the order of 10^{10} impostor comparisons. If text appears in each box it give the same quantity as that coded by the color. Grey indicates FMR is at the intended FMR target level. Light red colors present a security vulnerability to, for example, a passport gate. Each +1 increase in $\log 10 \text{ FMR}$ corresponds to a factor of 10 increase in FMR. The matrix is not quite symmetric because images in the enrollment and verification sets are different.

Cross region FMR at threshold T = 0.926 for algorithm imagus_000, giving FMR(T) = 0.0001 globally.

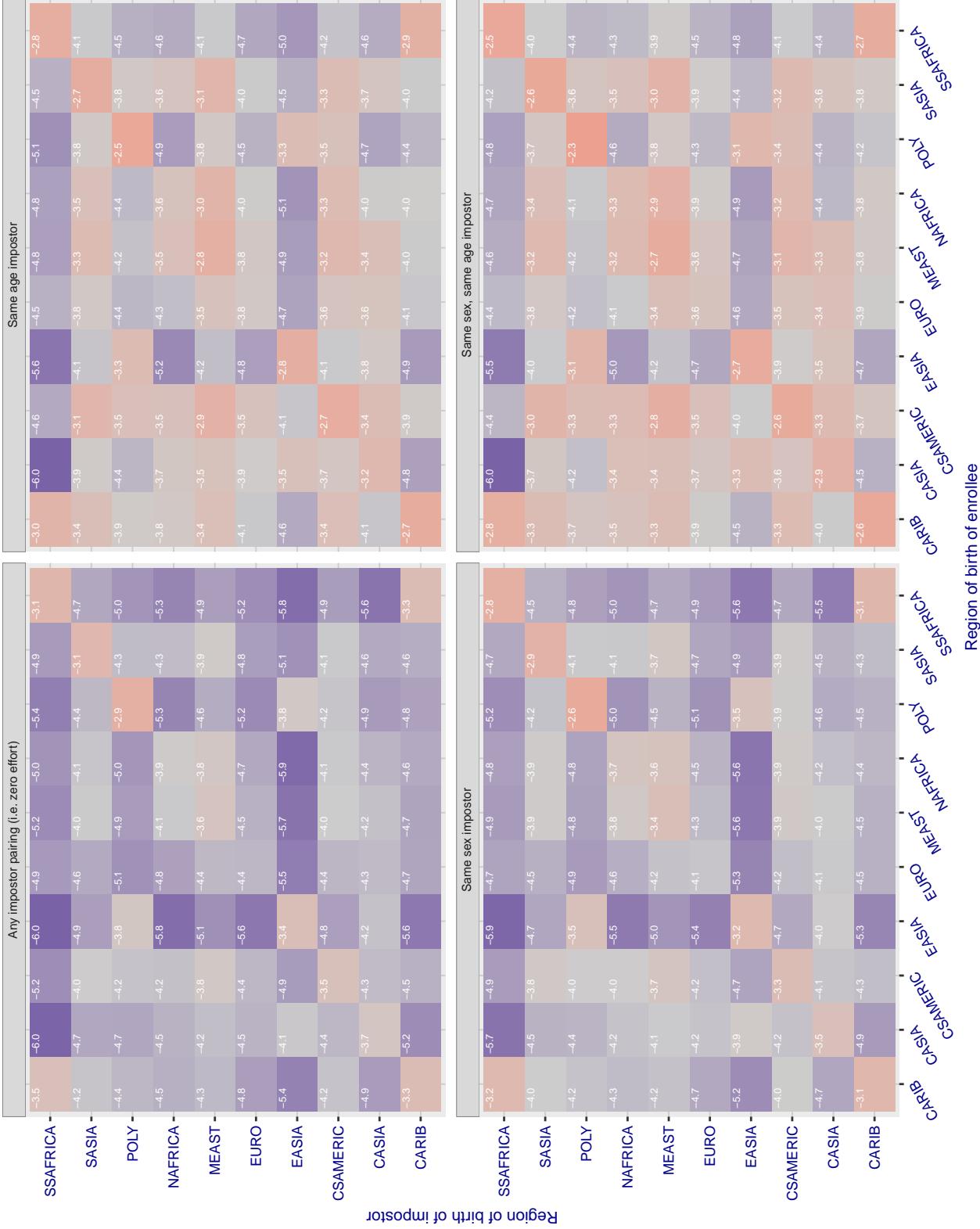


Figure 186: For algorithm imagus-000 operating on visa images, the heatmap shows false match rates observed over impostor comparisons of faces from different individuals who were born in the given region pair. False matches are counted against a recognition threshold fixed globally to give the target FMR in the plot title, computed over all on the order of 10^{10} impostor comparisons. If text appears in each box it give the same quantity as that coded by the color. Grey indicates FMR is at the intended FMR target level. Light red colors present a security vulnerability to, for example, a passport gate. Each +1 increase in $\log_{10} FMR$ corresponds to a factor of 10 increase in FMR. The matrix is not quite symmetric because images in the enrollment and verification sets are different.

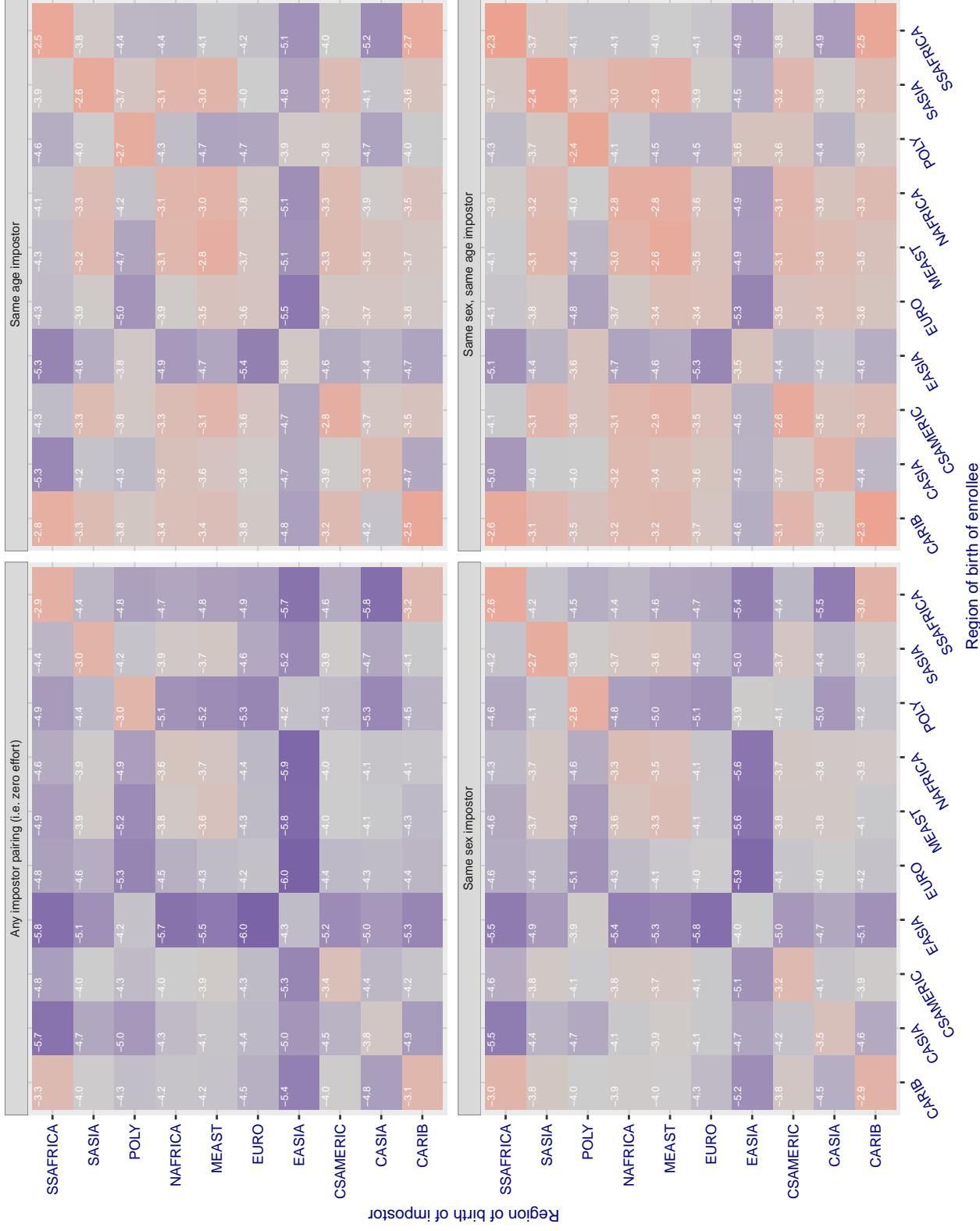
Cross region FMR at threshold T = 1.375 for algorithm imperial_000, giving FMR(T) = 0.0001 globally.

Figure 187: For algorithm imperial-000 operating on visa images, the heatmap shows false match rates observed over impostor comparisons of faces from different individuals who were born in the given region pair. False matches are counted against a recognition threshold fixed globally to give the target FMR in the plot title, computed over all on the order of 10^{10} impostor comparisons. If text appears in each box it give the same quantity as that coded by the color. Grey indicates FMR is at the intended FMR target level. Light red colors present a security vulnerability to, for example, a passport gate. Each +1 increase in $\log_{10} \text{FMR}$ corresponds to a factor of 10 increase in FMR. The matrix is not quite symmetric because images in the enrollment and verification sets are different.

Cross region FMR at threshold T = 1.358 for algorithm imperial_002, giving FMR(T) = 0.0001 globally.

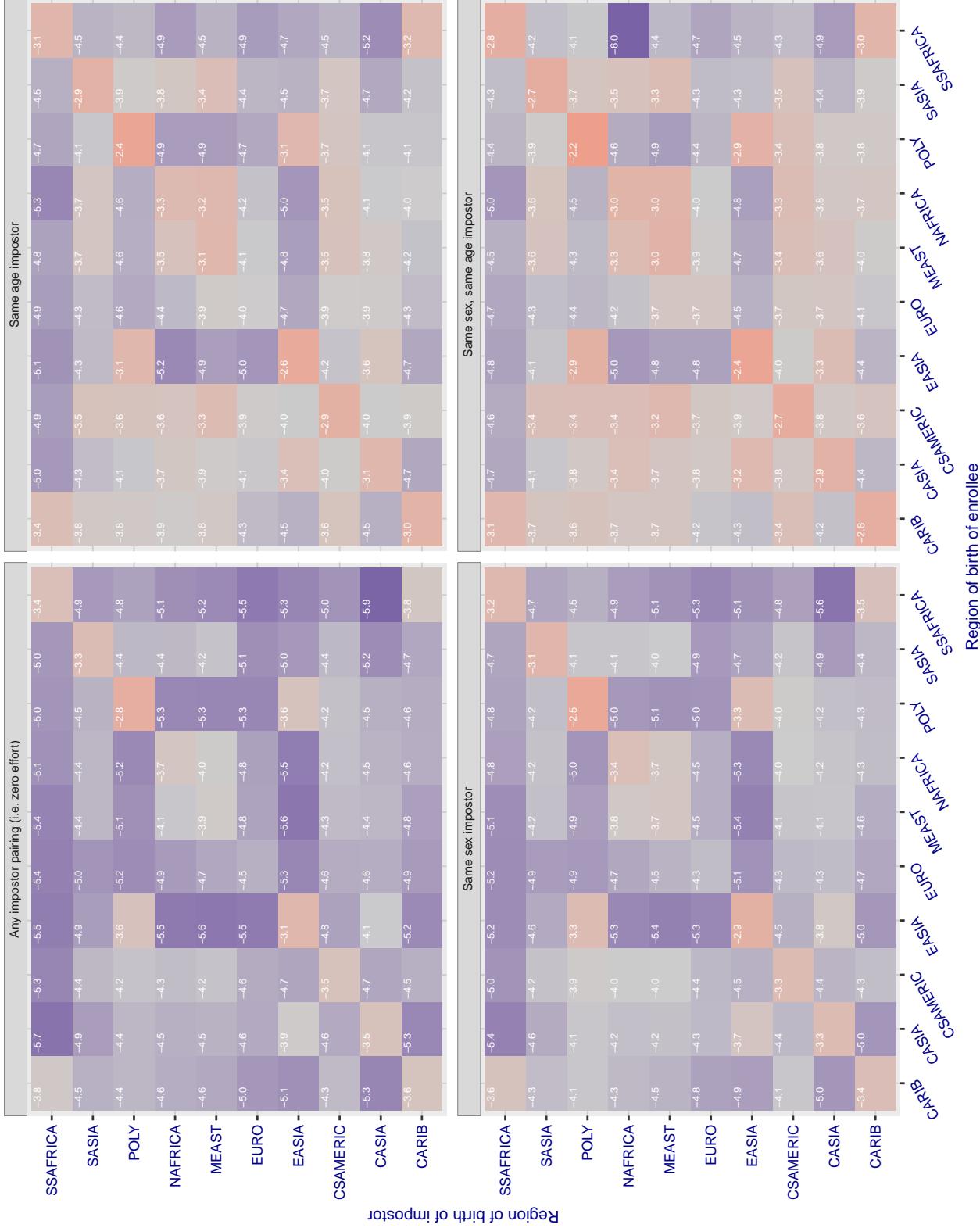


Figure 188: For algorithm imperial-002 operating on visa images, the heatmap shows false match rates observed over impostor comparisons of faces from different individuals who were born in the given region pair. False matches are counted against a recognition threshold fixed globally to give the target FMR in the plot title, computed over all on the order of 10^{10} impostor comparisons. If text appears in each box it give the same quantity as that coded by the color. Grey indicates FMR is at the intended FMR target level. Light red colors present a security vulnerability to, for example, a passport gate. Each +1 increase in $\log_{10} \text{FMR}$ corresponds to a factor of 10 increase in FMR. The matrix is not quite symmetric because images in the enrollment and verification sets are different.

Cross region FMR at threshold T = 1.427 for algorithm incode_003, giving $\text{FMR}(\text{T}) = 0.0001$ globally.

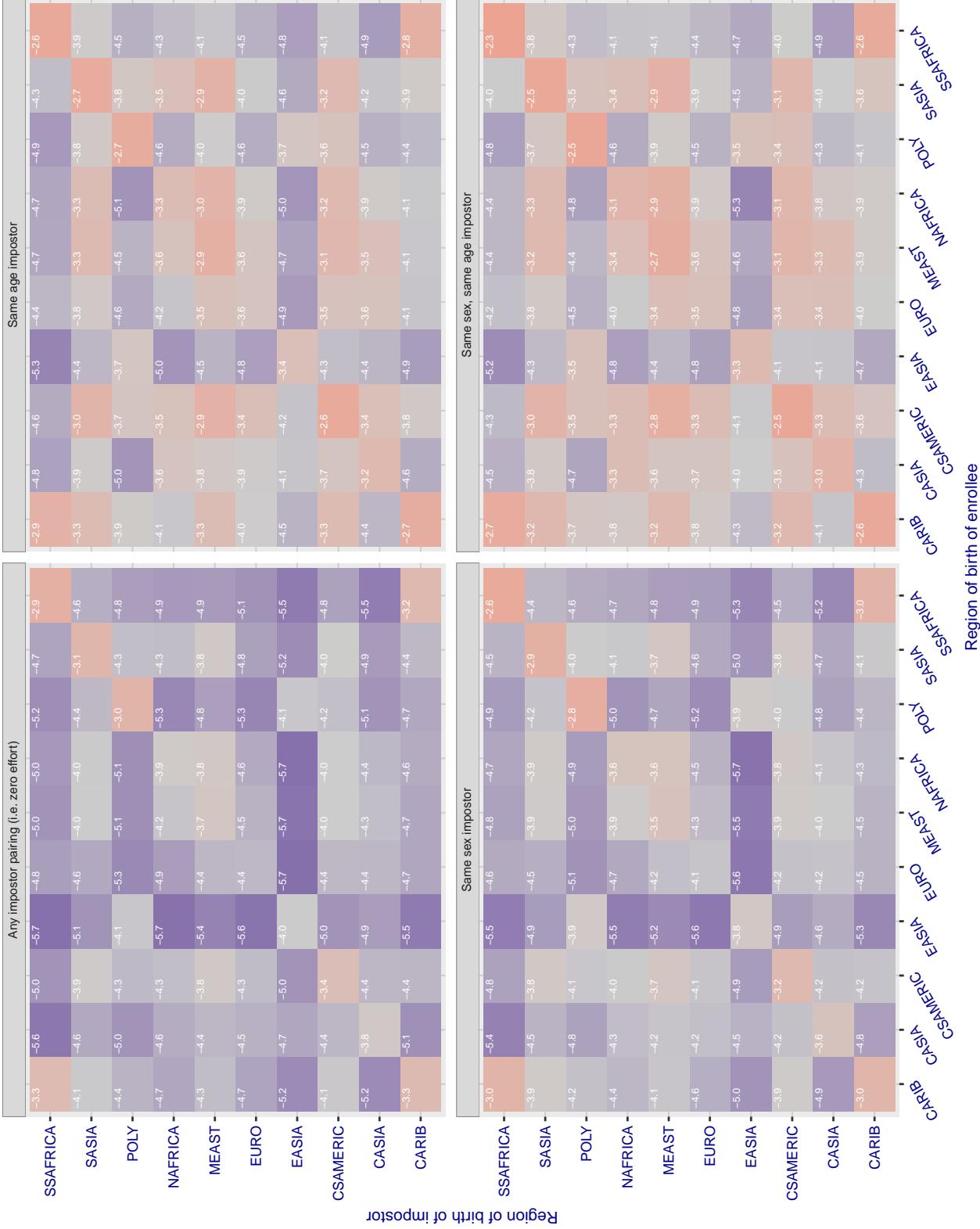


Figure 189: For algorithm incode-003 operating on visa images, the heatmap shows false match rates observed over impostor comparisons of faces from different individuals who were born in the given region pair. False matches are counted against a recognition threshold fixed globally to give the target FMR in the plot title, computed over all on the order of 10^{10} impostor comparisons. If text appears in each box it give the same quantity as that coded by the color. Grey indicates FMR is at the intended FMR target level. Light red colors present a security vulnerability to, for example, a passport gate. Each +1 increase in $\log_{10} \text{FMR}$ corresponds to a factor of 10 increase in FMR. The matrix is not quite symmetric because images in the enrollment and verification sets are different.

Cross region FMR at threshold T = 1.398 for algorithm incode_004, giving $\text{FMR}(\text{T}) = 0.0001$ globally.

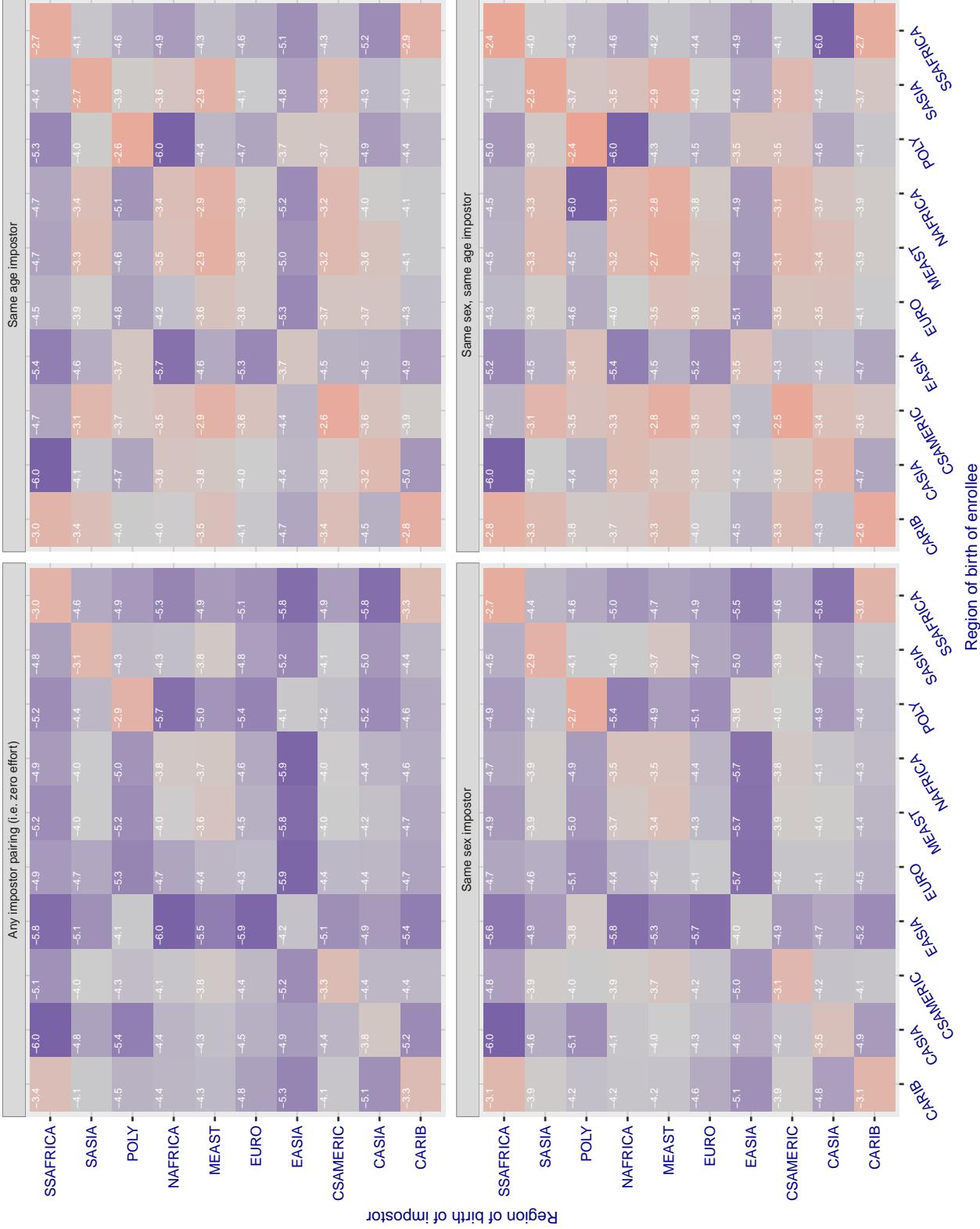


Figure 190: For algorithm incode-004 operating on visa images, the heatmap shows false match rates observed over impostor comparisons of faces from different individuals who were born in the given region pair. False matches are counted against a recognition threshold fixed globally to give the target FMR in the plot title, computed over all on the order of 10^{10} impostor comparisons. If text appears in each box it give the same quantity as that coded by the color. Grey indicates FMR is at the intended FMR target level. Light red colors present a security vulnerability to, for example, a passport gate. Each +1 increase in $\log_{10} \text{FMR}$ corresponds to a factor of 10 increase in FMR. The matrix is not quite symmetric because images in the enrollment and verification sets are different.

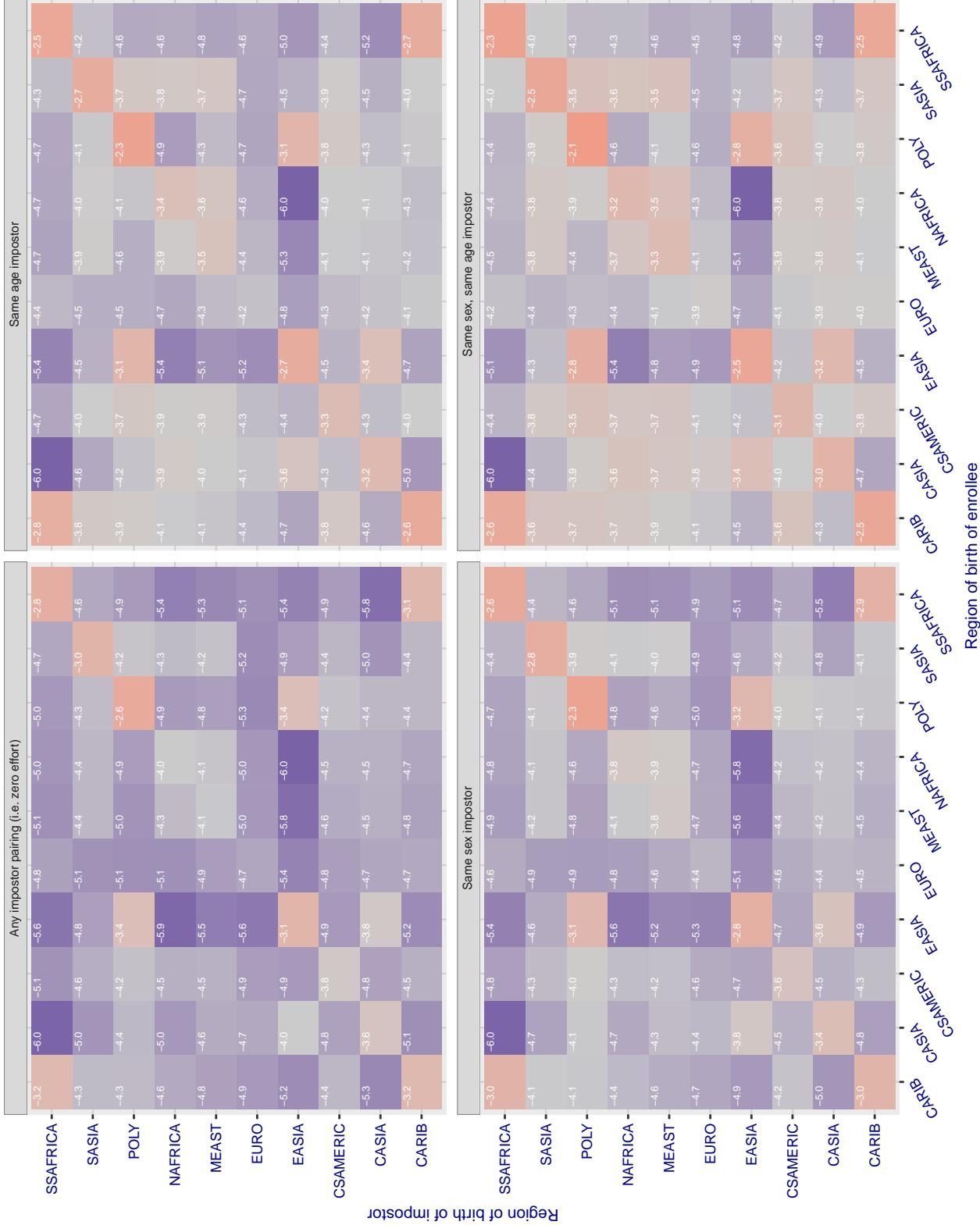
Cross region FMR at threshold T = 29.232 for algorithm innovatrics_004, giving FMR(T) = 0.0001 globally.

Figure 191: For algorithm innovatrics-004 operating on visa images, the heatmap shows false match rates observed over impostor comparisons of faces from different individuals who were born in the given region pair. False matches are counted against a recognition threshold fixed globally to give the target FMR in the plot title, computed over all on the order of 10^{10} impostor comparisons. If text appears in each box it give the same quantity as that coded by the color. Grey indicates FMR is at the intended FMR target level. Light red colors present a security vulnerability to, for example, a passport gate. Each +1 increase in $\log_{10} FMR$ corresponds to a factor of 10 increase in FMR. The matrix is not quite symmetric because images in the enrollment and verification sets are different.

Cross region FMR at threshold T = 27.987 for algorithm innovatrics_006, giving FMR(T) = 0.0001 globally.

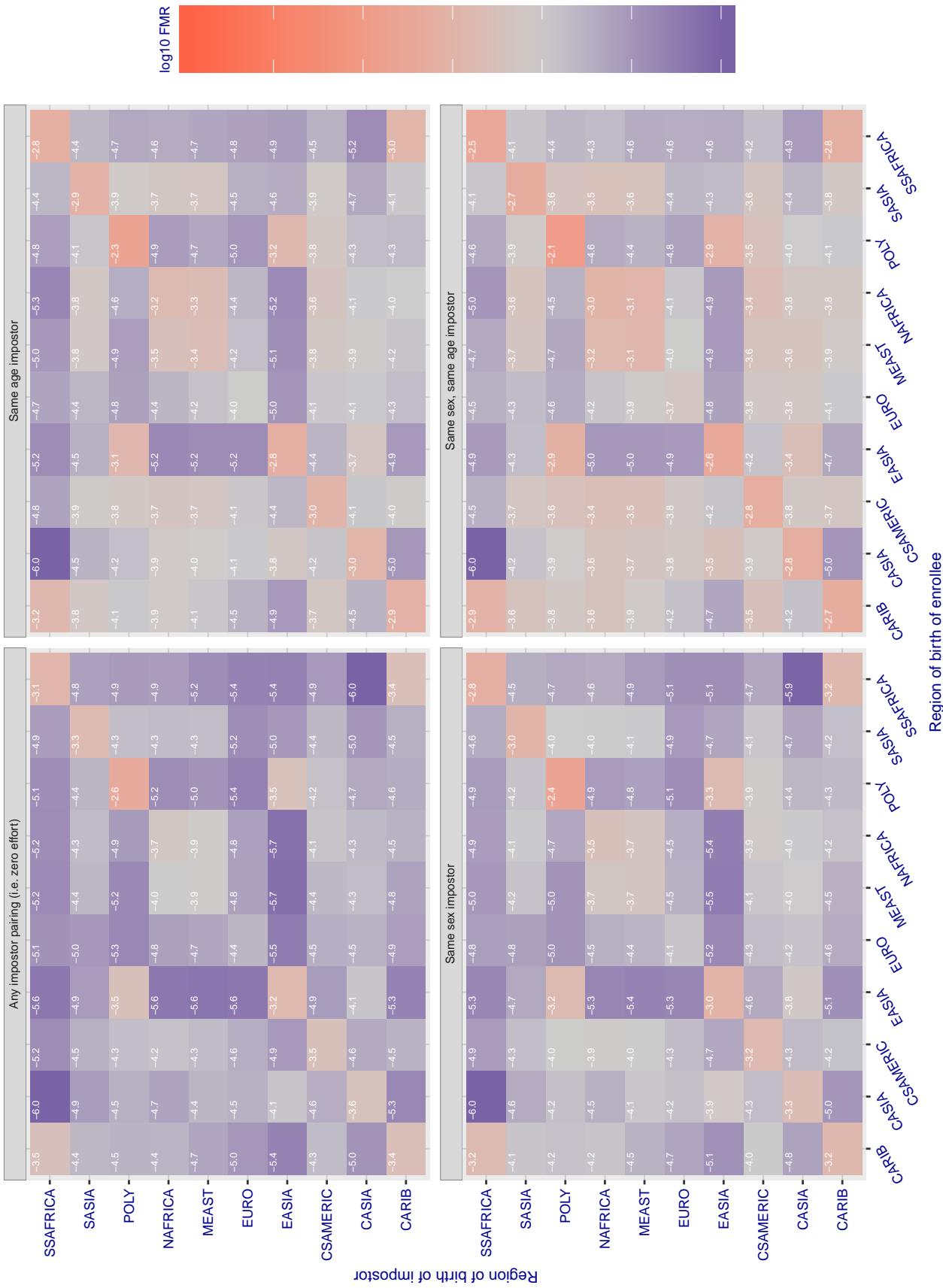


Figure 192: For algorithm innovatrics-006 operating on visa images, the heatmap shows false match rates observed over impostor comparisons of faces from different individuals who were born in the given region pair. False matches are counted against a recognition threshold fixed globally to give the target FMR in the plot title, computed over all on the order of 10^{10} impostor comparisons. If text appears in each box it give the same quantity as that coded by the color. Grey indicates FMR is at the intended FMR target level. Light red colors present a security vulnerability to, for example, a passport gate. Each +1 increase in $\log_{10} FMR$ corresponds to a factor of 10 increase in FMR. The matrix is not quite symmetric because images in the enrollment and verification sets are different.

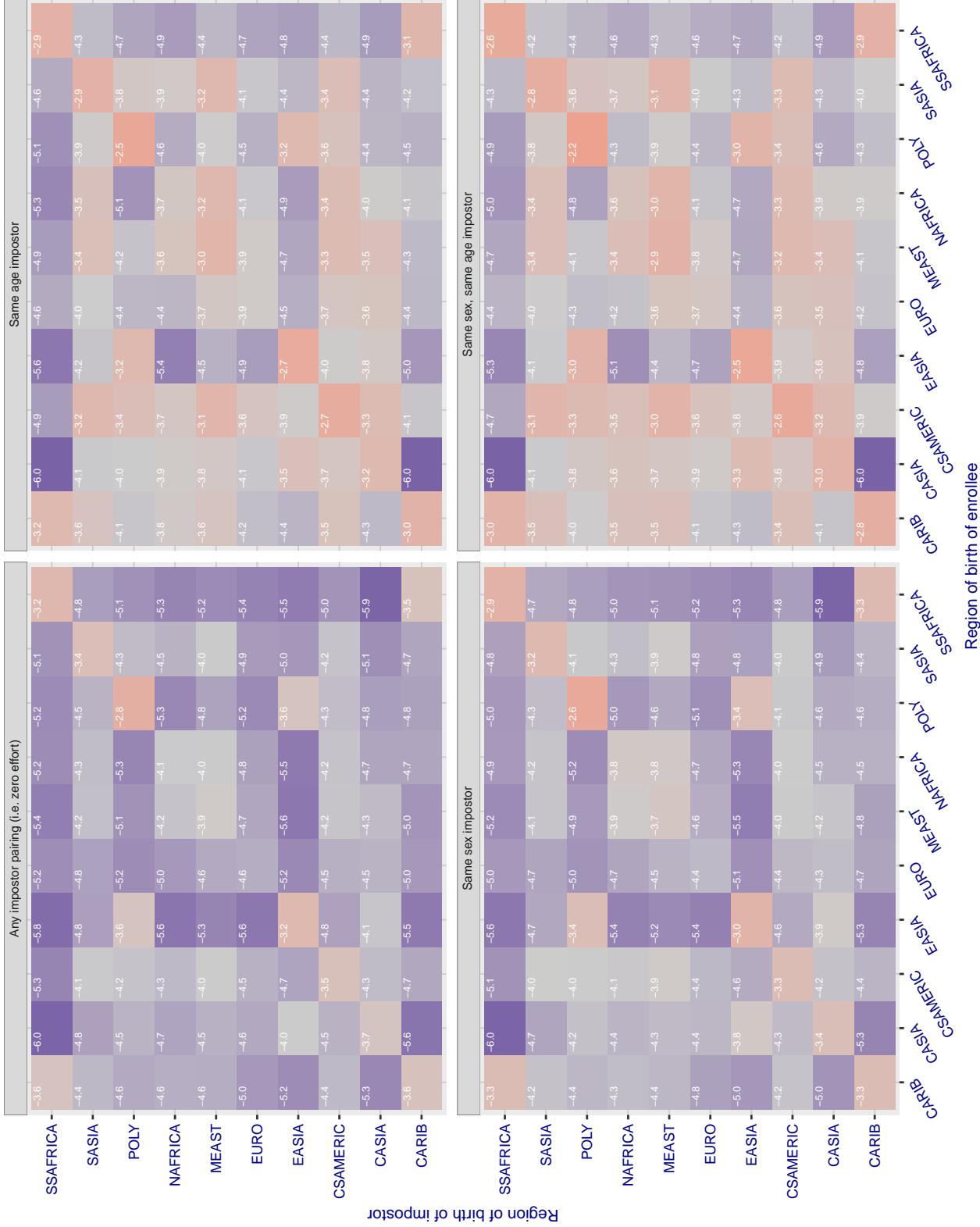
Cross region FMR at threshold T = 0.705 for algorithm intellicloudai_001, giving FMR(T) = 0.00001 globally.

Figure 193: For algorithm intellicloudai-001 operating on visa images, the heatmap shows false match rates observed over impostor comparisons of faces from different individuals who were born in the given region pair. False matches are counted against a recognition threshold fixed globally to give the target FMR in the plot title, computed over all on the order of 10^{10} impostor comparisons. If text appears in each box it give the same quantity as that coded by the color. Grey indicates FMR is at the intended FMR target level. Light red colors present a security vulnerability to, for example, a passport gate. Each +1 increase in $\log_{10} \text{FMR}$ corresponds to a factor of 10 increase in FMR. The matrix is not quite symmetric because images in the enrollment and verification sets are different.

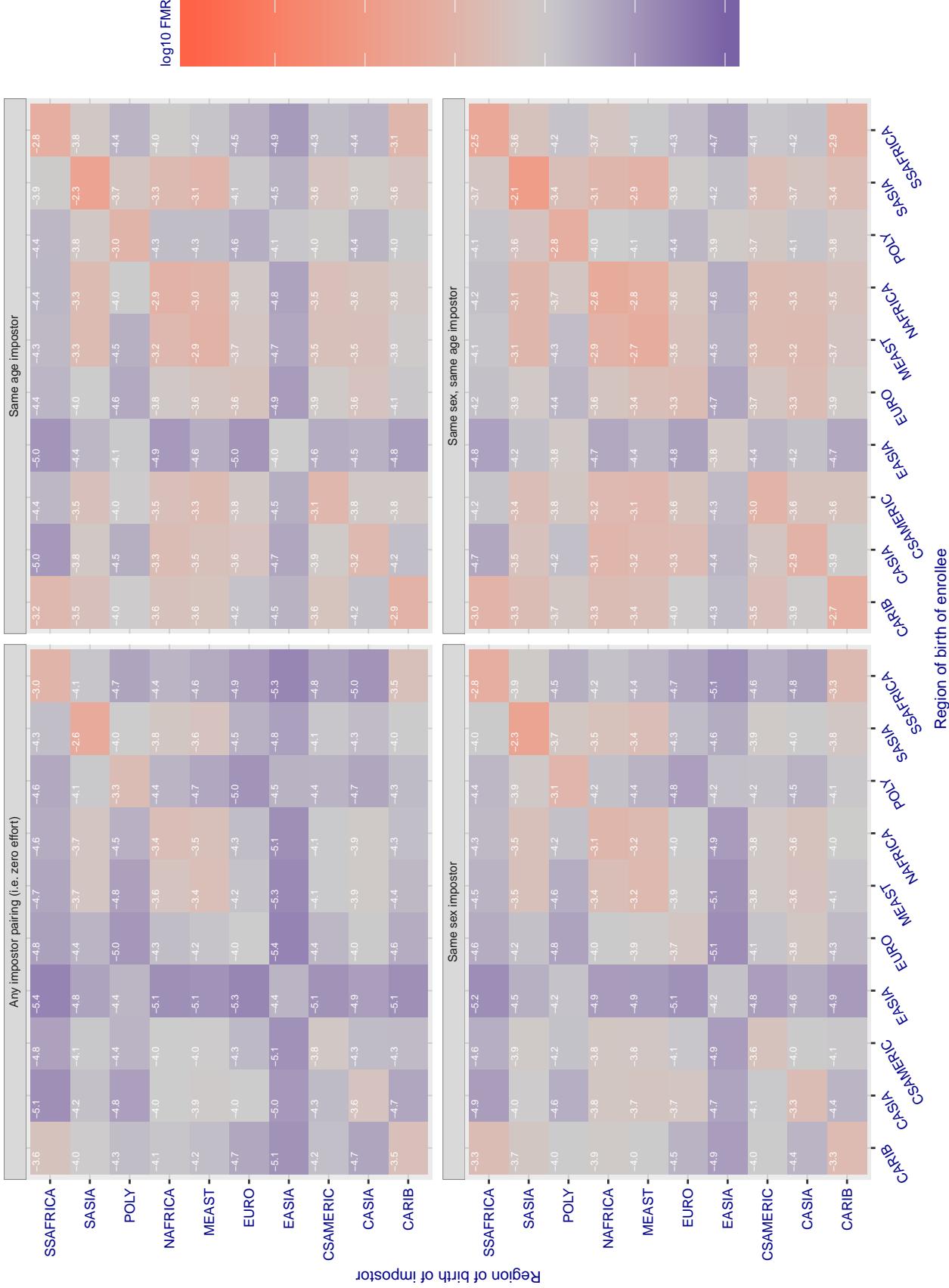
Cross region FMR at threshold T = 0.300 for algorithm intellifusion_001, giving FMR(T) = 0.00001 globally.

Figure 194: For algorithm intellifusion-001 operating on visa images, the heatmap shows false match rates observed over impostor comparisons of faces from different individuals who were born in the given region pair. False matches are counted against a recognition threshold fixed globally to give the target FMR in the plot title, computed over all on the order of 10^{10} impostor comparisons. If text appears in each box it give the same quantity as that coded by the color. Grey indicates FMR is at the intended FMR target level. Light red colors present a security vulnerability to, for example, a passport gate. Each +1 increase in $\log_{10} \text{FMR}$ corresponds to a factor of 10 increase in FMR. The matrix is not quite symmetric because images in the enrollment and verification sets are different.

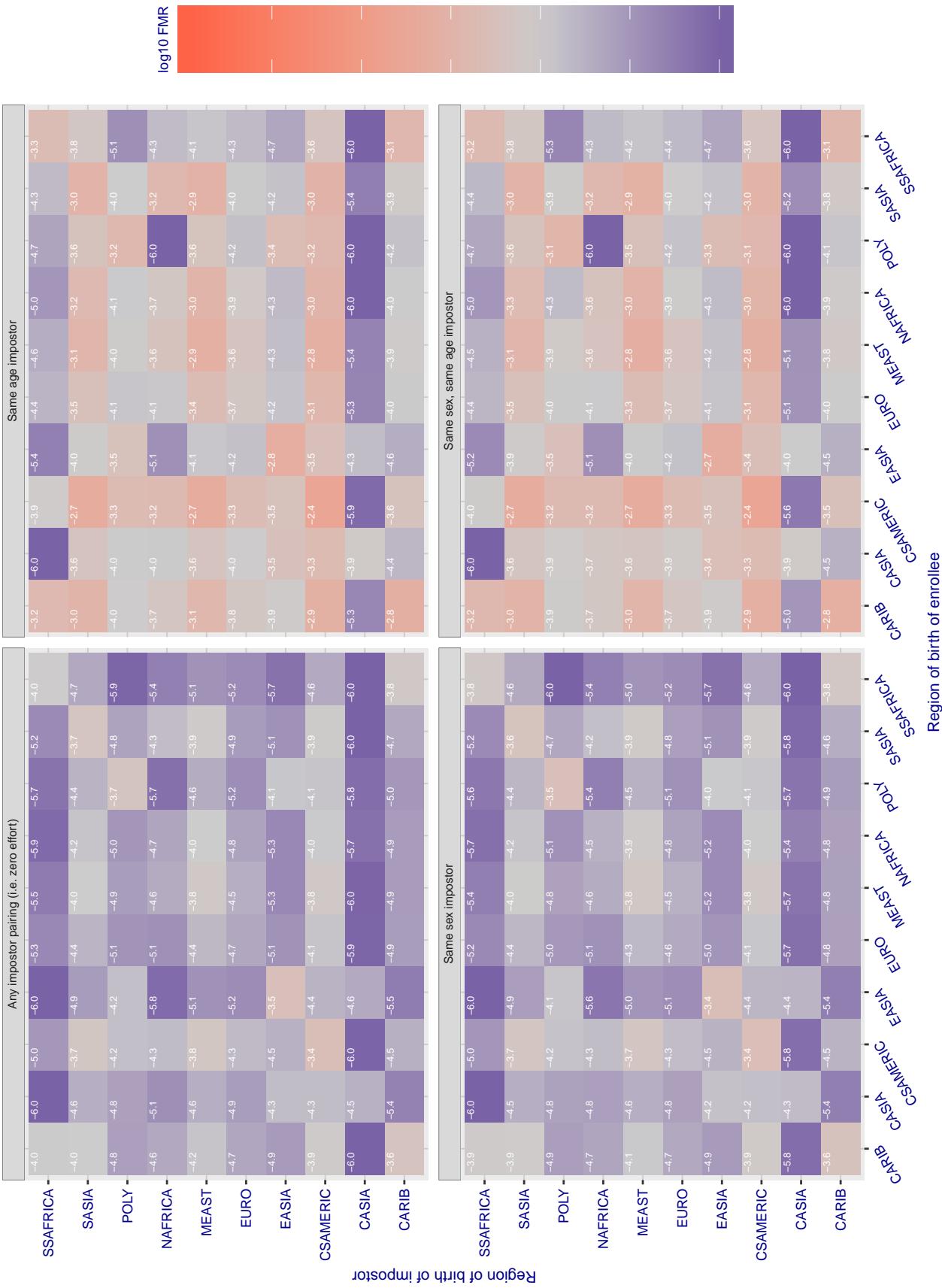
Cross region FMR at threshold T = 49.664 for algorithm intellivision_001, giving FMR(T) = 0.0001 globally.

Figure 195: For algorithm intellivision-001 operating on visa images, the heatmap shows false match rates observed over impostor comparisons of faces from different individuals who were born in the given region pair. False matches are counted against a recognition threshold fixed globally to give the target FMR in the plot title, computed over all on the order of 10^{10} impostor comparisons. If text appears in each box it give the same quantity as that coded by the color. Grey indicates FMR is at the intended FMR target level. Light red colors present a security vulnerability to, for example, a passport gate. Each +1 increase in $\log_{10} FMR$ corresponds to a factor of 10 increase in FMR. The matrix is not quite symmetric because images in the enrollment and verification sets are different.

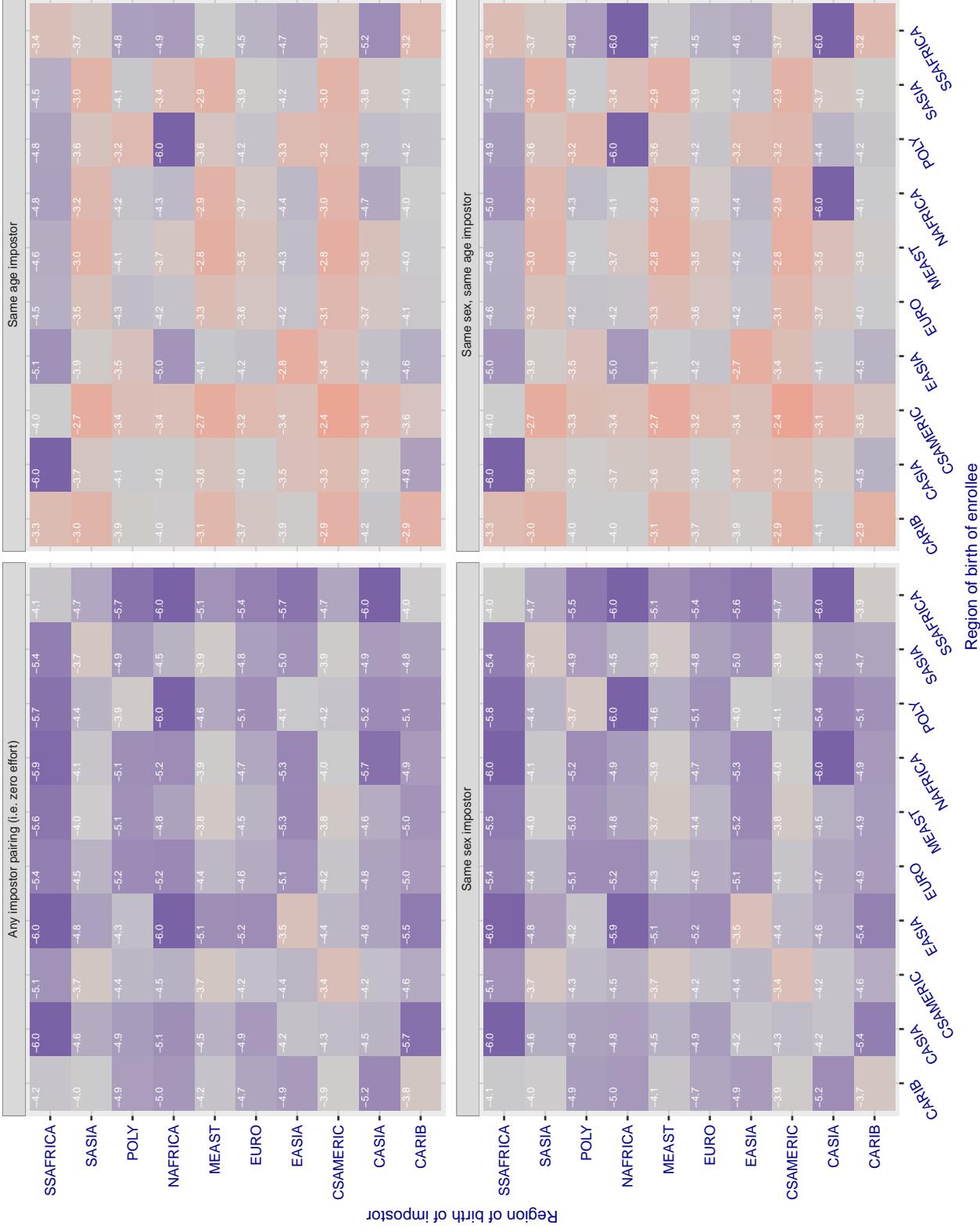
Cross region FMR at threshold T = 44.160 for algorithm intellivision_002, giving FMR(T) = 0.0001 globally.

Figure 196: For algorithm intellivision-002 operating on visa images, the heatmap shows false match rates observed over impostor comparisons of faces from different individuals who were born in the given region pair. False matches are counted against a recognition threshold fixed globally to give the target FMR in the plot title, computed over all on the order of 10^{10} impostor comparisons. If text appears in each box it give the same quantity as that coded by the color. Grey indicates FMR is at the intended FMR target level. Light red colors present a security vulnerability to, for example, a passport gate. Each +1 increase in $\log_{10} FMR$ corresponds to a factor of 10 increase in FMR. The matrix is not quite symmetric because images in the enrollment and verification sets are different.

Cross region FMR at threshold T = 594.014 for algorithm intelresearch_000, giving FMR(T) = 0.0001 globally.

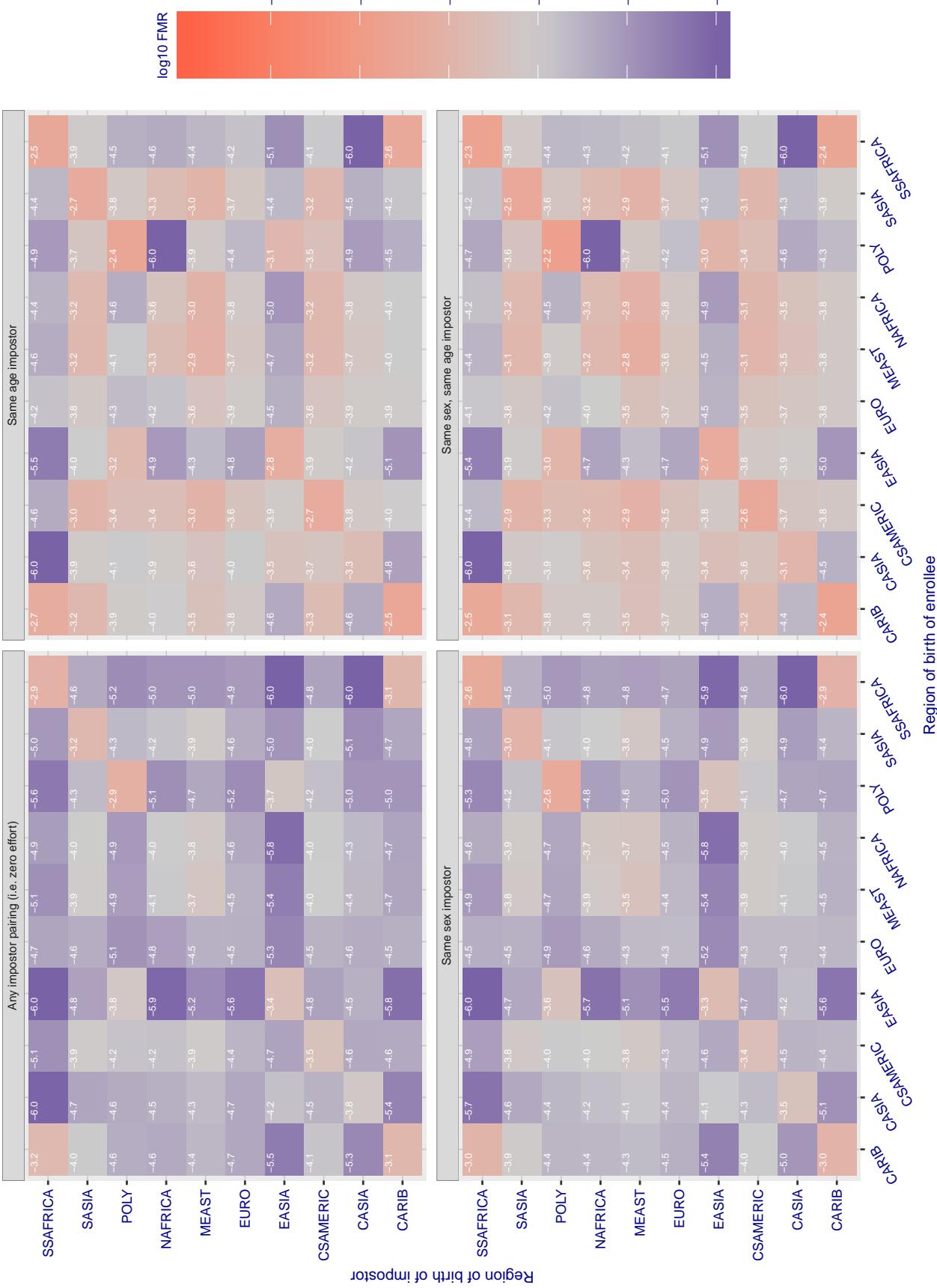


Figure 197: For algorithm intelresearch-000 operating on visa images, the heatmap shows false match rates observed over impostor comparisons of faces from different individuals who were born in the given region pair. False matches are counted against a recognition threshold fixed globally to give the target FMR in the plot title, computed over all on the order of 10^{10} impostor comparisons. If text appears in each box it give the same quantity as that coded by the color. Grey indicates FMR is at the intended FMR target level. Light red colors present a security vulnerability to, for example, a passport gate. Each +1 increase in $\log_{10} FMR$ corresponds to a factor of 10 increase in FMR . The matrix is not quite symmetric because images in the enrollment and verification sets are different.

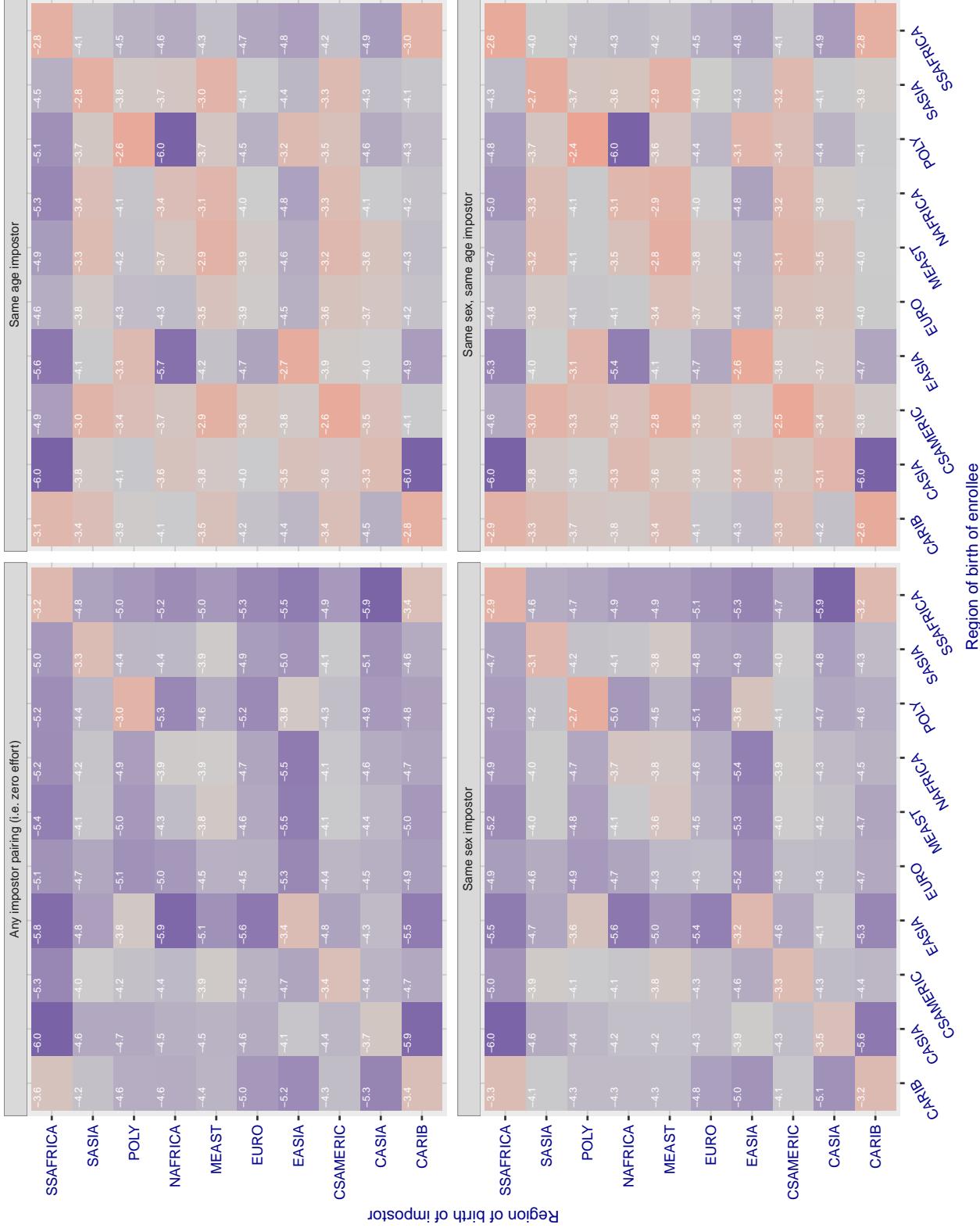
Cross region FMR at threshold T = 1.389 for algorithm intsysmsu_000, giving FMR(T) = 0.0001 globally.

Figure 198: For algorithm intsysmsu-000 operating on visa images, the heatmap shows false match rates observed over impostor comparisons of faces from different individuals who were born in the given region pair. False matches are counted against a recognition threshold fixed globally to give the target FMR in the plot title, computed over all on the order of 10^{10} impostor comparisons. If text appears in each box it give the same quantity as that coded by the color. Grey indicates FMR is at the intended FMR target level. Light red colors present a security vulnerability to, for example, a passport gate. Each +1 increase in $\log_{10} FMR$ corresponds to a factor of 10 increase in FMR. The matrix is not quite symmetric because images in the enrollment and verification sets are different.

Cross region FMR at threshold T = 1.361 for algorithm iiface_000, giving FMR(T) = 0.0001 globally.

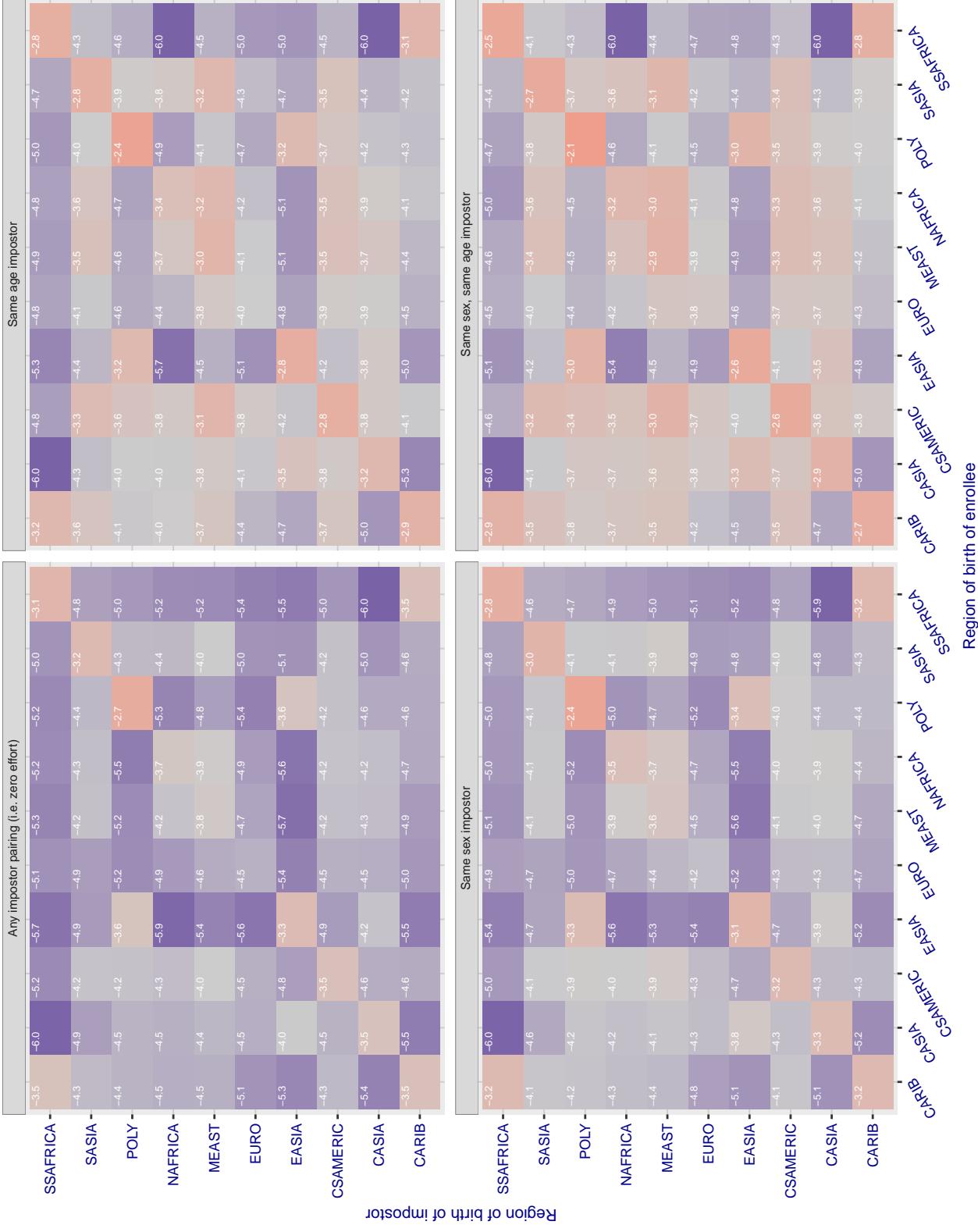


Figure 199: For algorithm iiface-000 operating on visa images, the heatmap shows false match rates observed over impostor comparisons of faces from different individuals who were born in the given region pair. False matches are counted against a recognition threshold fixed globally to give the target FMR in the plot title, computed over all on the order of 10^{10} impostor comparisons. If text appears in each box it give the same quantity as that coded by the color. Grey indicates FMR is at the intended FMR target level. Light red colors present a security vulnerability to, for example, a passport gate. Each +1 increase in $\log_{10} \text{FMR}$ corresponds to a factor of 10 increase in FMR. The matrix is not quite symmetric because images in the enrollment and verification sets are different.

Cross region FMR at threshold T = 0.985 for algorithm isap_001, giving FMR(T) = 0.0001 globally.

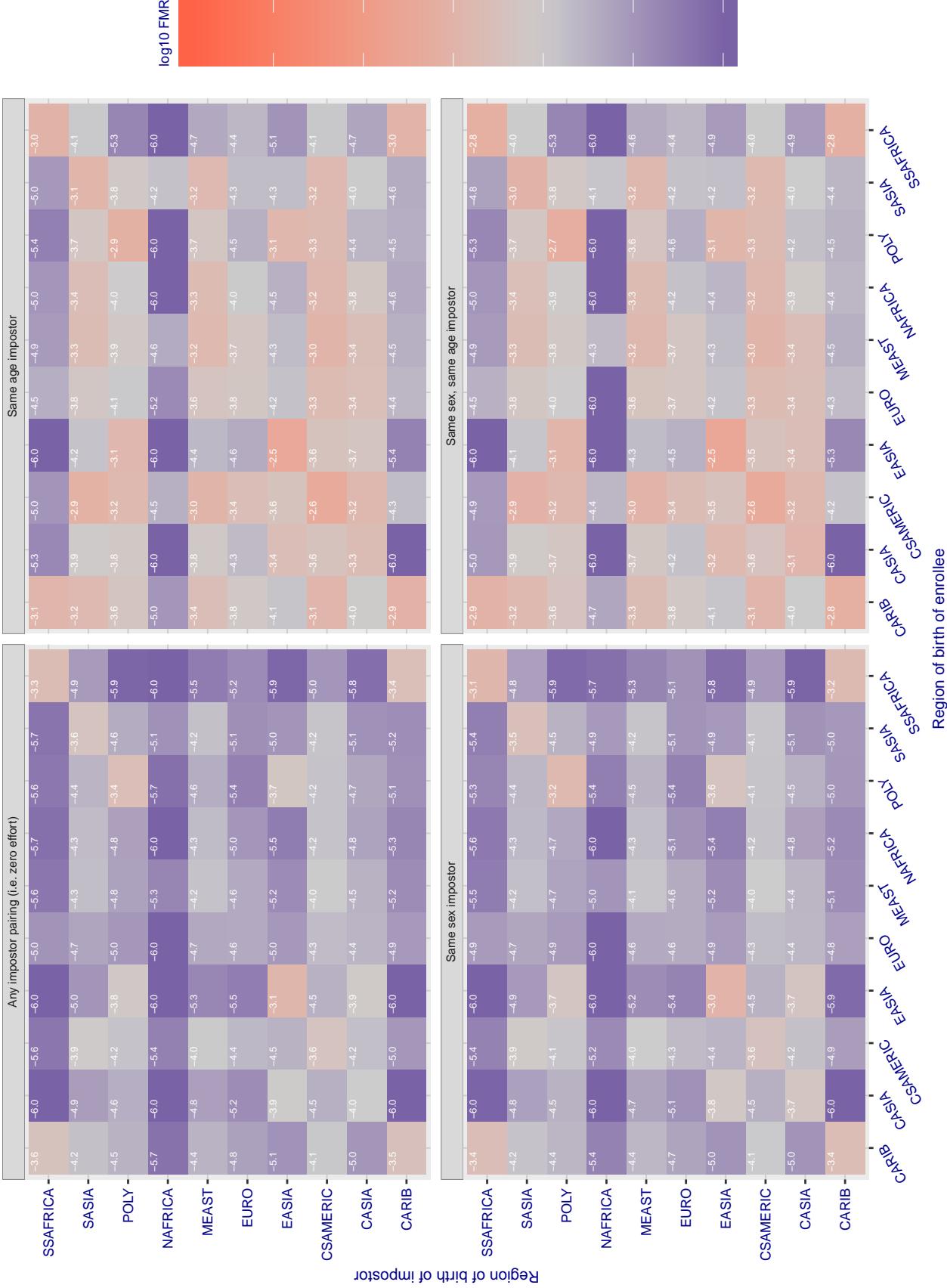


Figure 20: For algorithm isap-001 operating on visa images, the heatmap shows false match rates observed over impostor comparisons of faces from different individuals who were born in the given region pair. False matches are counted against a recognition threshold fixed globally to give the target FMR in the plot title, computed over all on the order of 10^{10} impostor comparisons. If text appears in each box it give the same quantity as that coded by the color. Grey indicates FMR is at the intended FMR target level. Light red colors present a security vulnerability to, for example, a passport gate. Each +1 increase in $\log 10$ FMR corresponds to a factor of 10 increase in FMR. The matrix is not quite symmetric because images in the enrollment and verification sets are different.

Cross region FMR at threshold T = 23.498 for algorithm isityou_000, giving FMR(T) = 0.0001 globally.

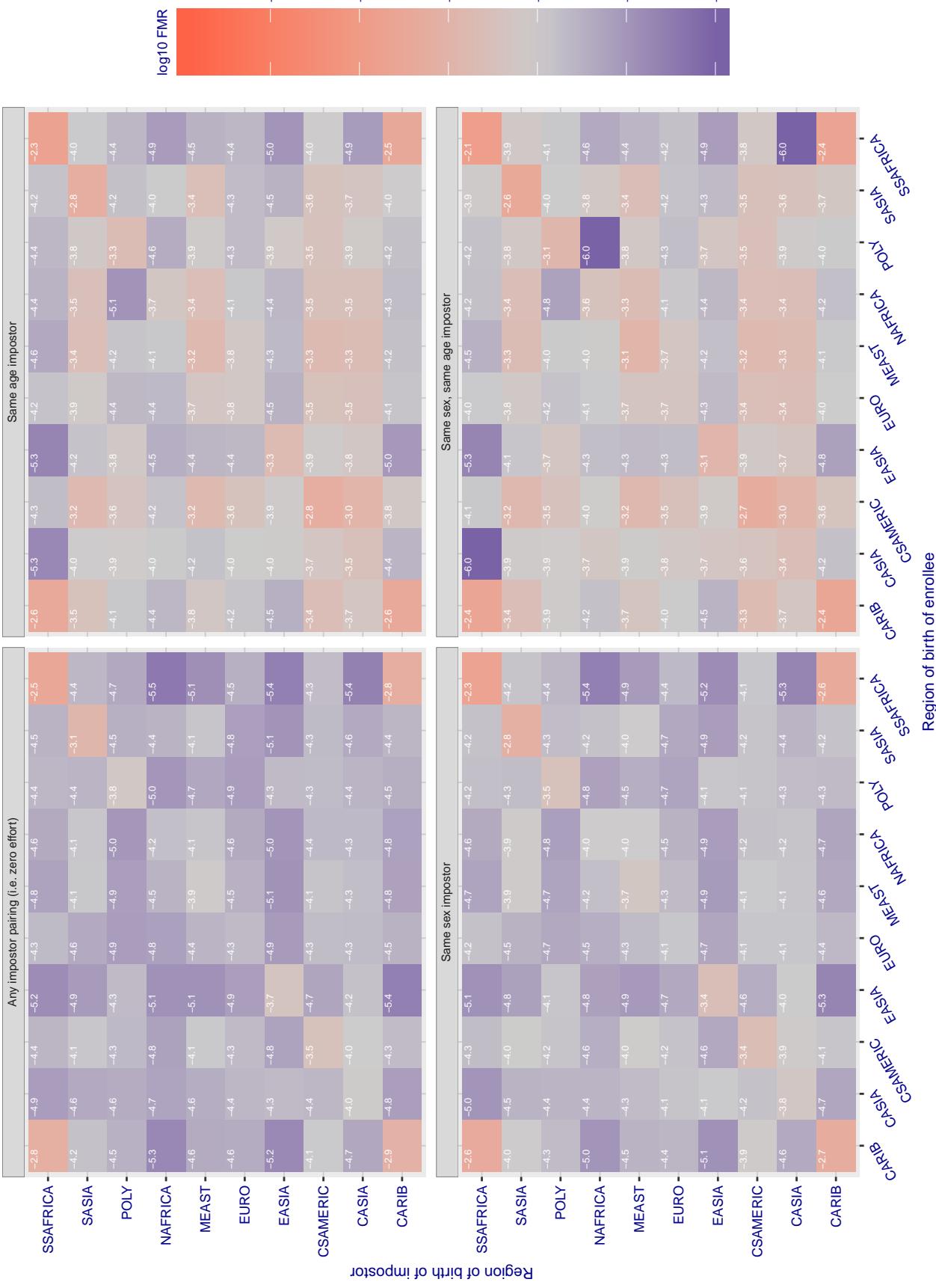


Figure 201: For algorithm isityou-000 operating on visa images, the heatmap shows false match rates observed over impostor comparisons of faces from different individuals who were born in the given region pair. False matches are counted against a recognition threshold fixed globally to give the target FMR in the plot title, computed over all on the order of 10^{10} impostor comparisons. If text appears in each box it give the same quantity as that coded by the color. Grey indicates FMR is at the intended FMR target level. Light red colors present a security vulnerability to, for example, a passport gate. Each +1 increase in $\log_{10} FMR$ corresponds to a factor of 10 increase in FMR. The matrix is not quite symmetric because images in the enrollment and verification sets are different.

Cross region FMR at threshold T = 0.693 for algorithm isystems_001, giving FMR(T) = 0.0001 globally.

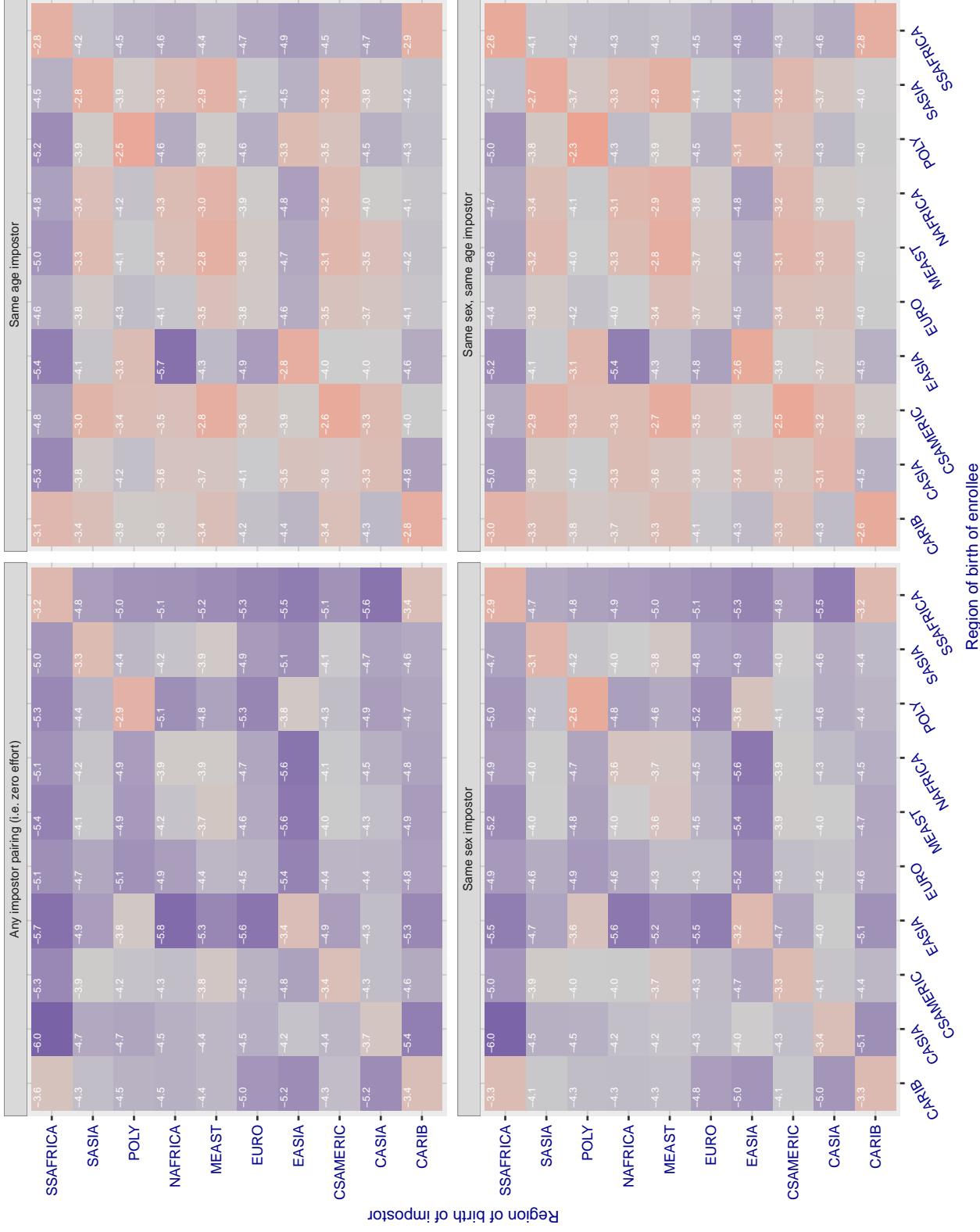


Figure 202: For algorithm isystems-001 operating on visa images, the heatmap shows false match rates observed over impostor comparisons of faces from different individuals who were born in the given region pair. False matches are counted against a recognition threshold fixed globally to give the target FMR in the plot title, computed over all on the order of 10^{10} impostor comparisons. If text appears in each box it give the same quantity as that coded by the color. Grey indicates FMR is at the intended FMR target level. Light red colors present a security vulnerability to, for example, a passport gate. Each +1 increase in $\log_{10} \text{FMR}$ corresponds to a factor of 10 increase in FMR. The matrix is not quite symmetric because images in the enrollment and verification sets are different.

Cross region FMR at threshold T = 0.690 for algorithm isystems_002, giving FMR(T) = 0.0001 globally.

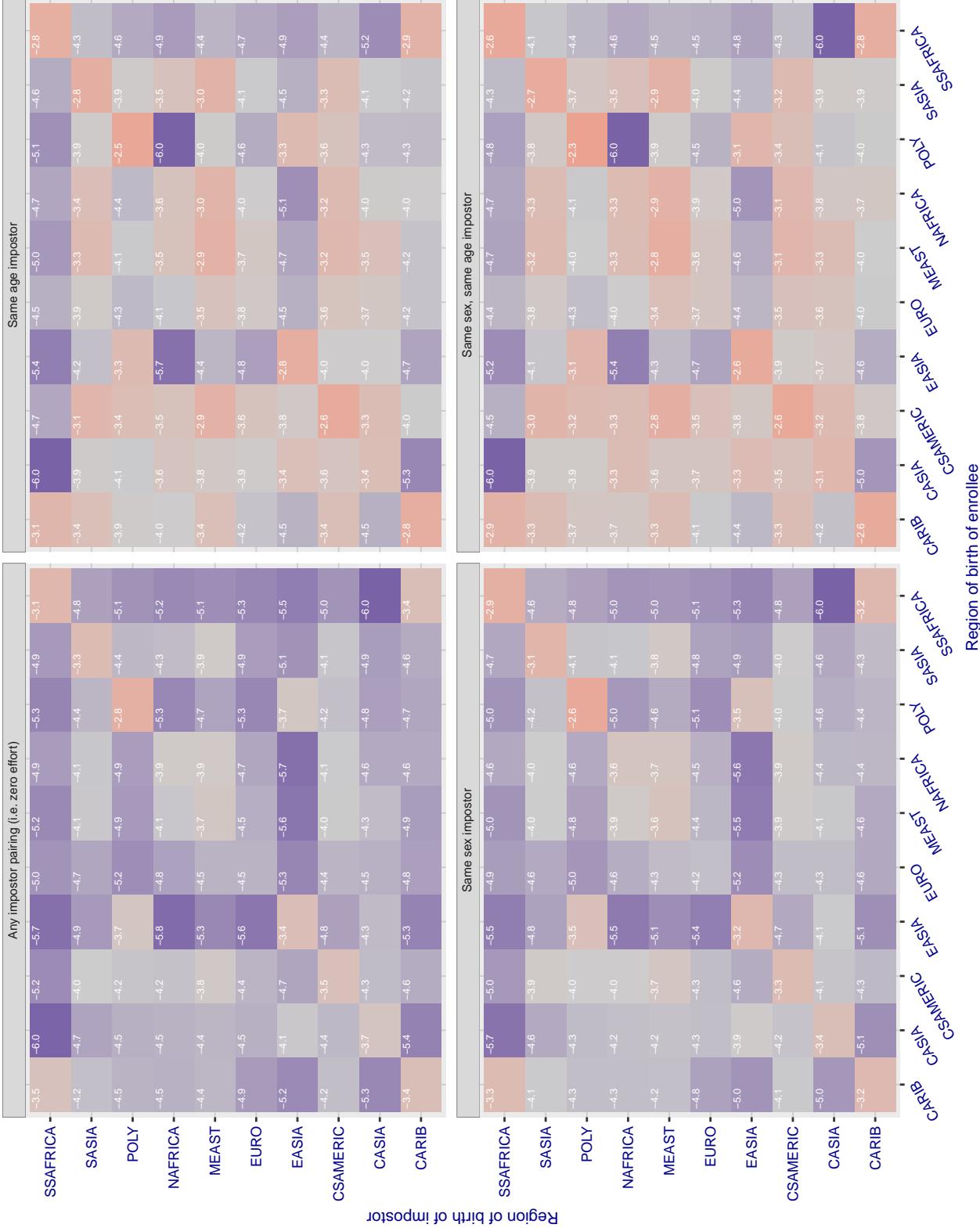


Figure 203: For algorithm isystems-002 operating on visa images, the heatmap shows false match rates observed over impostor comparisons of faces from different individuals who were born in the given region pair. False matches are counted against a recognition threshold fixed globally to give the target FMR in the plot title, computed over all on the order of 10^{10} impostor comparisons. If text appears in each box it give the same quantity as that coded by the color. Grey indicates FMR is at the intended FMR target level. Light red colors present a security vulnerability to, for example, a passport gate. Each +1 increase in $\log_{10} \text{FMR}$ corresponds to a factor of 10 increase in FMR. The matrix is not quite symmetric because images in the enrollment and verification sets are different.

Cross region FMR at threshold T = 49.879 for algorithm itmo_005, giving FMR(T) = 0.0001 globally.

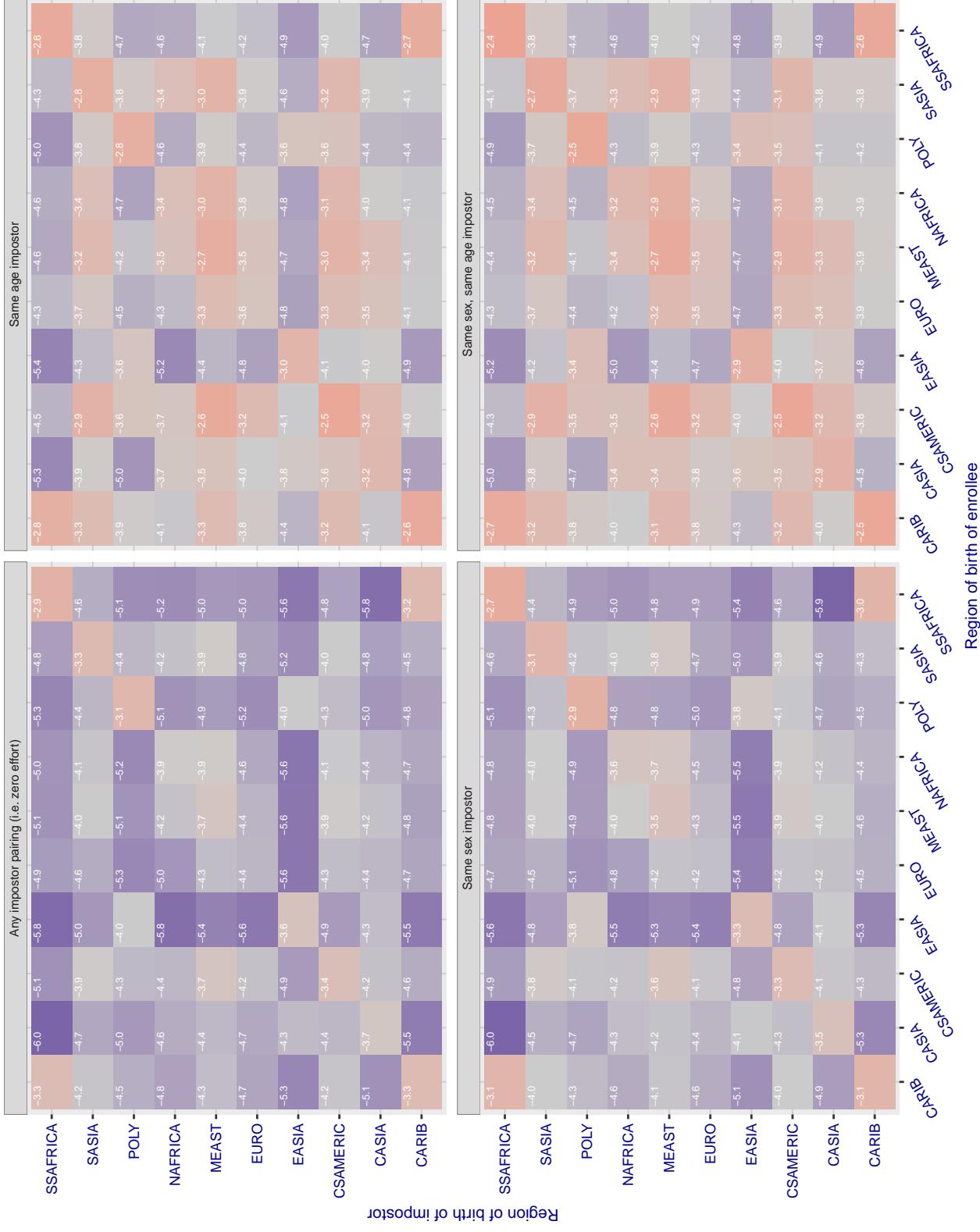


Figure 204: For algorithm itmo-005 operating on visa images, the heatmap shows false match rates observed over impostor comparisons of faces from different individuals who were born in the given region pair. False matches are counted against a recognition threshold fixed globally to give the target FMR in the plot title, computed over all on the order of 10^{10} impostor comparisons. If text appears in each box it give the same quantity as that coded by the color. Grey indicates FMR is at the intended FMR target level. Light red colors present a security vulnerability to, for example, a passport gate. Each +1 increase in $\log 10$ FMR corresponds to a factor of 10 increase in FMR. The matrix is not quite symmetric because images in the enrollment and verification sets are different.

Cross region FMR at threshold T = 49.789 for algorithm itmo_006, giving FMR(T) = 0.0001 globally.

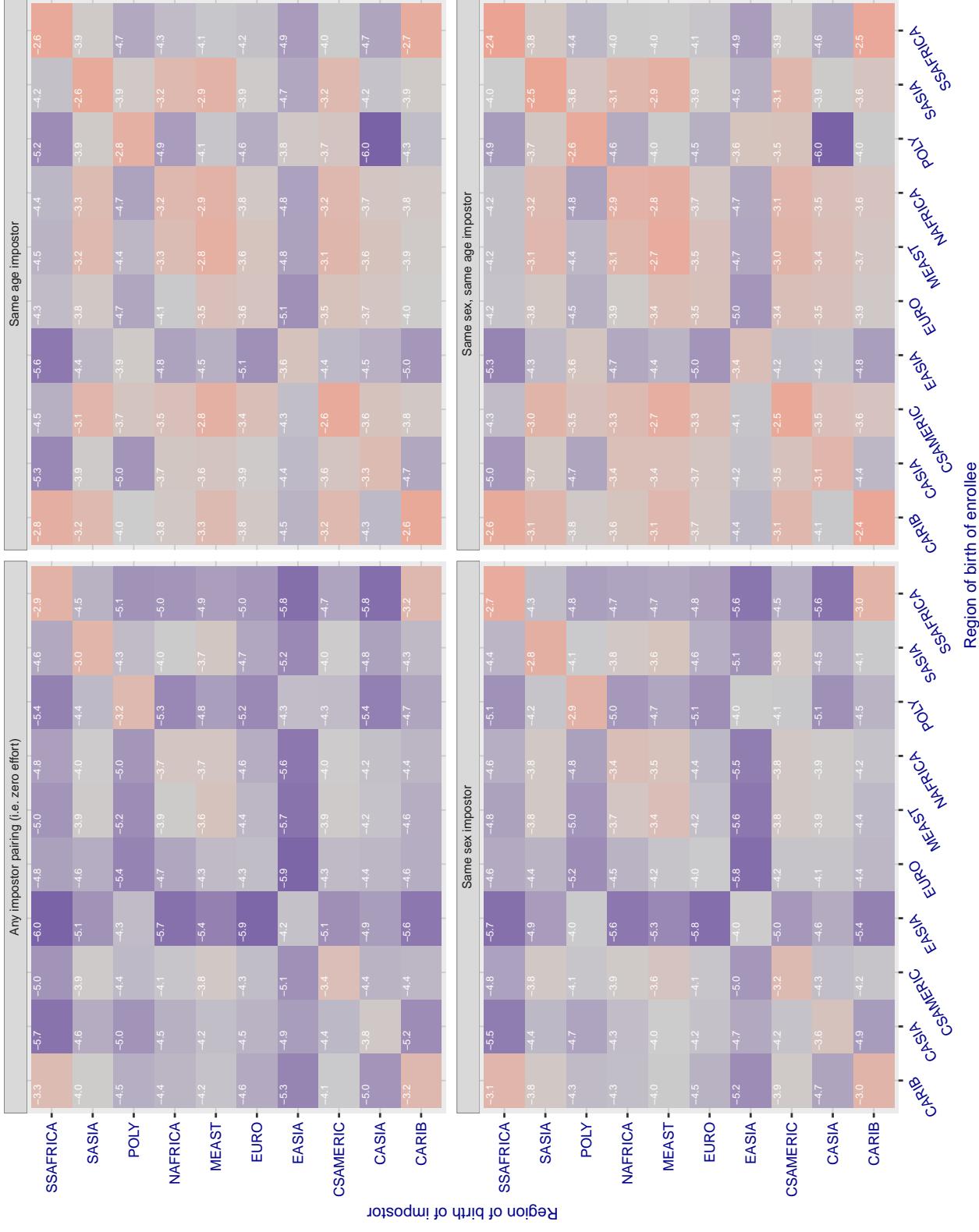


Figure 205: For algorithm itmo-006 operating on visa images, the heatmap shows false match rates observed over impostor comparisons of faces from different individuals who were born in the given region pair. False matches are counted against a recognition threshold fixed globally to give the target FMR in the plot title, computed over all on the order of 10^{10} impostor comparisons. If text appears in each box it give the same quantity as that coded by the color. Grey indicates FMR is at the intended FMR target level. Light red colors present a security vulnerability to, for example, a passport gate. Each +1 increase in \log_{10} FMR corresponds to a factor of 10 increase in FMR. The matrix is not quite symmetric because images in the enrollment and verification sets are different.

Cross region FMR at threshold T = 1.301 for algorithm kakao_001, giving FMR(T) = 0.0001 globally.

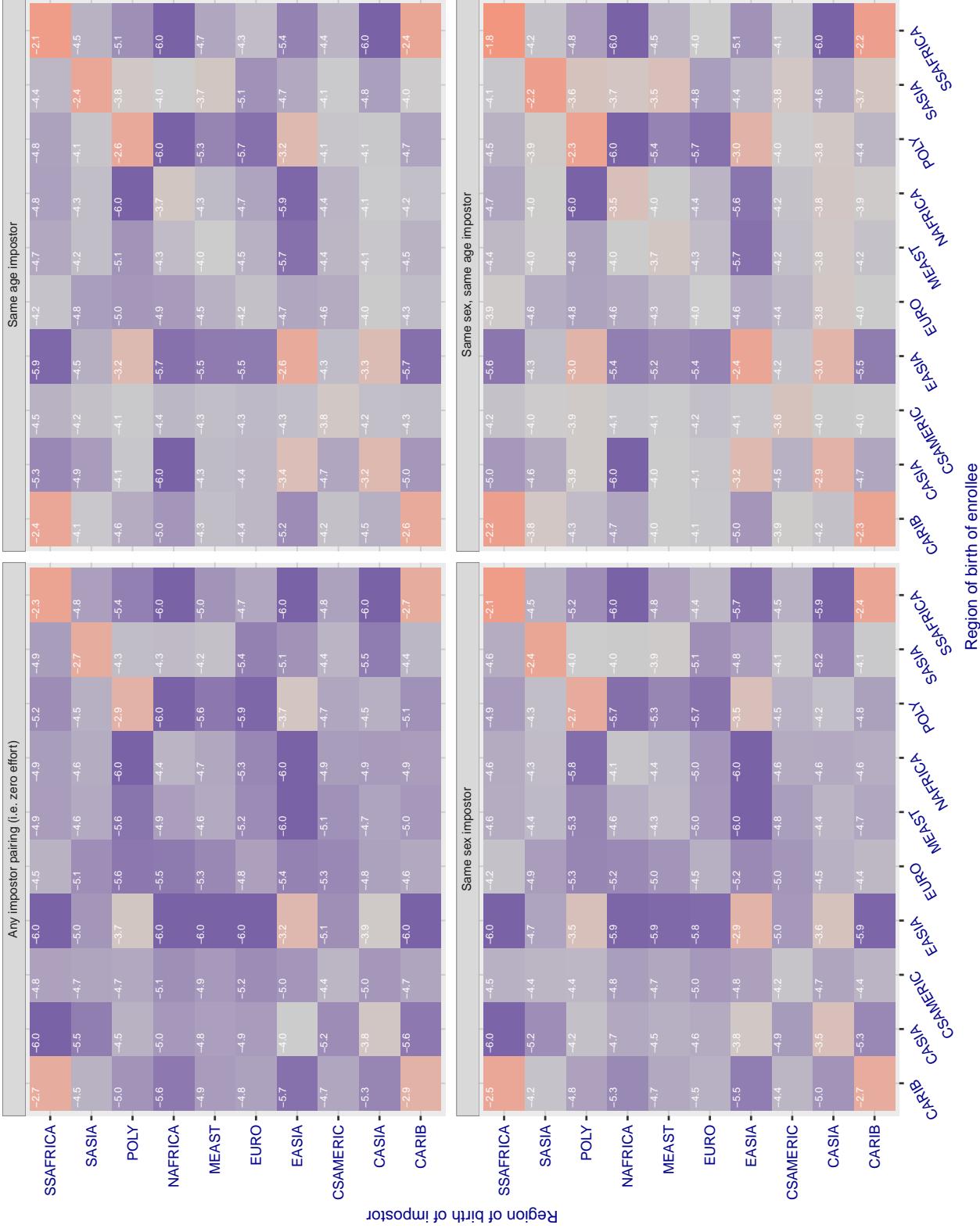


Figure 206: For algorithm kakao-001 operating on visa images, the heatmap shows false match rates observed over impostor comparisons of faces from different individuals who were born in the given region pair. False matches are counted against a recognition threshold fixed globally to give the target FMR in the plot title, computed over all on the order of 10^{10} impostor comparisons. If text appears in each box it give the same quantity as that coded by the color. Grey indicates FMR is at the intended FMR target level. Light red colors present a security vulnerability to, for example, a passport gate. Each +1 increase in $\log_{10} \text{FMR}$ corresponds to a factor of 10 increase in FMR. The matrix is not quite symmetric because images in the enrollment and verification sets are different.

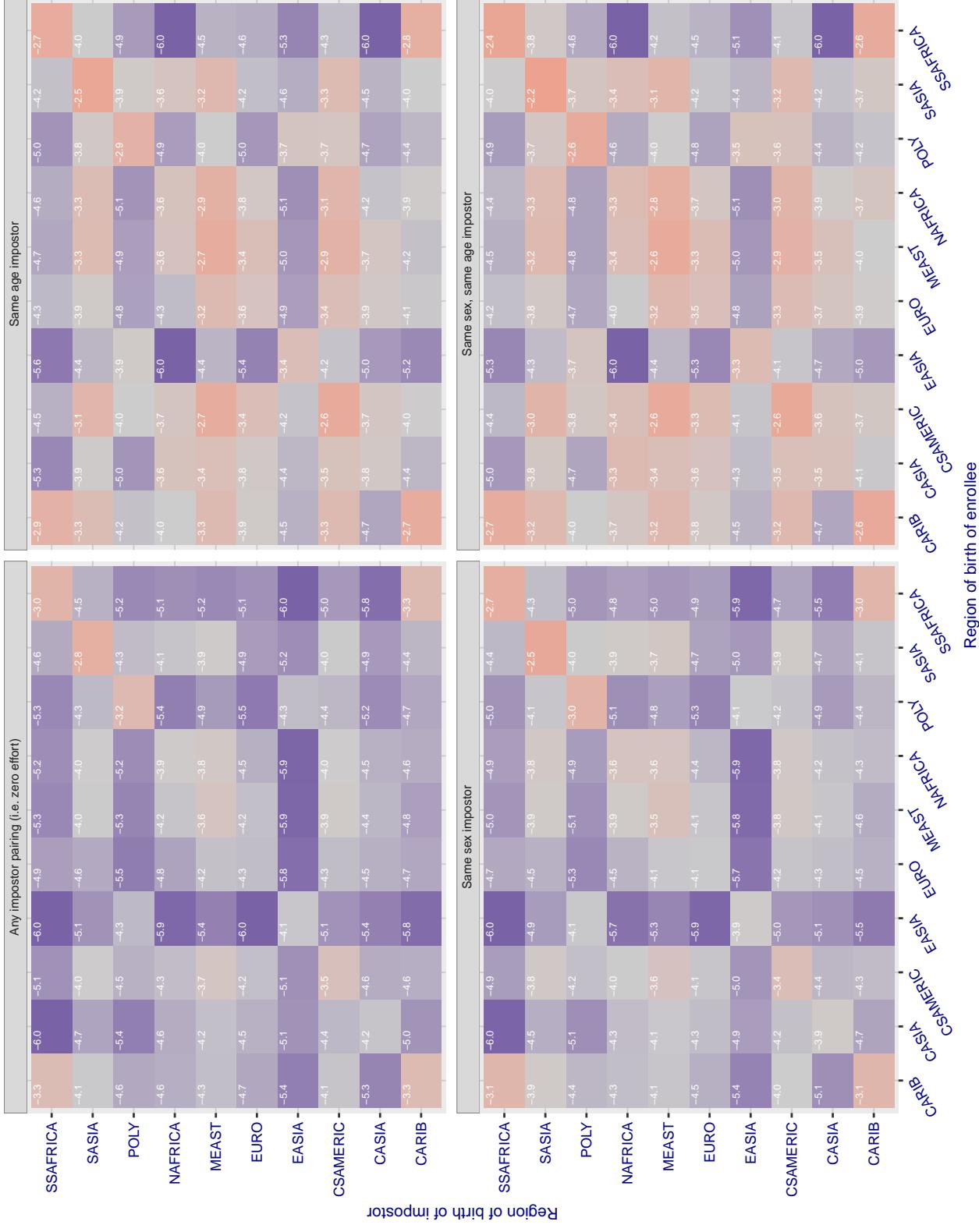
Cross region FMR at threshold T = 0.929 for algorithm kakao_002, giving FMR(T) = 0.0001 globally.

Figure 207: For algorithm kakao-002 operating on visa images, the heatmap shows false match rates observed over impostor comparisons of faces from different individuals who were born in the given region pair. False matches are counted against a recognition threshold fixed globally to give the target FMR in the plot title, computed over all on the order of 10^{10} impostor comparisons. If text appears in each box it give the same quantity as that coded by the color. Grey indicates FMR is at the intended FMR target level. Light red colors present a security vulnerability to, for example, a passport gate. Each +1 increase in $\log_{10} \text{FMR}$ corresponds to a factor of 10 increase in FMR. The matrix is not quite symmetric because images in the enrollment and verification sets are different.

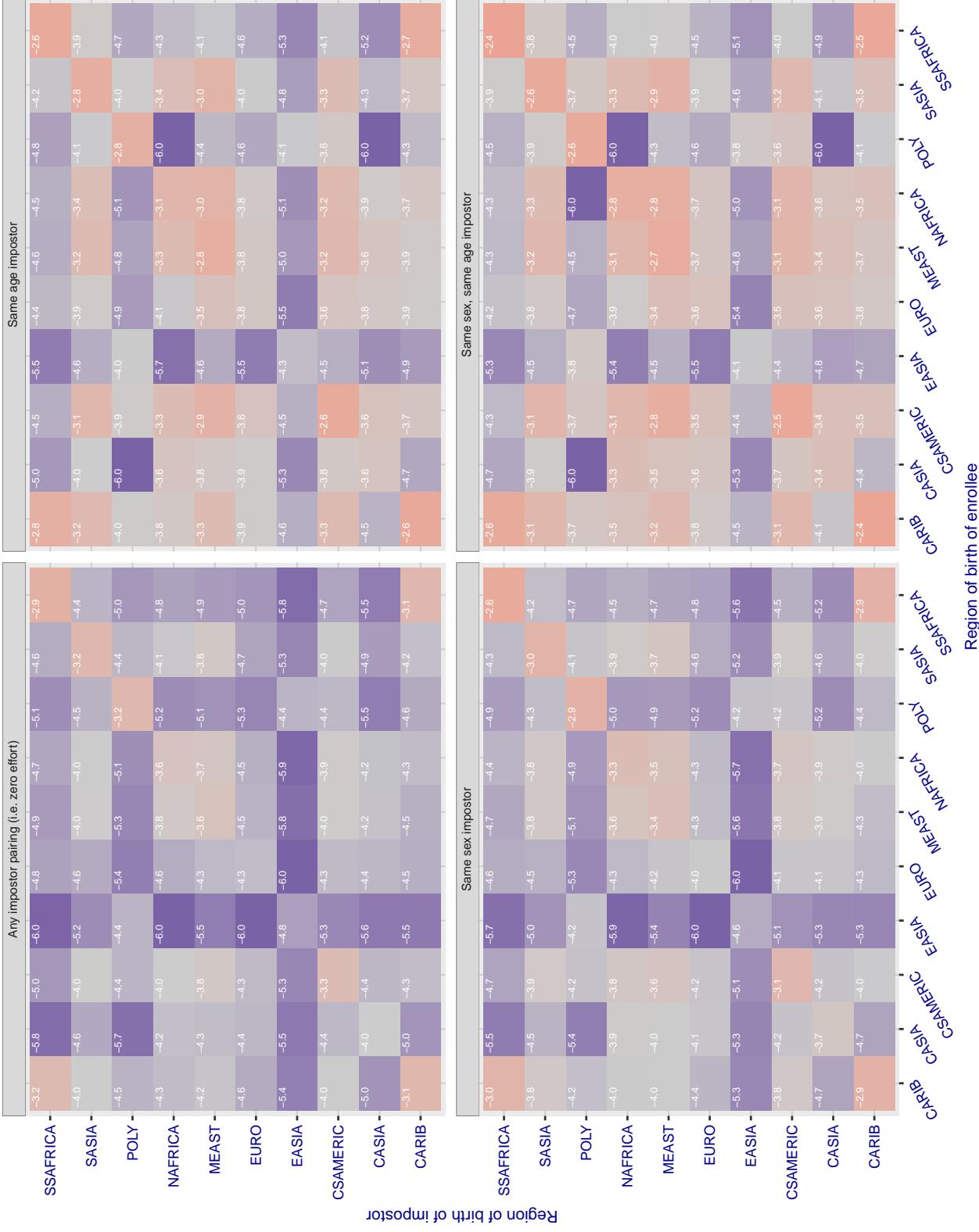
Cross region FMR at threshold T = 0.686 for algorithm kedacom_000, giving FMR(T) = 0.0001 globally.

Figure 208: For algorithm kedacom-000 operating on visa images, the heatmap shows false match rates observed over impostor comparisons of faces from different individuals who were born in the given region pair. False matches are counted against a recognition threshold fixed globally to give the target FMR in the plot title, computed over all on the order of 10^{10} impostor comparisons. If text appears in each box it give the same quantity as that coded by the color. Grey indicates FMR is at the intended FMR target level. Light red colors present a security vulnerability to, for example, a passport gate. Each +1 increase in $\log_{10} \text{FMR}$ corresponds to a factor of 10 increase in FMR. The matrix is not quite symmetric because images in the enrollment and verification sets are different.

Cross region FMR at threshold T = 0.500 for algorithm kneron_003, giving FMR(T) = 0.0001 globally.

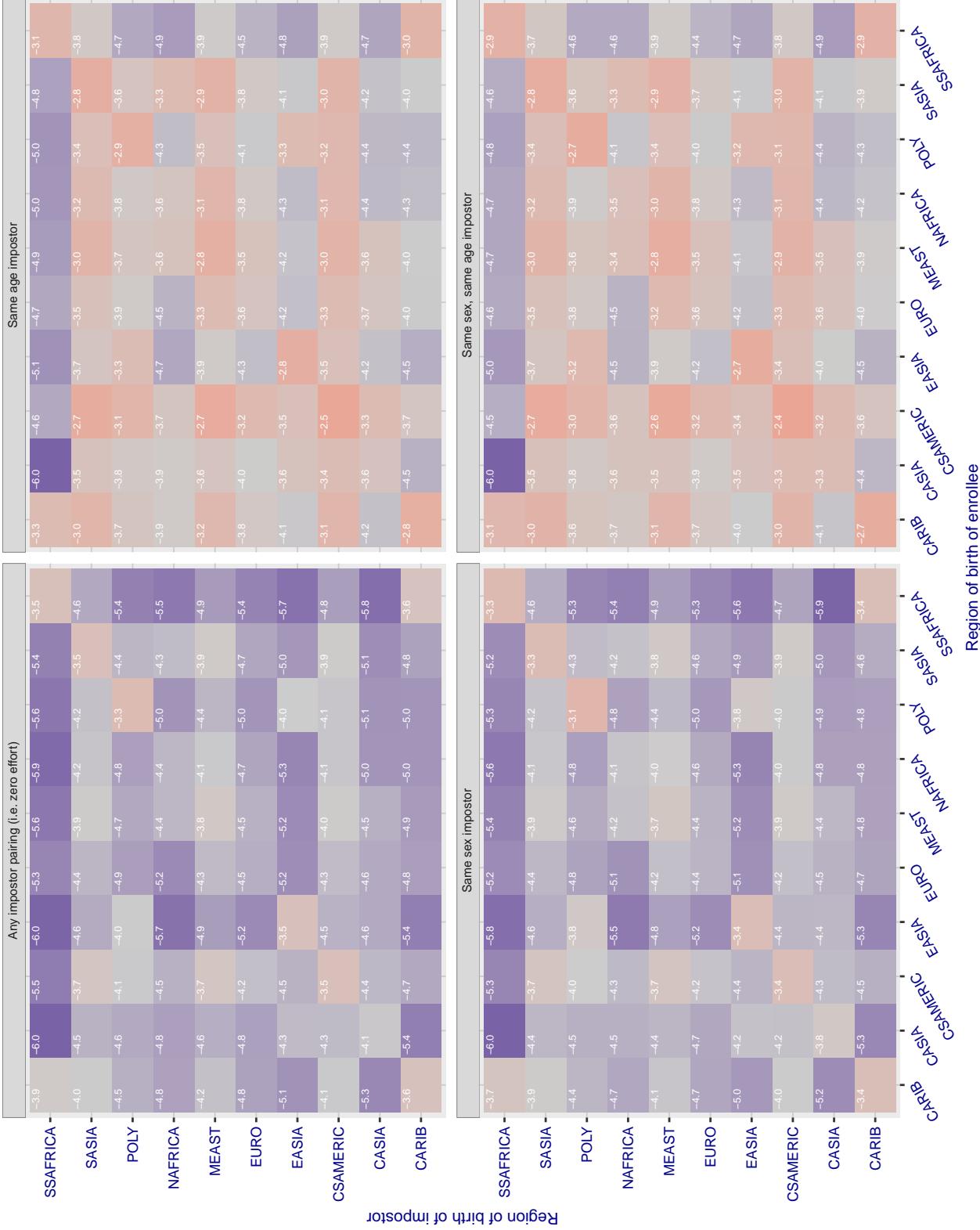


Figure 209: For algorithm kneron-003 operating on visa images, the heatmap shows false match rates observed over impostor comparisons of faces from different individuals who were born in the given region pair. False matches are counted against a recognition threshold fixed globally to give the target FMR in the plot title, computed over all on the order of 10^{10} impostor comparisons. If text appears in each box it give the same quantity as that coded by the color. Grey indicates FMR is at the intended FMR target level. Light red colors present a security vulnerability to, for example, a passport gate. Each +1 increase in $\log_{10} FMR$ corresponds to a factor of 10 increase in FMR. The matrix is not quite symmetric because images in the enrollment and verification sets are different.

Cross region FMR at threshold T = 0.701 for algorithm lookman_002, giving FMR(T) = 0.0001 globally.

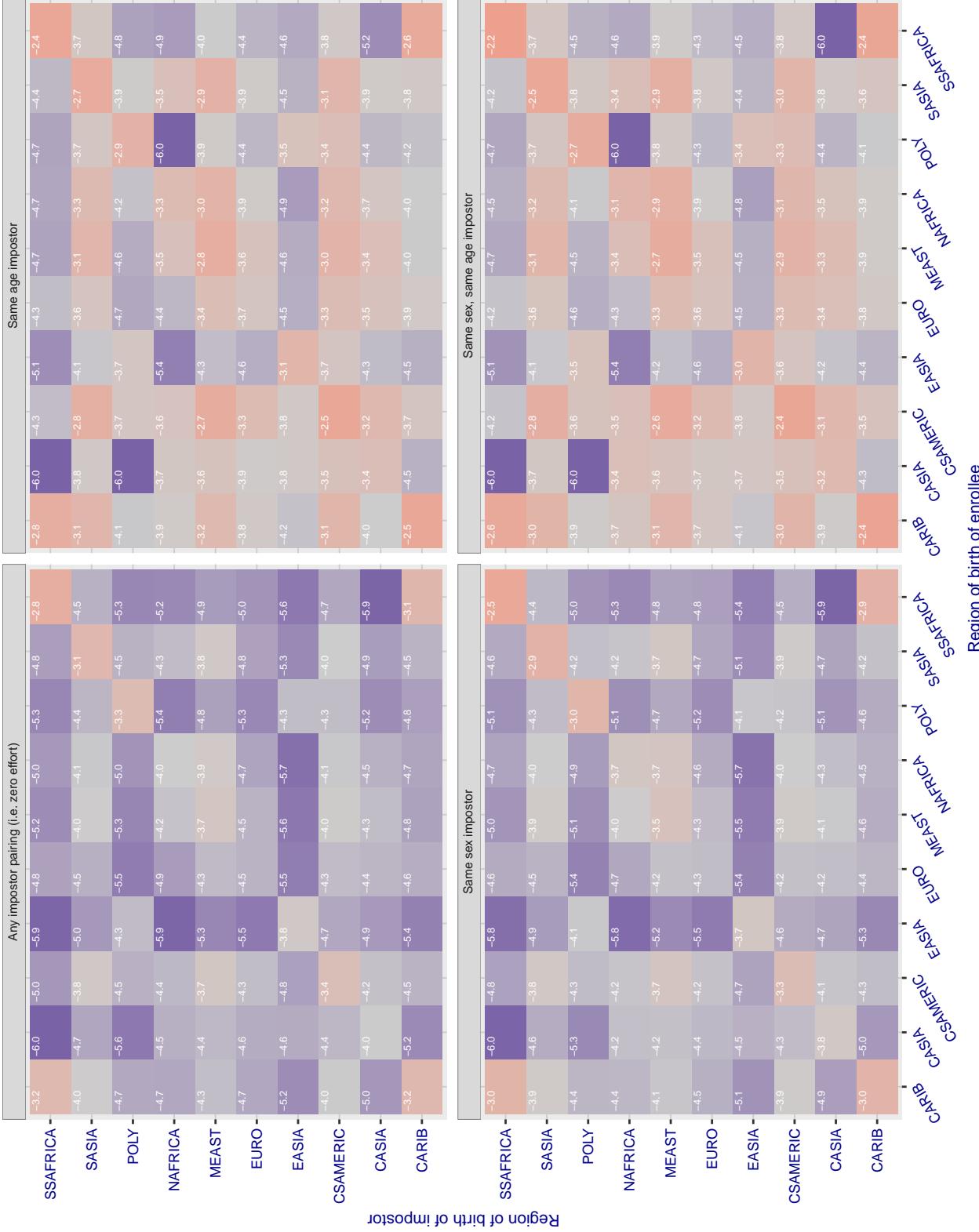


Figure 210: For algorithm lookman-002 operating on visa images, the heatmap shows false match rates observed over impostor comparisons of faces from different individuals who were born in the given region pair. False matches are counted against a recognition threshold fixed globally to give the target FMR in the plot title, computed over all on the order of 10^{10} impostor comparisons. If text appears in each box it give the same quantity as that coded by the color. Grey indicates FMR is at the intended FMR target level. Light red colors present a security vulnerability to, for example, a passport gate. Each +1 increase in $\log_{10} \text{FMR}$ corresponds to a factor of 10 increase in FMR. The matrix is not quite symmetric because images in the enrollment and verification sets are different.

Cross region FMR at threshold $T = 0.733$ for algorithm `lookman_004`, giving $FMR(T) = 0.0001$ globally.

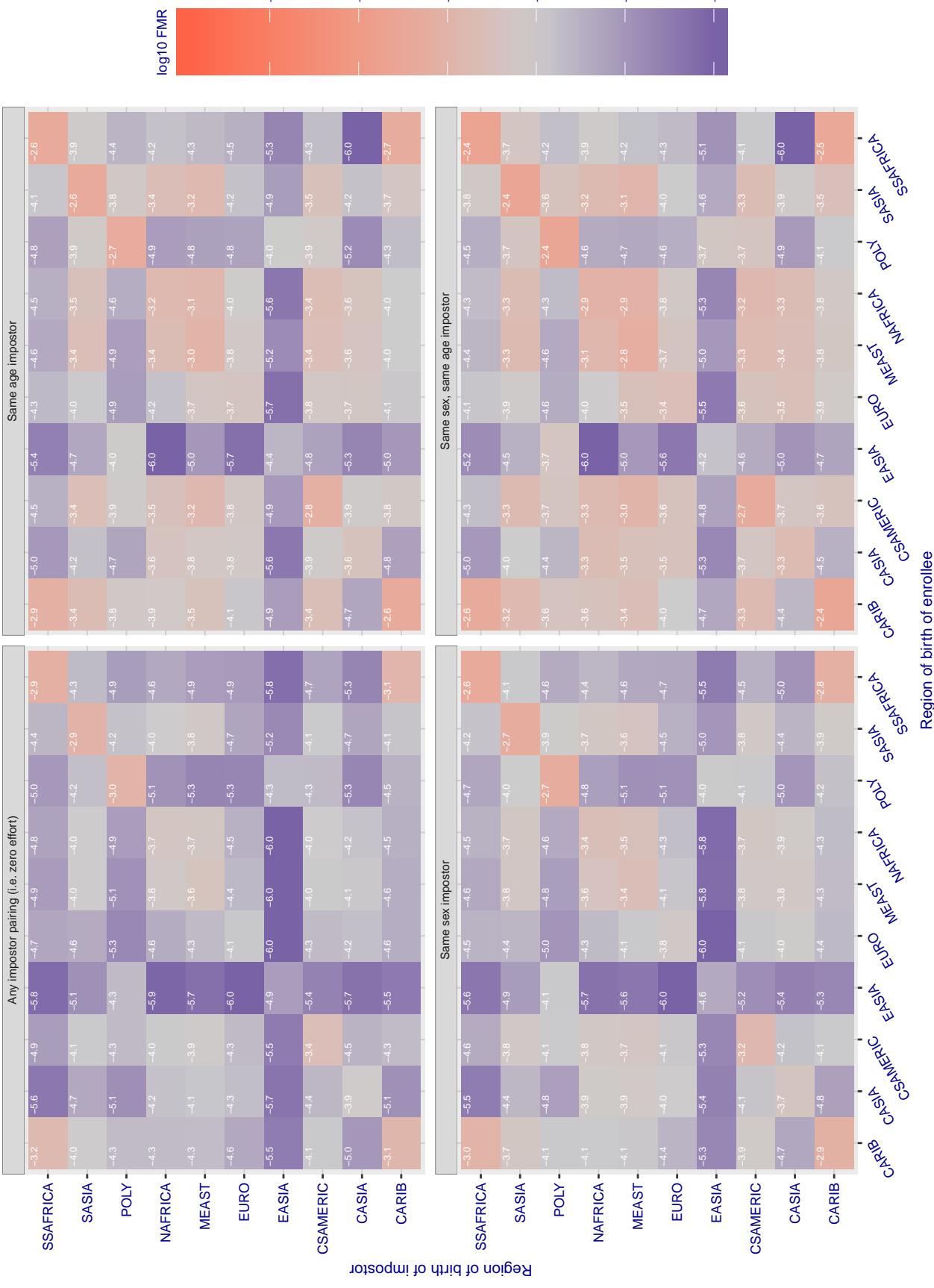


Figure 211: For algorithm lookman-004 operating on visa images, the heatmap shows false match rates observed over impostor comparisons of faces from different individuals who were born in the given region pair. False matches are counted against a recognition threshold fixed globally to give the target FMR in the plot title, computed over all on the order of 10^{10} impostor comparisons. If text appears in each box it give the same quantity as that coded by the color. Grey indicates FMR is at the intended FMR target level. Light red colors present a security vulnerability to, for example, a passport gate. Each +1 increase in $\log_{10} FMR$ corresponds to a factor of 10 increase in FMR . The matrix is not quite symmetric because images in the enrollment and verification sets are different.

Cross region FMR at threshold T = 74.511 for algorithm megvii_001, giving FMR(T) = 0.0001 globally.

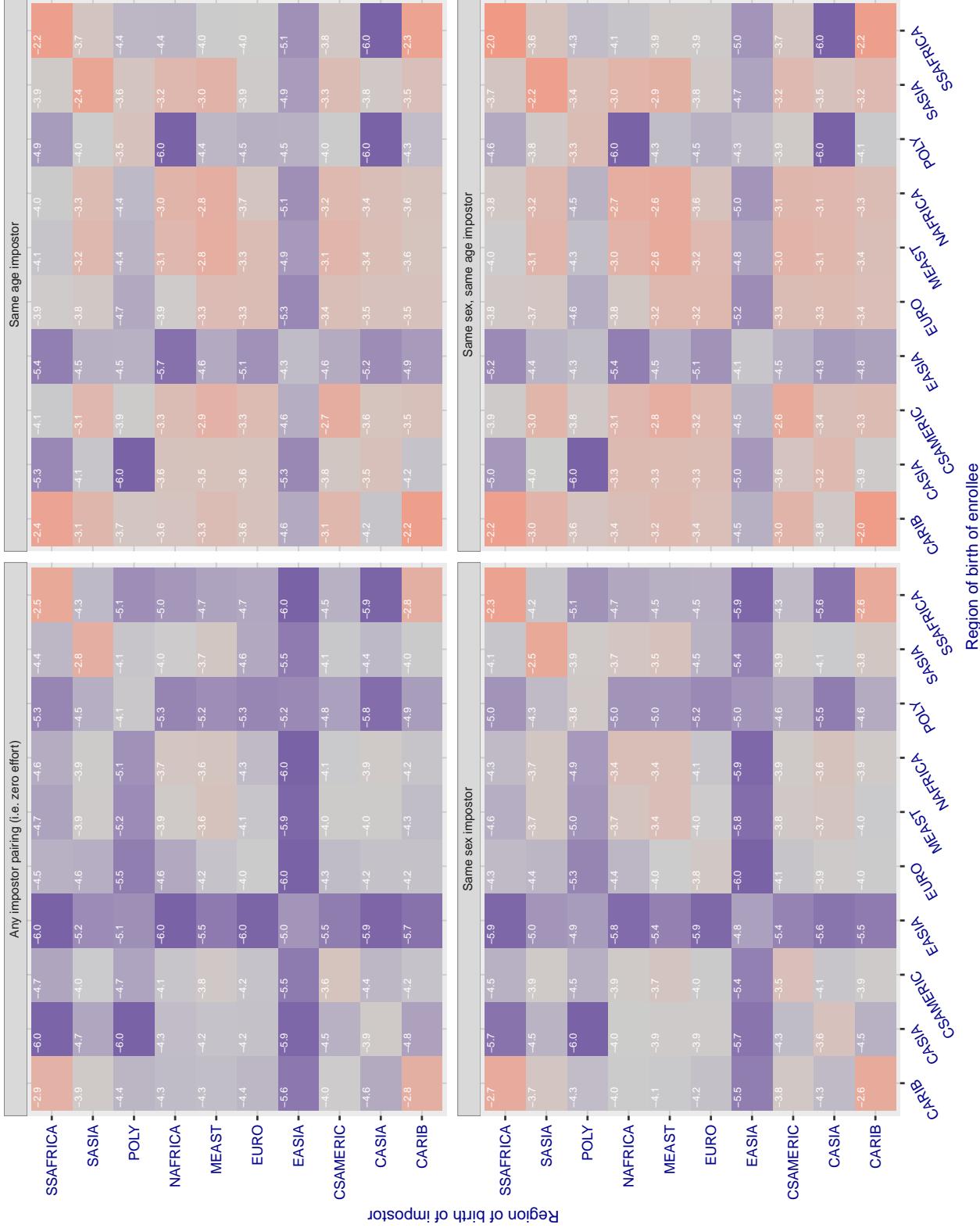


Figure 212: For algorithm megvii-001 operating on visa images, the heatmap shows false match rates observed over impostor comparisons of faces from different individuals who were born in the given region pair. False matches are counted against a recognition threshold fixed globally to give the target FMR in the plot title, computed over all on the order of 10^{10} impostor comparisons. If text appears in each box it give the same quantity as that coded by the color. Grey indicates FMR is at the intended FMR target level. Light red colors present a security vulnerability to, for example, a passport gate. Each +1 increase in $\log_{10} \text{FMR}$ corresponds to a factor of 10 increase in FMR. The matrix is not quite symmetric because images in the enrollment and verification sets are different.

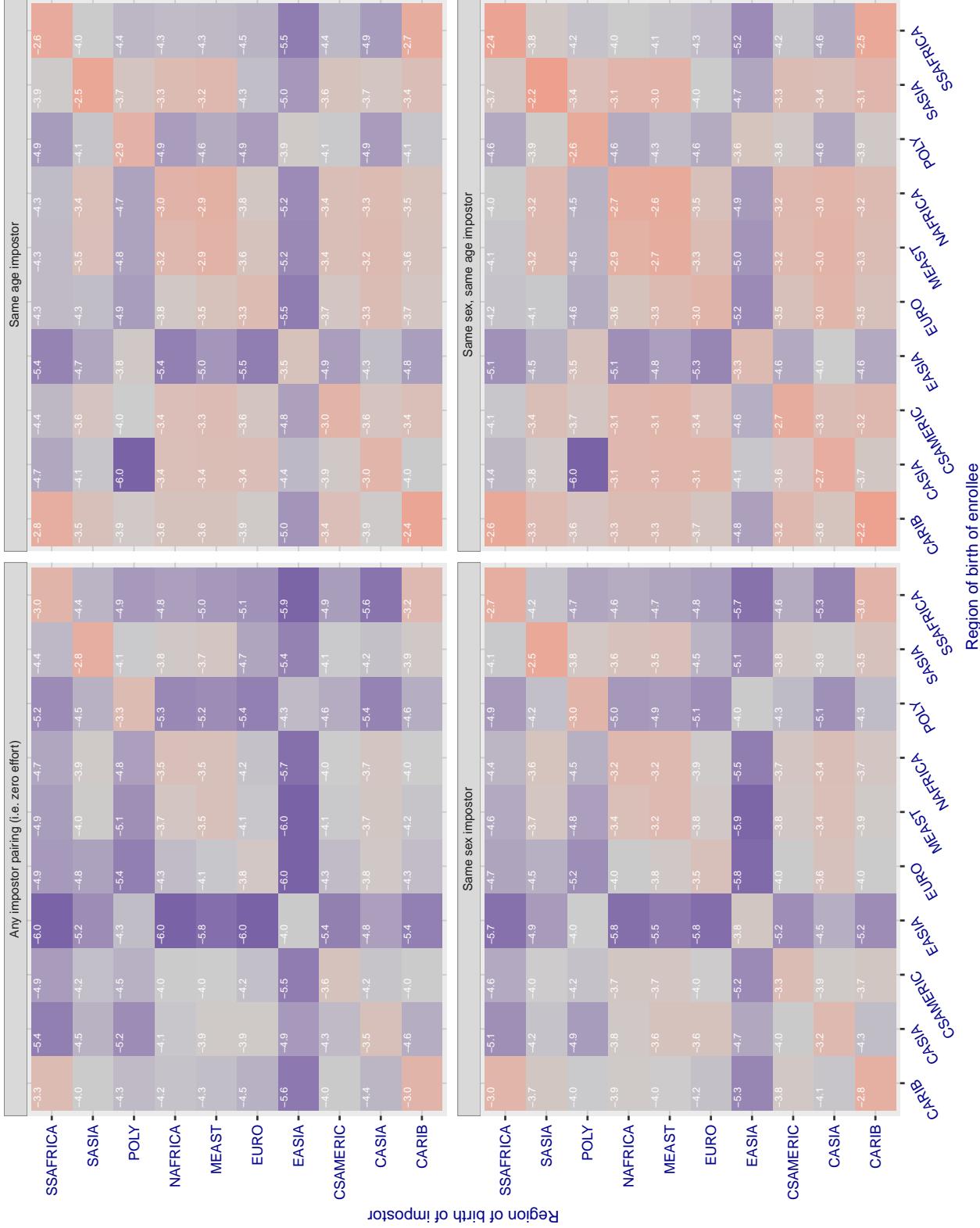
Cross region FMR at threshold T = 66.384 for algorithm megvii_002, giving FMR(T) = 0.0001 globally.

Figure 213: For algorithm megvii-002 operating on visa images, the heatmap shows false match rates observed over impostor comparisons of faces from different individuals who were born in the given region pair. False matches are counted against a recognition threshold fixed globally to give the target FMR in the plot title, computed over all on the order of 10^{10} impostor comparisons. If text appears in each box it give the same quantity as that coded by the color. Grey indicates FMR is at the intended FMR target level. Light red colors present a security vulnerability to, for example, a passport gate. Each +1 increase in $\log_{10} \text{FMR}$ corresponds to a factor of 10 increase in FMR. The matrix is not quite symmetric because images in the enrollment and verification sets are different.

Cross region FMR at threshold T = 0.425 for algorithm meiya_001, giving FMR(T) = 0.0001 globally.

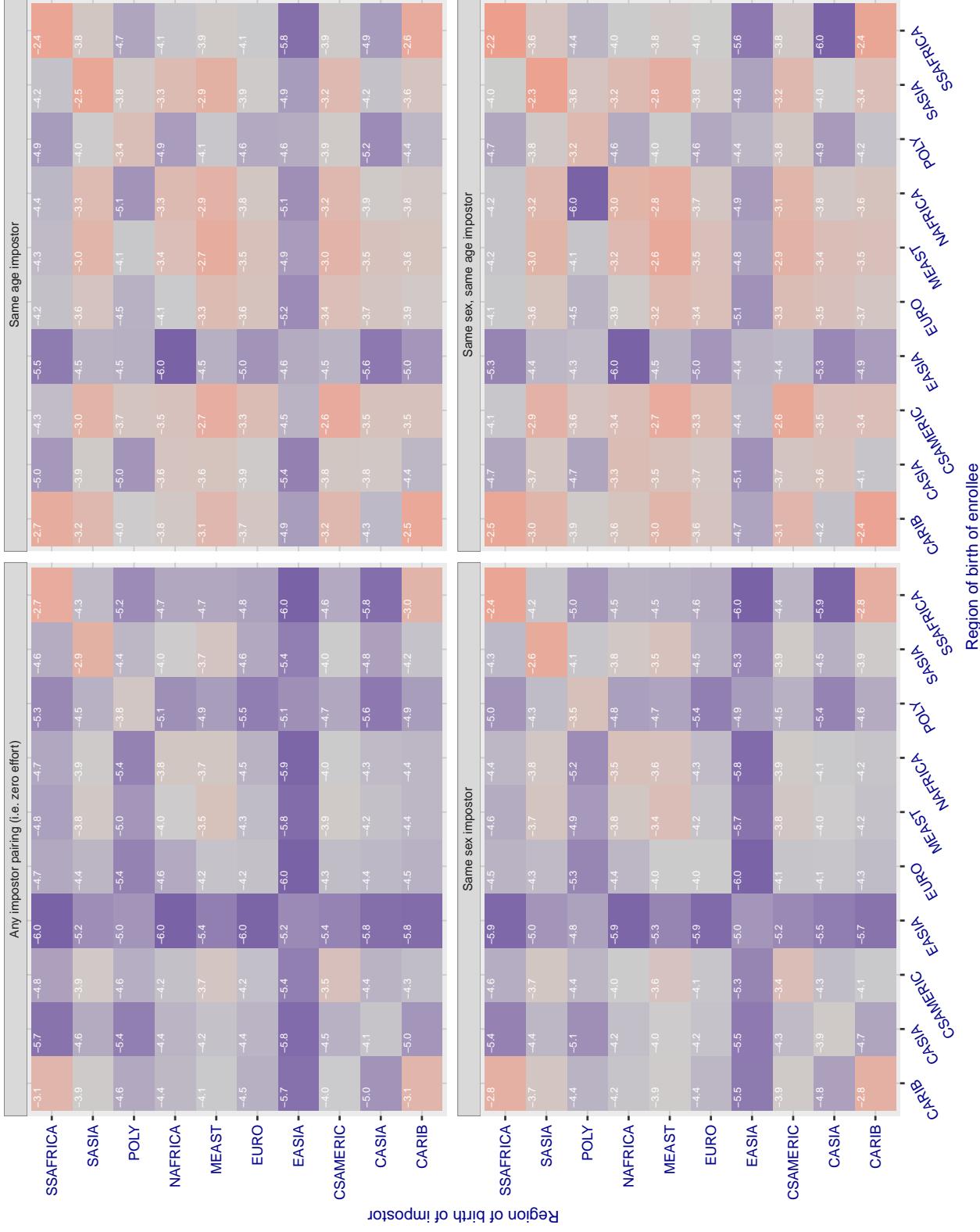


Figure 214: For algorithm meiya-001 operating on visa images, the heatmap shows false match rates observed over impostor comparisons of faces from different individuals who were born in the given region pair. False matches are counted against a recognition threshold fixed globally to give the target FMR in the plot title, computed over all on the order of 10^{10} impostor comparisons. If text appears in each box it give the same quantity as that coded by the color. Grey indicates FMR is at the intended FMR target level. Light red colors present a security vulnerability to, for example, a passport gate. Each +1 increase in $\log_{10} FMR$ corresponds to a factor of 10 increase in FMR. The matrix is not quite symmetric because images in the enrollment and verification sets are different.

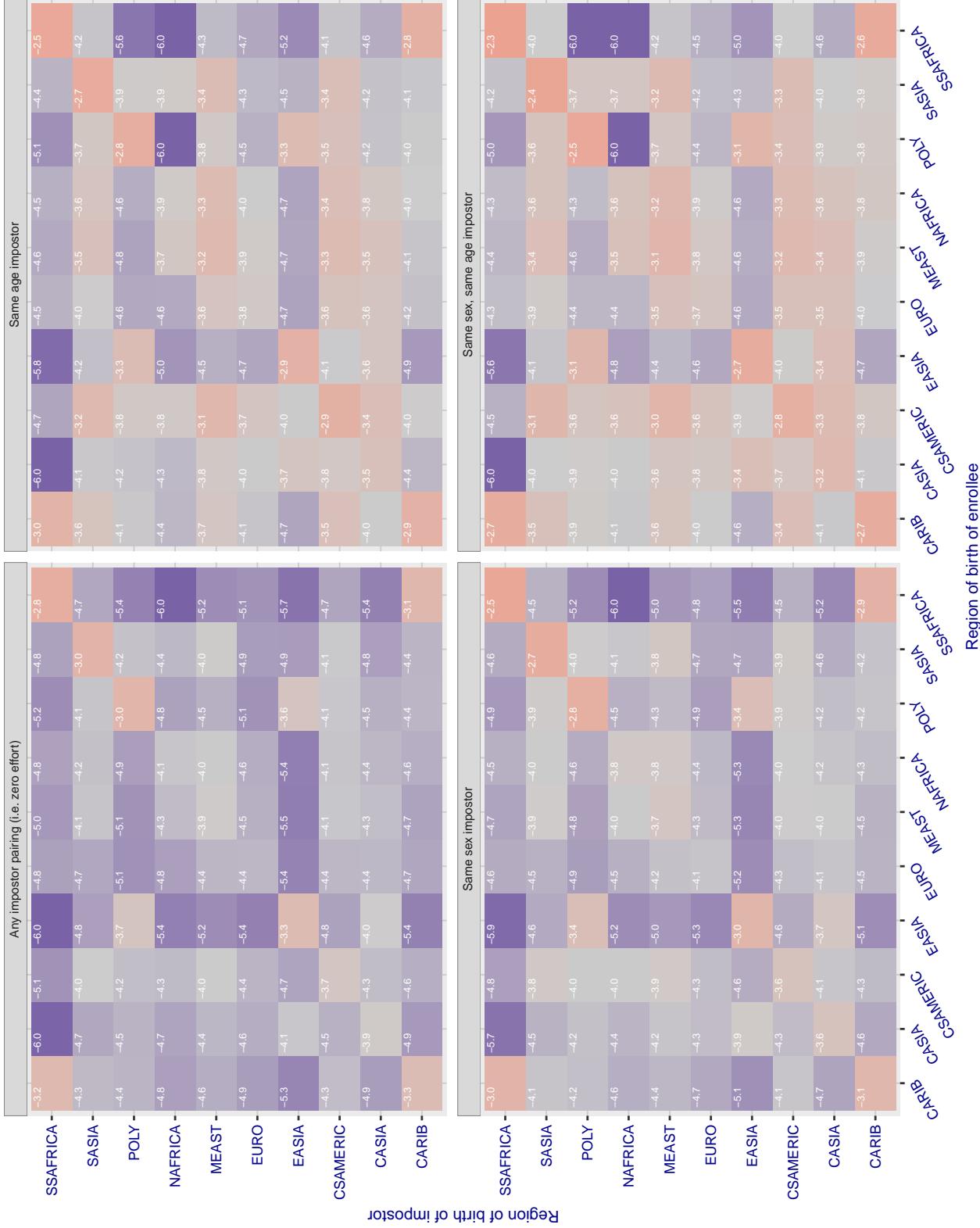
Cross region FMR at threshold T = 0.668 for algorithm microfocus_001, giving FMR(T) = 0.0001 globally.

Figure 215: For algorithm microfocus-001 operating on visa images, the heatmap shows false match rates observed over impostor comparisons of faces from different individuals who were born in the given region pair. False matches are counted against a recognition threshold fixed globally to give the target FMR in the plot title, computed over all on the order of 10^{10} impostor comparisons. If text appears in each box it give the same quantity as that coded by the color. Grey indicates FMR is at the intended FMR target level. Light red colors present a security vulnerability to, for example, a passport gate. Each +1 increase in $\log_{10} \text{FMR}$ corresponds to a factor of 10 increase in FMR. The matrix is not quite symmetric because images in the enrollment and verification sets are different.

Cross region FMR at threshold T = 0.602 for algorithm microfocus_002, giving FMR(T) = 0.0001 globally.

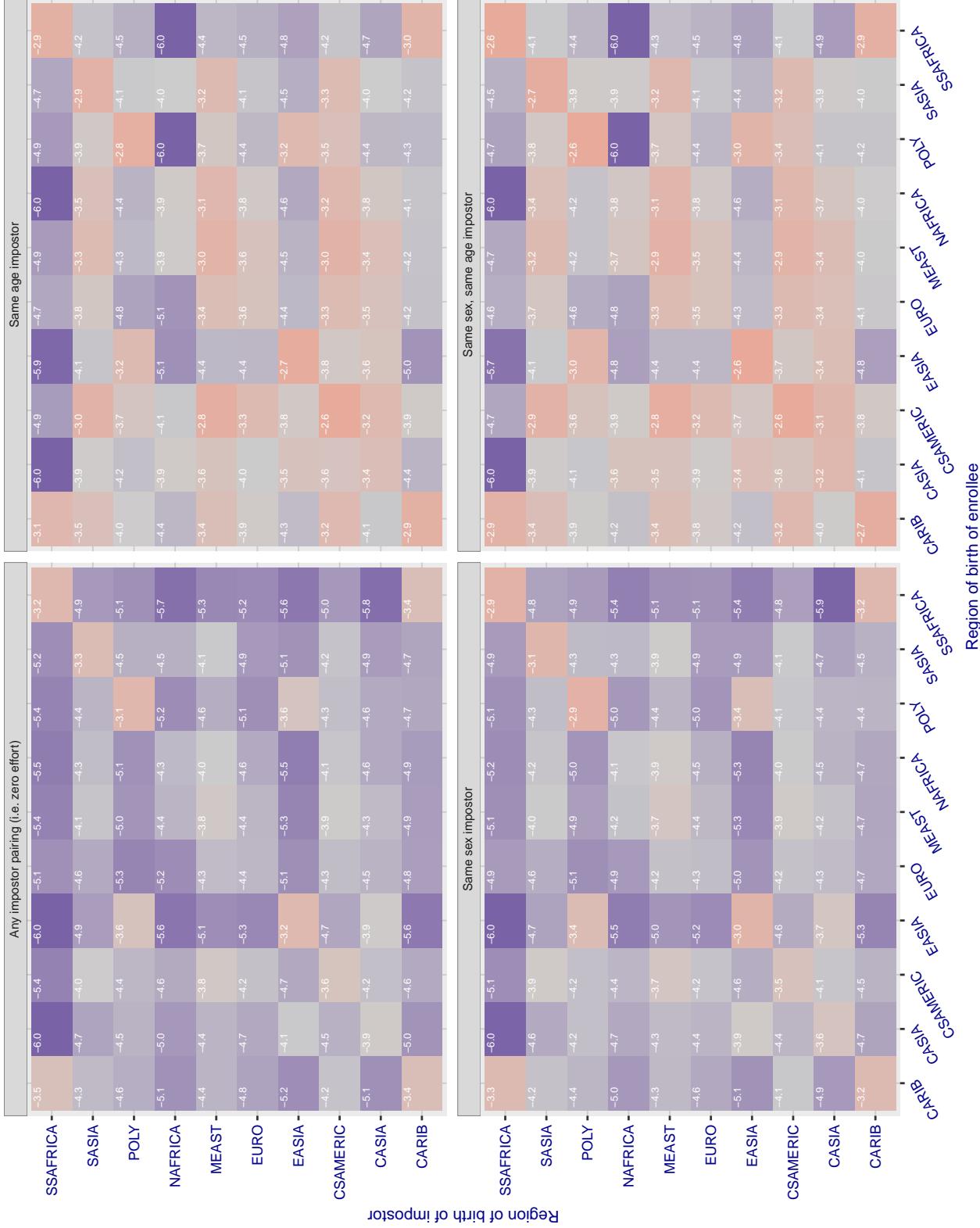


Figure 216: For algorithm microfocus-002 operating on visa images, the heatmap shows false match rates observed over impostor comparisons of faces from different individuals who were born in the given region pair. False matches are counted against a recognition threshold fixed globally to give the target FMR in the plot title, computed over all on the order of 10^{10} impostor comparisons. If text appears in each box it give the same quantity as that coded by the color. Grey indicates FMR is at the intended FMR target level. Light red colors present a security vulnerability to, for example, a passport gate. Each +1 increase in $\log_{10} FMR$ corresponds to a factor of 10 increase in FMR. The matrix is not quite symmetric because images in the enrollment and verification sets are different.

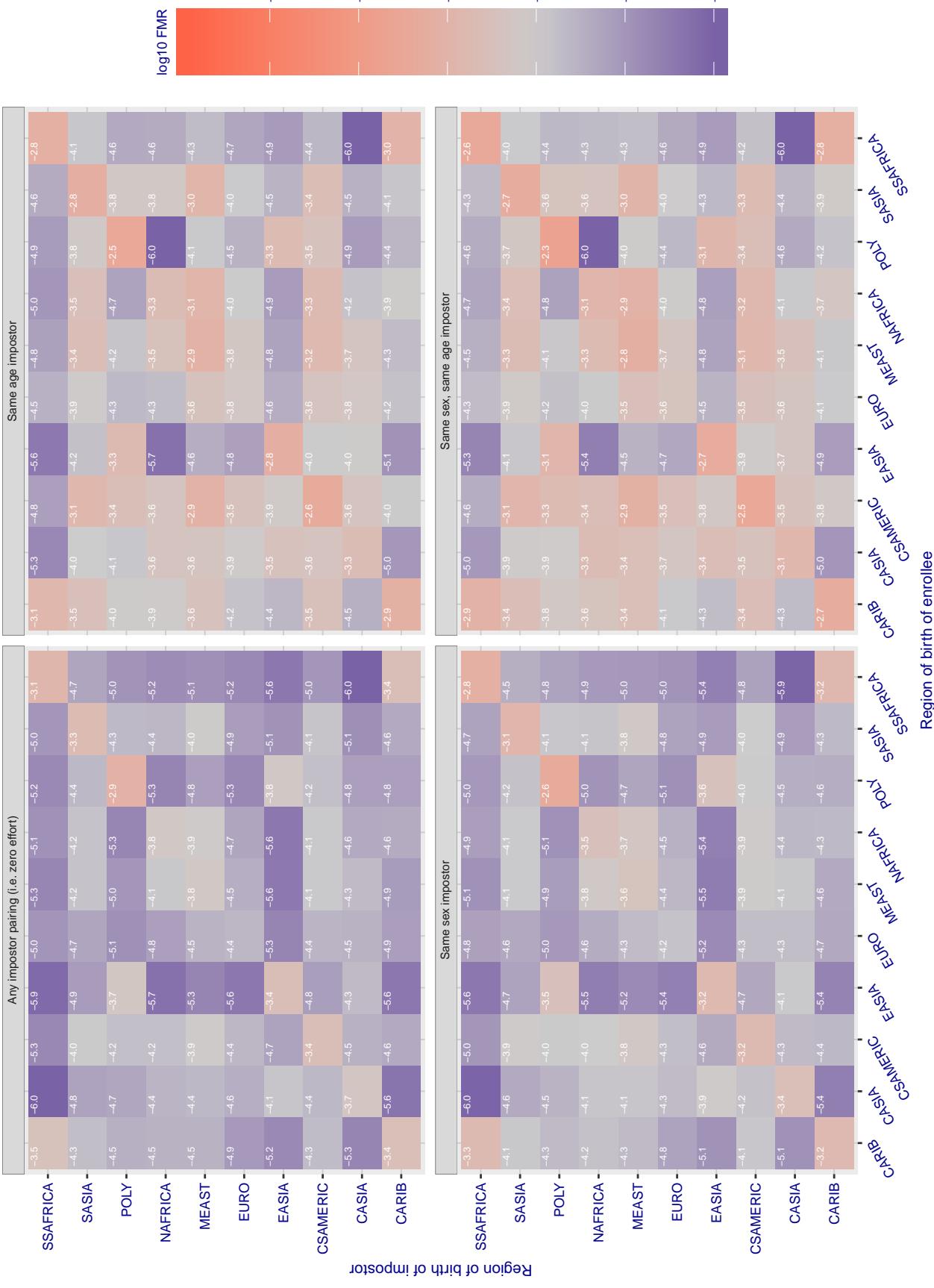
Cross region FMR at threshold T = 1.394 for algorithm mt_000, giving FMR(T) = 0.0001 globally.

Figure 217: For algorithm mt-000 operating on visa images, the heatmap shows false match rates observed over impostor comparisons of faces from different individuals who were born in the given region pair. False matches are counted against a recognition threshold fixed globally to give the target FMR in the plot title, computed over all on the order of 10^{10} impostor comparisons. If text appears in each box it give the same quantity as that coded by the color. Grey indicates FMR is at the intended FMR target level. Light red colors present a security vulnerability to, for example, a passport gate. Each +1 increase in $\log_{10} \text{FMR}$ corresponds to a factor of 10 increase in FMR. The matrix is not quite symmetric because images in the enrollment and verification sets are different.

Cross region FMR at threshold T = 46.101 for algorithm neurotechnology_005, giving FMR(T) = 0.0001 globally.

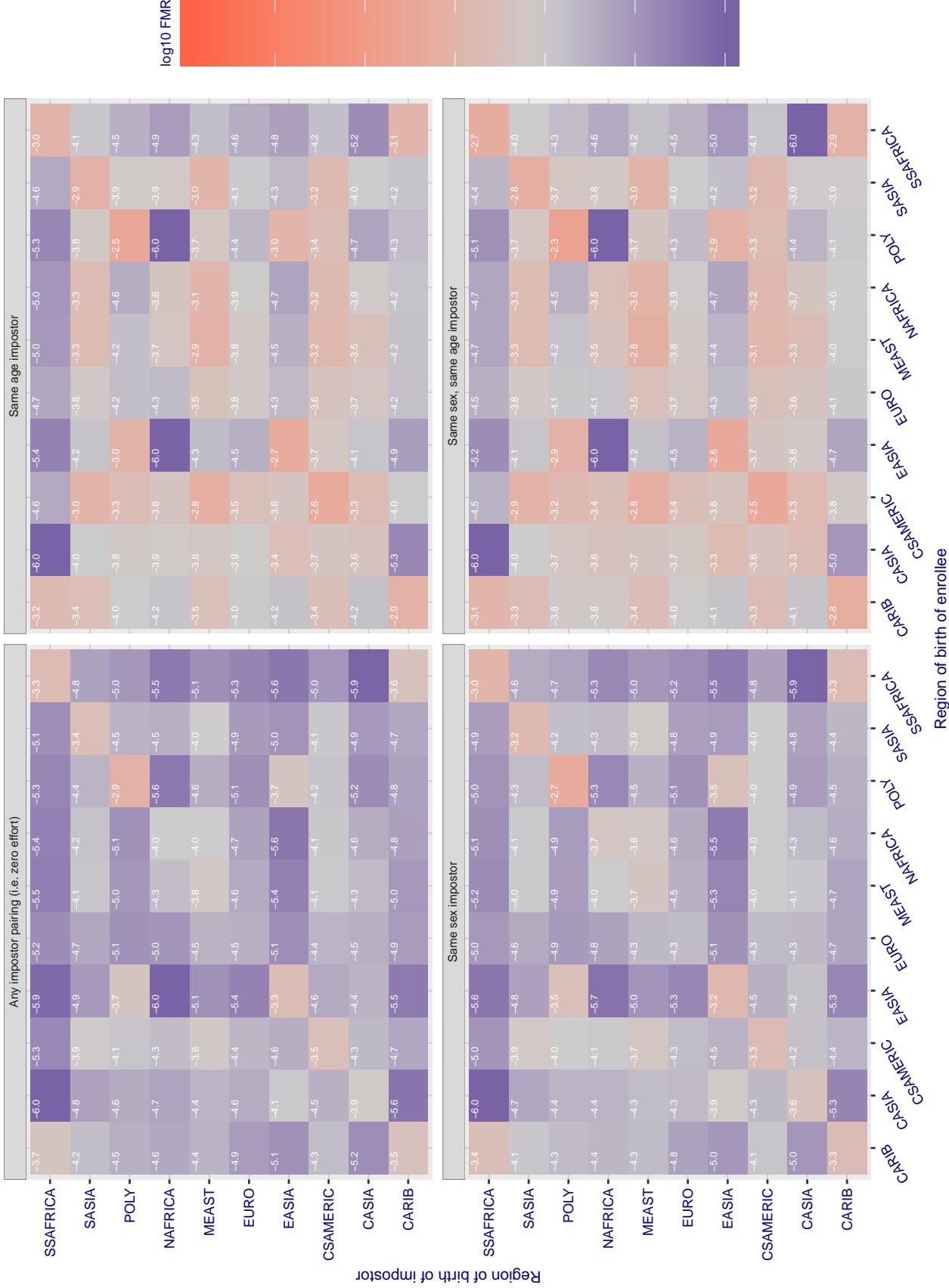


Figure 218: For algorithm neurotechnology-005 operating on visa images, the heatmap shows false match rates observed over impostor comparisons of faces from different individuals who were born in the given region pair. False matches are counted against a recognition threshold fixed globally to give the target FMR in the plot title, computed over all on the order of 10^{10} impostor comparisons. If text appears in each box it give the same quantity as that coded by the color. Grey indicates FMR is at the intended FMR target level. Light red colors present a security vulnerability to, for example, a passport gate. Each +1 increase in $\log_{10} \text{FMR}$ corresponds to a factor of 10 increase in FMR. The matrix is not quite symmetric because images in the enrollment and verification sets are different.

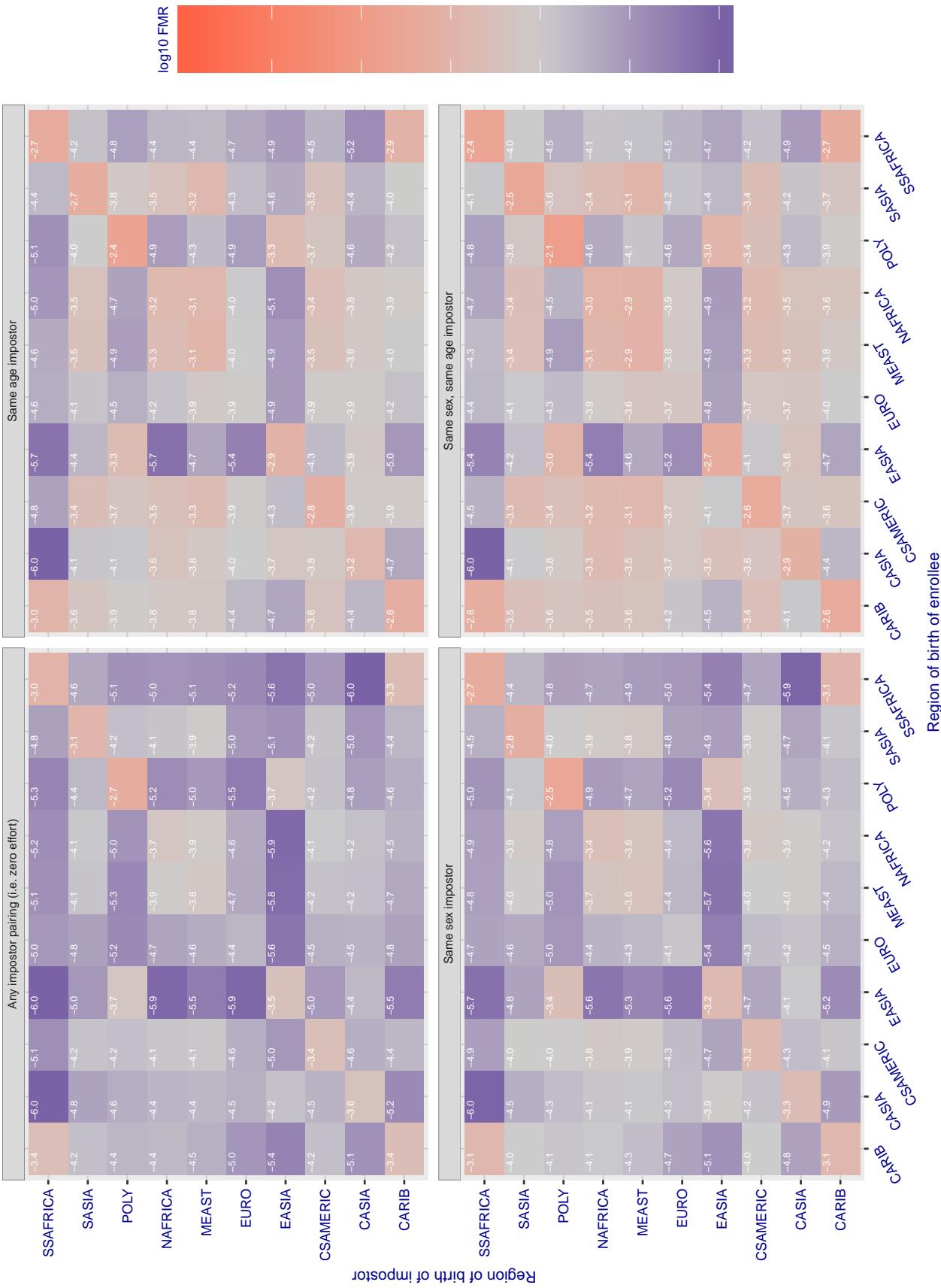
Cross region FMR at threshold T = 2044.000 for algorithm neurotechnology_006, giving FMR(T) = 0.0001 globally.

Figure 219: For algorithm neurotechnology-006 operating on visa images, the heatmap shows false match rates observed over impostor comparisons of faces from different individuals who were born in the given region pair. False matches are counted against a recognition threshold fixed globally to give the target FMR in the plot title, computed over all on the order of 10^{10} impostor comparisons. If text appears in each box it give the same quantity as that coded by the color. Grey indicates FMR is at the intended FMR target level. Light red colors present a security vulnerability to, for example, a passport gate. Each +1 increase in $\log_{10} \text{FMR}$ corresponds to a factor of 10 increase in FMR. The matrix is not quite symmetric because images in the enrollment and verification sets are different.

Cross region FMR at threshold T = 1.000 for algorithm nodeflux_001, giving FMR(T) = 0.0001 globally.

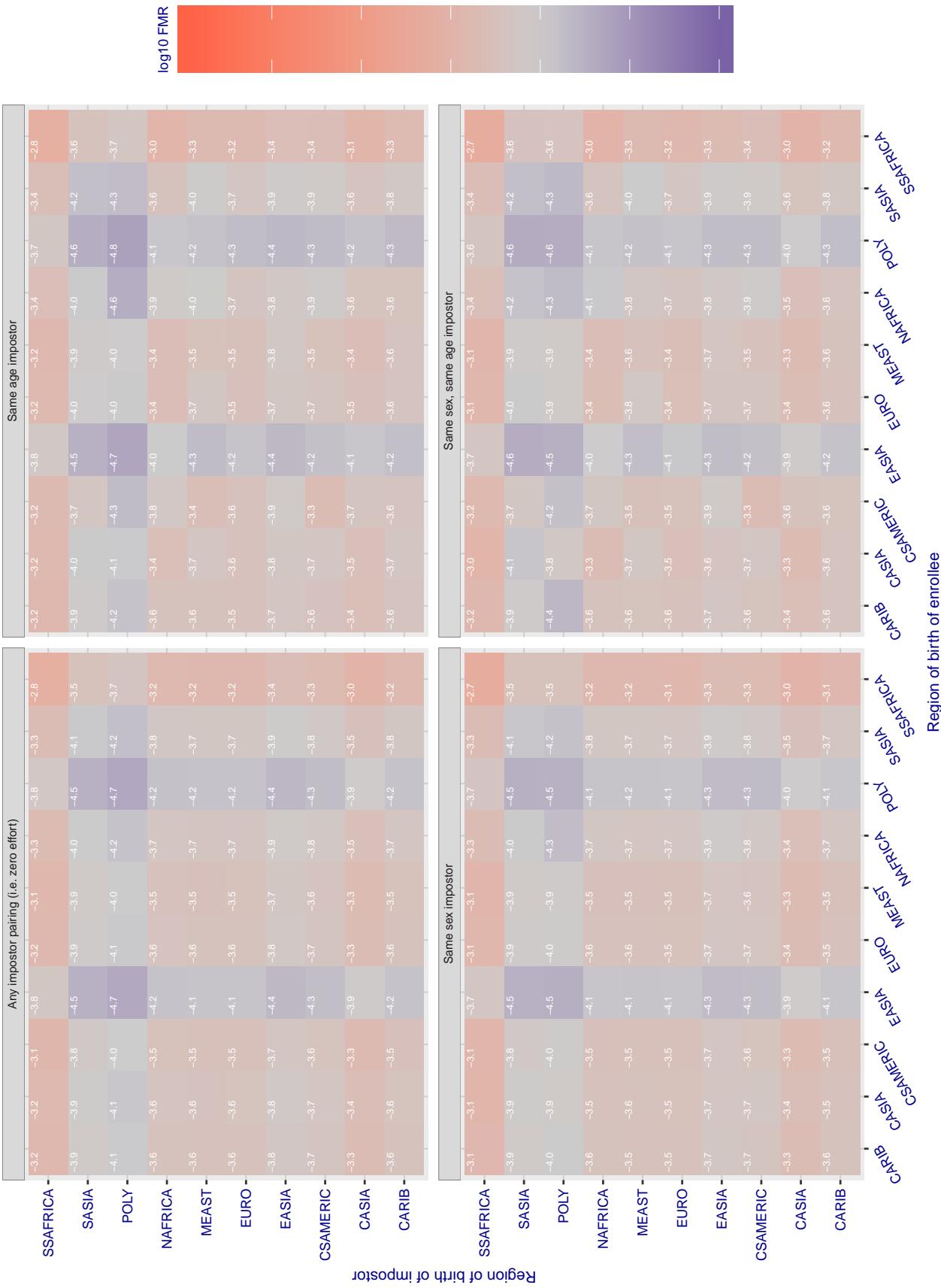


Figure 220: For algorithm nodeflux-001 operating on visa images, the heatmap shows false match rates observed over impostor comparisons of faces from different individuals who were born in the given region pair. False matches are counted against a recognition threshold fixed globally to give the target FMR in the plot title, computed over all on the order of 10^{10} impostor comparisons. If text appears in each box it give the same quantity as that coded by the color. Grey indicates FMR is at the intended FMR target level. Light red colors present a security vulnerability to, for example, a passport gate. Each +1 increase in $\log_{10} FMR$ corresponds to a factor of 10 increase in FMR. The matrix is not quite symmetric because images in the enrollment and verification sets are different.

Cross region FMR at threshold T = 0.455 for algorithm nodeflux_002, giving FMR(T) = 0.0001 globally.

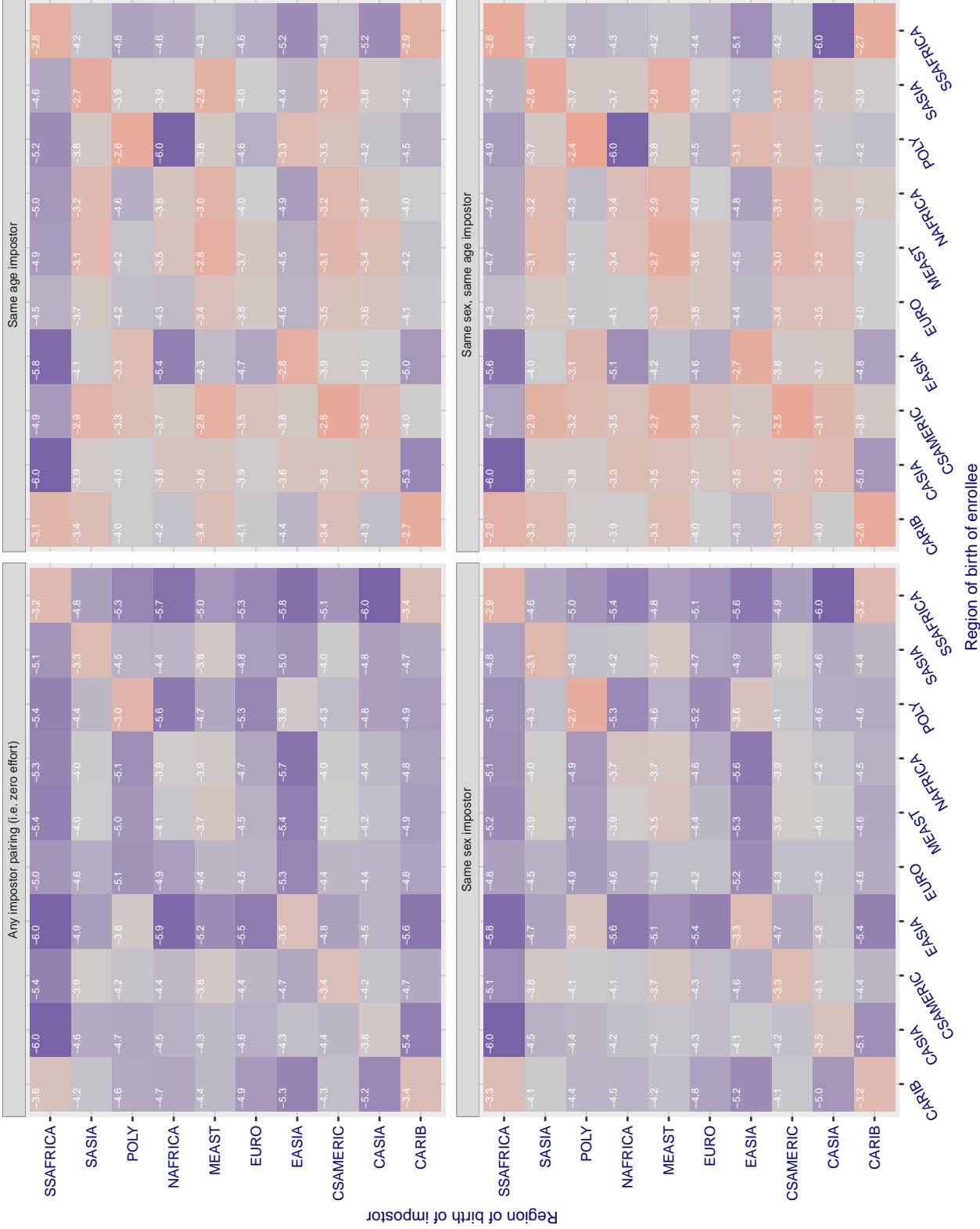


Figure 221: For algorithm nodeflux-002 operating on visa images, the heatmap shows false match rates observed over impostor comparisons of faces from different individuals who were born in the given region pair. False matches are counted against a recognition threshold fixed globally to give the target FMR in the plot title, computed over all on the order of 10^{10} impostor comparisons. If text appears in each box it give the same quantity as that coded by the color. Grey indicates FMR is at the intended FMR target level. Light red colors present a security vulnerability to, for example, a passport gate. Each +1 increase in $\log_{10} \text{FMR}$ corresponds to a factor of 10 increase in FMR. The matrix is not quite symmetric because images in the enrollment and verification sets are different.

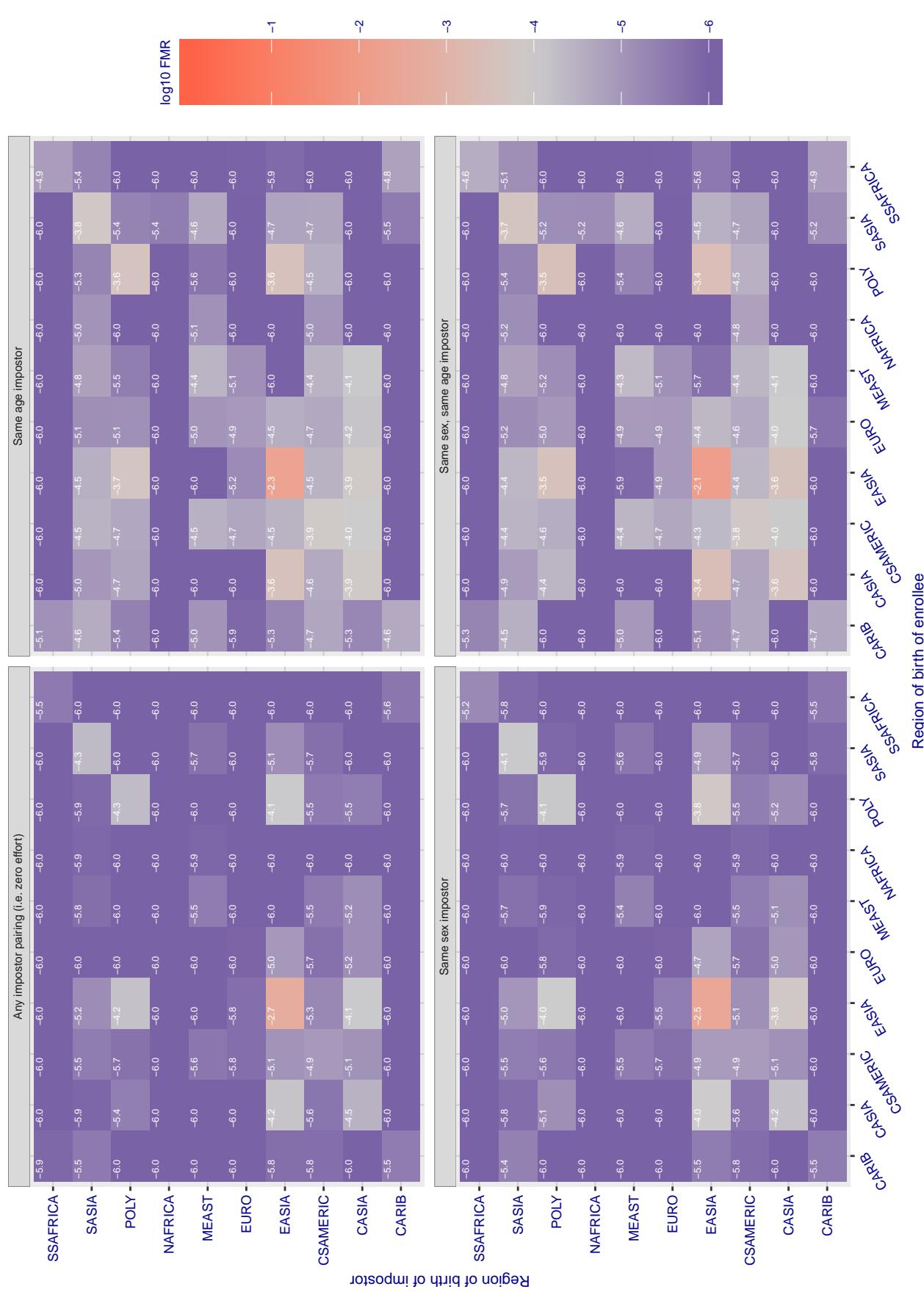
Cross region FMR at threshold T = 16846383821648700779774369791310334462380752812000954299625965117711518105060865483

Figure 222: For algorithm notiontag-000 operating on visa images, the heatmap shows false match rates observed over impostor comparisons of faces from different individuals who were born in the given region pair. False matches are counted against a recognition threshold fixed globally to give the target FMR in the plot title, computed over all on the order of 10^{10} impostor comparisons. If text appears in each box it give the same quantity as that coded by the color. Grey indicates FMR is at the intended FMR target level. Light red colors present a security vulnerability to, for example, a passport gate. Each +1 increase in $\log_{10} FMR$ corresponds to a factor of 10 increase in FMR. The matrix is not quite symmetric because images in the enrollment and verification sets are different.

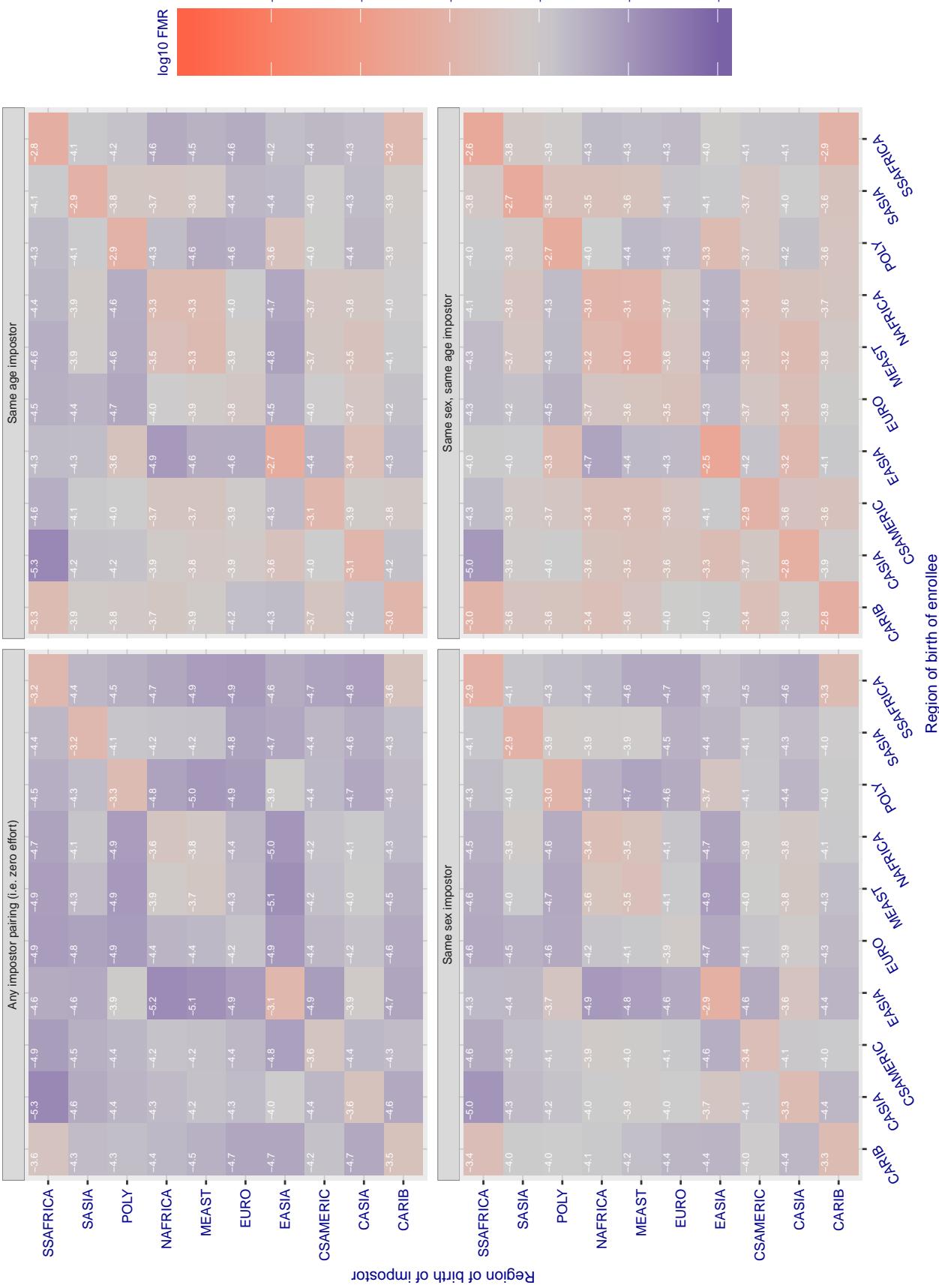
Cross region FMR at threshold T = 1.997 for algorithm ntechlab_006, giving FMR(T) = 0.0001 globally.

Figure 223: For algorithm ntechlab-006 operating on visa images, the heatmap shows false match rates observed over impostor comparisons of faces from different individuals who were born in the given region pair. False matches are counted against a recognition threshold fixed globally to give the target FMR in the plot title, computed over all on the order of 10^{10} impostor comparisons. If text appears in each box it give the same quantity as that coded by the color. Grey indicates FMR is at the intended FMR target level. Light red colors present a security vulnerability to, for example, a passport gate. Each +1 increase in $\log_{10} \text{FMR}$ corresponds to a factor of 10 increase in FMR. The matrix is not quite symmetric because images in the enrollment and verification sets are different.

Cross region FMR at threshold T = 1.416 for algorithm ntechlab_007, giving FMR(T) = 0.0001 globally.

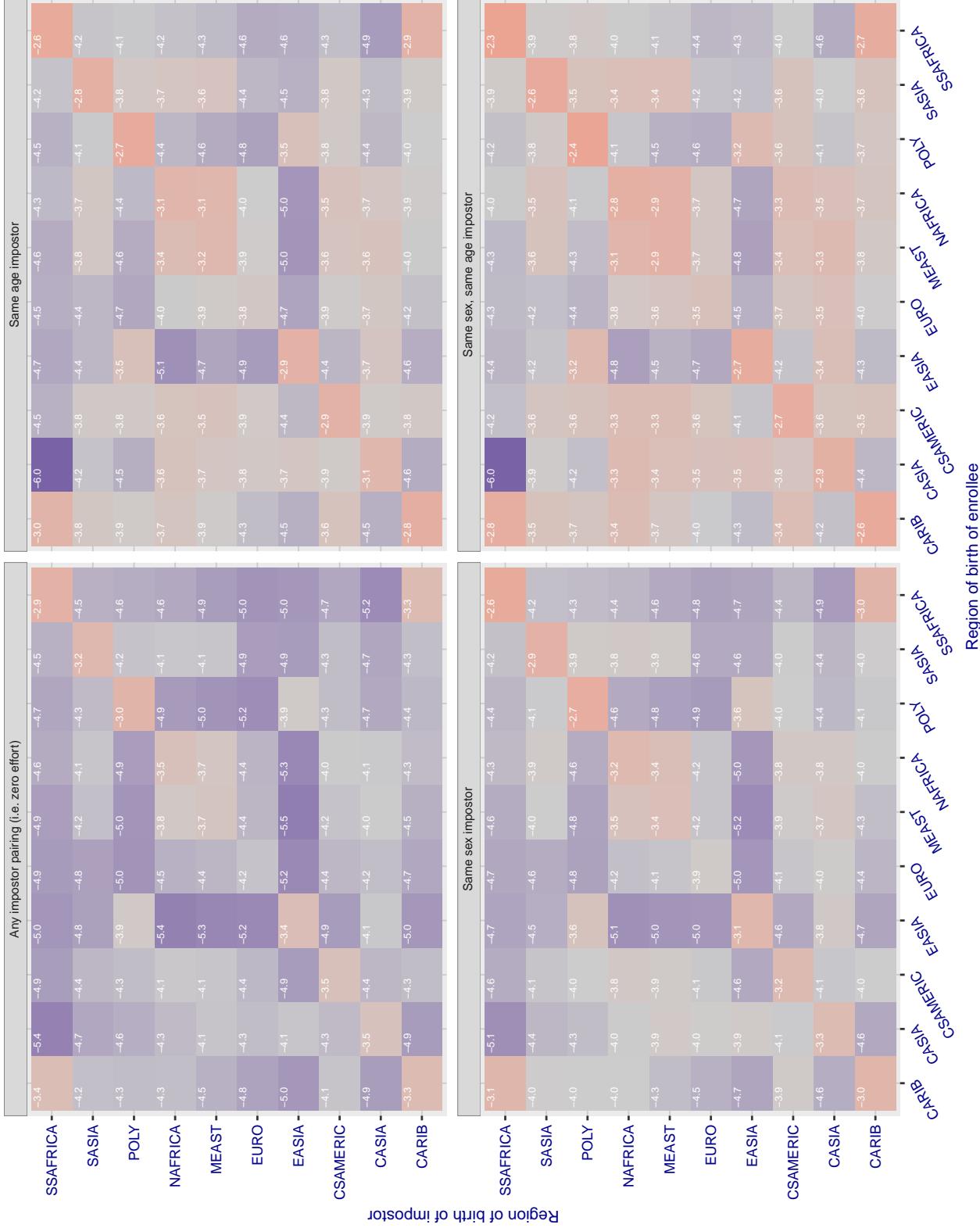


Figure 224: For algorithm ntechlab-007 operating on visa images, the heatmap shows false match rates observed over impostor comparisons of faces from different individuals who were born in the given region pair. False matches are counted against a recognition threshold fixed globally to give the target FMR in the plot title, computed over all on the order of 10^{10} impostor comparisons. If text appears in each box it give the same quantity as that coded by the color. Grey indicates FMR is at the intended FMR target level. Light red colors present a security vulnerability to, for example, a passport gate. Each +1 increase in $\log_{10} FMR$ corresponds to a factor of 10 increase in FMR. The matrix is not quite symmetric because images in the enrollment and verification sets are different.

Cross region FMR at threshold T = 0.428 for algorithm pixelall_002, giving FMR(T) = 0.0001 globally.

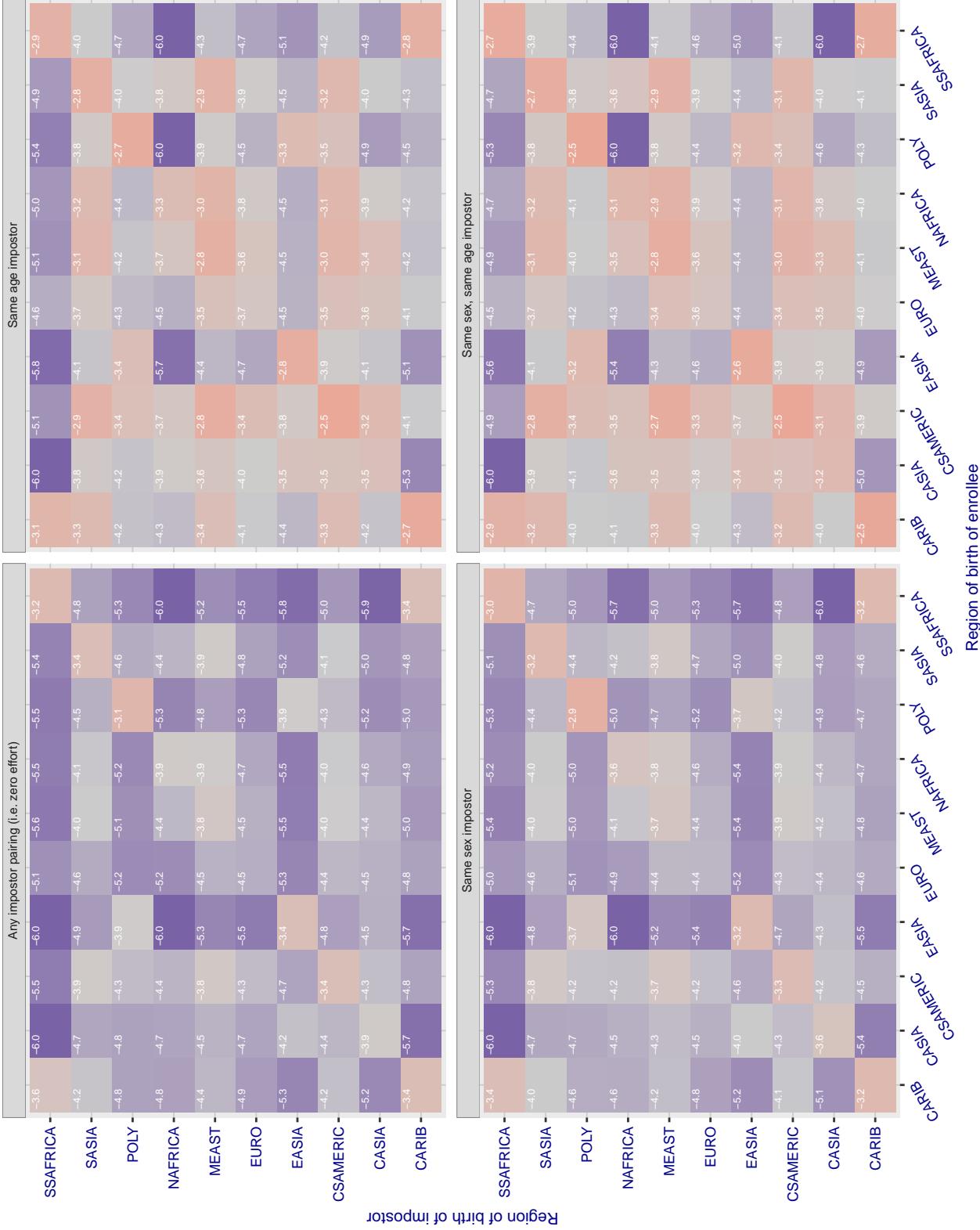


Figure 225: For algorithm pixelall-002 operating on visa images, the heatmap shows false match rates observed over impostor comparisons of faces from different individuals who were born in the given region pair. False matches are counted against a recognition threshold fixed globally to give the target FMR in the plot title, computed over all on the order of 10^{10} impostor comparisons. If text appears in each box it give the same quantity as that coded by the color. Grey indicates FMR is at the intended FMR target level. Light red colors present a security vulnerability to, for example, a passport gate. Each +1 increase in $\log_{10} \text{FMR}$ corresponds to a factor of 10 increase in FMR. The matrix is not quite symmetric because images in the enrollment and verification sets are different.

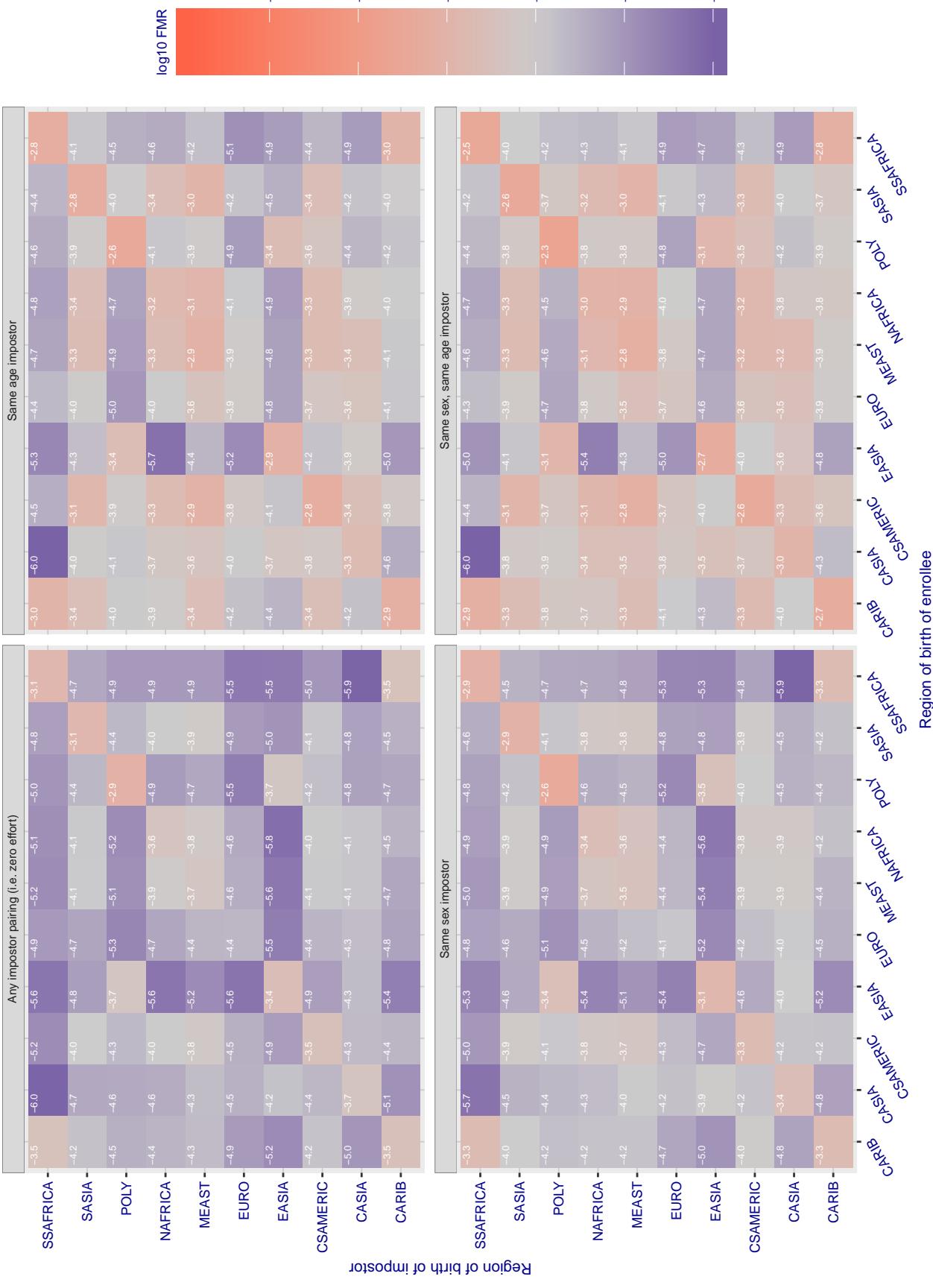
Cross region FMR at threshold T = 0.337 for algorithm psl_001, giving FMR(T) = 0.0001 globally.

Figure 226: For algorithm psl-001 operating on visa images, the heatmap shows false match rates observed over impostor comparisons of faces from different individuals who were born in the given region pair. False matches are counted against a recognition threshold fixed globally to give the target FMR in the plot title, computed over all on the order of 10^{10} impostor comparisons. If text appears in each box it give the same quantity as that coded by the color. Grey indicates FMR is at the intended FMR target level. Light red colors present a security vulnerability to, for example, a passport gate. Each +1 increase in $\log 10$ FMR corresponds to a factor of 10 increase in FMR. The matrix is not quite symmetric because images in the enrollment and verification sets are different.

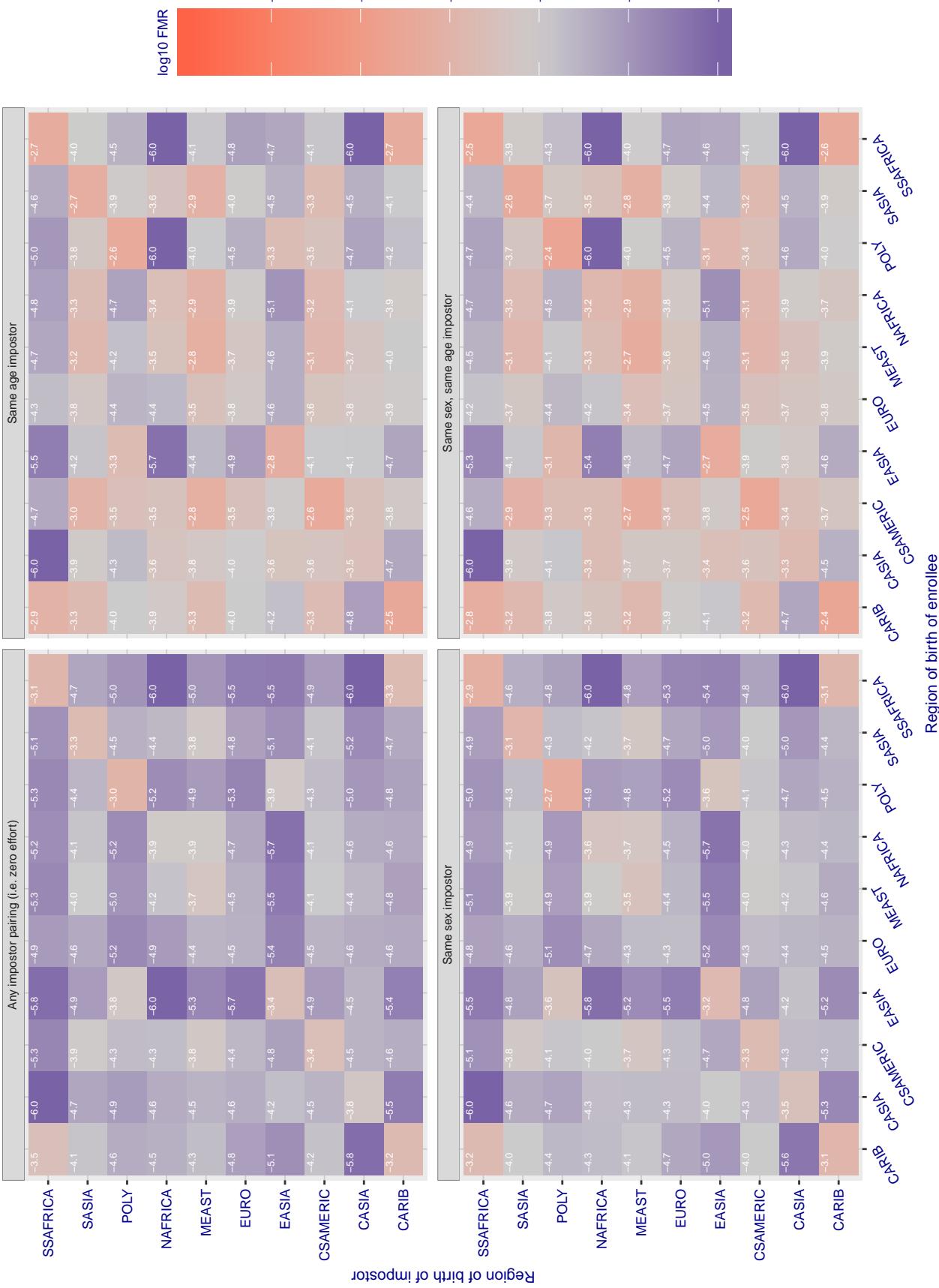
Cross region FMR at threshold T = 0.353 for algorithm psl_002, giving FMR(T) = 0.0001 globally.

Figure 227: For algorithm psl-002 operating on visa images, the heatmap shows false match rates observed over impostor comparisons of faces from different individuals who were born in the given region pair. False matches are counted against a recognition threshold fixed globally to give the target FMR in the plot title, computed over all on the order of 10^{10} impostor comparisons. If text appears in each box it give the same quantity as that coded by the color. Grey indicates FMR is at the intended FMR target level. Light red colors present a security vulnerability to, for example, a passport gate. Each +1 increase in $\log 10 \text{ FMR}$ corresponds to a factor of 10 increase in FMR. The matrix is not quite symmetric because images in the enrollment and verification sets are different.

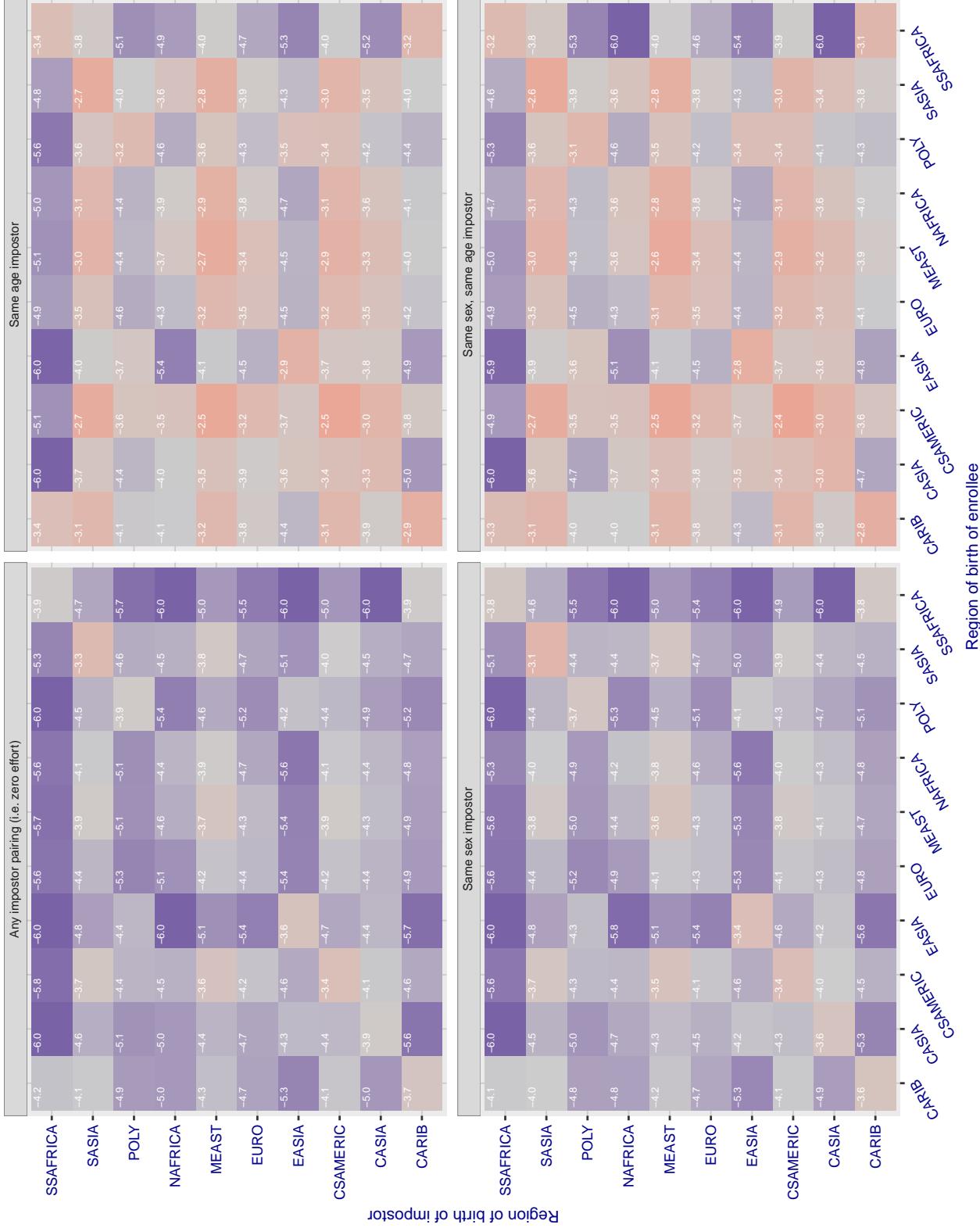
Cross region FMR at threshold T = 0.779 for algorithm rankone_006, giving FMR(T) = 0.0001 globally.

Figure 228: For algorithm rankone-006 operating on visa images, the heatmap shows false match rates observed over impostor comparisons of faces from different individuals who were born in the given region pair. False matches are counted against a recognition threshold fixed globally to give the target FMR in the plot title, computed over all on the order of 10^{10} impostor comparisons. If text appears in each box it give the same quantity as that coded by the color. Grey indicates FMR is at the intended FMR target level. Light red colors present a security vulnerability to, for example, a passport gate. Each +1 increase in $\log_{10} \text{FMR}$ corresponds to a factor of 10 increase in FMR. The matrix is not quite symmetric because images in the enrollment and verification sets are different.

Cross region FMR at threshold $T = 0.661$ for algorithm rankone_007, giving $FMR(T) = 0.0001$ globally.

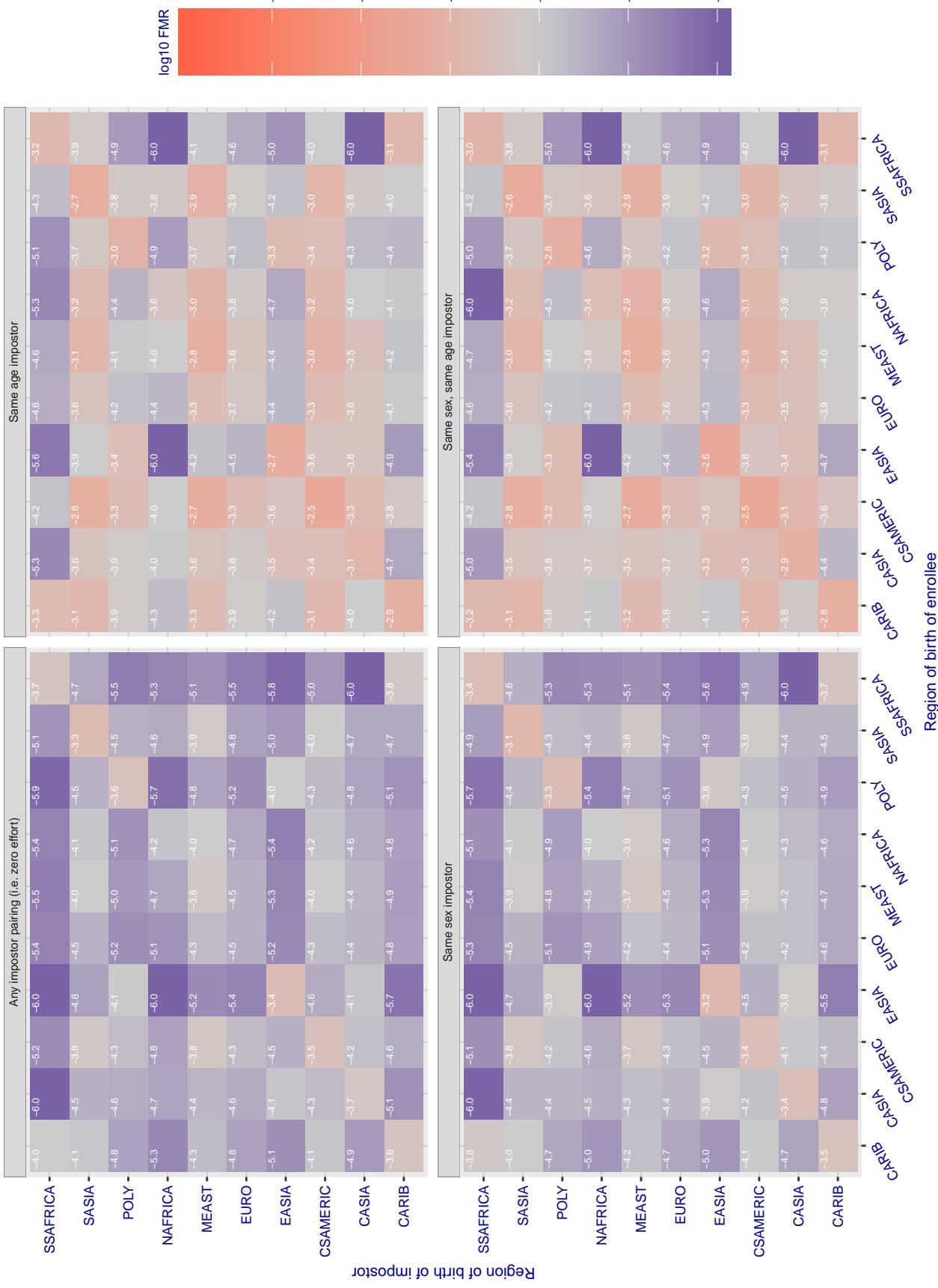


Figure 229: For algorithm rankone-007 operating on visa images, the heatmap shows false match rates observed over impostor comparisons of faces from different individuals who were born in the given region pair. False matches are counted against a recognition threshold fixed globally to give the target FMR in the plot title, computed over all on the order of 10^{10} impostor comparisons. If text appears in each box it give the same quantity as that coded by the color. Grey indicates FMR is at the intended FMR target level. Light red colors present a security vulnerability to, for example, a passport gate. Each +1 increase in \log_{10} FMR corresponds to a factor of 10 increase in FMR. The matrix is not quite symmetric because images in the enrollment and verification sets are different.

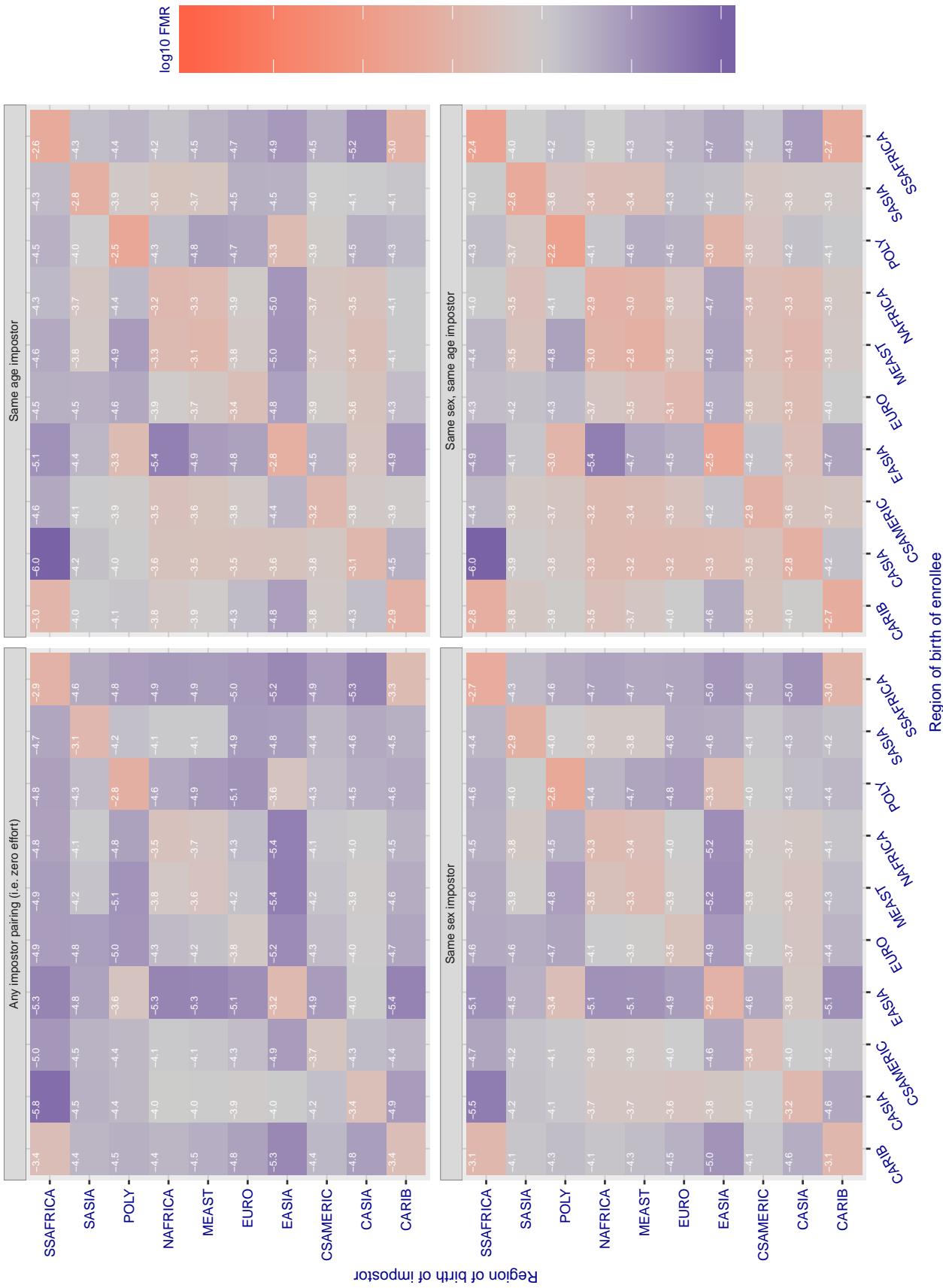
Cross region FMR at threshold T = 0.8883 for algorithm realnetworks_002, giving FMR(T) = 0.00001 globally.

Figure 230: For algorithm realnetworks-002 operating on visa images, the heatmap shows false match rates observed over impostor comparisons of faces from different individuals who were born in the given region pair. False matches are counted against a recognition threshold fixed globally to give the target FMR in the plot title, computed over all on the order of 10^{10} impostor comparisons. If text appears in each box it give the same quantity as that coded by the color. Grey indicates FMR is at the intended FMR target level. Light red colors present a security vulnerability to, for example, a passport gate. Each +1 increase in $\log_{10} \text{FMR}$ corresponds to a factor of 10 increase in FMR. The matrix is not quite symmetric because images in the enrollment and verification sets are different.

Cross region FMR at threshold T = 0.886 for algorithm realnetworks_003, giving FMR(T) = 0.0001 globally.

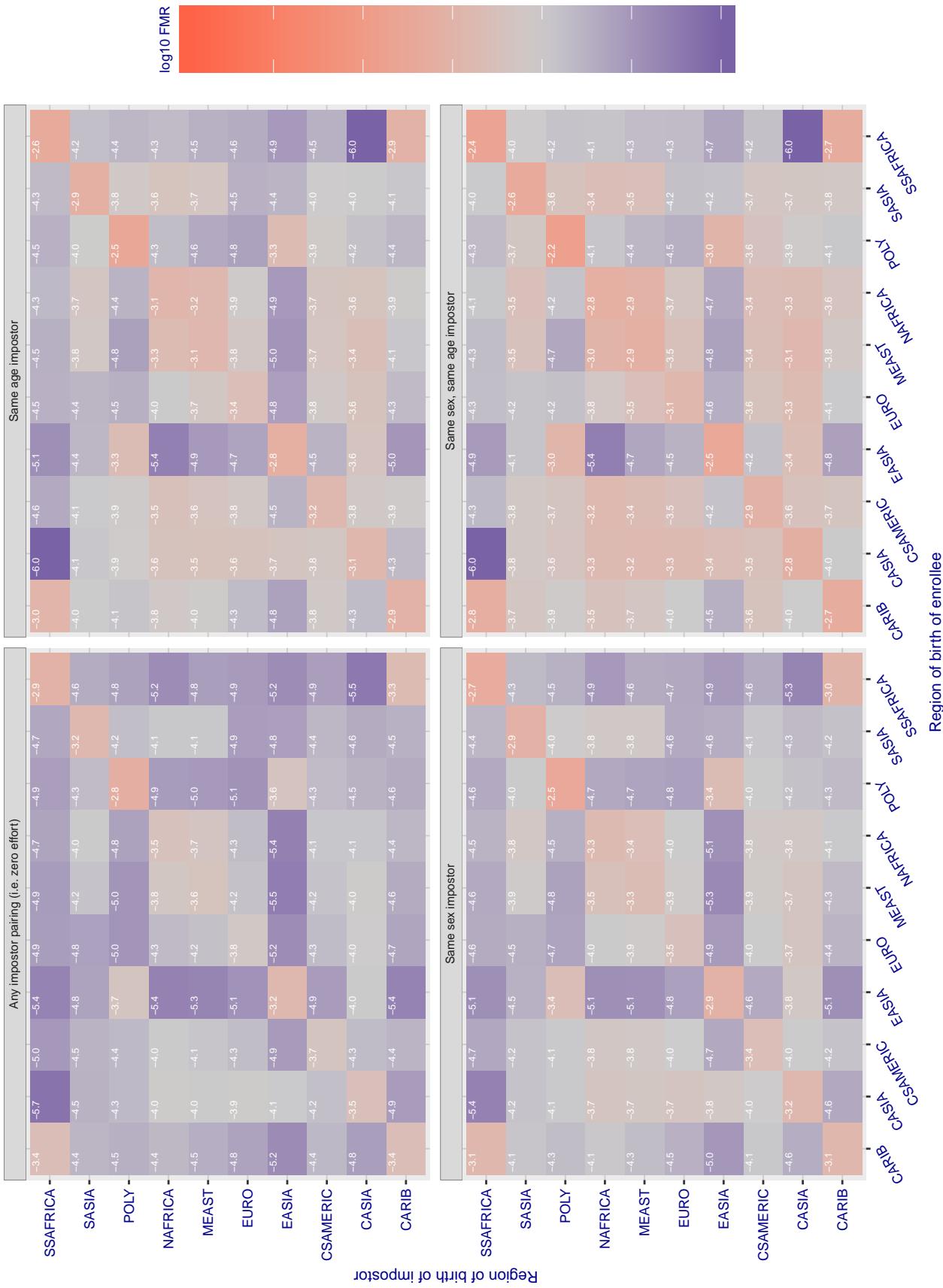


Figure 231: For algorithm realnetworks-003 operating on visa images, the heatmap shows false match rates observed over impostor comparisons of faces from different individuals who were born in the given region pair. False matches are counted against a recognition threshold fixed globally to give the target FMR in the plot title, computed over all on the order of 10^{10} impostor comparisons. If text appears in each box it give the same quantity as that coded by the color. Grey indicates FMR is at the intended FMR target level. Light red colors present a security vulnerability to, for example, a passport gate. Each +1 increase in $\log_{10} FMR$ corresponds to a factor of 10 increase in FMR. The matrix is not quite symmetric because images in the enrollment and verification sets are different.

Cross region FMR at threshold T = 70.373 for algorithm remarkai_000, giving FMR(T) = 0.0001 globally.

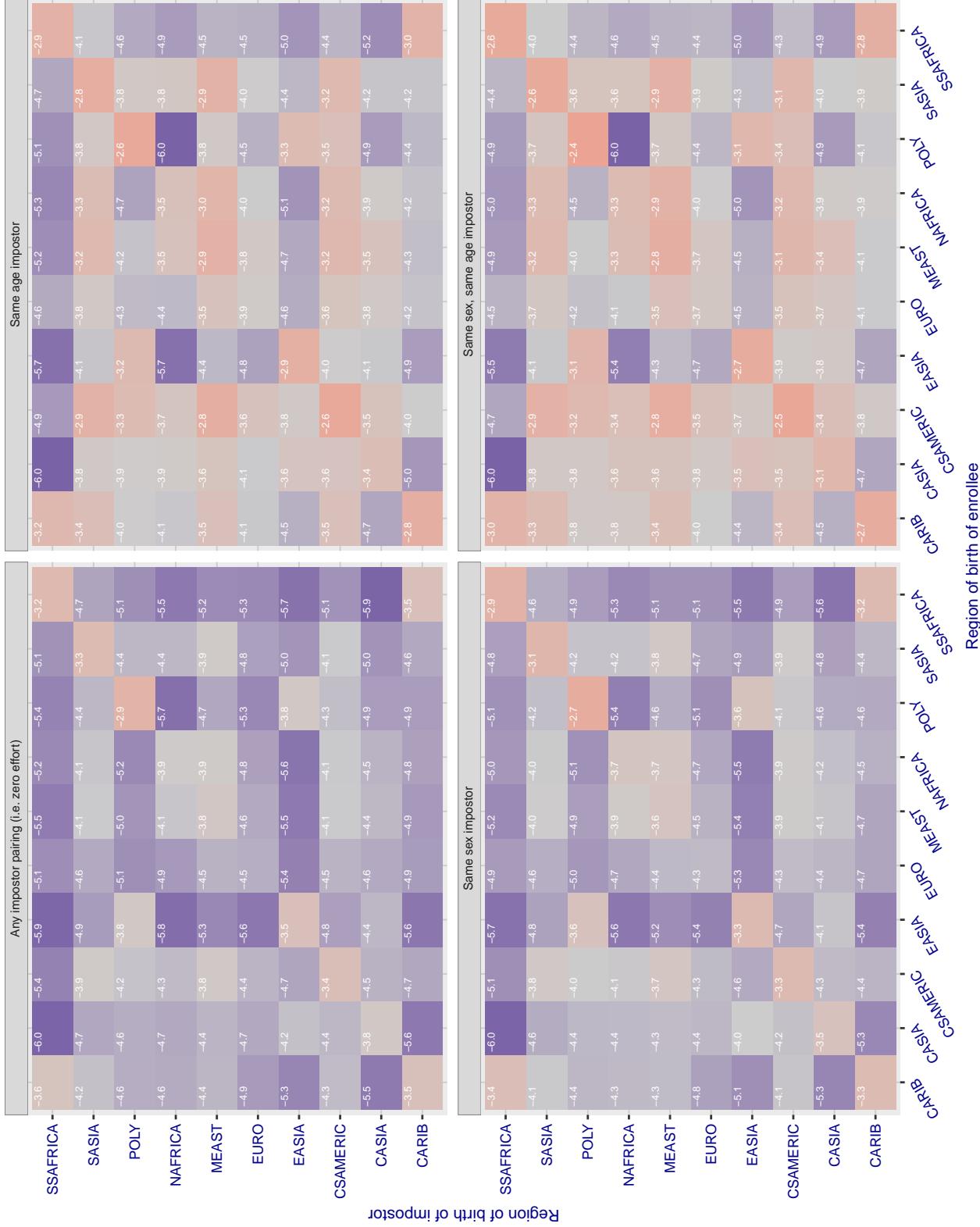


Figure 232: For algorithm remarkai-000 operating on visa images, the heatmap shows false match rates observed over impostor comparisons of faces from different individuals who were born in the given region pair. False matches are counted against a recognition threshold fixed globally to give the target FMR in the plot title, computed over all on the order of 10^{10} impostor comparisons. If text appears in each box it give the same quantity as that coded by the color. Grey indicates FMR is at the intended FMR target level. Light red colors present a security vulnerability to, for example, a passport gate. Each +1 increase in $\log_{10} \text{FMR}$ corresponds to a factor of 10 increase in FMR. The matrix is not quite symmetric because images in the enrollment and verification sets are different.

Cross region FMR at threshold T = 70.384 for algorithm remarkai_001, giving FMR(T) = 0.0001 globally.

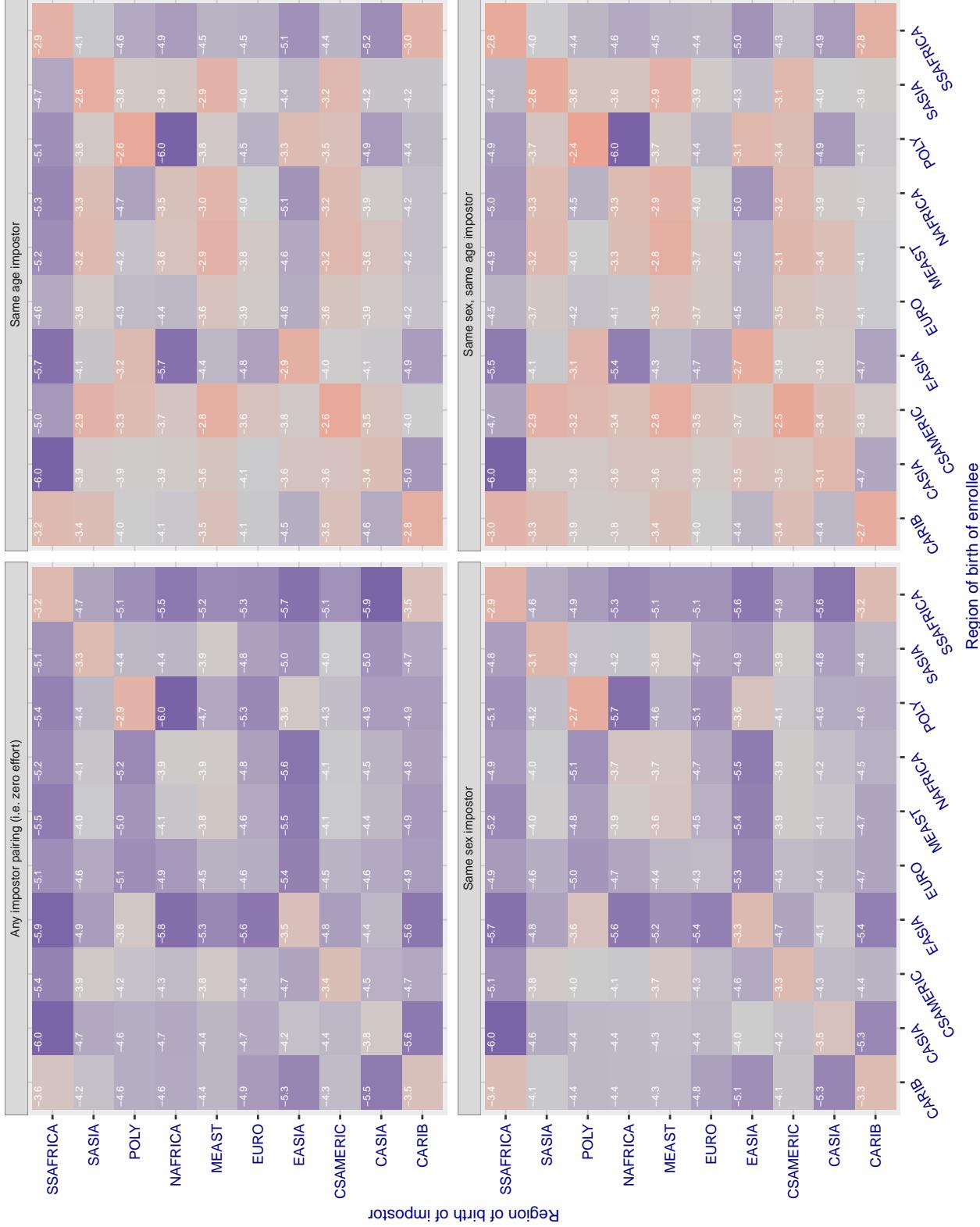


Figure 233: For algorithm remarkai-001 operating on visa images, the heatmap shows false match rates observed over impostor comparisons of faces from different individuals who were born in the given region pair. False matches are counted against a recognition threshold fixed globally to give the target FMR in the plot title, computed over all on the order of 10^{10} impostor comparisons. If text appears in each box it give the same quantity as that coded by the color. Grey indicates FMR is at the intended FMR target level. Light red colors present a security vulnerability to, for example, a passport gate. Each +1 increase in $\log_{10} FMR$ corresponds to a factor of 10 increase in FMR. The matrix is not quite symmetric because images in the enrollment and verification sets are different.

Cross region FMR at threshold T = 0.663 for algorithm rokid_000, giving $FMR(T) = 0.0001$ globally.

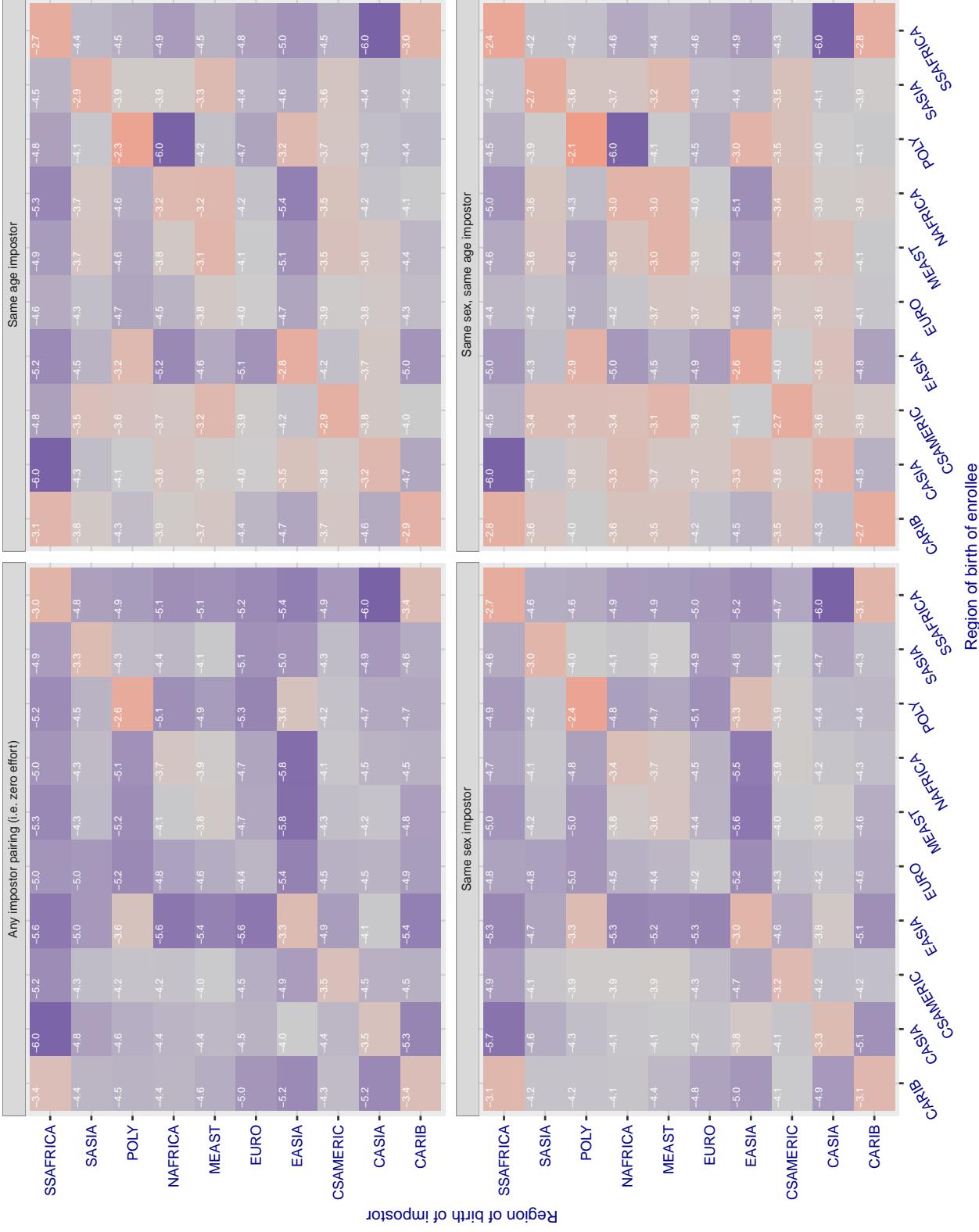


Figure 234: For algorithm rokid-000 operating on visa images, the heatmap shows false match rates observed over impostor comparisons of faces from different individuals who were born in the given region pair. False matches are counted against a recognition threshold fixed globally to give the target FMR in the plot title, computed over all on the order of 10^{10} impostor comparisons. If text appears in each box it give the same quantity as that coded by the color. Grey indicates FMR is at the intended FMR target level. Light red colors present a security vulnerability to, for example, a passport gate. Each +1 increase in $\log_{10} FMR$ corresponds to a factor of 10 increase in FMR. The matrix is not quite symmetric because images in the enrollment and verification sets are different.

Cross region FMR at threshold T = 0.682 for algorithm saffe_001, giving FMR(T) = 0.0001 globally.

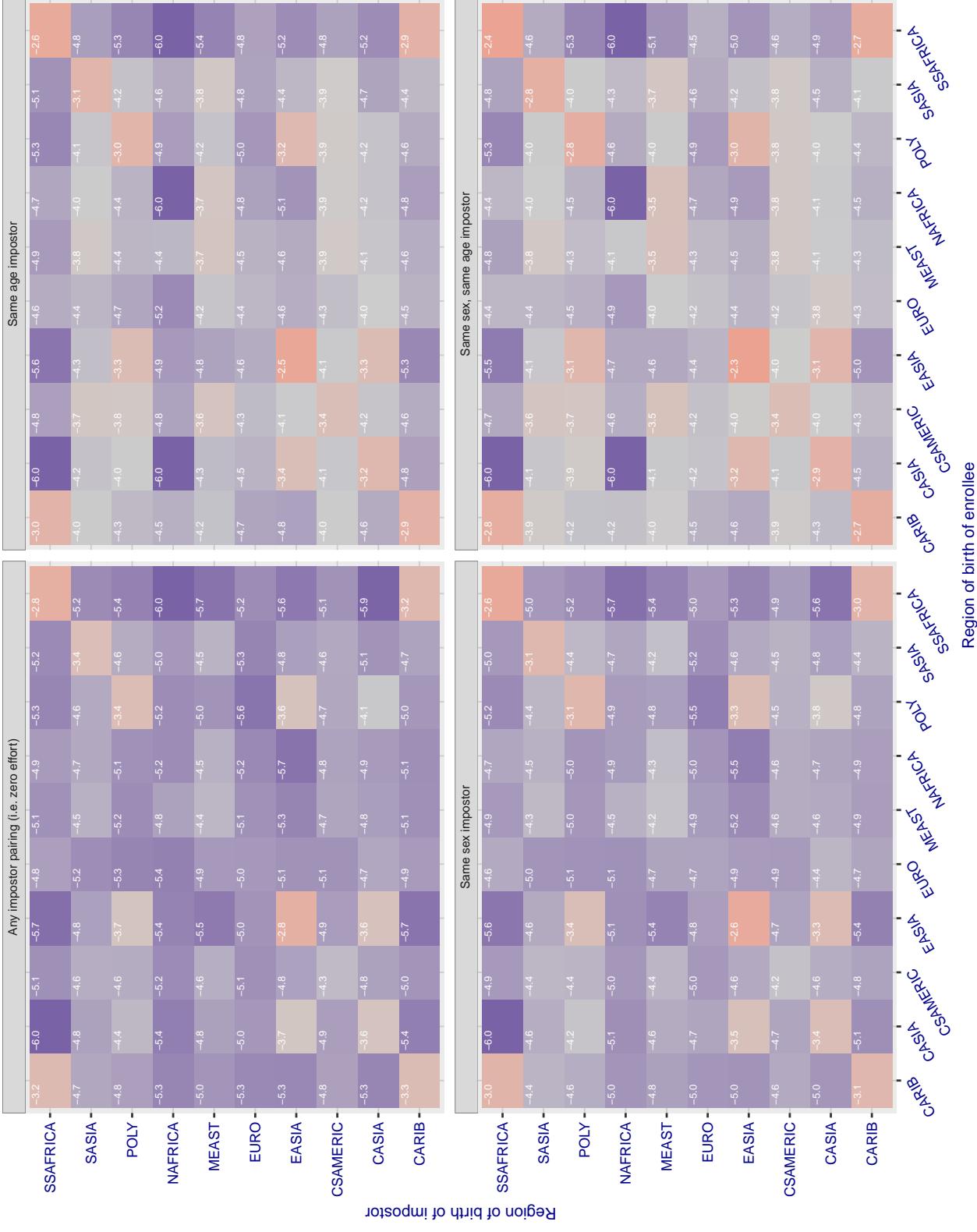


Figure 235: For algorithm saffe-001 operating on visa images, the heatmap shows false match rates observed over impostor comparisons of faces from different individuals who were born in the given region pair. False matches are counted against a recognition threshold fixed globally to give the target FMR in the plot title, computed over all on the order of 10^{10} impostor comparisons. If text appears in each box it give the same quantity as that coded by the color. Grey indicates FMR is at the intended FMR target level. Light red colors present a security vulnerability to, for example, a passport gate. Each +1 increase in \log_{10} FMR corresponds to a factor of 10 increase in FMR. The matrix is not quite symmetric because images in the enrollment and verification sets are different.

Cross region FMR at threshold T = 0.383 for algorithm saffe_002, giving FMR(T) = 0.0001 globally.

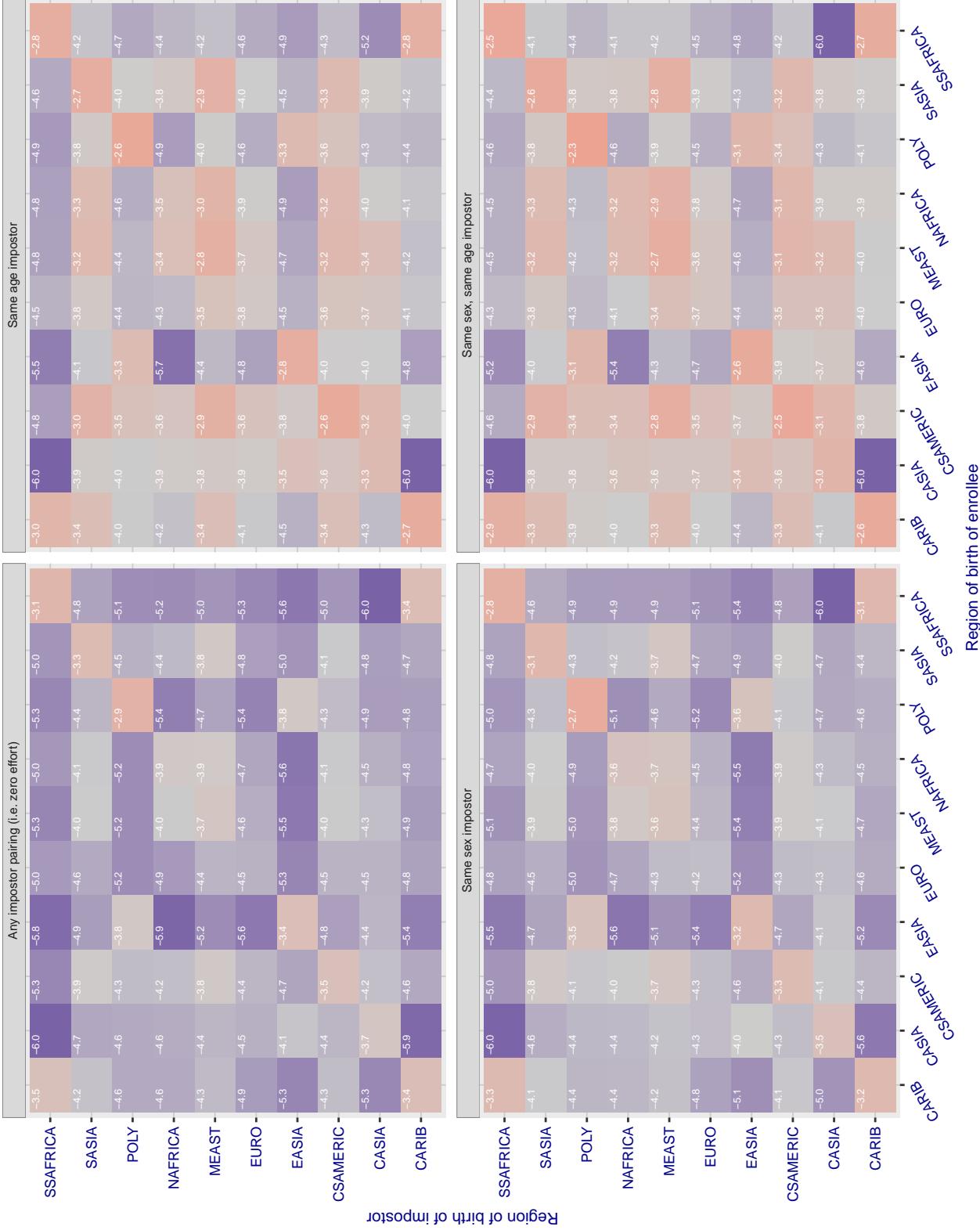


Figure 236: For algorithm saffe-002 operating on visa images, the heatmap shows false match rates observed over impostor comparisons of faces from different individuals who were born in the given region pair. False matches are counted against a recognition threshold fixed globally to give the target FMR in the plot title, computed over all on the order of 10^{10} impostor comparisons. If text appears in each box it give the same quantity as that coded by the color. Grey indicates FMR is at the intended FMR target level. Light red colors present a security vulnerability to, for example, a passport gate. Each +1 increase in $\log 10 \text{ FMR}$ corresponds to a factor of 10 increase in FMR. The matrix is not quite symmetric because images in the enrollment and verification sets are different.

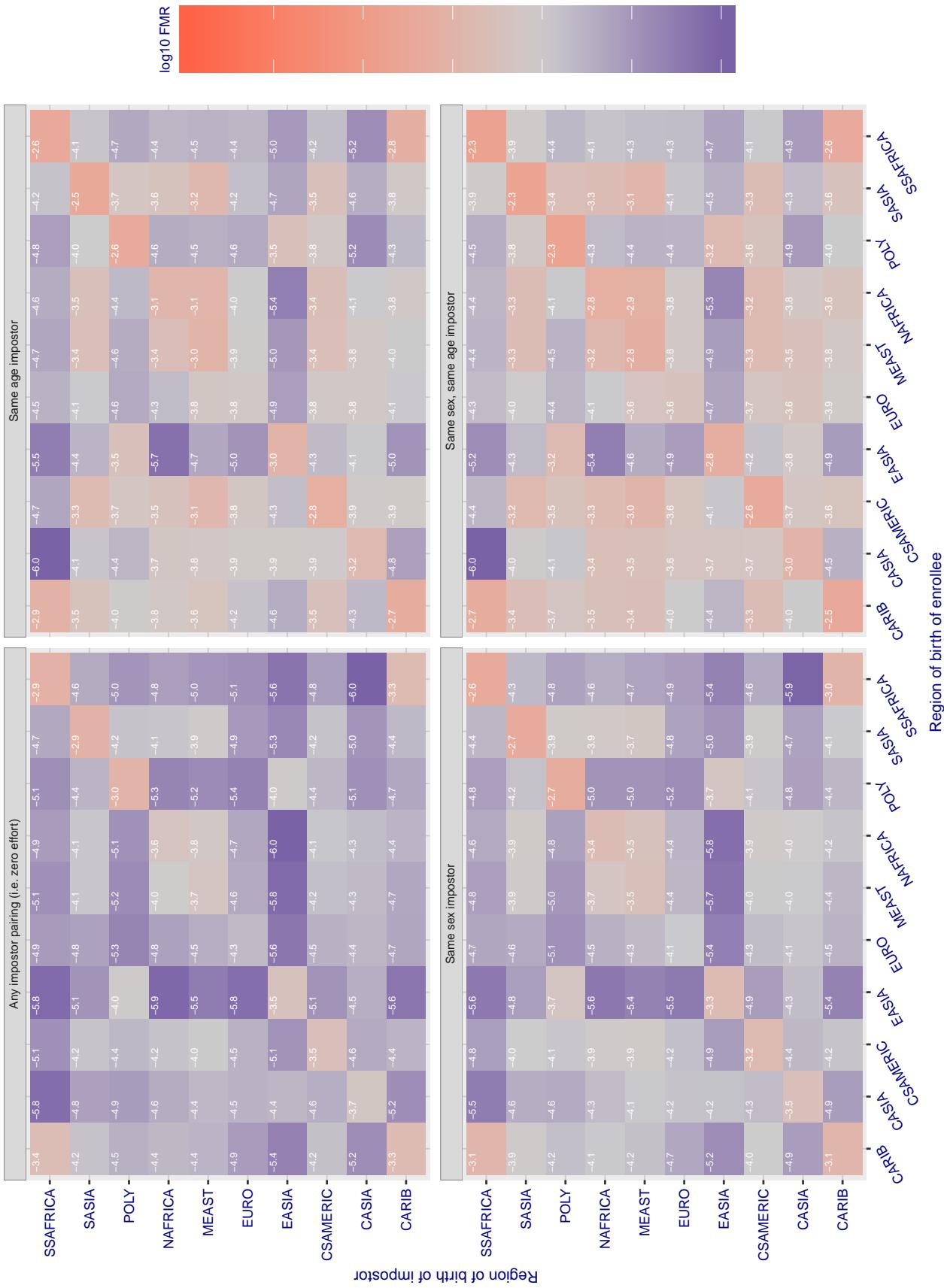
Cross region FMR at threshold T = 0.390 for algorithm sensetime_001, giving FMR(T) = 0.0001 globally.

Figure 237: For algorithm sensetime-001 operating on visa images, the heatmap shows false match rates observed over impostor comparisons of faces from different individuals who were born in the given region pair. False matches are counted against a recognition threshold fixed globally to give the target FMR in the plot title, computed over all on the order of 10^{10} impostor comparisons. If text appears in each box it give the same quantity as that coded by the color. Grey indicates FMR is at the intended FMR target level. Light red colors present a security vulnerability to, for example, a passport gate. Each +1 increase in $\log_{10} \text{FMR}$ corresponds to a factor of 10 increase in FMR. The matrix is not quite symmetric because images in the enrollment and verification sets are different.

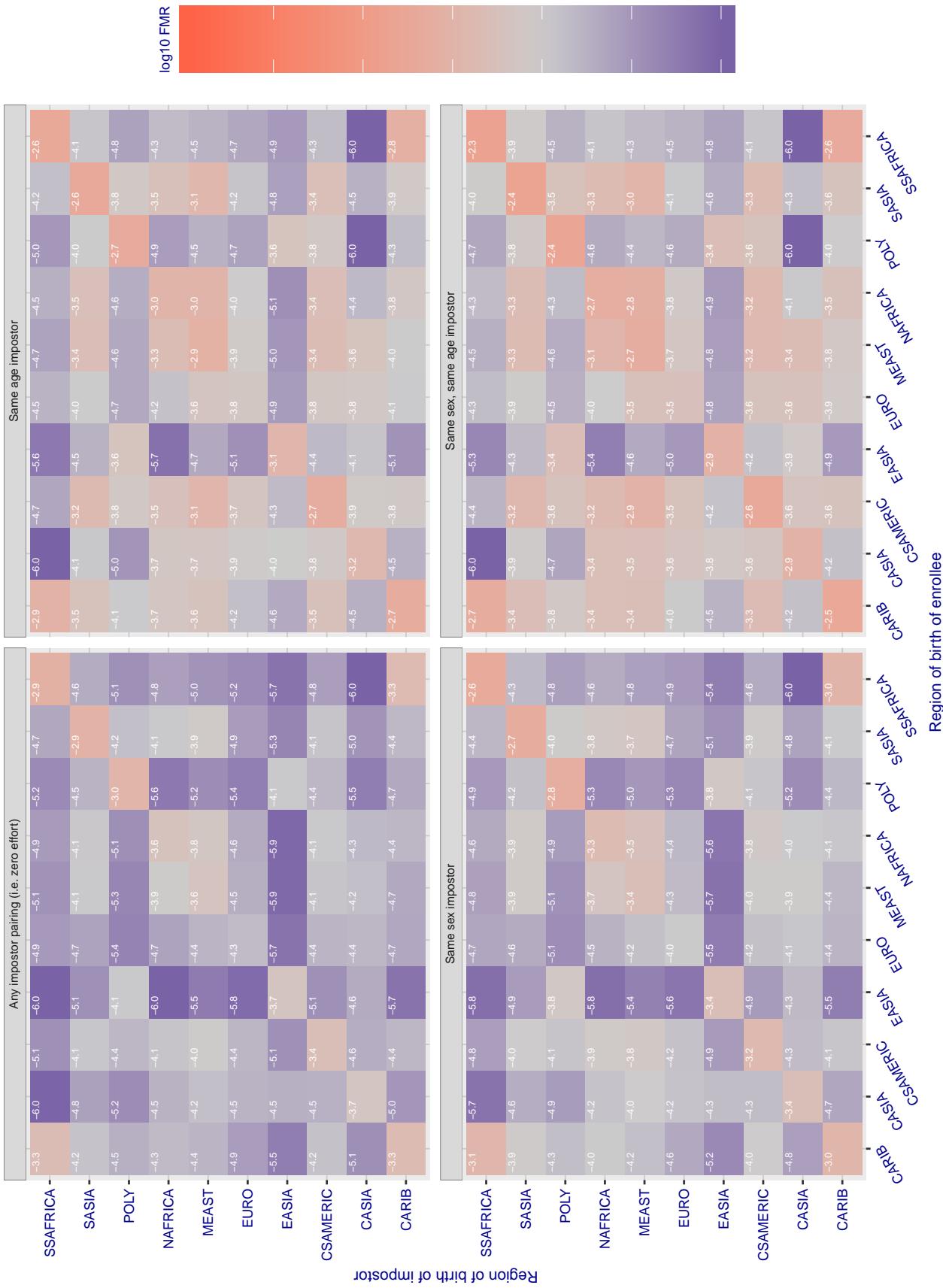
Cross region FMR at threshold T = 0.390 for algorithm sensetime_002, giving FMR(T) = 0.0001 globally.

Figure 238: For algorithm sensetime-002 operating on visa images, the heatmap shows false match rates observed over impostor comparisons of faces from different individuals who were born in the given region pair. False matches are counted against a recognition threshold fixed globally to give the target FMR in the plot title, computed over all on the order of 10^{10} impostor comparisons. If text appears in each box it give the same quantity as that coded by the color. Grey indicates FMR is at the intended FMR target level. Light red colors present a security vulnerability to, for example, a passport gate. Each +1 increase in $\log_{10} \text{FMR}$ corresponds to a factor of 10 increase in FMR. The matrix is not quite symmetric because images in the enrollment and verification sets are different.

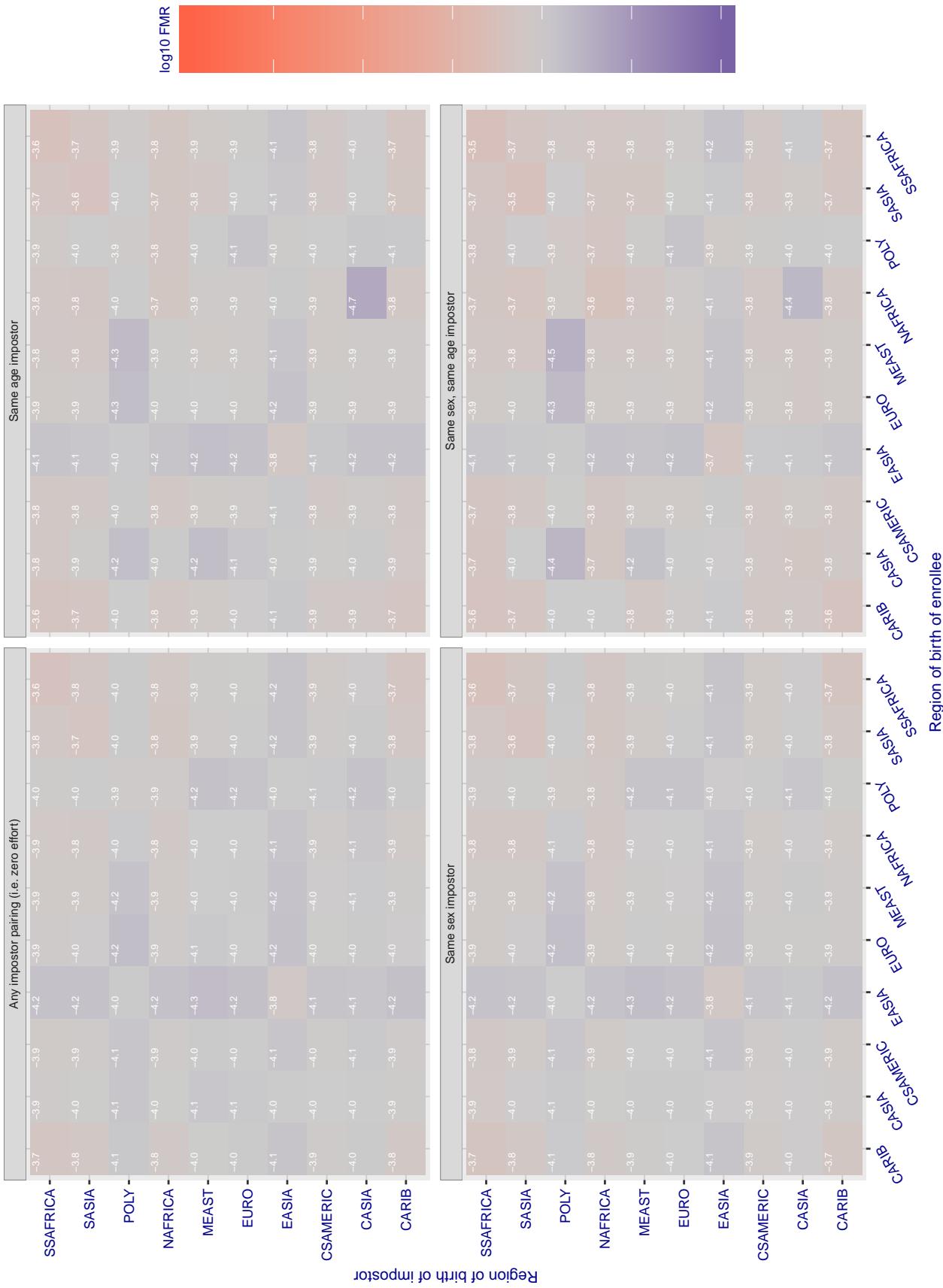
Cross region FMR at threshold T = 0.970 for algorithm shaman_000, giving FMR(T) = 0.0001 globally.

Figure 239: For algorithm shaman-000 operating on visa images, the heatmap shows false match rates observed over impostor comparisons of faces from different individuals who were born in the given region pair. False matches are counted against a recognition threshold fixed globally to give the target FMR in the plot title, computed over all on the order of 10^{10} impostor comparisons. If text appears in each box it give the same quantity as that coded by the color. Grey indicates FMR is at the intended FMR target level. Light red colors present a security vulnerability to, for example, a passport gate. Each +1 increase in $\log_{10} \text{FMR}$ corresponds to a factor of 10 increase in FMR. The matrix is not quite symmetric because images in the enrollment and verification sets are different.

Cross region FMR at threshold T = 0.725 for algorithm shaman_001, giving FMR(T) = 0.0001 globally.

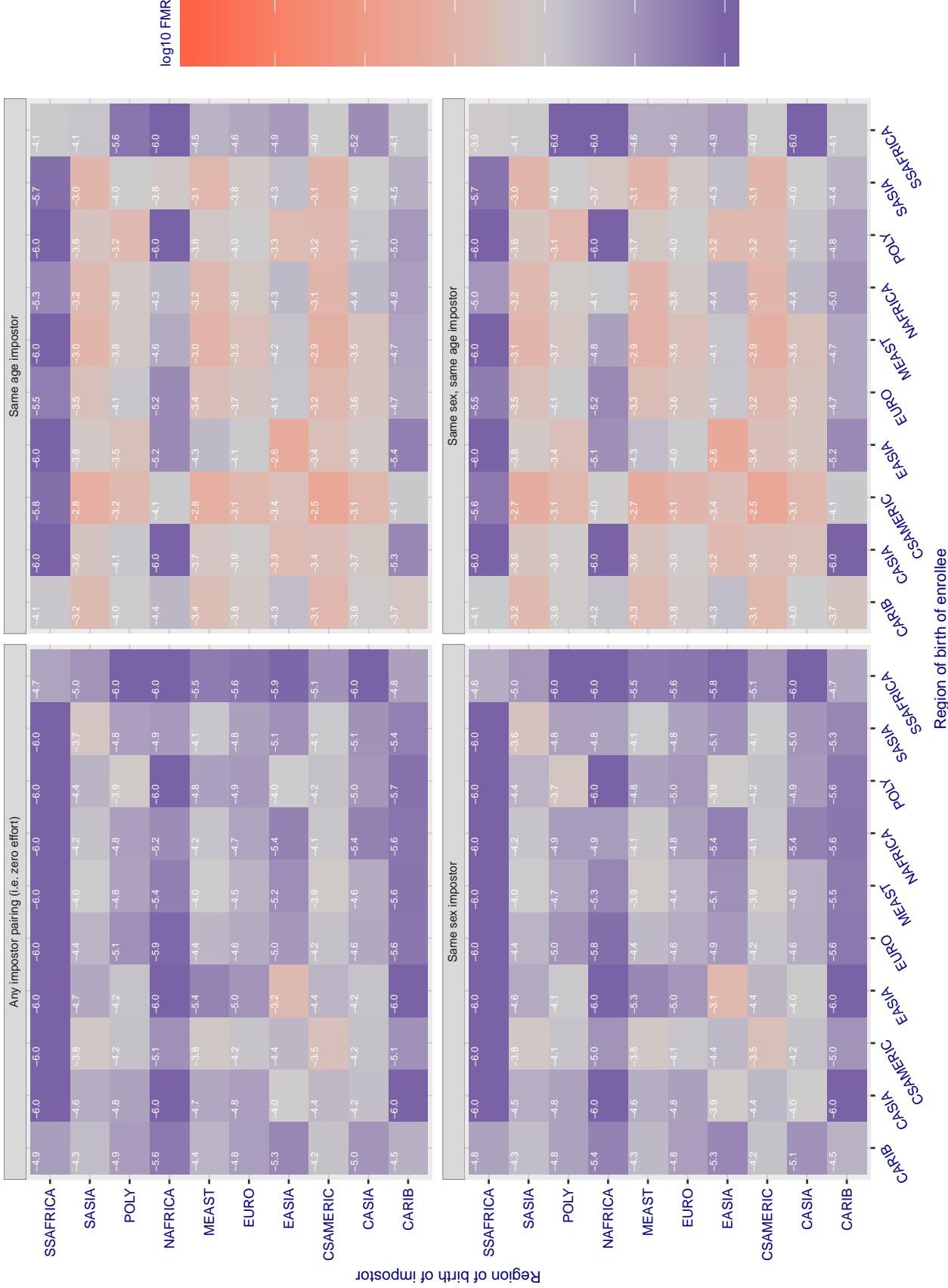


Figure 240: For algorithm shaman-001 operating on visa images, the heatmap shows false match rates observed over impostor comparisons of faces from different individuals who were born in the given region pair. False matches are counted against a recognition threshold fixed globally to give the target FMR in the plot title, computed over all on the order of 10^{10} impostor comparisons. If text appears in each box it give the same quantity as that coded by the color. Grey indicates FMR is at the intended FMR target level. Light red colors present a security vulnerability to, for example, a passport gate. Each +1 increase in $\log_{10} FMR$ corresponds to a factor of 10 increase in FMR. The matrix is not quite symmetric because images in the enrollment and verification sets are different.

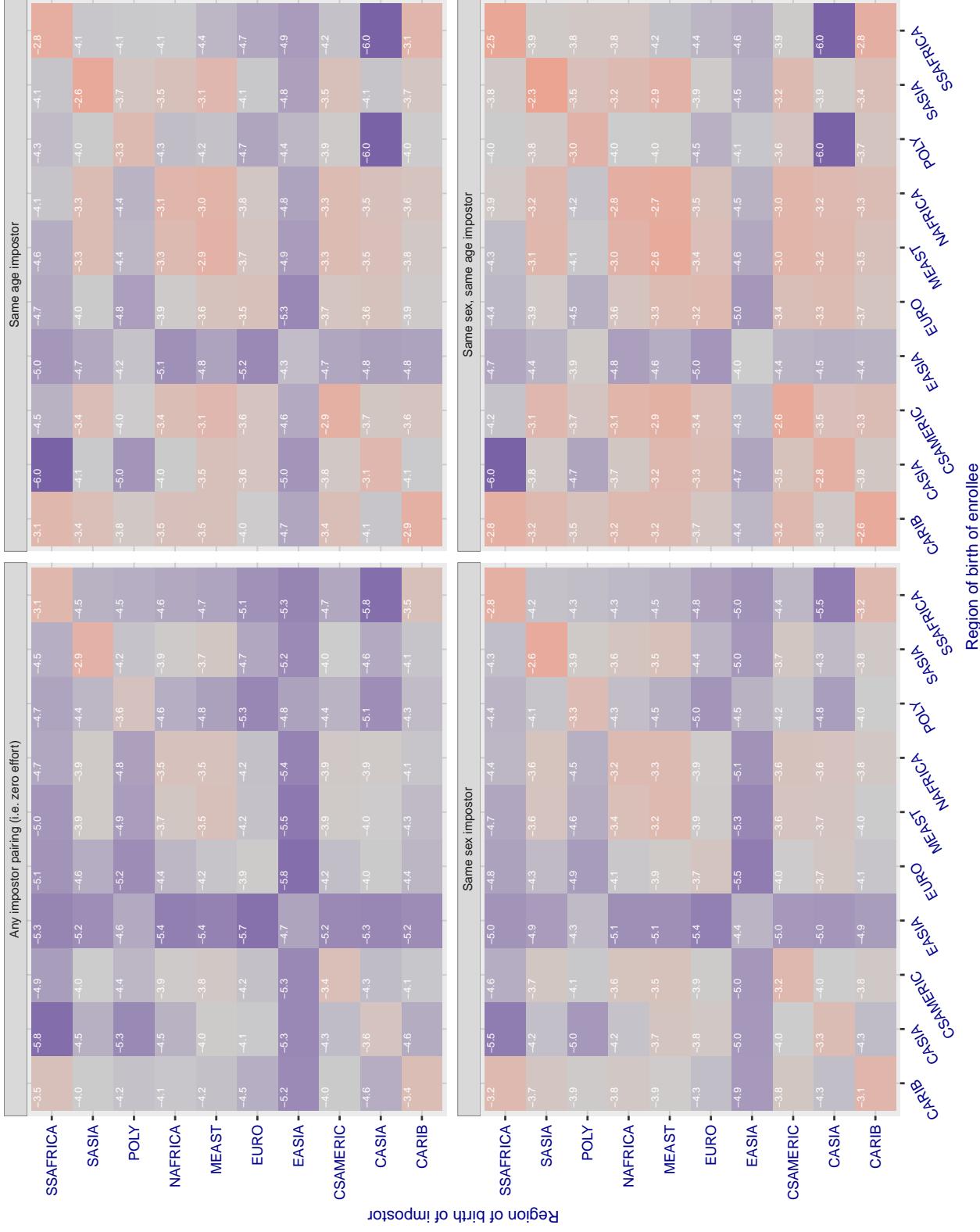
Cross region FMR at threshold T = 0.400 for algorithm shu_001, giving FMR(T) = 0.0001 globally.

Figure 241: For algorithm shu-001 operating on visa images, the heatmap shows false match rates observed over impostor comparisons of faces from different individuals who were born in the given region pair. False matches are counted against a recognition threshold fixed globally to give the target FMR in the plot title, computed over all on the order of 10^{10} impostor comparisons. If text appears in each box it give the same quantity as that coded by the color. Grey indicates FMR is at the intended FMR target level. Light red colors present a security vulnerability to, for example, a passport gate. Each +1 increase in $\log 10 \text{FMR}$ corresponds to a factor of 10 increase in FMR. The matrix is not quite symmetric because images in the enrollment and verification sets are different.

Cross region FMR at threshold T = 0.390 for algorithm siat_002, giving FMR(T) = 0.0001 globally.

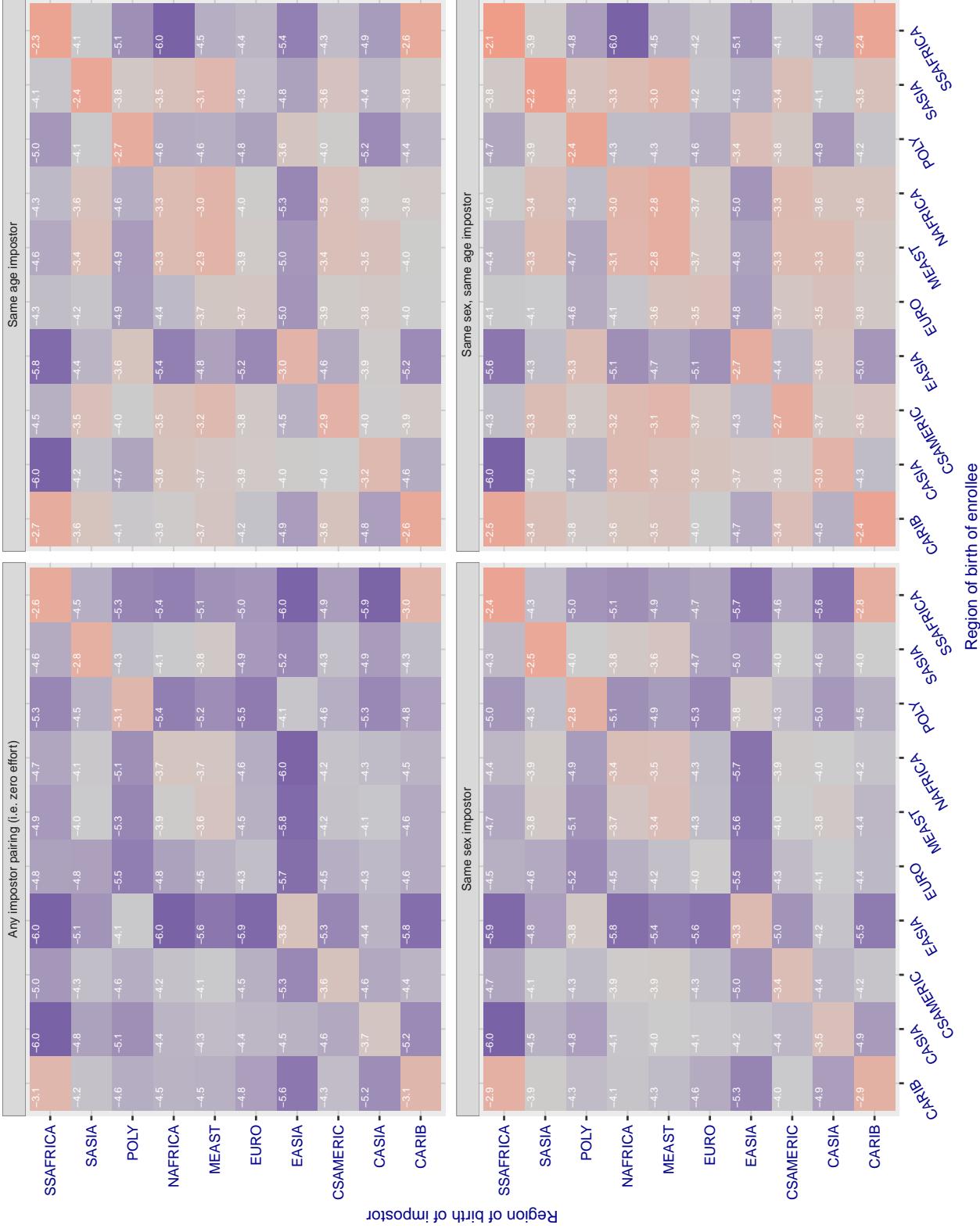


Figure 242: For algorithm siat-002 operating on visa images, the heatmap shows false match rates observed over impostor comparisons of faces from different individuals who were born in the given region pair. False matches are counted against a recognition threshold fixed globally to give the target FMR in the plot title, computed over all on the order of 10^{10} impostor comparisons. If text appears in each box it give the same quantity as that coded by the color. Grey indicates FMR is at the intended FMR target level. Light red colors present a security vulnerability to, for example, a passport gate. Each +1 increase in \log_{10} FMR corresponds to a factor of 10 increase in FMR. The matrix is not quite symmetric because images in the enrollment and verification sets are different.

Cross region FMR at threshold T = 0.393 for algorithm siat_004, giving FMR(T) = 0.0001 globally.

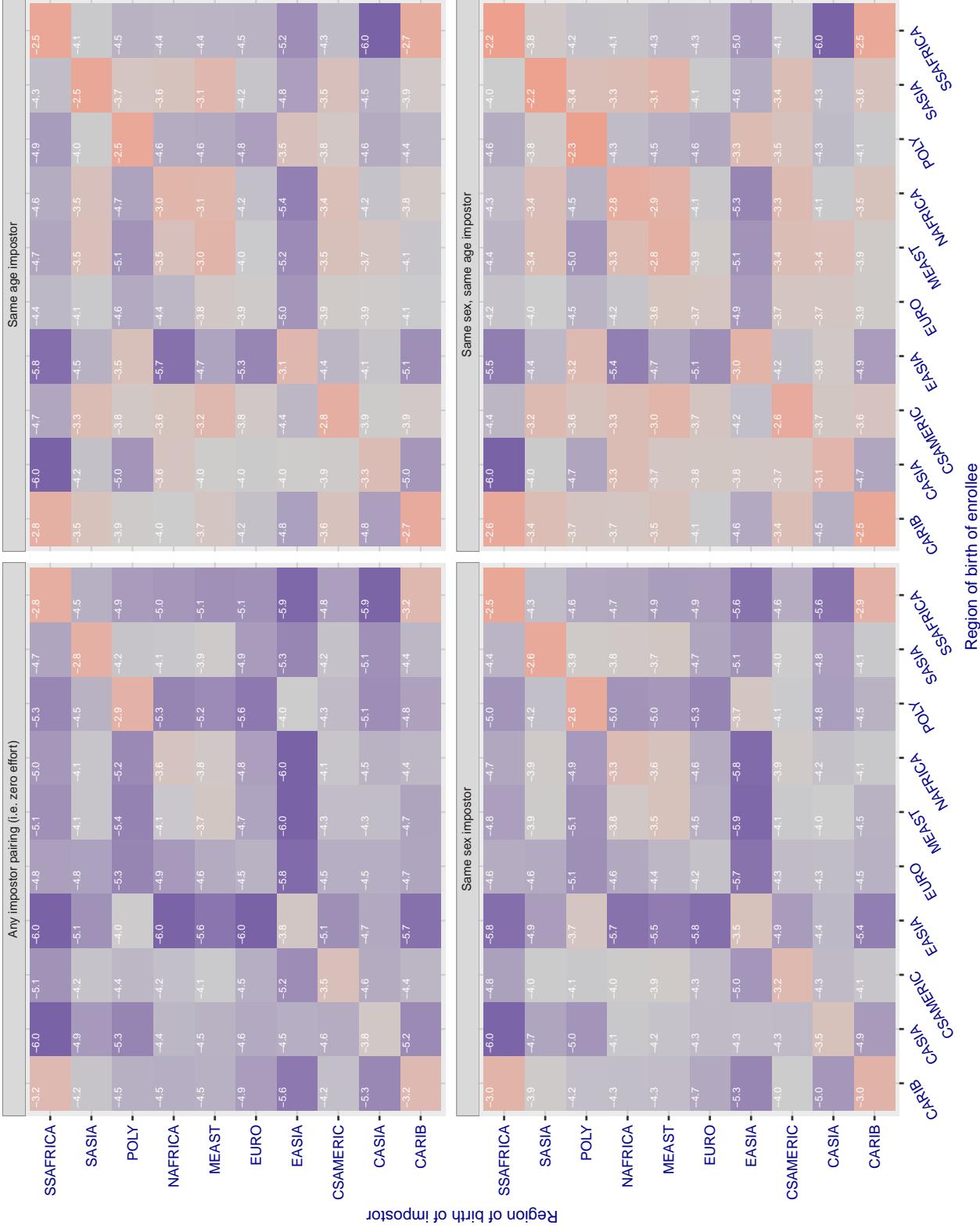


Figure 243: For algorithm siat-004 operating on visa images, the heatmap shows false match rates observed over impostor comparisons of faces from different individuals who were born in the given region pair. False matches are counted against a recognition threshold fixed globally to give the target FMR in the plot title, computed over all on the order of 10^{10} impostor comparisons. If text appears in each box it give the same quantity as that coded by the color. Grey indicates FMR is at the intended FMR target level. Light red colors present a security vulnerability to, for example, a passport gate. Each +1 increase in $\log 10$ FMR corresponds to a factor of 10 increase in FMR. The matrix is not quite symmetric because images in the enrollment and verification sets are different.

Cross region FMR at threshold T = 0.598 for algorithm smilart_002, giving $\text{FMR}(\text{T}) = 0.0001$ globally.

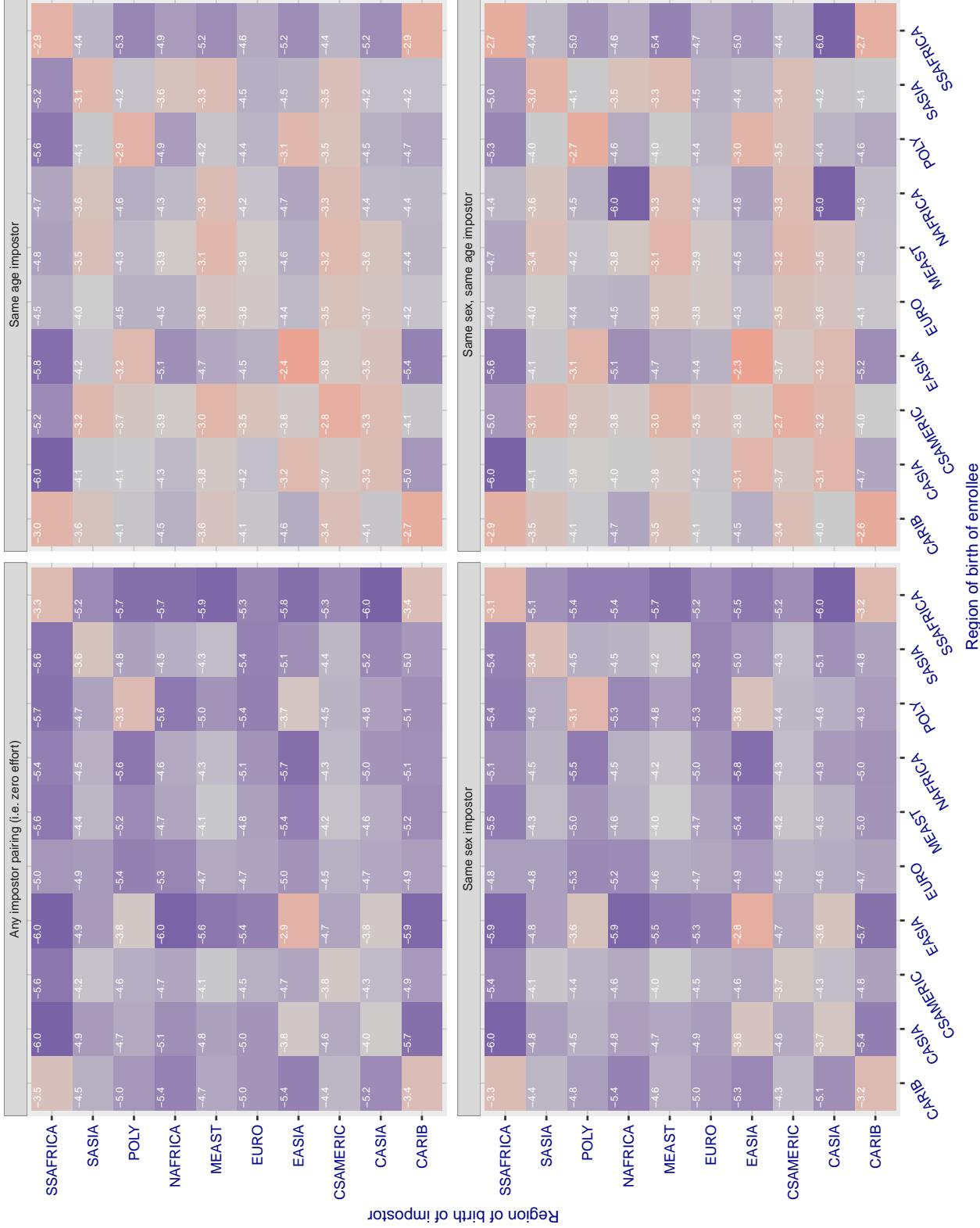


Figure 244: For algorithm smilart-002 operating on visa images, the heatmap shows false match rates observed over impostor comparisons of faces from different individuals who were born in the given region pair. False matches are counted against a recognition threshold fixed globally to give the target FMR in the plot title, computed over all on the order of 10^{10} impostor comparisons. If text appears in each box it give the same quantity as that coded by the color. Grey indicates FMR is at the intended FMR target level. Light red colors present a security vulnerability to, for example, a passport gate. Each +1 increase in $\log_{10} \text{FMR}$ corresponds to a factor of 10 increase in FMR. The matrix is not quite symmetric because images in the enrollment and verification sets are different.

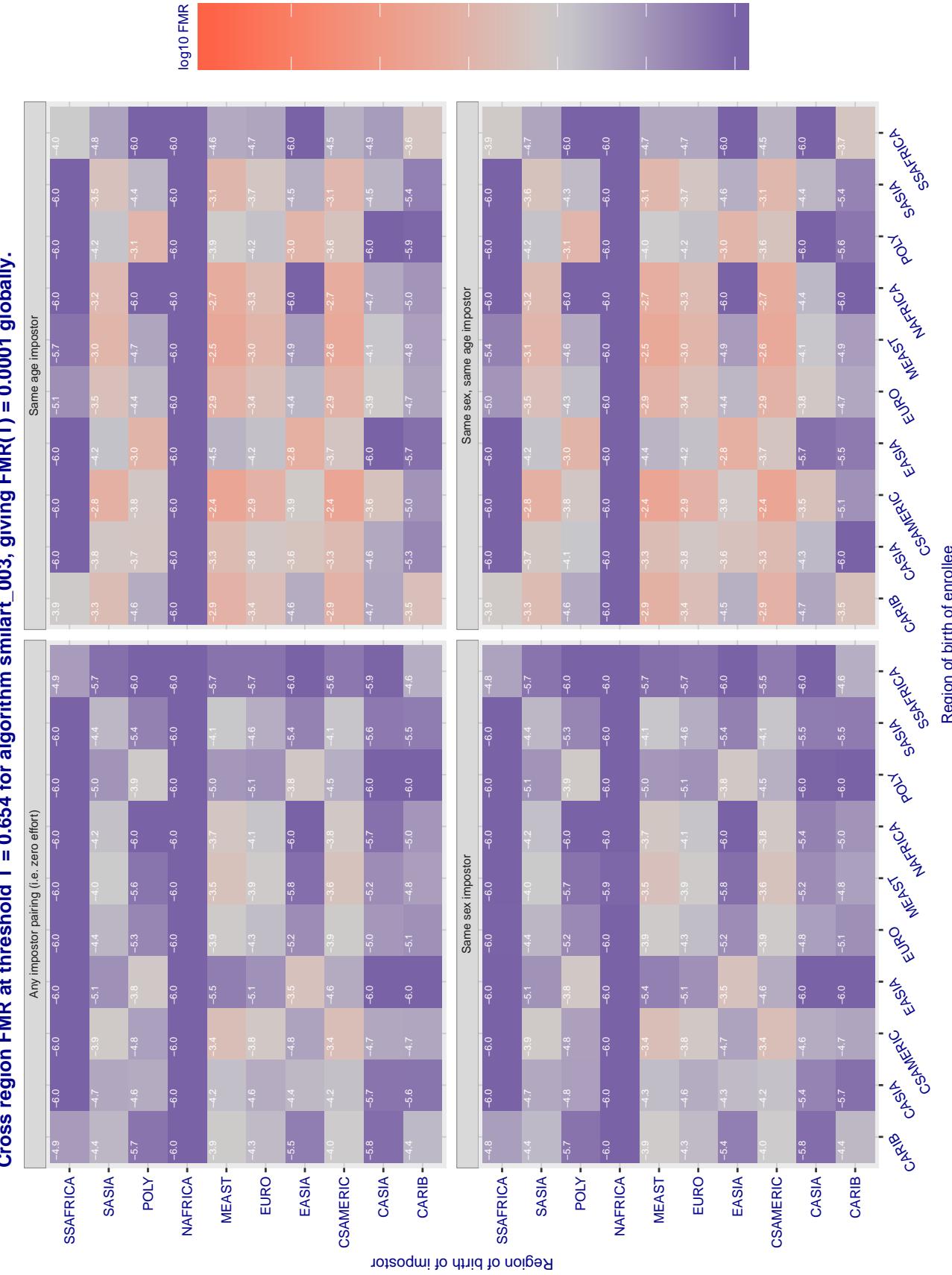


Figure 245: For algorithm *smilart-003* operating on visa images, the heatmap shows false match rates observed over impostor comparisons of faces from different individuals who were born in the given region pair. False matches are counted against a recognition threshold fixed globally to give the target FMR in the plot title, computed over all on the order of 10^{10} impostor comparisons. If text appears in each box it give the same quantity as that coded by the color. Grey indicates FMR is at the intended FMR target level. Light red colors present a security vulnerability to, for example, a passport gate. Each +1 increase in \log_{10} FMR corresponds to a factor of 10 increase in FMR. The matrix is not quite symmetric because images in the enrollment and verification sets are different.

Cross region FMR at threshold T = 0.314 for algorithm starhybrid_001, giving FMR(T) = 0.0001 globally.

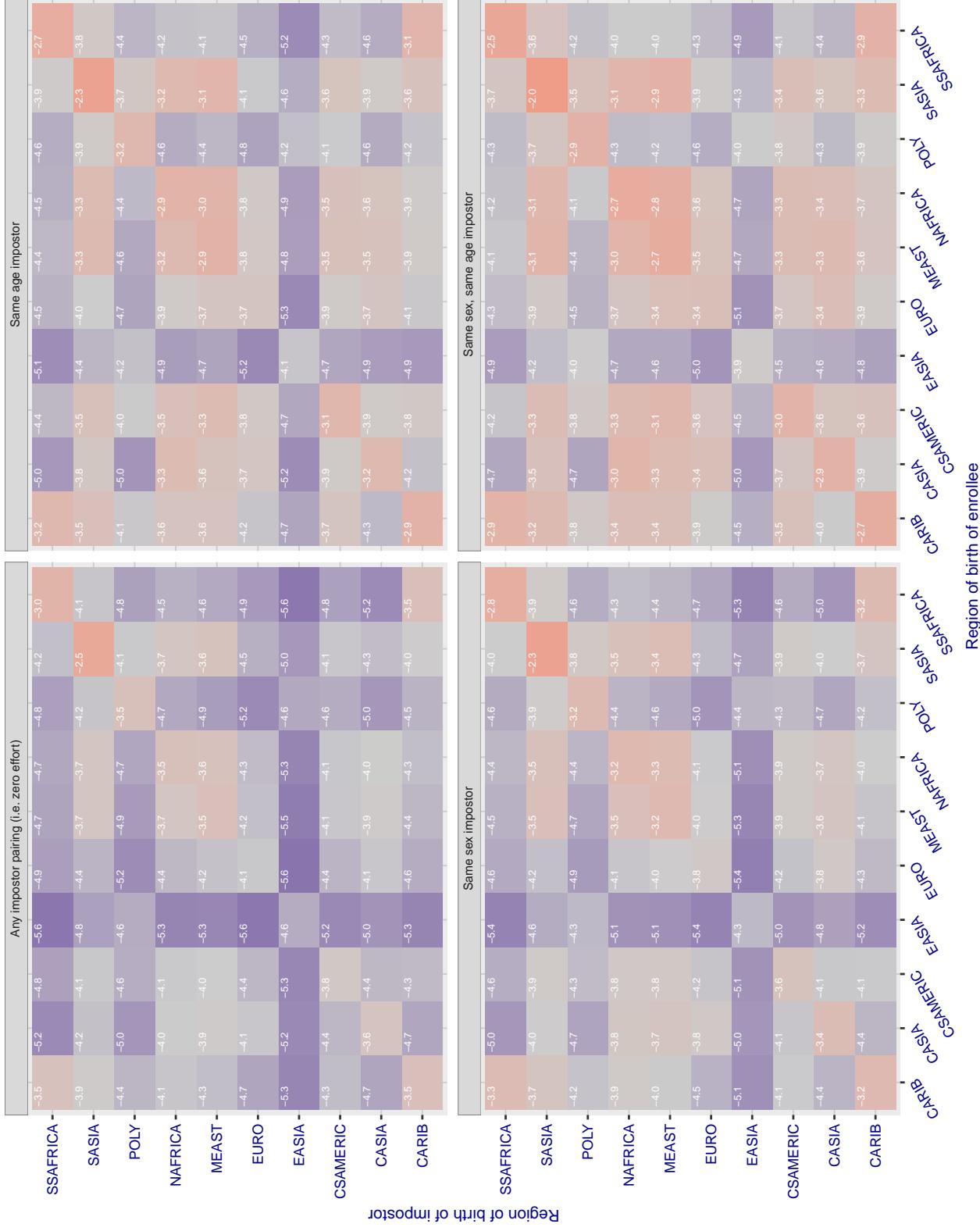


Figure 246: For algorithm starhybrid-001 operating on visa images, the heatmap shows false match rates observed over impostor comparisons of faces from different individuals who were born in the given region pair. False matches are counted against a recognition threshold fixed globally to give the target FMR in the plot title, computed over all on the order of 10^{10} impostor comparisons. If text appears in each box it give the same quantity as that coded by the color. Grey indicates FMR is at the intended FMR target level. Light red colors present a security vulnerability to, for example, a passport gate. Each +1 increase in $\log_{10} \text{FMR}$ corresponds to a factor of 10 increase in FMR. The matrix is not quite symmetric because images in the enrollment and verification sets are different.

Cross region FMR at threshold T = 0.221 for algorithm **synesis_004**, giving FMR(T) = 0.0001 globally.

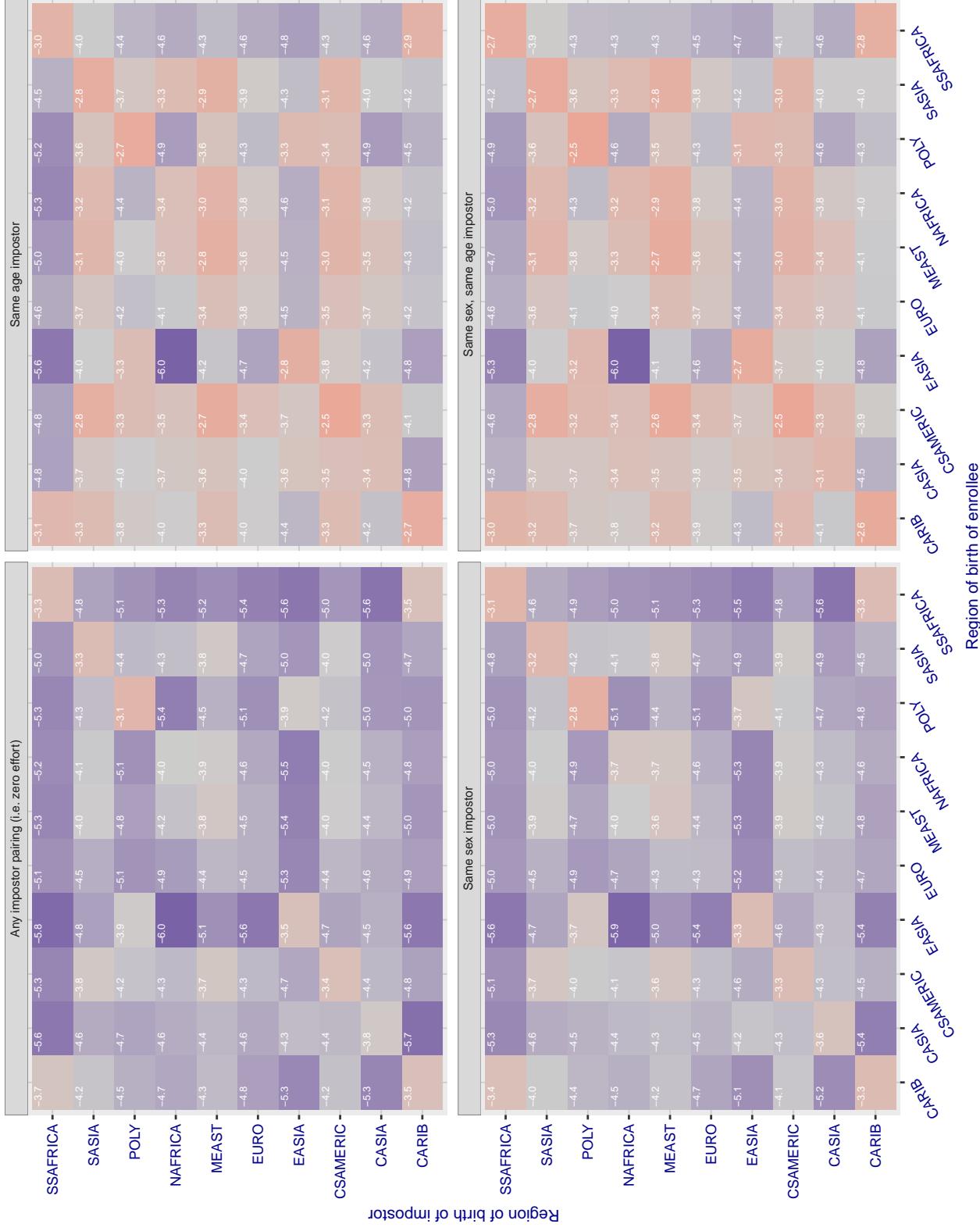


Figure 247: For algorithm **synesis-004** operating on visa images, the heatmap shows false match rates observed over impostor comparisons of faces from different individuals who were born in the given region pair. False matches are counted against a recognition threshold fixed globally to give the target FMR in the plot title, computed over all on the order of 10^{10} impostor comparisons. If text appears in each box it give the same quantity as that coded by the color. Grey indicates FMR is at the intended FMR target level. Light red colors present a security vulnerability to, for example, a passport gate. Each +1 increase in $\log_{10} FMR$ corresponds to a factor of 10 increase in FMR. The matrix is not quite symmetric because images in the enrollment and verification sets are different.

Cross region FMR at threshold T = 0.356 for algorithm **synesis_005**, giving FMR(T) = 0.0001 globally.

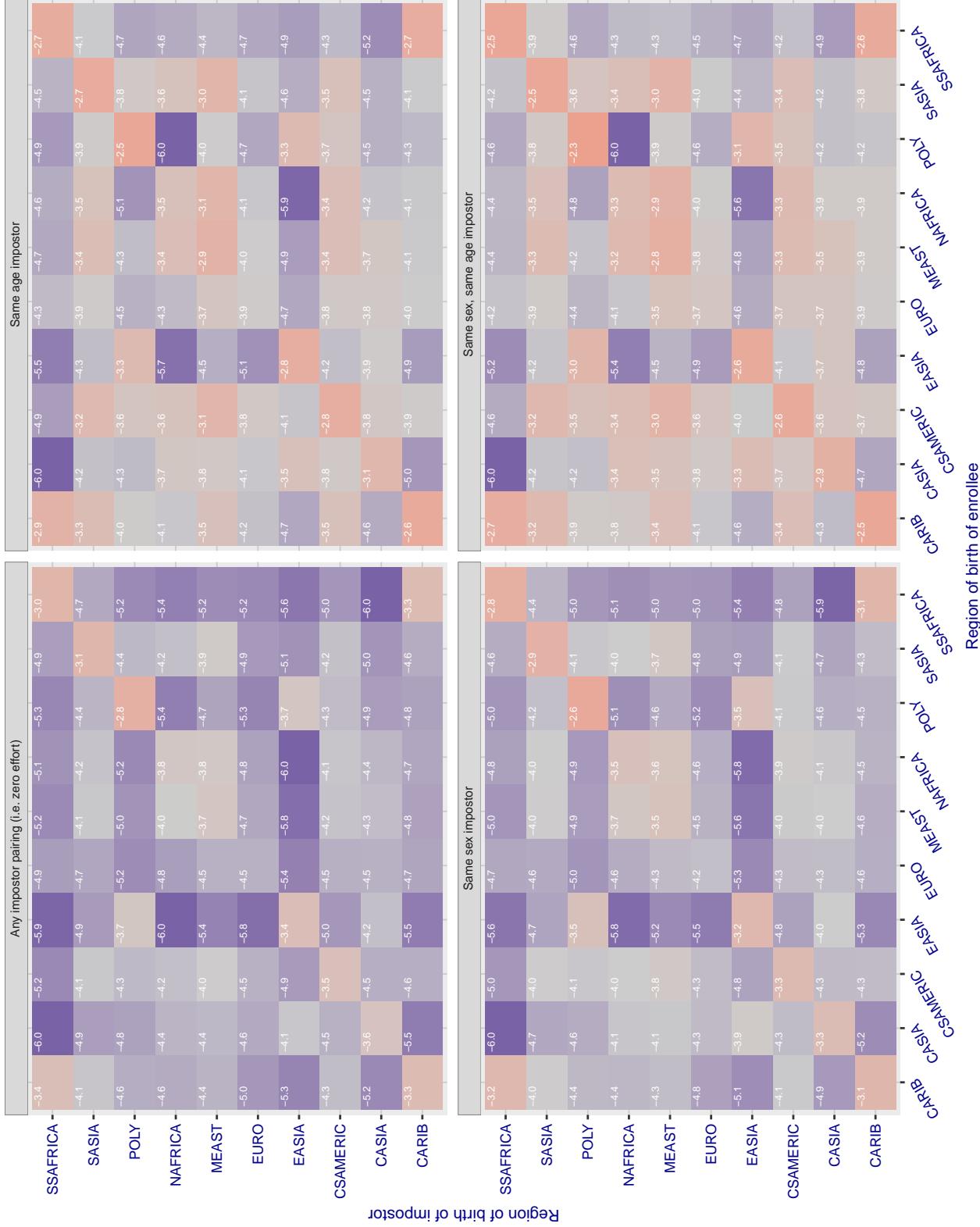


Figure 248: For algorithm **synesis-005** operating on visa images, the heatmap shows false match rates observed over impostor comparisons of faces from different individuals who were born in the given region pair. False matches are counted against a recognition threshold fixed globally to give the target FMR in the plot title, computed over all on the order of 10^{10} impostor comparisons. If text appears in each box it give the same quantity as that coded by the color. Grey indicates FMR is at the intended FMR target level. Light red colors present a security vulnerability to, for example, a passport gate. Each +1 increase in $\log_{10} \text{FMR}$ corresponds to a factor of 10 increase in FMR. The matrix is not quite symmetric because images in the enrollment and verification sets are different.

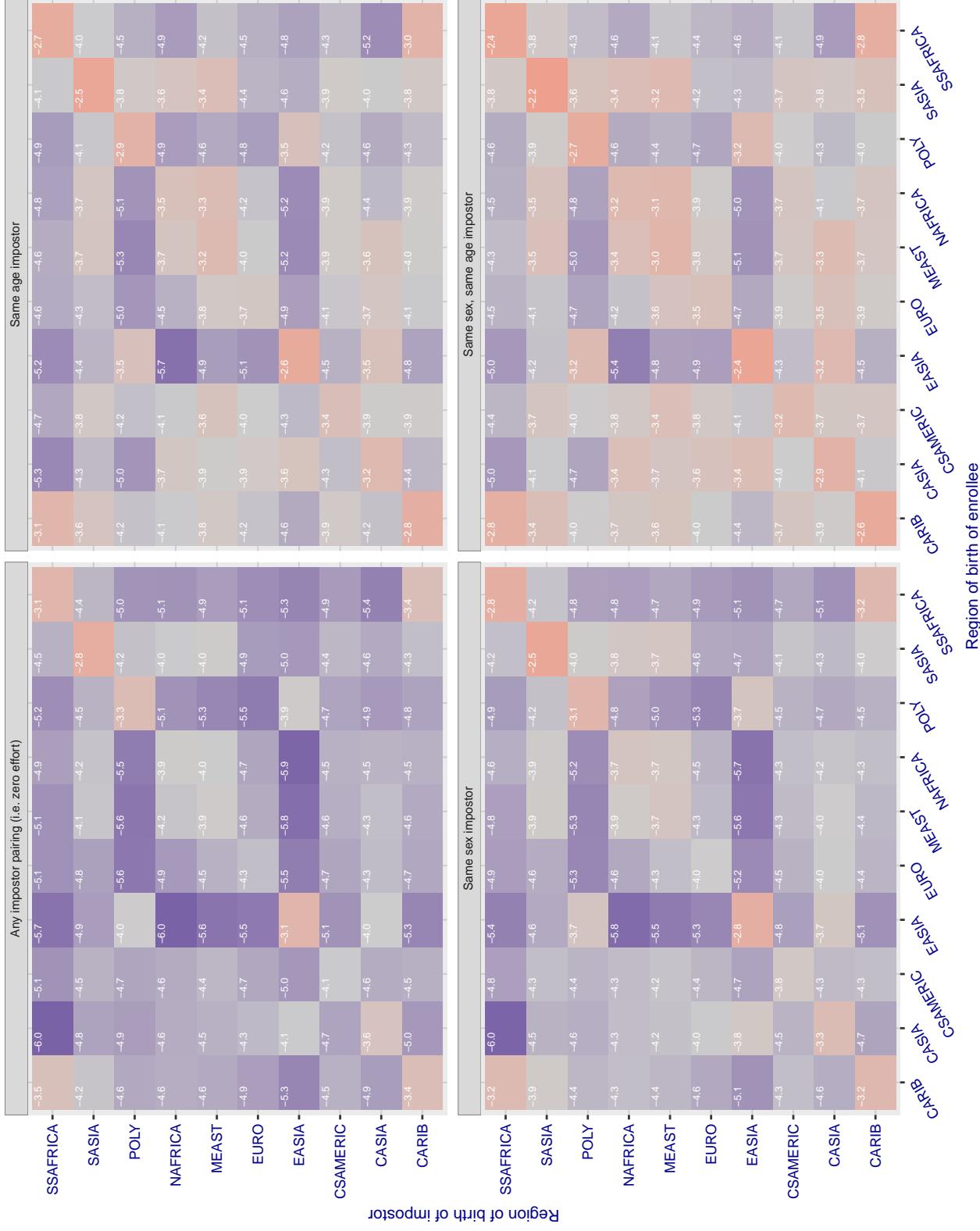
Cross region FMR at threshold T = 147.661 for algorithm tech5_002, giving FMR(T) = 0.0001 globally.

Figure 249: For algorithm tech5-002 operating on visa images, the heatmap shows false match rates observed over impostor comparisons of faces from different individuals who were born in the given region pair. False matches are counted against a recognition threshold fixed globally to give the target FMR in the plot title, computed over all on the order of 10^{10} impostor comparisons. If text appears in each box it give the same quantity as that coded by the color. Grey indicates FMR is at the intended FMR target level. Light red colors present a security vulnerability to, for example, a passport gate. Each +1 increase in $\log_{10} \text{FMR}$ corresponds to a factor of 10 increase in FMR. The matrix is not quite symmetric because images in the enrollment and verification sets are different.

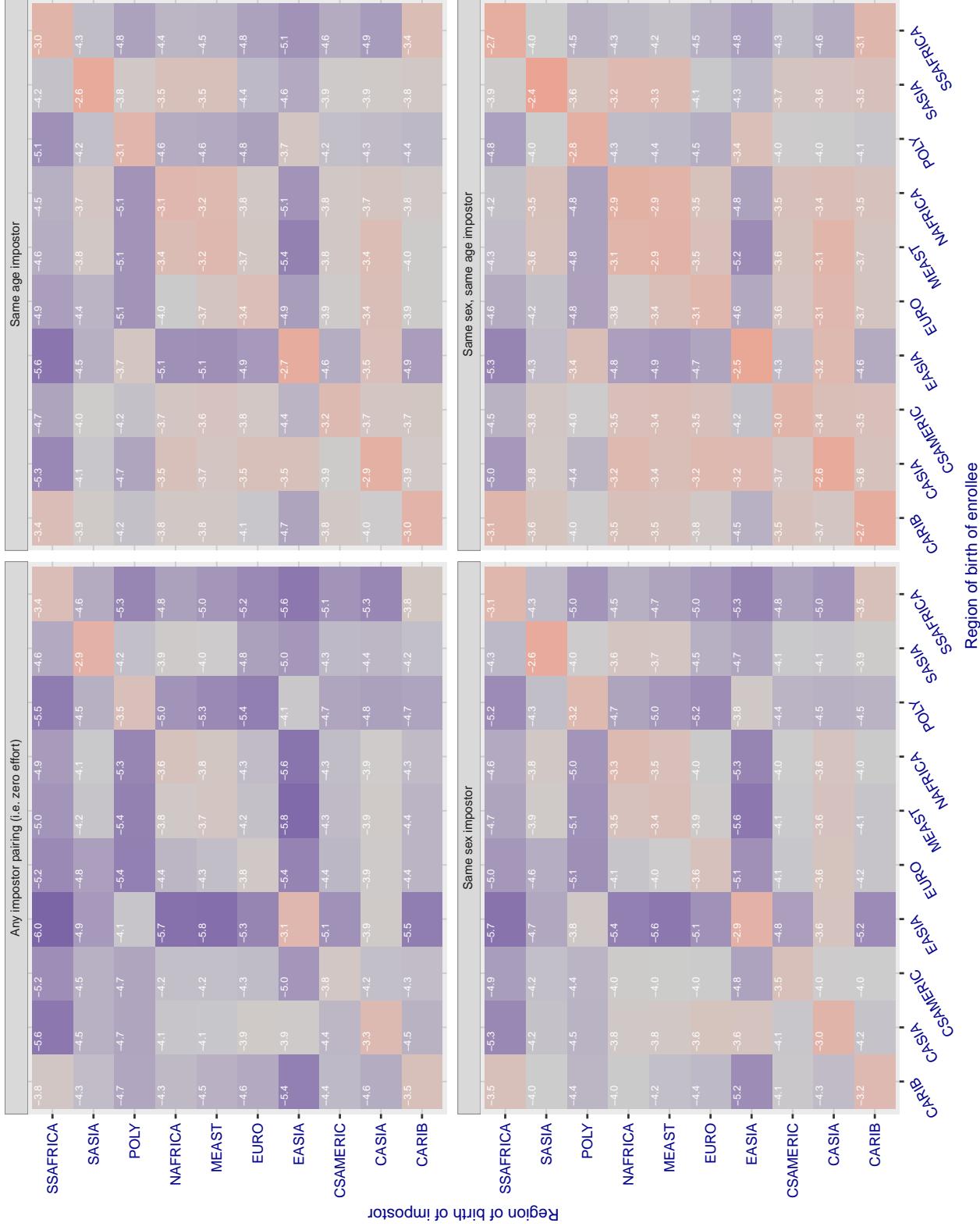
Cross region FMR at threshold T = 147.080 for algorithm tech5_003, giving FMR(T) = 0.0001 globally.

Figure 250: For algorithm tech5-003 operating on visa images, the heatmap shows false match rates observed over impostor comparisons of faces from different individuals who were born in the given region pair. False matches are counted against a recognition threshold fixed globally to give the target FMR in the plot title, computed over all on the order of 10^{10} impostor comparisons. If text appears in each box it give the same quantity as that coded by the color. Grey indicates FMR is at the intended FMR target level. Light red colors present a security vulnerability to, for example, a passport gate. Each +1 increase in $\log_{10} \text{FMR}$ corresponds to a factor of 10 increase in FMR. The matrix is not quite symmetric because images in the enrollment and verification sets are different.

Cross region FMR at threshold T = 0.896 for algorithm tevian_003, giving FMR(T) = 0.0001 globally.

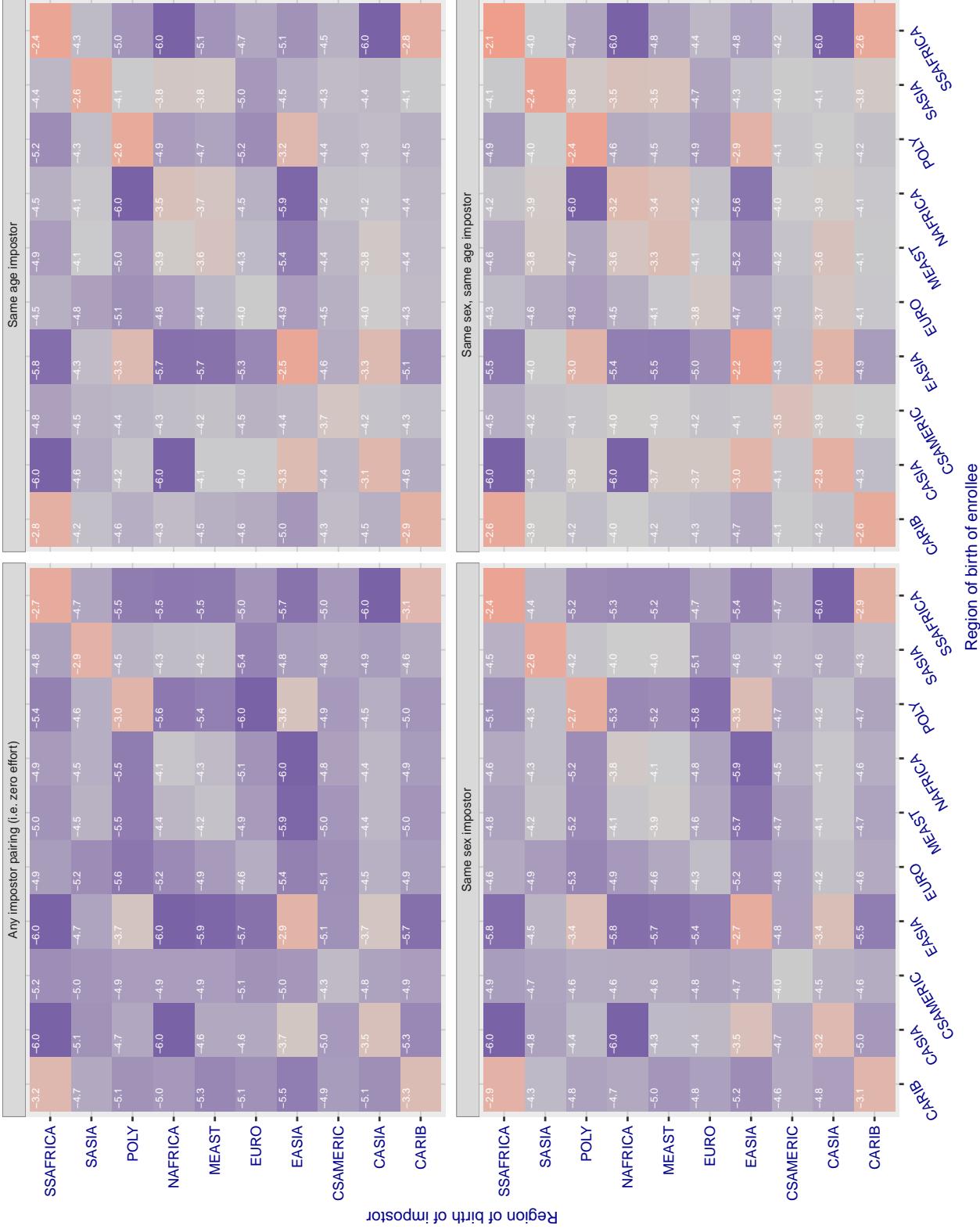


Figure 251: For algorithm tevian-003 operating on visa images, the heatmap shows false match rates observed over impostor comparisons of faces from different individuals who were born in the given region pair. False matches are counted against a recognition threshold fixed globally to give the target FMR in the plot title, computed over all on the order of 10^{10} impostor comparisons. If text appears in each box it give the same quantity as that coded by the color. Grey indicates FMR is at the intended FMR target level. Light red colors present a security vulnerability to, for example, a passport gate. Each +1 increase in $\log_{10} \text{FMR}$ corresponds to a factor of 10 increase in FMR. The matrix is not quite symmetric because images in the enrollment and verification sets are different.

Cross region FMR at threshold T = 0.896 for algorithm tevian_004, giving FMR(T) = 0.0001 globally.

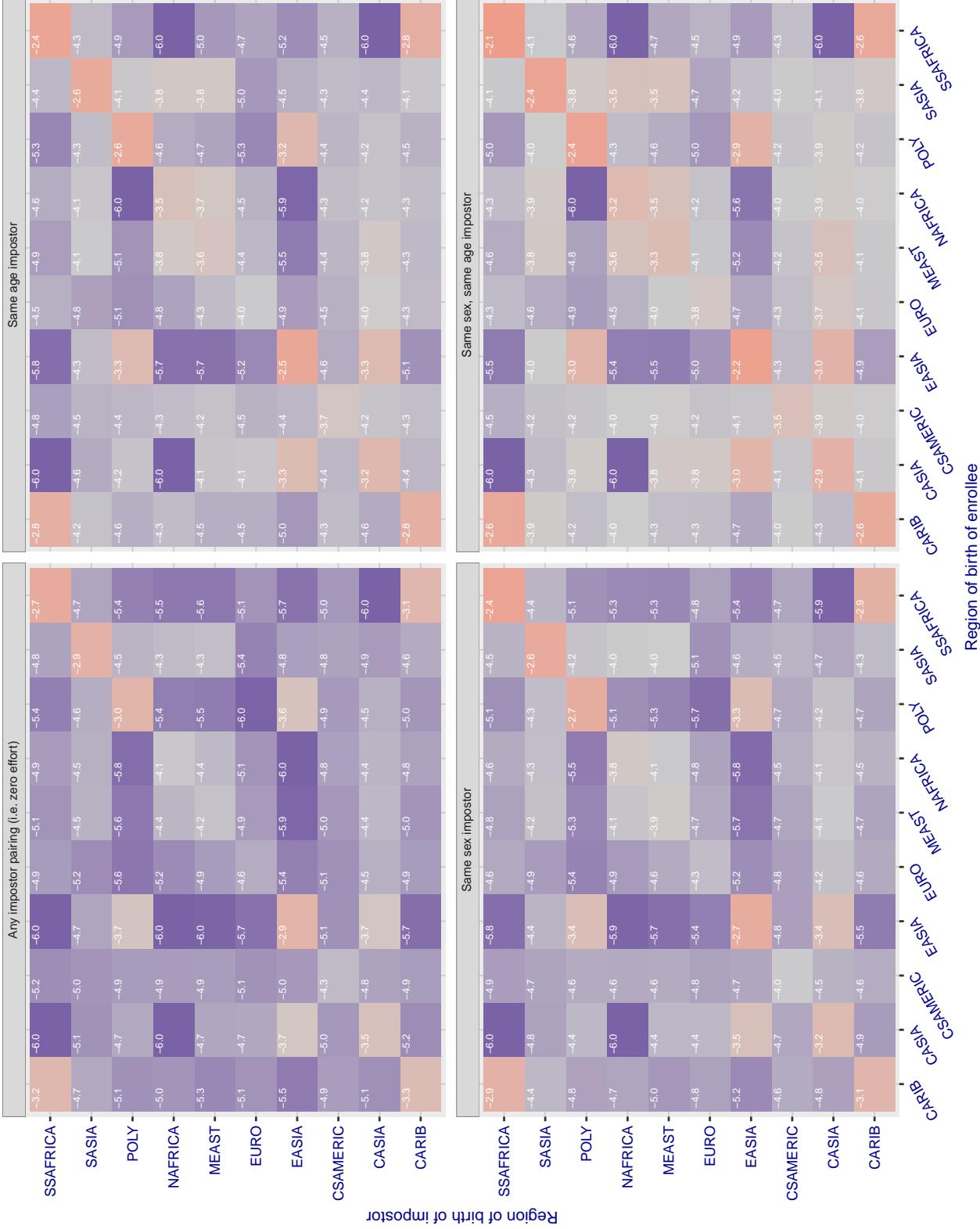


Figure 252: For algorithm tevian-004 operating on visa images, the heatmap shows false match rates observed over impostor comparisons of faces from different individuals who were born in the given region pair. False matches are counted against a recognition threshold fixed globally to give the target FMR in the plot title, computed over all on the order of 10^{10} impostor comparisons. If text appears in each box it give the same quantity as that coded by the color. Grey indicates FMR is at the intended FMR target level. Light red colors present a security vulnerability to, for example, a passport gate. Each +1 increase in $\log_{10} \text{FMR}$ corresponds to a factor of 10 increase in FMR. The matrix is not quite symmetric because images in the enrollment and verification sets are different.

Cross region FMR at threshold T = 151.011 for algorithm tiger_002, giving $\text{FMR}(\text{T}) = 0.0001$ globally.

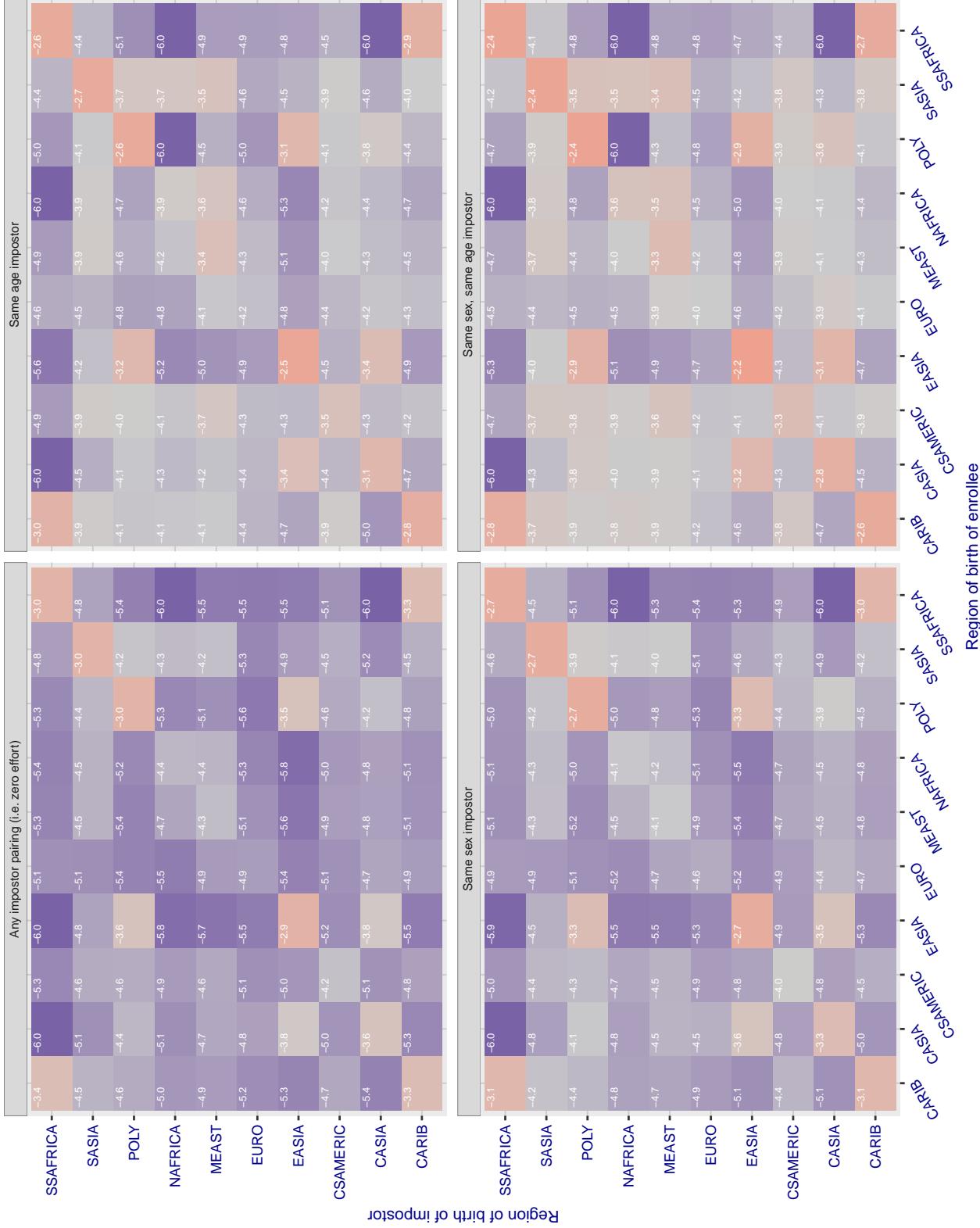


Figure 253: For algorithm tiger-002 operating on visa images, the heatmap shows false match rates observed over impostor comparisons of faces from different individuals who were born in the given region pair. False matches are counted against a recognition threshold fixed globally to give the target FMR in the plot title, computed over all on the order of 10^{10} impostor comparisons. If text appears in each box it give the same quantity as that coded by the color. Grey indicates FMR is at the intended FMR target level. Light red colors present a security vulnerability to, for example, a passport gate. Each +1 increase in $\log 10 \text{ FMR}$ corresponds to a factor of 10 increase in FMR. The matrix is not quite symmetric because images in the enrollment and verification sets are different.

Cross region FMR at threshold $T = 149.313$ for algorithm tiger_003, giving $FMR(T) = 0.0001$ globally.

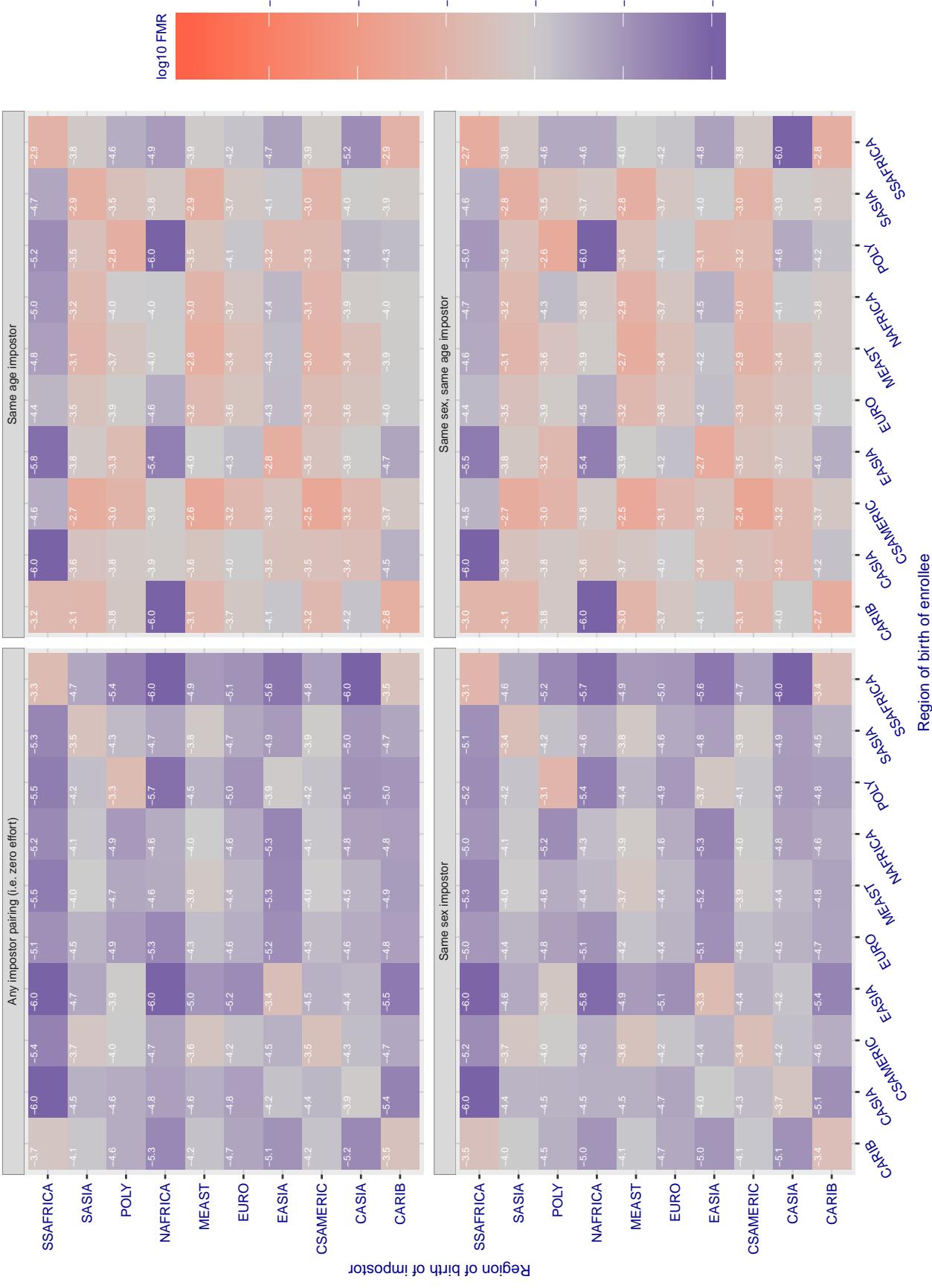


Figure 254: For algorithm tiger-003 operating on visa images, the heatmap shows false match rates observed over impostor comparisons of faces from different individuals who were born in the given region pair. False matches are counted against a recognition threshold fixed globally to give the target FMR in the plot title, computed over all on the order of 10^{10} impostor comparisons. If text appears in each box it give the same quantity as that coded by the color. Grey indicates FMR is at the intended FMR target level. Light red colors present a security vulnerability to, for example, a passport gate. Each +1 increase in $\log_{10} \text{FMR}$ corresponds to a factor of 10 increase in FMR. The matrix is not quite symmetric because images in the enrollment and verification sets are different.

Cross region FMR at threshold T = 43.677 for algorithm tongyi_005, giving FMR(T) = 0.0001 globally.

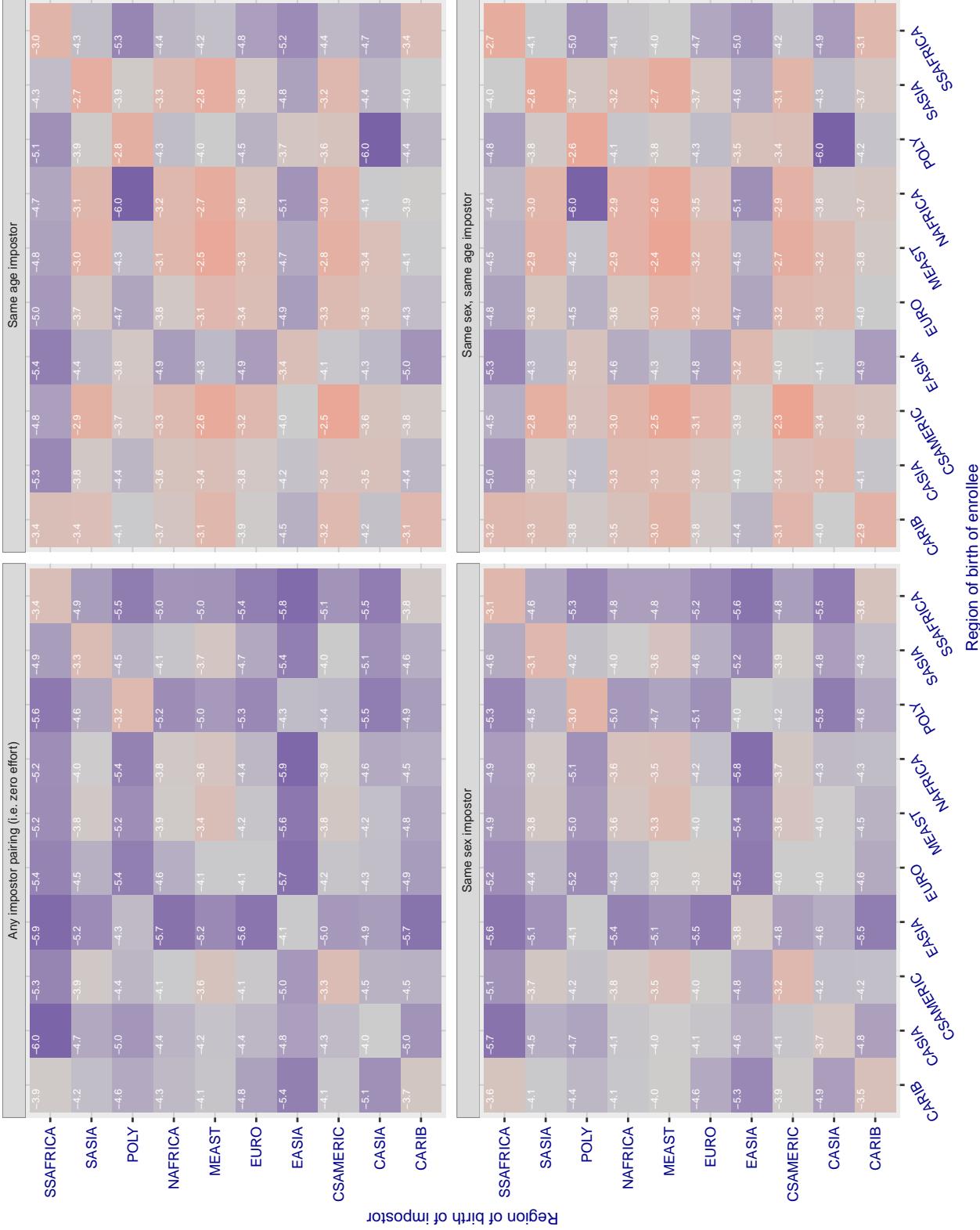


Figure 255: For algorithm tongyi-005 operating on visa images, the heatmap shows false match rates observed over impostor comparisons of faces from different individuals who were born in the given region pair. False matches are counted against a recognition threshold fixed globally to give the target FMR in the plot title, computed over all on the order of 10^{10} impostor comparisons. If text appears in each box it give the same quantity as that coded by the color. Grey indicates FMR is at the intended FMR target level. Light red colors present a security vulnerability to, for example, a passport gate. Each +1 increase in $\log_{10} \text{FMR}$ corresponds to a factor of 10 increase in FMR. The matrix is not quite symmetric because images in the enrollment and verification sets are different.

Cross region FMR at threshold T = 0.628 for algorithm toshiba_002, giving FMR(T) = 0.0001 globally.

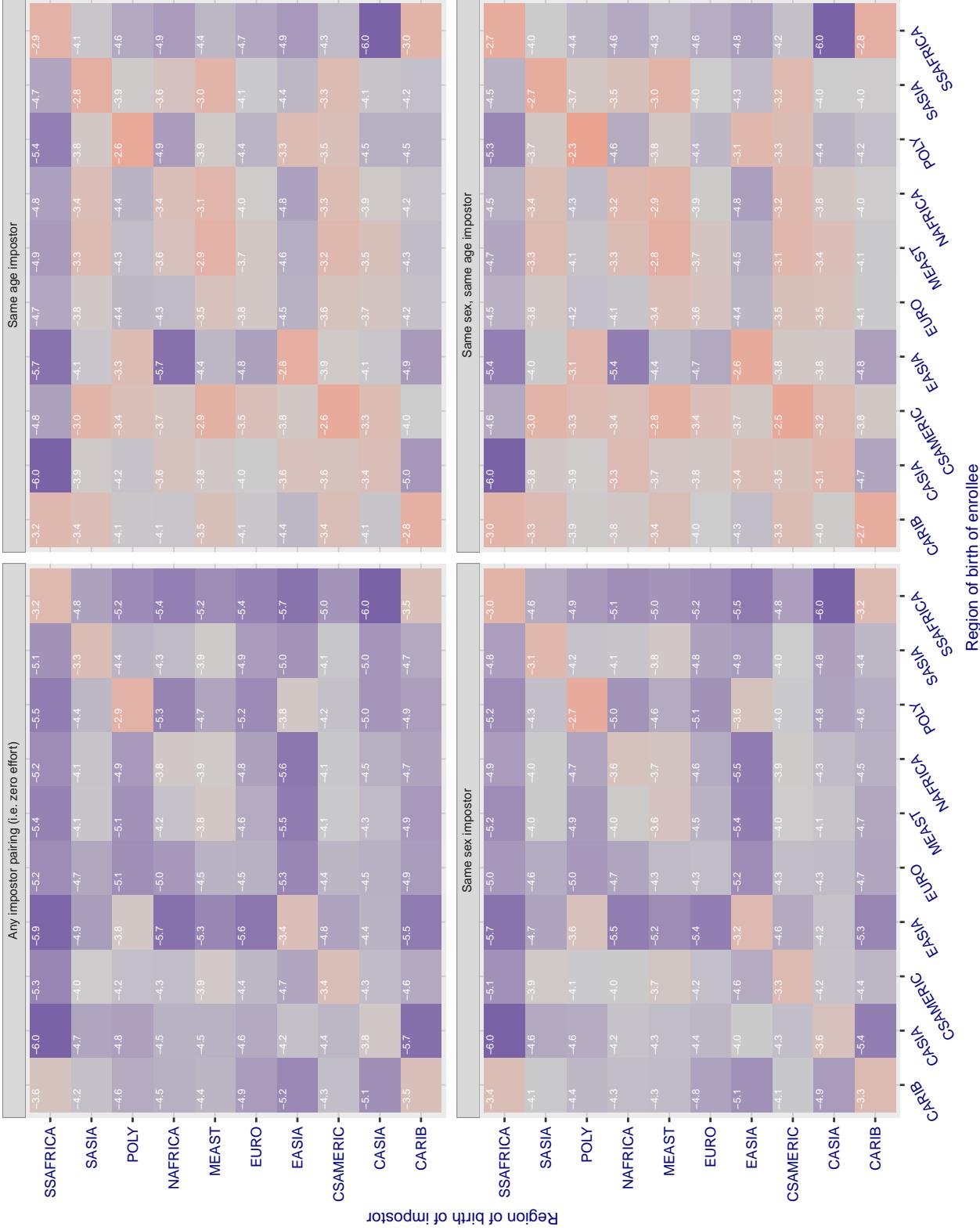


Figure 256: For algorithm toshiba-002 operating on visa images, the heatmap shows false match rates observed over impostor comparisons of faces from different individuals who were born in the given region pair. False matches are counted against a recognition threshold fixed globally to give the target FMR in the plot title, computed over all on the order of 10^{10} impostor comparisons. If text appears in each box it give the same quantity as that coded by the color. Grey indicates FMR is at the intended FMR target level. Light red colors present a security vulnerability to, for example, a passport gate. Each +1 increase in $\log_{10} FMR$ corresponds to a factor of 10 increase in FMR. The matrix is not quite symmetric because images in the enrollment and verification sets are different.

Cross region FMR at threshold T = 0.626 for algorithm toshiba_003, giving FMR(T) = 0.0001 globally.

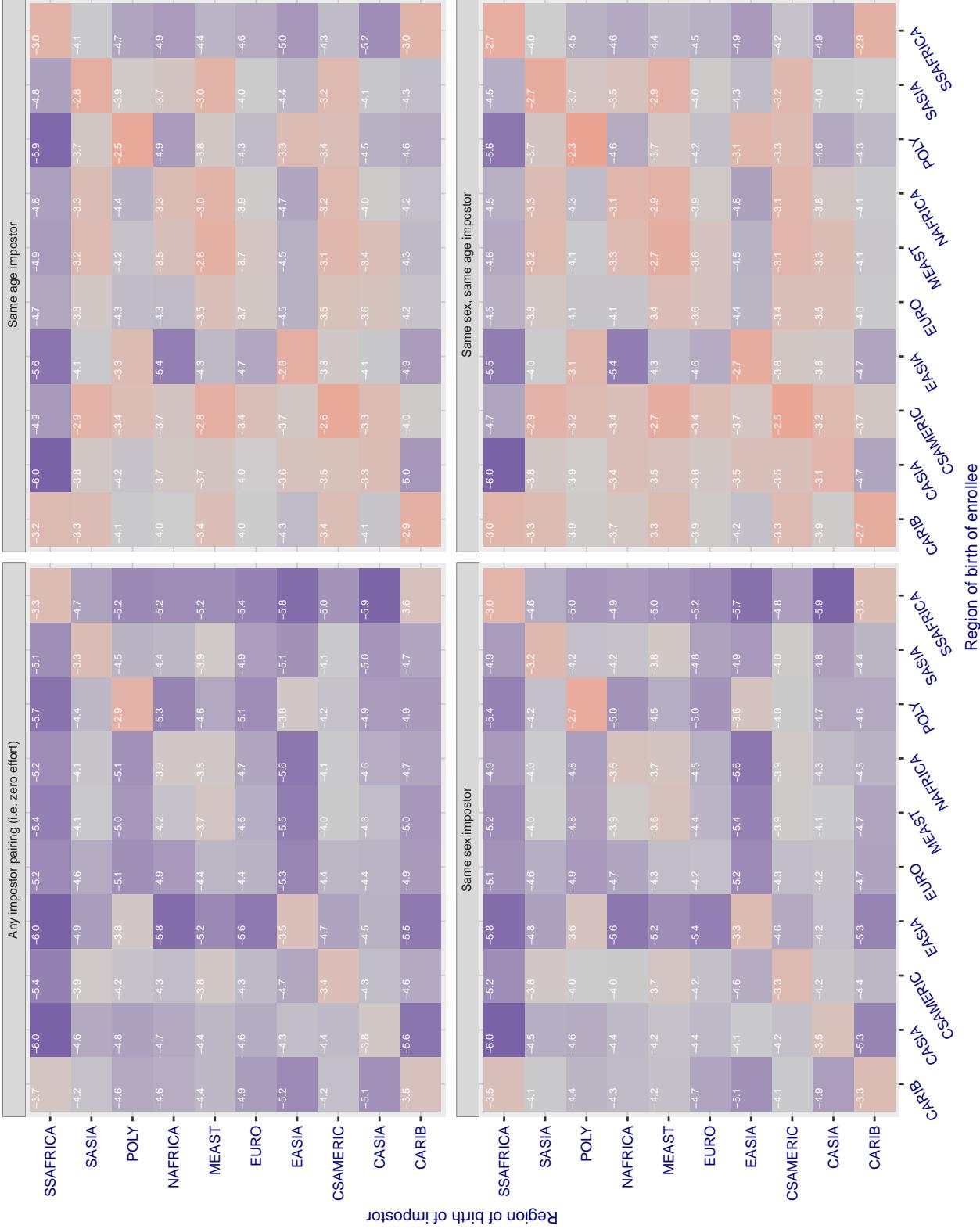


Figure 257: For algorithm toshiba-003 operating on visa images, the heatmap shows false match rates observed over impostor comparisons of faces from different individuals who were born in the given region pair. False matches are counted against a recognition threshold fixed globally to give the target FMR in the plot title, computed over all on the order of 10^{10} impostor comparisons. If text appears in each box it give the same quantity as that coded by the color. Grey indicates FMR is at the intended FMR target level. Light red colors present a security vulnerability to, for example, a passport gate. Each +1 increase in $\log_{10} FMR$ corresponds to a factor of 10 increase in FMR. The matrix is not quite symmetric because images in the enrollment and verification sets are different.

Cross region FMR at threshold T = 0.151 for algorithm ulsee_001, giving FMR(T) = 0.0001 globally.

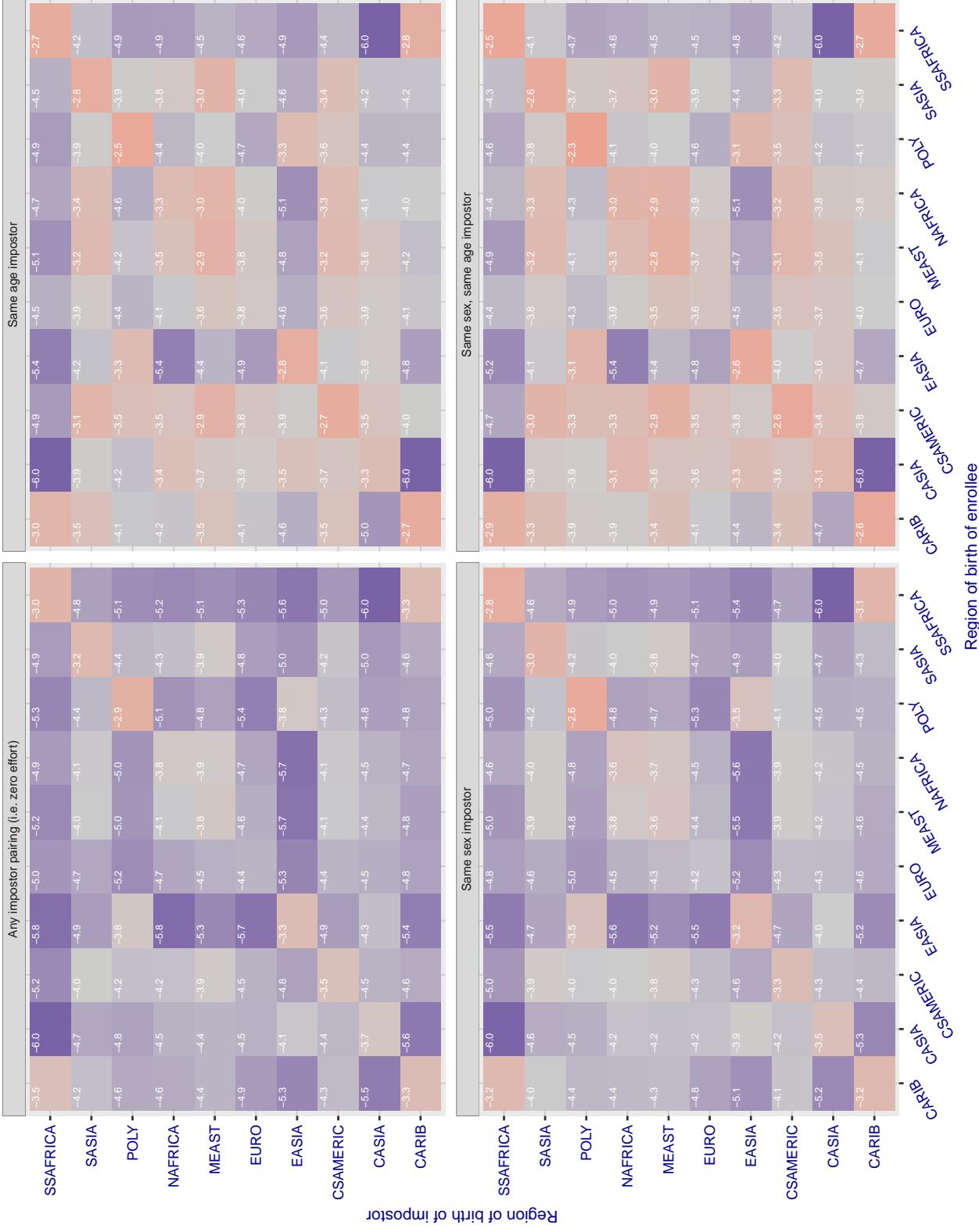


Figure 258: For algorithm ulsee_001 operating on visa images, the heatmap shows false match rates observed over impostor comparisons of faces from different individuals who were born in the given region pair. False matches are counted against a recognition threshold fixed globally to give the target FMR in the plot title, computed over all on the order of 10^{10} impostor comparisons. If text appears in each box it give the same quantity as that coded by the color. Grey indicates FMR is at the intended FMR target level. Light red colors present a security vulnerability to, for example, a passport gate. Each +1 increase in $\log 10$ FMR corresponds to a factor of 10 increase in FMR. The matrix is not quite symmetric because images in the enrollment and verification sets are different.

Cross region FMR at threshold T = 0.771 for algorithm uluface_002, giving FMR(T) = 0.0001 globally.

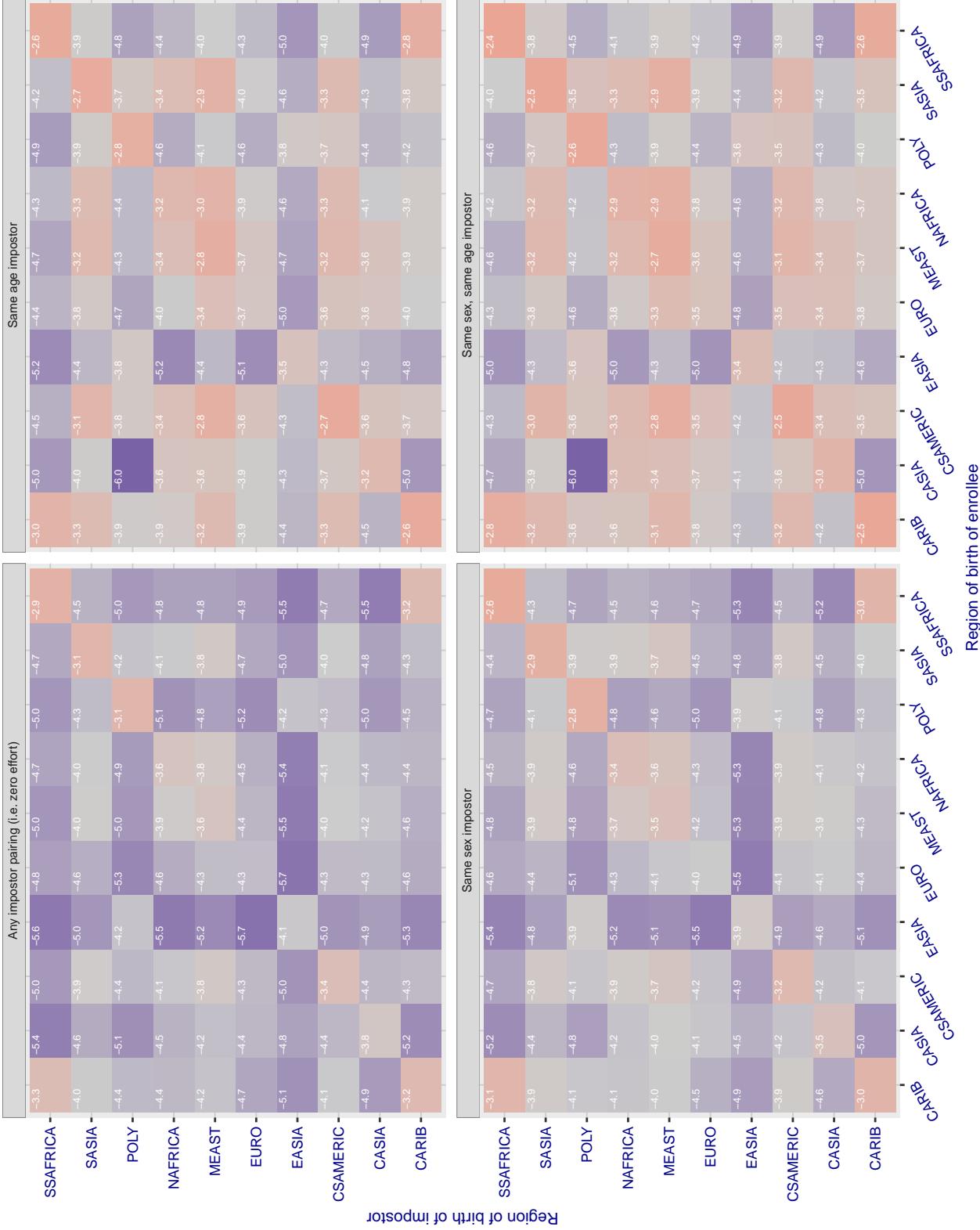


Figure 259: For algorithm uluface-002 operating on visa images, the heatmap shows false match rates observed over impostor comparisons of faces from different individuals who were born in the given region pair. False matches are counted against a recognition threshold fixed globally to give the target FMR in the plot title, computed over all on the order of 10^{10} impostor comparisons. If text appears in each box it give the same quantity as that coded by the color. Grey indicates FMR is at the intended FMR target level. Light red colors present a security vulnerability to, for example, a passport gate. Each +1 increase in $\log_{10} FMR$ corresponds to a factor of 10 increase in FMR. The matrix is not quite symmetric because images in the enrollment and verification sets are different.

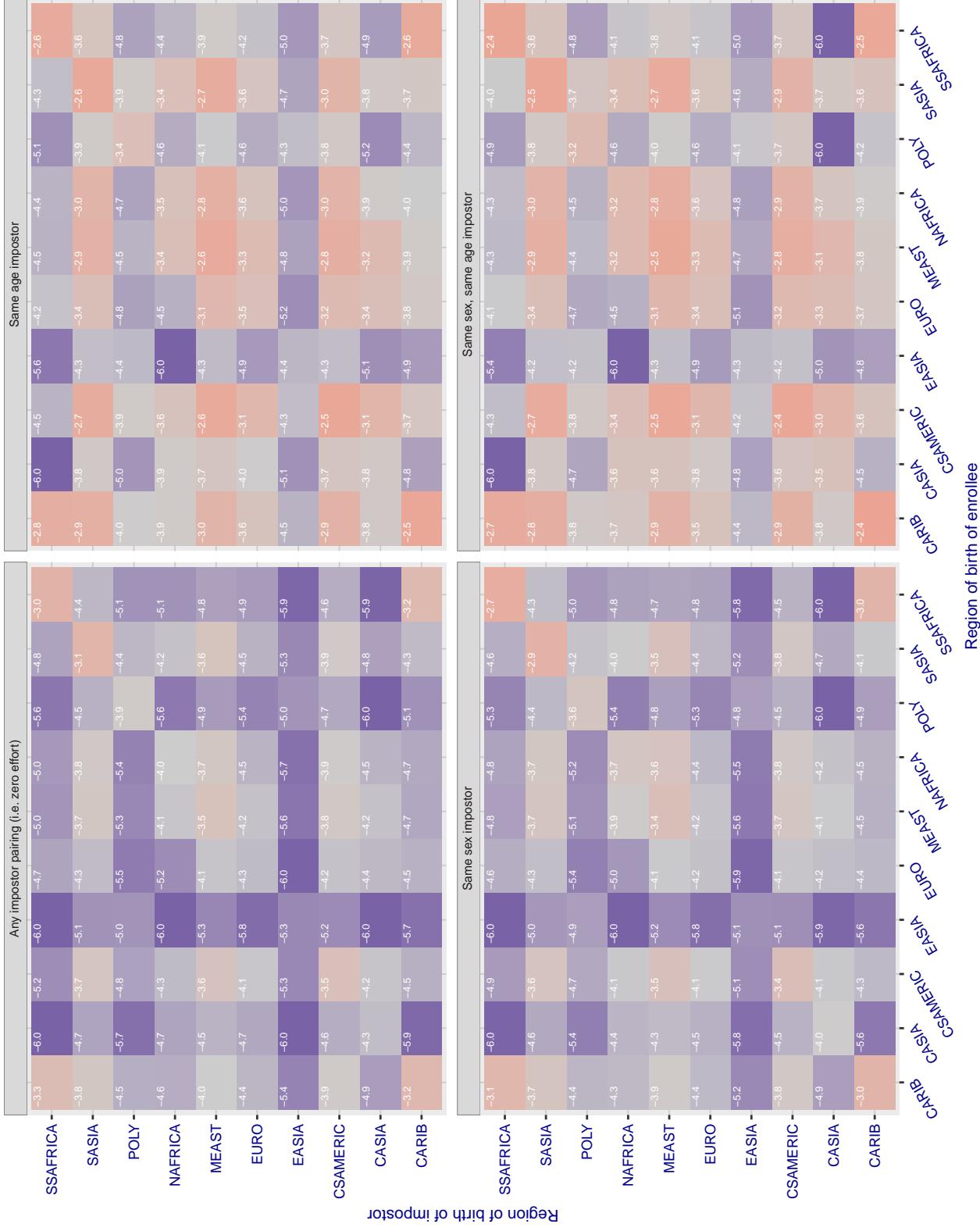
Cross region FMR at threshold T = 0.482 for algorithm upc_001, giving FMR(T) = 0.0001 globally.

Figure 260: For algorithm upc-001 operating on visa images, the heatmap shows false match rates observed over impostor comparisons of faces from different individuals who were born in the given region pair. False matches are counted against a recognition threshold fixed globally to give the target FMR in the plot title, computed over all on the order of 10^{10} impostor comparisons. If text appears in each box it give the same quantity as that coded by the color. Grey indicates FMR is at the intended FMR target level. Light red colors present a security vulnerability to, for example, a passport gate. Each +1 increase in \log_{10} FMR corresponds to a factor of 10 increase in FMR. The matrix is not quite symmetric because images in the enrollment and verification sets are different.

Cross region FMR at threshold T = 0.428 for algorithm vcog_002, giving FMR(T) = 0.0001 globally.

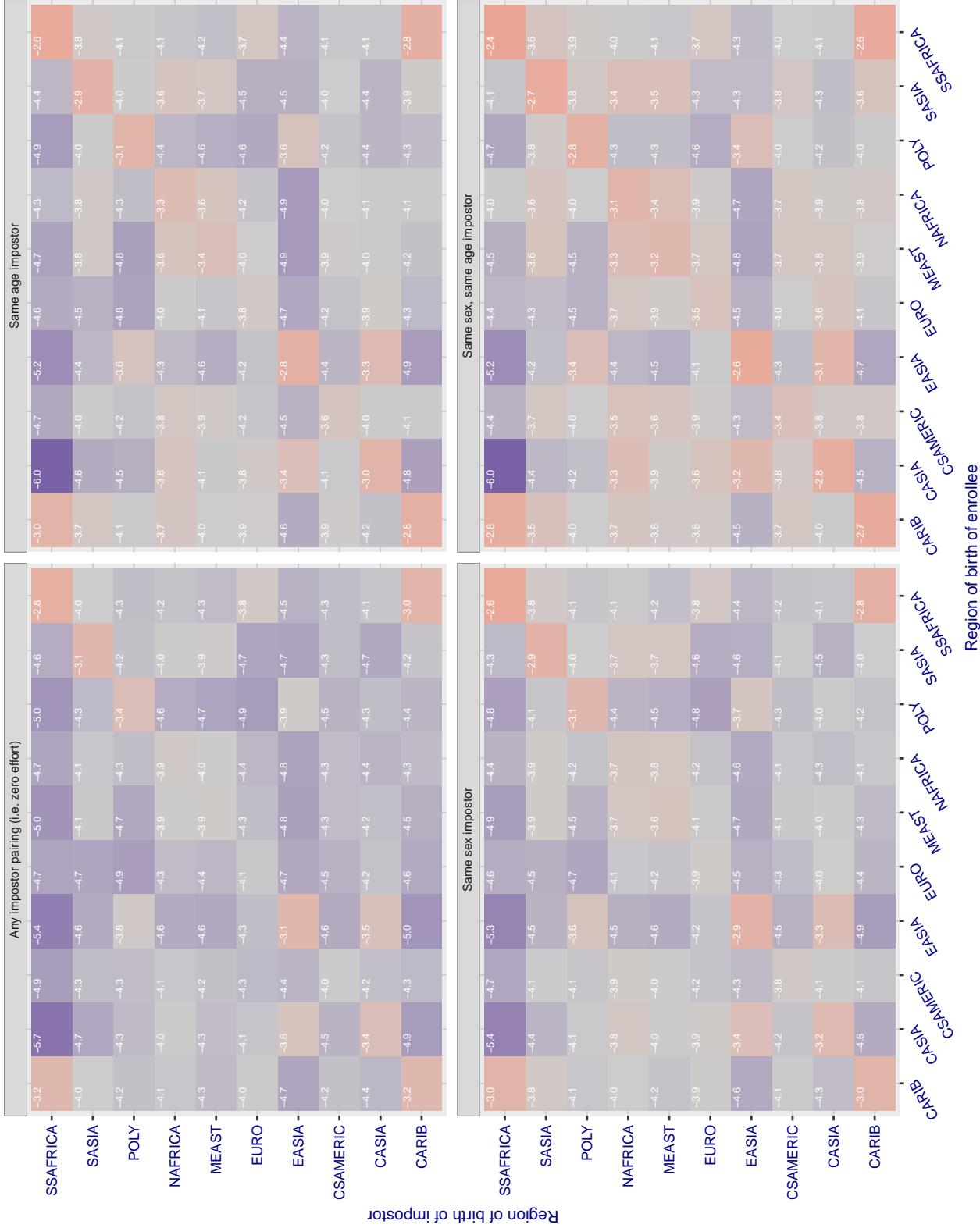


Figure 261: For algorithm vcog-002 operating on visa images, the heatmap shows false match rates observed over impostor comparisons of faces from different individuals who were born in the given region pair. False matches are counted against a recognition threshold fixed globally to give the target FMR in the plot title, computed over all on the order of 10^{10} impostor comparisons. If text appears in each box it give the same quantity as that coded by the color. Grey indicates FMR is at the intended FMR target level. Light red colors present a security vulnerability to, for example, a passport gate. Each +1 increase in $\log 10 \text{ FMR}$ corresponds to a factor of 10 increase in FMR. The matrix is not quite symmetric because images in the enrollment and verification sets are different.

Cross region FMR at threshold T = 71.529 for algorithm vd_001, giving FMR(T) = 0.0001 globally.

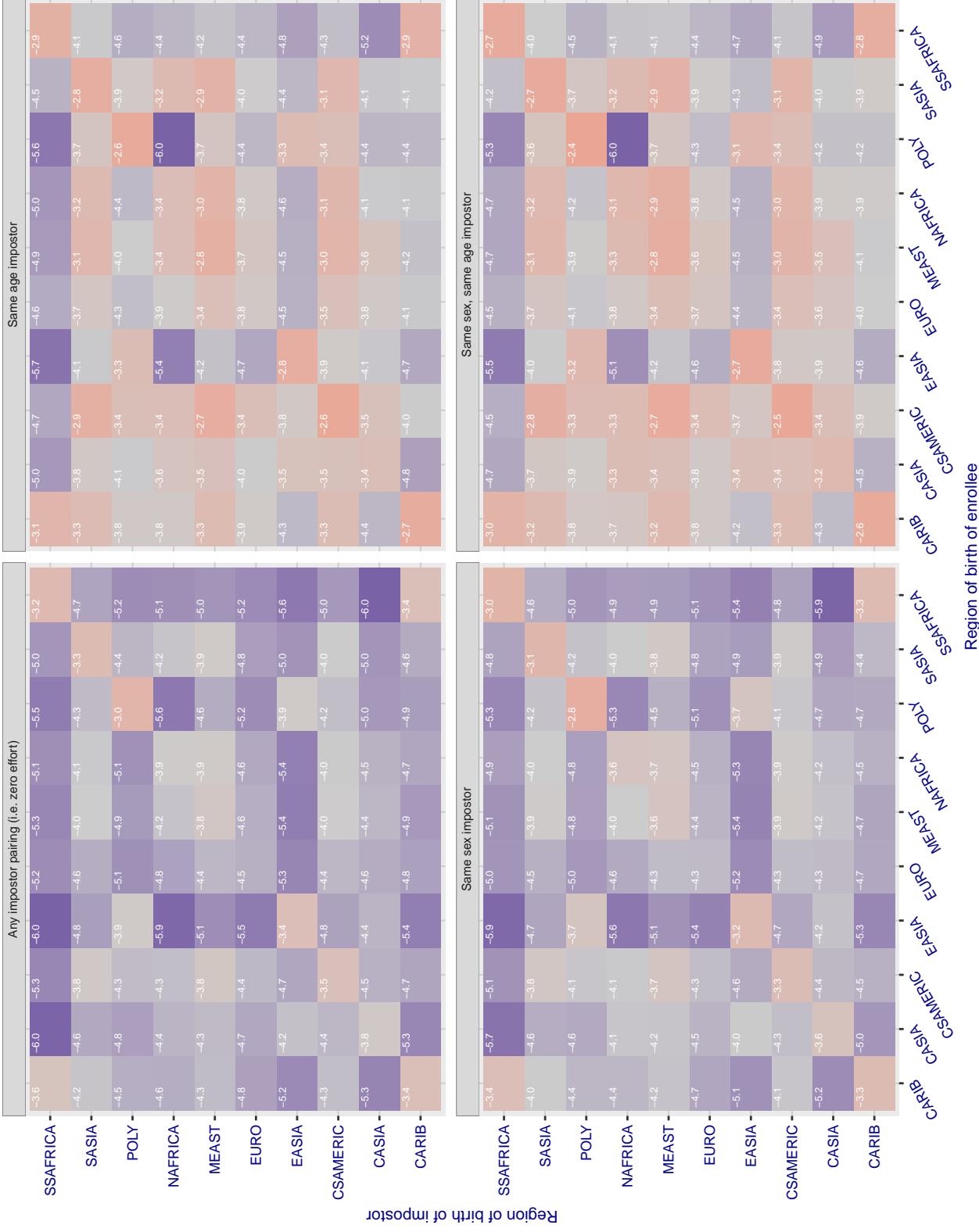


Figure 262: For algorithm vd_001 operating on visa images, the heatmap shows false match rates observed over impostor comparisons of faces from different individuals who were born in the given region pair. False matches are counted against a recognition threshold fixed globally to give the target FMR in the plot title, computed over all on the order of 10^{10} impostor comparisons. If text appears in each box it give the same quantity as that coded by the color. Grey indicates FMR is at the intended FMR target level. Light red colors present a security vulnerability to, for example, a passport gate. Each +1 increase in $\log 10$ FMR corresponds to a factor of 10 increase in FMR. The matrix is not quite symmetric because images in the enrollment and verification sets are different.

Cross region FMR at threshold T = 3.325 for algorithm veridas_001, giving FMR(T) = 0.00001 globally.

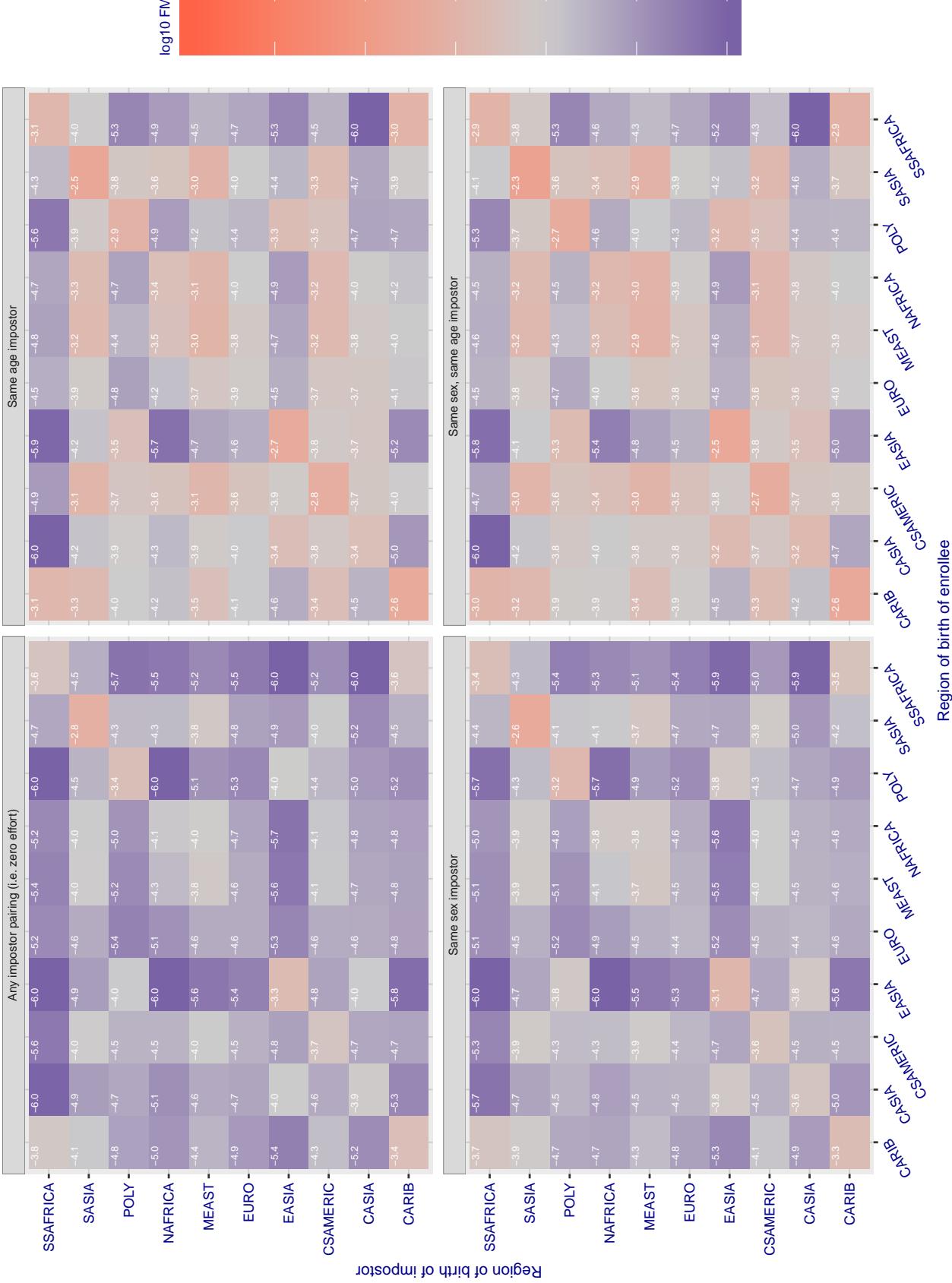


Figure 263: For algorithm veridas-001 operating on visa images, the heatmap shows false match rates observed over impostor comparisons of faces from different individuals who were born in the given region pair. False matches are counted against a recognition threshold fixed globally to give the target FMR in the plot title, computed over all on the order of 10^{10} impostor comparisons. If text appears in each box it give the same quantity as that coded by the color. Grey indicates FMR is at the intended FMR target level. Light red colors present a security vulnerability to, for example, a passport gate. Each +1 increase in $\log_{10} FMR$ corresponds to a factor of 10 increase in FMR. The matrix is not quite symmetric because images in the enrollment and verification sets are different.

Cross region FMR at threshold T = 3.389 for algorithm veridas_002, giving FMR(T) = 0.0001 globally.

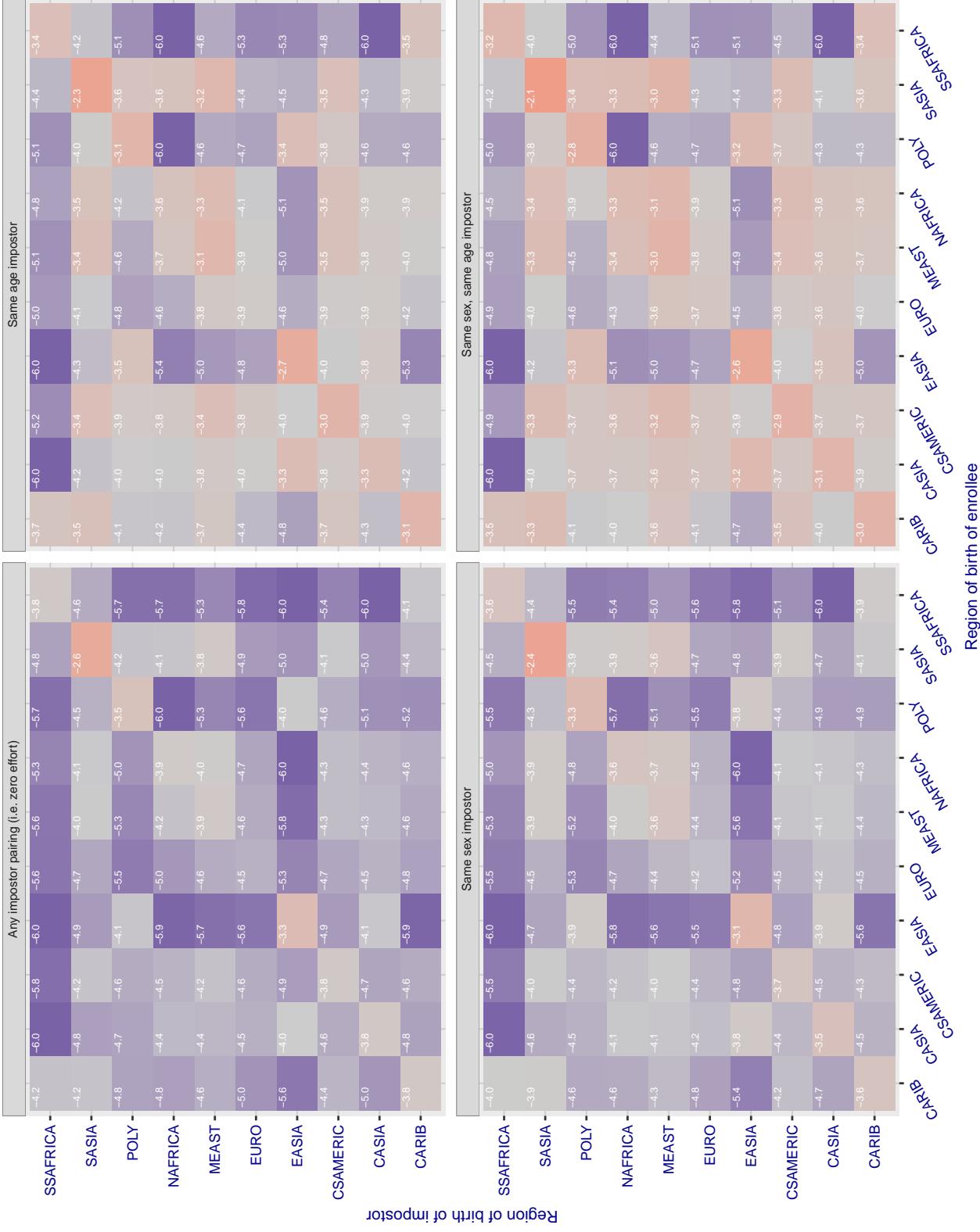


Figure 264: For algorithm veridas-002 operating on visa images, the heatmap shows false match rates observed over impostor comparisons of faces from different individuals who were born in the given region pair. False matches are counted against a recognition threshold fixed globally to give the target FMR in the plot title, computed over all on the order of 10^{10} impostor comparisons. If text appears in each box it give the same quantity as that coded by the color. Grey indicates FMR is at the intended FMR target level. Light red colors present a security vulnerability to, for example, a passport gate. Each +1 increase in $\log_{10} FMR$ corresponds to a factor of 10 increase in FMR. The matrix is not quite symmetric because images in the enrollment and verification sets are different.

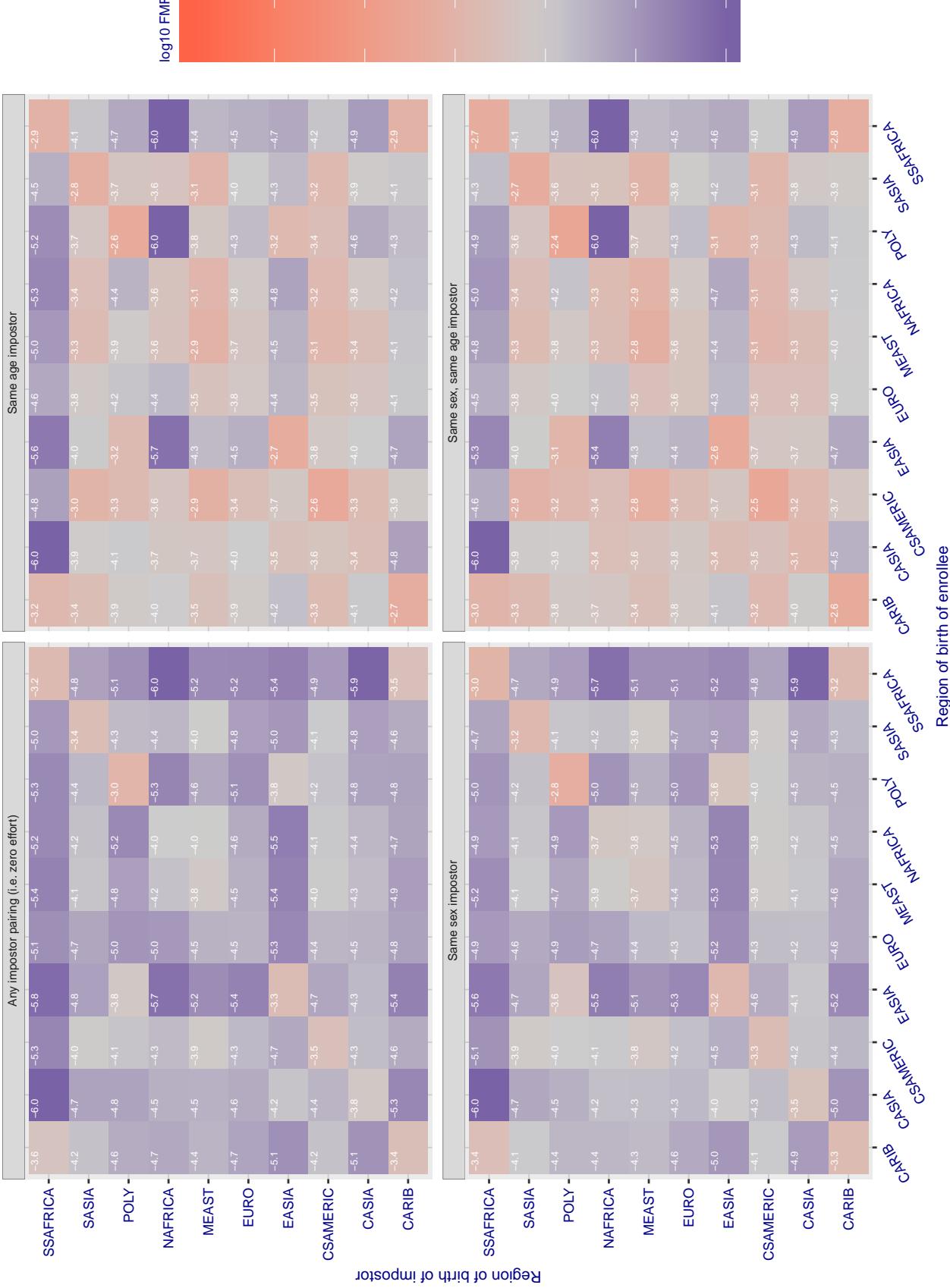
Cross region FMR at threshold T = 2.859 for algorithm via_000, giving FMR(T) = 0.00001 globally.

Figure 265: For algorithm via_000 operating on visa images, the heatmap shows false match rates observed over impostor comparisons of faces from different individuals who were born in the given region pair. False matches are counted against a recognition threshold fixed globally to give the target FMR in the plot title, computed over all on the order of 10^{10} impostor comparisons. If text appears in each box it give the same quantity as that coded by the color. Grey indicates FMR is at the intended FMR target level. Light red colors present a security vulnerability to, for example, a passport gate. Each +1 increase in $\log 10 \text{ FMR}$ corresponds to a factor of 10 increase in FMR. The matrix is not quite symmetric because images in the enrollment and verification sets are different.

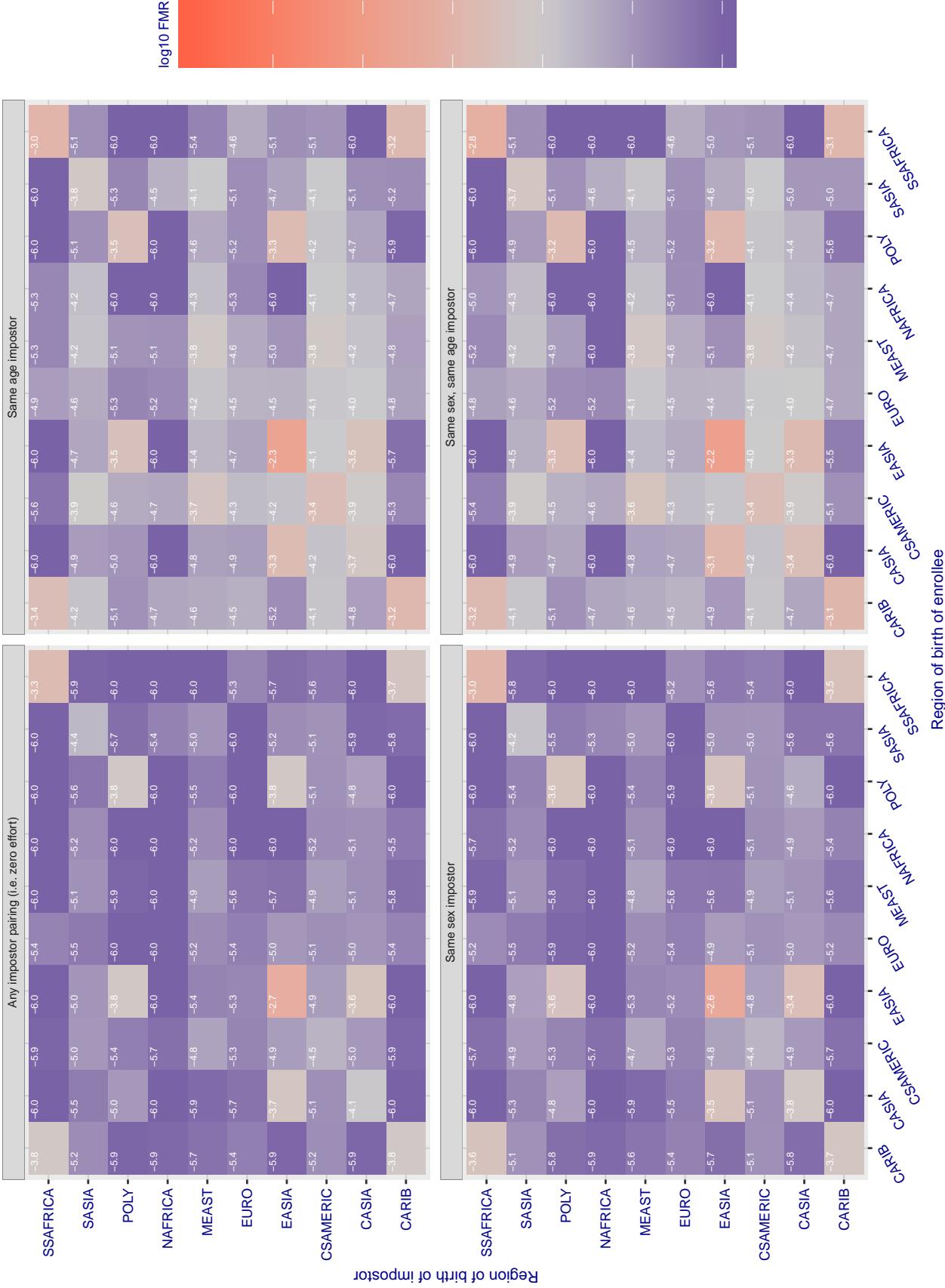
Cross region FMR at threshold T = 0.842 for algorithm videonetics_001, giving FMR(T) = 0.0001 globally.

Figure 266: For algorithm videonetics-001 operating on visa images, the heatmap shows false match rates observed over impostor comparisons of faces from different individuals who were born in the given region pair. False matches are counted against a recognition threshold fixed globally to give the target FMR in the plot title, computed over all on the order of 10^{10} impostor comparisons. If text appears in each box it give the same quantity as that coded by the color. Grey indicates FMR is at the intended FMR target level. Light red colors present a security vulnerability to, for example, a passport gate. Each +1 increase in $\log_{10} FMR$ corresponds to a factor of 10 increase in FMR. The matrix is not quite symmetric because images in the enrollment and verification sets are different.

Cross region FMR at threshold T = 3.057 for algorithm vigilantsolutions_006, giving FMR(T) = 0.0001 globally.

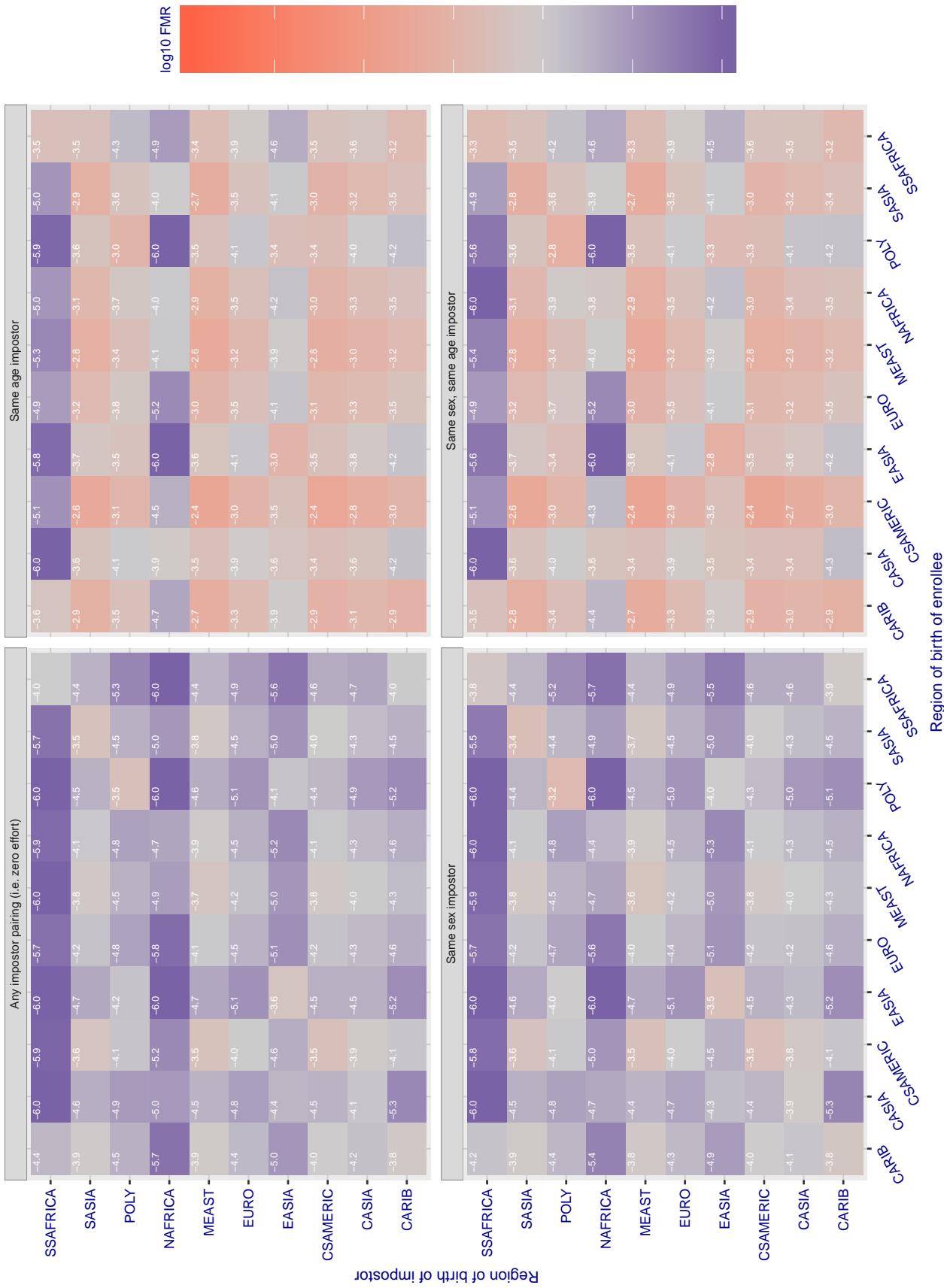


Figure 267: For algorithm vigilantsolutions-006 operating on visa images, the heatmap shows false match rates observed over impostor comparisons of faces from different individuals who were born in the given region pair. False matches are counted against a recognition threshold fixed globally to give the target FMR in the plot title, computed over all on the order of 10^{10} impostor comparisons. If text appears in each box it give the same quantity as that coded by the color. Grey indicates FMR is at the intended FMR target level. Light red colors present a security vulnerability to, for example, a passport gate. Each +1 increase in $\log_{10} FMR$ corresponds to a factor of 10 increase in FMR. The matrix is not quite symmetric because images in the enrollment and verification sets are different.

Cross region FMR at threshold T = 2.926 for algorithm vigilantsolutions_007, giving FMR(T) = 0.0001 globally.

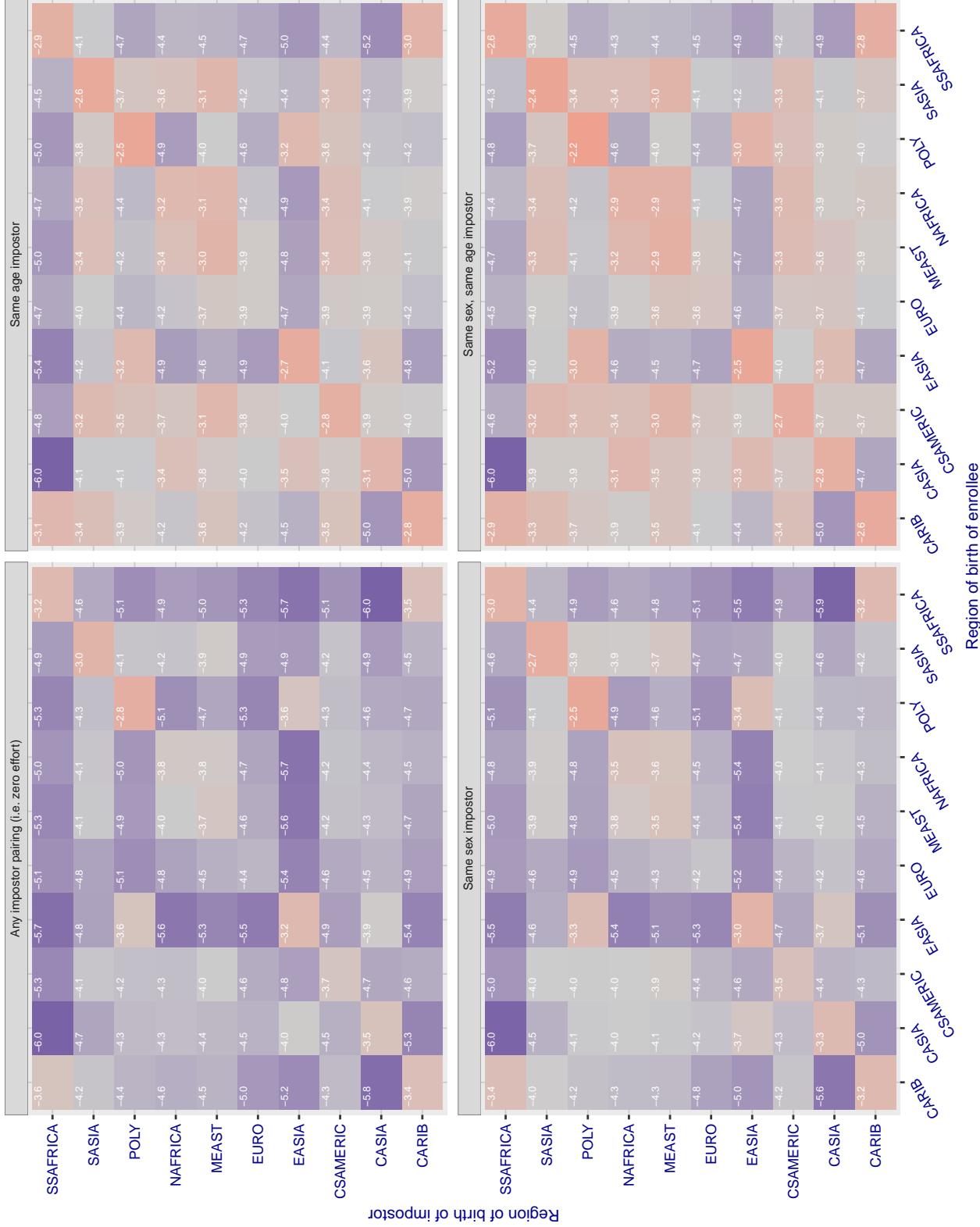


Figure 268: For algorithm vigilantsolutions-007 operating on visa images, the heatmap shows false match rates observed over impostor comparisons of faces from different individuals who were born in the given region pair. False matches are counted against a recognition threshold fixed globally to give the target FMR in the plot title, computed over all on the order of 10^{10} impostor comparisons. If text appears in each box it give the same quantity as that coded by the color. Grey indicates FMR is at the intended FMR target level. Light red colors present a security vulnerability to, for example, a passport gate. Each +1 increase in $\log_{10} FMR$ corresponds to a factor of 10 increase in FMR. The matrix is not quite symmetric because images in the enrollment and verification sets are different.

Cross region FMR at threshold T = 0.432 for algorithm vion_000, giving FMR(T) = 0.0001 globally.

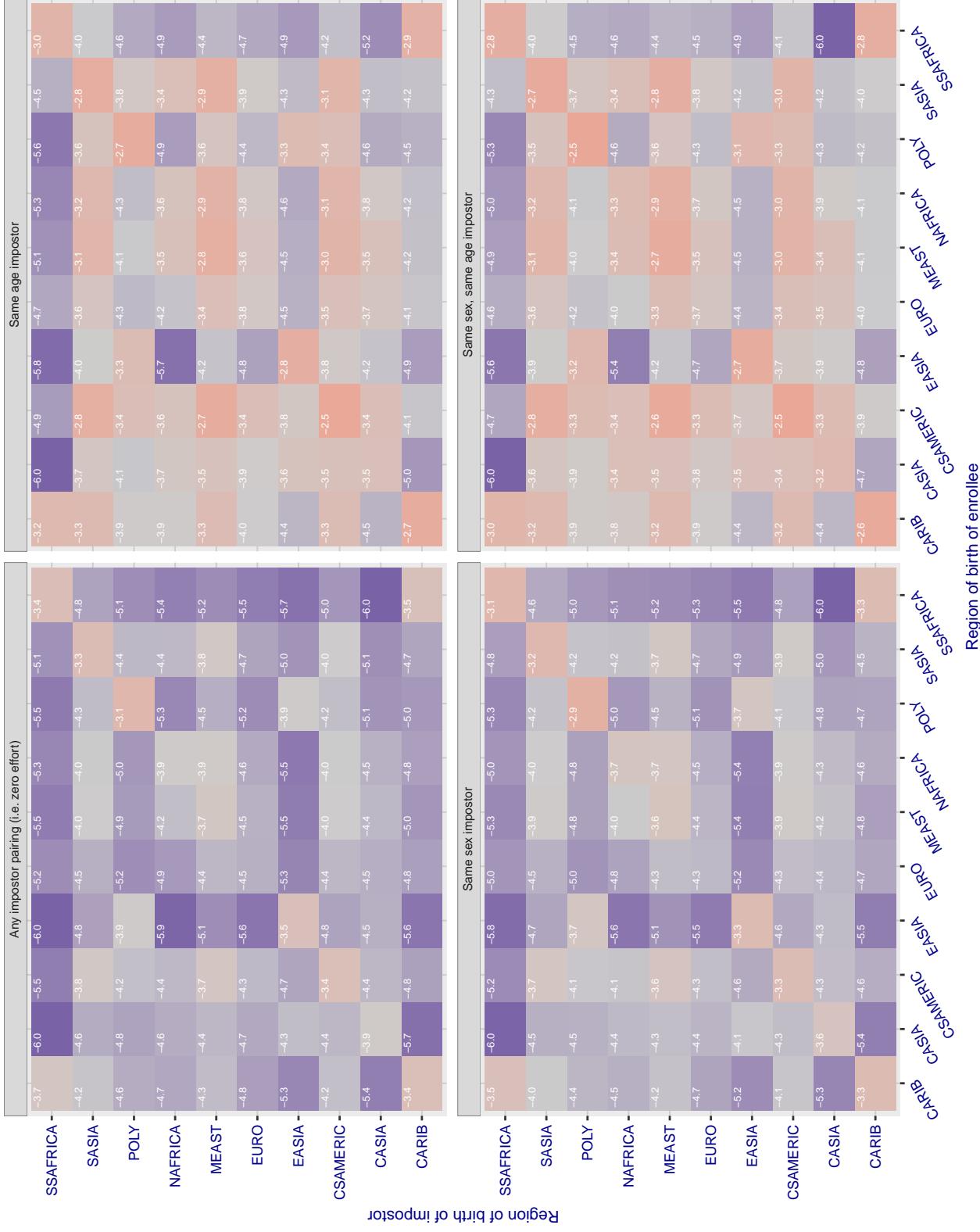


Figure 269: For algorithm vion-000 operating on visa images, the heatmap shows false match rates observed over impostor comparisons of faces from different individuals who were born in the given region pair. False matches are counted against a recognition threshold fixed globally to give the target FMR in the plot title, computed over all on the order of 10^{10} impostor comparisons. If text appears in each box it give the same quantity as that coded by the color. Grey indicates FMR is at the intended FMR target level. Light red colors present a security vulnerability to, for example, a passport gate. Each +1 increase in $\log_{10} \text{FMR}$ corresponds to a factor of 10 increase in FMR. The matrix is not quite symmetric because images in the enrollment and verification sets are different.

Cross region FMR at threshold T = 0.433 for algorithm visionbox_000, giving FMR(T) = 0.0001 globally.

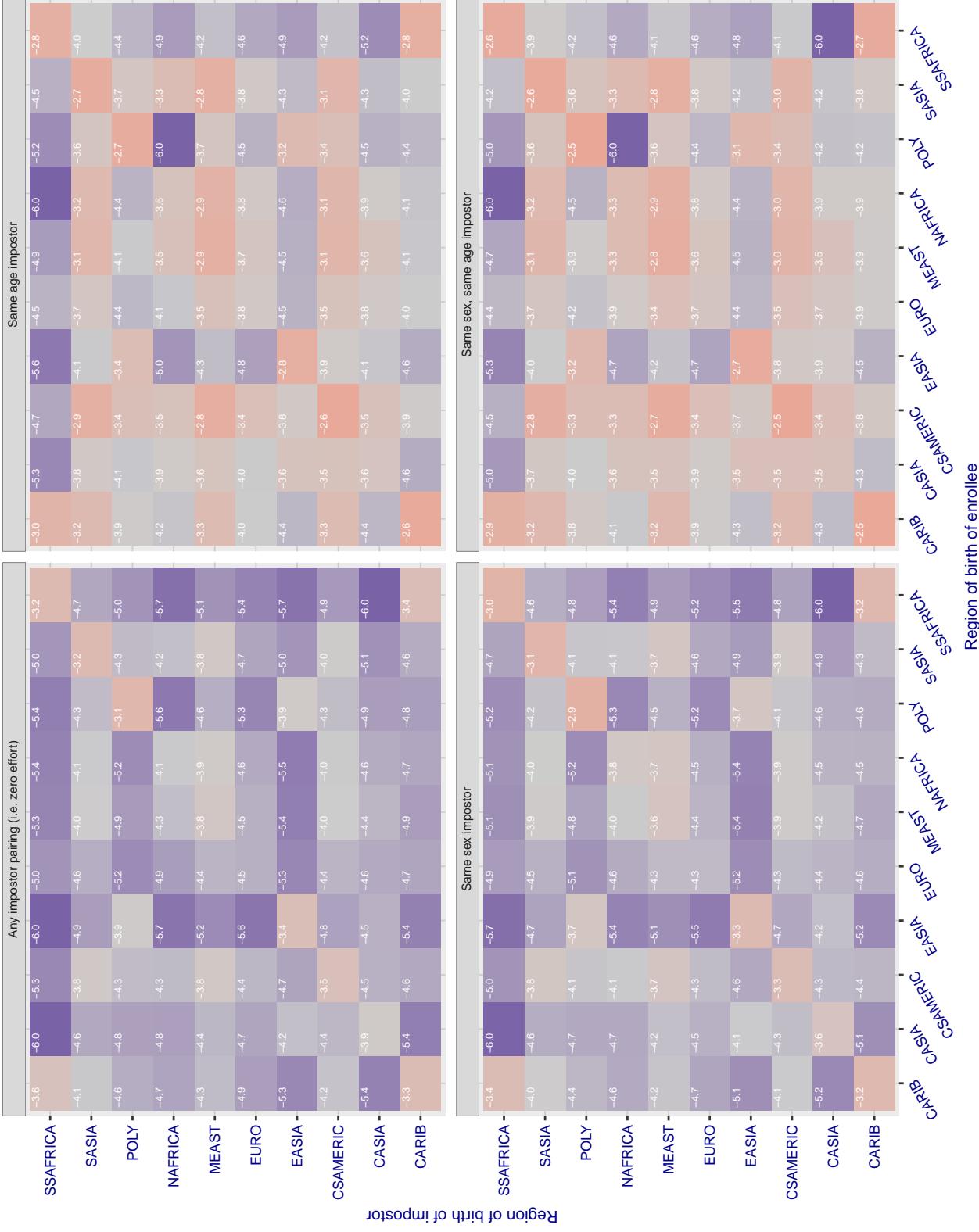


Figure 270: For algorithm visionbox-000 operating on visa images, the heatmap shows false match rates observed over impostor comparisons of faces from different individuals who were born in the given region pair. False matches are counted against a recognition threshold fixed globally to give the target FMR in the plot title, computed over all on the order of 10^{10} impostor comparisons. If text appears in each box it give the same quantity as that coded by the color. Grey indicates FMR is at the intended FMR target level. Light red colors present a security vulnerability to, for example, a passport gate. Each +1 increase in $\log_{10} FMR$ corresponds to a factor of 10 increase in FMR. The matrix is not quite symmetric because images in the enrollment and verification sets are different.

Cross region FMR at threshold T = 0.382 for algorithm visionbox_001, giving FMR(T) = 0.00001 globally.

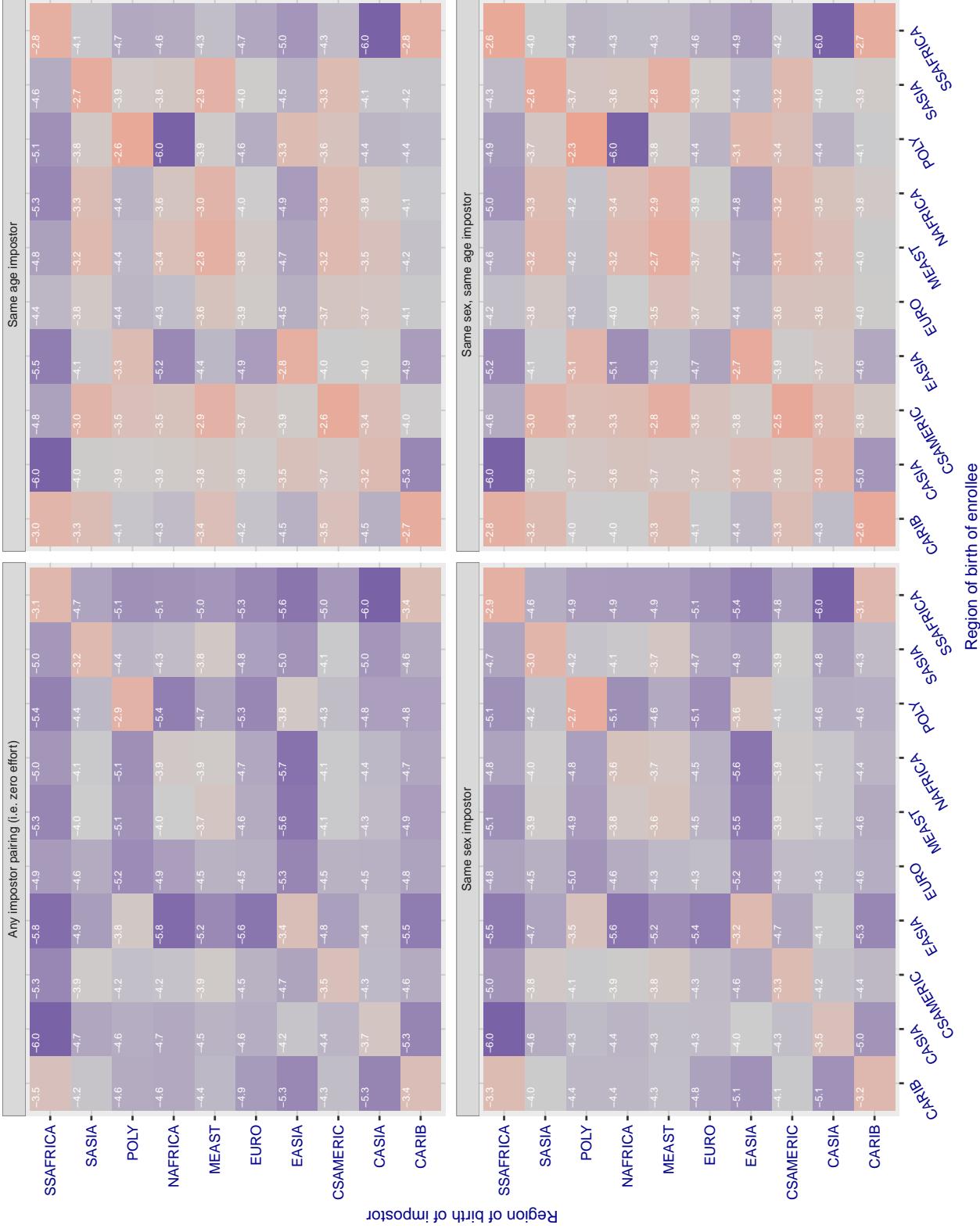


Figure 271: For algorithm visionbox-001 operating on visa images, the heatmap shows false match rates observed over impostor comparisons of faces from different individuals who were born in the given region pair. False matches are counted against a recognition threshold fixed globally to give the target FMR in the plot title, computed over all on the order of 10^{10} impostor comparisons. If text appears in each box it give the same quantity as that coded by the color. Grey indicates FMR is at the intended FMR target level. Light red colors present a security vulnerability to, for example, a passport gate. Each +1 increase in $\log_{10} FMR$ corresponds to a factor of 10 increase in FMR. The matrix is not quite symmetric because images in the enrollment and verification sets are different.

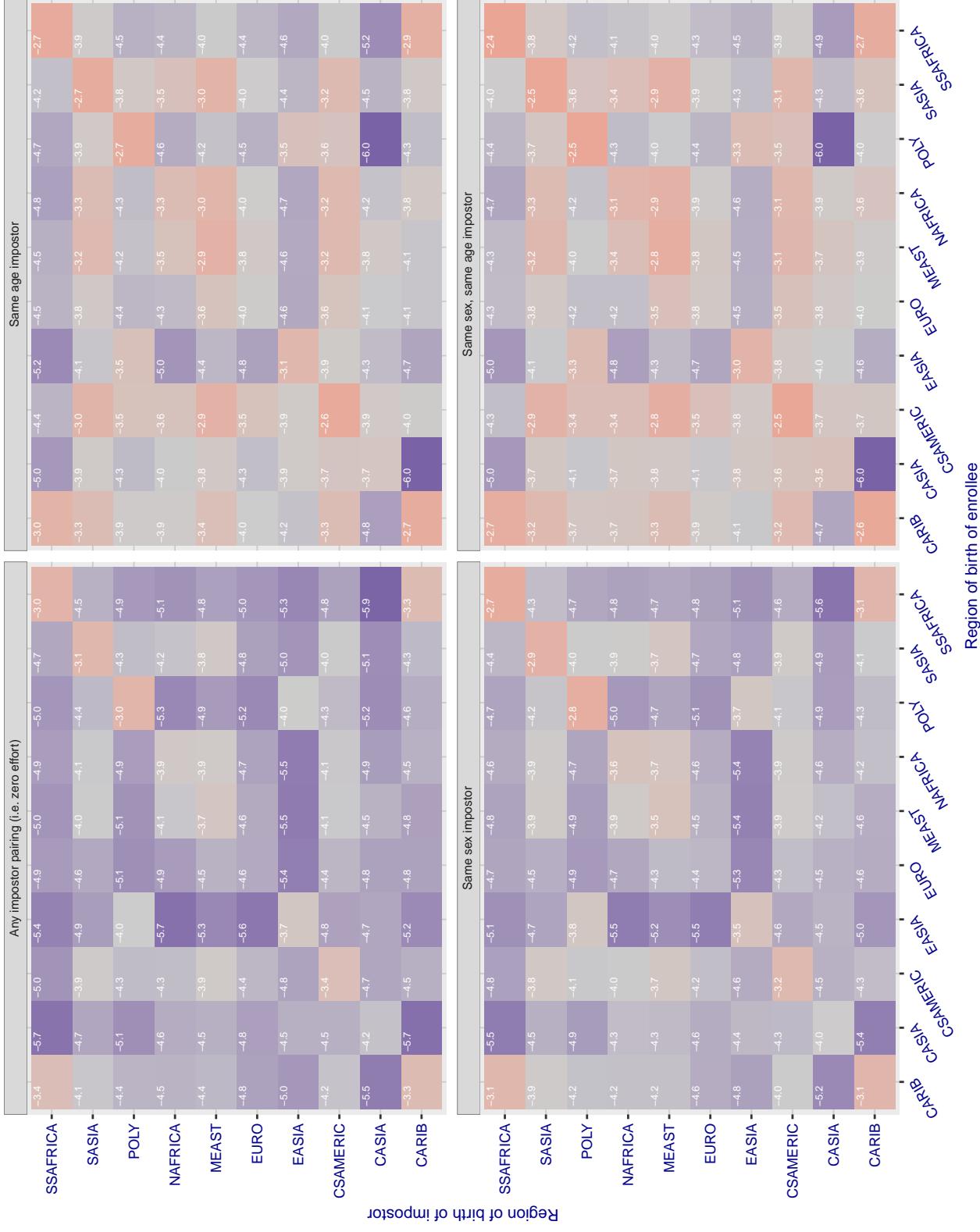
Cross region FMR at threshold T = 0.669 for algorithm visionlabs_006, giving FMR(T) = 0.0001 globally.

Figure 272: For algorithm visionlabs-006 operating on visa images, the heatmap shows false match rates observed over impostor comparisons of faces from different individuals who were born in the given region pair. False matches are counted against a recognition threshold fixed globally to give the target FMR in the plot title, computed over all on the order of 10^{10} impostor comparisons. If text appears in each box it give the same quantity as that coded by the color. Grey indicates FMR is at the intended FMR target level. Light red colors present a security vulnerability to, for example, a passport gate. Each +1 increase in $\log_{10} \text{FMR}$ corresponds to a factor of 10 increase in FMR. The matrix is not quite symmetric because images in the enrollment and verification sets are different.

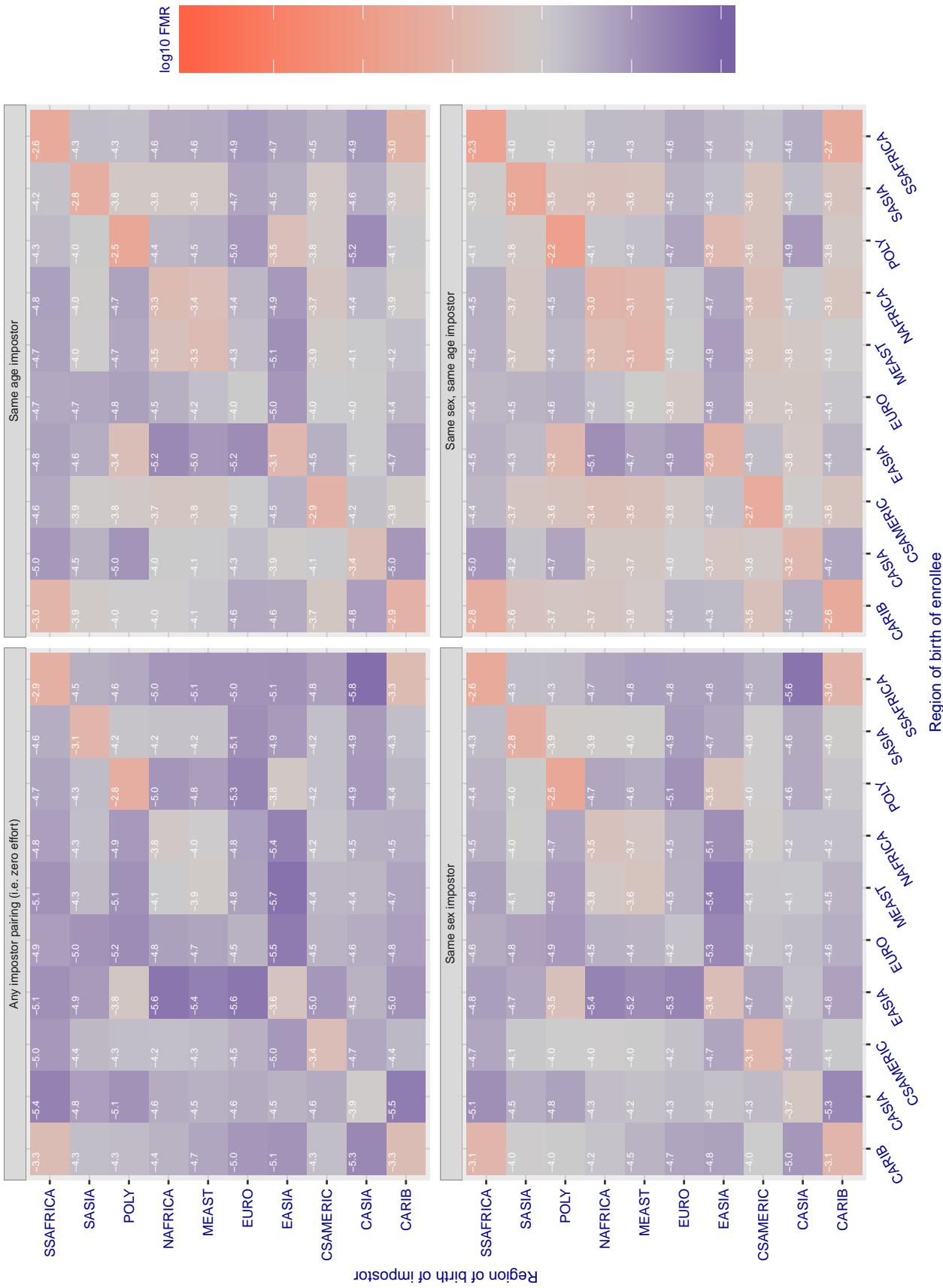
Cross region FMR at threshold T = 0.657 for algorithm visionlabs_007, giving FMR(T) = 0.0001 globally.

Figure 273: For algorithm visionlabs-007 operating on visa images, the heatmap shows false match rates observed over impostor comparisons of faces from different individuals who were born in the given region pair. False matches are counted against a recognition threshold fixed globally to give the target FMR in the plot title, computed over all on the order of 10^{10} impostor comparisons. If text appears in each box it give the same quantity as that coded by the color. Grey indicates FMR is at the intended FMR target level. Light red colors present a security vulnerability to, for example, a passport gate. Each +1 increase in $\log_{10} \text{FMR}$ corresponds to a factor of 10 increase in FMR. The matrix is not quite symmetric because images in the enrollment and verification sets are different.

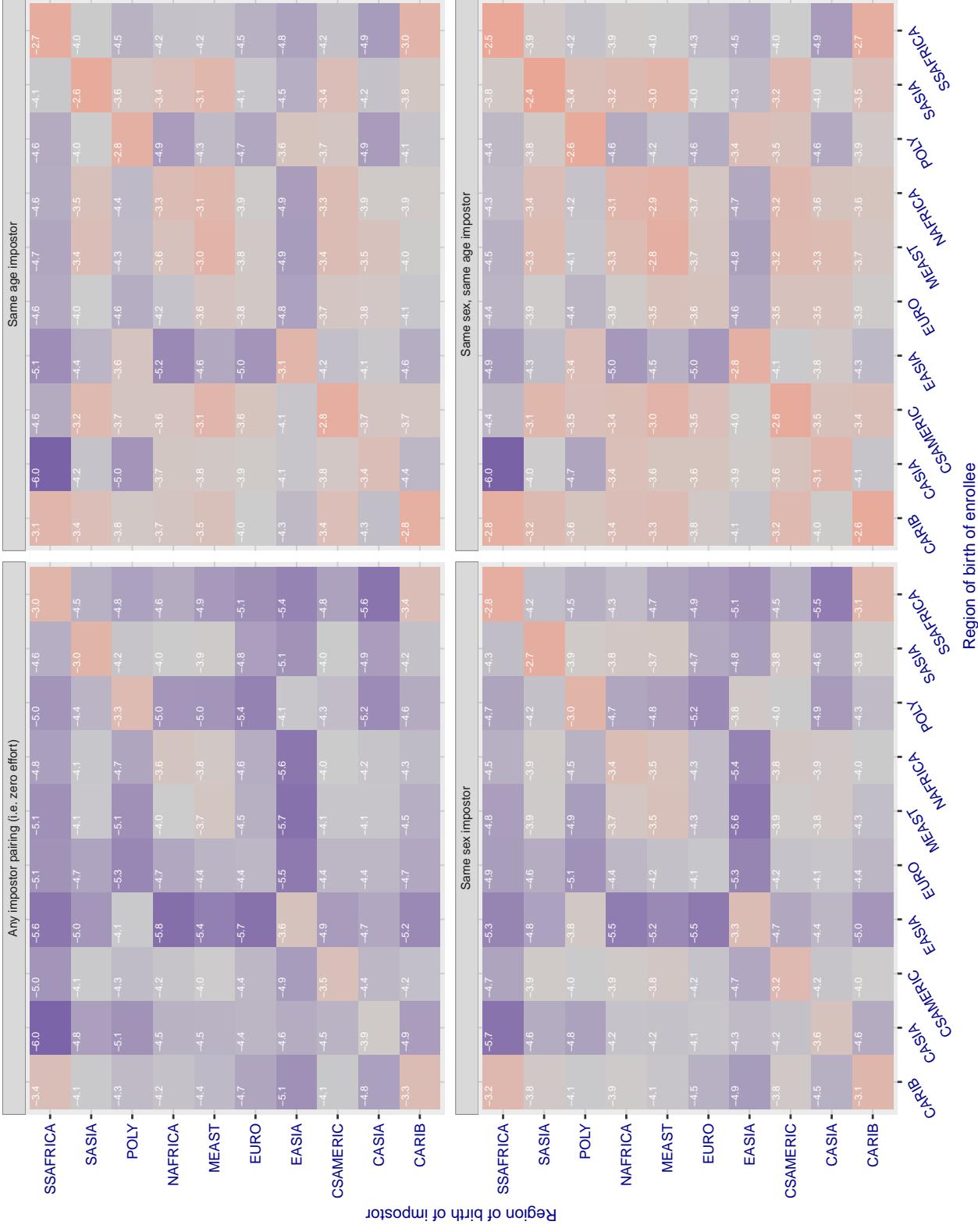
Cross region FMR at threshold T = 995.898 for algorithm vocord_006, giving FMR(T) = 0.0001 globally.

Figure 274: For algorithm vocord-006 operating on visa images, the heatmap shows false match rates observed over impostor comparisons of faces from different individuals who were born in the given region pair. False matches are counted against a recognition threshold fixed globally to give the target FMR in the plot title, computed over all on the order of 10^{10} impostor comparisons. If text appears in each box it give the same quantity as that coded by the color. Grey indicates FMR is at the intended FMR target level. Light red colors present a security vulnerability to, for example, a passport gate. Each +1 increase in $\log_{10} FMR$ corresponds to a factor of 10 increase in FMR. The matrix is not quite symmetric because images in the enrollment and verification sets are different.

Cross region FMR at threshold T = 995.241 for algorithm vocord_007, giving FMR(T) = 0.0001 globally.

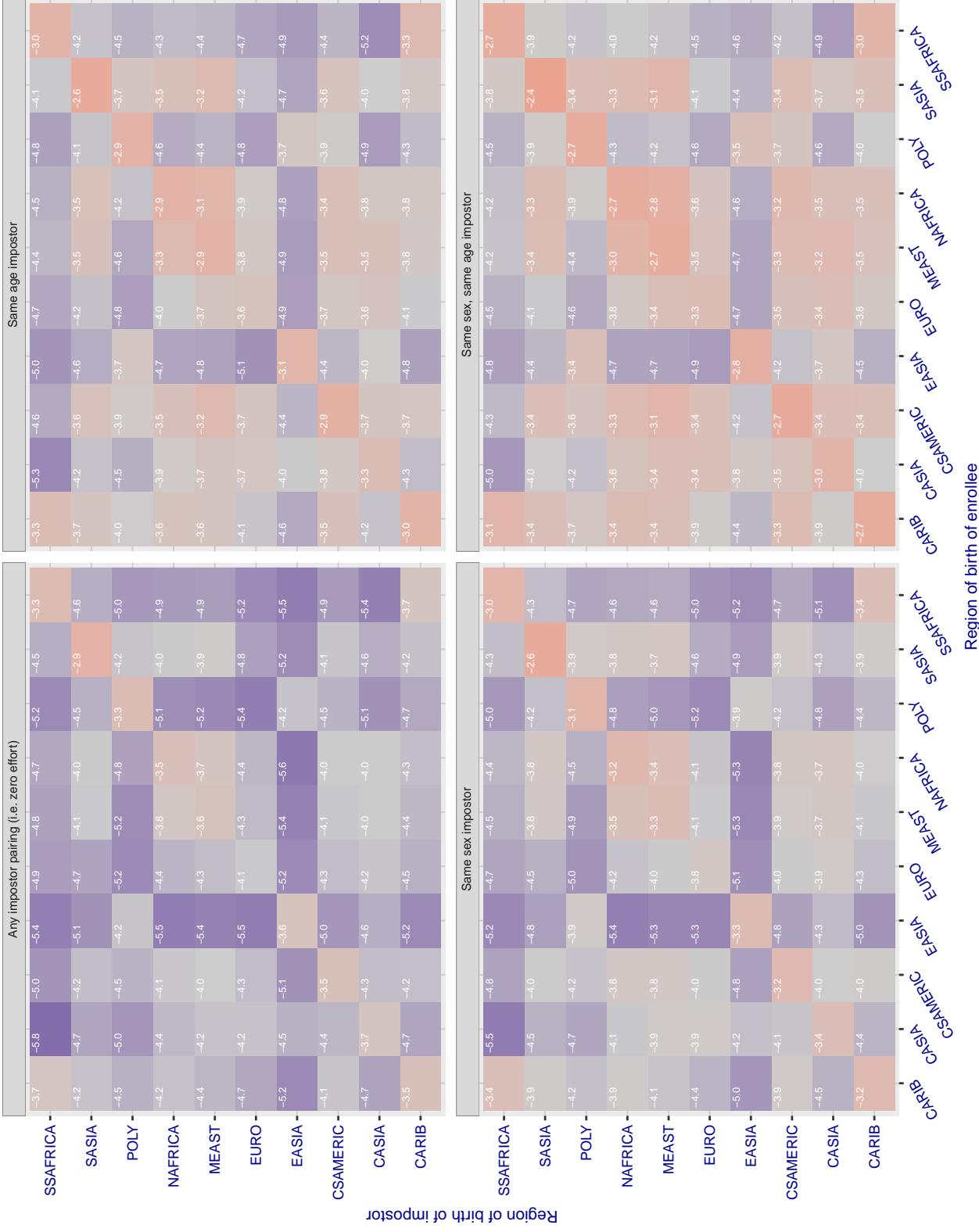


Figure 275: For algorithm vocord-007 operating on visa images, the heatmap shows false match rates observed over impostor comparisons of faces from different individuals who were born in the given region pair. False matches are counted against a recognition threshold fixed globally to give the target FMR in the plot title, computed over all on the order of 10^{10} impostor comparisons. If text appears in each box it give the same quantity as that coded by the color. Grey indicates FMR is at the intended FMR target level. Light red colors present a security vulnerability to, for example, a passport gate. Each +1 increase in $\log_{10} FMR$ corresponds to a factor of 10 increase in FMR. The matrix is not quite symmetric because images in the enrollment and verification sets are different.

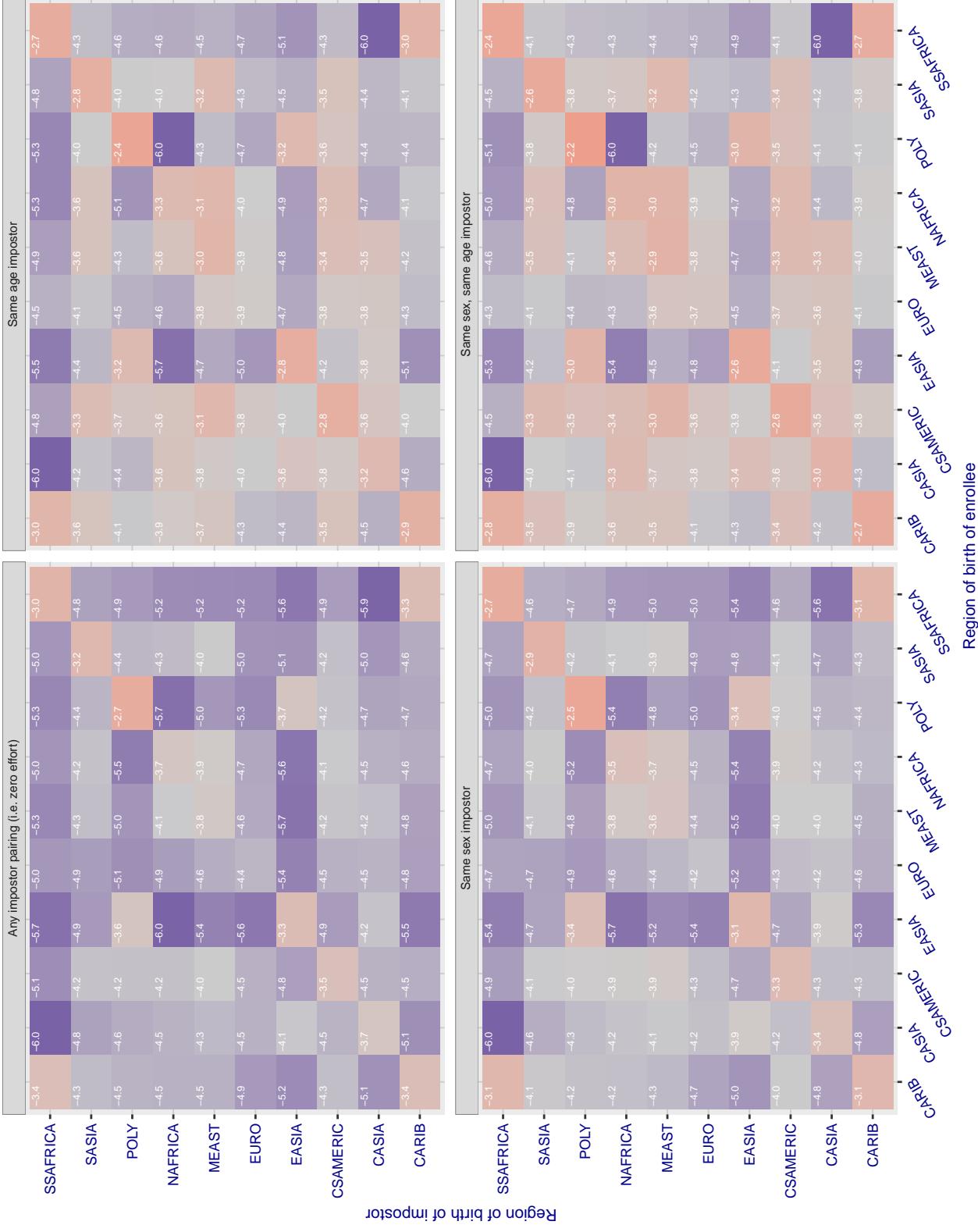
Cross region FMR at threshold T = 0.400 for algorithm winsense_000, giving FMR(T) = 0.0001 globally.

Figure 276: For algorithm winsense-000 operating on visa images, the heatmap shows false match rates observed over impostor comparisons of faces from different individuals who were born in the given region pair. False matches are counted against a recognition threshold fixed globally to give the target FMR in the plot title, computed over all on the order of 10^{10} impostor comparisons. If text appears in each box it give the same quantity as that coded by the color. Grey indicates FMR is at the intended FMR target level. Light red colors present a security vulnerability to, for example, a passport gate. Each +1 increase in $\log_{10} FMR$ corresponds to a factor of 10 increase in FMR. The matrix is not quite symmetric because images in the enrollment and verification sets are different.

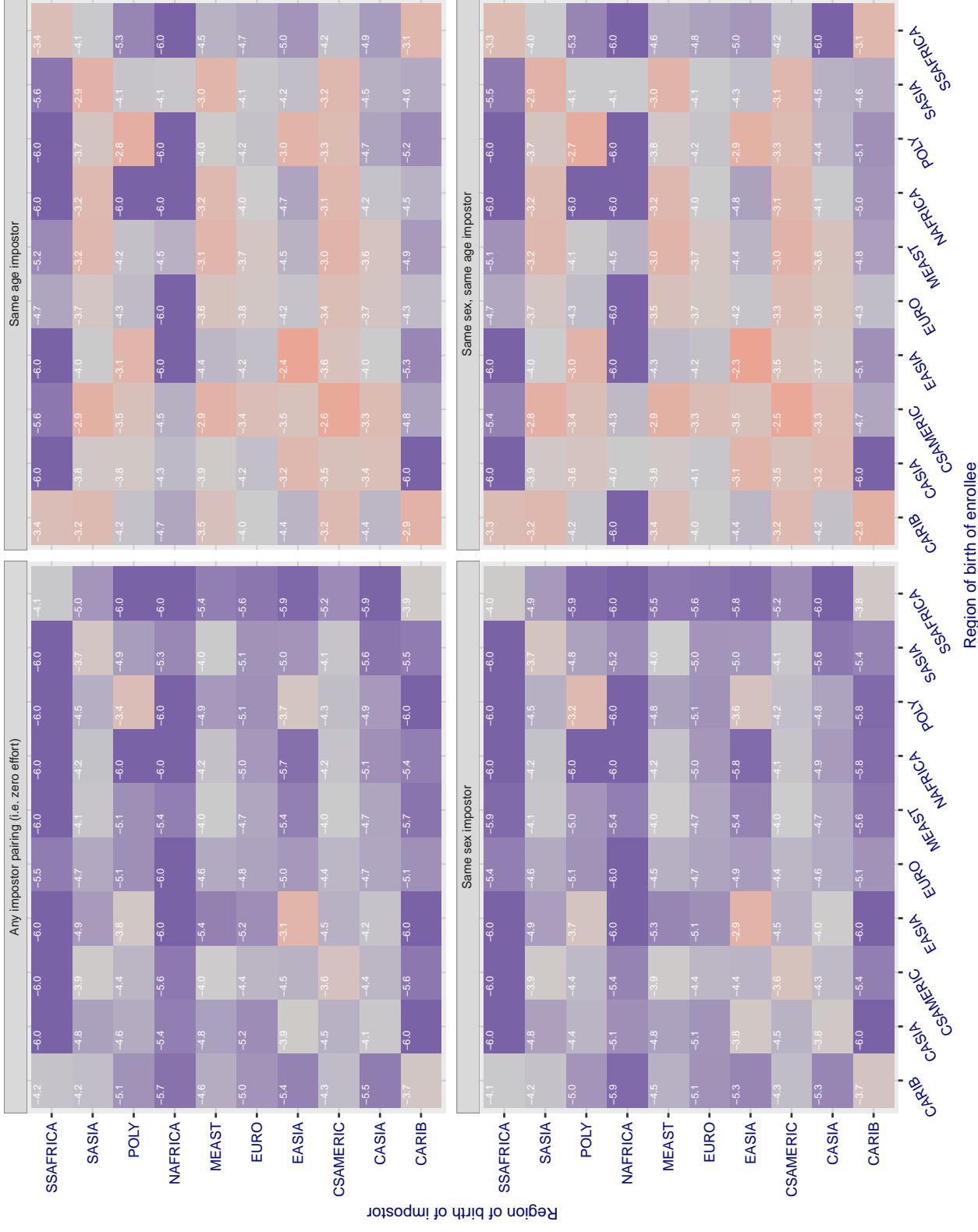
Cross region FMR at threshold T = 5.544 for algorithm yisheng_004, giving FMR(T) = 0.0001 globally.

Figure 277: For algorithm yisheng-004 operating on visa images, the heatmap shows false match rates observed over impostor comparisons of faces from different individuals who were born in the given region pair. False matches are counted against a recognition threshold fixed globally to give the target FMR in the plot title, computed over all on the order of 10^{10} impostor comparisons. If text appears in each box it give the same quantity as that coded by the color. Grey indicates FMR is at the intended FMR target level. Light red colors present a security vulnerability to, for example, a passport gate. Each +1 increase in $\log_{10} \text{FMR}$ corresponds to a factor of 10 increase in FMR. The matrix is not quite symmetric because images in the enrollment and verification sets are different.

Cross region FMR at threshold T = 37.698 for algorithm yitu_003, giving FMR(T) = 0.0001 globally.

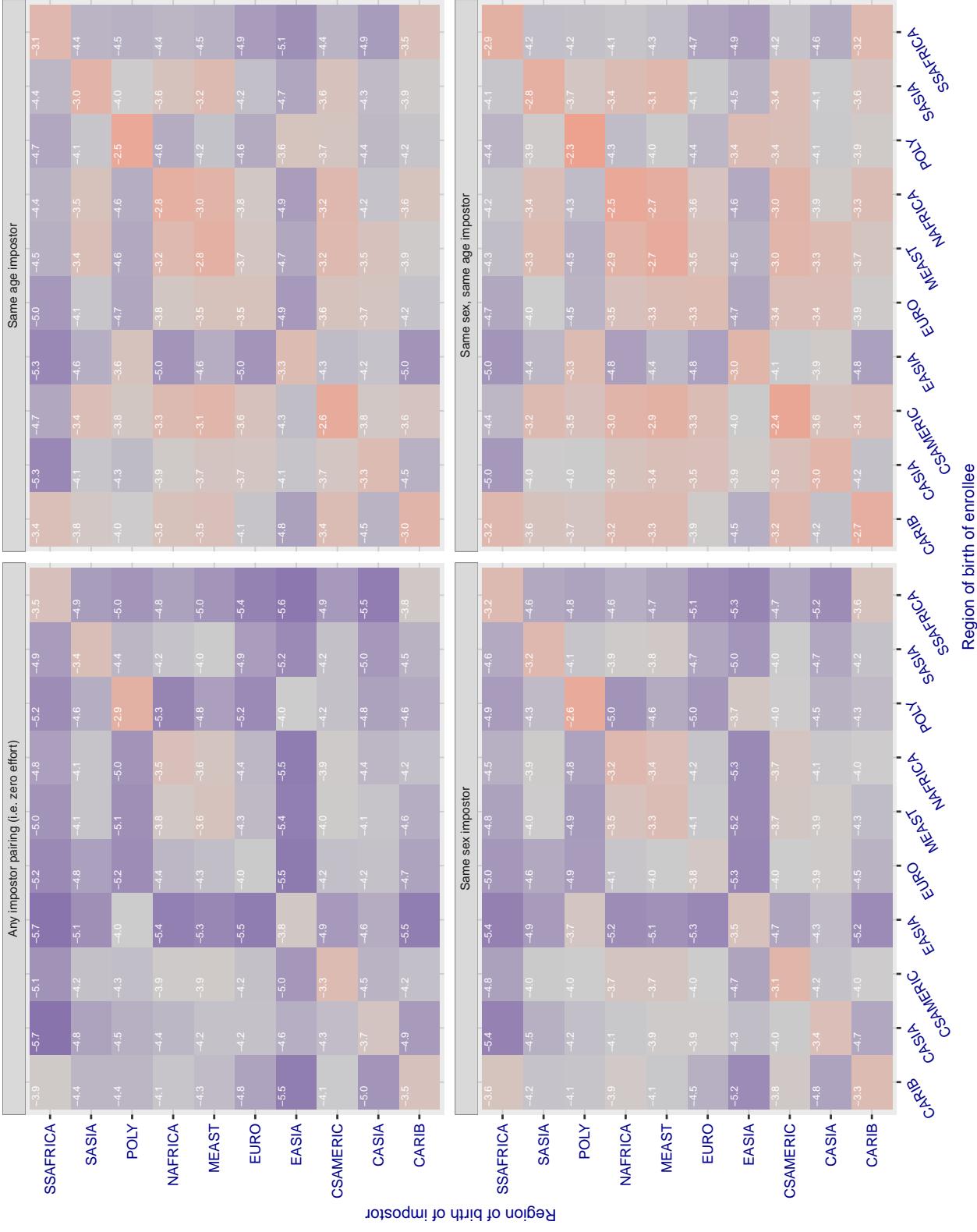


Figure 278: For algorithm yitu-003 operating on visa images, the heatmap shows false match rates observed over impostor comparisons of faces from different individuals who were born in the given region pair. False matches are counted against a recognition threshold fixed globally to give the target FMR in the plot title, computed over all on the order of 10^{10} impostor comparisons. If text appears in each box it give the same quantity as that coded by the color. Grey indicates FMR is at the intended FMR target level. Light red colors present a security vulnerability to, for example, a passport gate. Each +1 increase in $\log 10 \text{ FMR}$ corresponds to a factor of 10 increase in FMR. The matrix is not quite symmetric because images in the enrollment and verification sets are different.

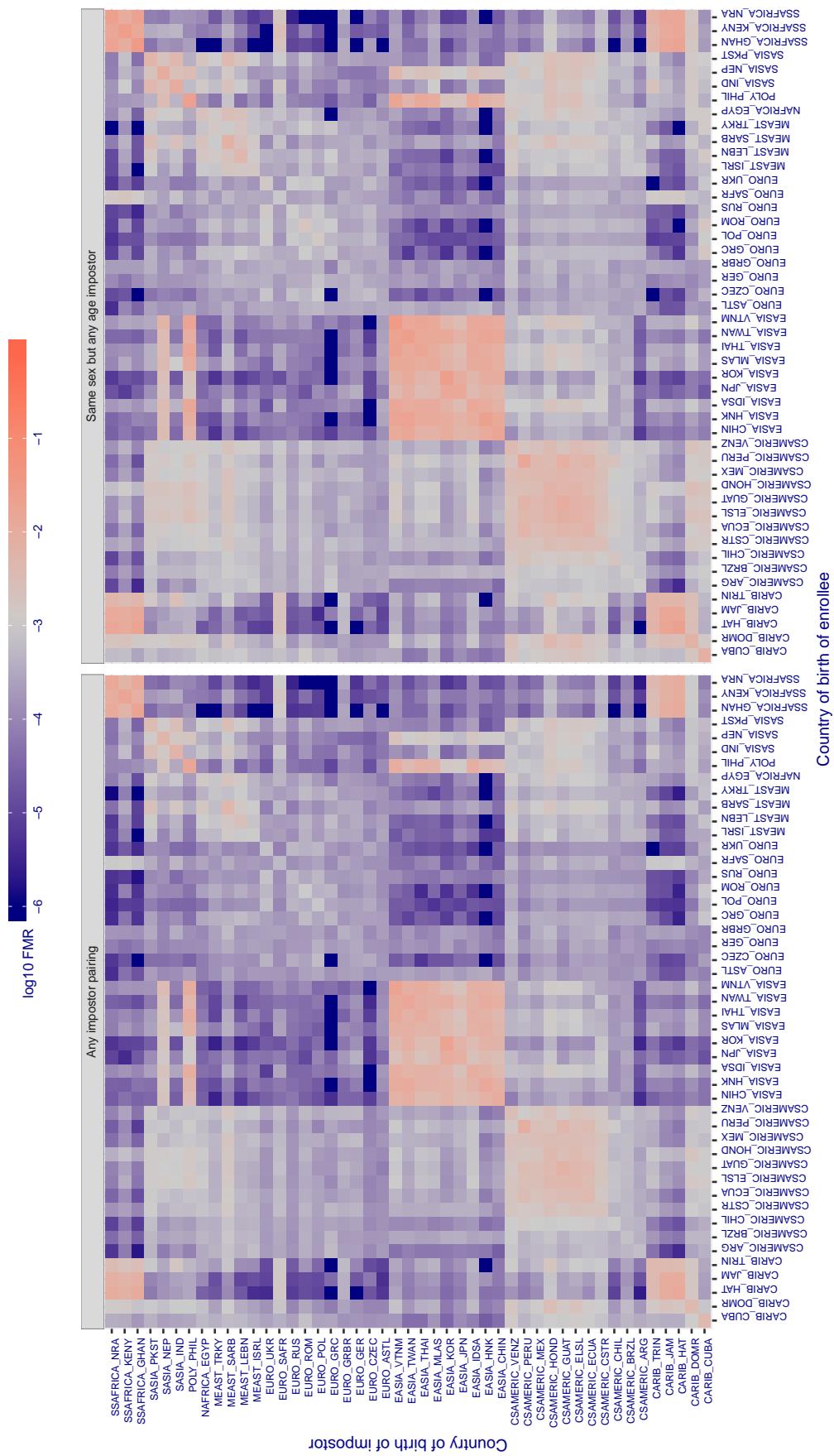
Cross country FMR at threshold T = 2.575 for algorithm 3divi_003, giving $\text{FMR}(\text{T}) = 0.001$ globally.

Figure 279: For algorithm 3divi-003 operating on visa images, the heatmap shows false match rates observed over impostor comparisons of faces from different individuals who were born in the given country pair. False matches are counted against a recognition threshold fixed globally to give the target FMR in the plot title, computed over all on the order of 10^{10} impostor comparisons. If text appears in each box it give the same quantity as that coded by the color. Grey indicates FMR is at the intended FMR target level. Light red colors present a security vulnerability to, for example, a passport gate. Each $+1$ increase in $\log_{10} \text{FMR}$ corresponds to a factor of 10 increase in FMR . The matrix is not quite symmetric because images in the enrollment and verification sets are different.

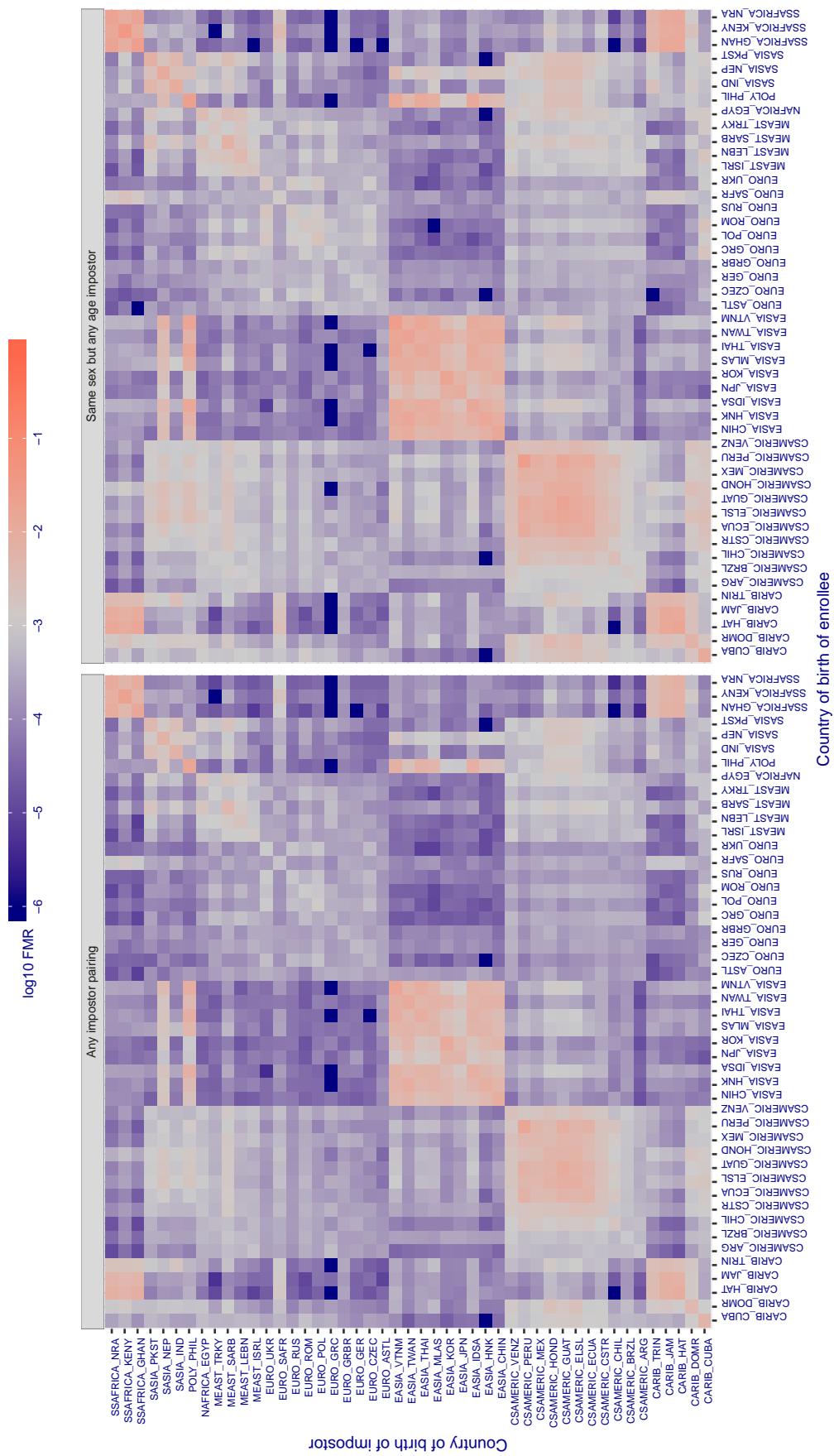
Cross country FMR at threshold T = 2.692 for algorithm 3divi_004, giving $\text{FMR}(\text{T}) = 0.001$ globally.

Figure 280: For algorithm 3divi-004 operating on visa images, the heatmap shows false match rates observed over impostor comparisons of faces from different individuals who were born in the given country pair. False matches are counted against a recognition threshold fixed globally to give the target FMR in the plot title, computed over all on the order of 10^{10} impostor comparisons. If text appears in each box it give the same quantity as that coded by the color. Grey indicates FMR is at the intended FMR target level. Light red colors present a security vulnerability to, for example, a passport gate. Each +1 increase in $\log_{10} \text{FMR}$ corresponds to a factor of 10 increase in FMR . The matrix is not quite symmetric because images in the enrollment and verification sets are different.

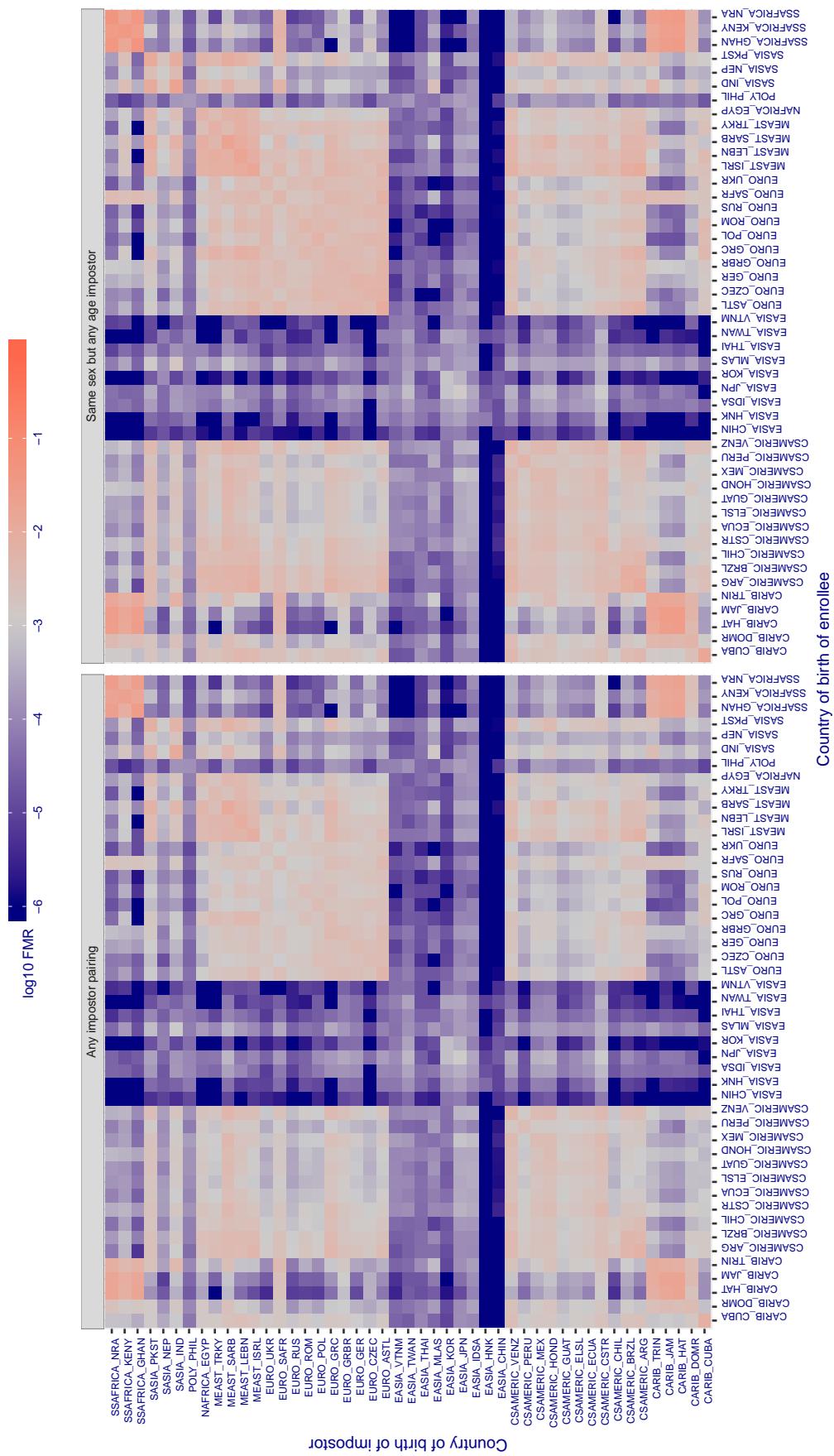
Cross country FMR at threshold T = 0.632 for algorithm adera_001, giving $FMR(T) = 0.001$ globally.

Figure 281: For algorithm adera-001 operating on visa images, the heatmap shows false match rates observed over impostor comparisons of faces from different individuals who were born in the given country pair. False matches are counted against a recognition threshold fixed globally to give the target FMR in the plot title, computed over all on the order of 10^{10} impostor comparisons. If text appears in each box it give the same quantity as that coded by the color. Grey indicates FMR is at the intended FMR target level. Light red colors present a security vulnerability to, for example, a passport gate. Each +1 increase in $\log_{10} FMR$ corresponds to a factor of 10 increase in FMR . The matrix is not quite symmetric because images in the enrollment and verification sets are different.

Cross country FMR at threshold $T = 0.6662$ for algorithm alchera_000, giving $FMR(T) = 0.001$ globally.

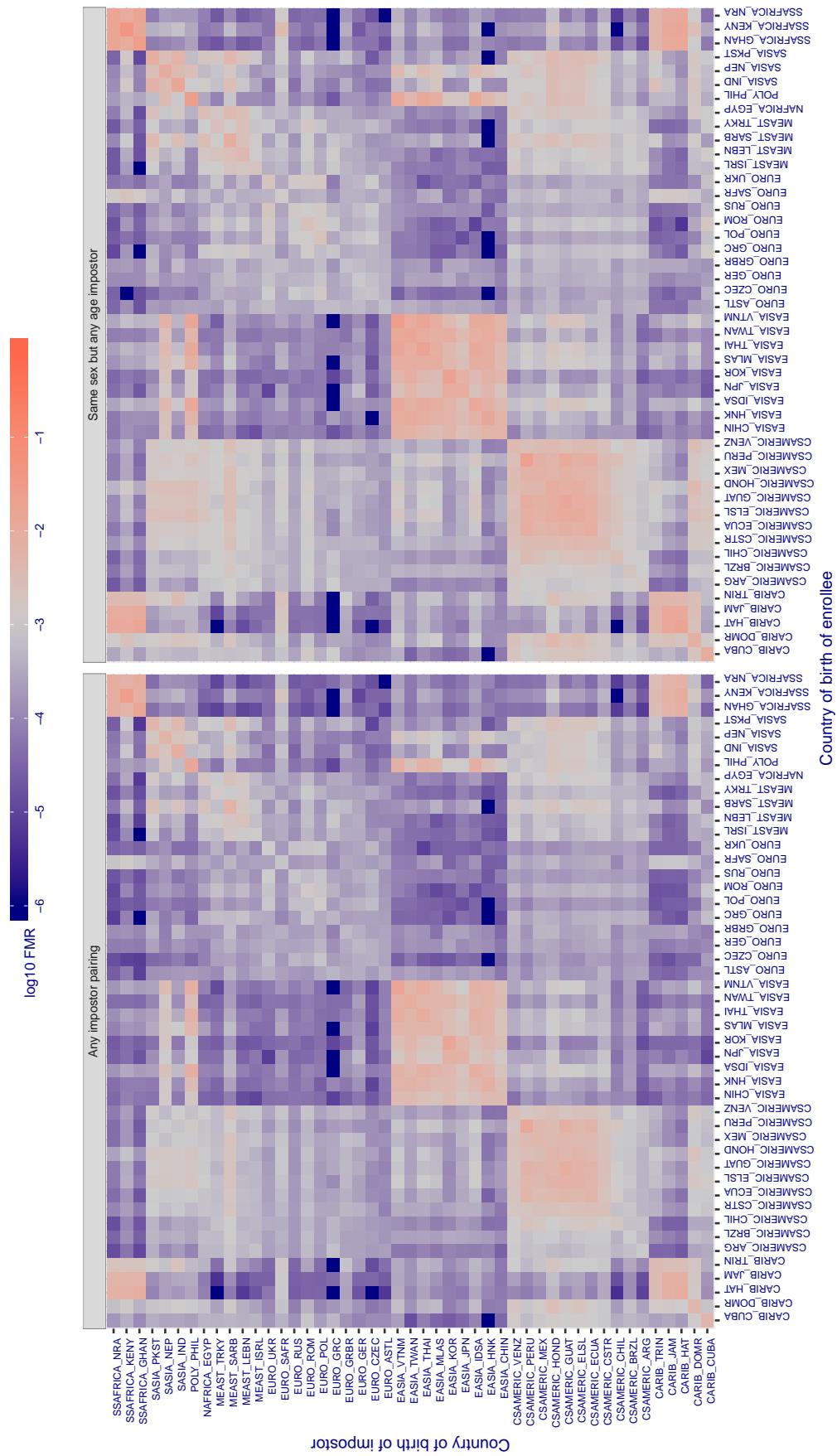


Figure 282: For algorithm alchera-000 operating on visa images, the heatmap shows false match rates observed over impostor comparisons of faces from different individuals who were born in the given country pair. False matches are counted against a recognition threshold fixed globally to give the target FMR in the plot title, computed over all on the order of 10^{10} impostor comparisons. If text appears in each box it give the same quantity as that coded by the color. Grey indicates FMR is at the intended FMR target level. Light red colors present a security vulnerability to, for example, a passport gate. Each +1 increase in $\log_{10} FMR$ corresponds to a factor of 10 increase in FMR . The matrix is not quite symmetric because images in the enrollment and verification sets are different.

Cross country FMR at threshold $T = 0.667$ for algorithm alchera_001, giving $FMR(T) = 0.001$ globally.

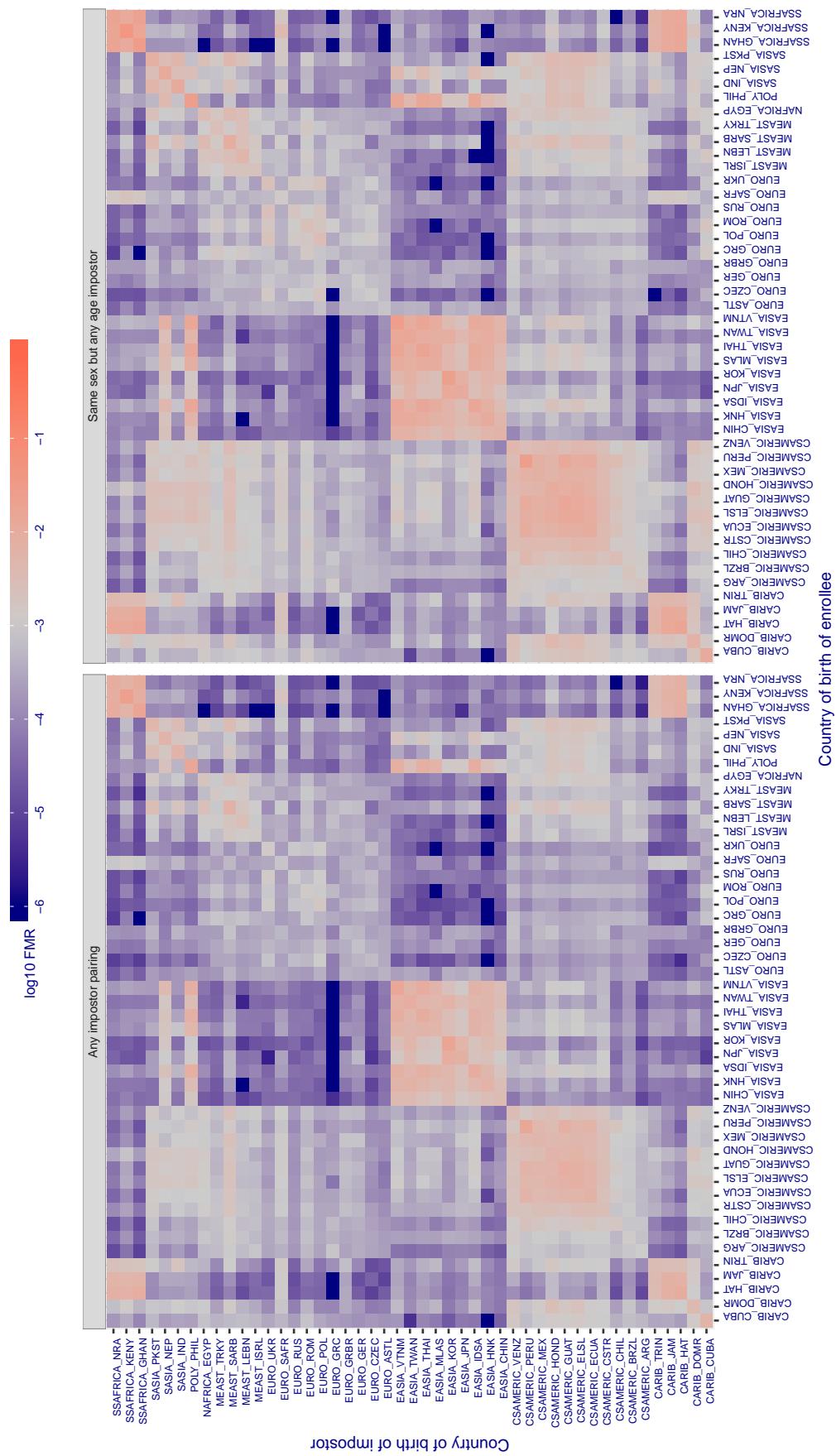


Figure 283: For algorithm alchera-001 operating on visa images, the heatmap shows false match rates observed over impostor comparisons of faces from different individuals who were born in the given country pair. False matches are counted against a recognition threshold fixed globally to give the target FMR in the plot title, computed over all on the order of 10^{10} impostor comparisons. If text appears in each box it give the same quantity as that coded by the color. Grey indicates FMR is at the intended FMR target level. Light red colors present a security vulnerability to, for example, a passport gate. Each +1 increase in $\log_{10} FMR$ corresponds to a factor of 10 increase in FMR . The matrix is not quite symmetric because images in the enrollment and verification sets are different.

Cross country FMR at threshold T = 0.339 for algorithm allgovision_000, giving $\text{FMR}(T) = 0.001$ globally.

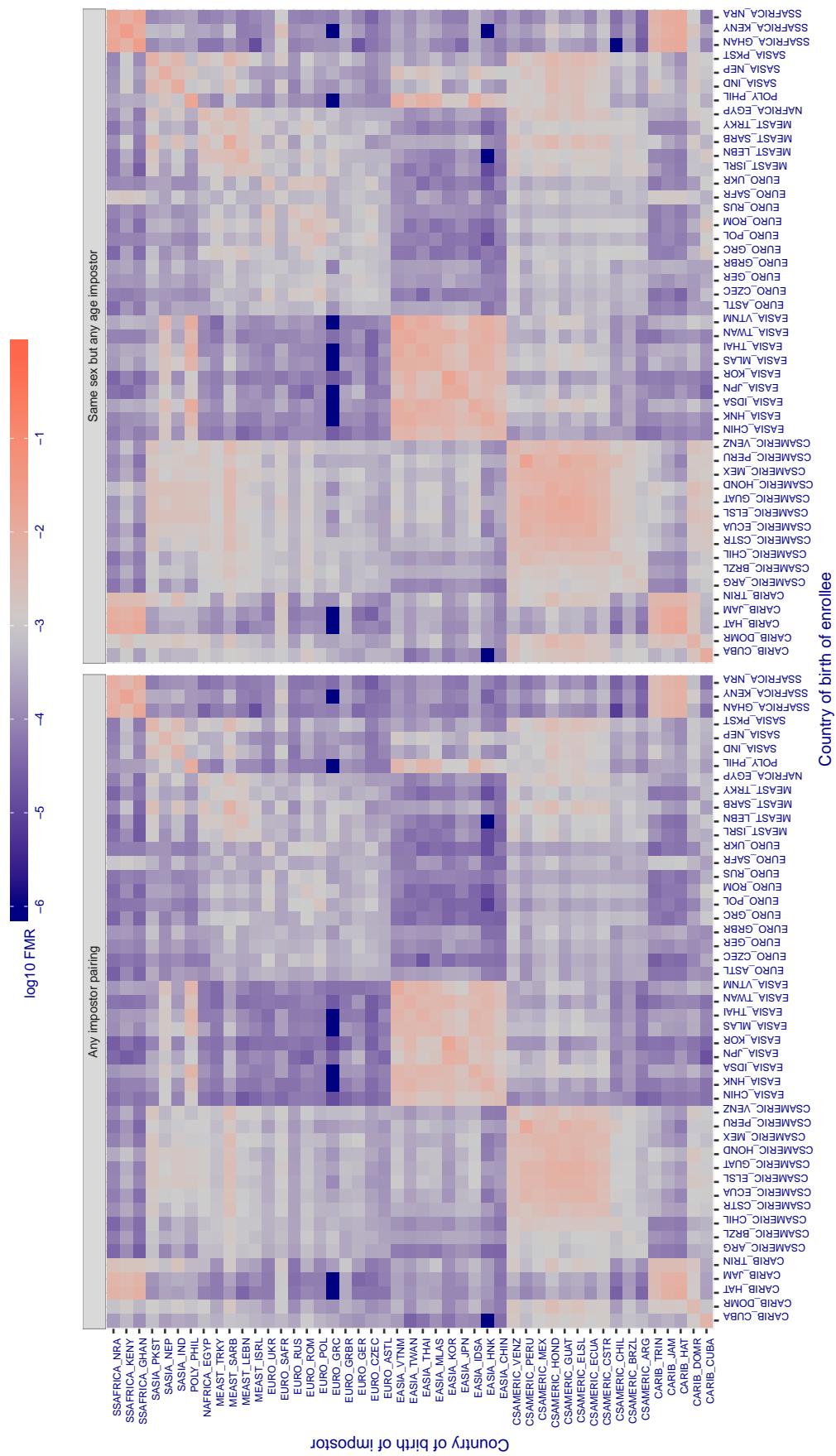


Figure 284: For algorithm allgovision-000 operating on visa images, the heatmap shows false match rates observed over impostor comparisons of faces from different individuals who were born in the given country pair. False matches are counted against a recognition threshold fixed globally to give the target FMR in the plot title, computed over all on the order of 10^{10} impostor comparisons. If text appears in each box it give the same quantity as that coded by the color. Grey indicates FMR is at the intended FMR target level. Light red colors present a security vulnerability to, for example, a passport gate. Each +1 increase in $\log_{10} \text{FMR}$ corresponds to a factor of 10 increase in FMR. The matrix is not quite symmetric because images in the enrollment and verification sets are different.

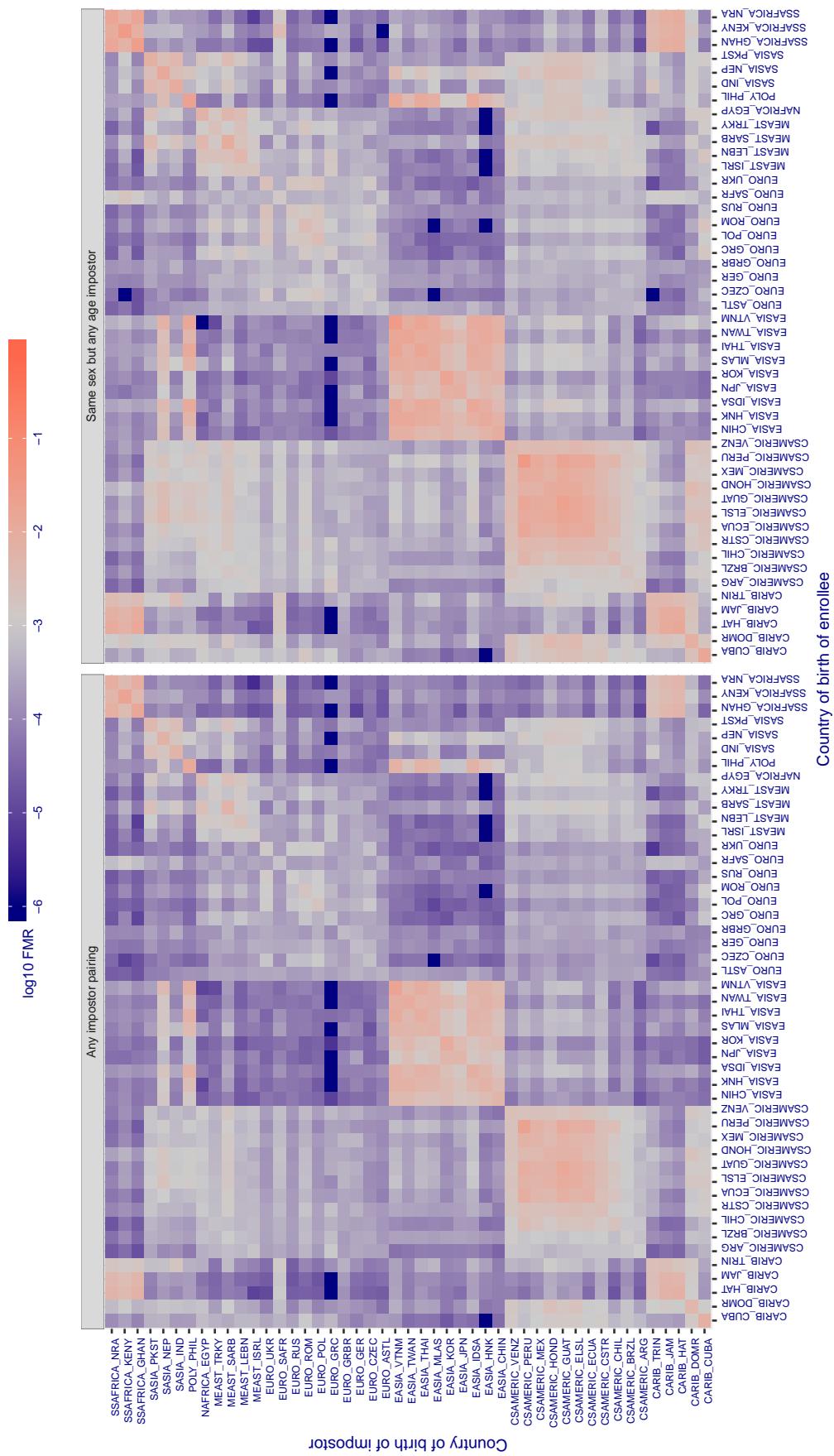
Cross country FMR at threshold T = 0.313 for algorithm alphaface_001, giving FMR(T) = 0.001 globally.

Figure 285: For algorithm alphaface-001 operating on visa images, the heatmap shows false match rates observed over impostor comparisons of faces from different individuals who were born in the given country pair. False matches are counted against a recognition threshold fixed globally to give the target FMR in the plot title, computed over all on the order of 10^{10} impostor comparisons. If text appears in each box it give the same quantity as that coded by the color. Grey indicates FMR is at the intended FMR target level. Light red colors present a security vulnerability to, for example, a passport gate. Each +1 increase in $\log_{10} FMR$ corresponds to a factor of 10 increase in FMR. The matrix is not quite symmetric because images in the enrollment and verification sets are different.

Cross country FMR at threshold T = 3.524 for algorithm amplifiedgroup_001, giving FMR(T) = 0.001 globally.

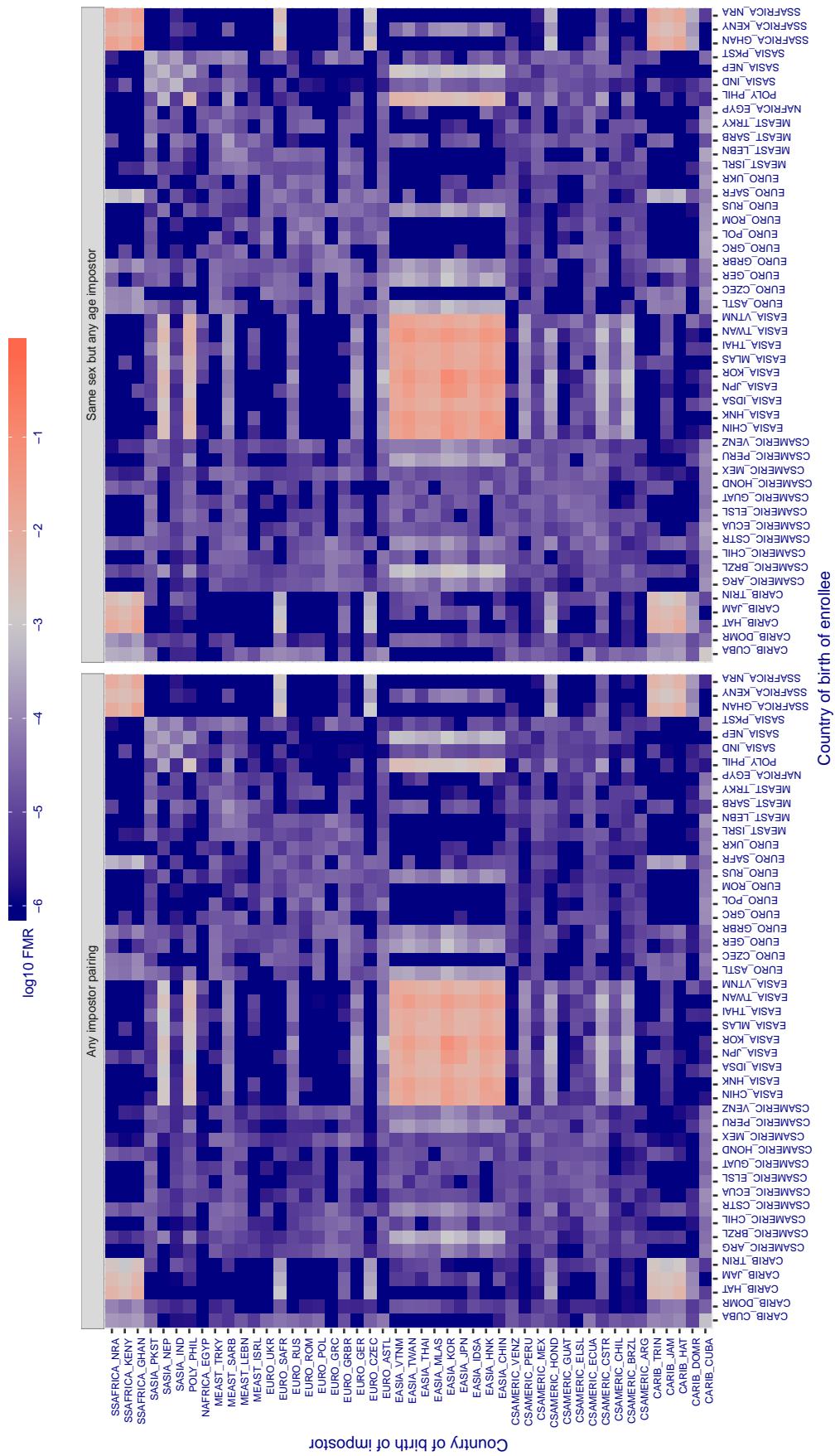


Figure 286: For algorithm amplifiedgroup-001 operating on visa images, the heatmap shows false match rates observed over impostor comparisons of faces from different individuals who were born in the given country pair. False matches are counted against a recognition threshold fixed globally to give the target FMR in the plot title, computed over all on the order of 10^{10} impostor comparisons. If text appears in each box it give the same quantity as that coded by the color. Grey indicates FMR is at the intended FMR target level. Light red colors present a security vulnerability to, for example, a passport gate. Each +1 increase in $\log_{10} FMR$ corresponds to a factor of 10 increase in FMR. The matrix is not quite symmetric because images in the enrollment and verification sets are different.

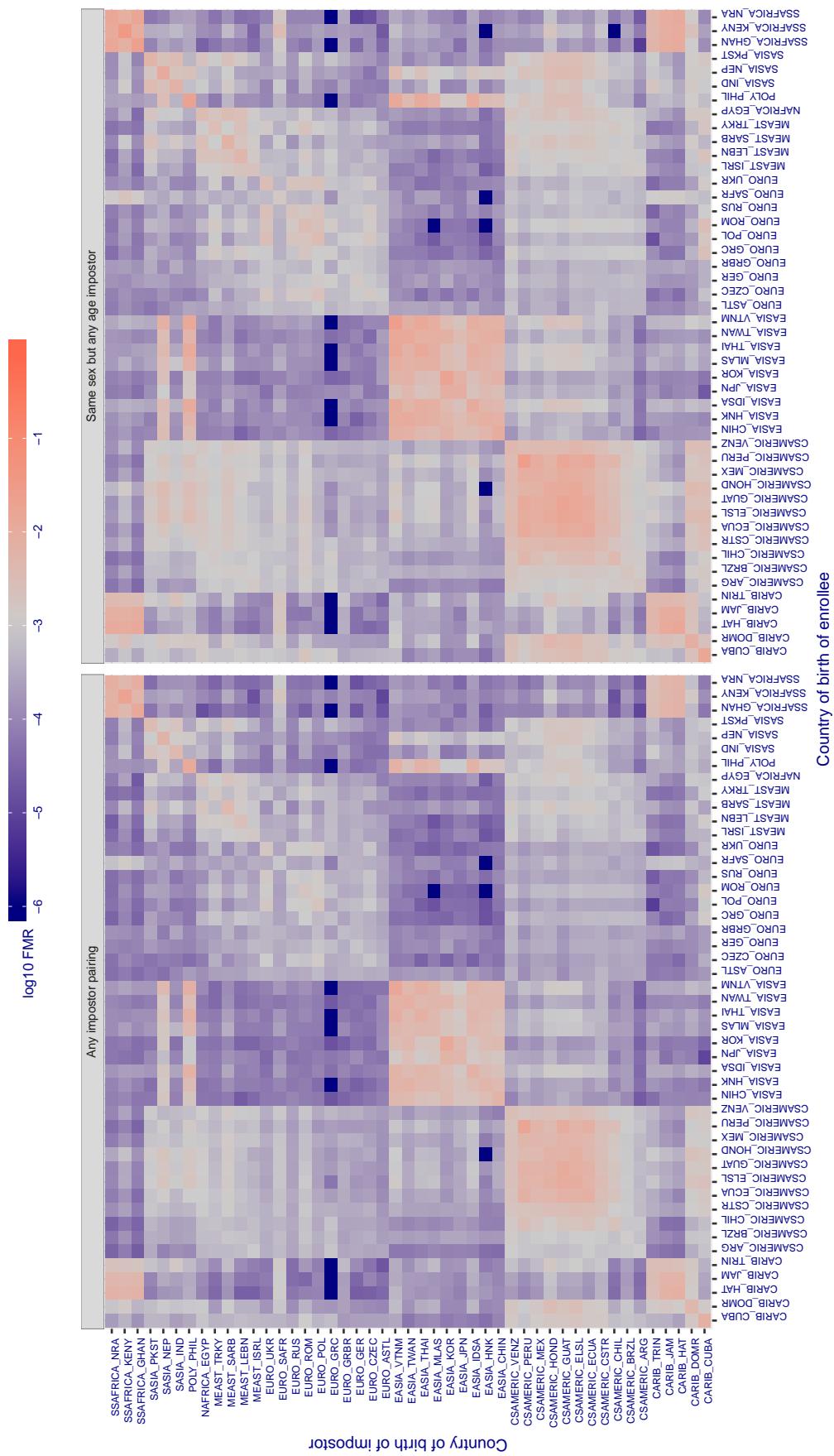
Cross country FMR at threshold T = 0.313 for algorithm anke_003, giving $\text{FMR}(T) = 0.001$ globally.

Figure 287: For algorithm anke-003 operating on visa images, the heatmap shows false match rates observed over impostor comparisons of faces from different individuals who were born in the given country pair. False matches are counted against a recognition threshold fixed globally to give the target FMR in the plot title, computed over all on the order of 10^{10} impostor comparisons. If text appears in each box it give the same quantity as that coded by the color. Grey indicates FMR is at the intended FMR target level. Light red colors present a security vulnerability to, for example, a passport gate. Each $+1$ increase in $\log_{10} \text{FMR}$ corresponds to a factor of 10 increase in FMR . The matrix is not quite symmetric because images in the enrollment and verification sets are different.

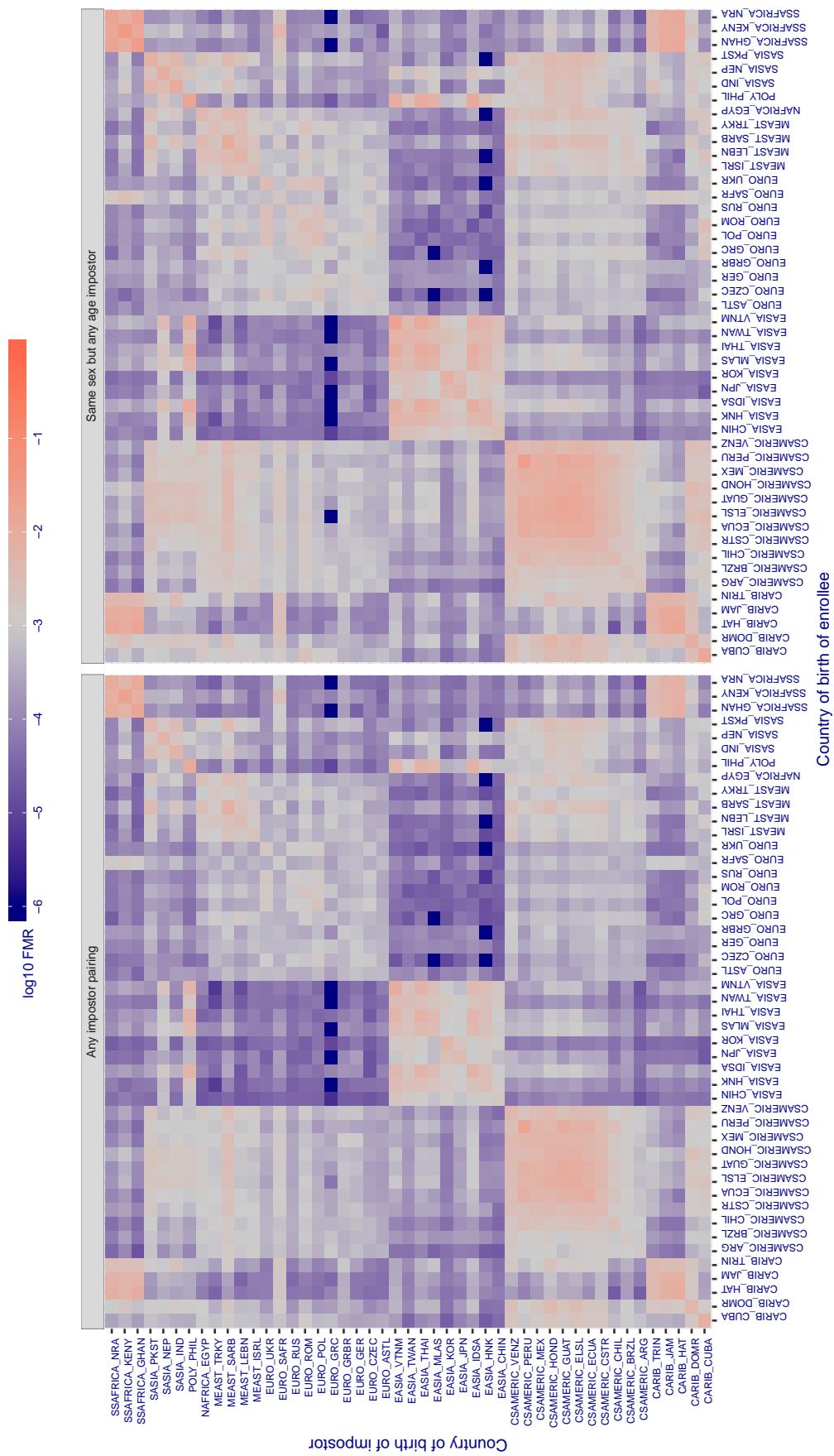
Cross country FMR at threshold T = 0.309 for algorithm anke_004, giving $\text{FMR}(\text{T}) = 0.001$ globally.

Figure 288: For algorithm anke-004 operating on visa images, the heatmap shows false match rates observed over impostor comparisons of faces from different individuals who were born in the given country pair. False matches are counted against a recognition threshold fixed globally to give the target FMR in the plot title, computed over all on the order of 10^{10} impostor comparisons. If text appears in each box it give the same quantity as that coded by the color. Grey indicates FMR is at the intended FMR target level. Light red colors present a security vulnerability to, for example, a passport gate. Each $+1$ increase in $\log_{10} \text{FMR}$ corresponds to a factor of 10 increase in FMR . The matrix is not quite symmetric because images in the enrollment and verification sets are different.

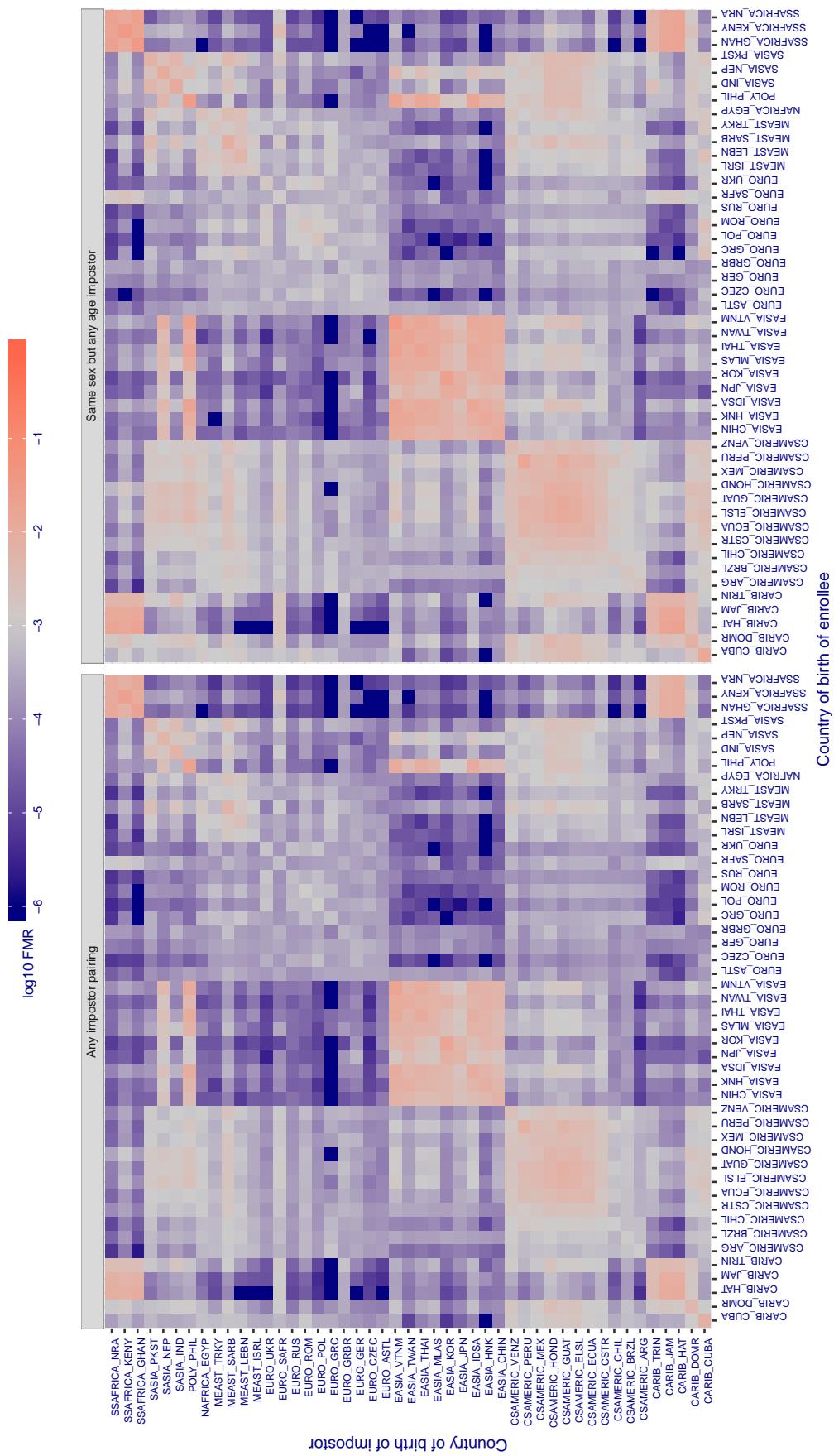
Cross country FMR at threshold T = 1.431 for algorithm anyvision_002, giving FMR(T) = 0.001 globally.

Figure 289: For algorithm anyvision-002 operating on visa images, the heatmap shows false match rates observed over impostor comparisons of faces from different individuals who were born in the given country pair. False matches are counted against a recognition threshold fixed globally to give the target FMR in the plot title, computed over all on the order of 10^{10} impostor comparisons. If text appears in each box it give the same quantity as that coded by the color. Grey indicates FMR is at the intended FMR target level. Light red colors present a security vulnerability to, for example, a passport gate. Each +1 increase in $\log_{10} FMR$ corresponds to a factor of 10 increase in FMR. The matrix is not quite symmetric because images in the enrollment and verification sets are different.

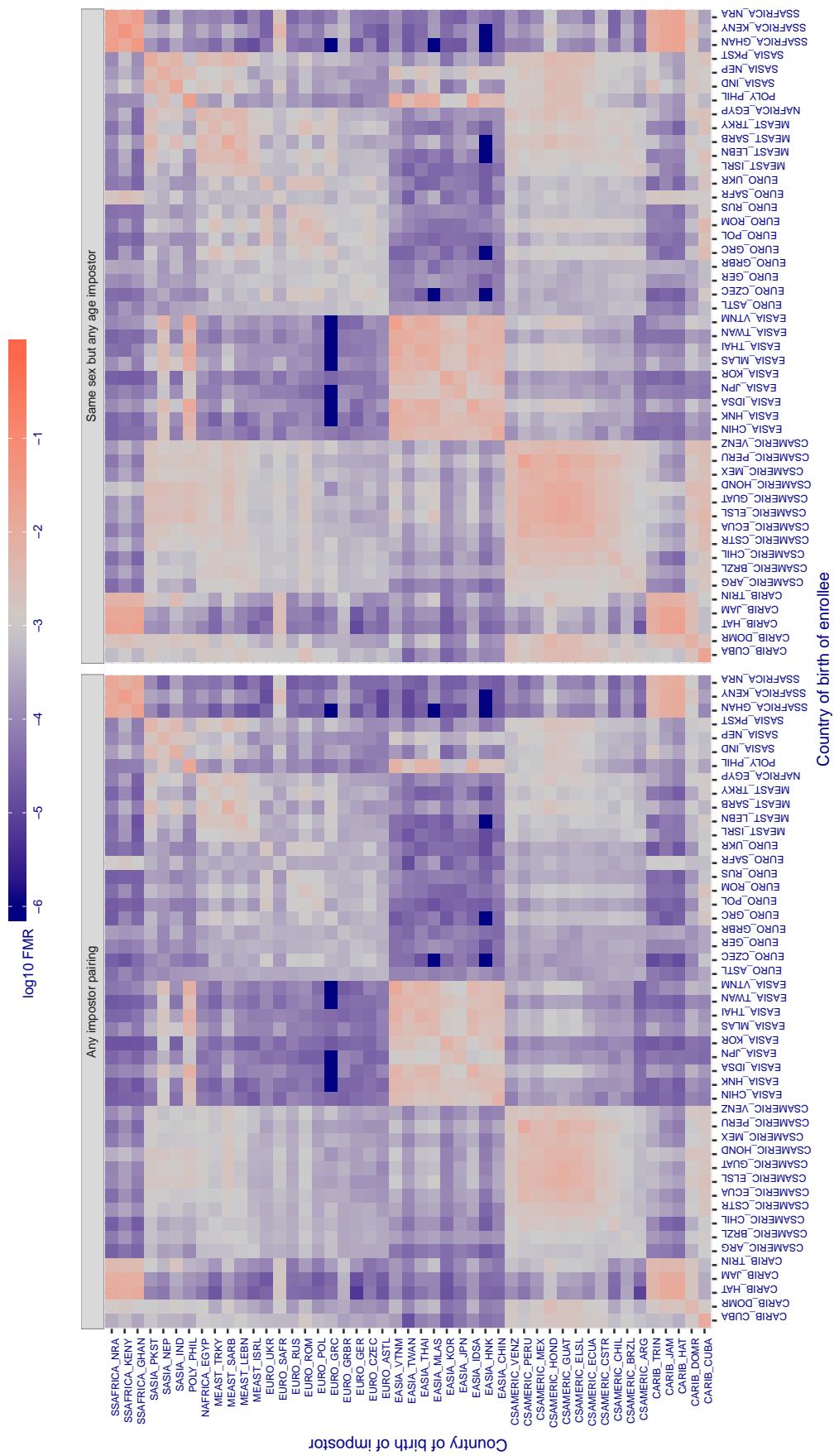
Cross country FMR at threshold T = 1.297 for algorithm anyvision_004, giving FMR(T) = 0.001 globally.

Figure 290: For algorithm anyvision-004 operating on visa images, the heatmap shows false match rates observed over impostor comparisons of faces from different individuals who were born in the given country pair. False matches are counted against a recognition threshold fixed globally to give the target FMR in the plot title, computed over all on the order of 10^{10} impostor comparisons. If text appears in each box it give the same quantity as that coded by the color. Grey indicates FMR is at the intended FMR target level. Light red colors present a security vulnerability to, for example, a passport gate. Each +1 increase in $\log_{10} \text{FMR}$ corresponds to a factor of 10 increase in FMR. The matrix is not quite symmetric because images in the enrollment and verification sets are different.

Cross country FMR at threshold T = 2.758 for algorithm aware_003, giving $\text{FMR}(\text{T}) = 0.001$ globally.

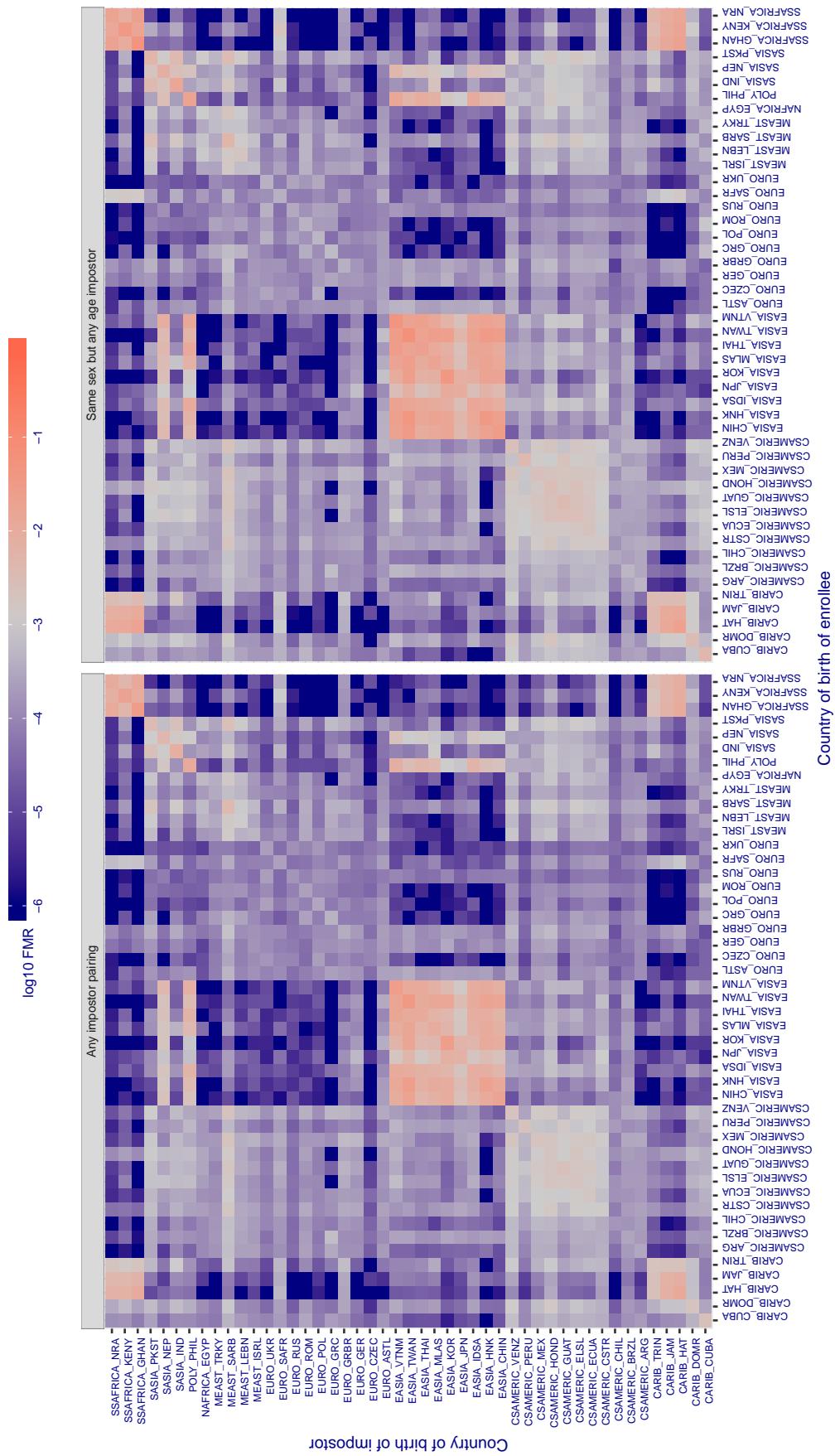


Figure 291: For algorithm aware-003 operating on visa images, the heatmap shows false match rates observed over impostor comparisons of faces from different individuals who were born in the given country pair. False matches are counted against a recognition threshold fixed globally to give the target FMR in the plot title, computed over all on the order of 10^{10} impostor comparisons. If text appears in each box it give the same quantity as that coded by the color. Grey indicates FMR is at the intended FMR target level. Light red colors present a security vulnerability to, for example, a passport gate. Each +1 increase in $\log_{10} \text{FMR}$ corresponds to a factor of 10 increase in FMR . The matrix is not quite symmetric because images in the enrollment and verification sets are different.

Cross country FMR at threshold T = 3.681 for algorithm aware_004, giving $\text{FMR}(\text{T}) = 0.001$ globally.

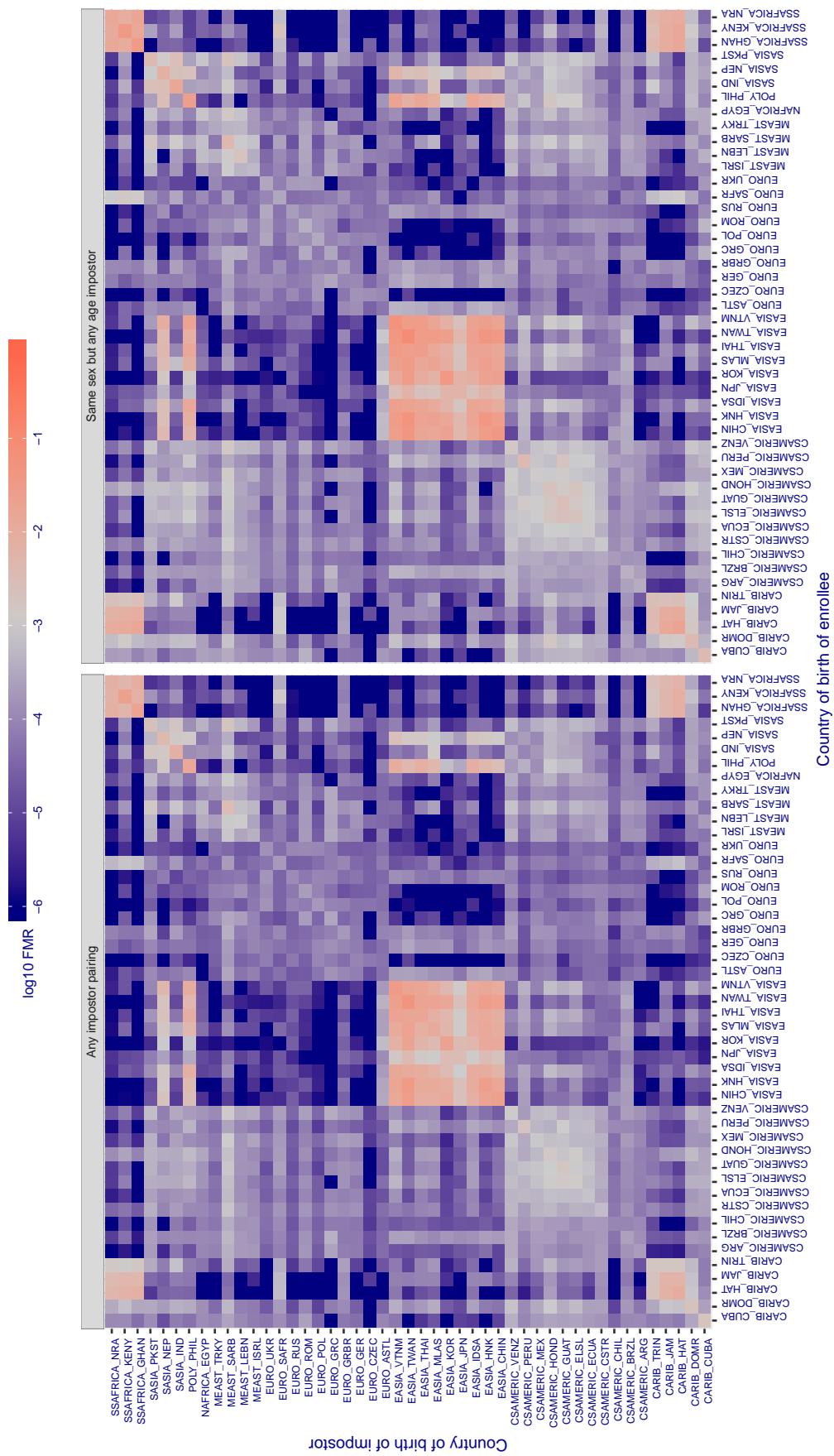


Figure 292: For algorithm aware-004 operating on visa images, the heatmap shows false match rates observed over impostor comparisons of faces from different individuals who were born in the given country pair. False matches are counted against a recognition threshold fixed globally to give the target FMR in the plot title, computed over all on the order of 10^{10} impostor comparisons. If text appears in each box it give the same quantity as that coded by the color. Grey indicates FMR is at the intended FMR target level. Light red colors present a security vulnerability to, for example, a passport gate. Each +1 increase in $\log_{10} \text{FMR}$ corresponds to a factor of 10 increase in FMR . The matrix is not quite symmetric because images in the enrollment and verification sets are different.

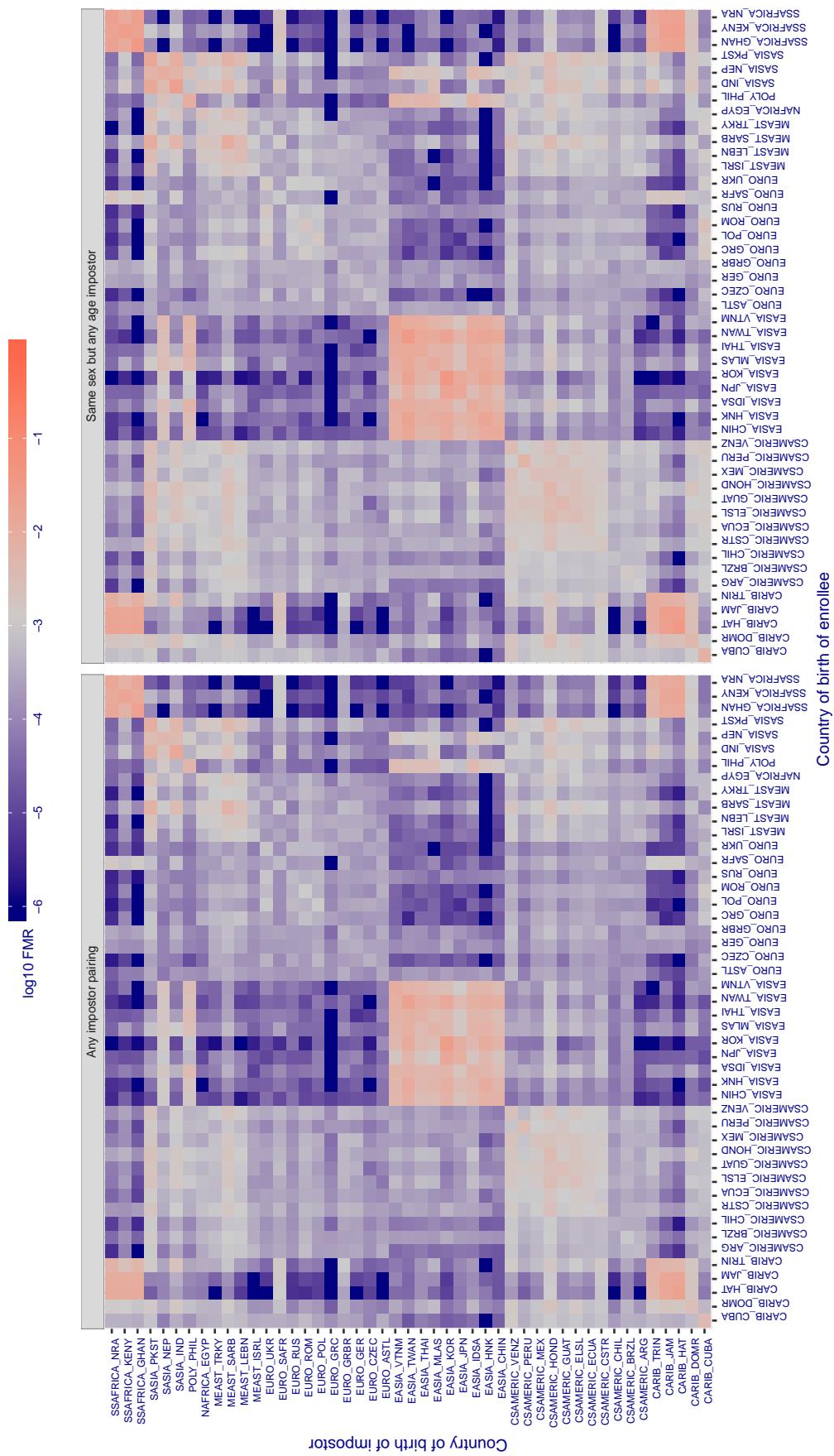
Cross country FMR at threshold T = 0.800 for algorithm ayonix_000, giving FMR(T) = 0.001 globally.

Figure 293: For algorithm ayonix-000 operating on visa images, the heatmap shows false match rates observed over impostor comparisons of faces from different individuals who were born in the given country pair. False matches are counted against a recognition threshold fixed globally to give the target FMR in the plot title, computed over all on the order of 10^{10} impostor comparisons. If text appears in each box it give the same quantity as that coded by the color. Grey indicates FMR is at the intended FMR target level. Light red colors present a security vulnerability to, for example, a passport gate. Each +1 increase in $\log_{10} FMR$ corresponds to a factor of 10 increase in FMR. The matrix is not quite symmetric because images in the enrollment and verification sets are different.

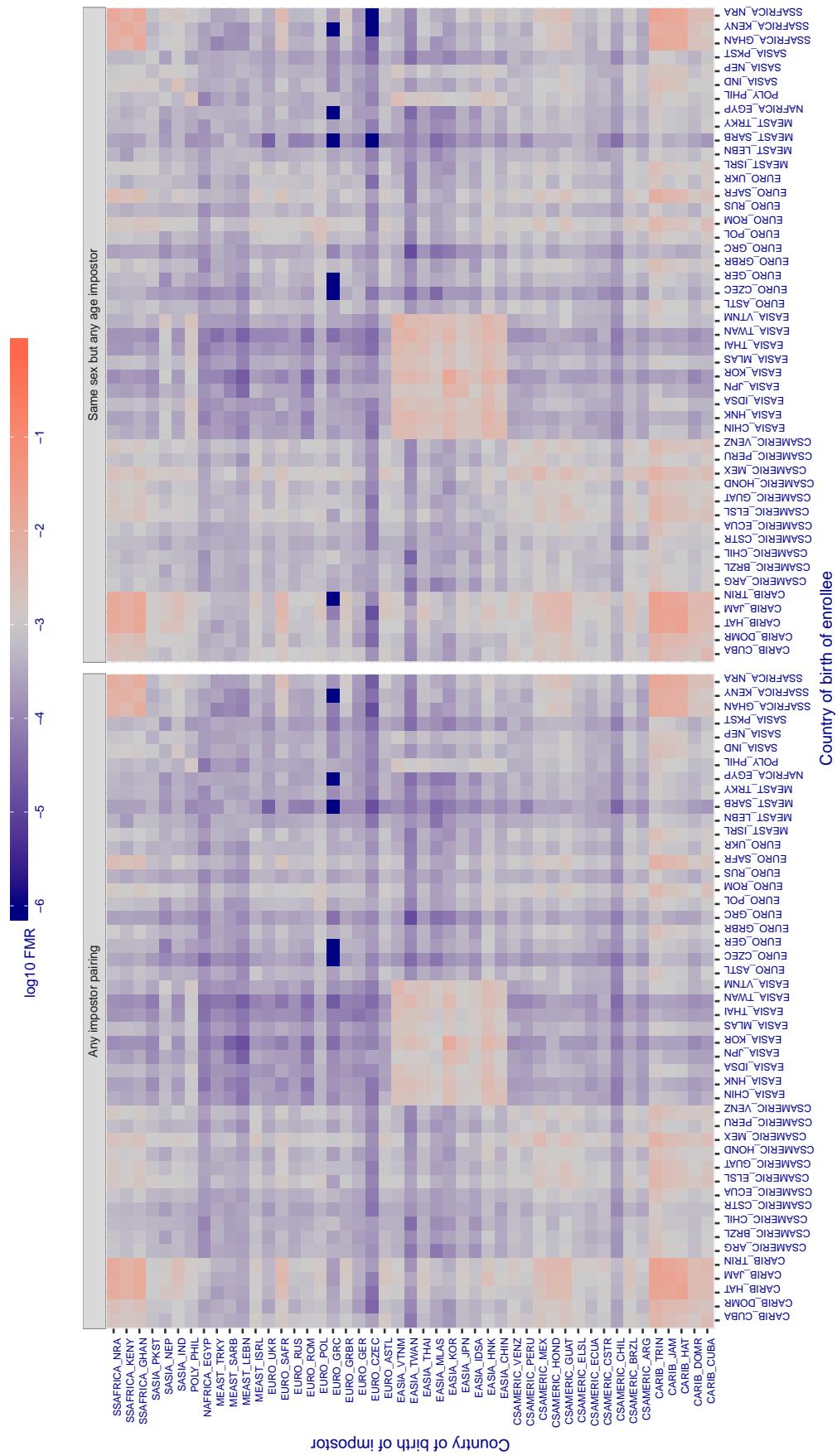
Cross country FMR at threshold T = 0.649 for algorithm bm_001, giving $\text{FMR}(\text{T}) = 0.001$ globally.

Figure 294: For algorithm *bm-001* operating on visa images, the heatmap shows false match rates observed over impostor comparisons of faces from different individuals who were born in the given country pair. False matches are counted against a recognition threshold fixed globally to give the target FMR in the plot title, computed over all on the order of 10^{10} impostor comparisons. If text appears in each box it give the same quantity as that coded by the color. Grey indicates FMR is at the intended FMR target level. Light red colors present a security vulnerability to, for example, a passport gate. Each +1 increase in $\log_{10} \text{FMR}$ corresponds to a factor of 10 increase in FMR . The matrix is not quite symmetric because images in the enrollment and verification sets are different.

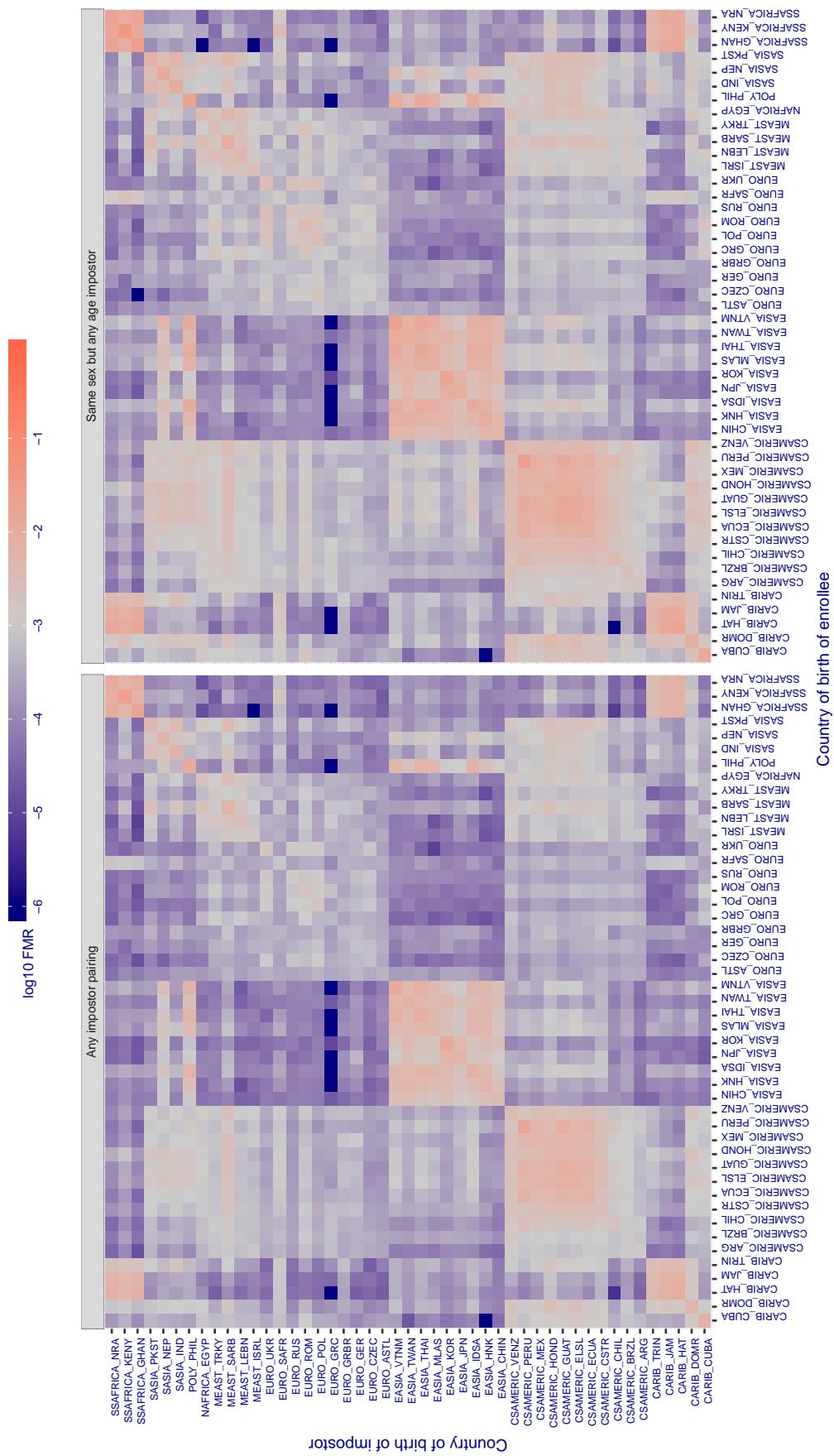
Cross country FMR at threshold T = 0.306 for algorithm camvi_002, giving FMR(T) = 0.001 globally.

Figure 295: For algorithm camvi-002 operating on visa images, the heatmap shows false match rates observed over impostor comparisons of faces from different individuals who were born in the given country pair. False matches are counted against a recognition threshold fixed globally to give the target FMR in the plot title, computed over all on the order of 10^{10} impostor comparisons. If text appears in each box it give the same quantity as that coded by the color. Grey indicates FMR is at the intended FMR target level. Light red colors present a security vulnerability to, for example, a passport gate. Each +1 increase in $\log_{10} \text{FMR}$ corresponds to a factor of 10 increase in FMR. The matrix is not quite symmetric because images in the enrollment and verification sets are different.

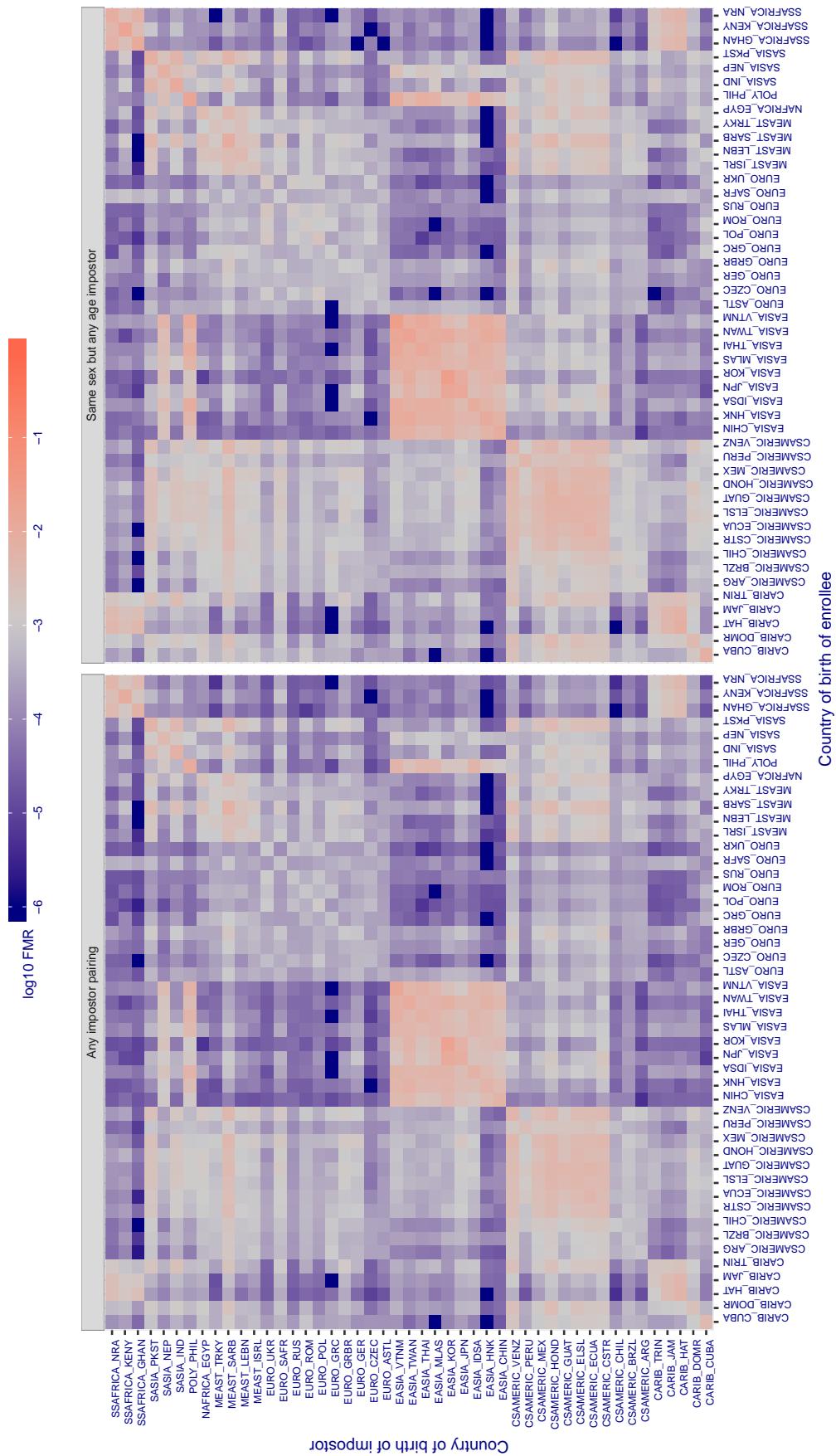
Cross country FMR at threshold T = 0.272 for algorithm camvi_004, giving $\text{FMR}(\text{T}) = 0.001$ globally.

Figure 296: For algorithm camvi-004 operating on visa images, the heatmap shows false match rates observed over impostor comparisons of faces from different individuals who were born in the given country pair. False matches are counted against a recognition threshold fixed globally to give the target FMR in the plot title, computed over all on the order of 10^{10} impostor comparisons. If text appears in each box it give the same quantity as that coded by the color. Grey indicates FMR is at the intended FMR target level. Light red colors present a security vulnerability to, for example, a passport gate. Each +1 increase in $\log_{10} \text{FMR}$ corresponds to a factor of 10 increase in FMR . The matrix is not quite symmetric because images in the enrollment and verification sets are different.

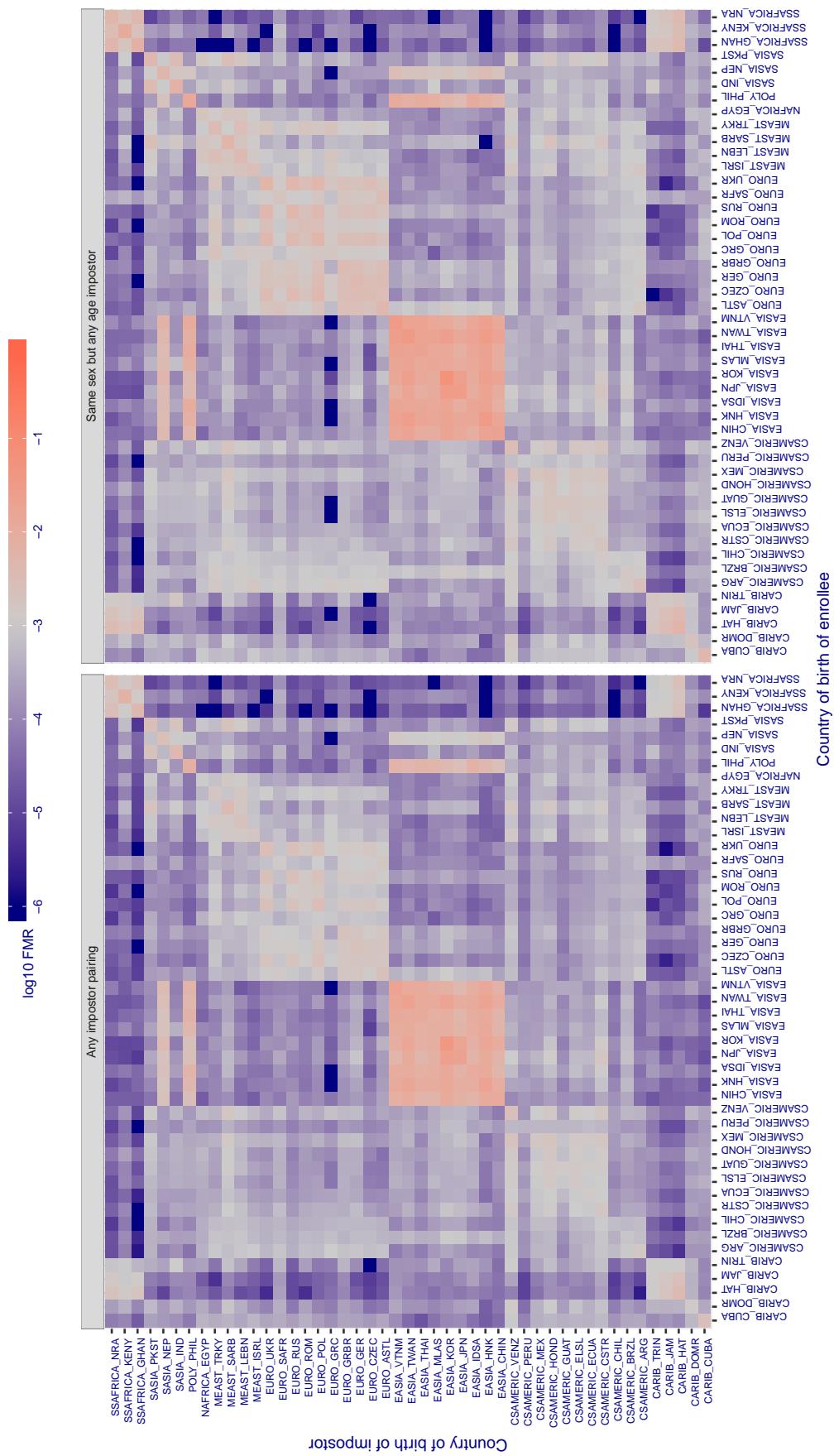
Cross country FMR at threshold T = 0.346 for algorithm ceiec_001, giving FMR(T) = 0.001 globally.

Figure 297: For algorithm ceiec-001 operating on visa images, the heatmap shows false match rates observed over impostor comparisons of faces from different individuals who were born in the given country pair. False matches are counted against a recognition threshold fixed globally to give the target FMR in the plot title, computed over all on the order of 10^{10} impostor comparisons. If text appears in each box it give the same quantity as that coded by the color. Grey indicates FMR is at the intended FMR target level. Light red colors present a security vulnerability to, for example, a passport gate. Each +1 increase in $\log_{10} \text{FMR}$ corresponds to a factor of 10 increase in FMR. The matrix is not quite symmetric because images in the enrollment and verification sets are different.

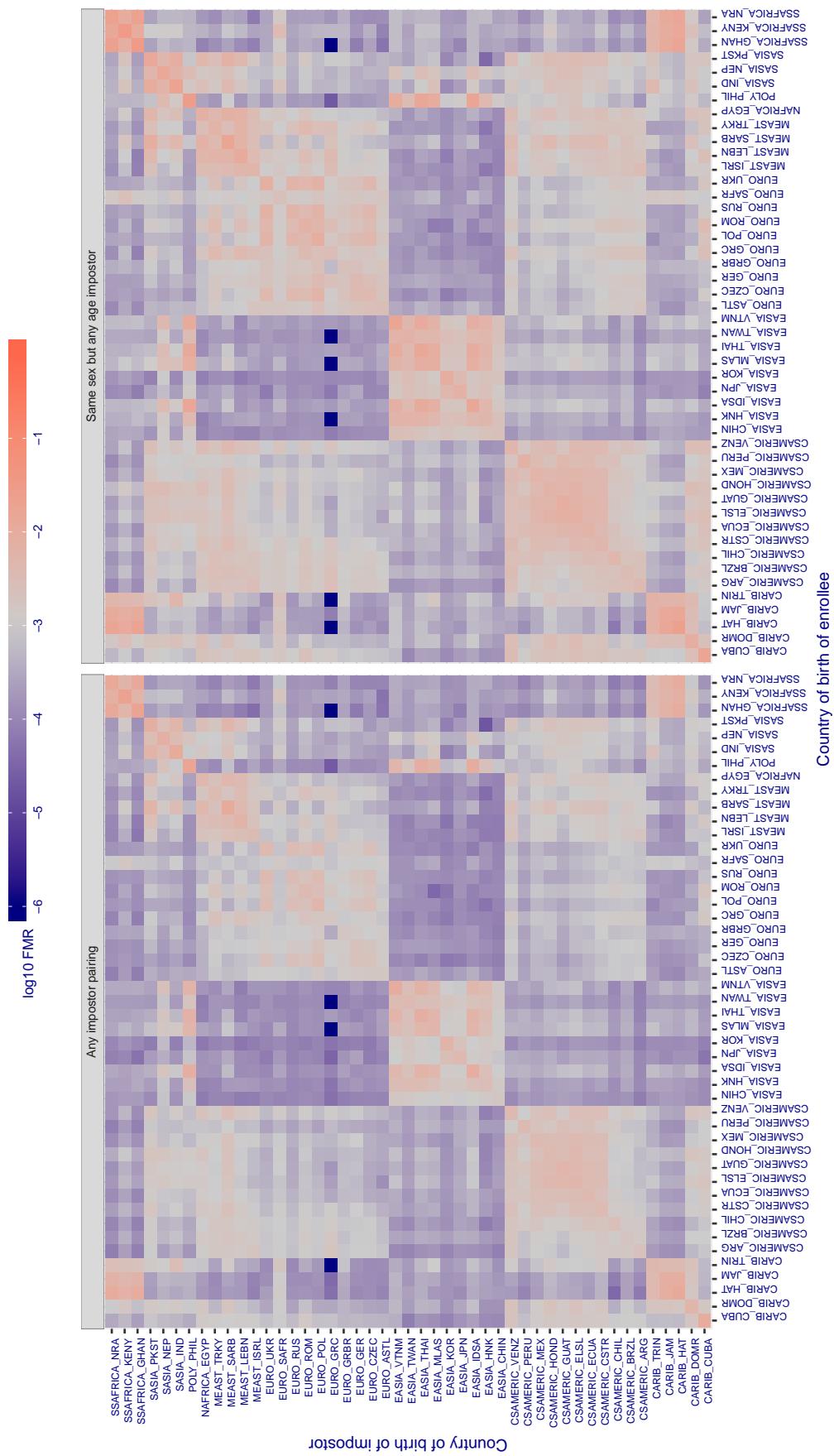
Cross country FMR at threshold T = 0.247 for algorithm ceiec_002, giving FMR(T) = 0.001 globally.

Figure 298: For algorithm ceiec-002 operating on visa images, the heatmap shows false match rates observed over impostor comparisons of faces from different individuals who were born in the given country pair. False matches are counted against a recognition threshold fixed globally to give the target FMR in the plot title, computed over all on the order of 10^{10} impostor comparisons. If text appears in each box it give the same quantity as that coded by the color. Grey indicates FMR is at the intended FMR target level. Light red colors present a security vulnerability to, for example, a passport gate. Each +1 increase in $\log_{10} \text{FMR}$ corresponds to a factor of 10 increase in FMR. The matrix is not quite symmetric because images in the enrollment and verification sets are different.

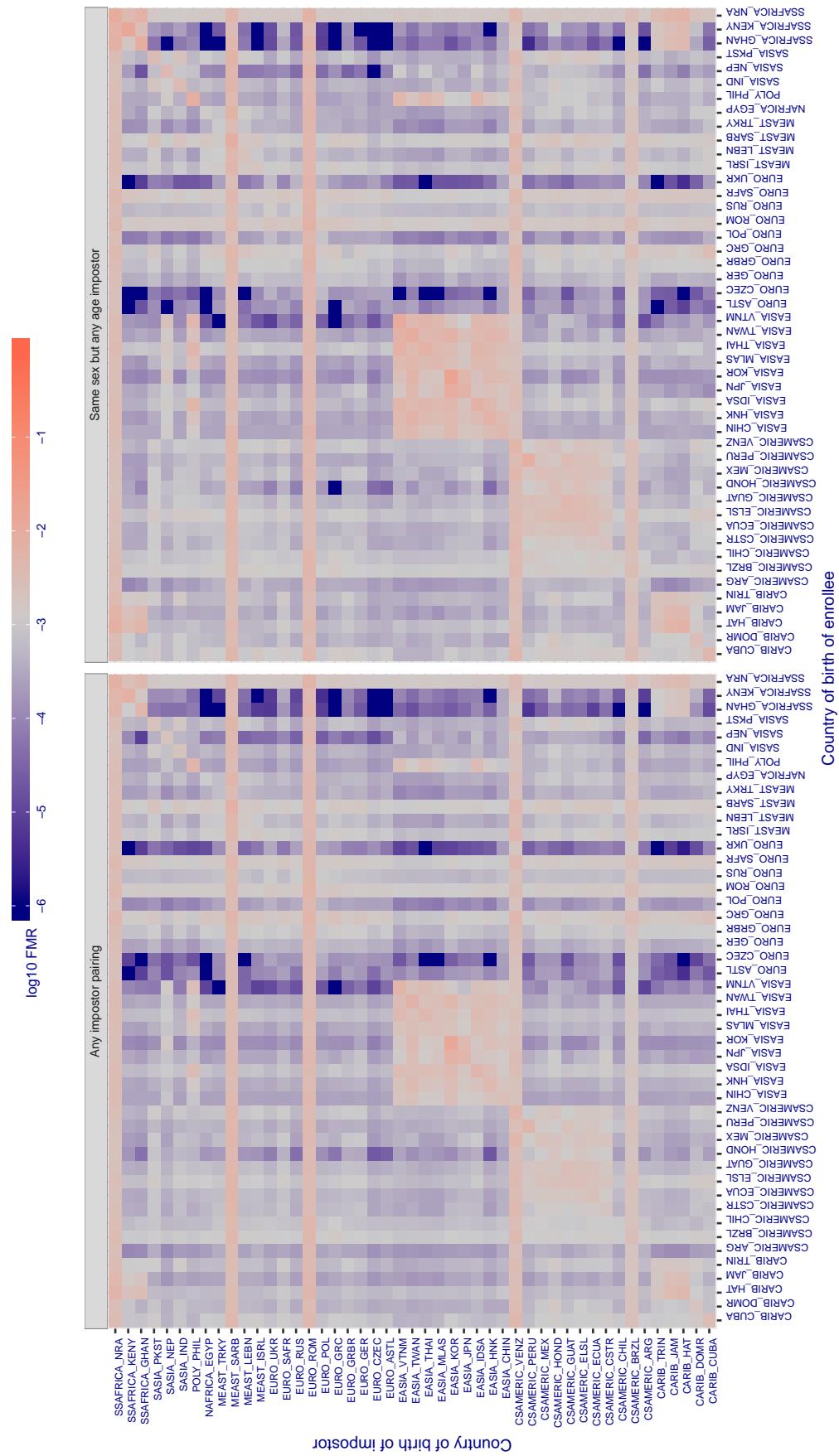
Cross country FMR at threshold T = 0.365 for algorithm chtface_001, giving $FMR(T) = 0.001$ globally.

Figure 299: For algorithm chtface-001 operating on visa images, the heatmap shows false match rates observed over impostor comparisons of faces from different individuals who were born in the given country pair. False matches are counted against a recognition threshold fixed globally to give the target FMR in the plot title, computed over all on the order of 10^{10} impostor comparisons. If text appears in each box it give the same quantity as that coded by the color. Grey indicates FMR is at the intended FMR target level. Light red colors present a security vulnerability to, for example, a passport gate. Each +1 increase in $\log_{10} FMR$ corresponds to a factor of 10 increase in FMR . The matrix is not quite symmetric because images in the enrollment and verification sets are different.

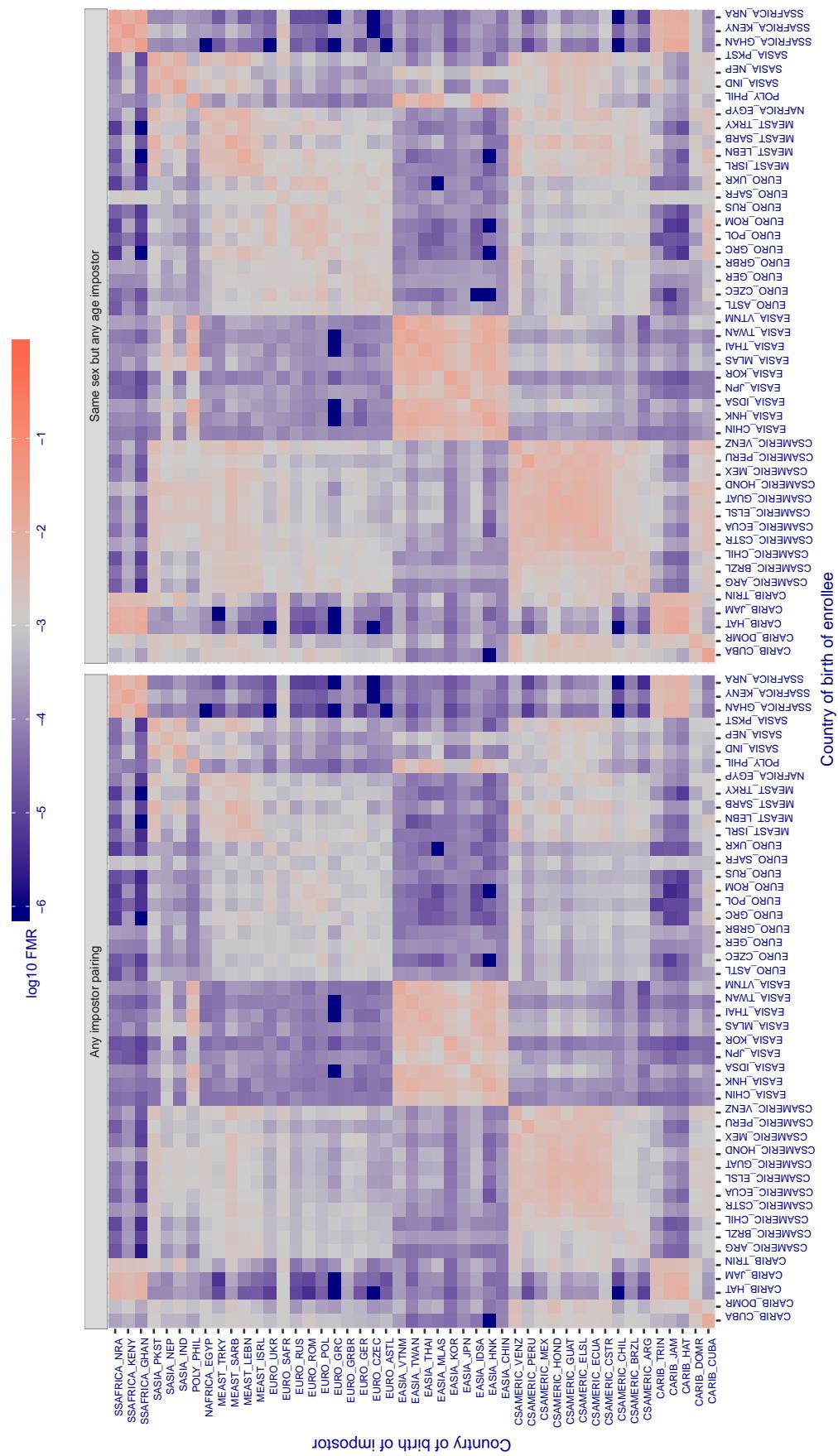
Cross country FMR at threshold T = 2845.000 for algorithm cogent_003, giving FMR(T) = 0.001 globally.

Figure 300: For algorithm cogent-003 operating on visa images, the heatmap shows false match rates observed over impostor comparisons of faces from different individuals who were born in the given country pair. False matches are counted against a recognition threshold fixed globally to give the target FMR in the plot title, computed over all on the order of 10^{10} impostor comparisons. If text appears in each box it give the same quantity as that coded by the color. Grey indicates FMR is at the intended FMR target level. Light red colors present a security vulnerability to, for example, a passport gate. Each +1 increase in $\log_{10} \text{FMR}$ corresponds to a factor of 10 increase in FMR. The matrix is not quite symmetric because images in the enrollment and verification sets are different.

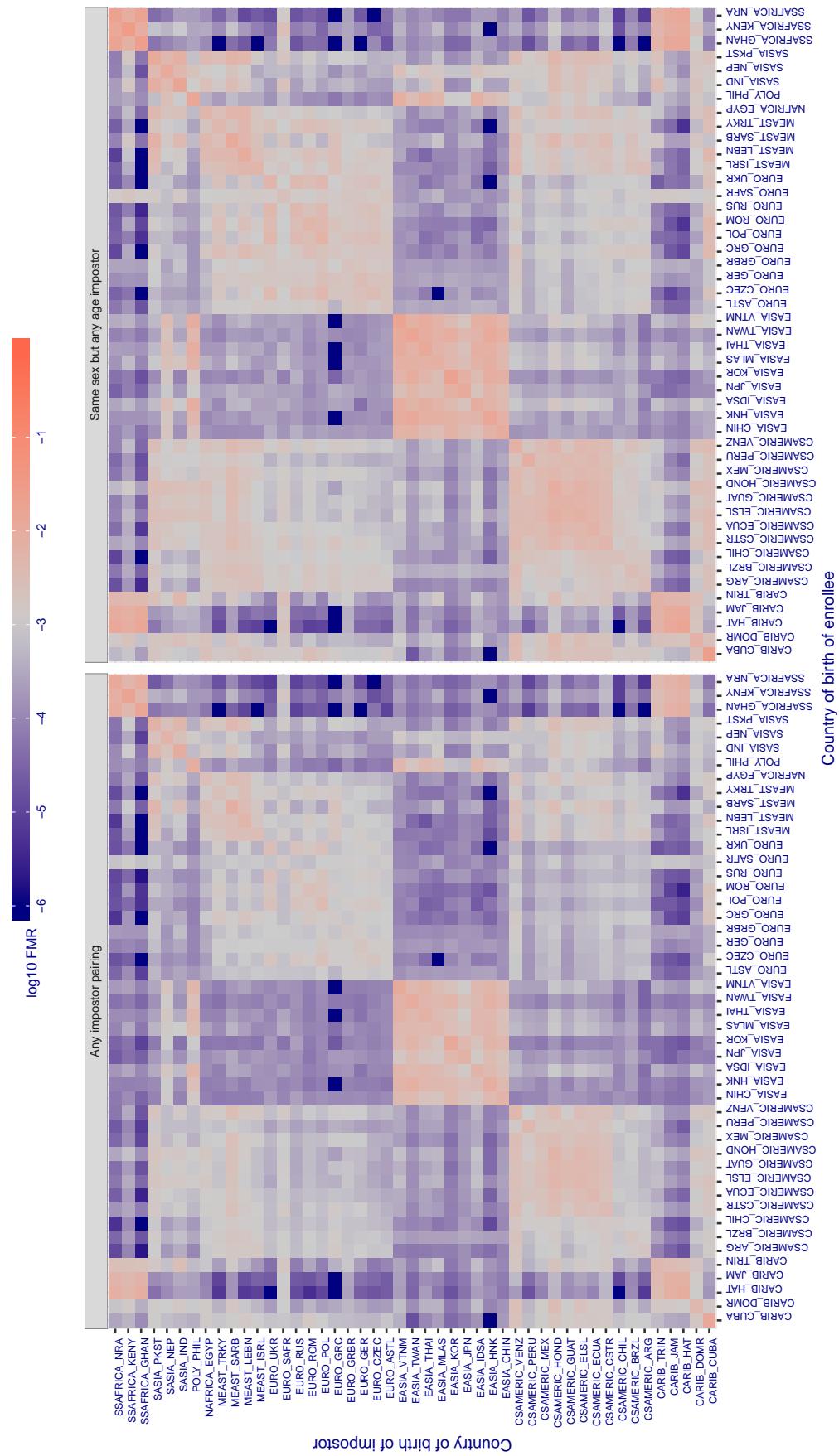
Cross country FMR at threshold T = 2939.000 for algorithm cogent_004, giving FMR(T) = 0.001 globally.

Figure 301: For algorithm cogent-004 operating on visa images, the heatmap shows false match rates observed over impostor comparisons of faces from different individuals who were born in the given country pair. False matches are counted against a recognition threshold fixed globally to give the target FMR in the plot title, computed over all on the order of 10^{10} impostor comparisons. If text appears in each box it give the same quantity as that coded by the color. Grey indicates FMR is at the intended FMR target level. Light red colors present a security vulnerability to, for example, a passport gate. Each +1 increase in $\log_{10} \text{FMR}$ corresponds to a factor of 10 increase in FMR. The matrix is not quite symmetric because images in the enrollment and verification sets are different.

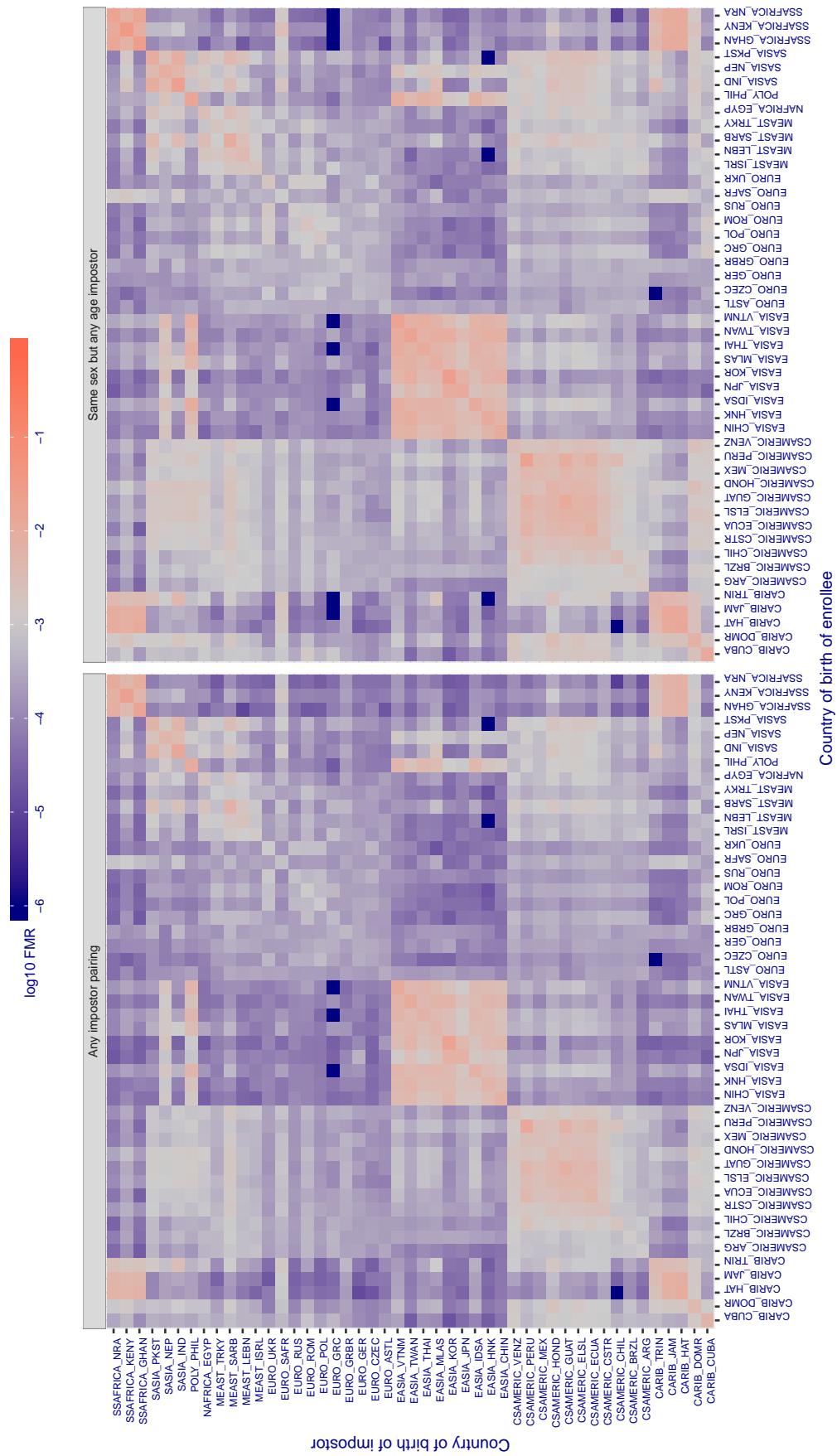
Cross country FMR at threshold T = 0.522 for algorithm cognitec_000, giving FMR(T) = 0.001 globally.

Figure 302: For algorithm cognitec-000 operating on visa images, the heatmap shows false match rates observed over impostor comparisons of faces from different individuals who were born in the given country pair. False matches are counted against a recognition threshold fixed globally to give the target FMR in the plot title, computed over all on the order of 10^{10} impostor comparisons. If text appears in each box it give the same quantity as that coded by the color. Grey indicates FMR is at the intended FMR target level. Light red colors present a security vulnerability to, for example, a passport gate. Each +1 increase in $\log_{10} \text{FMR}$ corresponds to a factor of 10 increase in FMR. The matrix is not quite symmetric because images in the enrollment and verification sets are different.

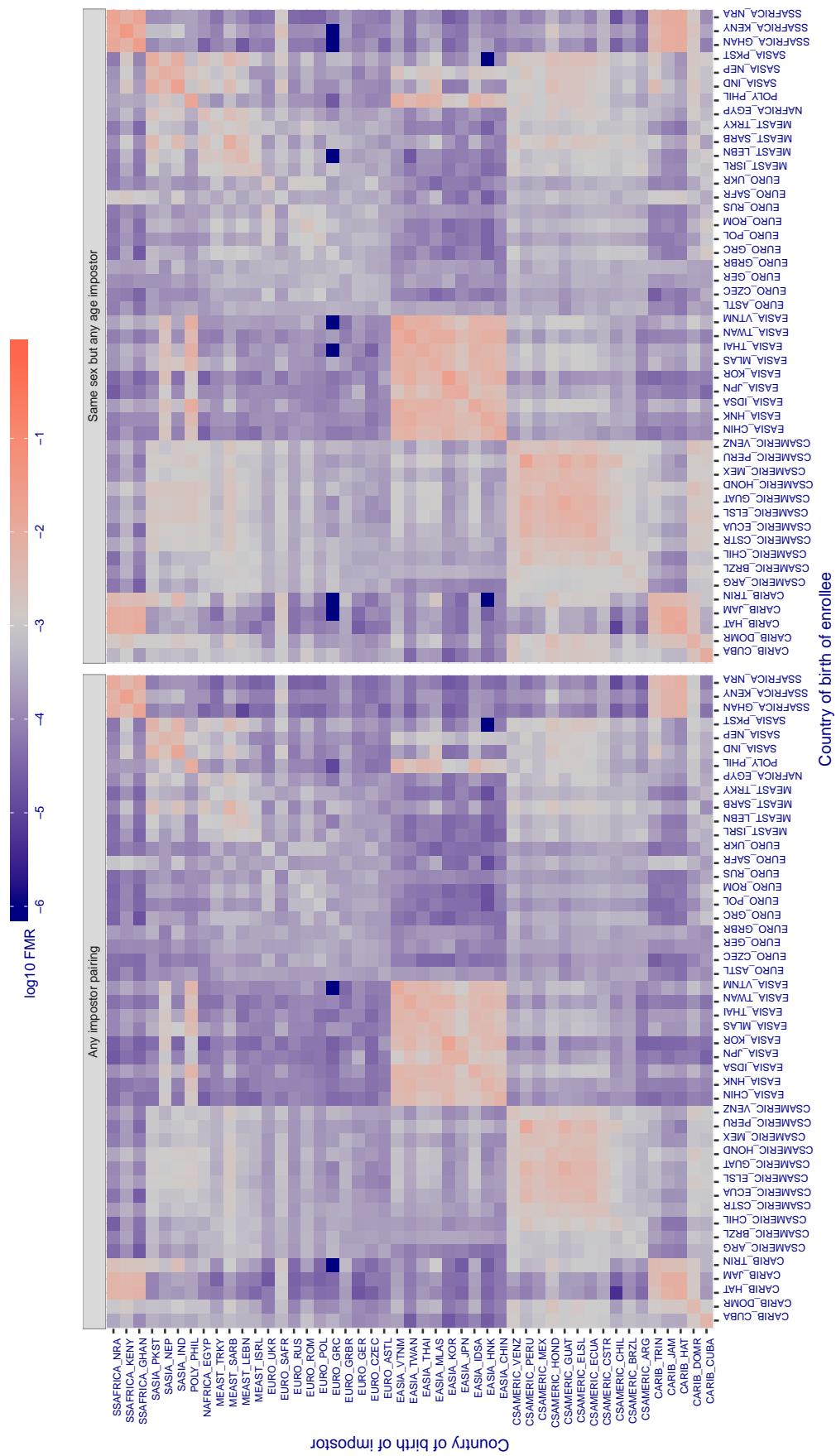
Cross country FMR at threshold T = 0.522 for algorithm cognitec_001, giving FMR(T) = 0.001 globally.

Figure 303: For algorithm cognitec-001 operating on visa images, the heatmap shows false match rates observed over impostor comparisons of faces from different individuals who were born in the given country pair. False matches are counted against a recognition threshold fixed globally to give the target FMR in the plot title, computed over all on the order of 10^{10} impostor comparisons. If text appears in each box it give the same quantity as that coded by the color. Grey indicates FMR is at the intended FMR target level. Light red colors present a security vulnerability to, for example, a passport gate. Each +1 increase in $\log_{10} \text{FMR}$ corresponds to a factor of 10 increase in FMR. The matrix is not quite symmetric because images in the enrollment and verification sets are different.

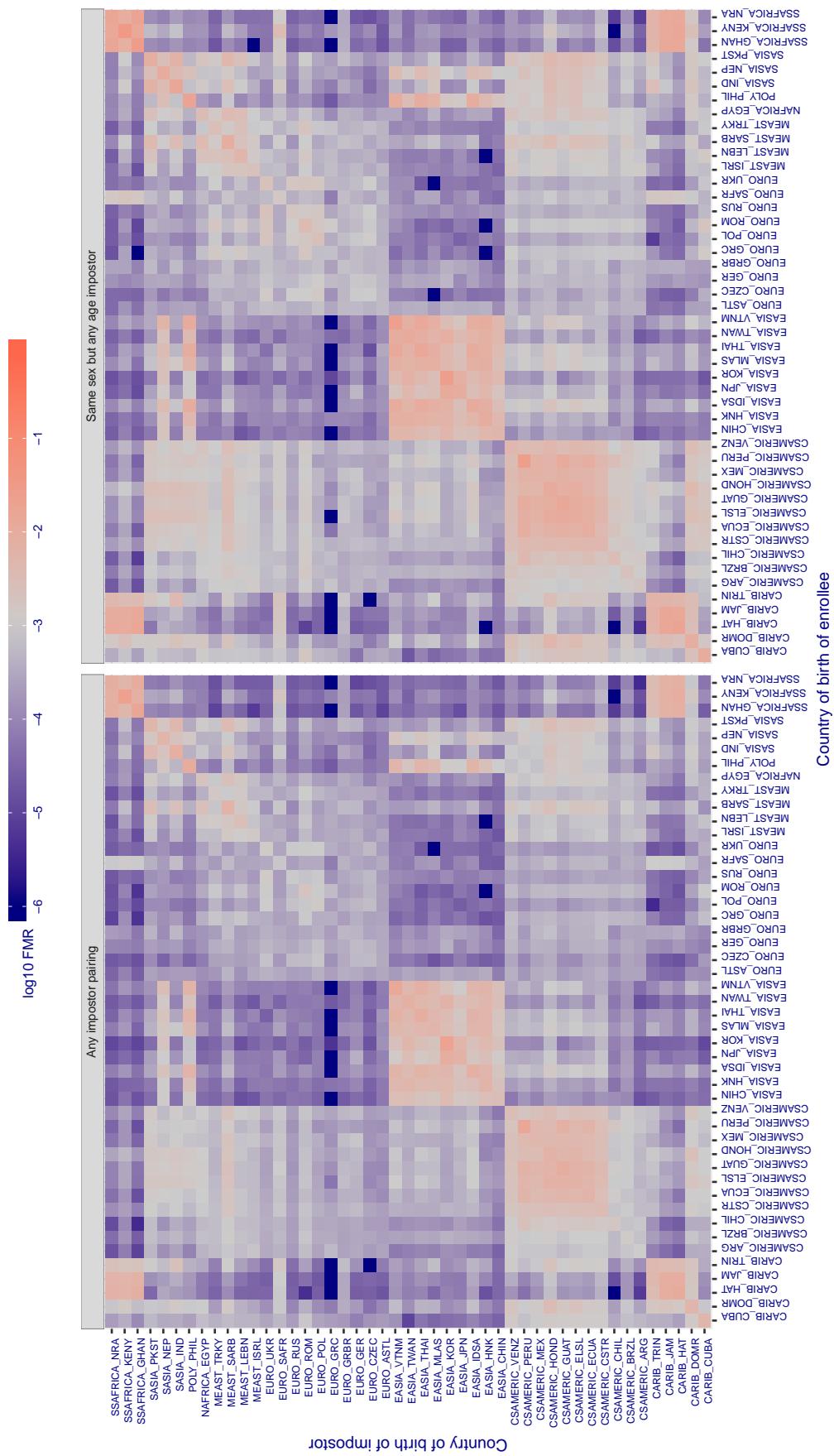
Cross country FMR at threshold T = 3.572 for algorithm ctbcbank_000, giving $FMR(T) = 0.001$ globally.

Figure 304: For algorithm ctbcbank-000 operating on visa images, the heatmap shows false match rates observed over impostor comparisons of faces from different individuals who were born in the given country pair. False matches are counted against a recognition threshold fixed globally to give the target FMR in the plot title, computed over all on the order of 10^{10} impostor comparisons. If text appears in each box it give the same quantity as that coded by the color. Grey indicates FMR is at the intended FMR target level. Light red colors present a security vulnerability to, for example, a passport gate. Each +1 increase in $\log_{10} FMR$ corresponds to a factor of 10 increase in FMR . The matrix is not quite symmetric because images in the enrollment and verification sets are different.

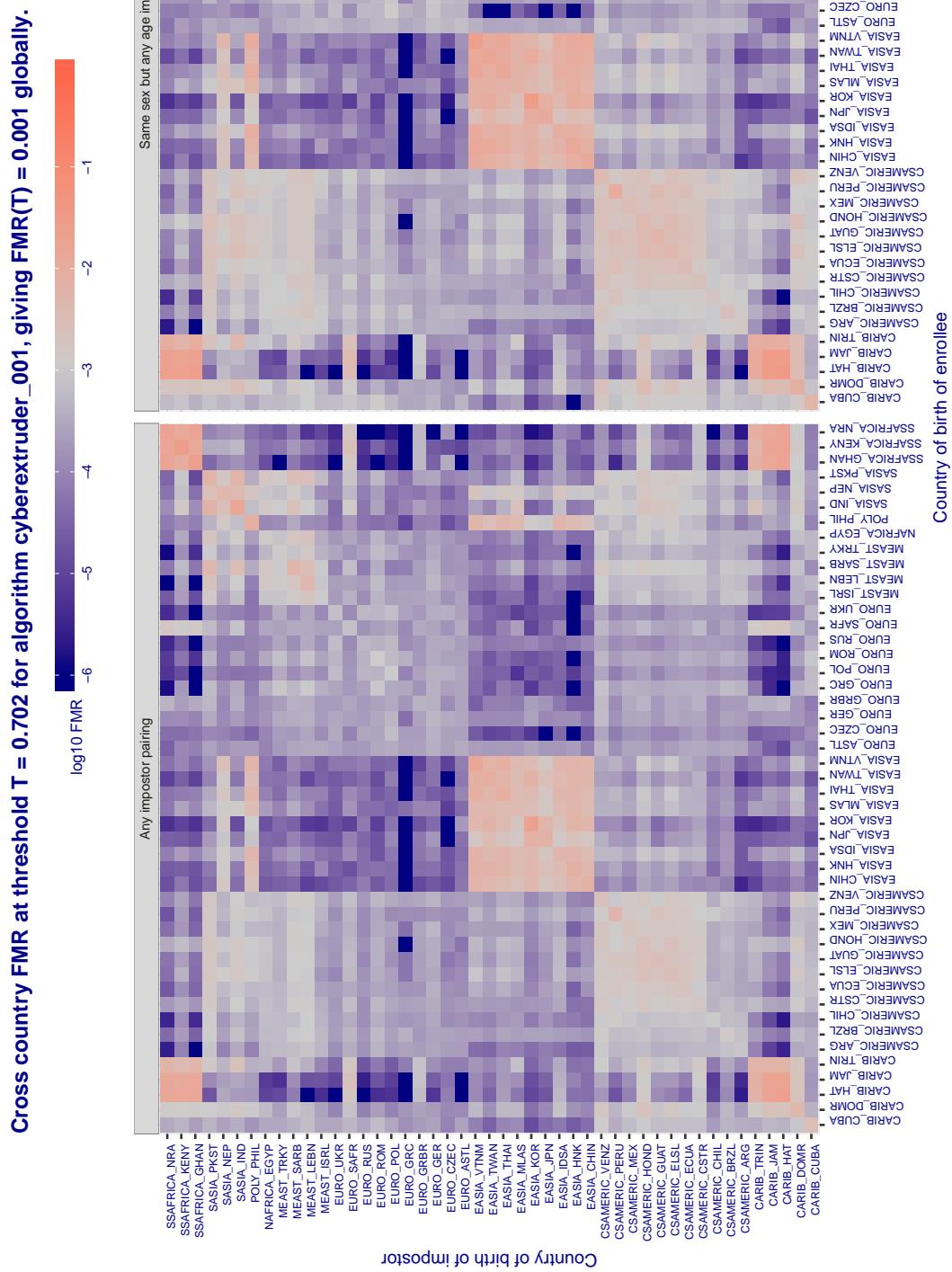


Figure 305: For algorithm cyberextruder-001 operating on visa images, the heatmap shows false match rates observed over impostor comparisons of faces from different individuals who were born in the given country pair. False matches are counted against a recognition threshold fixed globally to give the target FMR in the plot title, computed over all on the order of 10^{10} impostor comparisons. If text appears in each box it give the same quantity as that coded by the color. Grey indicates FMR is at the intended FMR target level. Light red colors present a security vulnerability to, for example, a passport gate. Each +1 increase in $\log_{10} \text{FMR}$ corresponds to a factor of 10 increase in FMR . The matrix is not quite symmetric because images in the enrollment and verification sets are different.

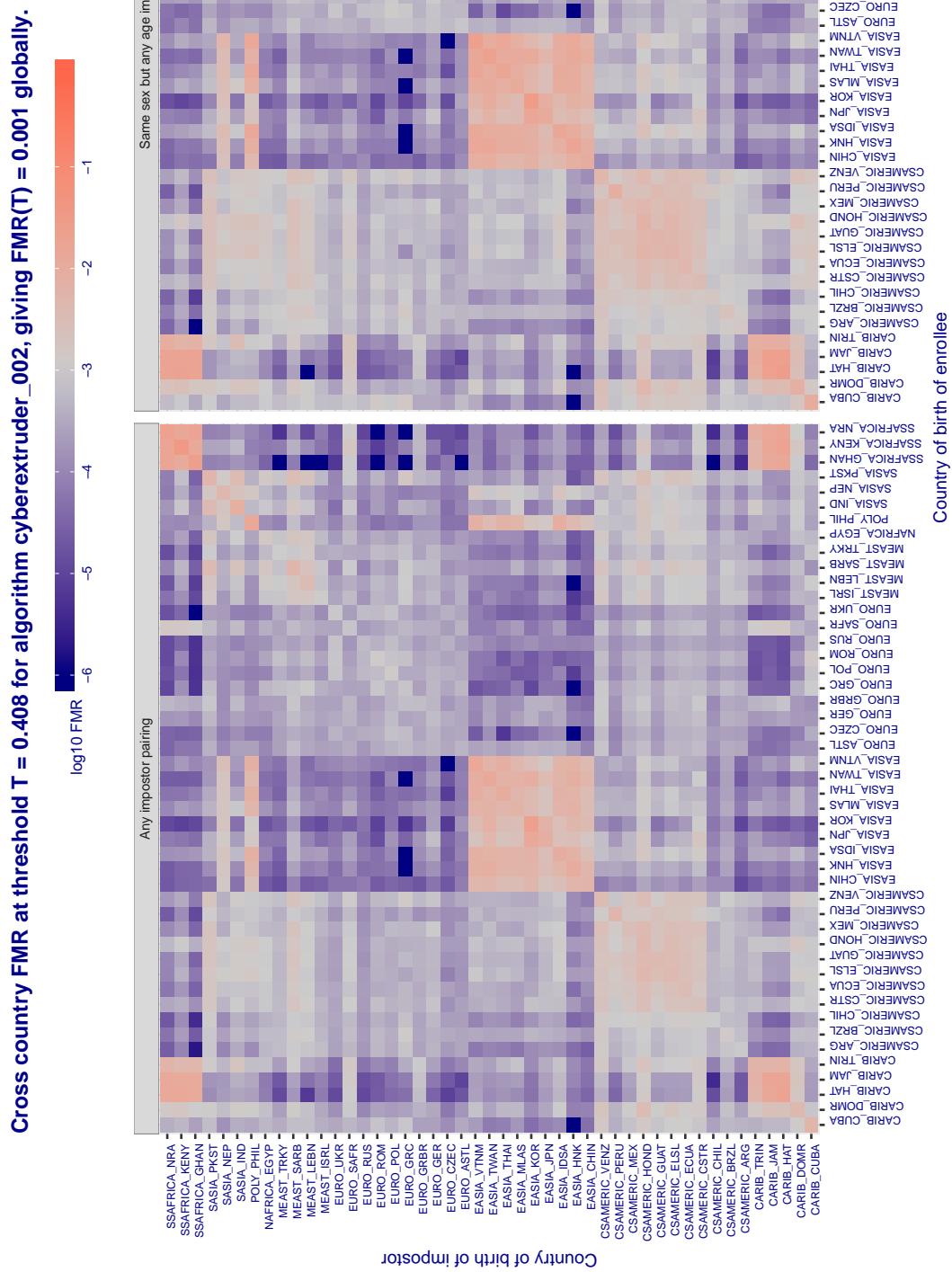


Figure 306: For algorithm cyberextruder-002 operating on visa images, the heatmap shows false match rates observed over impostor comparisons of faces from different individuals who were born in the given country pair. False matches are counted against a recognition threshold fixed globally to give the target FMR in the plot title, computed over all on the order of 10^{10} impostor comparisons. If text appears in each box it give the same quantity as that coded by the color. Grey indicates FMR is at the intended FMR target level. Light red colors present a security vulnerability to, for example, a passport gate. Each +1 increase in $\log_{10} \text{FMR}$ corresponds to a factor of 10 increase in FMR. The matrix is not quite symmetric because images in the enrollment and verification sets are different.

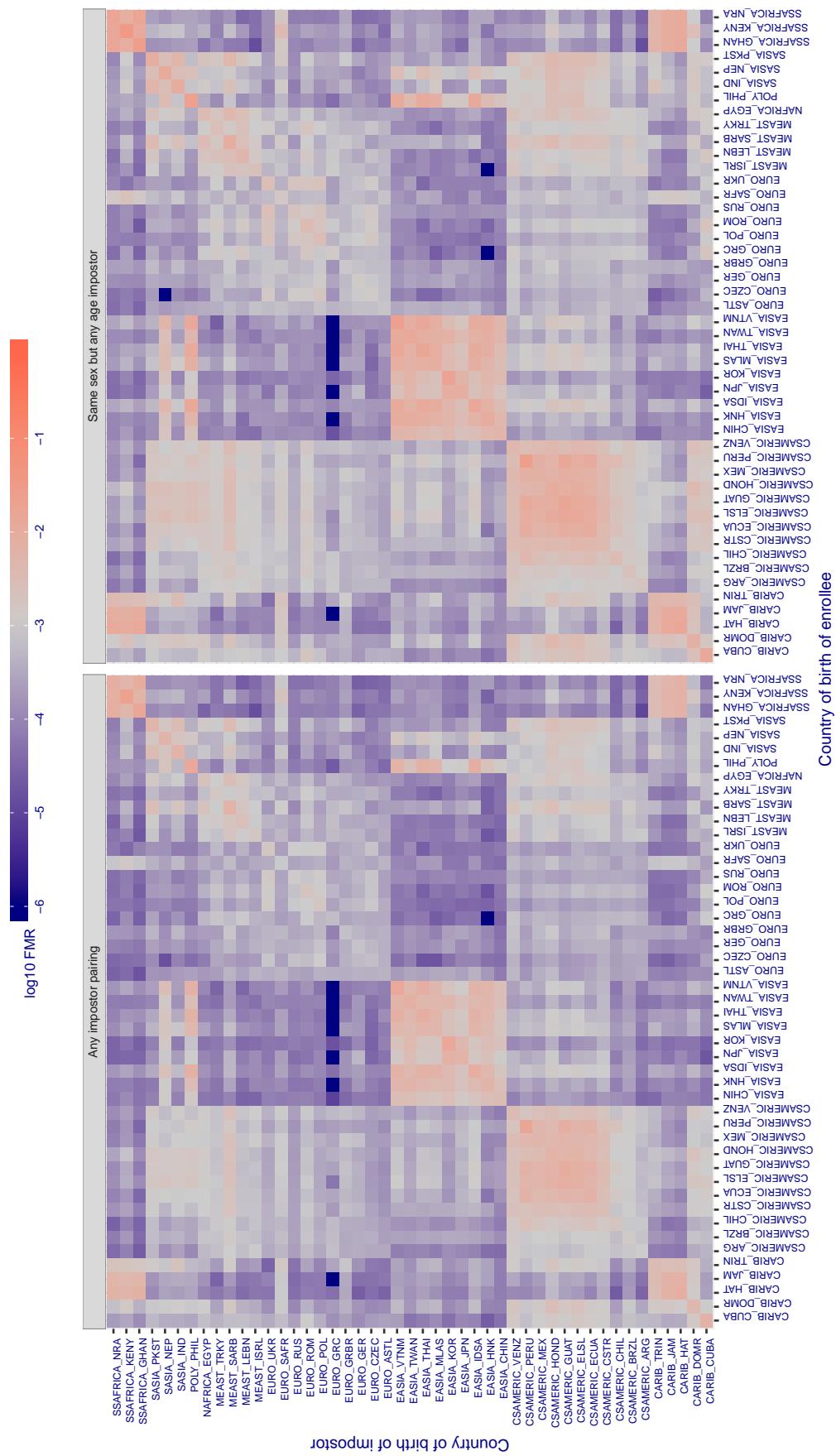
Cross country FMR at threshold T = 1.322 for algorithm cyberlink_001, giving $FMR(T) = 0.001$ globally.

Figure 307: For algorithm cyberlink-001 operating on visa images, the heatmap shows false match rates observed over impostor comparisons of faces from different individuals who were born in the given country pair. False matches are counted against a recognition threshold fixed globally to give the target FMR in the plot title, computed over all on the order of 10^{10} impostor comparisons. If text appears in each box it give the same quantity as that coded by the color. Grey indicates FMR is at the intended FMR target level. Light red colors present a security vulnerability to, for example, a passport gate. Each +1 increase in $\log_{10} FMR$ corresponds to a factor of 10 increase in FMR . The matrix is not quite symmetric because images in the enrollment and verification sets are different.

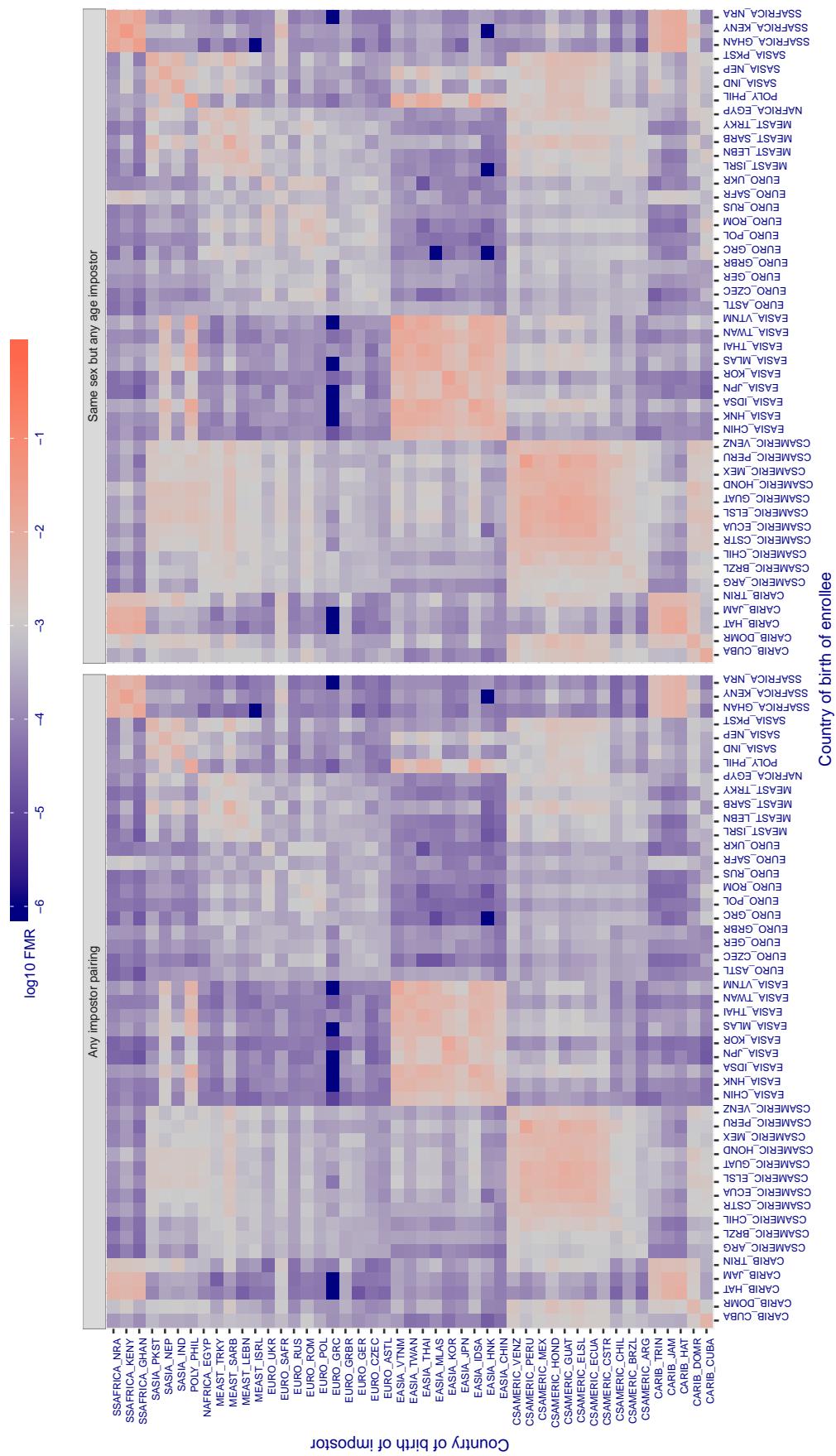
Cross country FMR at threshold T = 1.322 for algorithm cyberlink_002, giving $FMR(T) = 0.001$ globally.

Figure 308: For algorithm cyberlink-002 operating on visa images, the heatmap shows false match rates observed over impostor comparisons of faces from different individuals who were born in the given country pair. False matches are counted against a recognition threshold fixed globally to give the target FMR in the plot title, computed over all on the order of 10^{10} impostor comparisons. If text appears in each box it give the same quantity as that coded by the color. Grey indicates FMR is at the intended FMR target level. Light red colors present a security vulnerability to, for example, a passport gate. Each +1 increase in $\log_{10} FMR$ corresponds to a factor of 10 increase in FMR . The matrix is not quite symmetric because images in the enrollment and verification sets are different.

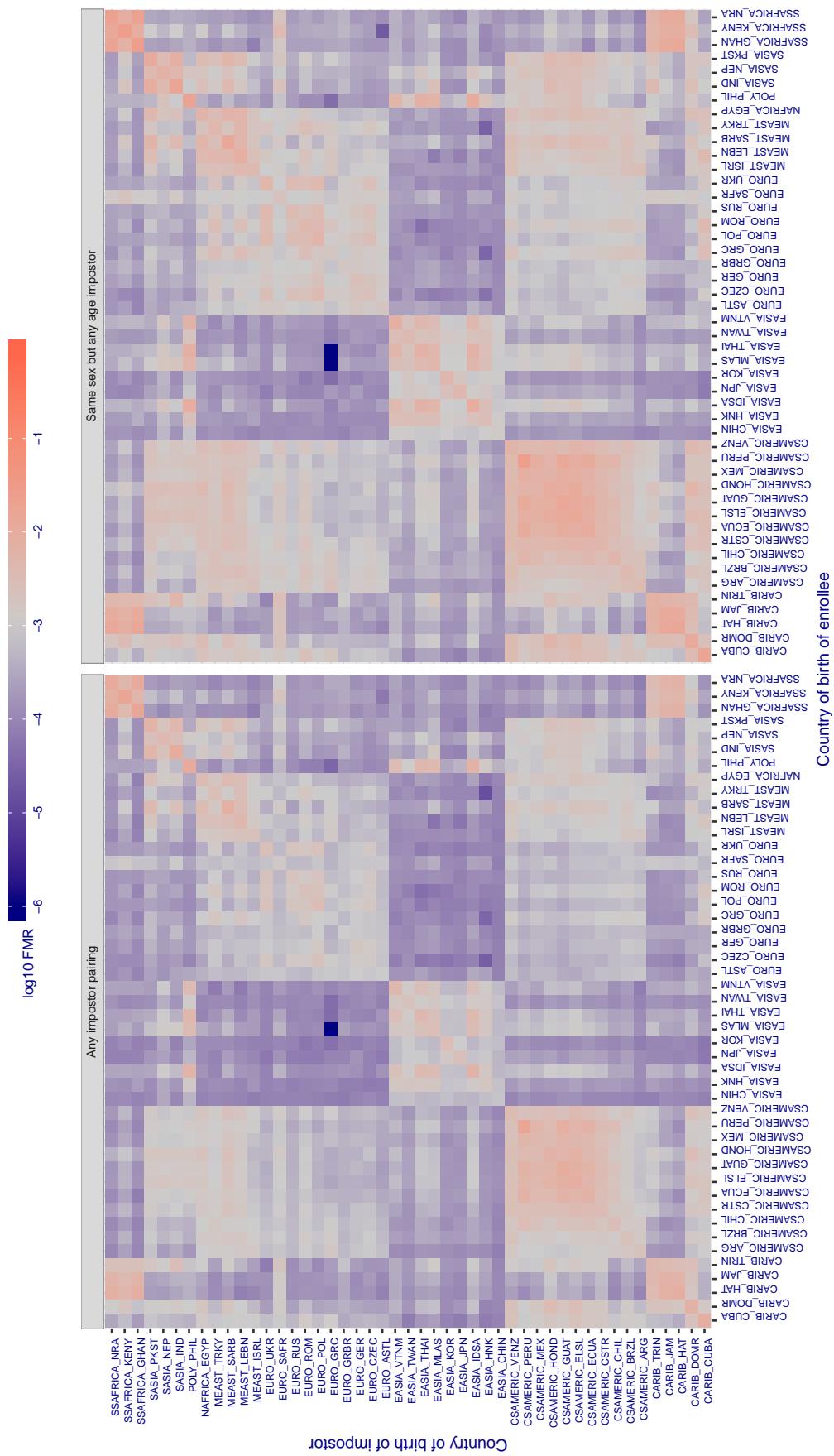
Cross country FMR at threshold T = 5958.000 for algorithm dahua_002, giving $FMR(T) = 0.001$ globally.

Figure 309: For algorithm dahua-002 operating on visa images, the heatmap shows false match rates observed over impostor comparisons of faces from different individuals who were born in the given country pair. False matches are counted against a recognition threshold fixed globally to give the target FMR in the plot title, computed over all on the order of 10^{10} impostor comparisons. If text appears in each box it give the same quantity as that coded by the color. Grey indicates FMR is at the intended FMR target level. Light red colors present a security vulnerability to, for example, a passport gate. Each +1 increase in $\log_{10} FMR$ corresponds to a factor of 10 increase in FMR . The matrix is not quite symmetric because images in the enrollment and verification sets are different.

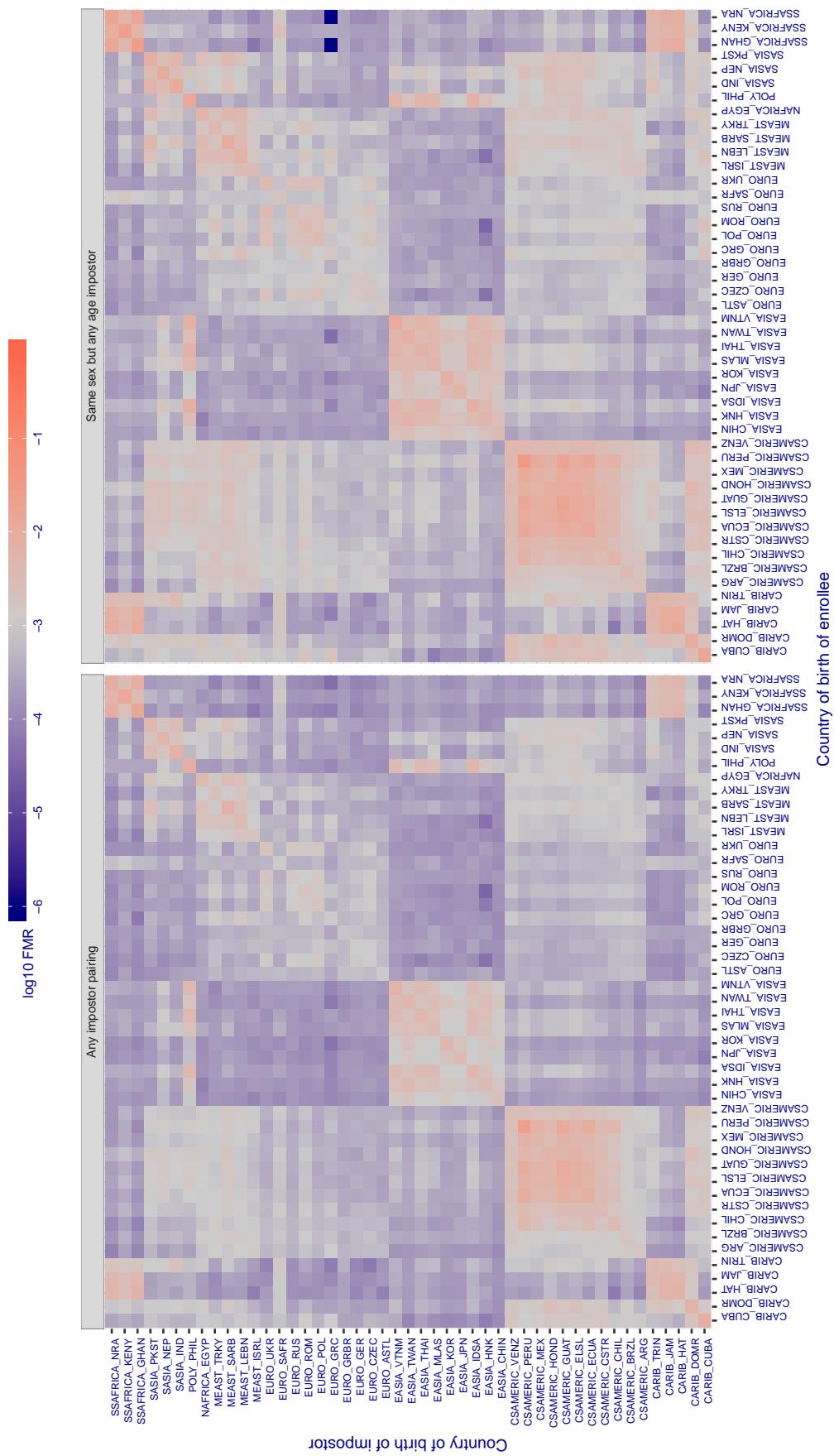
Cross country FMR at threshold T = 5392.000 for algorithm dahua_003, giving $FMR(T) = 0.001$ globally.

Figure 310: For algorithm dahua-003 operating on visa images, the heatmap shows false match rates observed over impostor comparisons of faces from different individuals who were born in the given country pair. False matches are counted against a recognition threshold fixed globally to give the target FMR in the plot title, computed over all on the order of 10^{10} impostor comparisons. If text appears in each box it give the same quantity as that coded by the color. Grey indicates FMR is at the intended FMR target level. Light red colors present a security vulnerability to, for example, a passport gate. Each +1 increase in $\log_{10} FMR$ corresponds to a factor of 10 increase in FMR . The matrix is not quite symmetric because images in the enrollment and verification sets are different.

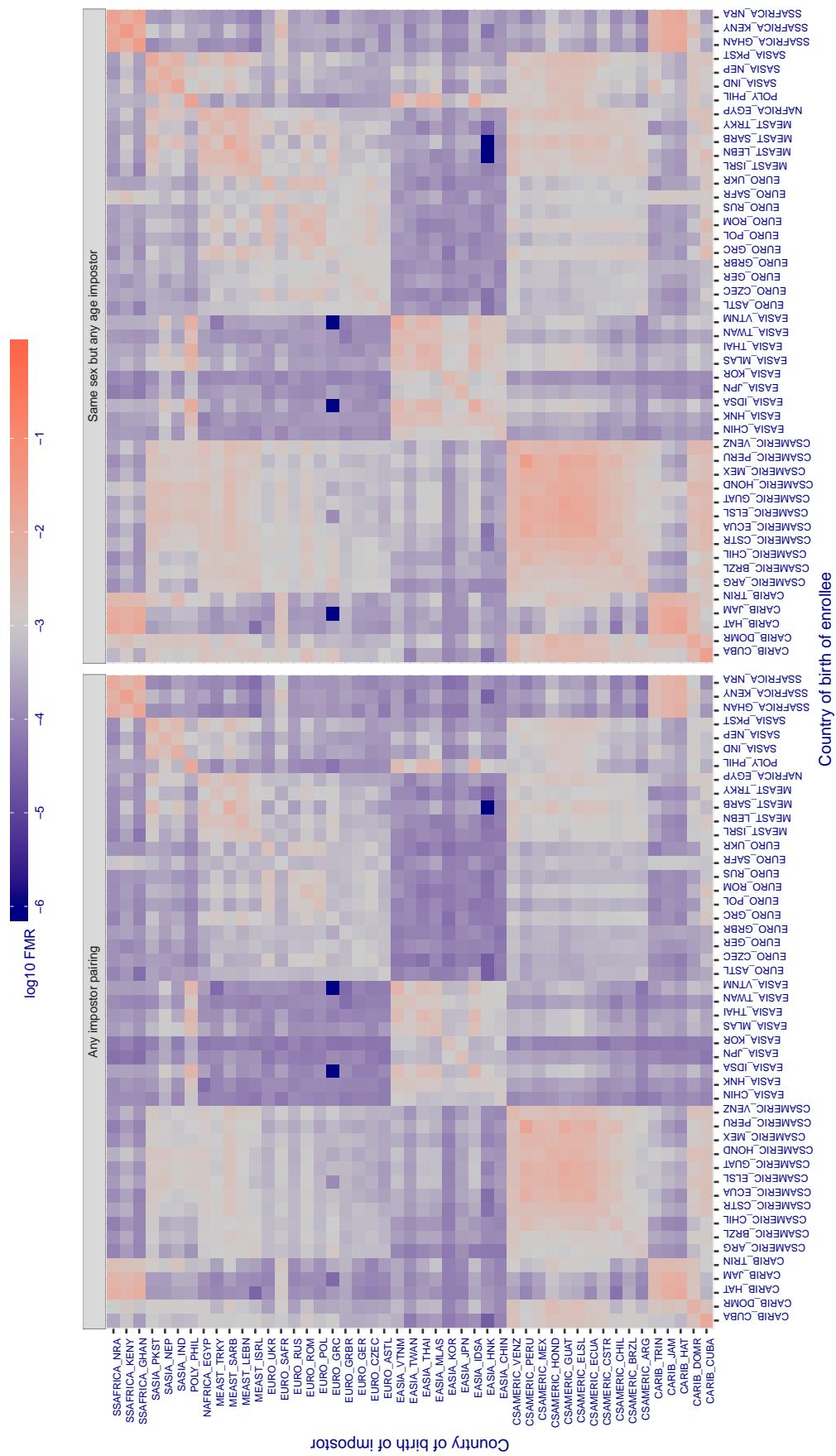
Cross country FMR at threshold T = 1.293 for algorithm deepglint_001, giving FMR(T) = 0.001 globally.

Figure 311: For algorithm deepglint-001 operating on visa images, the heatmap shows false match rates observed over impostor comparisons of faces from different individuals who were born in the given country pair. False matches are counted against a recognition threshold fixed globally to give the target FMR in the plot title, computed over all on the order of 10^{10} impostor comparisons. If text appears in each box it give the same quantity as that coded by the color. Grey indicates FMR is at the intended FMR target level. Light red colors present a security vulnerability to, for example, a passport gate. Each +1 increase in $\log_{10} FMR$ corresponds to a factor of 10 increase in FMR. The matrix is not quite symmetric because images in the enrollment and verification sets are different.

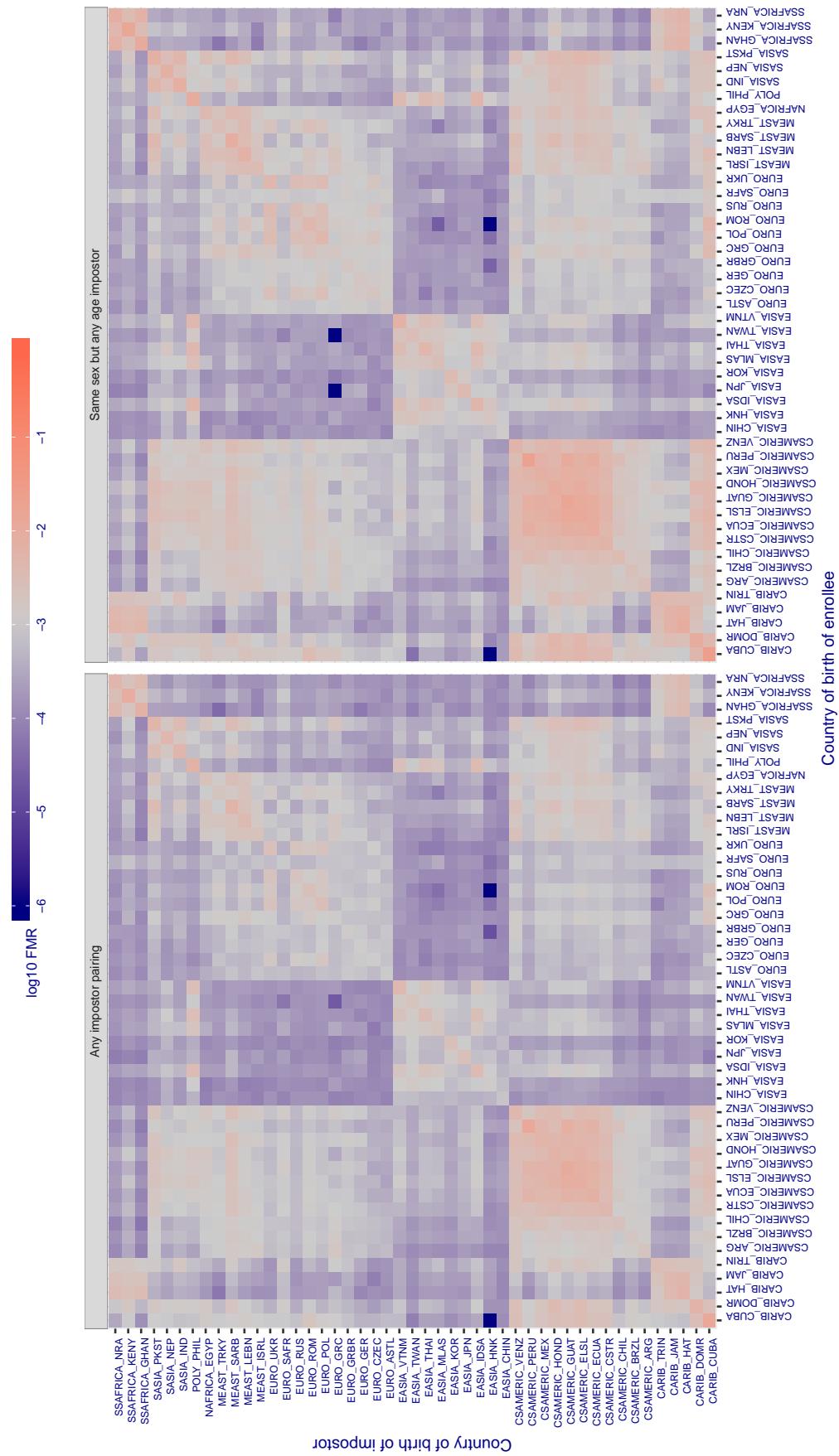
Cross country FMR at threshold T = 1.300 for algorithm deepsea_001, giving FMR(T) = 0.001 globally.

Figure 312: For algorithm deepsea-001 operating on visa images, the heatmap shows false match rates observed over impostor comparisons of faces from different individuals who were born in the given country pair. False matches are counted against a recognition threshold fixed globally to give the target FMR in the plot title, computed over all on the order of 10^{10} impostor comparisons. If text appears in each box it give the same quantity as that coded by the color. Grey indicates FMR is at the intended FMR target level. Light red colors present a security vulnerability to, for example, a passport gate. Each +1 increase in $\log_{10} FMR$ corresponds to a factor of 10 increase in FMR. The matrix is not quite symmetric because images in the enrollment and verification sets are different.

Cross country FMR at threshold T = 75.231 for algorithm dermalog_005, giving FMR(T) = 0.001 globally.

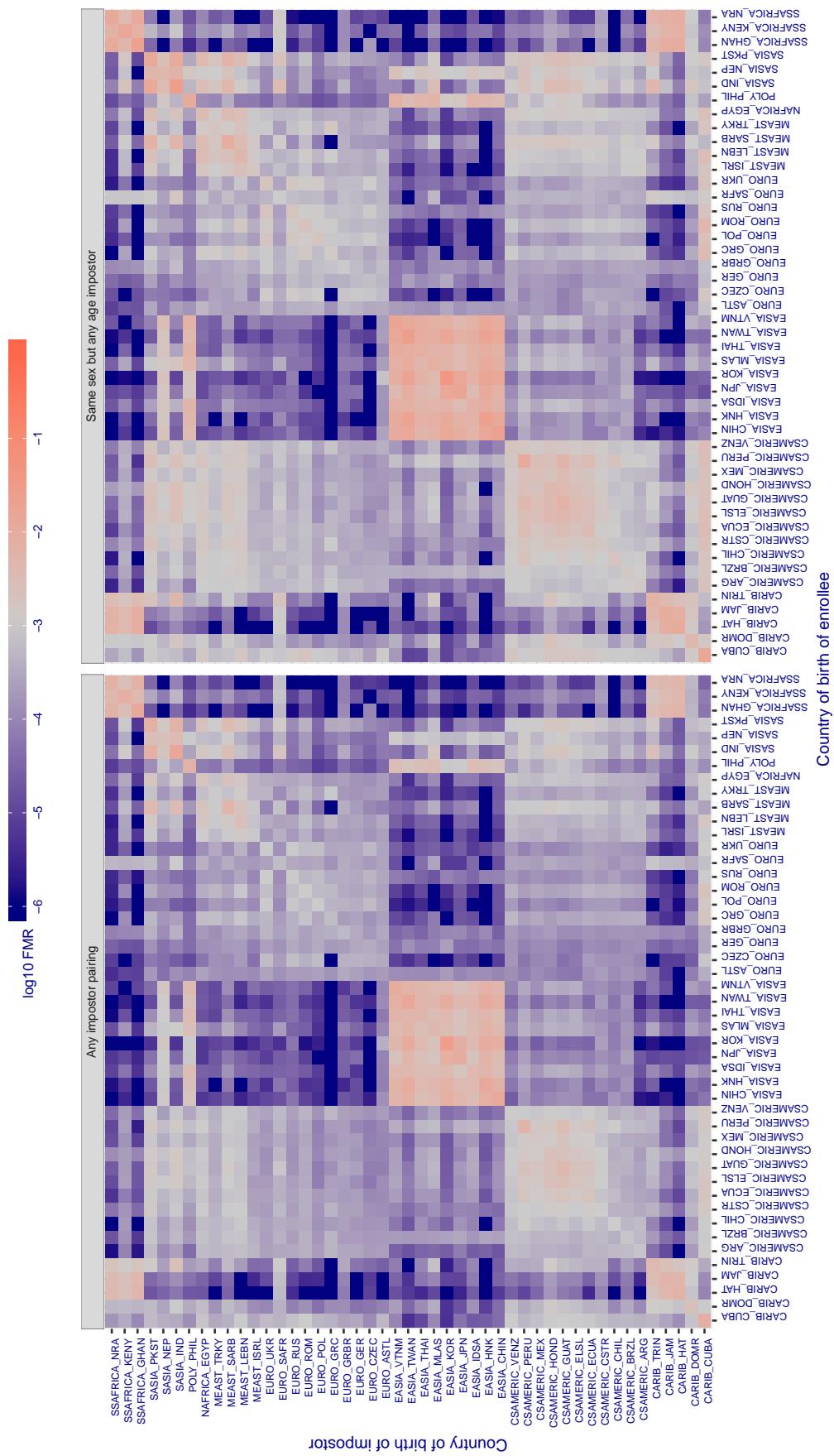


Figure 313: For algorithm dermalog-005 operating on visa images, the heatmap shows false match rates observed over impostor comparisons of faces from different individuals who were born in the given country pair. False matches are counted against a recognition threshold fixed globally to give the target FMR in the plot title, computed over all on the order of 10^{10} impostor comparisons. If text appears in each box it give the same quantity as that coded by the color. Grey indicates FMR is at the intended FMR target level. Light red colors present a security vulnerability to, for example, a passport gate. Each +1 increase in $\log_{10} FMR$ corresponds to a factor of 10 increase in FMR. The matrix is not quite symmetric because images in the enrollment and verification sets are different.

Cross country FMR at threshold T = 76.496 for algorithm dermalog_006, giving FMR(T) = 0.001 globally.

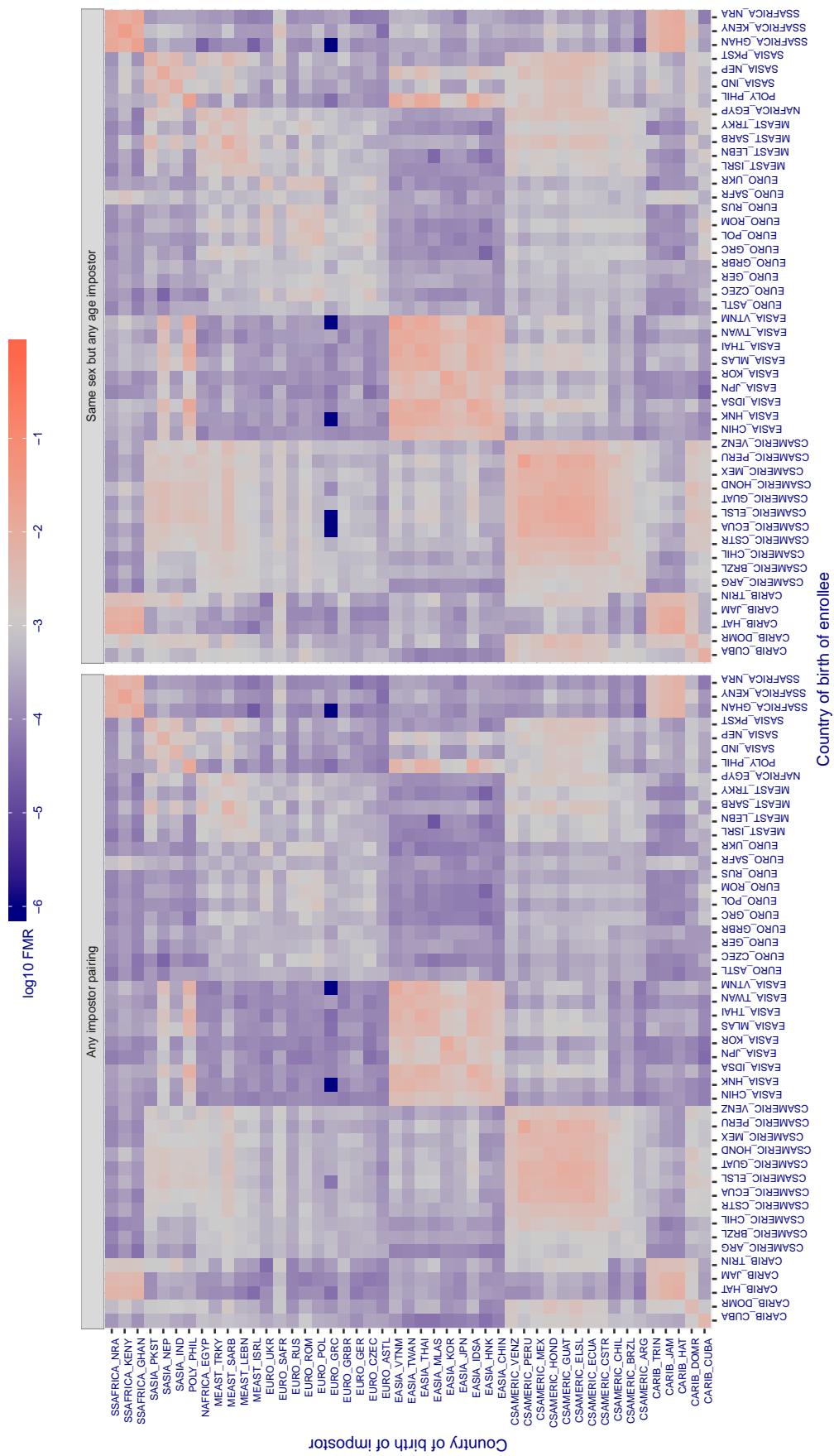


Figure 314: For algorithm dermalog-006 operating on visa images, the heatmap shows false match rates observed over impostor comparisons of faces from different individuals who were born in the given country pair. False matches are counted against a recognition threshold fixed globally to give the target FMR in the plot title, computed over all on the order of 10^{10} impostor comparisons. If text appears in each box it give the same quantity as that coded by the color. Grey indicates FMR is at the intended FMR target level. Light red colors present a security vulnerability to, for example, a passport gate. Each +1 increase in $\log_{10} \text{FMR}$ corresponds to a factor of 10 increase in FMR. The matrix is not quite symmetric because images in the enrollment and verification sets are different.

Cross country FMR at threshold T = 0.547 for algorithm digitalbarriers_002, giving FMR(T) = 0.001 globally.

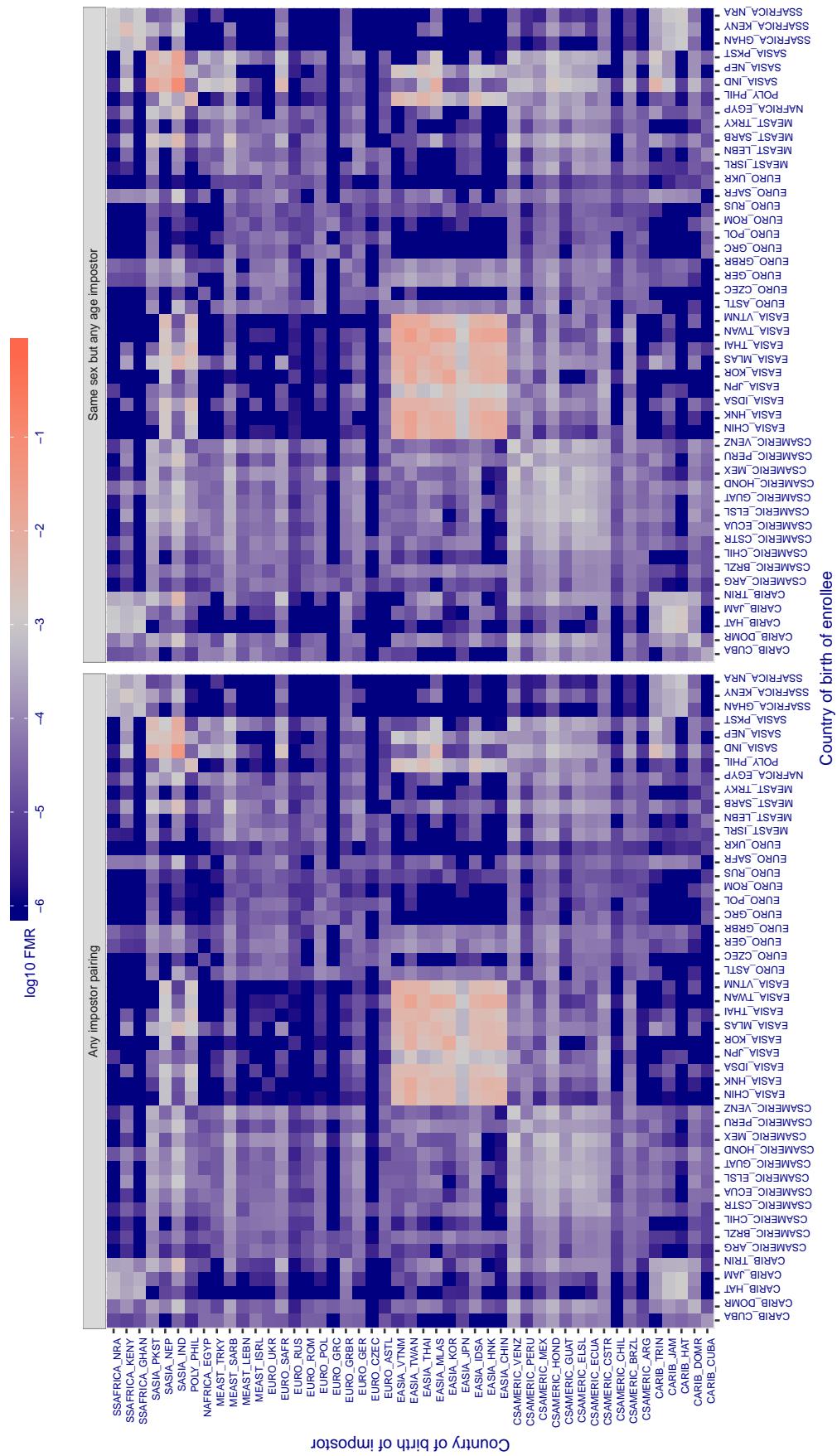


Figure 315: For algorithm digitalbarriers-002 operating on visa images, the heatmap shows false match rates observed over impostor comparisons of faces from different individuals who were born in the given country pair. False matches are counted against a recognition threshold fixed globally to give the target FMR in the plot title, computed over all on the order of 10^{10} impostor comparisons. If text appears in each box it give the same quantity as that coded by the color. Grey indicates FMR is at the intended FMR target level. Light red colors present a security vulnerability to, for example, a passport gate. Each +1 increase in $\log_{10} \text{FMR}$ corresponds to a factor of 10 increase in FMR. The matrix is not quite symmetric because images in the enrollment and verification sets are different.

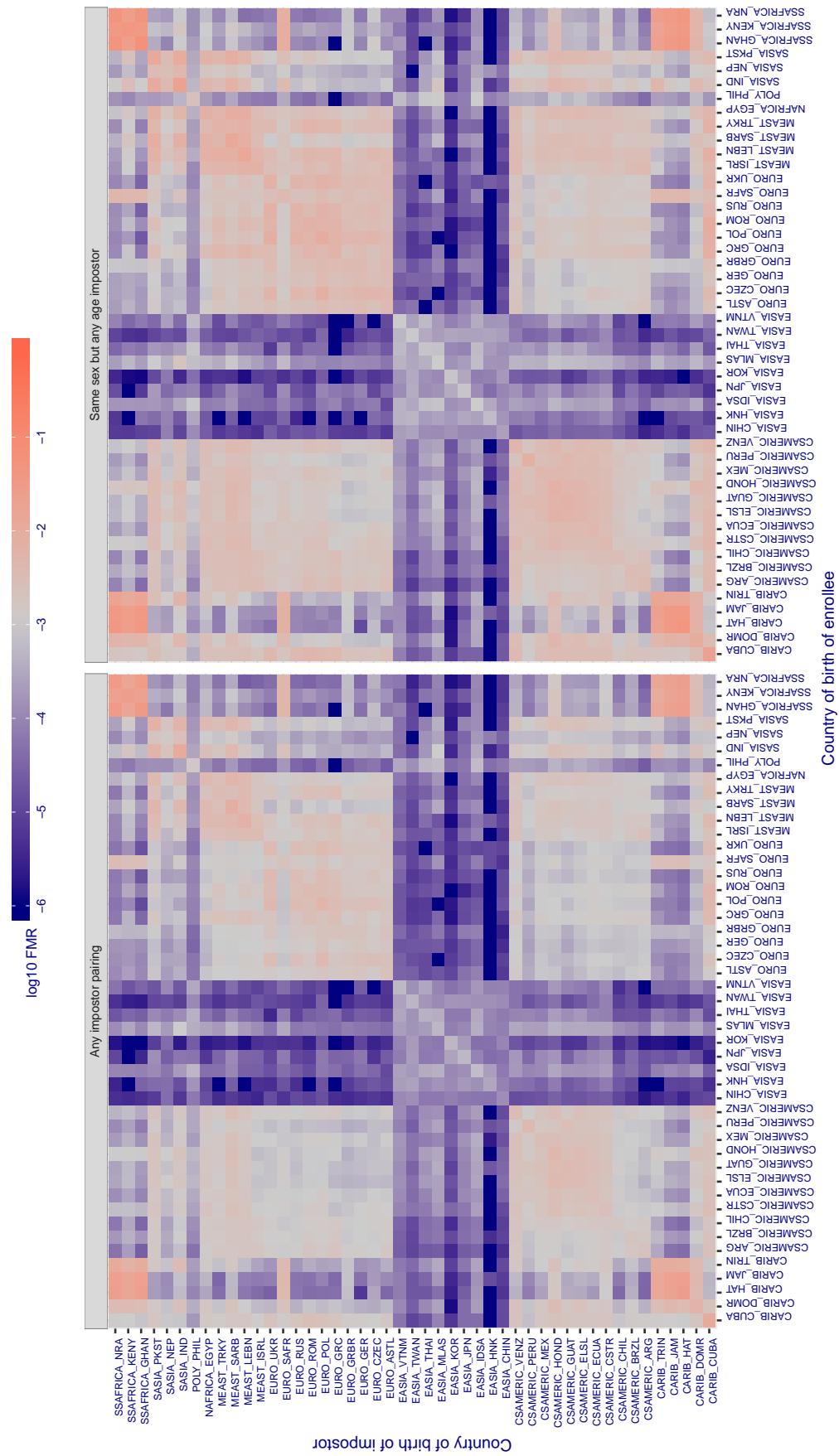
Cross country FMR at threshold T = 0.974 for algorithm dsk_000, giving $FMR(T) = 0.001$ globally.

Figure 316: For algorithm dsk-000 operating on visa images, the heatmap shows false match rates observed over impostor comparisons of faces from different individuals who were born in the given country pair. False matches are counted against a recognition threshold fixed globally to give the target FMR in the plot title, computed over all on the order of 10^{10} impostor comparisons. If text appears in each box it give the same quantity as that coded by the color. Grey indicates FMR is at the intended FMR target level. Light red colors present a security vulnerability to, for example, a passport gate. Each +1 increase in $\log_{10} FMR$ corresponds to a factor of 10 increase in FMR. The matrix is not quite symmetric because images in the enrollment and verification sets are different.

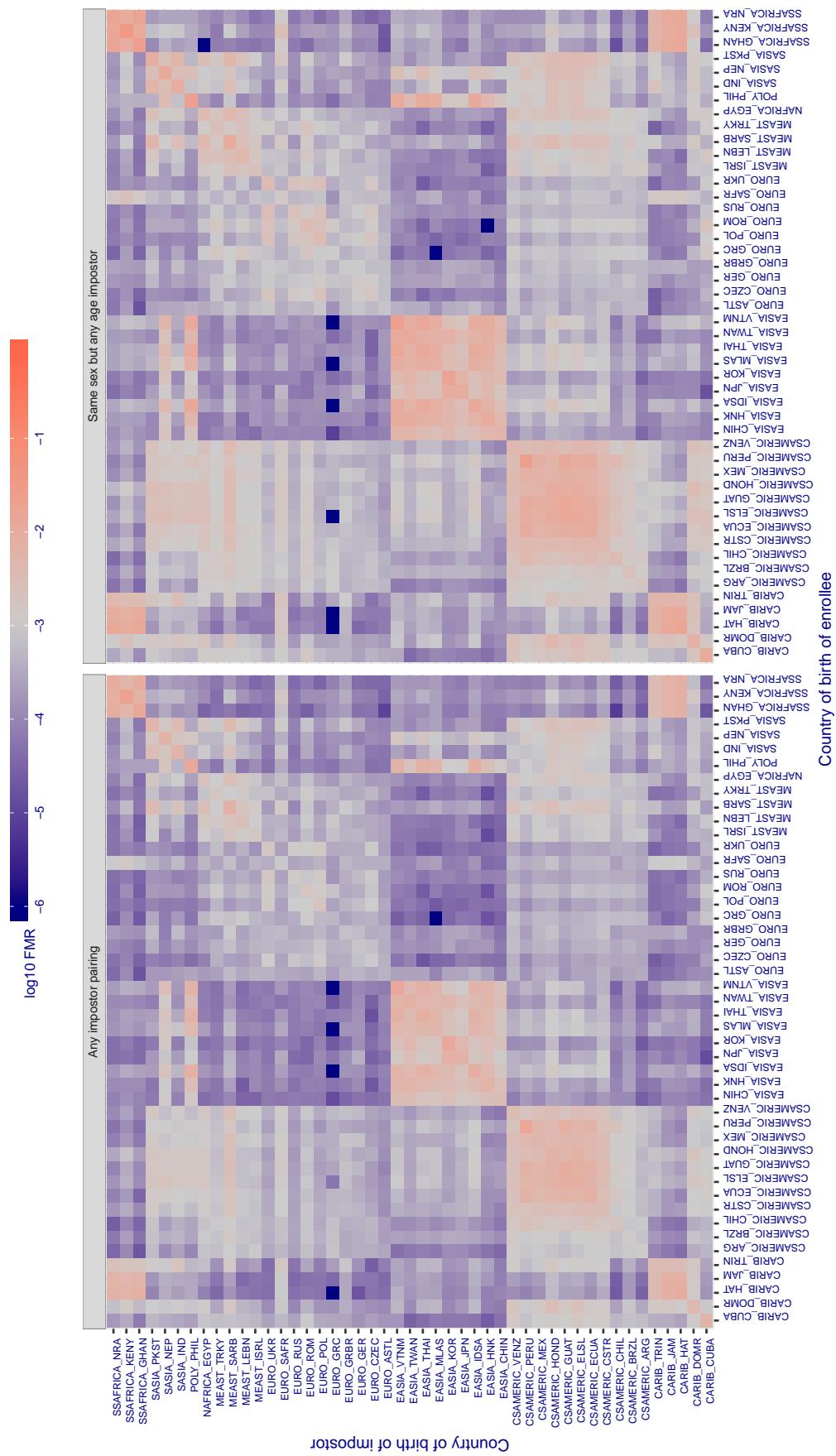
Cross country FMR at threshold T = 48.749 for algorithm einetworks_000, giving $FMR(T) = 0.001$ globally.

Figure 317: For algorithm einetworks-000 operating on visa images, the heatmap shows false match rates observed over impostor comparisons of faces from different individuals who were born in the given country pair. False matches are counted against a recognition threshold fixed globally to give the target FMR in the plot title, computed over all on the order of 10^{10} impostor comparisons. If text appears in each box it give the same quantity as that coded by the color. Grey indicates FMR is at the intended FMR target level. Light red colors present a security vulnerability to, for example, a passport gate. Each +1 increase in $\log_{10} FMR$ corresponds to a factor of 10 increase in FMR. The matrix is not quite symmetric because images in the enrollment and verification sets are different.

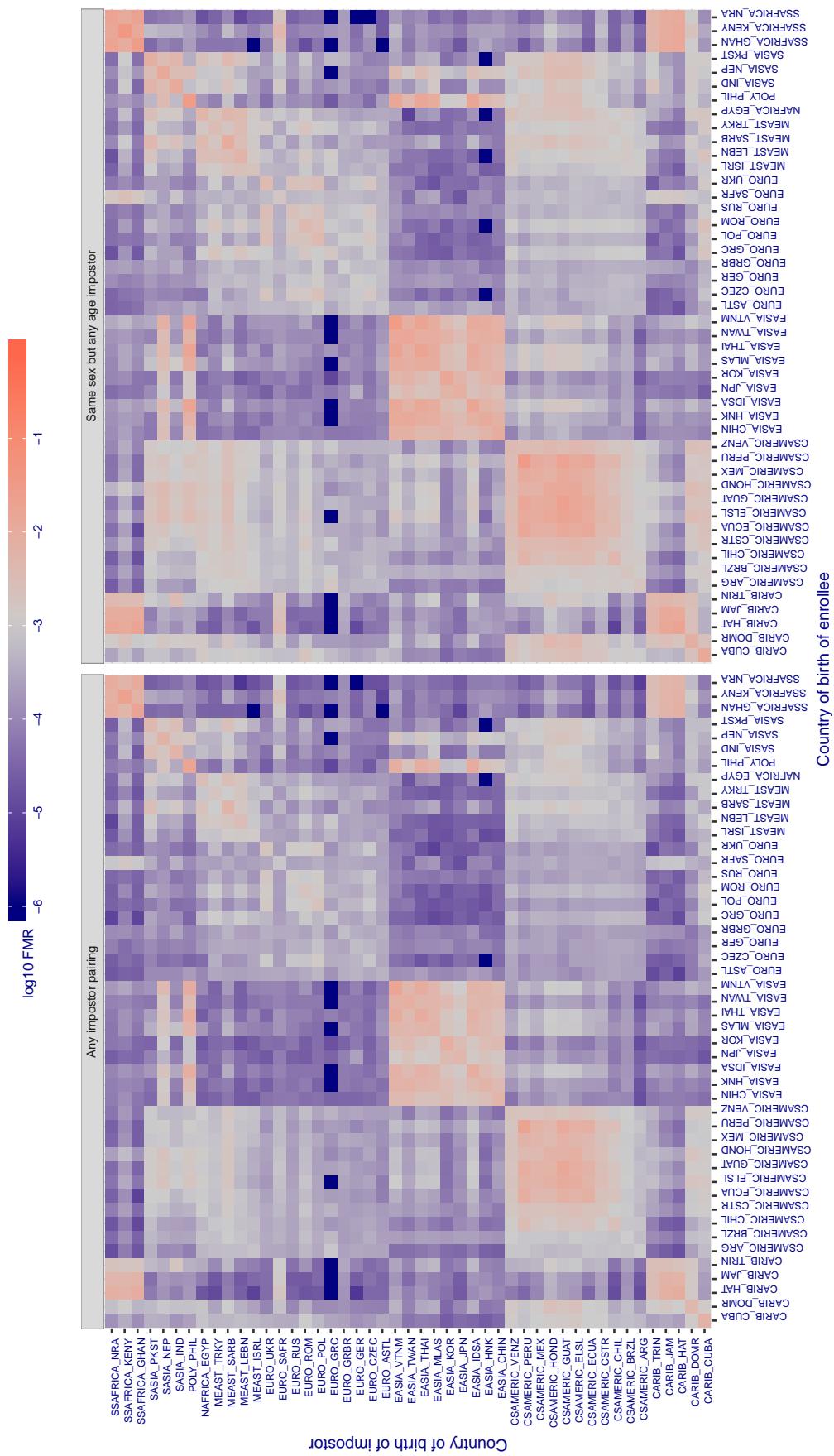
Cross country FMR at threshold T = 2.426 for algorithm everai_002, giving FMR(T) = 0.001 globally.

Figure 318: For algorithm everai-002 operating on visa images, the heatmap shows false match rates observed over impostor comparisons of faces from different individuals who were born in the given country pair. False matches are counted against a recognition threshold fixed globally to give the target FMR in the plot title, computed over all on the order of 10^{10} impostor comparisons. If text appears in each box it give the same quantity as that coded by the color. Grey indicates FMR is at the intended FMR target level. Light red colors present a security vulnerability to, for example, a passport gate. Each +1 increase in $\log_{10} \text{FMR}$ corresponds to a factor of 10 increase in FMR. The matrix is not quite symmetric because images in the enrollment and verification sets are different.

Cross country FMR at threshold T = 0.311 for algorithm f8_001, giving FMR(T) = 0.001 globally.

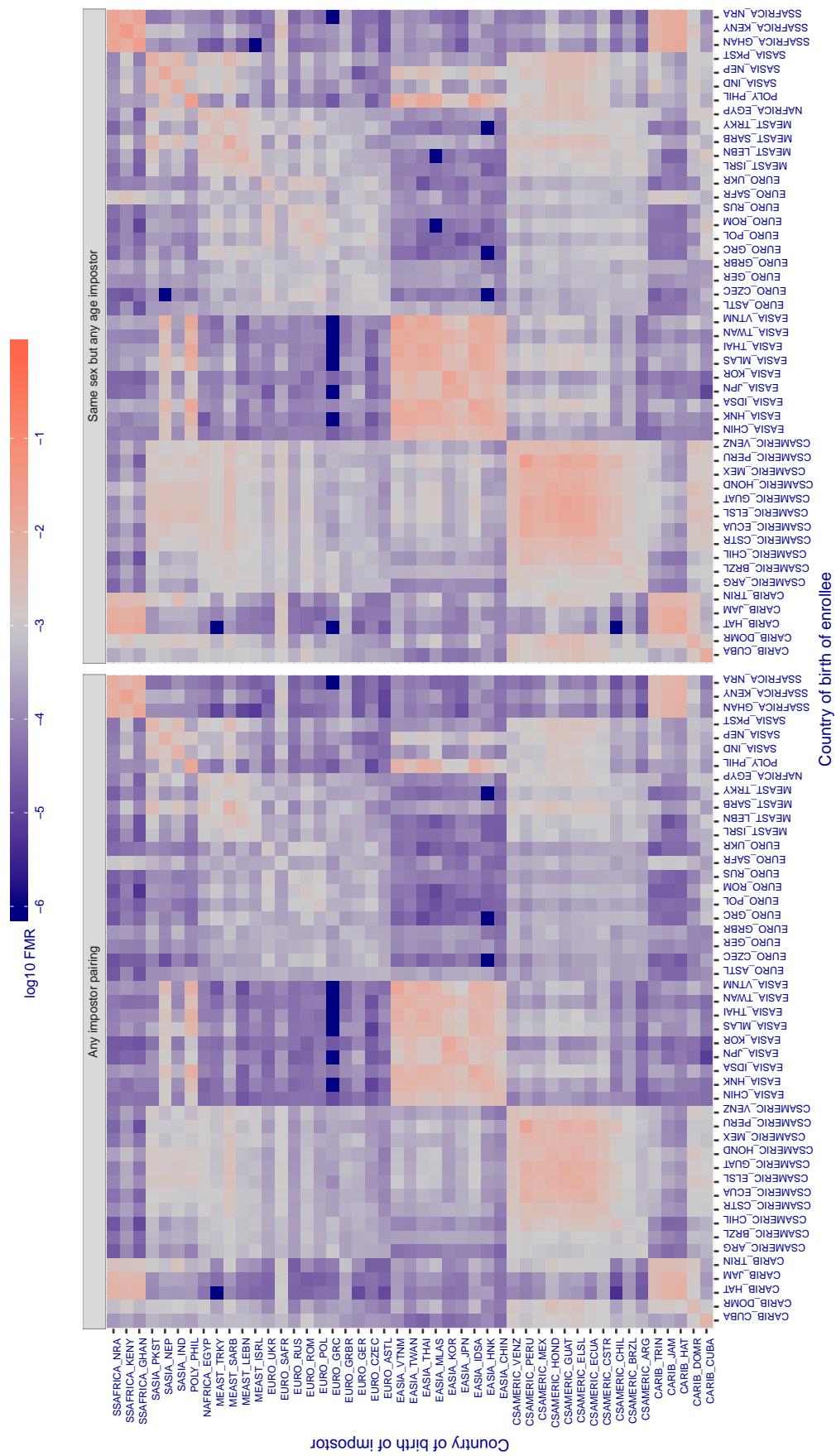


Figure 319: For algorithm f8-001 operating on visa images, the heatmap shows false match rates observed over impostor comparisons of faces from different individuals who were born in the given country pair. False matches are counted against a recognition threshold fixed globally to give the target FMR in the plot title, computed over all on the order of 10^{10} impostor comparisons. If text appears in each box it give the same quantity as that coded by the color. Grey indicates FMR is at the intended FMR target level. Light red colors present a security vulnerability to, for example, a passport gate. Each +1 increase in $\log_{10} \text{FMR}$ corresponds to a factor of 10 increase in FMR. The matrix is not quite symmetric because images in the enrollment and verification sets are different.

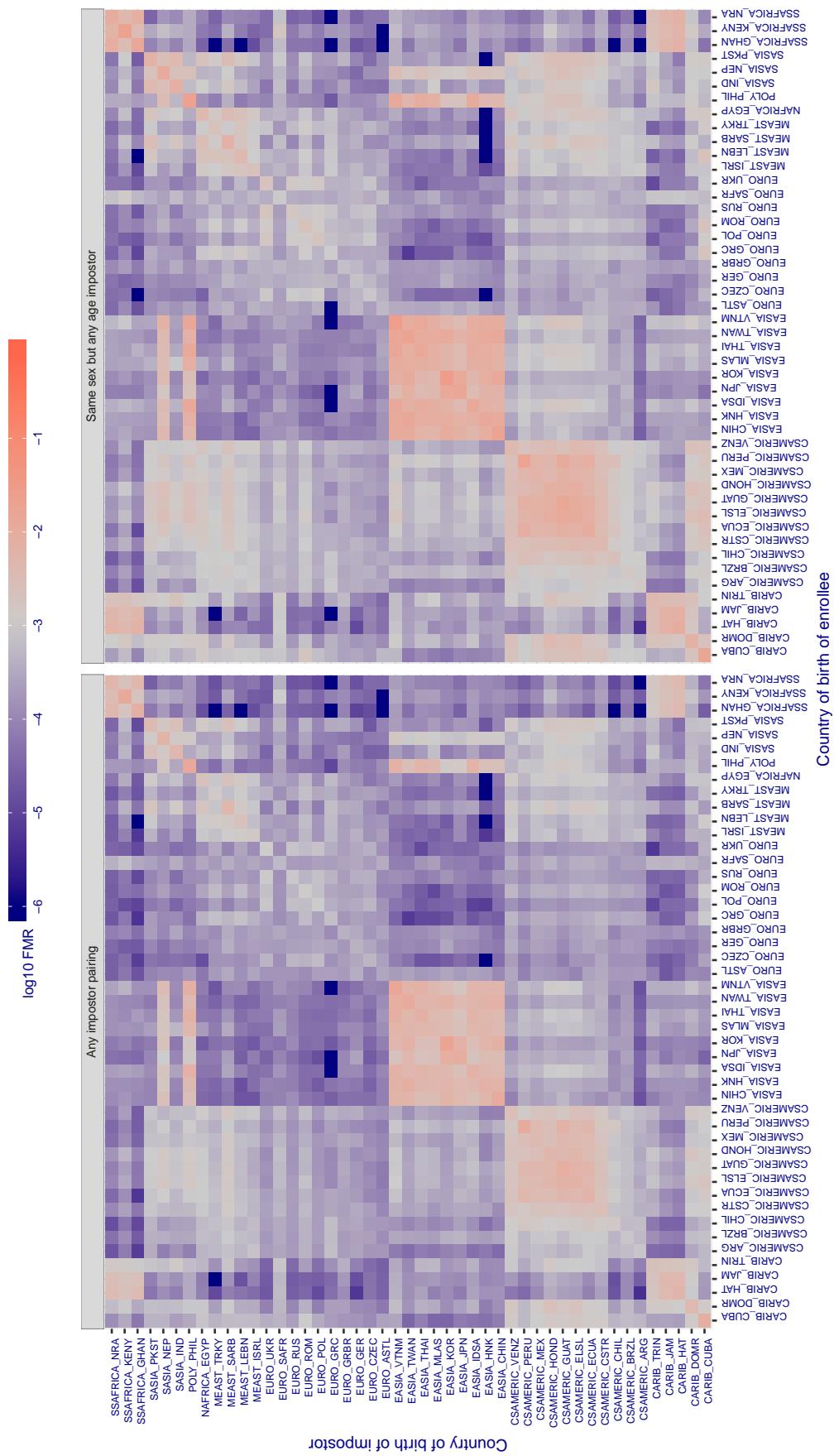
Cross country FMR at threshold T = 1.300 for algorithm facesoft_000, giving $FMR(T) = 0.001$ globally.

Figure 320: For algorithm facesoft-000 operating on visa images, the heatmap shows false match rates observed over impostor comparisons of faces from different individuals who were born in the given country pair. False matches are counted against a recognition threshold fixed globally to give the target FMR in the plot title, computed over all on the order of 10^{10} impostor comparisons. If text appears in each box it give the same quantity as that coded by the color. Grey indicates FMR is at the intended FMR target level. Light red colors present a security vulnerability to, for example, a passport gate. Each +1 increase in $\log_{10} FMR$ corresponds to a factor of 10 increase in FMR. The matrix is not quite symmetric because images in the enrollment and verification sets are different.

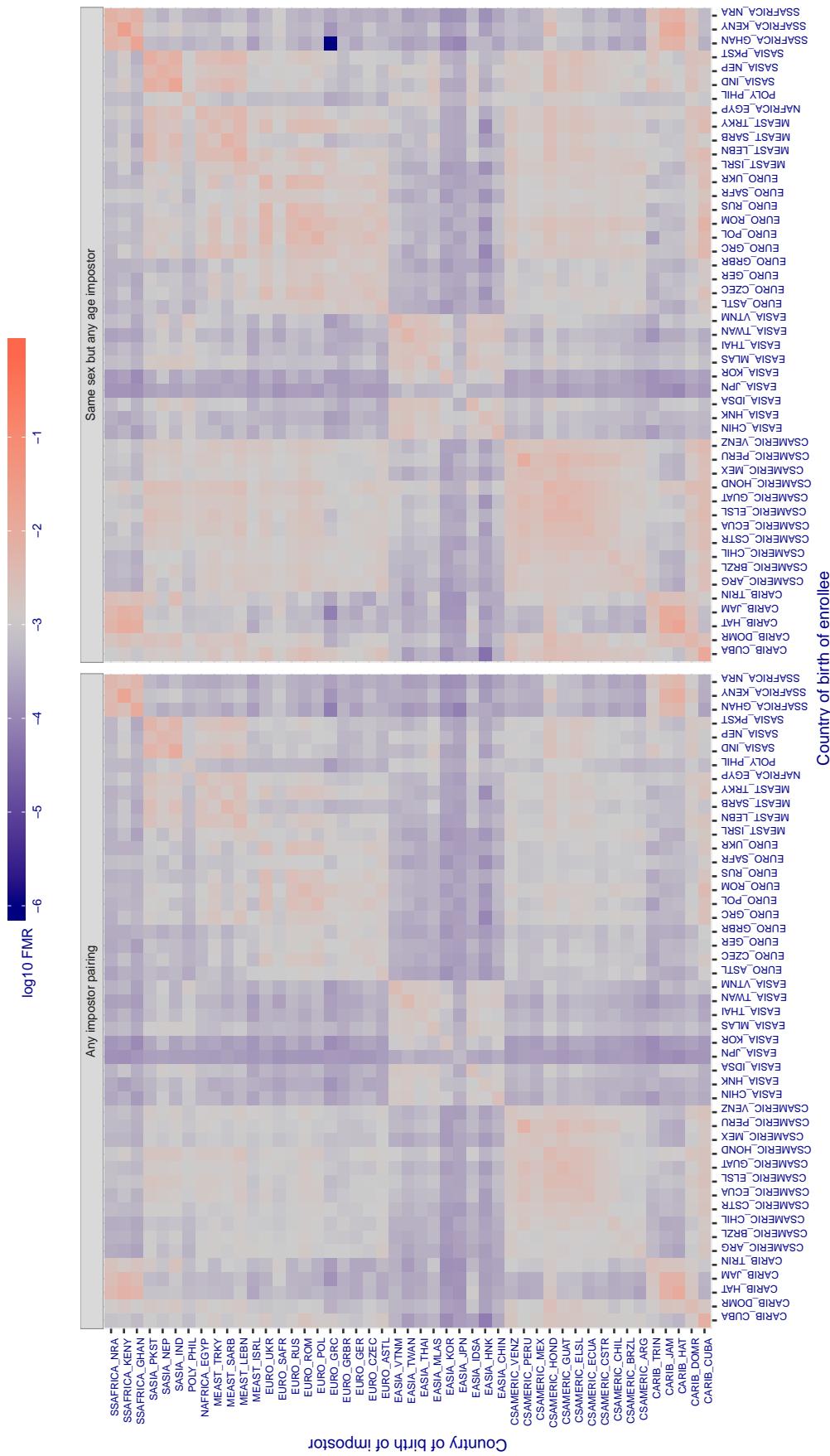
Cross country FMR at threshold T = 0.591 for algorithm glory_000, giving FMR(T) = 0.001 globally.

Figure 321: For algorithm *glory-000* operating on visa images, the heatmap shows false match rates observed over impostor comparisons of faces from different individuals who were born in the given country pair. False matches are counted against a recognition threshold fixed globally to give the target FMR in the plot title, computed over all on the order of 10^{10} impostor comparisons. If text appears in each box it give the same quantity as that coded by the color. Grey indicates FMR is at the intended FMR target level. Light red colors present a security vulnerability to, for example, a passport gate. Each +1 increase in $\log_{10} FMR$ corresponds to a factor of 10 increase in FMR. The matrix is not quite symmetric because images in the enrollment and verification sets are different.

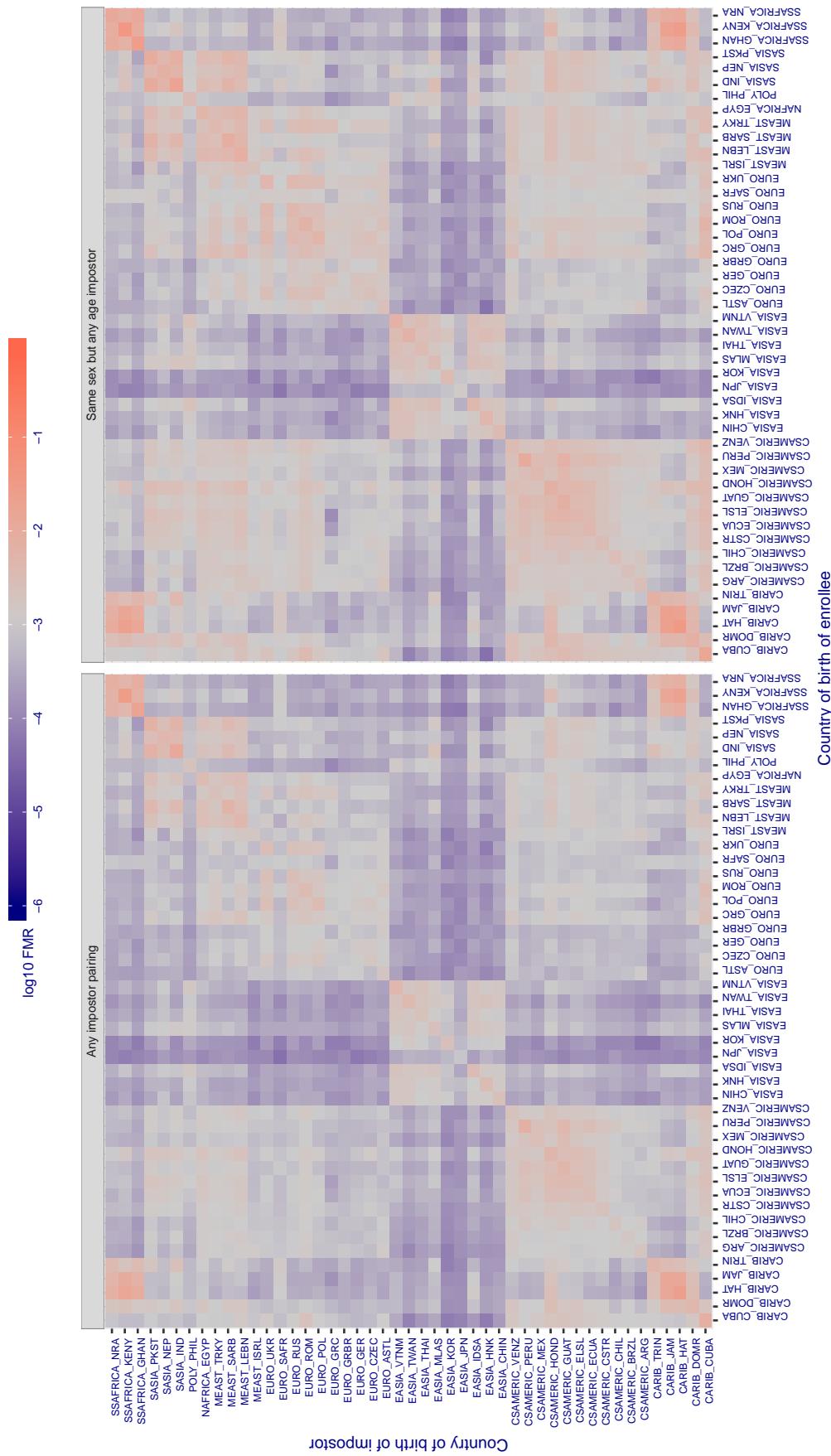
Cross country FMR at threshold T = 0.596 for algorithm glory_001, giving FMR(T) = 0.001 globally.

Figure 322: For algorithm *glory-001* operating on visa images, the heatmap shows false match rates observed over impostor comparisons of faces from different individuals who were born in the given country pair. False matches are counted against a recognition threshold fixed globally to give the target FMR in the plot title, computed over all on the order of 10^{10} impostor comparisons. If text appears in each box it give the same quantity as that coded by the color. Grey indicates FMR is at the intended FMR target level. Light red colors present a security vulnerability to, for example, a passport gate. Each +1 increase in $\log_{10} FMR$ corresponds to a factor of 10 increase in FMR. The matrix is not quite symmetric because images in the enrollment and verification sets are different.

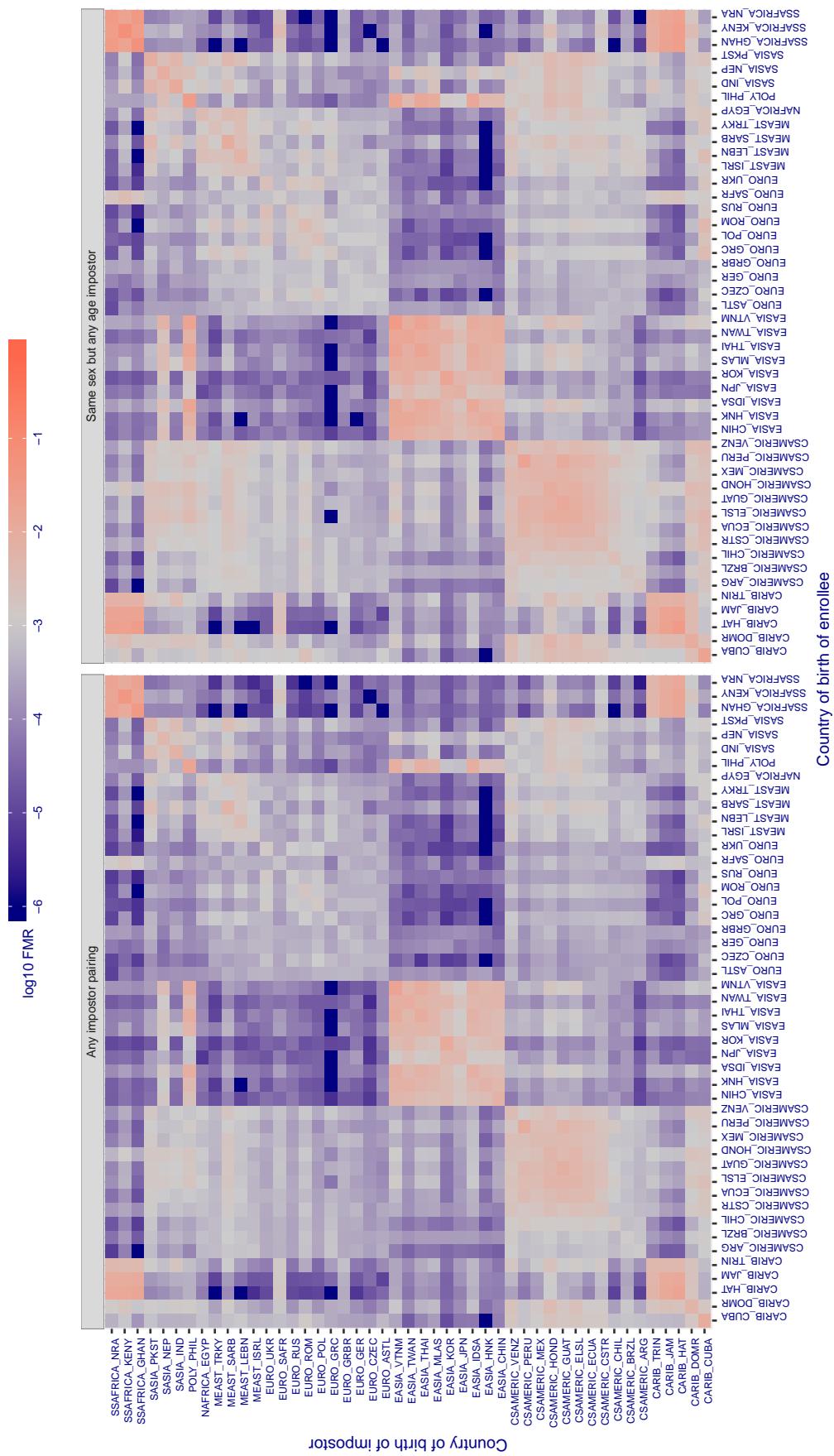
Cross country FMR at threshold T = 0.402 for algorithm gorilla_002, giving FMR(T) = 0.001 globally.

Figure 323: For algorithm gorilla-002 operating on visa images, the heatmap shows false match rates observed over impostor comparisons of faces from different individuals who were born in the given country pair. False matches are counted against a recognition threshold fixed globally to give the target FMR in the plot title, computed over all on the order of 10^{10} impostor comparisons. If text appears in each box it give the same quantity as that coded by the color. Grey indicates FMR is at the intended FMR target level. Light red colors present a security vulnerability to, for example, a passport gate. Each +1 increase in $\log_{10} FMR$ corresponds to a factor of 10 increase in FMR. The matrix is not quite symmetric because images in the enrollment and verification sets are different.

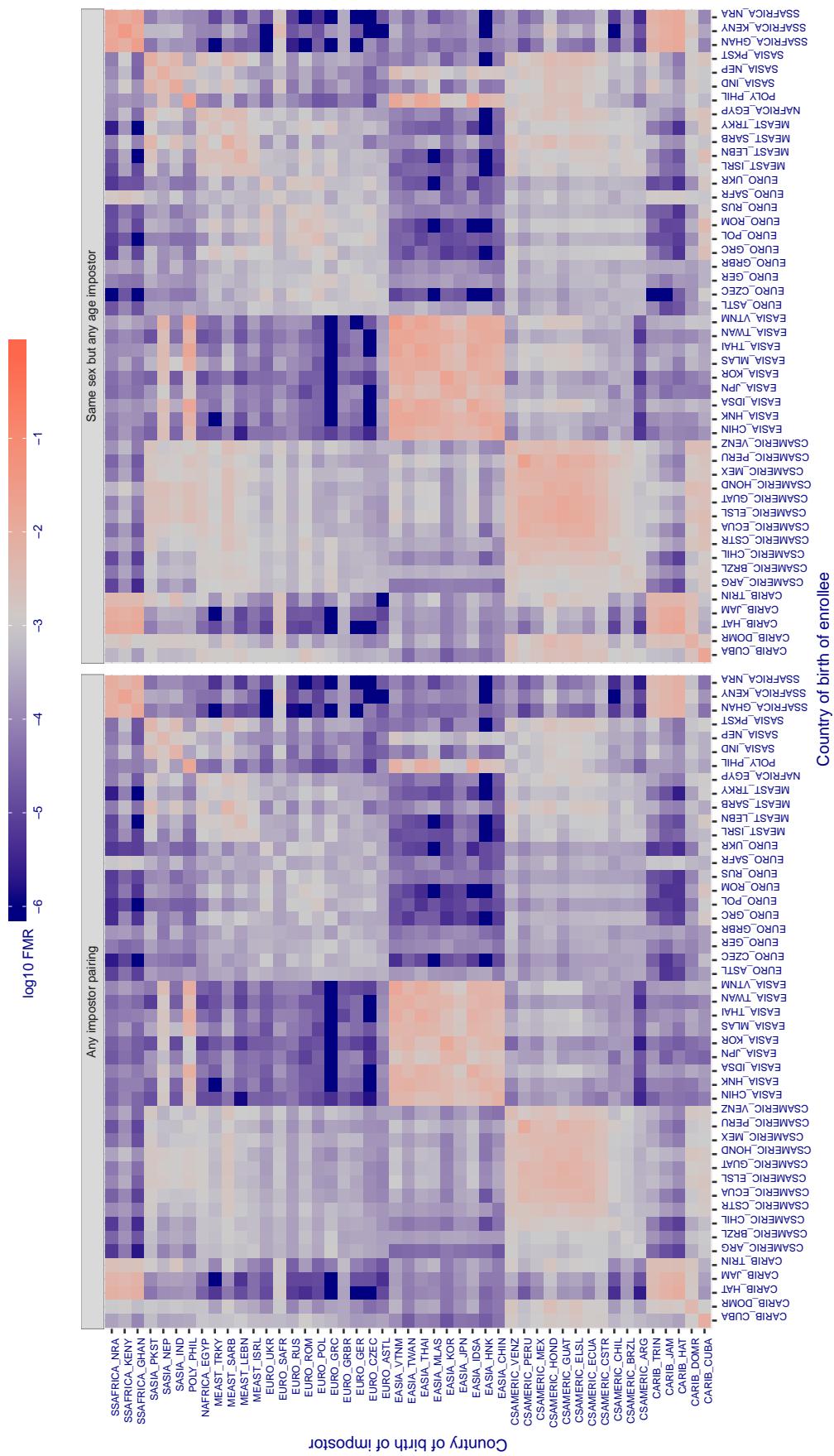
Cross country FMR at threshold T = 0.357 for algorithm gorilla_003, giving FMR(T) = 0.001 globally.

Figure 324: For algorithm gorilla-003 operating on visa images, the heatmap shows false match rates observed over impostor comparisons of faces from different individuals who were born in the given country pair. False matches are counted against a recognition threshold fixed globally to give the target FMR in the plot title, computed over all on the order of 10^{10} impostor comparisons. If text appears in each box it give the same quantity as that coded by the color. Grey indicates FMR is at the intended FMR target level. Light red colors present a security vulnerability to, for example, a passport gate. Each +1 increase in $\log_{10} \text{FMR}$ corresponds to a factor of 10 increase in FMR. The matrix is not quite symmetric because images in the enrollment and verification sets are different.

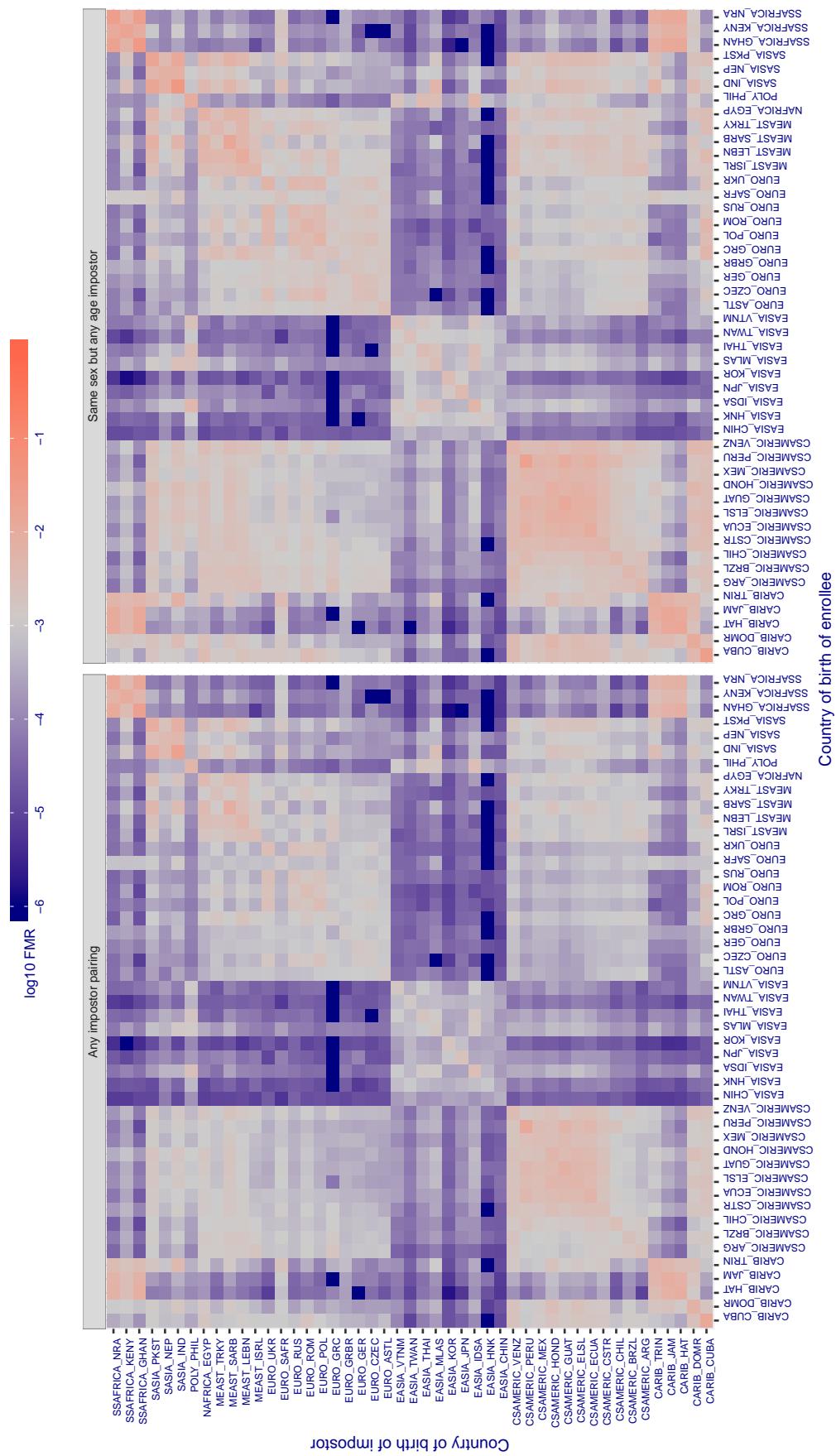
Cross country FMR at threshold T = 63.025 for algorithm hik_001, giving $FMR(T) = 0.001$ globally.

Figure 325: For algorithm hik-001 operating on visa images, the heatmap shows false match rates observed over impostor comparisons of faces from different individuals who were born in the given country pair. False matches are counted against a recognition threshold fixed globally to give the target FMR in the plot title, computed over all on the order of 10^{10} impostor comparisons. If text appears in each box it give the same quantity as that coded by the color. Grey indicates FMR is at the intended FMR target level. Light red colors present a security vulnerability to, for example, a passport gate. Each +1 increase in $\log_{10} FMR$ corresponds to a factor of 10 increase in FMR. The matrix is not quite symmetric because images in the enrollment and verification sets are different.

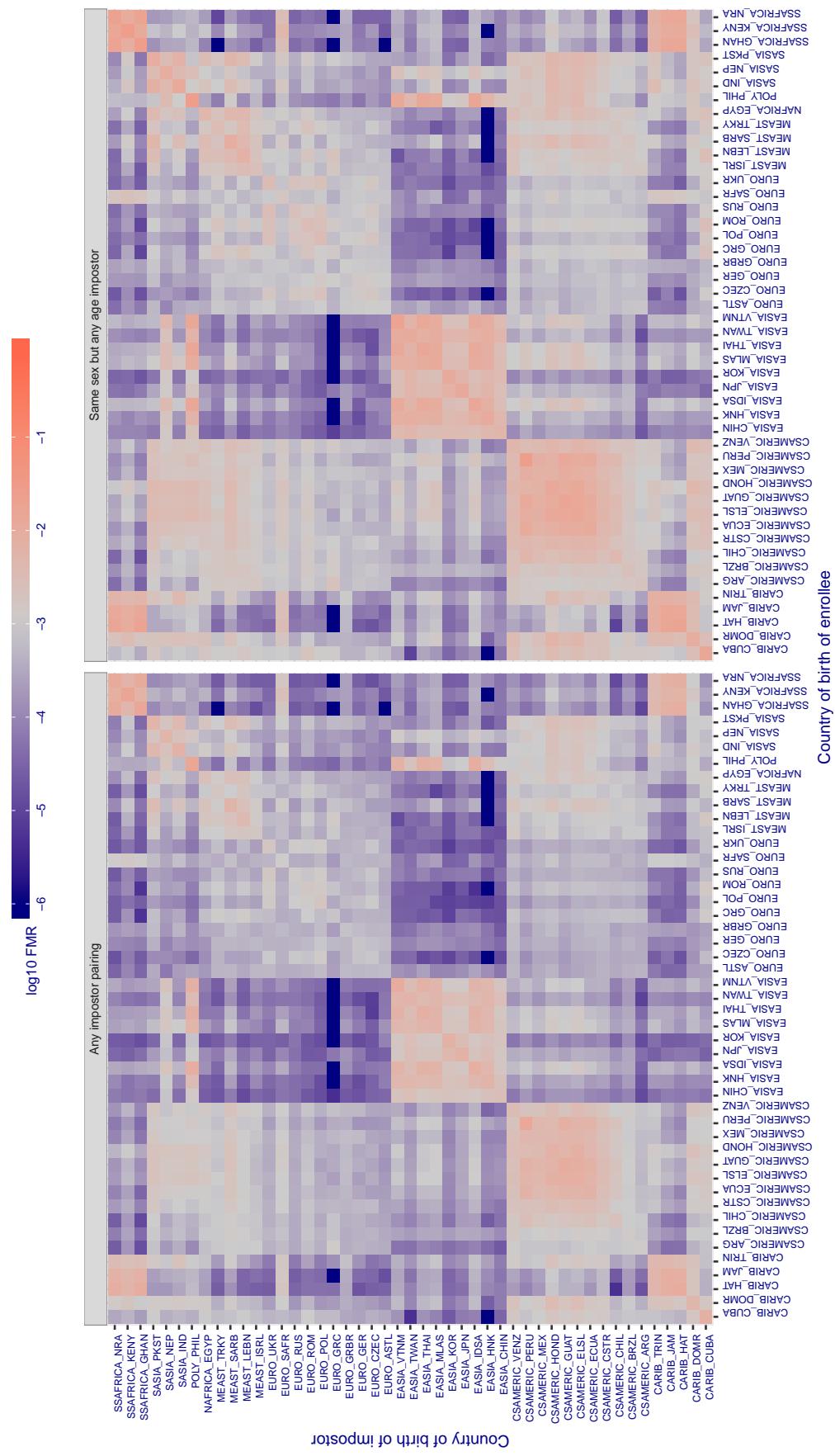
Cross country FMR at threshold T = 0.727 for algorithm hr_001, giving FMR(T) = 0.001 globally.

Figure 326: For algorithm hr-001 operating on visa images, the heatmap shows false match rates observed over impostor comparisons of faces from different individuals who were born in the given country pair. False matches are counted against a recognition threshold fixed globally to give the target FMR in the plot title, computed over all on the order of 10^{10} impostor comparisons. If text appears in each box it give the same quantity as that coded by the color. Grey indicates FMR is at the intended FMR target level. Light red colors present a security vulnerability to, for example, a passport gate. Each +1 increase in $\log_{10} \text{FMR}$ corresponds to a factor of 10 increase in FMR. The matrix is not quite symmetric because images in the enrollment and verification sets are different.

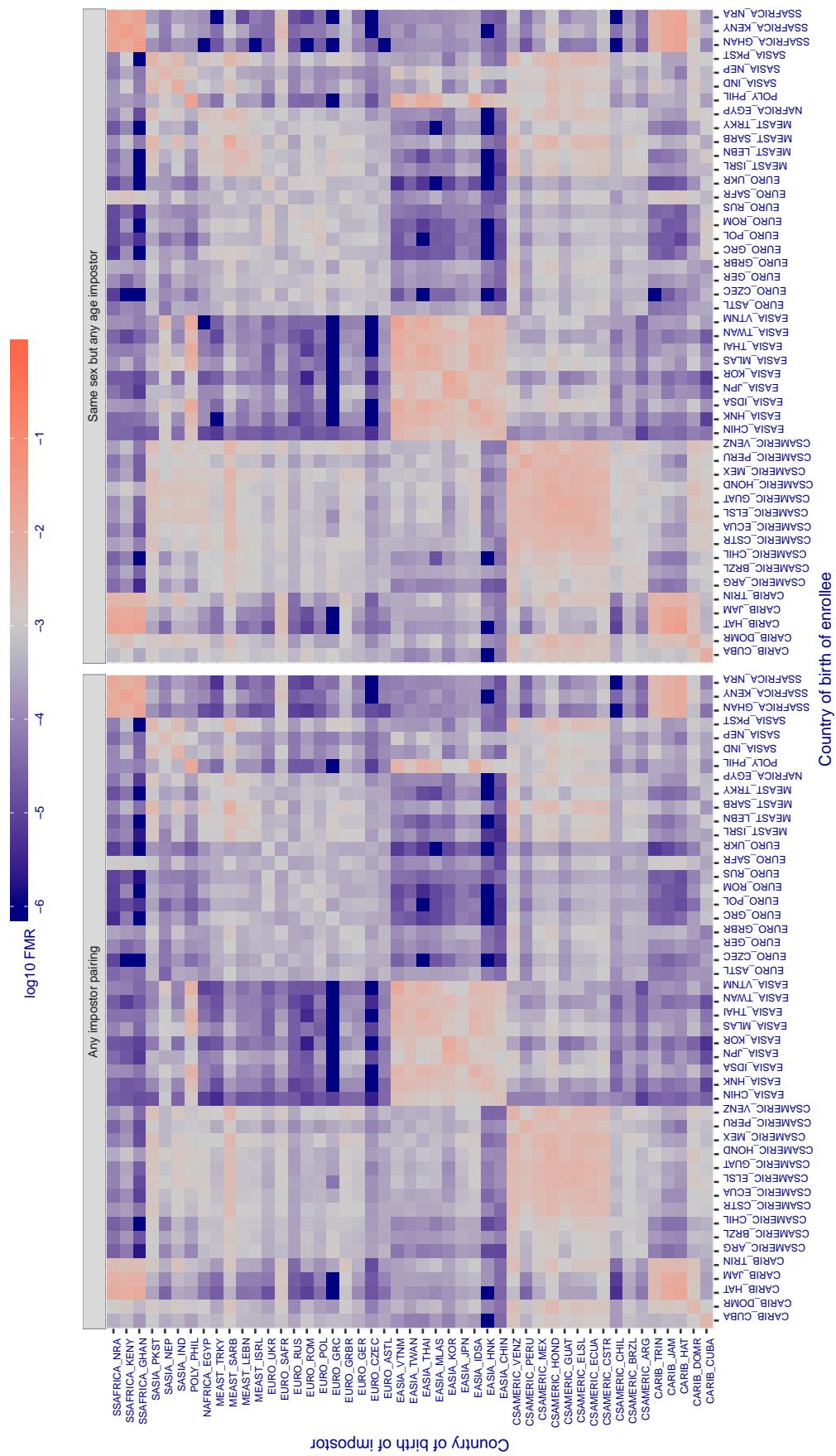
Cross country FMR at threshold T = 36641.000 for algorithm id3_003, giving FMR(T) = 0.001 globally.

Figure 327: For algorithm id3-003 operating on visa images, the heatmap shows false match rates observed over impostor comparisons of faces from different individuals who were born in the given country pair. False matches are counted against a recognition threshold fixed globally to give the target FMR in the plot title, computed over all on the order of 10^{10} impostor comparisons. If text appears in each box it give the same quantity as that coded by the color. Grey indicates FMR is at the intended FMR target level. Light red colors present a security vulnerability to, for example, a passport gate. Each +1 increase in $\log_{10} \text{FMR}$ corresponds to a factor of 10 increase in FMR. The matrix is not quite symmetric because images in the enrollment and verification sets are different.

Cross country FMR at threshold T = 36163.000 for algorithm id3_004, giving $\text{FMR}(T) = 0.001$ globally.

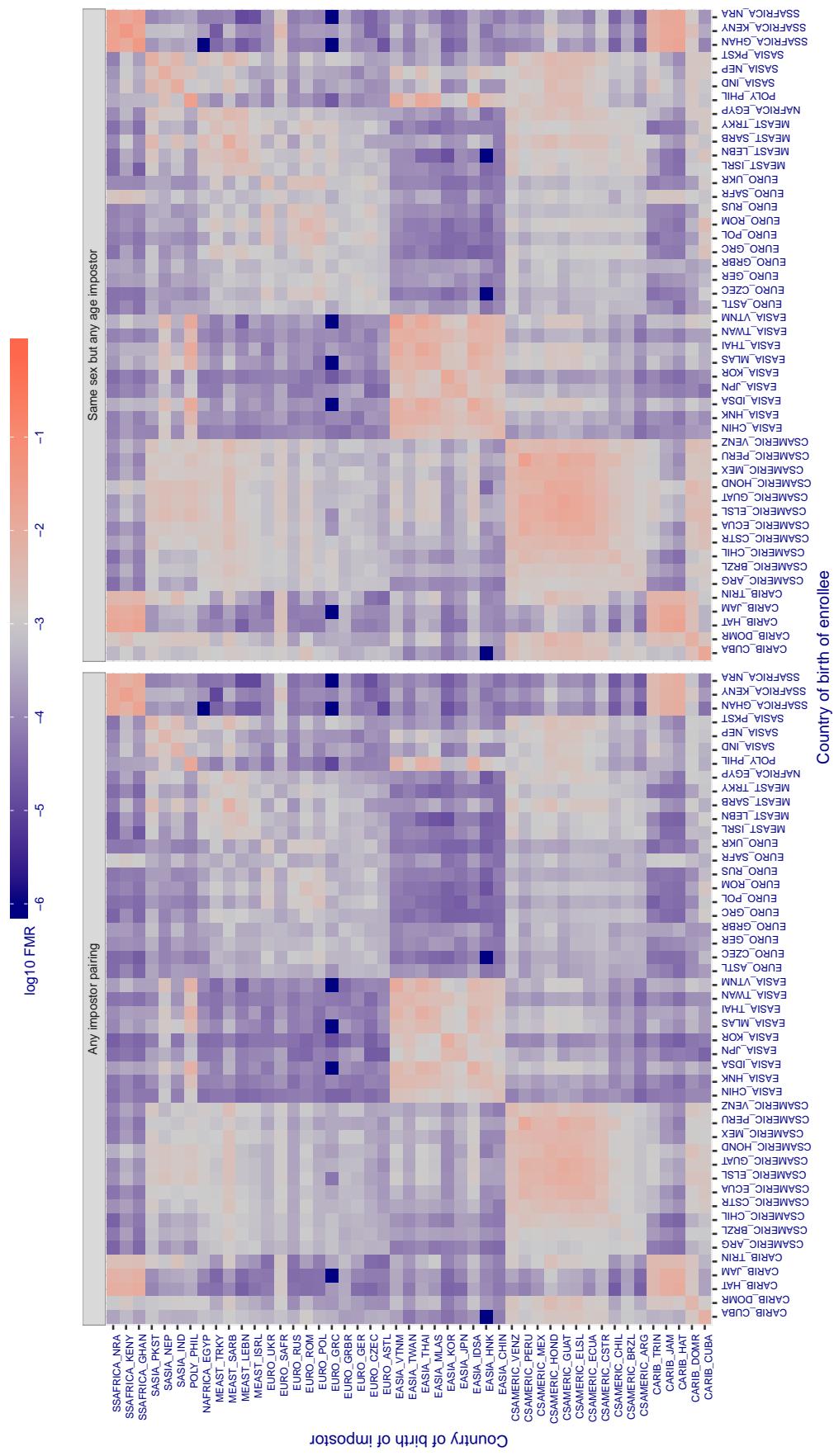


Figure 328: For algorithm id3_004 operating on visa images, the heatmap shows false match rates observed over impostor comparisons of faces from different individuals who were born in the given country pair. False matches are counted against a recognition threshold fixed globally to give the target FMR in the plot title, computed over all on the order of 10^{10} impostor comparisons. If text appears in each box it give the same quantity as that coded by the color. Grey indicates FMR is at the intended FMR target level. Light red colors present a security vulnerability to, for example, a passport gate. Each +1 increase in $\log_{10} \text{FMR}$ corresponds to a factor of 10 increase in FMR. The matrix is not quite symmetric because images in the enrollment and verification sets are different.

Cross country FMR at threshold T = 3136.629 for algorithm idemia_003, giving $FMR(T) = 0.001$ globally.

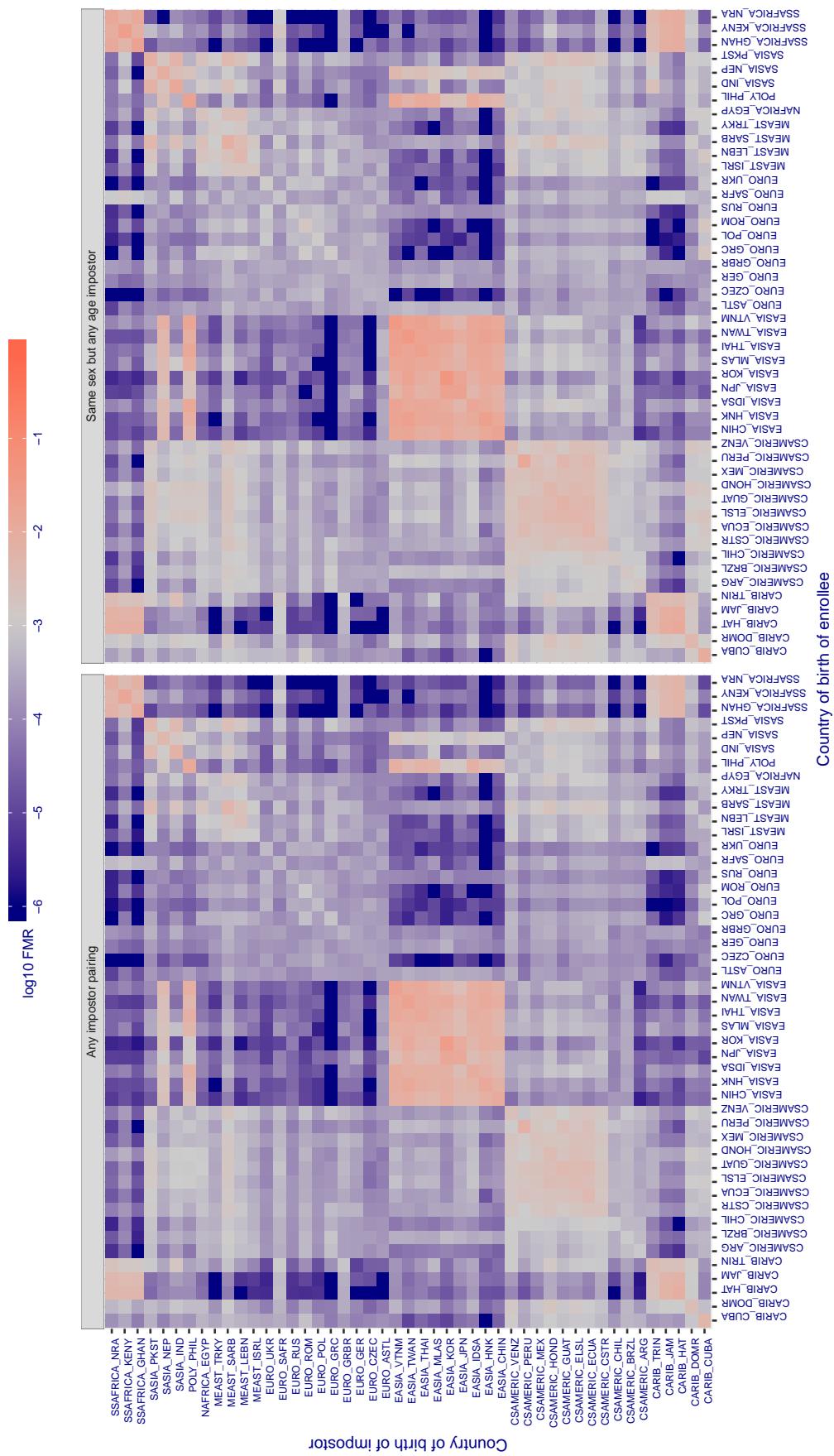


Figure 329: For algorithm idemia-003 operating on visa images, the heatmap shows false match rates observed over impostor comparisons of faces from different individuals who were born in the given country pair. False matches are counted against a recognition threshold fixed globally to give the target FMR in the plot title, computed over all on the order of 10^{10} impostor comparisons. If text appears in each box it give the same quantity as that coded by the color. Grey indicates FMR is at the intended FMR target level. Light red colors present a security vulnerability to, for example, a passport gate. Each +1 increase in $\log_{10} FMR$ corresponds to a factor of 10 increase in FMR . The matrix is not quite symmetric because images in the enrollment and verification sets are different.

Cross country FMR at threshold T = 3261.090 for algorithm idemia_004, giving FMR(T) = 0.001 globally.

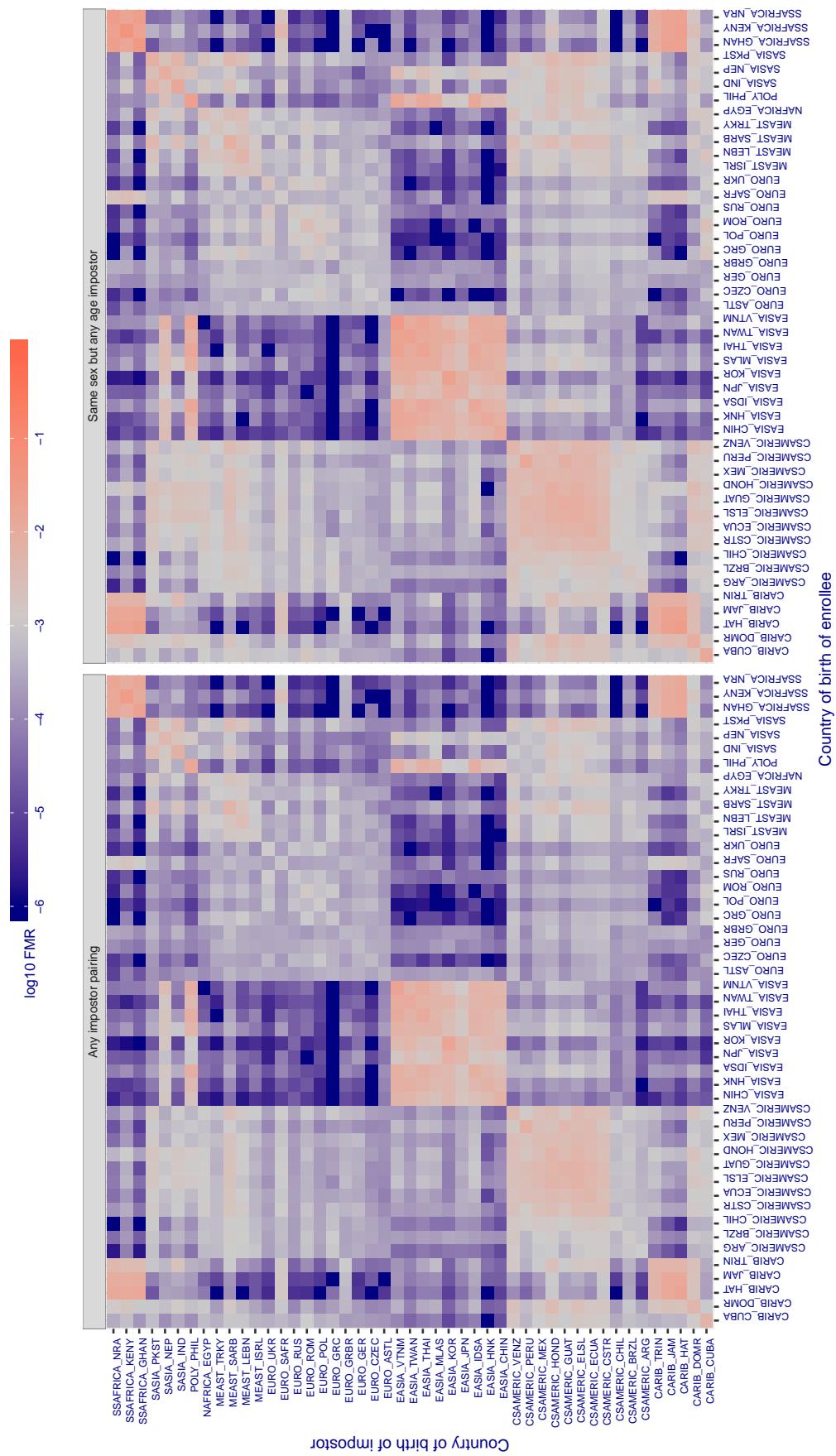


Figure 330: For algorithm idemia-004 operating on visa images, the heatmap shows false match rates observed over impostor comparisons of faces from different individuals who were born in the given country pair. False matches are counted against a recognition threshold fixed globally to give the target FMR in the plot title, computed over all on the order of 10^{10} impostor comparisons. If text appears in each box it give the same quantity as that coded by the color. Grey indicates FMR is at the intended FMR target level. Light red colors present a security vulnerability to, for example, a passport gate. Each +1 increase in $\log_{10} FMR$ corresponds to a factor of 10 increase in FMR. The matrix is not quite symmetric because images in the enrollment and verification sets are different.

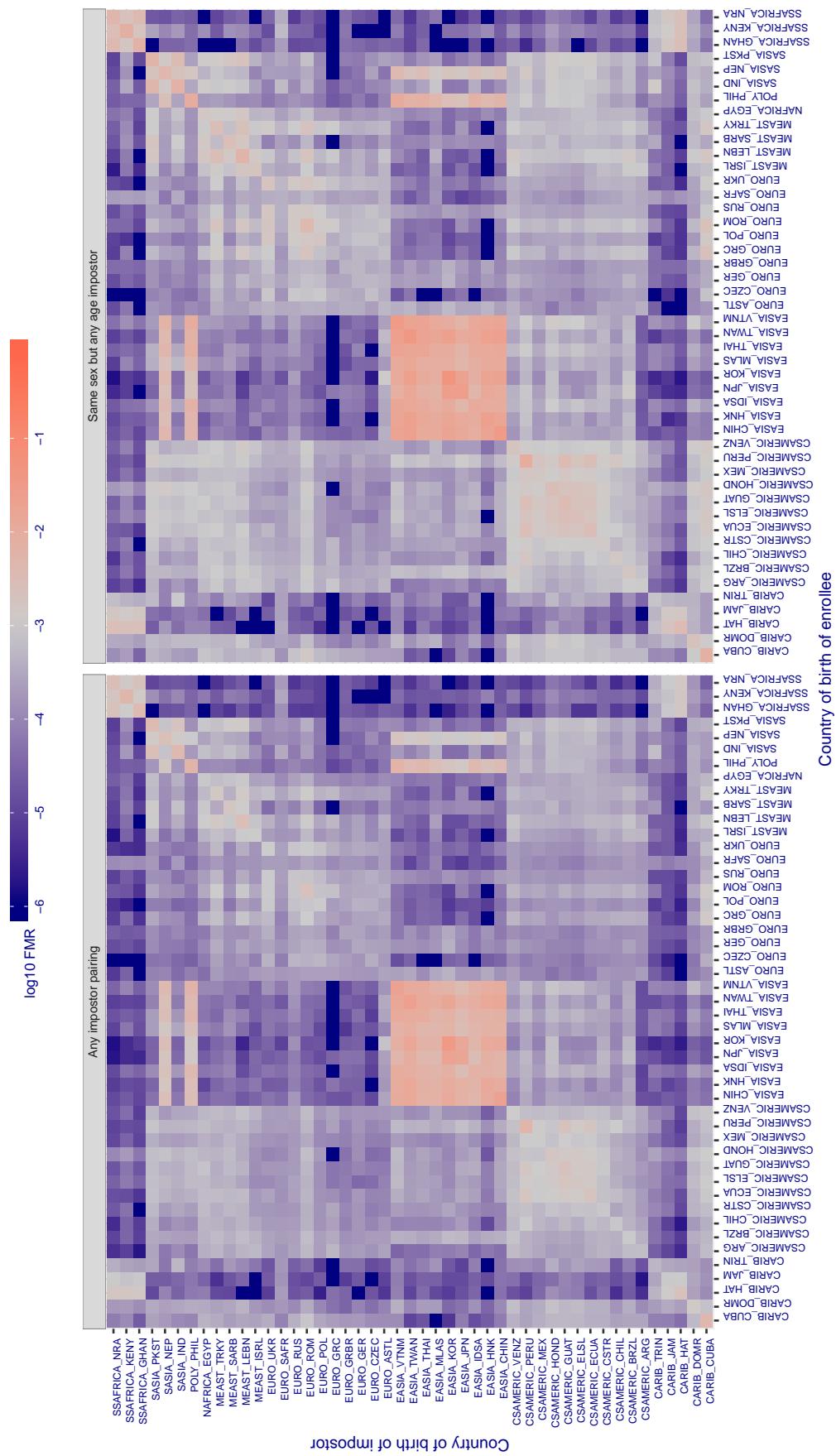
Cross country FMR at threshold T = 0.721 for algorithm iit_000, giving FMR(T) = 0.001 globally.

Figure 331: For algorithm iit-000 operating on visa images, the heatmap shows false match rates observed over impostor comparisons of faces from different individuals who were born in the given country pair. False matches are counted against a recognition threshold fixed globally to give the target FMR in the plot title, computed over all on the order of 10^{10} impostor comparisons. If text appears in each box it give the same quantity as that coded by the color. Grey indicates FMR is at the intended FMR target level. Light red colors present a security vulnerability to, for example, a passport gate. Each +1 increase in $\log_{10} \text{FMR}$ corresponds to a factor of 10 increase in FMR. The matrix is not quite symmetric because images in the enrollment and verification sets are different.

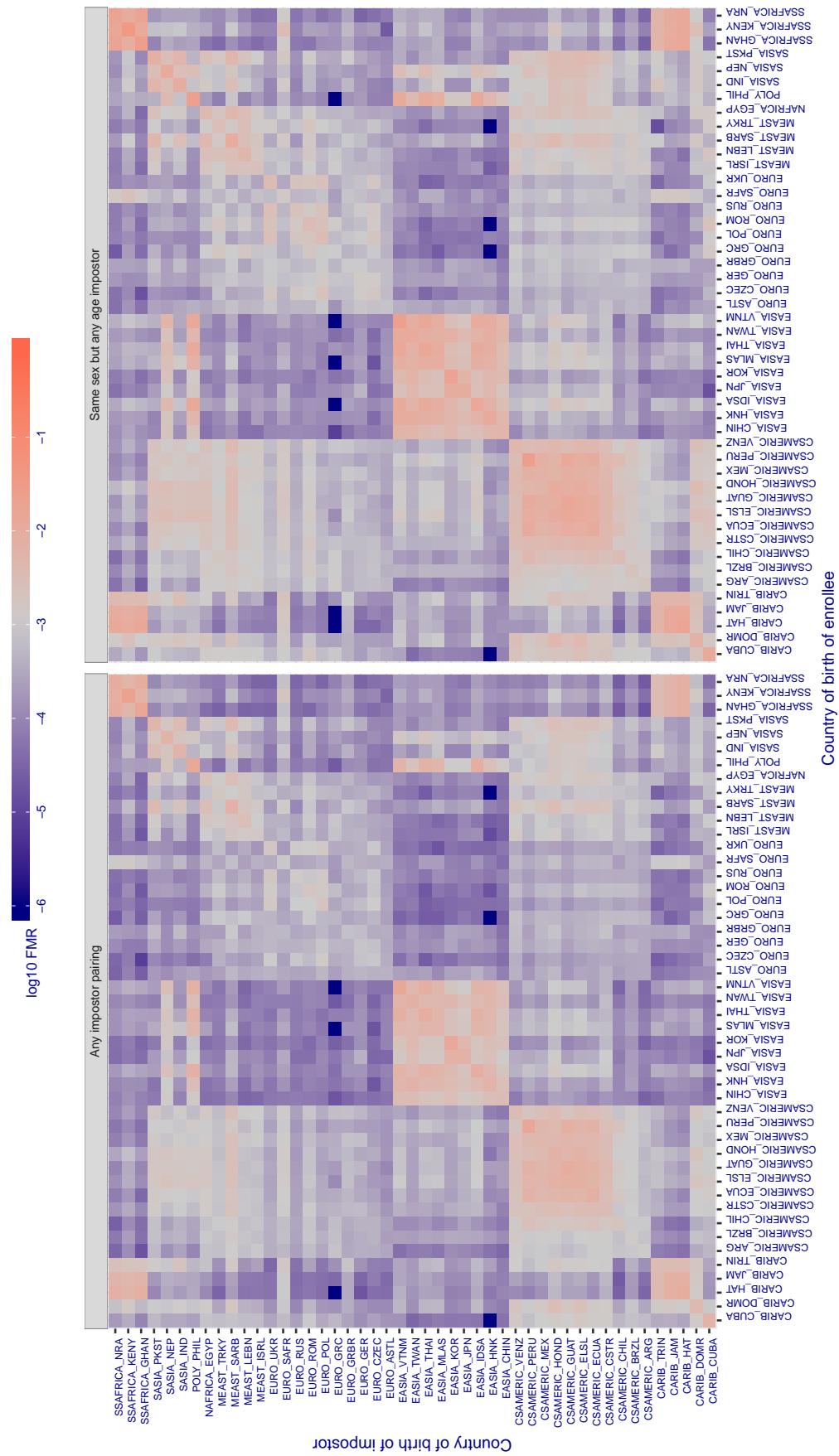
Cross country FMR at threshold T = 0.647 for algorithm iit_001, giving FMR(T) = 0.001 globally.

Figure 332: For algorithm iit-001 operating on visa images, the heatmap shows false match rates observed over impostor comparisons of faces from different individuals who were born in the given country pair. False matches are counted against a recognition threshold fixed globally to give the target FMR in the plot title, computed over all on the order of 10^{10} impostor comparisons. If text appears in each box it give the same quantity as that coded by the color. Grey indicates FMR is at the intended FMR target level. Light red colors present a security vulnerability to, for example, a passport gate. Each +1 increase in $\log_{10} \text{FMR}$ corresponds to a factor of 10 increase in FMR. The matrix is not quite symmetric because images in the enrollment and verification sets are different.

Cross country FMR at threshold T = 0.809 for algorithm imagus_000, giving $FMR(T) = 0.001$ globally.

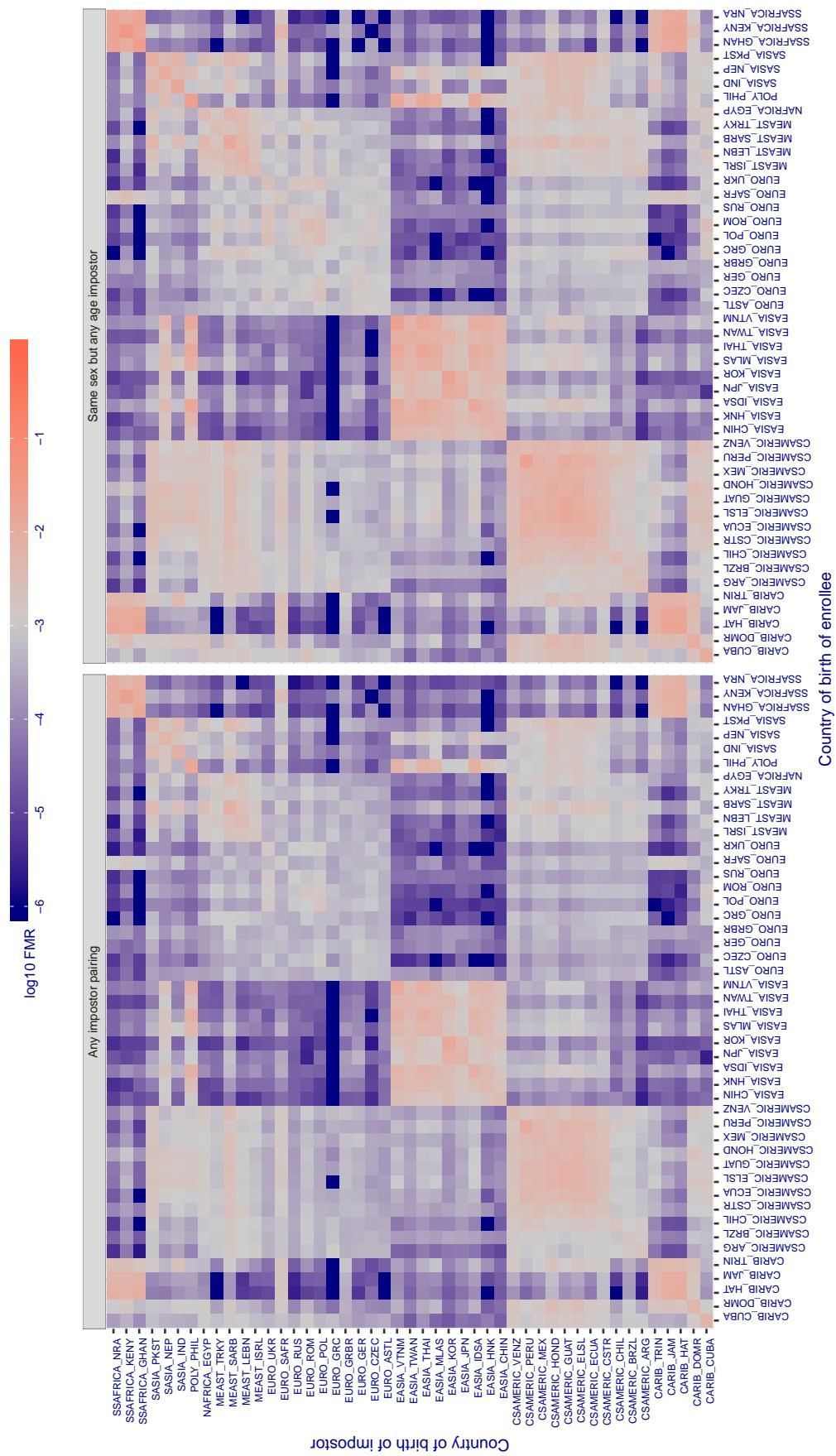


Figure 333: For algorithm imagus-000 operating on visa images, the heatmap shows false match rates observed over impostor comparisons of faces from different individuals who were born in the given country pair. False matches are counted against a recognition threshold fixed globally to give the target FMR in the plot title, computed over all on the order of 10^{10} impostor comparisons. If text appears in each box it give the same quantity as that coded by the color. Grey indicates FMR is at the intended FMR target level. Light red colors present a security vulnerability to, for example, a passport gate. Each +1 increase in $\log_{10} FMR$ corresponds to a factor of 10 increase in FMR. The matrix is not quite symmetric because images in the enrollment and verification sets are different.

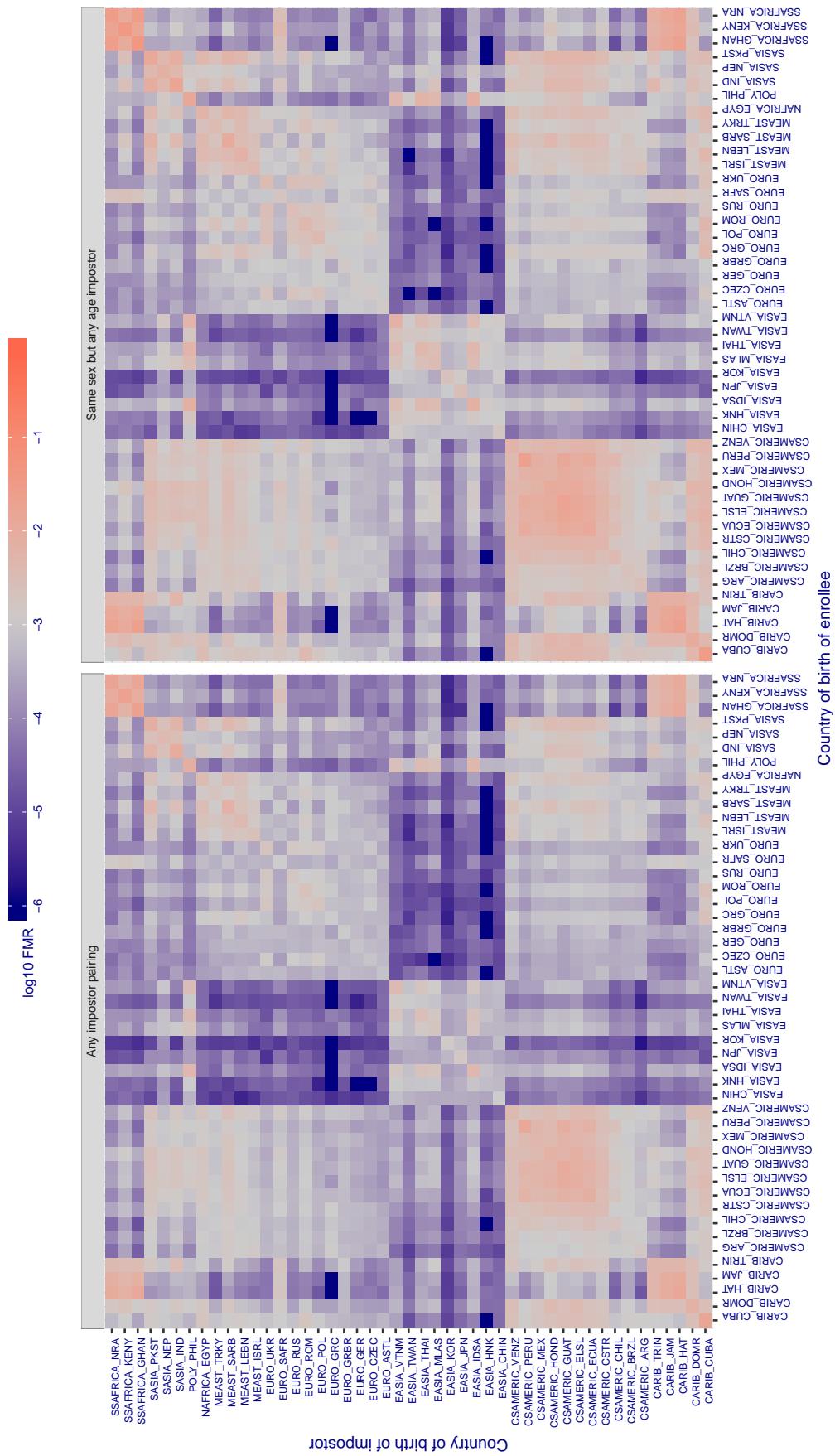
Cross country FMR at threshold T = 1.302 for algorithm imperial_000, giving $FMR(T) = 0.001$ globally.

Figure 334: For algorithm imperial-000 operating on visa images, the heatmap shows false match rates observed over impostor comparisons of faces from different individuals who were born in the given country pair. False matches are counted against a recognition threshold fixed globally to give the target FMR in the plot title, computed over all on the order of 10^{10} impostor comparisons. If text appears in each box it give the same quantity as that coded by the color. Grey indicates FMR is at the intended FMR target level. Light red colors present a security vulnerability to, for example, a passport gate. Each +1 increase in \log_{10} FMR corresponds to a factor of 10 increase in FMR. The matrix is not quite symmetric because images in the enrollment and verification sets are different.

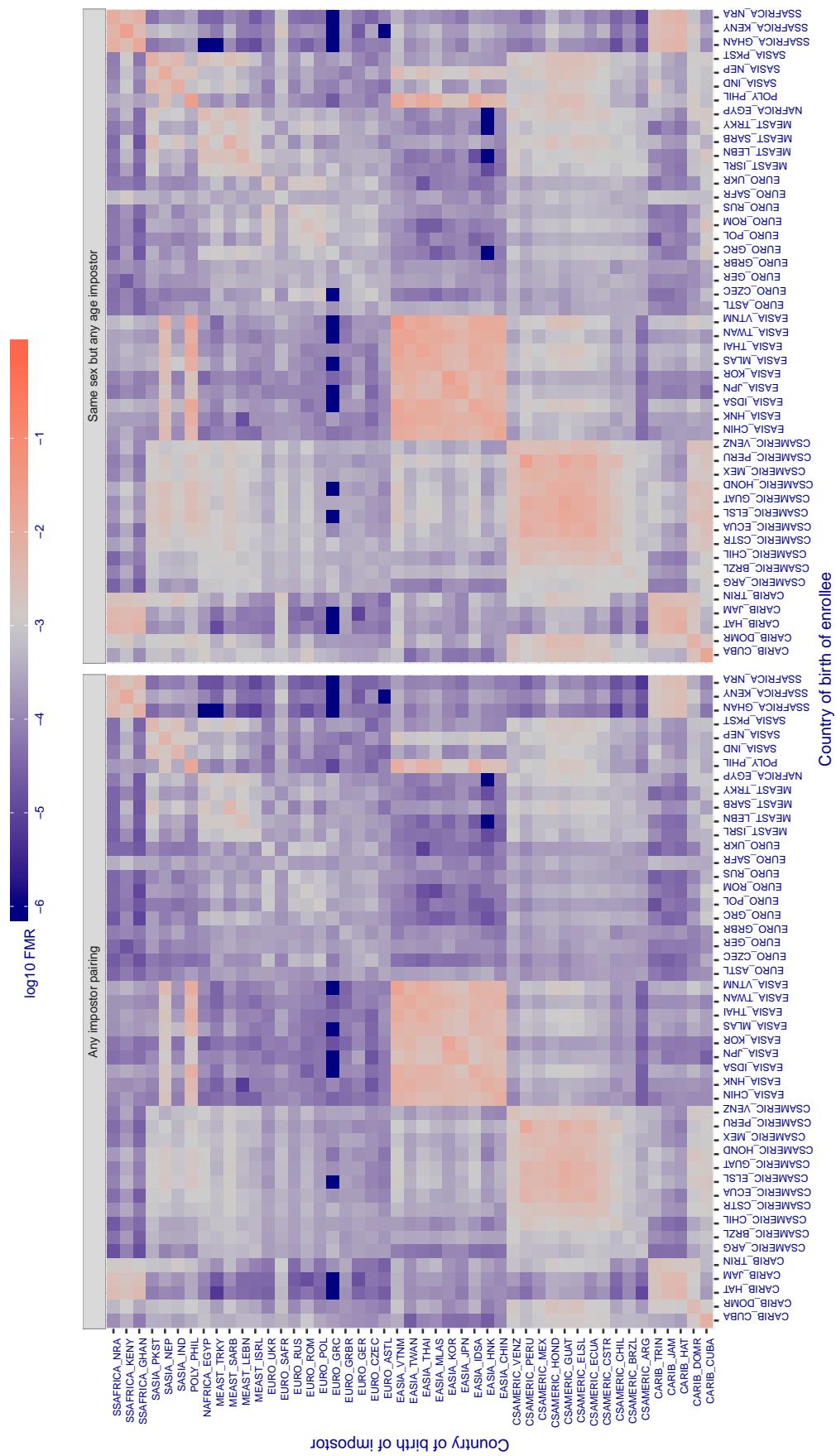
Cross country FMR at threshold T = 1.285 for algorithm imperial_002, giving $\text{FMR}(T) = 0.001$ globally.

Figure 335: For algorithm imperial-002 operating on visa images, the heatmap shows false match rates observed over impostor comparisons of faces from different individuals who were born in the given country pair. False matches are counted against a recognition threshold fixed globally to give the target FMR in the plot title, computed over all on the order of 10^{10} impostor comparisons. If text appears in each box it give the same quantity as that coded by the color. Grey indicates FMR is at the intended FMR target level. Light red colors present a security vulnerability to, for example, a passport gate. Each +1 increase in $\log_{10} \text{FMR}$ corresponds to a factor of 10 increase in FMR. The matrix is not quite symmetric because images in the enrollment and verification sets are different.

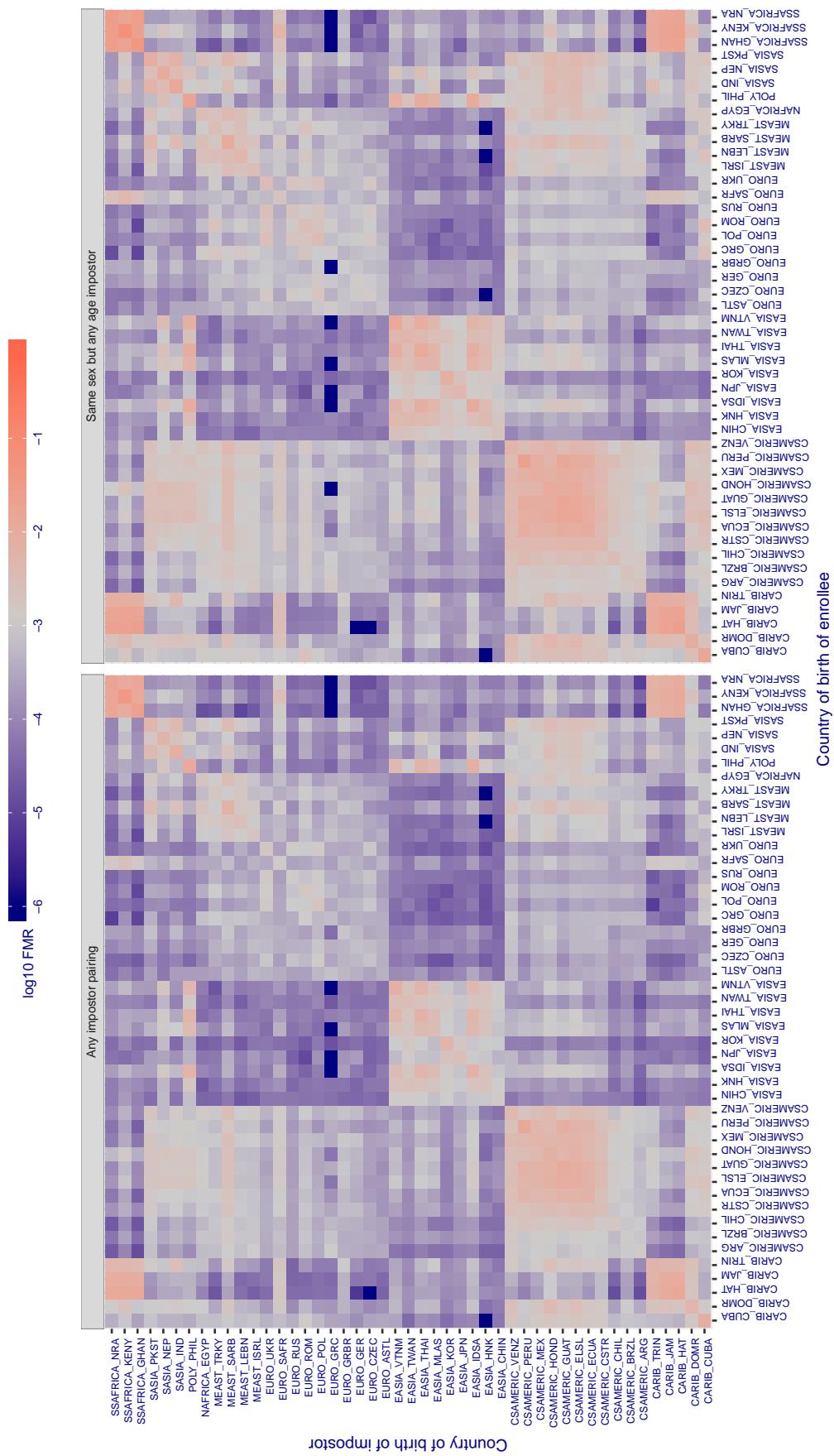
Cross country FMR at threshold T = 1.340 for algorithm incode_003, giving FMR(T) = 0.001 globally.

Figure 336: For algorithm incode-003 operating on visa images, the heatmap shows false match rates observed over impostor comparisons of faces from different individuals who were born in the given country pair. False matches are counted against a recognition threshold fixed globally to give the target FMR in the plot title, computed over all on the order of 10^{10} impostor comparisons. If text appears in each box it give the same quantity as that coded by the color. Grey indicates FMR is at the intended FMR target level. Light red colors present a security vulnerability to, for example, a passport gate. Each +1 increase in $\log_{10} FMR$ corresponds to a factor of 10 increase in FMR. The matrix is not quite symmetric because images in the enrollment and verification sets are different.

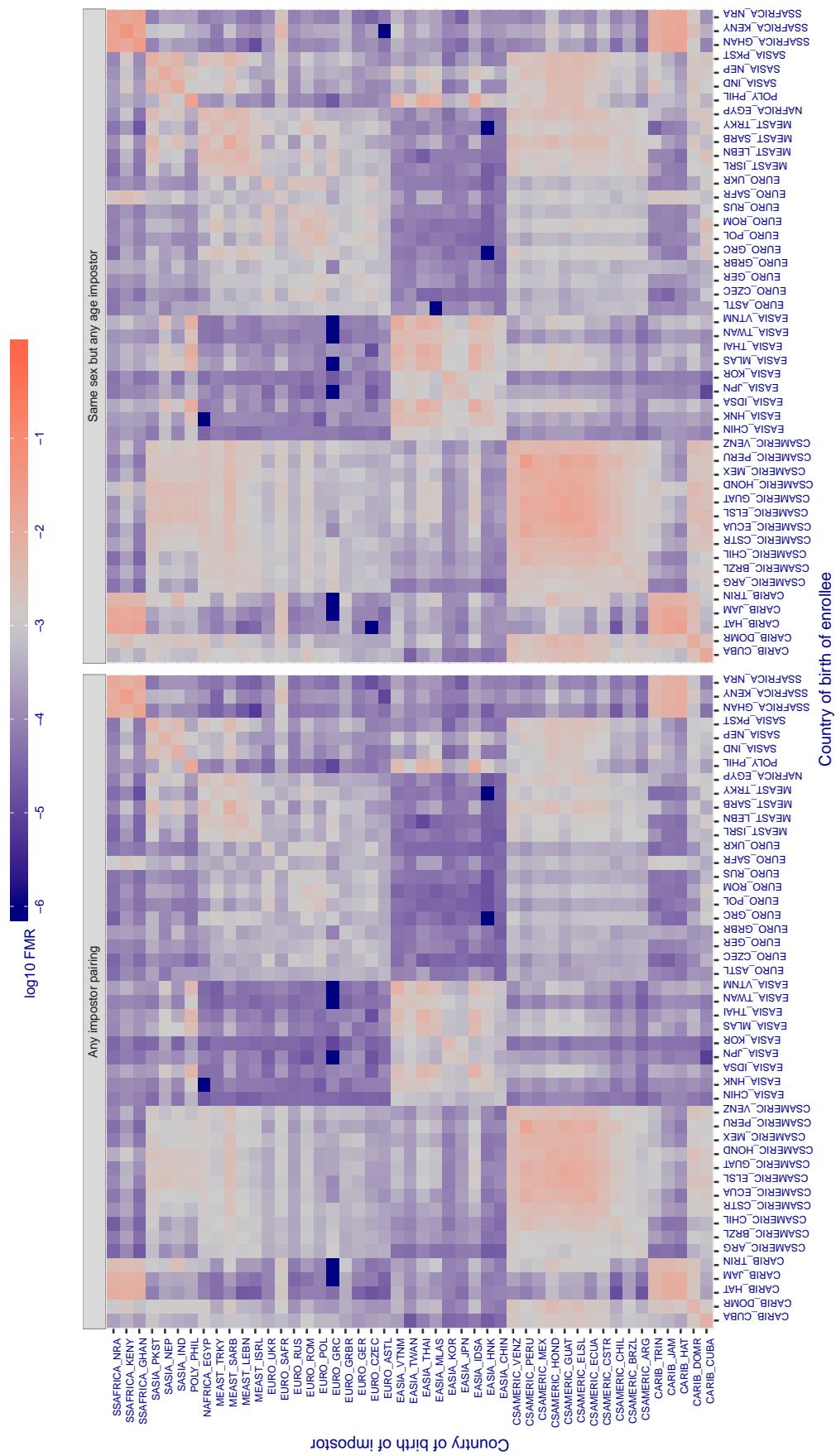
Cross country FMR at threshold T = 1.314 for algorithm incode_004, giving $FMR(T) = 0.001$ globally.

Figure 337: For algorithm incode-004 operating on visa images, the heatmap shows false match rates observed over impostor comparisons of faces from different individuals who were born in the given country pair. False matches are counted against a recognition threshold fixed globally to give the target FMR in the plot title, computed over all on the order of 10^{10} impostor comparisons. If text appears in each box it give the same quantity as that coded by the color. Grey indicates FMR is at the intended FMR target level. Light red colors present a security vulnerability to, for example, a passport gate. Each +1 increase in $\log_{10} FMR$ corresponds to a factor of 10 increase in FMR . The matrix is not quite symmetric because images in the enrollment and verification sets are different.

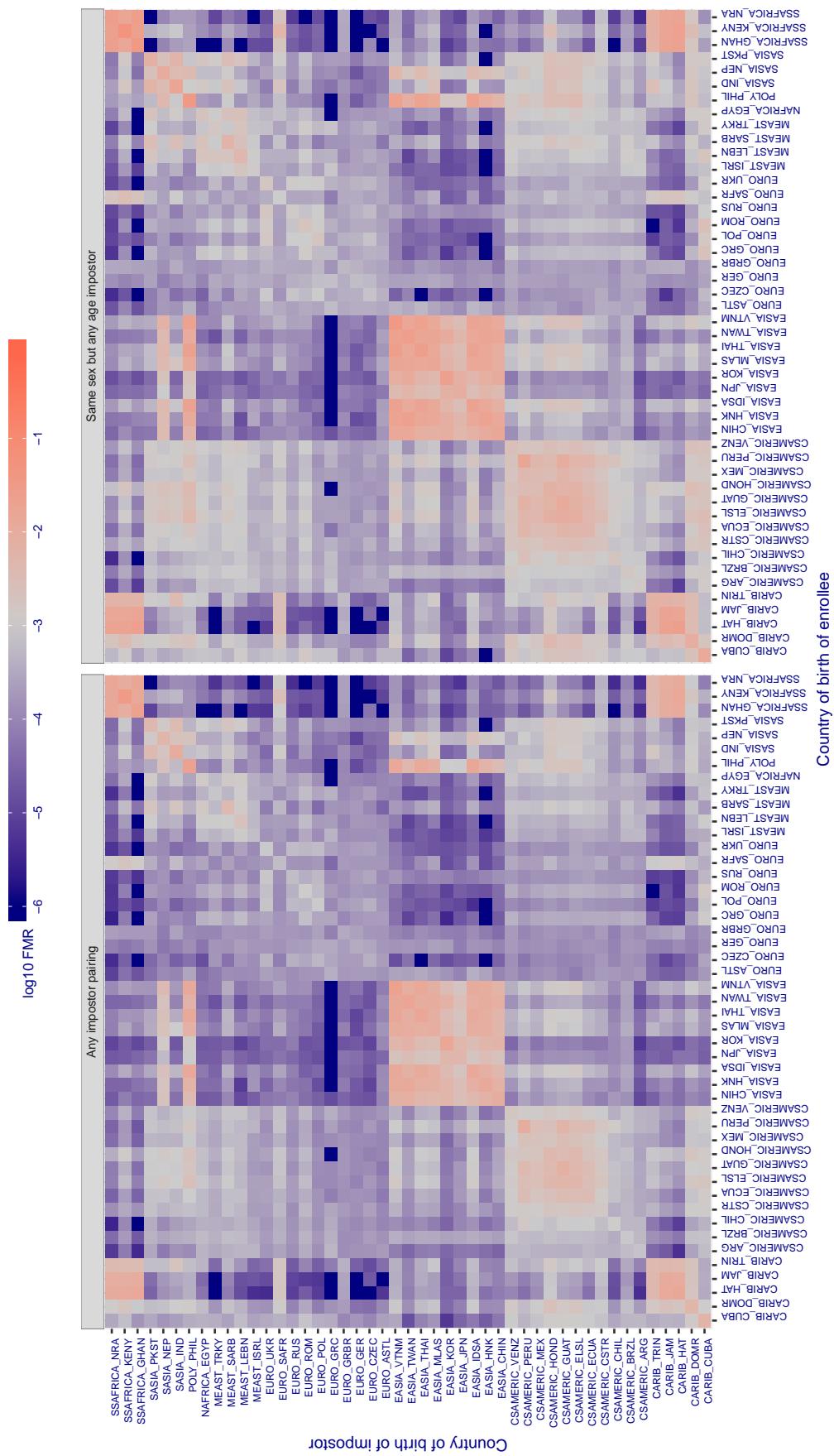
Cross country FMR at threshold T = 21.422 for algorithm innovatrics_004, giving $FMR(T) = 0.001$ globally.

Figure 338: For algorithm innovatrics-004 operating on visa images, the heatmap shows false match rates observed over impostor comparisons of faces from different individuals who were born in the given country pair. False matches are counted against a recognition threshold fixed globally to give the target FMR in the plot title, computed over all on the order of 10^{10} impostor comparisons. If text appears in each box it give the same quantity as that coded by the color. Grey indicates FMR is at the intended FMR target level. Light red colors present a security vulnerability to, for example, a passport gate. Each +1 increase in $\log_{10} FMR$ corresponds to a factor of 10 increase in FMR. The matrix is not quite symmetric because images in the enrollment and verification sets are different.

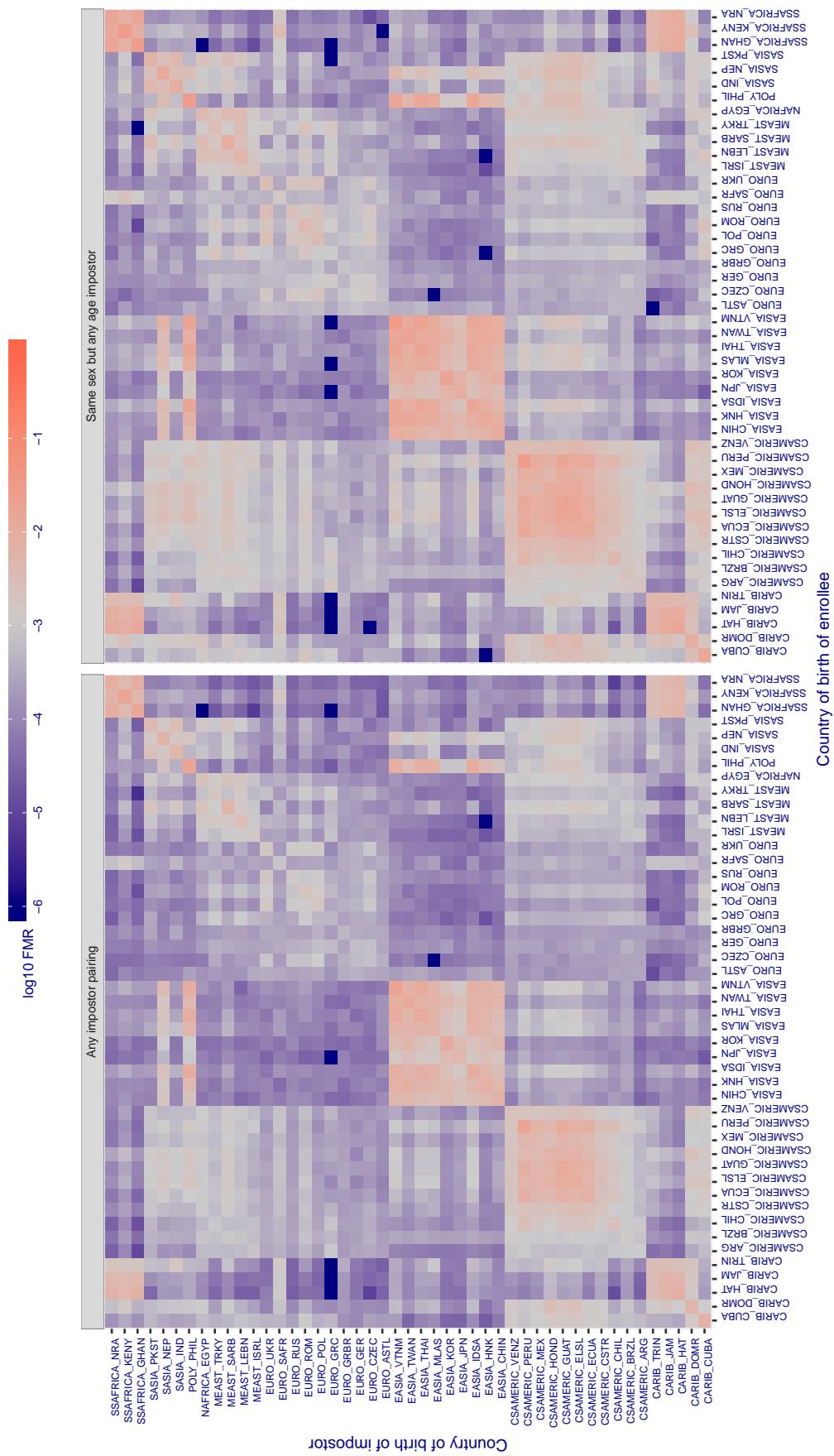
Cross country FMR at threshold T = 20.505 for algorithm innovatrics_006, giving FMR(T) = 0.001 globally.

Figure 339: For algorithm innovatrics-006 operating on visa images, the heatmap shows false match rates observed over impostor comparisons of faces from different individuals who were born in the given country pair. False matches are counted against a recognition threshold fixed globally to give the target FMR in the plot title, computed over all on the order of 10^{10} impostor comparisons. If text appears in each box it give the same quantity as that coded by the color. Grey indicates FMR is at the intended FMR target level. Light red colors present a security vulnerability to, for example, a passport gate. Each +1 increase in $\log_{10} \text{FMR}$ corresponds to a factor of 10 increase in FMR. The matrix is not quite symmetric because images in the enrollment and verification sets are different.

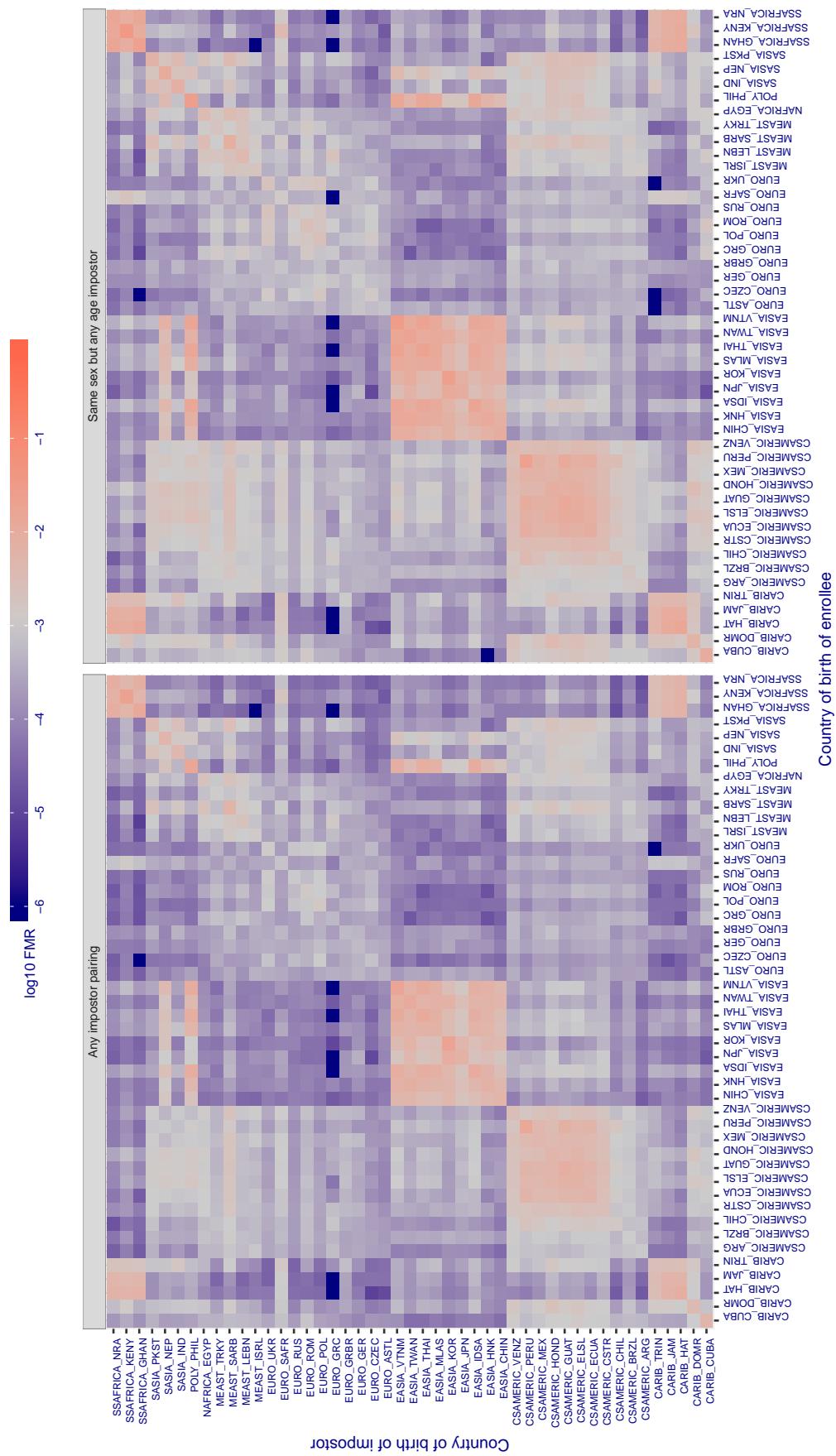
Cross country FMR at threshold T = 0.6662 for algorithm intellicloudai_001, giving FMR(T) = 0.001 globally.

Figure 340: For algorithm intellicloudai-001 operating on visa images, the heatmap shows false match rates observed over impostor comparisons of faces from different individuals who were born in the given country pair. False matches are counted against a recognition threshold fixed globally to give the target FMR in the plot title, computed over all on the order of 10^{10} impostor comparisons. If text appears in each box it give the same quantity as that coded by the color. Grey indicates FMR is at the intended FMR target level. Light red colors present a security vulnerability to, for example, a passport gate. Each +1 increase in $\log_{10} FMR$ corresponds to a factor of 10 increase in FMR. The matrix is not quite symmetric because images in the enrollment and verification sets are different.

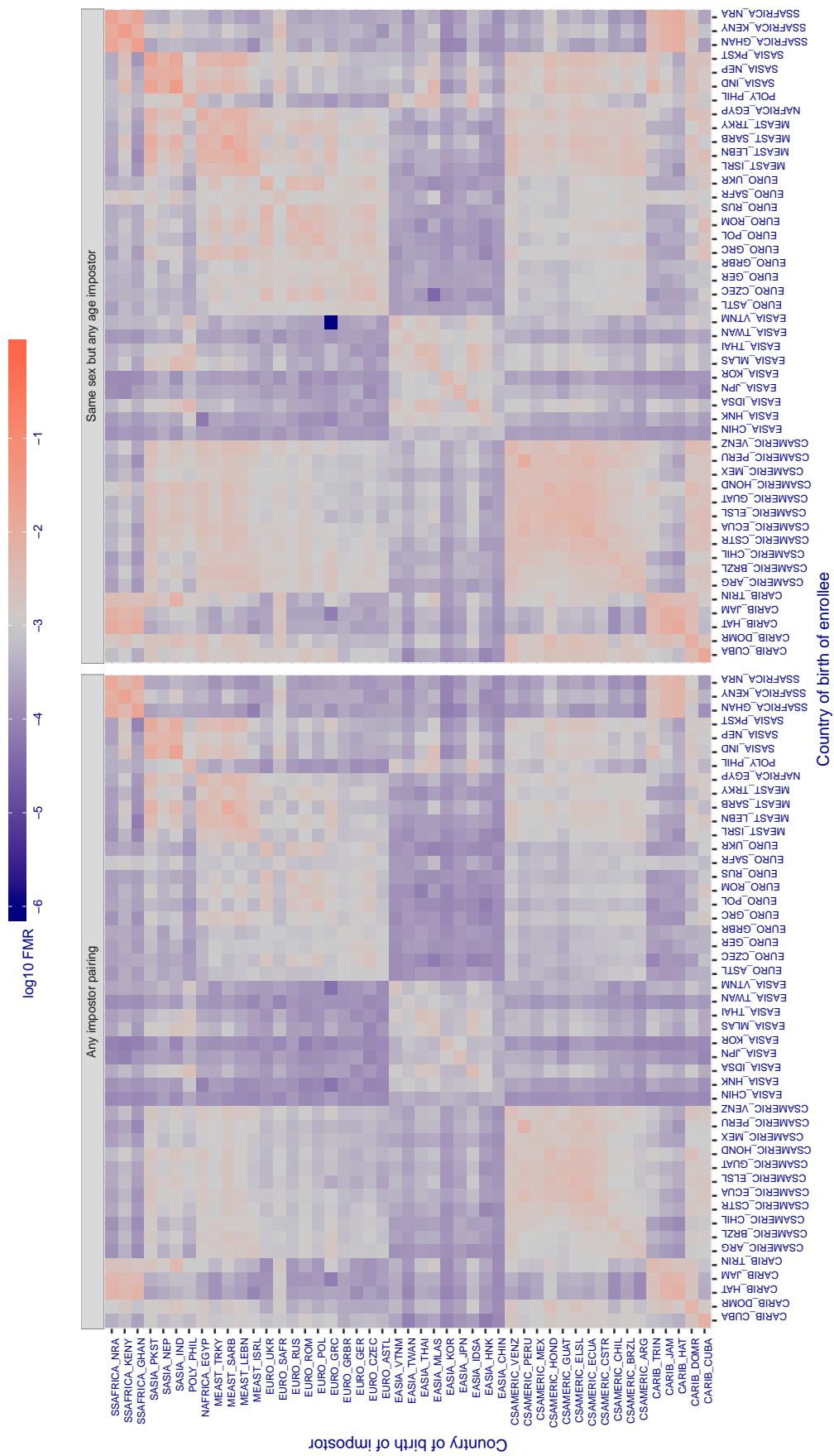
Cross country FMR at threshold T = 0.240 for algorithm intellifusion_001, giving $\text{FMR}(\text{T}) = 0.001$ globally.

Figure 341: For algorithm intellifusion-001 operating on visa images, the heatmap shows false match rates observed over impostor comparisons of faces from different individuals who were born in the given country pair. False matches are counted against a recognition threshold fixed globally to give the target FMR in the plot title, computed over all on the order of 10^{10} impostor comparisons. If text appears in each box it give the same quantity as that coded by the color. Grey indicates FMR is at the intended FMR target level. Light red colors present a security vulnerability to, for example, a passport gate. Each +1 increase in $\log_{10} \text{FMR}$ corresponds to a factor of 10 increase in FMR. The matrix is not quite symmetric because images in the enrollment and verification sets are different.

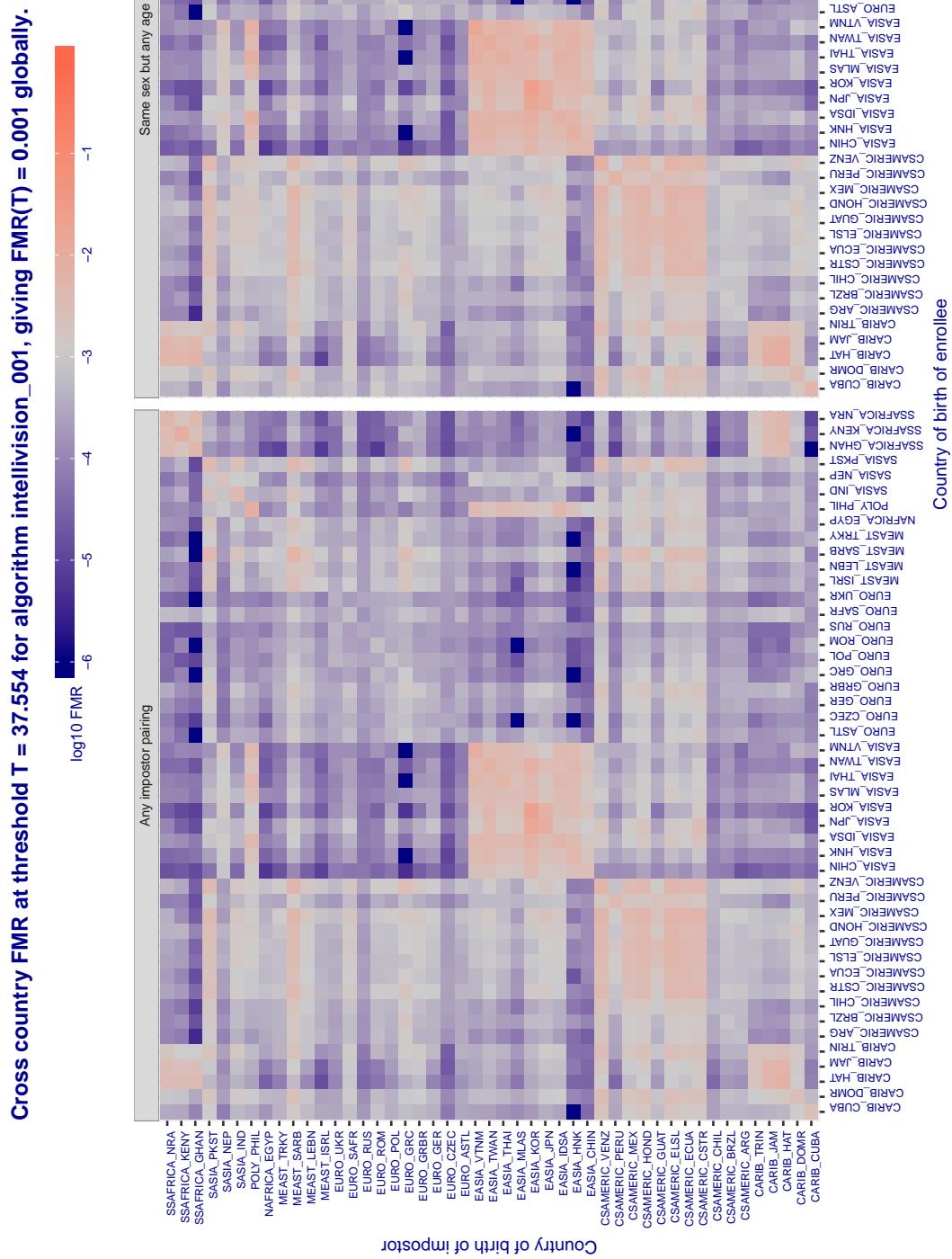


Figure 342: For algorithm intellivision-001 operating on visa images, the heatmap shows false match rates observed over impostor comparisons of faces from different individuals who were born in the given country pair. False matches are counted against a recognition threshold fixed globally to give the target FMR in the plot title, computed over all on the order of 10^{10} impostor comparisons. If text appears in each box it give the same quantity as that coded by the color. Grey indicates FMR is at the intended FMR target level. Light red colors present a security vulnerability to, for example, a passport gate. Each +1 increase in $\log_{10} \text{FMR}$ corresponds to a factor of 10 increase in FMR . The matrix is not quite symmetric because images in the enrollment and verification sets are different.

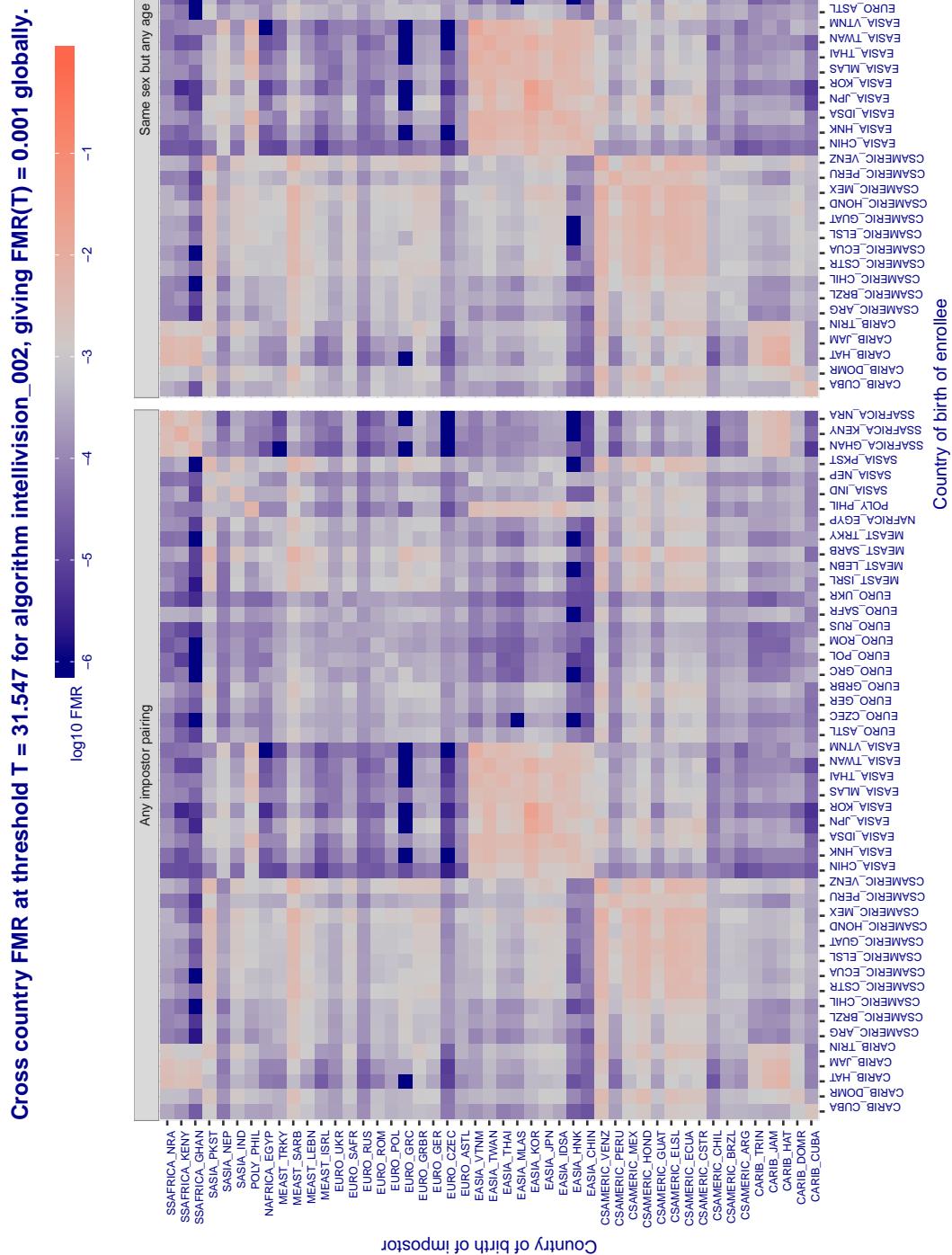


Figure 343: For algorithm intellivision-002 operating on visa images, the heatmap shows false match rates observed over impostor comparisons of faces from different individuals who were born in the given country pair. False matches are counted against a recognition threshold fixed globally to give the target FMR in the plot title, computed over all on the order of 10^{10} impostor comparisons. If text appears in each box it give the same quantity as that coded by the color. Grey indicates FMR is at the intended FMR target level. Light red colors present a security vulnerability to, for example, a passport gate. Each +1 increase in $\log_{10} \text{FMR}$ corresponds to a factor of 10 increase in FMR . The matrix is not quite symmetric because images in the enrollment and verification sets are different.

Cross country FMR at threshold T = 565.207 for algorithm intelresearch_000, giving $FMR(T) = 0.001$ globally.

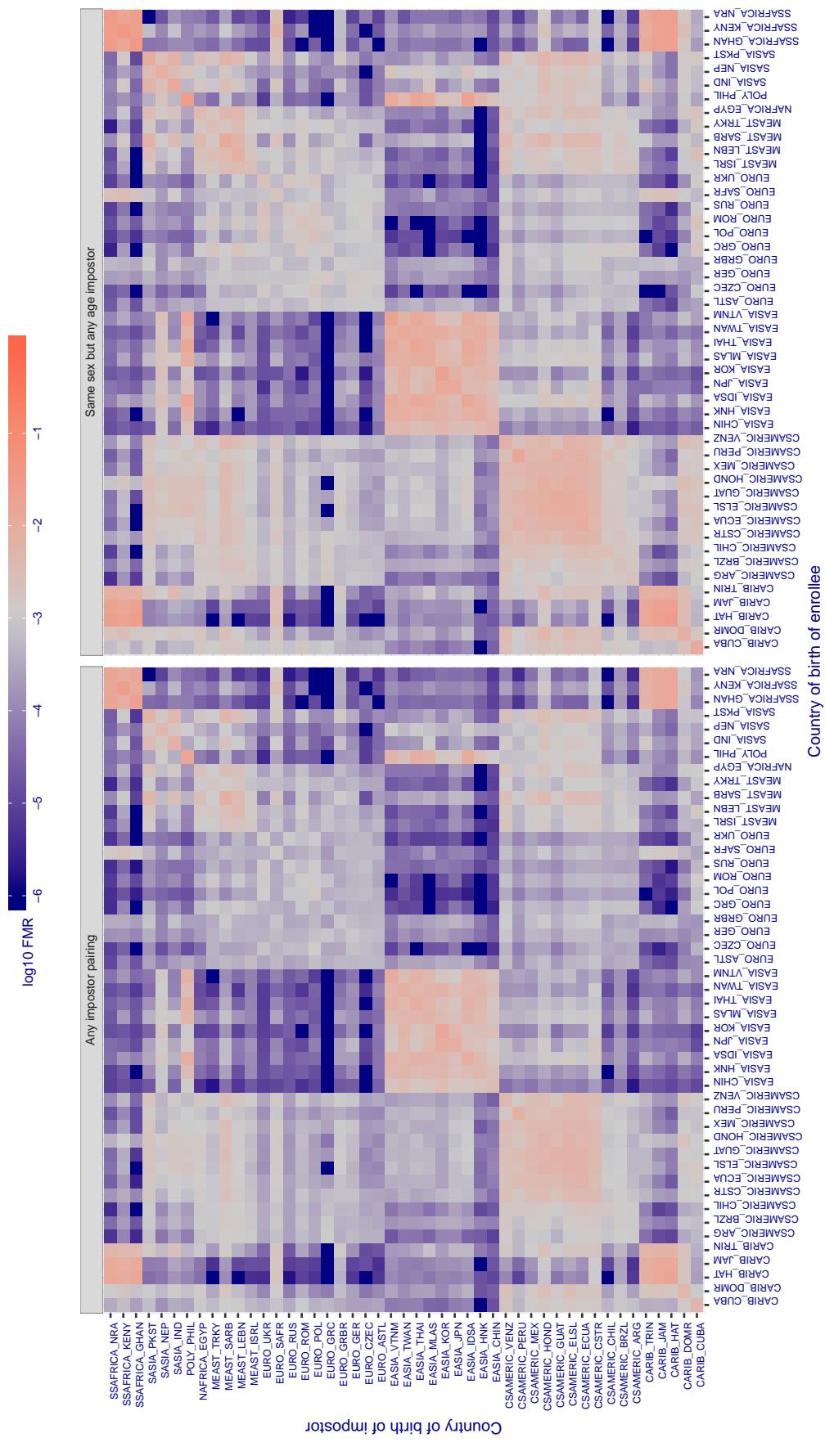


Figure 344: For algorithm intelresearch-000 operating on visa images, the heatmap shows false match rates observed over impostor comparisons of faces from different individuals who were born in the given country pair. False matches are counted against a recognition threshold fixed globally to give the target FMR in the plot title, computed over all on the order of 10^{10} impostor comparisons. If text appears in each box it give the same quantity as that coded by the color. Grey indicates FMR is at the intended FMR target level. Light red colors present a security vulnerability to, for example, a passport gate. Each +1 increase in $\log_{10} FMR$ corresponds to a factor of 10 increase in FMR . The matrix is not quite symmetric because images in the enrollment and verification sets are different.

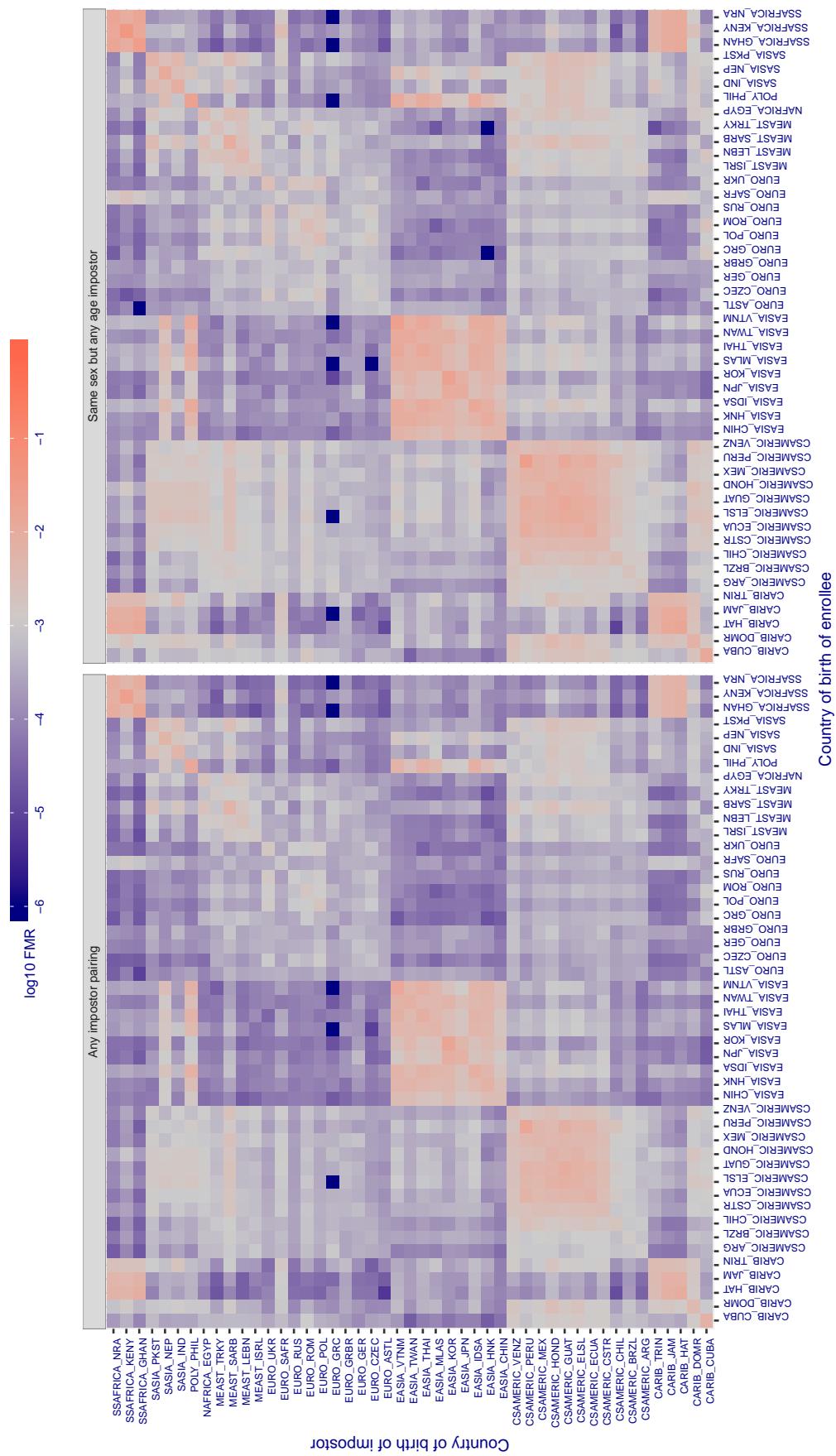
Cross country FMR at threshold T = 1.306 for algorithm intsysmsu_000, giving FMR(T) = 0.001 globally.

Figure 345: For algorithm intsysmsu-000 operating on visa images, the heatmap shows false match rates observed over impostor comparisons of faces from different individuals who were born in the given country pair. False matches are counted against a recognition threshold fixed globally to give the target FMR in the plot title, computed over all on the order of 10^{10} impostor comparisons. If text appears in each box it give the same quantity as that coded by the color. Grey indicates FMR is at the intended FMR target level. Light red colors present a security vulnerability to, for example, a passport gate. Each +1 increase in $\log_{10} FMR$ corresponds to a factor of 10 increase in FMR. The matrix is not quite symmetric because images in the enrollment and verification sets are different.

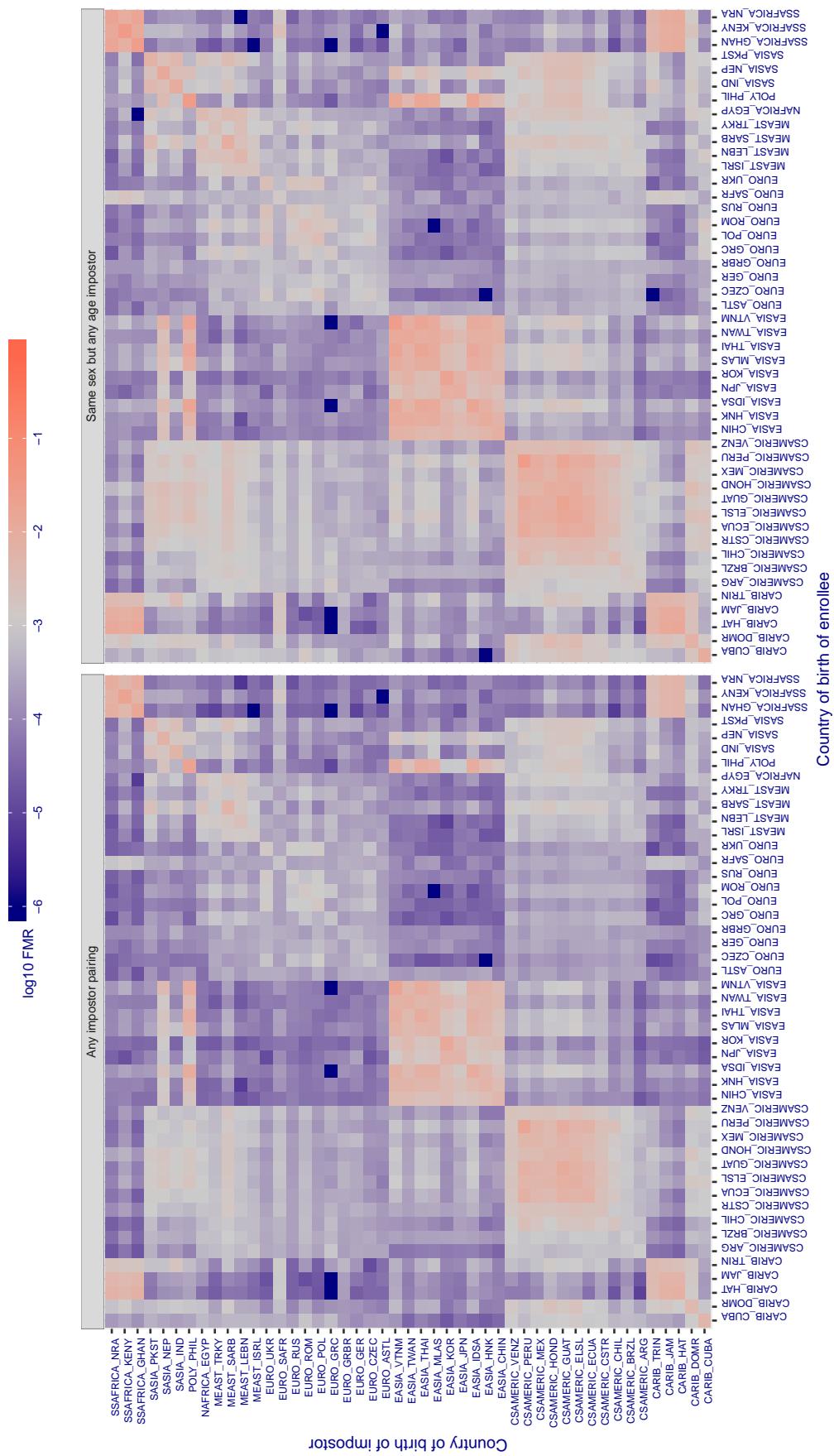
Cross country FMR at threshold T = 1.280 for algorithm iqface_000, giving FMR(T) = 0.001 globally.

Figure 346: For algorithm iqface-000 operating on visa images, the heatmap shows false match rates observed over impostor comparisons of faces from different individuals who were born in the given country pair. False matches are counted against a recognition threshold fixed globally to give the target FMR in the plot title, computed over all on the order of 10^{10} impostor comparisons. If text appears in each box it give the same quantity as that coded by the color. Grey indicates FMR is at the intended FMR target level. Light red colors present a security vulnerability to, for example, a passport gate. Each +1 increase in $\log_{10} \text{FMR}$ corresponds to a factor of 10 increase in FMR. The matrix is not quite symmetric because images in the enrollment and verification sets are different.

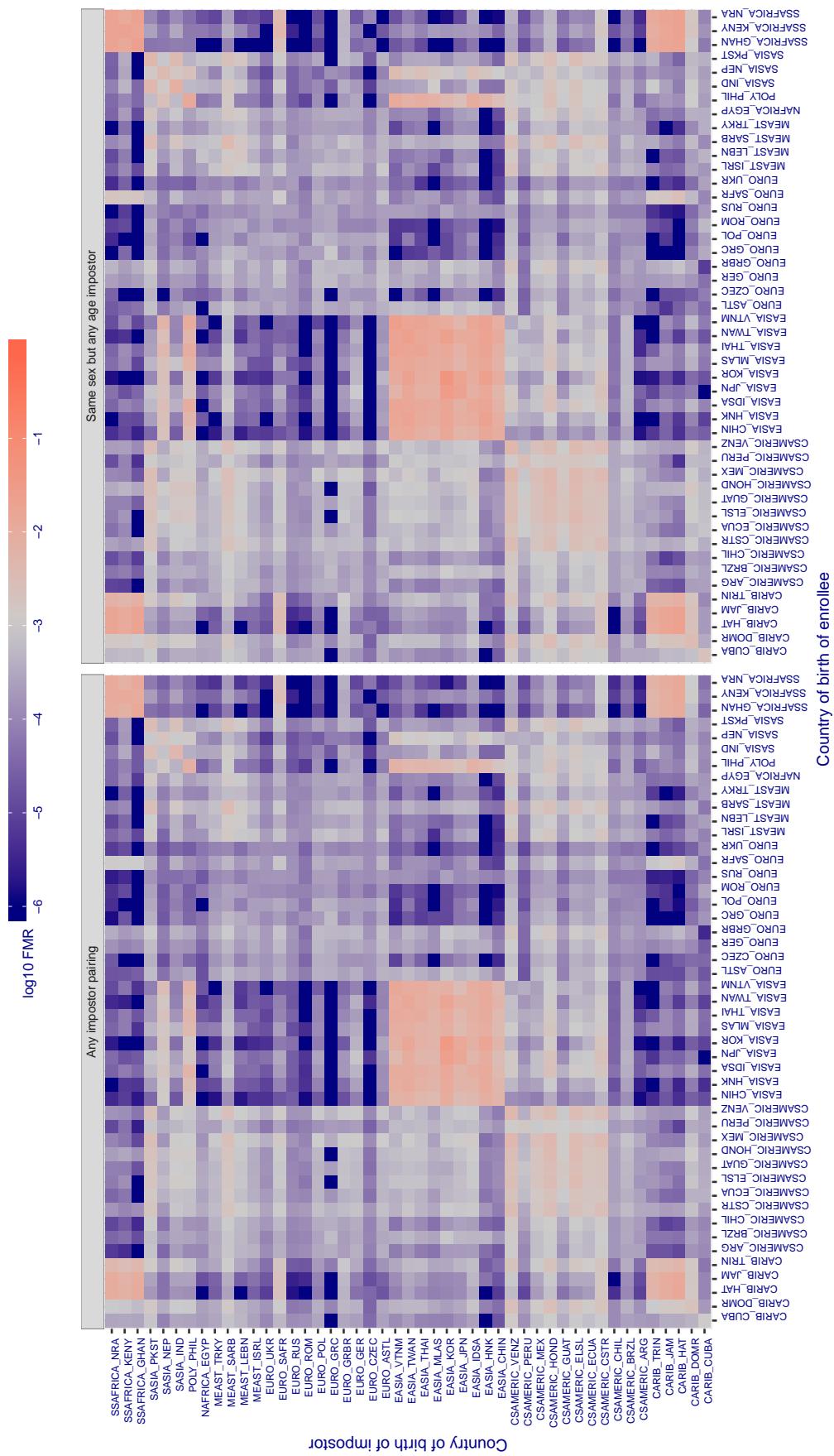
Cross country FMR at threshold T = 0.982 for algorithm isap_001, giving FMR(T) = 0.001 globally.

Figure 347: For algorithm isap-001 operating on visa images, the heatmap shows false match rates observed over impostor comparisons of faces from different individuals who were born in the given country pair. False matches are counted against a recognition threshold fixed globally to give the target FMR in the plot title, computed over all on the order of 10^{10} impostor comparisons. If text appears in each box it give the same quantity as that coded by the color. Grey indicates FMR is at the intended FMR target level. Light red colors present a security vulnerability to, for example, a passport gate. Each +1 increase in $\log_{10} \text{FMR}$ corresponds to a factor of 10 increase in FMR. The matrix is not quite symmetric because images in the enrollment and verification sets are different.

Cross country FMR at threshold T = 20.648 for algorithm isityou_000, giving FMR(T) = 0.001 globally.

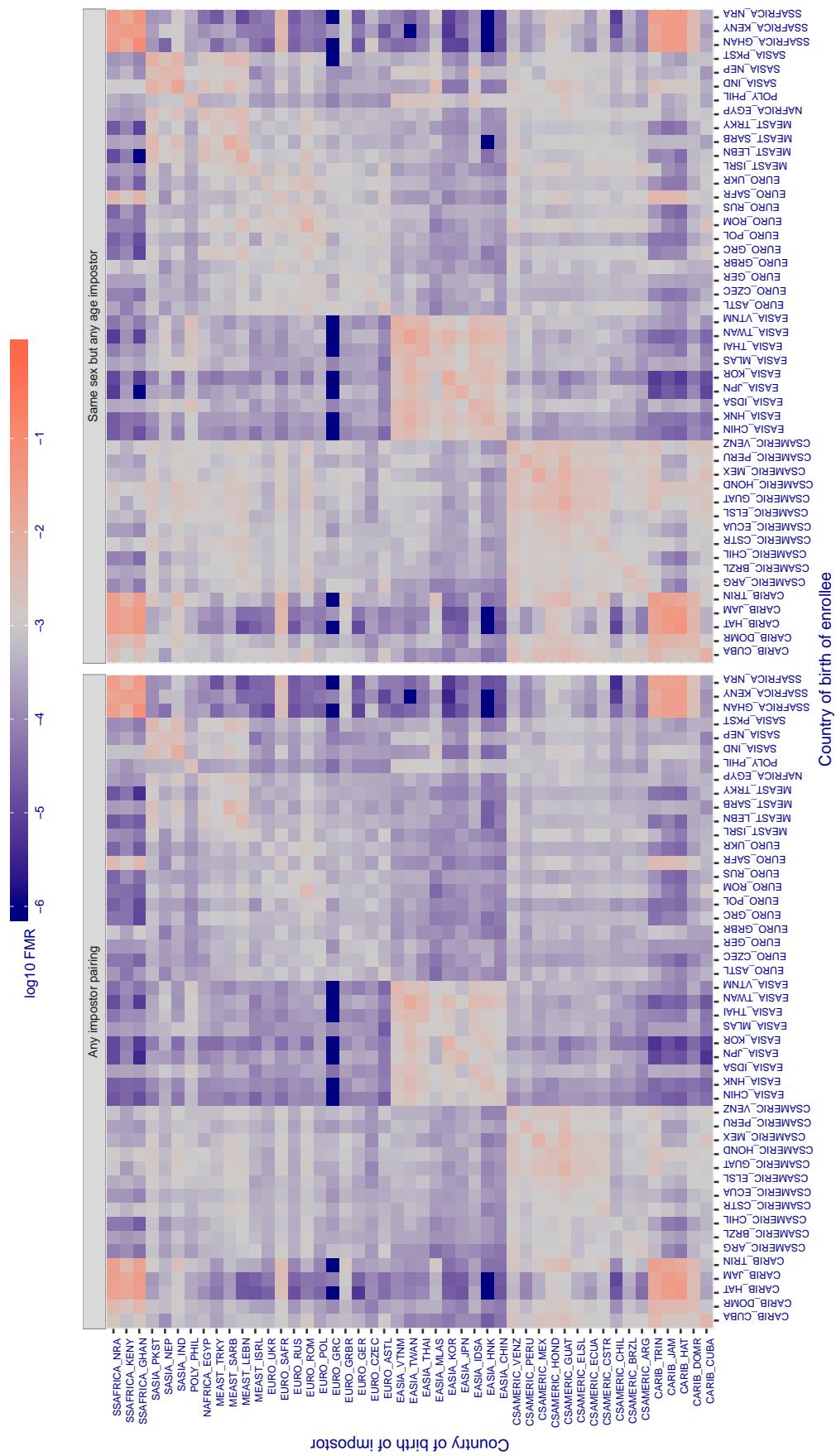


Figure 348: For algorithm isityou-000 operating on visa images, the heatmap shows false match rates observed over impostor comparisons of faces from different individuals who were born in the given country pair. False matches are counted against a recognition threshold fixed globally to give the target FMR in the plot title, computed over all on the order of 10^{10} impostor comparisons. If text appears in each box it give the same quantity as that coded by the color. Grey indicates FMR is at the intended FMR target level. Light red colors present a security vulnerability to, for example, a passport gate. Each +1 increase in $\log_{10} FMR$ corresponds to a factor of 10 increase in FMR. The matrix is not quite symmetric because images in the enrollment and verification sets are different.

Cross country FMR at threshold T = 0.649 for algorithm systems_001, giving FMR(T) = 0.001 globally.

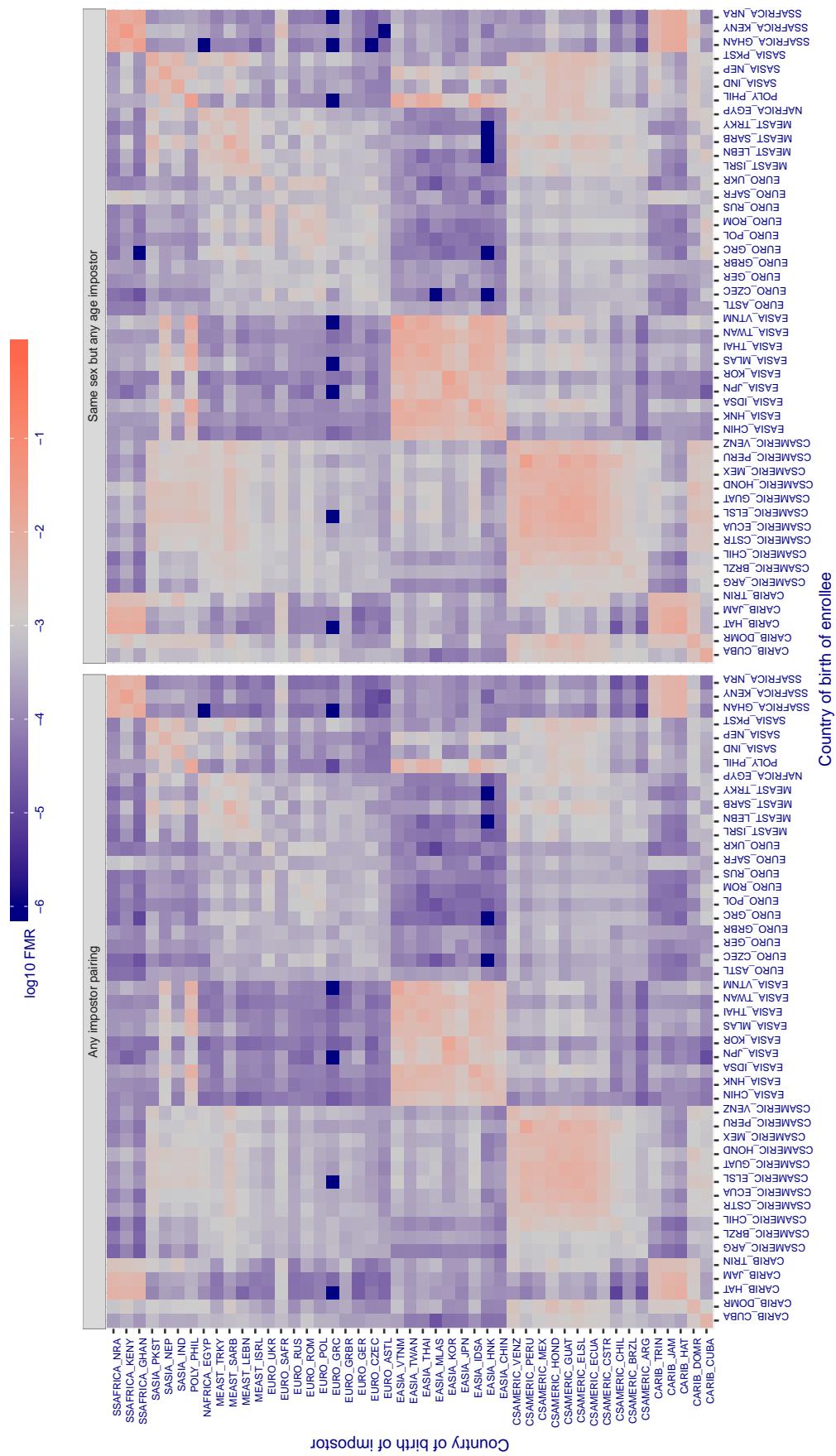


Figure 349: For algorithm systems-001 operating on visa images, the heatmap shows false match rates observed over impostor comparisons of faces from different individuals who were born in the given country pair. False matches are counted against a recognition threshold fixed globally to give the target FMR in the plot title, computed over all on the order of 10^{10} impostor comparisons. If text appears in each box it give the same quantity as that coded by the color. Grey indicates FMR is at the intended FMR target level. Light red colors present a security vulnerability to, for example, a passport gate. Each +1 increase in $\log_{10} FMR$ corresponds to a factor of 10 increase in FMR. The matrix is not quite symmetric because images in the enrollment and verification sets are different.

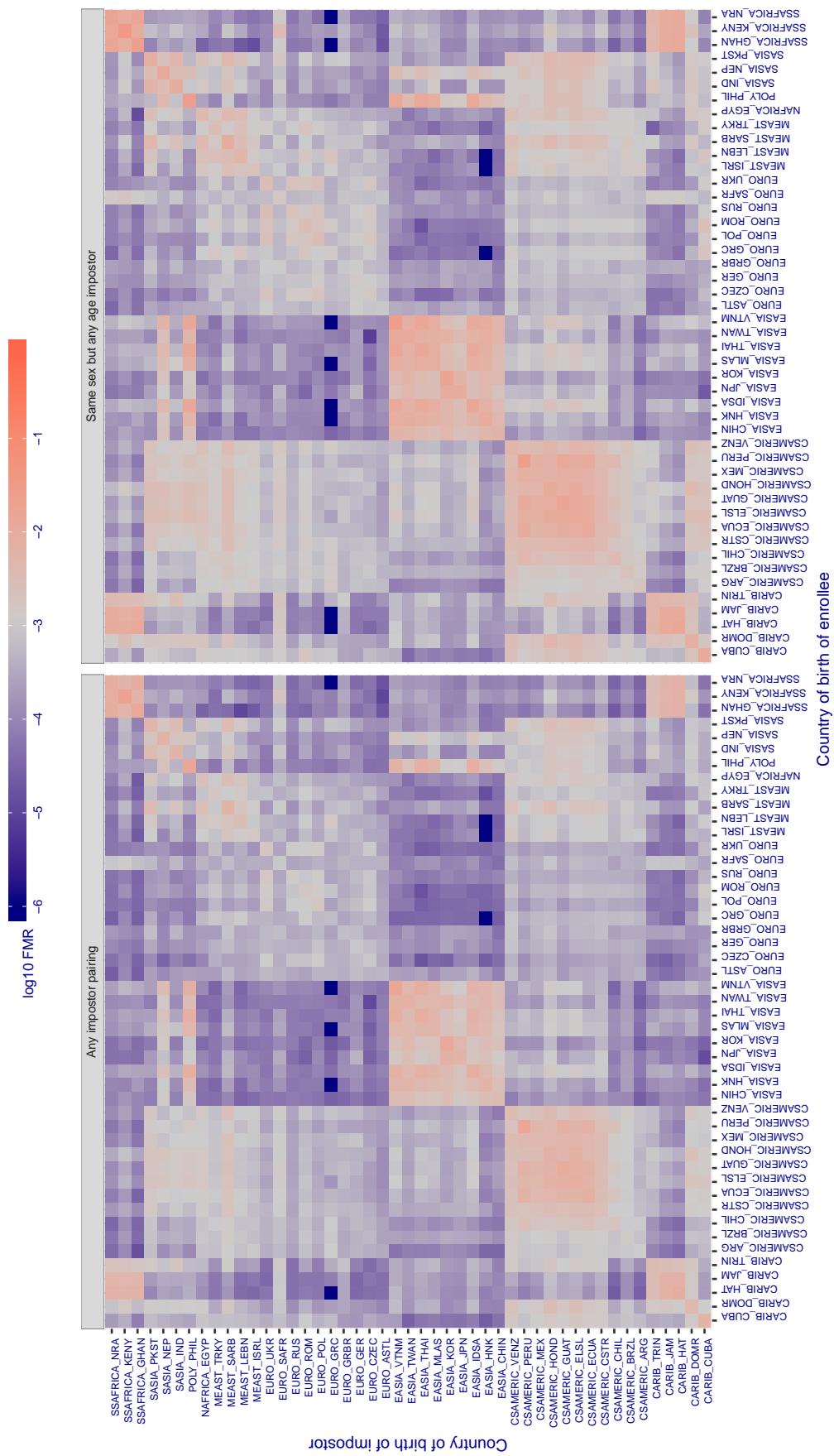
Cross country FMR at threshold T = 0.647 for algorithm systems_002, giving FMR(T) = 0.001 globally.

Figure 350: For algorithm systems-002 operating on visa images, the heatmap shows false match rates observed over impostor comparisons of faces from different individuals who were born in the given country pair. False matches are counted against a recognition threshold fixed globally to give the target FMR in the plot title, computed over all on the order of 10^{10} impostor comparisons. If text appears in each box it give the same quantity as that coded by the color. Grey indicates FMR is at the intended FMR target level. Light red colors present a security vulnerability to, for example, a passport gate. Each +1 increase in $\log_{10} FMR$ corresponds to a factor of 10 increase in FMR. The matrix is not quite symmetric because images in the enrollment and verification sets are different.

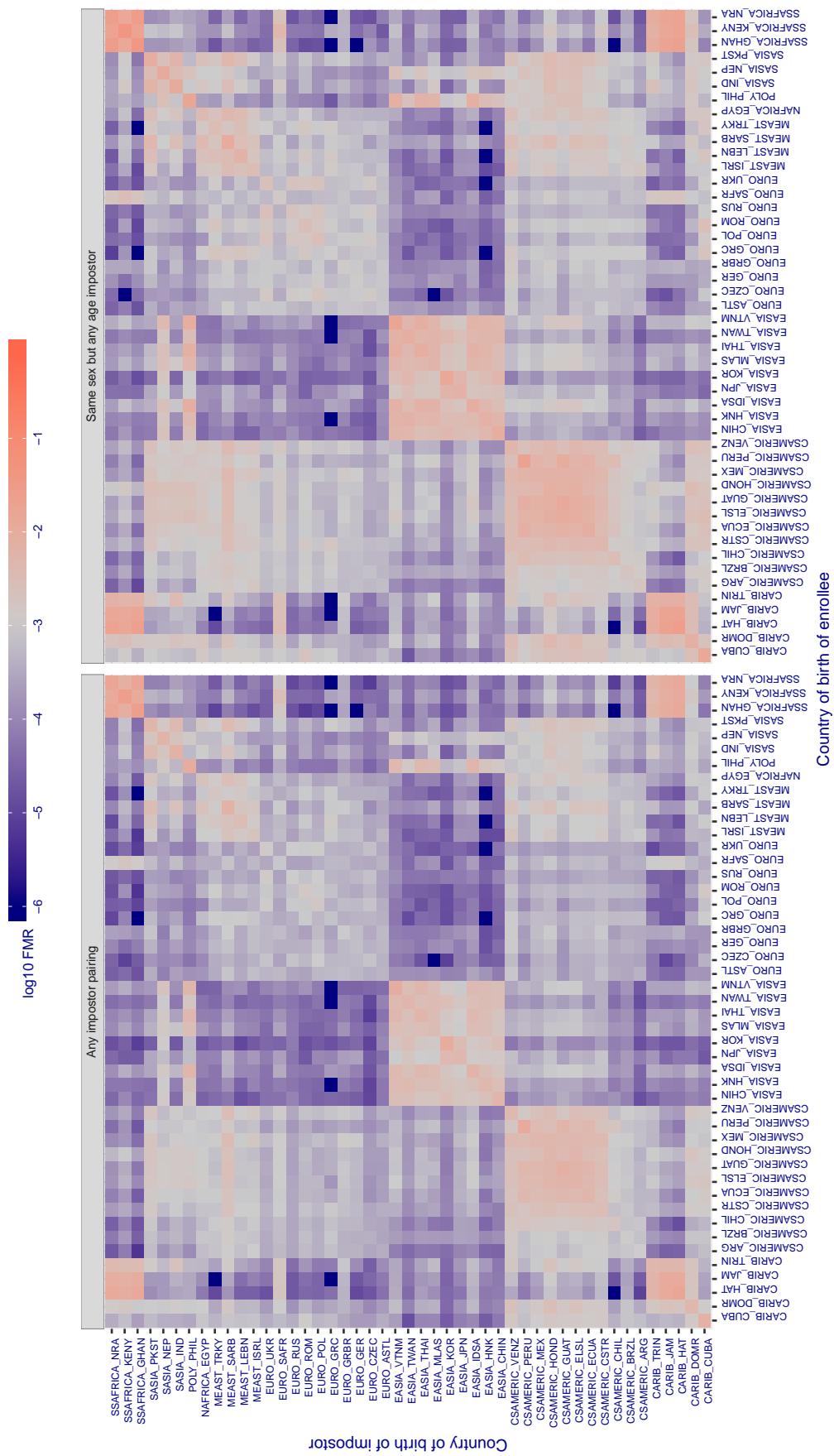
Cross country FMR at threshold T = 10.316 for algorithm itmo_005, giving FMR(T) = 0.001 globally.

Figure 351: For algorithm itmo-005 operating on visa images, the heatmap shows false match rates observed over impostor comparisons of faces from different individuals who were born in the given country pair. False matches are counted against a recognition threshold fixed globally to give the target FMR in the plot title, computed over all on the order of 10^{10} impostor comparisons. If text appears in each box it give the same quantity as that coded by the color. Grey indicates FMR is at the intended FMR target level. Light red colors present a security vulnerability to, for example, a passport gate. Each +1 increase in $\log_{10} \text{FMR}$ corresponds to a factor of 10 increase in FMR. The matrix is not quite symmetric because images in the enrollment and verification sets are different.

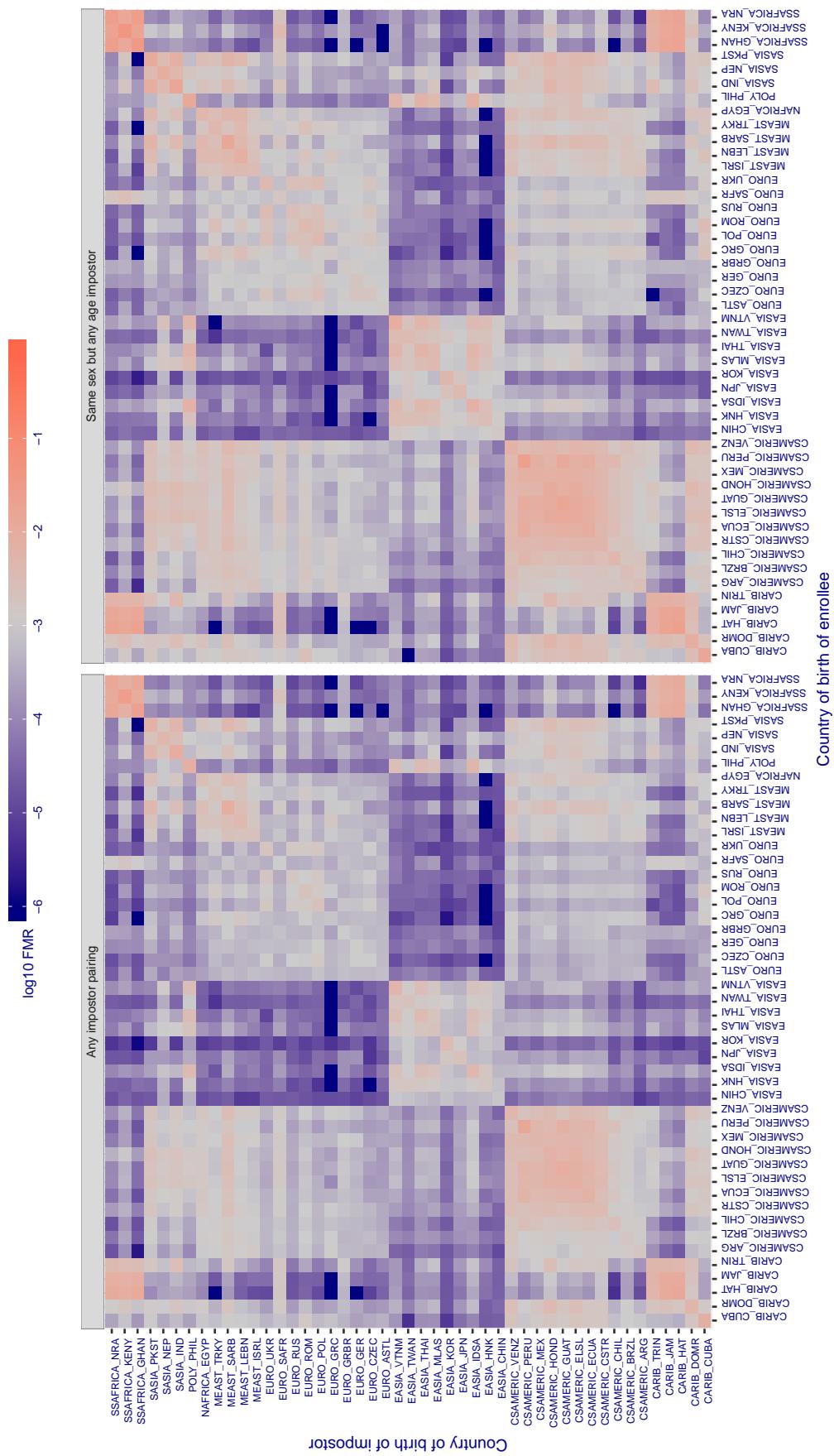
Cross country FMR at threshold T = 12.030 for algorithm itmo_006, giving FMR(T) = 0.001 globally.

Figure 352: For algorithm itmo-006 operating on visa images, the heatmap shows false match rates observed over impostor comparisons of faces from different individuals who were born in the given country pair. False matches are counted against a recognition threshold fixed globally to give the target FMR in the plot title, computed over all on the order of 10^{10} impostor comparisons. If text appears in each box it give the same quantity as that coded by the color. Grey indicates FMR is at the intended FMR target level. Light red colors present a security vulnerability to, for example, a passport gate. Each +1 increase in $\log_{10} \text{FMR}$ corresponds to a factor of 10 increase in FMR. The matrix is not quite symmetric because images in the enrollment and verification sets are different.

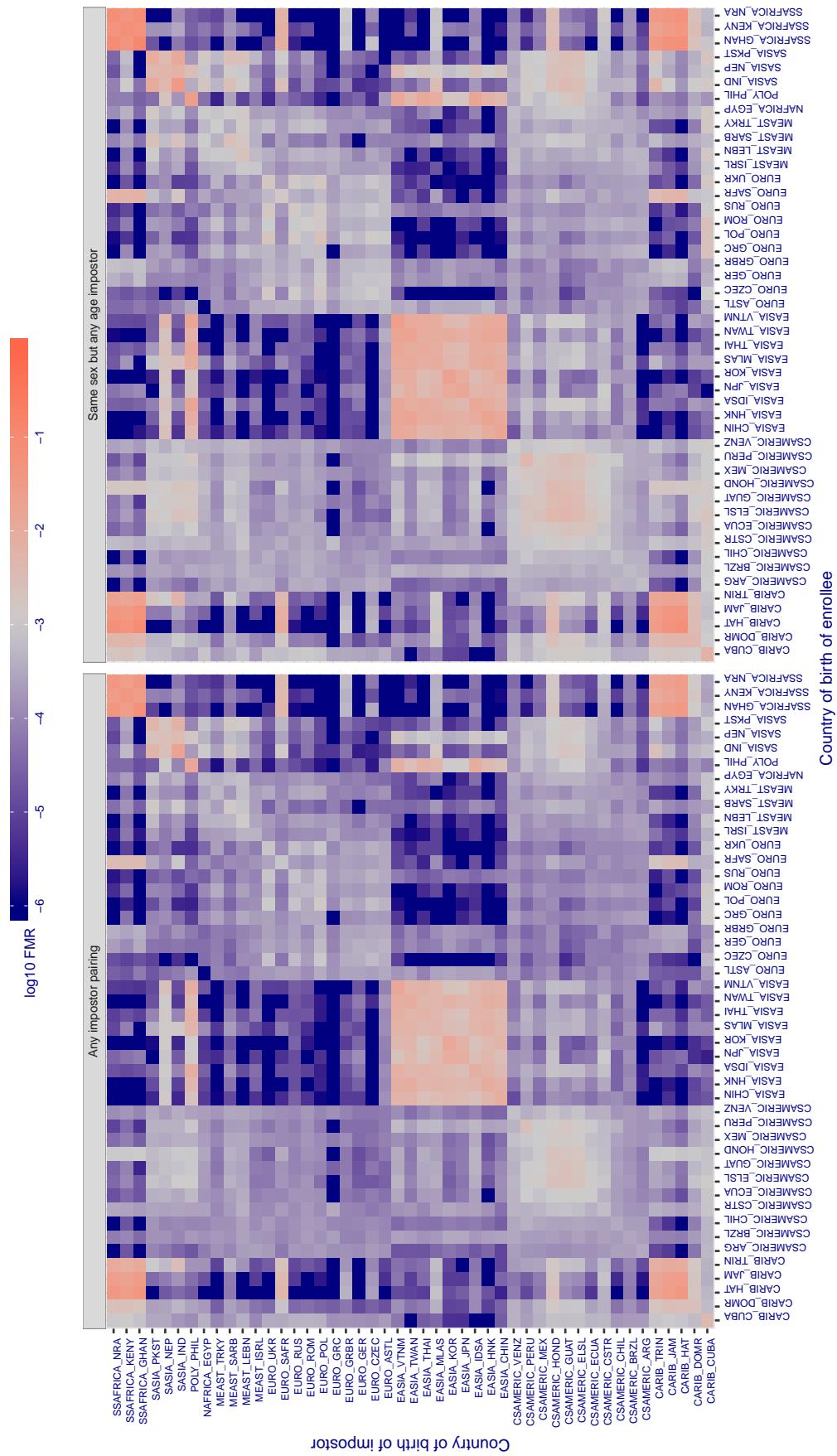
Cross country FMR at threshold T = 1.192 for algorithm kakao_001, giving $\text{FMR}(\text{T}) = 0.001$ globally.

Figure 353: For algorithm kakao-001 operating on visa images, the heatmap shows false match rates observed over impostor comparisons of faces from different individuals who were born in the given country pair. False matches are counted against a recognition threshold fixed globally to give the target FMR in the plot title, computed over all on the order of 10^{10} impostor comparisons. If text appears in each box it give the same quantity as that coded by the color. Grey indicates FMR is at the intended FMR target level. Light red colors present a security vulnerability to, for example, a passport gate. Each +1 increase in $\log_{10} \text{FMR}$ corresponds to a factor of 10 increase in FMR . The matrix is not quite symmetric because images in the enrollment and verification sets are different.

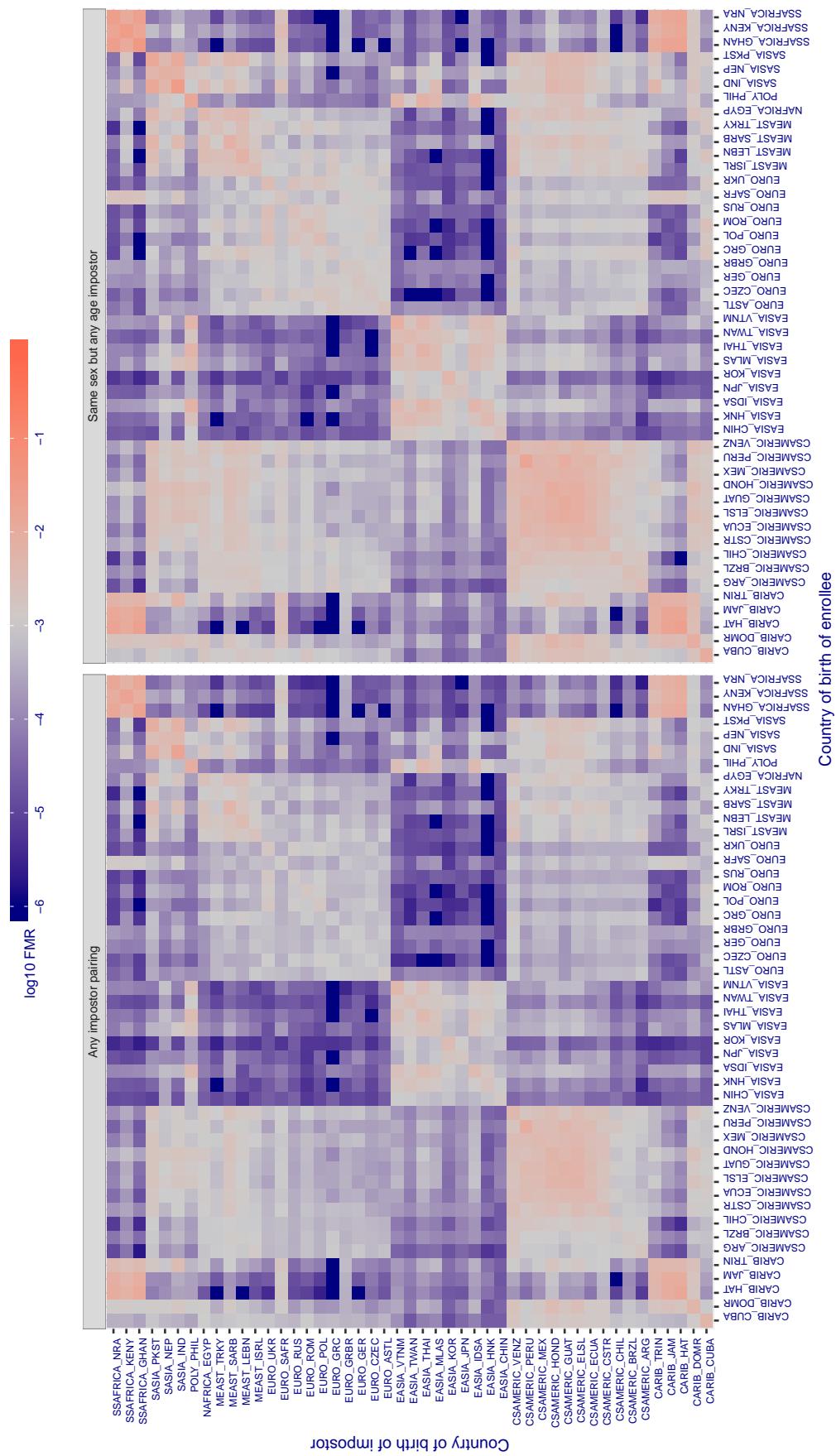
Cross country FMR at threshold T = 0.854 for algorithm kakao_002, giving $FMR(T) = 0.001$ globally.

Figure 354: For algorithm kakao-002 operating on visa images, the heatmap shows false match rates observed over impostor comparisons of faces from different individuals who were born in the given country pair. False matches are counted against a recognition threshold fixed globally to give the target FMR in the plot title, computed over all on the order of 10^{10} impostor comparisons. If text appears in each box it give the same quantity as that coded by the color. Grey indicates FMR is at the intended FMR target level. Light red colors present a security vulnerability to, for example, a passport gate. Each +1 increase in $\log_{10} FMR$ corresponds to a factor of 10 increase in FMR . The matrix is not quite symmetric because images in the enrollment and verification sets are different.

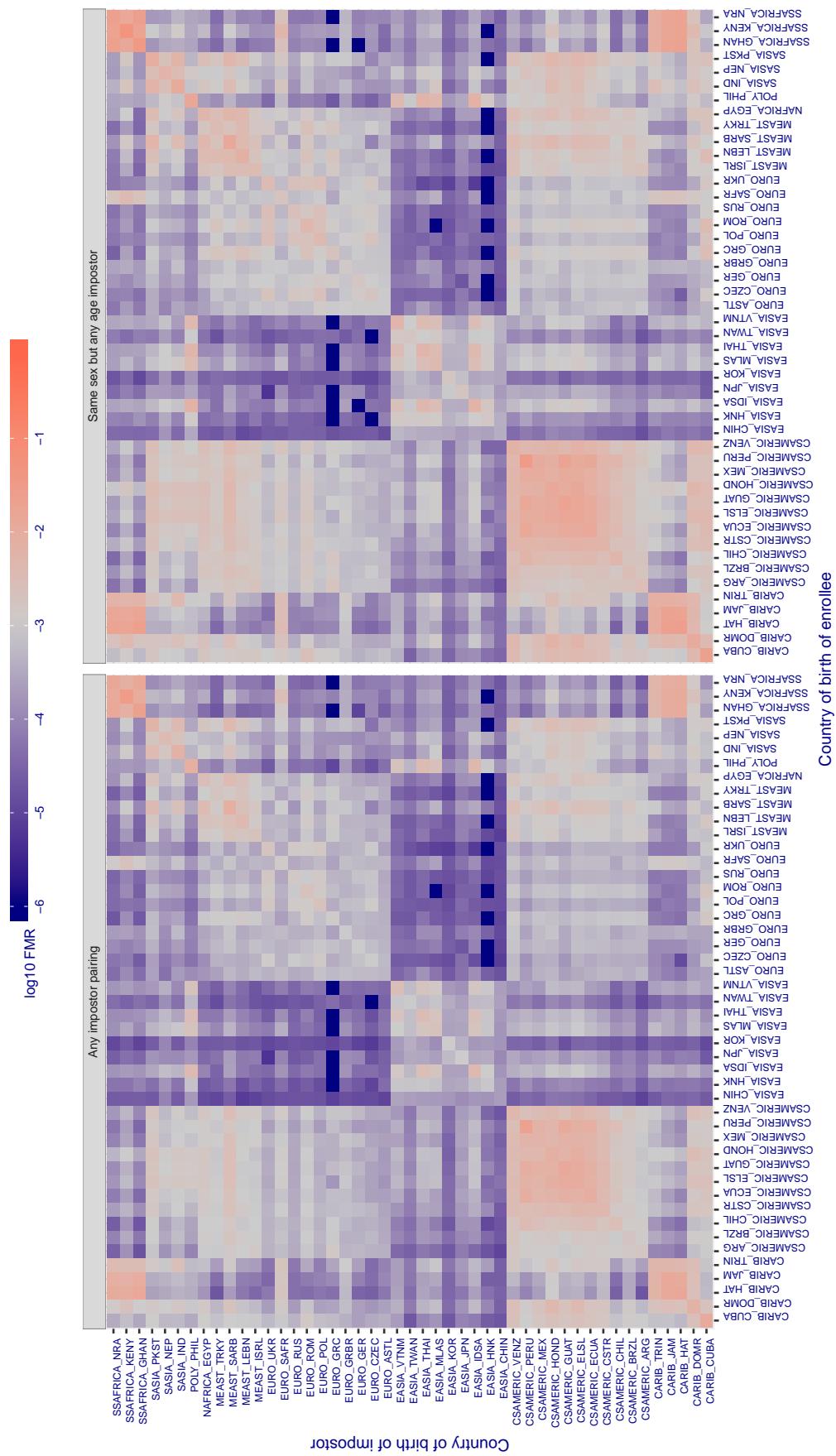
Cross country FMR at threshold T = 0.650 for algorithm kedacom_000, giving $FMR(T) = 0.001$ globally.

Figure 355: For algorithm kedacom-000 operating on visa images, the heatmap shows false match rates observed over impostor comparisons of faces from different individuals who were born in the given country pair. False matches are counted against a recognition threshold fixed globally to give the target FMR in the plot title, computed over all on the order of 10^{10} impostor comparisons. If text appears in each box it give the same quantity as that coded by the color. Grey indicates FMR is at the intended FMR target level. Light red colors present a security vulnerability to, for example, a passport gate. Each +1 increase in $\log_{10} FMR$ corresponds to a factor of 10 increase in FMR . The matrix is not quite symmetric because images in the enrollment and verification sets are different.

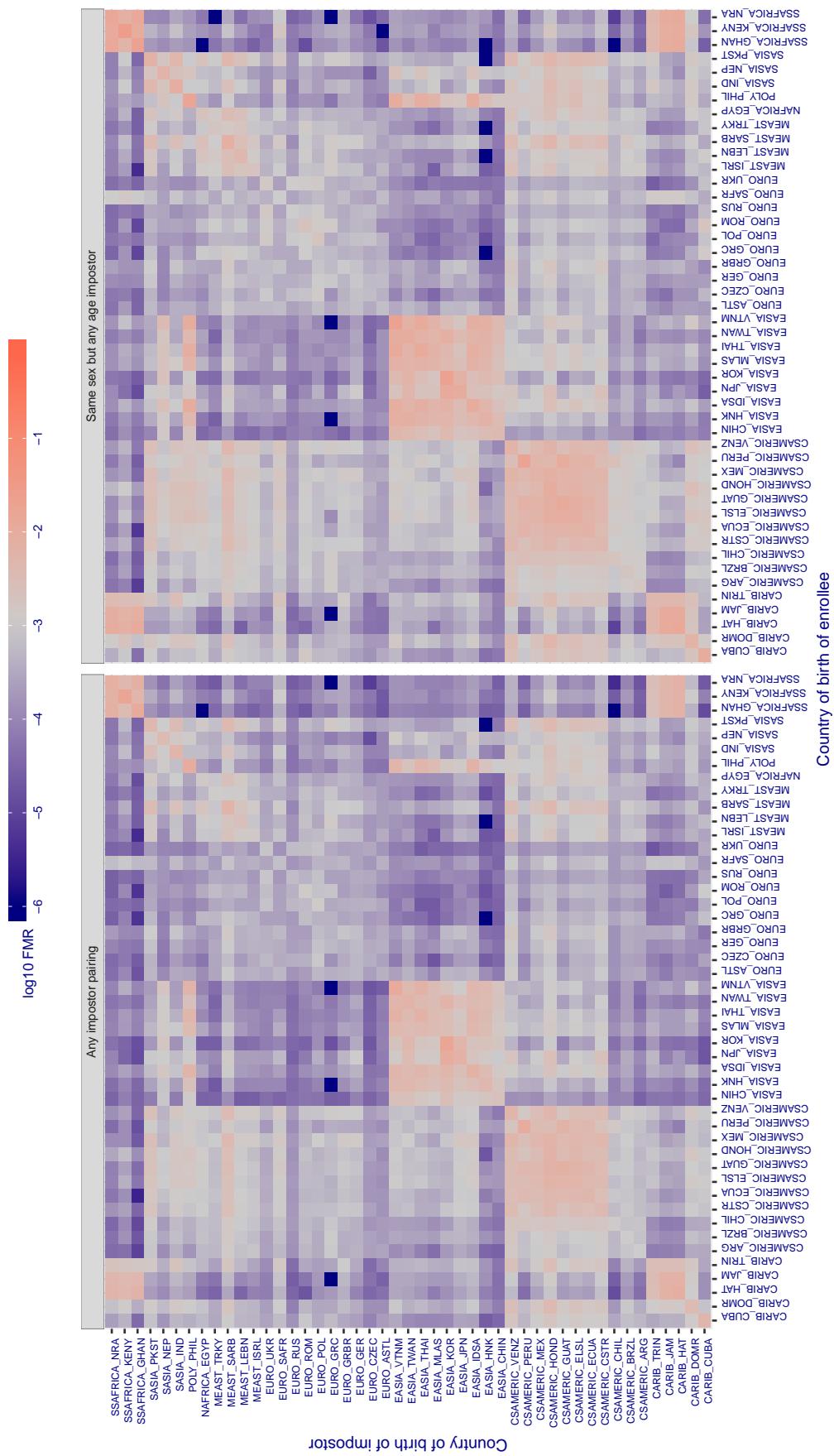
Cross country FMR at threshold T = 0.397 for algorithm kneron_003, giving $\text{FMR}(\text{T}) = 0.001$ globally.

Figure 356: For algorithm kneron-003 operating on visa images, the heatmap shows false match rates observed over impostor comparisons of faces from different individuals who were born in the given country pair. False matches are counted against a recognition threshold fixed globally to give the target FMR in the plot title, computed over all on the order of 10^{10} impostor comparisons. If text appears in each box it give the same quantity as that coded by the color. Grey indicates FMR is at the intended FMR target level. Light red colors present a security vulnerability to, for example, a passport gate. Each +1 increase in $\log_{10} \text{FMR}$ corresponds to a factor of 10 increase in FMR . The matrix is not quite symmetric because images in the enrollment and verification sets are different.

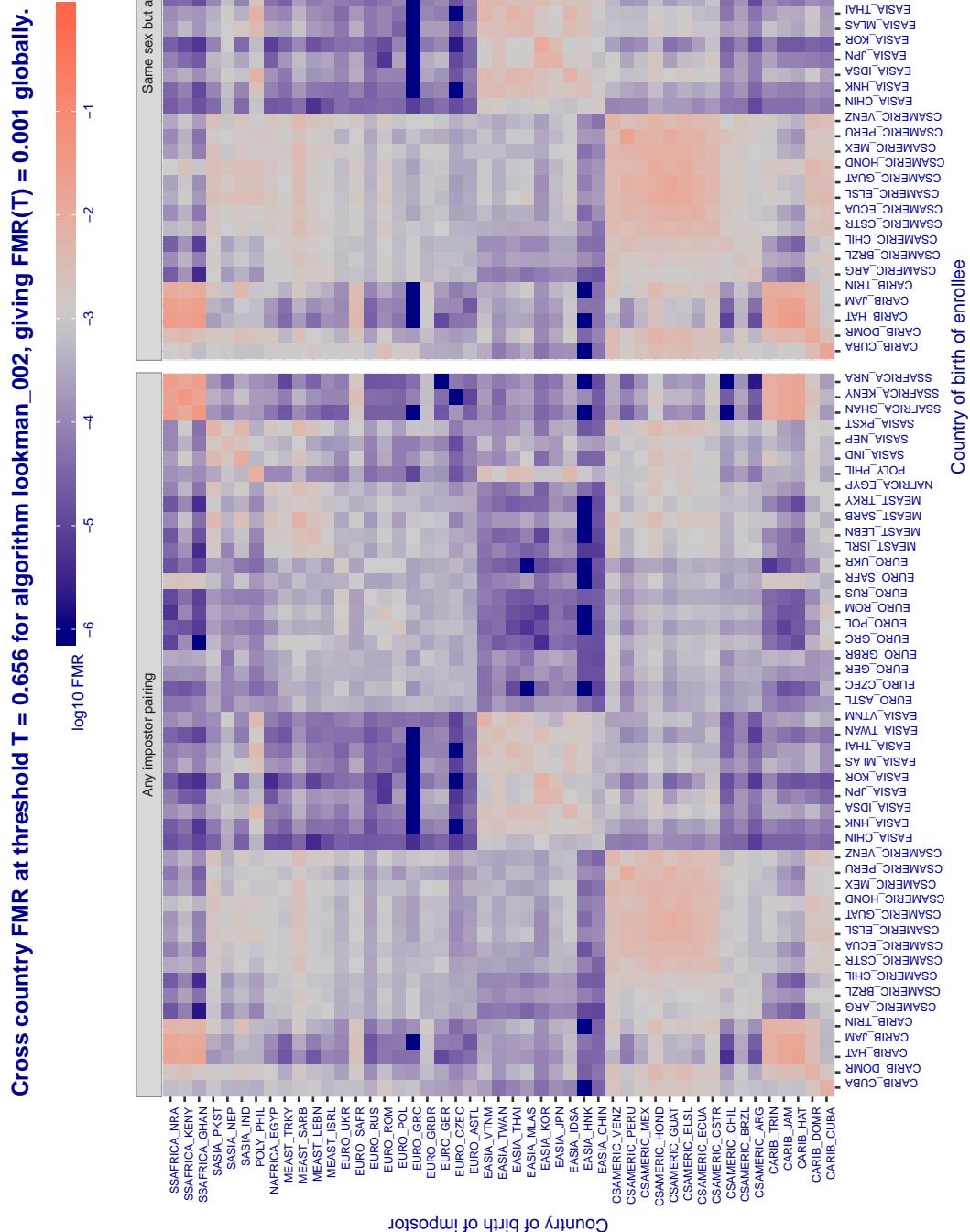


Figure 357: For algorithm lookman-002 operating on visa images, the heatmap shows false match rates observed over impostor comparisons of faces from different individuals who were born in the given country pair. False matches are counted against a recognition threshold fixed globally to give the target FMR in the plot title, computed over all on the order of 10^{10} impostor comparisons. If text appears in each box it give the same quantity as that coded by the color. Grey indicates FMR is at the intended FMR target level. Light red colors present a security vulnerability to, for example, a passport gate. Each +1 increase in $\log_{10} \text{FMR}$ corresponds to a factor of 10 increase in FMR . The matrix is not quite symmetric because images in the enrollment and verification sets are different.

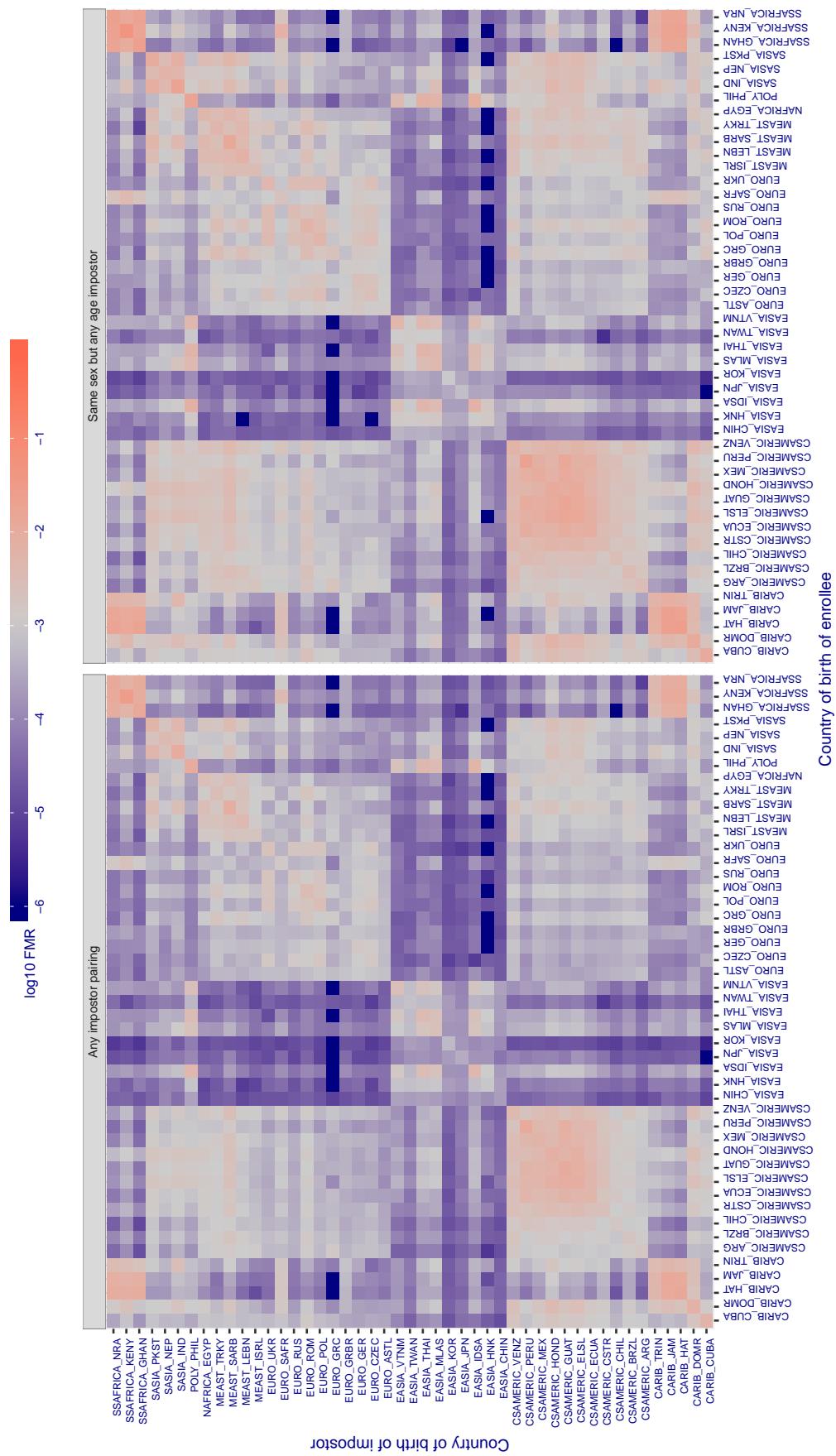
Cross country FMR at threshold T = 0.703 for algorithm lookman_004, giving FMR(T) = 0.001 globally.

Figure 358: For algorithm lookman-004 operating on visa images, the heatmap shows false match rates observed over impostor comparisons of faces from different individuals who were born in the given country pair. False matches are counted against a recognition threshold fixed globally to give the target FMR in the plot title, computed over all on the order of 10^{10} impostor comparisons. If text appears in each box it give the same quantity as that coded by the color. Grey indicates FMR is at the intended FMR target level. Light red colors present a security vulnerability to, for example, a passport gate. Each +1 increase in $\log_{10} \text{FMR}$ corresponds to a factor of 10 increase in FMR. The matrix is not quite symmetric because images in the enrollment and verification sets are different.

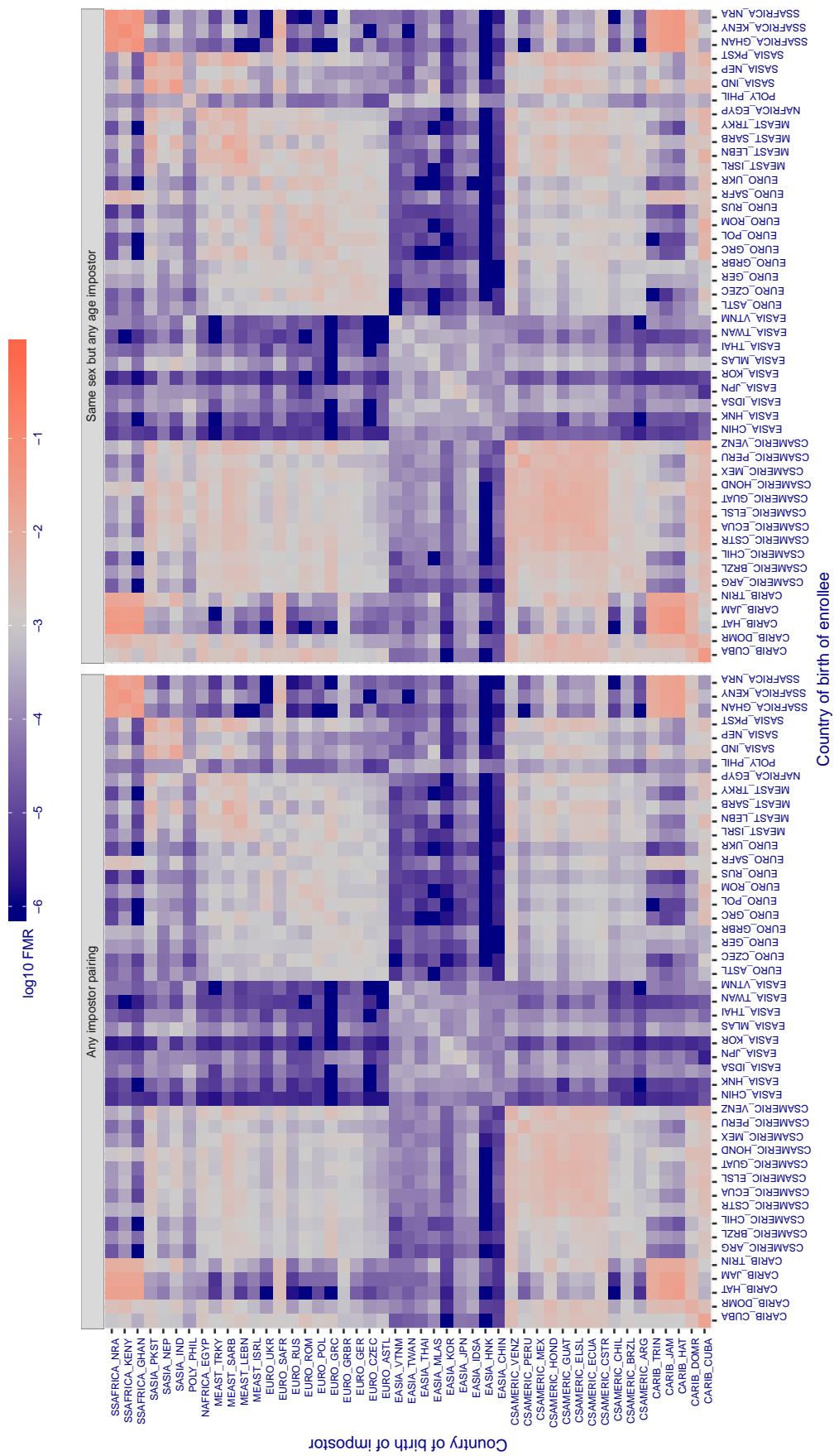
Cross country FMR at threshold T = 66.706 for algorithm megvii_001, giving FMR(T) = 0.001 globally.

Figure 359: For algorithm megvii-001 operating on visa images, the heatmap shows false match rates observed over impostor comparisons of faces from different individuals who were born in the given country pair. False matches are counted against a recognition threshold fixed globally to give the target FMR in the plot title, computed over all on the order of 10^{10} impostor comparisons. If text appears in each box it give the same quantity as that coded by the color. Grey indicates FMR is at the intended FMR target level. Light red colors present a security vulnerability to, for example, a passport gate. Each +1 increase in $\log_{10} \text{FMR}$ corresponds to a factor of 10 increase in FMR. The matrix is not quite symmetric because images in the enrollment and verification sets are different.

Cross country FMR at threshold T = 58.026 for algorithm megvii_002, giving FMR(T) = 0.001 globally.

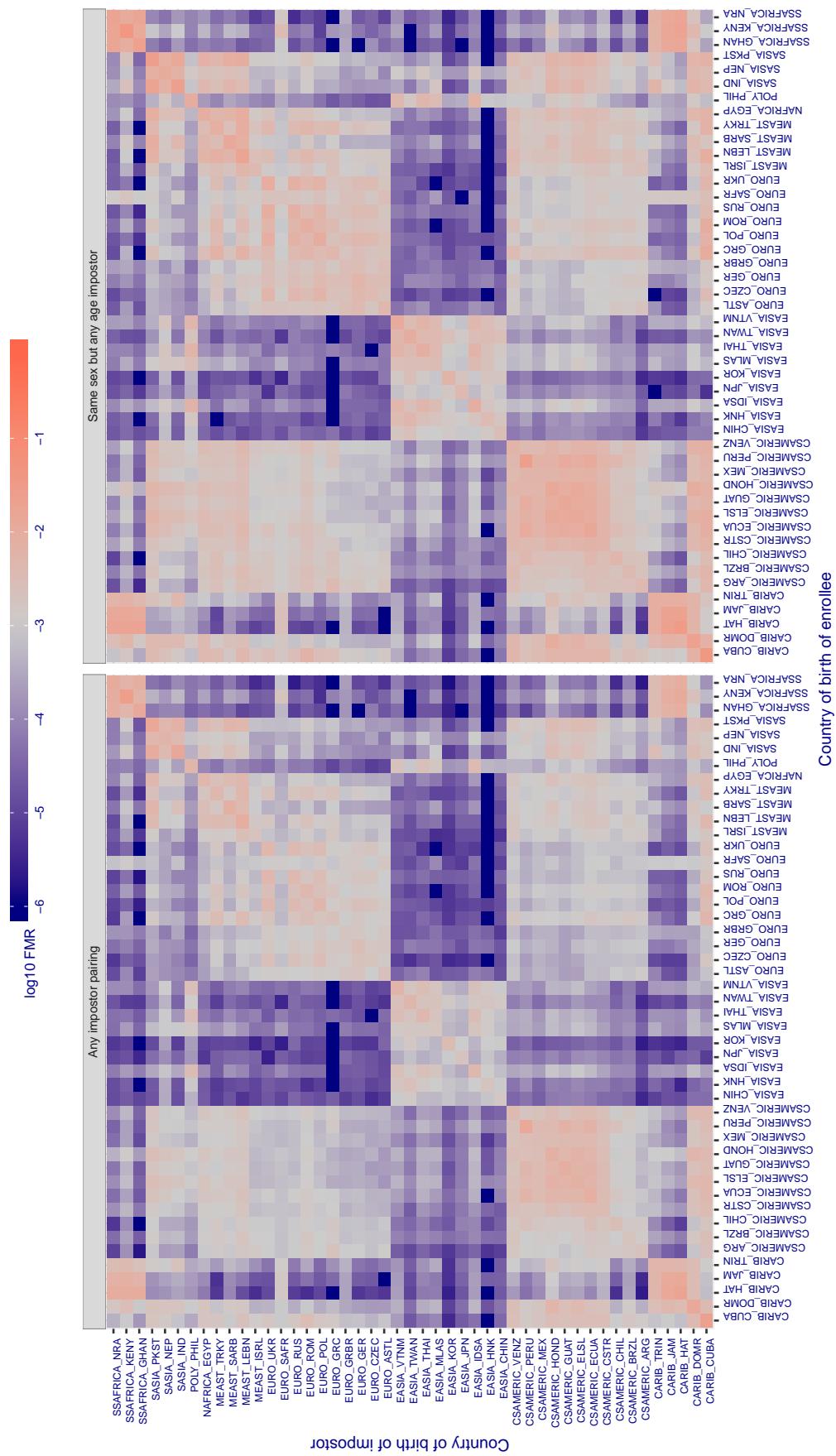


Figure 360: For algorithm megvii-002 operating on visa images, the heatmap shows false match rates observed over impostor comparisons of faces from different individuals who were born in the given country pair. False matches are counted against a recognition threshold fixed globally to give the target FMR in the plot title, computed over all on the order of 10^{10} impostor comparisons. If text appears in each box it give the same quantity as that coded by the color. Grey indicates FMR is at the intended FMR target level. Light red colors present a security vulnerability to, for example, a passport gate. Each +1 increase in $\log_{10} \text{FMR}$ corresponds to a factor of 10 increase in FMR. The matrix is not quite symmetric because images in the enrollment and verification sets are different.

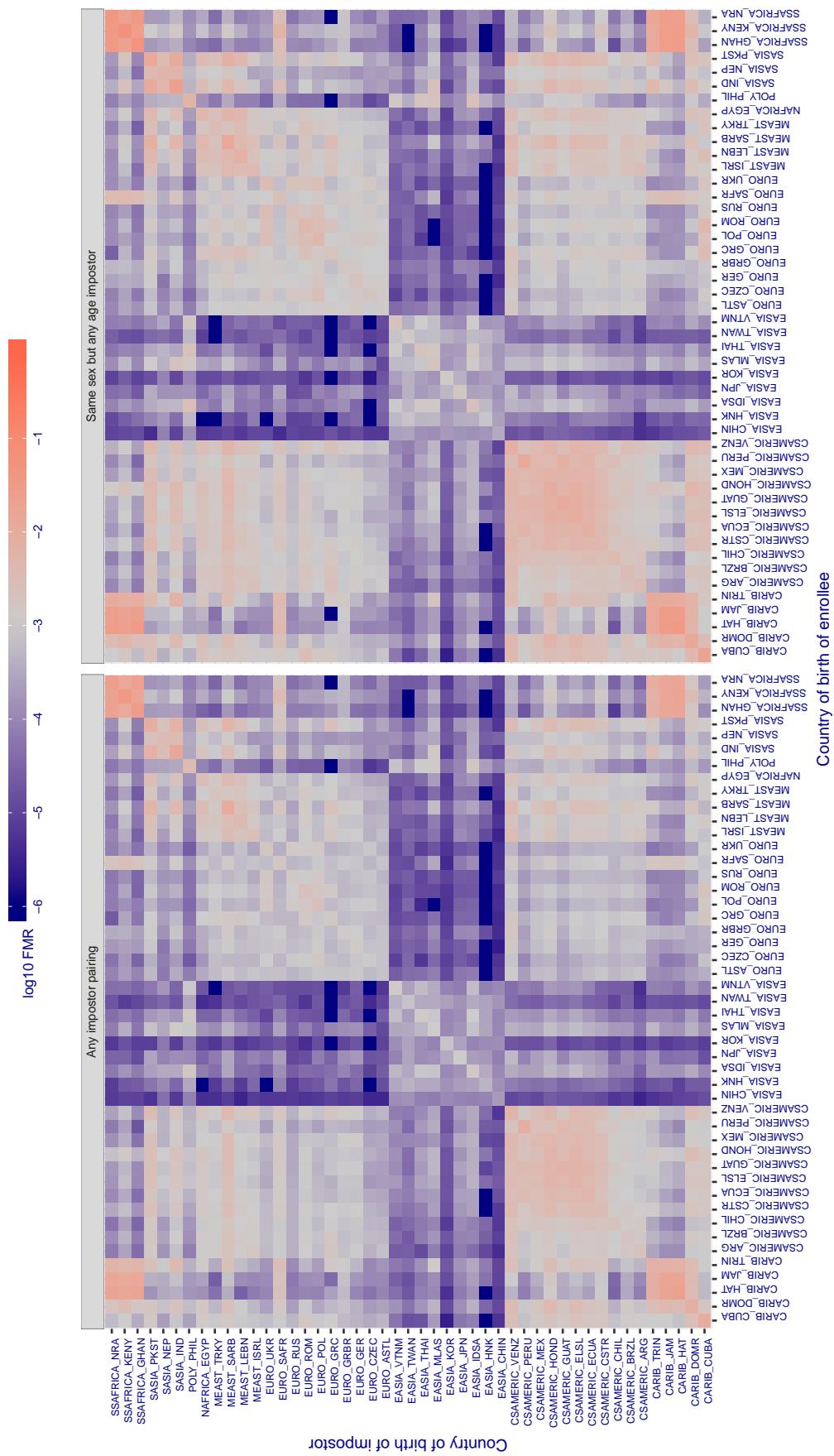
Cross country FMR at threshold T = 0.345 for algorithm meiya_001, giving FMR(T) = 0.001 globally.

Figure 361: For algorithm meiya-001 operating on visa images, the heatmap shows false match rates observed over impostor comparisons of faces from different individuals who were born in the given country pair. False matches are counted against a recognition threshold fixed globally to give the target FMR in the plot title, computed over all on the order of 10^{10} impostor comparisons. If text appears in each box it give the same quantity as that coded by the color. Grey indicates FMR is at the intended FMR target level. Light red colors present a security vulnerability to, for example, a passport gate. Each +1 increase in $\log_{10} \text{FMR}$ corresponds to a factor of 10 increase in FMR. The matrix is not quite symmetric because images in the enrollment and verification sets are different.

Cross country FMR at threshold T = 0.624 for algorithm microfocus_001, giving FMR(T) = 0.001 globally.

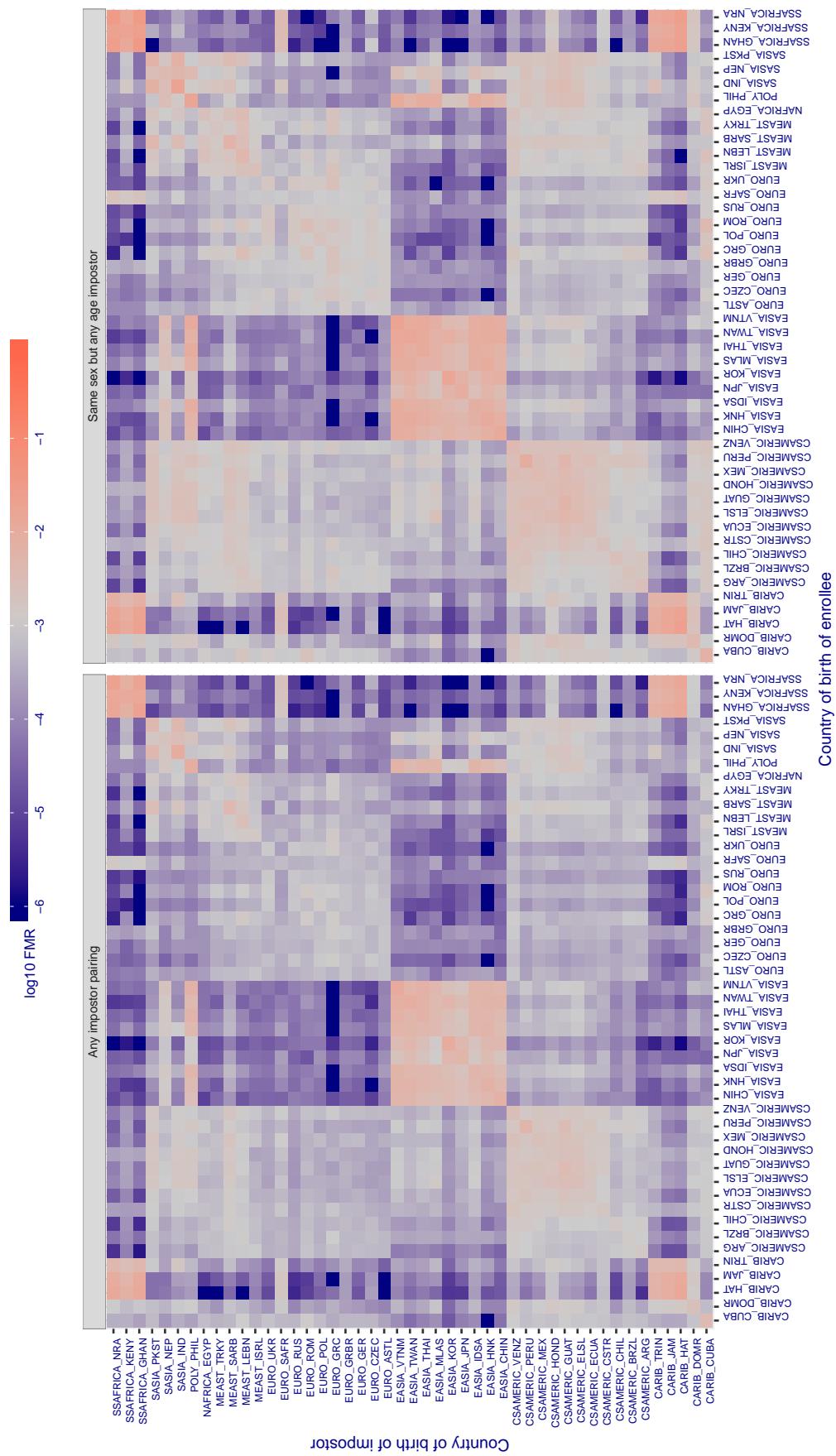


Figure 362: For algorithm microfocus-001 operating on visa images, the heatmap shows false match rates observed over impostor comparisons of faces from different individuals who were born in the given country pair. False matches are counted against a recognition threshold fixed globally to give the target FMR in the plot title, computed over all on the order of 10^{10} impostor comparisons. If text appears in each box it give the same quantity as that coded by the color. Grey indicates FMR is at the intended FMR target level. Light red colors present a security vulnerability to, for example, a passport gate. Each +1 increase in $\log_{10} FMR$ corresponds to a factor of 10 increase in FMR. The matrix is not quite symmetric because images in the enrollment and verification sets are different.

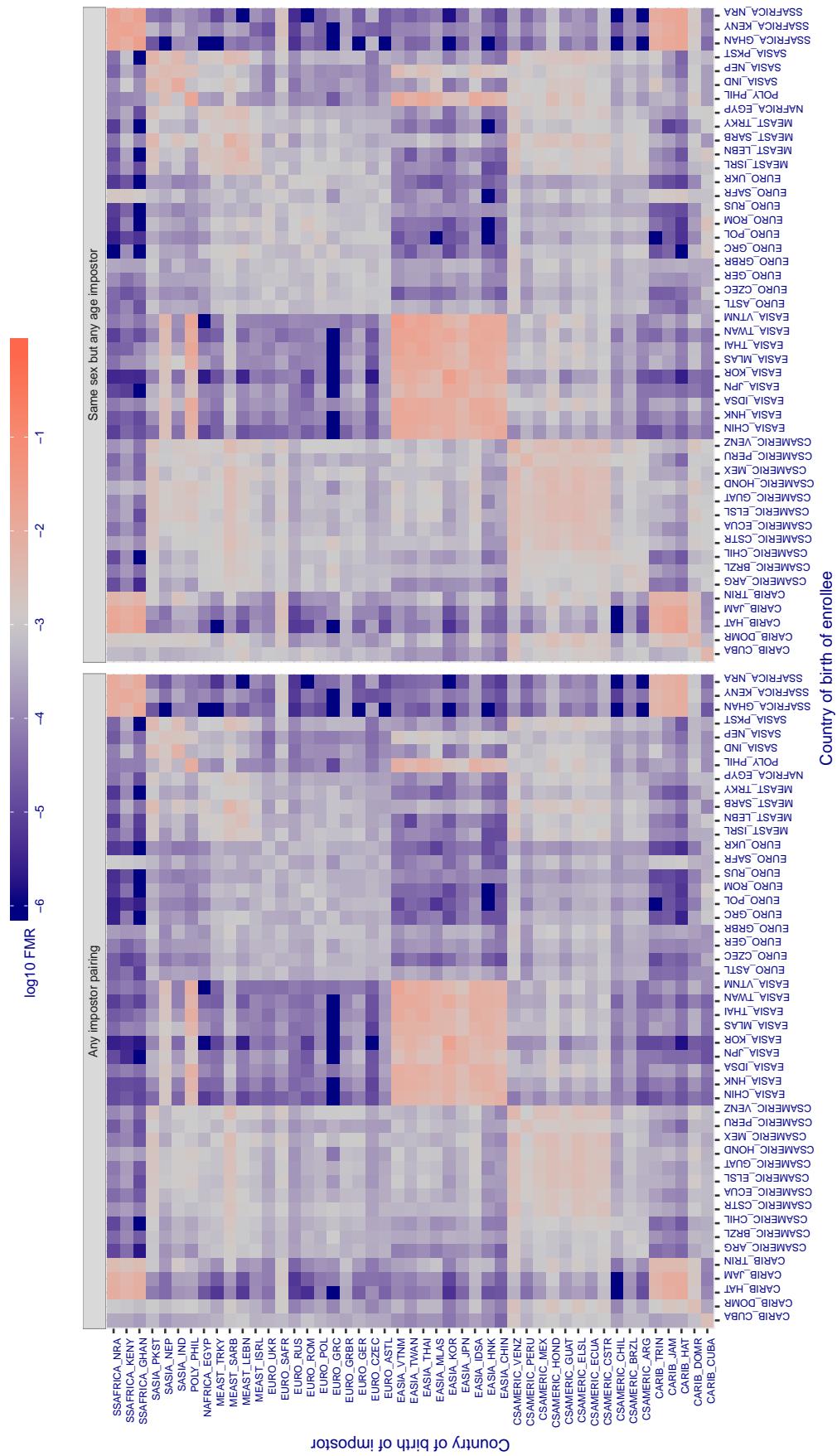
Cross country FMR at threshold T = 0.542 for algorithm microfocus_002, giving FMR(T) = 0.001 globally.

Figure 363: For algorithm microfocus-002 operating on visa images, the heatmap shows false match rates observed over impostor comparisons of faces from different individuals who were born in the given country pair. False matches are counted against a recognition threshold fixed globally to give the target FMR in the plot title, computed over all on the order of 10^{10} impostor comparisons. If text appears in each box it give the same quantity as that coded by the color. Grey indicates FMR is at the intended FMR target level. Light red colors present a security vulnerability to, for example, a passport gate. Each +1 increase in $\log_{10} FMR$ corresponds to a factor of 10 increase in FMR. The matrix is not quite symmetric because images in the enrollment and verification sets are different.

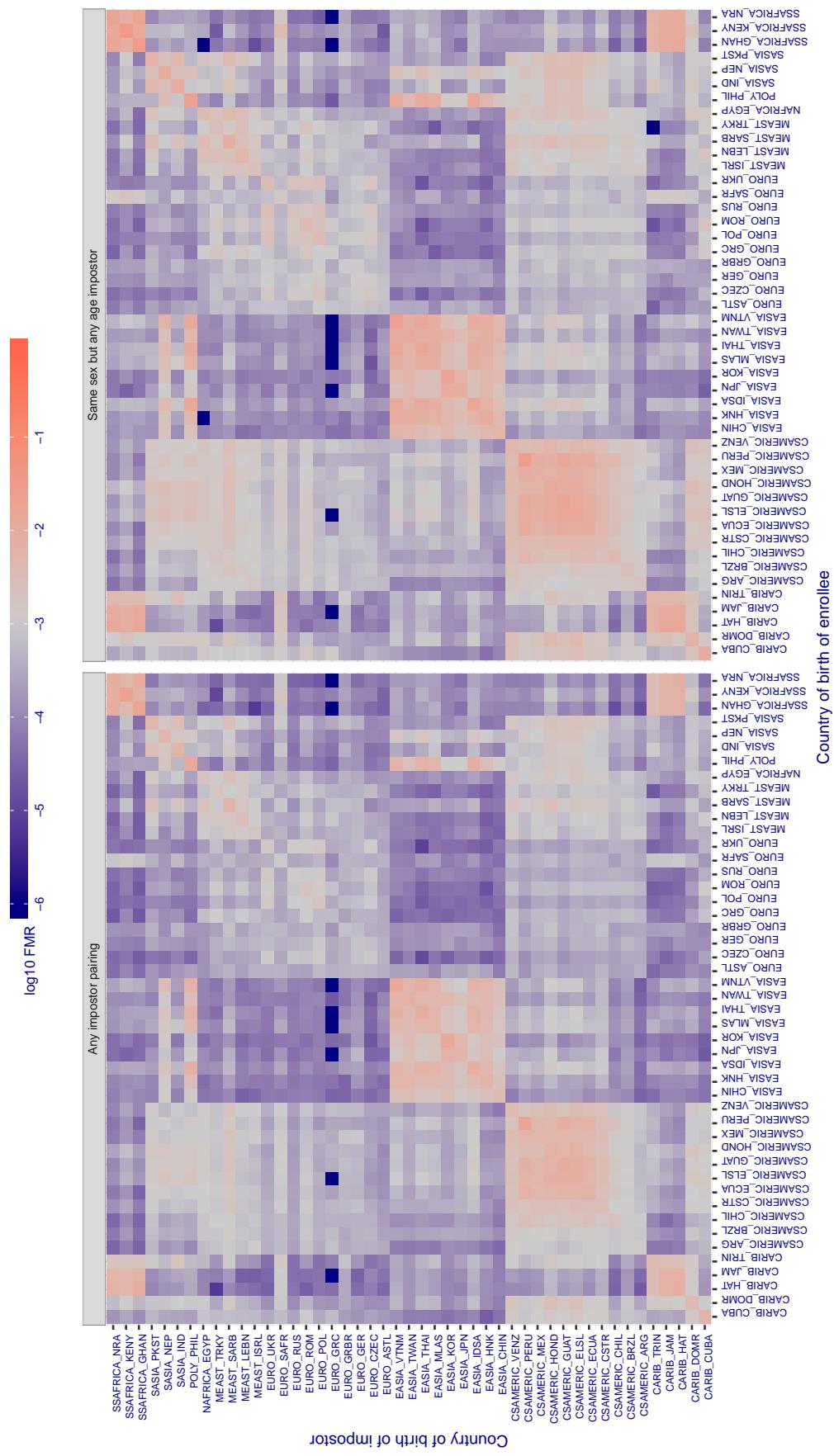
Cross country FMR at threshold T = 1.310 for algorithm mt_000, giving FMR(T) = 0.001 globally.

Figure 364: For algorithm mt-000 operating on visa images, the heatmap shows false match rates observed over impostor comparisons of faces from different individuals who were born in the given country pair. False matches are counted against a recognition threshold fixed globally to give the target FMR in the plot title, computed over all on the order of 10^{10} impostor comparisons. If text appears in each box it give the same quantity as that coded by the color. Grey indicates FMR is at the intended FMR target level. Light red colors present a security vulnerability to, for example, a passport gate. Each +1 increase in $\log_{10} \text{FMR}$ corresponds to a factor of 10 increase in FMR. The matrix is not quite symmetric because images in the enrollment and verification sets are different.

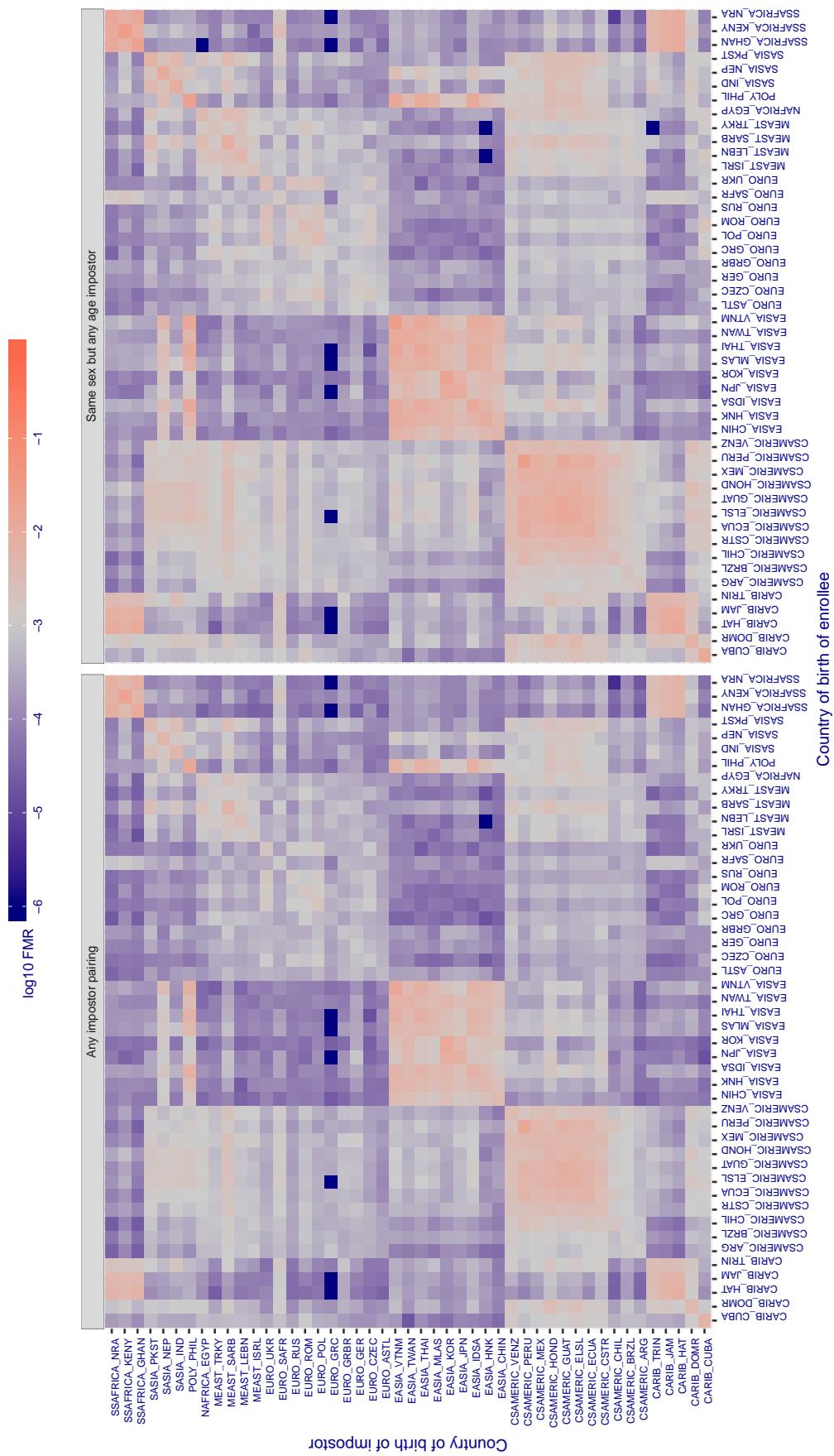
Cross country FMR at threshold T = 33.449 for algorithm neurotechnology_005, giving FMR(T) = 0.001 globally.

Figure 365: For algorithm neurotechnology-005 operating on visa images, the heatmap shows false match rates observed over impostor comparisons of faces from different individuals who were born in the given country pair. False matches are counted against a recognition threshold fixed globally to give the target FMR in the plot title, computed over all on the order of 10^{10} impostor comparisons. If text appears in each box it give the same quantity as that coded by the color. Grey indicates FMR is at the intended FMR target level. Light red colors present a security vulnerability to, for example, a passport gate. Each +1 increase in $\log_{10} \text{FMR}$ corresponds to a factor of 10 increase in FMR. The matrix is not quite symmetric because images in the enrollment and verification sets are different.

Cross country FMR at threshold T = 1686.000 for algorithm neurotechnology_006, giving FMR(T) = 0.001 globally.

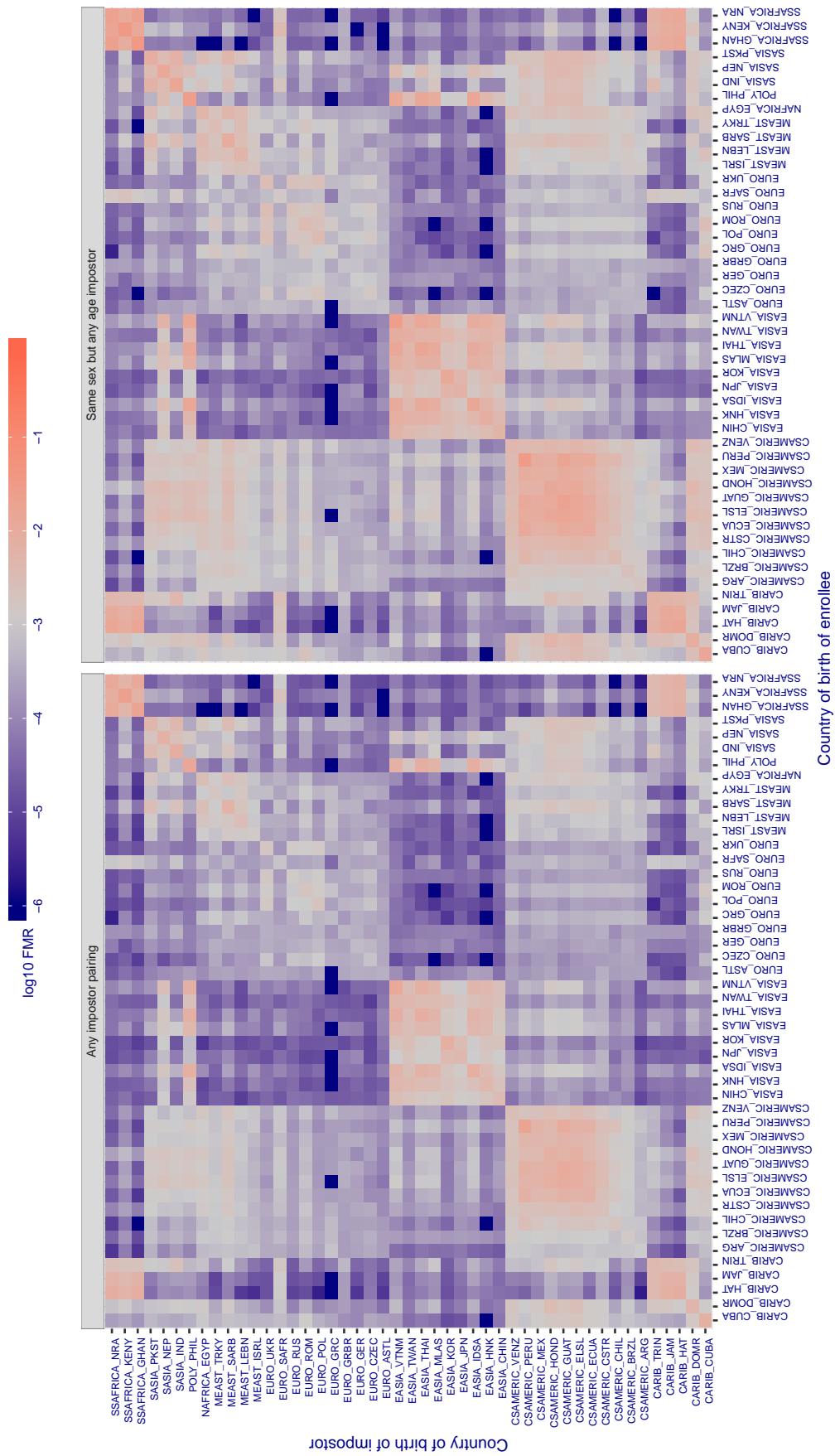


Figure 366: For algorithm neurotechnology-006 operating on visa images, the heatmap shows false match rates observed over impostor comparisons of faces from different individuals who were born in the given country pair. False matches are counted against a recognition threshold fixed globally to give the target FMR in the plot title, computed over all on the order of 10^{10} impostor comparisons. If text appears in each box it give the same quantity as that coded by the color. Grey indicates FMR is at the intended FMR target level. Light red colors present a security vulnerability to, for example, a passport gate. Each +1 increase in $\log_{10} \text{FMR}$ corresponds to a factor of 10 increase in FMR. The matrix is not quite symmetric because images in the enrollment and verification sets are different.

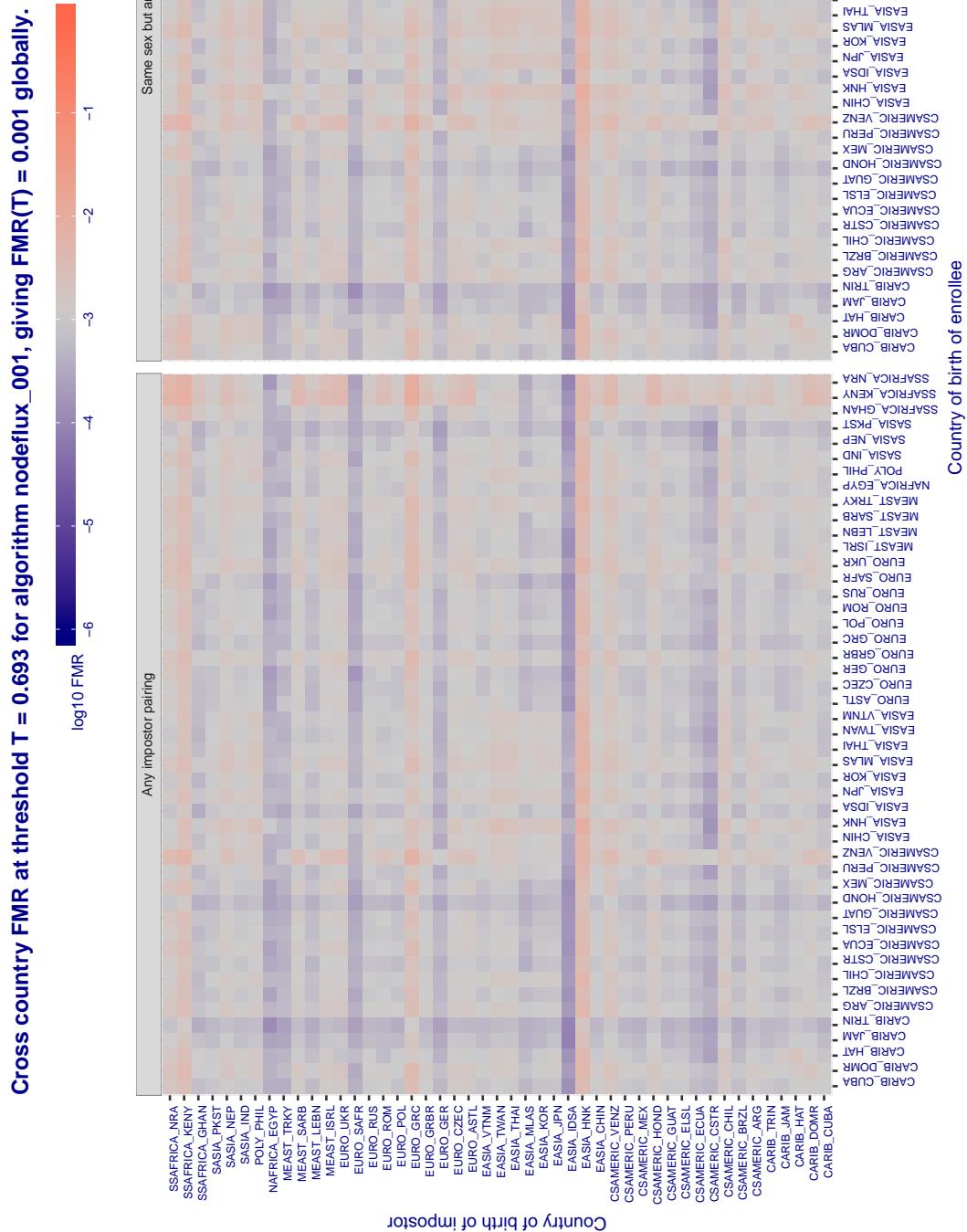


Figure 367: For algorithm nodeflux-001 operating on visa images, the heatmap shows false match rates observed over impostor comparisons of faces from different individuals who were born in the given country pair. False matches are counted against a recognition threshold fixed globally to give the target FMR in the plot title, computed over all on the order of 10^{10} impostor comparisons. If text appears in each box it give the same quantity as that coded by the color. Grey indicates FMR is at the intended FMR target level. Light red colors present a security vulnerability to, for example, a passport gate. Each +1 increase in $\log_{10} FMR$ corresponds to a factor of 10 increase in FMR. The matrix is not quite symmetric because images in the enrollment and verification sets are different.

Cross country FMR at threshold T = 0.420 for algorithm nodeflux_002, giving FMR(T) = 0.001 globally.

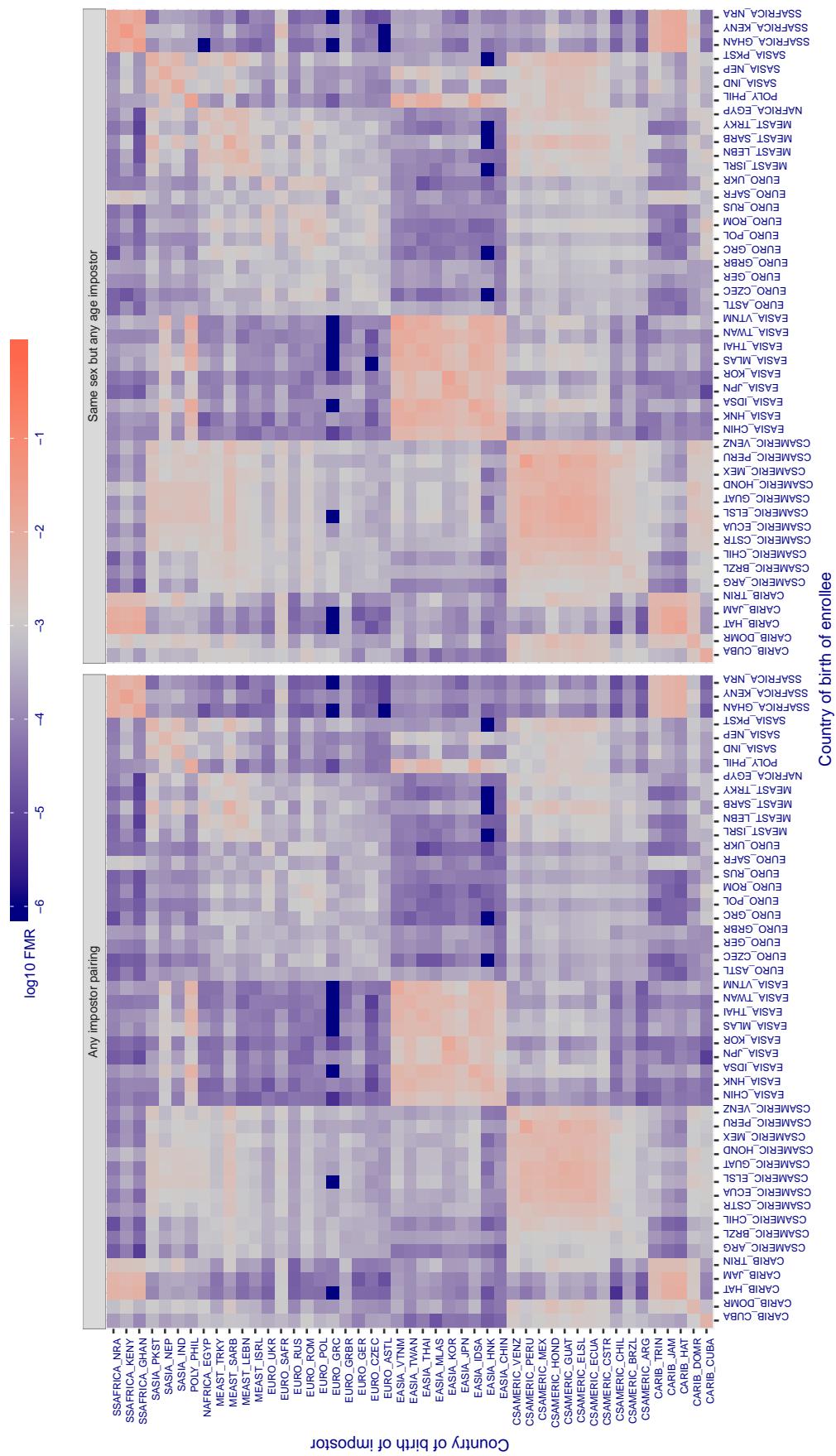


Figure 368: For algorithm nodeflux-002 operating on visa images, the heatmap shows false match rates observed over impostor comparisons of faces from different individuals who were born in the given country pair. False matches are counted against a recognition threshold fixed globally to give the target FMR in the plot title, computed over all on the order of 10^{10} impostor comparisons. If text appears in each box it give the same quantity as that coded by the color. Grey indicates FMR is at the intended FMR target level. Light red colors present a security vulnerability to, for example, a passport gate. Each +1 increase in $\log_{10} \text{FMR}$ corresponds to a factor of 10 increase in FMR. The matrix is not quite symmetric because images in the enrollment and verification sets are different.

Cross country FMR at threshold T = 1338139146338239954308032998197392108861073498206667481318591787294160965343825654106871

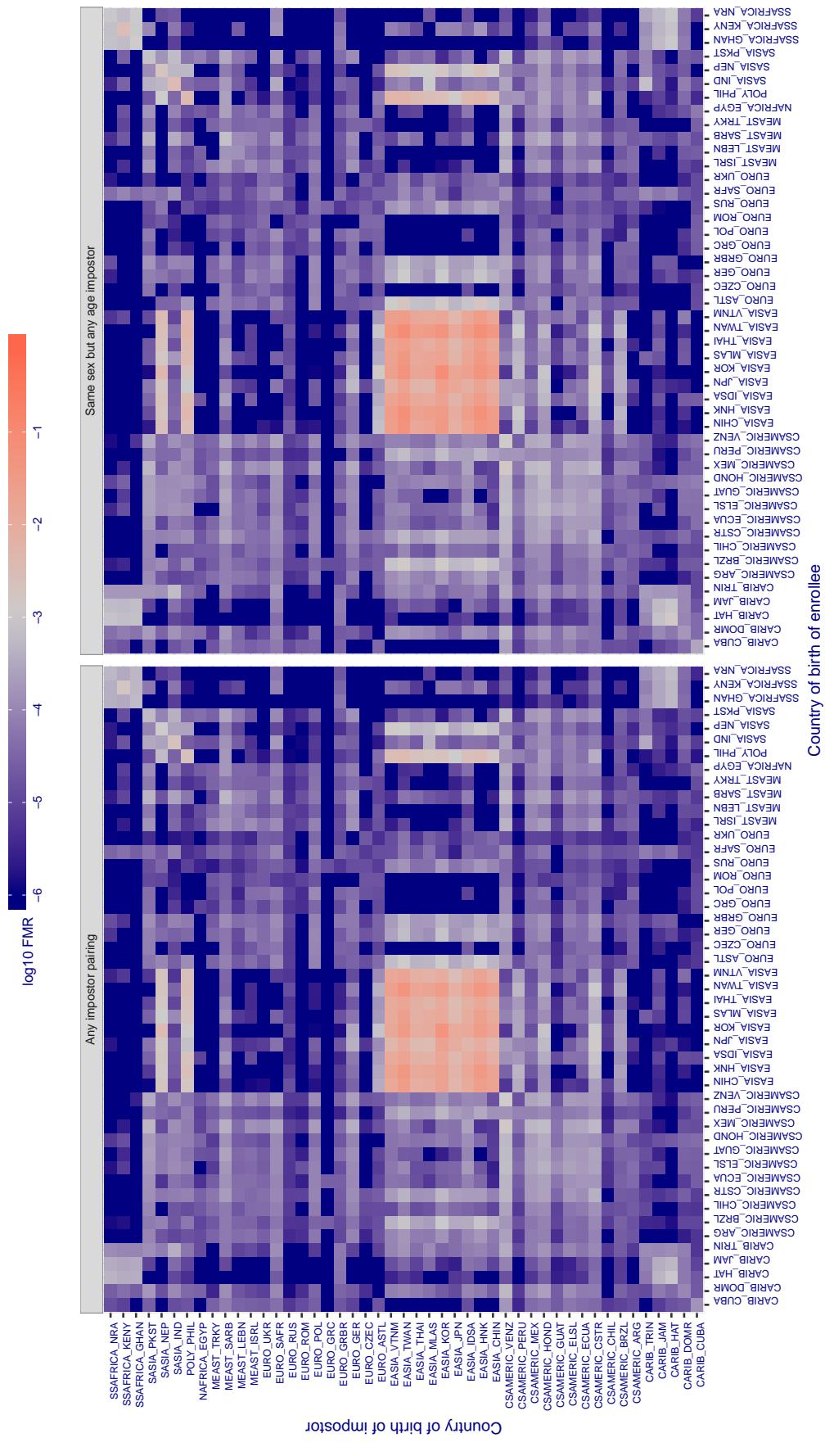


Figure 369: For algorithm notiontag-000 operating on visa images, the heatmap shows false match rates observed over impostor comparisons of faces from different individuals who were born in the given country pair. False matches are counted against a recognition threshold fixed globally to give the target FMR in the plot title, computed over all on the order of 10^{10} impostor comparisons. If text appears in each box it give the same quantity as that coded by the color. Grey indicates FMR is at the intended FMR target level. Light red colors present a security vulnerability to, for example, a passport gate. Each +1 increase in $\log_{10} FMR$ corresponds to a factor of 10 increase in FMR. The matrix is not quite symmetric because images in the enrollment and verification sets are different.

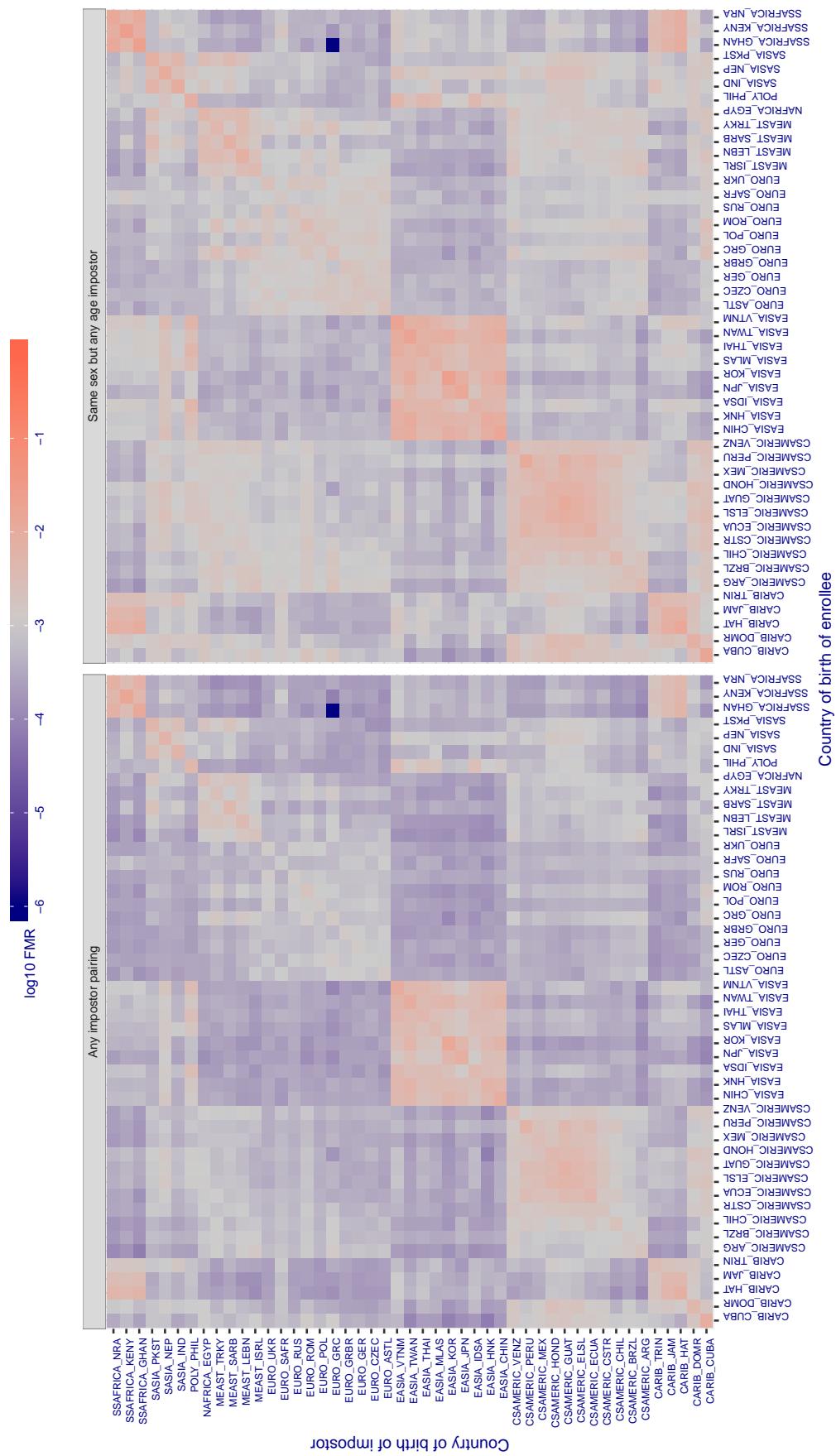
Cross country FMR at threshold T = 1.929 for algorithm ntechlab_006, giving FMR(T) = 0.001 globally.

Figure 370: For algorithm ntechlab-006 operating on visa images, the heatmap shows false match rates observed over impostor comparisons of faces from different individuals who were born in the given country pair. False matches are counted against a recognition threshold fixed globally to give the target FMR in the plot title, computed over all on the order of 10^{10} impostor comparisons. If text appears in each box it give the same quantity as that coded by the color. Grey indicates FMR is at the intended FMR target level. Light red colors present a security vulnerability to, for example, a passport gate. Each +1 increase in $\log_{10} FMR$ corresponds to a factor of 10 increase in FMR. The matrix is not quite symmetric because images in the enrollment and verification sets are different.

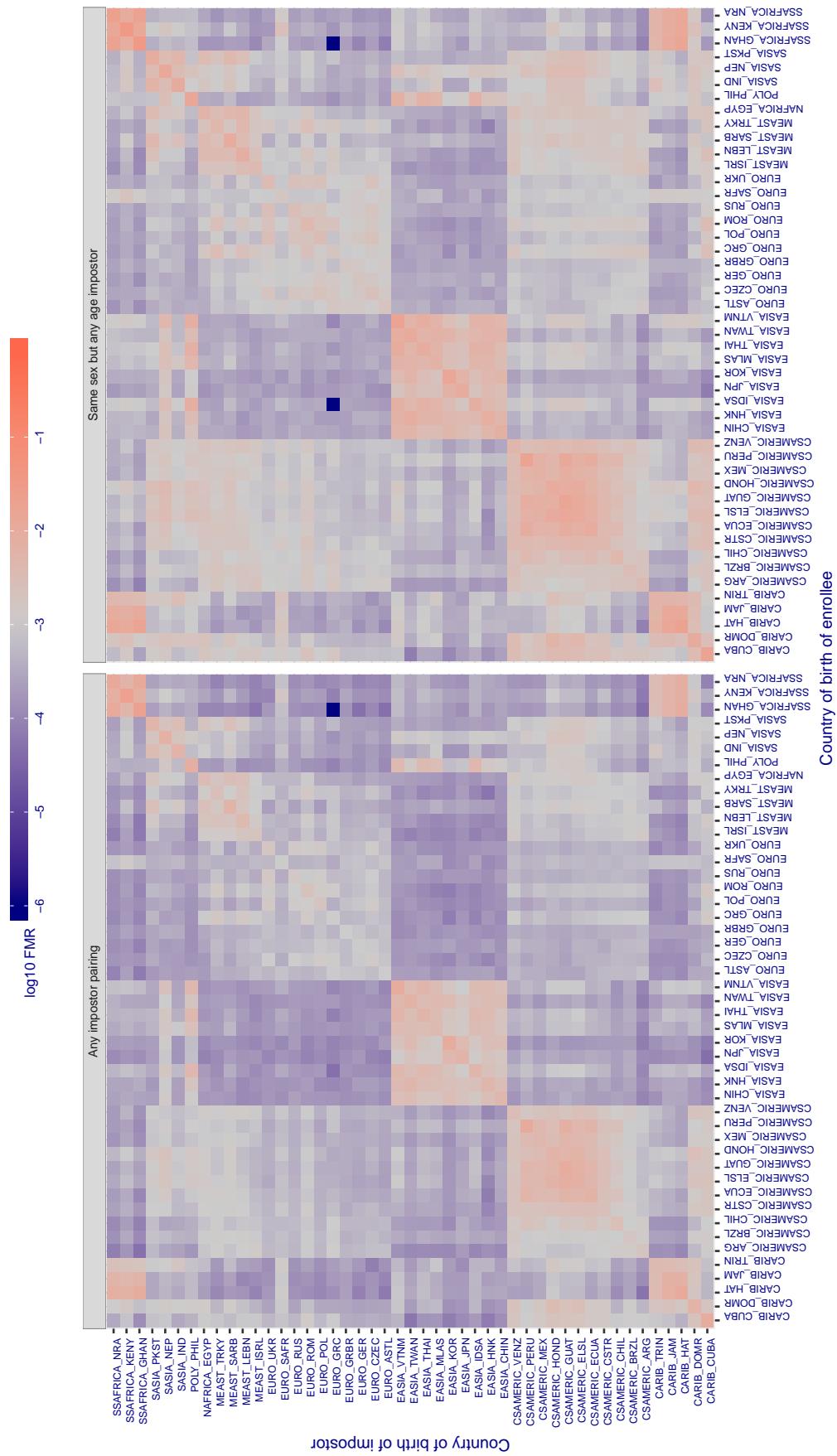
Cross country FMR at threshold T = 1.319 for algorithm ntechlab_007, giving $\text{FMR}(\text{T}) = 0.001$ globally.

Figure 371: For algorithm ntechlab-007 operating on visa images, the heatmap shows false match rates observed over impostor comparisons of faces from different individuals who were born in the given country pair. False matches are counted against a recognition threshold fixed globally to give the target FMR in the plot title, computed over all on the order of 10^{10} impostor comparisons. If text appears in each box it give the same quantity as that coded by the color. Grey indicates FMR is at the intended FMR target level. Light red colors present a security vulnerability to, for example, a passport gate. Each +1 increase in $\log_{10} \text{FMR}$ corresponds to a factor of 10 increase in FMR. The matrix is not quite symmetric because images in the enrollment and verification sets are different.

Cross country FMR at threshold T = 0.334 for algorithm pixelall_002, giving $\text{FMR}(\text{T}) = 0.001$ globally.

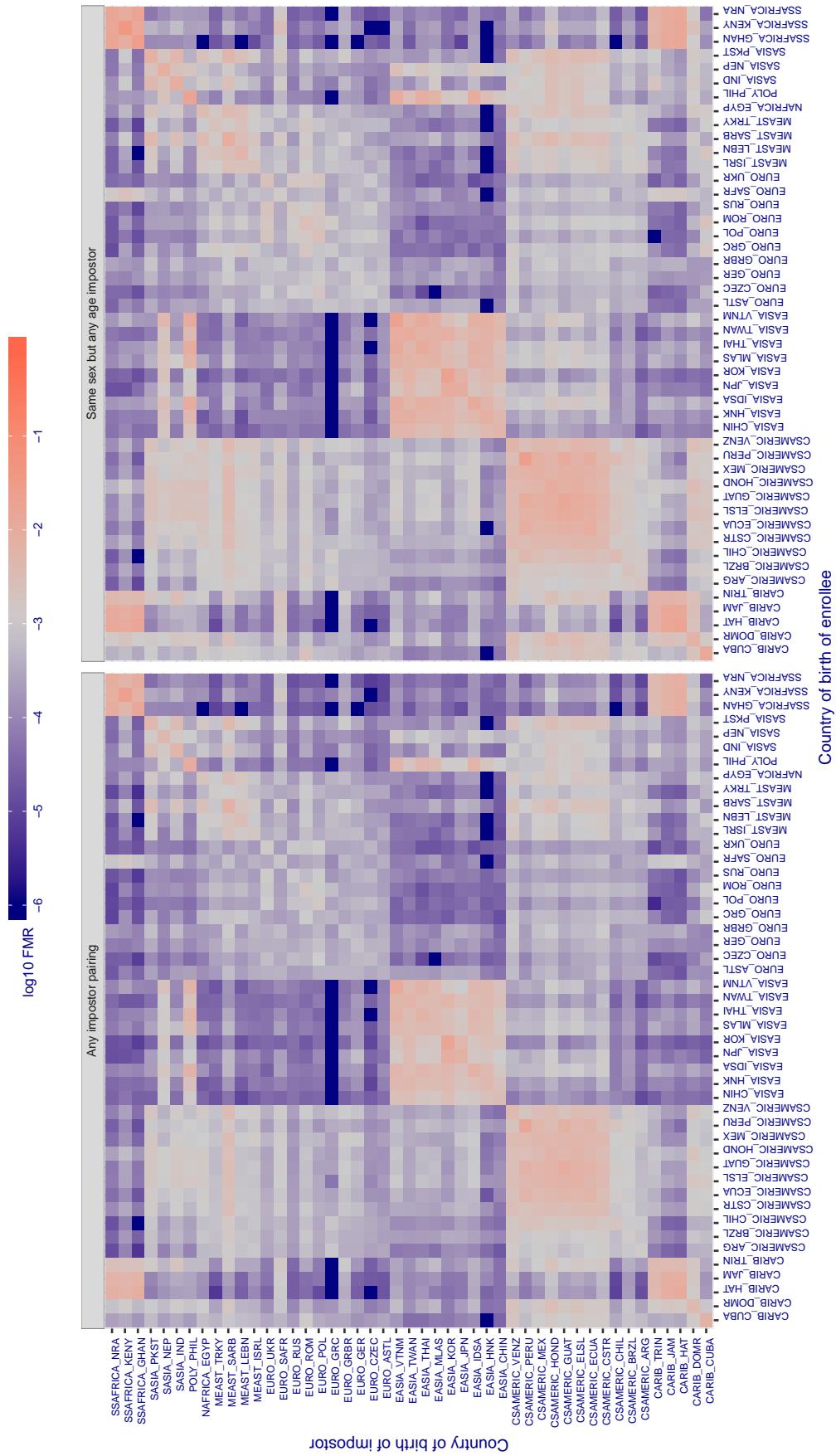


Figure 372: For algorithm pixelall-002 operating on visa images, the heatmap shows false match rates observed over impostor comparisons of faces from different individuals who were born in the given country pair. False matches are counted against a recognition threshold fixed globally to give the target FMR in the plot title, computed over all on the order of 10^{10} impostor comparisons. If text appears in each box it give the same quantity as that coded by the color. Grey indicates FMR is at the intended FMR target level. Light red colors present a security vulnerability to, for example, a passport gate. Each +1 increase in $\log_{10} \text{FMR}$ corresponds to a factor of 10 increase in FMR . The matrix is not quite symmetric because images in the enrollment and verification sets are different.

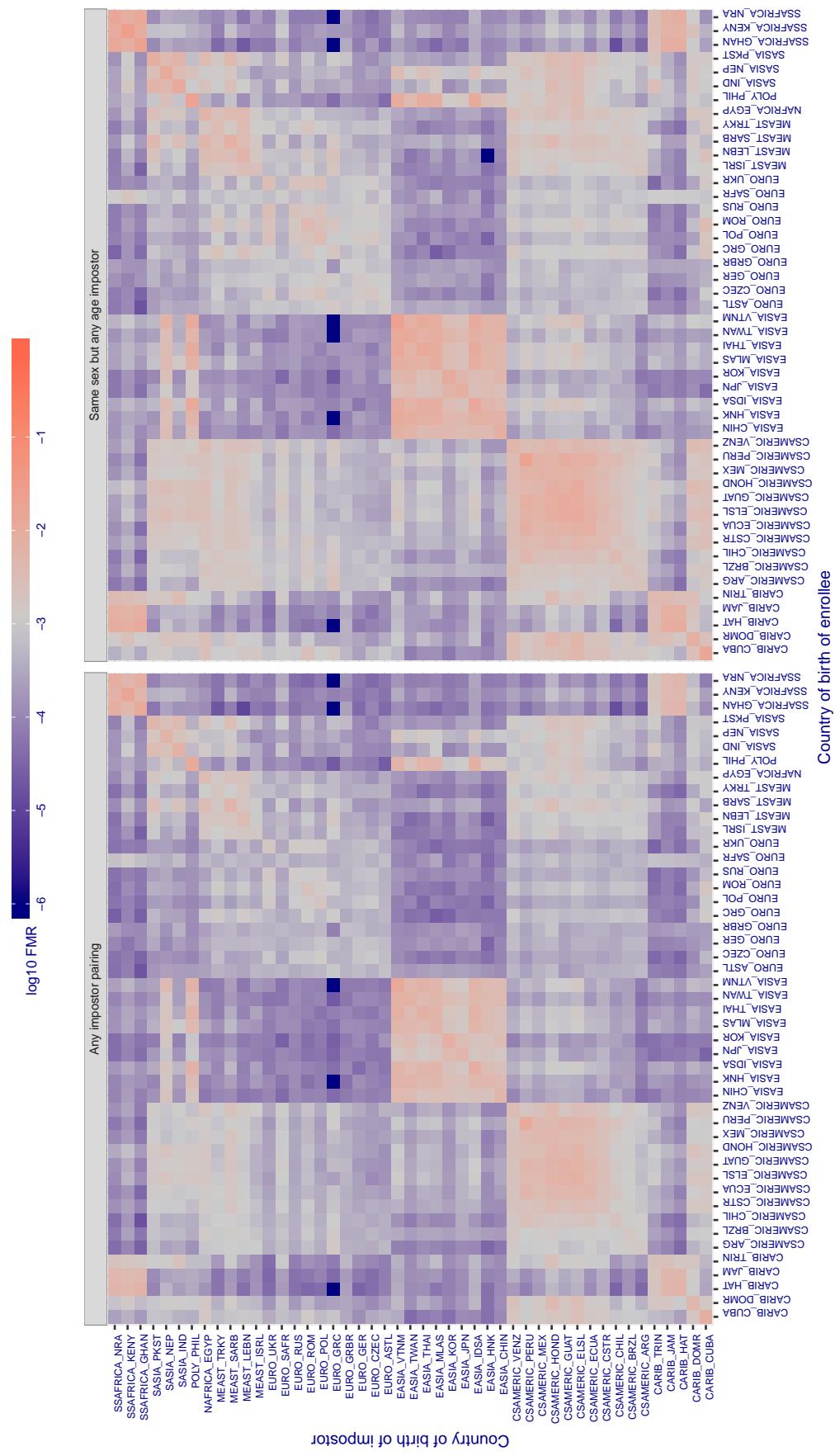
Cross country FMR at threshold T = 0.253 for algorithm psl_001, giving $FMR(T) = 0.001$ globally.

Figure 373: For algorithm psl_001 operating on visa images, the heatmap shows false match rates observed over impostor comparisons of faces from different individuals who were born in the given country pair. False matches are counted against a recognition threshold fixed globally to give the target FMR in the plot title, computed over all on the order of 10^{10} impostor comparisons. If text appears in each box it give the same quantity as that coded by the color. Grey indicates FMR is at the intended FMR target level. Light red colors present a security vulnerability to, for example, a passport gate. Each +1 increase in $\log_{10} FMR$ corresponds to a factor of 10 increase in FMR. The matrix is not quite symmetric because images in the enrollment and verification sets are different.

Cross country FMR at threshold T = 0.272 for algorithm psl_002, giving $FMR(T) = 0.001$ globally.

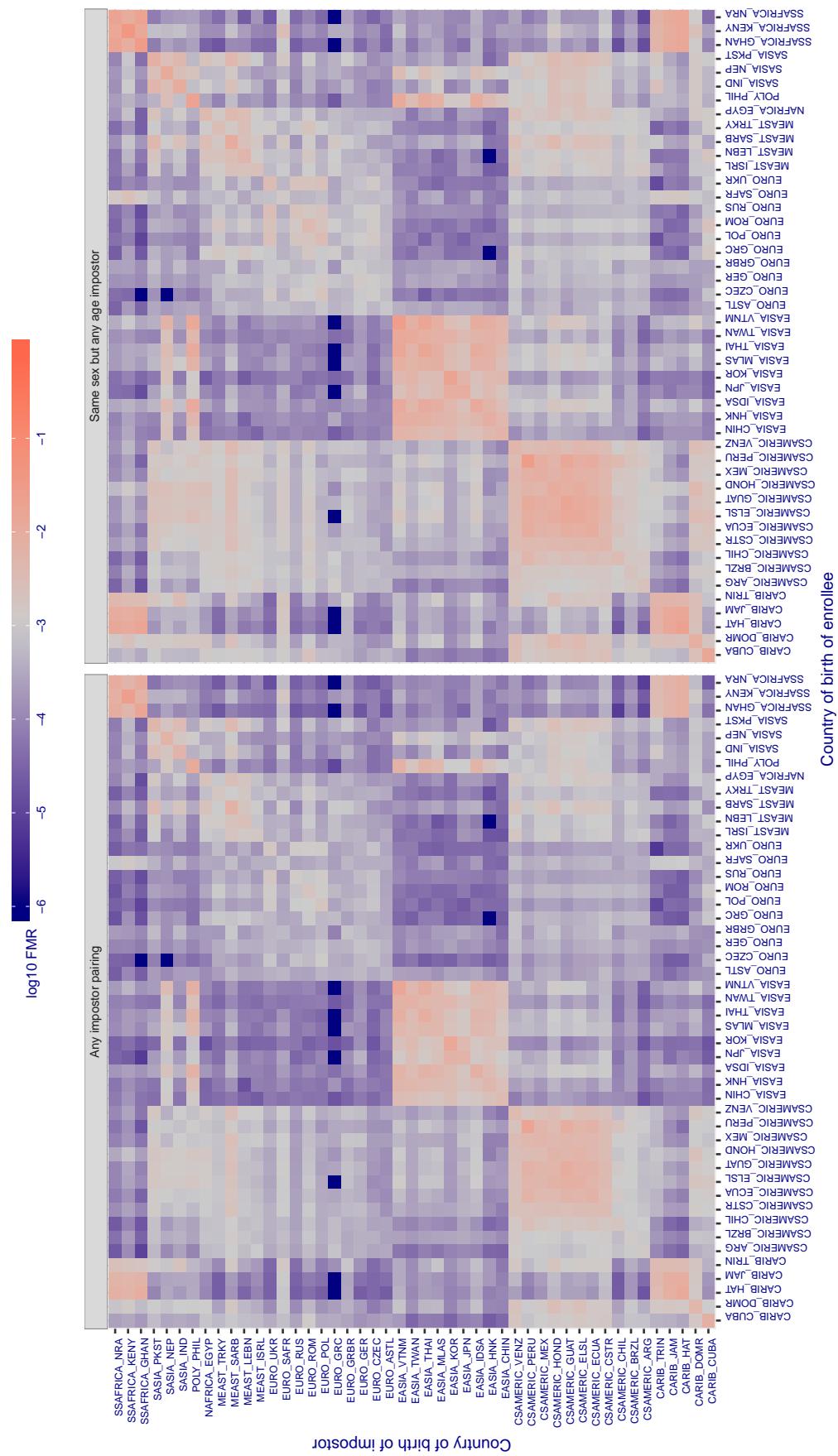


Figure 374: For algorithm psl_002 operating on visa images, the heatmap shows false match rates observed over impostor comparisons of faces from different individuals who were born in the given country pair. False matches are counted against a recognition threshold fixed globally to give the target FMR in the plot title, computed over all on the order of 10^{10} impostor comparisons. If text appears in each box it give the same quantity as that coded by the color. Grey indicates FMR is at the intended FMR target level. Light red colors present a security vulnerability to, for example, a passport gate. Each +1 increase in $\log_{10} FMR$ corresponds to a factor of 10 increase in FMR. The matrix is not quite symmetric because images in the enrollment and verification sets are different.

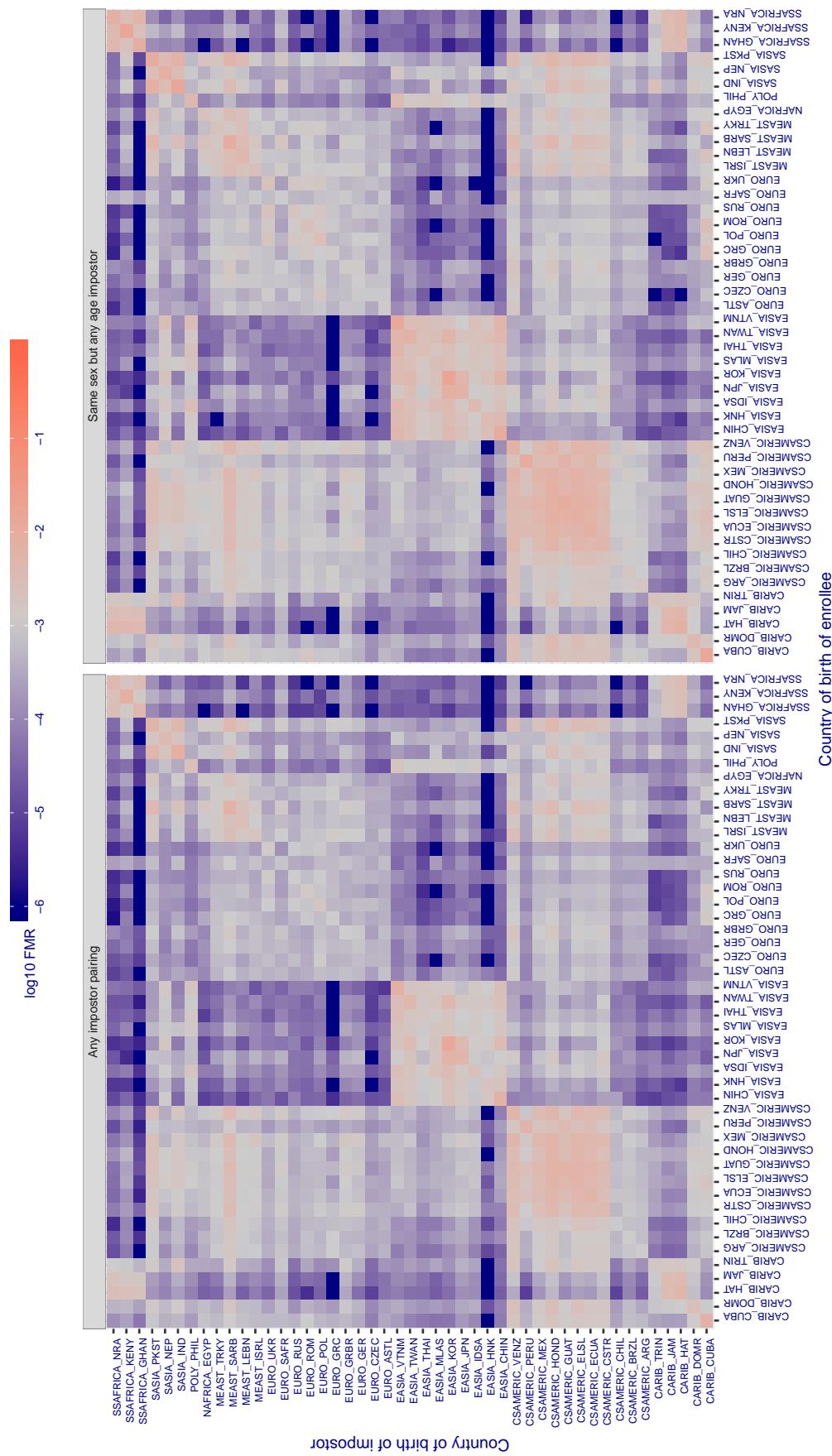
Cross country FMR at threshold T = 0.613 for algorithm rankone_006, giving $\text{FMR}(\text{T}) = 0.001$ globally.

Figure 375: For algorithm rankone-006 operating on visa images, the heatmap shows false match rates observed over impostor comparisons of faces from different individuals who were born in the given country pair. False matches are counted against a recognition threshold fixed globally to give the target FMR in the plot title, computed over all on the order of 10^{10} impostor comparisons. If text appears in each box it give the same quantity as that coded by the color. Grey indicates FMR is at the intended FMR target level. Light red colors present a security vulnerability to, for example, a passport gate. Each +1 increase in $\log_{10} \text{FMR}$ corresponds to a factor of 10 increase in FMR . The matrix is not quite symmetric because images in the enrollment and verification sets are different.

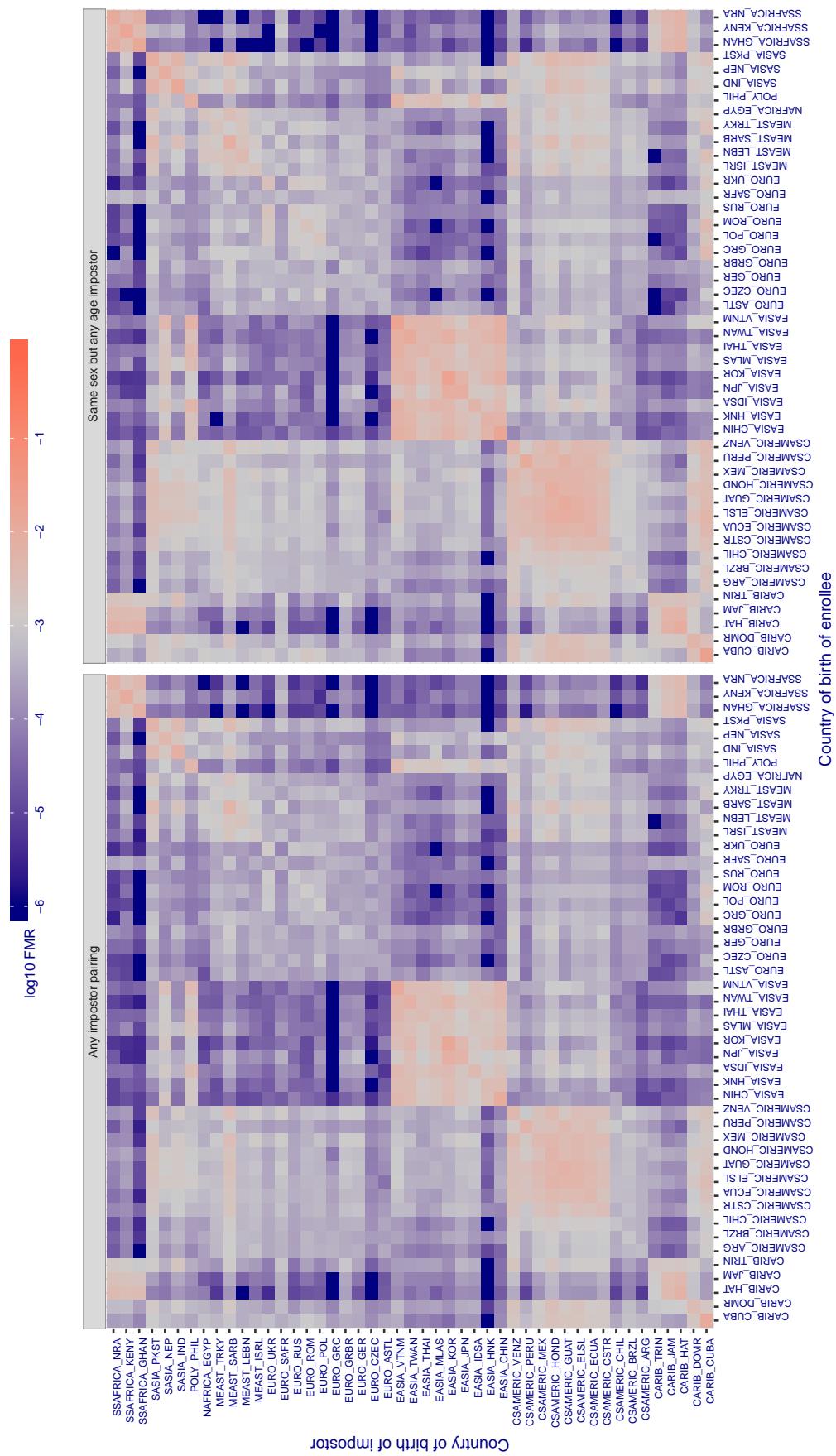
Cross country FMR at threshold T = 0.536 for algorithm rankone_007, giving $\text{FMR}(\text{T}) = 0.001$ globally.

Figure 376: For algorithm rankone-007 operating on visa images, the heatmap shows false match rates observed over impostor comparisons of faces from different individuals who were born in the given country pair. False matches are counted against a recognition threshold fixed globally to give the target FMR in the plot title, computed over all on the order of 10^{10} impostor comparisons. If text appears in each box it give the same quantity as that coded by the color. Grey indicates FMR is at the intended FMR target level. Light red colors present a security vulnerability to, for example, a passport gate. Each +1 increase in $\log_{10} \text{FMR}$ corresponds to a factor of 10 increase in FMR . The matrix is not quite symmetric because images in the enrollment and verification sets are different.

Cross country FMR at threshold T = 0.814 for algorithm realnetworks_002, giving $FMR(T) = 0.001$ globally.

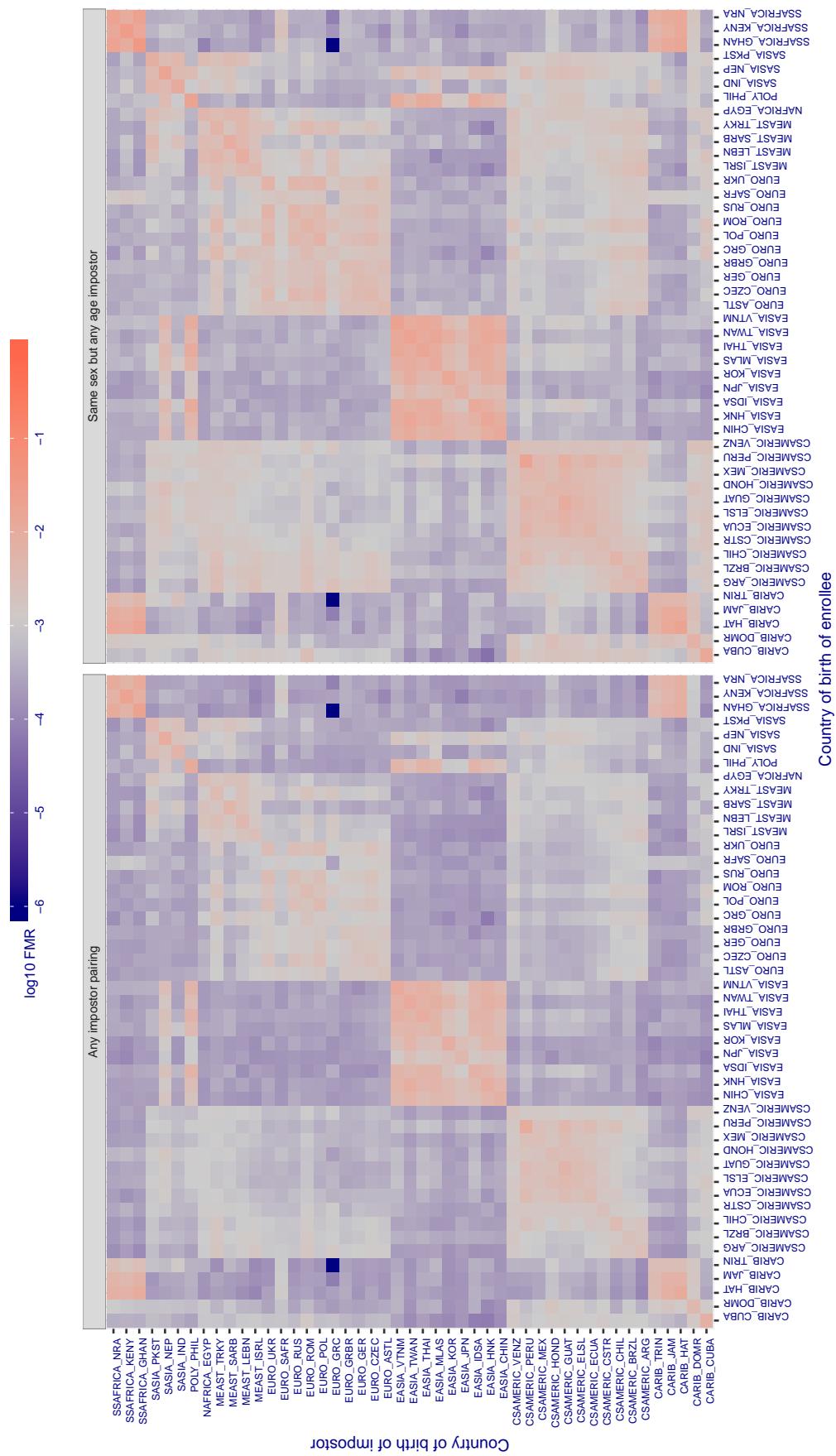


Figure 377: For algorithm realnetworks-002 operating on visa images, the heatmap shows false match rates observed over impostor comparisons of faces from different individuals who were born in the given country pair. False matches are counted against a recognition threshold fixed globally to give the target FMR in the plot title, computed over all on the order of 10^{10} impostor comparisons. If text appears in each box it give the same quantity as that coded by the color. Grey indicates FMR is at the intended FMR target level. Light red colors present a security vulnerability to, for example, a passport gate. Each +1 increase in $\log_{10} FMR$ corresponds to a factor of 10 increase in FMR. The matrix is not quite symmetric because images in the enrollment and verification sets are different.

Cross country FMR at threshold T = 0.817 for algorithm realnetworks_003, giving $\text{FMR}(\text{T}) = 0.001$ globally.

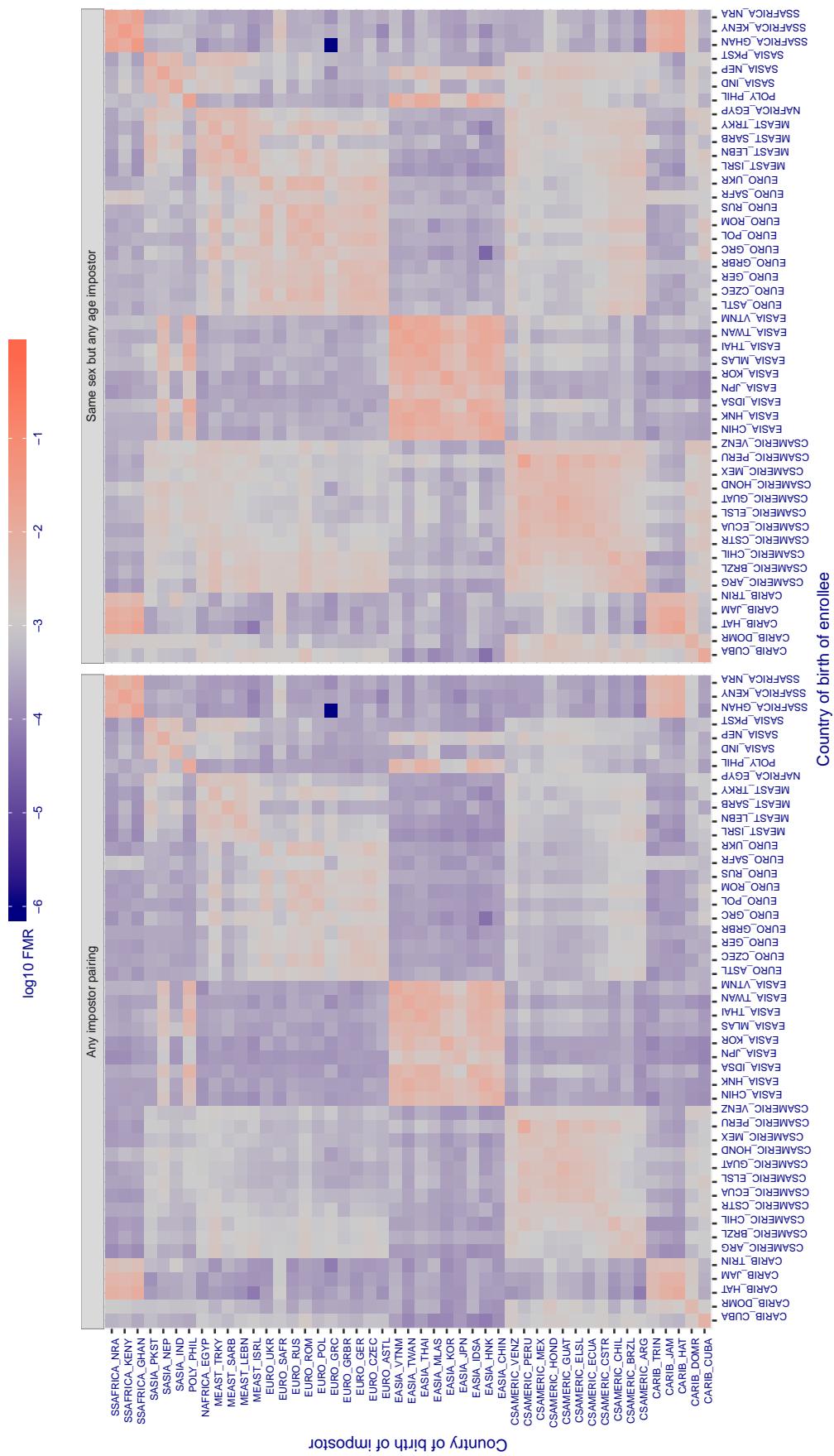


Figure 378: For algorithm *reannetworks-003* operating on visa images, the heatmap shows false match rates observed over impostor comparisons of faces from different individuals who were born in the given country pair. False matches are counted against a recognition threshold fixed globally to give the target FMR in the plot title, computed over all on the order of 10^{10} impostor comparisons. If text appears in each box it give the same quantity as that coded by the color. Grey indicates FMR is at the intended FMR target level. Light red colors present a security vulnerability to, for example, a passport gate. Each +1 increase in $\log_{10} \text{FMR}$ corresponds to a factor of 10 increase in FMR . The matrix is not quite symmetric because images in the enrollment and verification sets are different.

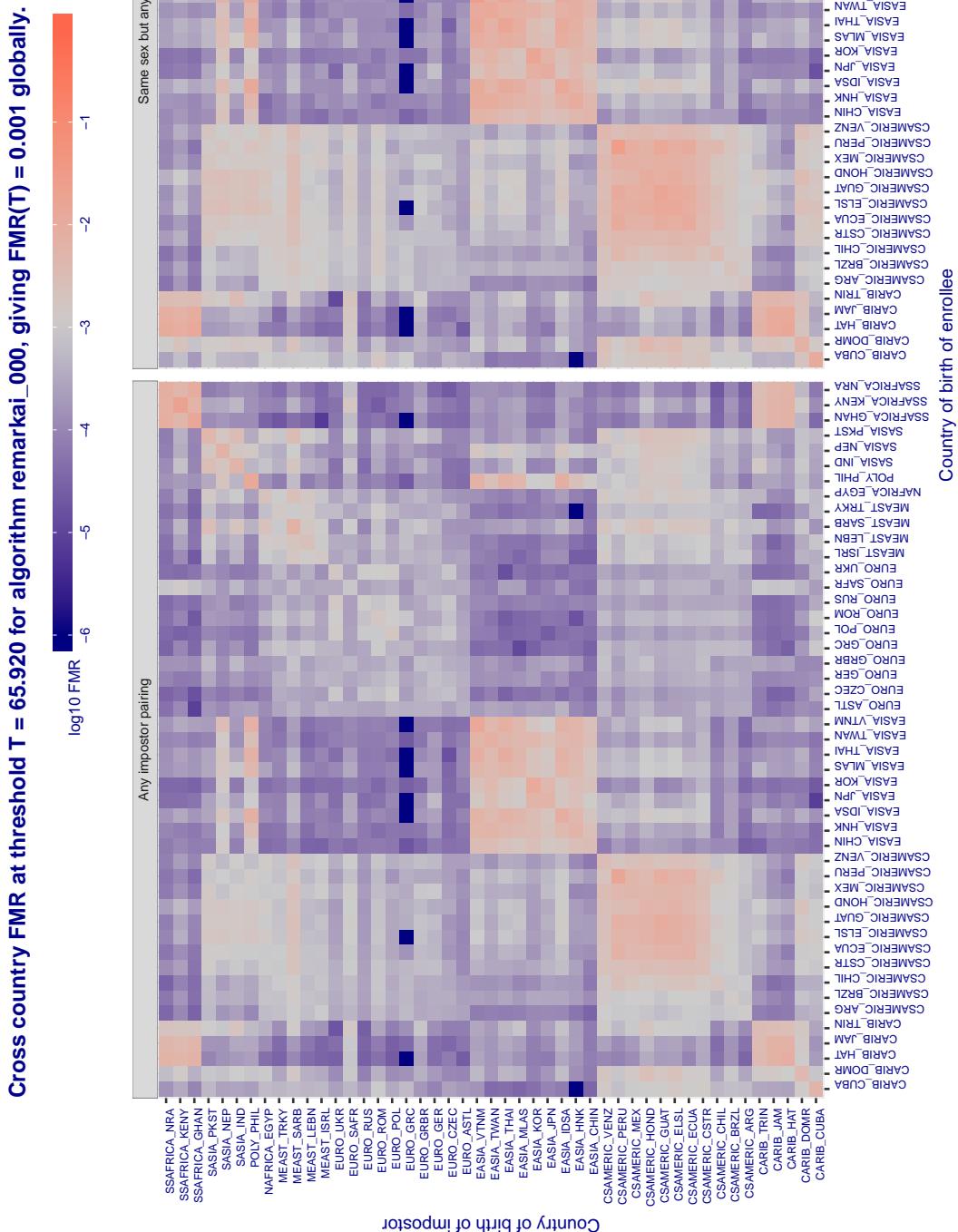


Figure 379: For algorithm remarkai-000 operating on visa images, the heatmap shows false match rates observed over impostor comparisons of faces from different individuals who were born in the given country pair. False matches are counted against a recognition threshold fixed globally to give the target FMR in the plot title, computed over all on the order of 10^{10} impostor comparisons. If text appears in each box it give the same quantity as that coded by the color. Grey indicates FMR is at the intended FMR target level. Light red colors present a security vulnerability to, for example, a passport gate. Each +1 increase in \log_{10} FMR corresponds to a factor of 10 increase in FMR. The matrix is not quite symmetric because images in the enrollment and verification sets are different.

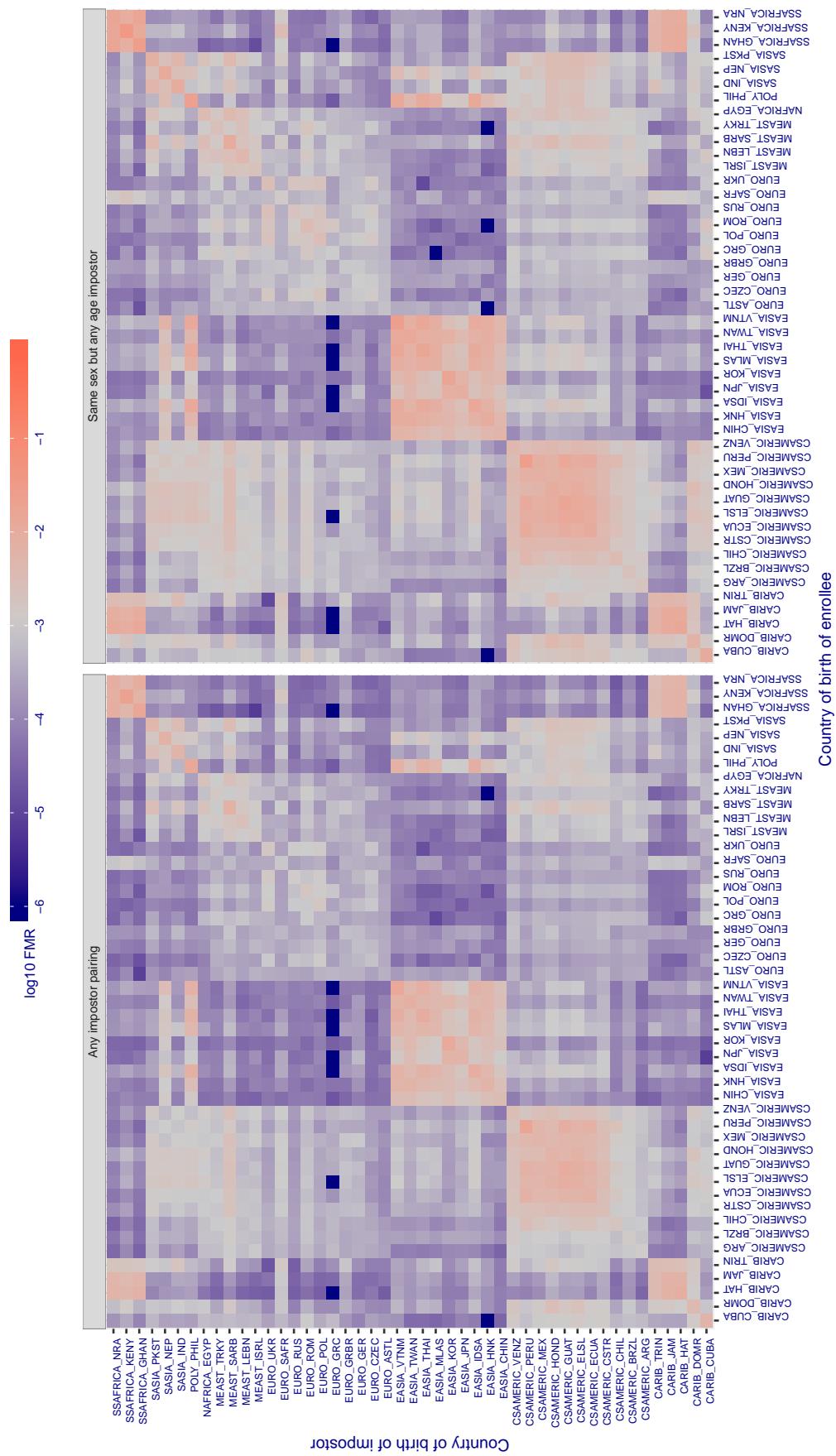
Cross country FMR at threshold T = 65.928 for algorithm remarkai_001, giving FMR(T) = 0.001 globally.

Figure 380: For algorithm remarkai-001 operating on visa images, the heatmap shows false match rates observed over impostor comparisons of faces from different individuals who were born in the given country pair. False matches are counted against a recognition threshold fixed globally to give the target FMR in the plot title, computed over all on the order of 10^{10} impostor comparisons. If text appears in each box it give the same quantity as that coded by the color. Grey indicates FMR is at the intended FMR target level. Light red colors present a security vulnerability to, for example, a passport gate. Each +1 increase in $\log_{10} \text{FMR}$ corresponds to a factor of 10 increase in FMR. The matrix is not quite symmetric because images in the enrollment and verification sets are different.

Cross country FMR at threshold T = 0.624 for algorithm rokid_000, giving FMR(T) = 0.001 globally.

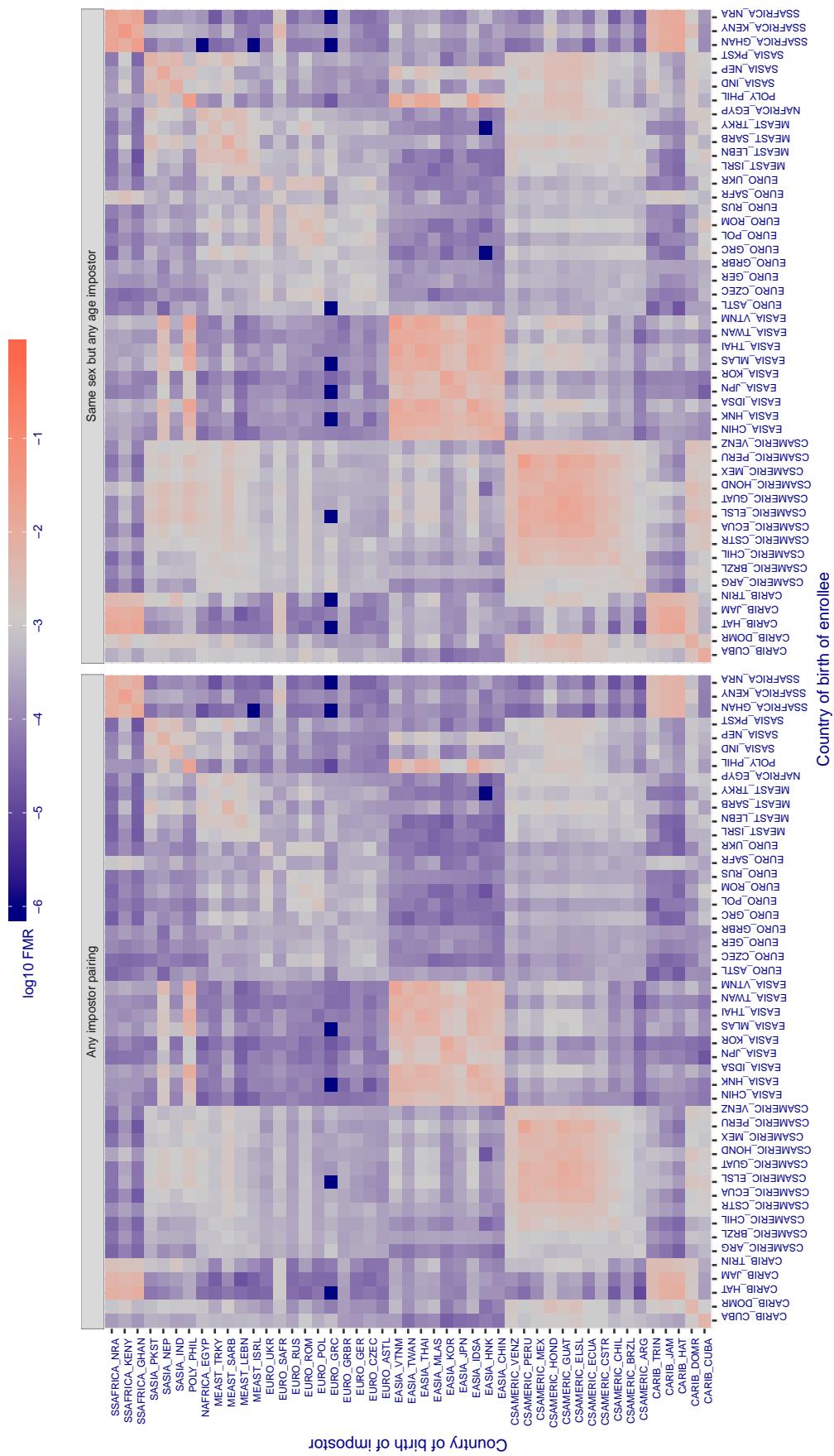


Figure 381: For algorithm rokid-000 operating on visa images, the heatmap shows false match rates observed over impostor comparisons of faces from different individuals who were born in the given country pair. False matches are counted against a recognition threshold fixed globally to give the target FMR in the plot title, computed over all on the order of 10^{10} impostor comparisons. If text appears in each box it give the same quantity as that coded by the color. Grey indicates FMR is at the intended FMR target level. Light red colors present a security vulnerability to, for example, a passport gate. Each +1 increase in $\log_{10} \text{FMR}$ corresponds to a factor of 10 increase in FMR. The matrix is not quite symmetric because images in the enrollment and verification sets are different.

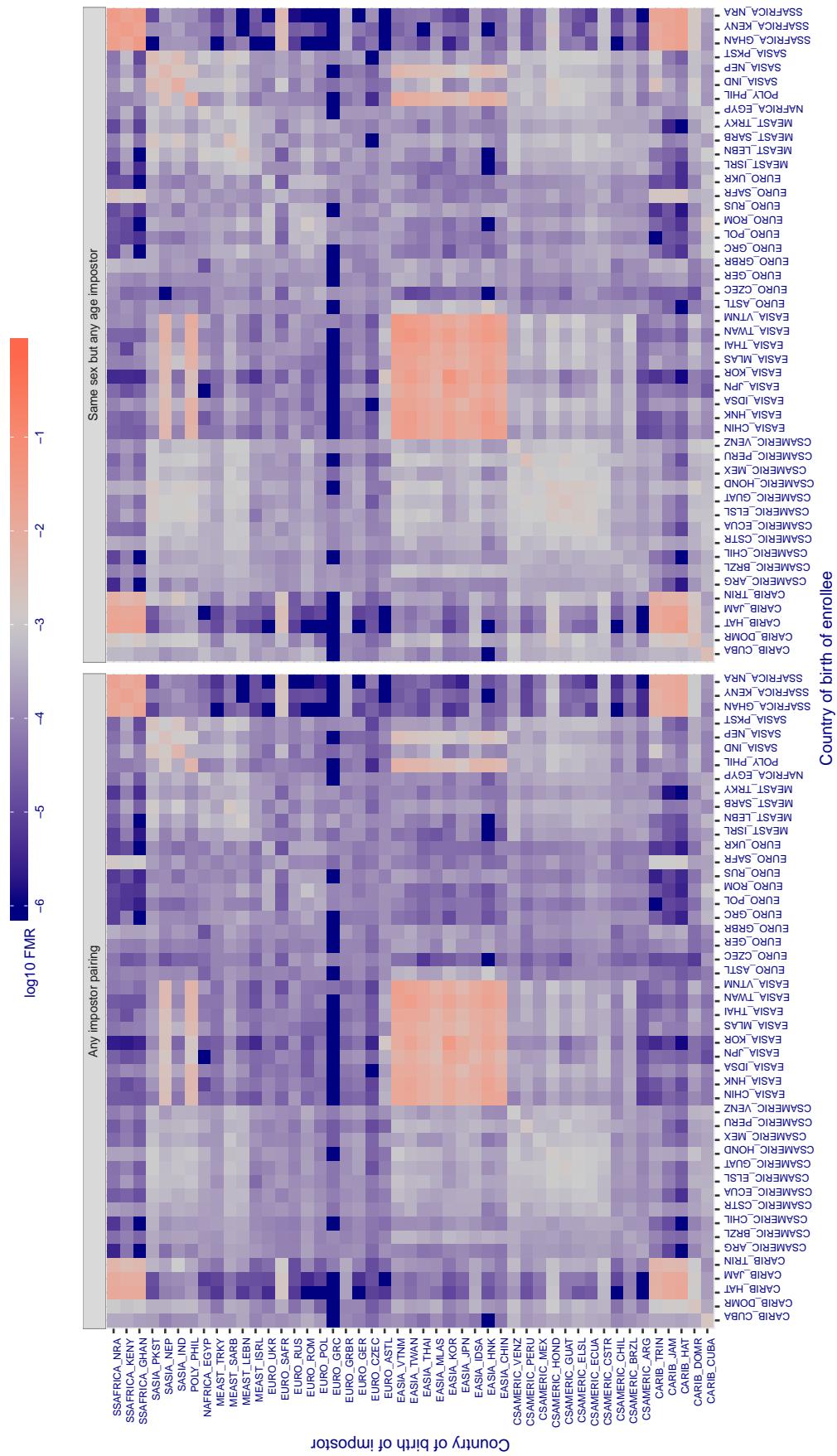
Cross country FMR at threshold T = 0.609 for algorithm saffe_001, giving FMR(T) = 0.001 globally.

Figure 382: For algorithm saffe-001 operating on visa images, the heatmap shows false match rates observed over impostor comparisons of faces from different individuals who were born in the given country pair. False matches are counted against a recognition threshold fixed globally to give the target FMR in the plot title, computed over all on the order of 10^{10} impostor comparisons. If text appears in each box it give the same quantity as that coded by the color. Grey indicates FMR is at the intended FMR target level. Light red colors present a security vulnerability to, for example, a passport gate. Each +1 increase in $\log_{10} \text{FMR}$ corresponds to a factor of 10 increase in FMR. The matrix is not quite symmetric because images in the enrollment and verification sets are different.

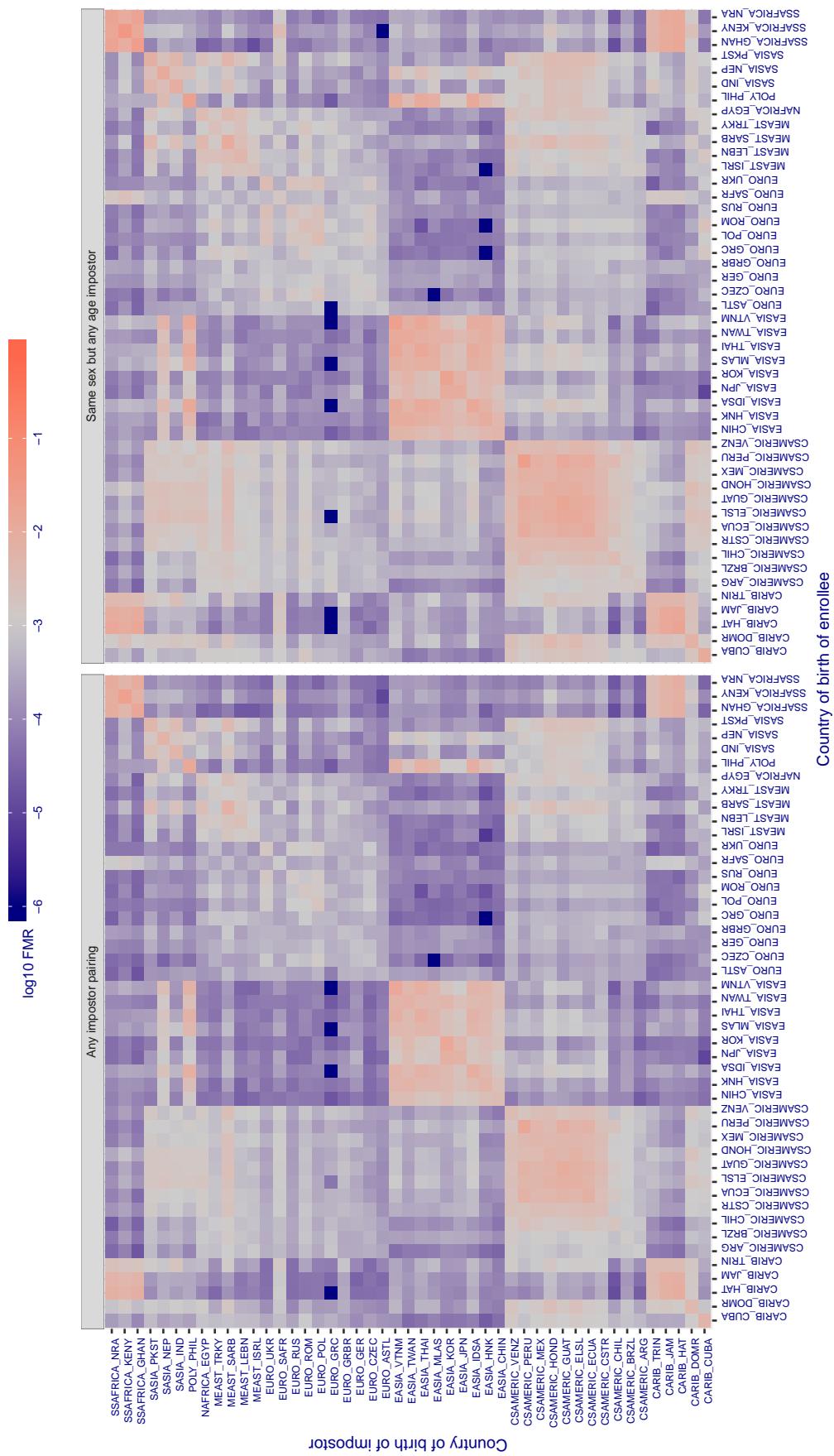
Cross country FMR at threshold T = 0.295 for algorithm safe_002, giving $FMR(T) = 0.001$ globally.

Figure 383: For algorithm safe-002 operating on visa images, the heatmap shows false match rates observed over impostor comparisons of faces from different individuals who were born in the given country pair. False matches are counted against a recognition threshold fixed globally to give the target FMR in the plot title, computed over all on the order of 10^{10} impostor comparisons. If text appears in each box it give the same quantity as that coded by the color. Grey indicates FMR is at the intended FMR target level. Light red colors present a security vulnerability to, for example, a passport gate. Each +1 increase in $\log_{10} FMR$ corresponds to a factor of 10 increase in FMR . The matrix is not quite symmetric because images in the enrollment and verification sets are different.

Cross country FMR at threshold T = 0.368 for algorithm sensetime_001, giving $\text{FMR}(T) = 0.001$ globally.

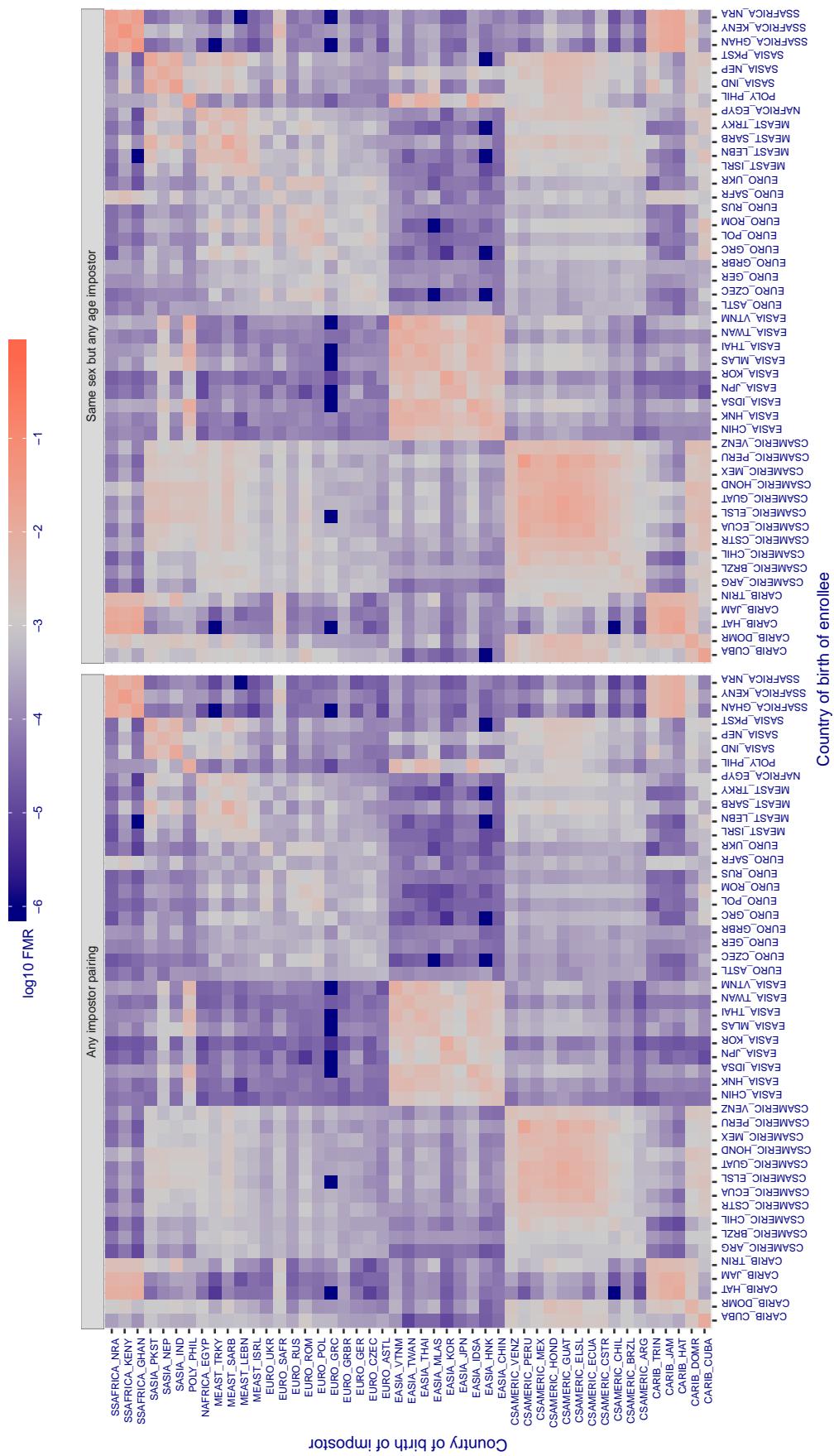


Figure 384: For algorithm sensetime-001 operating on visa images, the heatmap shows false match rates observed over impostor comparisons of faces from different individuals who were born in the given country pair. False matches are counted against a recognition threshold fixed globally to give the target FMR in the plot title, computed over all on the order of 10^{10} impostor comparisons. If text appears in each box it give the same quantity as that coded by the color. Grey indicates FMR is at the intended FMR target level. Light red colors present a security vulnerability to, for example, a passport gate. Each +1 increase in $\log_{10} \text{FMR}$ corresponds to a factor of 10 increase in FMR . The matrix is not quite symmetric because images in the enrollment and verification sets are different.

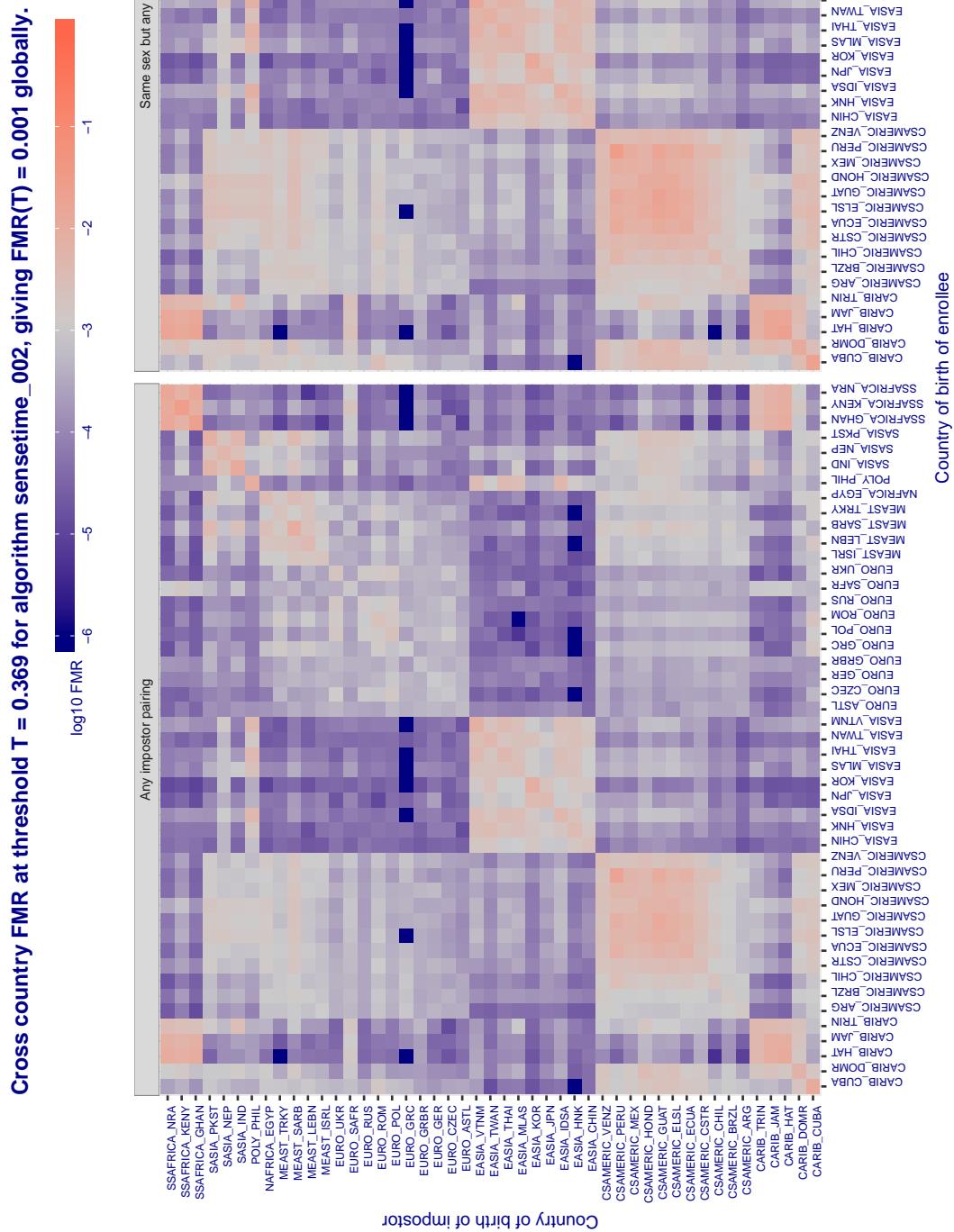


Figure 385: For algorithm sensetime-002 operating on visa images, the heatmap shows false match rates observed over impostor comparisons of faces from different individuals who were born in the given country pair. False matches are counted against a recognition threshold fixed globally to give the target FMR in the plot title, computed over all on the order of 10^{10} impostor comparisons. If text appears in each box it give the same quantity as that coded by the color. Grey indicates FMR is at the intended FMR target level. Light red colors present a security vulnerability to, for example, a passport gate. Each +1 increase in $\log_{10} \text{FMR}$ corresponds to a factor of 10 increase in FMR . The matrix is not quite symmetric because images in the enrollment and verification sets are different.

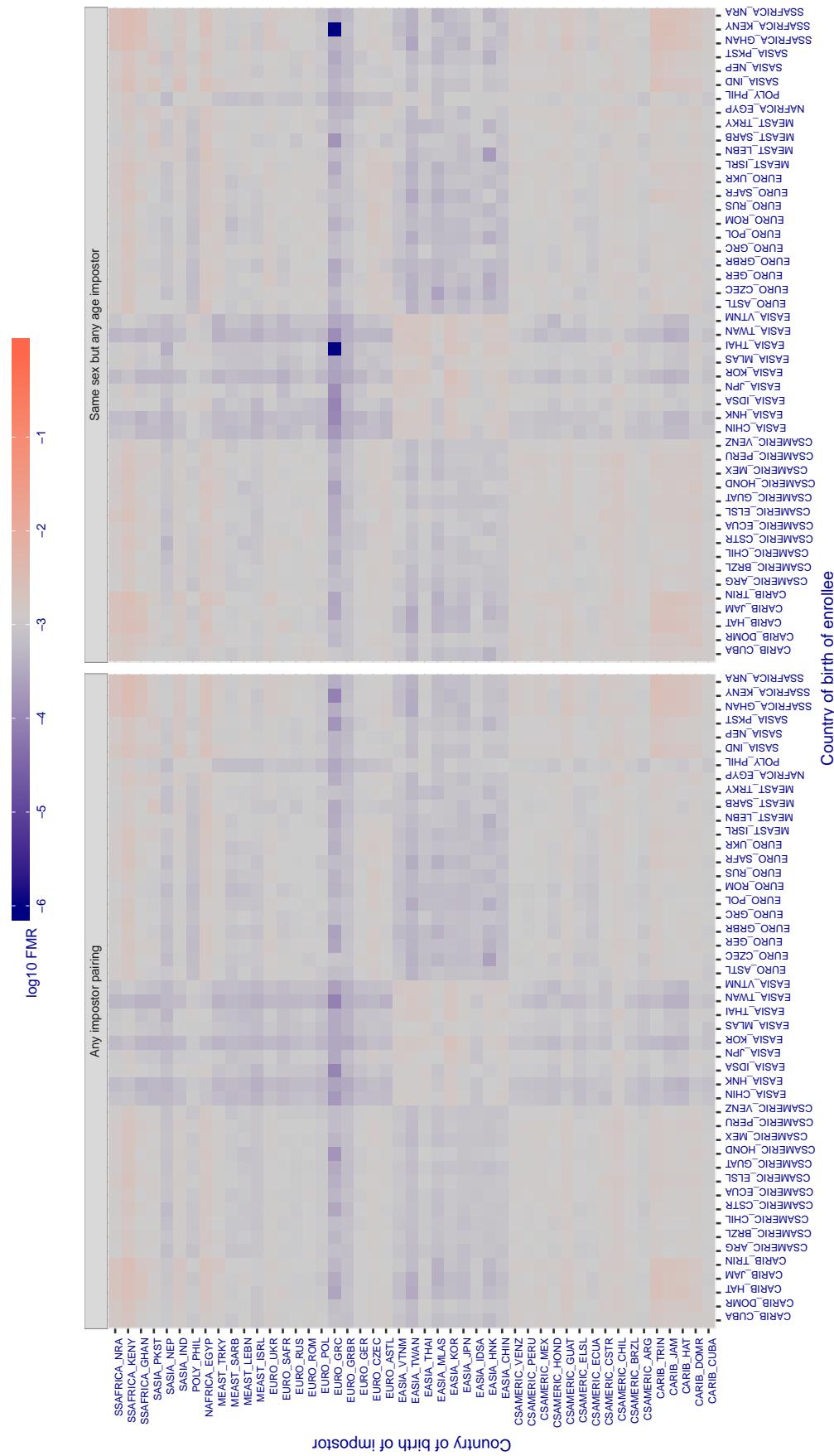
Cross country FMR at threshold T = 0.939 for algorithm shaman_000, giving $\text{FMR}(T) = 0.001$ globally.

Figure 386: For algorithm shaman-000 operating on visa images, the heatmap shows false match rates observed over impostor comparisons of faces from different individuals who were born in the given country pair. False matches are counted against a recognition threshold fixed globally to give the target FMR in the plot title, computed over all on the order of 10^{10} impostor comparisons. If text appears in each box it give the same quantity as that coded by the color. Grey indicates FMR is at the intended FMR target level. Light red colors present a security vulnerability to, for example, a passport gate. Each +1 increase in $\log_{10} \text{FMR}$ corresponds to a factor of 10 increase in FMR . The matrix is not quite symmetric because images in the enrollment and verification sets are different.

Cross country FMR at threshold T = 0.599 for algorithm shaman_001, giving $\text{FMR}(T) = 0.001$ globally.

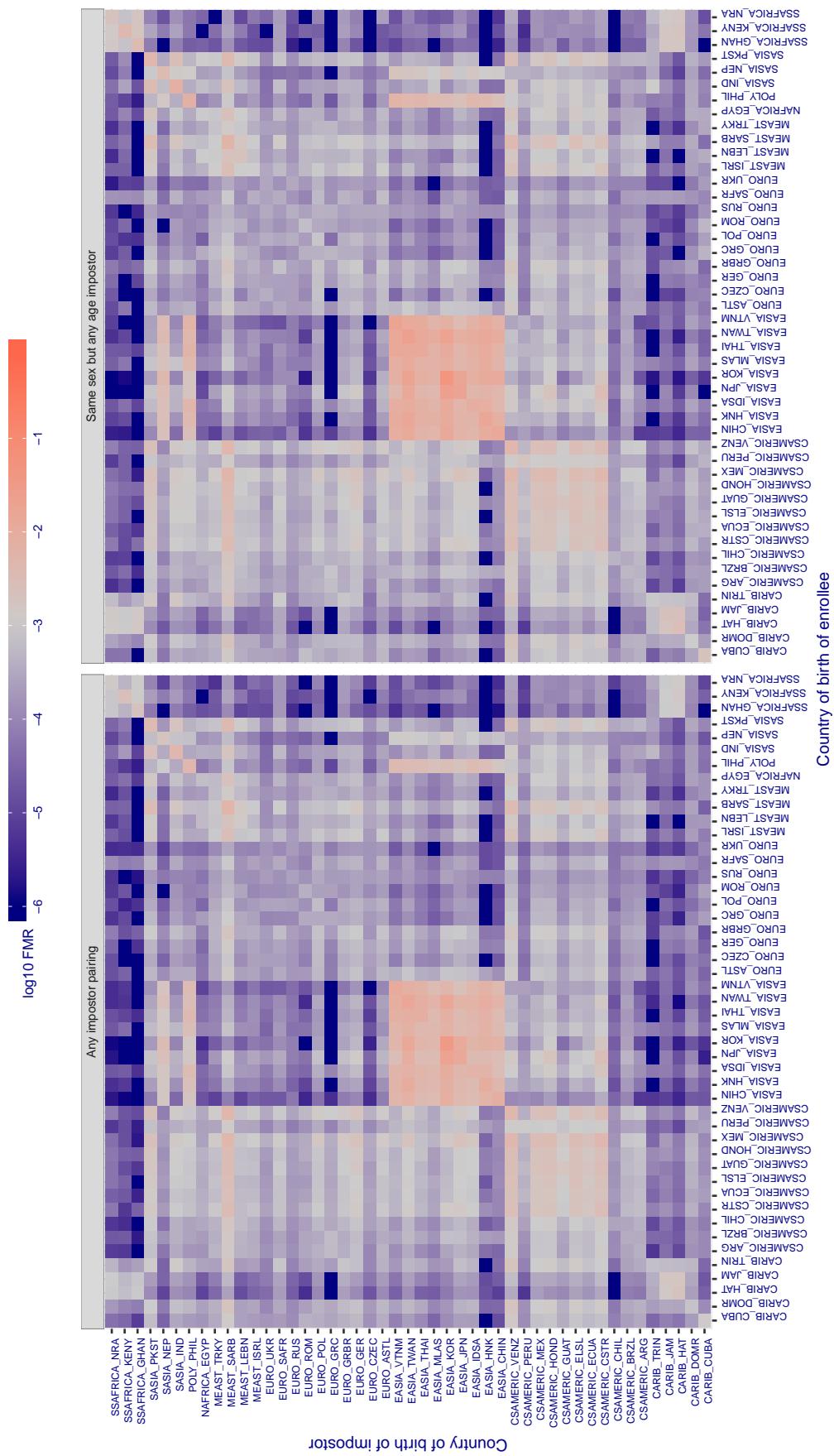


Figure 387: For algorithm shaman-001 operating on visa images, the heatmap shows false match rates observed over impostor comparisons of faces from different individuals who were born in the given country pair. False matches are counted against a recognition threshold fixed globally to give the target FMR in the plot title, computed over all on the order of 10^{10} impostor comparisons. If text appears in each box it give the same quantity as that coded by the color. Grey indicates FMR is at the intended FMR target level. Light red colors present a security vulnerability to, for example, a passport gate. Each +1 increase in $\log_{10} \text{FMR}$ corresponds to a factor of 10 increase in FMR . The matrix is not quite symmetric because images in the enrollment and verification sets are different.

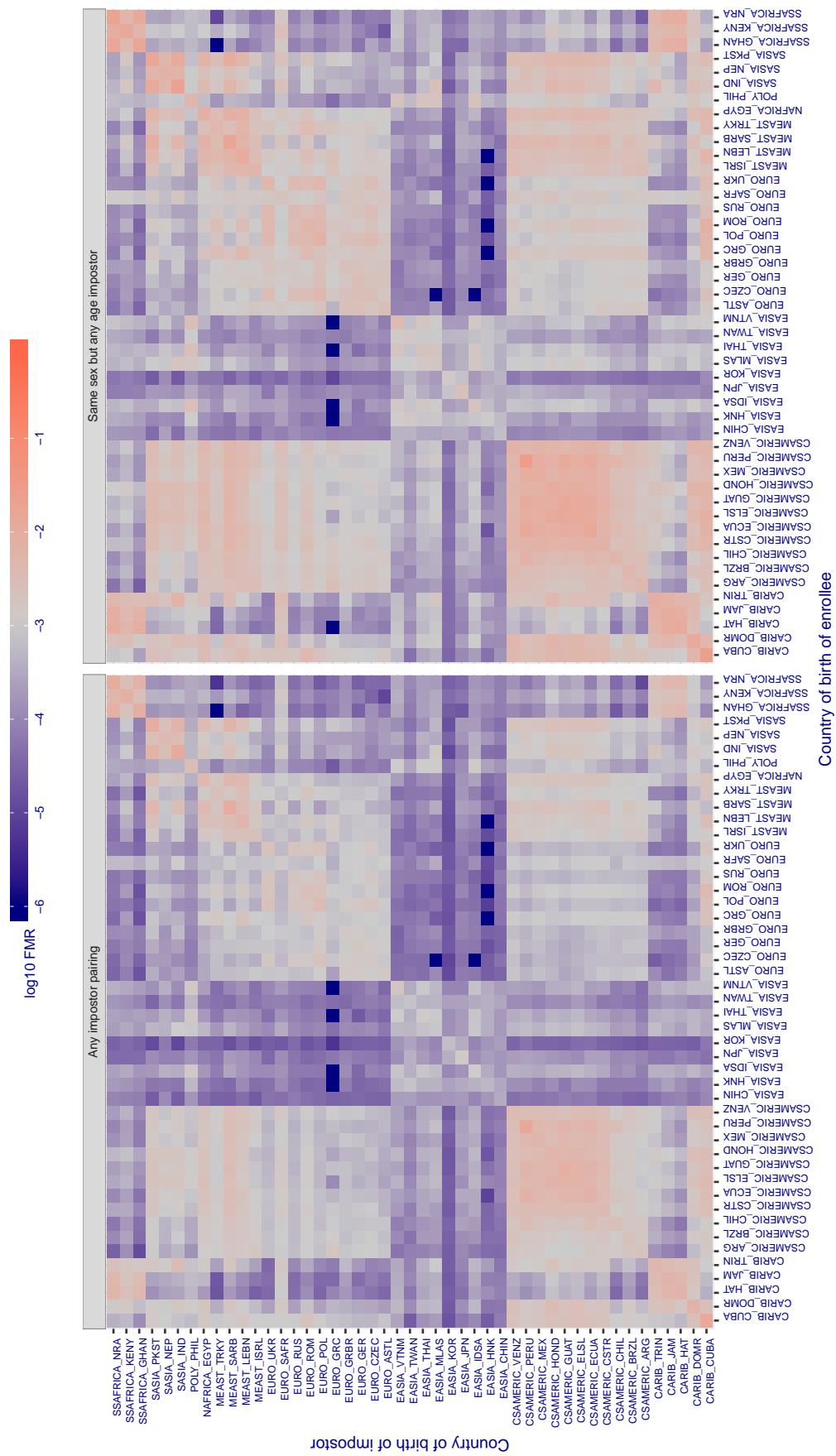
Cross country FMR at threshold T = 0.316 for algorithm shu_001, giving FMR(T) = 0.001 globally.

Figure 388: For algorithm shu-001 operating on visa images, the heatmap shows false match rates observed over impostor comparisons of faces from different individuals who were born in the given country pair. False matches are counted against a recognition threshold fixed globally to give the target FMR in the plot title, computed over all on the order of 10^{10} impostor comparisons. If text appears in each box it give the same quantity as that coded by the color. Grey indicates FMR is at the intended FMR target level. Light red colors present a security vulnerability to, for example, a passport gate. Each +1 increase in $\log_{10} \text{FMR}$ corresponds to a factor of 10 increase in FMR. The matrix is not quite symmetric because images in the enrollment and verification sets are different.

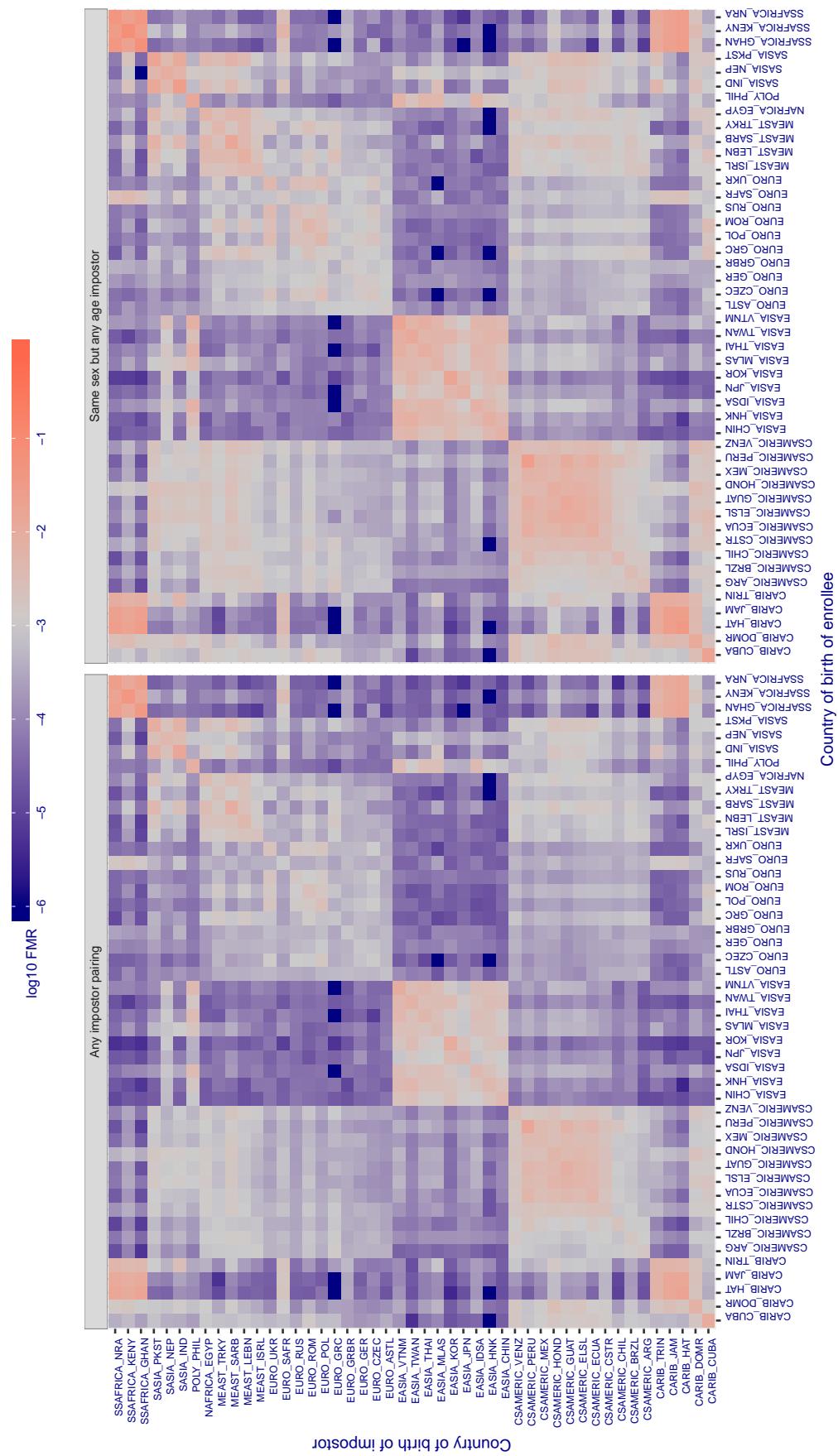
Cross country FMR at threshold T = 0.370 for algorithm siat_002, giving $FMR(T) = 0.001$ globally.

Figure 389: For algorithm siat-002 operating on visa images, the heatmap shows false match rates observed over impostor comparisons of faces from different individuals who were born in the given country pair. False matches are counted against a recognition threshold fixed globally to give the target FMR in the plot title, computed over all on the order of 10^{10} impostor comparisons. If text appears in each box it give the same quantity as that coded by the color. Grey indicates FMR is at the intended FMR target level. Light red colors present a security vulnerability to, for example, a passport gate. Each +1 increase in $\log_{10} FMR$ corresponds to a factor of 10 increase in FMR. The matrix is not quite symmetric because images in the enrollment and verification sets are different.

Cross country FMR at threshold T = 0.371 for algorithm siat_004, giving $FMR(T) = 0.001$ globally.

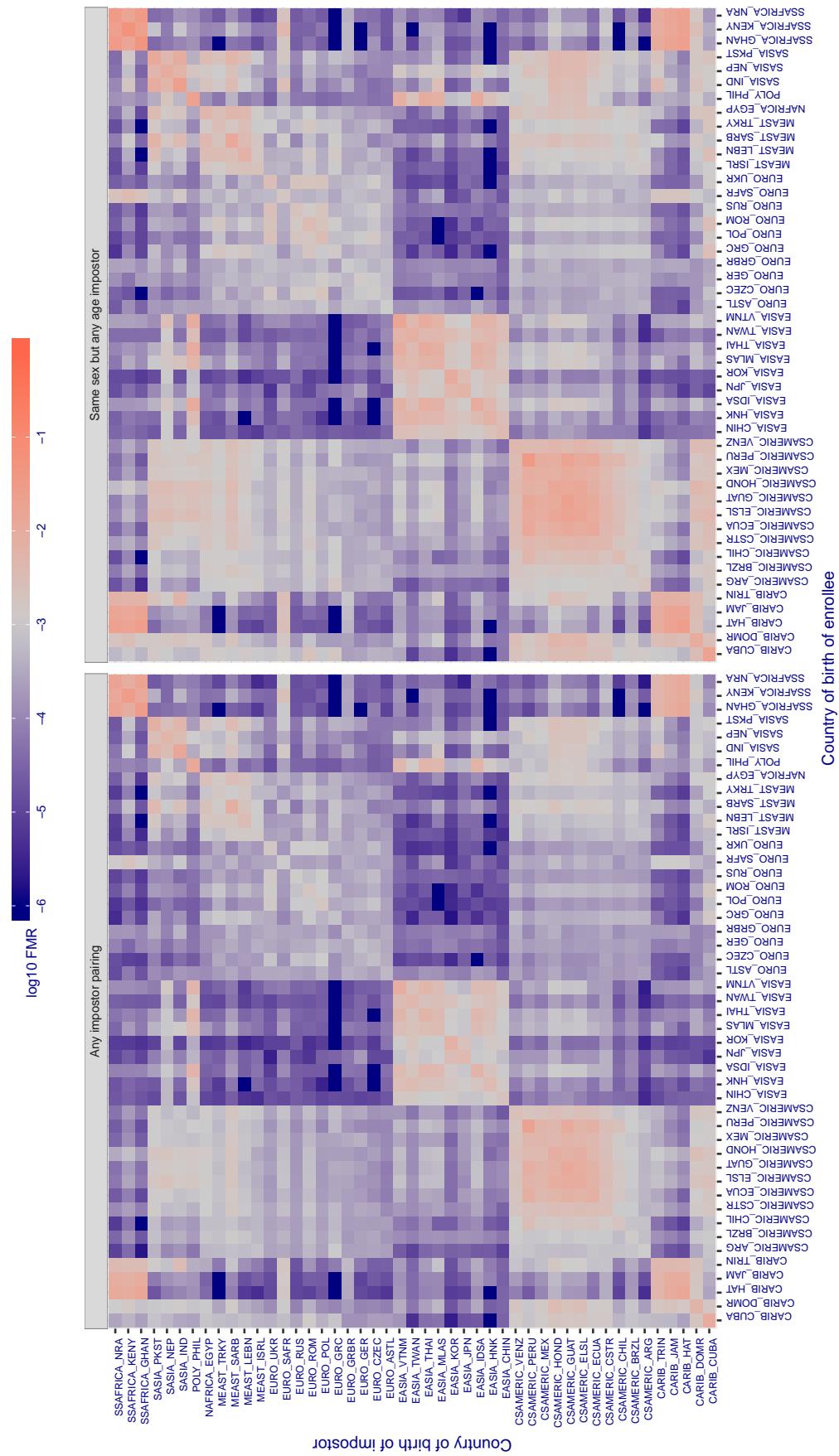


Figure 390: For algorithm siat-004 operating on visa images, the heatmap shows false match rates observed over impostor comparisons of faces from different individuals who were born in the given country pair. False matches are counted against a recognition threshold fixed globally to give the target FMR in the plot title, computed over all on the order of 10^{10} impostor comparisons. If text appears in each box it give the same quantity as that coded by the color. Grey indicates FMR is at the intended FMR target level. Light red colors present a security vulnerability to, for example, a passport gate. Each +1 increase in $\log_{10} FMR$ corresponds to a factor of 10 increase in FMR. The matrix is not quite symmetric because images in the enrollment and verification sets are different.

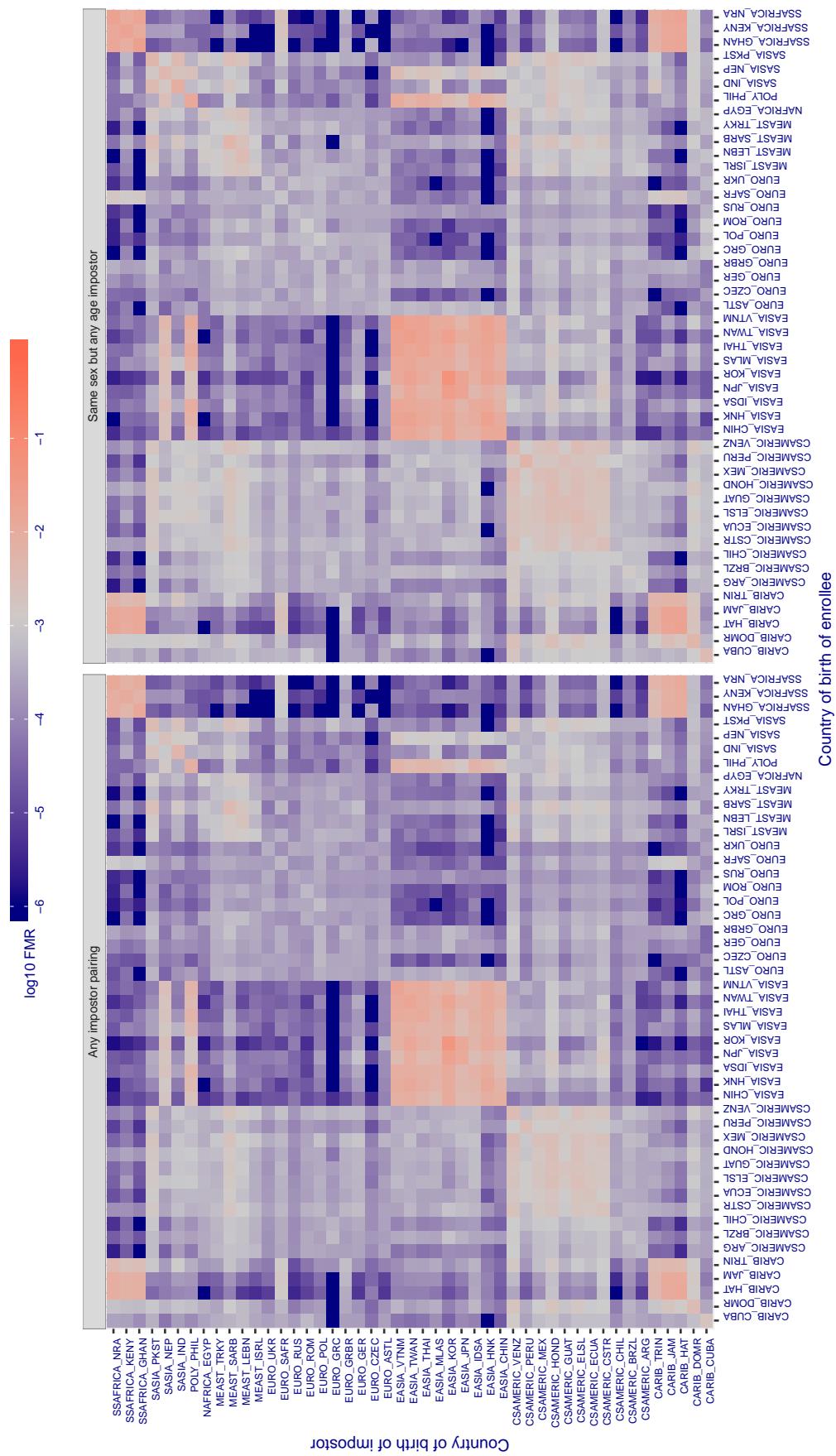
Cross country FMR at threshold T = 0.488 for algorithm similart_002, giving $FMR(T) = 0.001$ globally.

Figure 391: For algorithm similart-002 operating on visa images, the heatmap shows false match rates observed over impostor comparisons of faces from different individuals who were born in the given country pair. False matches are counted against a recognition threshold fixed globally to give the target FMR in the plot title, computed over all on the order of 10^{10} impostor comparisons. If text appears in each box it give the same quantity as that coded by the color. Grey indicates FMR is at the intended FMR target level. Light red colors present a security vulnerability to, for example, a passport gate. Each +1 increase in $\log_{10} FMR$ corresponds to a factor of 10 increase in FMR . The matrix is not quite symmetric because images in the enrollment and verification sets are different.

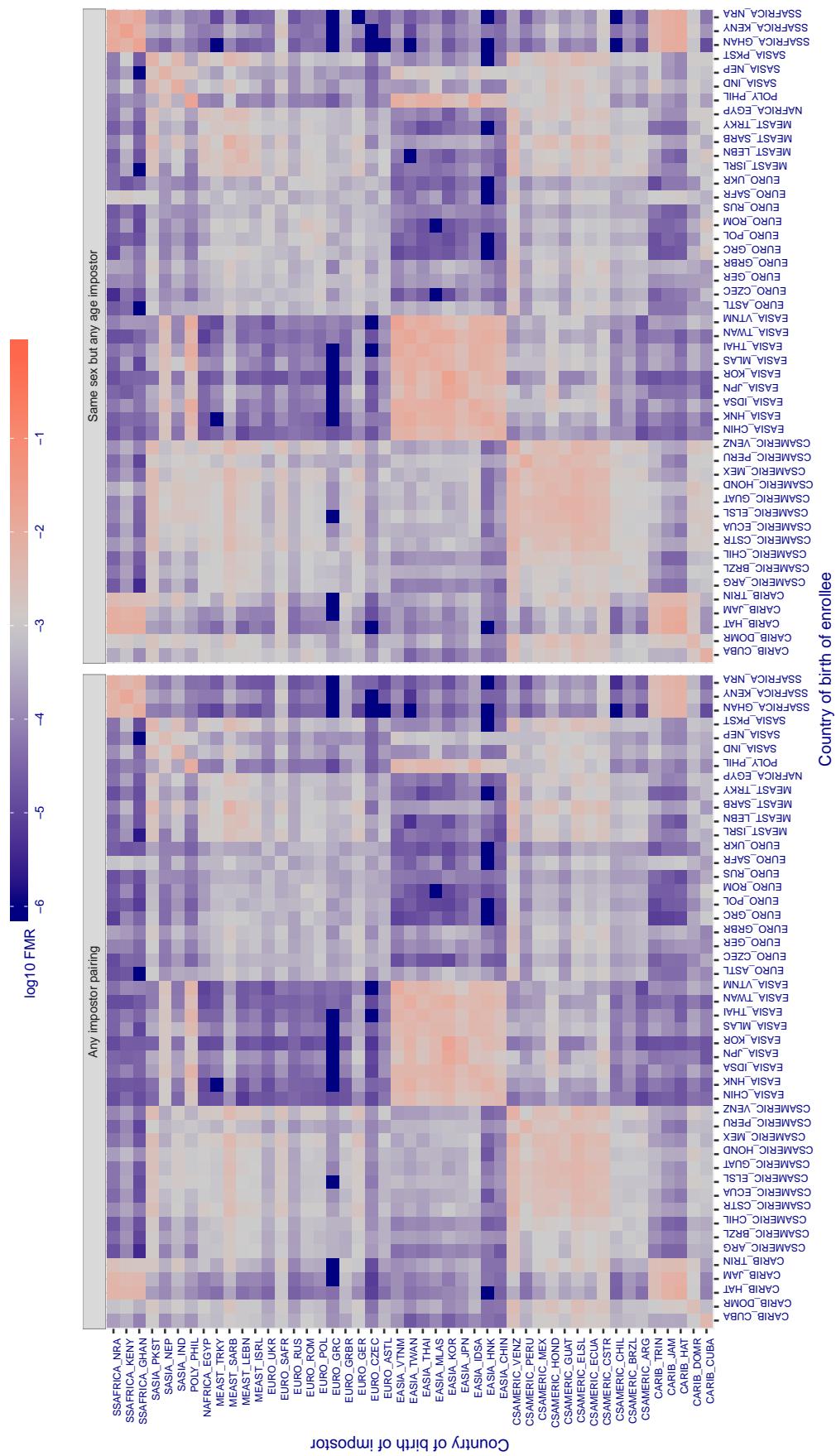
Cross country FMR at threshold T = 0.388 for algorithm similart_003, giving $FMR(T) = 0.001$ globally.

Figure 392: For algorithm similart-003 operating on visa images, the heatmap shows false match rates observed over impostor comparisons of faces from different individuals who were born in the given country pair. False matches are counted against a recognition threshold fixed globally to give the target FMR in the plot title, computed over all on the order of 10^{10} impostor comparisons. If text appears in each box it give the same quantity as that coded by the color. Grey indicates FMR is at the intended FMR target level. Light red colors present a security vulnerability to, for example, a passport gate. Each +1 increase in $\log_{10} FMR$ corresponds to a factor of 10 increase in FMR . The matrix is not quite symmetric because images in the enrollment and verification sets are different.

Cross country FMR at threshold T = 0.251 for algorithm starhybrid_001, giving FMR(T) = 0.001 globally.

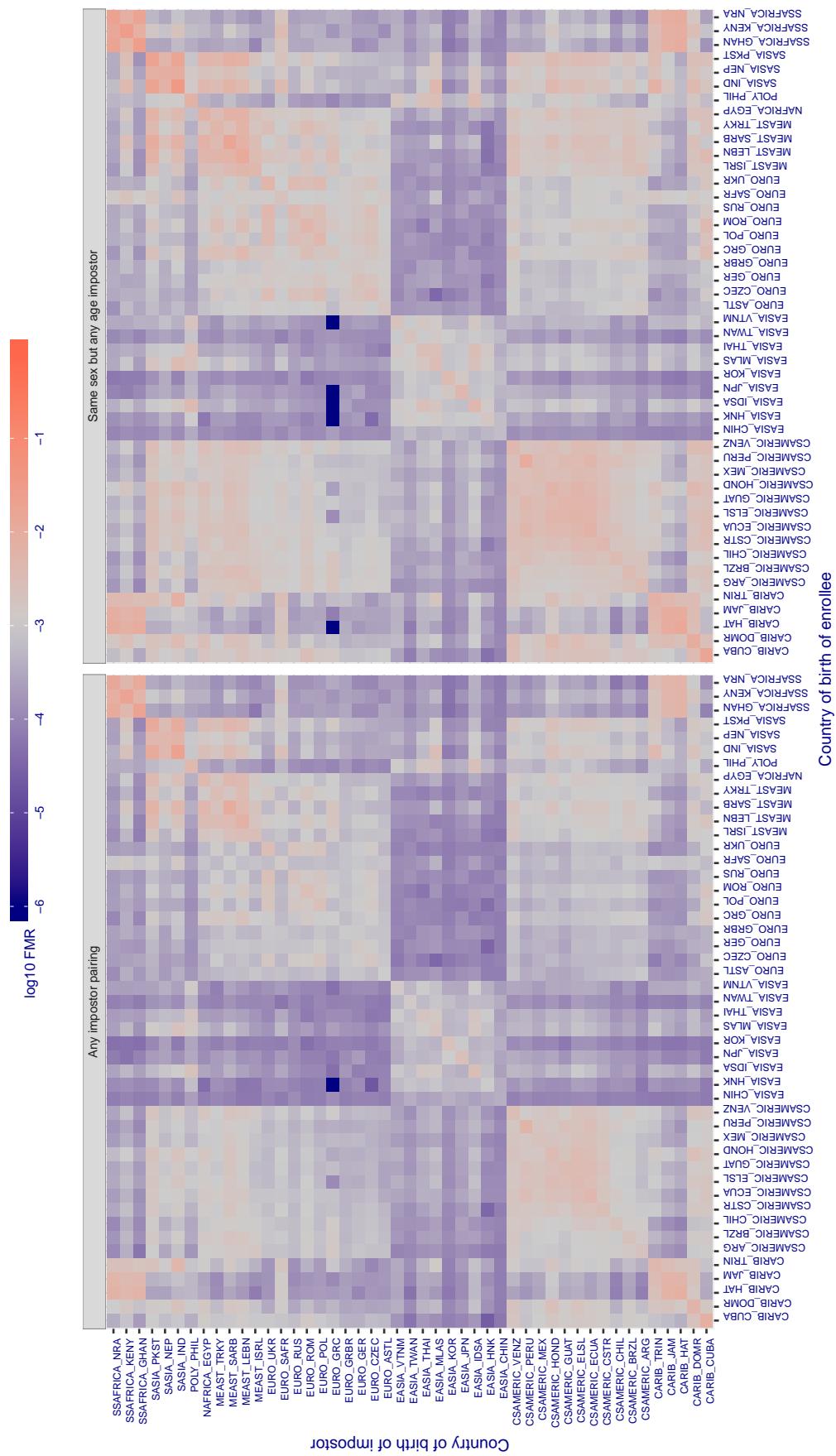


Figure 393: For algorithm starhybrid-001 operating on visa images, the heatmap shows false match rates observed over impostor comparisons of faces from different individuals who were born in the given country pair. False matches are counted against a recognition threshold fixed globally to give the target FMR in the plot title, computed over all on the order of 10^{10} impostor comparisons. If text appears in each box it give the same quantity as that coded by the color. Grey indicates FMR is at the intended FMR target level. Light red colors present a security vulnerability to, for example, a passport gate. Each +1 increase in $\log_{10} FMR$ corresponds to a factor of 10 increase in FMR. The matrix is not quite symmetric because images in the enrollment and verification sets are different.

Cross country FMR at threshold T = 0.047 for algorithm synesis_004, giving $\text{FMR}(T) = 0.001$ globally.

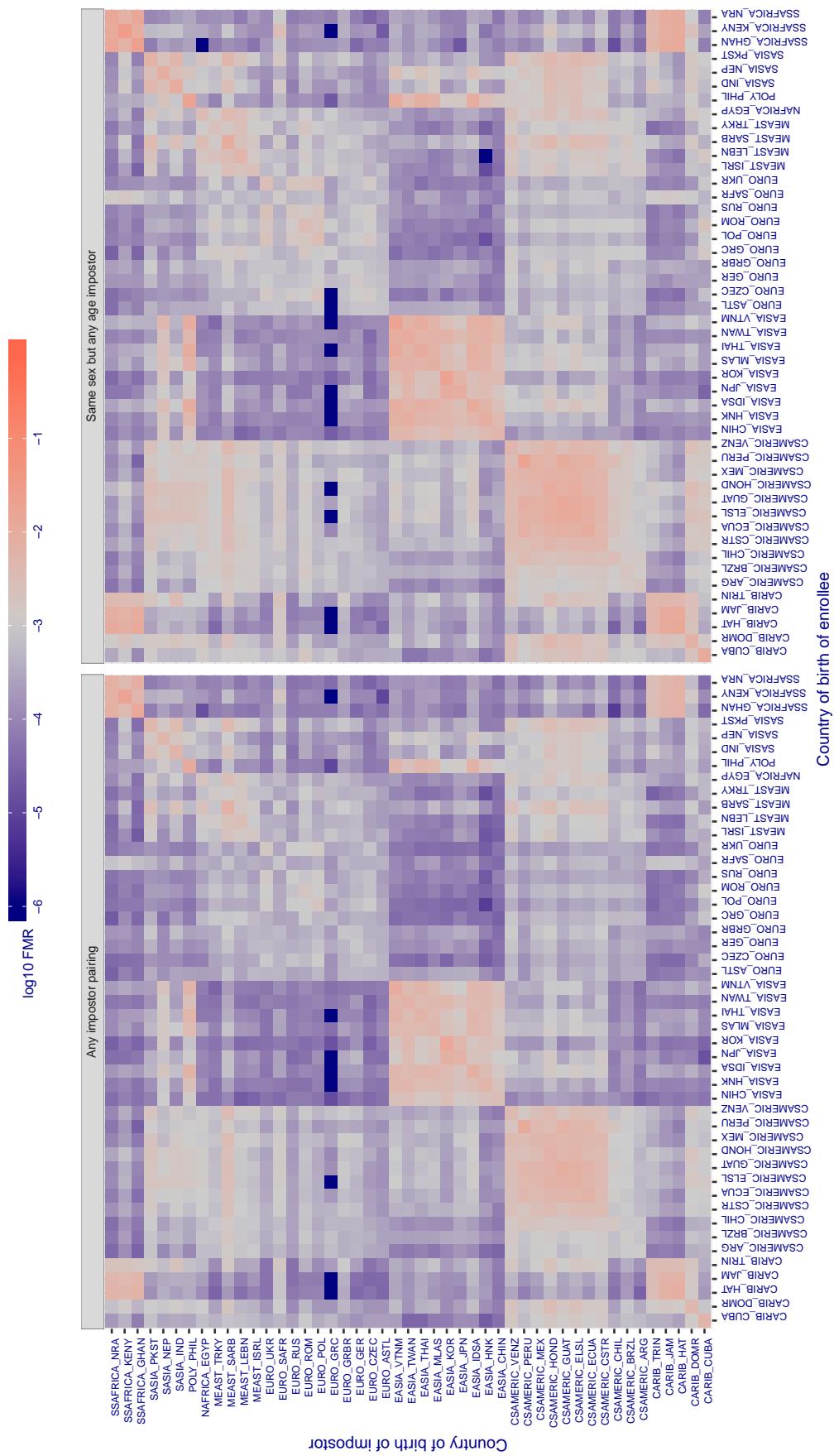


Figure 394: For algorithm synesis-004 operating on visa images, the heatmap shows false match rates observed over impostor comparisons of faces from different individuals who were born in the given country pair. False matches are counted against a recognition threshold fixed globally to give the target FMR in the plot title, computed over all on the order of 10^{10} impostor comparisons. If text appears in each box it give the same quantity as that coded by the color. Grey indicates FMR is at the intended FMR target level. Light red colors present a security vulnerability to, for example, a passport gate. Each +1 increase in $\log_{10} \text{FMR}$ corresponds to a factor of 10 increase in FMR . The matrix is not quite symmetric because images in the enrollment and verification sets are different.

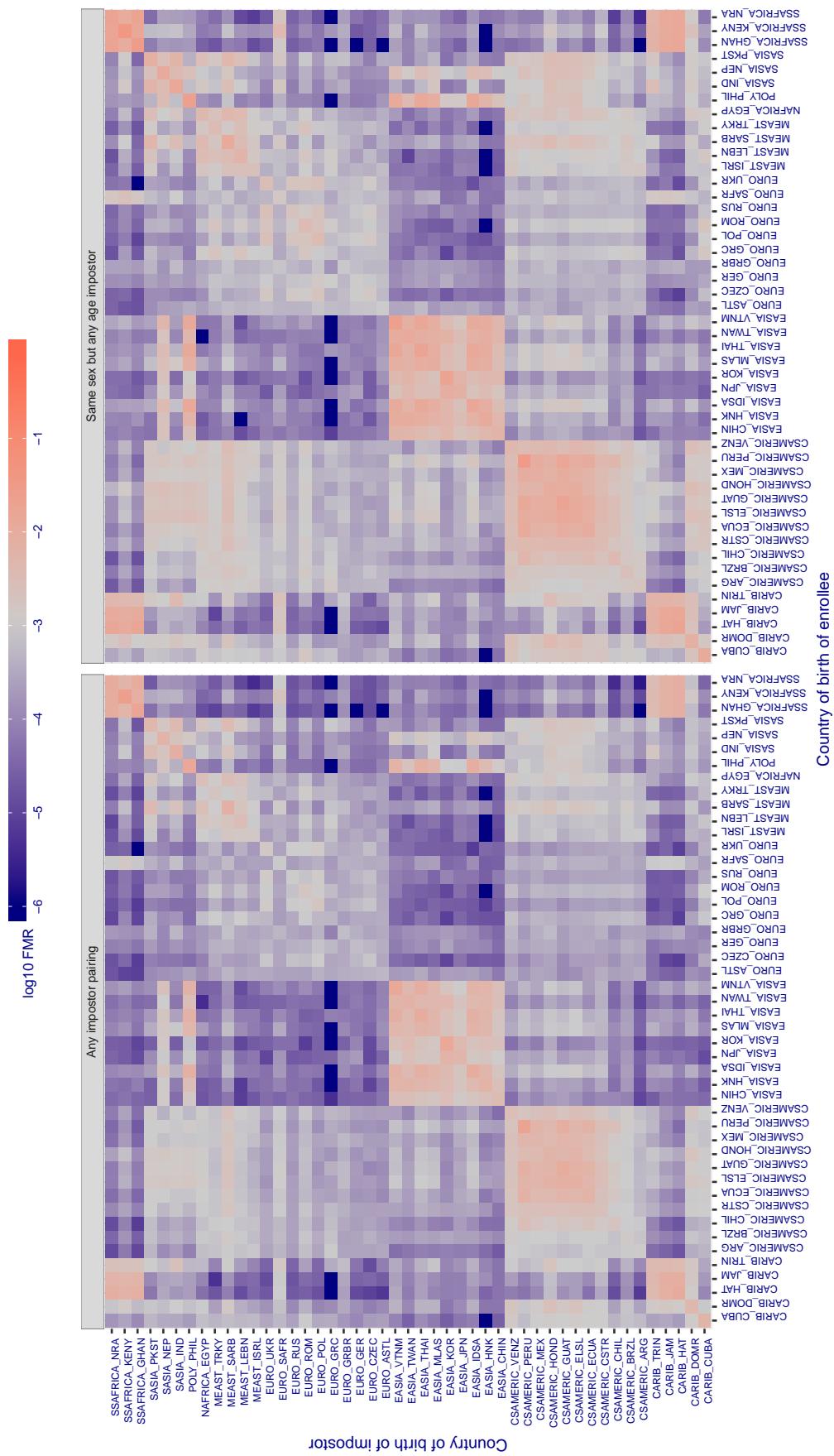
Cross country FMR at threshold T = 0.274 for algorithm synthesis_005, giving $\text{FMR}(T) = 0.001$ globally.

Figure 395: For algorithm synthesis-005 operating on visa images, the heatmap shows false match rates observed over impostor comparisons of faces from different individuals who were born in the given country pair. False matches are counted against a recognition threshold fixed globally to give the target FMR in the plot title, computed over all on the order of 10^{10} impostor comparisons. If text appears in each box it give the same quantity as that coded by the color. Grey indicates FMR is at the intended FMR target level. Light red colors present a security vulnerability to, for example, a passport gate. Each +1 increase in $\log_{10} \text{FMR}$ corresponds to a factor of 10 increase in FMR . The matrix is not quite symmetric because images in the enrollment and verification sets are different.

Cross country FMR at threshold T = 147.234 for algorithm tech5_002, giving $FMR(T) = 0.001$ globally.

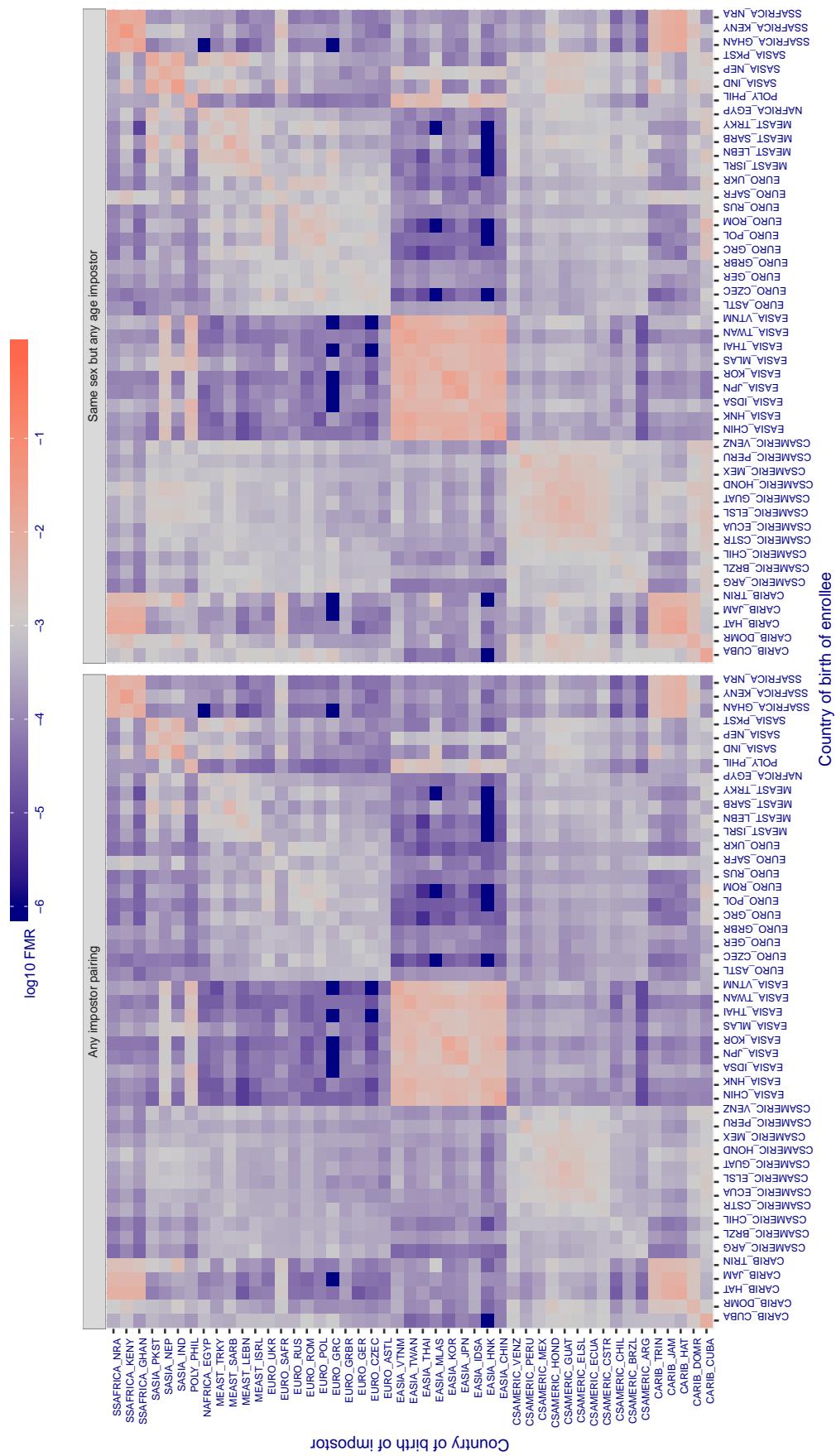


Figure 396: For algorithm tech5-002 operating on visa images, the heatmap shows false match rates observed over impostor comparisons of faces from different individuals who were born in the given country pair. False matches are counted against a recognition threshold fixed globally to give the target FMR in the plot title, computed over all on the order of 10^{10} impostor comparisons. If text appears in each box it give the same quantity as that coded by the color. Grey indicates FMR is at the intended FMR target level. Light red colors present a security vulnerability to, for example, a passport gate. Each +1 increase in $\log_{10} FMR$ corresponds to a factor of 10 increase in FMR. The matrix is not quite symmetric because images in the enrollment and verification sets are different.

Cross country FMR at threshold T = 146.607 for algorithm tech5_003, giving $FMR(T) = 0.001$ globally.

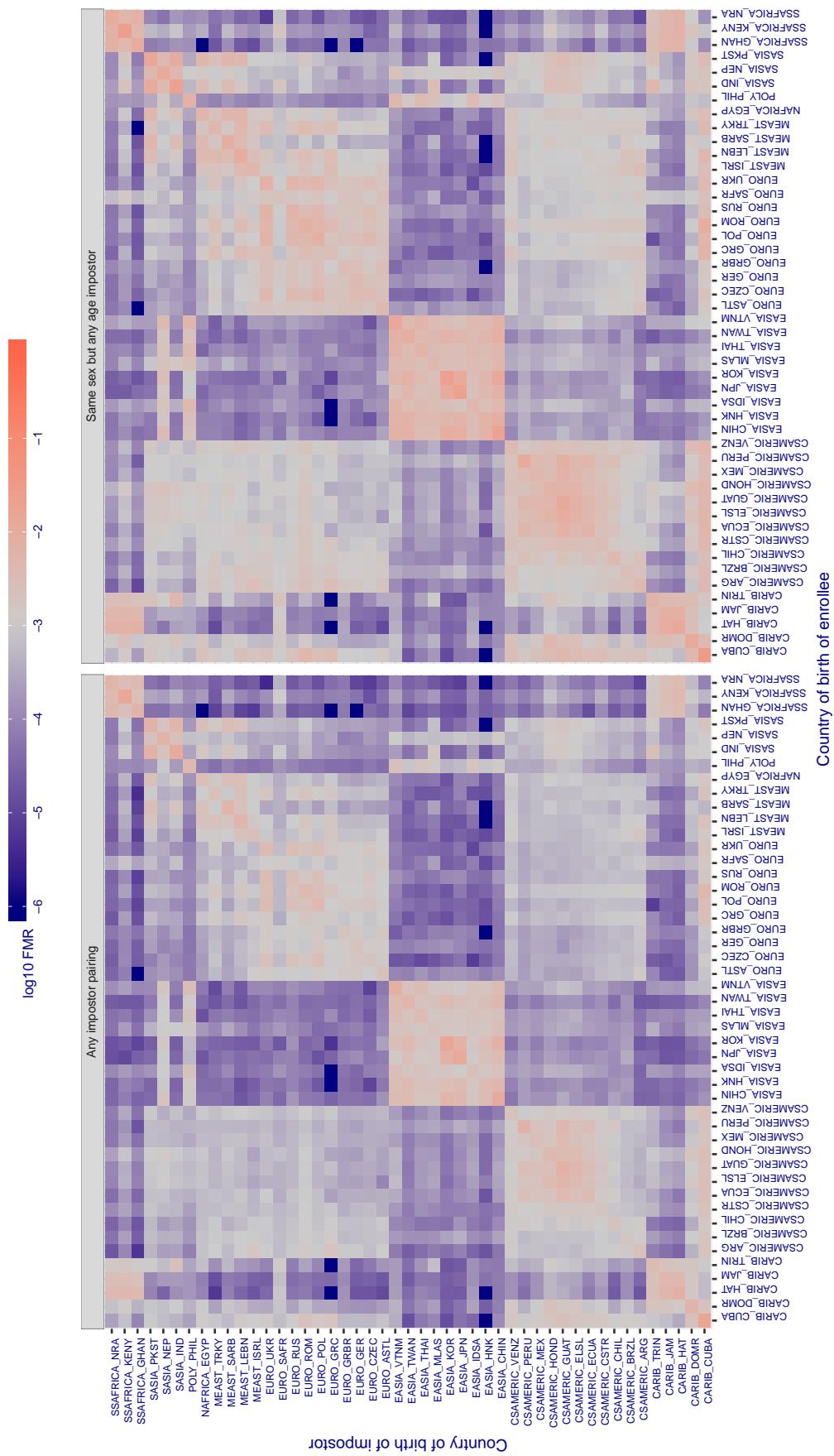


Figure 397: For algorithm tech5-003 operating on visa images, the heatmap shows false match rates observed over impostor comparisons of faces from different individuals who were born in the given country pair. False matches are counted against a recognition threshold fixed globally to give the target FMR in the plot title, computed over all on the order of 10^{10} impostor comparisons. If text appears in each box it give the same quantity as that coded by the color. Grey indicates FMR is at the intended FMR target level. Light red colors present a security vulnerability to, for example, a passport gate. Each +1 increase in $\log_{10} FMR$ corresponds to a factor of 10 increase in FMR. The matrix is not quite symmetric because images in the enrollment and verification sets are different.

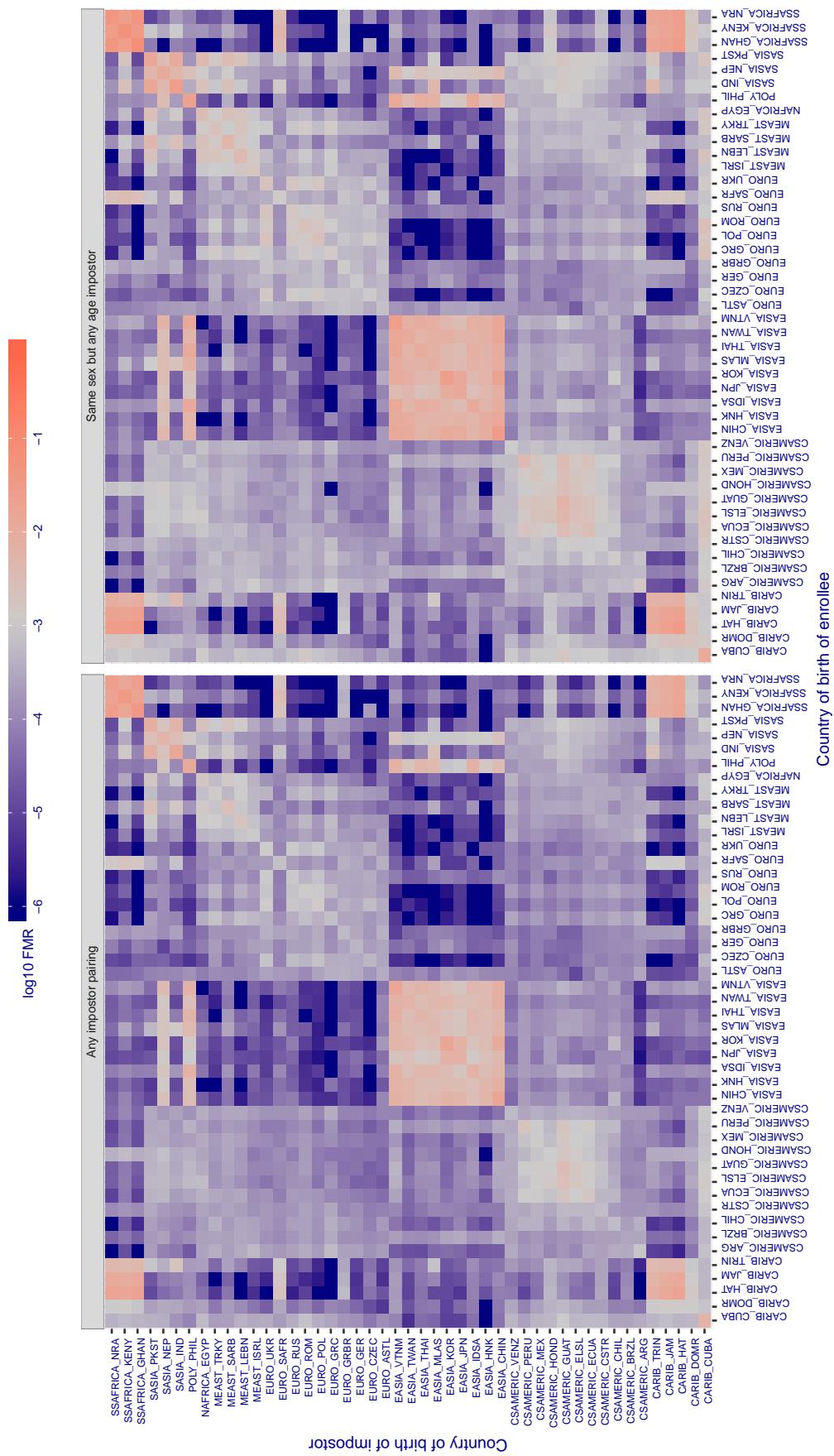
Cross country FMR at threshold T = 0.769 for algorithm tevian_003, giving $FMR(T) = 0.001$ globally.

Figure 398: For algorithm tevian-003 operating on visa images, the heatmap shows false match rates observed over impostor comparisons of faces from different individuals who were born in the given country pair. False matches are counted against a recognition threshold fixed globally to give the target FMR in the plot title, computed over all on the order of 10^{10} impostor comparisons. If text appears in each box it give the same quantity as that coded by the color. Grey indicates FMR is at the intended FMR target level. Light red colors present a security vulnerability to, for example, a passport gate. Each +1 increase in $\log_{10} FMR$ corresponds to a factor of 10 increase in FMR . The matrix is not quite symmetric because images in the enrollment and verification sets are different.

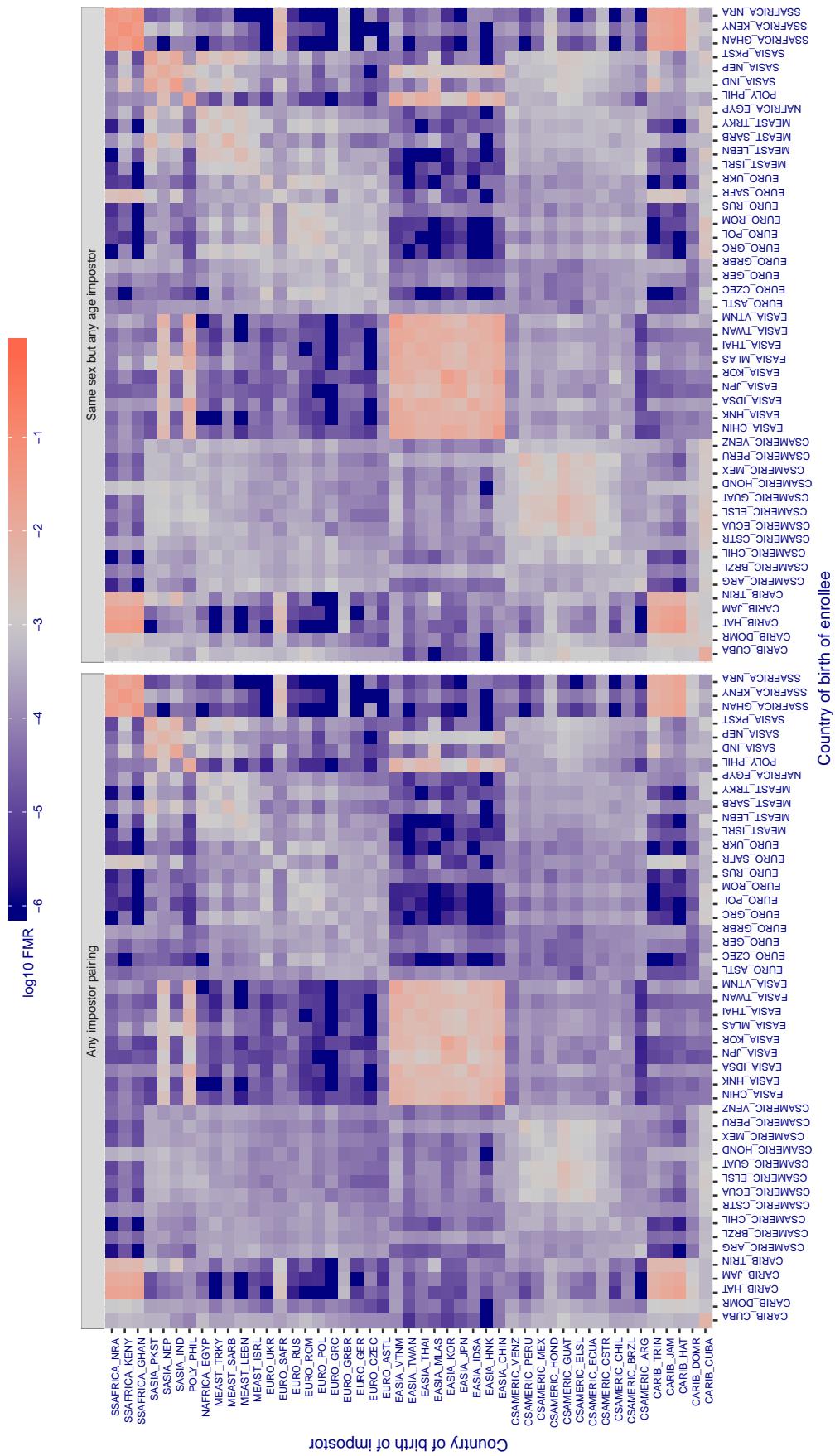
Cross country FMR at threshold T = 0.769 for algorithm tevian_004, giving $\text{FMR}(\text{T}) = 0.001$ globally.

Figure 399: For algorithm tevian-004 operating on visa images, the heatmap shows false match rates observed over impostor comparisons of faces from different individuals who were born in the given country pair. False matches are counted against a recognition threshold fixed globally to give the target FMR in the plot title, computed over all on the order of 10^{10} impostor comparisons. If text appears in each box it give the same quantity as that coded by the color. Grey indicates FMR is at the intended FMR target level. Light red colors present a security vulnerability to, for example, a passport gate. Each +1 increase in $\log_{10} \text{FMR}$ corresponds to a factor of 10 increase in FMR . The matrix is not quite symmetric because images in the enrollment and verification sets are different.

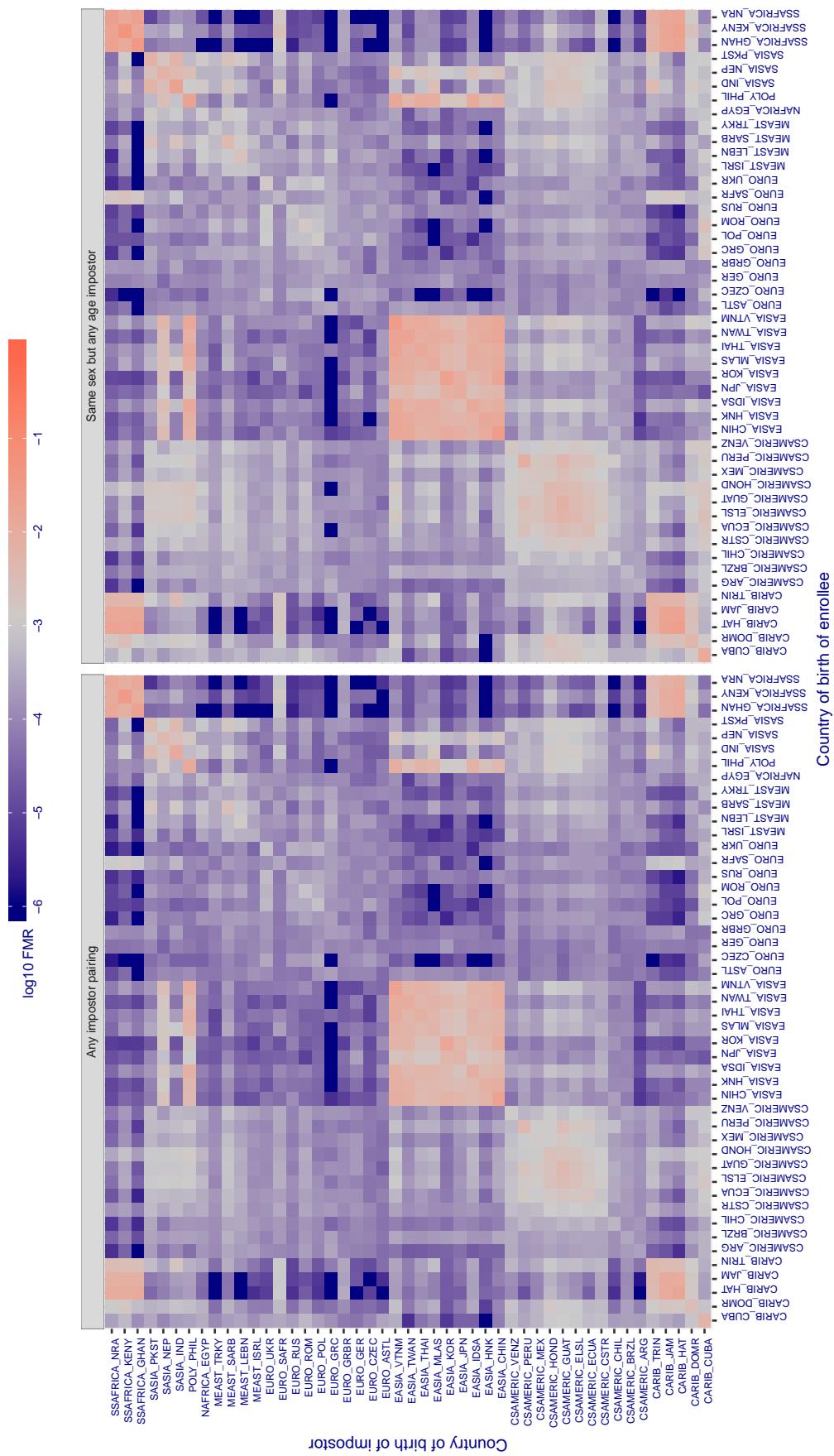
Cross country FMR at threshold T = 143.194 for algorithm tiger_002, giving $FMR(T) = 0.001$ globally.

Figure 400: For algorithm tiger-002 operating on visa images, the heatmap shows false match rates observed over impostor comparisons of faces from different individuals who were born in the given country pair. False matches are counted against a recognition threshold fixed globally to give the target FMR in the plot title, computed over all on the order of 10^{10} impostor comparisons. If text appears in each box it give the same quantity as that coded by the color. Grey indicates FMR is at the intended FMR target level. Light red colors present a security vulnerability to, for example, a passport gate. Each +1 increase in $\log_{10} FMR$ corresponds to a factor of 10 increase in FMR . The matrix is not quite symmetric because images in the enrollment and verification sets are different.

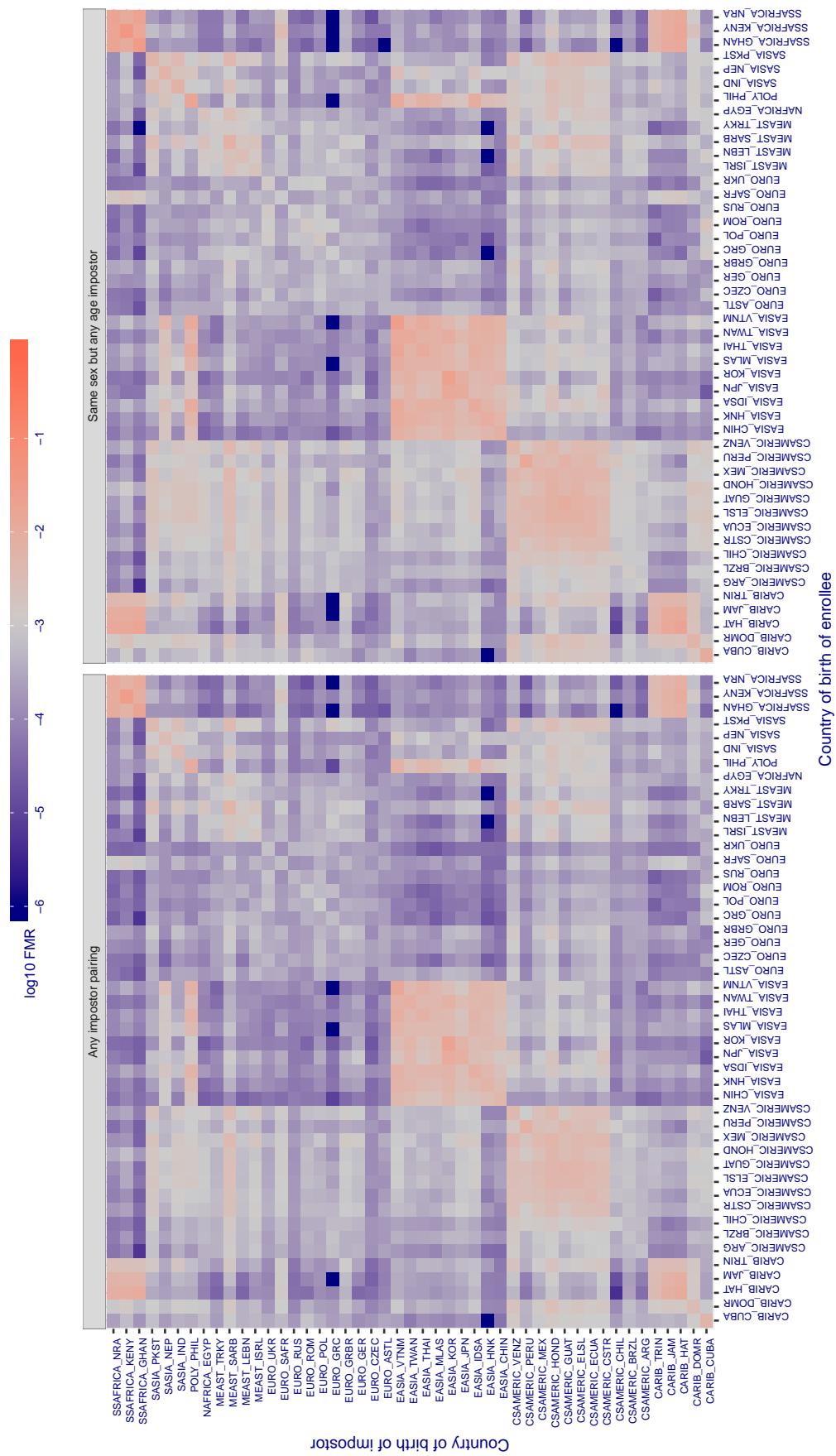
Cross country FMR at threshold T = 139.101 for algorithm tiger_003, giving $FMR(T) = 0.001$ globally.

Figure 401: For algorithm tiger-003 operating on visa images, the heatmap shows false match rates observed over impostor comparisons of faces from different individuals who were born in the given country pair. False matches are counted against a recognition threshold fixed globally to give the target FMR in the plot title, computed over all on the order of 10^{10} impostor comparisons. If text appears in each box it give the same quantity as that coded by the color. Grey indicates FMR is at the intended FMR target level. Light red colors present a security vulnerability to, for example, a passport gate. Each +1 increase in $\log_{10} FMR$ corresponds to a factor of 10 increase in FMR . The matrix is not quite symmetric because images in the enrollment and verification sets are different.

Cross country FMR at threshold T = 43.483 for algorithm tongyi_005, giving $FMR(T) = 0.001$ globally.

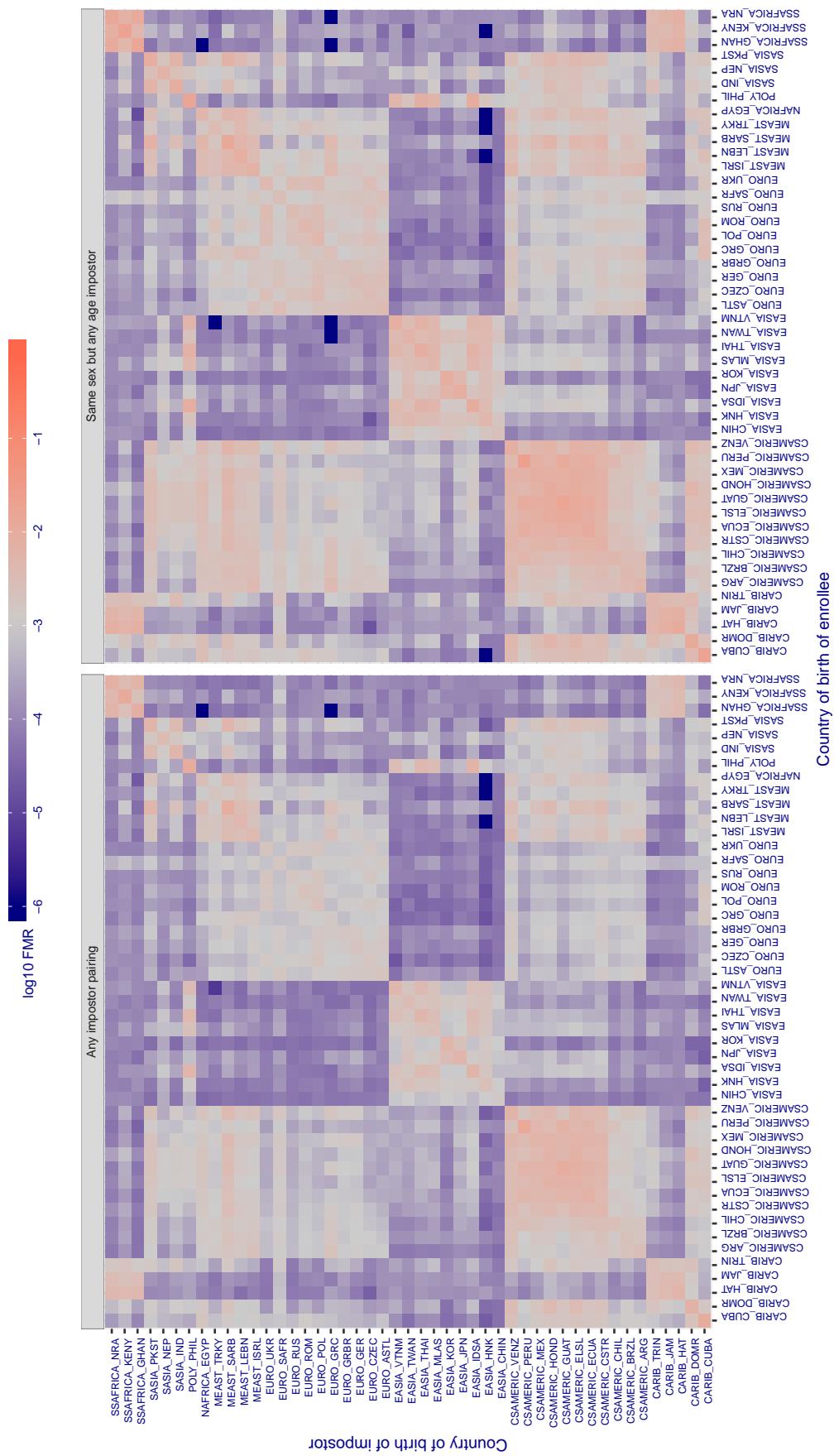


Figure 402: For algorithm tongyi-005 operating on visa images, the heatmap shows false match rates observed over impostor comparisons of faces from different individuals who were born in the given country pair. False matches are counted against a recognition threshold fixed globally to give the target FMR in the plot title, computed over all on the order of 10^{10} impostor comparisons. If text appears in each box it give the same quantity as that coded by the color. Grey indicates FMR is at the intended FMR target level. Light red colors present a security vulnerability to, for example, a passport gate. Each +1 increase in $\log_{10} FMR$ corresponds to a factor of 10 increase in FMR . The matrix is not quite symmetric because images in the enrollment and verification sets are different.

Cross country FMR at threshold T = 0.599 for algorithm toshiba_002, giving $FMR(T) = 0.001$ globally.

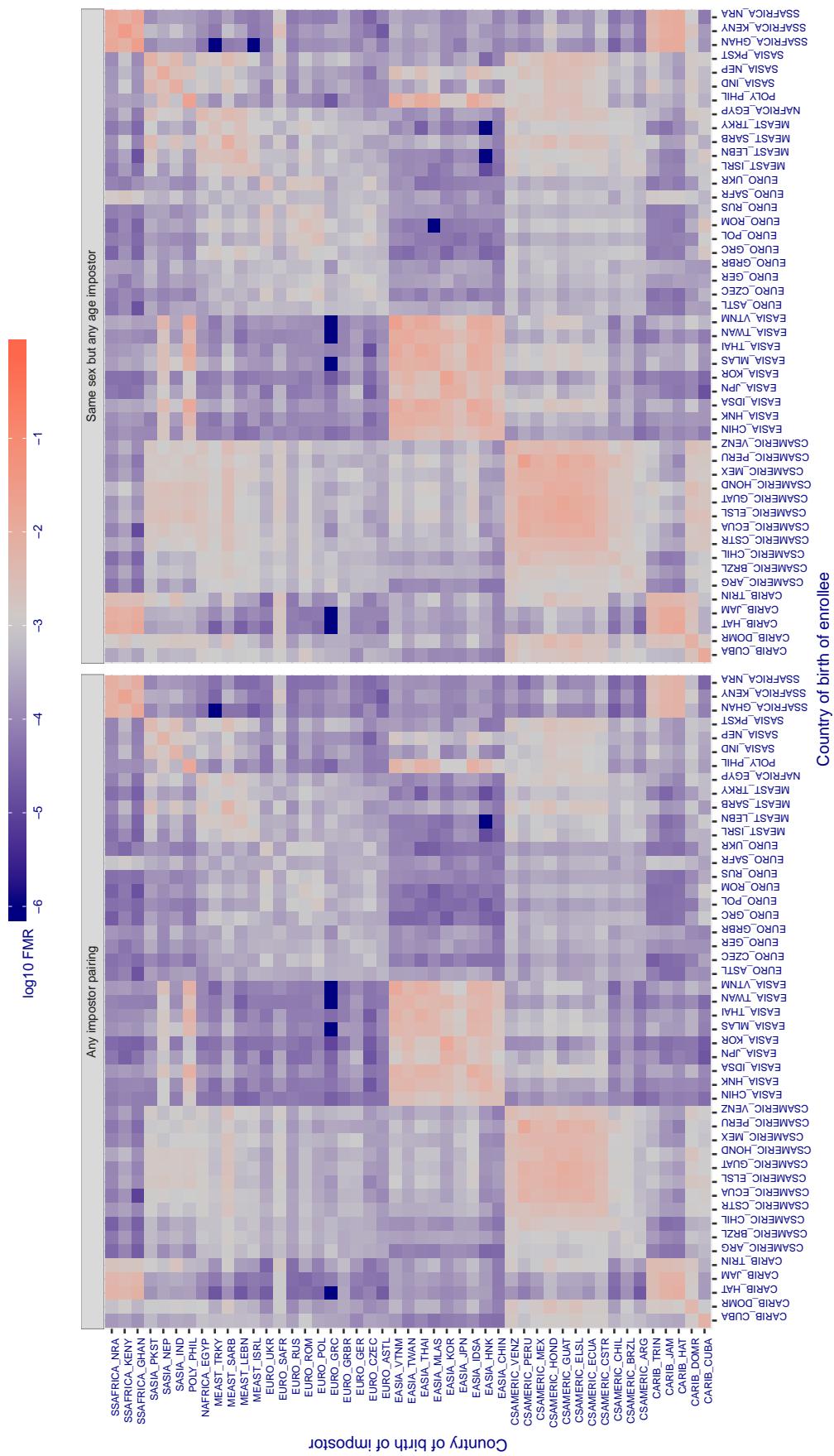


Figure 403: For algorithm toshiba-002 operating on visa images, the heatmap shows false match rates observed over impostor comparisons of faces from different individuals who were born in the given country pair. False matches are counted against a recognition threshold fixed globally to give the target FMR in the plot title, computed over all on the order of 10^{10} impostor comparisons. If text appears in each box it give the same quantity as that coded by the color. Grey indicates FMR is at the intended FMR target level. Light red colors present a security vulnerability to, for example, a passport gate. Each +1 increase in $\log_{10} FMR$ corresponds to a factor of 10 increase in FMR . The matrix is not quite symmetric because images in the enrollment and verification sets are different.

Cross country FMR at threshold T = 0.596 for algorithm toshiba_003, giving $FMR(T) = 0.001$ globally.

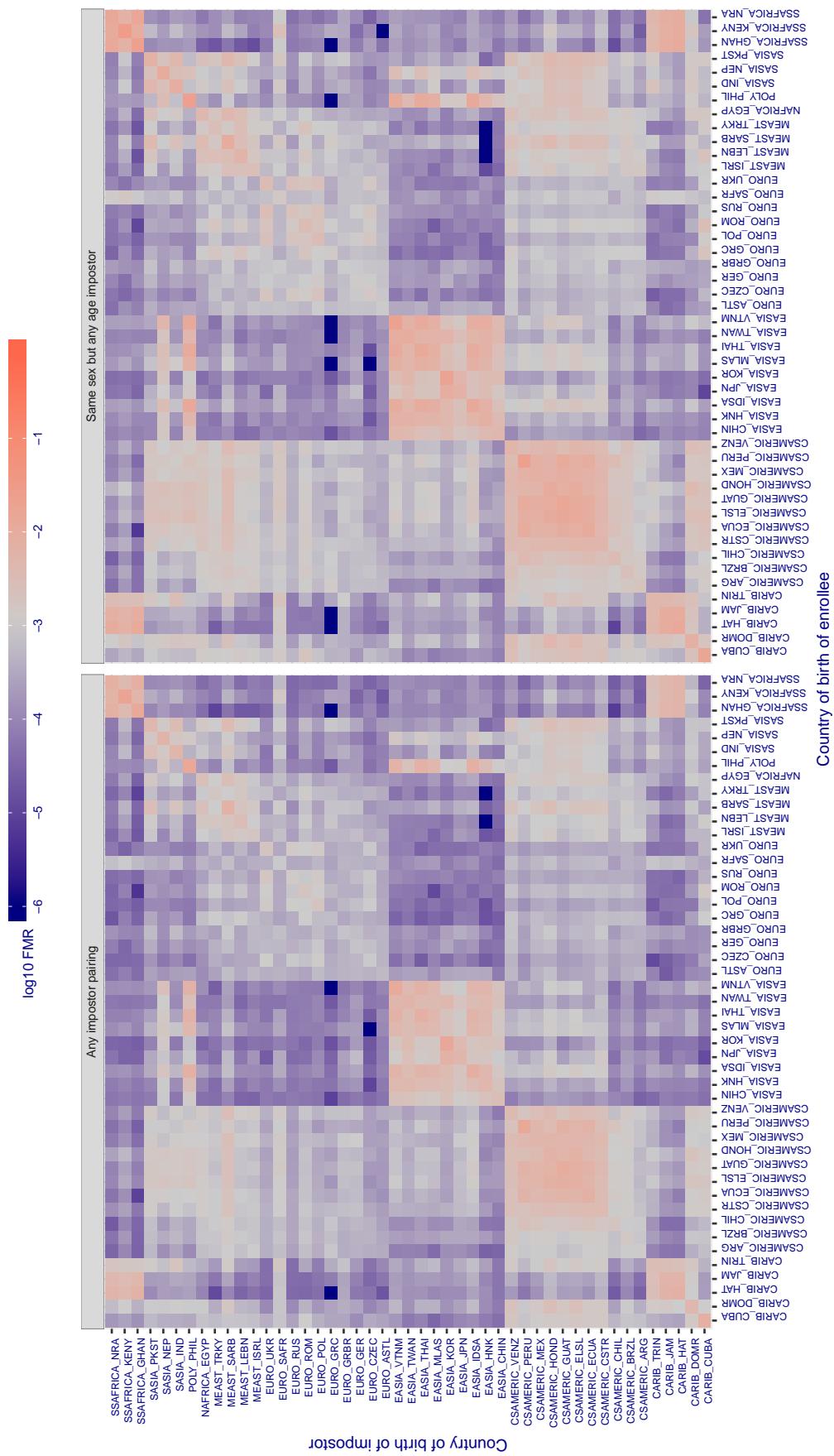


Figure 404: For algorithm toshiba-003 operating on visa images, the heatmap shows false match rates observed over impostor comparisons of faces from different individuals who were born in the given country pair. False matches are counted against a recognition threshold fixed globally to give the target FMR in the plot title, computed over all on the order of 10^{10} impostor comparisons. If text appears in each box it give the same quantity as that coded by the color. Grey indicates FMR is at the intended FMR target level. Light red colors present a security vulnerability to, for example, a passport gate. Each +1 increase in $\log_{10} FMR$ corresponds to a factor of 10 increase in FMR . The matrix is not quite symmetric because images in the enrollment and verification sets are different.

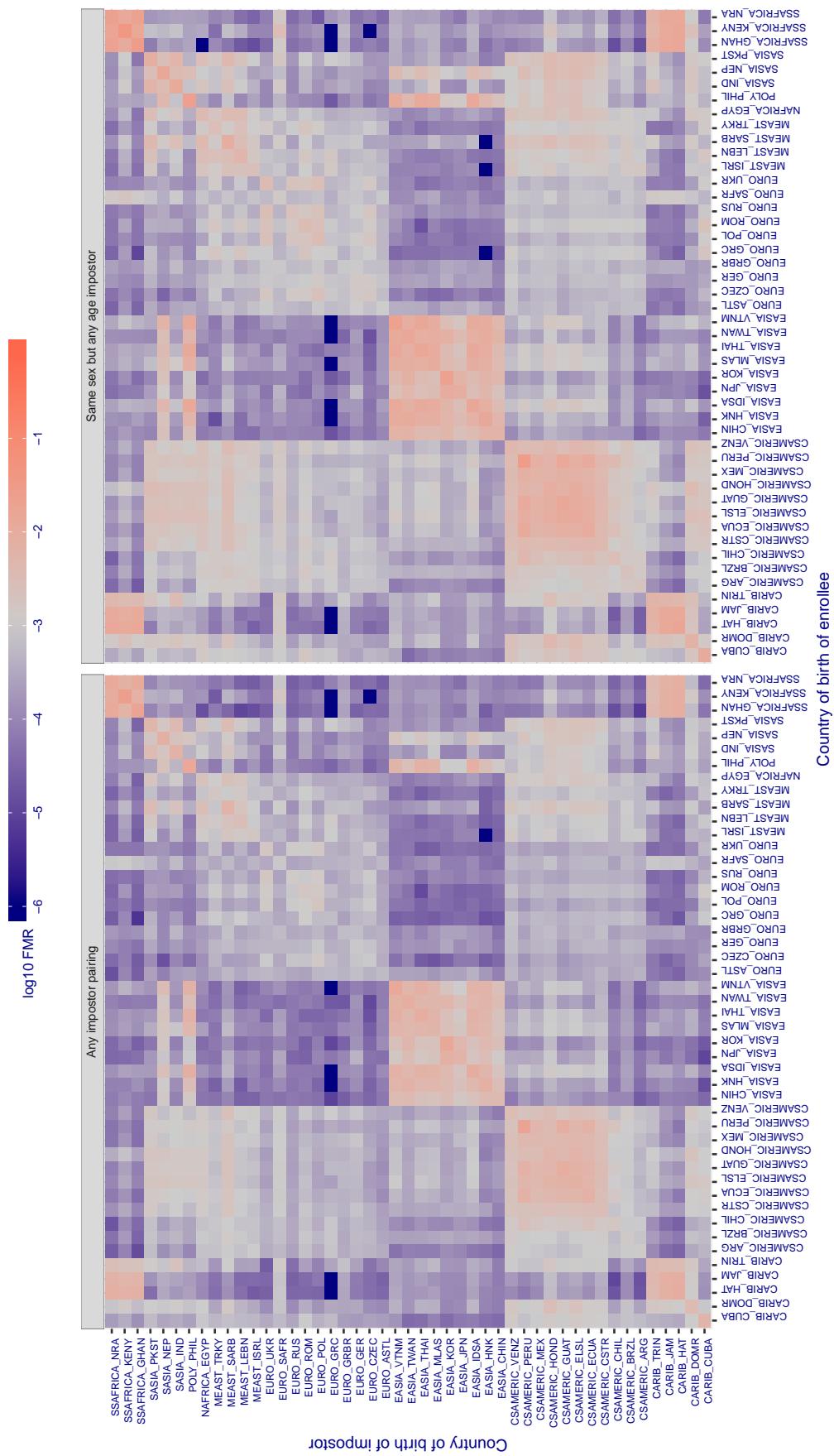
Cross country FMR at threshold T = 0.048 for algorithm ulsee_001, giving FMR(T) = 0.001 globally.

Figure 405: For algorithm ulsee-001 operating on visa images, the heatmap shows false match rates observed over impostor comparisons of faces from different individuals who were born in the given country pair. False matches are counted against a recognition threshold fixed globally to give the target FMR in the plot title, computed over all on the order of 10^{10} impostor comparisons. If text appears in each box it give the same quantity as that coded by the color. Grey indicates FMR is at the intended FMR target level. Light red colors present a security vulnerability to, for example, a passport gate. Each +1 increase in $\log_{10} \text{FMR}$ corresponds to a factor of 10 increase in FMR. The matrix is not quite symmetric because images in the enrollment and verification sets are different.

Cross country FMR at threshold $T = 0.681$ for algorithm uluface_002, giving $FMR(T) = 0.001$ globally.

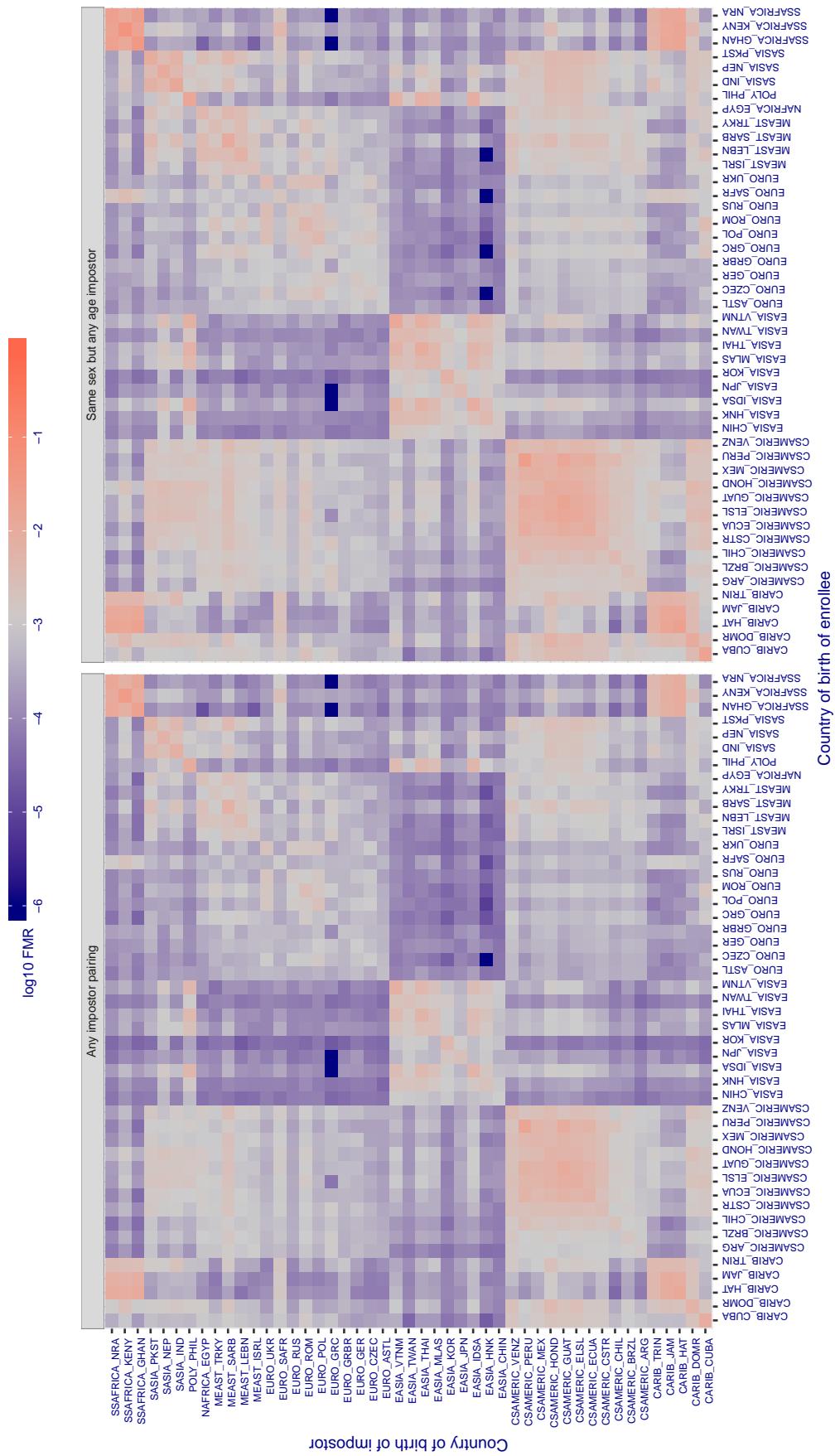


Figure 406: For algorithm uluface-002 operating on visa images, the heatmap shows false match rates observed over impostor comparisons of faces from different individuals who were born in the given country pair. False matches are counted against a recognition threshold fixed globally to give the target FMR in the plot title, computed over all on the order of 10^{10} impostor comparisons. If text appears in each box it give the same quantity as that coded by the color. Grey indicates FMR is at the intended FMR target level. Light red colors present a security vulnerability to, for example, a passport gate. Each +1 increase in $\log_{10} FMR$ corresponds to a factor of 10 increase in FMR . The matrix is not quite symmetric because images in the enrollment and verification sets are different.

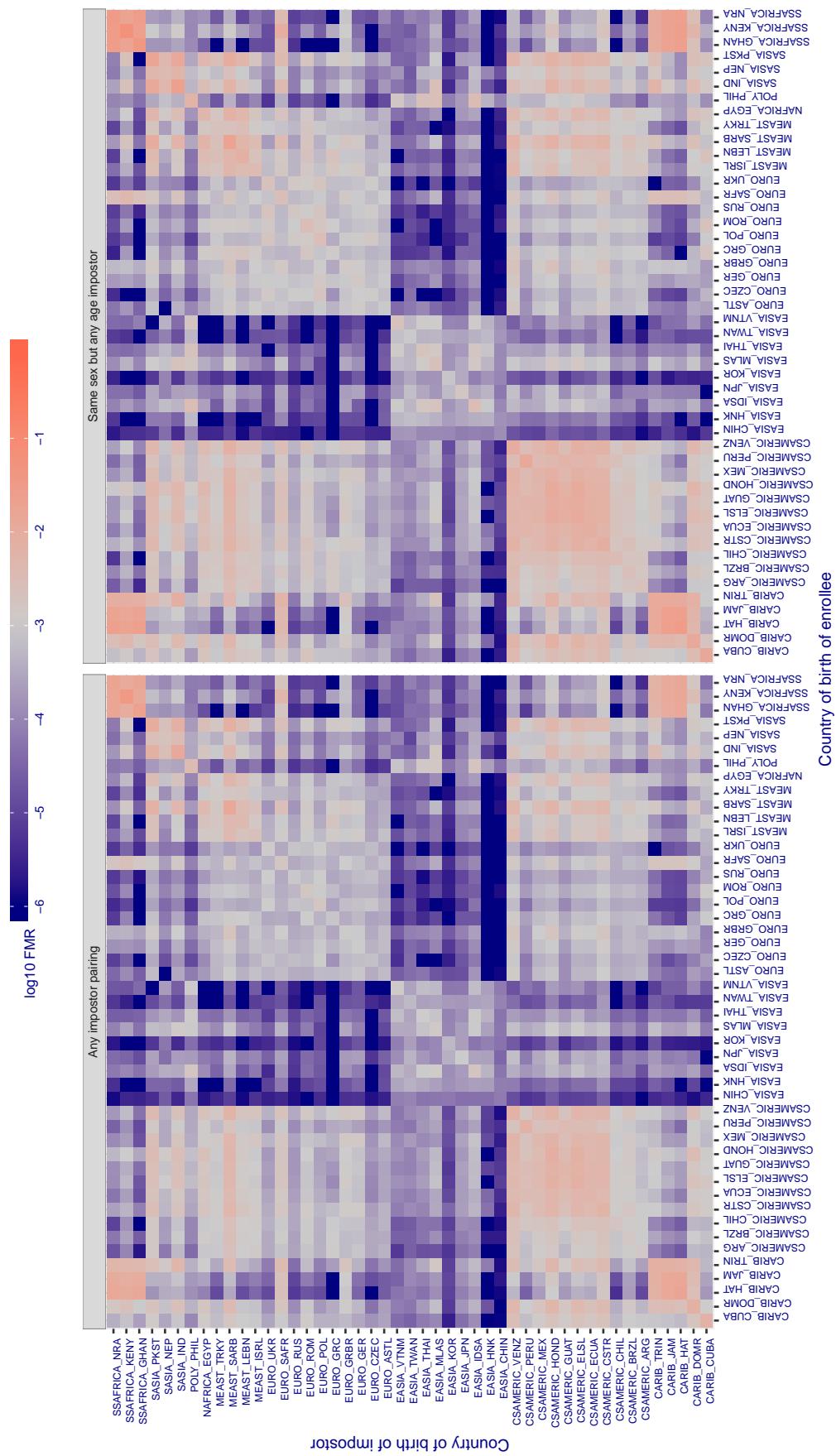
Cross country FMR at threshold T = 0.384 for algorithm upc_001, giving FMR(T) = 0.001 globally.

Figure 407: For algorithm upc-001 operating on visa images, the heatmap shows false match rates observed over impostor comparisons of faces from different individuals who were born in the given country pair. False matches are counted against a recognition threshold fixed globally to give the target FMR in the plot title, computed over all on the order of 10^{10} impostor comparisons. If text appears in each box it give the same quantity as that coded by the color. Grey indicates FMR is at the intended FMR target level. Light red colors present a security vulnerability to, for example, a passport gate. Each +1 increase in \log_{10} FMR corresponds to a factor of 10 increase in FMR. The matrix is not quite symmetric because images in the enrollment and verification sets are different.

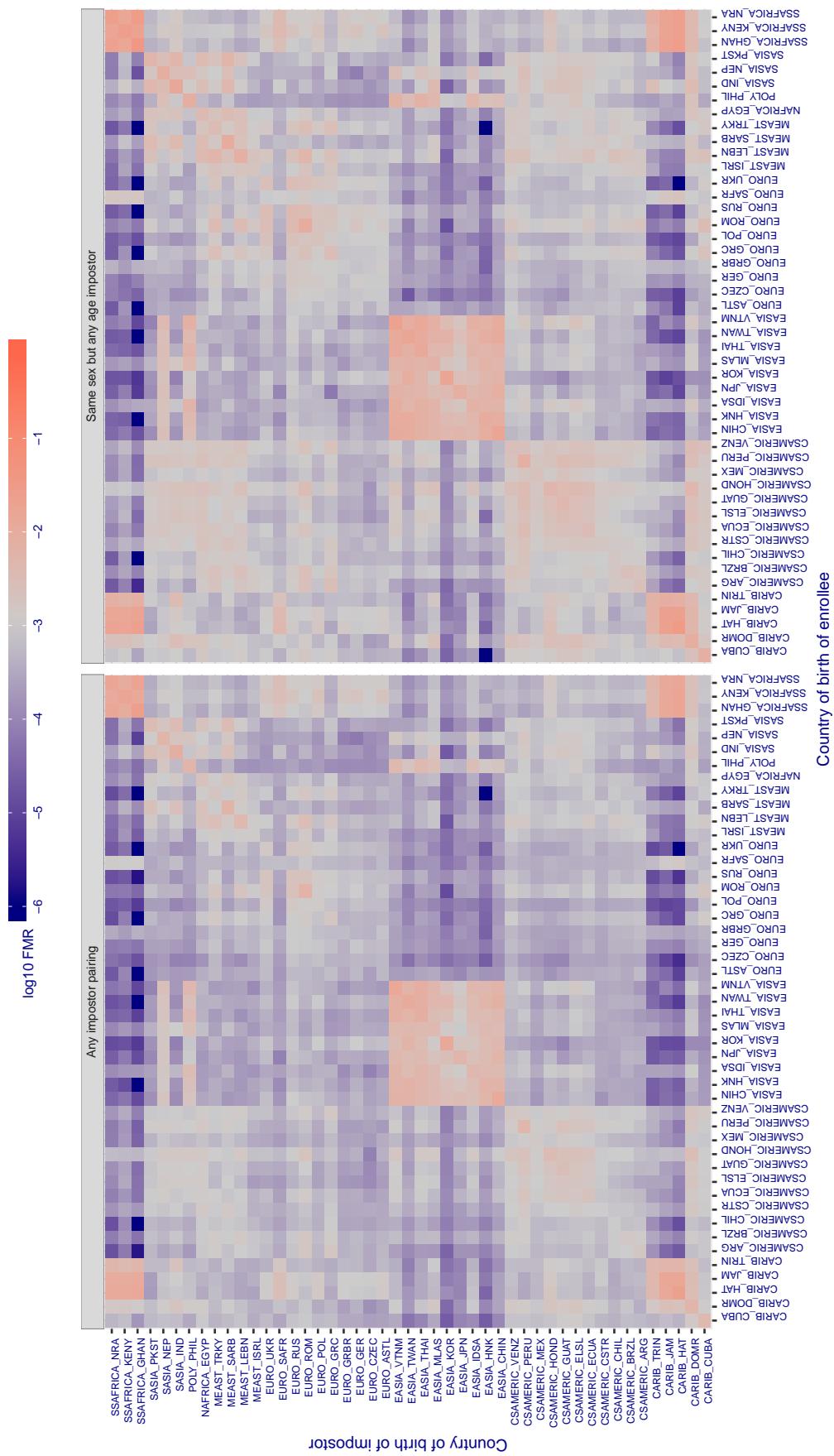
Cross country FMR at threshold T = 0.310 for algorithm vcog_002, giving FMR(T) = 0.001 globally.

Figure 408: For algorithm vcog-002 operating on visa images, the heatmap shows false match rates observed over impostor comparisons of faces from different individuals who were born in the given country pair. False matches are counted against a recognition threshold fixed globally to give the target FMR in the plot title, computed over all on the order of 10^{10} impostor comparisons. If text appears in each box it give the same quantity as that coded by the color. Grey indicates FMR is at the intended FMR target level. Light red colors present a security vulnerability to, for example, a passport gate. Each +1 increase in $\log_{10} \text{FMR}$ corresponds to a factor of 10 increase in FMR. The matrix is not quite symmetric because images in the enrollment and verification sets are different.

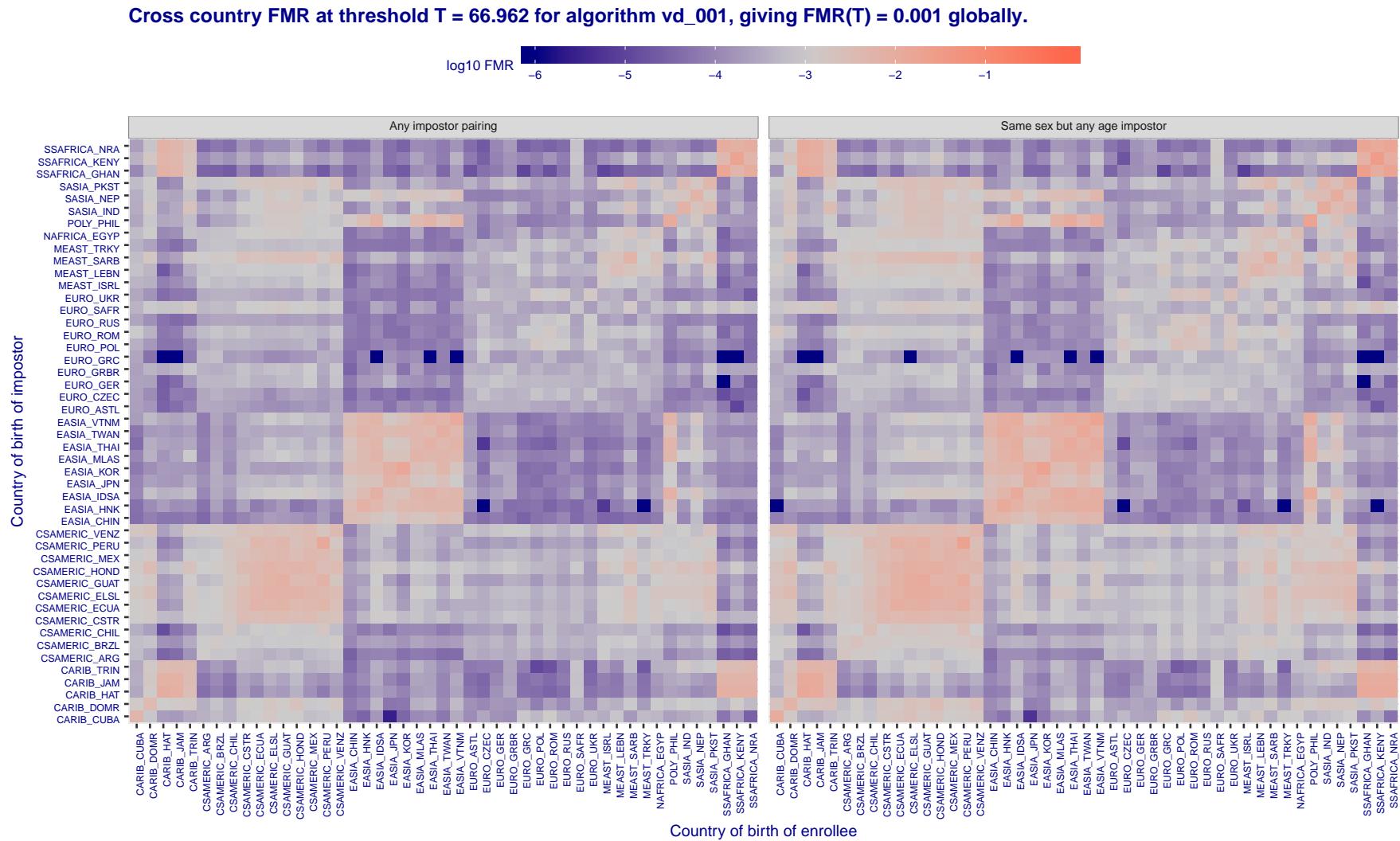


Figure 409: For algorithm vd-001 operating on visa images, the heatmap shows false match rates observed over impostor comparisons of faces from different individuals who were born in the given country pair. False matches are counted against a recognition threshold fixed globally to give the target FMR in the plot title, computed over all on the order of 10^{10} impostor comparisons. If text appears in each box it give the same quantity as that coded by the color. Grey indicates FMR is at the intended FMR target level. Light red colors present a security vulnerability to, for example, a passport gate. Each +1 increase in \log_{10} FMR corresponds to a factor of 10 increase in FMR. The matrix is not quite symmetric because images in the enrollment and verification sets are different.

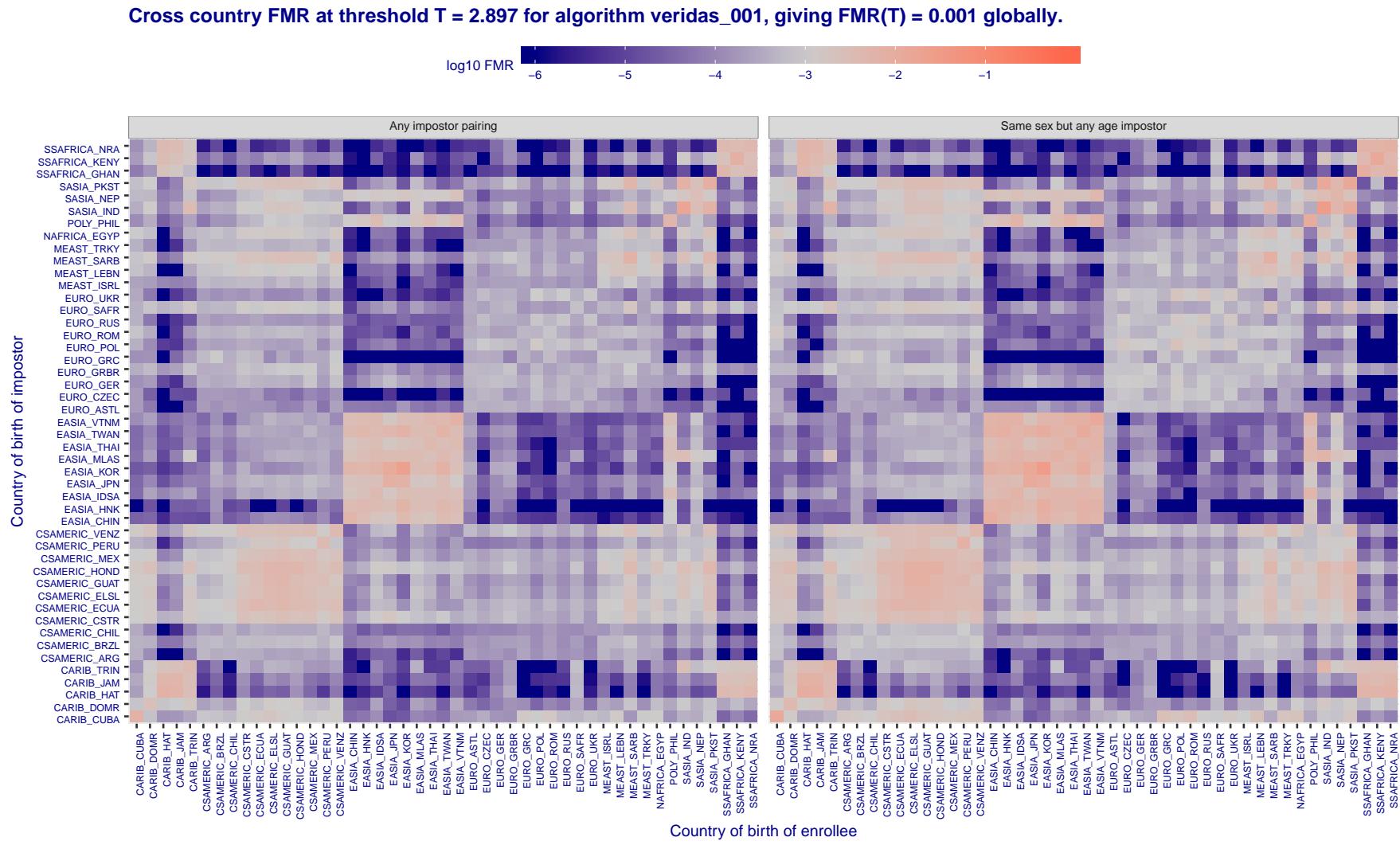


Figure 410: For algorithm veridas-001 operating on visa images, the heatmap shows false match rates observed over impostor comparisons of faces from different individuals who were born in the given country pair. False matches are counted against a recognition threshold fixed globally to give the target FMR in the plot title, computed over all on the order of 10^{10} impostor comparisons. If text appears in each box it give the same quantity as that coded by the color. Grey indicates FMR is at the intended FMR target level. Light red colors present a security vulnerability to, for example, a passport gate. Each +1 increase in \log_{10} FMR corresponds to a factor of 10 increase in FMR. The matrix is not quite symmetric because images in the enrollment and verification sets are different.

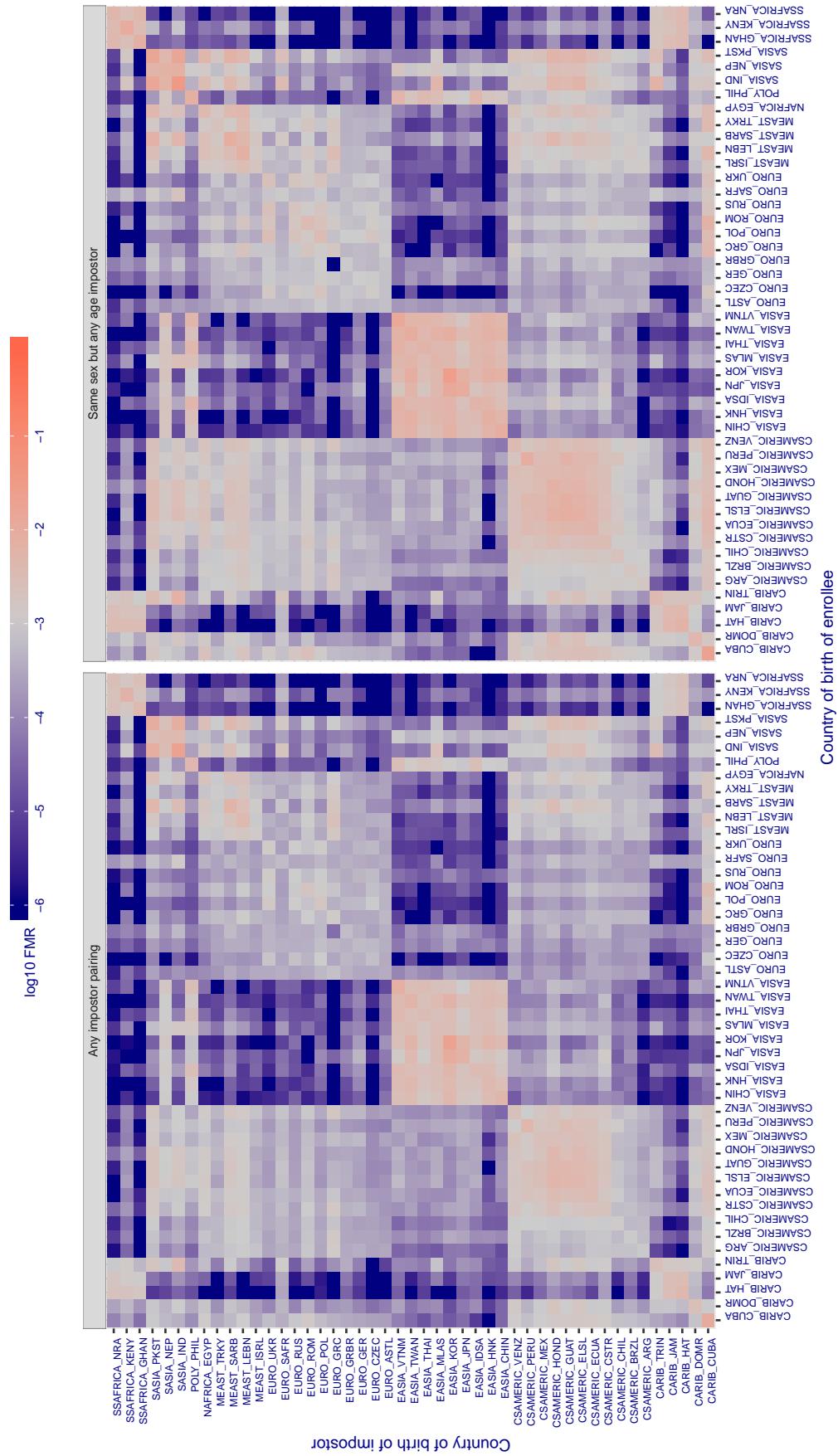
Cross country FMR at threshold T = 3.010 for algorithm veridas_002, giving $FMR(T) = 0.001$ globally.

Figure 411: For algorithm veridas-002 operating on visa images, the heatmap shows false match rates observed over impostor comparisons of faces from different individuals who were born in the given country pair. False matches are counted against a recognition threshold fixed globally to give the target FMR in the plot title, computed over all on the order of 10^{10} impostor comparisons. If text appears in each box it give the same quantity as that coded by the color. Grey indicates FMR is at the intended FMR target level. Light red colors present a security vulnerability to, for example, a passport gate. Each +1 increase in $\log_{10} FMR$ corresponds to a factor of 10 increase in FMR . The matrix is not quite symmetric because images in the enrollment and verification sets are different.

Cross country FMR at threshold T = 2.677 for algorithm via_000, giving FMR(T) = 0.001 globally.

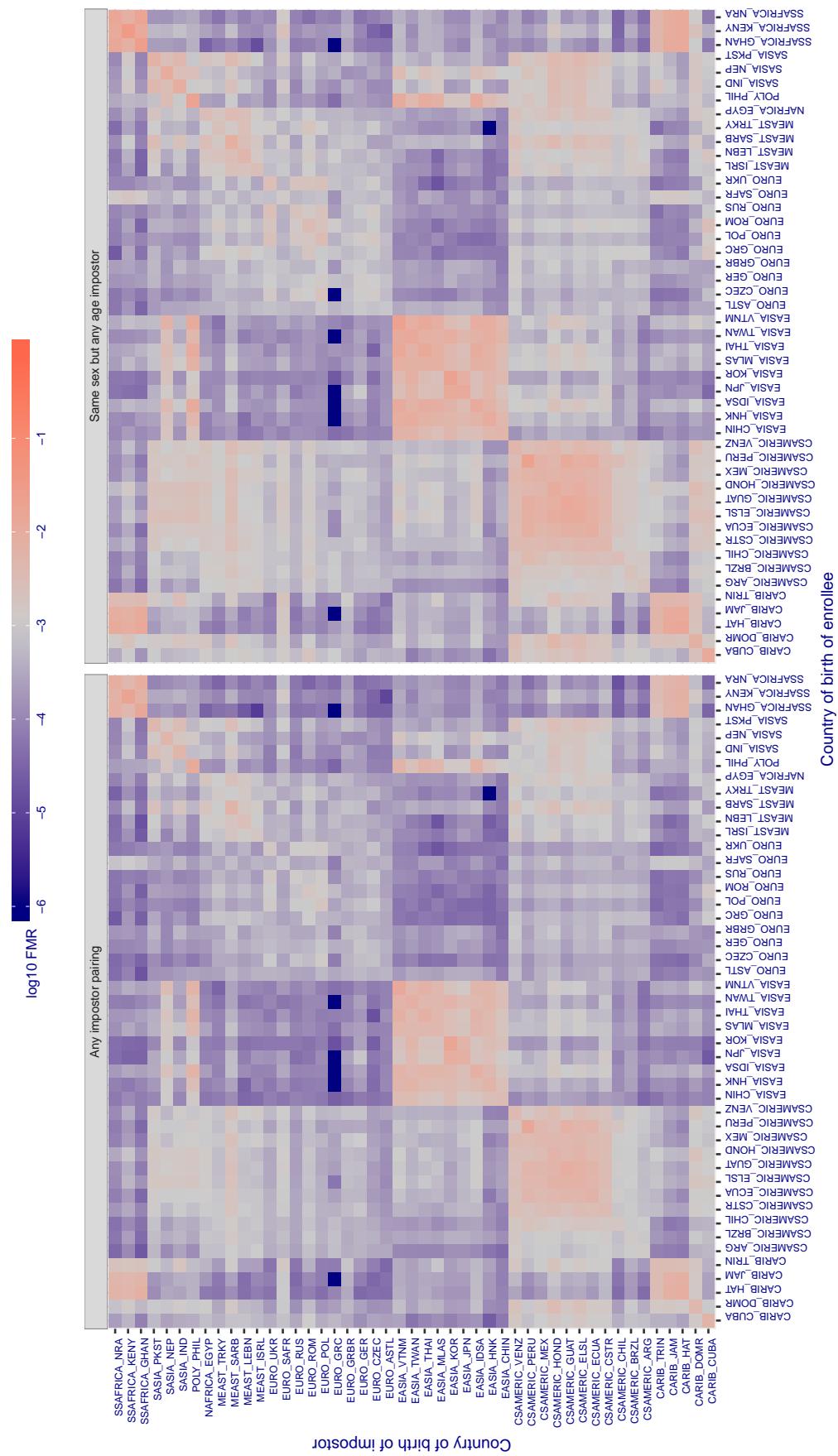


Figure 412: For algorithm via-000 operating on visa images, the heatmap shows false match rates observed over impostor comparisons of faces from different individuals who were born in the given country pair. False matches are counted against a recognition threshold fixed globally to give the target FMR in the plot title, computed over all on the order of 10^{10} impostor comparisons. If text appears in each box it give the same quantity as that coded by the color. Grey indicates FMR is at the intended FMR target level. Light red colors present a security vulnerability to, for example, a passport gate. Each +1 increase in \log_{10} FMR corresponds to a factor of 10 increase in FMR. The matrix is not quite symmetric because images in the enrollment and verification sets are different.

Cross country FMR at threshold T = 0.755 for algorithm videonetics_001, giving $\text{FMR}(T) = 0.001$ globally.

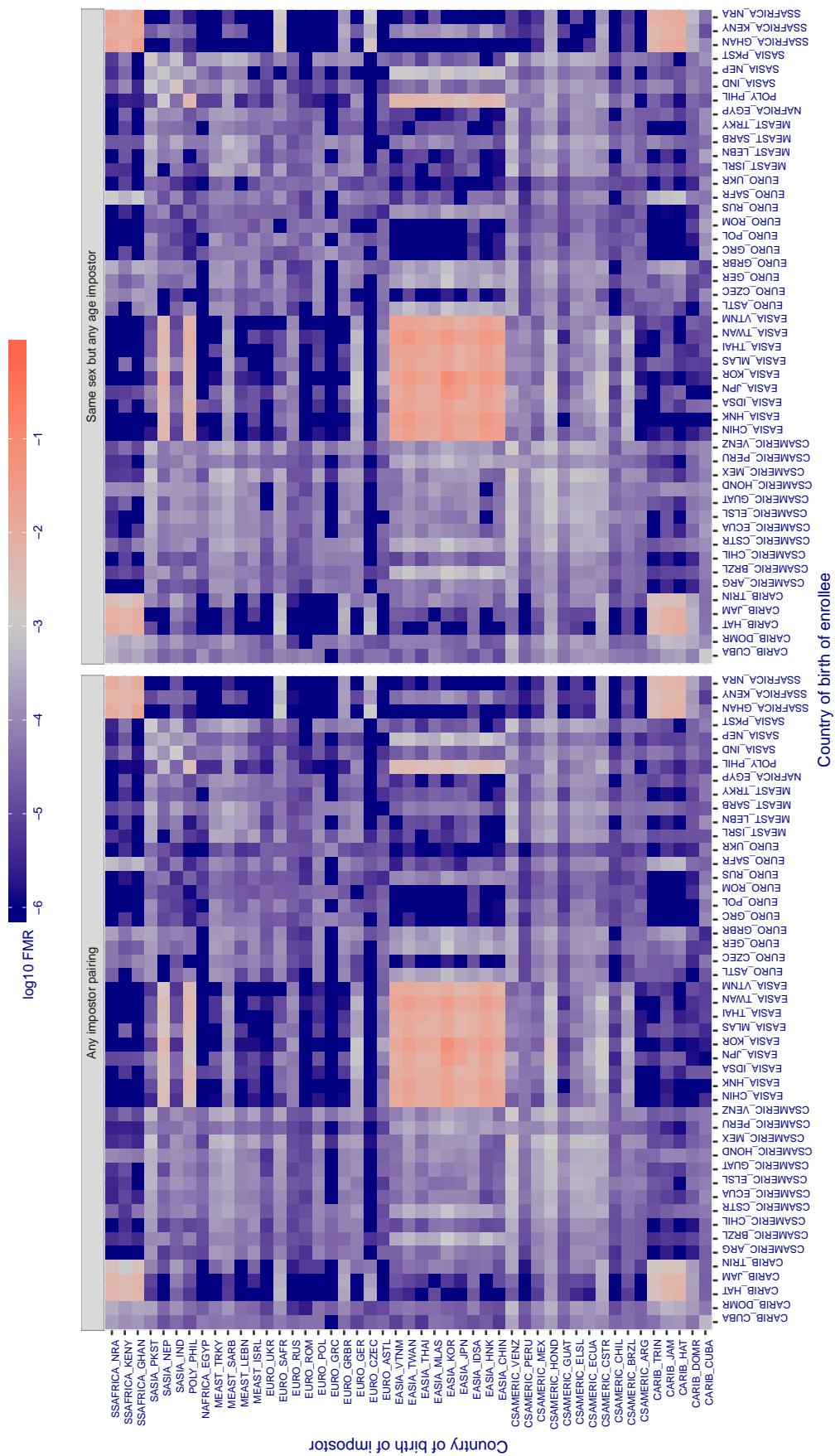


Figure 413: For algorithm videonetics-001 operating on visa images, the heatmap shows false match rates observed over impostor comparisons of faces from different individuals who were born in the given country pair. False matches are counted against a recognition threshold fixed globally to give the target FMR in the plot title, computed over all on the order of 10^{10} impostor comparisons. If text appears in each box it give the same quantity as that coded by the color. Grey indicates FMR is at the intended FMR target level. Light red colors present a security vulnerability to, for example, a passport gate. Each +1 increase in $\log_{10} \text{FMR}$ corresponds to a factor of 10 increase in FMR. The matrix is not quite symmetric because images in the enrollment and verification sets are different.

Cross country FMR at threshold T = 2.809 for algorithm vigilantsolutions_006, giving $\text{FMR}(T) = 0.001$ globally.

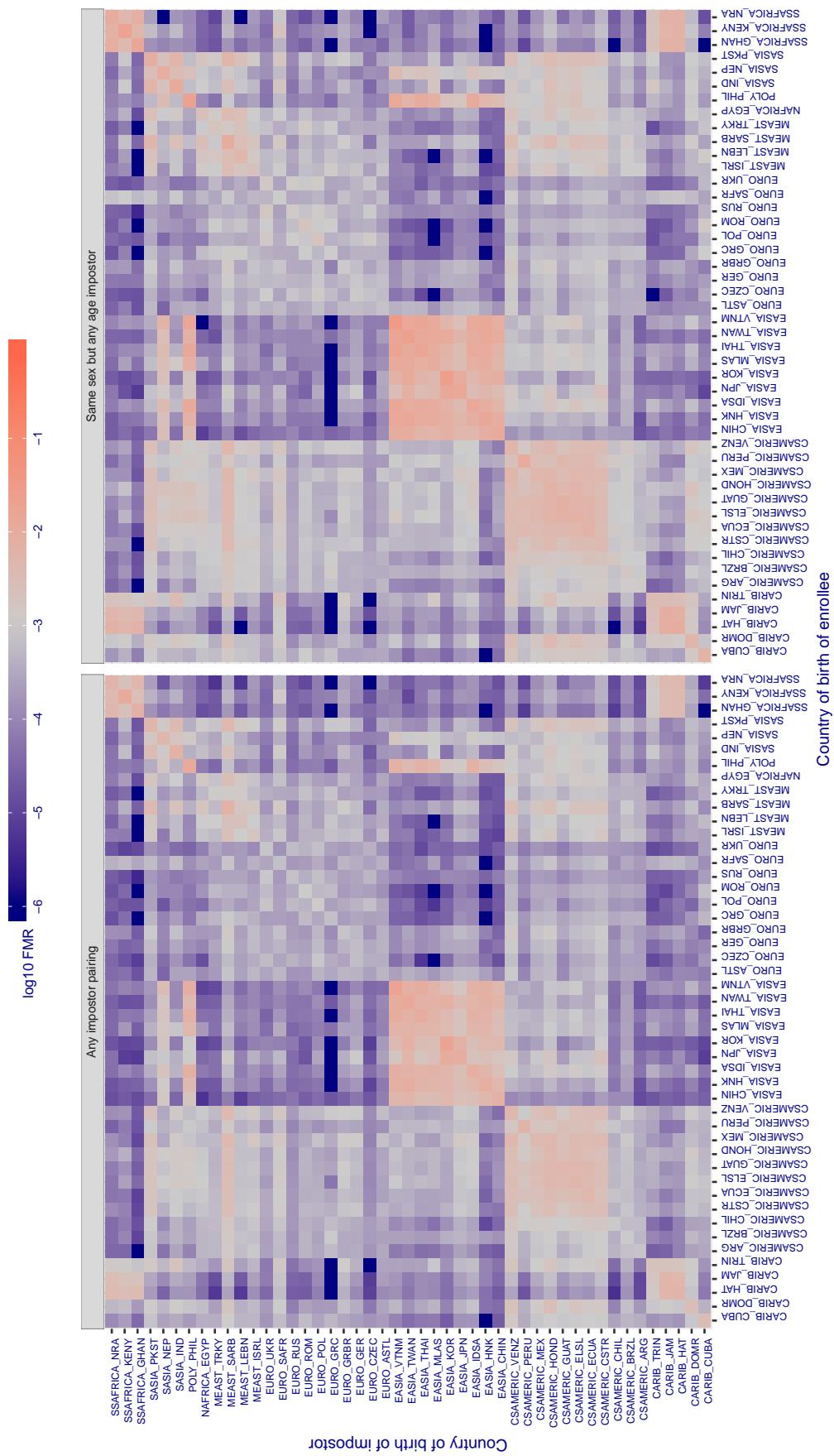


Figure 414: For algorithm vigilantsolutions-006 operating on visa images, the heatmap shows false match rates observed over impostor comparisons of faces from different individuals who were born in the given country pair. False matches are counted against a recognition threshold fixed globally to give the target FMR in the plot title, computed over all on the order of 10^{10} impostor comparisons. If text appears in each box it give the same quantity as that coded by the color. Grey indicates FMR is at the intended FMR target level. Light red colors present a security vulnerability to, for example, a passport gate. Each +1 increase in $\log_{10} \text{FMR}$ corresponds to a factor of 10 increase in FMR . The matrix is not quite symmetric because images in the enrollment and verification sets are different.

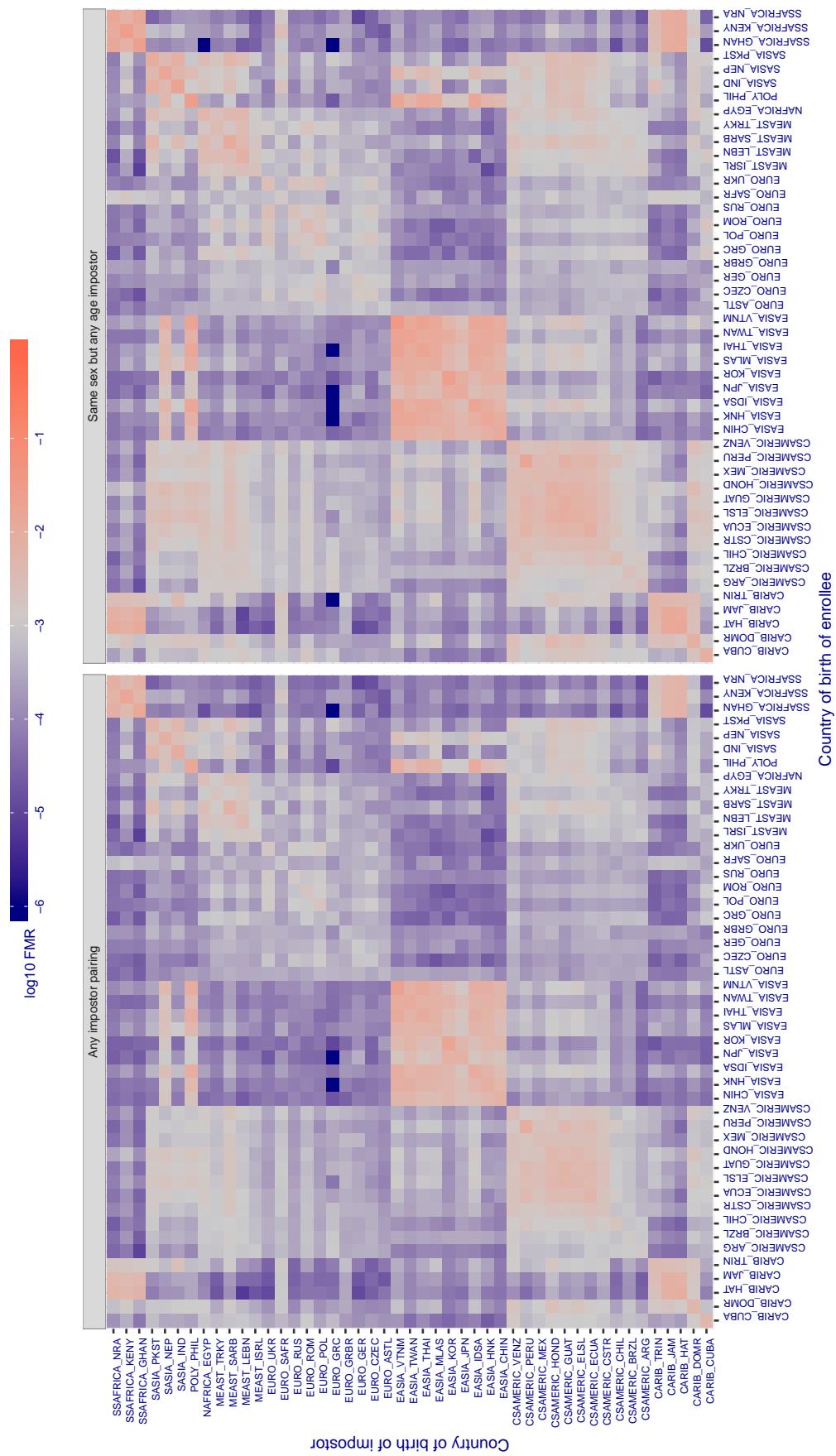
Cross country FMR at threshold T = 2.755 for algorithm vigilantsolutions_007, giving $\text{FMR}(T) = 0.001$ globally.

Figure 415: For algorithm vigilantsolutions-007 operating on visa images, the heatmap shows false match rates observed over impostor comparisons of faces from different individuals who were born in the given country pair. False matches are counted against a recognition threshold fixed globally to give the target FMR in the plot title, computed over all on the order of 10^{10} impostor comparisons. If text appears in each box it give the same quantity as that coded by the color. Grey indicates FMR is at the intended FMR target level. Light red colors present a security vulnerability to, for example, a passport gate. Each +1 increase in $\log_{10} \text{FMR}$ corresponds to a factor of 10 increase in FMR . The matrix is not quite symmetric because images in the enrollment and verification sets are different.

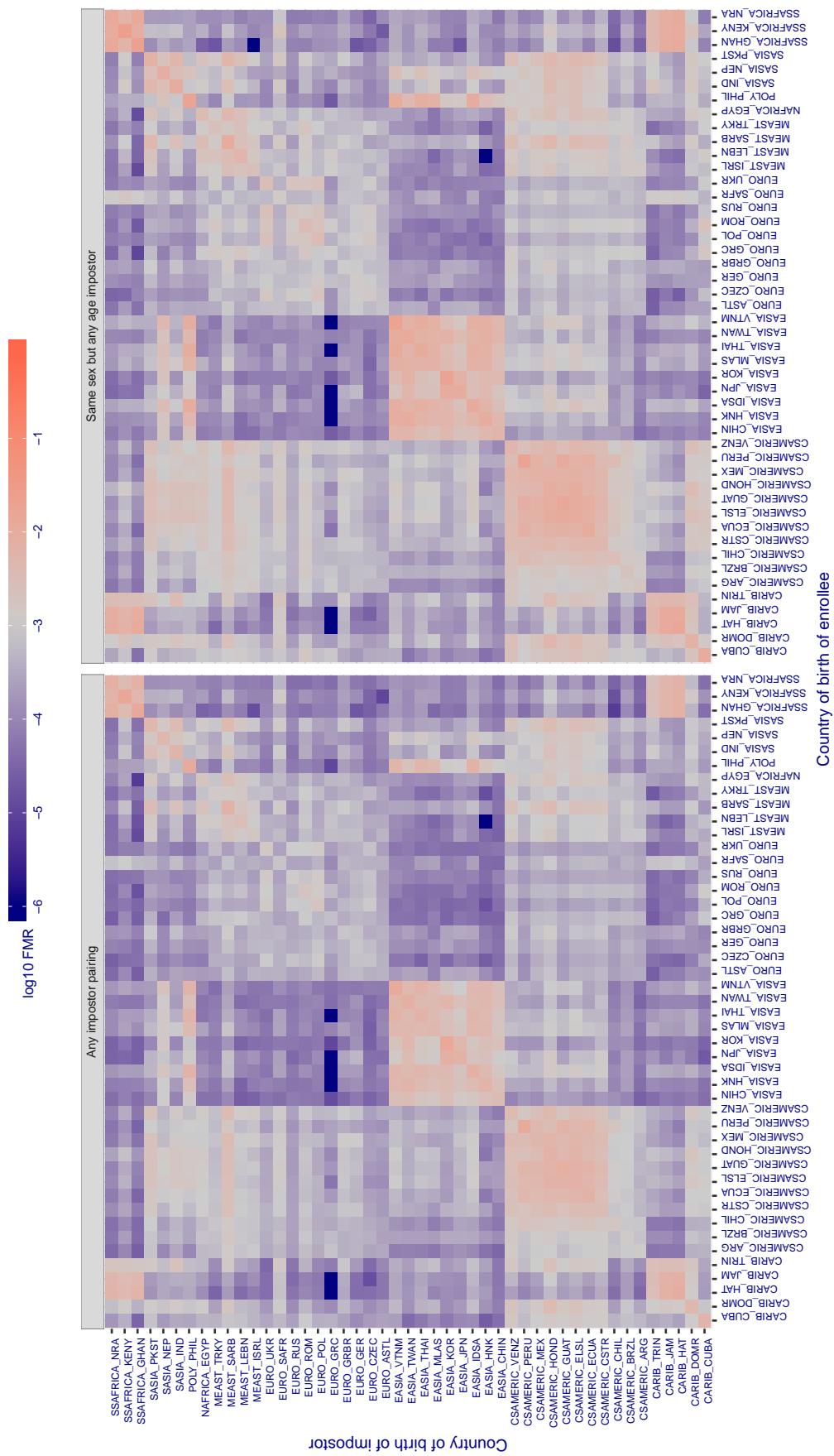
Cross country FMR at threshold T = 0.336 for algorithm vion_000, giving $FMR(T) = 0.001$ globally.

Figure 416: For algorithm vion-000 operating on visa images, the heatmap shows false match rates observed over impostor comparisons of faces from different individuals who were born in the given country pair. False matches are counted against a recognition threshold fixed globally to give the target FMR in the plot title, computed over all on the order of 10^{10} impostor comparisons. If text appears in each box it give the same quantity as that coded by the color. Grey indicates FMR is at the intended FMR target level. Light red colors present a security vulnerability to, for example, a passport gate. Each +1 increase in $\log_{10} FMR$ corresponds to a factor of 10 increase in FMR. The matrix is not quite symmetric because images in the enrollment and verification sets are different.

Cross country FMR at threshold T = 0.340 for algorithm visionbox_000, giving $FMR(T) = 0.001$ globally.

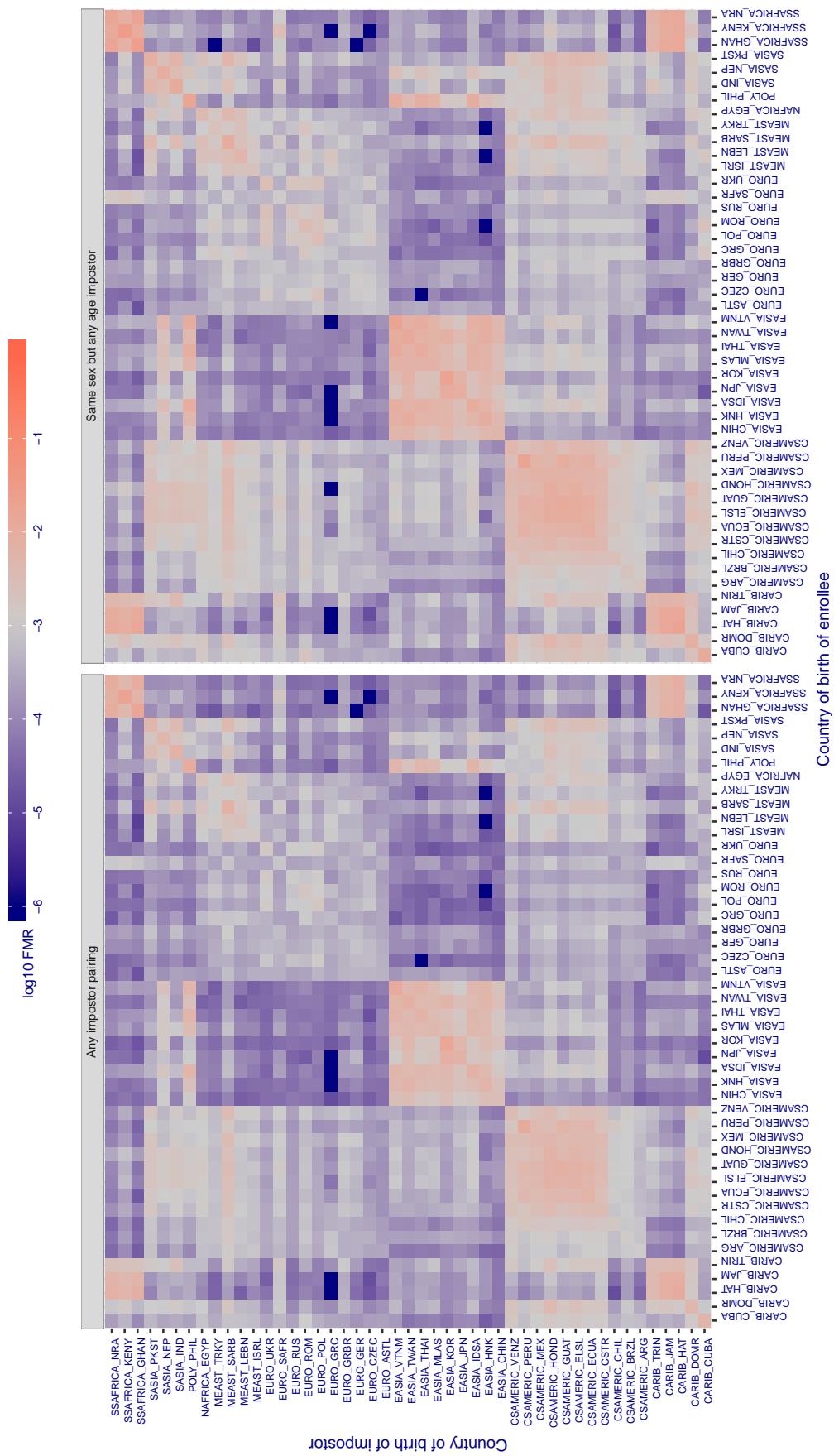


Figure 417: For algorithm visionbox-000 operating on visa images, the heatmap shows false match rates observed over impostor comparisons of faces from different individuals who were born in the given country pair. False matches are counted against a recognition threshold fixed globally to give the target FMR in the plot title, computed over all on the order of 10^{10} impostor comparisons. If text appears in each box it give the same quantity as that coded by the color. Grey indicates FMR is at the intended FMR target level. Light red colors present a security vulnerability to, for example, a passport gate. Each +1 increase in $\log_{10} FMR$ corresponds to a factor of 10 increase in FMR . The matrix is not quite symmetric because images in the enrollment and verification sets are different.

Cross country FMR at threshold T = 0.296 for algorithm visionbox_001, giving $FMR(T) = 0.001$ globally.

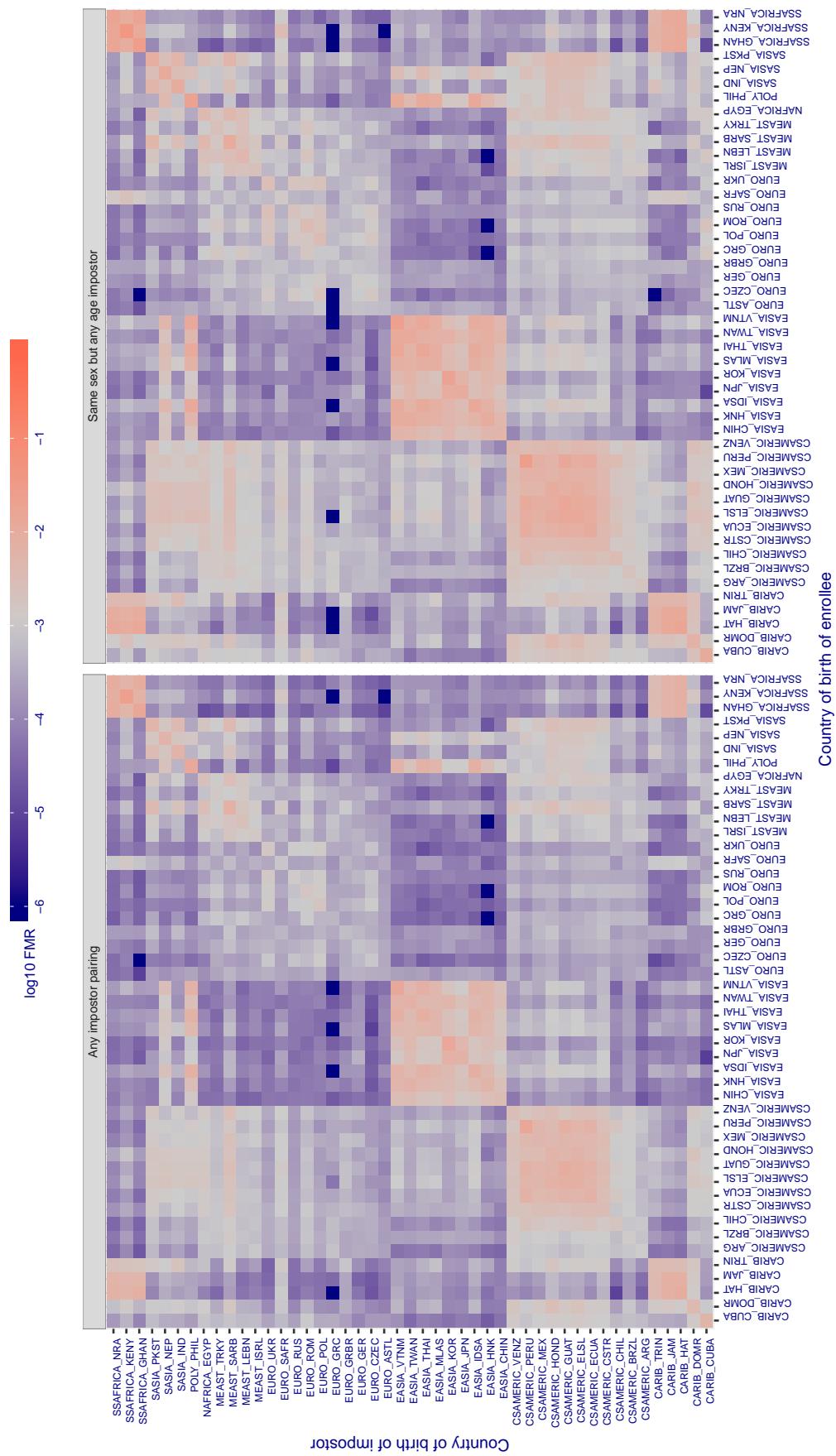


Figure 418: For algorithm visionbox-001 operating on visa images, the heatmap shows false match rates observed over impostor comparisons of faces from different individuals who were born in the given country pair. False matches are counted against a recognition threshold fixed globally to give the target FMR in the plot title, computed over all on the order of 10^{10} impostor comparisons. If text appears in each box it give the same quantity as that coded by the color. Grey indicates FMR is at the intended FMR target level. Light red colors present a security vulnerability to, for example, a passport gate. Each +1 increase in $\log_{10} FMR$ corresponds to a factor of 10 increase in FMR. The matrix is not quite symmetric because images in the enrollment and verification sets are different.

Cross country FMR at threshold T = 0.444 for algorithm visionlabs_006, giving $\text{FMR}(T) = 0.001$ globally.

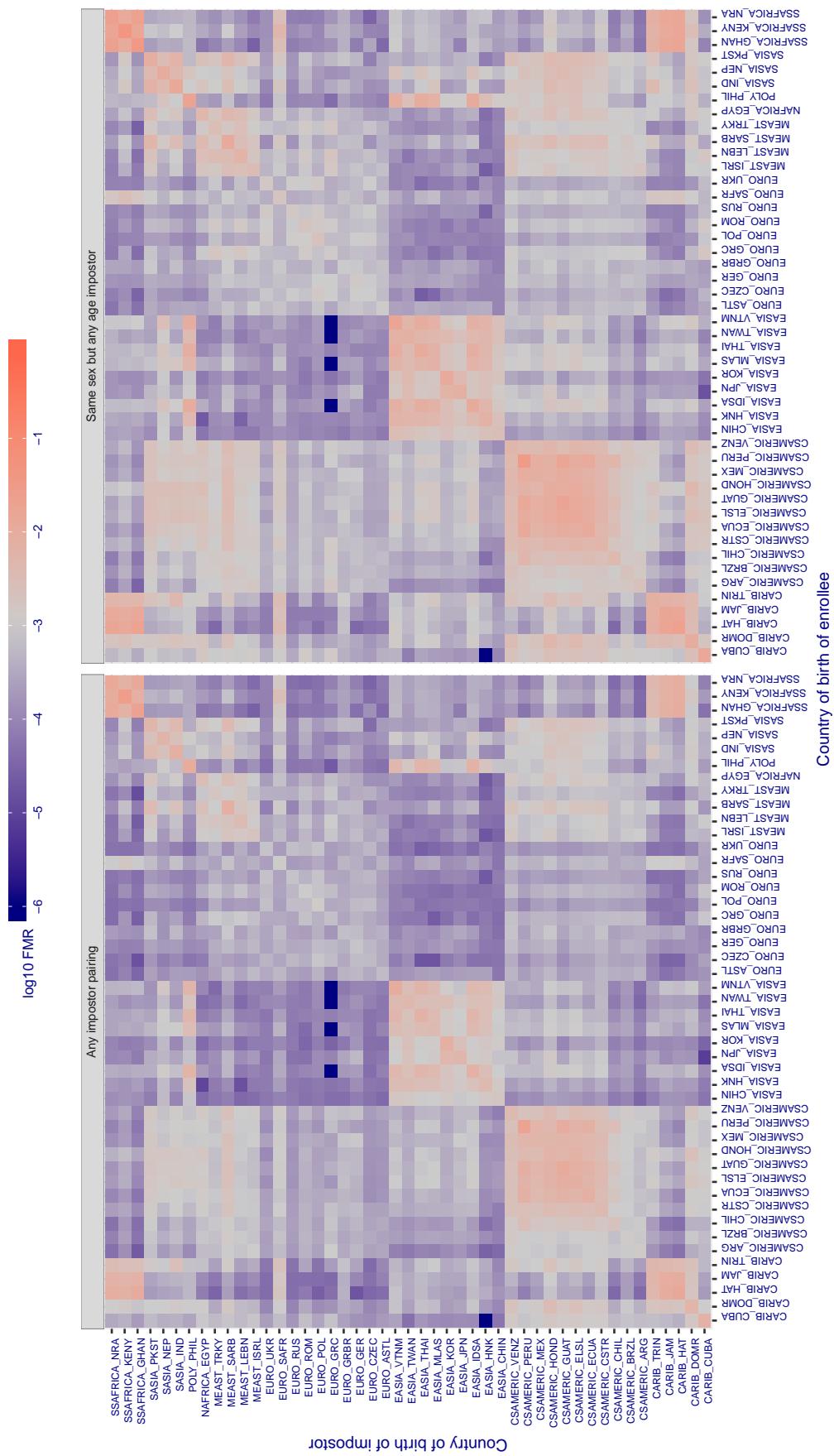


Figure 419: For algorithm visionlabs-006 operating on visa images, the heatmap shows false match rates observed over impostor comparisons of faces from different individuals who were born in the given country pair. False matches are counted against a recognition threshold fixed globally to give the target FMR in the plot title, computed over all on the order of 10^{10} impostor comparisons. If text appears in each box it give the same quantity as that coded by the color. Grey indicates FMR is at the intended FMR target level. Light red colors present a security vulnerability to, for example, a passport gate. Each +1 increase in $\log_{10} \text{FMR}$ corresponds to a factor of 10 increase in FMR . The matrix is not quite symmetric because images in the enrollment and verification sets are different.

Cross country FMR at threshold T = 0.459 for algorithm visionlabs_007, giving $\text{FMR}(T) = 0.001$ globally.

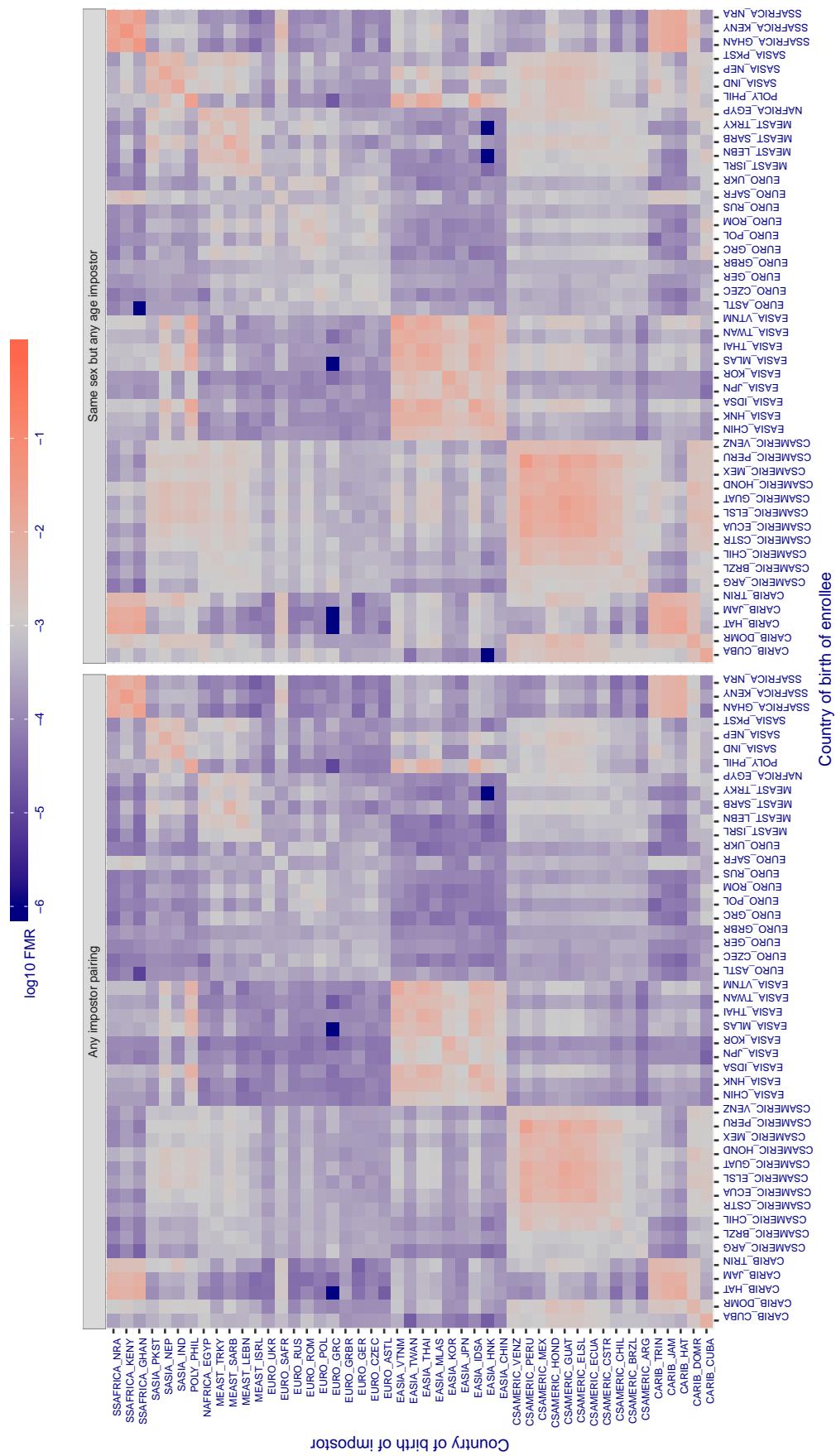


Figure 420: For algorithm visionlabs-007 operating on visa images, the heatmap shows false match rates observed over impostor comparisons of faces from different individuals who were born in the given country pair. False matches are counted against a recognition threshold fixed globally to give the target FMR in the plot title, computed over all on the order of 10^{10} impostor comparisons. If text appears in each box it give the same quantity as that coded by the color. Grey indicates FMR is at the intended FMR target level. Light red colors present a security vulnerability to, for example, a passport gate. Each +1 increase in $\log_{10} \text{FMR}$ corresponds to a factor of 10 increase in FMR . The matrix is not quite symmetric because images in the enrollment and verification sets are different.

Cross country FMR at threshold T = 995.311 for algorithm vocord_006, giving $FMR(T) = 0.001$ globally.

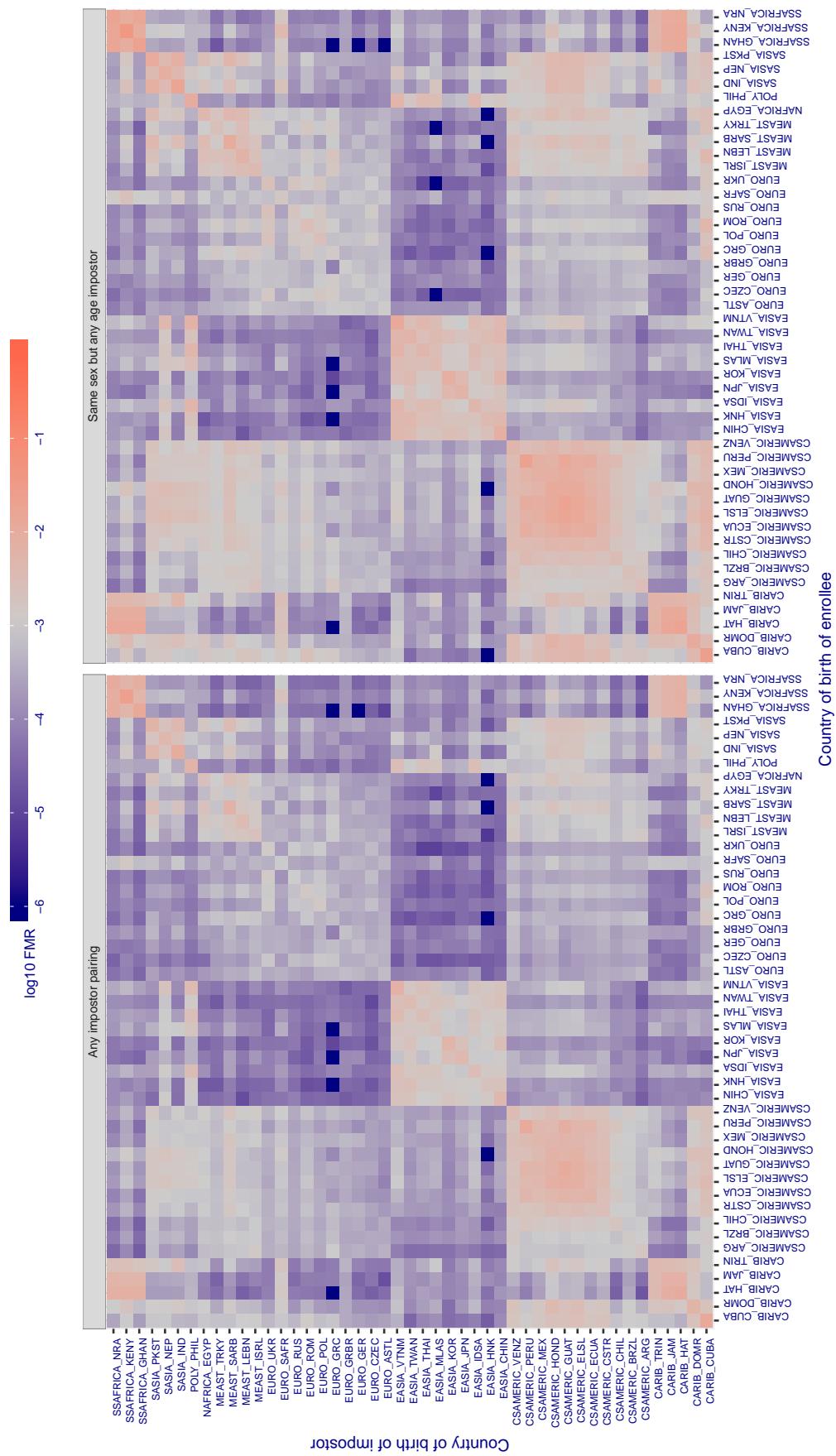


Figure 421: For algorithm vocord-006 operating on visa images, the heatmap shows false match rates observed over impostor comparisons of faces from different individuals who were born in the given country pair. False matches are counted against a recognition threshold fixed globally to give the target FMR in the plot title, computed over all on the order of 10^{10} impostor comparisons. If text appears in each box it give the same quantity as that coded by the color. Grey indicates FMR is at the intended FMR target level. Light red colors present a security vulnerability to, for example, a passport gate. Each +1 increase in $\log_{10} FMR$ corresponds to a factor of 10 increase in FMR . The matrix is not quite symmetric because images in the enrollment and verification sets are different.

Cross country FMR at threshold T = 994.723 for algorithm vocord_007, giving $FMR(T) = 0.001$ globally.

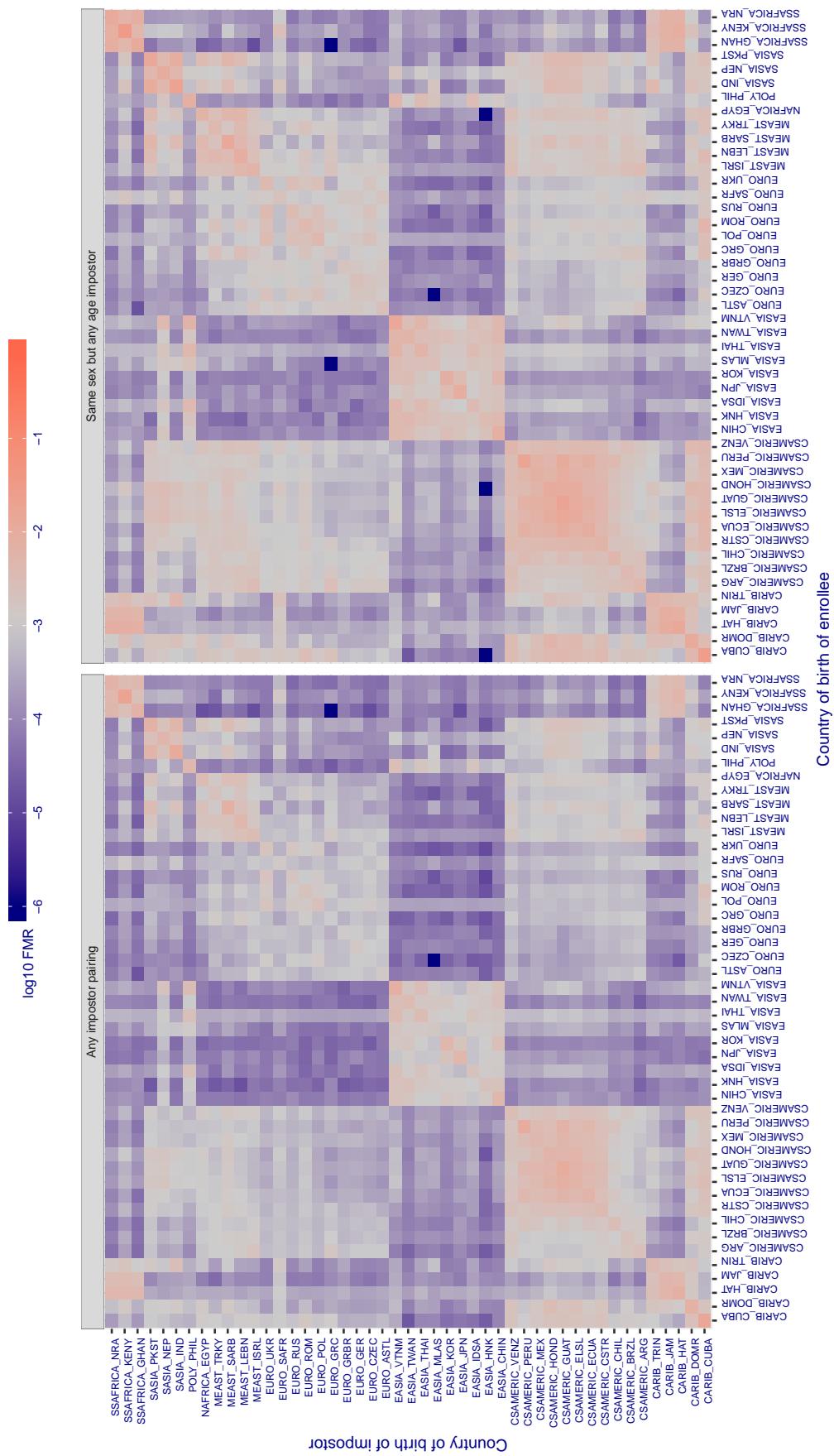


Figure 422: For algorithm vocord-007 operating on visa images, the heatmap shows false match rates observed over impostor comparisons of faces from different individuals who were born in the given country pair. False matches are counted against a recognition threshold fixed globally to give the target FMR in the plot title, computed over all on the order of 10^{10} impostor comparisons. If text appears in each box it give the same quantity as that coded by the color. Grey indicates FMR is at the intended FMR target level. Light red colors present a security vulnerability to, for example, a passport gate. Each +1 increase in $\log_{10} FMR$ corresponds to a factor of 10 increase in FMR . The matrix is not quite symmetric because images in the enrollment and verification sets are different.

Cross country FMR at threshold T = 0.314 for algorithm winsense_000, giving FMR(T) = 0.001 globally.

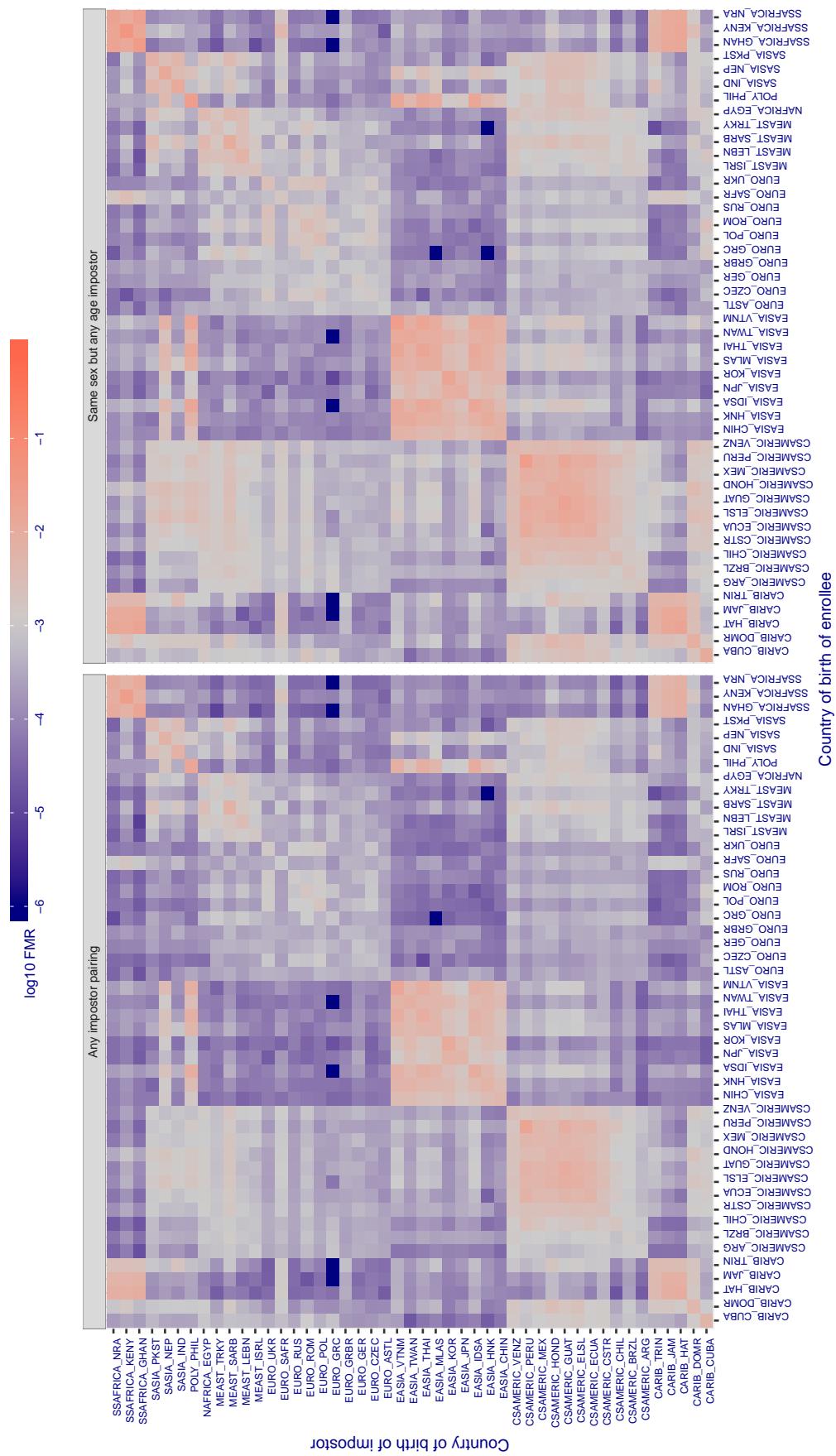


Figure 423: For algorithm winsense-000 operating on visa images, the heatmap shows false match rates observed over impostor comparisons of faces from different individuals who were born in the given country pair. False matches are counted against a recognition threshold fixed globally to give the target FMR in the plot title, computed over all on the order of 10^{10} impostor comparisons. If text appears in each box it give the same quantity as that coded by the color. Grey indicates FMR is at the intended FMR target level. Light red colors present a security vulnerability to, for example, a passport gate. Each +1 increase in $\log_{10} \text{FMR}$ corresponds to a factor of 10 increase in FMR. The matrix is not quite symmetric because images in the enrollment and verification sets are different.

Cross country FMR at threshold T = 5.333 for algorithm yisheng_004, giving $\text{FMR}(T) = 0.001$ globally.

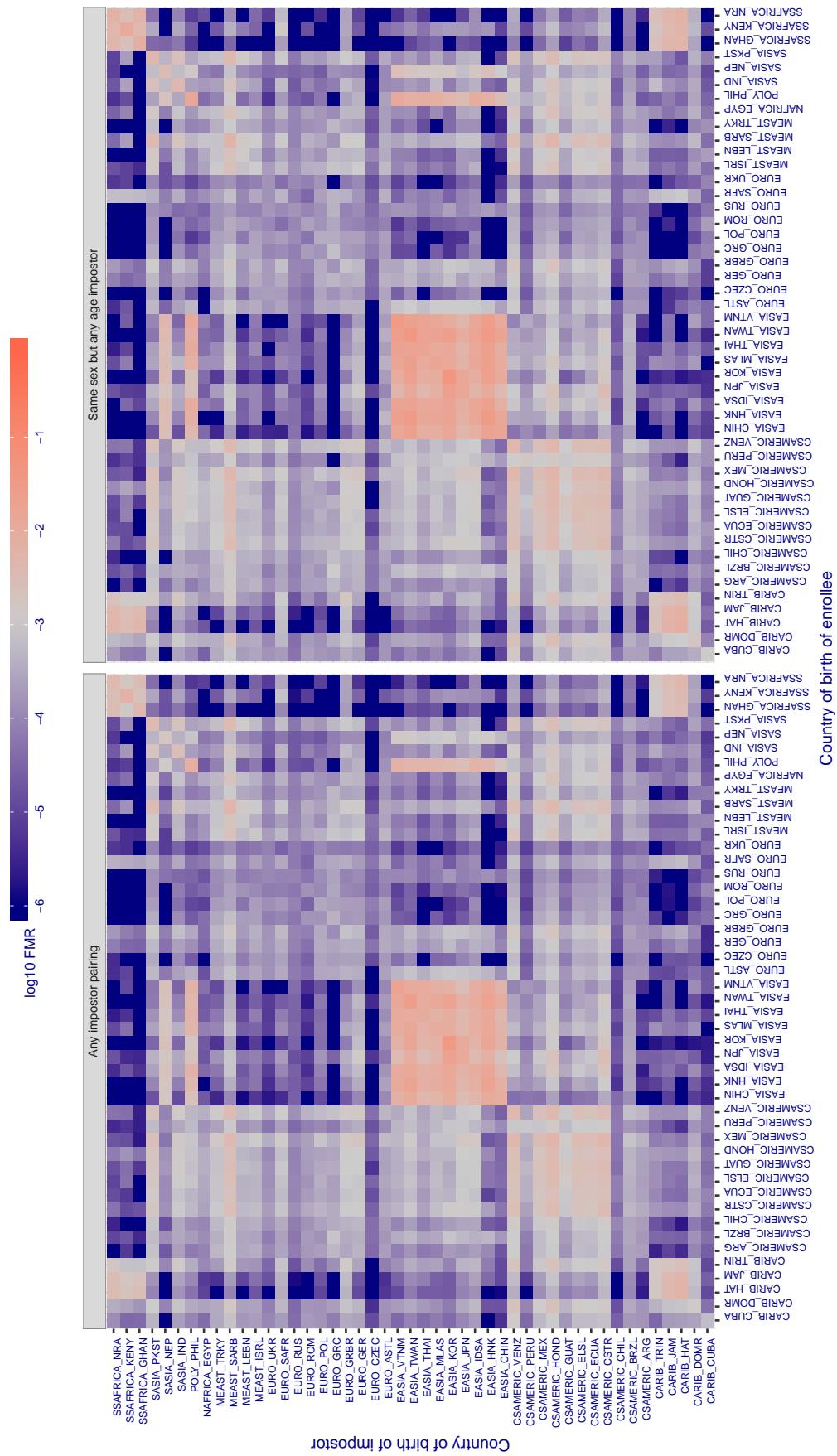


Figure 424: For algorithm yisheng-004 operating on visa images, the heatmap shows false match rates observed over impostor comparisons of faces from different individuals who were born in the given country pair. False matches are counted against a recognition threshold fixed globally to give the target FMR in the plot title, computed over all on the order of 10^{10} impostor comparisons. If text appears in each box it give the same quantity as that coded by the color. Grey indicates FMR is at the intended FMR target level. Light red colors present a security vulnerability to, for example, a passport gate. Each +1 increase in $\log_{10} \text{FMR}$ corresponds to a factor of 10 increase in FMR . The matrix is not quite symmetric because images in the enrollment and verification sets are different.

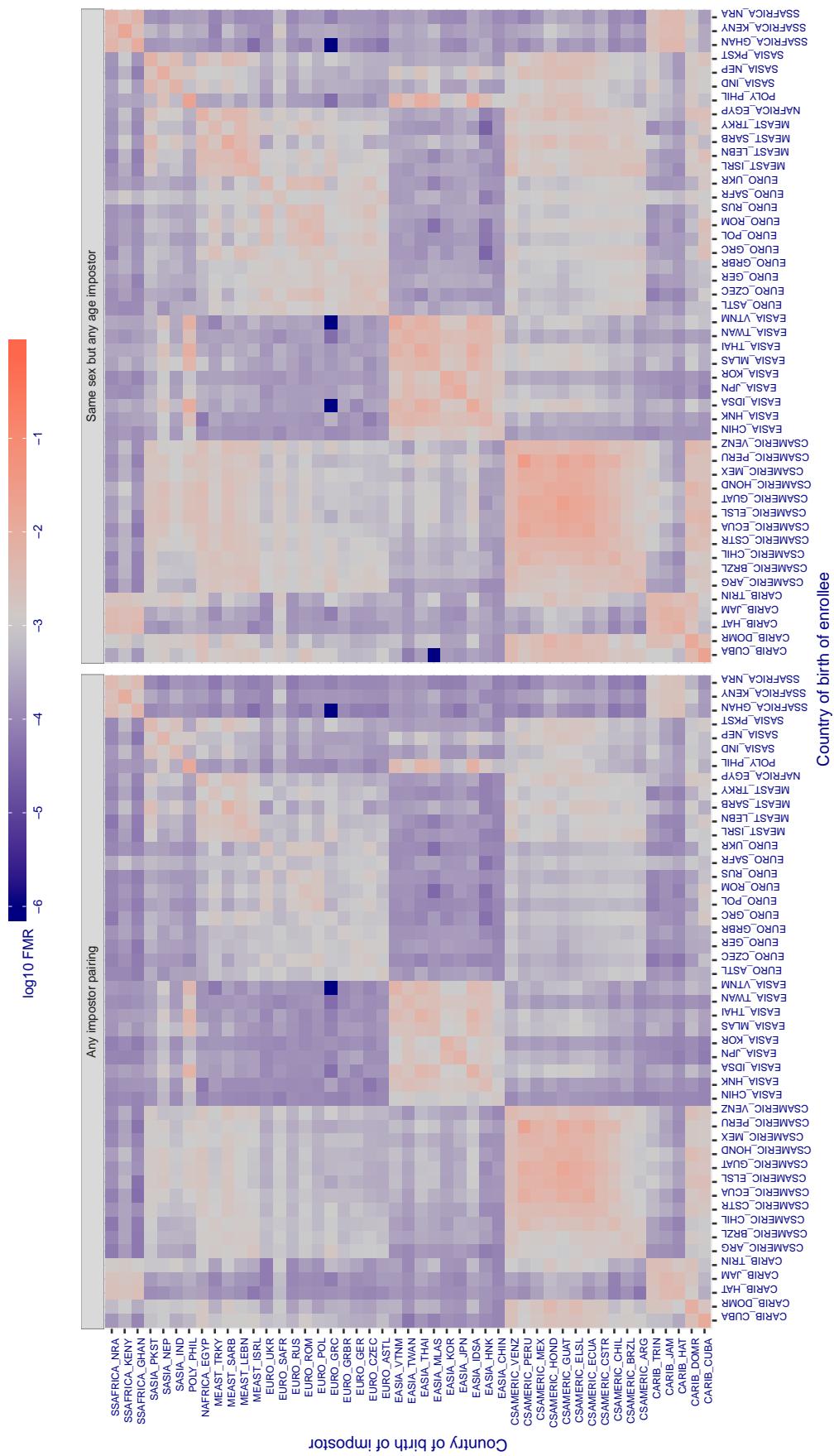
Cross country FMR at threshold T = 37.550 for algorithm yitu_003, giving FMR(T) = 0.001 globally.

Figure 425: For algorithm yitu-003 operating on visa images, the heatmap shows false match rates observed over impostor comparisons of faces from different individuals who were born in the given country pair. False matches are counted against a recognition threshold fixed globally to give the target FMR in the plot title, computed over all on the order of 10^{10} impostor comparisons. If text appears in each box it give the same quantity as that coded by the color. Grey indicates FMR is at the intended FMR target level. Light red colors present a security vulnerability to, for example, a passport gate. Each +1 increase in $\log_{10} \text{FMR}$ corresponds to a factor of 10 increase in FMR. The matrix is not quite symmetric because images in the enrollment and verification sets are different.

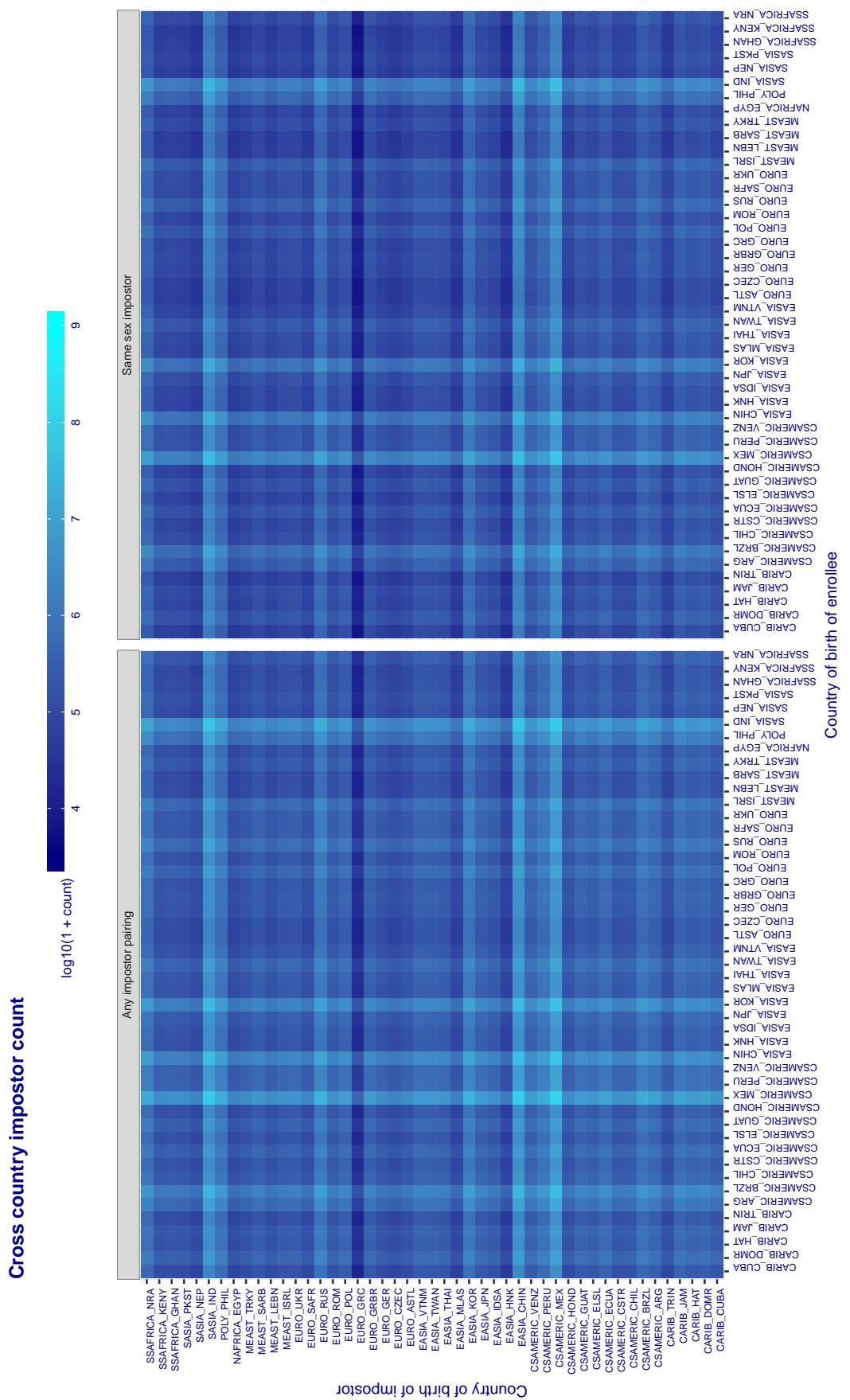


Figure 426: For visa images, the heatmap shows the count of impostor comparisons of faces from different individuals who were born in the given country pair.

3.6.2 Effect of age on impostors

Background: This section shows the effect of age on the impostor distribution. The ideal behaviour is that the age of the enrollee and the impostor would not affect impostor scores. This would support FMR stability over sub-populations.

Goals:

- ▷ To show the effect of relative ages of the impostor and enrollee on false match rates.
- ▷ To determine whether some algorithms have better impostor distribution stability.

Methods:

- ▷ Define 14 age group bins, spanning 0 to over 100 years old.
- ▷ Compute FMR over all impostor comparisons for which the subjects in the enrollee and impostor images have ages in two bins.
- ▷ Compute FMR over all impostor comparisons for which the subjects are additionally of the same sex, and born in the same geographic region.

Results:

The notable aspects are:

- ▷ Diagonal dominance: Impostors are more likely to be matched against their same age group.
- ▷ Same sex and same region impostors are more successful. On the diagonal, an impostor is more likely to succeed by posing as someone of the same sex. If $\Delta \log_{10} \text{FMR} = 0.2$, then same-sex same-region FMR exceeds the all-pairs FMR by factor of $10^{0.2} = 1.6$.
- ▷ Young children impostors give elevated FMR against young children. Older adult impostor give elevated FMR against older adults. These effects are quite large, for example if $\Delta \log_{10} \text{FMR} = 1.0$ larger than a 32 year old, then these groups have higher FMR by a factor of $10^1 = 10$. This would imply an FMR above 0.01 for a nominal (global) FMR = 0.001.
- ▷ Algorithms vary.
- ▷ We computed the same quantities for a global FMR = 0.0001. The effects are similar.

Note the calculations in this section include impostors paired across all countries of birth.

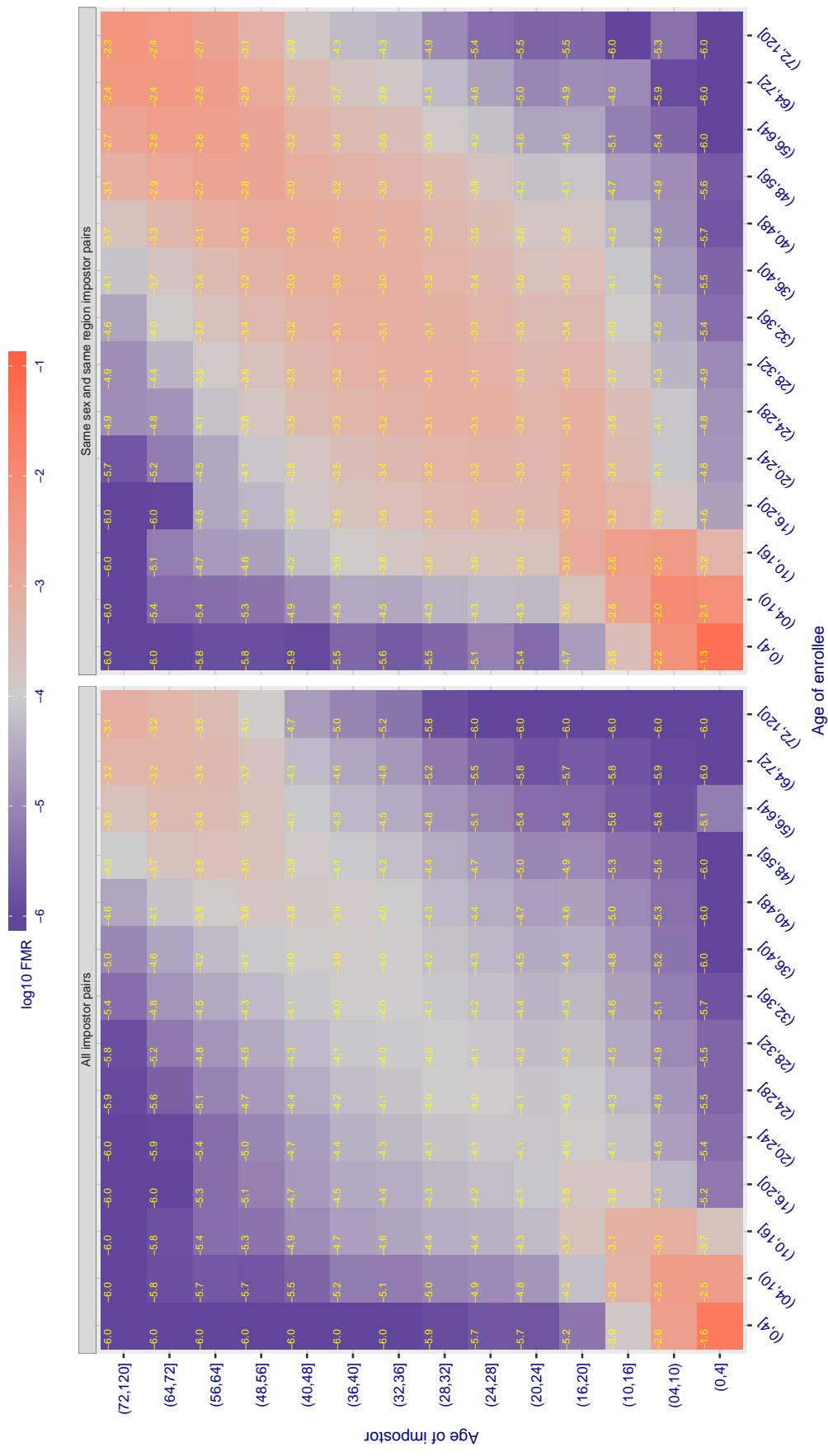
Cross age FMR at threshold T = 2.740 for algorithm 3divi_003, giving $FMR(T) = 0.0001$ globally.

Figure 427: For algorithm 3divi-003 operating on visa images, the heatmap shows false match observed over impostor comparisons of faces from different individuals who have the given age pair. False matches are counted against a recognition threshold fixed globally to give $FMR = 0.0001$ over all on the order of 10^{10} impostor comparisons. The text in each box gives the same quantity as that coded by the color. Light colors present a security vulnerability to, for example, a passport gate.

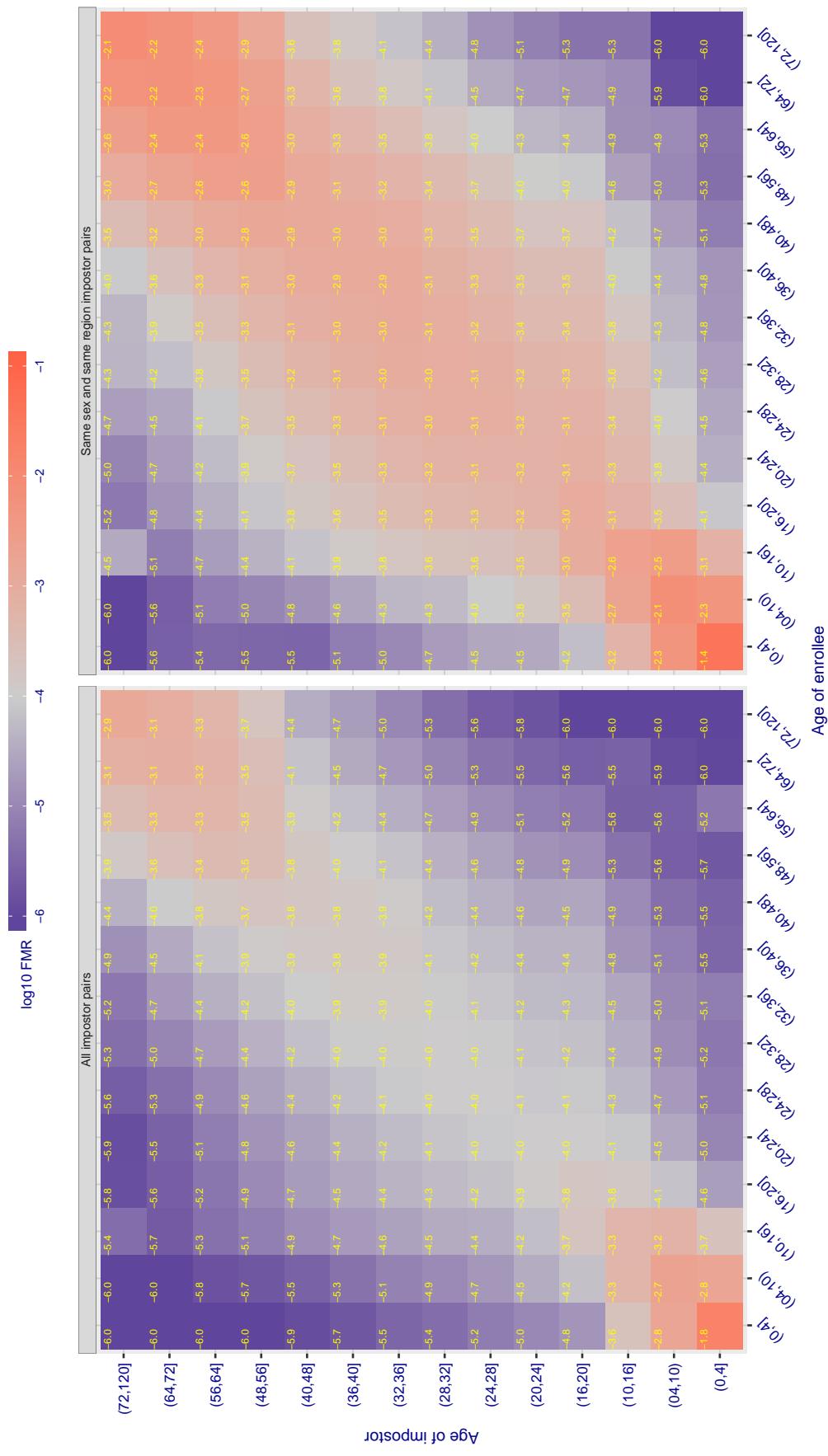
Cross age FMR at threshold T = 2.857 for algorithm 3divi_004, giving $FMR(T) = 0.0001$ globally.

Figure 428: For algorithm 3divi-004 operating on visa images, the heatmap shows false match observed over impostor comparisons of faces from different individuals who have the given age pair. False matches are counted against a recognition threshold fixed globally to give $FMR = 0.0001$ over all on the order of 10^{10} impostor comparisons. The text in each box gives the same quantity as that coded by the color. Light colors present a security vulnerability to, for example, a passport gate.

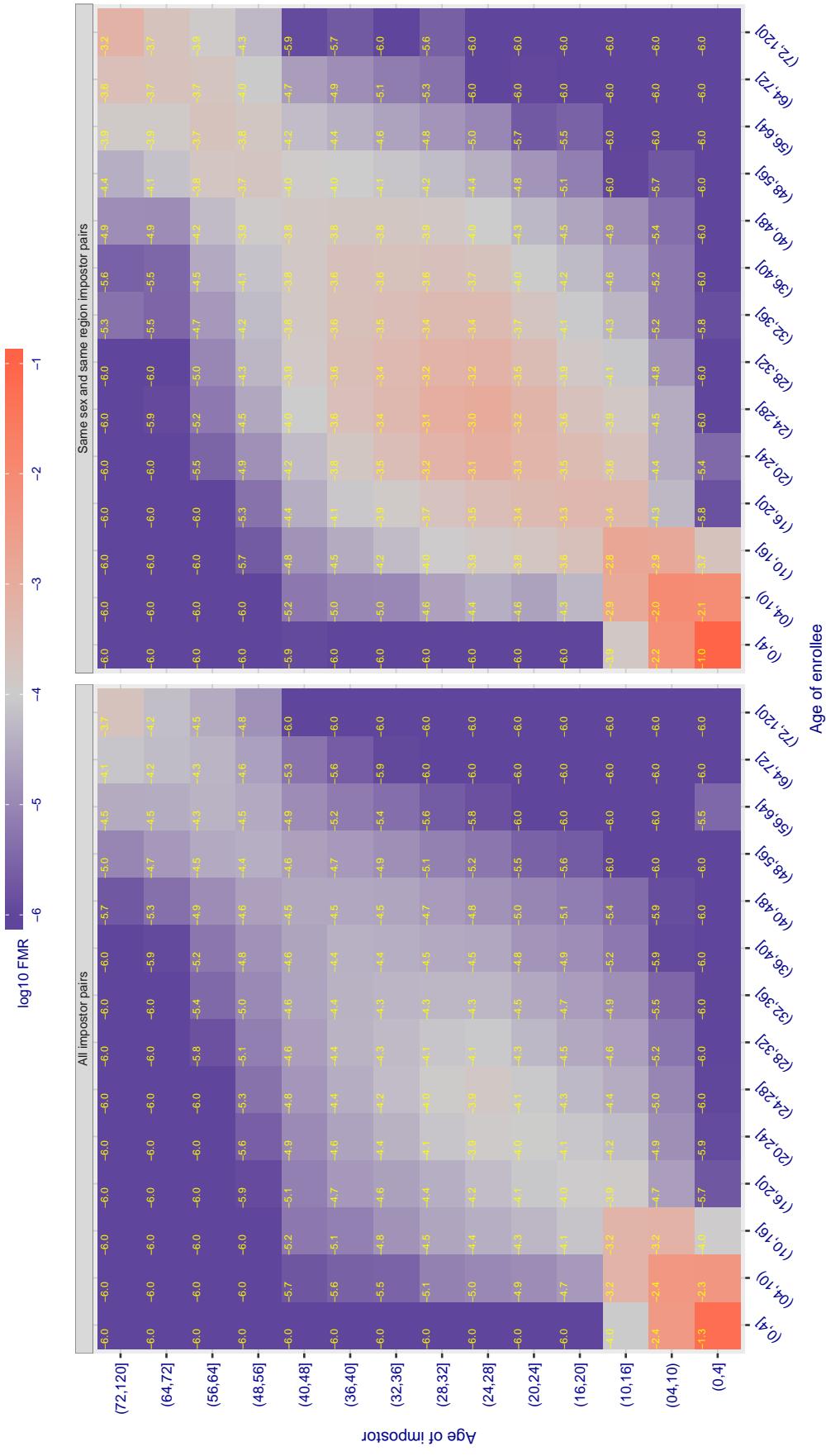


Figure 429: For algorithm adera-001 operating on visa images, the heatmap shows false match observed over impostor comparisons of faces from different individuals who have the given age pair. False matches are counted against a recognition threshold fixed globally to give $FMR = 0.0001$ over all on the order of 10^{10} impostor comparisons. The text in each box gives the same quantity as that coded by the color. Light colors present a security vulnerability to, for example, a passport gate.

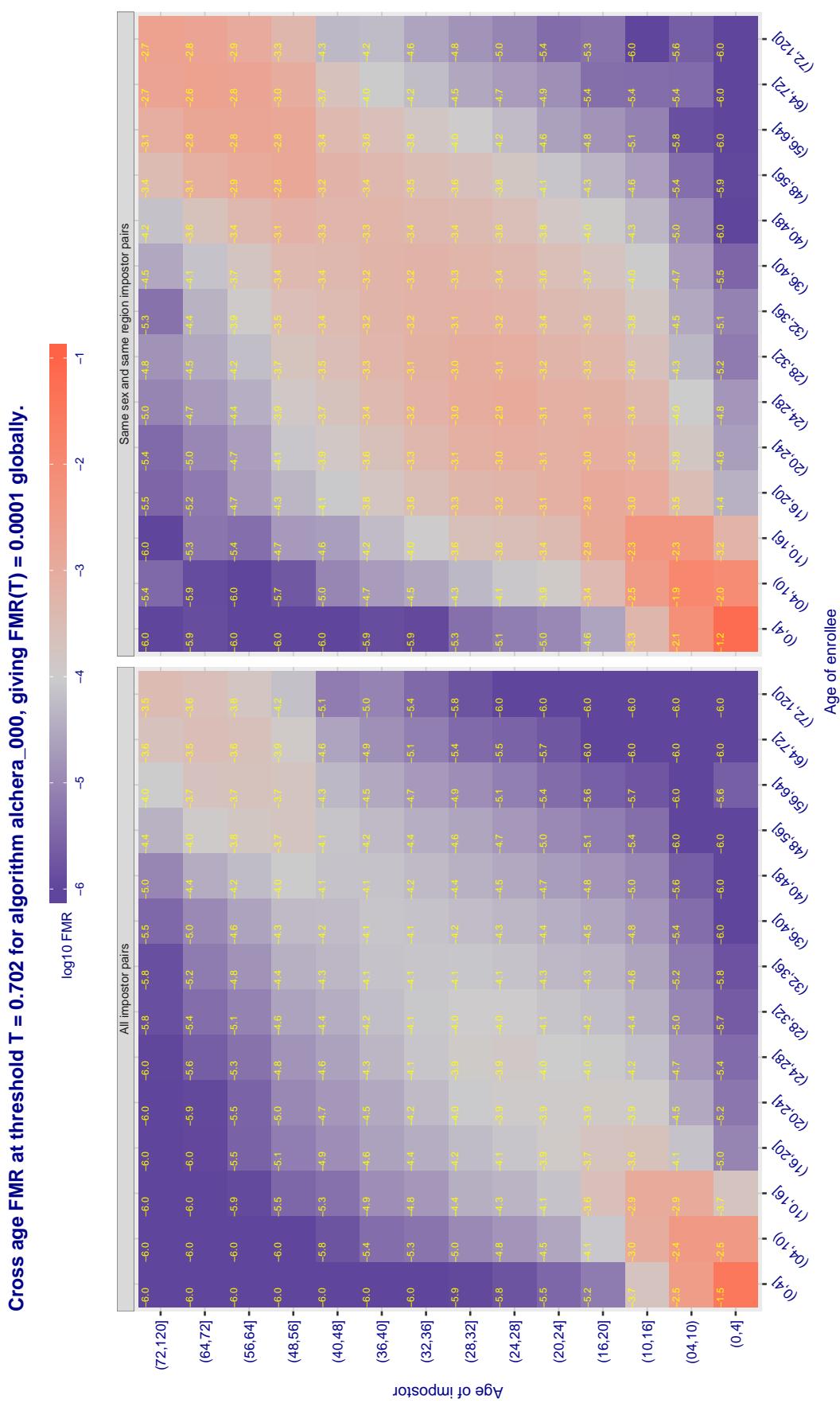


Figure 430: For algorithm alchera-000 operating on visa images, the heatmap shows false match observed over impostor comparisons of faces from different individuals who have the given age pair. False matches are counted against a recognition threshold fixed globally to give $FMR = 0.0001$ over all on the order of 10^{10} impostor comparisons. The text in each box gives the same quantity as that coded by the color. Light colors present a security vulnerability to, for example, a passport gate.

Cross age FMR at threshold T = 0.713 for algorithm alchera_001, giving FMR(T) = 0.0001 globally.

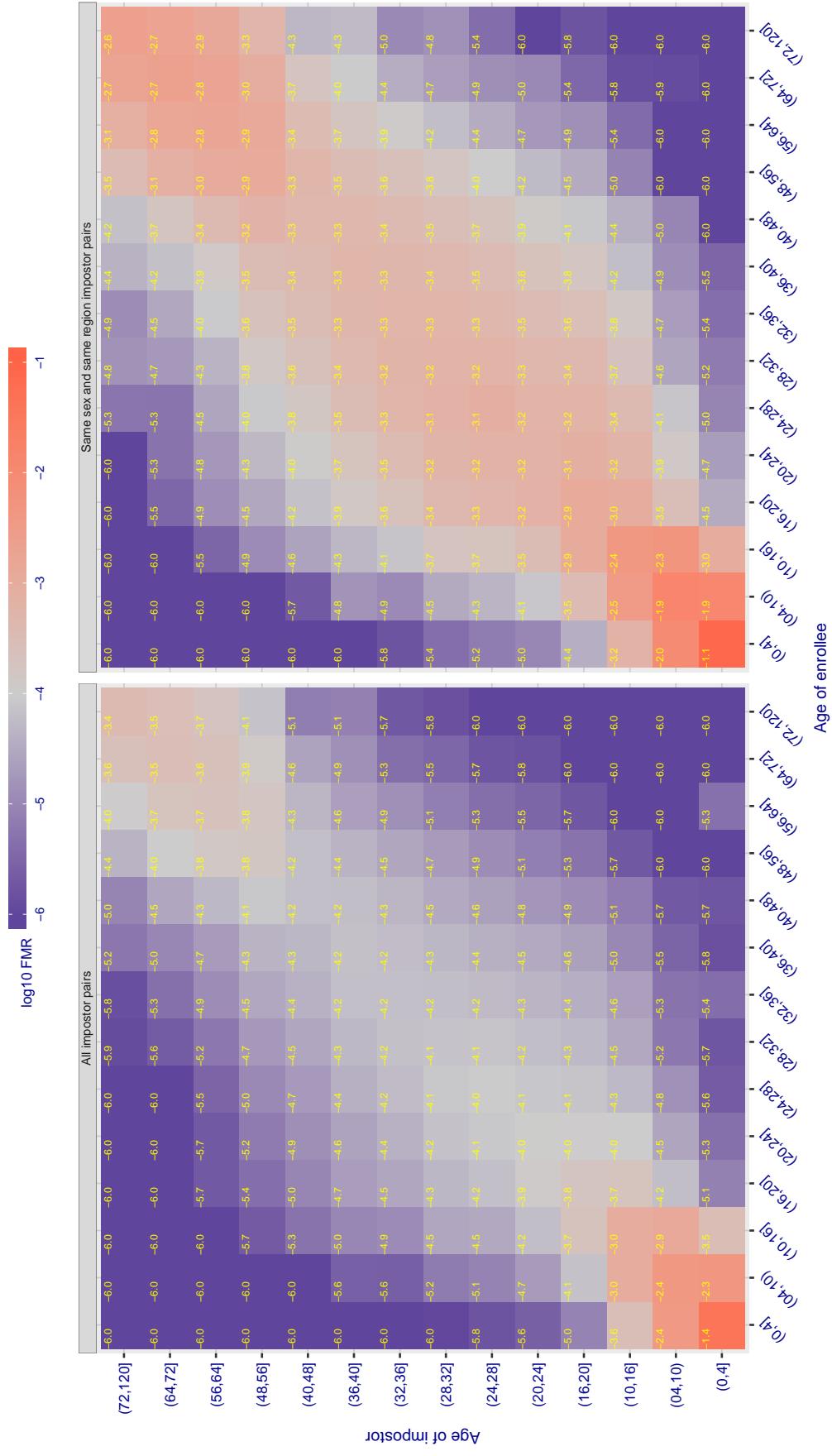


Figure 431: For algorithm alchera-001 operating on visa images, the heatmap shows false match observed over impostor comparisons of faces from different individuals who have the given age pair. False matches are counted against a recognition threshold fixed globally to give $FMR = 0.0001$ over all on the order of 10^{10} impostor comparisons. The text in each box gives the same quantity as that coded by the color. Light colors present a security vulnerability to, for example, a passport gate.

Cross age FMR at threshold T = 0.433 for algorithm allgovision_000, giving $FMR(T) = 0.0001$ globally.

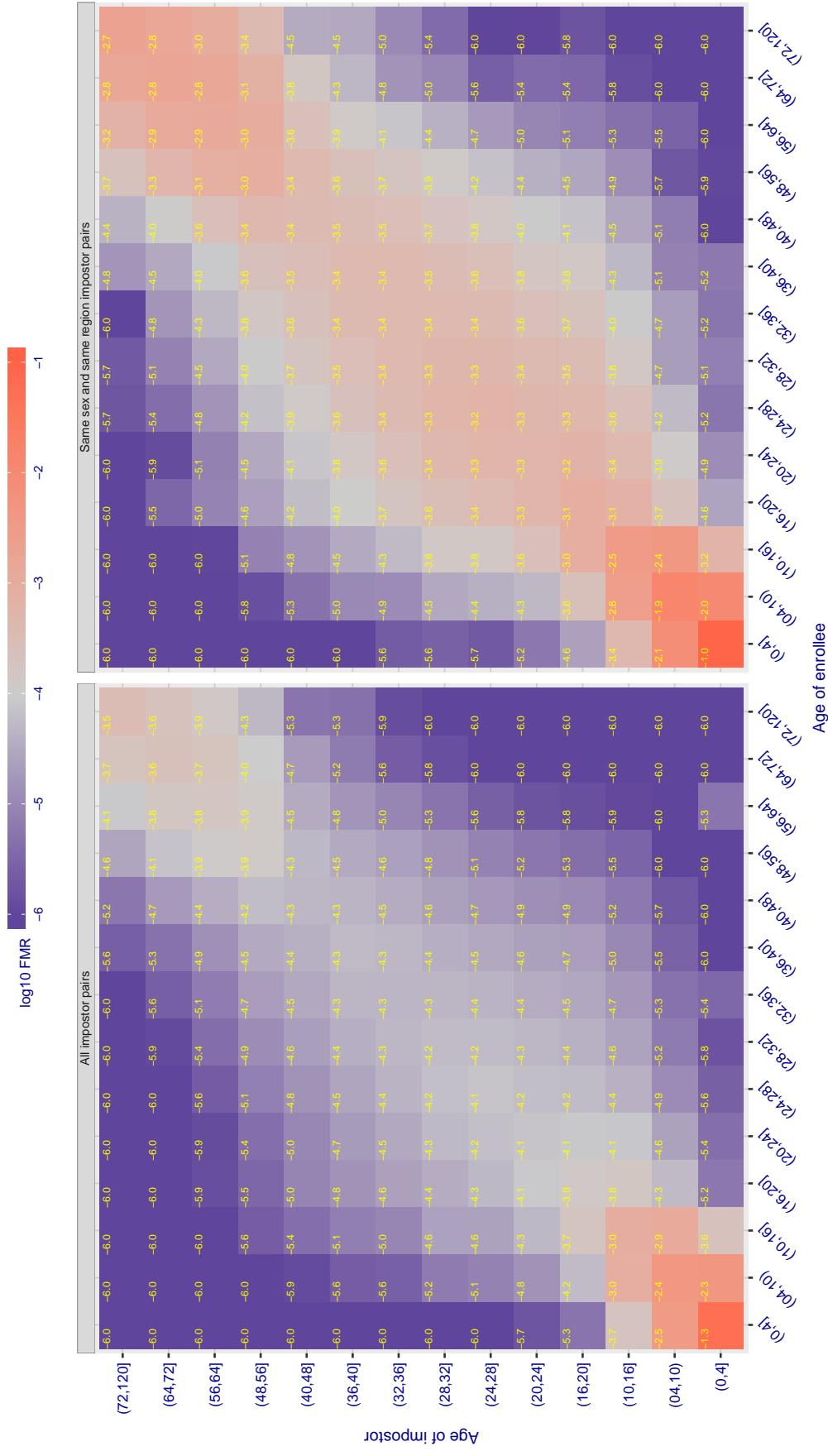


Figure 432: For algorithm allgovision-000 operating on visa images, the heatmap shows false match observed over impostor comparisons of faces from different individuals who have the given age pair. False matches are counted against a recognition threshold fixed globally to give $FMR = 0.0001$ over all on the order of 10^{10} impostor comparisons. The text in each box gives the same quantity as that coded by the color. Light colors present a security vulnerability to, for example, a passport gate.

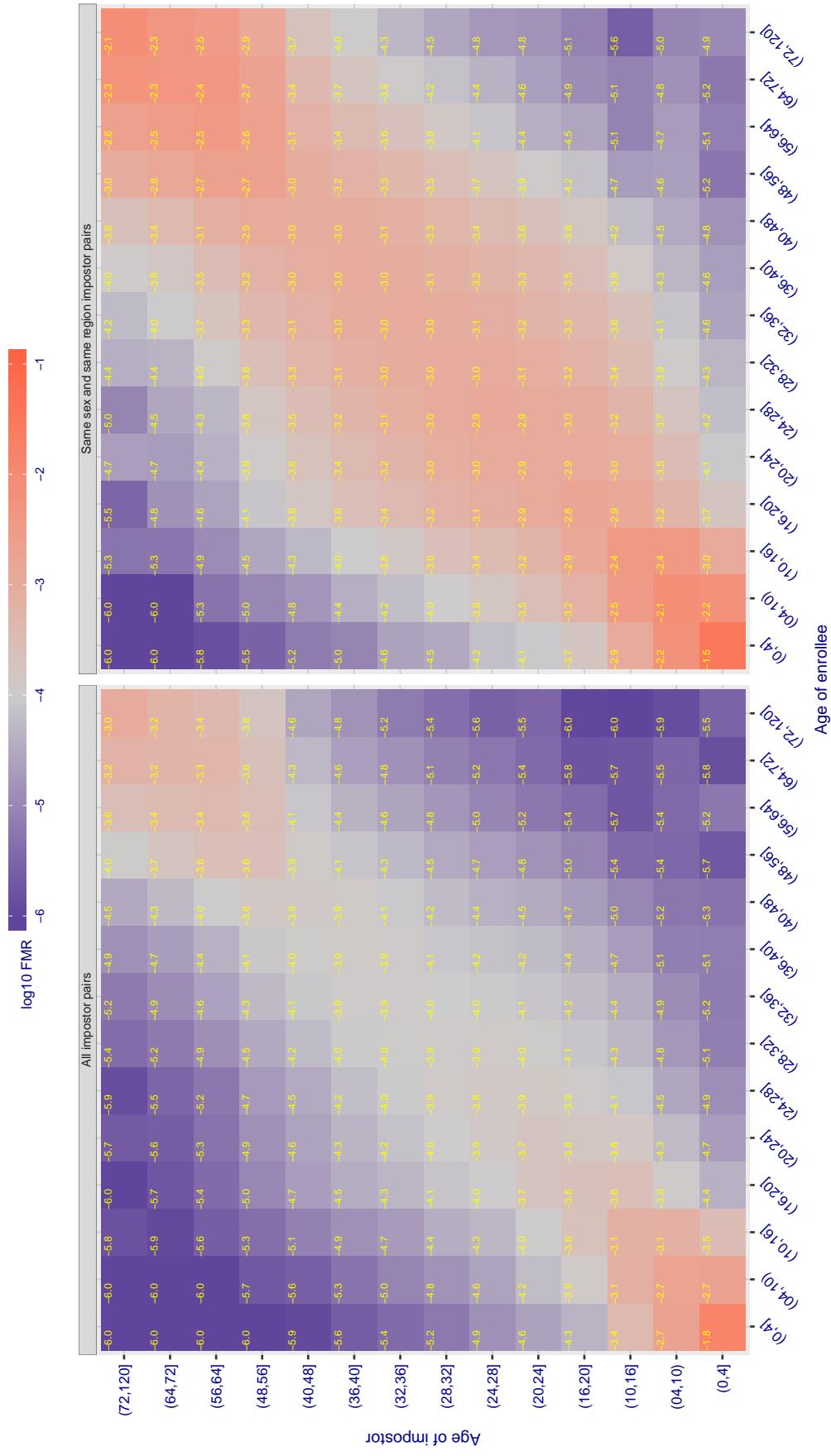
Cross age FMR at threshold T = 0.396 for algorithm alphaface_001, giving $FMR(T) = 0.0001$ globally.

Figure 433: For algorithm alphaface-001 operating on visa images, the heatmap shows false match observed over impostor comparisons of faces from different individuals who have the given age pair. False matches are counted against a recognition threshold fixed globally to give $FMR = 0.001$ over all on the order of 10^{10} impostor comparisons. The text in each box gives the same quantity as that coded by the color. Light colors present a security vulnerability to, for example, a passport gate.

Cross age FMR at threshold T = 3.640 for algorithm amplifiedgroup_001, giving $FMR(T) = 0.0001$ globally.

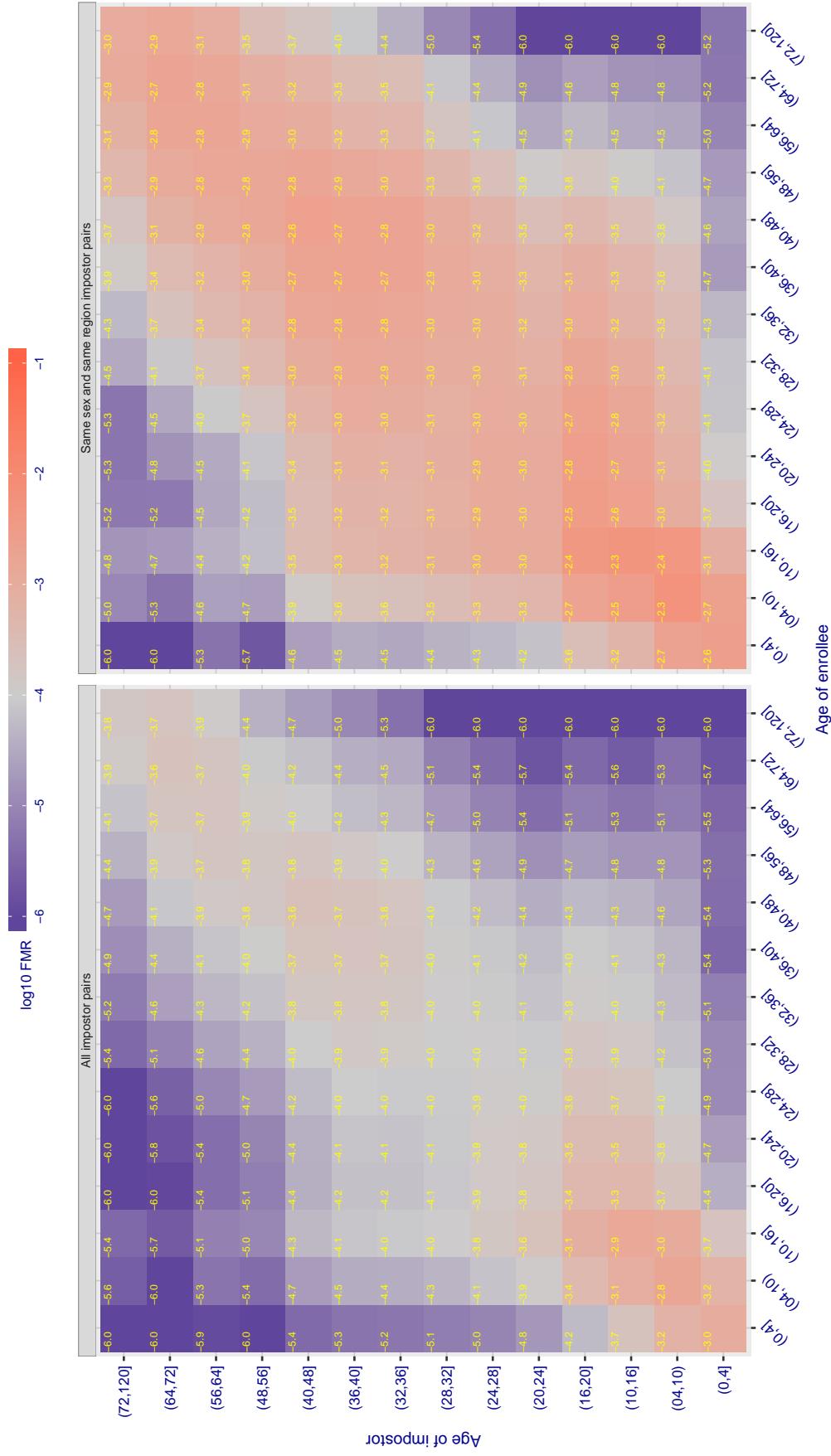


Figure 434: For algorithm amplifiedgroup-001 operating on visa images, the heatmap shows false match observed over impostor comparisons of faces from different individuals who have the given age pair. False matches are counted against a recognition threshold fixed globally to give $FMR = 0.0001$ over all on the order of 10^{10} impostor comparisons. The text in each box gives the same quantity as that coded by the color. Light colors present a security vulnerability to, for example, a passport gate.

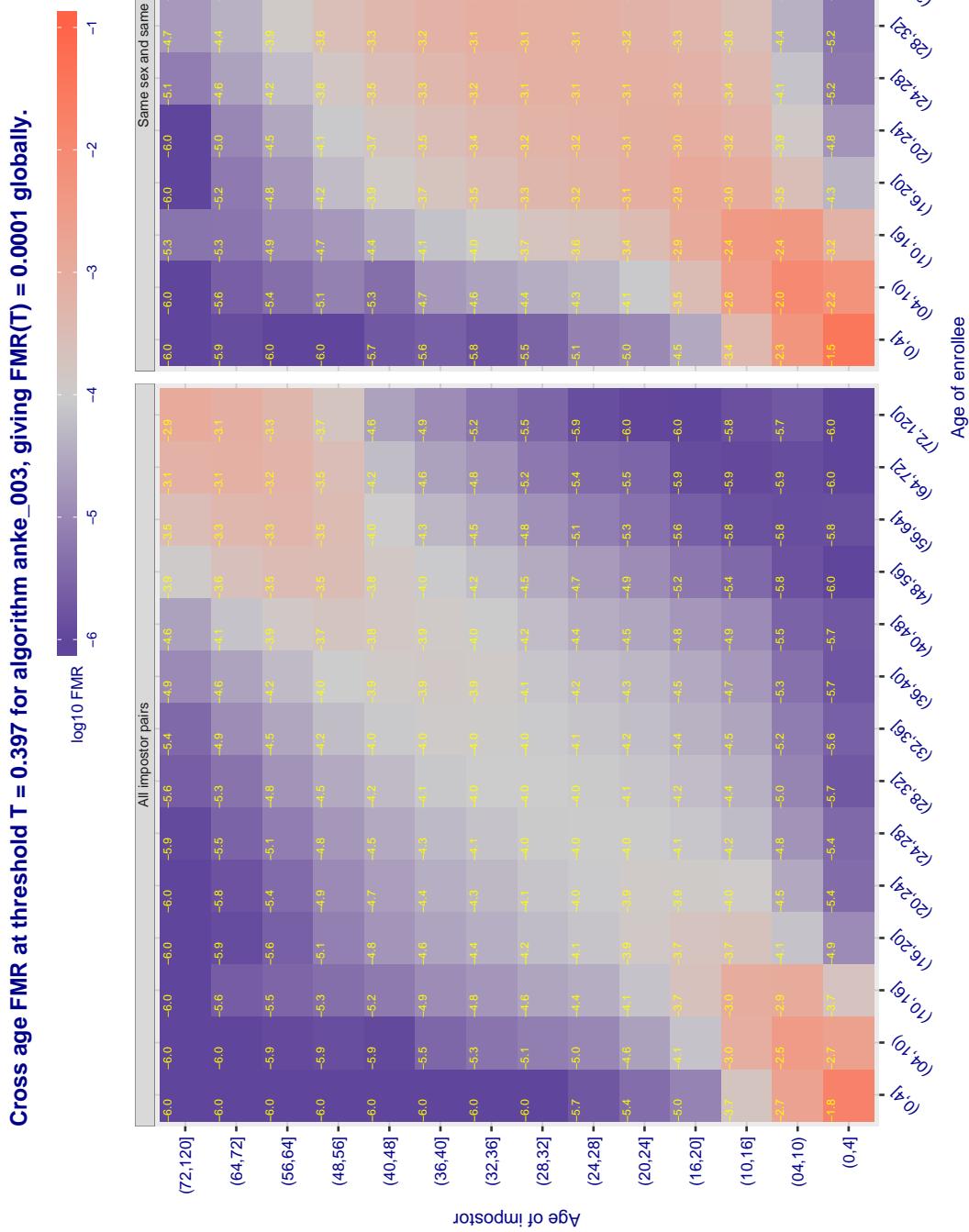


Figure 435: For algorithm anke-003 operating on visa images, the heatmap shows false match observed over impostor comparisons of faces from different individuals who have the given age pair. False matches are counted against a recognition threshold fixed globally to give $FMR = 0.0001$ over all on the order of 10^{10} impostor comparisons. The text in each box gives the same quantity as that coded by the color. Light colors present a security vulnerability to, for example, a passport gate.

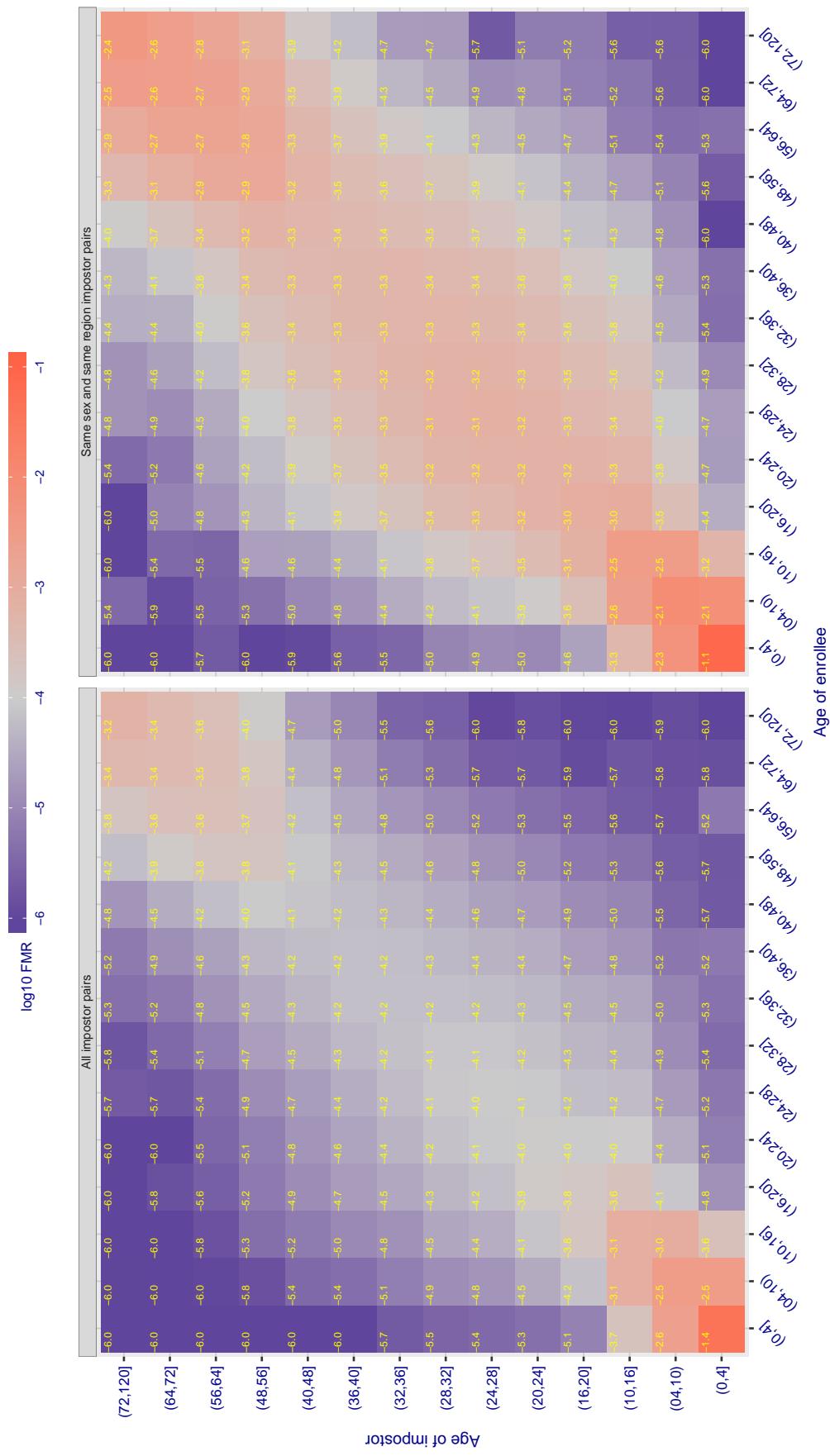
Cross age FMR at threshold T = 0.397 for algorithm anke_004, giving $FMR(T) = 0.0001$ globally.

Figure 436: For algorithm anke-004 operating on visa images, the heatmap shows false match observed over imposter comparisons of faces from different individuals who have the given age pair. False matches are counted against a recognition threshold fixed globally to give $FMR = 0.0001$ over all on the order of 10^{10} impostor comparisons. The text in each box gives the same quantity as that coded by the color. Light colors present a security vulnerability to, for example, a passport gate.

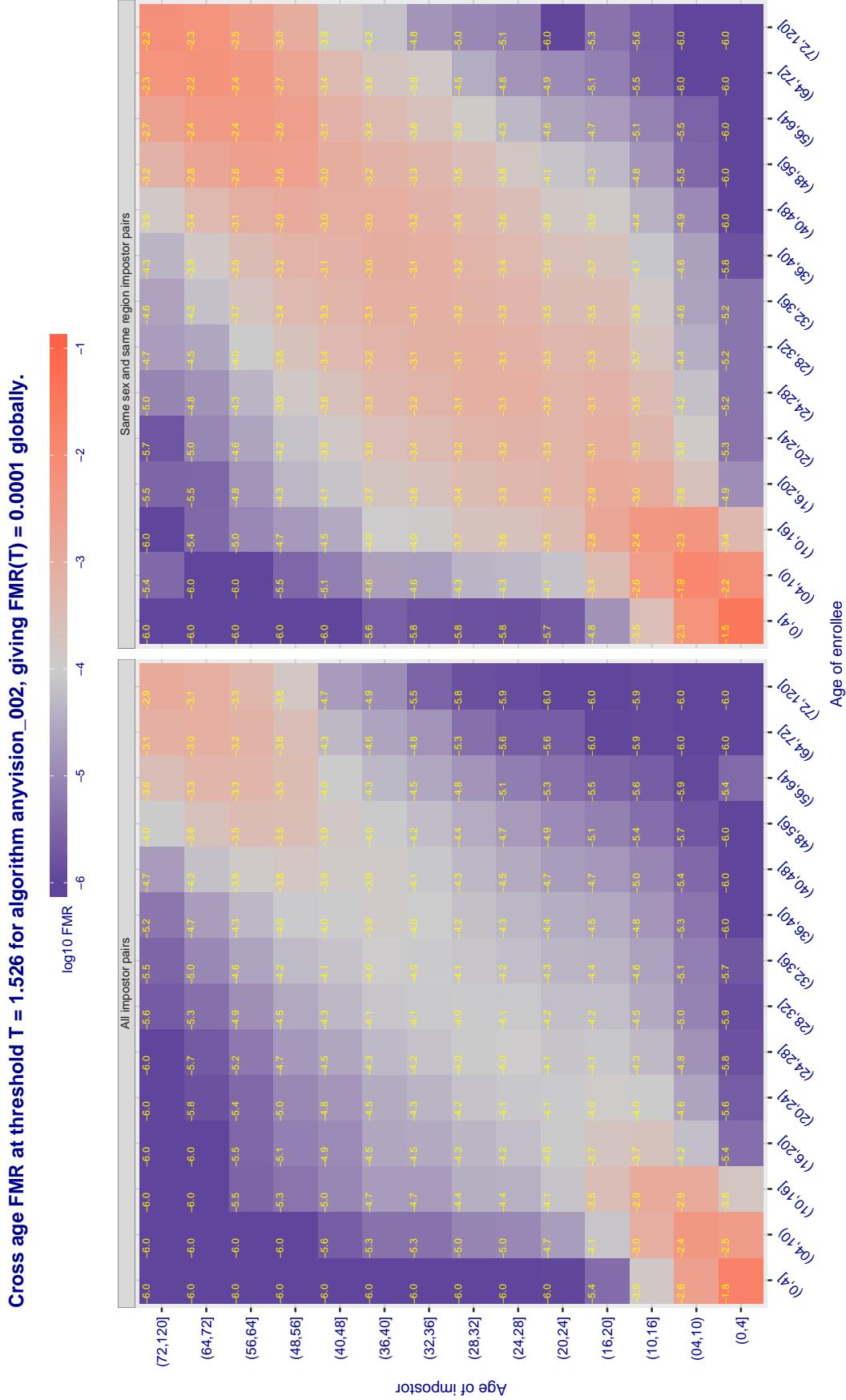


Figure 437: For algorithm anyvision-002 operating on visa images, the heatmap shows false match observed over impostor comparisons of faces from different individuals who have the given age pair. False matches are counted against a recognition threshold fixed globally to give $FMR = 0.001$ over all on the order of 10^{10} impostor comparisons. The text in each box gives the same quantity as that coded by the color. Light colors present a security vulnerability to, for example, a passport gate.

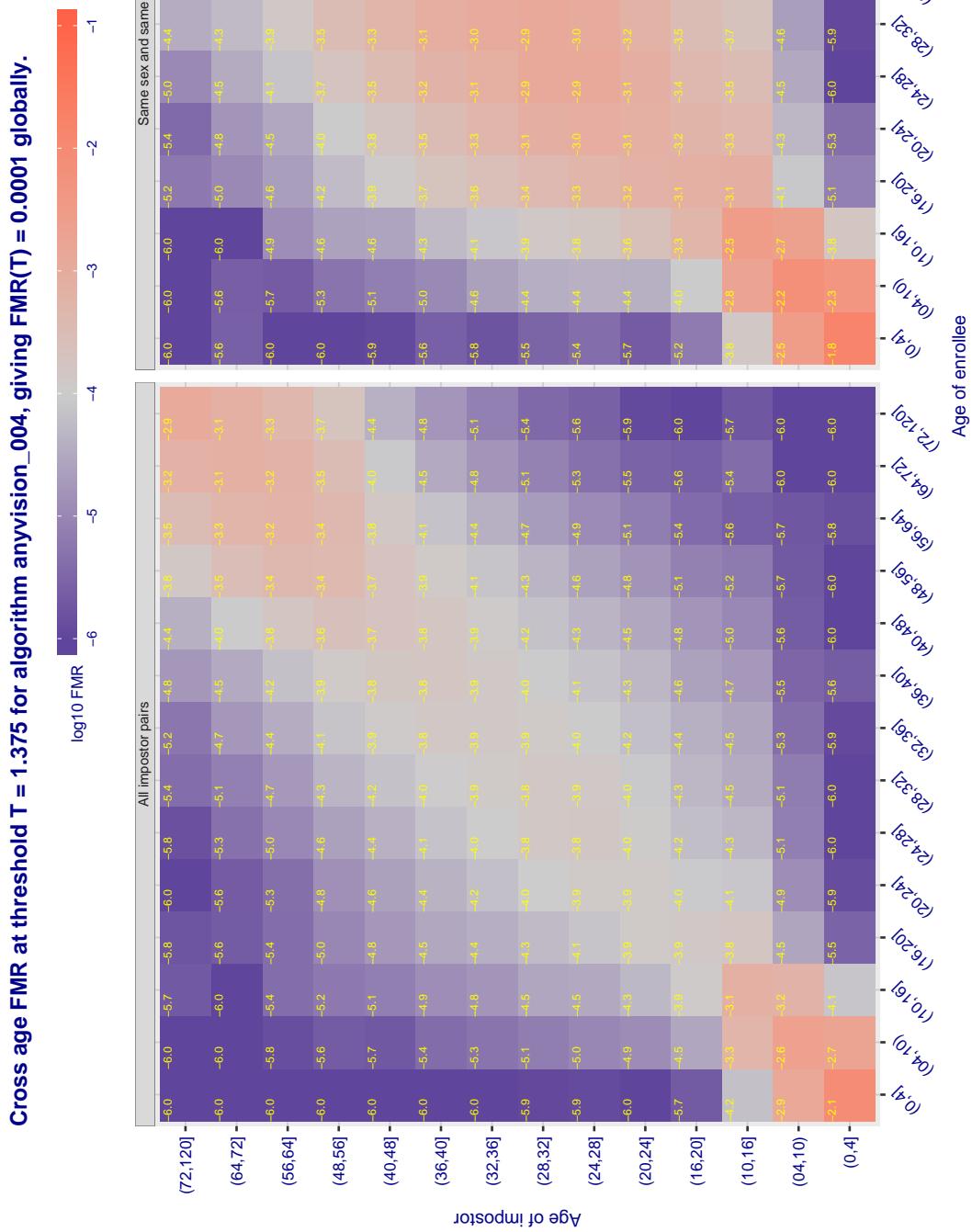


Figure 438: For algorithm anyvision-004 operating on visa images, the heatmap shows false match observed over impostor comparisons of faces from different individuals who have the given age pair. False matches are counted against a recognition threshold fixed globally to give $FMR = 0.001$ over all on the order of 10^{10} impostor comparisons. The text in each box gives the same quantity as that coded by the color. Light colors present a security vulnerability to, for example, a passport gate.

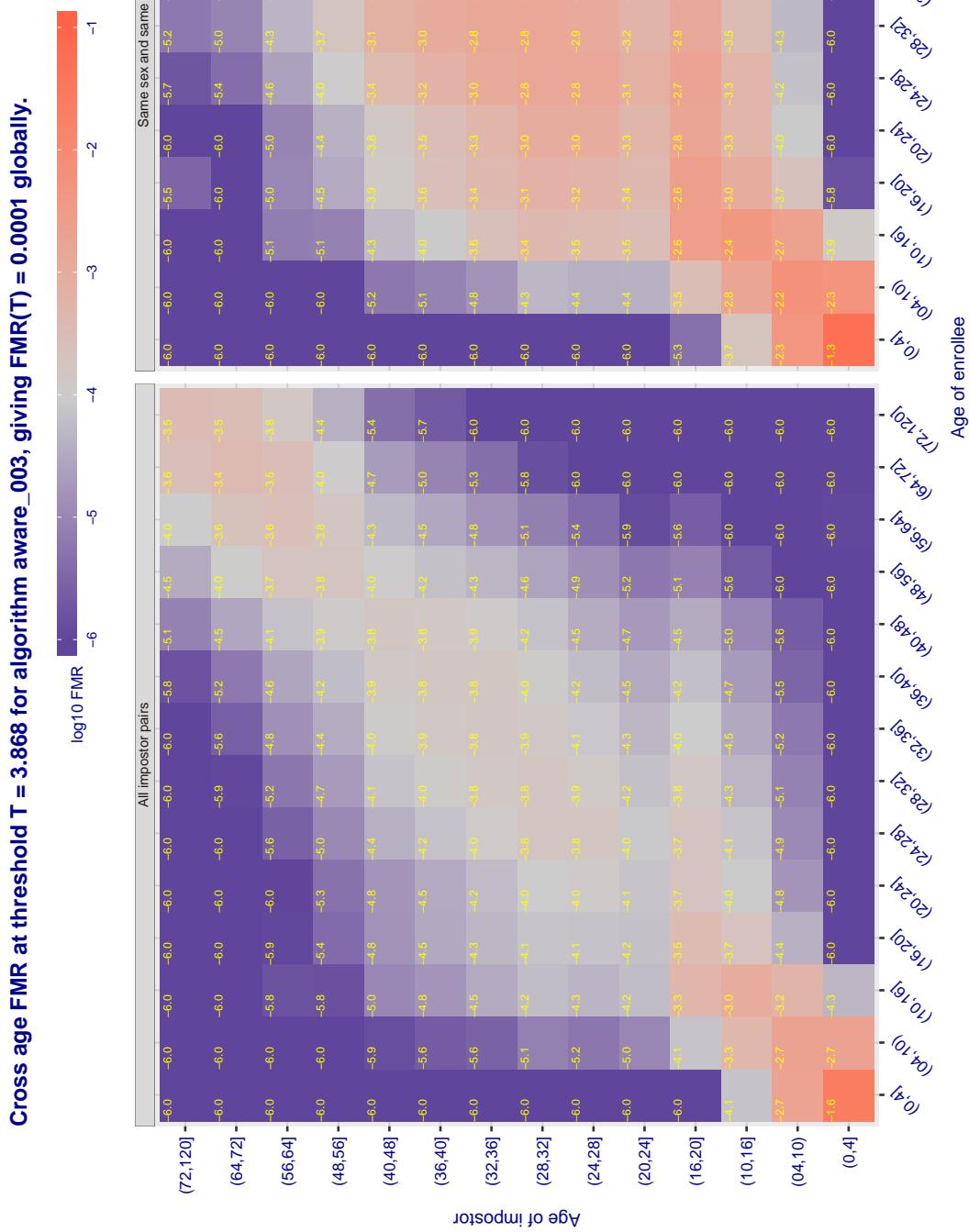


Figure 439: For algorithm aware-003 operating on visa images, the heatmap shows false match observed over impostor comparisons of faces from different individuals who have the given age pair. False matches are counted against a recognition threshold fixed globally to give $FMR = 0.0001$ over all on the order of 10^{10} impostor comparisons. The text in each box gives the same quantity as that coded by the color. Light colors present a security vulnerability to, for example, a passport gate.

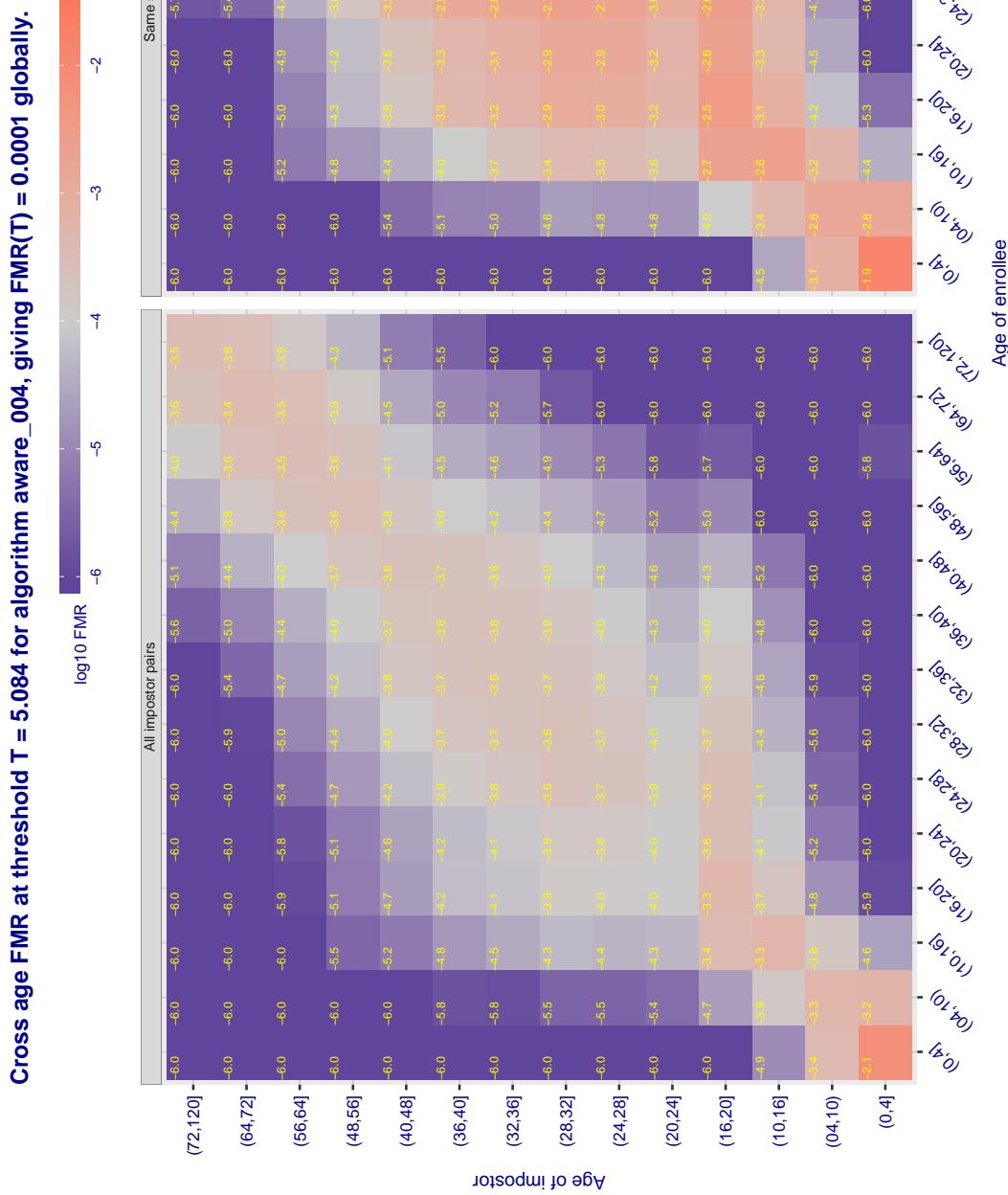


Figure 440: For algorithm aware-004 operating on visa images, the heatmap shows false match observed over impostor comparisons of faces from different individuals who have the given age pair. False matches are counted against a recognition threshold fixed globally to give $FMR = 0.0001$ over all on the order of 10^{10} impostor comparisons. The text in each box gives the same quantity as that coded by the color. Light colors present a security vulnerability to, for example, a passport gate.

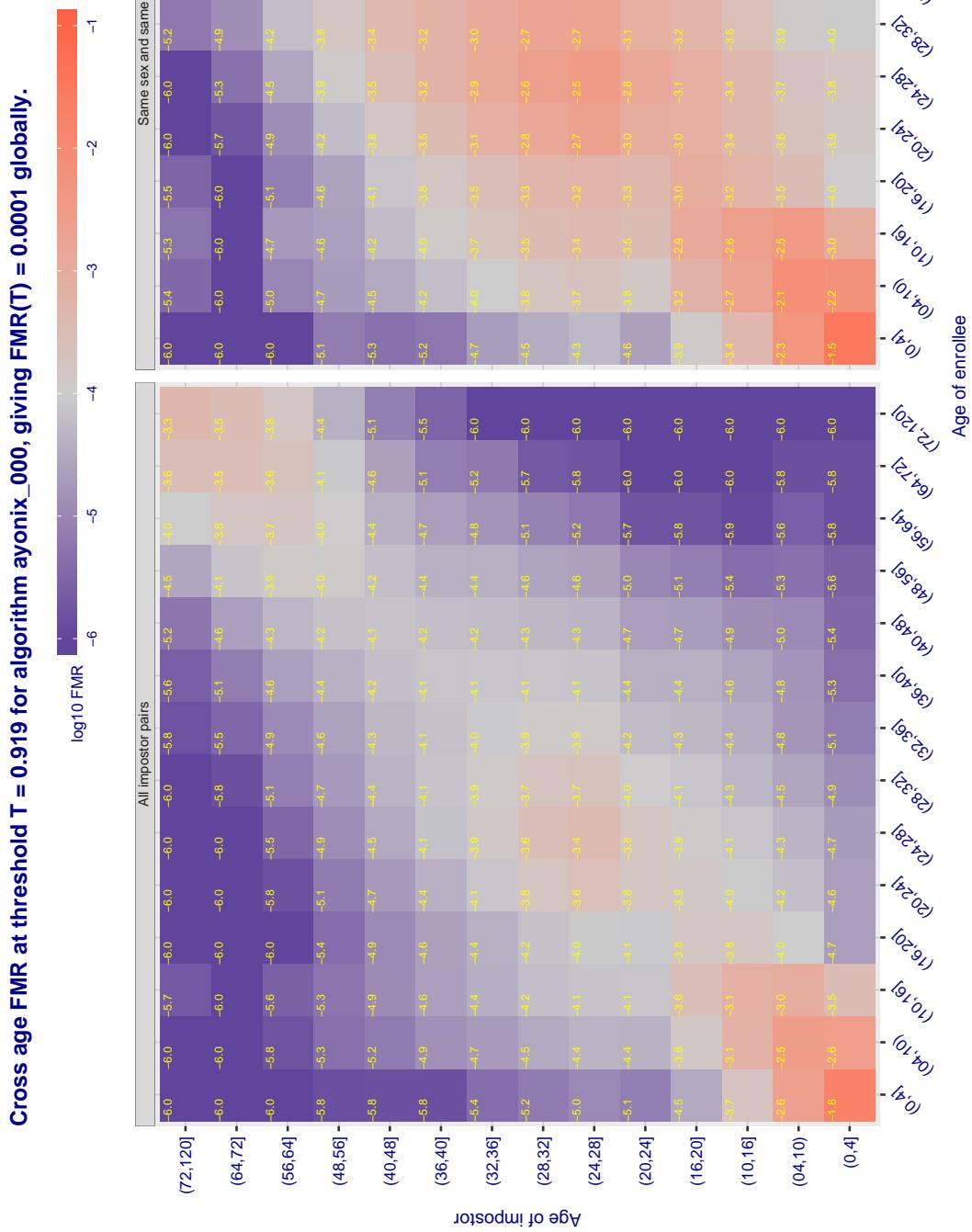


Figure 441: For algorithm ayonix-000 operating on visa images, the heatmap shows false match observed over impostor comparisons of faces from different individuals who have the given age pair. False matches are counted against a recognition threshold fixed globally to give $FMR = 0.0001$ over all on the order of 10^{10} impostor comparisons. The text in each box gives the same quantity as that coded by the color. Light colors present a security vulnerability to, for example, a passport gate.

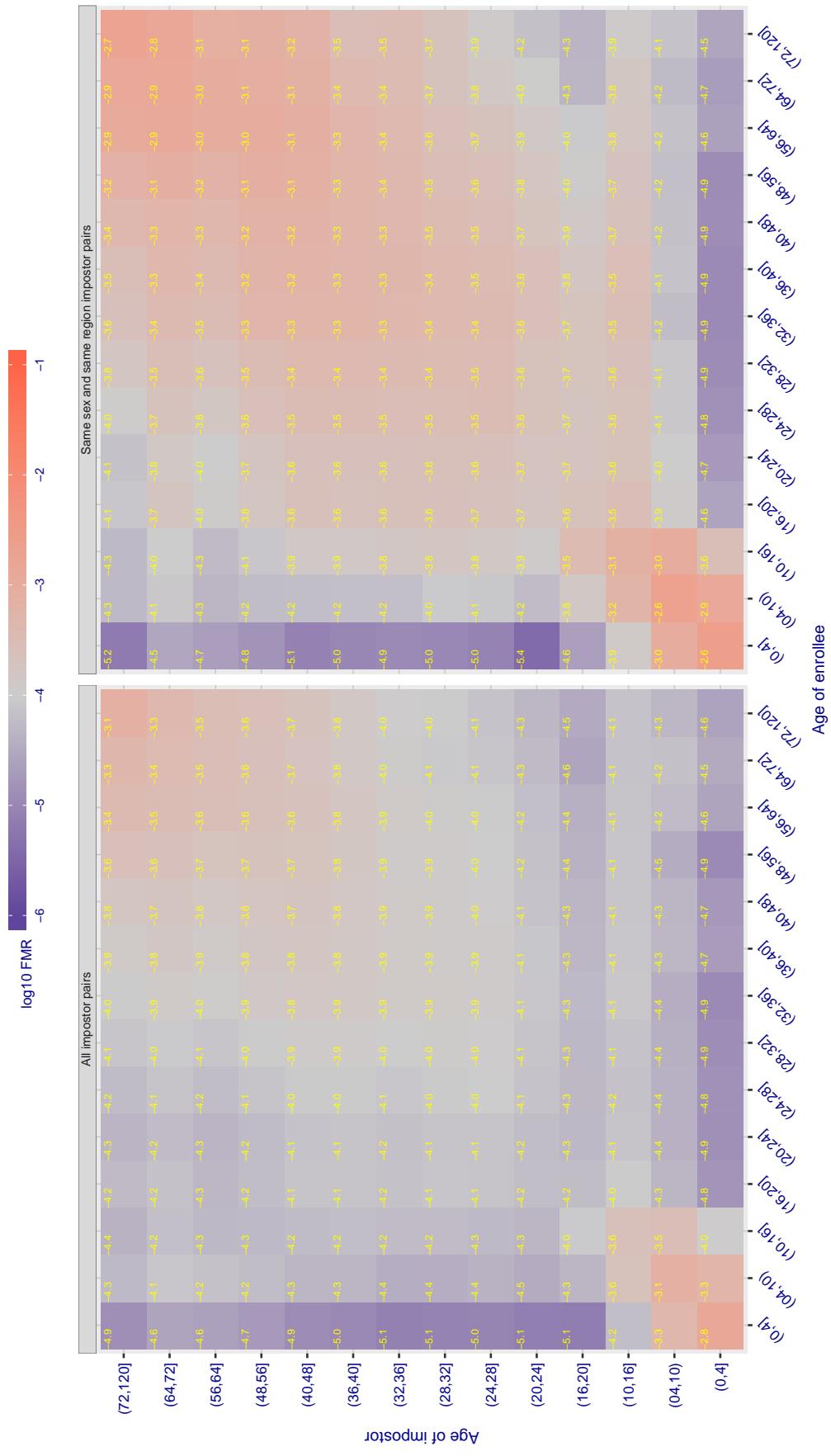
Cross age FMR at threshold T = 0.731 for algorithm bm_001, giving $FMR(T) = 0.0001$ globally.

Figure 442: For algorithm bm-001 operating on visa images, the heatmap shows false match observed over impostor comparisons of faces from different individuals who have the given age pair. False matches are counted against a recognition threshold fixed globally to give $FMR = 0.0001$ over all on the order of 10^{10} impostor comparisons. The text in each box gives the same quantity as that coded by the color. Light colors present a security vulnerability to, for example, a passport gate.

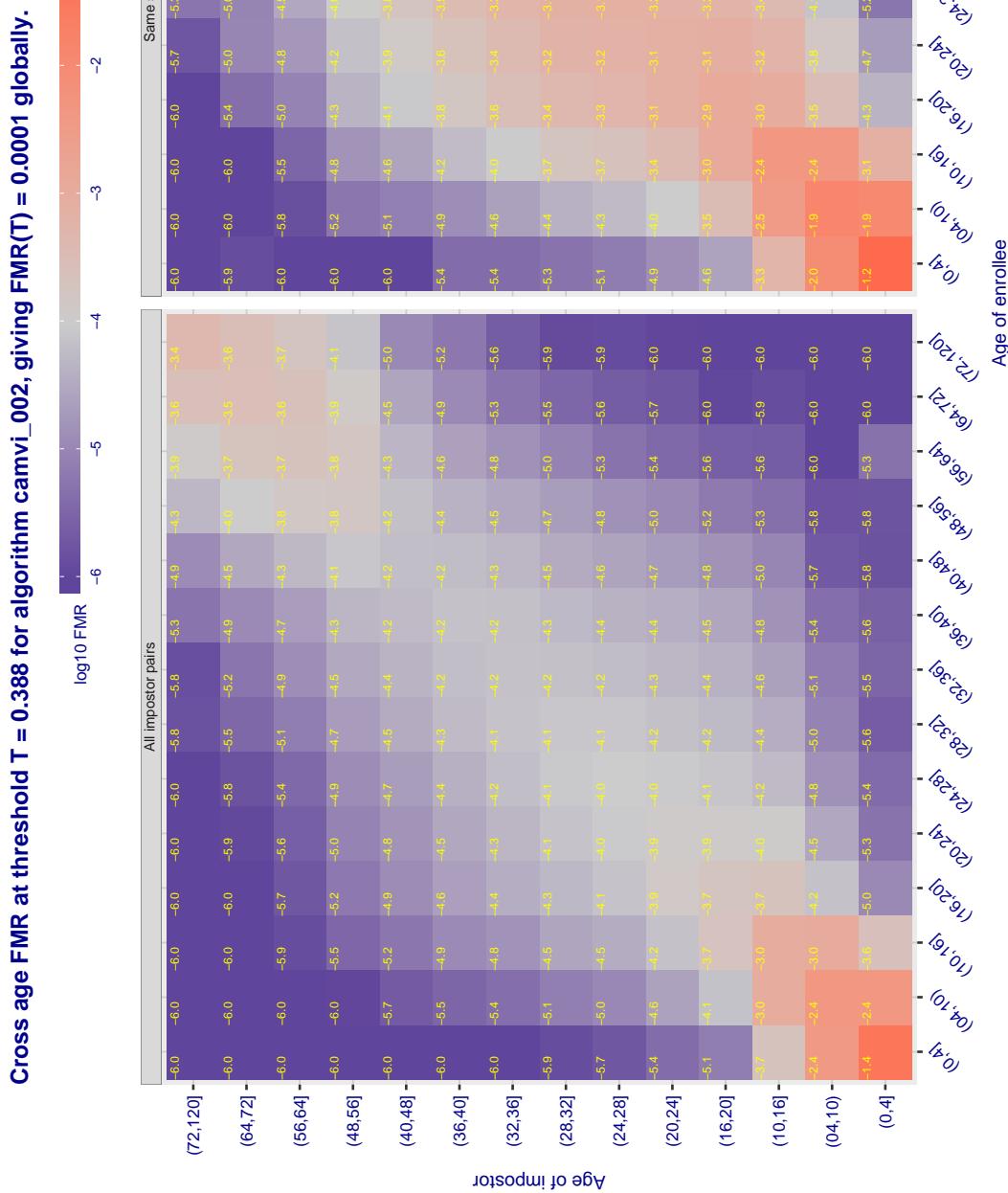


Figure 443: For algorithm camvi-002 operating on visa images, the heatmap shows false match observed over impostor comparisons of faces from different individuals who have the given age pair. False matches are counted against a recognition threshold fixed globally to give $FMR = 0.0001$ over all on the order of 10^{10} impostor comparisons. The text in each box gives the same quantity as that coded by the color. Light colors present a security vulnerability to, for example, a passport gate.

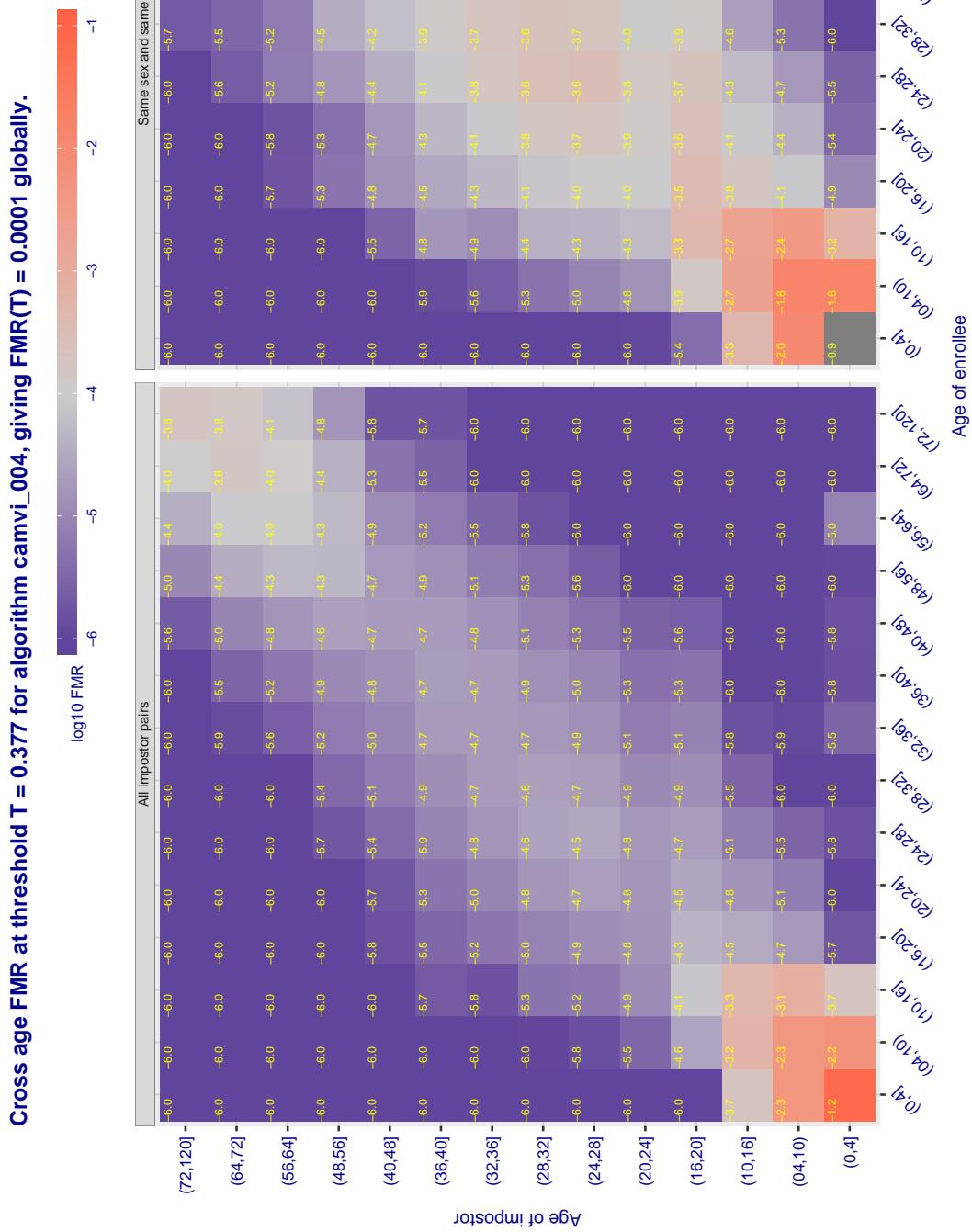


Figure 44: For algorithm camvi-004 operating on visa images, the heatmap shows false match observed over impostor comparisons of faces from different individuals who have the given age pair. False matches are counted against a recognition threshold fixed globally to give $FMR = 0.0001$ over all on the order of 10^{10} impostor comparisons. The text in each box gives the same quantity as that coded by the color. Light colors present a security vulnerability to, for example, a passport gate.

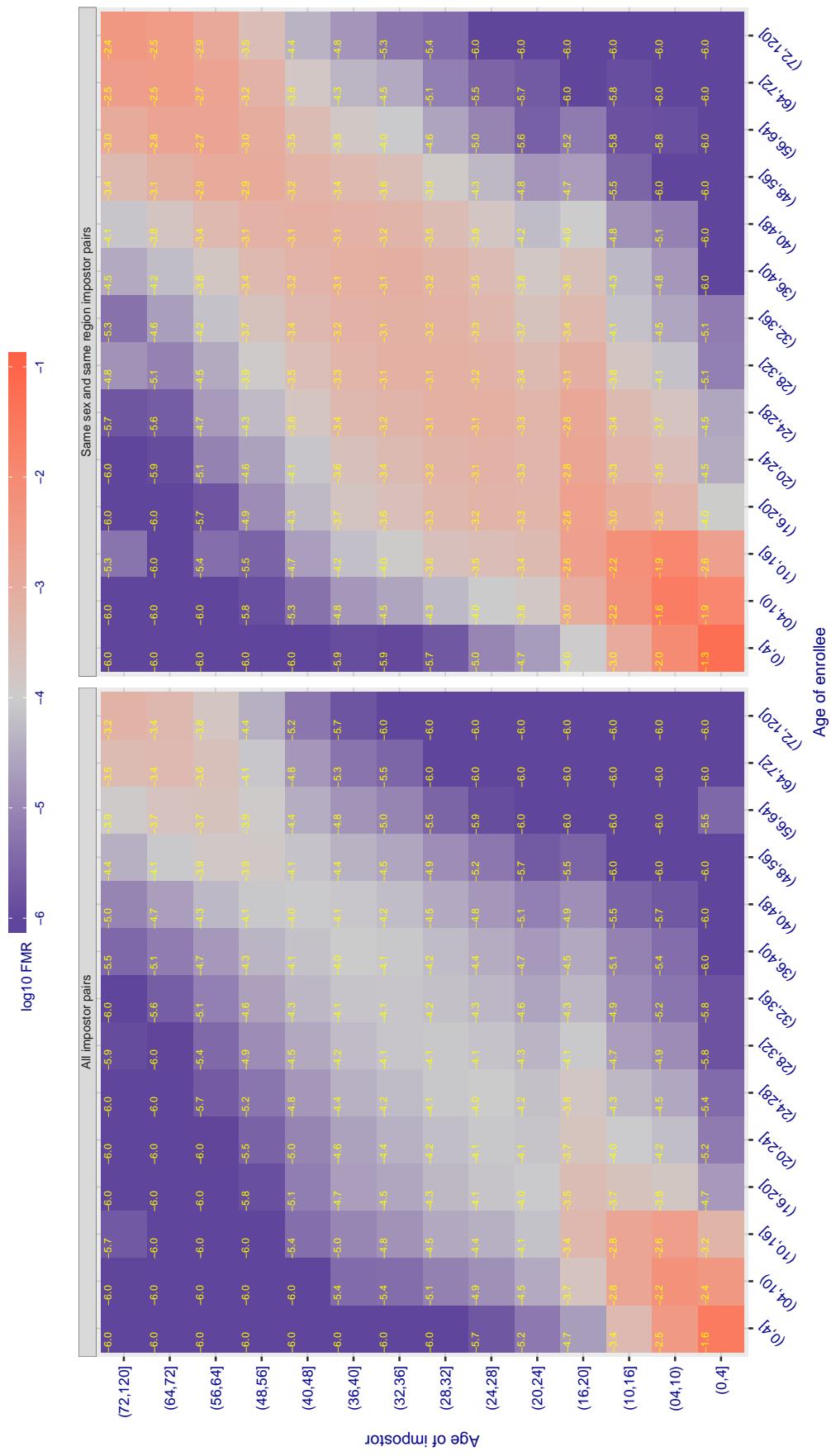
Cross age FMR at threshold T = 0.436 for algorithm ceiec_001, giving $FMR(T) = 0.0001$ globally.

Figure 445: For algorithm ceiec-001 operating on visa images, the heatmap shows false match observed over impostor comparisons of faces from different individuals who have the given age pair. False matches are counted against a recognition threshold fixed globally to give $FMR = 0.0001$ over all on the order of 10^{10} impostor comparisons. The text in each box gives the same quantity as that coded by the color. Light colors present a security vulnerability to, for example, a passport gate.

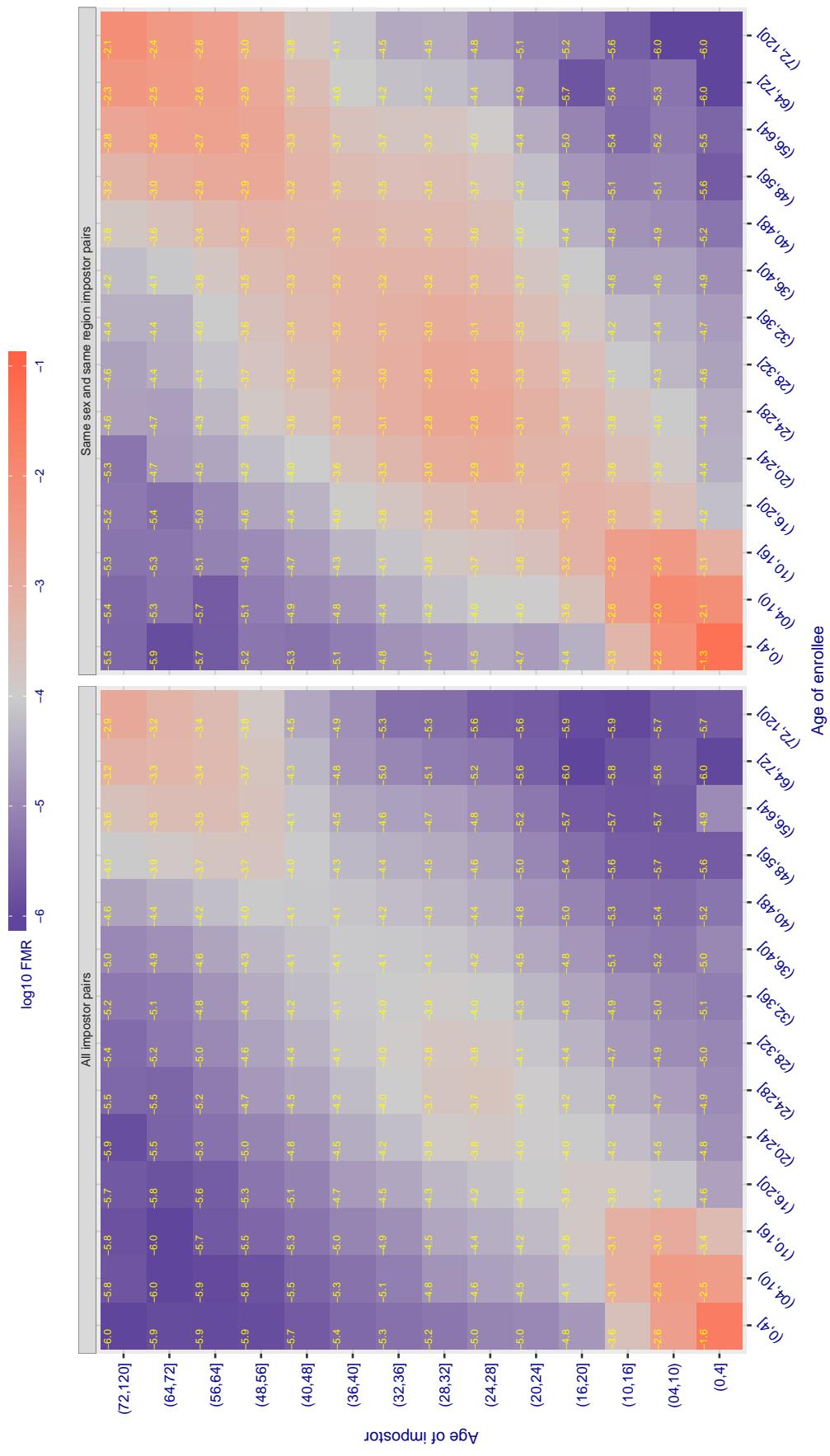
Cross age FMR at threshold T = 0.325 for algorithm ceiec_002, giving $FMR(T) = 0.0001$ globally.

Figure 446: For algorithm ceiec-002 operating on visa images, the heatmap shows false match observed over impostor comparisons of faces from different individuals who have the given age pair. False matches are counted against a recognition threshold fixed globally to give $FMR = 0.0001$ over all on the order of 10^{10} impostor comparisons. The text in each box gives the same quantity as that coded by the color. Light colors present a security vulnerability to, for example, a passport gate.

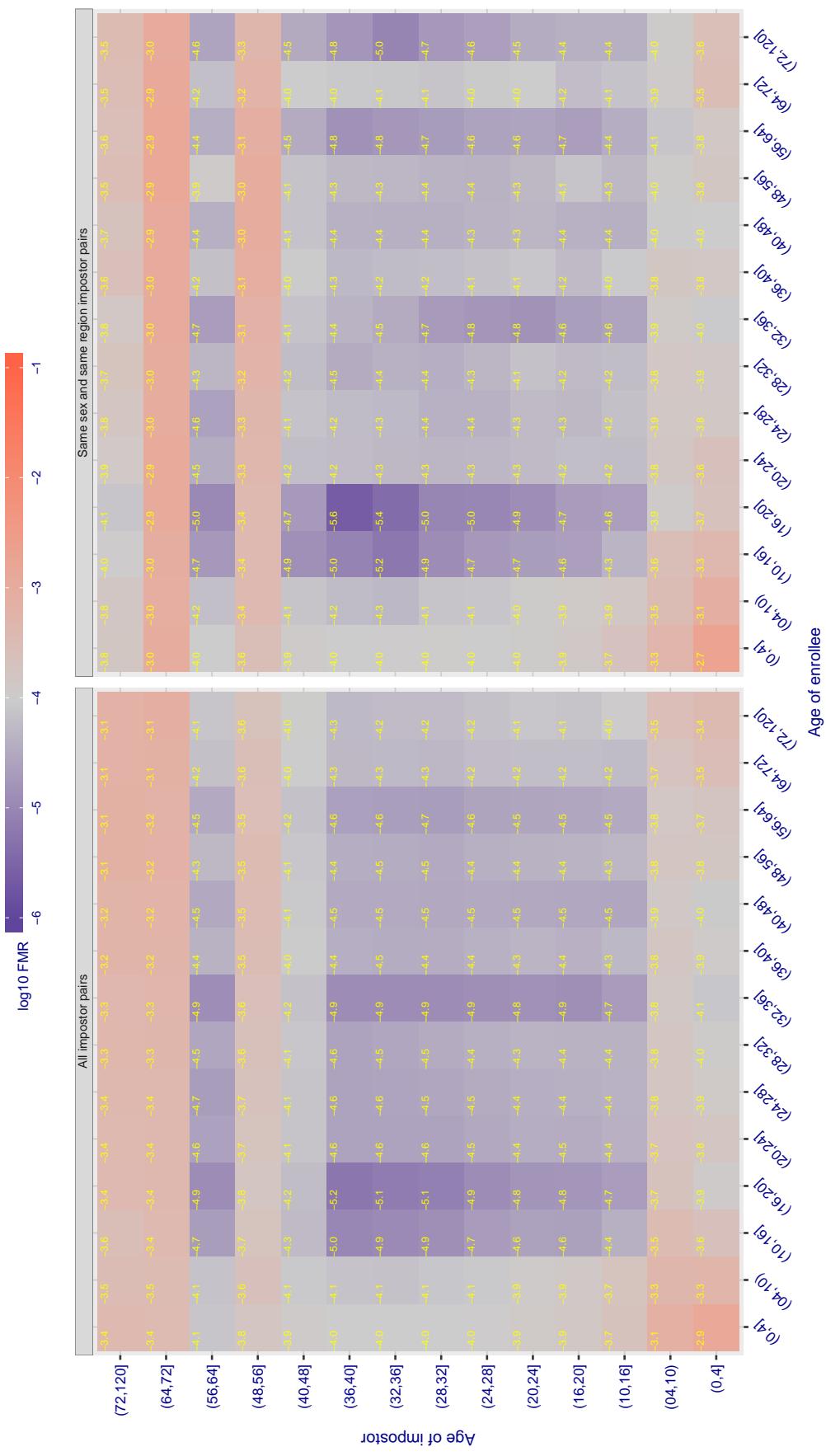
Cross age FMR at threshold T = 106.748 for algorithm chtface_001, giving $FMR(T) = 0.0001$ globally.

Figure 447: For algorithm chtface-001 operating on visa images, the heatmap shows false match observed over impostor comparisons of faces from different individuals who have the given age pair. False matches are counted against a recognition threshold fixed globally to give $FMR = 0.0001$ over all on the order of 10^{10} impostor comparisons. The text in each box gives the same quantity as that coded by the color. Light colors present a security vulnerability to, for example, a passport gate.

Cross age FMR at threshold T = 2972.000 for algorithm cogent_003, giving FMR(T) = 0.0001 globally.

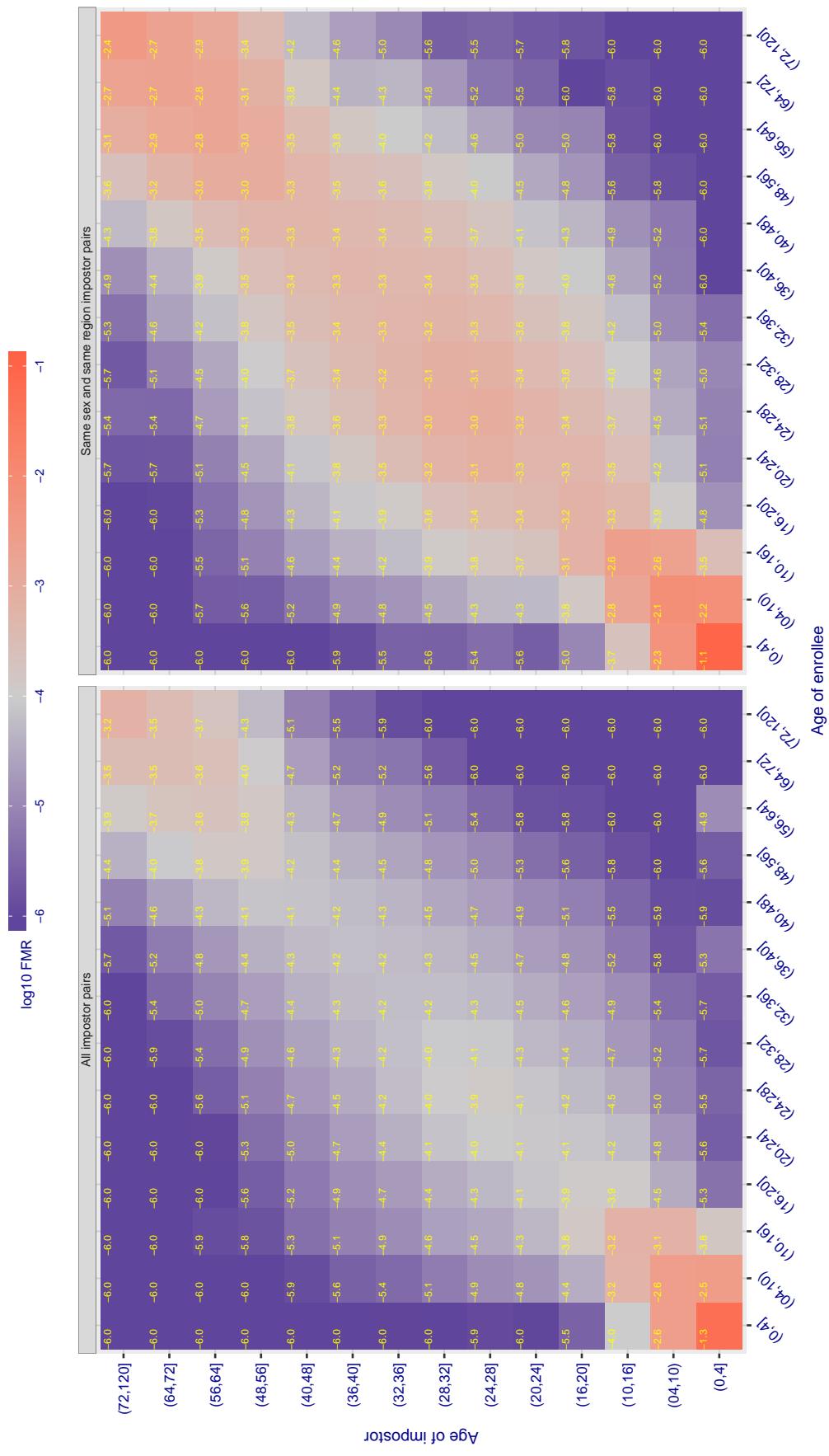


Figure 448: For algorithm cogent-003 operating on visa images, the heatmap shows false match observed over impostor comparisons of faces from different individuals who have the given age pair. False matches are counted against a recognition threshold fixed globally to give $FMR = 0.0001$ over all on the order of 10^{10} impostor comparisons. The text in each box gives the same quantity as that coded by the color. Light colors present a security vulnerability to, for example, a passport gate.

Cross age FMR at threshold T = 3156.000 for algorithm cogent_004, giving FMR(T) = 0.0001 globally.

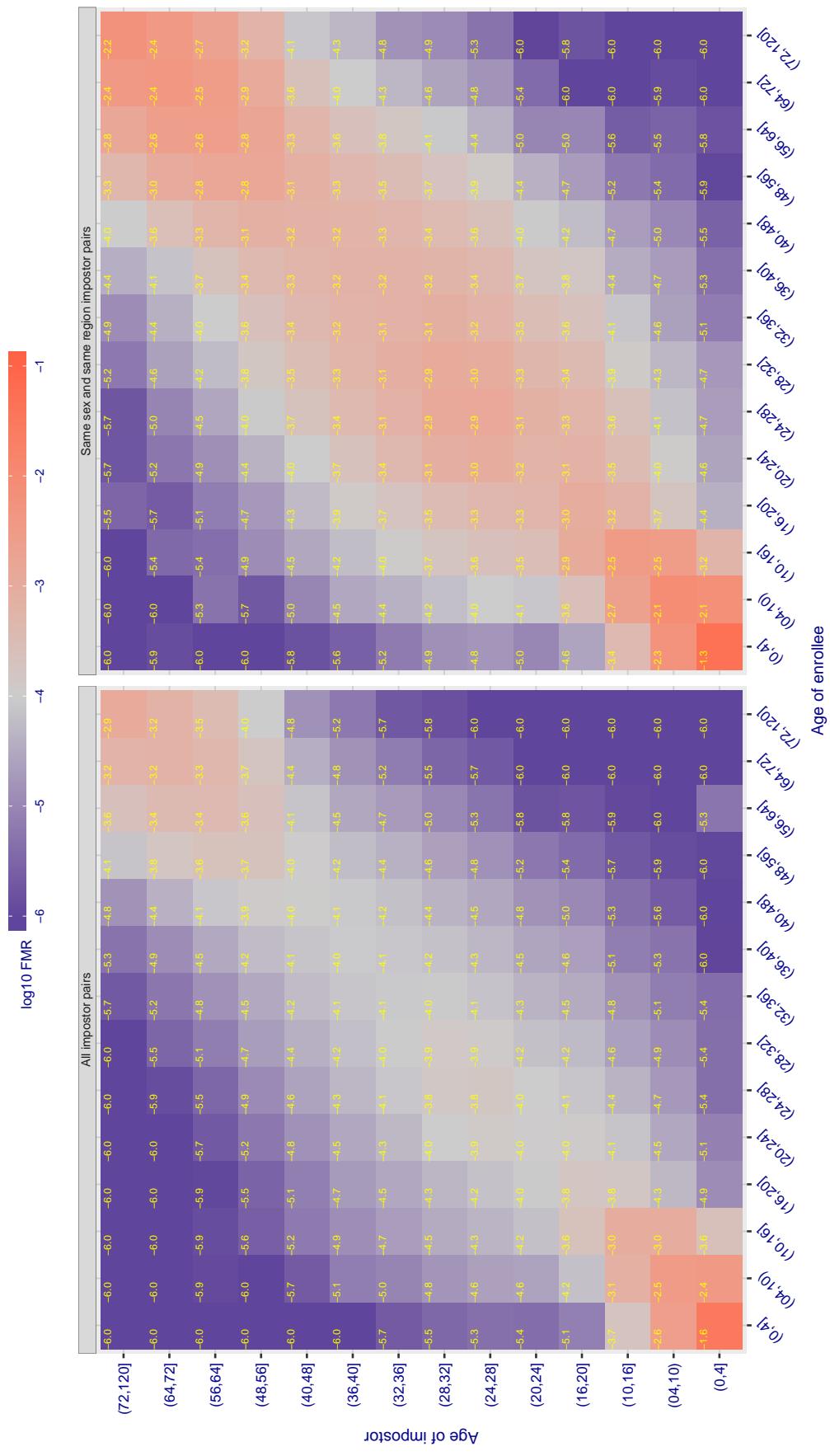


Figure 449: For algorithm cogent-004 operating on visa images, the heatmap shows false match observed over impostor comparisons of faces from different individuals who have the given age pair. False matches are counted against a recognition threshold fixed globally to give $FMR = 0.0001$ over all on the order of 10^{10} impostor comparisons. The text in each box gives the same quantity as that coded by the color. Light colors present a security vulnerability to, for example, a passport gate.

Cross age FMR at threshold T = 0.565 for algorithm cognitec_000, giving FMR(T) = 0.0001 globally.

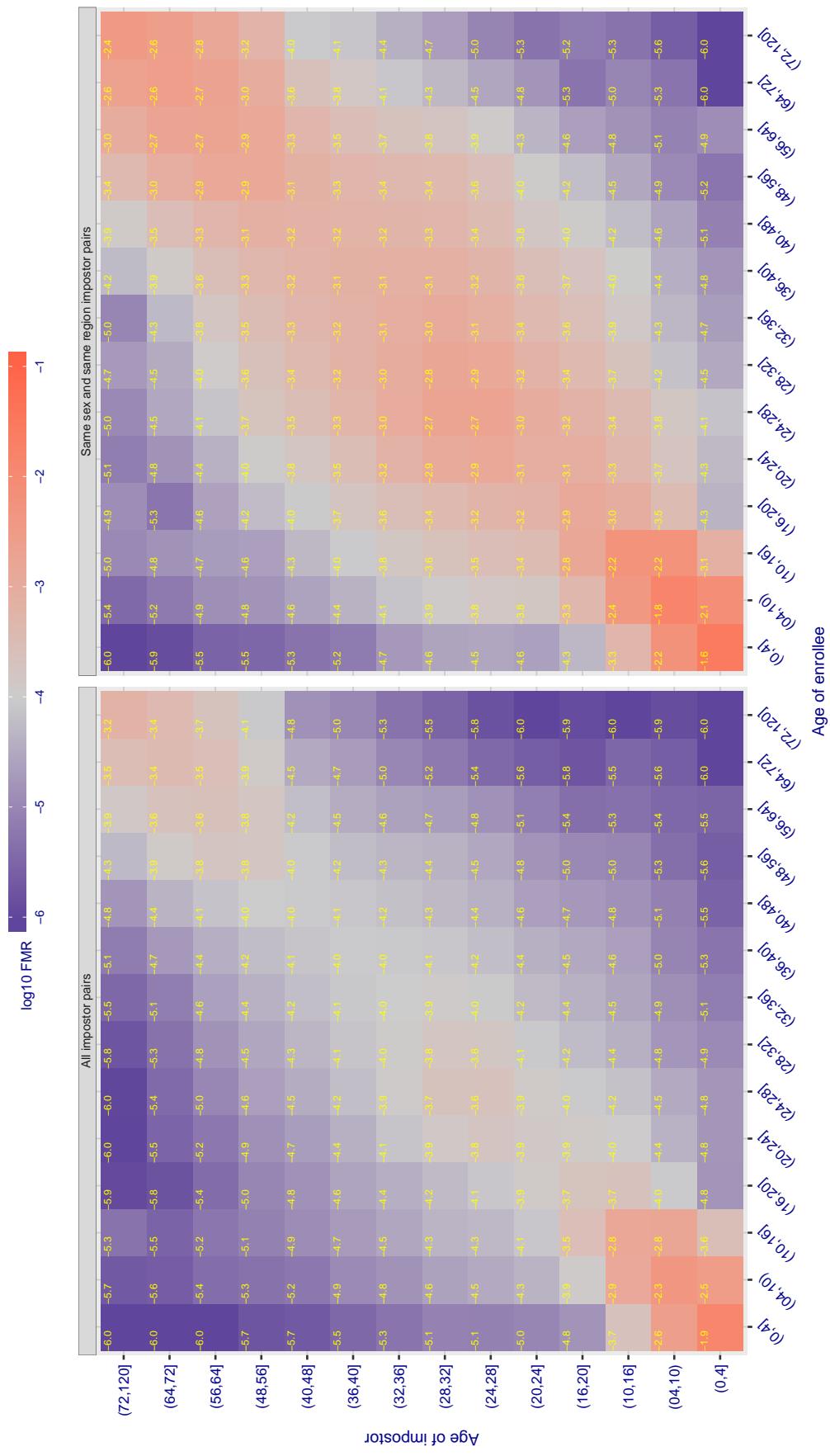


Figure 450: For algorithm cognitec-000 operating on visa images, the heatmap shows false match observed over impostor comparisons of faces from different individuals who have the given age pair. False matches are counted against a recognition threshold fixed globally to give FMR = 0.0001 over all on the order of 10^{10} impostor comparisons. The text in each box gives the same quantity as that coded by the color. Light colors present a security vulnerability to, for example, a passport gate.

Cross age FMR at threshold T = 0.565 for algorithm cognitec_001, giving FMR(T) = 0.0001 globally.

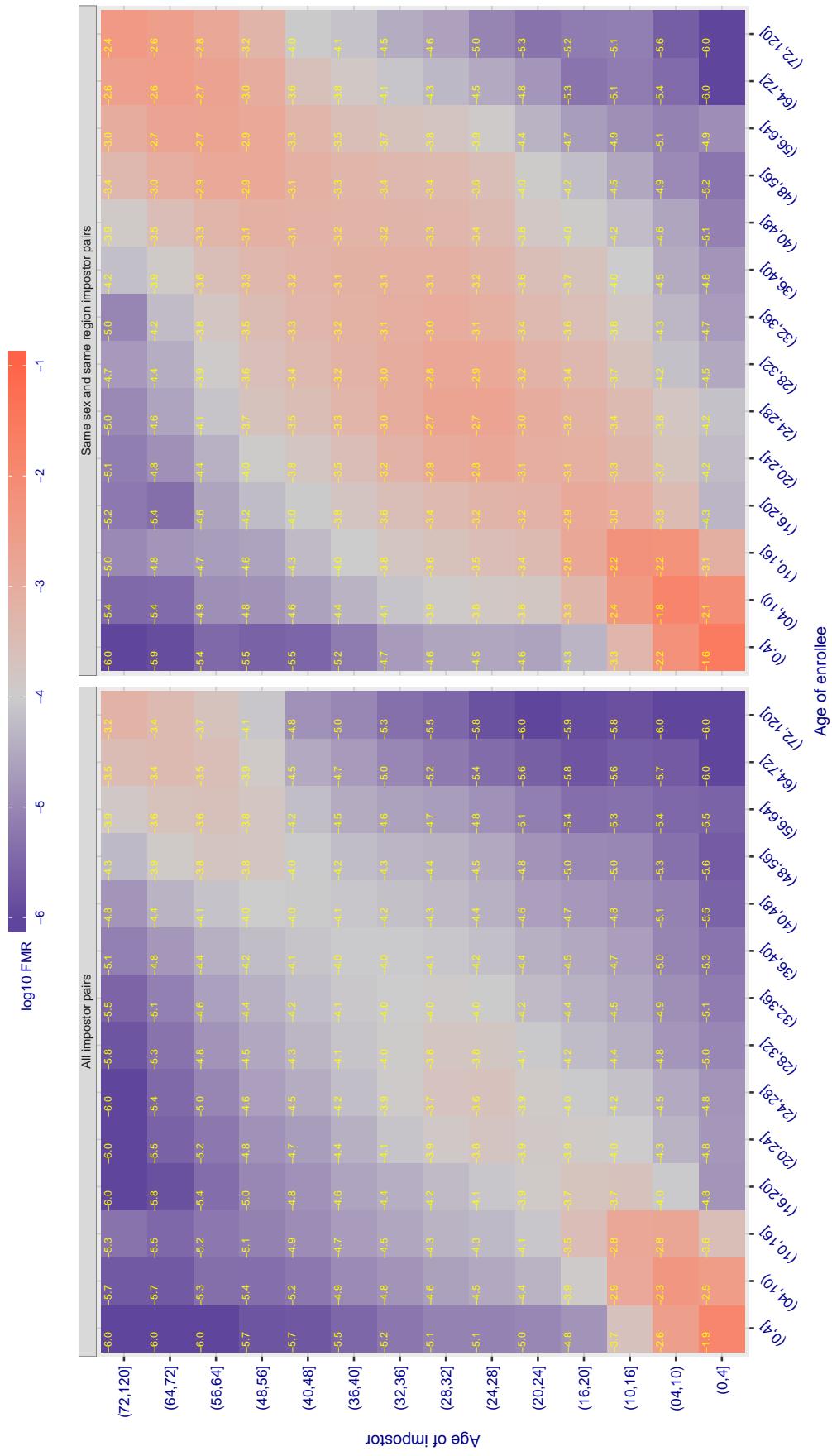


Figure 451: For algorithm cognitec-001 operating on visa images, the heatmap shows false match observed over impostor comparisons of faces from different individuals who have the given age pair. False matches are counted against a recognition threshold fixed globally to give FMR = 0.0001 over all on the order of 10^{10} impostor comparisons. The text in each box gives the same quantity as that coded by the color. Light colors present a security vulnerability to, for example, a passport gate.

Cross age FMR at threshold T = 3.730 for algorithm ctbcbank_000, giving FMR(T) = 0.0001 globally.

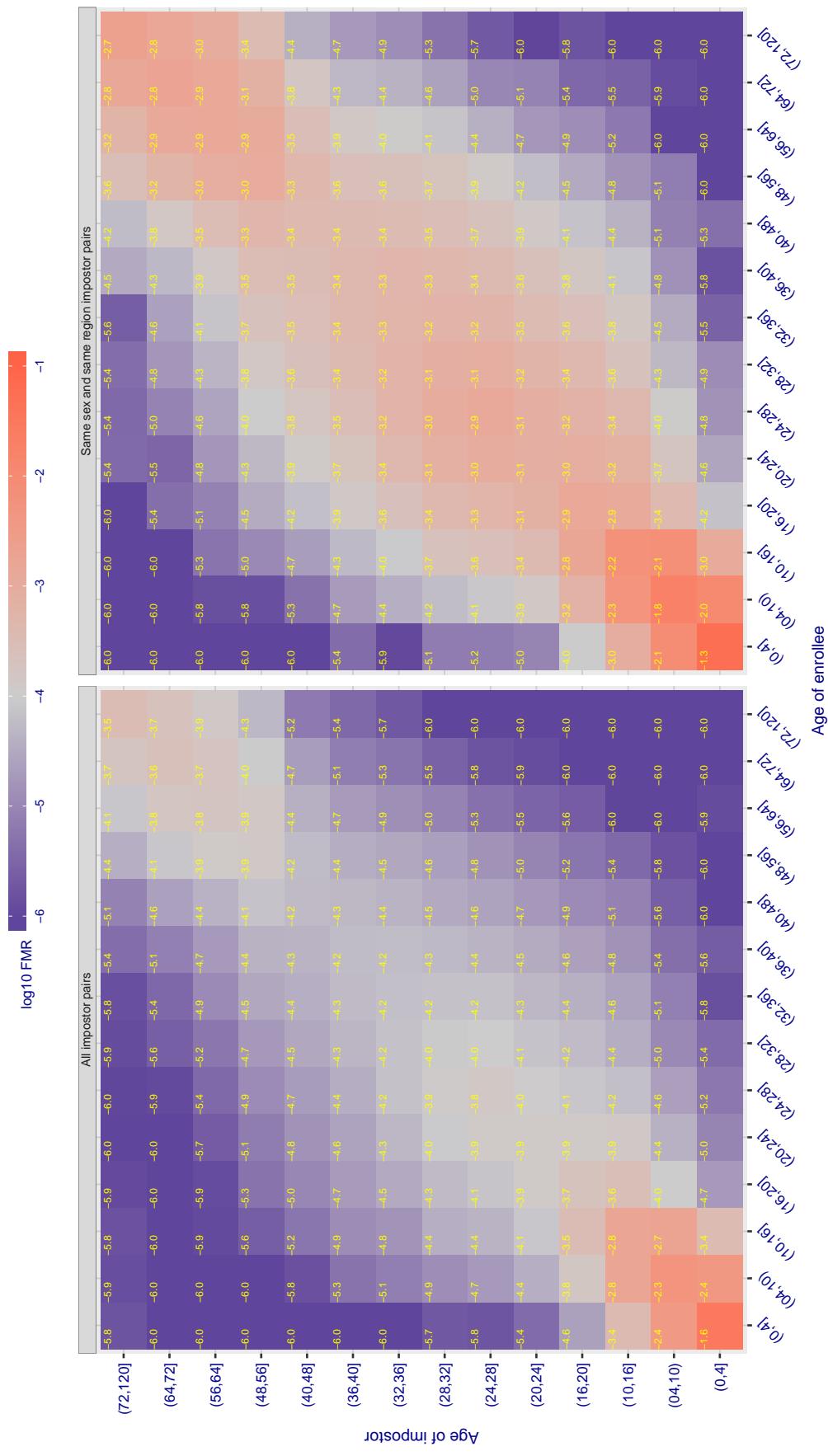


Figure 452: For algorithm ctbcbank-000 operating on visa images, the heatmap shows false match observed over impostor comparisons of faces from different individuals who have the given age pair. False matches are counted against a recognition threshold fixed globally to give $FMR = 0.0001$ over all on the order of 10^{10} impostor comparisons. The text in each box gives the same quantity as that coded by the color. Light colors present a security vulnerability to, for example, a passport gate.

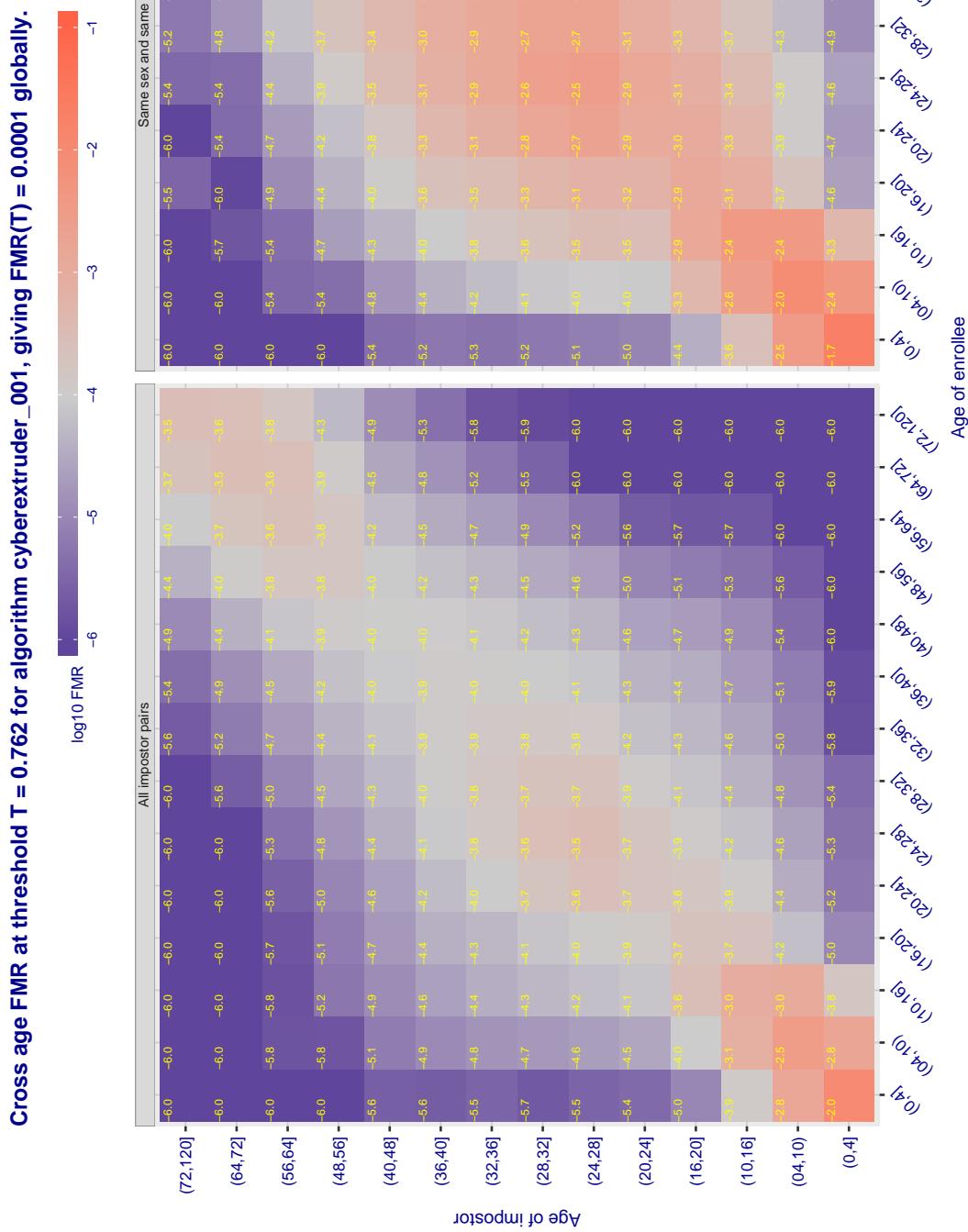


Figure 453: For algorithm *cyberextruder-001* operating on visa images, the heatmap shows false match observed over impostor comparisons of faces from different individuals who have the given age pair. False matches are counted against a recognition threshold fixed globally to give $FMR = 0.0001$ over all on the order of 10^{10} impostor comparisons. The text in each box gives the same quantity as that coded by the color. Light colors present a security vulnerability to, for example, a passport gate.

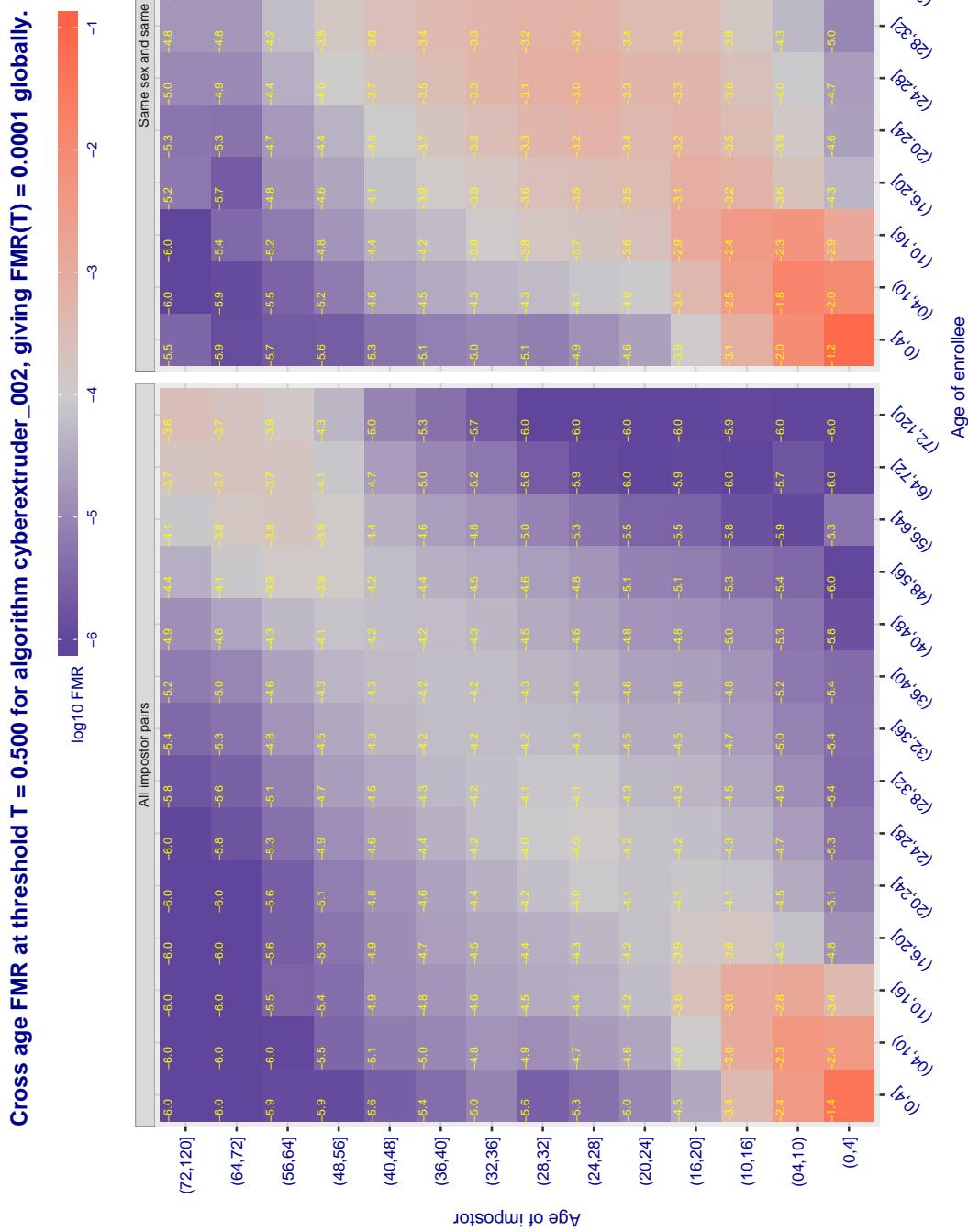


Figure 454: For algorithm *cyberextruder-002* operating on visa images, the heatmap shows false match observed over impostor comparisons of faces from different individuals who have the given age pair. False matches are counted against a recognition threshold fixed globally to give $FMR = 0.0001$ over all on the order of 10^{10} impostor comparisons. The text in each box gives the same quantity as that coded by the color. Light colors present a security vulnerability to, for example, a passport gate.

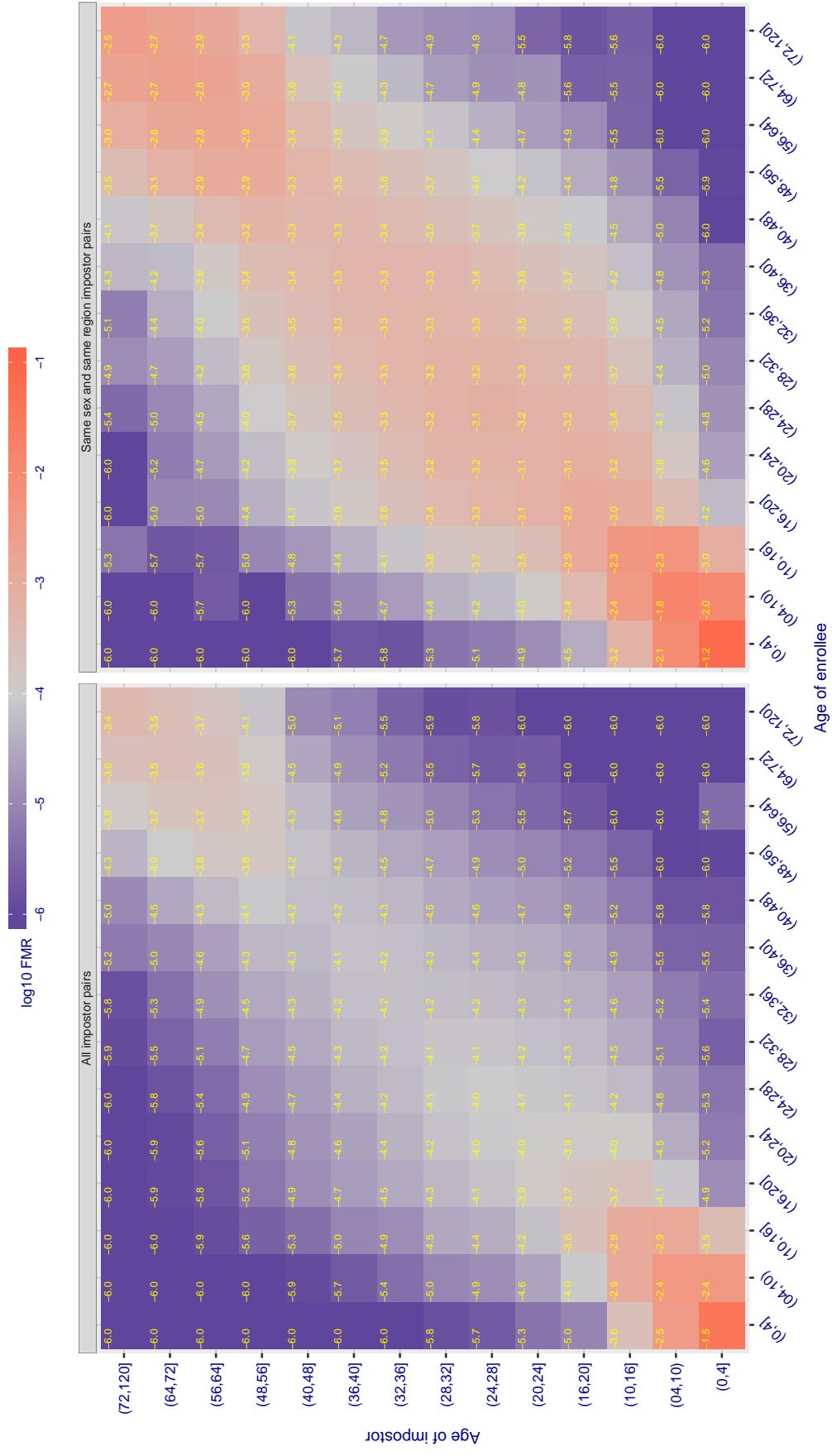
Cross age FMR at threshold T = 1.403 for algorithm cyberlink_001, giving $FMR(T) = 0.0001$ globally.

Figure 455: For algorithm cyberlink-001 operating on visa images, the heatmap shows false match observed over impostor comparisons of faces from different individuals who have the given age pair. False matches are counted against a recognition threshold fixed globally to give $FMR = 0.0001$ over all on the order of 10^{10} impostor comparisons. The text in each box gives the same quantity as that coded by the color. Light colors present a security vulnerability to, for example, a passport gate.

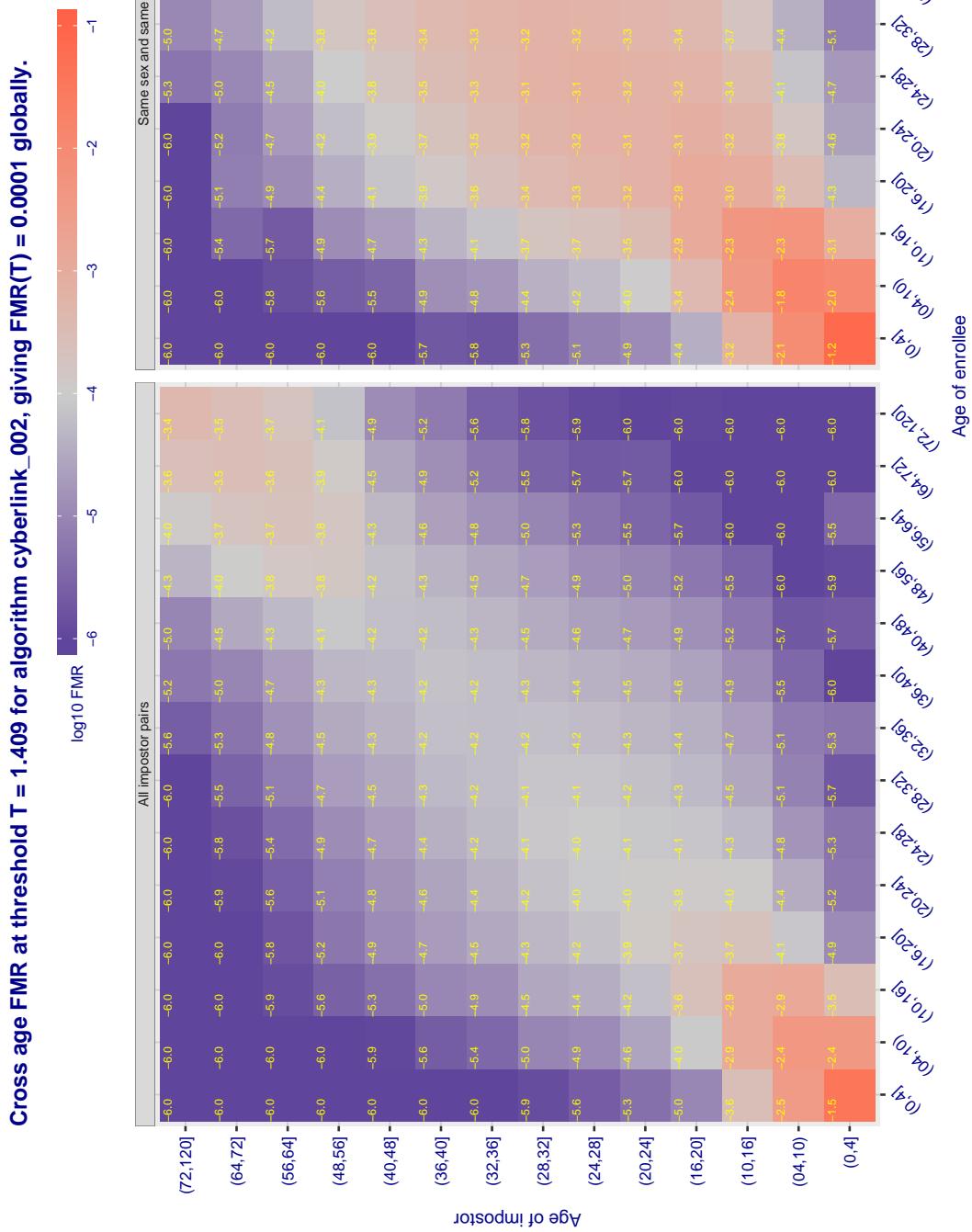


Figure 456: For algorithm cyberlink-002 operating on visa images, the heatmap shows false match observed over impostor comparisons of faces from different individuals who have the given age pair. False matches are counted against a recognition threshold fixed globally to give $FMR = 0.0001$ over all on the order of 10^{10} impostor comparisons. The text in each box gives the same quantity as that coded by the color. Light colors present a security vulnerability to, for example, a passport gate.

Cross age FMR at threshold T = 6696.000 for algorithm dahua_002, giving $FMR(T) = 0.0001$ globally.

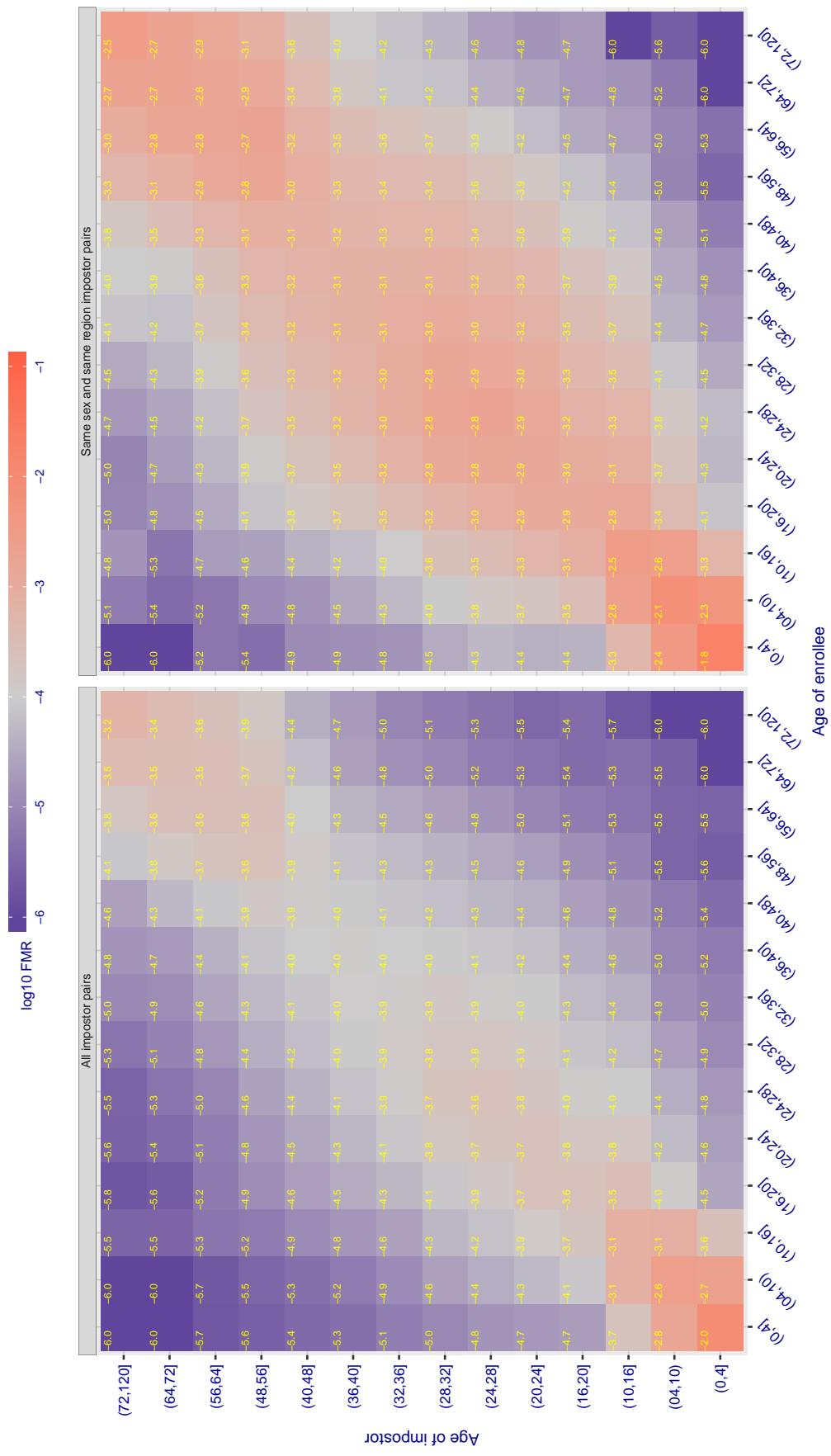


Figure 457: For algorithm dahua-002 operating on visa images, the heatmap shows false match observed over impostor comparisons of faces from different individuals who have the given age pair. False matches are counted against a recognition threshold fixed globally to give $FMR = 0.0001$ over all on the order of 10^{10} impostor comparisons. The text in each box gives the same quantity as that coded by the color. Light colors present a security vulnerability to, for example, a passport gate.

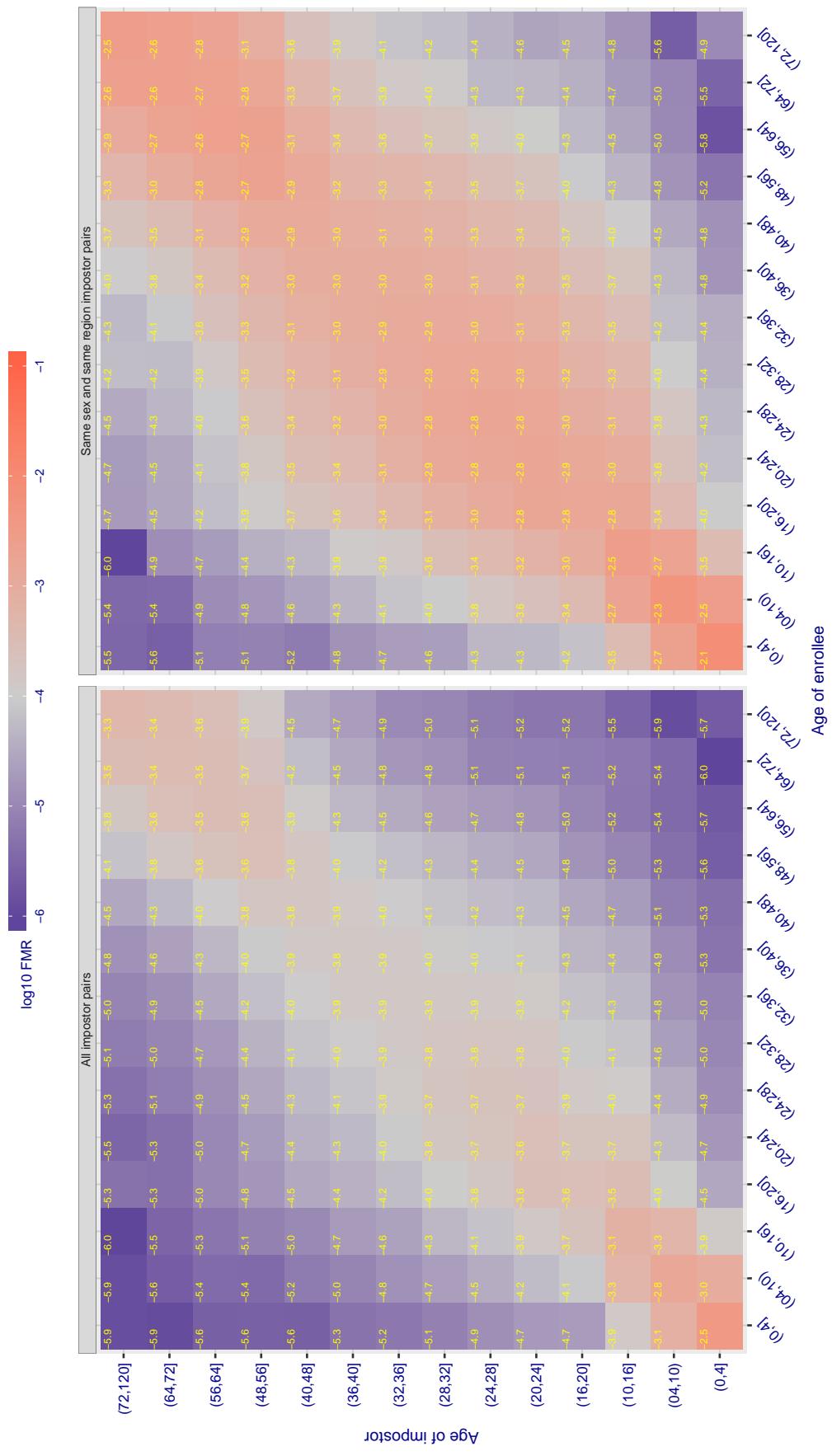
Cross age FMR at threshold T = 6034.000 for algorithm dahua_003, giving $FMR(T) = 0.0001$ globally.

Figure 458: For algorithm dahua-003 operating on visa images, the heatmap shows false match observed over impostor comparisons of faces from different individuals who have the given age pair. False matches are counted against a recognition threshold fixed globally to give $FMR = 0.0001$ over all on the order of 10^{10} impostor comparisons. The text in each box gives the same quantity as that coded by the color. Light colors present a security vulnerability to, for example, a passport gate.

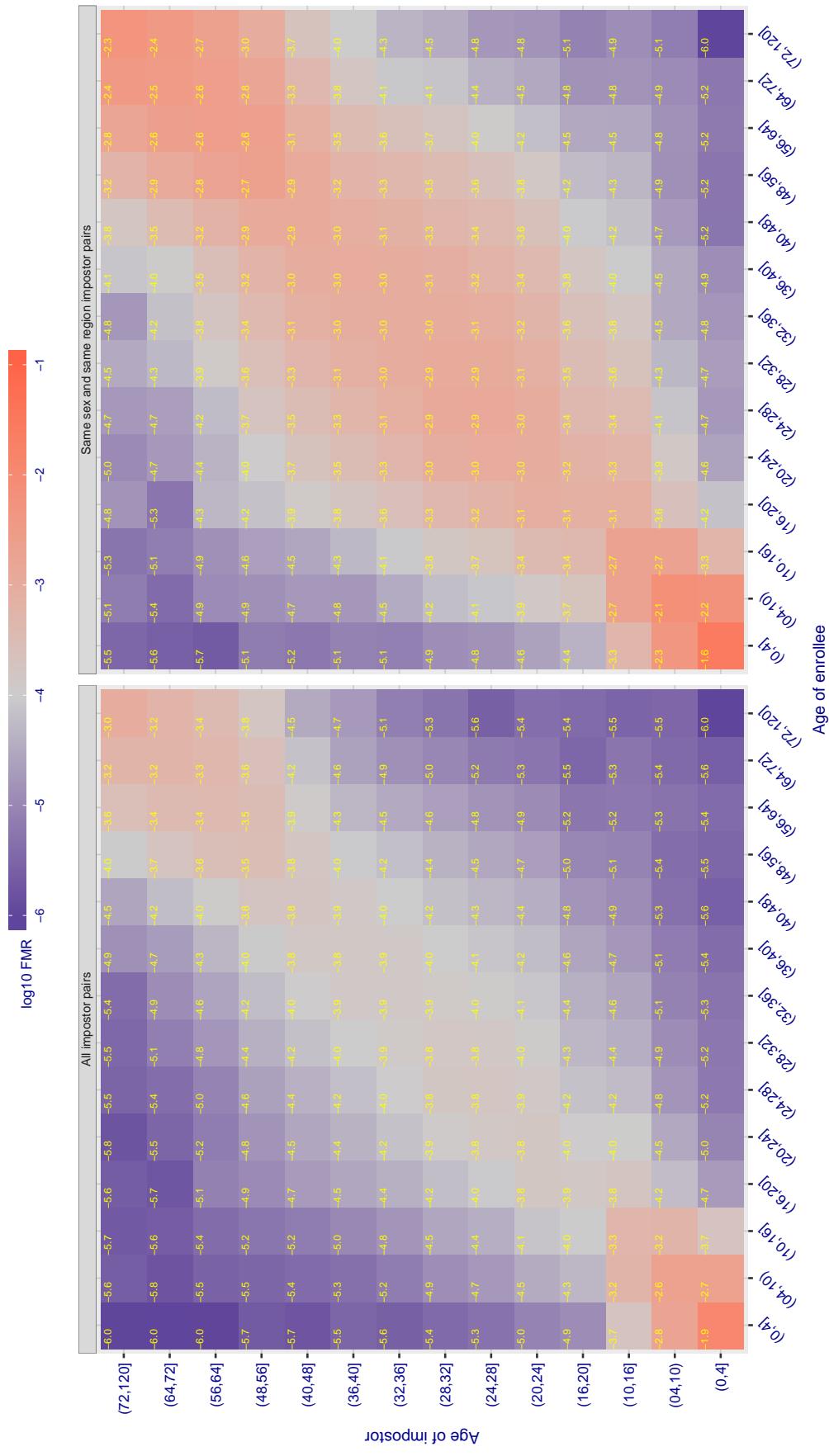
Cross age FMR at threshold T = 1.359 for algorithm `deepglint_001`, giving $\text{FMR}(\text{T}) = 0.0001$ globally.

Figure 459: For algorithm `deepglint-001` operating on visa images, the heatmap shows false match observed over impostor comparisons of faces from different individuals who have the given age pair. False matches are counted against a recognition threshold fixed globally to give $\text{FMR} = 0.001$ over all on the order of 10^{10} impostor comparisons. The text in each box gives the same quantity as that coded by the color. Light colors present a security vulnerability to, for example, a passport gate.

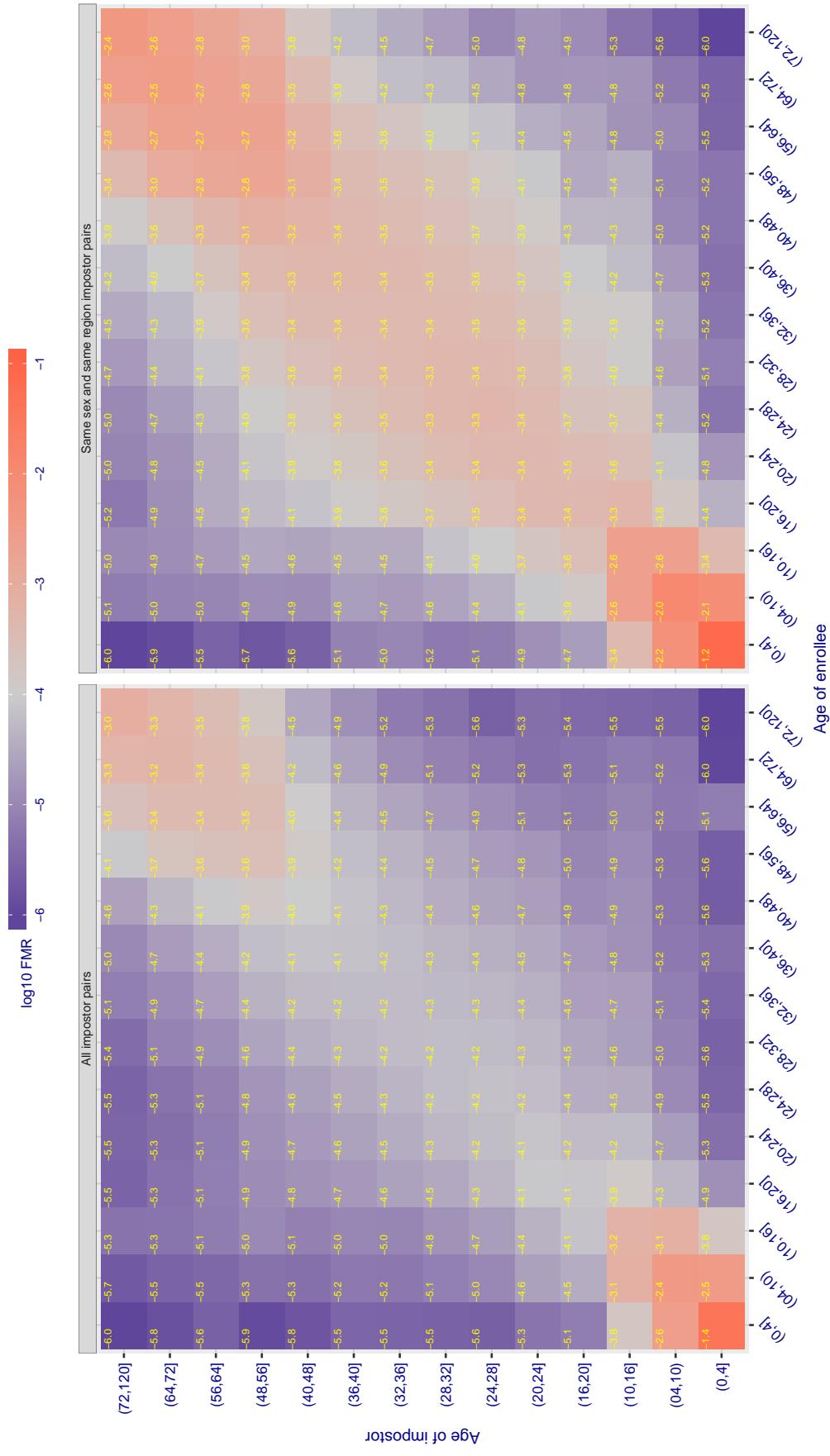
Cross age FMR at threshold T = 1.371 for algorithm deepsea_001, giving $FMR(T) = 0.0001$ globally.

Figure 460: For algorithm deepsea-001 operating on visa images, the heatmap shows false match observed over impostor comparisons of faces from different individuals who have the given age pair. False matches are counted against a recognition threshold fixed globally to give $FMR = 0.0001$ over all on the order of 10^{10} impostor comparisons. The text in each box gives the same quantity as that coded by the color. Light colors present a security vulnerability to, for example, a passport gate.

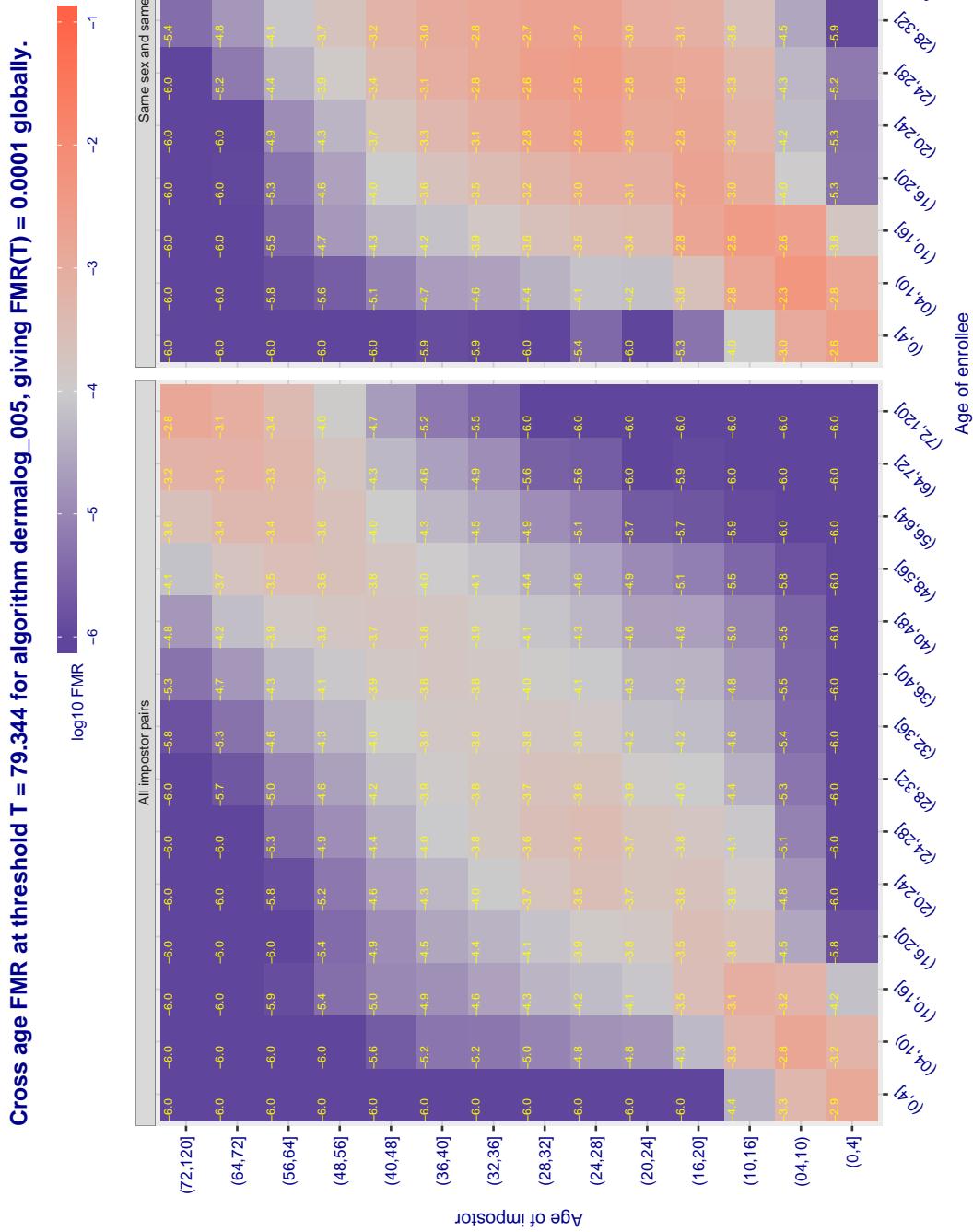


Figure 461: For algorithm dermalog-005 operating on visa images, the heatmap shows false match observed over impostor comparisons of faces from different individuals who have the given age pair. False matches are counted against a recognition threshold fixed globally to give $FMR = 0.0001$ over all on the order of 10^{10} impostor comparisons. The text in each box gives the same quantity as that coded by the color. Light colors present a security vulnerability to, for example, a passport gate.

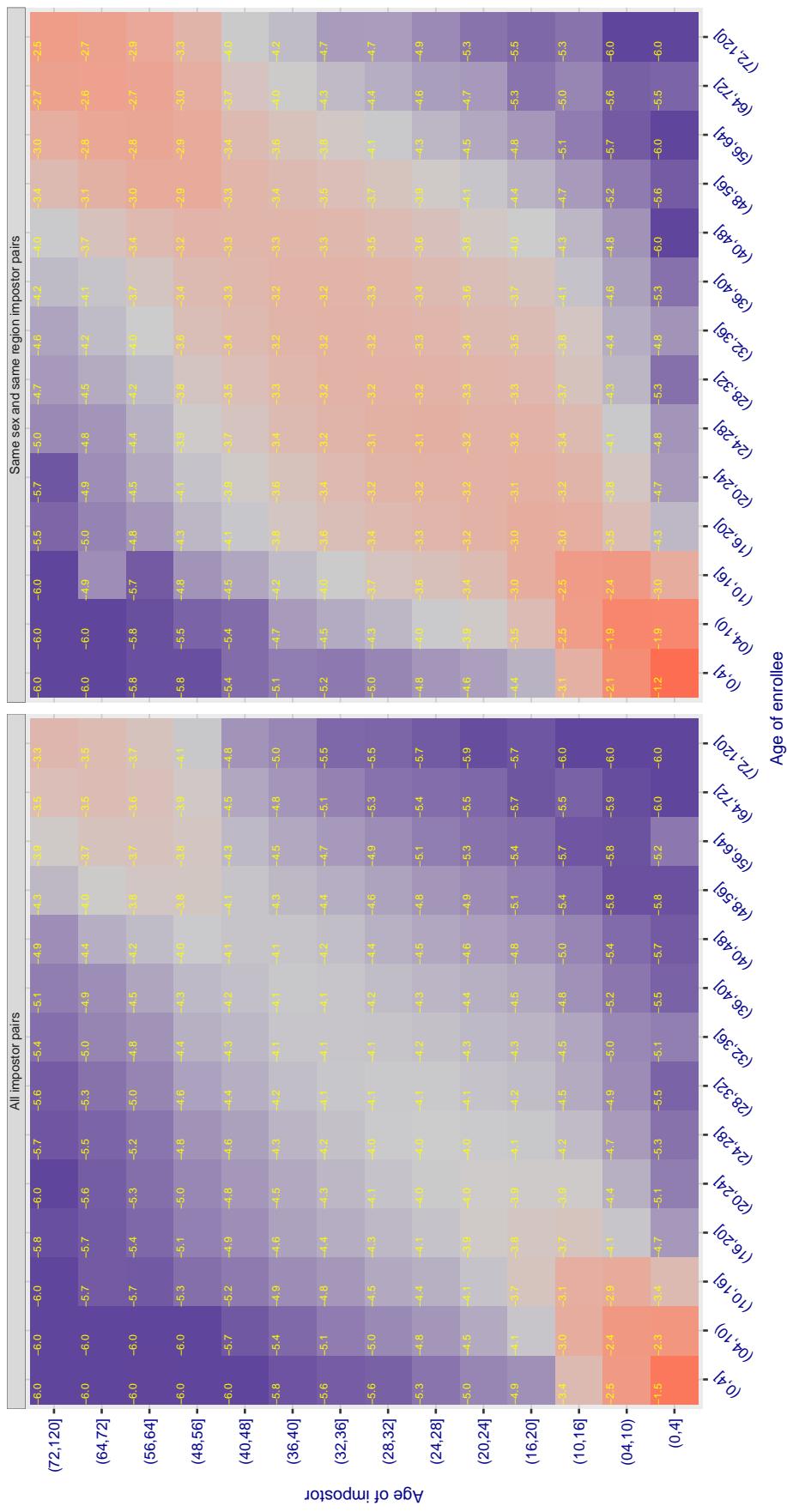
Cross age FMR at threshold T = 79.670 for algorithm dermalog_006, giving $FMR(T) = 0.0001$ globally.

Figure 462: For algorithm dermalog-006 operating on visa images, the heatmap shows false match observed over impostor comparisons of faces from different individuals who have the given age pair. False matches are counted against a recognition threshold fixed globally to give $FMR = 0.001$ over all on the order of 10^{10} impostor comparisons. The text in each box gives the same quantity as that coded by the color. Light colors present a security vulnerability to, for example, a passport gate.

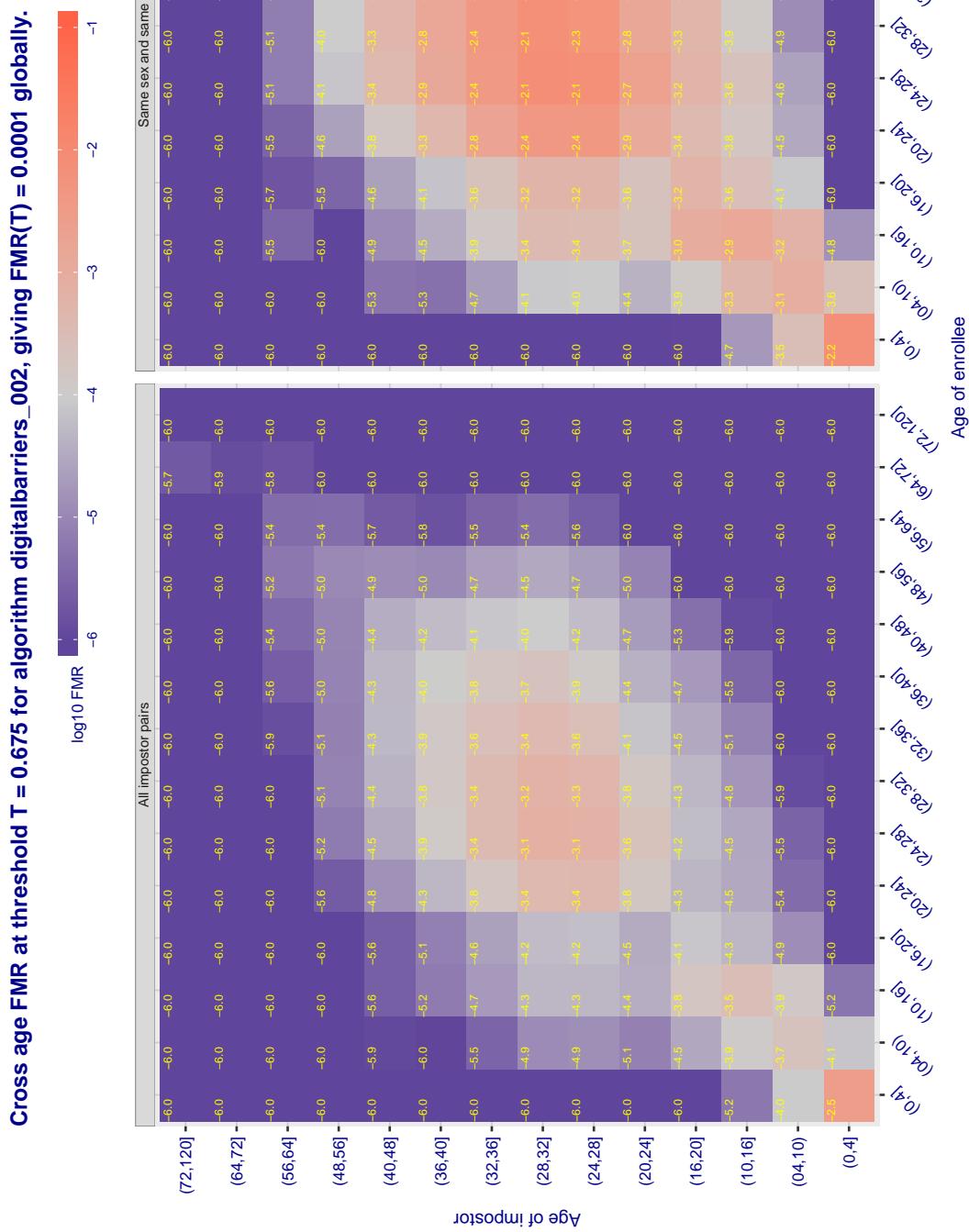


Figure 463: For algorithm digitalBarriers-002 operating on visa images, the heatmap shows false match observed over impostor comparisons of faces from different individuals who have the given age pair. False matches are counted against a recognition threshold fixed globally to give $FMR = 0.0001$ over all on the order of 10^{10} impostor comparisons. The text in each box gives the same quantity as that coded by the color. Light colors present a security vulnerability to, for example, a passport gate.

Cross age FMR at threshold T = 1.061 for algorithm dsk_000, giving FMR(T) = 0.0001 globally.

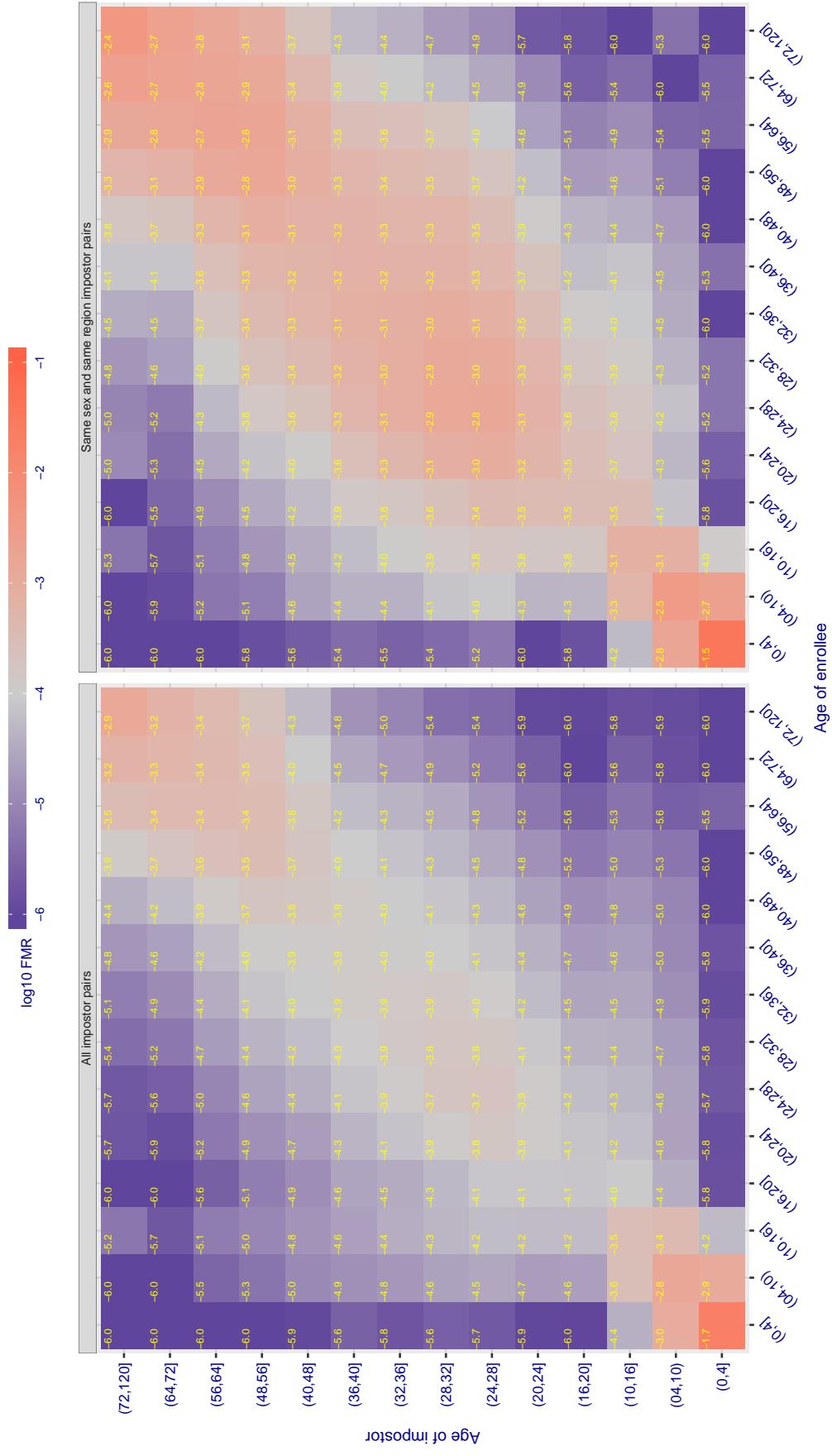


Figure 464: For algorithm dsk-000 operating on visa images, the heatmap shows false match observed over imposter comparisons of faces from different individuals who have the given age pair. False matches are counted against a recognition threshold fixed globally to give FMR = 0.0001 over all on the order of 10^{10} impostor comparisons. The text in each box gives the same quantity as that coded by the color. Light colors present a security vulnerability to, for example, a passport gate.

Cross age FMR at threshold T = 53.280 for algorithm einetworks_000, giving $FMR(T) = 0.00001$ globally.

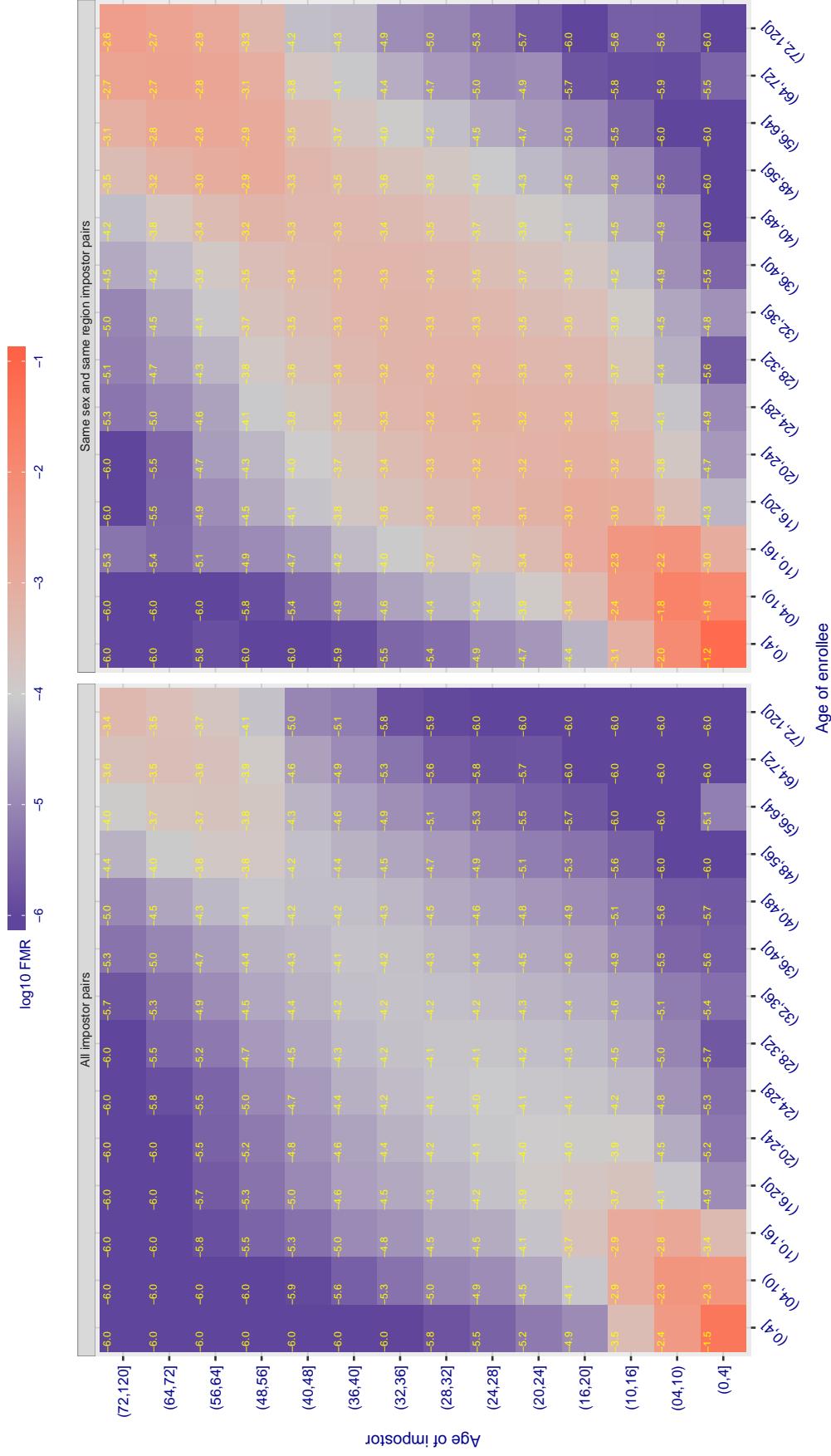


Figure 465: For algorithm einetworks-000 operating on visa images, the heatmap shows false match observed over impostor comparisons of faces from different individuals who have the given age pair. False matches are counted against a recognition threshold fixed globally to give $FMR = 0.0001$ over all on the order of 10^{10} impostor comparisons. The text in each box gives the same quantity as that coded by the color. Light colors present a security vulnerability to, for example, a passport gate.

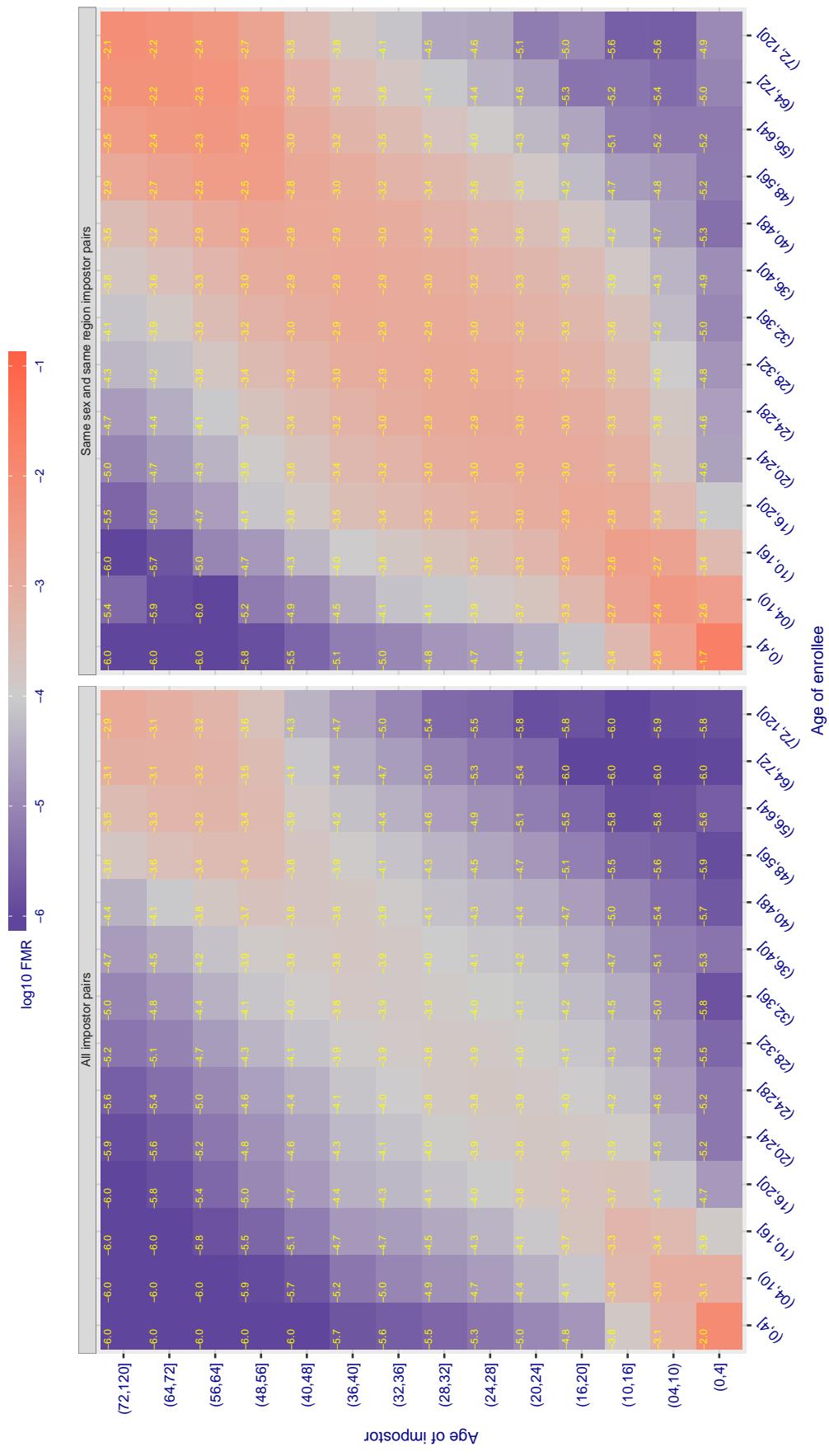
Cross age FMR at threshold T = 2.589 for algorithm everai_002, giving $\text{FMR}(\text{T}) = 0.0001$ globally.

Figure 466: For algorithm everai-002 operating on visa images, the heatmap shows false match observed over impostor comparisons of faces from different individuals who have the given age pair. False matches are counted against a recognition threshold fixed globally to give $\text{FMR} = 0.0001$ over all on the order of 10^{10} impostor comparisons. The text in each box gives the same quantity as that coded by the color. Light colors present a security vulnerability to, for example, a passport gate.

Cross age FMR at threshold T = 0.400 for algorithm f8_001, giving FMR(T) = 0.0001 globally.

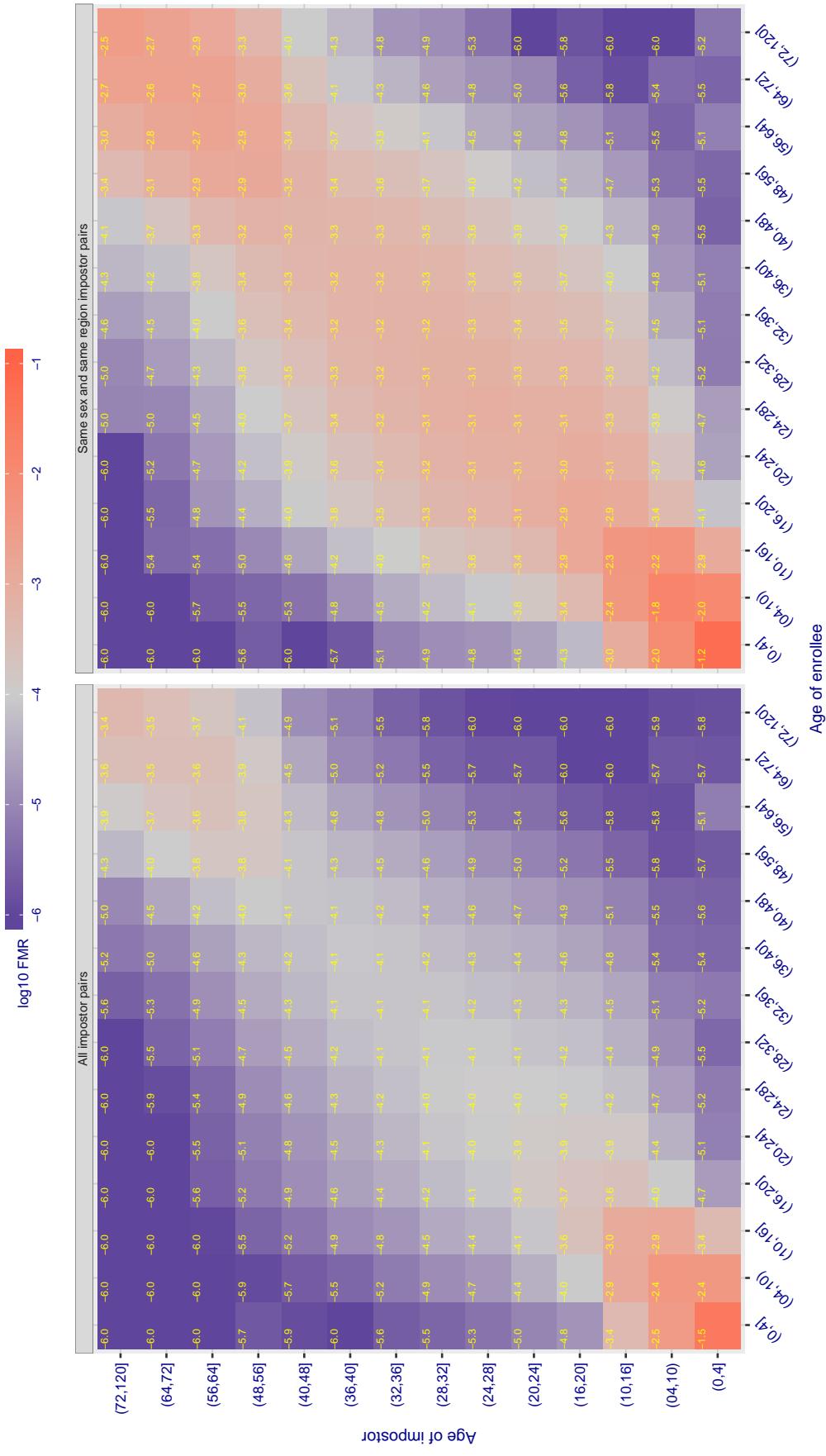


Figure 467: For algorithm f8_001 operating on visa images, the heatmap shows false match observed over impostor comparisons of faces from different individuals who have the given age pair. False matches are counted against a recognition threshold fixed globally to give $FMR = 0.0001$ over all on the order of 10^{10} impostor comparisons. The text in each box gives the same quantity as that coded by the color. Light colors present a security vulnerability to, for example, a passport gate.

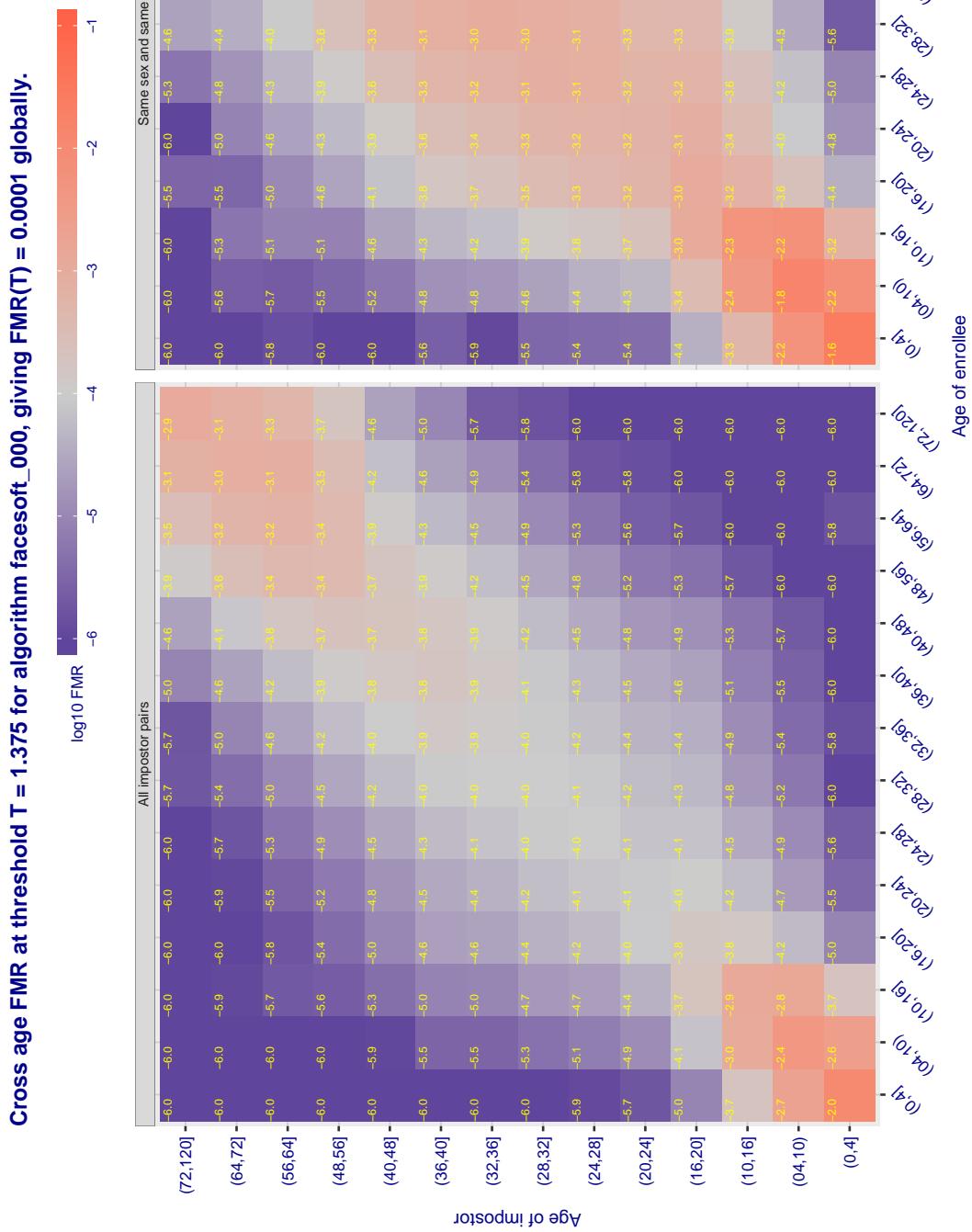


Figure 468: For algorithm facesoft-000 operating on visa images, the heatmap shows false match observed over impostor comparisons of faces from different individuals who have the given age pair. False matches are counted against a recognition threshold fixed globally to give $FMR = 0.0001$ over all on the order of 10^{10} impostor comparisons. The text in each box gives the same quantity as that coded by the color. Light colors present a security vulnerability to, for example, a passport gate.

Cross age FMR at threshold T = 0.611 for algorithm glory_000, giving FMR(T) = 0.0001 globally.

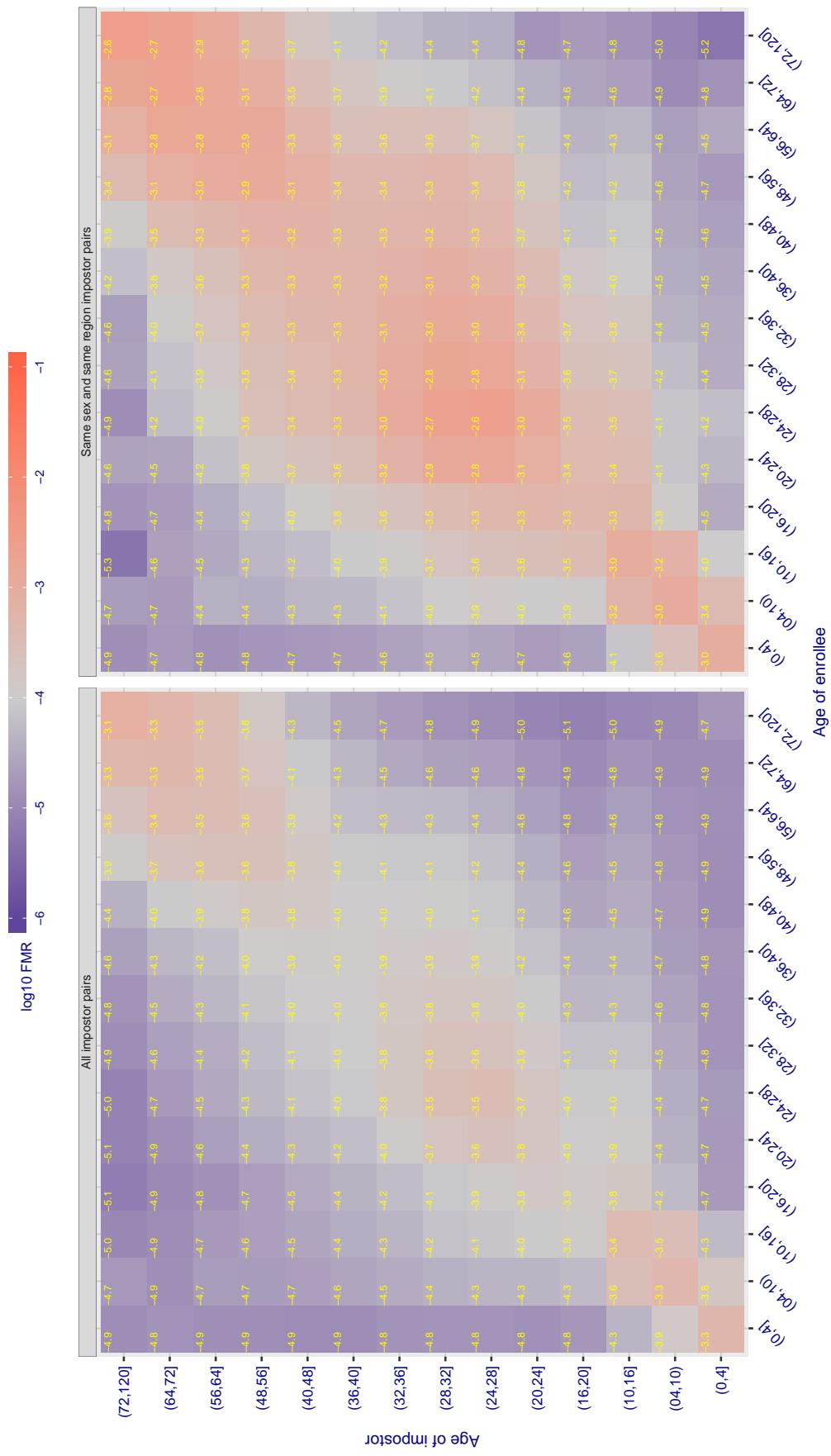


Figure 469: For algorithm glory-000 operating on visa images, the heatmap shows false match observed over impostor comparisons of faces from different individuals who have the given age pair. False matches are counted against a recognition threshold fixed globally to give FMR = 0.0001 over all on the order of 10^{10} impostor comparisons. The text in each box gives the same quantity as that coded by the color. Light colors present a security vulnerability to, for example, a passport gate.

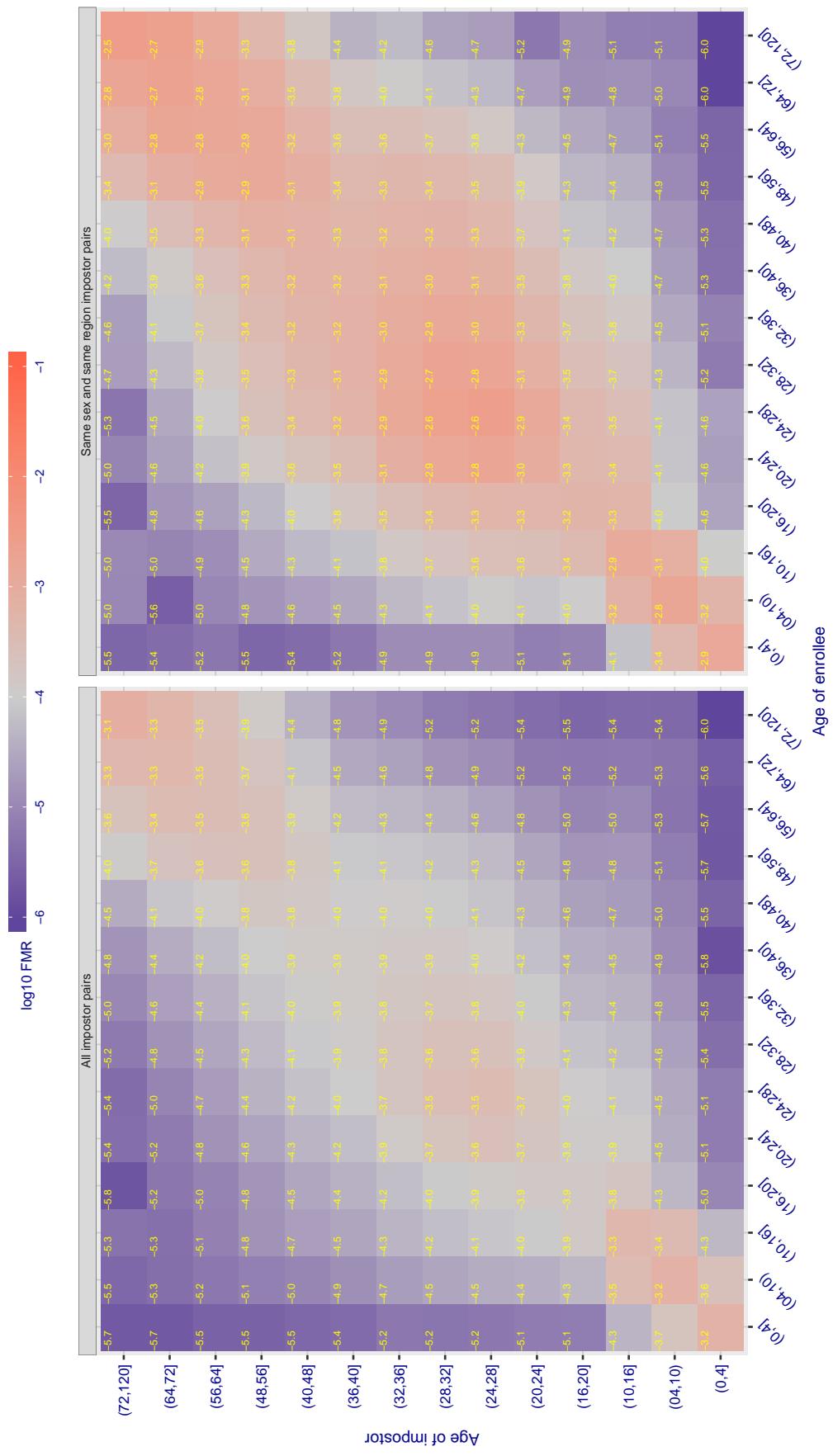
Cross age FMR at threshold T = 0.613 for algorithm glory_001, giving $FMR(T) = 0.0001$ globally.

Figure 470: For algorithm *glory-001* operating on visa images, the heatmap shows false match observed over impostor comparisons of faces from different individuals who have the given age pair. False matches are counted against a recognition threshold fixed globally to give $FMR = 0.0001$ over all on the order of 10^{10} impostor comparisons. The text in each box gives the same quantity as that coded by the color. Light colors present a security vulnerability to, for example, a passport gate.

Cross age FMR at threshold T = 0.483 for algorithm gorilla_002, giving FMR(T) = 0.0001 globally.

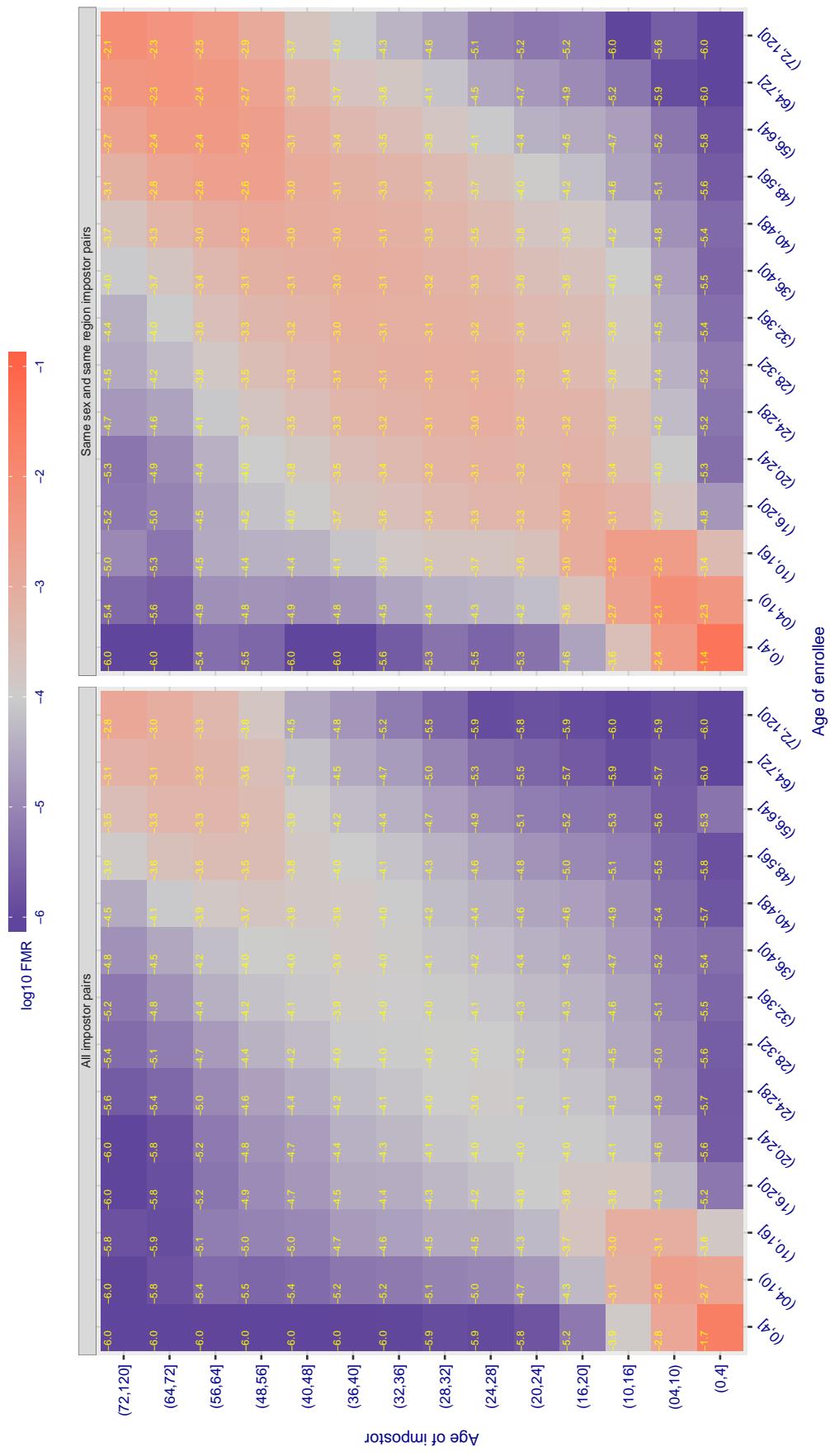


Figure 471: For algorithm gorilla-002 operating on visa images, the heatmap shows false match observed over impostor comparisons of faces from different individuals who have the given age pair. False matches are counted against a recognition threshold fixed globally to give FMR = 0.0001 over all on the order of 10^{10} impostor comparisons. The text in each box gives the same quantity as that coded by the color. Light colors present a security vulnerability to, for example, a passport gate.

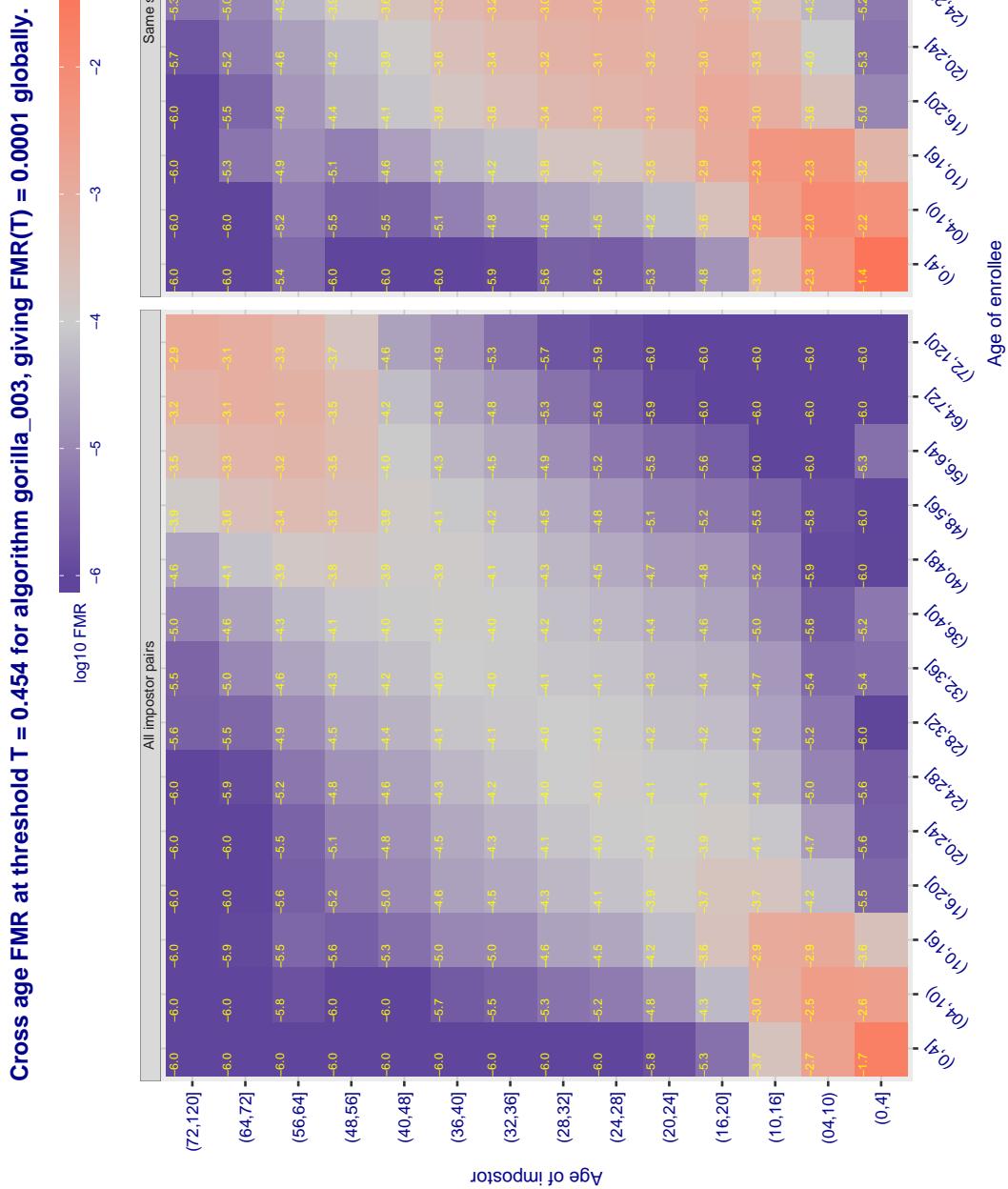


Figure 472: For algorithm gorilla-003 operating on visa images, the heatmap shows false match observed over impostor comparisons of faces from different individuals who have the given age pair. False matches are counted against a recognition threshold fixed globally to give $FMR = 0.0001$ over all on the order of 10^{10} impostor comparisons. The text in each box gives the same quantity as that coded by the color. Light colors present a security vulnerability to, for example, a passport gate.

Cross age FMR at threshold T = 66.565 for algorithm hik_001, giving FMR(T) = 0.0001 globally.

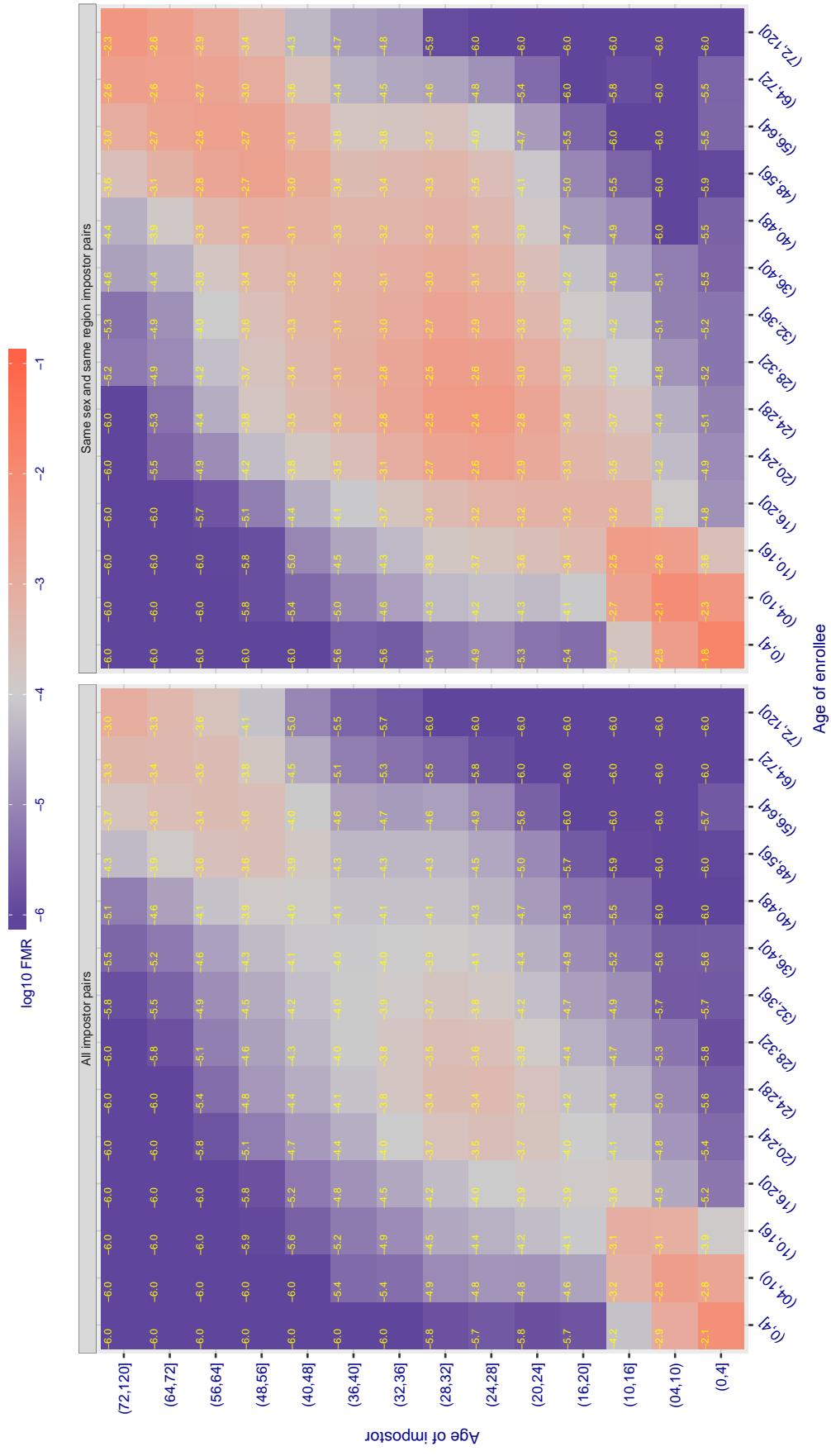


Figure 473: For algorithm hik-001 operating on visa images, the heatmap shows false match observed over impostor comparisons of faces from different individuals who have the given age pair. False matches are counted against a recognition threshold fixed globally to give $FMR = 0.0001$ over all on the order of 10^{10} impostor comparisons. The text in each box gives the same quantity as that coded by the color. Light colors present a security vulnerability to, for example, a passport gate.

Cross age FMR at threshold T = 0.823 for algorithm hr_001, giving FMR(T) = 0.0001 globally.

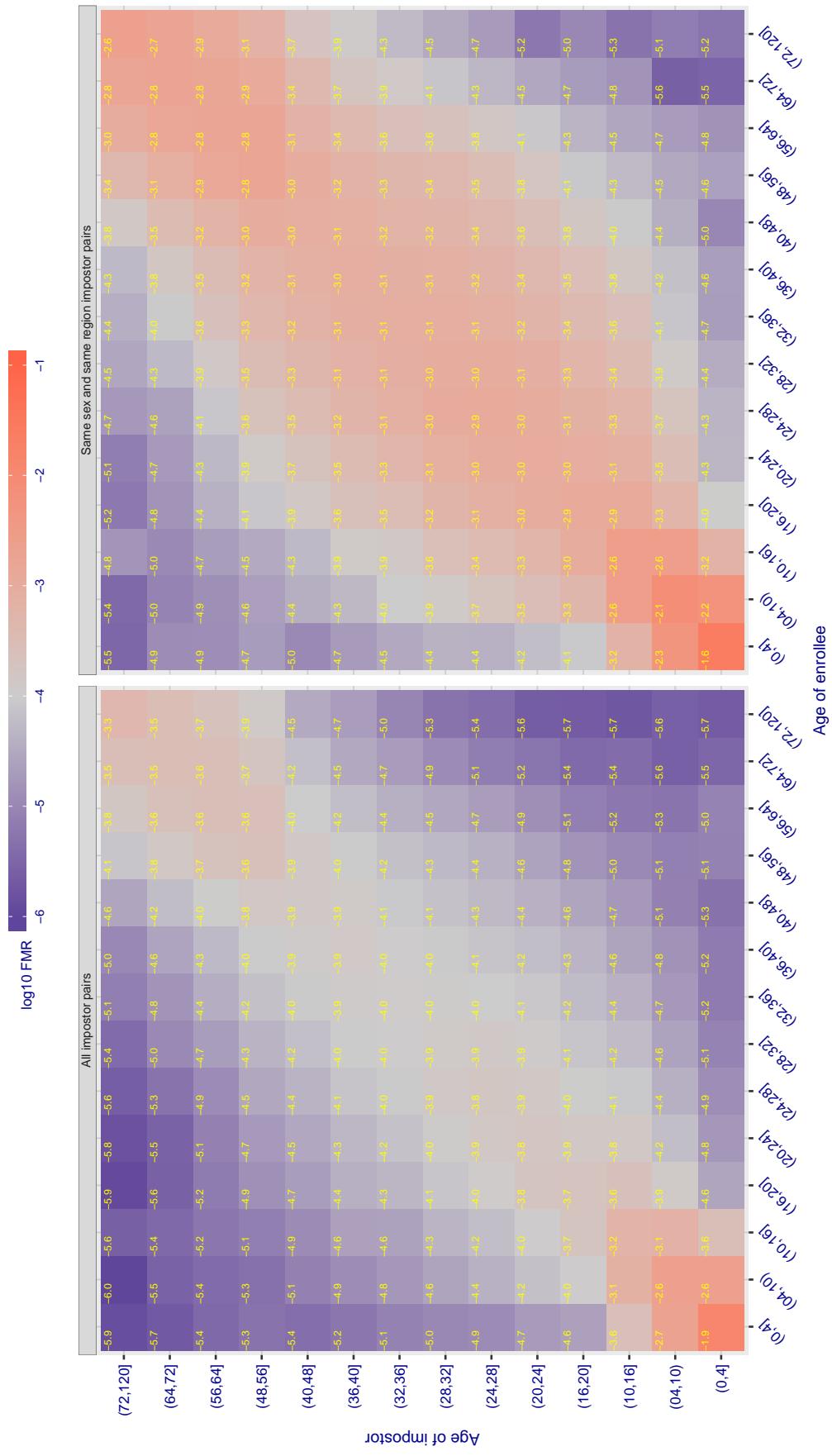


Figure 474: For algorithm hr-001 operating on visa images, the heatmap shows false match observed over impostor comparisons of faces from different individuals who have the given age pair. False matches are counted against a recognition threshold fixed globally to give FMR = 0.0001 over all on the order of 10^{10} impostor comparisons. The text in each box gives the same quantity as that coded by the color. Light colors present a security vulnerability to, for example, a passport gate.

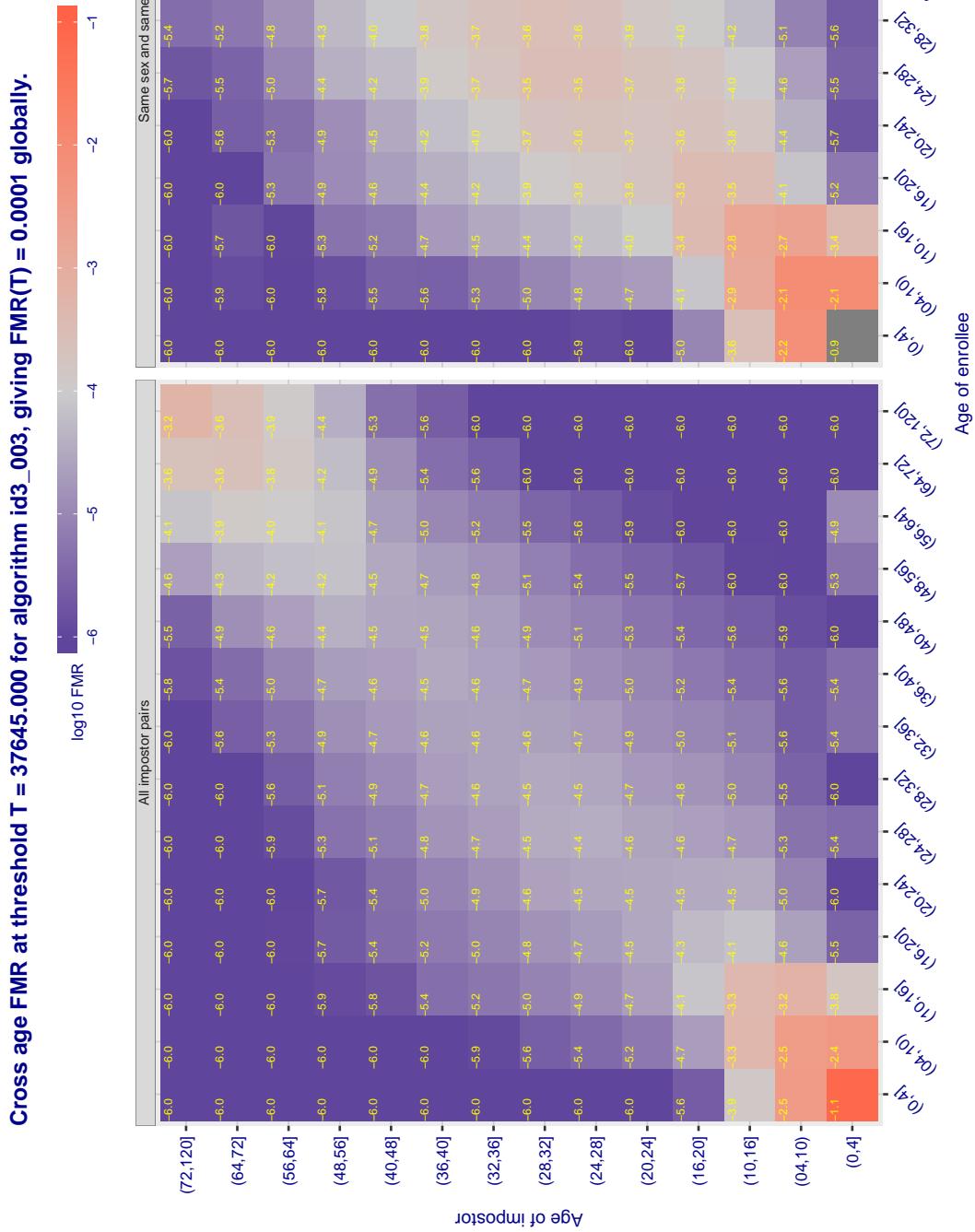
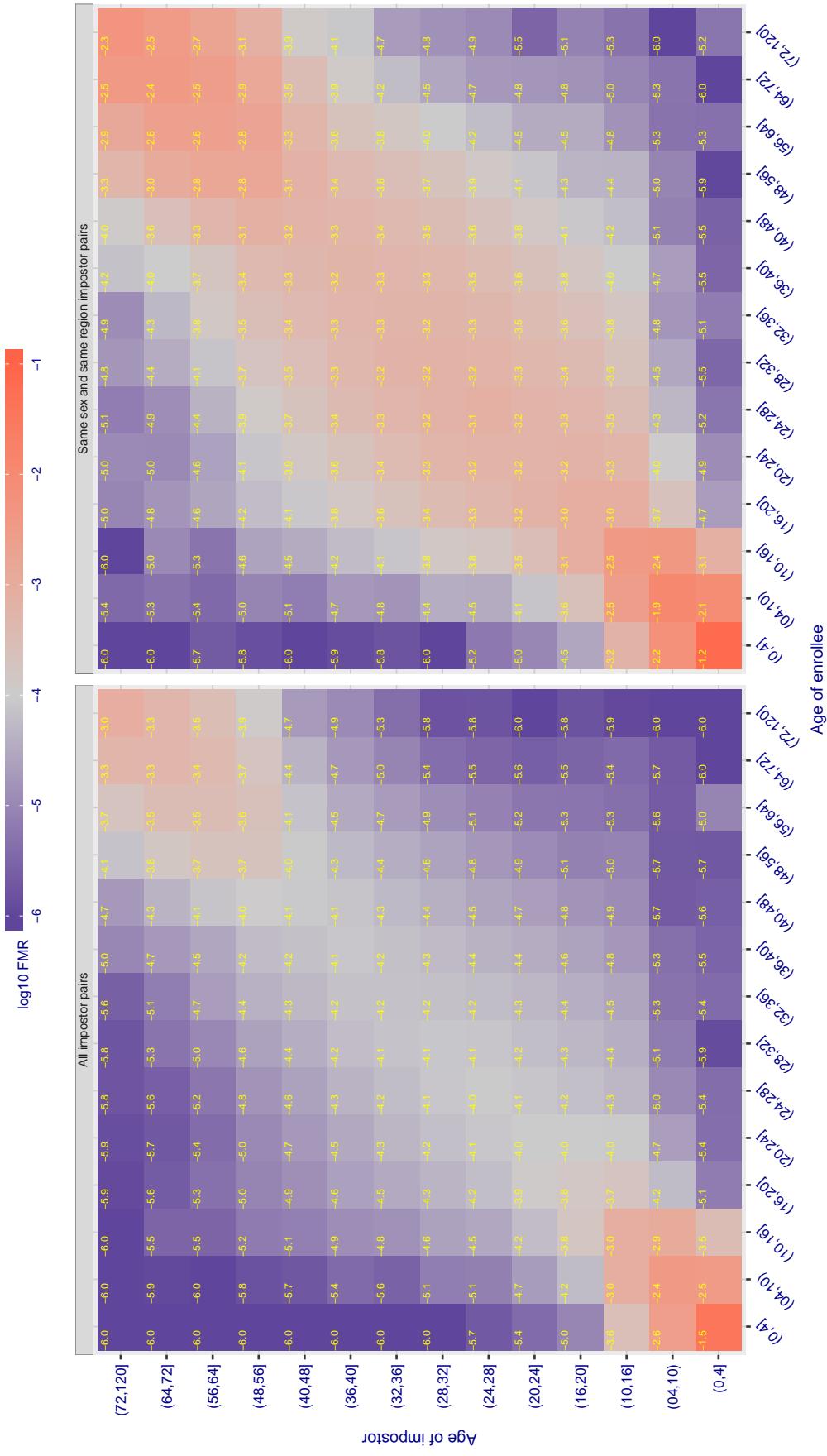


Figure 4/5: For algorithm id3-003 operating on visa images, the heatmap shows false match observed over impostor comparisons of faces from different individuals who have the given age pair. False matches are counted against a recognition threshold fixed globally to give $FMR = 0.0001$ over all on the order of 10^{10} impostor comparisons. The text in each box gives the same quantity as that coded by the color. Light colors present a security vulnerability to, for example, a passport gate.

Cross age FMR at threshold T = 37001.000 for algorithm id3_004, giving FMR(T) = 0.0001 globally.



Cross age FMR at threshold T = 3664.380 for algorithm idemia_003, giving FMR(T) = 0.0001 globally.

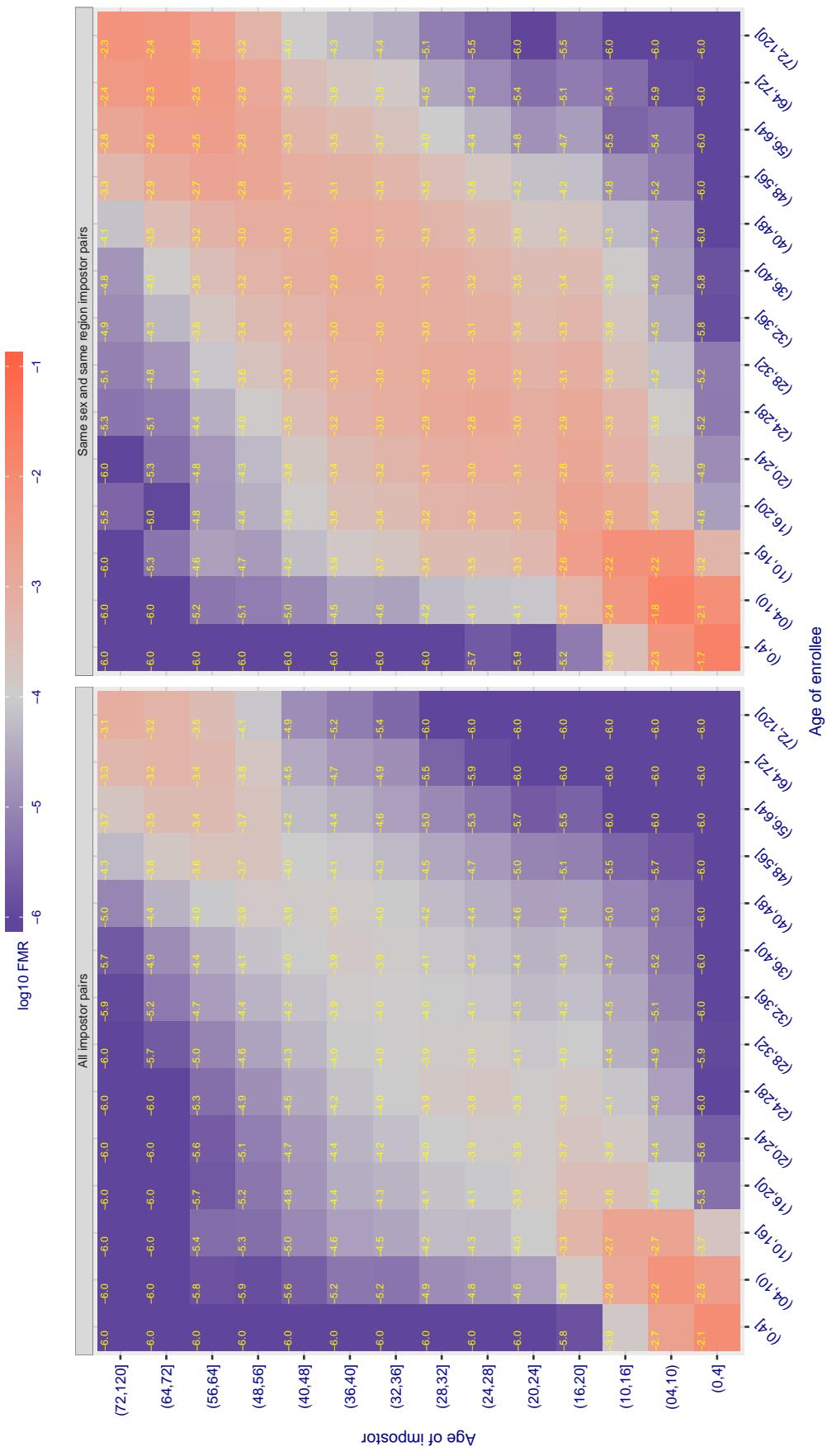


Figure 477: For algorithm idemia-003 operating on visa images, the heatmap shows false match observed over impostor comparisons of faces from different individuals who have the given age pair. False matches are counted against a recognition threshold fixed globally to give $FMR = 0.0001$ over all on the order of 10^{10} impostor comparisons. The text in each box gives the same quantity as that coded by the color. Light colors present a security vulnerability to, for example, a passport gate.

Cross age FMR at threshold T = 3925.463 for algorithm idemia_004, giving FMR(T) = 0.0001 globally.

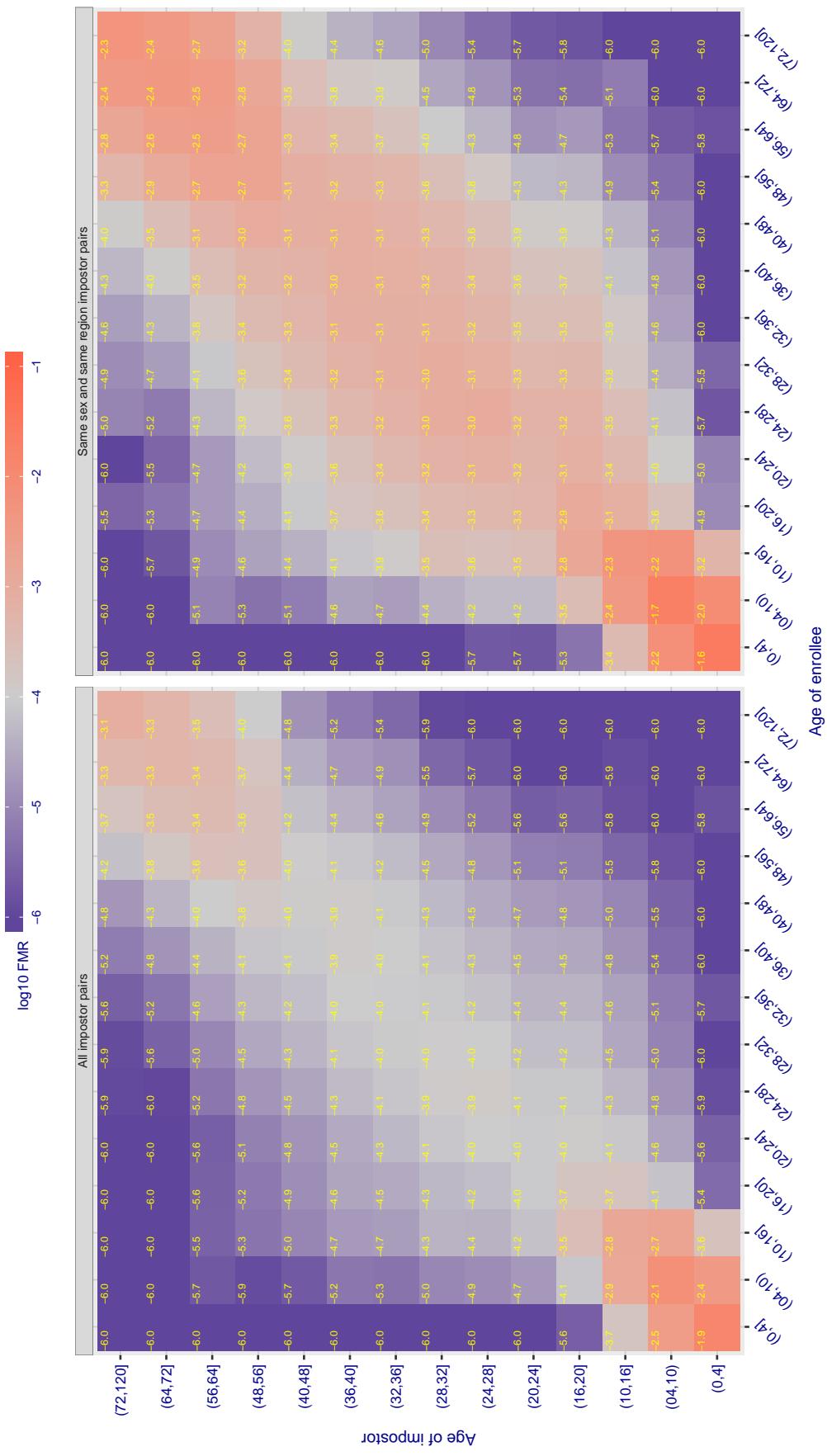


Figure 478: For algorithm idemia-004 operating on visa images, the heatmap shows false match observed over impostor comparisons of faces from different individuals who have the given age pair. False matches are counted against a recognition threshold fixed globally to give $FMR = 0.0001$ over all on the order of 10^{10} impostor comparisons. The text in each box gives the same quantity as that coded by the color. Light colors present a security vulnerability to, for example, a passport gate.

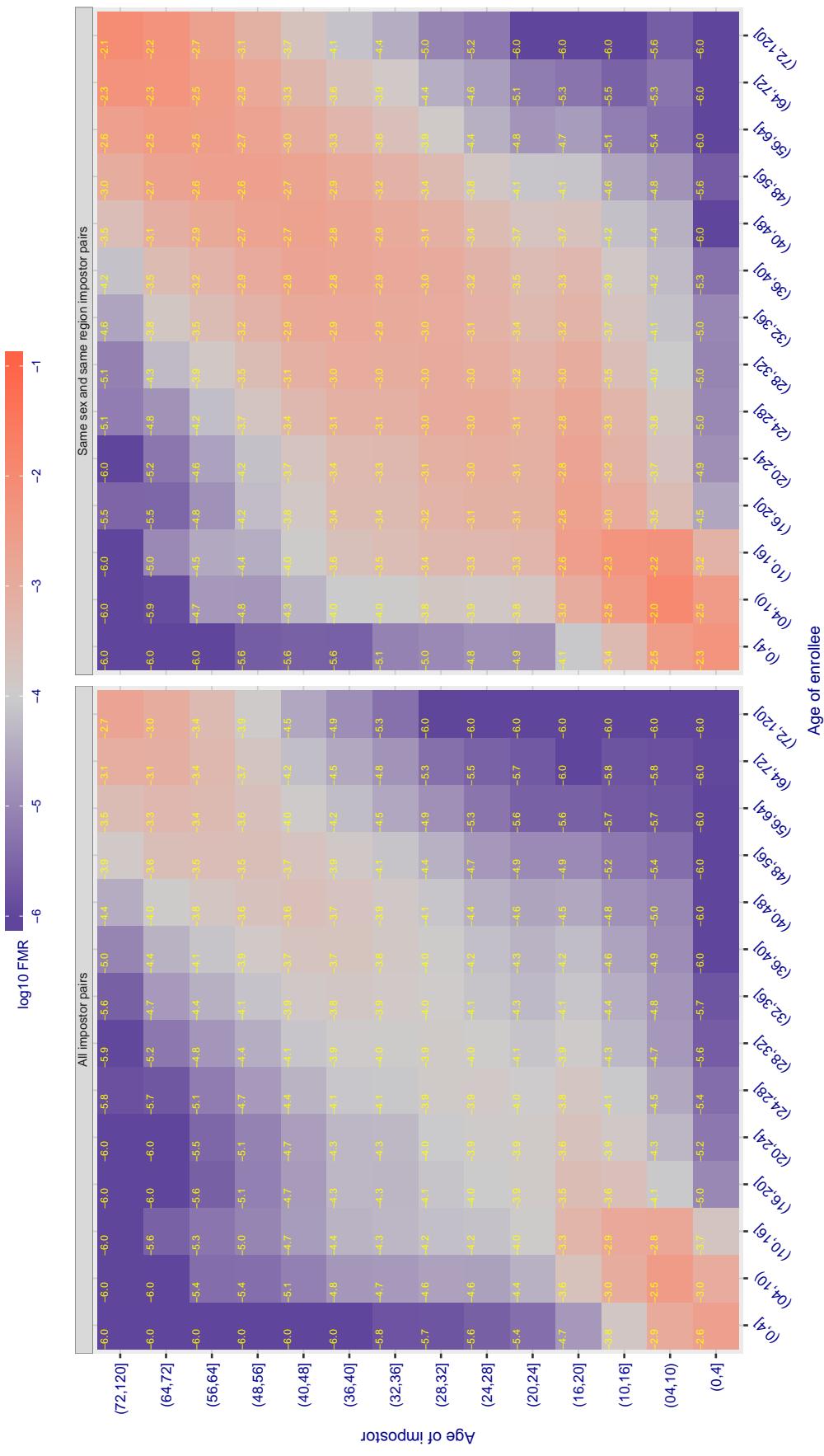


Figure 479: For algorithm *iit-000* operating on visa images, the heatmap shows false match observed over impostor comparisons of faces from different individuals who have the given age pair. False matches are counted against a recognition threshold fixed globally to give $FMR = 0.0001$ over all on the order of 10^{10} impostor comparisons. The text in each box gives the same quantity as that coded by the color. Light colors present a security vulnerability to, for example, a passport gate.

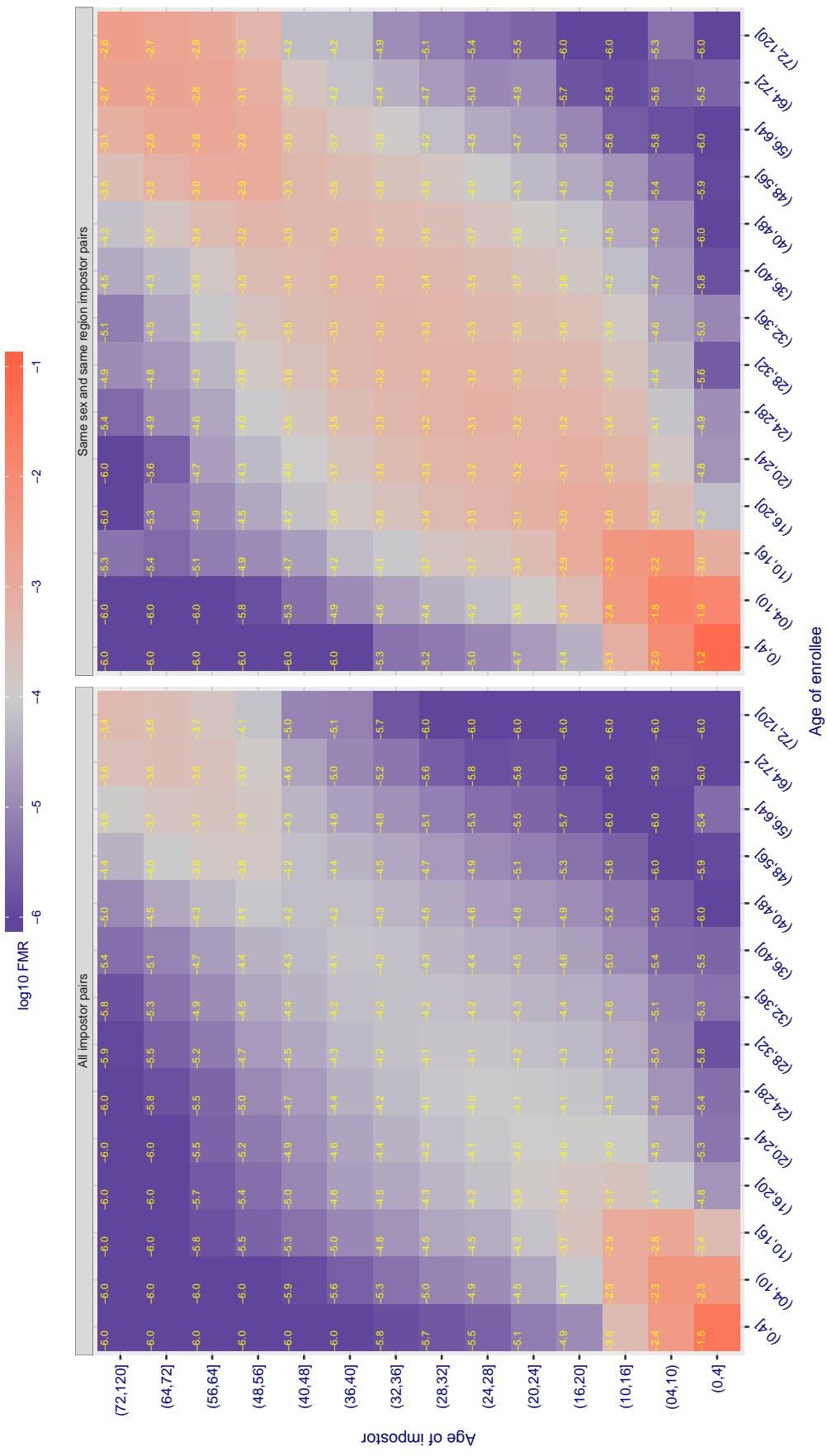


Figure 480: For algorithm *iit-001* operating on visa images, the heatmap shows false match observed over impostor comparisons of faces from different individuals who have the given age pair. False matches are counted against a recognition threshold fixed globally to give $FMR = 0.0001$ over all on the order of 10^{10} impostor comparisons. The text in each box gives the same quantity as that coded by the color. Light colors present a security vulnerability to, for example, a passport gate.

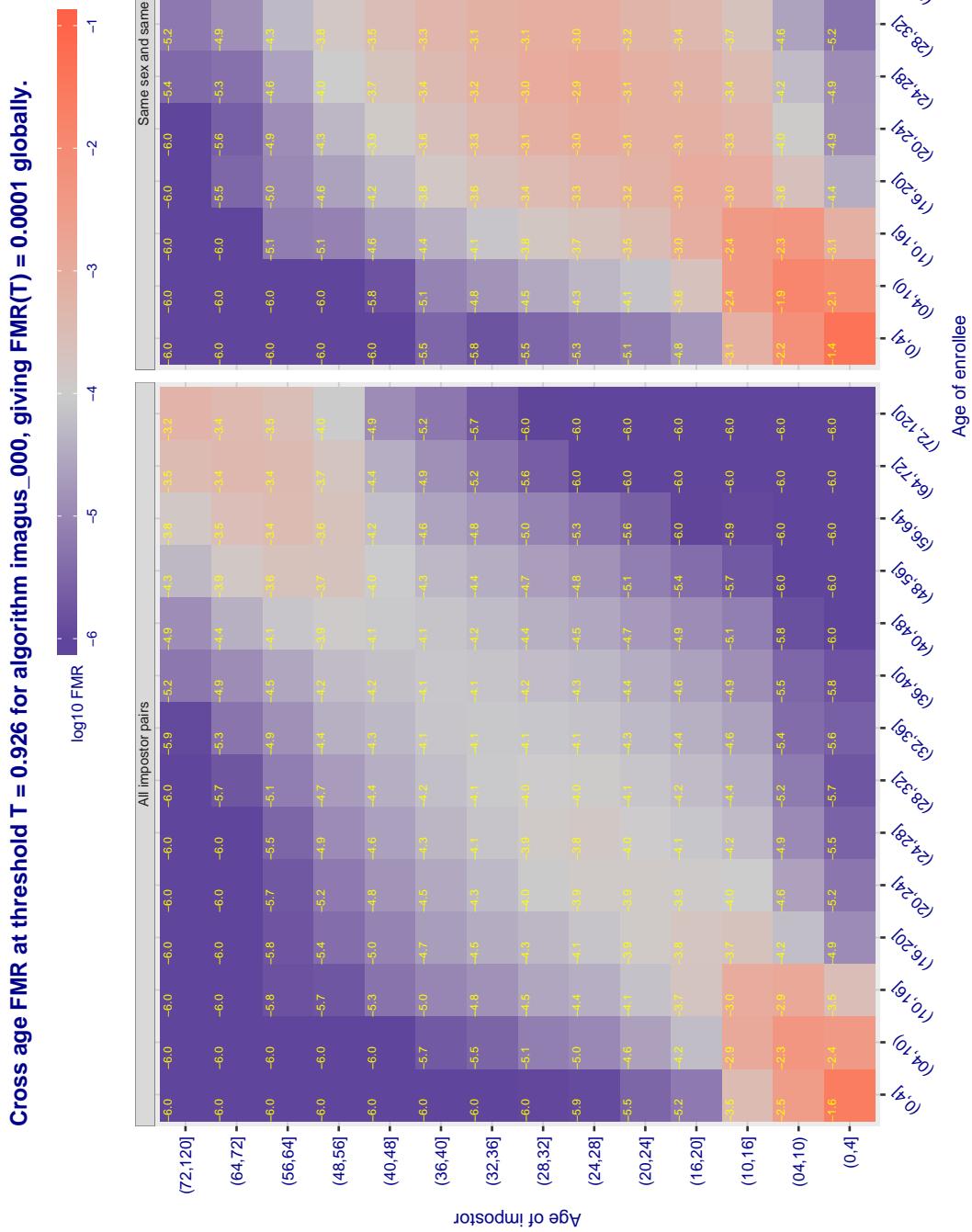


Figure 481: For algorithm `imags-000` operating on visa images, the heatmap shows false match observed over impostor comparisons of faces from different individuals who have the given age pair. False matches are counted against a recognition threshold fixed globally to give $FMR = 0.0001$ over all on the order of 10^{10} impostor comparisons. The text in each box gives the same quantity as that coded by the color. Light colors present a security vulnerability to, for example, a passport gate.

Cross age FMR at threshold T = 1.375 for algorithm imperial_000, giving FMR(T) = 0.0001 globally.

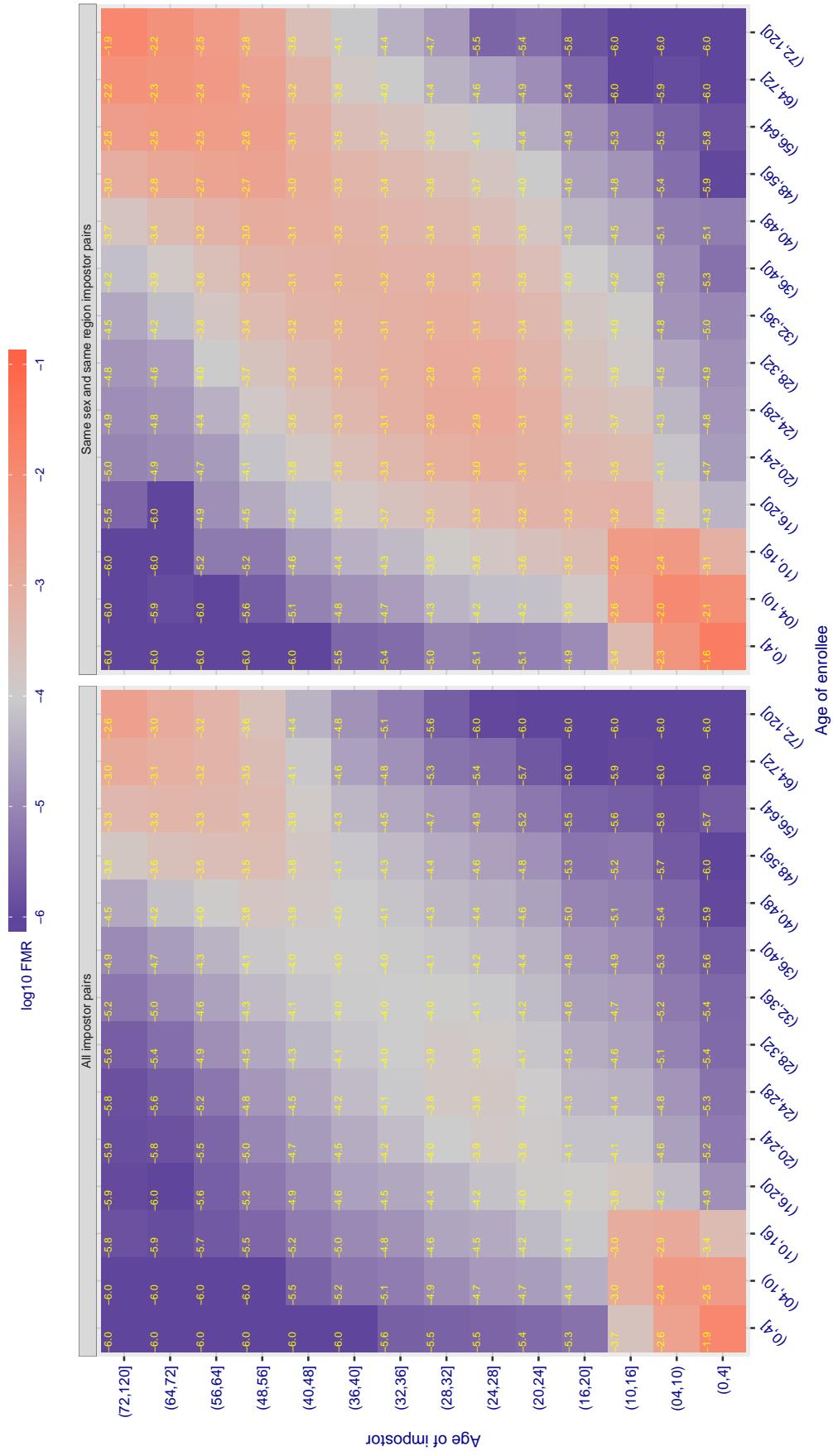


Figure 482: For algorithm imperial-000 operating on visa images, the heatmap shows false match observed over impostor comparisons of faces from different individuals who have the given age pair. False matches are counted against a recognition threshold fixed globally to give $FMR = 0.0001$ over all on the order of 10^{10} impostor comparisons. The text in each box gives the same quantity as that coded by the color. Light colors present a security vulnerability to, for example, a passport gate.

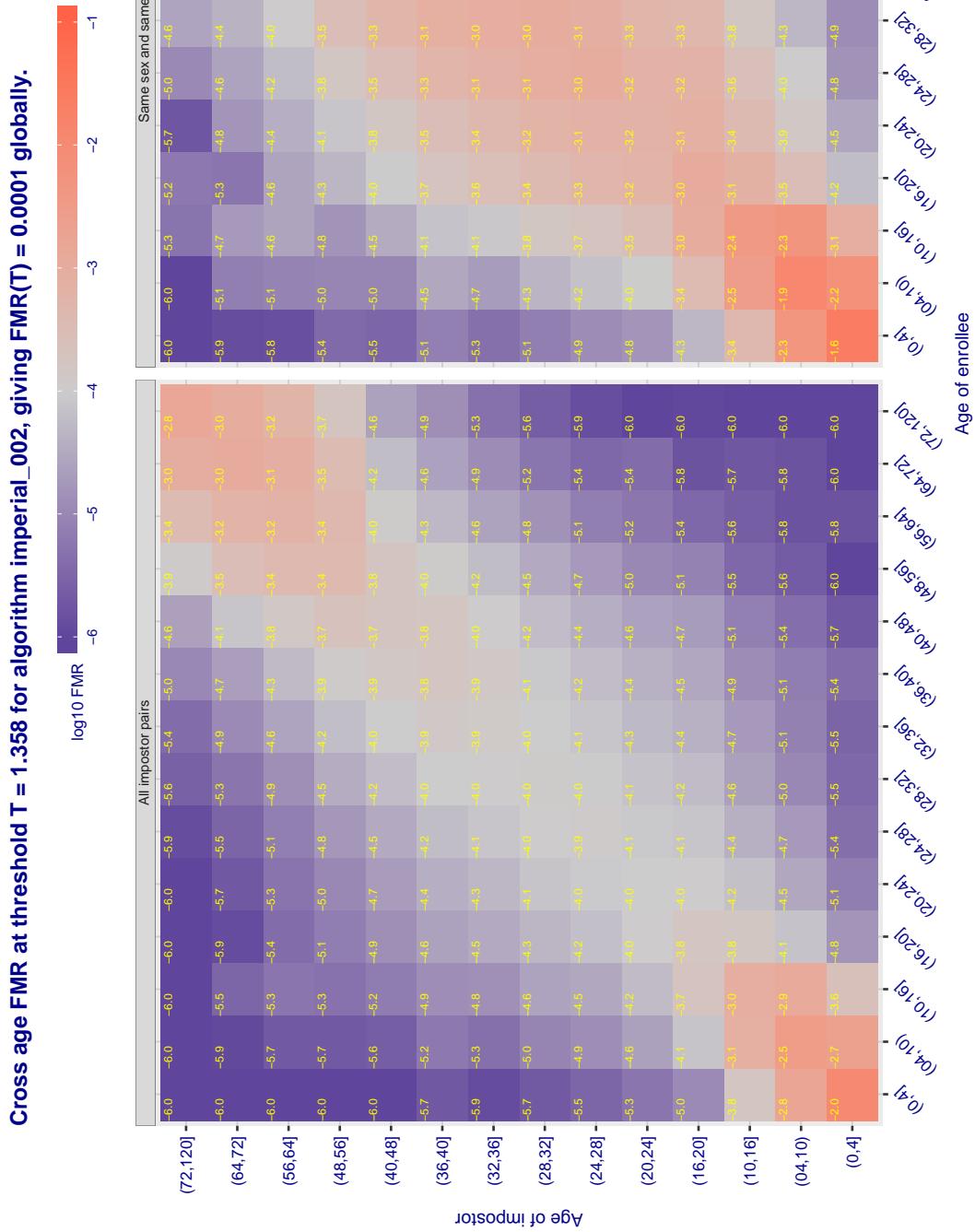


Figure 483: For algorithm imperial-002 operating on visa images, the heatmap shows false match observed over impostor comparisons of faces from different individuals who have the given age pair. False matches are counted against a recognition threshold fixed globally to give $FMR = 0.0001$ over all on the order of 10^{10} impostor comparisons. The text in each box gives the same quantity as that coded by the color. Light colors present a security vulnerability to, for example, a passport gate.

Cross age FMR at threshold T = 1.427 for algorithm incode_003, giving FMR(T) = 0.0001 globally.

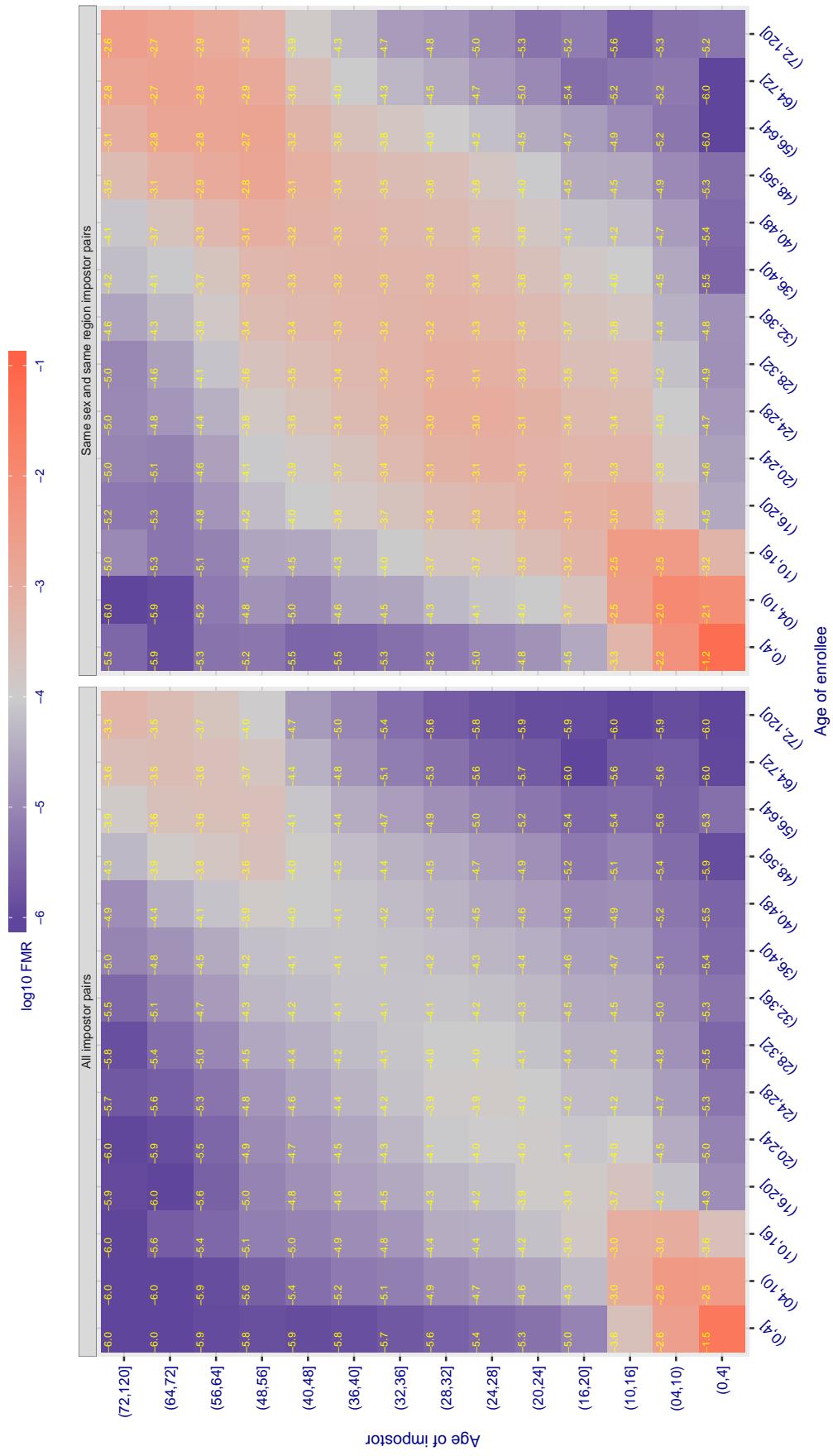


Figure 484: For algorithm incode-003 operating on visa images, the heatmap shows false match observed over impostor comparisons of faces from different individuals who have the given age pair. False matches are counted against a recognition threshold fixed globally to give FMR = 0.0001 over all on the order of 10^{10} impostor comparisons. The text in each box gives the same quantity as that coded by the color. Light colors present a security vulnerability to, for example, a passport gate.

Cross age FMR at threshold T = 1.398 for algorithm incode_004, giving FMR(T) = 0.0001 globally.

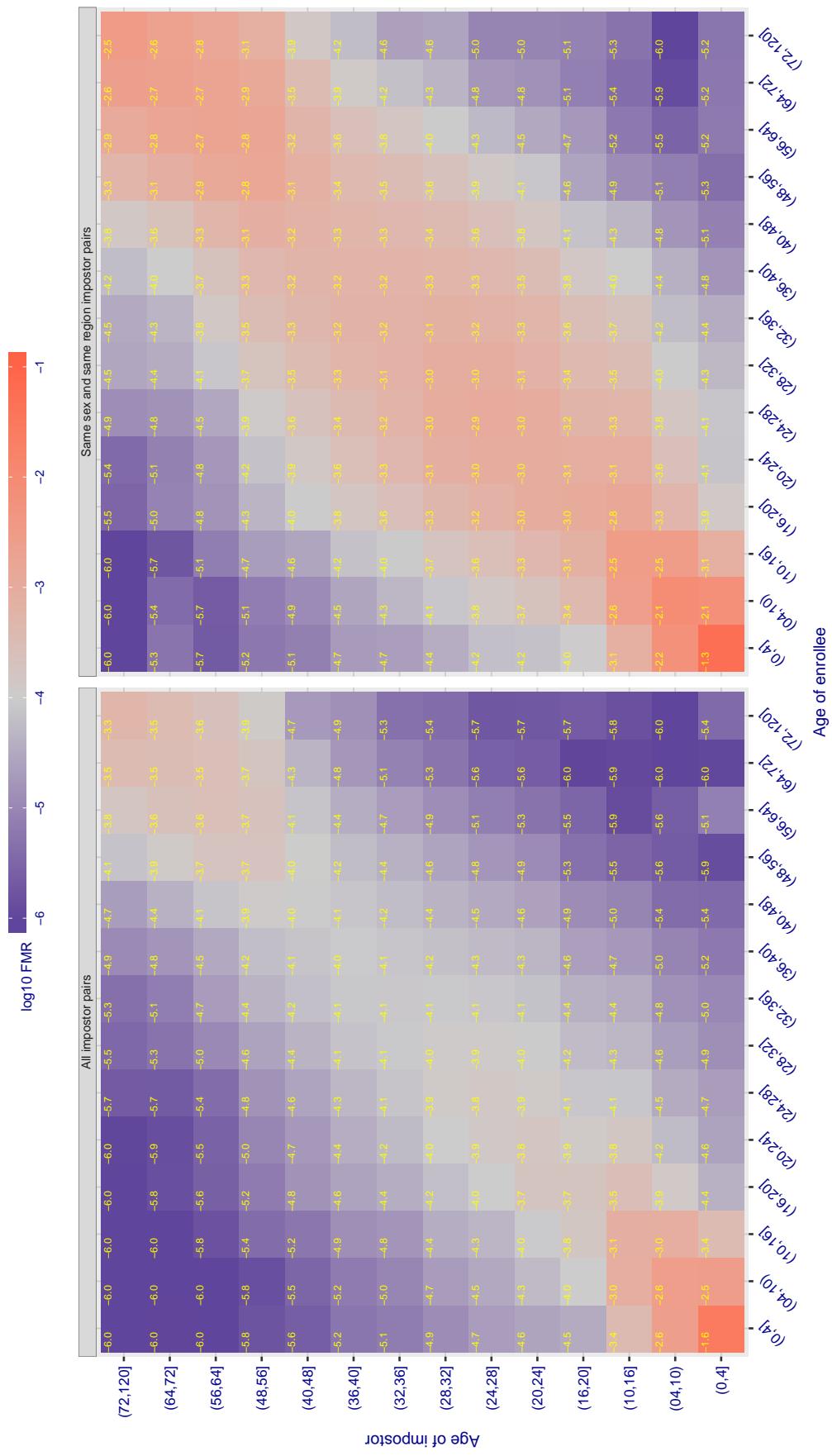


Figure 485: For algorithm incode_004 operating on visa images, the heatmap shows false match observed over impostor comparisons of faces from different individuals who have the given age pair. False matches are counted against a recognition threshold fixed globally to give $FMR = 0.0001$ over all on the order of 10^{10} impostor comparisons. The text in each box gives the same quantity as that coded by the color. Light colors present a security vulnerability to, for example, a passport gate.

Cross age FMR at threshold T = 29.232 for algorithm innovatrics_004, giving $FMR(T) = 0.0001$ globally.

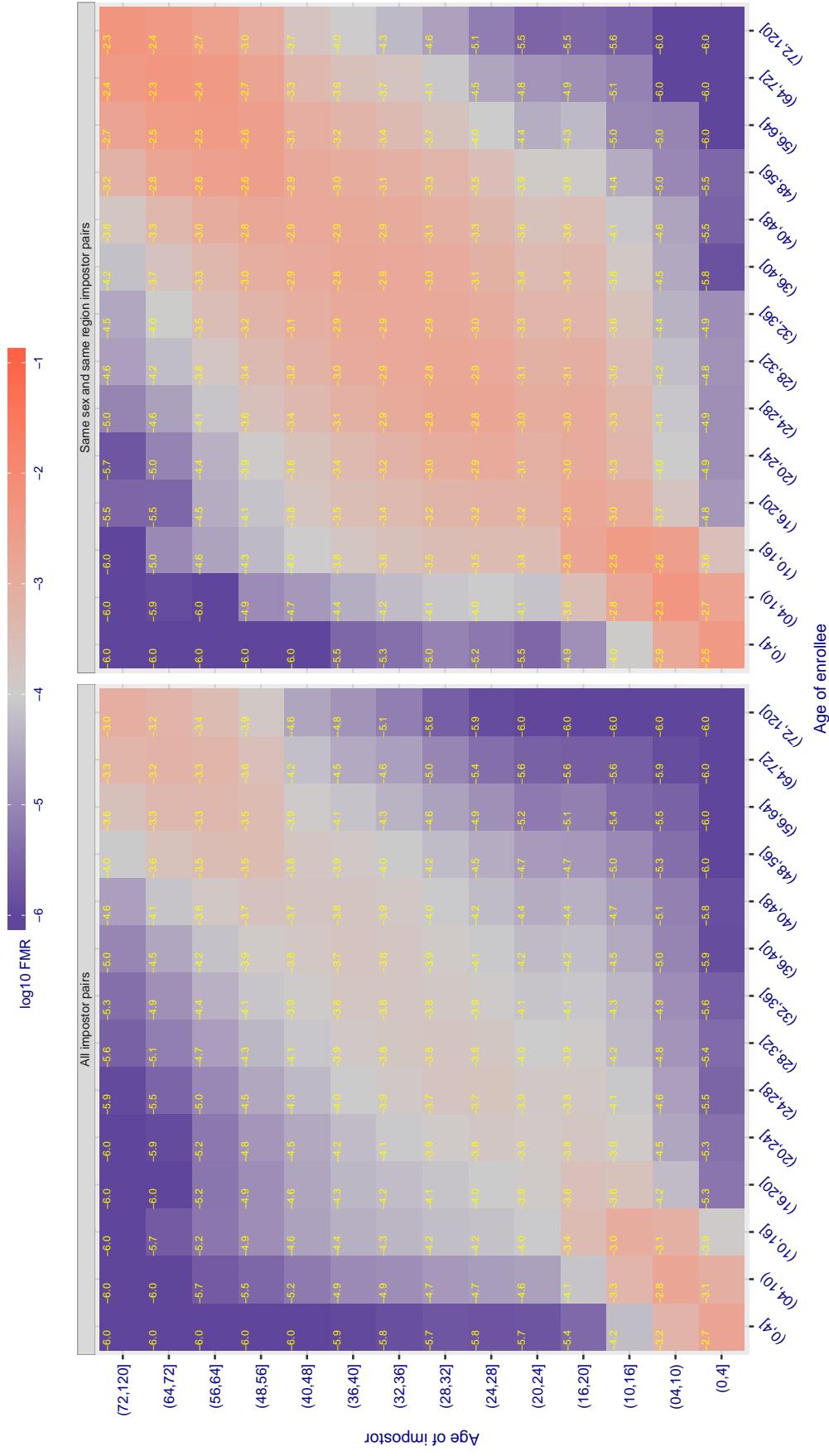


Figure 486: For algorithm innovatrics-004 operating on visa images, the heatmap shows false match observed over imposter comparisons of faces from different individuals who have the given age pair. False matches are counted against a recognition threshold fixed globally to give $FMR = 0.0001$ over all on the order of 10^{10} imposter comparisons. The text in each box gives the same quantity as that coded by the color. Light colors present a security vulnerability to, for example, a passport gate.

Cross age FMR at threshold T = 27.987 for algorithm innovatrics_006, giving $FMR(T) = 0.0001$ globally.

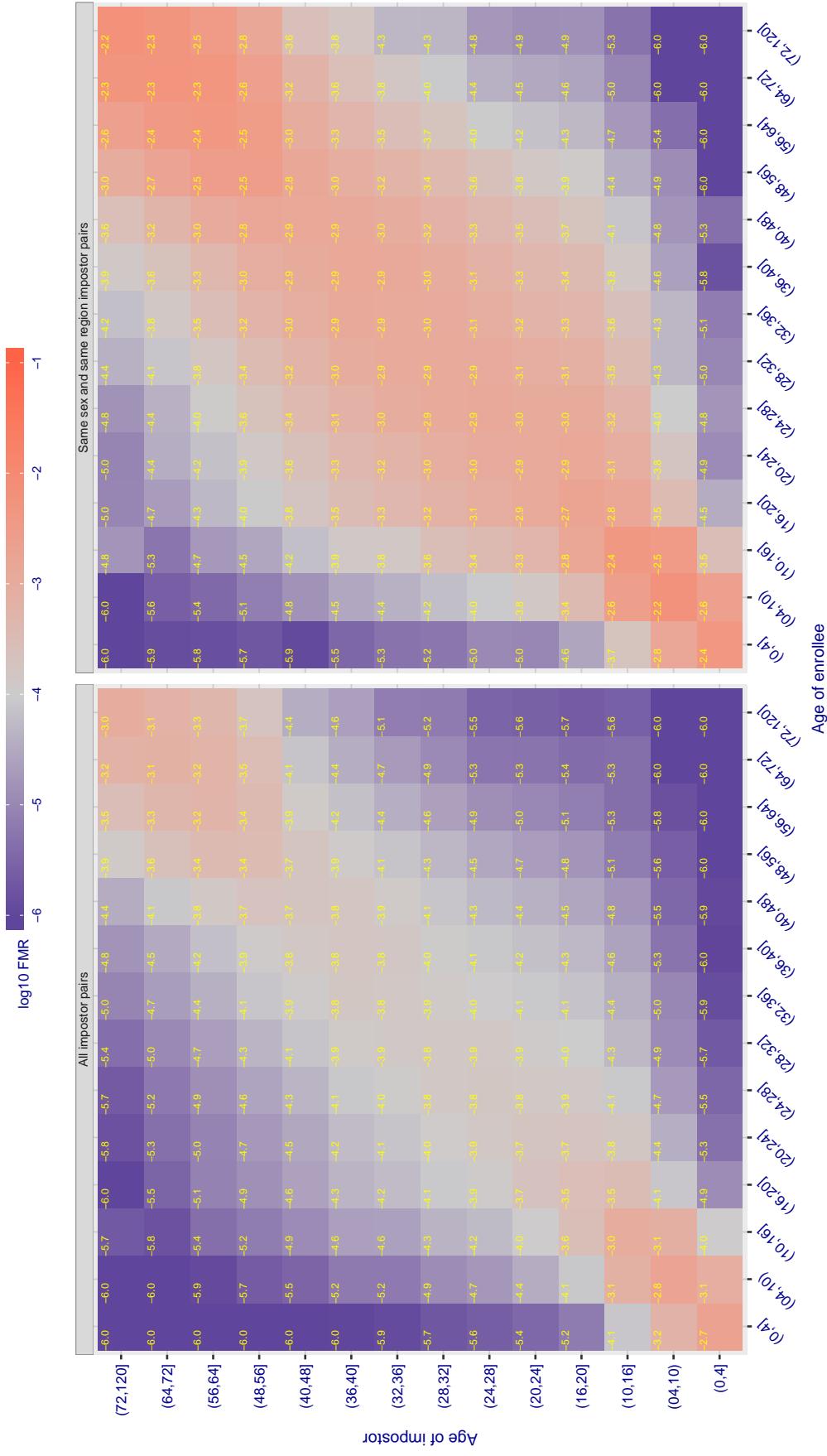


Figure 487: For algorithm innovatrics-006 operating on visa images, the heatmap shows false match observed over impostor comparisons of faces from different individuals who have the given age pair. False matches are counted against a recognition threshold fixed globally to give $FMR = 0.0001$ over all on the order of 10^{10} impostor comparisons. The text in each box gives the same quantity as that coded by the color. Light colors present a security vulnerability to, for example, a passport gate.

Cross age FMR at threshold T = 0.705 for algorithm intellicloudai_001, giving $FMR(T) = 0.0001$ globally.

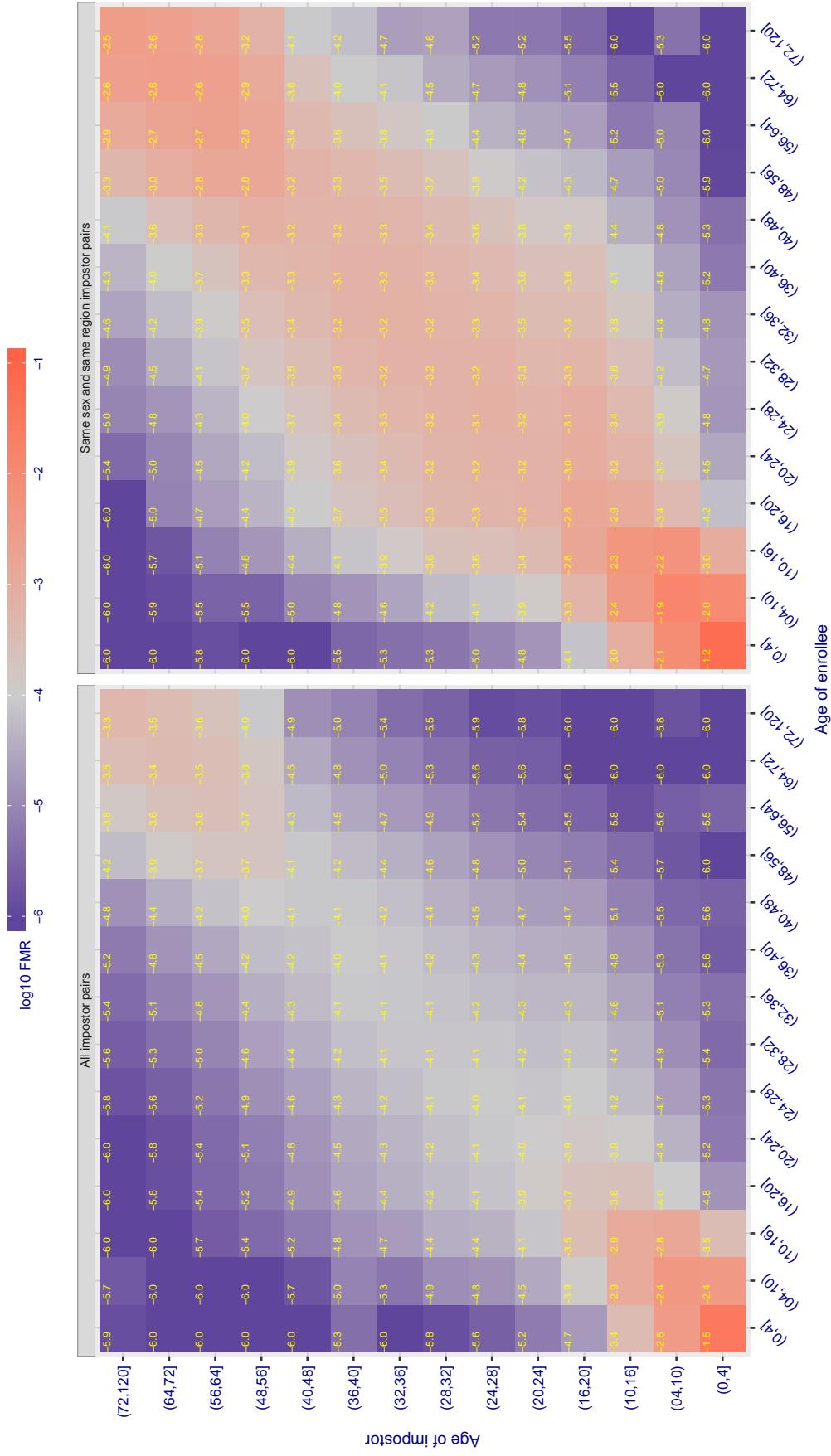


Figure 488: For algorithm intellicloudai-001 operating on visa images, the heatmap shows false match observed over impostor comparisons of faces from different individuals who have the given age pair. False matches are counted against a recognition threshold fixed globally to give $FMR = 0.0001$ over all on the order of 10^{10} impostor comparisons. The text in each box gives the same quantity as that coded by the color. Light colors present a security vulnerability to, for example, a passport gate.

Cross age FMR at threshold T = 0.300 for algorithm intellifusion_001, giving $FMR(T) = 0.0001$ globally.

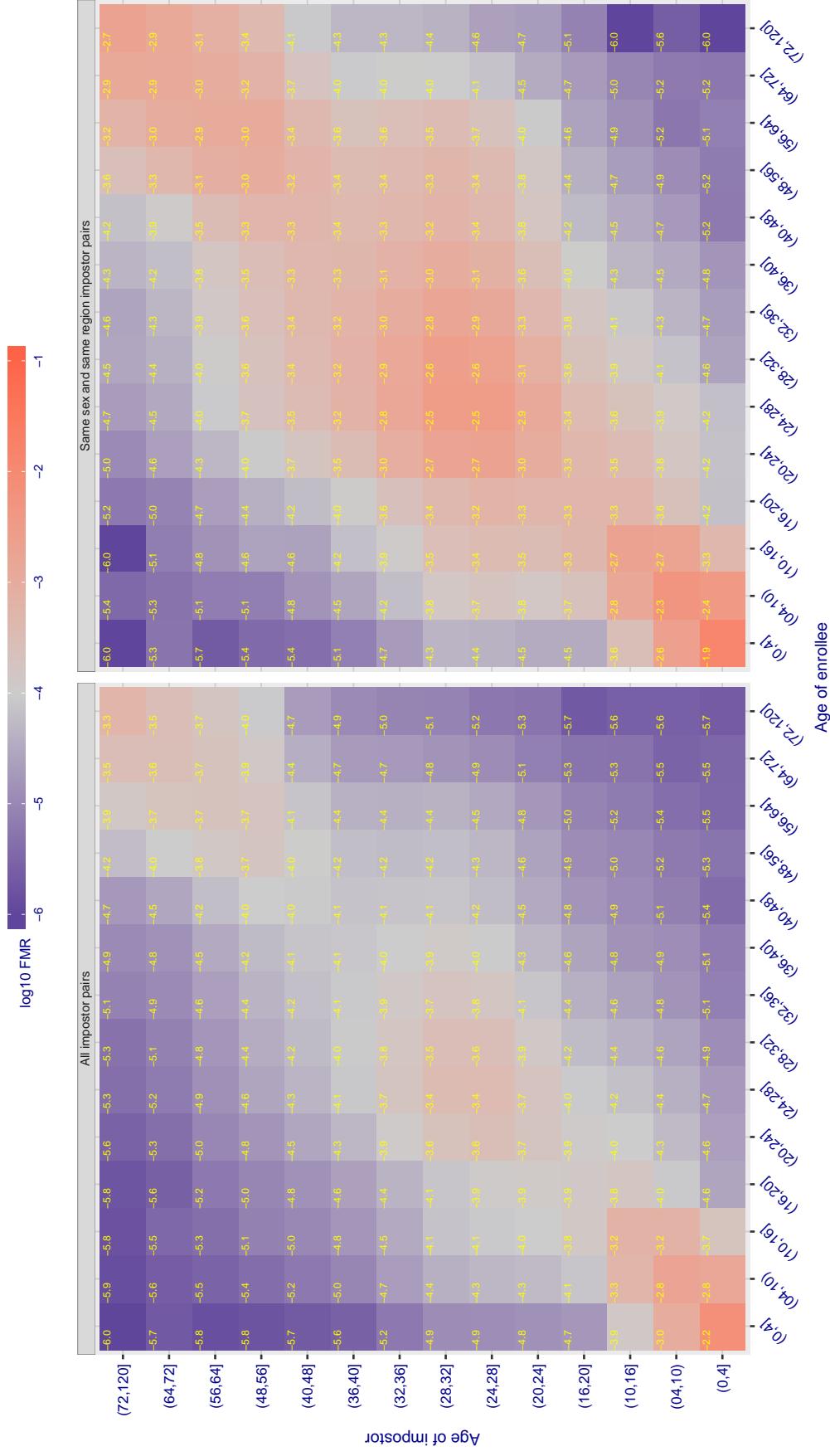


Figure 489: For algorithm intellifusion-001 operating on visa images, the heatmap shows false match observed over impostor comparisons of faces from different individuals who have the given age pair. False matches are counted against a recognition threshold fixed globally to give $FMR = 0.0001$ over all on the order of 10^{10} impostor comparisons. The text in each box gives the same quantity as that coded by the color. Light colors present a security vulnerability to, for example, a passport gate.

Cross age FMR at threshold T = 49.664 for algorithm intellivision_001, giving $FMR(T) = 0.0001$ globally.

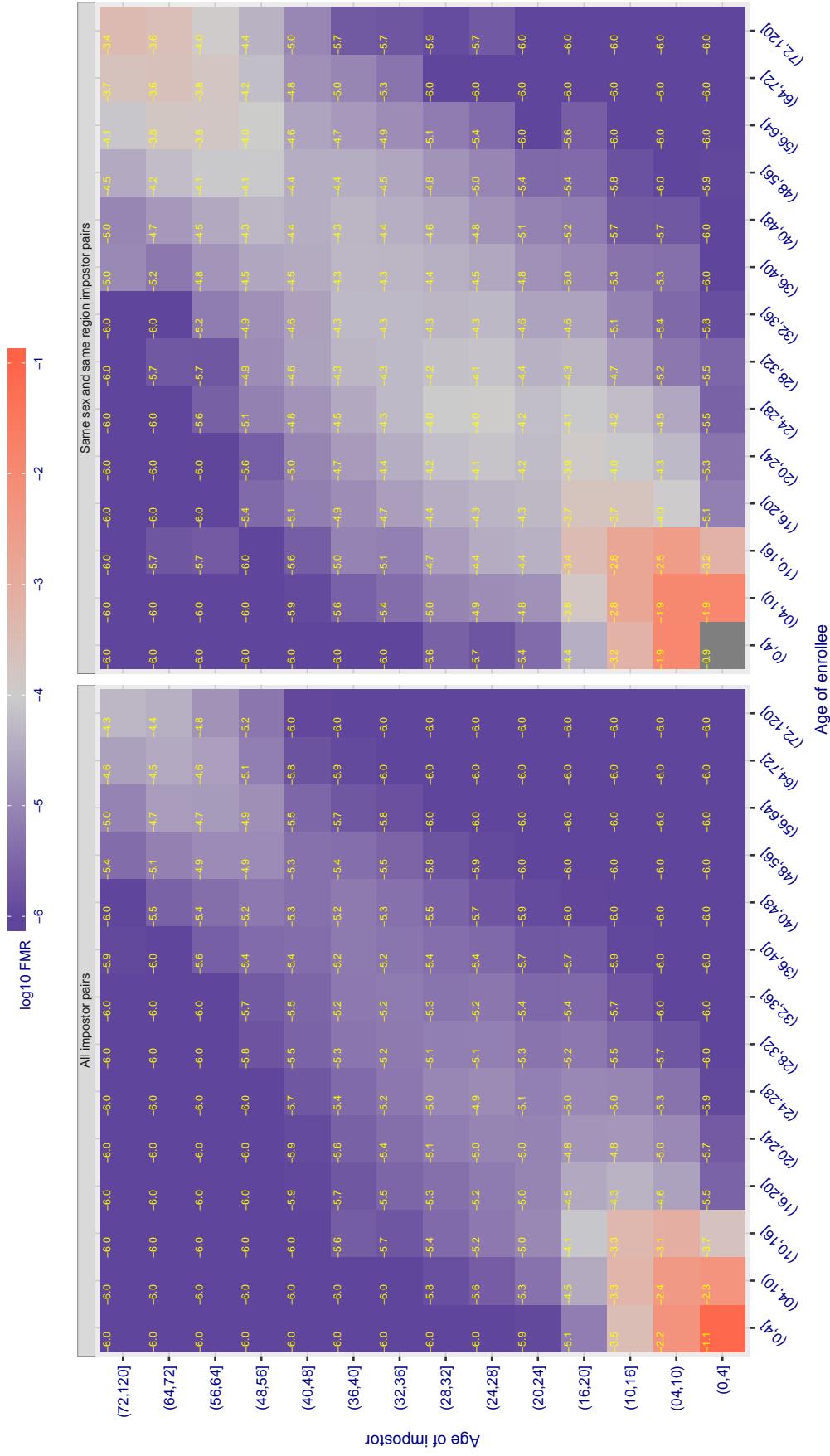


Figure 490: For algorithm intellivision_001 operating on visa images, the heatmap shows false match observed over impostor comparisons of faces from different individuals who have the given age pair. False matches are counted against a recognition threshold fixed globally to give $FMR = 0.0001$ over all on the order of 10^{10} impostor comparisons. The text in each box gives the same quantity as that coded by the color. Light colors present a security vulnerability to, for example, a passport gate.

Cross age FMR at threshold T = 44.160 for algorithm intellivision_002, giving $FMR(T) = 0.0001$ globally.

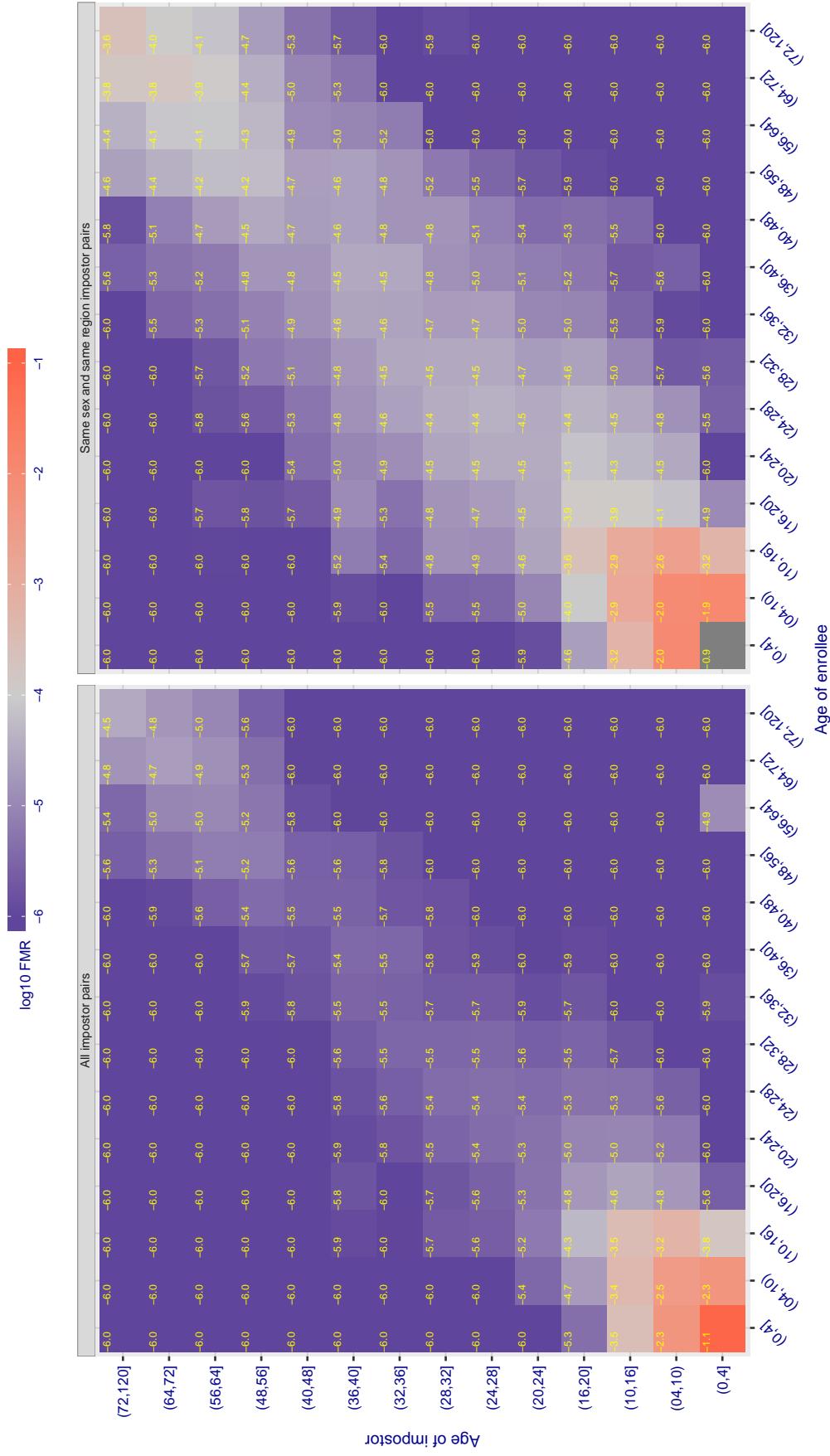


Figure 49I: For algorithm intellivision_002 operating on visa images, the heatmap shows false match observed over impostor comparisons of faces from different individuals who have the given age pair. False matches are counted against a recognition threshold fixed globally to give $FMR = 0.0001$ over all on the order of 10^{10} impostor comparisons. The text in each box gives the same quantity as that coded by the color. Light colors present a security vulnerability to, for example, a passport gate.

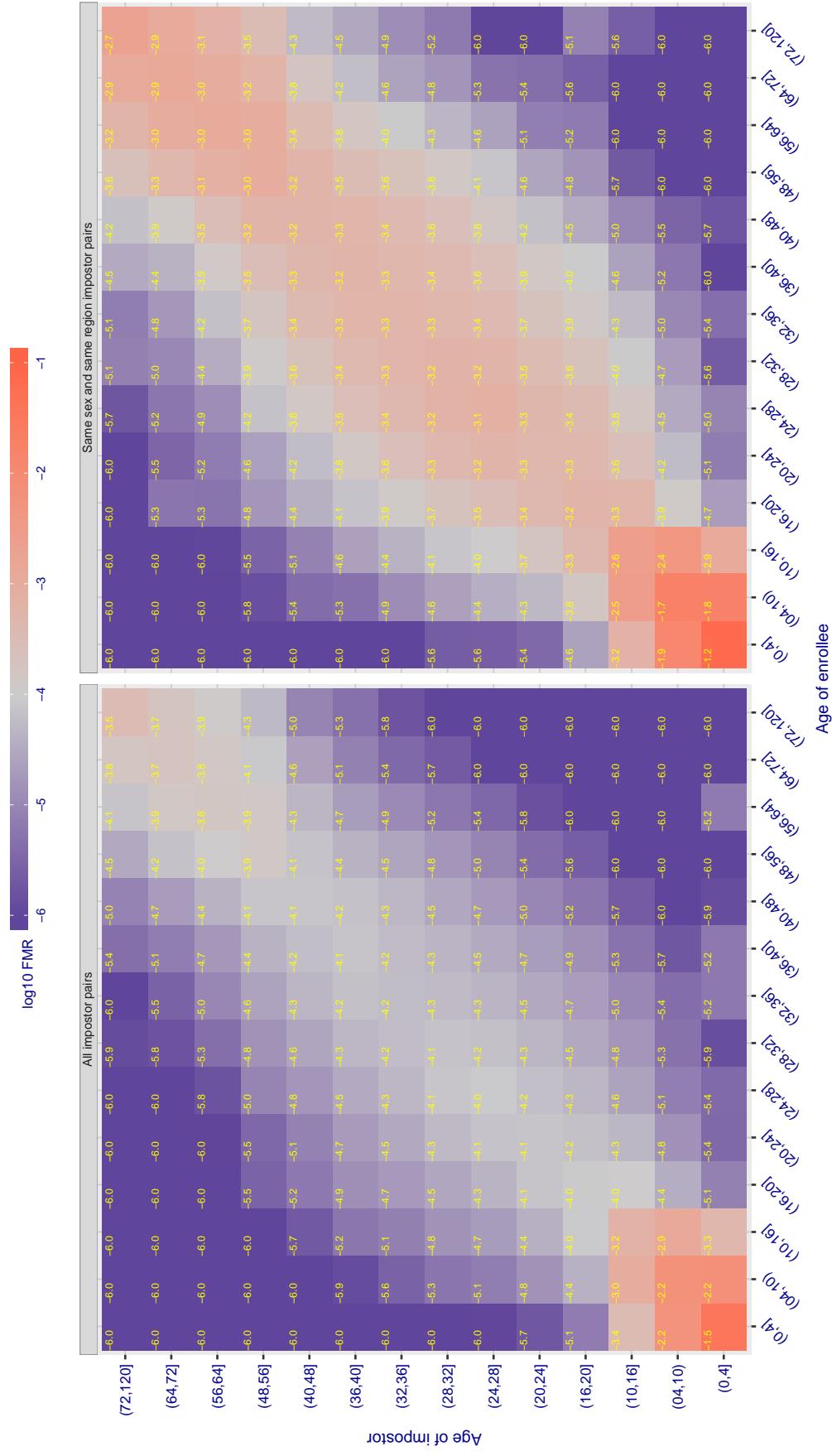
Cross age FMR at threshold T = 594.014 for algorithm intelresearch_000, giving $FMR(T) = 0.0001$ globally.

Figure 492: For algorithm intelresearch-000 operating on visa images, the heatmap shows false match observed over impostor comparisons of faces from different individuals who have the given age pair. False matches are counted against a recognition threshold fixed globally to give $FMR = 0.0001$ over all on the order of 10^{10} impostor comparisons. The text in each box gives the same quantity as that coded by the color. Light colors present a security vulnerability to, for example, a passport gate.

Cross age FMR at threshold T = 1.389 for algorithm intsysmsu_000, giving FMR(T) = 0.0001 globally.

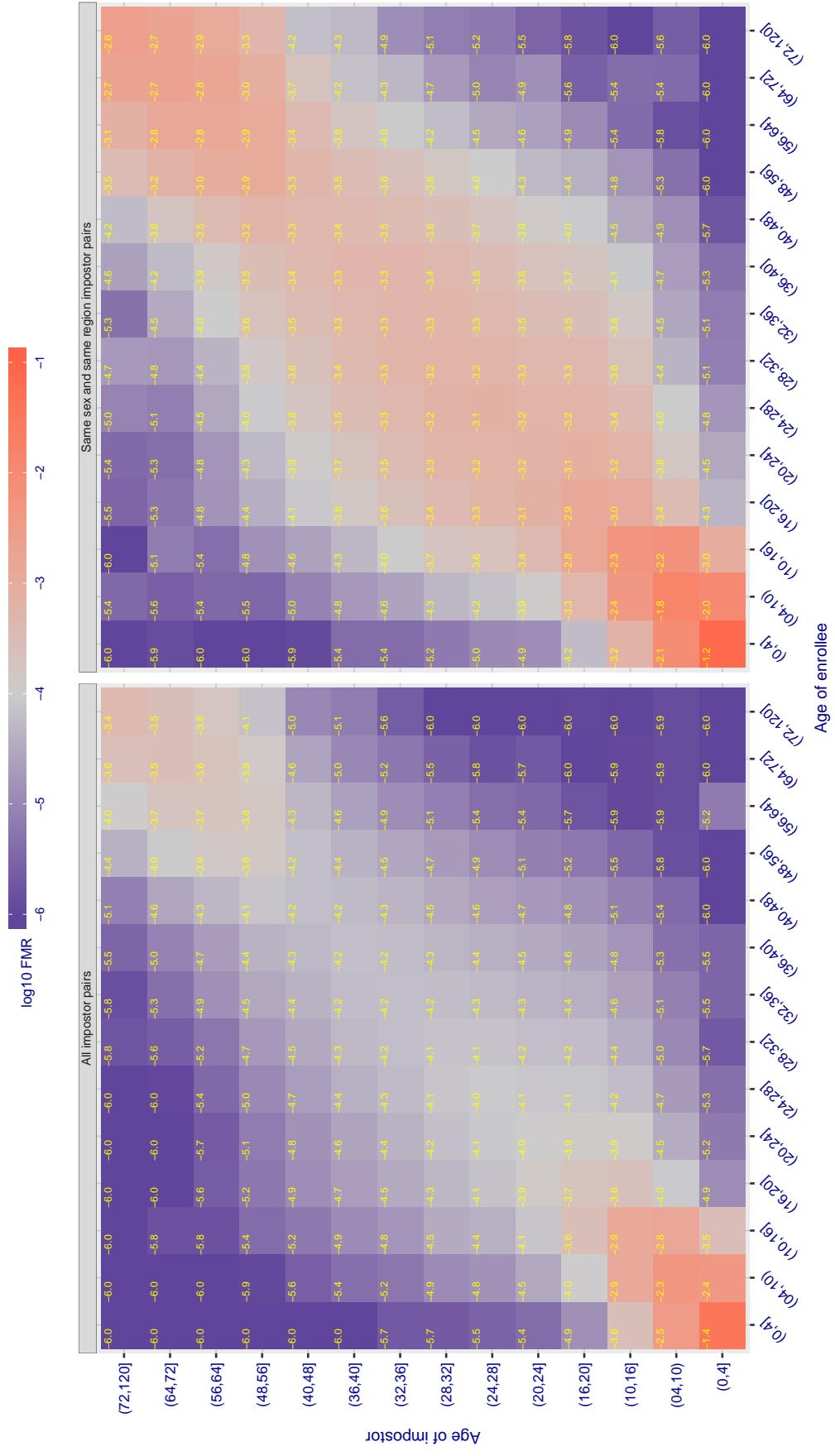


Figure 493: For algorithm intsysmsu-000 operating on visa images, the heatmap shows false match observed over impostor comparisons of faces from different individuals who have the given age pair. False matches are counted against a recognition threshold fixed globally to give $FMR = 0.001$ over all on the order of 10^{10} impostor comparisons. The text in each box gives the same quantity as that coded by the color. Light colors present a security vulnerability to, for example, a passport gate.

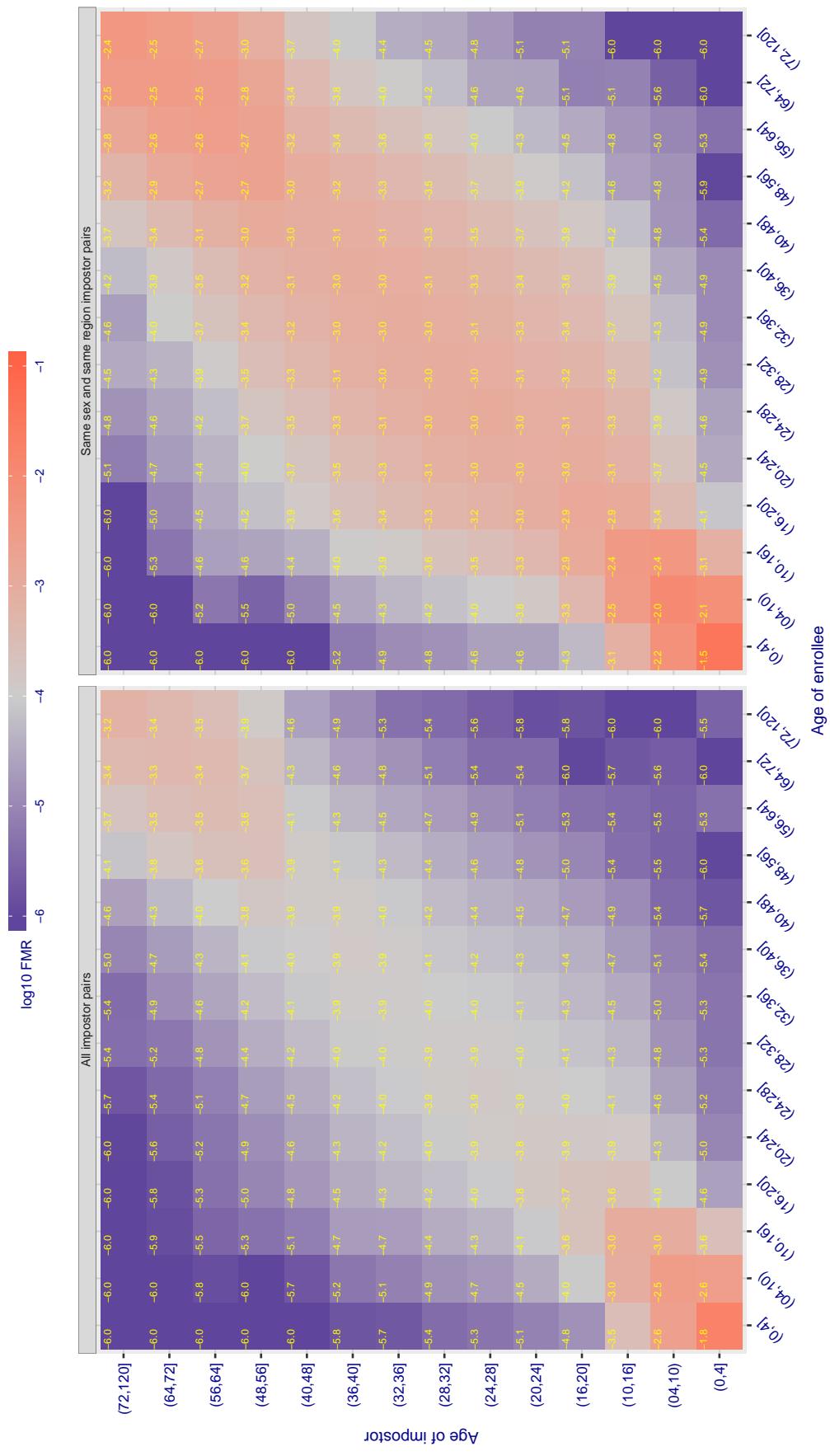
Cross age FMR at threshold T = 1.361 for algorithm iqface_000, giving $FMR(T) = 0.0001$ globally.

Figure 494: For algorithm iqface-000 operating on visa images, the heatmap shows false match observed over impostor comparisons of faces from different individuals who have the given age pair. False matches are counted against a recognition threshold fixed globally to give $FMR = 0.0001$ over all on the order of 10^{10} impostor comparisons. The text in each box gives the same quantity as that coded by the color. Light colors present a security vulnerability to, for example, a passport gate.

Cross age FMR at threshold T = 0.985 for algorithm isap_001, giving FMR(T) = 0.0001 globally.

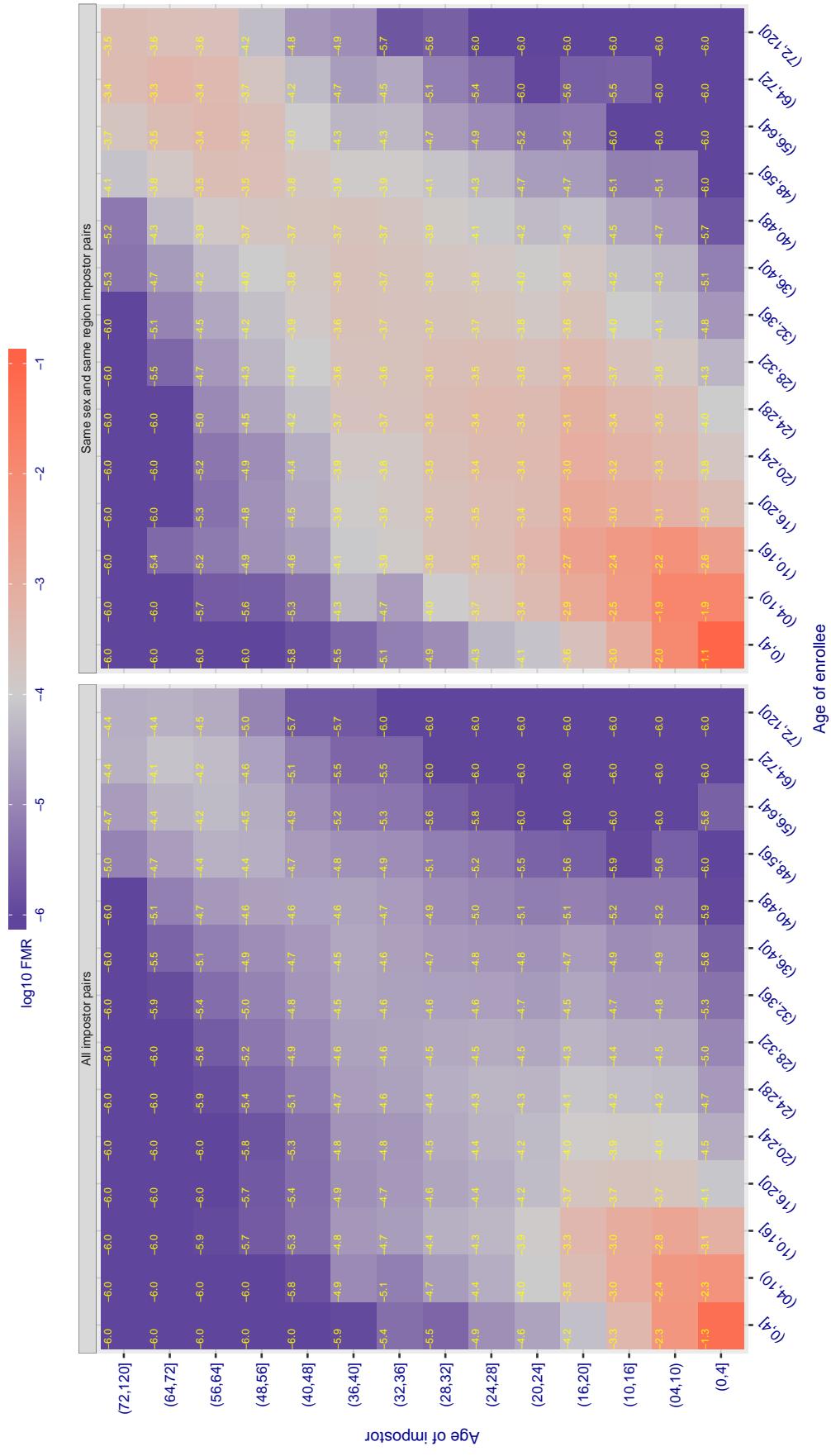


Figure 495: For algorithm isap_001 operating on visa images, the heatmap shows false match observed over imposter comparisons of faces from different individuals who have the given age pair. False matches are counted against a recognition threshold fixed globally to give FMR = 0.0001 over all on the order of 10^{10} impostor comparisons. The text in each box gives the same quantity as that coded by the color. Light colors present a security vulnerability to, for example, a passport gate.

Cross age FMR at threshold T = 23.498 for algorithm isityou_000, giving FMR(T) = 0.0001 globally.

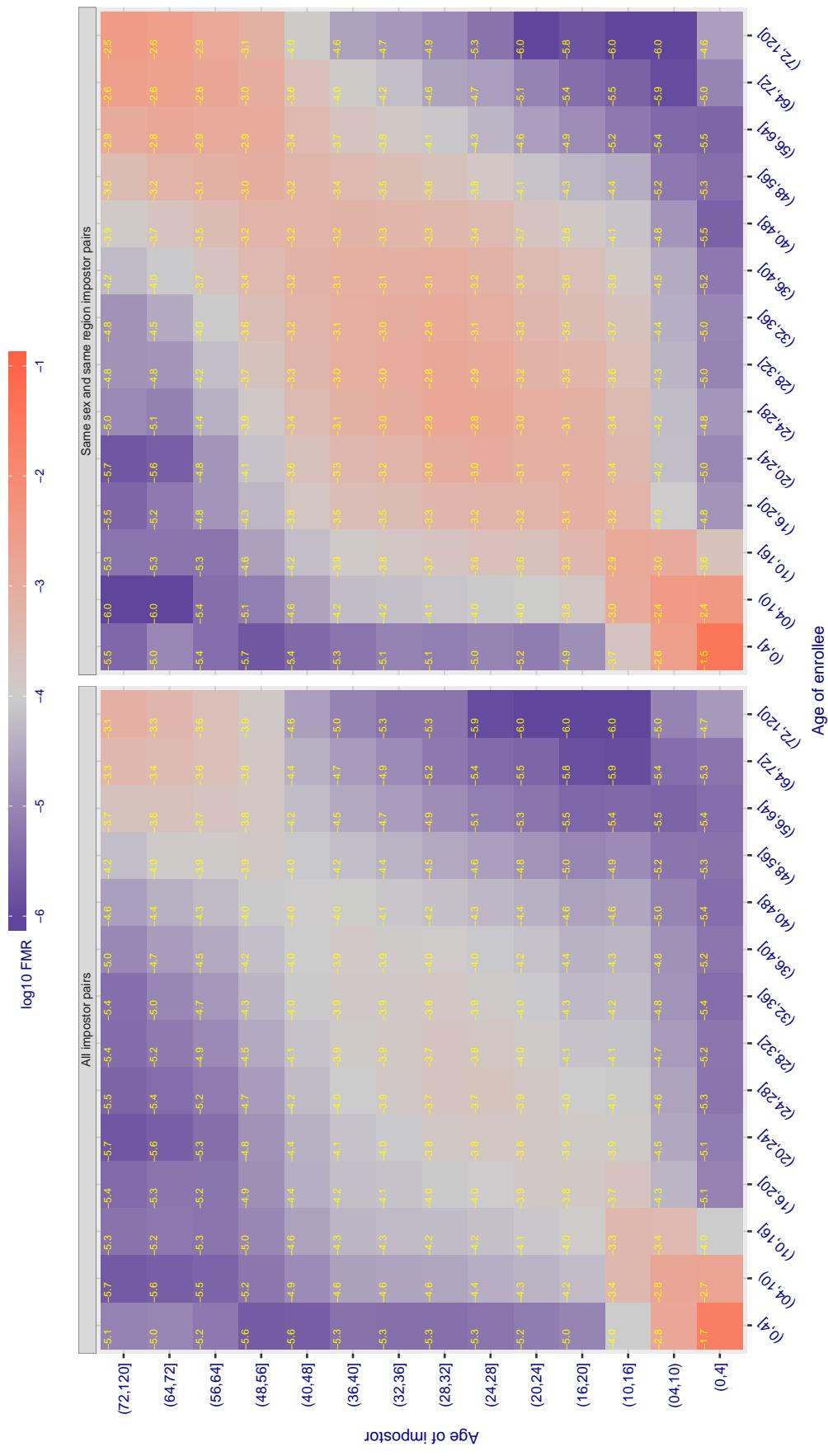


Figure 496: For algorithm isityou-000 operating on visa images, the heatmap shows false match observed over impostor comparisons of faces from different individuals who have the given age pair. False matches are counted against a recognition threshold fixed globally to give $FMR = 0.0001$ over all on the order of 10^{10} impostor comparisons. The text in each box gives the same quantity as that coded by the color. Light colors present a security vulnerability to, for example, a passport gate.

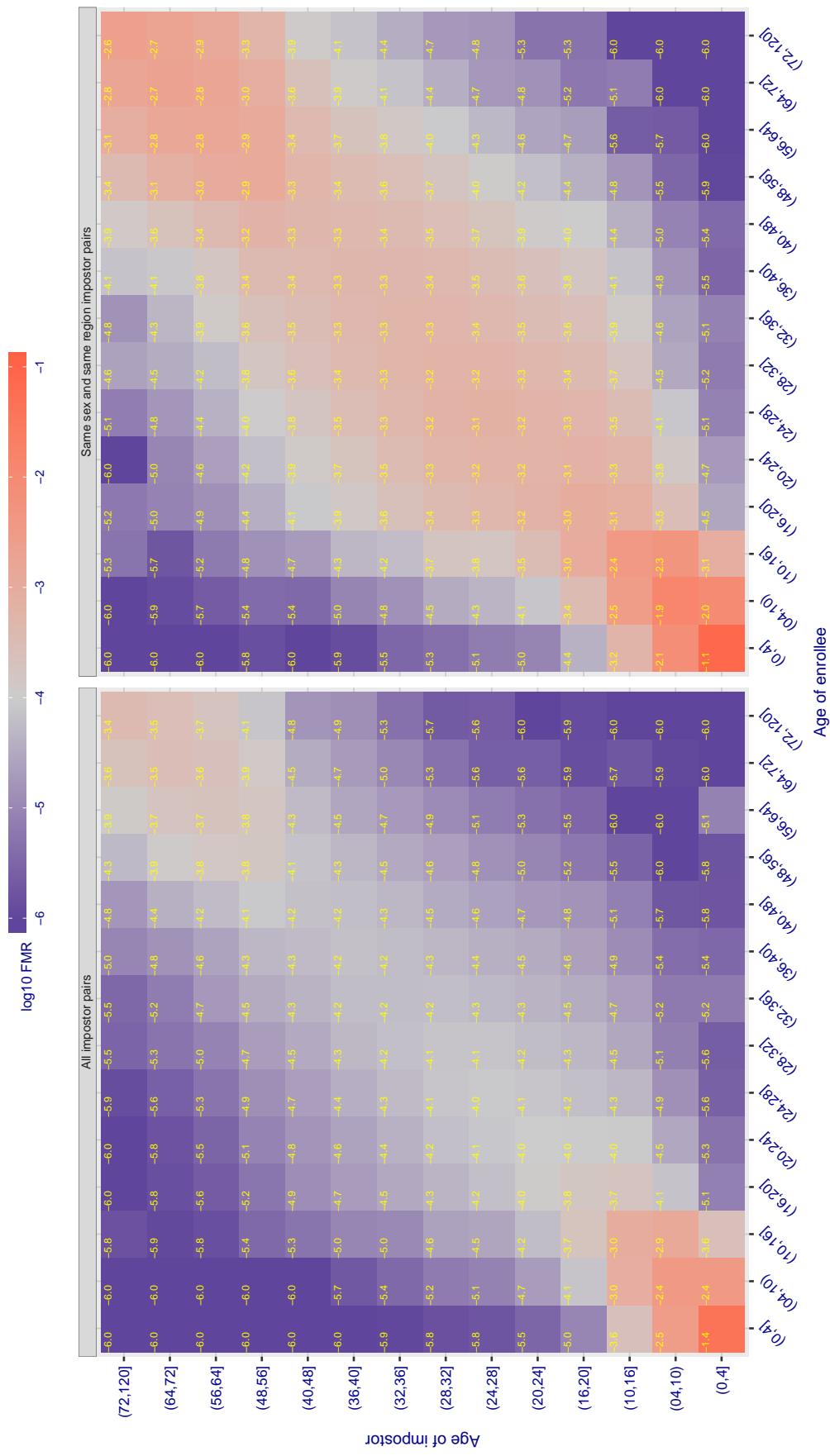
Cross age FMR at threshold T = 0.693 for algorithm **systems_001**, giving $\text{FMR}(\text{T}) = 0.0001$ globally.

Figure 497: For algorithm **systems-001** operating on visa images, the heatmap shows false match observed over impostor comparisons of faces from different individuals who have the given age pair. False matches are counted against a recognition threshold fixed globally to give $\text{FMR} = 0.0001$ over all on the order of 10^{10} impostor comparisons. The text in each box gives the same quantity as that coded by the color. Light colors present a security vulnerability to, for example, a passport gate.

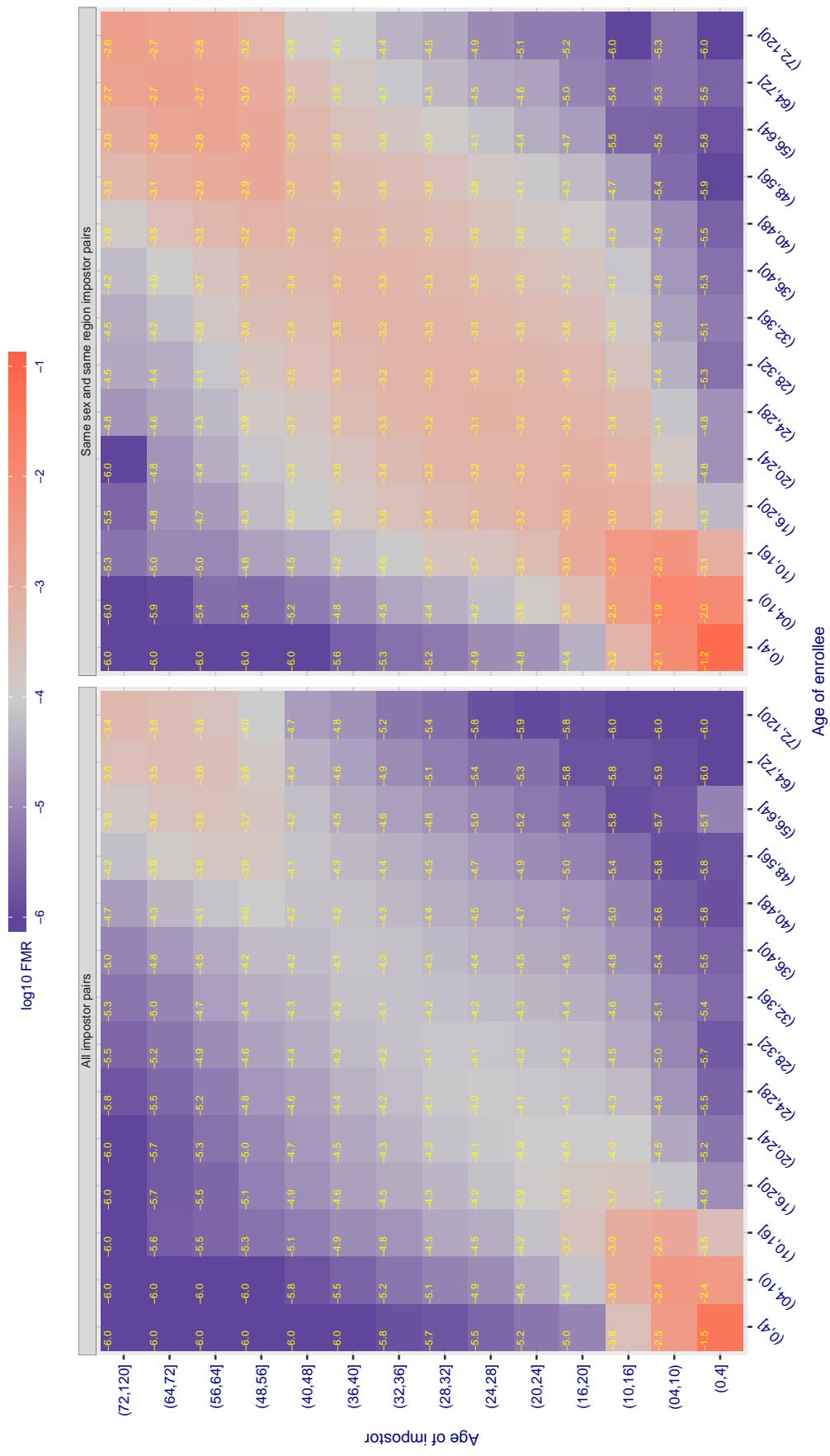
Cross age FMR at threshold T = 0.690 for algorithm **systems_002**, giving $\text{FMR}(\text{T}) = 0.0001$ globally.

Figure 498: For algorithm **systems-002** operating on visa images, the heatmap shows false match observed over impostor comparisons of faces from different individuals who have the given age pair. False matches are counted against a recognition threshold fixed globally to give $\text{FMR} = 0.0001$ over all on the order of 10^{10} impostor comparisons. The text in each box gives the same quantity as that coded by the color. Light colors present a security vulnerability to, for example, a passport gate.

Cross age FMR at threshold T = 49.879 for algorithm itmo_005, giving FMR(T) = 0.0001 globally.

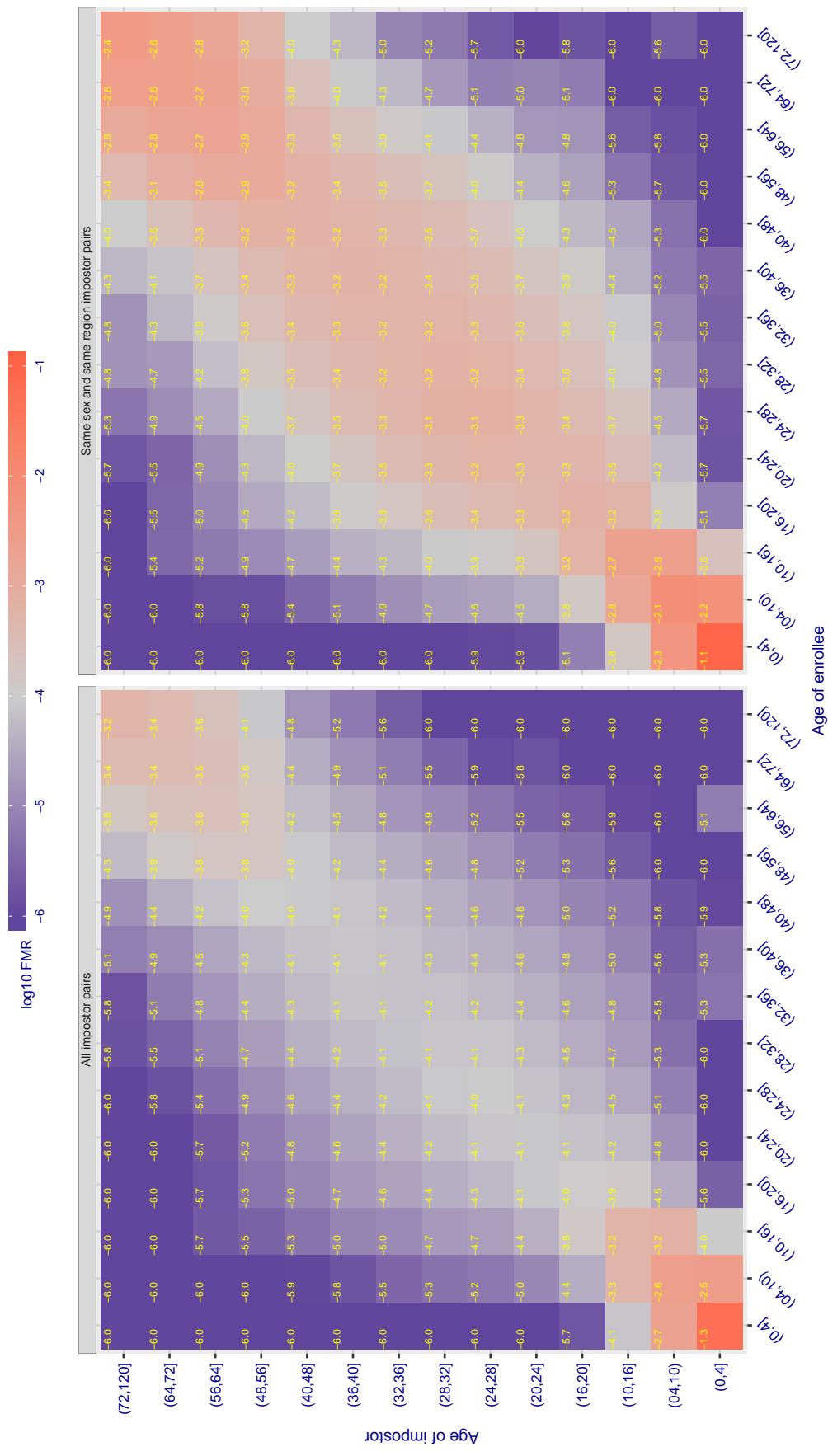


Figure 499: For algorithm itmo-005 operating on visa images, the heatmap shows false match observed over imposter comparisons of faces from different individuals who have the given age pair. False matches are counted against a recognition threshold fixed globally to give $FMR = 0.0001$ over all on the order of 10^{10} imposter comparisons. The text in each box gives the same quantity as that coded by the color. Light colors present a security vulnerability to, for example, a passport gate.

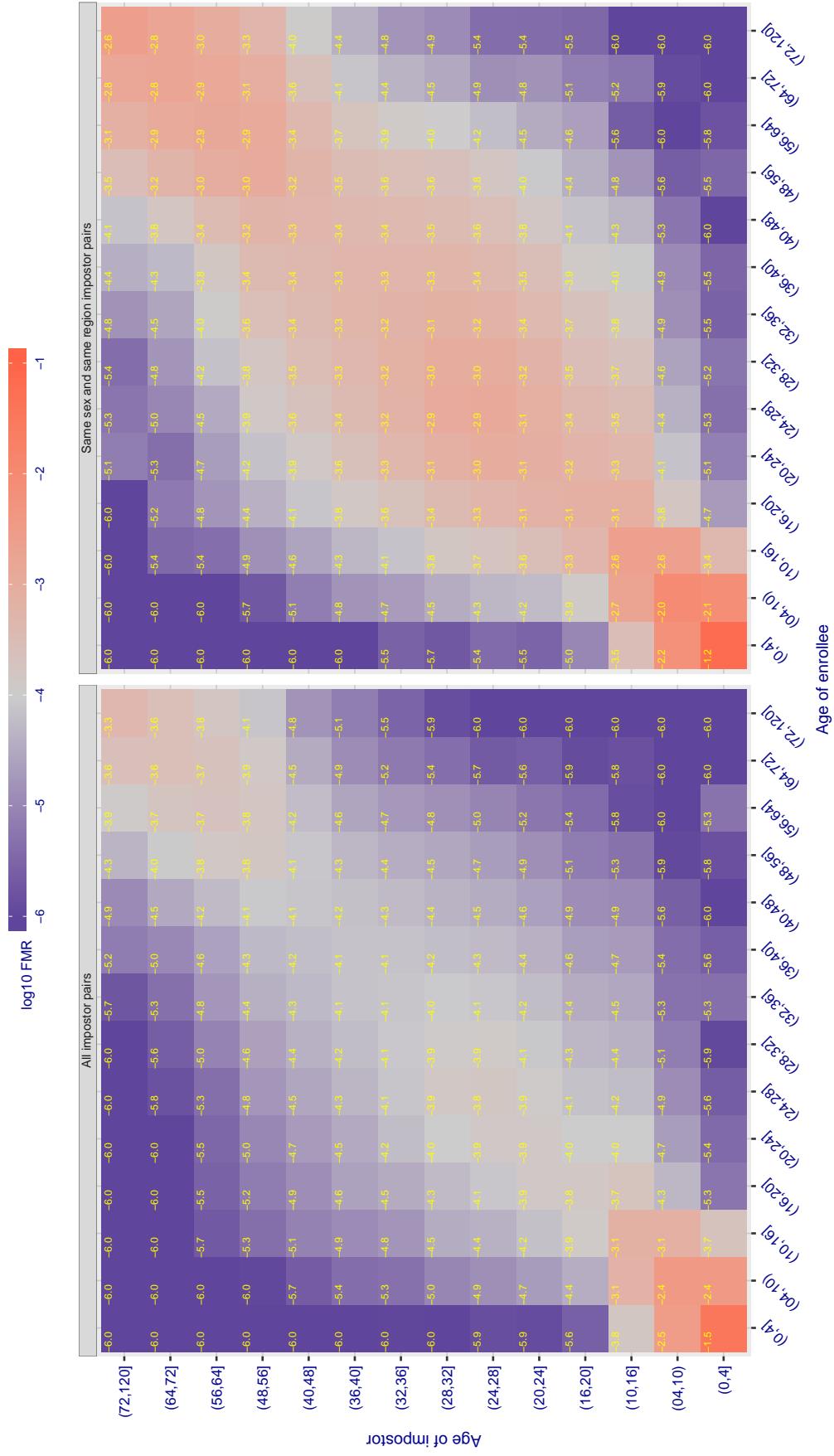
Cross age FMR at threshold T = 49.739 for algorithm itmo_006, giving $FMR(T) = 0.0001$ globally.

Figure 500: For algorithm itmo-006 operating on visa images, the heatmap shows false match observed over impostor comparisons of faces from different individuals who have the given age pair. False matches are counted against a recognition threshold fixed globally to give $FMR = 0.0001$ over all on the order of 10^{10} impostor comparisons. The text in each box gives the same quantity as that coded by the color. Light colors present a security vulnerability to, for example, a passport gate.

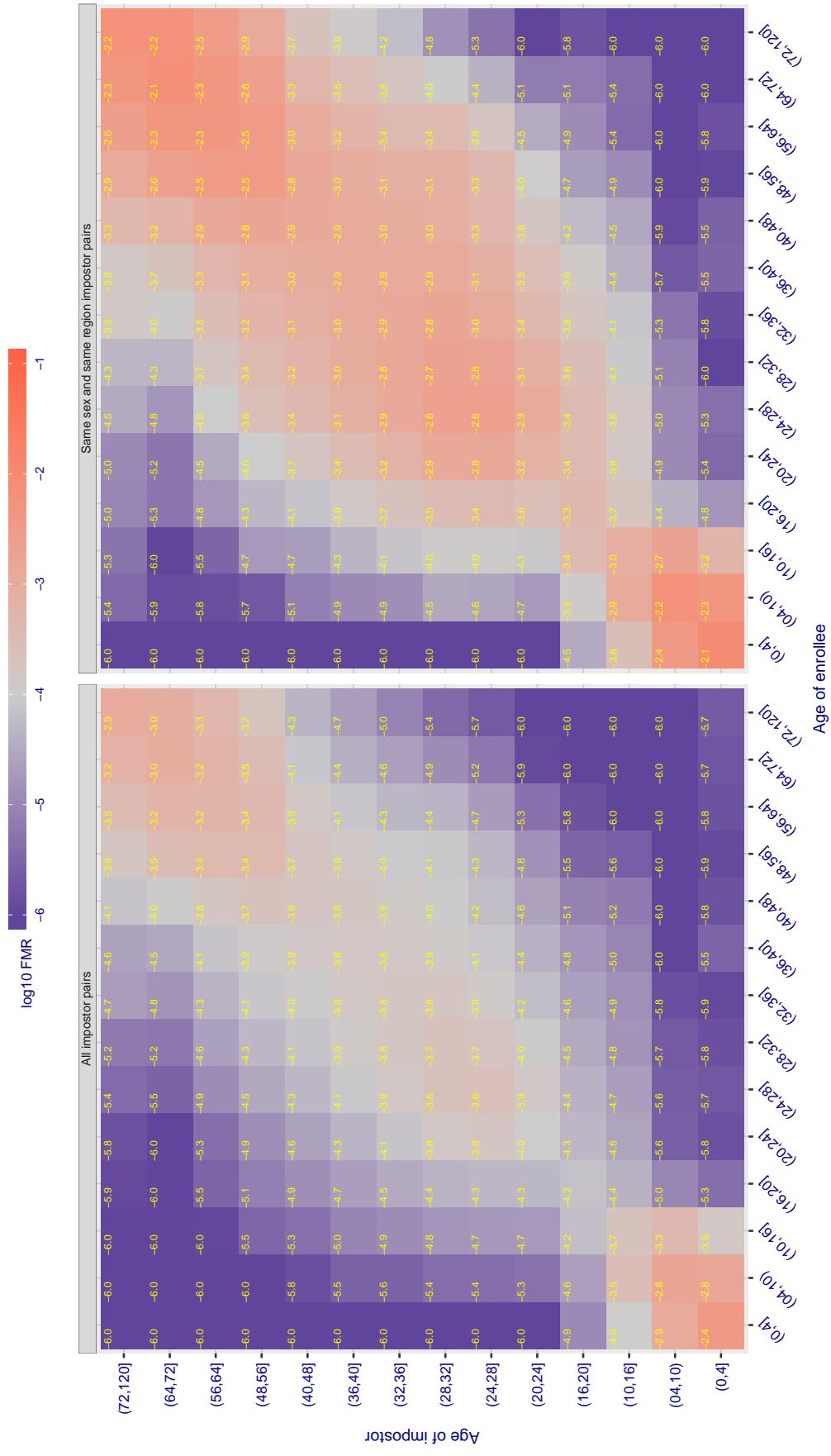
Cross age FMR at threshold T = 1.301 for algorithm kakao_001, giving $\text{FMR}(\text{T}) = 0.0001$ globally.

Figure 501: For algorithm kakao-001 operating on visa images, the heatmap shows false match observed over impostor comparisons of faces from different individuals who have the given age pair. False matches are counted against a recognition threshold fixed globally to give $\text{FMR} = 0.0001$ over all on the order of 10^{10} impostor comparisons. The text in each box gives the same quantity as that coded by the color. Light colors present a security vulnerability to, for example, a passport gate.

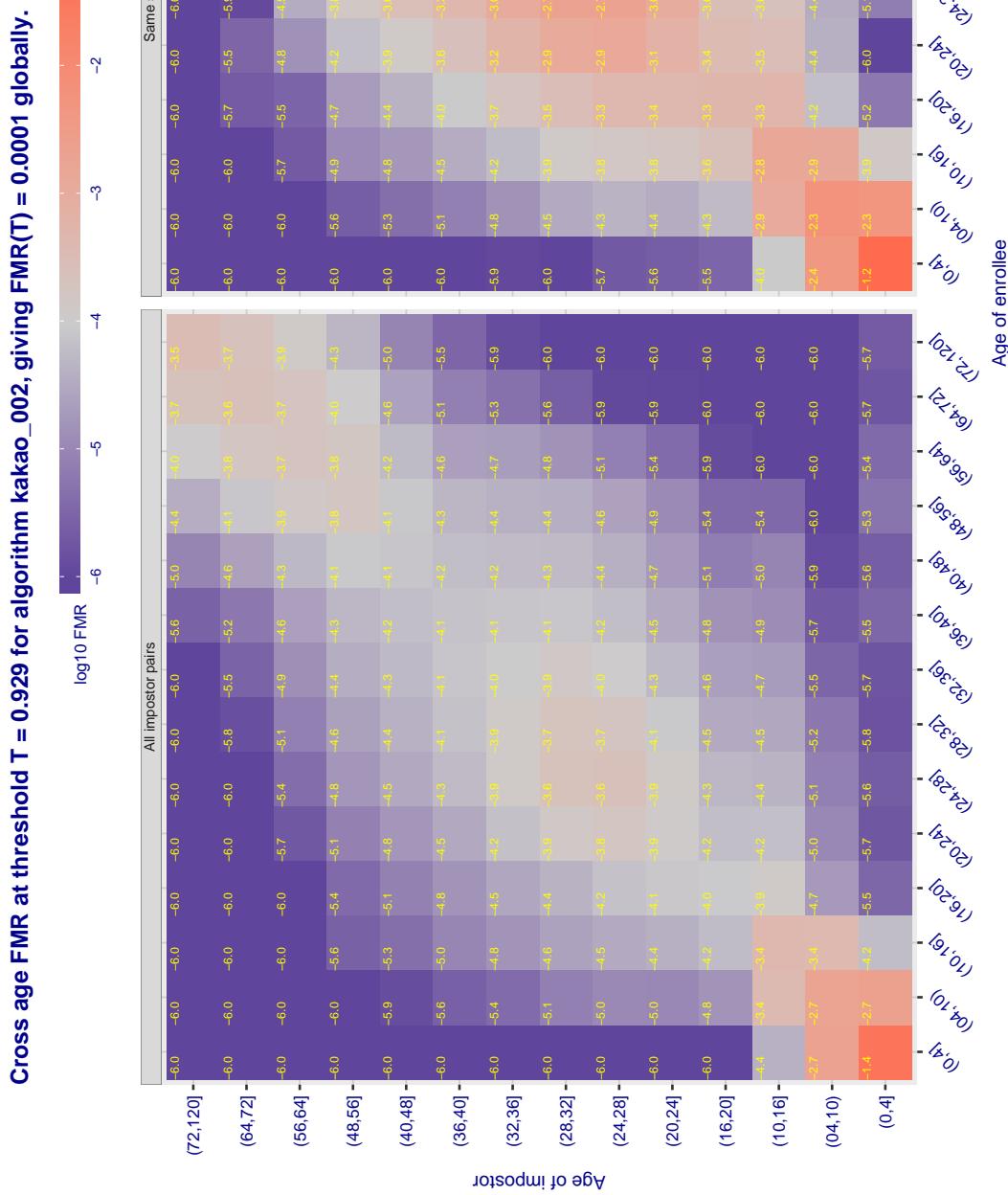


Figure 502: For algorithm kakao-002 operating on visa images, the heatmap shows false match observed over impostor comparisons of faces from different individuals who have the given age pair. False matches are counted against a recognition threshold fixed globally to give $FMR = 0.0001$ over all on the order of 10^{10} impostor comparisons. The text in each box gives the same quantity as that coded by the color. Light colors present a security vulnerability to, for example, a passport gate.

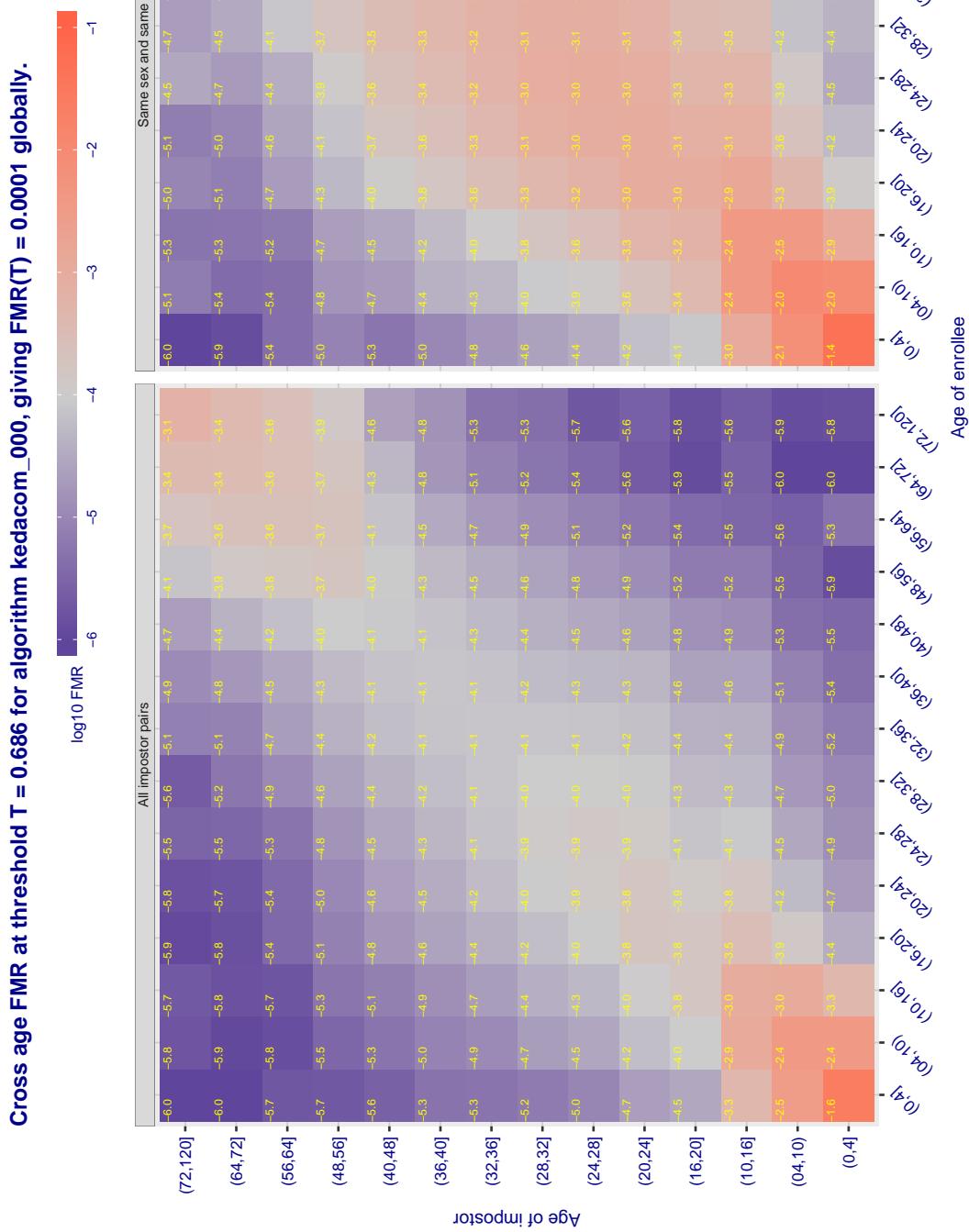


Figure 503: For algorithm kedacom-000 operating on visa images, the heatmap shows false match observed over impostor comparisons of faces from different individuals who have the given age pair. False matches are counted against a recognition threshold fixed globally to give $FMR = 0.0001$ over all on the order of 10^{10} impostor comparisons. The text in each box gives the same quantity as that coded by the color. Light colors present a security vulnerability to, for example, a passport gate.

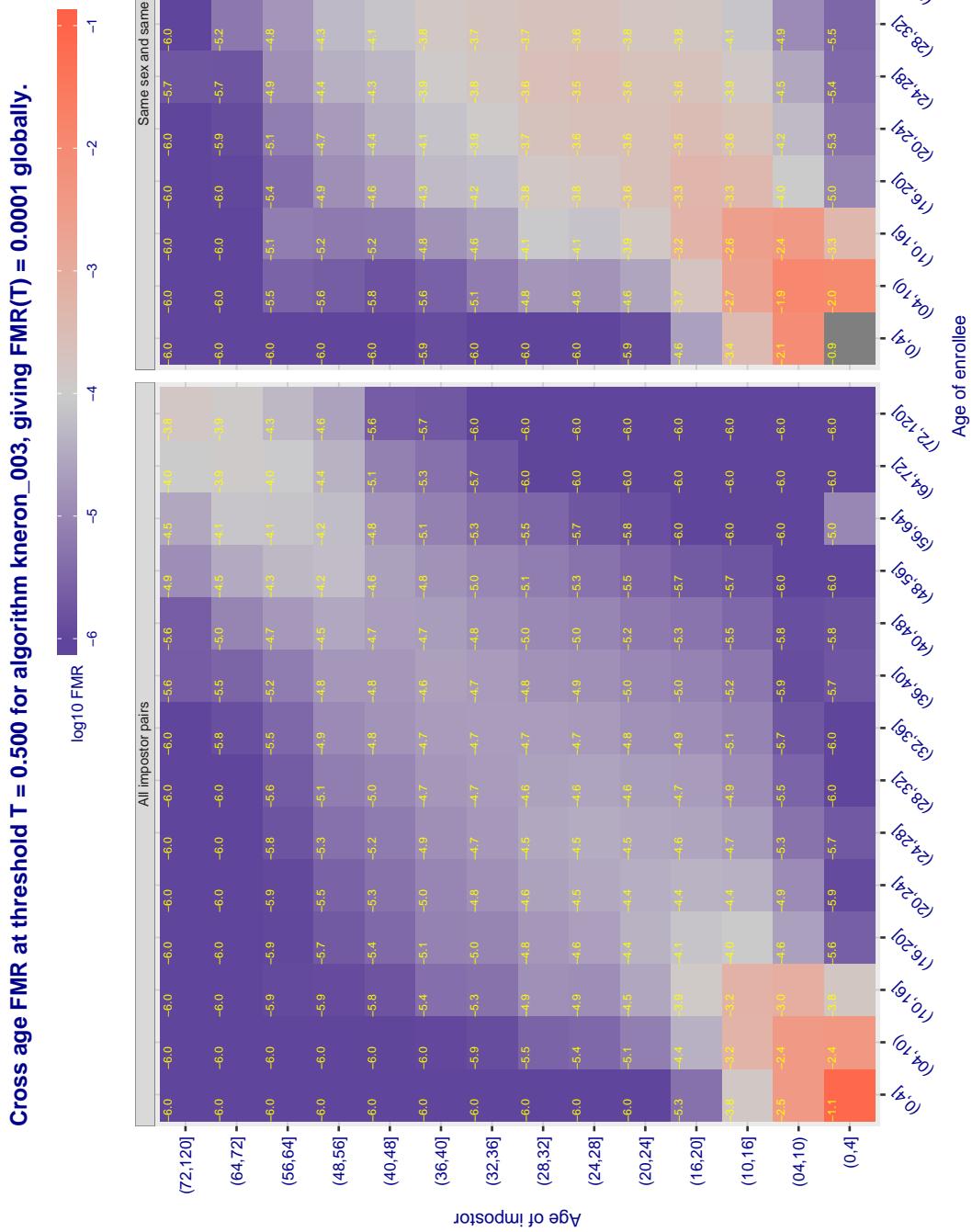


Figure 504: For algorithm kneron-003 operating on visa images, the heatmap shows false match observed over impostor comparisons of faces from different individuals who have the given age pair. False matches are counted against a recognition threshold fixed globally to give $FMR = 0.0001$ over all on the order of 10^{10} impostor comparisons. The text in each box gives the same quantity as that coded by the color. Light colors present a security vulnerability to, for example, a passport gate.

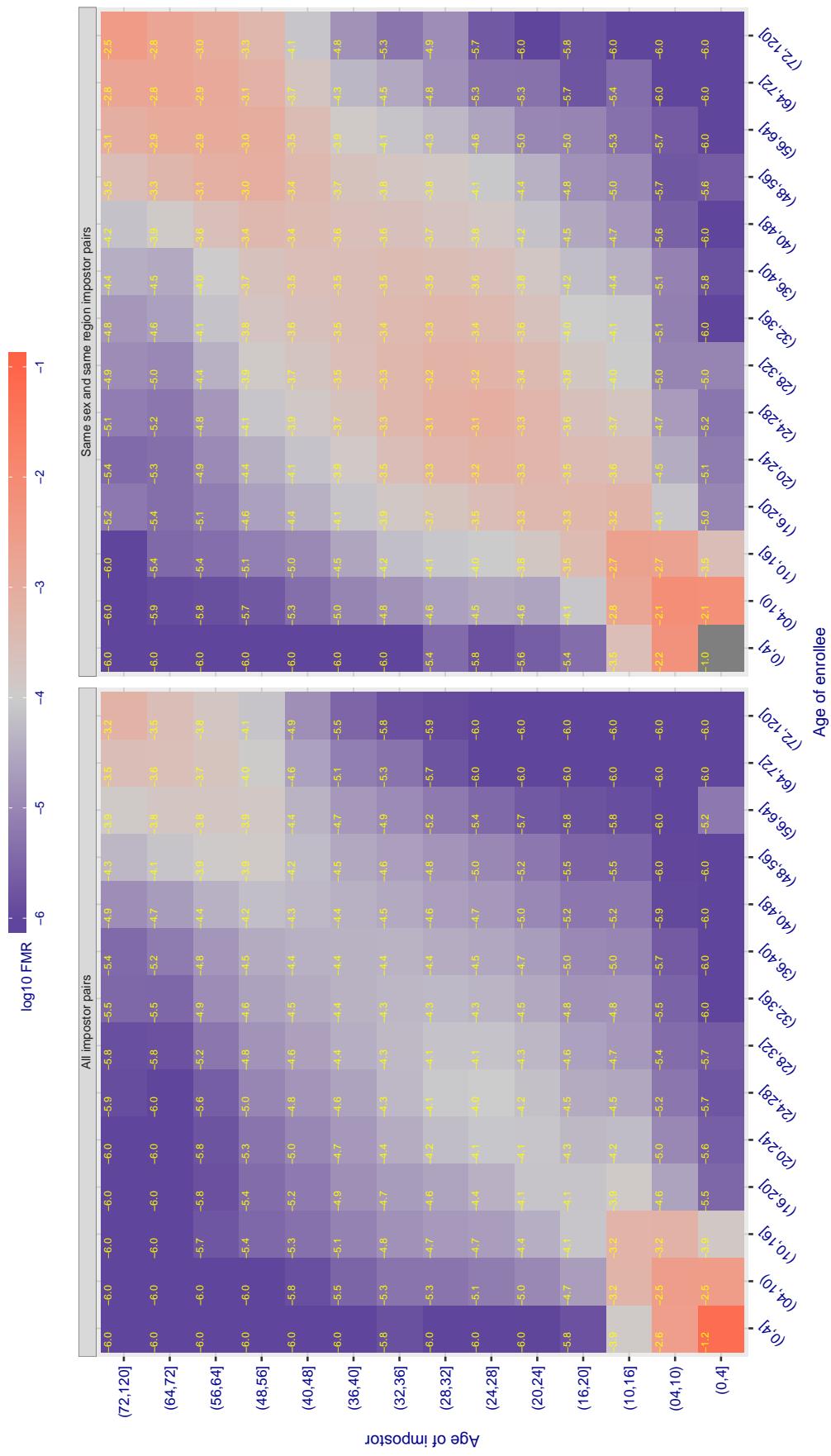
Cross age FMR at threshold T = 0.701 for algorithm lookman_002, giving $FMR(T) = 0.0001$ globally.

Figure 505: For algorithm lookman-002 operating on visa images, the heatmap shows false match observed over impostor comparisons of faces from different individuals who have the given age pair. False matches are counted against a recognition threshold fixed globally to give $FMR = 0.0001$ over all on the order of 10^{10} impostor comparisons. The text in each box gives the same quantity as that coded by the color. Light colors present a security vulnerability to, for example, a passport gate.

Cross age FMR at threshold T = 0.733 for algorithm lookman_004, giving FMR(T) = 0.0001 globally.

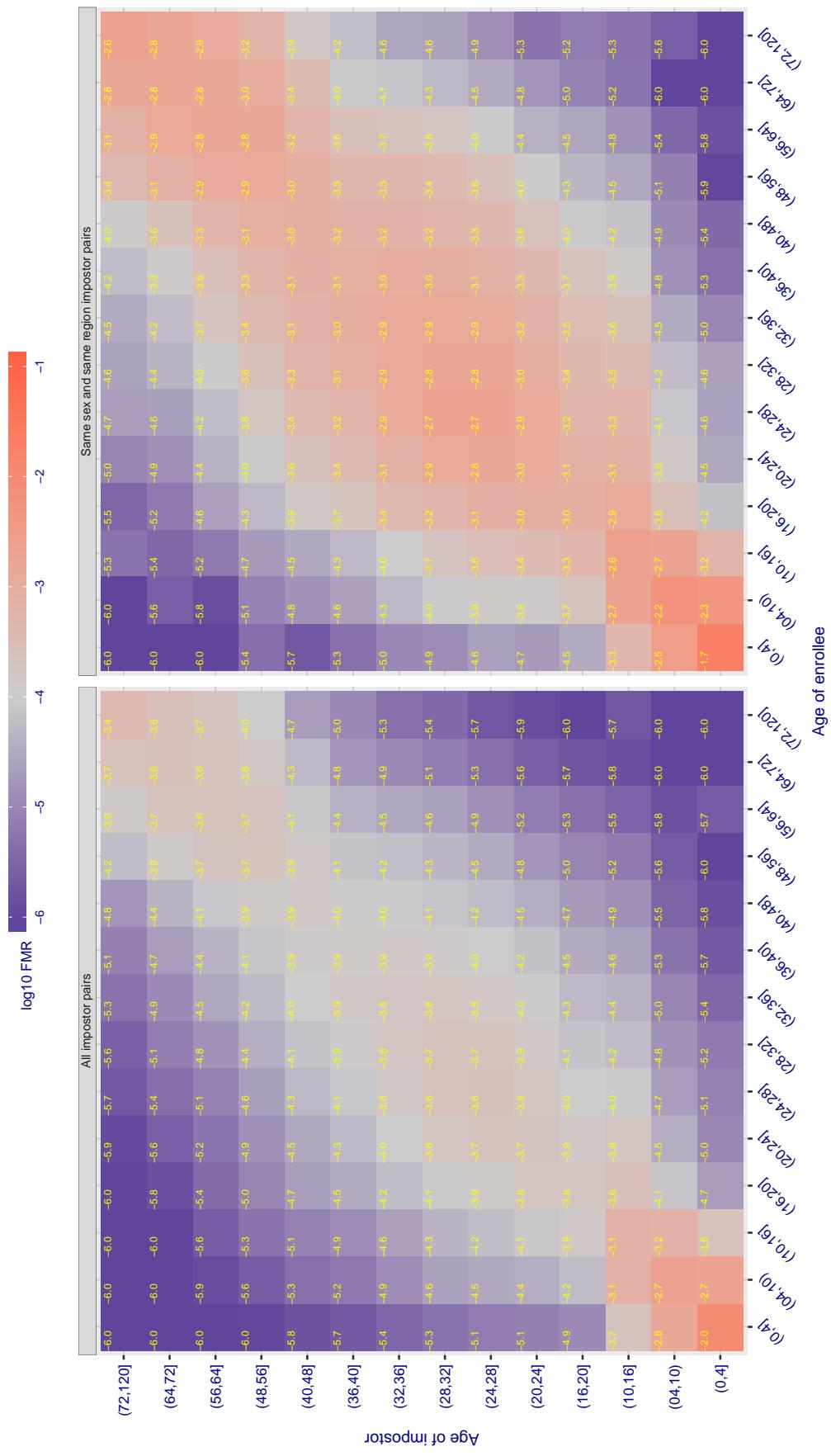


Figure 506: For algorithm lookman-004 operating on visa images, the heatmap shows false match observed over impostor comparisons of faces from different individuals who have the given age pair. False matches are counted against a recognition threshold fixed globally to give $FMR = 0.0001$ over all on the order of 10^{10} impostor comparisons. The text in each box gives the same quantity as that coded by the color. Light colors present a security vulnerability to, for example, a passport gate.

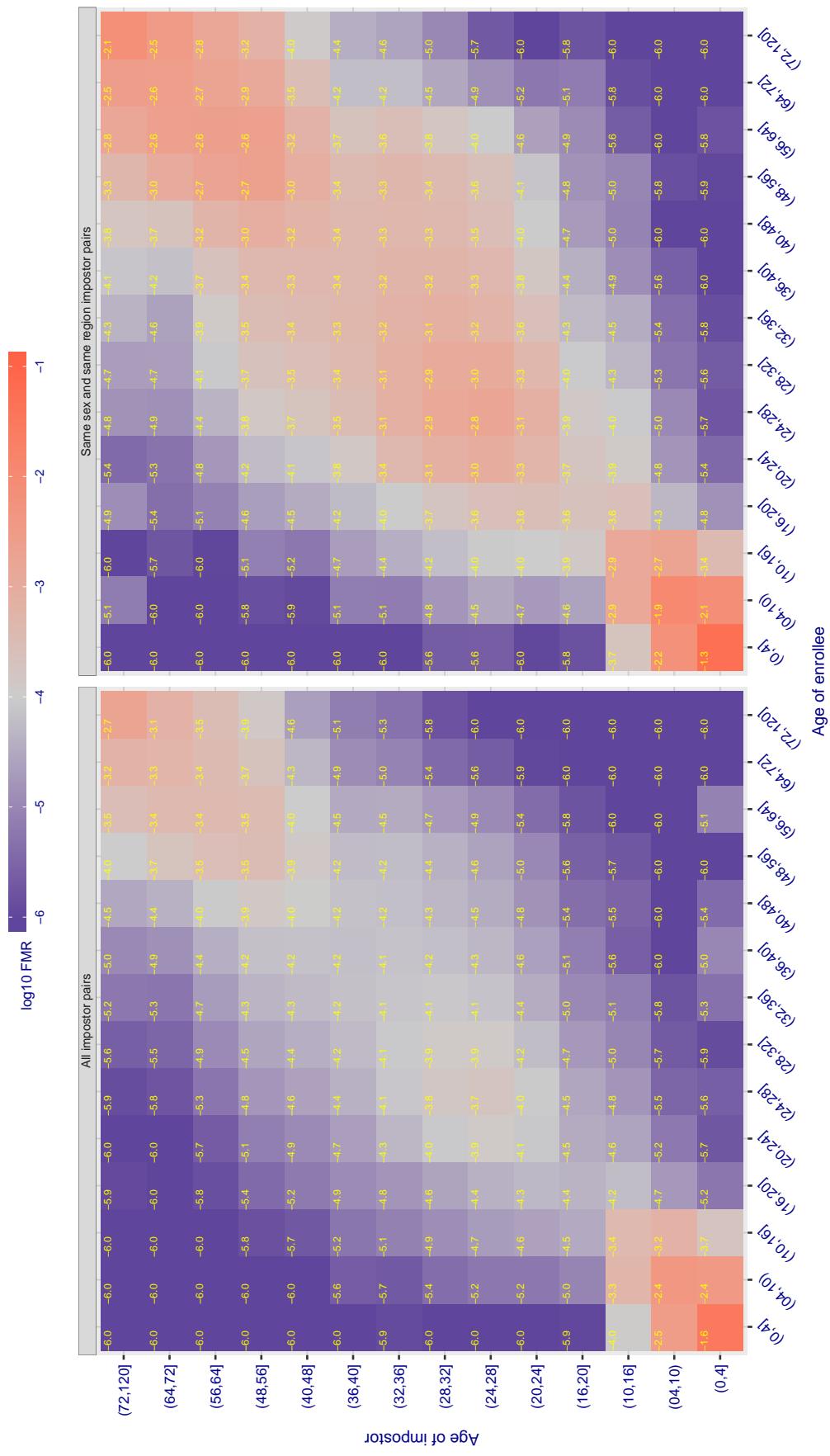
Cross age FMR at threshold T = 74.511 for algorithm megvii_001, giving $FMR(T) = 0.0001$ globally.

Figure 507: For algorithm megvii-001 operating on visa images, the heatmap shows false match observed over impostor comparisons of faces from different individuals who have the given age pair. False matches are counted against a recognition threshold fixed globally to give $FMR = 0.0001$ over all on the order of 10^{10} impostor comparisons. The text in each box gives the same quantity as that coded by the color. Light colors present a security vulnerability to, for example, a passport gate.

Cross age FMR at threshold T = 66.384 for algorithm megvii_002, giving FMR(T) = 0.0001 globally.

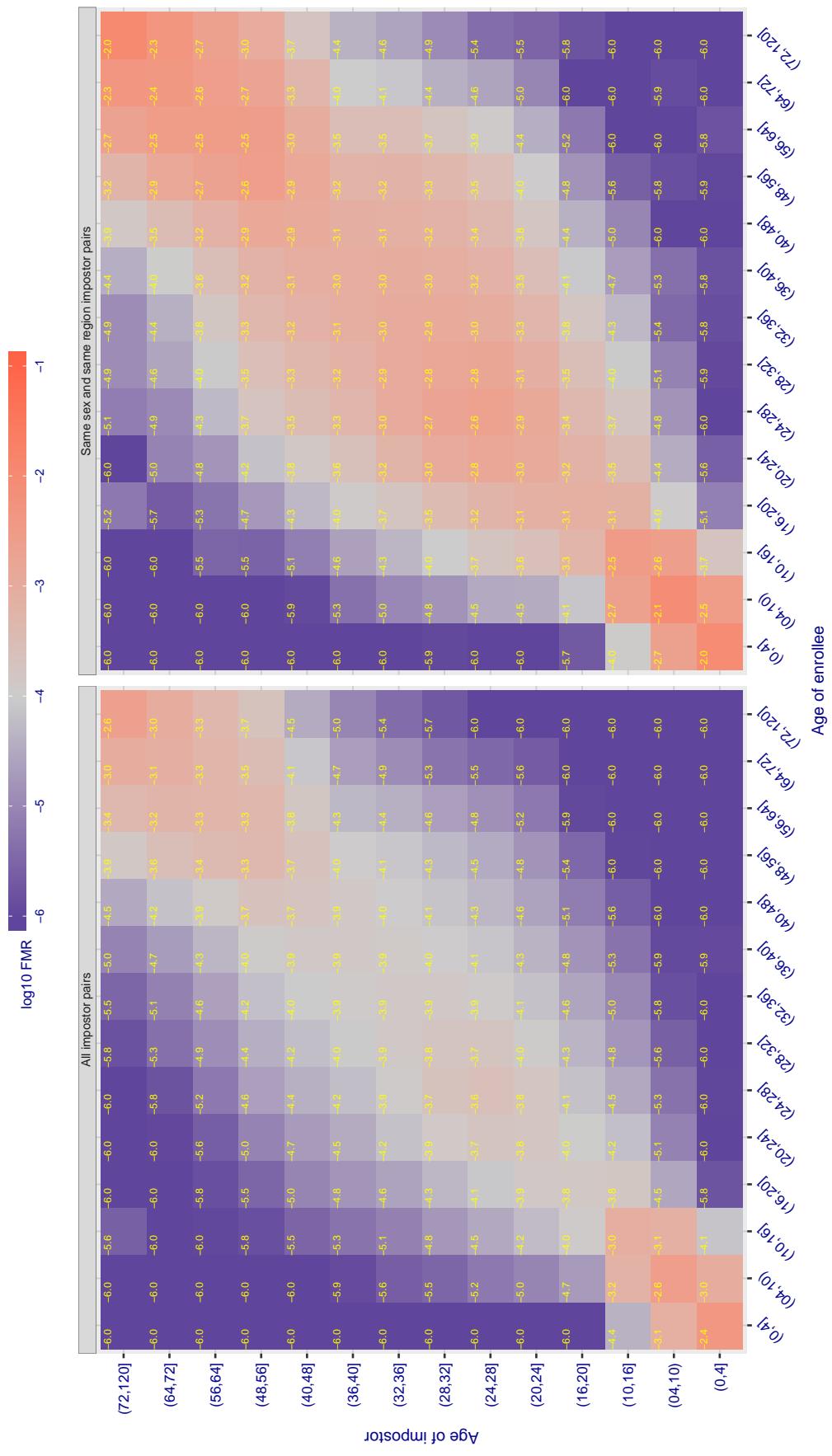


Figure 508: For algorithm megvii-002 operating on visa images, the heatmap shows false match observed over impostor comparisons of faces from different individuals who have the given age pair. False matches are counted against a recognition threshold fixed globally to give $FMR = 0.0001$ over all on the order of 10^{10} impostor comparisons. The text in each box gives the same quantity as that coded by the color. Light colors present a security vulnerability to, for example, a passport gate.

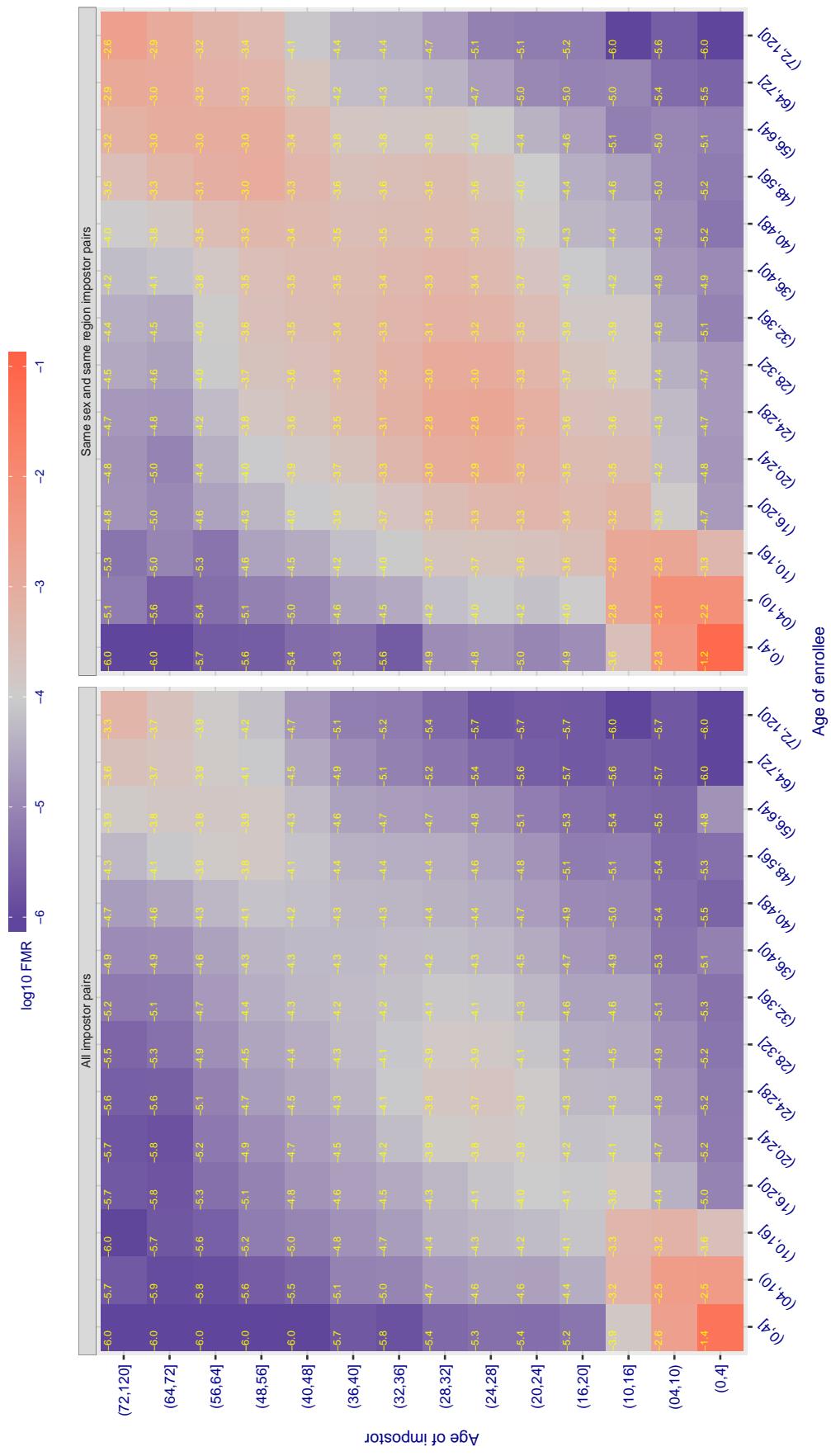
Cross age FMR at threshold T = 0.425 for algorithm meiya_001, giving $FMR(T) = 0.0001$ globally.

Figure 509: For algorithm meiya-001 operating on visa images, the heatmap shows false match observed over impostor comparisons of faces from different individuals who have the given age pair. False matches are counted against a recognition threshold fixed globally to give $FMR = 0.0001$ over all on the order of 10^{10} impostor comparisons. The text in each box gives the same quantity as that coded by the color. Light colors present a security vulnerability to, for example, a passport gate.

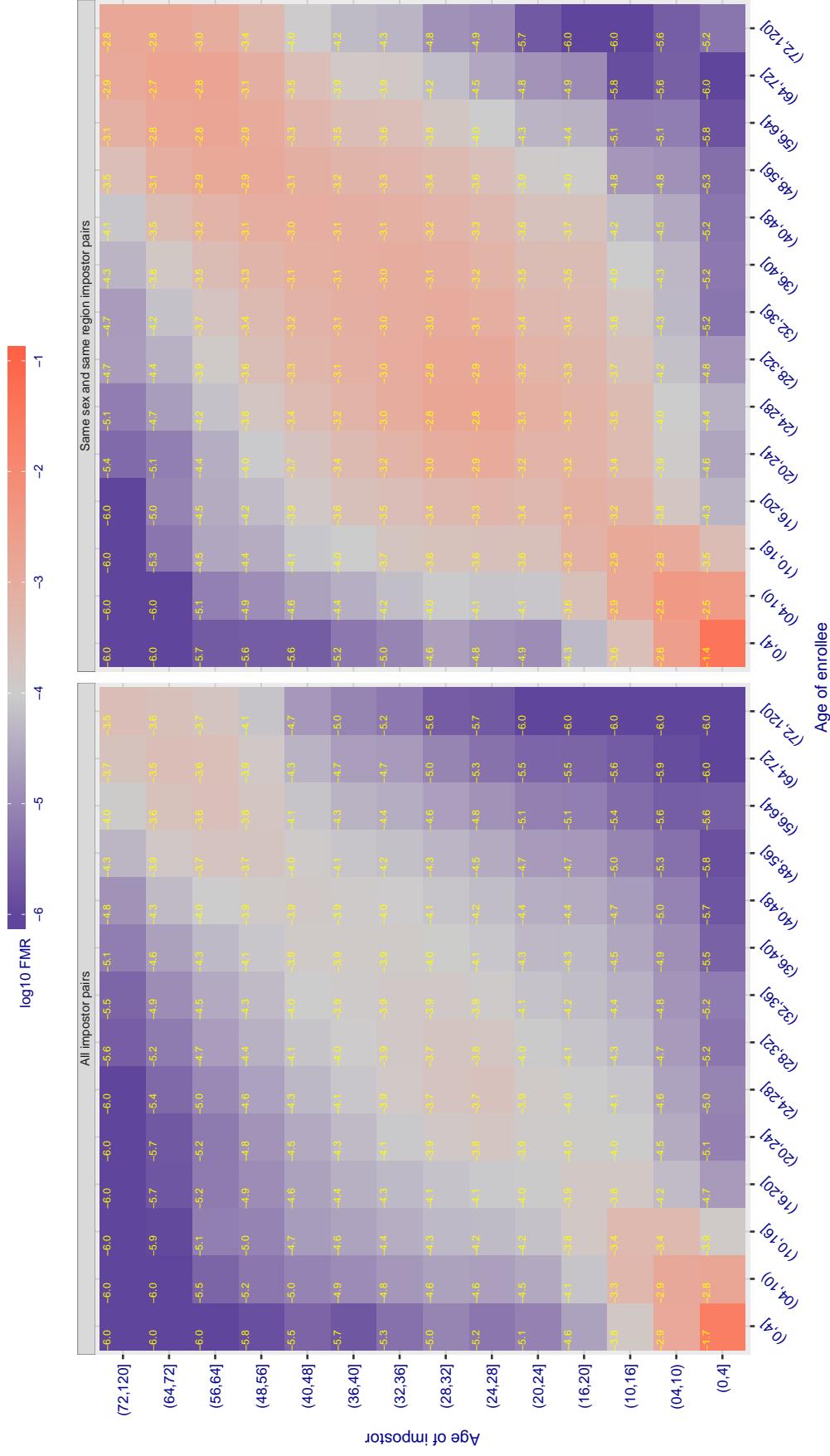
Cross age FMR at threshold T = 0.668 for algorithm microfocus_001, giving $FMR(T) = 0.0001$ globally.

Figure 510: For algorithm microfocus-001 operating on visa images, the heatmap shows false match observed over impostor comparisons of faces from different individuals who have the given age pair. False matches are counted against a recognition threshold fixed globally to give $FMR = 0.0001$ over all on the order of 10^{10} impostor comparisons. The text in each box gives the same quantity as that coded by the color. Light colors present a security vulnerability to, for example, a passport gate.

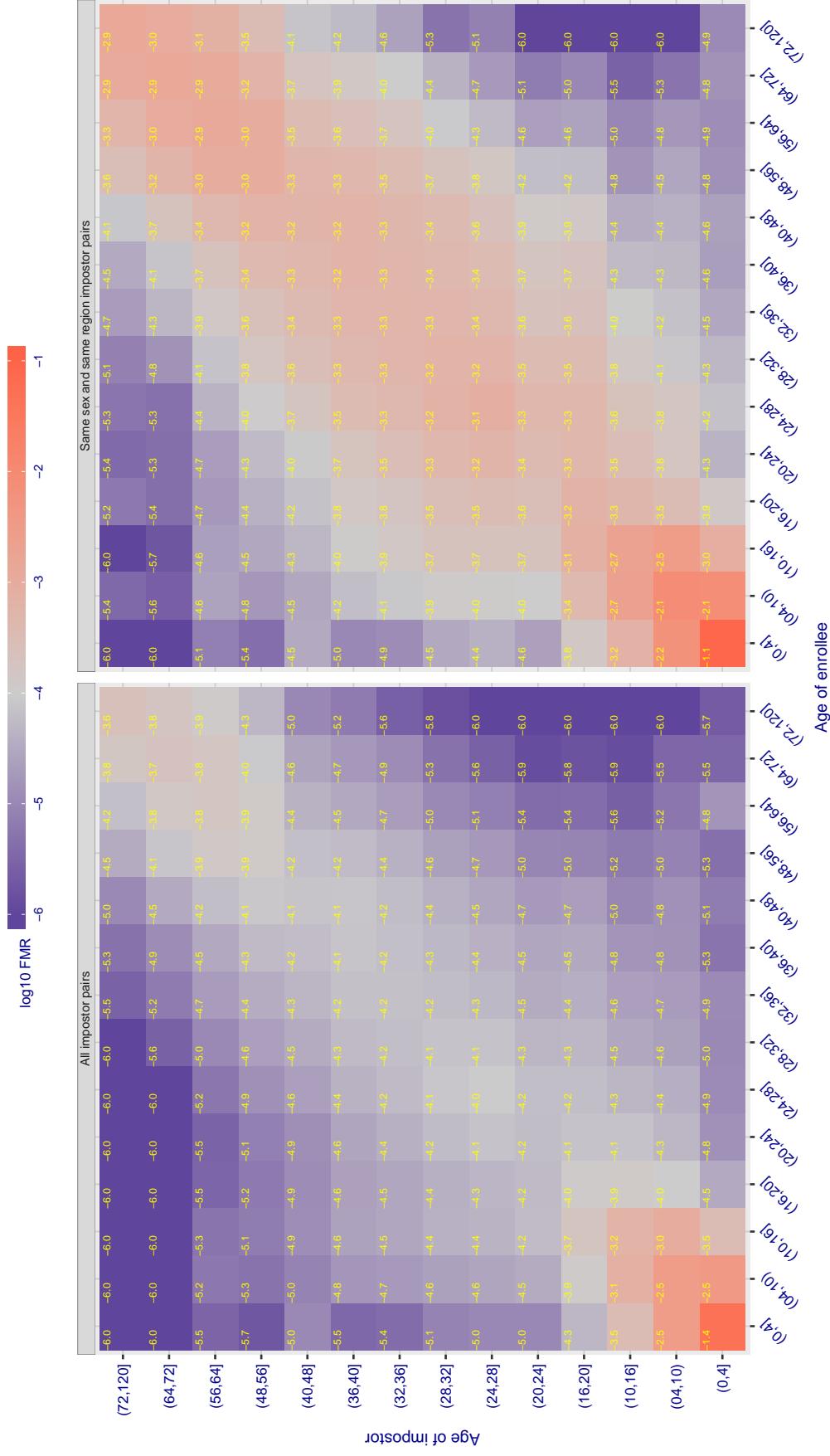
Cross age FMR at threshold T = 0.602 for algorithm microfocus_002, giving $FMR(T) = 0.0001$ globally.

Figure 511: For algorithm microfocus-002 operating on visa images, the heatmap shows false match observed over impostor comparisons of faces from different individuals who have the given age pair. False matches are counted against a recognition threshold fixed globally to give $FMR = 0.0001$ over all on the order of 10^{10} impostor comparisons. The text in each box gives the same quantity as that coded by the color. Light colors present a security vulnerability to, for example, a passport gate.

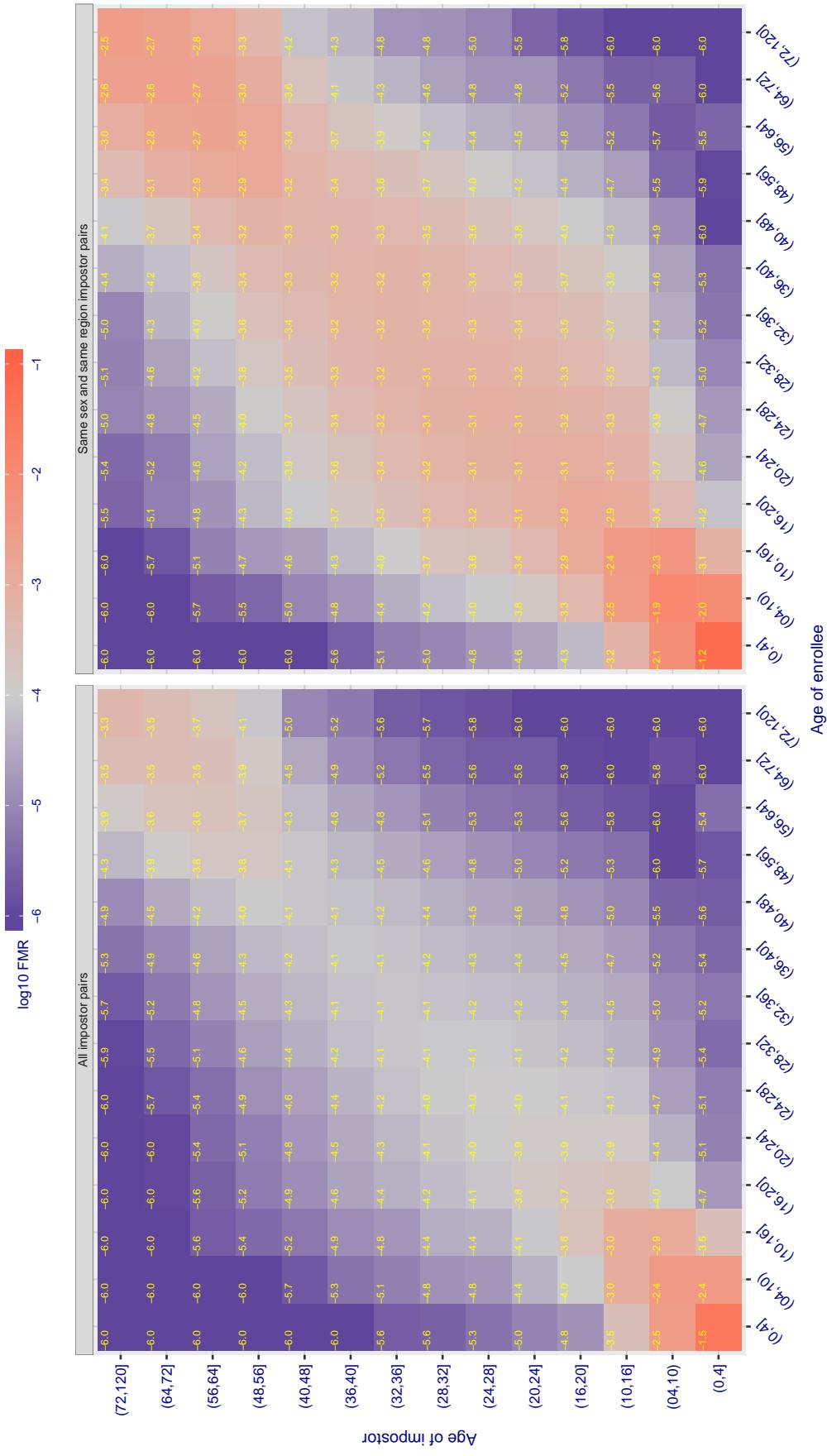
Cross age FMR at threshold T = 1.394 for algorithm mt_000, giving $FMR(T) = 0.0001$ globally.

Figure 512: For algorithm mt-000 operating on visa images, the heatmap shows false match observed over impostor comparisons of faces from different individuals who have the given age pair. False matches are counted against a recognition threshold fixed globally to give $FMR = 0.0001$ over all on the order of 10^{10} impostor comparisons. The text in each box gives the same quantity as that coded by the color. Light colors present a security vulnerability to, for example, a passport gate.

Cross age FMR at threshold T = 46.101 for algorithm neurotechnology_005, giving $FMR(T) = 0.0001$ globally.

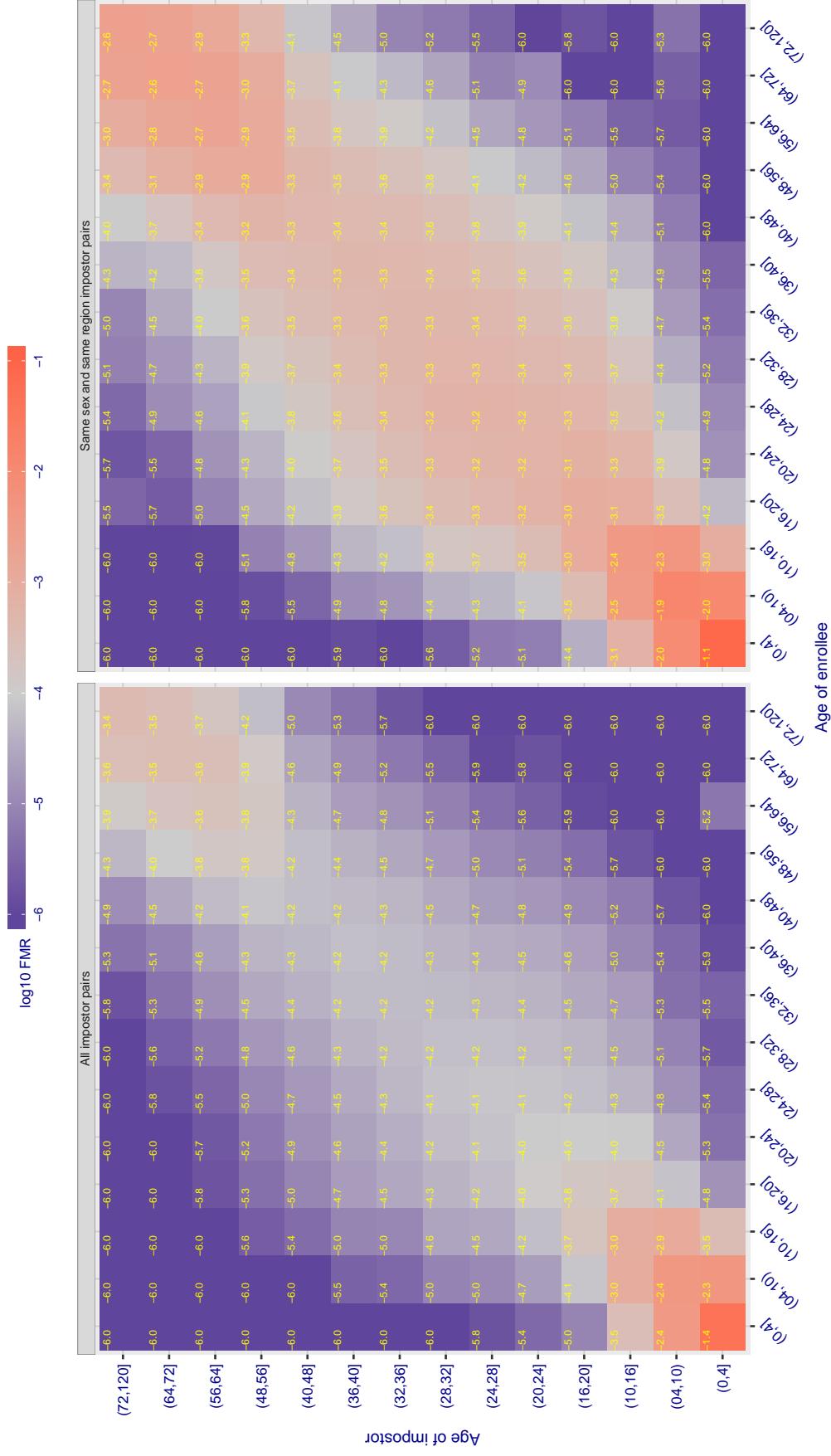


Figure 513: For algorithm neurotechnology_005 operating on visa images, the heatmap shows false match observed over impostor comparisons of faces from different individuals who have the given age pair. False matches are counted against a recognition threshold fixed globally to give $FMR = 0.0001$ over all on the order of 10^{10} impostor comparisons. The text in each box gives the same quantity as that coded by the color. Light colors present a security vulnerability to, for example, a passport gate.

Cross age FMR at threshold T = 2044.000 for algorithm neurotechnology_006, giving FMR(T) = 0.0001 globally.

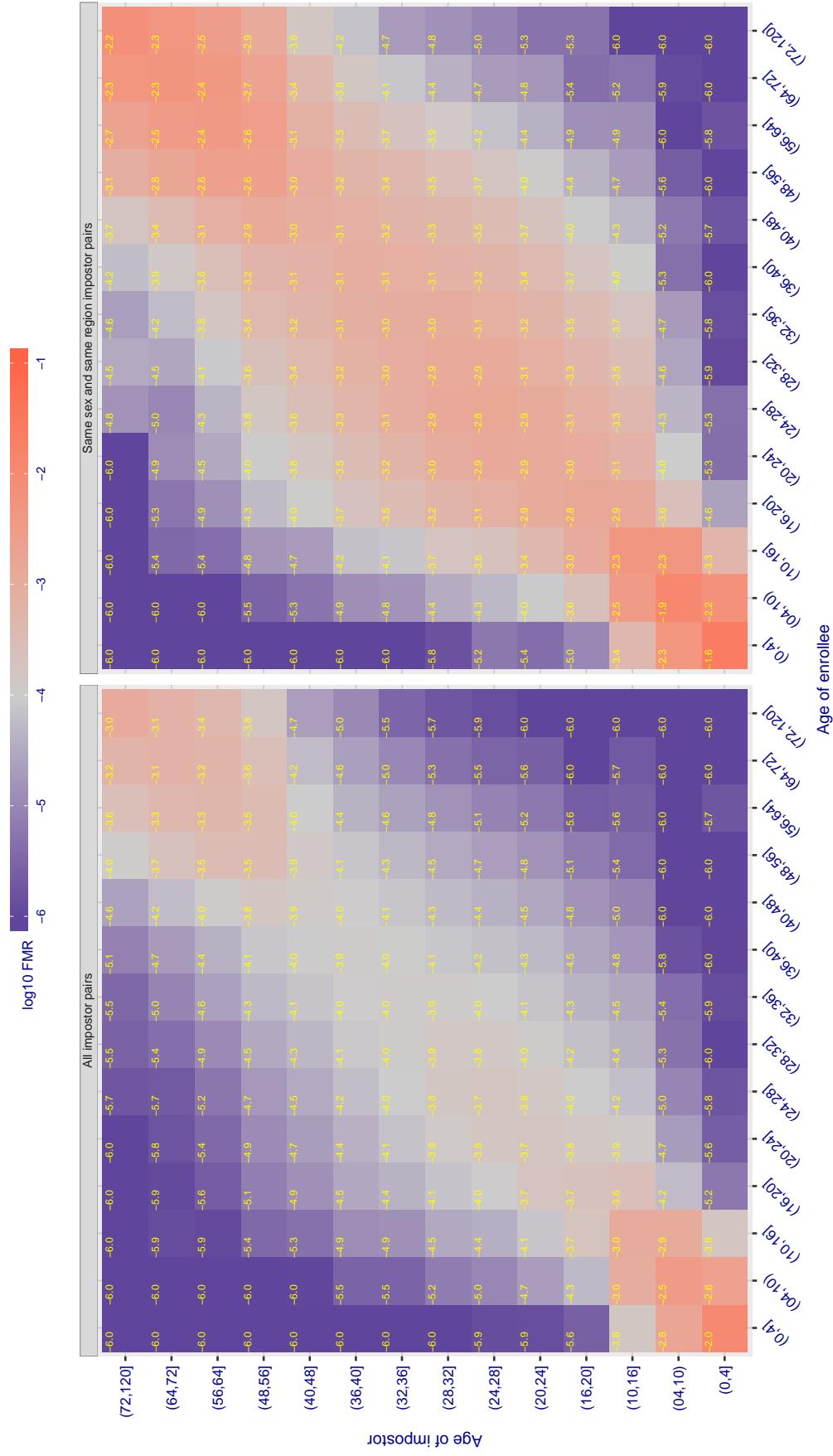
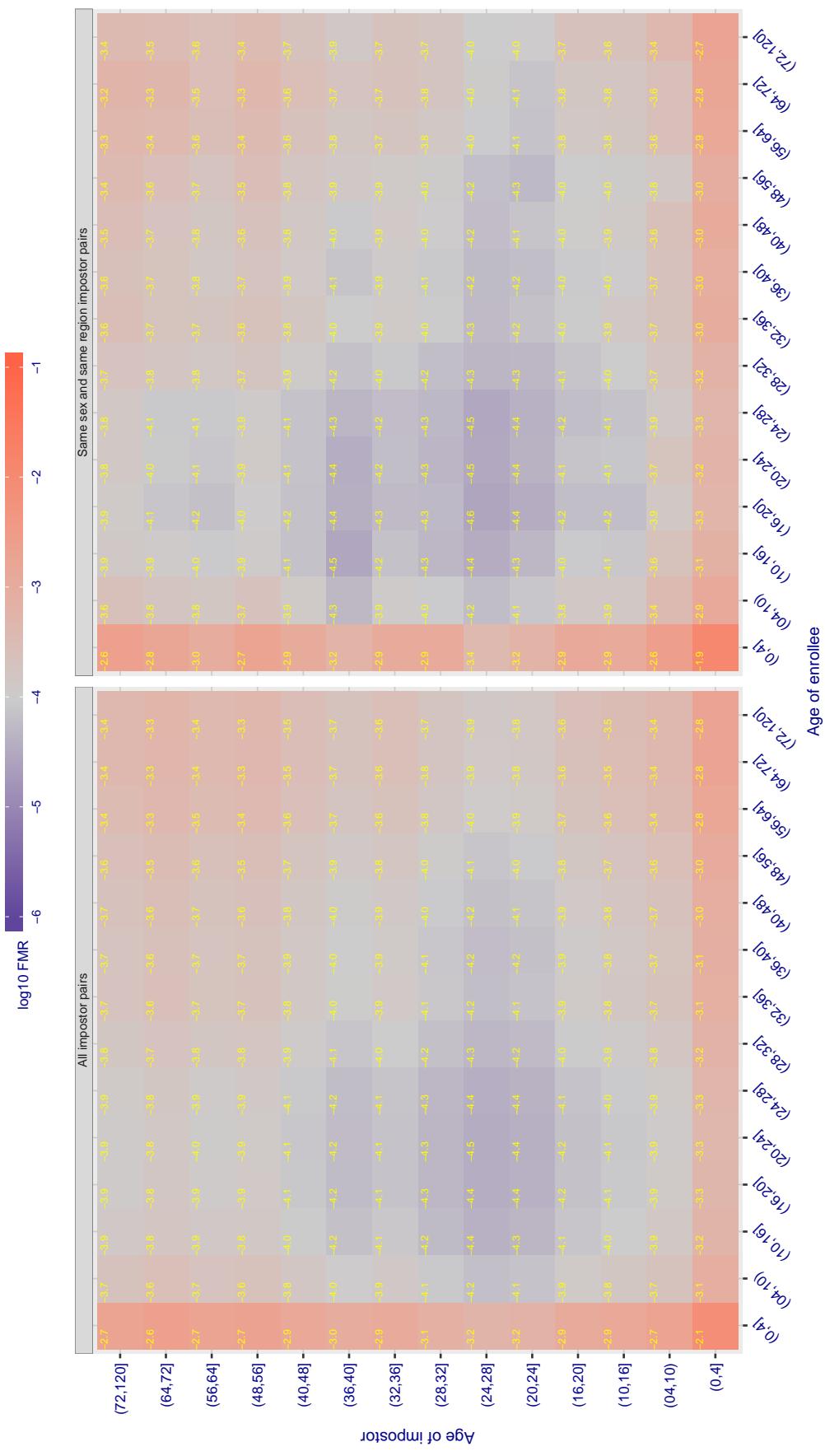


Figure 514: For algorithm neurotechnology-006 operating on visa images, the heatmap shows false match observed over impostor comparisons of faces from different individuals who have the given age pair. False matches are counted against a recognition threshold fixed globally to give $FMR = 0.0001$ over all on the order of 10^{10} impostor comparisons. The text in each box gives the same quantity as that coded by the color. Light colors present a security vulnerability to, for example, a passport gate.

Cross age FMR at threshold T = 1.000 for algorithm nodeflux_001, giving FMR(T) = 0.0001 globally.



FNMR(T)
F

Cross age FMR at threshold T = 0.455 for algorithm nodeflux_002, giving FMR(T) = 0.0001 globally.

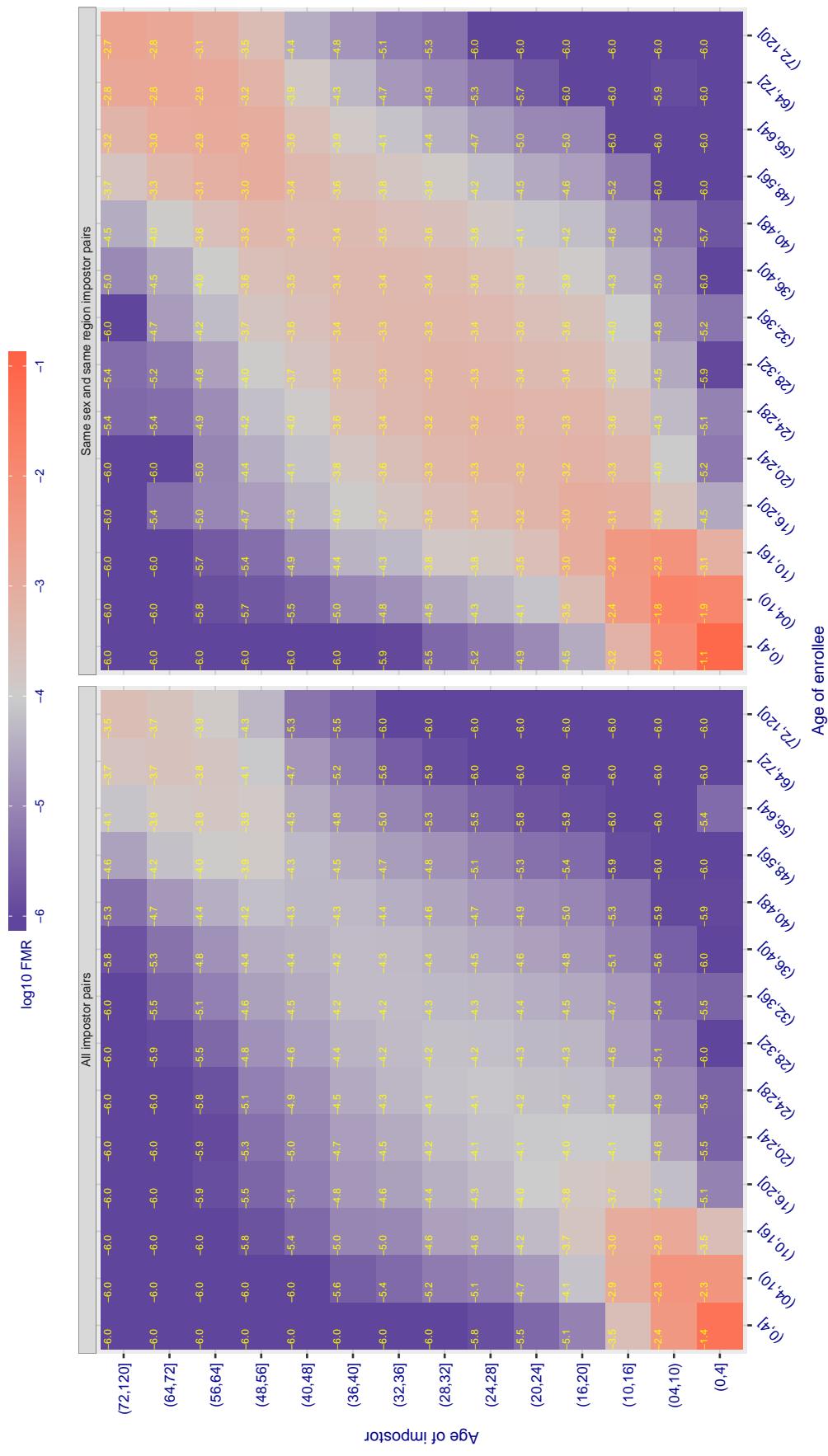


Figure 516: For algorithm nodeflux-002 operating on visa images, the heatmap shows false match observed over impostor comparisons of faces from different individuals who have the given age pair. False matches are counted against a recognition threshold fixed globally to give $FMR = 0.0001$ over all on the order of 10^{10} impostor comparisons. The text in each box gives the same quantity as that coded by the color. Light colors present a security vulnerability to, for example, a passport gate.

Cross age FMR at threshold T = 1684638382164870077977436979131033446238075281200095429962596511771151810506086548313212266745

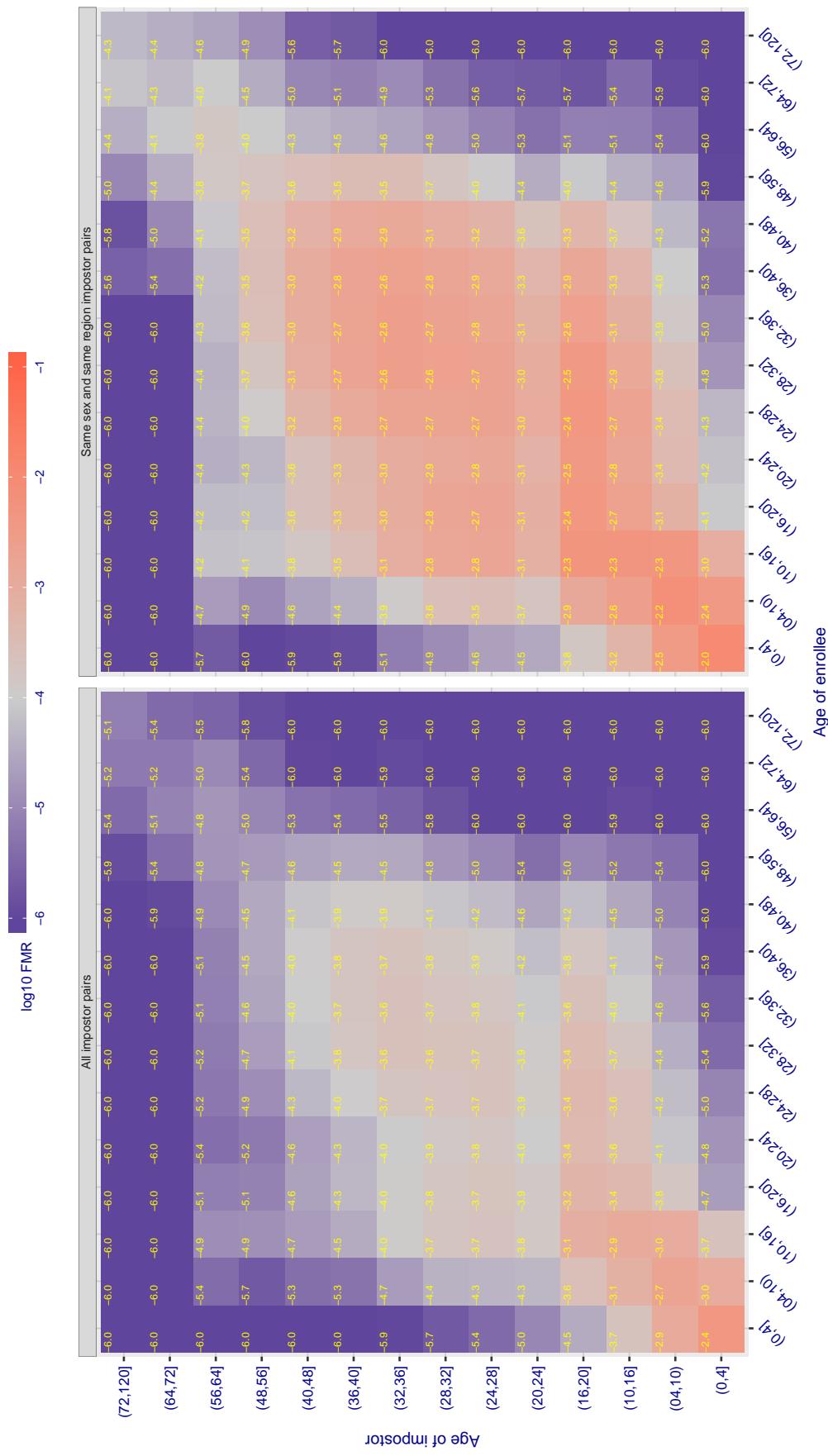


Figure 517: For algorithm notiontag-000 operating on visa images, the heatmap shows false match observed over impostor comparisons of faces from different individuals who have the given age pair. False matches are counted against a recognition threshold fixed globally to give FMR = 0.001 over all on the order of 10^{10} impostor comparisons. The text in each box gives the same quantity as that coded by the color. Light colors present a security vulnerability to, for example, a passport gate.

Cross age FMR at threshold T = 1.997 for algorithm ntechlab_006, giving FMR(T) = 0.0001 globally.

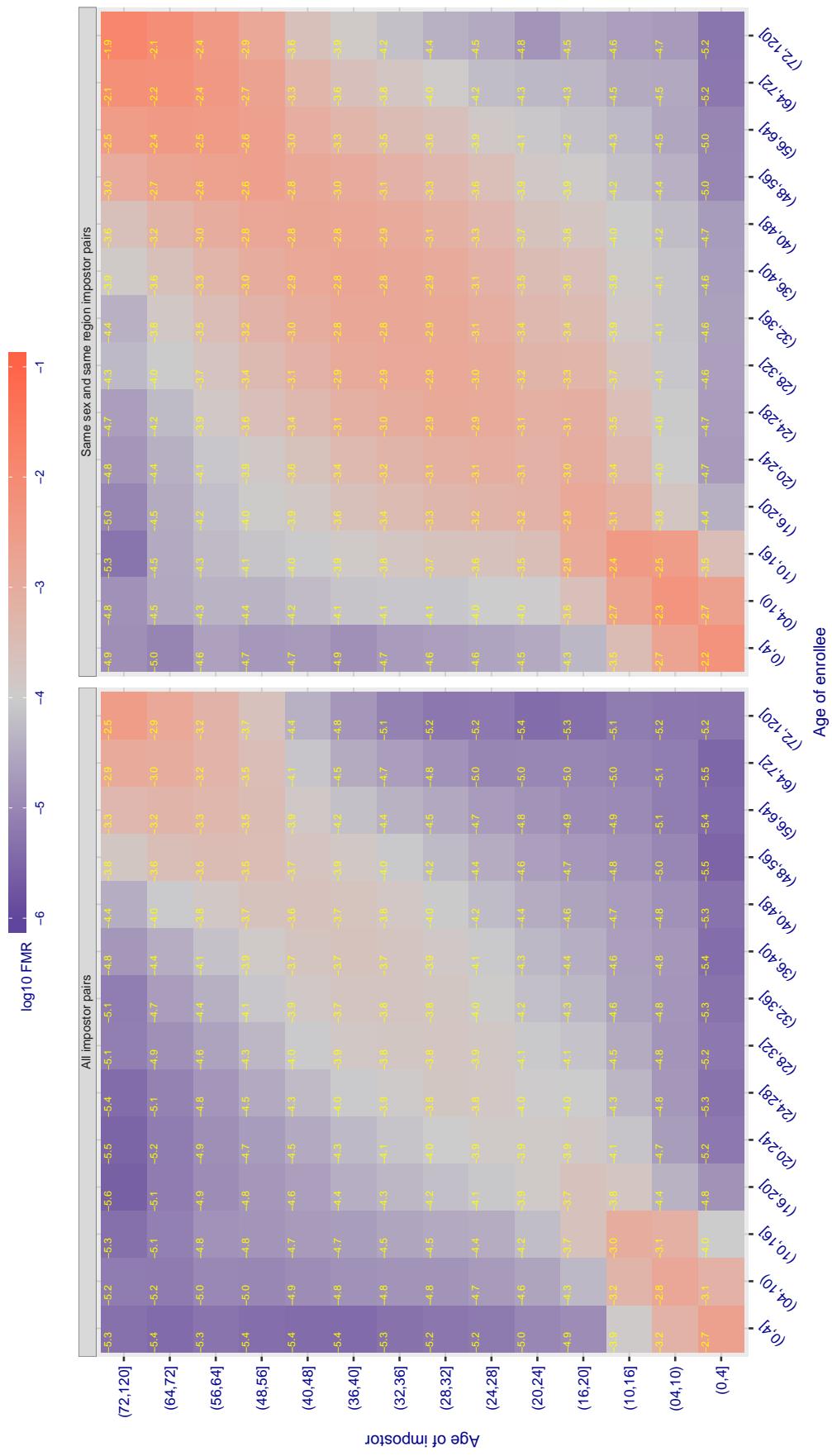


Figure 518: For algorithm ntechlab-006 operating on visa images, the heatmap shows false match observed over impostor comparisons of faces from different individuals who have the given age pair. False matches are counted against a recognition threshold fixed globally to give $FMR = 0.0001$ over all on the order of 10^{10} impostor comparisons. The text in each box gives the same quantity as that coded by the color. Light colors present a security vulnerability to, for example, a passport gate.

Cross age FMR at threshold T = 1.416 for algorithm ntechlab_007, giving FMR(T) = 0.0001 globally.

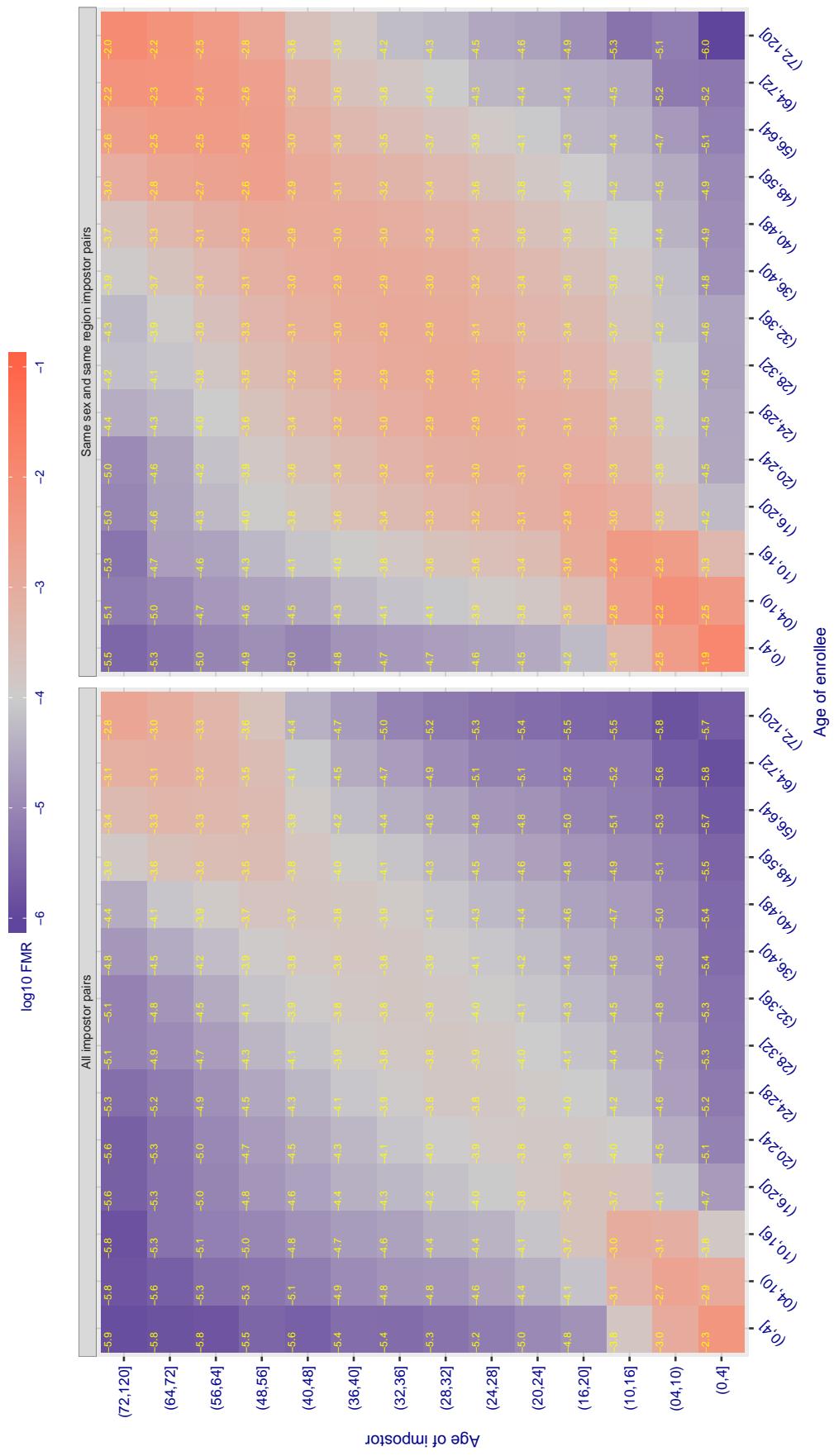


Figure 519: For algorithm ntechlab-007 operating on visa images, the heatmap shows false match observed over impostor comparisons of faces from different individuals who have the given age pair. False matches are counted against a recognition threshold fixed globally to give $FMR = 0.0001$ over all on the order of 10^{10} impostor comparisons. The text in each box gives the same quantity as that coded by the color. Light colors present a security vulnerability to, for example, a passport gate.

Cross age FMR at threshold T = 0.423 for algorithm pixelall_002, giving FMR(T) = 0.0001 globally.

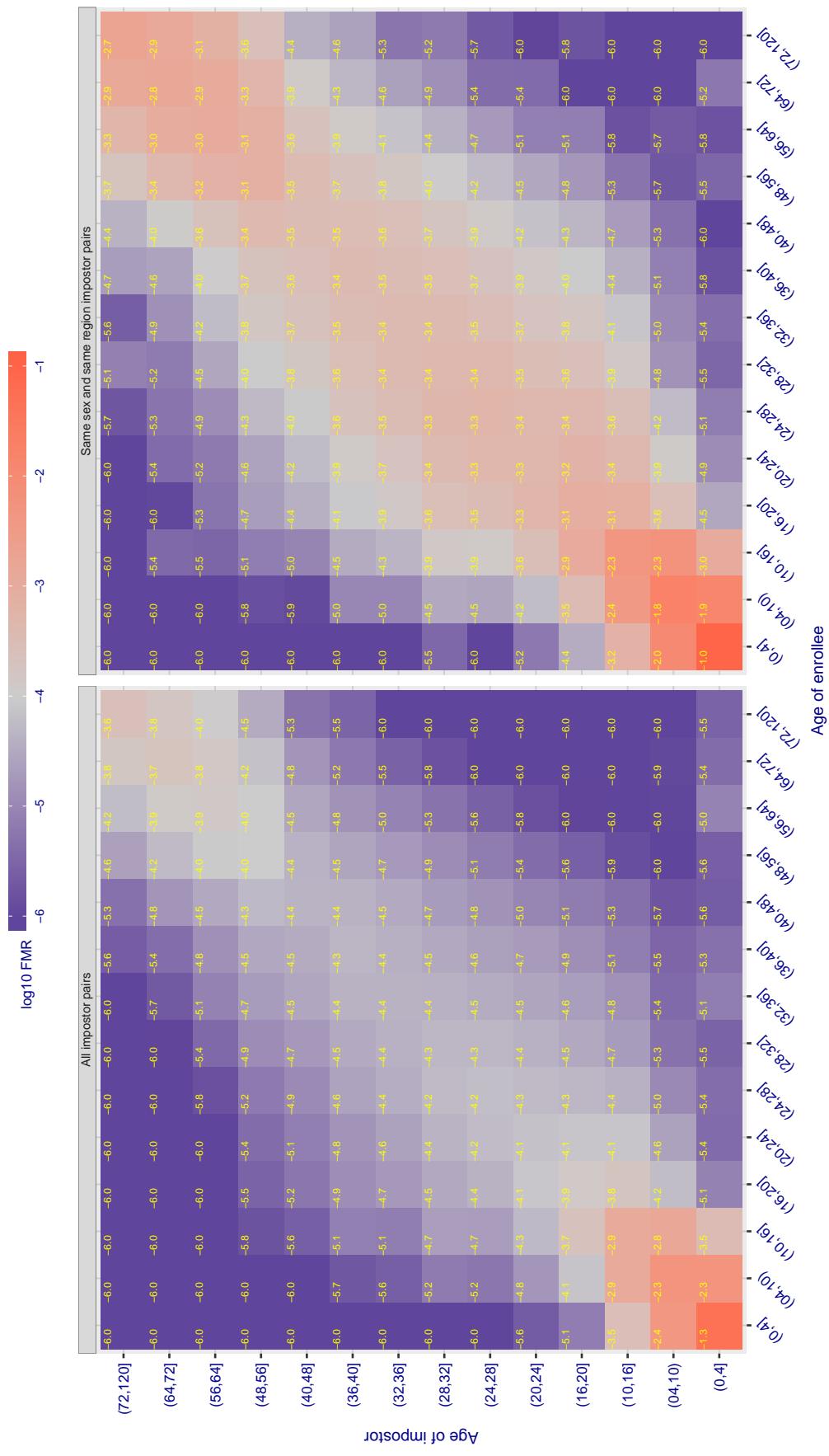


Figure 520: For algorithm pixelall-002 operating on visa images, the heatmap shows false match observed over impostor comparisons of faces from different individuals who have the given age pair. False matches are counted against a recognition threshold fixed globally to give $FMR = 0.0001$ over all on the order of 10^{10} impostor comparisons. The text in each box gives the same quantity as that coded by the color. Light colors present a security vulnerability to, for example, a passport gate.

Cross age FMR at threshold T = 0.337 for algorithm psI_001, giving FMR(T) = 0.0001 globally.

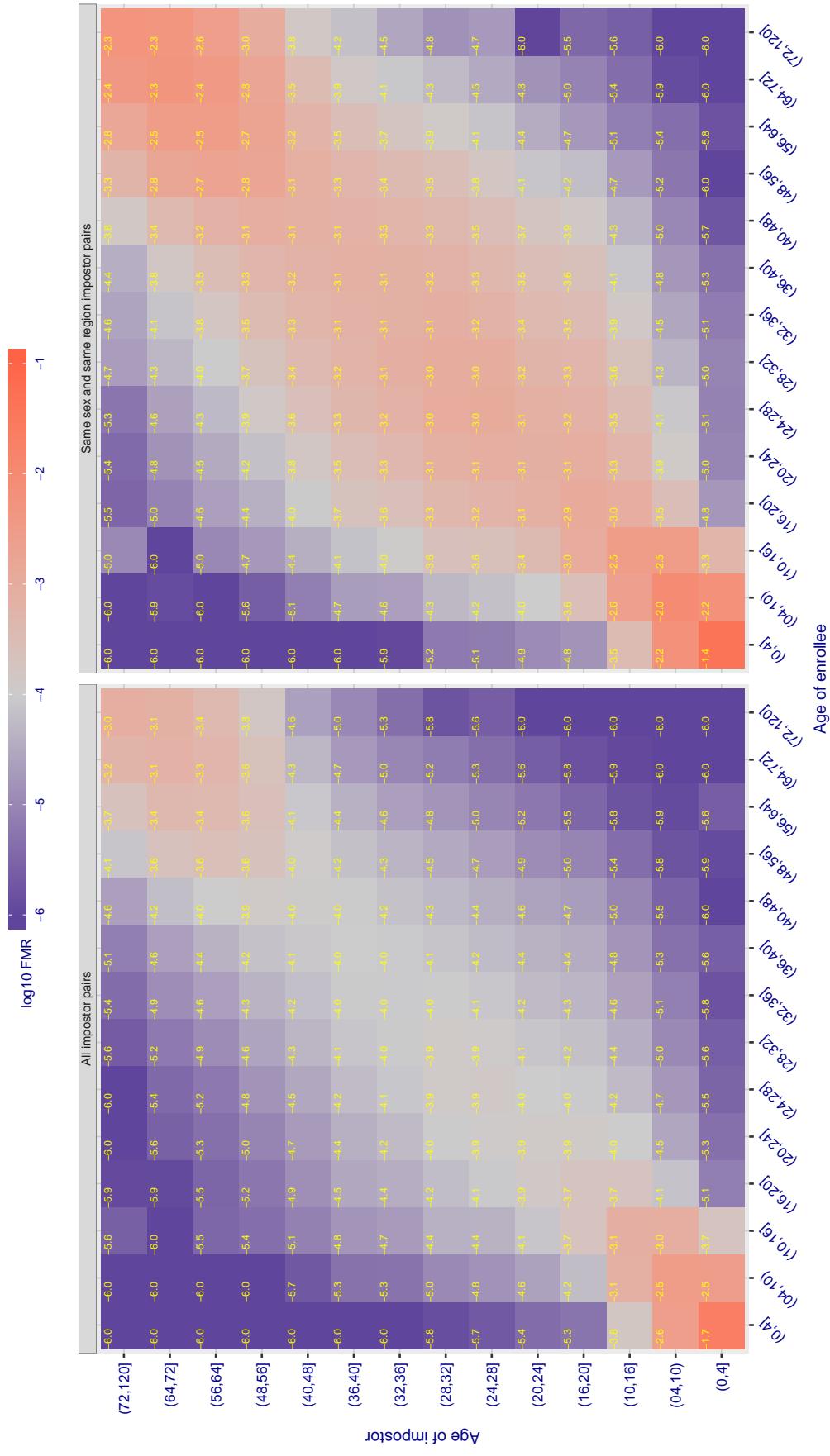


Figure 521: For algorithm psI-001 operating on visa images, the heatmap shows false match observed over impostor comparisons of faces from different individuals who have the given age pair. False matches are counted against a recognition threshold fixed globally to give $FMR = 0.0001$ over all on the order of 10^{10} impostor comparisons. The text in each box gives the same quantity as that coded by the color. Light colors present a security vulnerability to, for example, a passport gate.

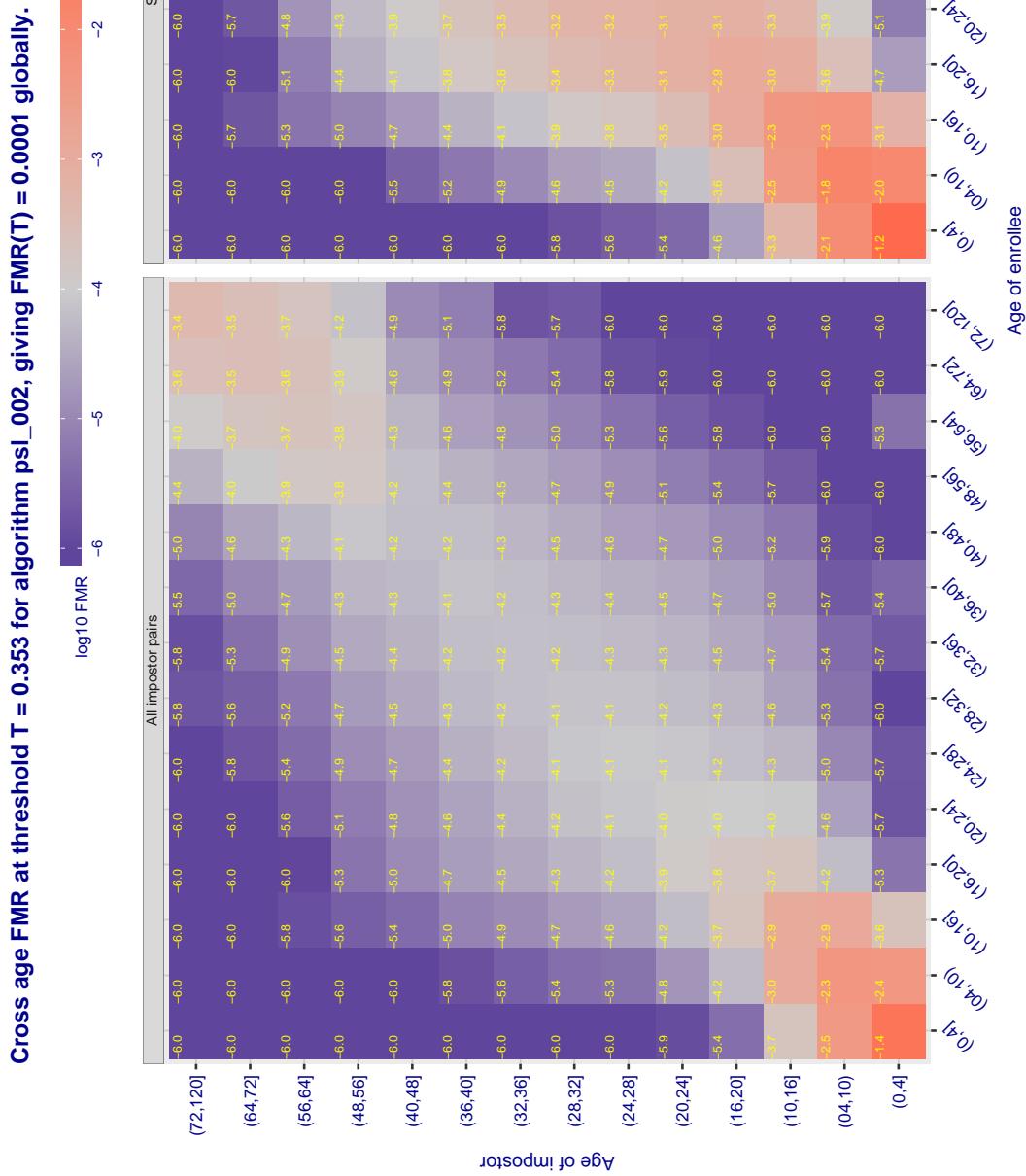


Figure 522: For algorithm psi-002 operating on visa images, the heatmap shows false match observed over impostor comparisons of faces from different individuals who have the given age pair. False matches are counted against a recognition threshold fixed globally to give $FMR = 0.0001$ over all on the order of 10^{10} impostor comparisons. The text in each box gives the same quantity as that coded by the color. Light colors present a security vulnerability to, for example, a passport gate.

Cross age FMR at threshold T = 0.779 for algorithm rankone_006, giving FMR(T) = 0.0001 globally.

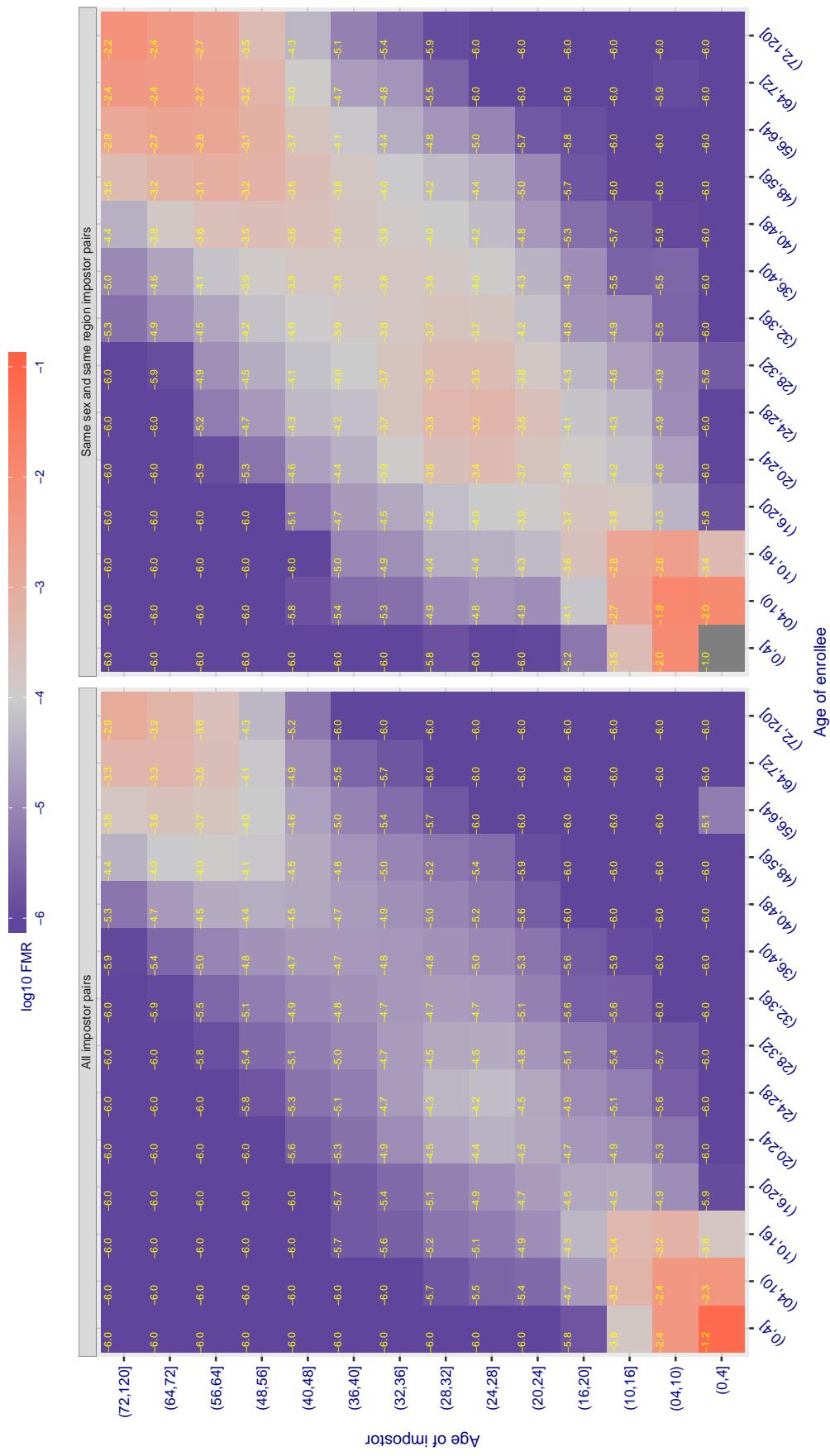


Figure 523: For algorithm rankone-006 operating on visa images, the heatmap shows false match observed over impostor comparisons of faces from different individuals who have the given age pair. False matches are counted against a recognition threshold fixed globally to give $FMR = 0.0001$ over all on the order of 10^{10} impostor comparisons. The text in each box gives the same quantity as that coded by the color. Light colors present a security vulnerability to, for example, a passport gate.

Cross age FMR at threshold T = 0.661 for algorithm rankone_007, giving FMR(T) = 0.0001 globally.

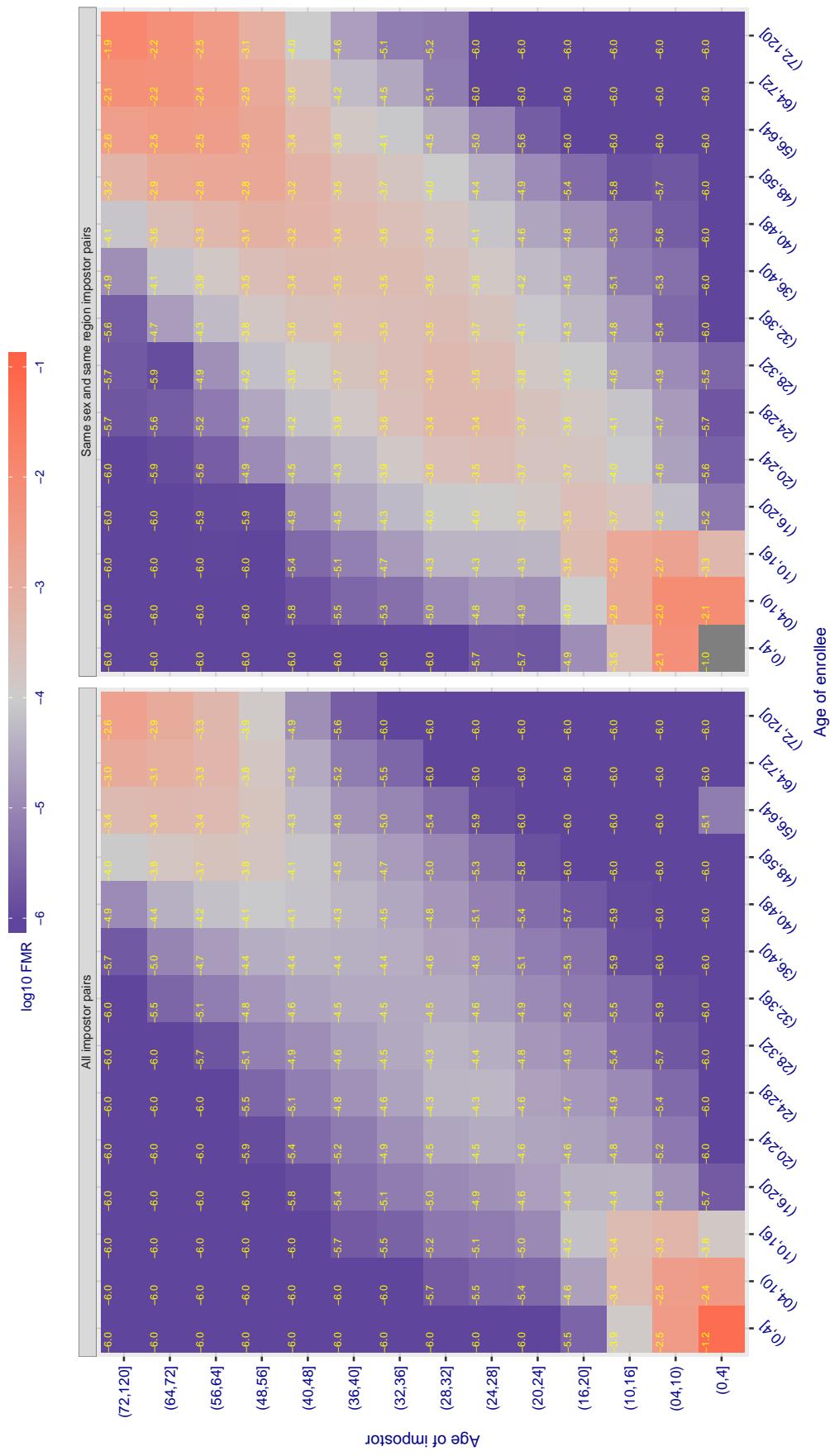


Figure 524: For algorithm rankone-007 operating on visa images, the heatmap shows false match observed over impostor comparisons of faces from different individuals who have the given age pair. False matches are counted against a recognition threshold fixed globally to give $FMR = 0.0001$ over all on the order of 10^{10} impostor comparisons. The text in each box gives the same quantity as that coded by the color. Light colors present a security vulnerability to, for example, a passport gate.

Cross age FMR at threshold T = 0.883 for algorithm realnetworks_002, giving FMR(T) = 0.0001 globally.

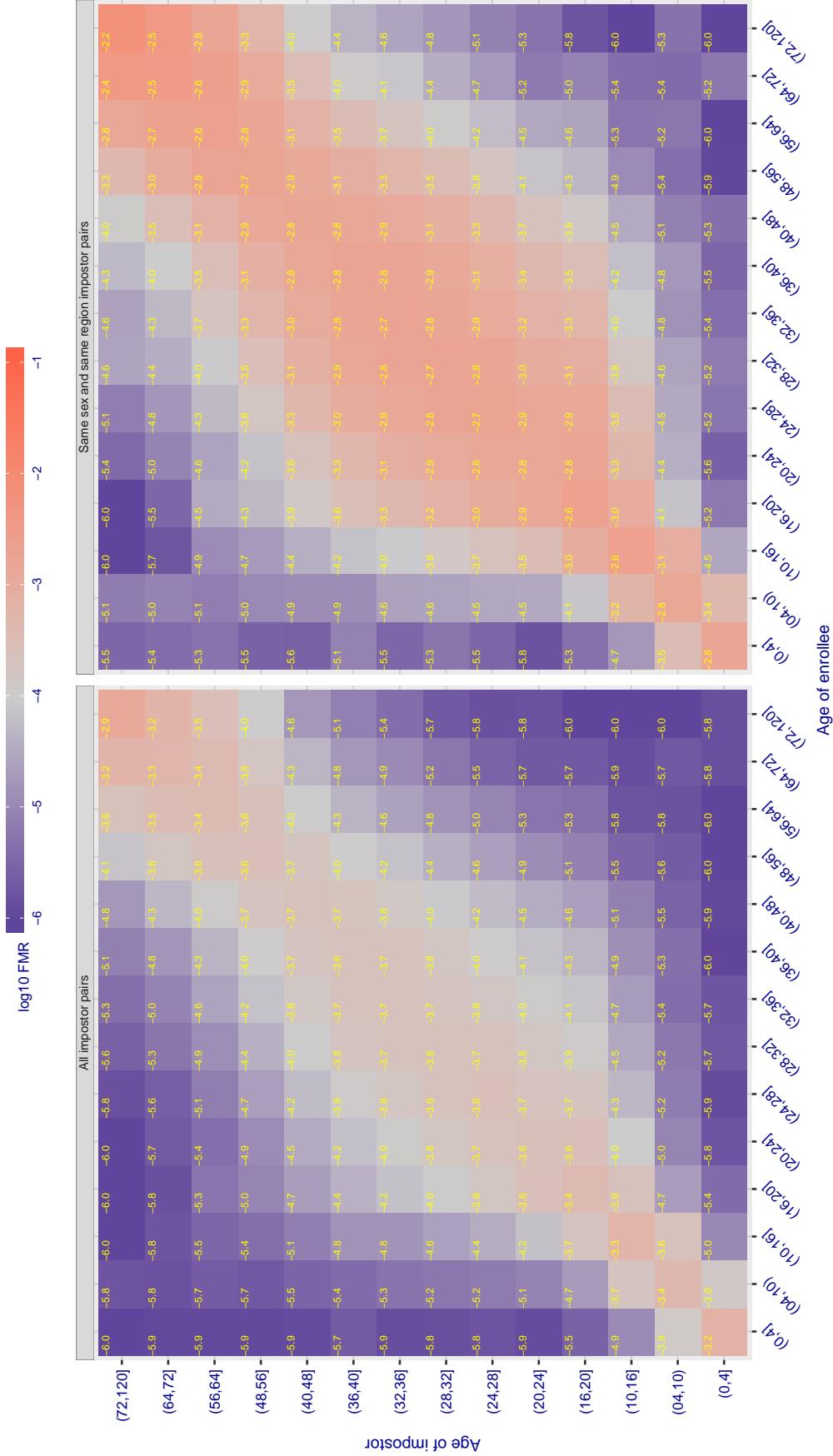


Figure 525: For algorithm realnetworks-002 operating on visa images, the heatmap shows false match observed over impostor comparisons of faces from different individuals who have the given age pair. False matches are counted against a recognition threshold fixed globally to give $FMR = 0.0001$ over all on the order of 10^{10} impostor comparisons. The text in each box gives the same quantity as that coded by the color. Light colors present a security vulnerability to, for example, a passport gate.

Cross age FMR at threshold T = 0.886 for algorithm realnetworks_003, giving $FMR(T) = 0.0001$ globally.

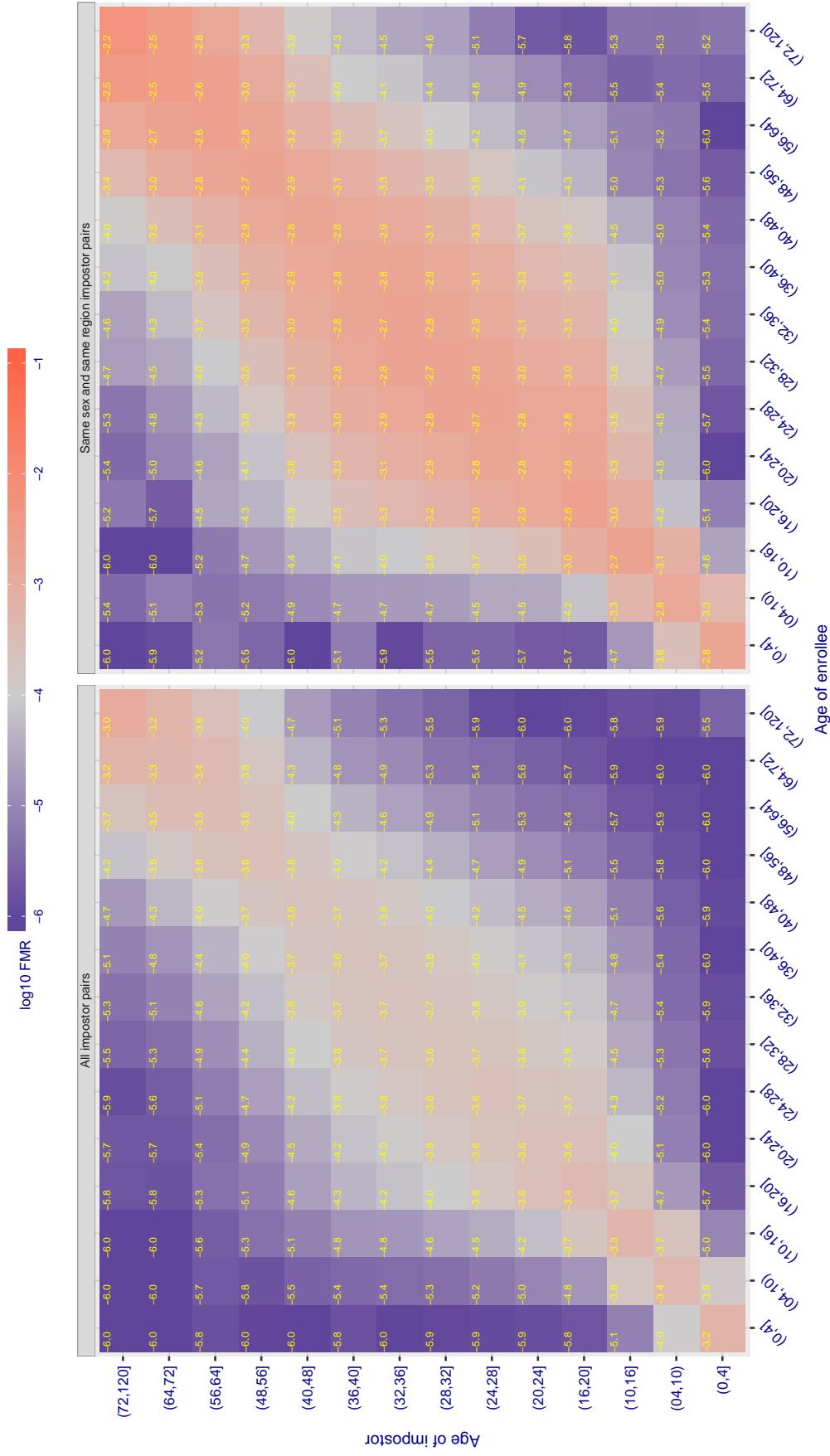
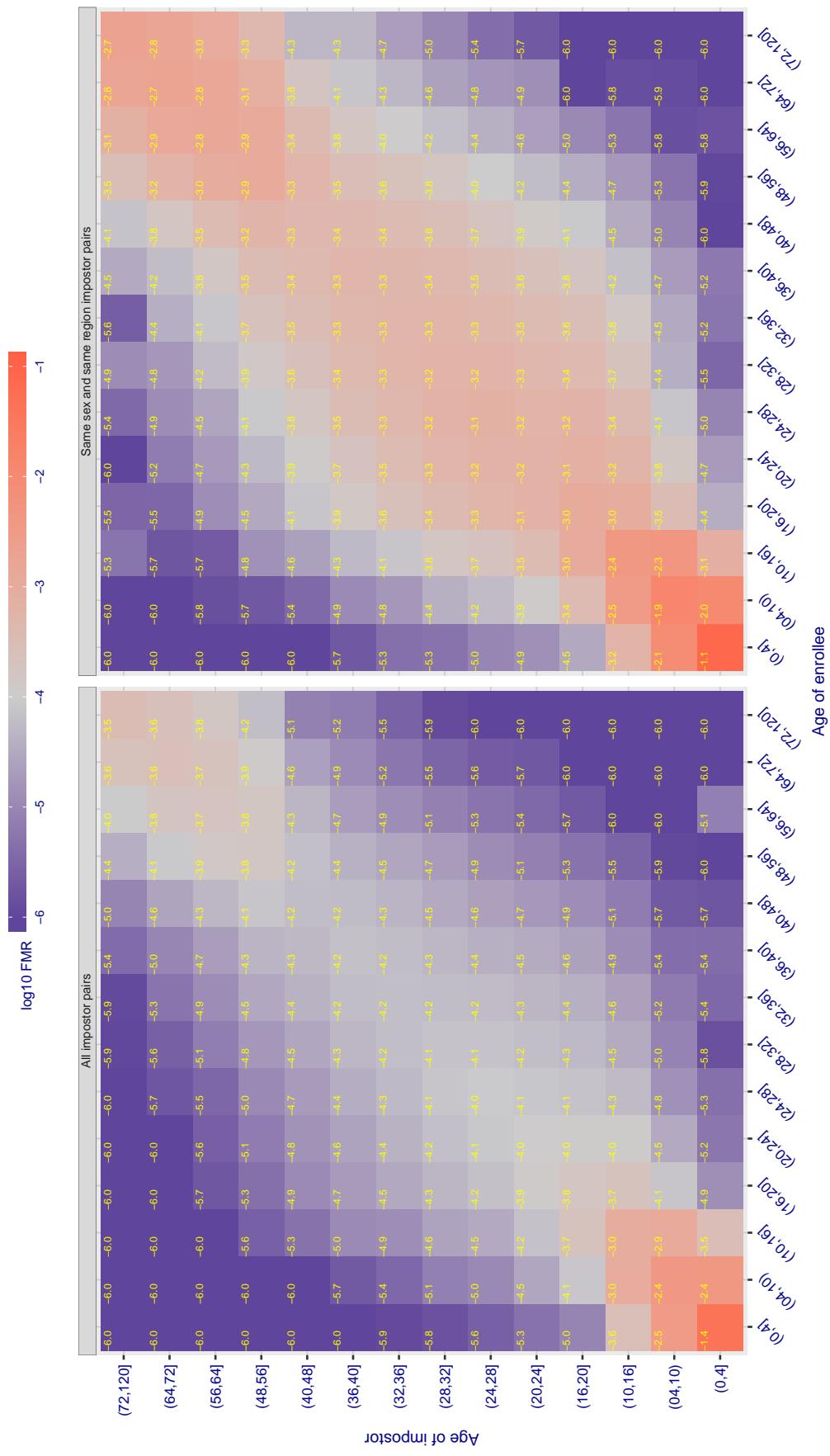


Figure 526: For algorithm realnetworks-003 operating on visa images, the heatmap shows false match observed over impostor comparisons of faces from different individuals who have the given age pair. False matches are counted against a recognition threshold fixed globally to give $FMR = 0.0001$ over all on the order of 10^{10} impostor comparisons. The text in each box gives the same quantity as that coded by the color. Light colors present a security vulnerability to, for example, a passport gate.

Cross age FMR at threshold T = 70.373 for algorithm remarkai_000, giving FMR(T) = 0.0001 globally.



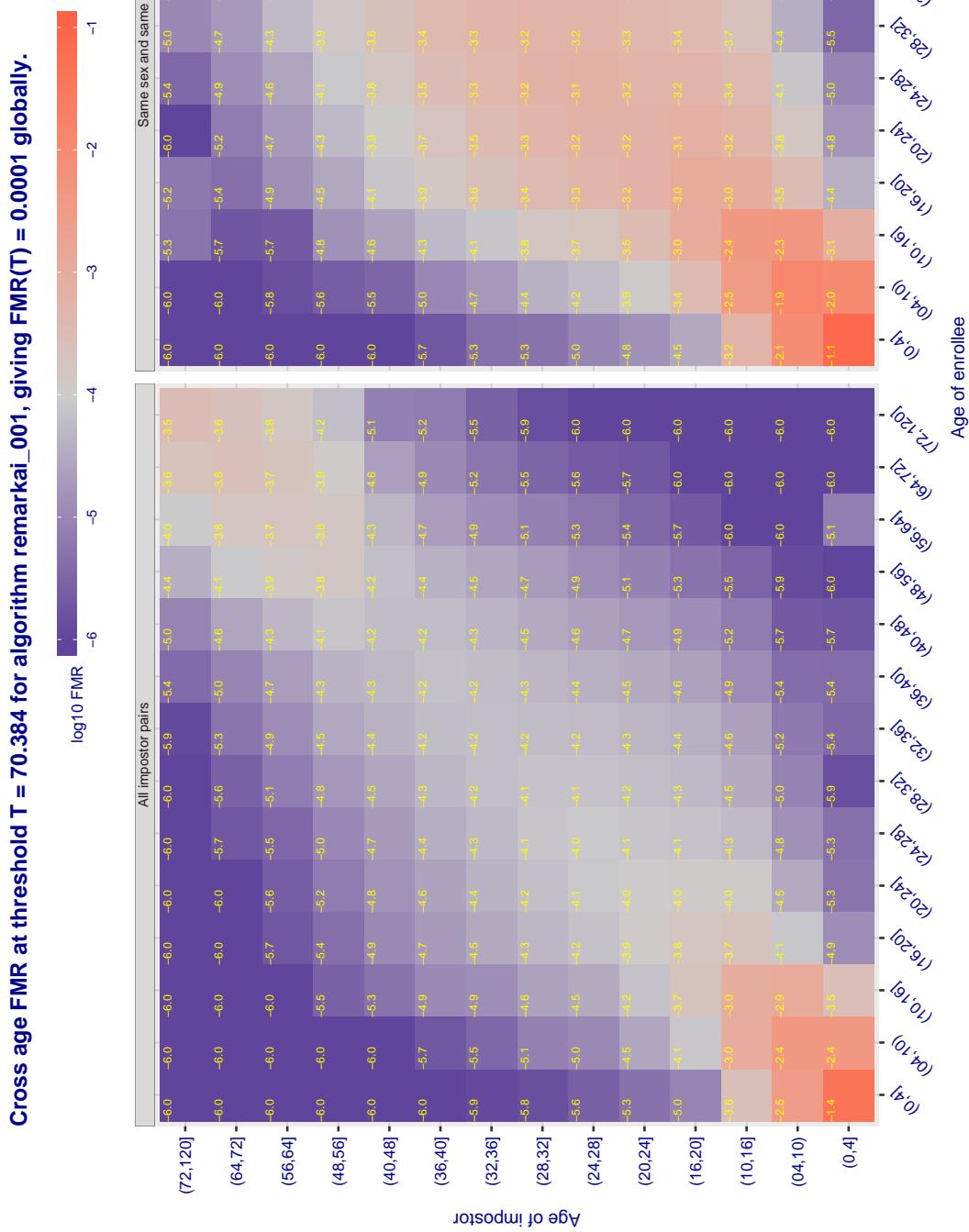


Figure 528: For algorithm *remarkai-001* operating on visa images, the heatmap shows false match observed over impostor comparisons of faces from different individuals who have the given age pair. False matches are counted against a recognition threshold fixed globally to give $FMR = 0.0001$ over all on the order of 10^{10} impostor comparisons. The text in each box gives the same quantity as that coded by the color. Light colors present a security vulnerability to, for example, a passport gate.

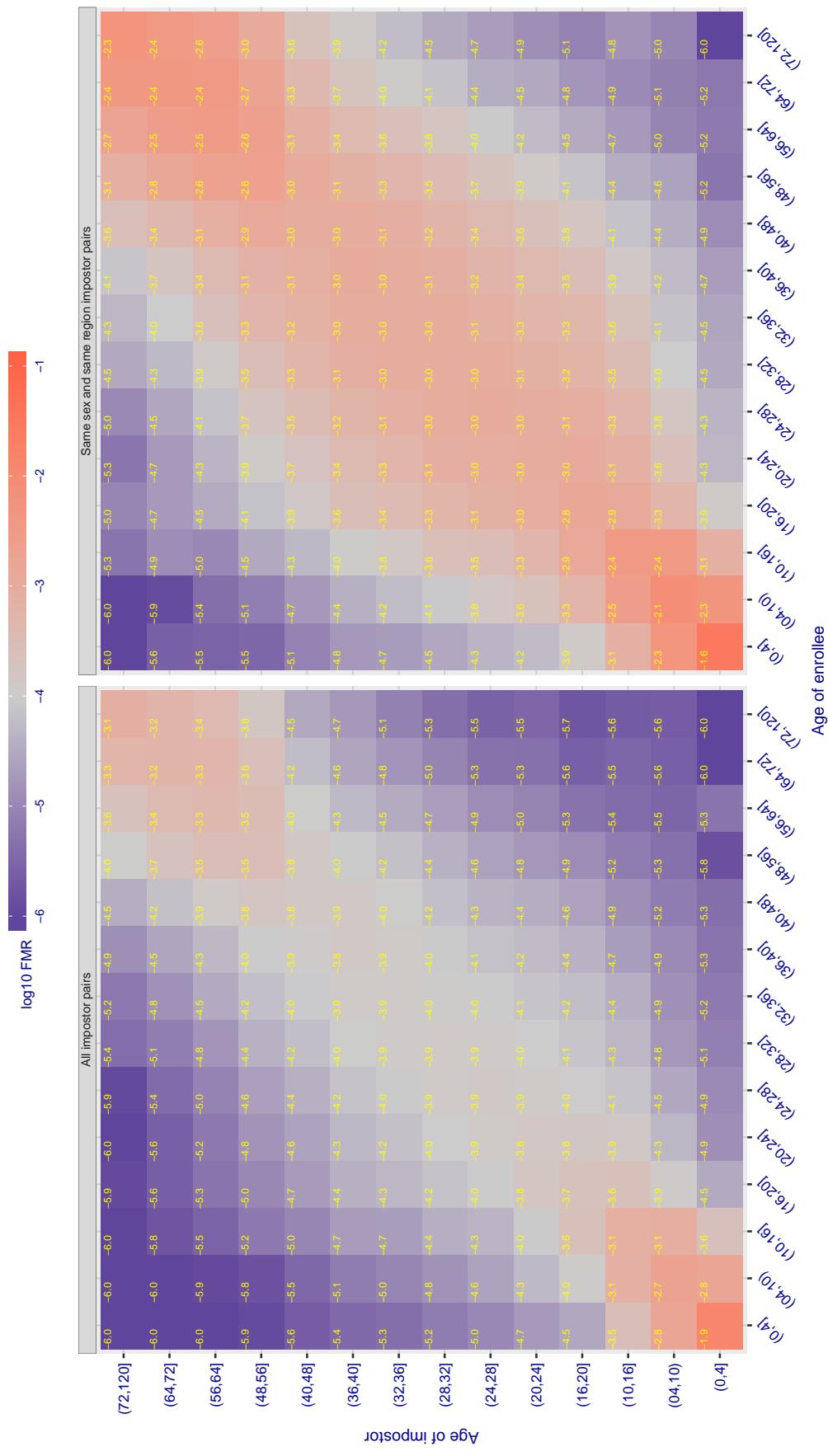
Cross age FMR at threshold T = 0.663 for algorithm rokid_000, giving $FMR(T) = 0.0001$ globally.

Figure 529: For algorithm rokid-000 operating on visa images, the heatmap shows false match observed over impostor comparisons of faces from different individuals who have the given age pair. False matches are counted against a recognition threshold fixed globally to give $FMR = 0.0001$ over all on the order of 10^{10} impostor comparisons. The text in each box gives the same quantity as that coded by the color. Light colors present a security vulnerability to, for example, a passport gate.

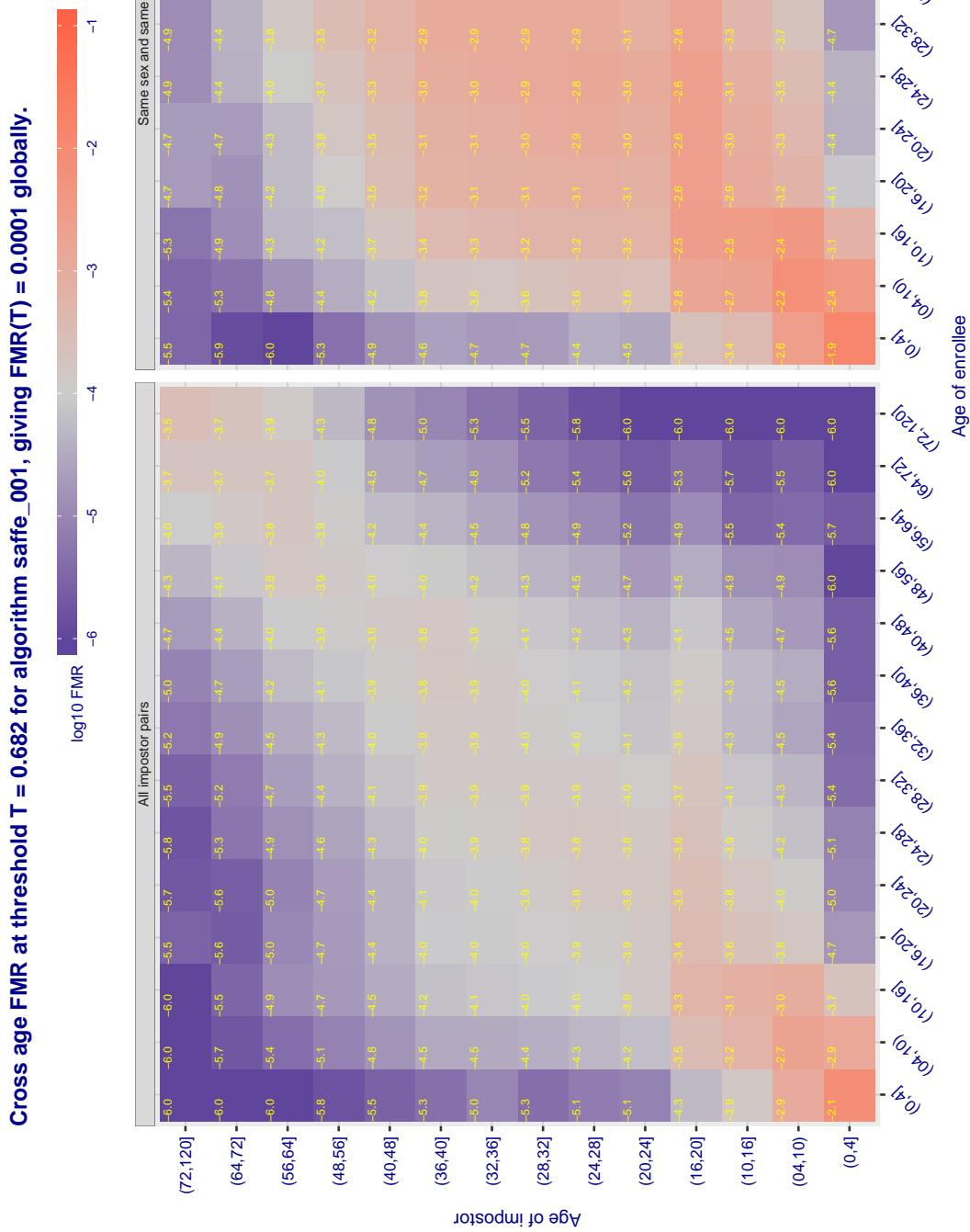


Figure 530: For algorithm safe-001 operating on visa images, the heatmap shows false match observed over impostor comparisons of faces from different individuals who have the given age pair. False matches are counted against a recognition threshold fixed globally to give $FMR = 0.0001$ over all on the order of 10^{10} impostor comparisons. The text in each box gives the same quantity as that coded by the color. Light colors present a security vulnerability to, for example, a passport gate.

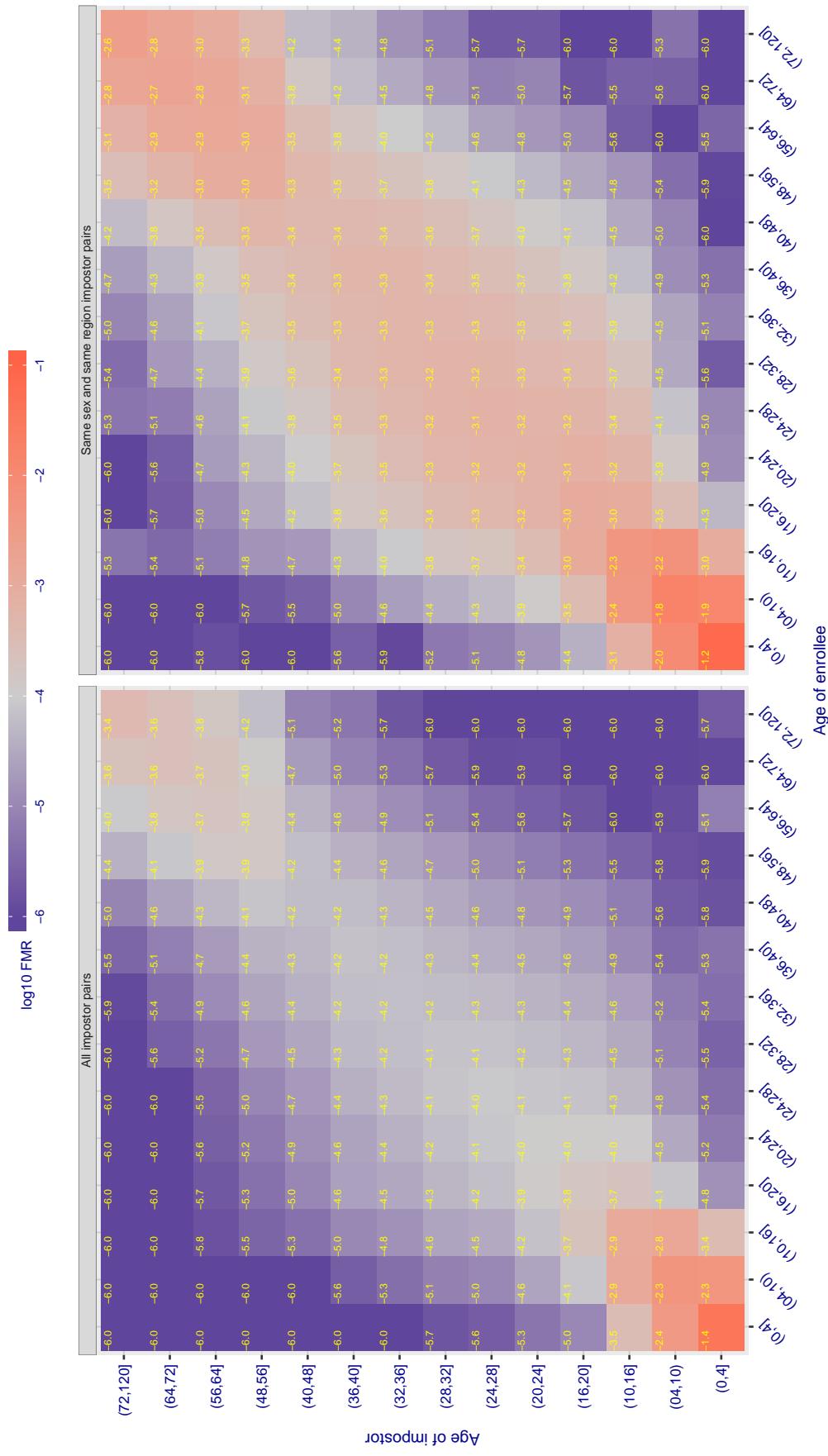
Cross age FMR at threshold T = 0.383 for algorithm saffe_002, giving $FMR(T) = 0.0001$ globally.

Figure 531: For algorithm saffe-002 operating on visa images, the heatmap shows false match observed over impostor comparisons of faces from different individuals who have the given age pair. False matches are counted against a recognition threshold fixed globally to give $FMR = 0.0001$ over all on the order of 10^{10} impostor comparisons. The text in each box gives the same quantity as that coded by the color. Light colors present a security vulnerability to, for example, a passport gate.

Cross age FMR at threshold T = 0.390 for algorithm sensetime_001, giving FMR(T) = 0.0001 globally.

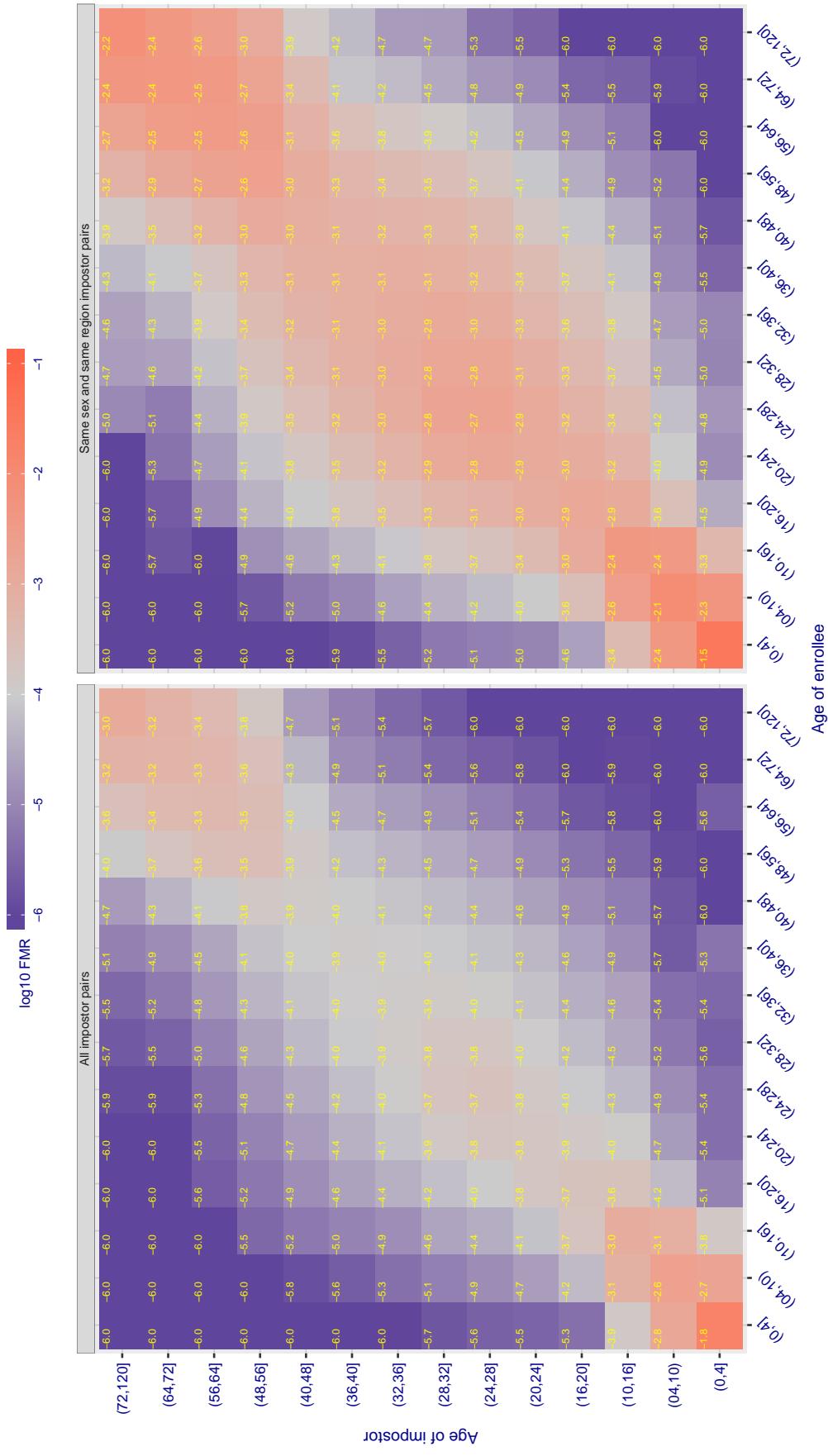
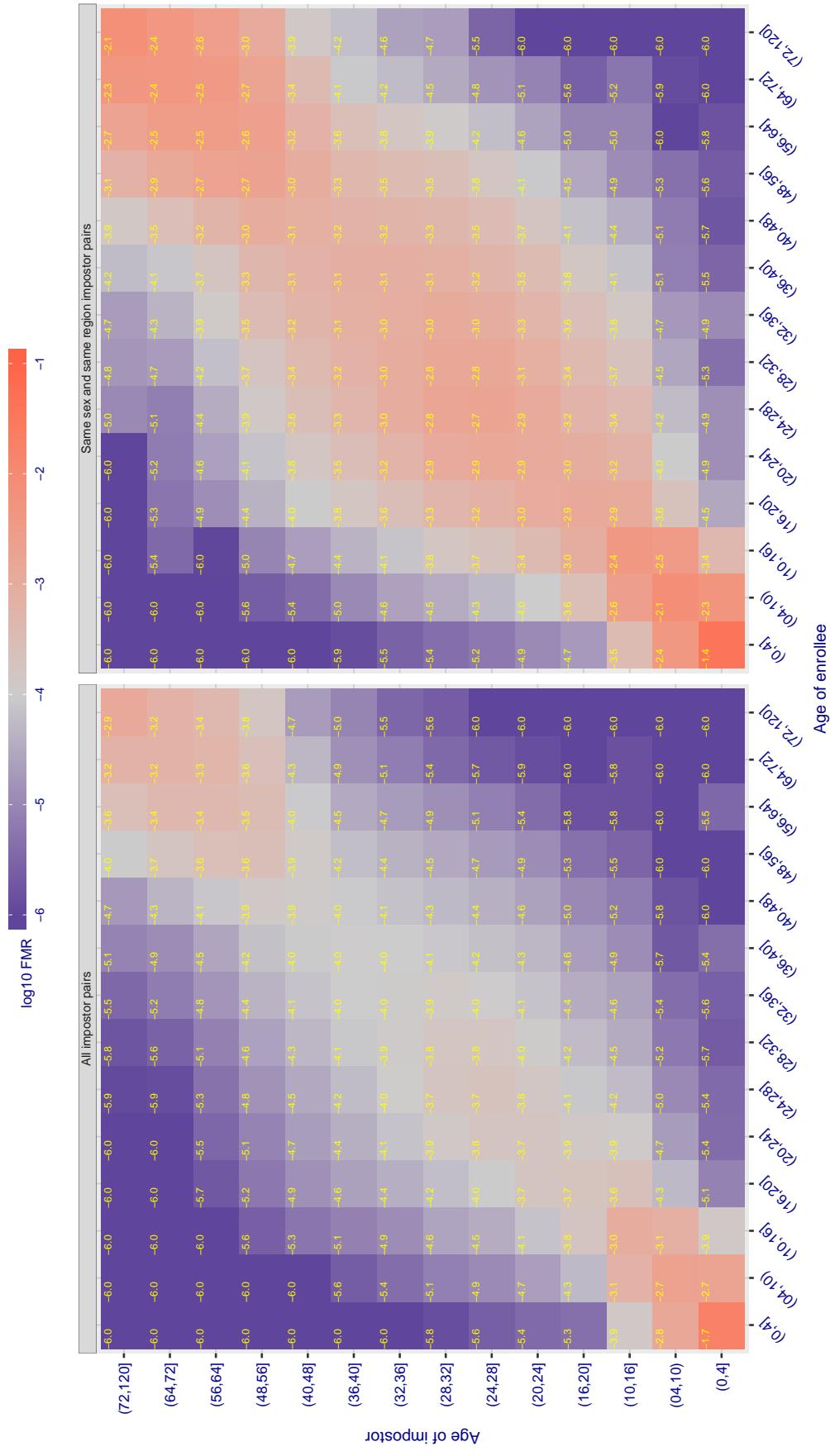


Figure 532: For algorithm sensetime-001 operating on visa images, the heatmap shows false match observed over impostor comparisons of faces from different individuals who have the given age pair. False matches are counted against a recognition threshold fixed globally to give $FMR = 0.0001$ over all on the order of 10^{10} impostor comparisons. The text in each box gives the same quantity as that coded by the color. Light colors present a security vulnerability to, for example, a passport gate.

Cross age FMR at threshold T = 0.390 for algorithm sensetime_002, giving FMR(T) = 0.0001 globally.



Cross age FMR at threshold T = 0.970 for algorithm shaman_000, giving FMR(T) = 0.0001 globally.

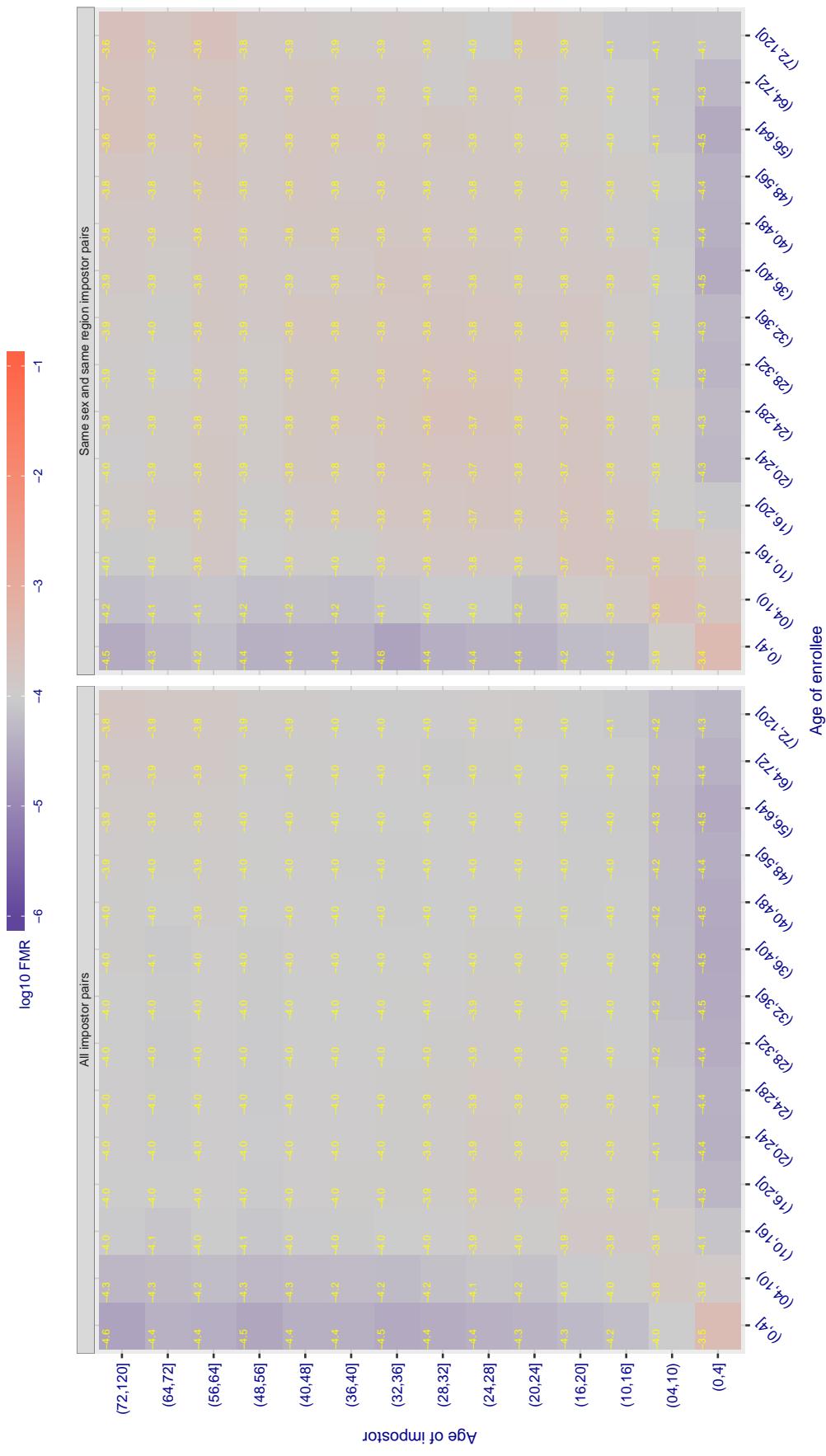


Figure 534: For algorithm shaman-000 operating on visa images, the heatmap shows false match observed over impostor comparisons of faces from different individuals who have the given age pair. False matches are counted against a recognition threshold fixed globally to give $FMR = 0.0001$ over all on the order of 10^{10} impostor comparisons. The text in each box gives the same quantity as that coded by the color. Light colors present a security vulnerability to, for example, a passport gate.

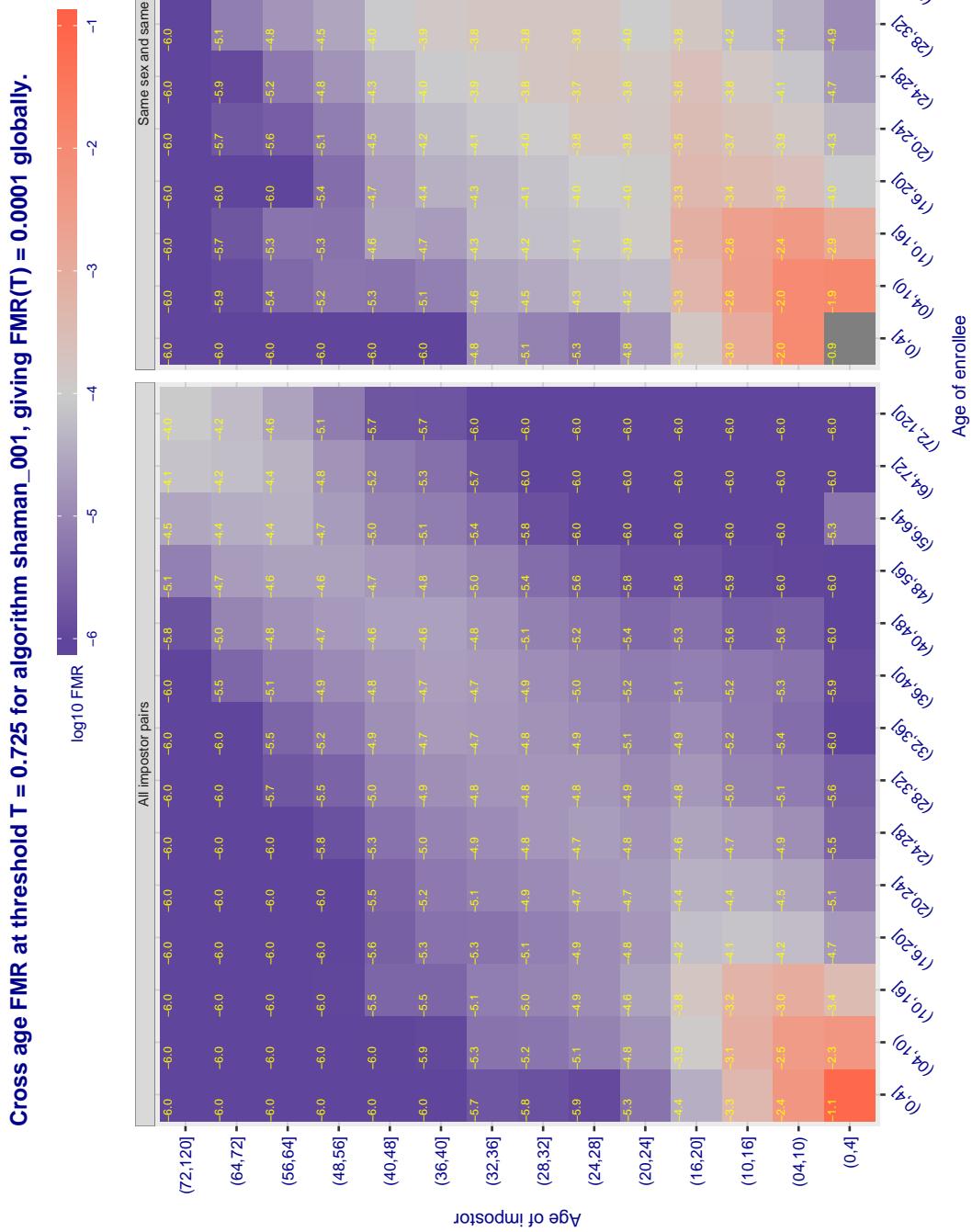


Figure 535: For algorithm shaman-001 operating on visa images, the heatmap shows false match observed over impostor comparisons of faces from different individuals who have the given age pair. False matches are counted against a recognition threshold fixed globally to give $FMR = 0.0001$ over all on the order of 10^{10} impostor comparisons. The text in each box gives the same quantity as that coded by the color. Light colors present a security vulnerability to, for example, a passport gate.

Cross age FMR at threshold T = 0.400 for algorithm shu_001, giving FMR(T) = 0.0001 globally.

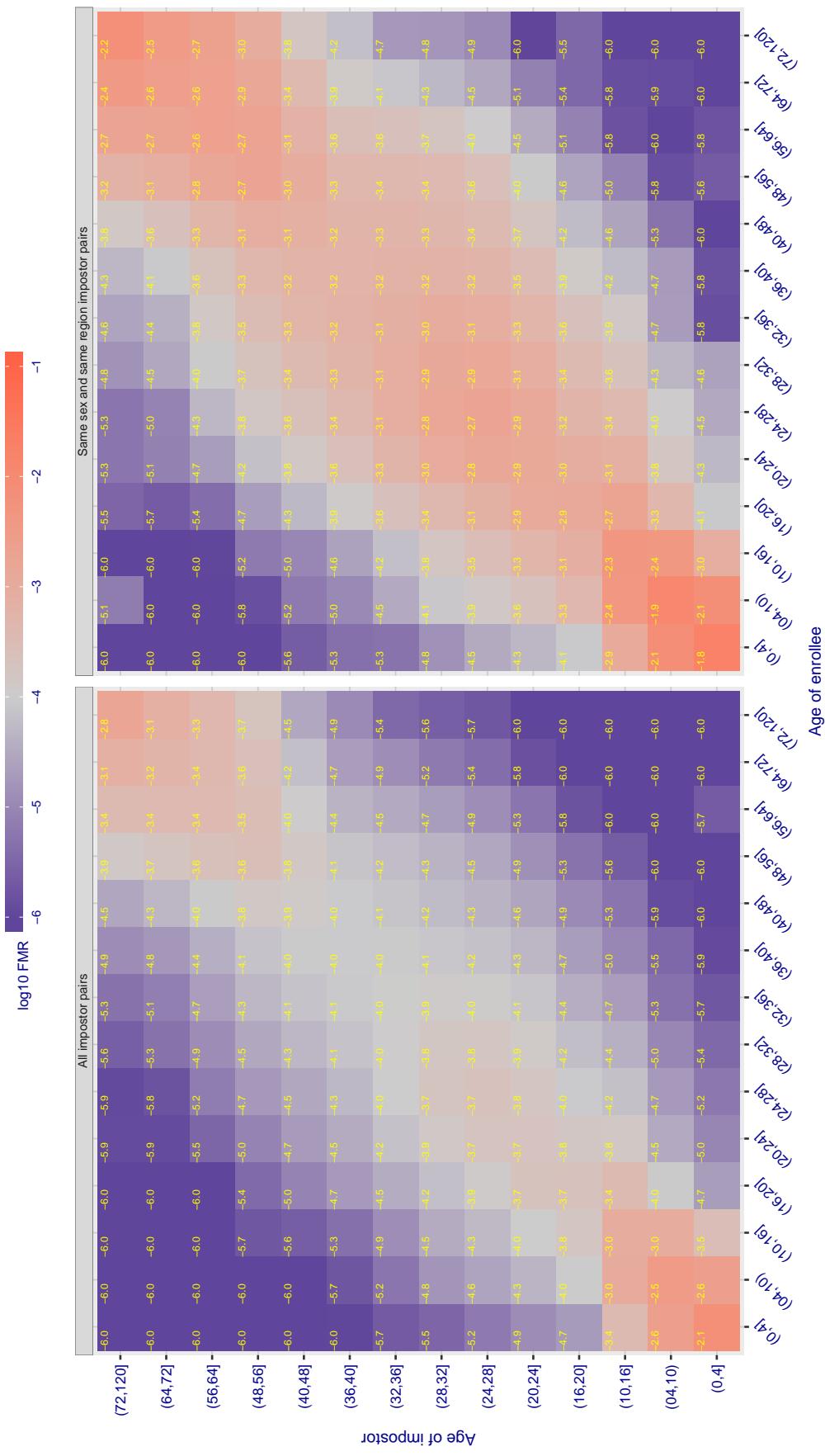


Figure 536: For algorithm shu-001 operating on visa images, the heatmap shows false match observed over imposter comparisons of faces from different individuals who have the given age pair. False matches are counted against a recognition threshold fixed globally to give $FMR = 0.0001$ over all on the order of 10^{10} imposter comparisons. The text in each box gives the same quantity as that coded by the color. Light colors present a security vulnerability to, for example, a passport gate.

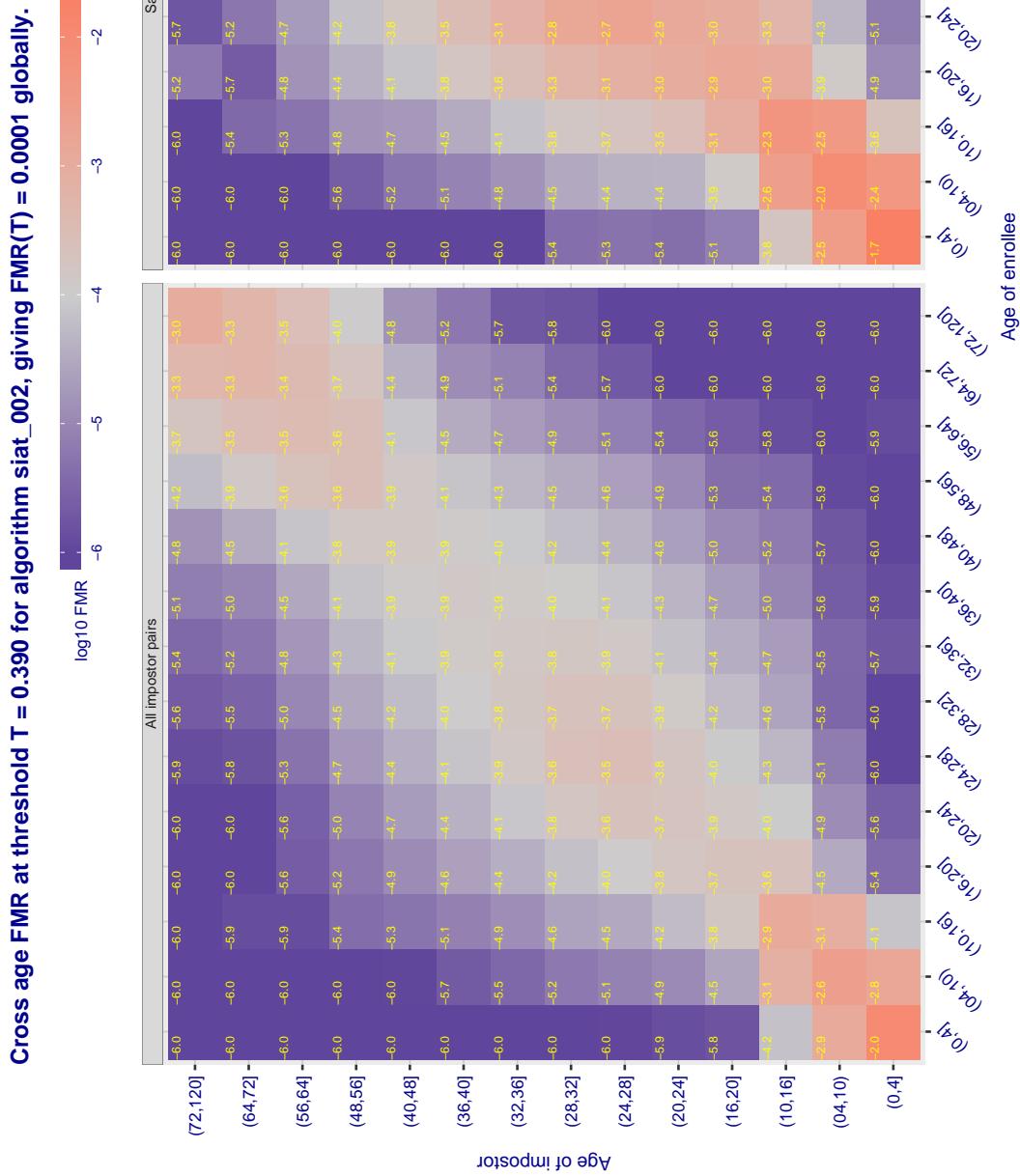


Figure 537: For algorithm siat-002 operating on visa images, the heatmap shows false match observed over impostor comparisons of faces from different individuals who have the given age pair. False matches are counted against a recognition threshold fixed globally to give $FMR = 0.0001$ over all on the order of 10^{10} impostor comparisons. The text in each box gives the same quantity as that coded by the color. Light colors present a security vulnerability to, for example, a passport gate.

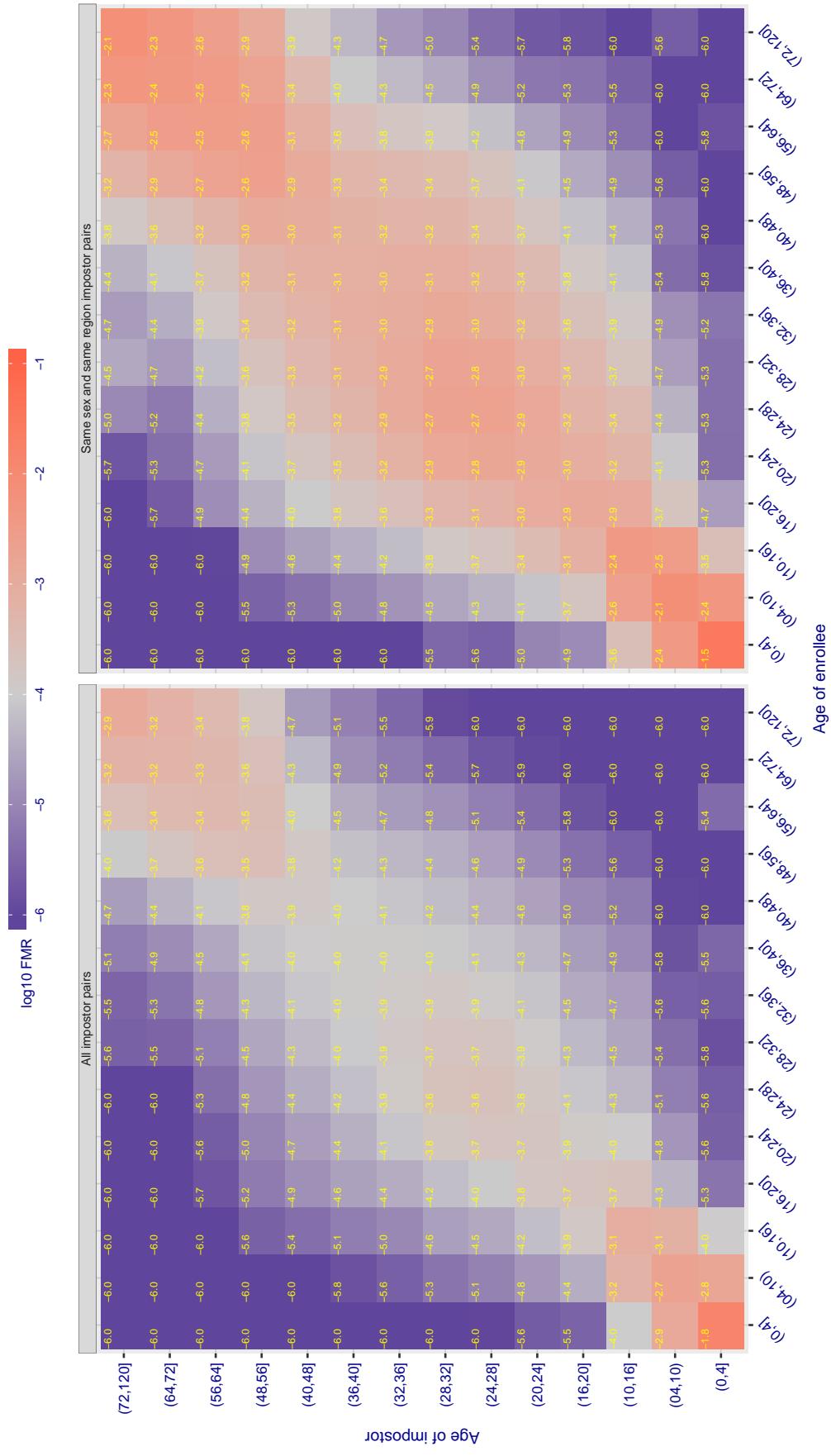
Cross age FMR at threshold T = 0.393 for algorithm siat_004, giving $FMR(T) = 0.0001$ globally.

Figure 538: For algorithm siat-004 operating on visa images, the heatmap shows false match observed over imposter comparisons of faces from different individuals who have the given age pair. False matches are counted against a recognition threshold fixed globally to give $FMR = 0.0001$ over all on the order of 10^{10} imposter comparisons. The text in each box gives the same quantity as that coded by the color. Light colors present a security vulnerability to, for example, a passport gate.

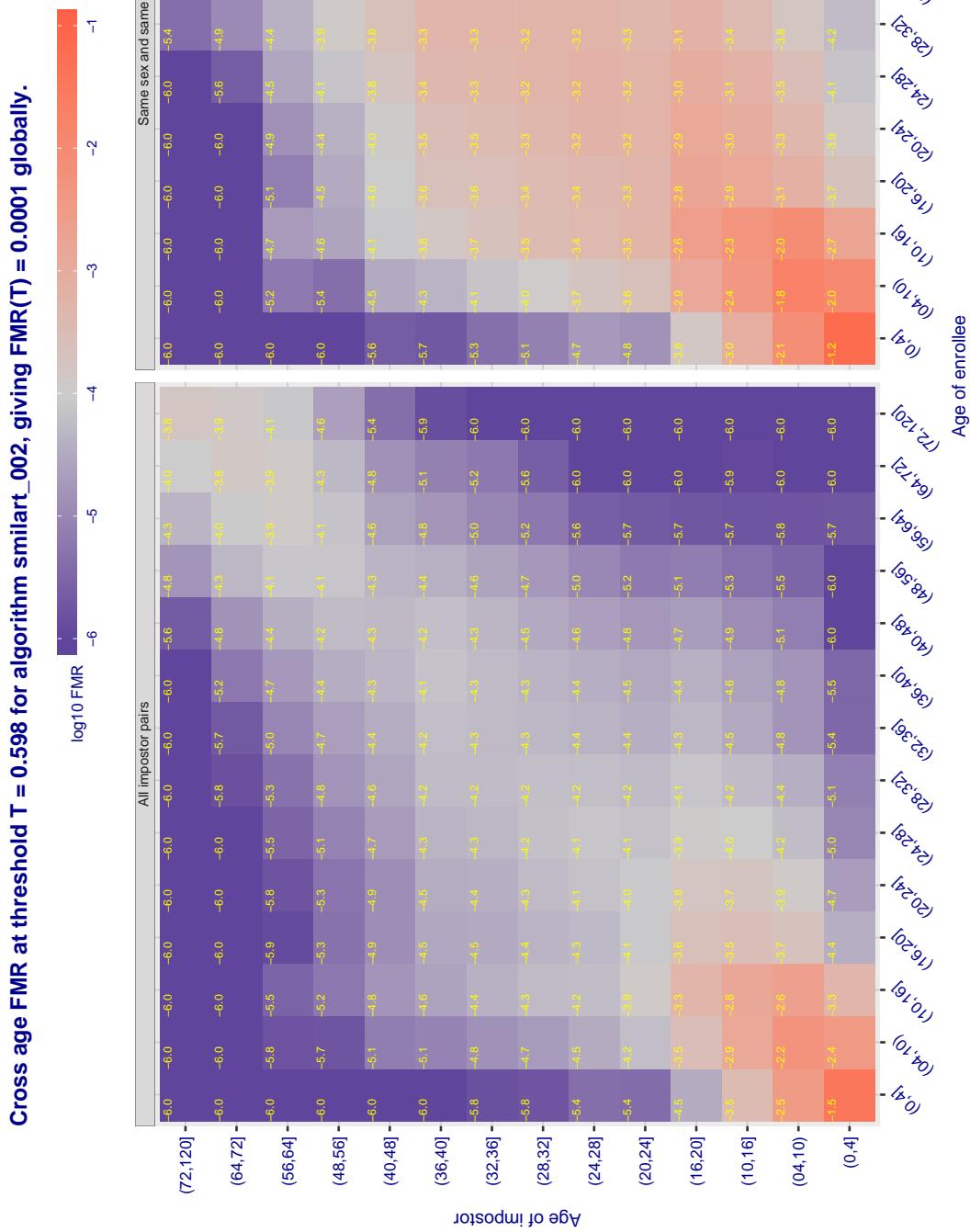


Figure 539: For algorithm smilart-002 operating on visa images, the heatmap shows false match observed over impostor comparisons of faces from different individuals who have the given age pair. False matches are counted against a recognition threshold fixed globally to give $FMR = 0.0001$ over all on the order of 10^{10} impostor comparisons. The text in each box gives the same quantity as that coded by the color. Light colors present a security vulnerability to, for example, a passport gate.

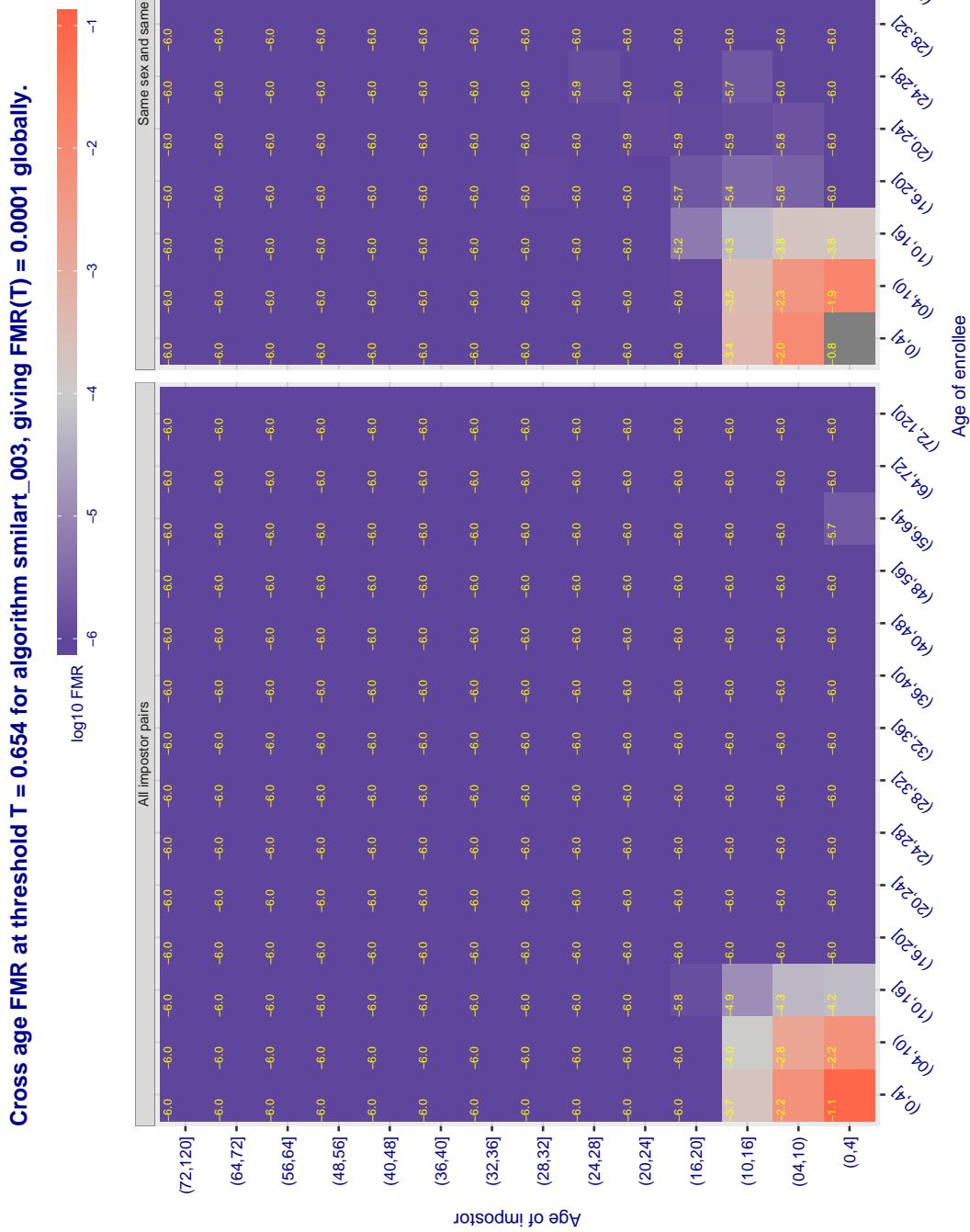


Figure 540: For algorithm smilart-003 operating on visa images, the heatmap shows false match observed over impostor comparisons of faces from different individuals who have the given age pair. False matches are counted against a recognition threshold fixed globally to give $FMR = 0.0001$ over all on the order of 10^{10} impostor comparisons. The text in each box gives the same quantity as that coded by the color. Light colors present a security vulnerability to, for example, a passport gate.

Cross age FMR at threshold T = 0.314 for algorithm starhybrid_001, giving FMR(T) = 0.0001 globally.

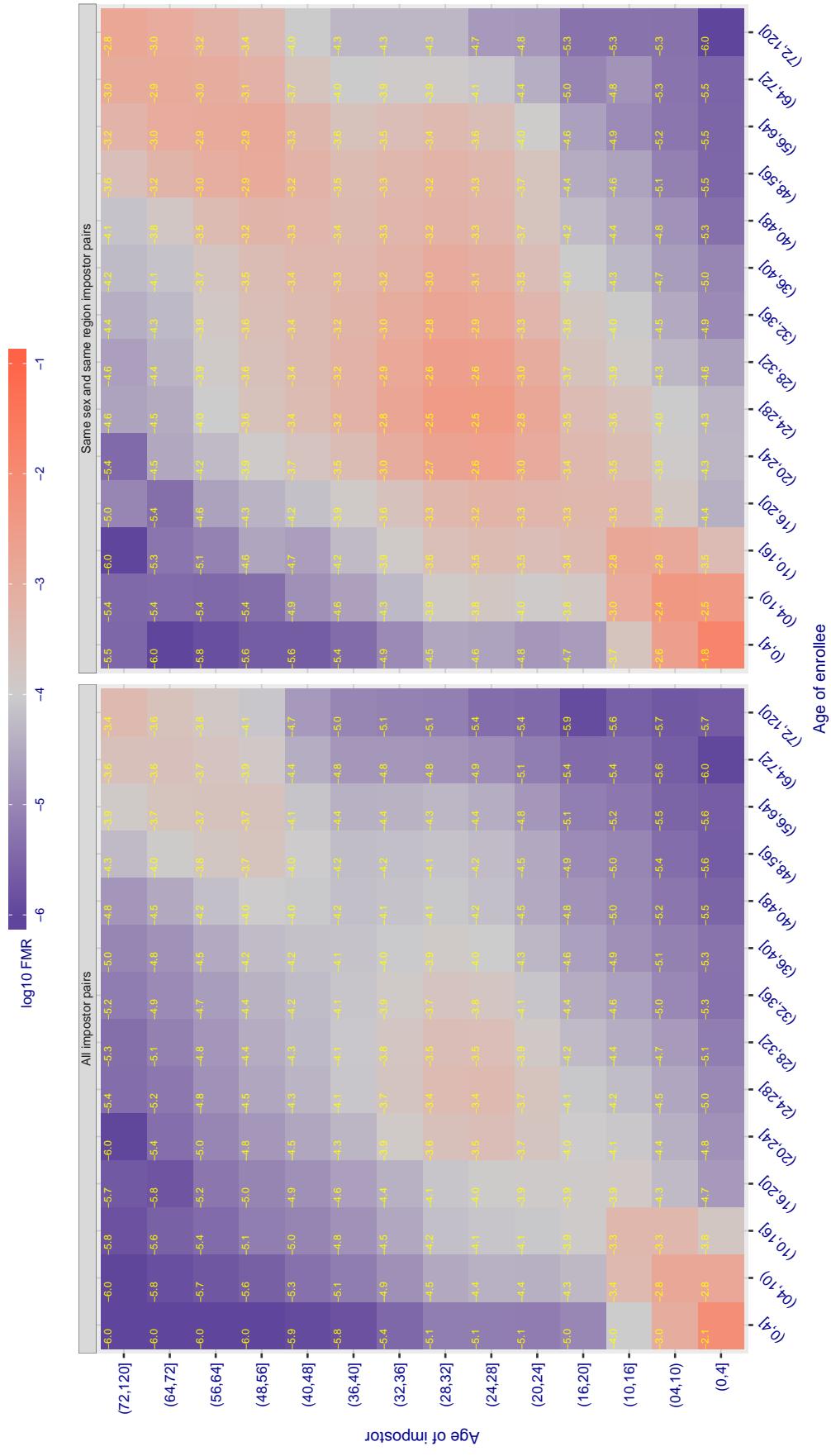


Figure 541: For algorithm starhybrid-001 operating on visa images, the heatmap shows false match observed over impostor comparisons of faces from different individuals who have the given age pair. False matches are counted against a recognition threshold fixed globally to give FMR = 0.0001 over all on the order of 10^{10} impostor comparisons. The text in each box gives the same quantity as that coded by the color. Light colors present a security vulnerability to, for example, a passport gate.

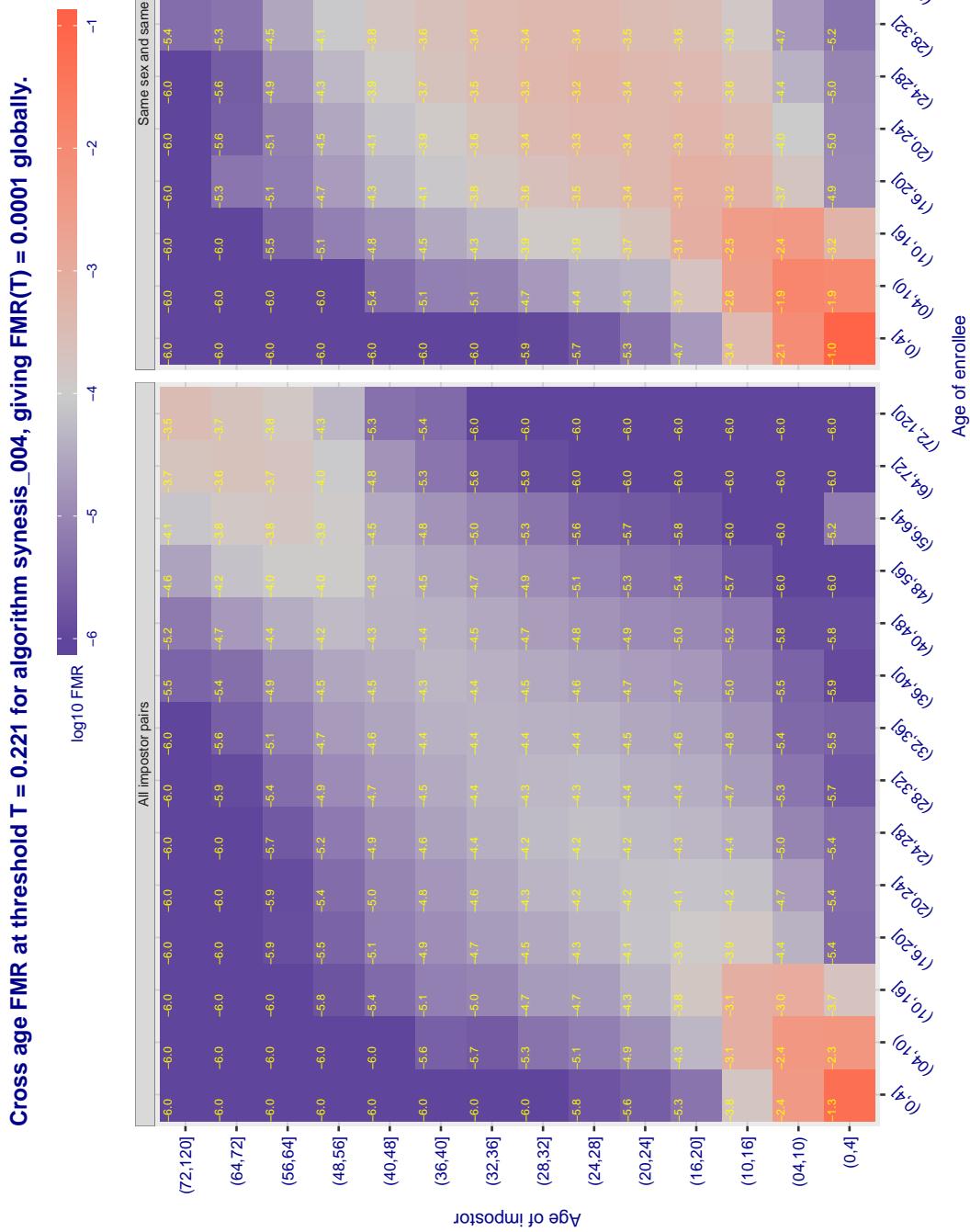


Figure 542: For algorithm *synesis-004* operating on visa images, the heatmap shows false match observed over impostor comparisons of faces from different individuals who have the given age pair. False matches are counted against a recognition threshold fixed globally to give $FMR = 0.0001$ over all on the order of 10^{10} impostor comparisons. The text in each box gives the same quantity as that coded by the color. Light colors present a security vulnerability to, for example, a passport gate.

Cross age FMR at threshold T = 0.356 for algorithm synthesis_005, giving FMR(T) = 0.0001 globally.

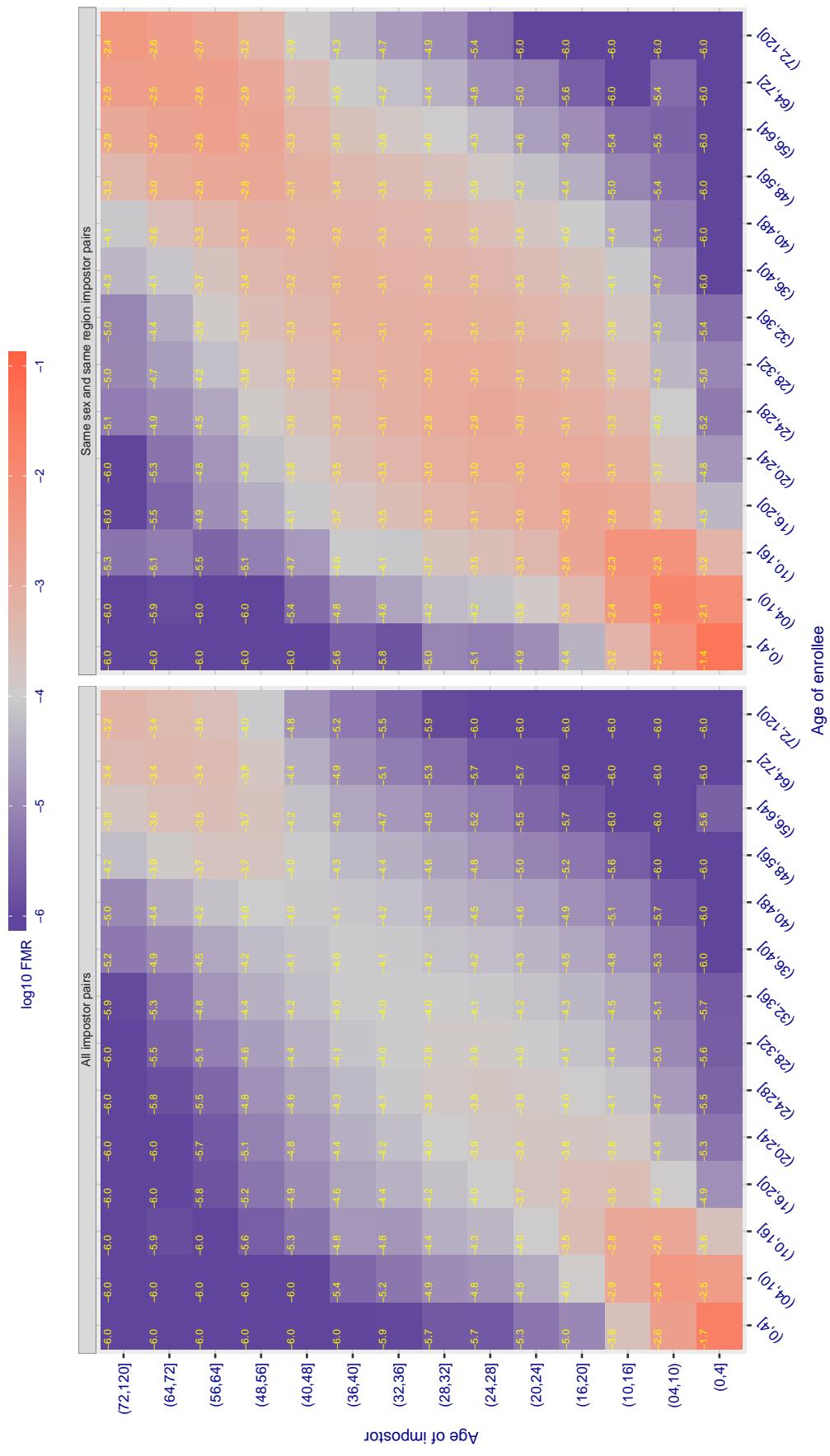


Figure 543: For algorithm synthesis-005 operating on visa images, the heatmap shows false match observed over impostor comparisons of faces from different individuals who have the given age pair. False matches are counted against a recognition threshold fixed globally to give $FMR = 0.0001$ over all on the order of 10^{10} impostor comparisons. The text in each box gives the same quantity as that coded by the color. Light colors present a security vulnerability to, for example, a passport gate.

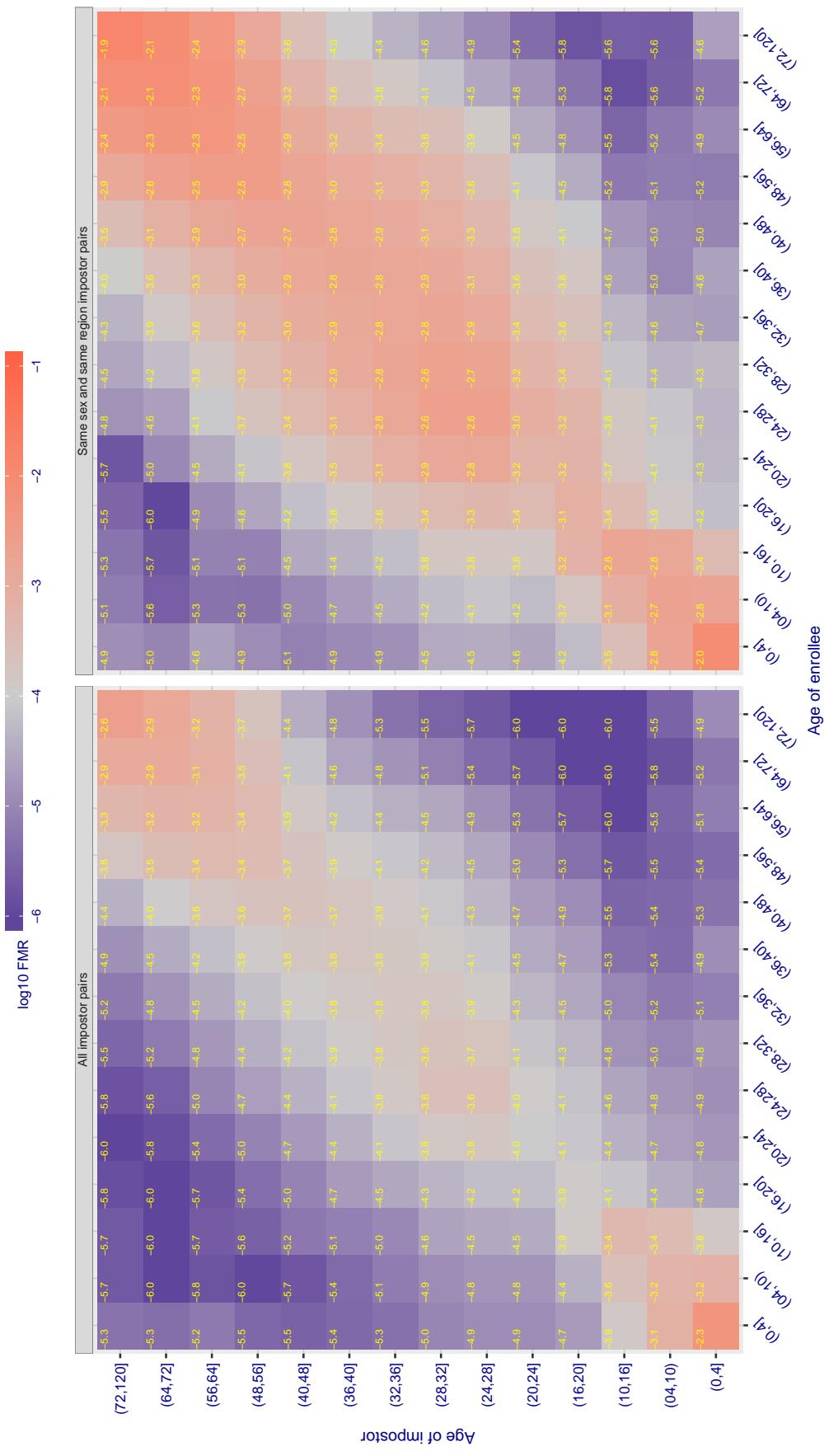
Cross age FMR at threshold T = 147.661 for algorithm tech5_002, giving $FMR(T) = 0.0001$ globally.

Figure 544: For algorithm tech5-002 operating on visa images, the heatmap shows false match observed over impostor comparisons of faces from different individuals who have the given age pair. False matches are counted against a recognition threshold fixed globally to give $FMR = 0.0001$ over all on the order of 10^{10} impostor comparisons. The text in each box gives the same quantity as that coded by the color. Light colors present a security vulnerability to, for example, a passport gate.

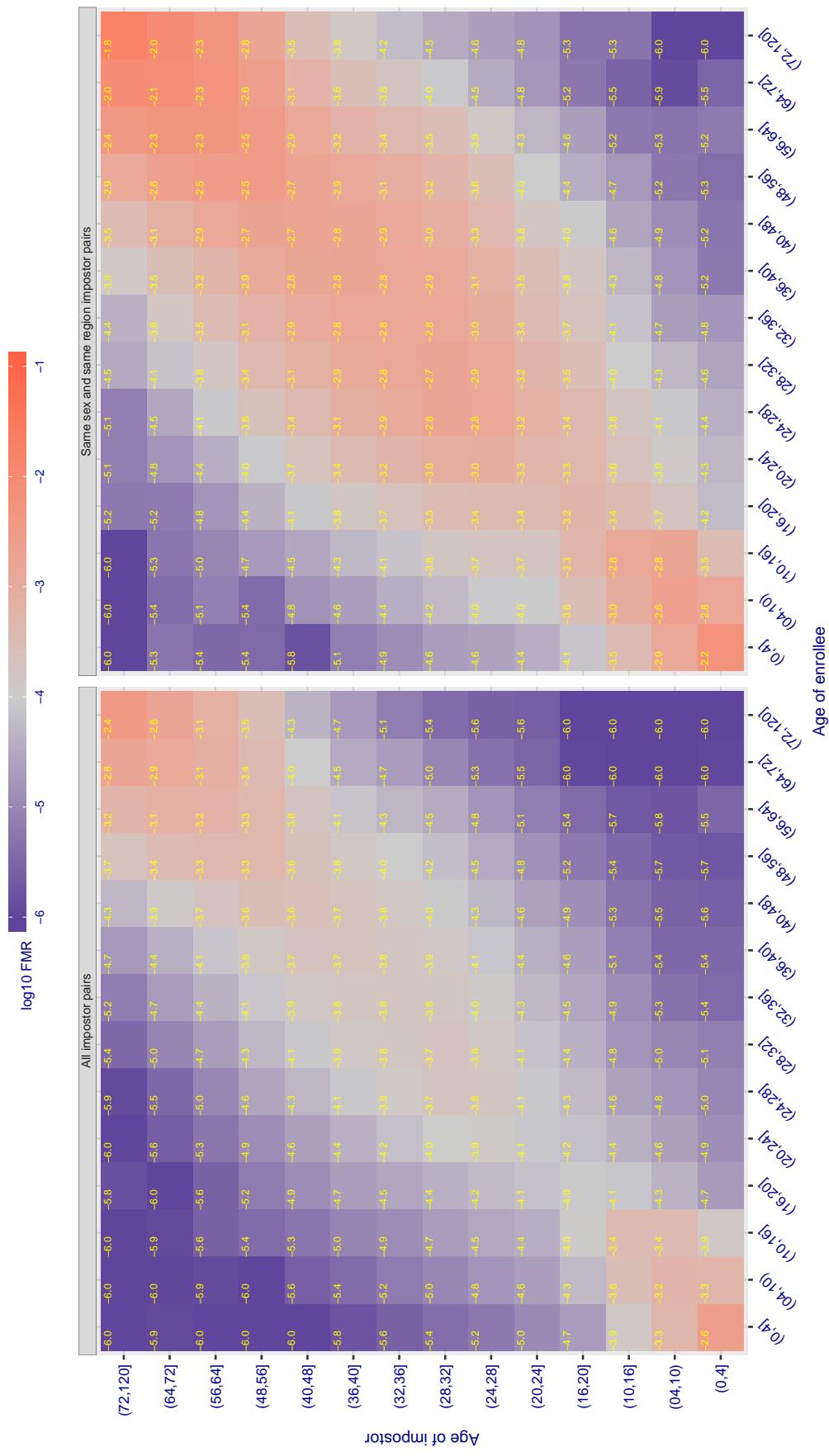
Cross age FMR at threshold T = 147.080 for algorithm tech5_003, giving $FMR(T) = 0.0001$ globally.

Figure 545: For algorithm tech5-003 operating on visa images, the heatmap shows false match observed over impostor comparisons of faces from different individuals who have the given age pair. False matches are counted against a recognition threshold fixed globally to give $FMR = 0.0001$ over all on the order of 10^{10} impostor comparisons. The text in each box gives the same quantity as that coded by the color. Light colors present a security vulnerability to, for example, a passport gate.

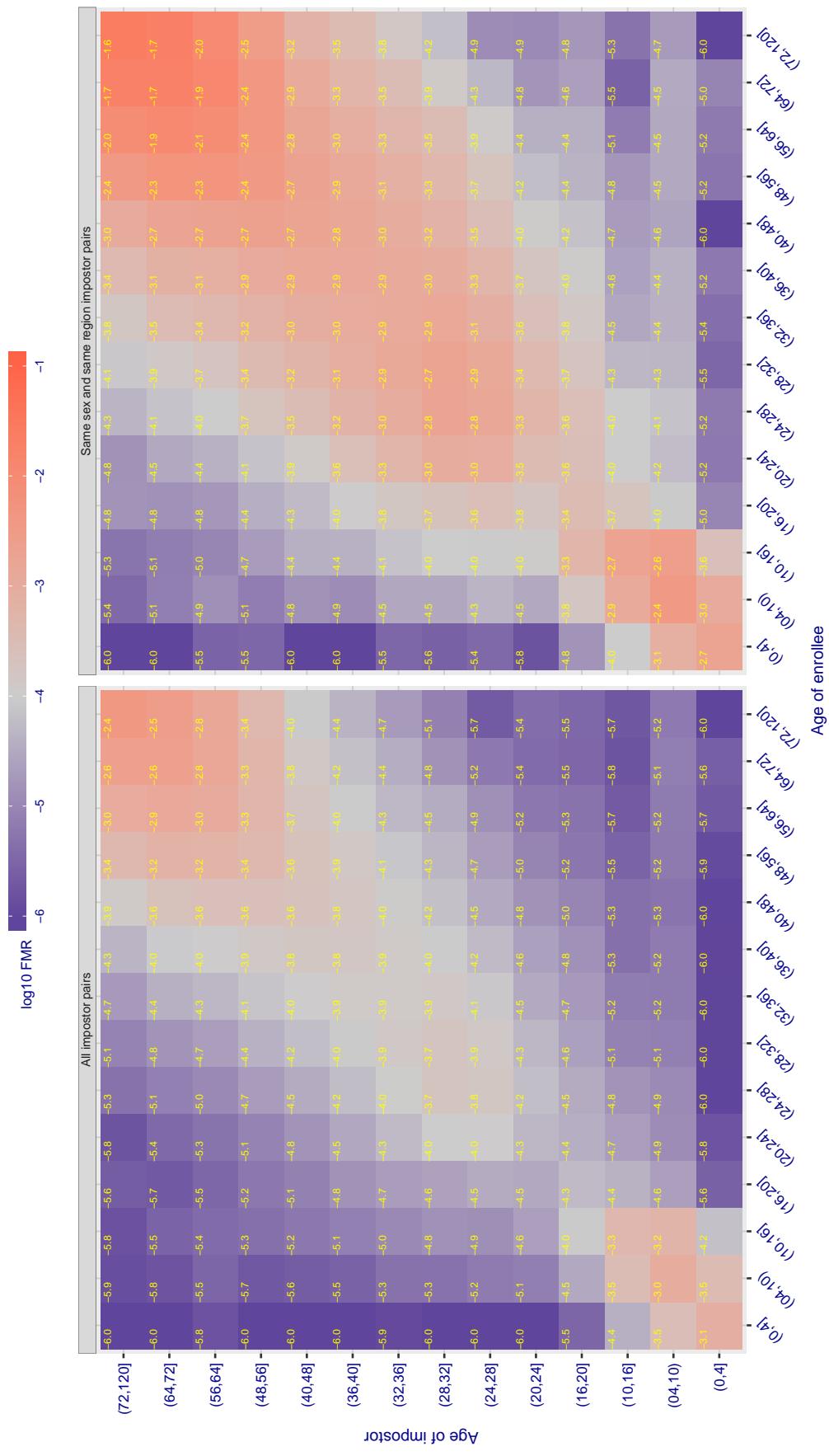
Cross age FMR at threshold T = 0.896 for algorithm tevian_003, giving $\text{FMR}(\text{T}) = 0.0001$ globally.

Figure 546: For algorithm tevian-003 operating on visa images, the heatmap shows false match observed over impostor comparisons of faces from different individuals who have the given age pair. False matches are counted against a recognition threshold fixed globally to give $\text{FMR} = 0.0001$ over all on the order of 10^{10} impostor comparisons. The text in each box gives the same quantity as that coded by the color. Light colors present a security vulnerability to, for example, a passport gate.

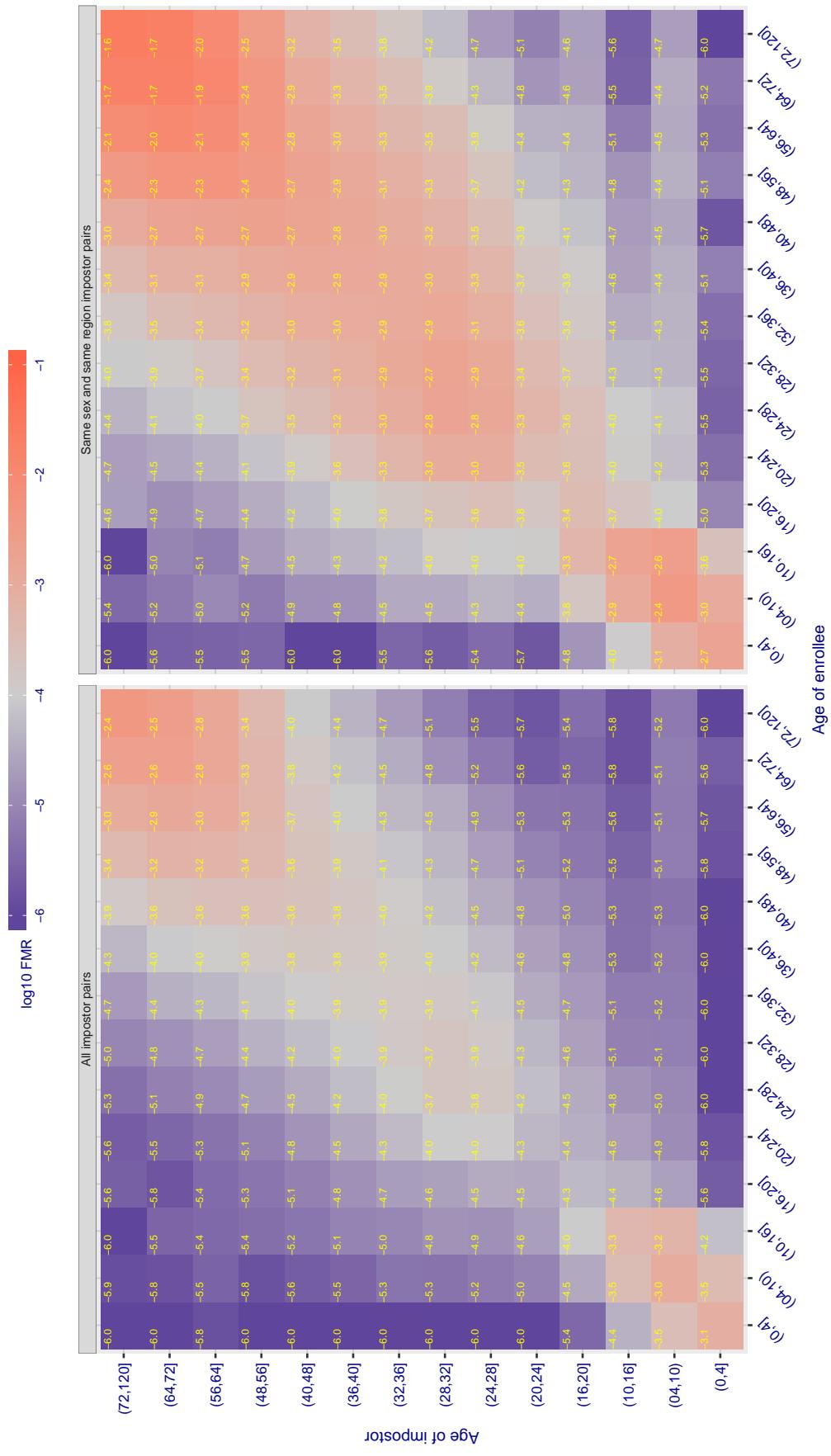
Cross age FMR at threshold T = 0.896 for algorithm tevian_004, giving $\text{FMR}(\text{T}) = 0.0001$ globally.

Figure 547: For algorithm tevian-004 operating on visa images, the heatmap shows false match observed over impostor comparisons of faces from different individuals who have the given age pair. False matches are counted against a recognition threshold fixed globally to give $\text{FMR} = 0.0001$ over all on the order of 10^{10} impostor comparisons. The text in each box gives the same quantity as that coded by the color. Light colors present a security vulnerability to, for example, a passport gate.

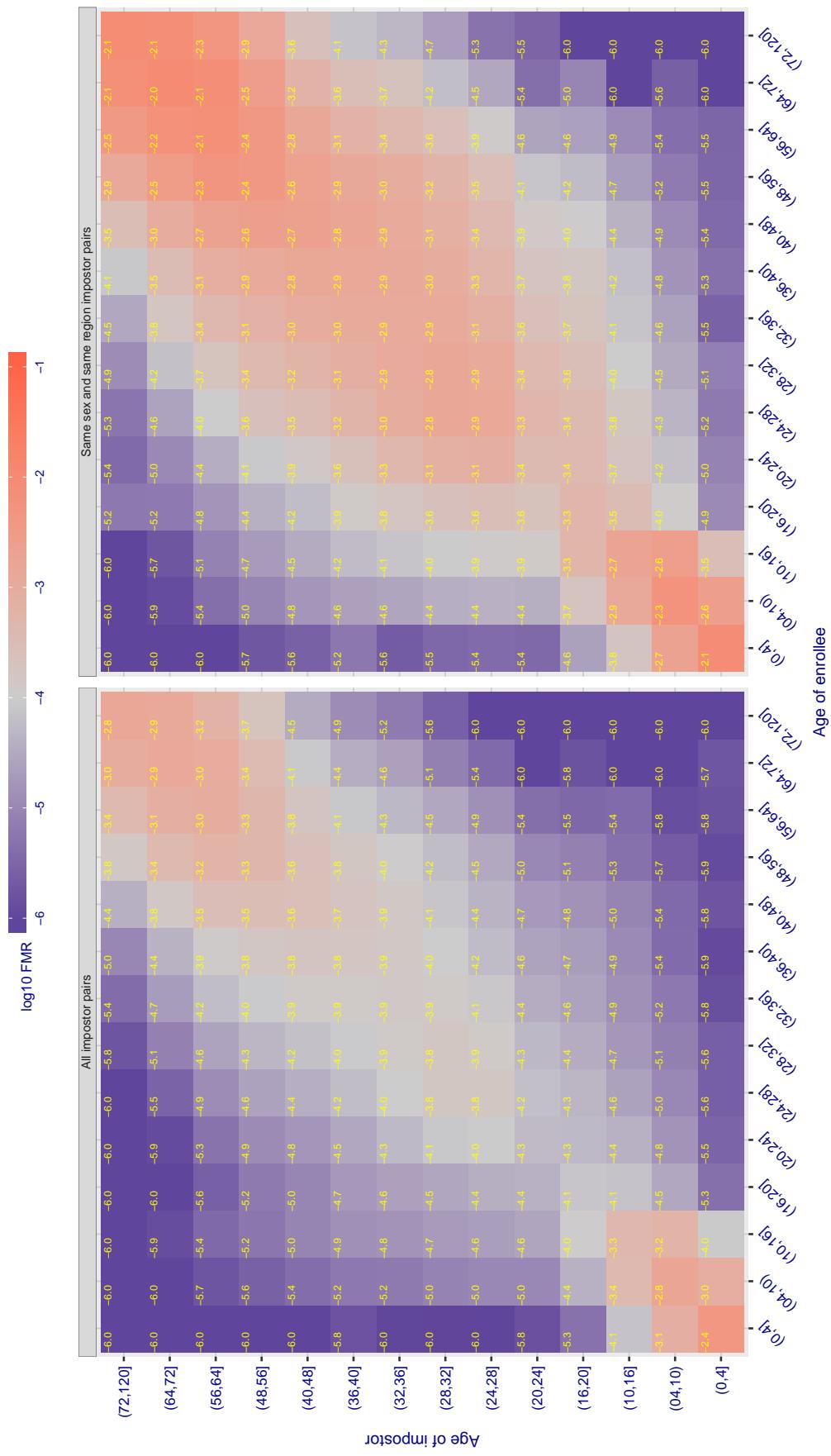
Cross age FMR at threshold T = 151.011 for algorithm tiger_002, giving $FMR(T) = 0.0001$ globally.

Figure 548: For algorithm tiger-002 operating on visa images, the heatmap shows false match observed over imposter comparisons of faces from different individuals who have the given age pair. False matches are counted against a recognition threshold fixed globally to give $FMR = 0.0001$ over all on the order of 10^{10} impostor comparisons. The text in each box gives the same quantity as that coded by the color. Light colors present a security vulnerability to, for example, a passport gate.

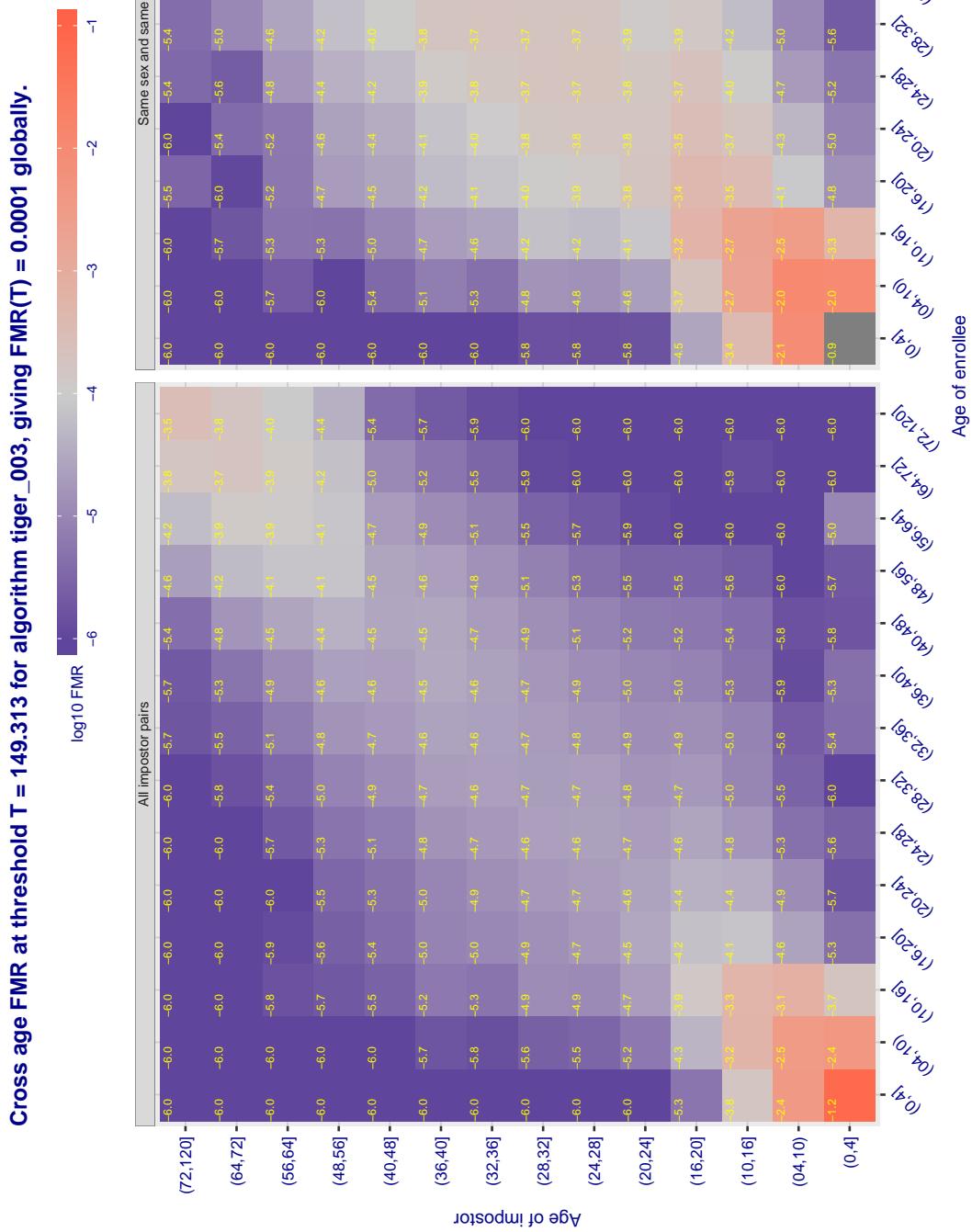


Figure 549: For algorithm tiger-003 operating on visa images, the heatmap shows false match observed over impostor comparisons of faces from different individuals who have the given age pair. False matches are counted against a recognition threshold fixed globally to give $FMR = 0.0001$ over all on the order of 10^{10} impostor comparisons. The text in each box gives the same quantity as that coded by the color. Light colors present a security vulnerability to, for example, a passport gate.

Cross age FMR at threshold T = 43.677 for algorithm tongyi_005, giving FMR(T) = 0.0001 globally.

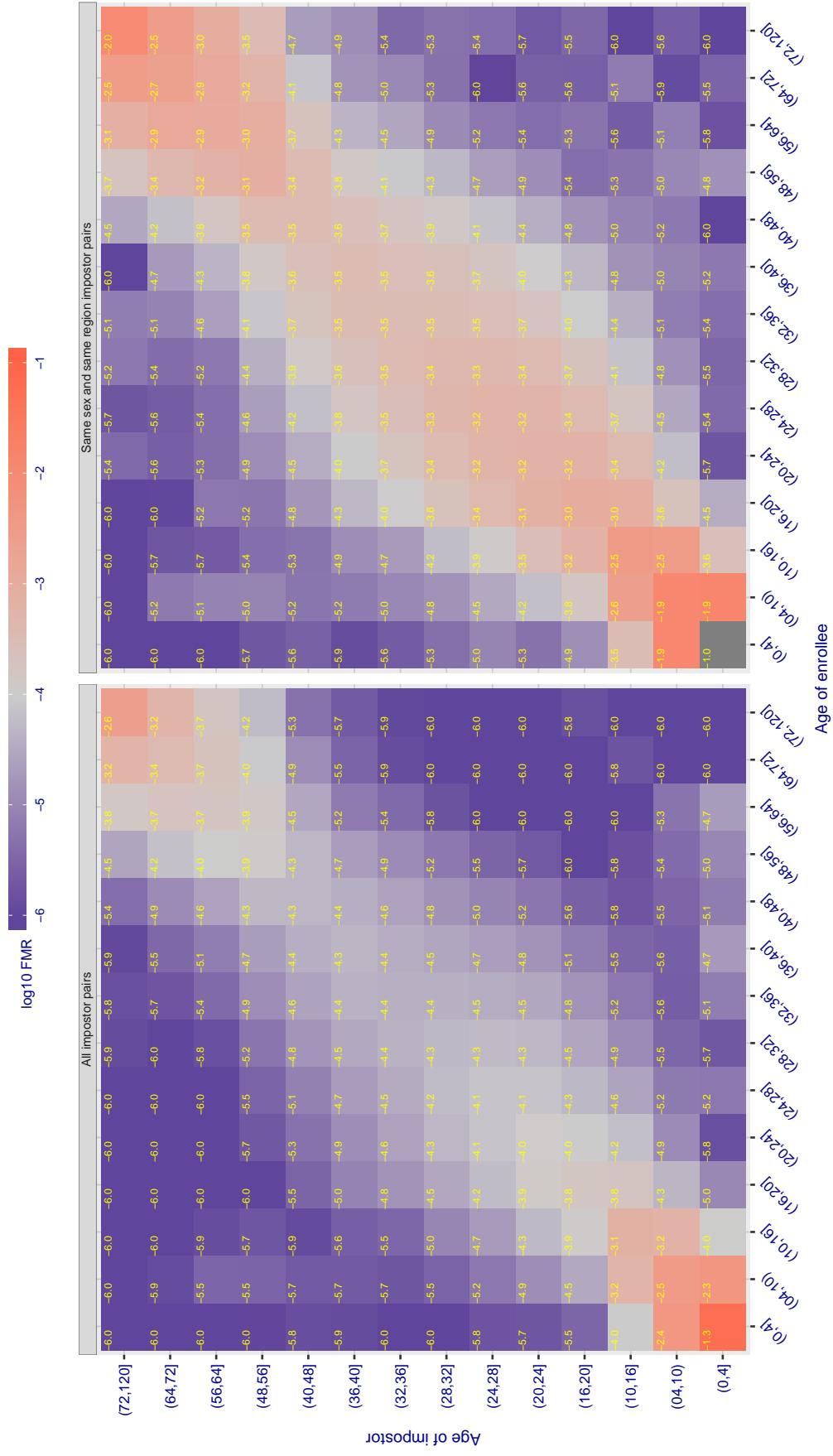


Figure 550: For algorithm tongyi-005 operating on visa images, the heatmap shows false match observed over impostor comparisons of faces from different individuals who have the given age pair. False matches are counted against a recognition threshold fixed globally to give FMR = 0.0001 over all on the order of 10^{10} impostor comparisons. The text in each box gives the same quantity as that coded by the color. Light colors present a security vulnerability to, for example, a passport gate.

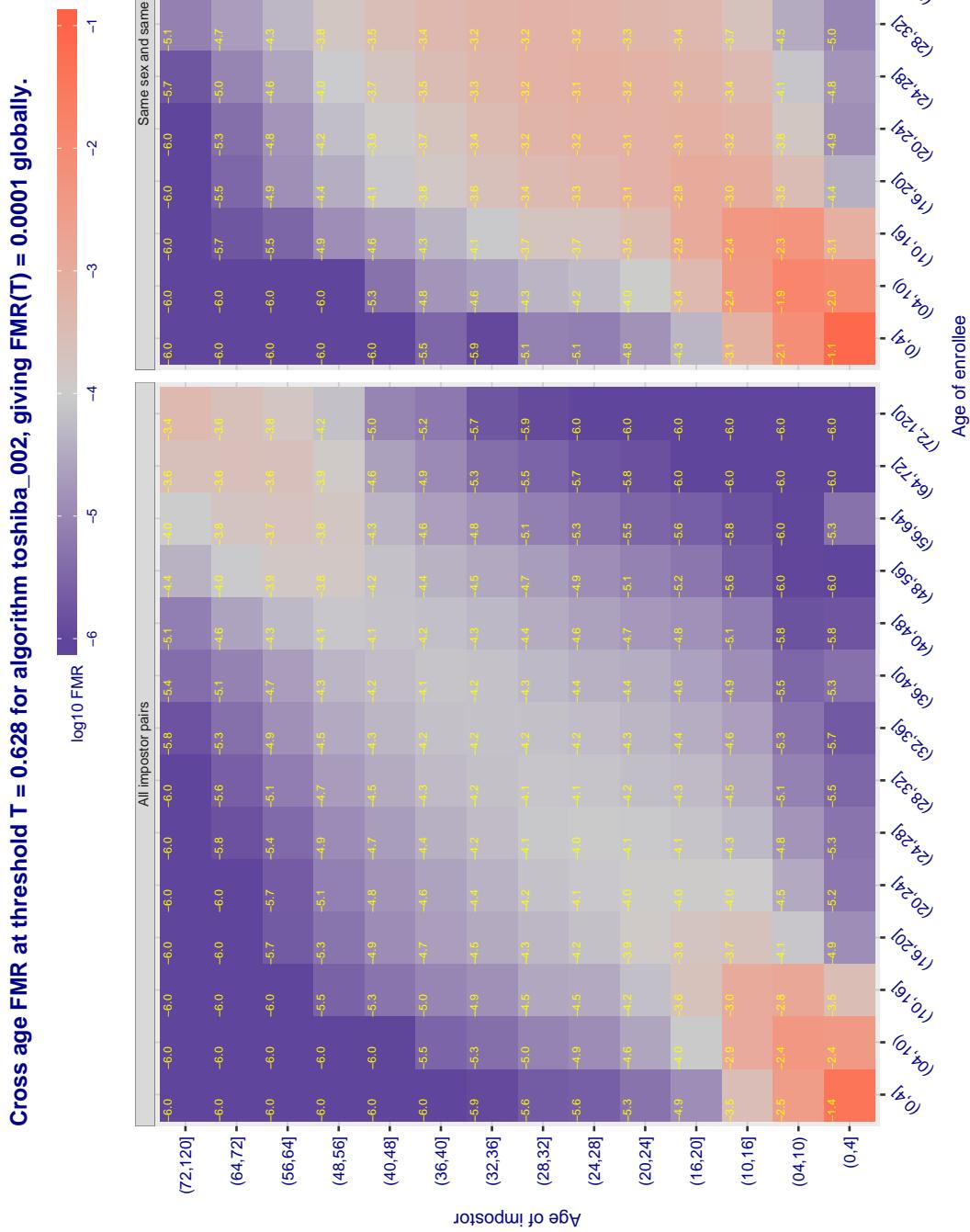


Figure 551: For algorithm toshiba-002 operating on visa images, the heatmap shows false match observed over impostor comparisons of faces from different individuals who have the given age pair. False matches are counted against a recognition threshold fixed globally to give $FMR = 0.0001$ over all on the order of 10^{10} impostor comparisons. The text in each box gives the same quantity as that coded by the color. Light colors present a security vulnerability to, for example, a passport gate.

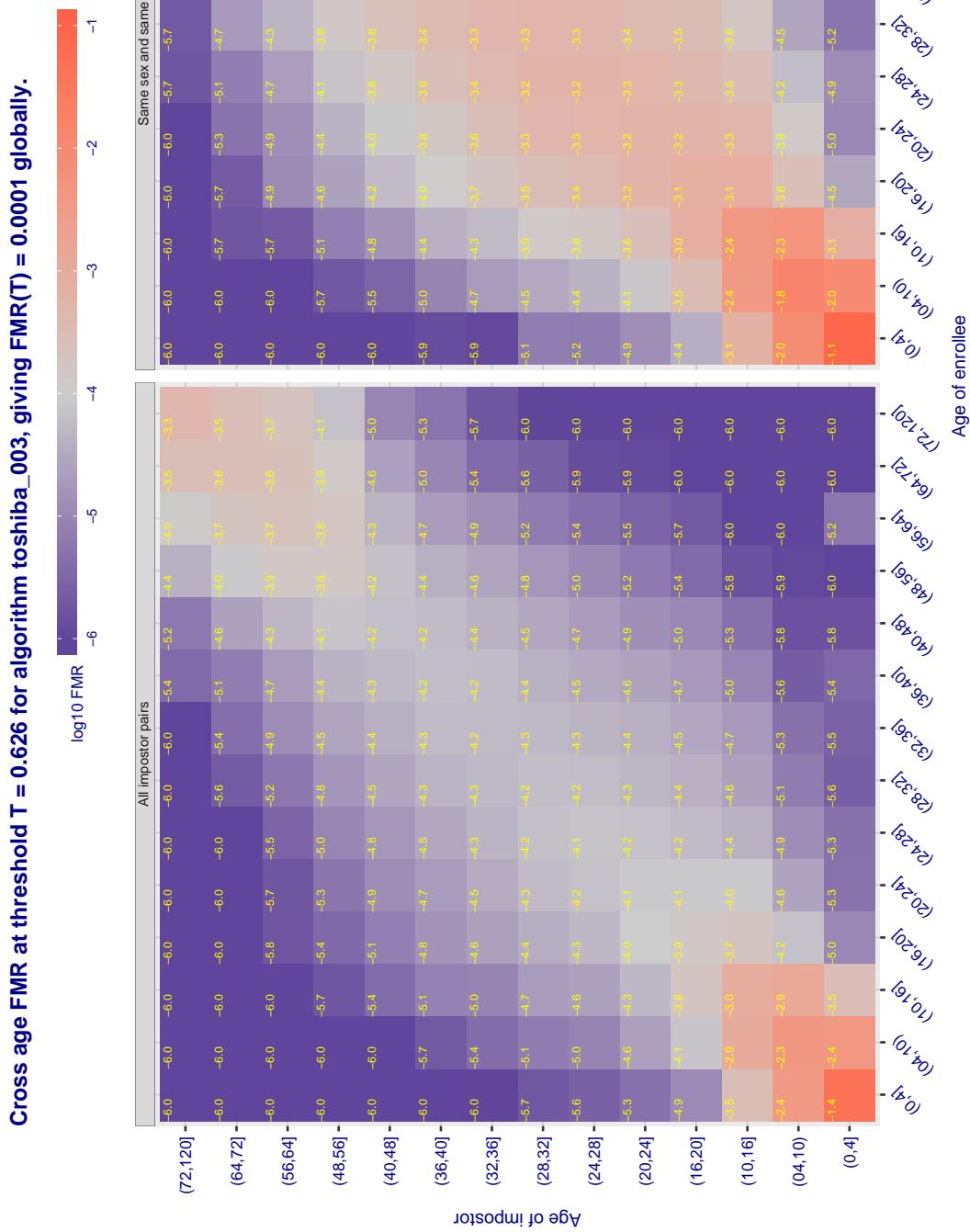


Figure 552: For algorithm toshiba-003 operating on visa images, the heatmap shows false match observed over impostor comparisons of faces from different individuals who have the given age pair. False matches are counted against a recognition threshold fixed globally to give $FMR = 0.0001$ over all on the order of 10^{10} impostor comparisons. The text in each box gives the same quantity as that coded by the color. Light colors present a security vulnerability to, for example, a passport gate.

Cross age FMR at threshold T = 0.151 for algorithm ulsee_001, giving FMR(T) = 0.0001 globally.

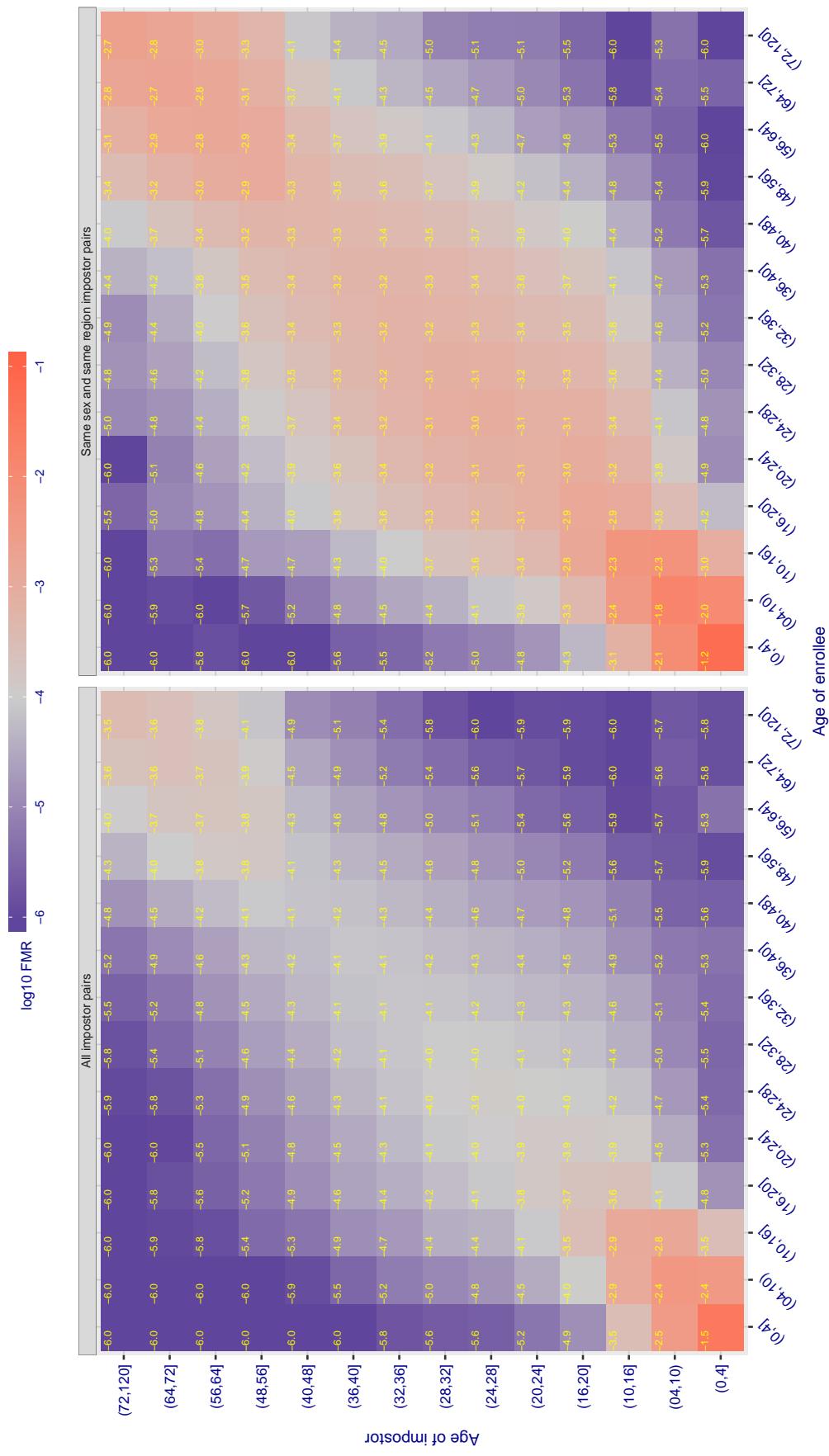


Figure 553: For algorithm ulsee-001 operating on visa images, the heatmap shows false match observed over impostor comparisons of faces from different individuals who have the given age pair. False matches are counted against a recognition threshold fixed globally to give $FMR = 0.0001$ over all on the order of 10^{10} impostor comparisons. The text in each box gives the same quantity as that coded by the color. Light colors present a security vulnerability to, for example, a passport gate.

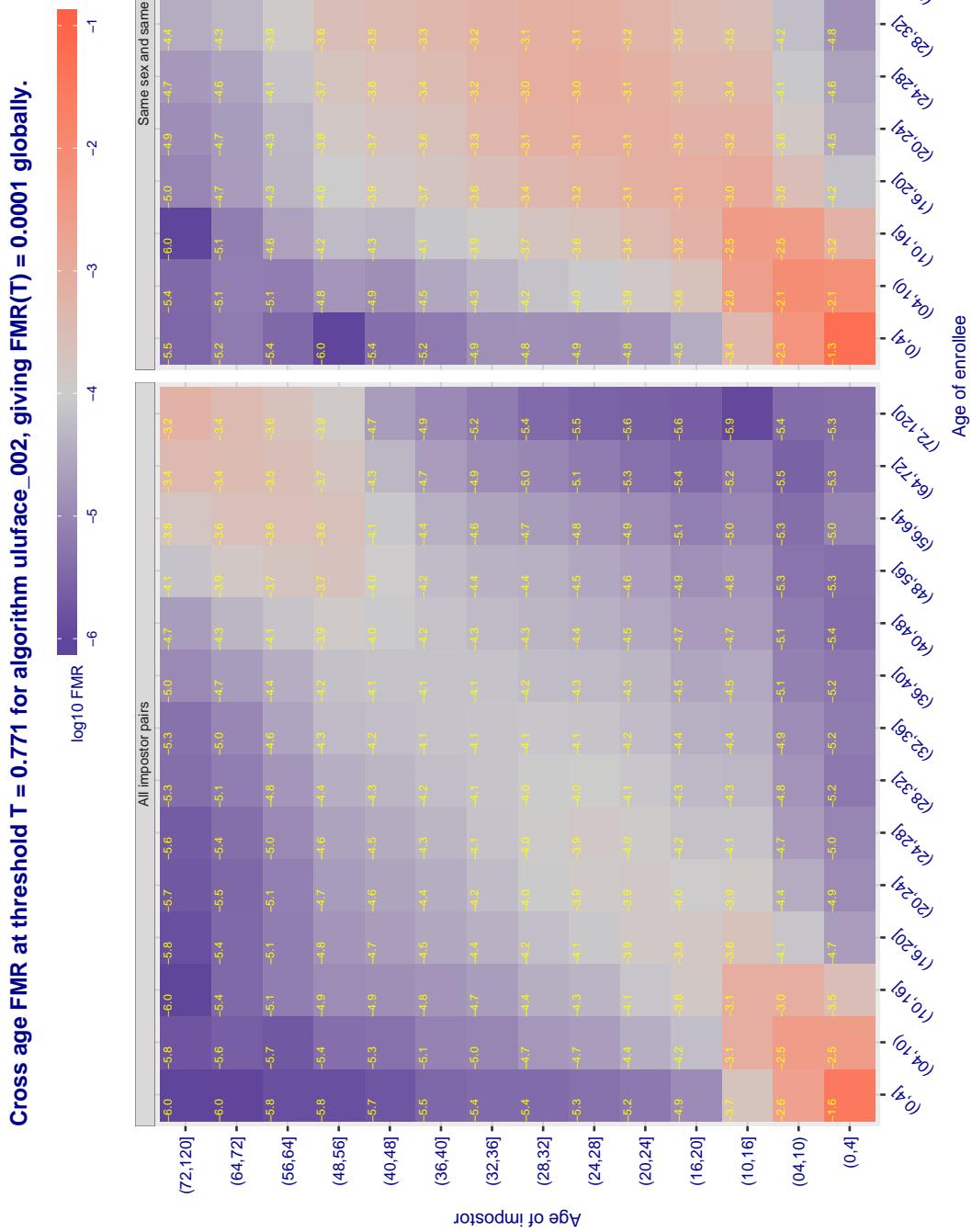


Figure 554: For algorithm uluface-002 operating on visa images, the heatmap shows false match observed over impostor comparisons of faces from different individuals who have the given age pair. False matches are counted against a recognition threshold fixed globally to give $FMR = 0.0001$ over all on the order of 10^{10} impostor comparisons. The text in each box gives the same quantity as that coded by the color. Light colors present a security vulnerability to, for example, a passport gate.

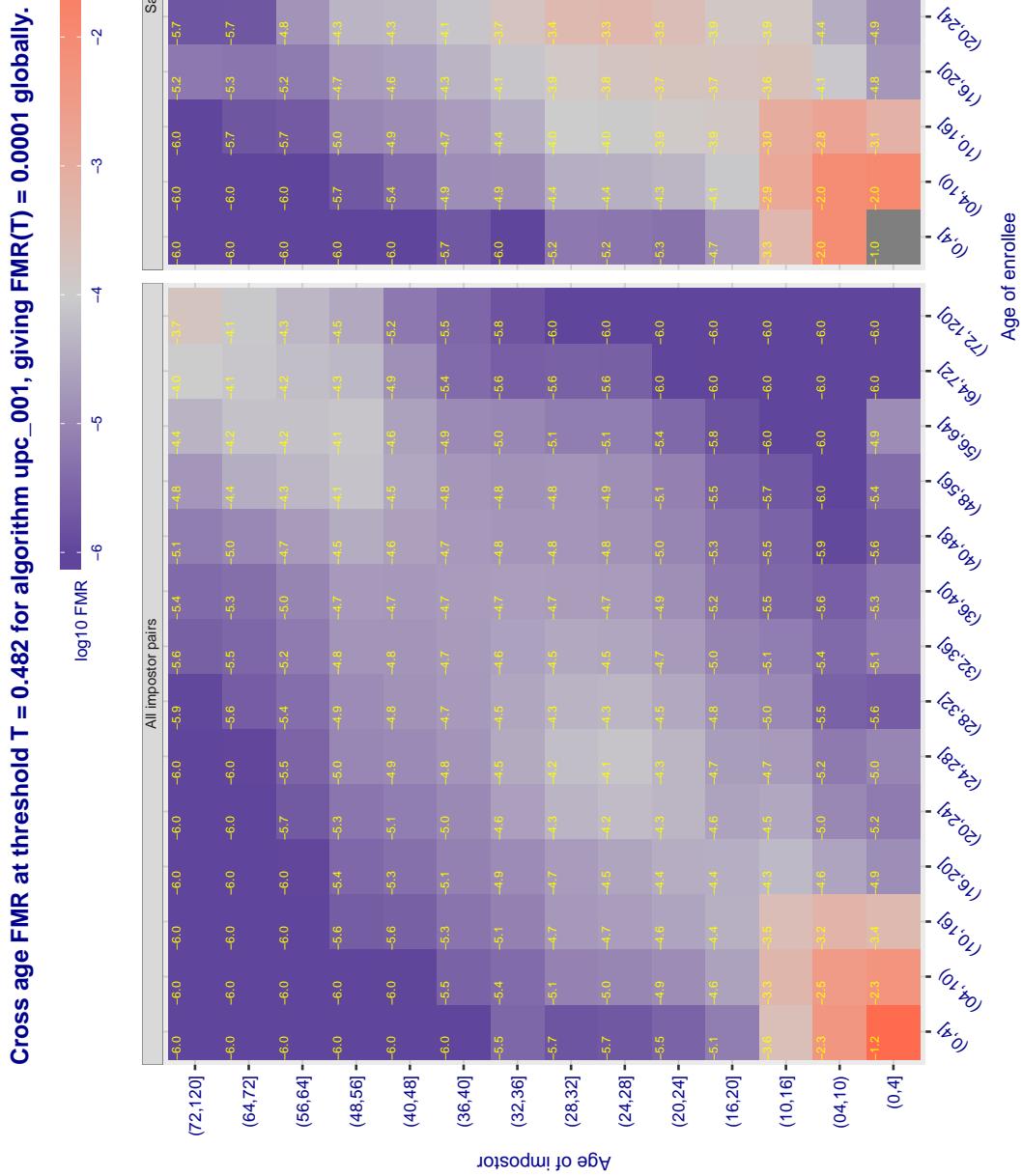


Figure 555: For algorithm upc-001 operating on visa images, the heatmap shows false match observed over impostor comparisons of faces from different individuals who have the given age pair. False matches are counted against a recognition threshold fixed globally to give $FMR = 0.0001$ over all on the order of 10^{10} impostor comparisons. The text in each box gives the same quantity as that coded by the color. Light colors present a security vulnerability to, for example, a passport gate.

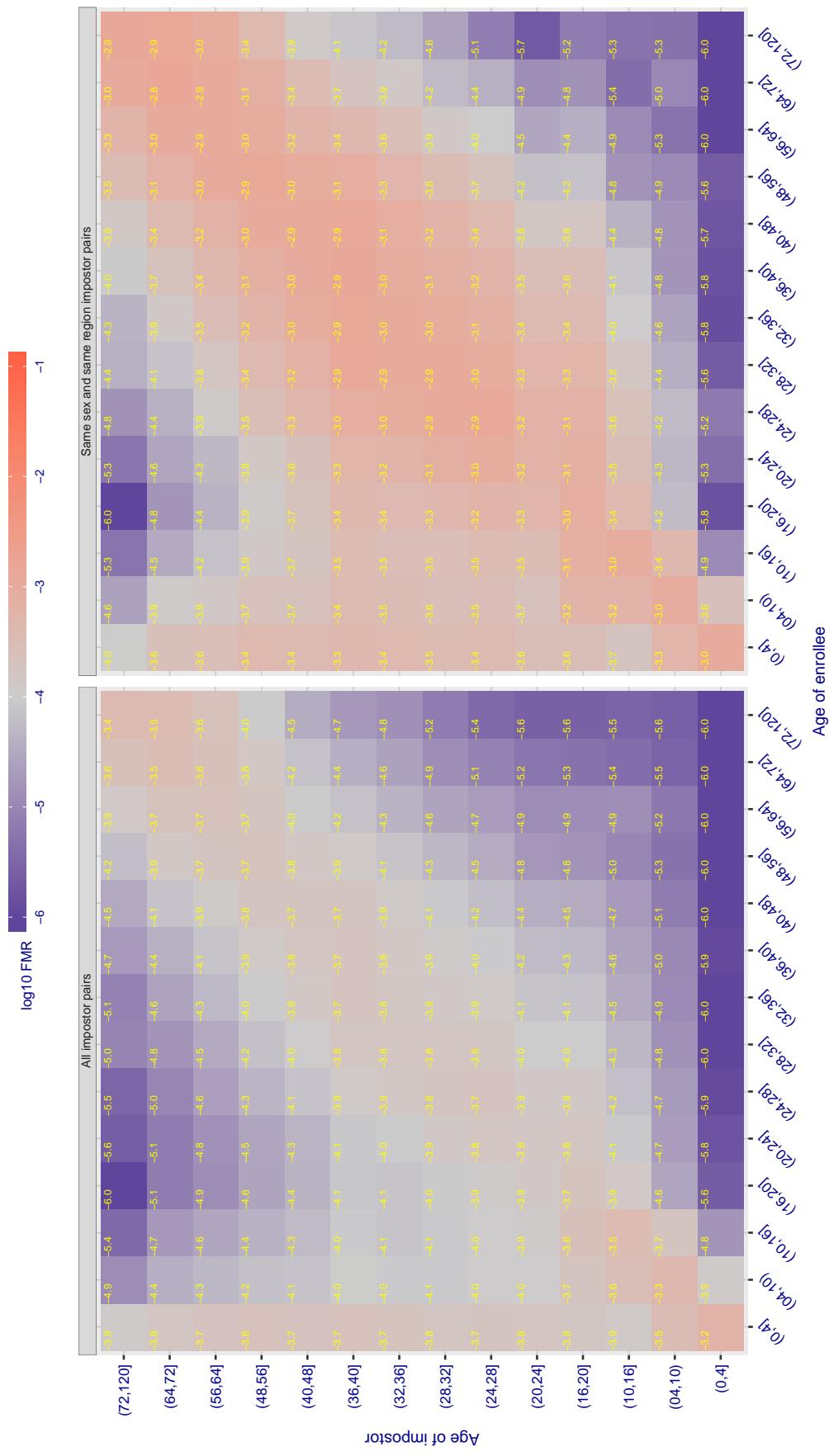
Cross age FMR at threshold T = 0.423 for algorithm vcog_002, giving $FMR(T) = 0.0001$ globally.

Figure 556: For algorithm vcog_002 operating on visa images, the heatmap shows false match observed over impostor comparisons of faces from different individuals who have the given age pair. False matches are counted against a recognition threshold fixed globally to give $FMR = 0.0001$ over all on the order of 10^{10} impostor comparisons. The text in each box gives the same quantity as that coded by the color. Light colors present a security vulnerability to, for example, a passport gate.

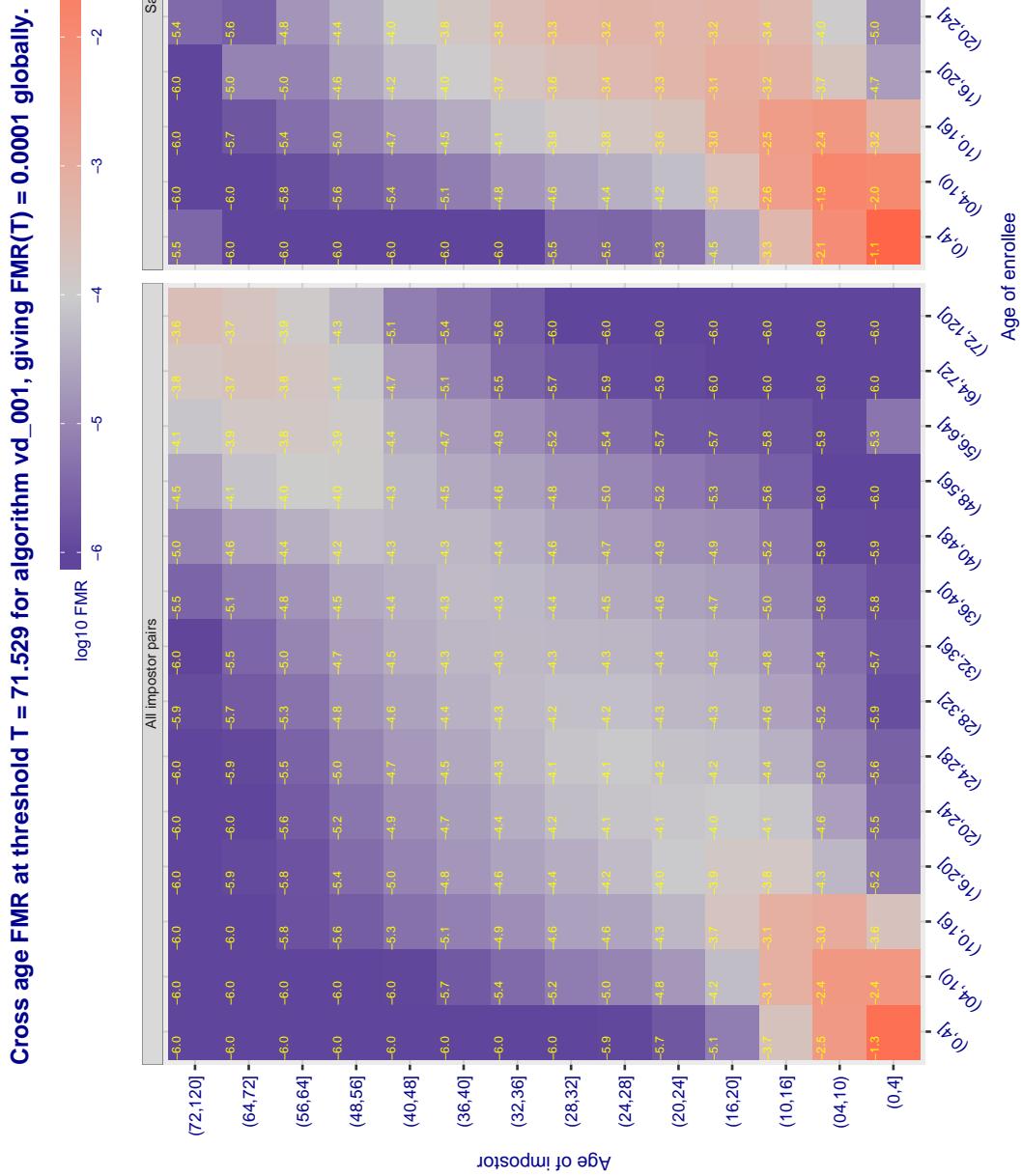


Figure 557: For algorithm vd-001 operating on visa images, the heatmap shows false match observed over impostor comparisons of faces from different individuals who have the given age pair. False matches are counted against a recognition threshold fixed globally to give $FMR = 0.0001$ over all on the order of 10^{10} impostor comparisons. The text in each box gives the same quantity as that coded by the color. Light colors present a security vulnerability to, for example, a passport gate.

Cross age FMR at threshold T = 3.325 for algorithm veridas_001, giving FMR(T) = 0.0001 globally.

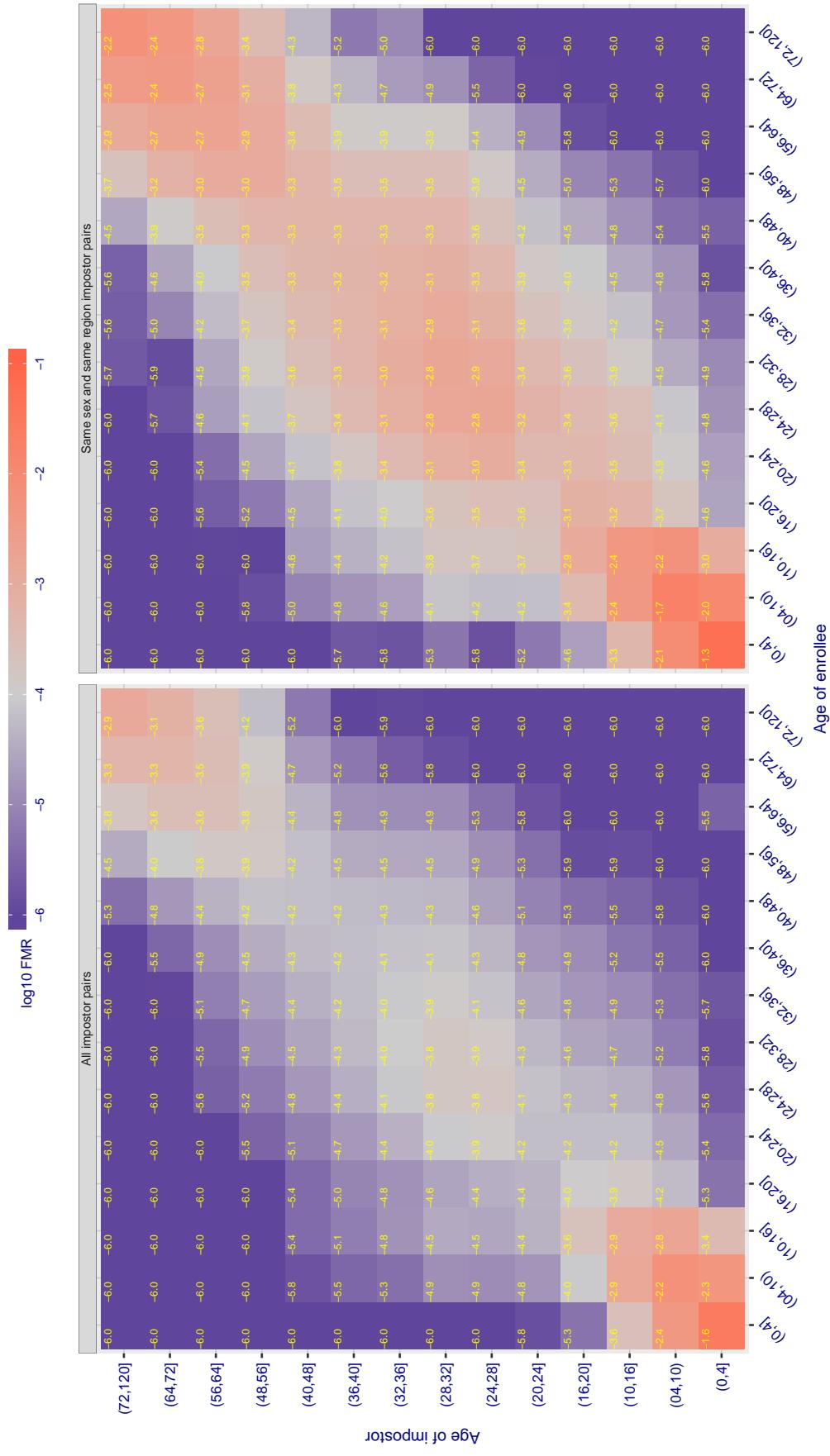


Figure 558: For algorithm veridas-001 operating on visa images, the heatmap shows false match observed over impostor comparisons of faces from different individuals who have the given age pair. False matches are counted against a recognition threshold fixed globally to give $FMR = 0.0001$ over all on the order of 10^{10} impostor comparisons. The text in each box gives the same quantity as that coded by the color. Light colors present a security vulnerability to, for example, a passport gate.

Cross age FMR at threshold T = 3.389 for algorithm veridas_002, giving FMR(T) = 0.0001 globally.

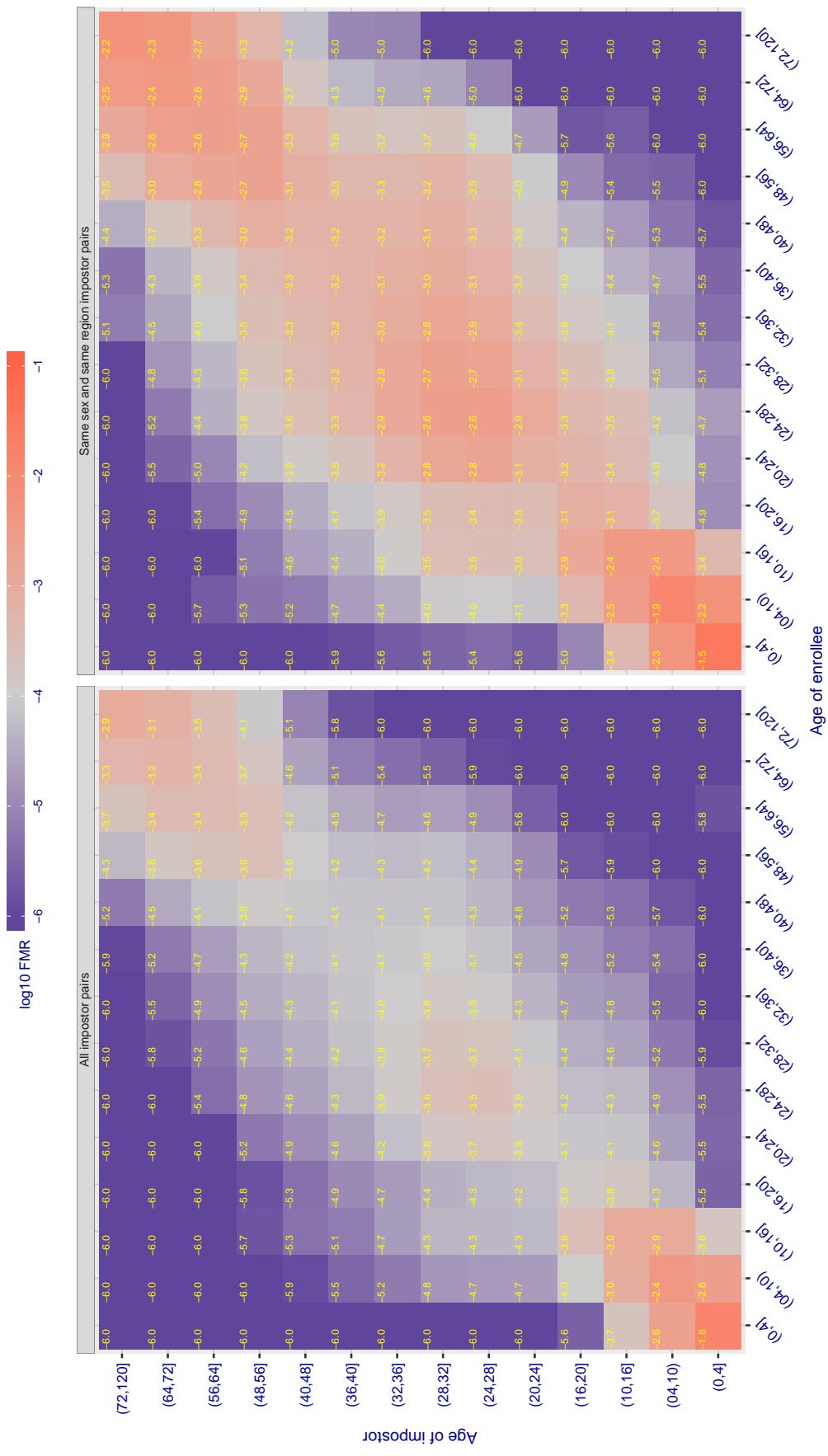


Figure 559: For algorithm veridas-002 operating on visa images, the heatmap shows false match observed over impostor comparisons of faces from different individuals who have the given age pair. False matches are counted against a recognition threshold fixed globally to give $FMR = 0.0001$ over all on the order of 10^{10} impostor comparisons. The text in each box gives the same quantity as that coded by the color. Light colors present a security vulnerability to, for example, a passport gate.

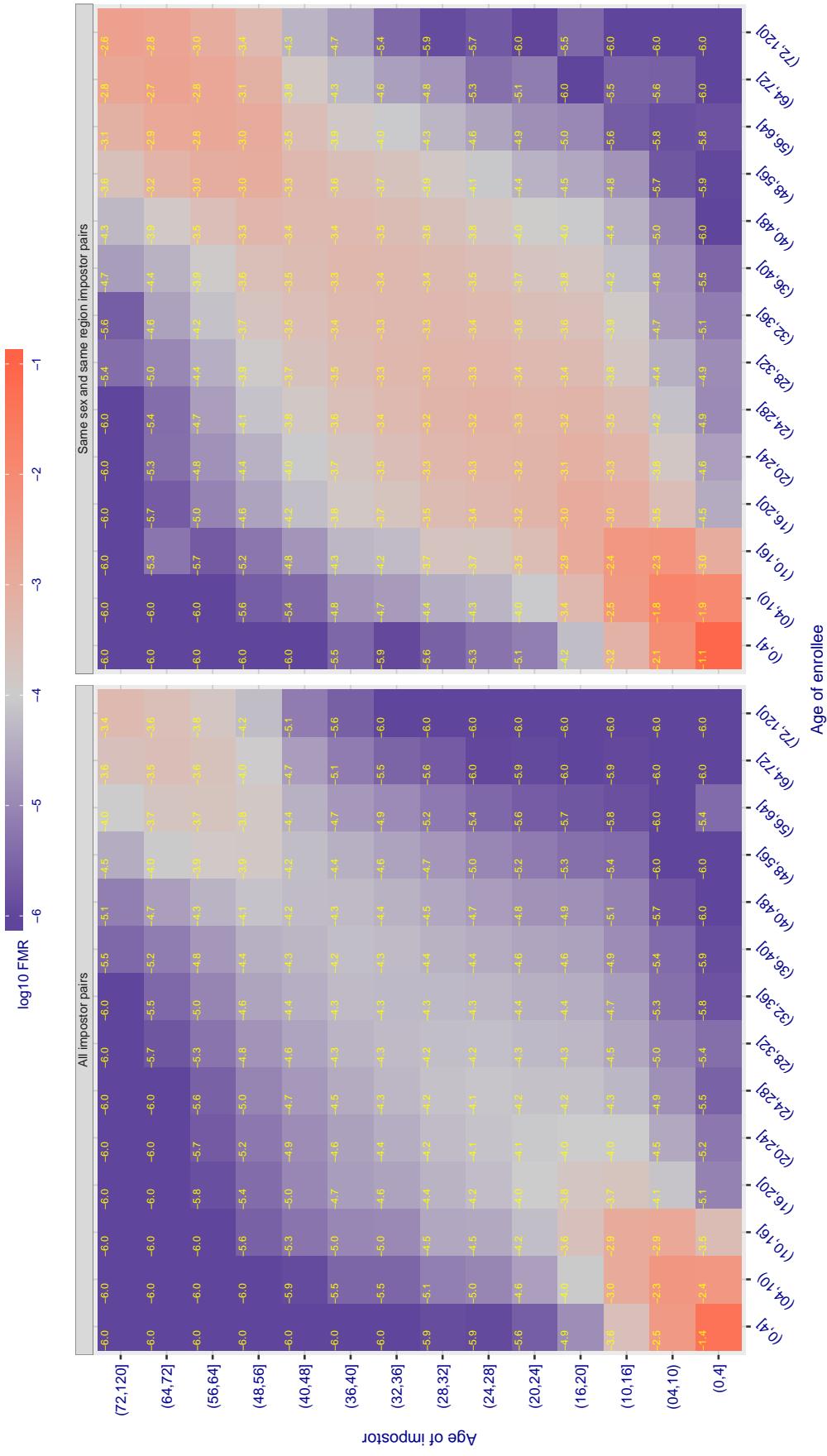
Cross age FMR at threshold T = 2.859 for algorithm via_000, giving $FMR(T) = 0.0001$ globally.

Figure 560: For algorithm via_000 operating on visa images, the heatmap shows false match observed over impostor comparisons of faces from different individuals who have the given age pair. False matches are counted against a recognition threshold fixed globally to give $FMR = 0.0001$ over all on the order of 10^{10} impostor comparisons. The text in each box gives the same quantity as that coded by the color. Light colors present a security vulnerability to, for example, a passport gate.

Cross age FMR at threshold T = 0.842 for algorithm videonetics_001, giving FMR(T) = 0.0001 globally.

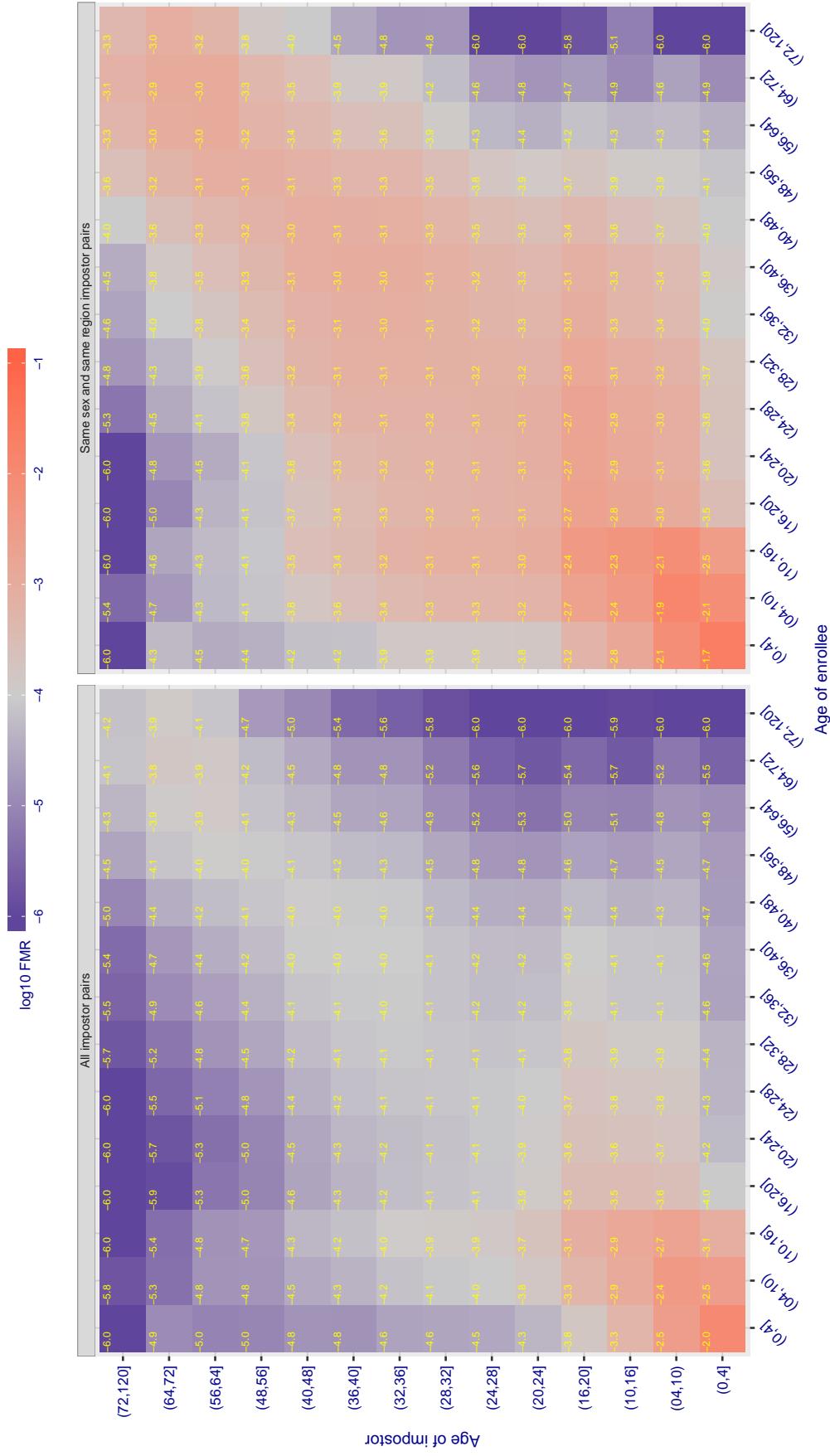


Figure 561: For algorithm videonetics-001 operating on visa images, the heatmap shows false match observed over impostor comparisons of faces from different individuals who have the given age pair. False matches are counted against a recognition threshold fixed globally to give $FMR = 0.0001$ over all on the order of 10^{10} impostor comparisons. The text in each box gives the same quantity as that coded by the color. Light colors present a security vulnerability to, for example, a passport gate.

Cross age FMR at threshold T = 3.057 for algorithm vigilantsolutions_006, giving FMR(T) = 0.0001 globally.

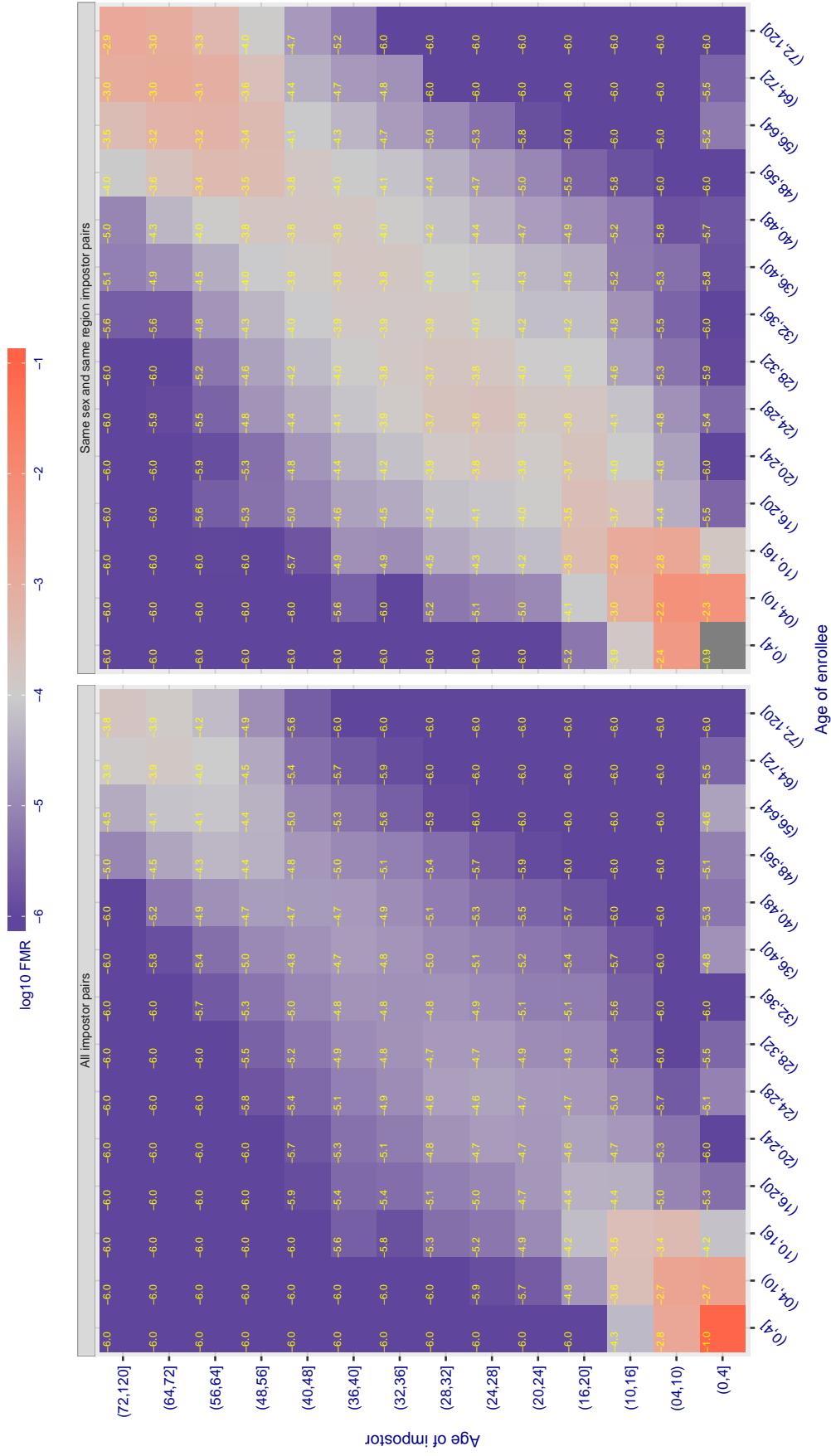


Figure 562: For algorithm vigilantsolutions-006 operating on visa images, the heatmap shows false match observed over impostor comparisons of faces from different individuals who have the given age pair. False matches are counted against a recognition threshold fixed globally to give $\text{FMR} = 0.0001$ over all on the order of 10^{10} impostor comparisons. The text in each box gives the same quantity as that coded by the color. Light colors present a security vulnerability to, for example, a passport gate.

Cross age FMR at threshold T = 2.926 for algorithm vigilantsolutions_007, giving FMR(T) = 0.0001 globally.

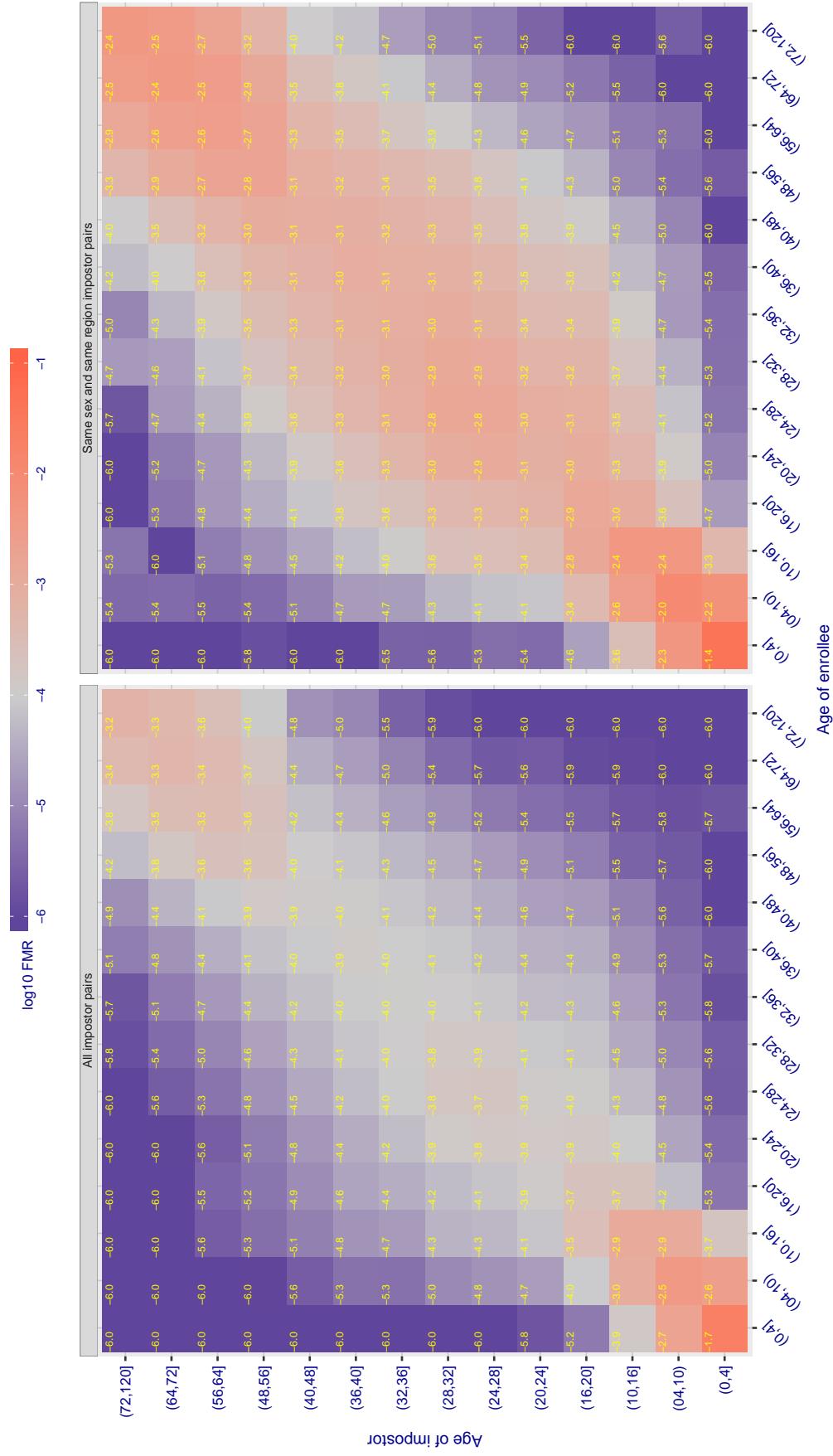


Figure 563: For algorithm vigilantsolutions-007 operating on visa images, the heatmap shows false match observed over impostor comparisons of faces from different individuals who have the given age pair. False matches are counted against a recognition threshold fixed globally to give $FMR = 0.0001$ over all on the order of 10^{10} impostor comparisons. The text in each box gives the same quantity as that coded by the color. Light colors present a security vulnerability to, for example, a passport gate.

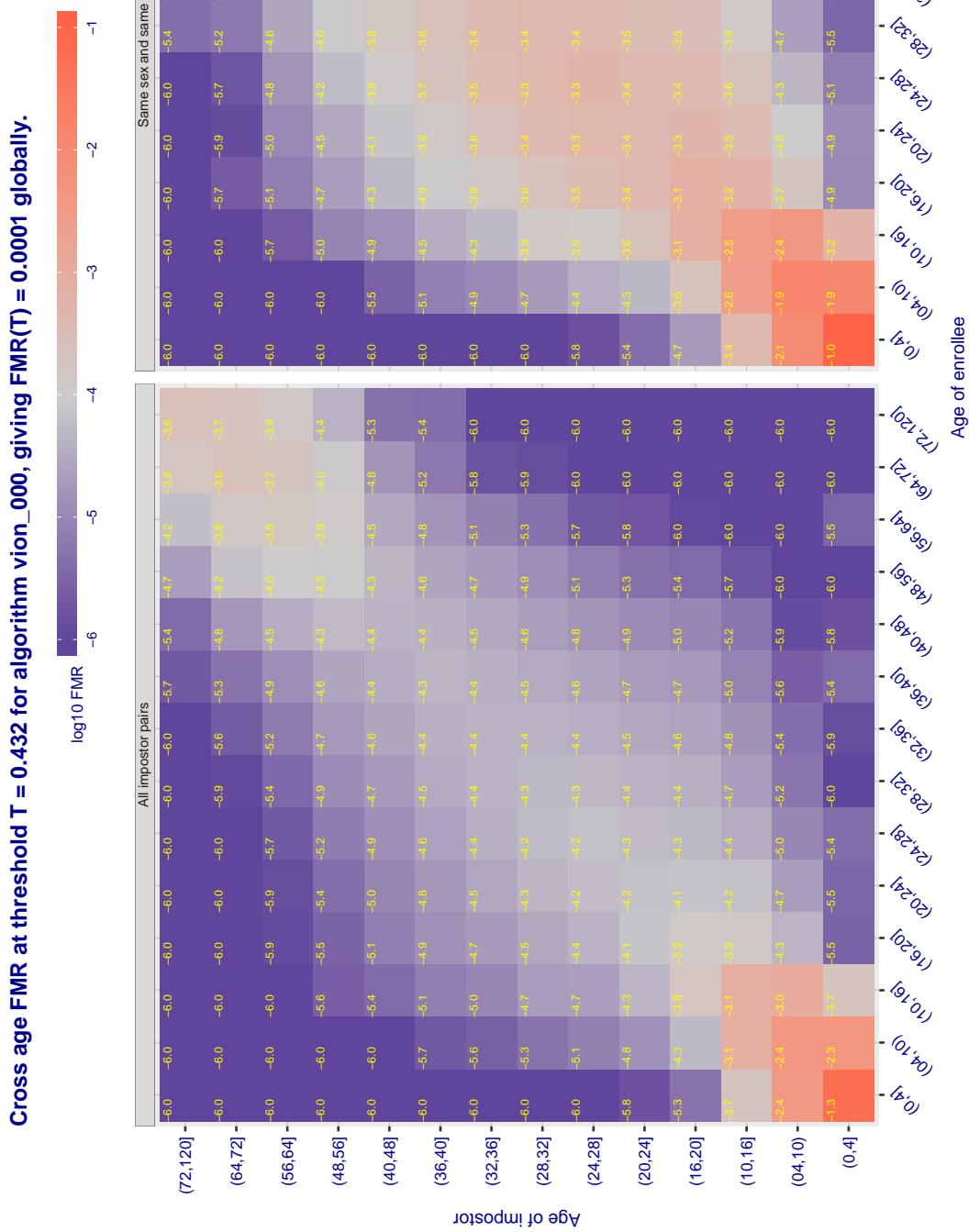


Figure 564: For algorithm vion-000 operating on visa images, the heatmap shows false match observed over impostor comparisons of faces from different individuals who have the given age pair. False matches are counted against a recognition threshold fixed globally to give $FMR = 0.0001$ over all on the order of 10^{10} impostor comparisons. The text in each box gives the same quantity as that coded by the color. Light colors present a security vulnerability to, for example, a passport gate.

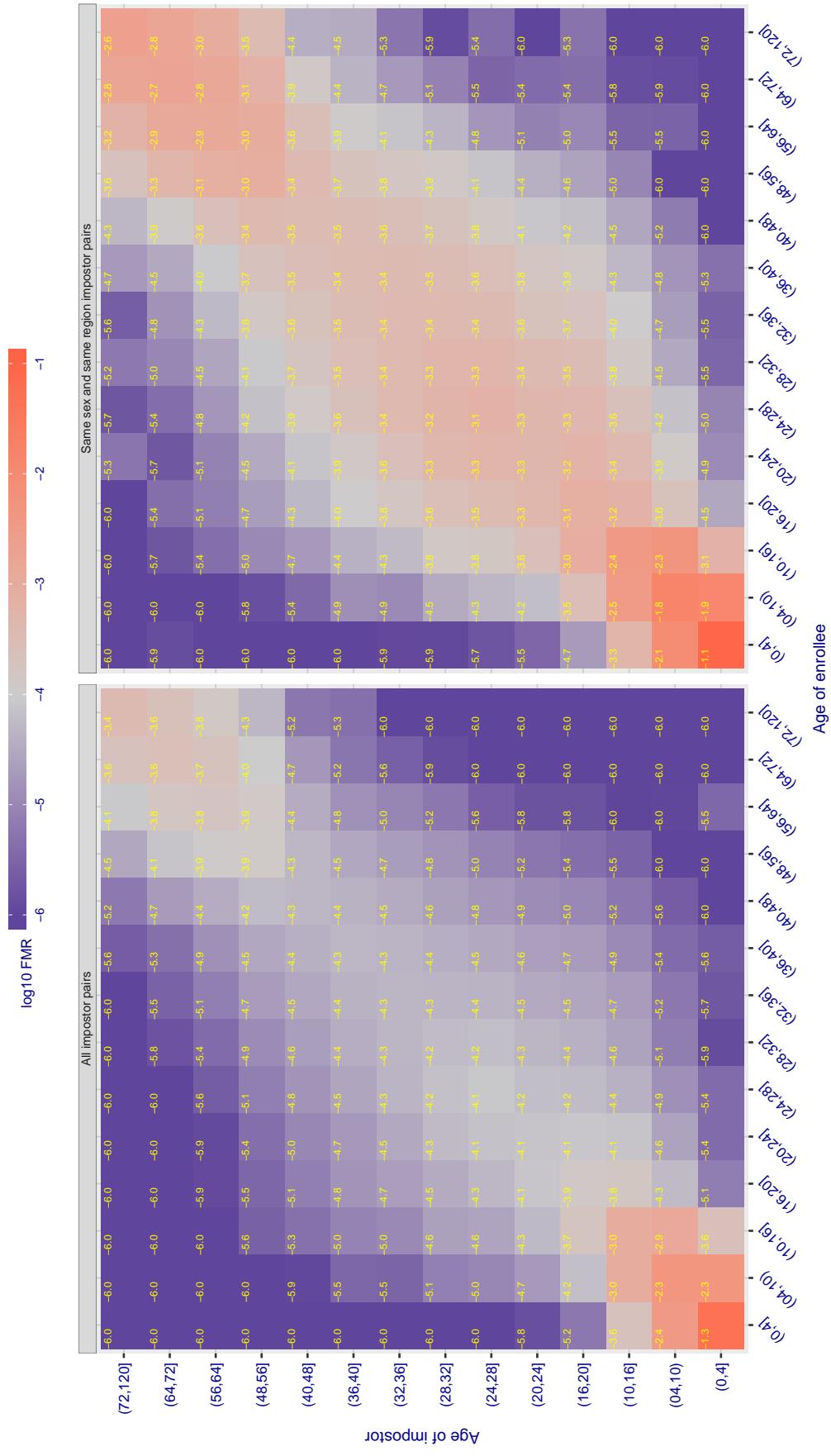
Cross age FMR at threshold T = 0.433 for algorithm visionbox_000, giving $FMR(T) = 0.0001$ globally.

Figure 565: For algorithm visionbox-000 operating on visa images, the heatmap shows false match observed over impostor comparisons of faces from different individuals who have the given age pair. False matches are counted against a recognition threshold fixed globally to give $FMR = 0.0001$ over all on the order of 10^{10} impostor comparisons. The text in each box gives the same quantity as that coded by the color. Light colors present a security vulnerability to, for example, a passport gate.

Cross age FMR at threshold T = 0.382 for algorithm visionbox_001, giving FMR(T) = 0.0001 globally.

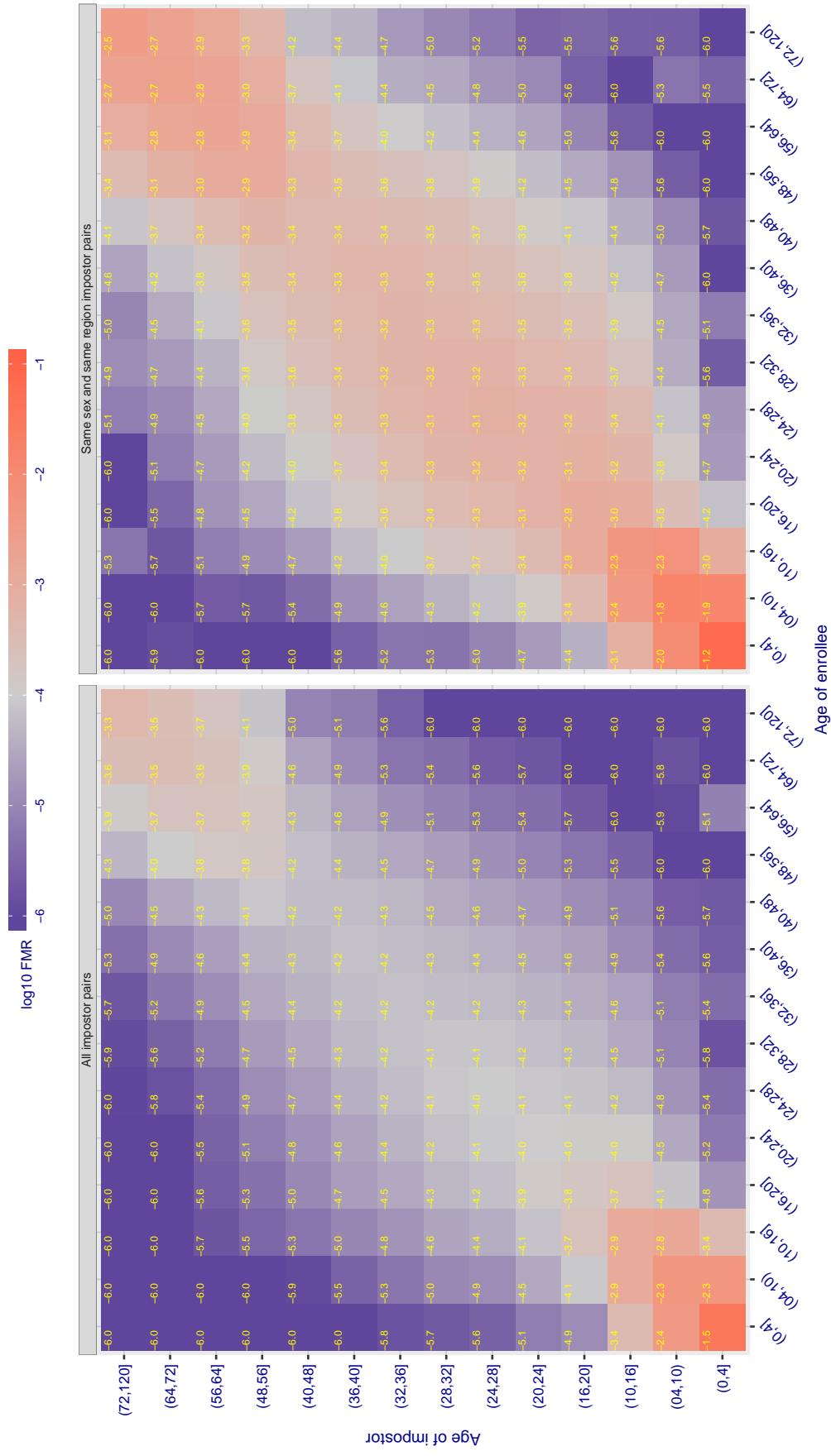


Figure 566: For algorithm visionbox-001 operating on visa images, the heatmap shows false match observed over impostor comparisons of faces from different individuals who have the given age pair. False matches are counted against a recognition threshold fixed globally to give FMR = 0.001 over all on the order of 10^{10} impostor comparisons. The text in each box gives the same quantity as that coded by the color. Light colors present a security vulnerability to, for example, a passport gate.

Cross age FMR at threshold T = 0.669 for algorithm visionlabs_006, giving FMR(T) = 0.0001 globally.

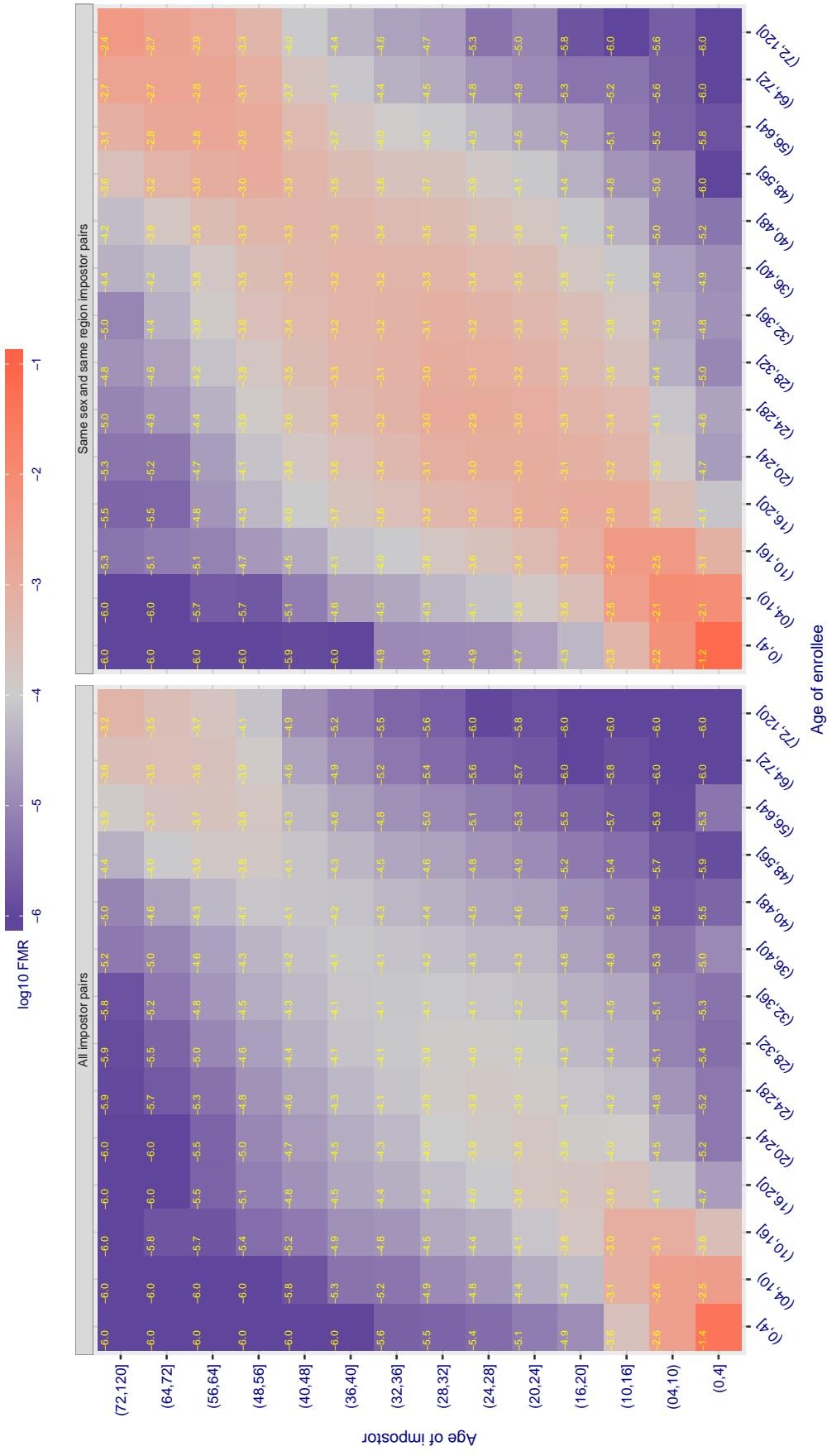


Figure 567: For algorithm visionlabs-006 operating on visa images, the heatmap shows false match observed over impostor comparisons of faces from different individuals who have the given age pair. False matches are counted against a recognition threshold fixed globally to give FMR = 0.001 over all on the order of 10^{10} impostor comparisons. The text in each box gives the same quantity as that coded by the color. Light colors present a security vulnerability to, for example, a passport gate.

Cross age FMR at threshold T = 0.657 for algorithm visionlabs_007, giving FMR(T) = 0.0001 globally.

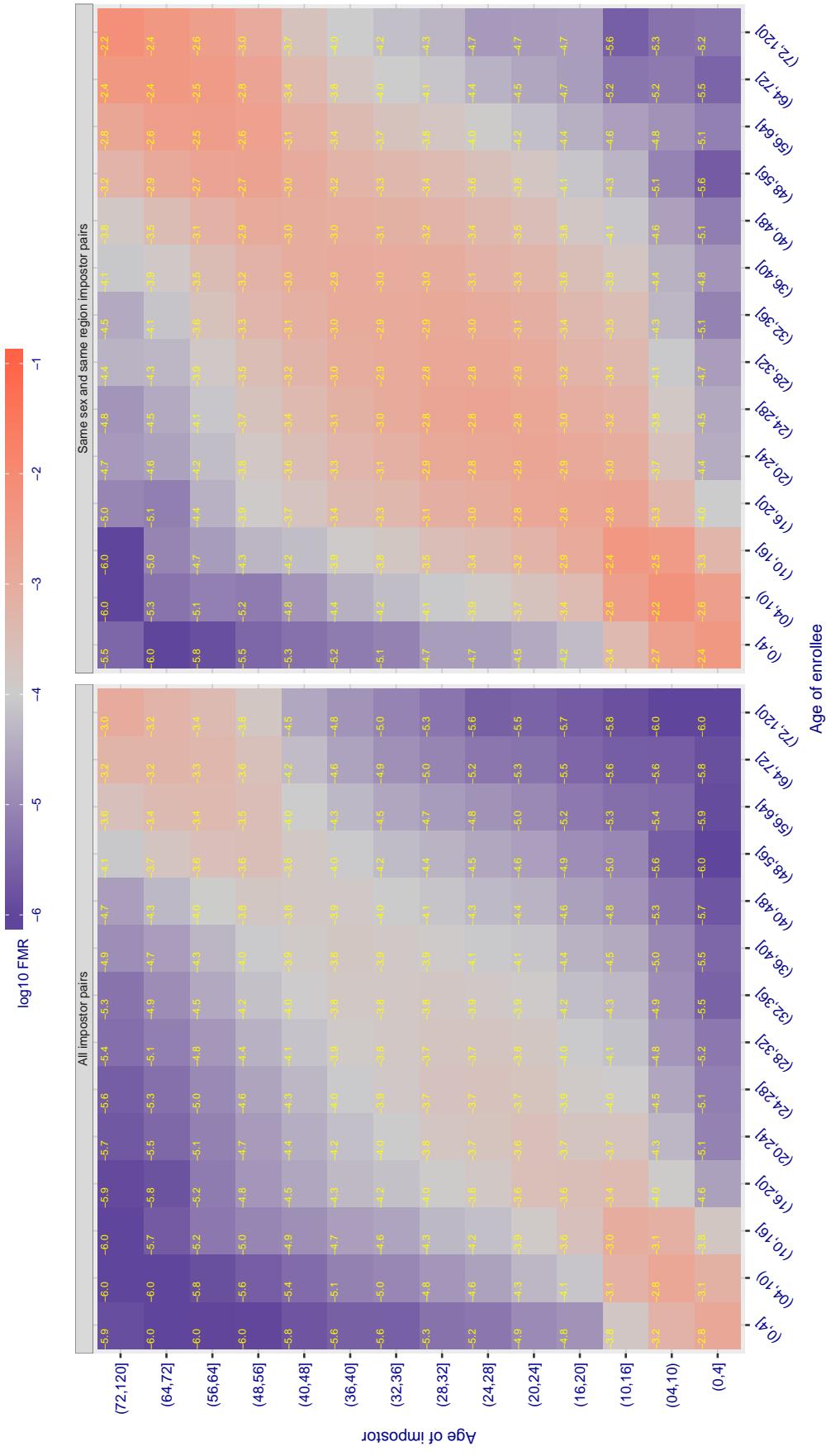


Figure 568: For algorithm visionlabs-007 operating on visa images, the heatmap shows false match observed over impostor comparisons of faces from different individuals who have the given age pair. False matches are counted against a recognition threshold fixed globally to give FMR = 0.001 over all on the order of 10^{10} impostor comparisons. The text in each box gives the same quantity as that coded by the color. Light colors present a security vulnerability to, for example, a passport gate.

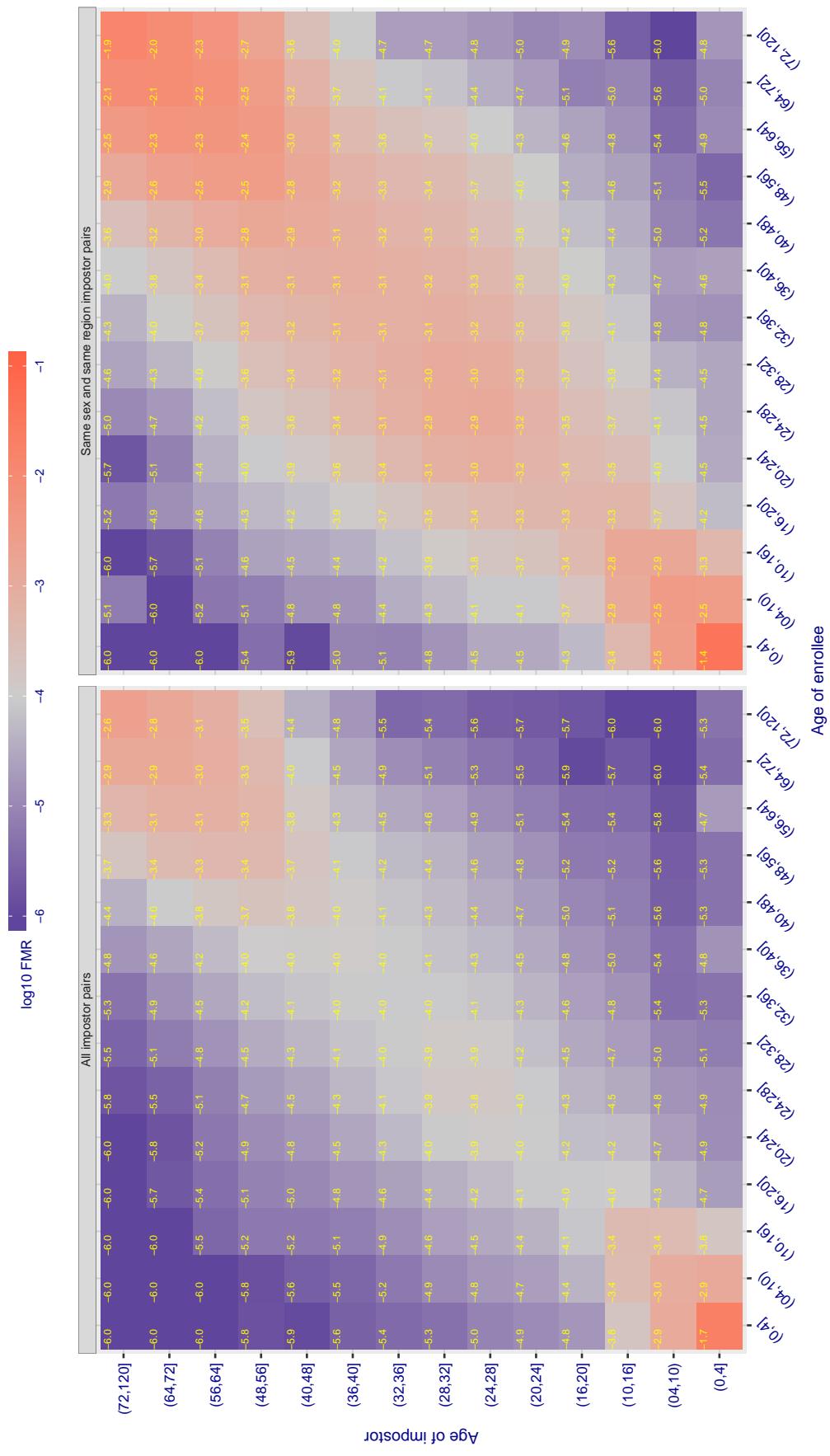
Cross age FMR at threshold T = 995.398 for algorithm vocord_006, giving $\text{FMR}(\text{T}) = 0.0001$ globally.

Figure 569: For algorithm vocord-006 operating on visa images, the heatmap shows false match observed over impostor comparisons of faces from different individuals who have the given age pair. False matches are counted against a recognition threshold fixed globally to give $\text{FMR} = 0.0001$ over all on the order of 10^{10} impostor comparisons. The text in each box gives the same quantity as that coded by the color. Light colors present a security vulnerability to, for example, a passport gate.

Cross age FMR at threshold T = 995.241 for algorithm vocord_007, giving FMR(T) = 0.0001 globally.

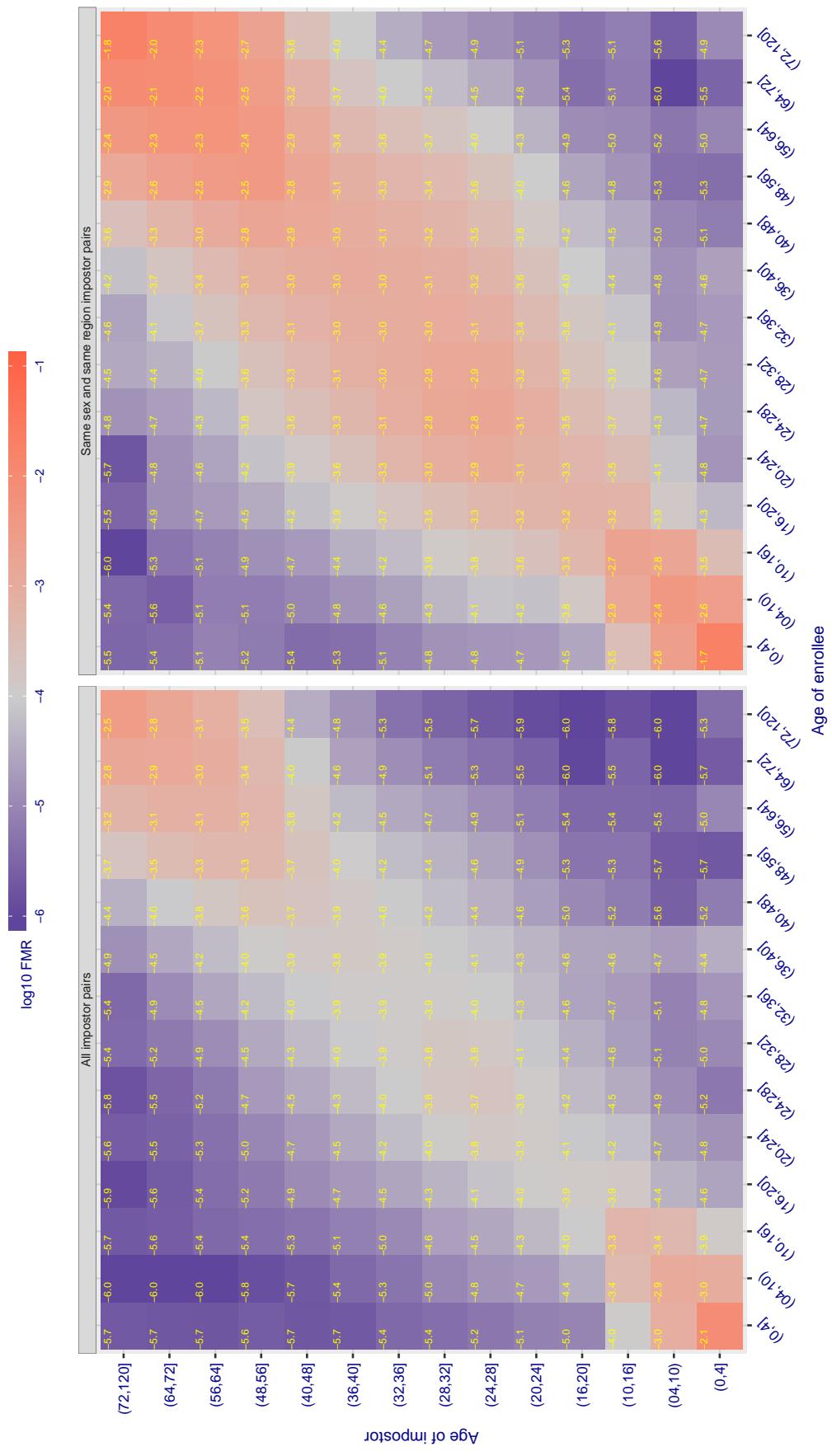


Figure 570: For algorithm vocord-007 operating on visa images, the heatmap shows false match observed over impostor comparisons of faces from different individuals who have the given age pair. False matches are counted against a recognition threshold fixed globally to give $FMR = 0.0001$ over all on the order of 10^{10} impostor comparisons. The text in each box gives the same quantity as that coded by the color. Light colors present a security vulnerability to, for example, a passport gate.

Cross age FMR at threshold T = 0.400 for algorithm winsense_000, giving FMR(T) = 0.0001 globally.

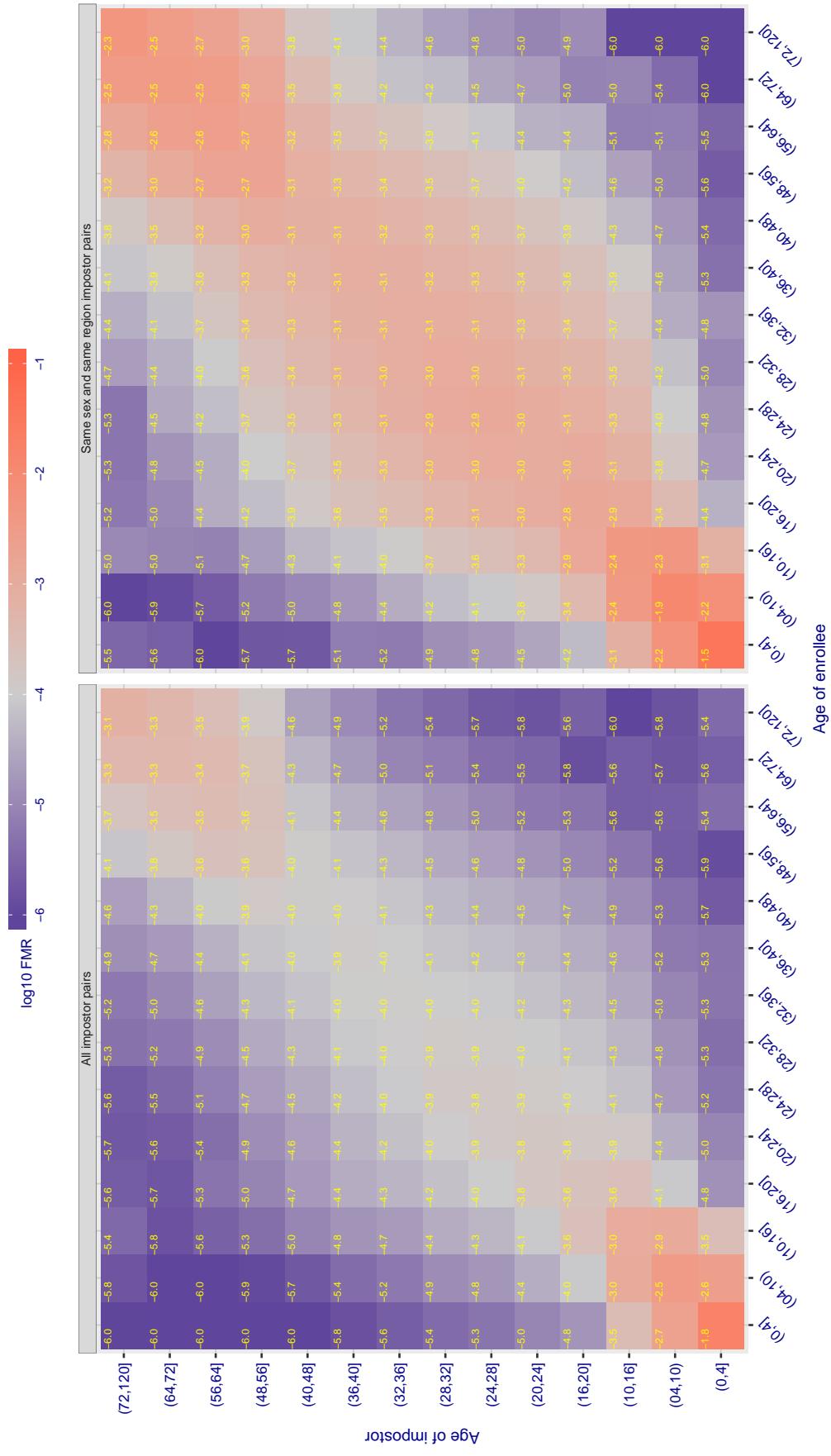


Figure 571: For algorithm winsense-000 operating on visa images, the heatmap shows false match observed over impostor comparisons of faces from different individuals who have the given age pair. False matches are counted against a recognition threshold fixed globally to give $FMR = 0.0001$ over all on the order of 10^{10} impostor comparisons. The text in each box gives the same quantity as that coded by the color. Light colors present a security vulnerability to, for example, a passport gate.

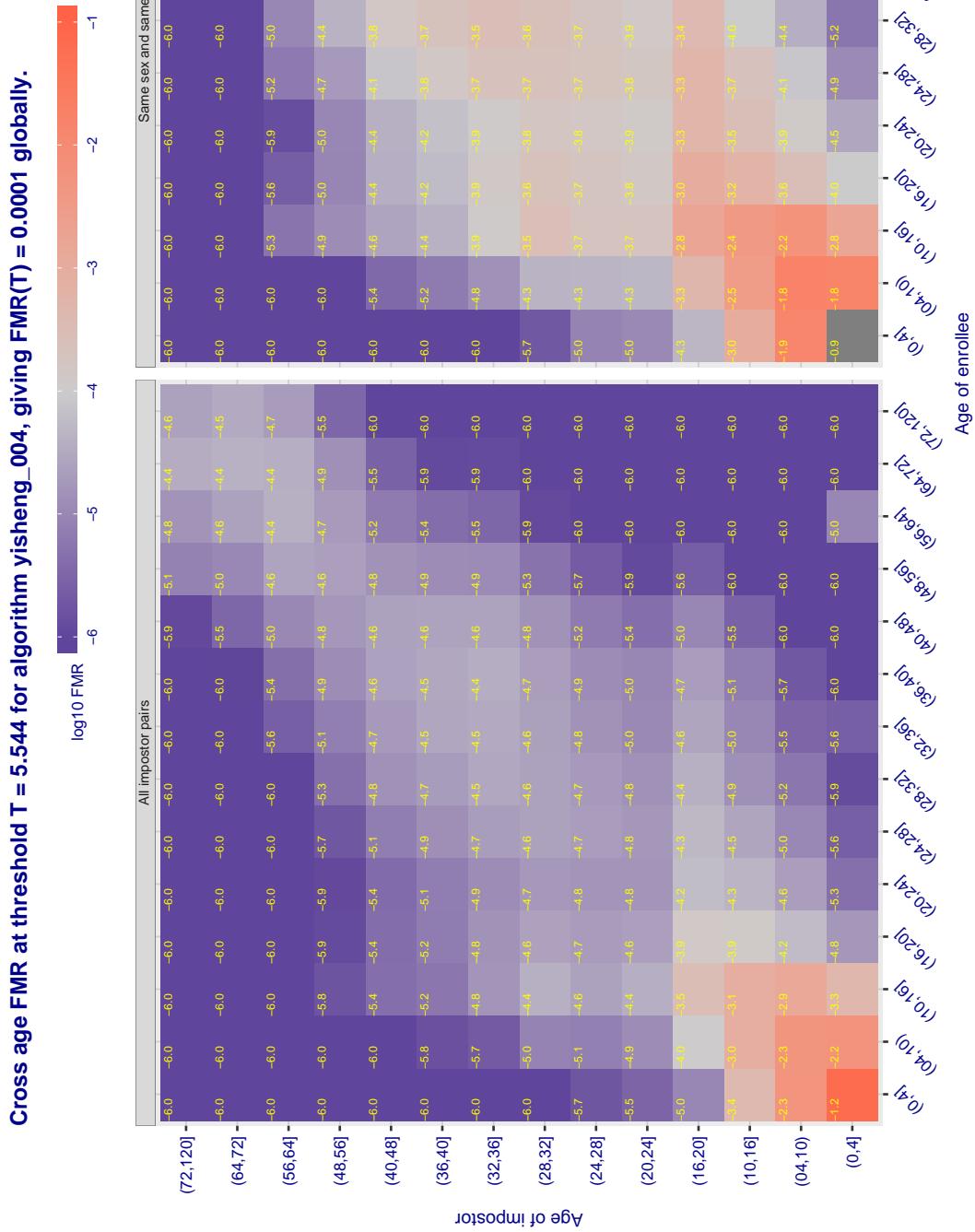


Figure 572: For algorithm *yisheng-004* operating on visa images, the heatmap shows false match observed over impostor comparisons of faces from different individuals who have the given age pair. False matches are counted against a recognition threshold fixed *globally* to give $FMR = 0.001$ over all on the order of 10^{10} impostor comparisons. The text in each box gives the same quantity as that coded by the color. Light colors present a security vulnerability to, for example, a passport gate.

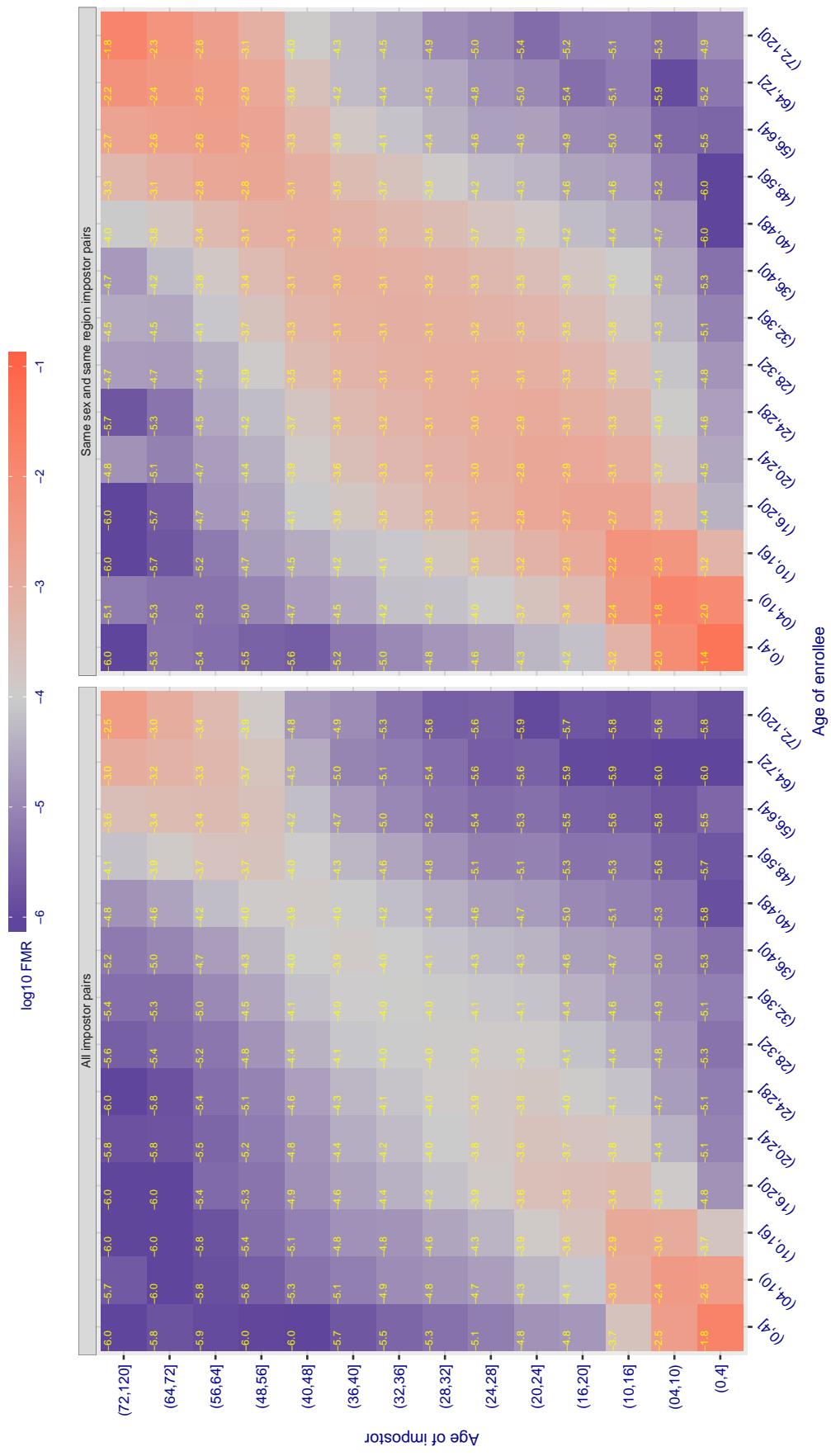
Cross age FMR at threshold T = 37.698 for algorithm yitu_003, giving $FMR(T) = 0.0001$ globally.

Figure 573: For algorithm yitu-003 operating on visa images, the heatmap shows false match observed over impostor comparisons of faces from different individuals who have the given age pair. False matches are counted against a recognition threshold fixed globally to give $FMR = 0.0001$ over all on the order of 10^{10} impostor comparisons. The text in each box gives the same quantity as that coded by the color. Light colors present a security vulnerability to, for example, a passport gate.

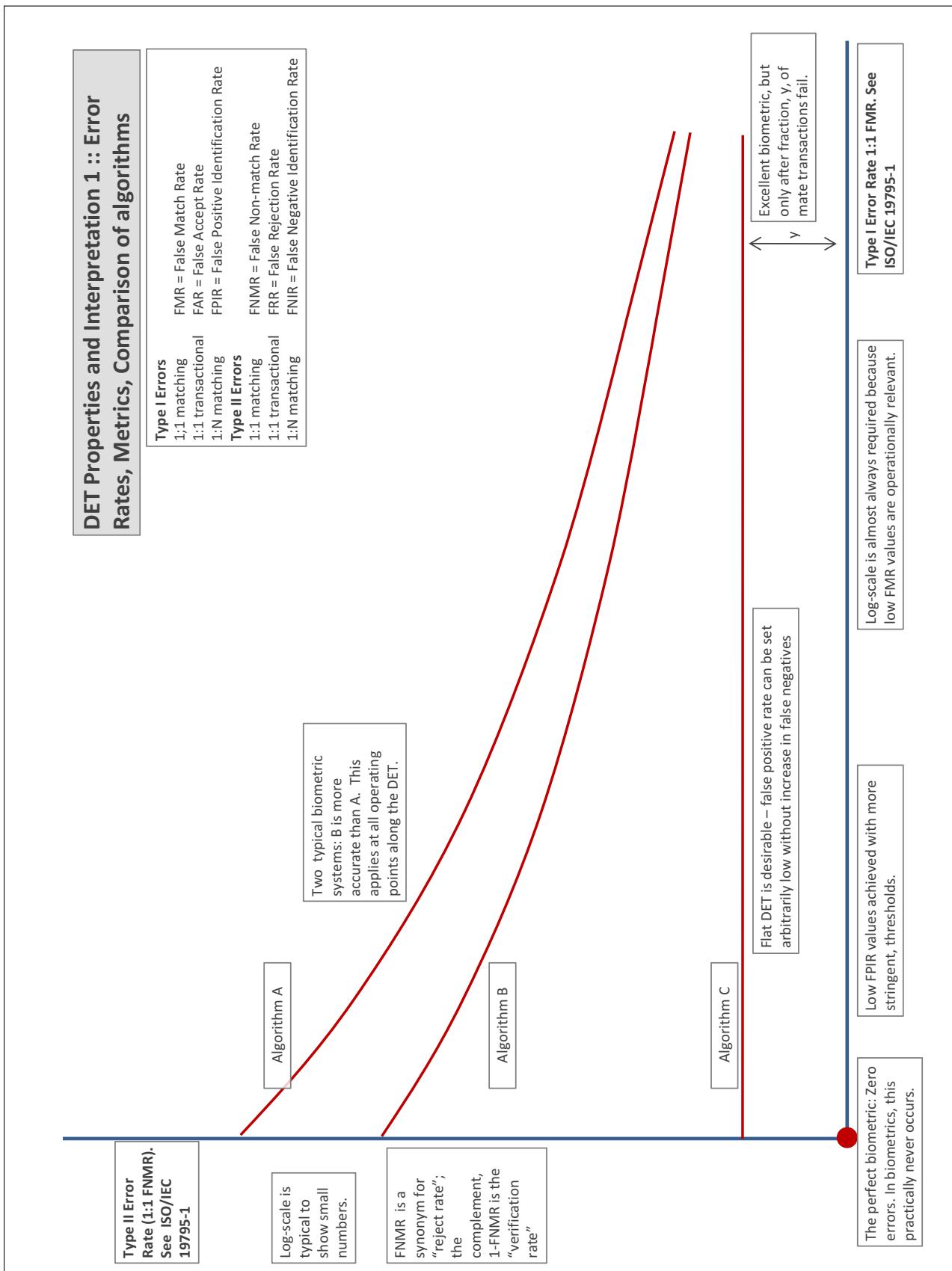
Accuracy Terms + Definitions

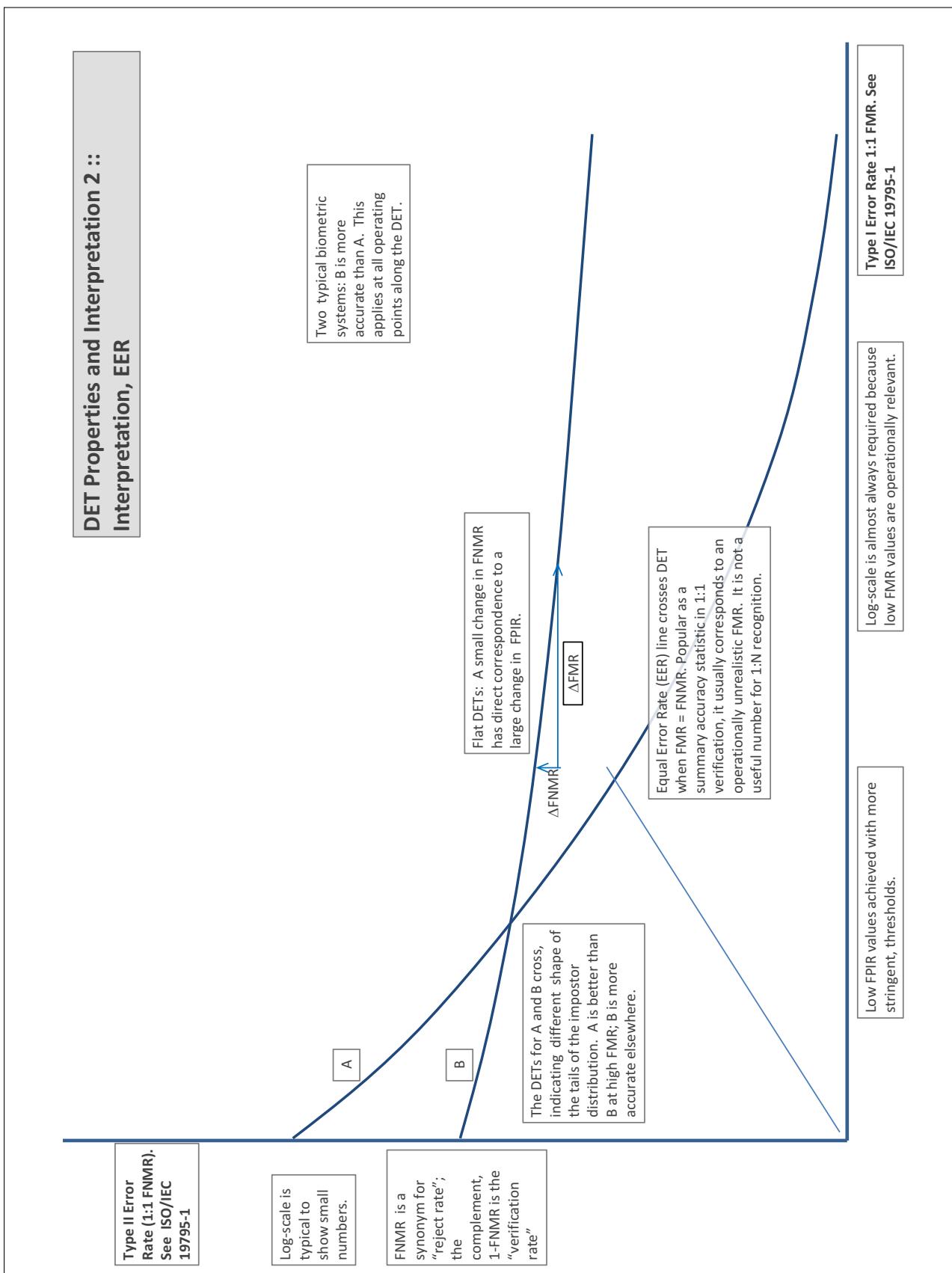
In biometrics, Type II errors occur when two samples of one person do not match – this is called a **false negative**. Correspondingly, Type I errors occur when samples from two persons do match – this is called a **false positive**. Matches are declared by a biometric system when the native comparison score from the recognition algorithm meets some **threshold**. Comparison scores can be either **similarity scores**, in which case higher values indicate that the samples are more likely to come from the same person, or **dissimilarity scores**, in which case higher values indicate different people. Similarity scores are traditionally computed by **fingerprint** and **face** recognition algorithms, while dissimilarities are used in **iris recognition**. In some cases, the dissimilarity score is a distance; this applies only when **metric** properties are obeyed. In any case, scores can be either **mate** scores, coming from a comparison of one person's samples, or **nonmate** scores, coming from comparison of different persons' samples. The words **genuine** or **authentic** are synonyms for mate, and the word **impostor** is used as a synonym for nonmatch. The words mate and nonmatch are traditionally used in identification applications (such as law enforcement search, or background checks) while genuine and impostor are used in verification applications (such as access control).

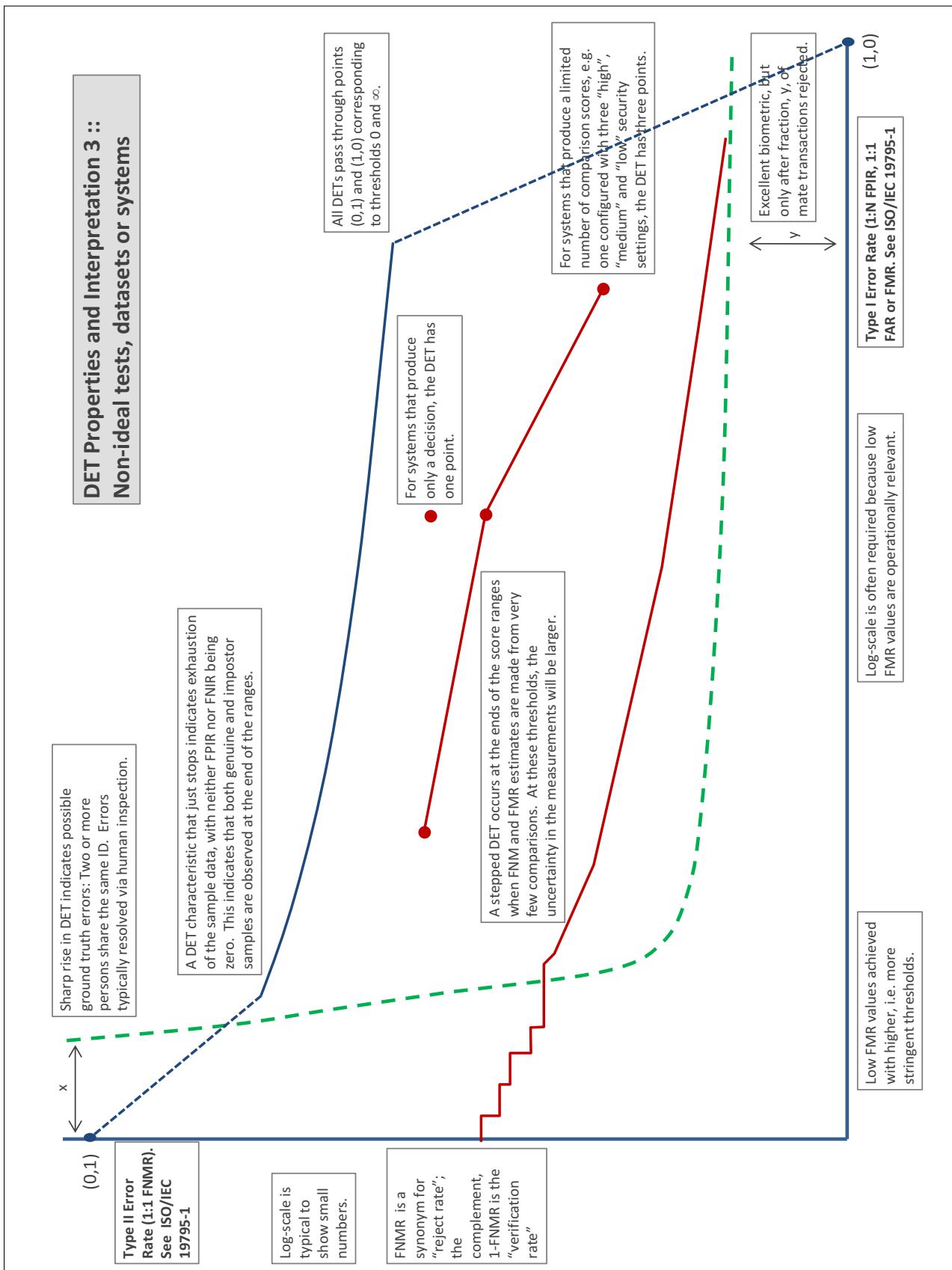
A **error tradeoff** characteristic represents the tradeoff between Type II and Type I classification errors. For verification this plots false non-match rate (FNMR) vs. false match rate (FMR) parametrically with T.

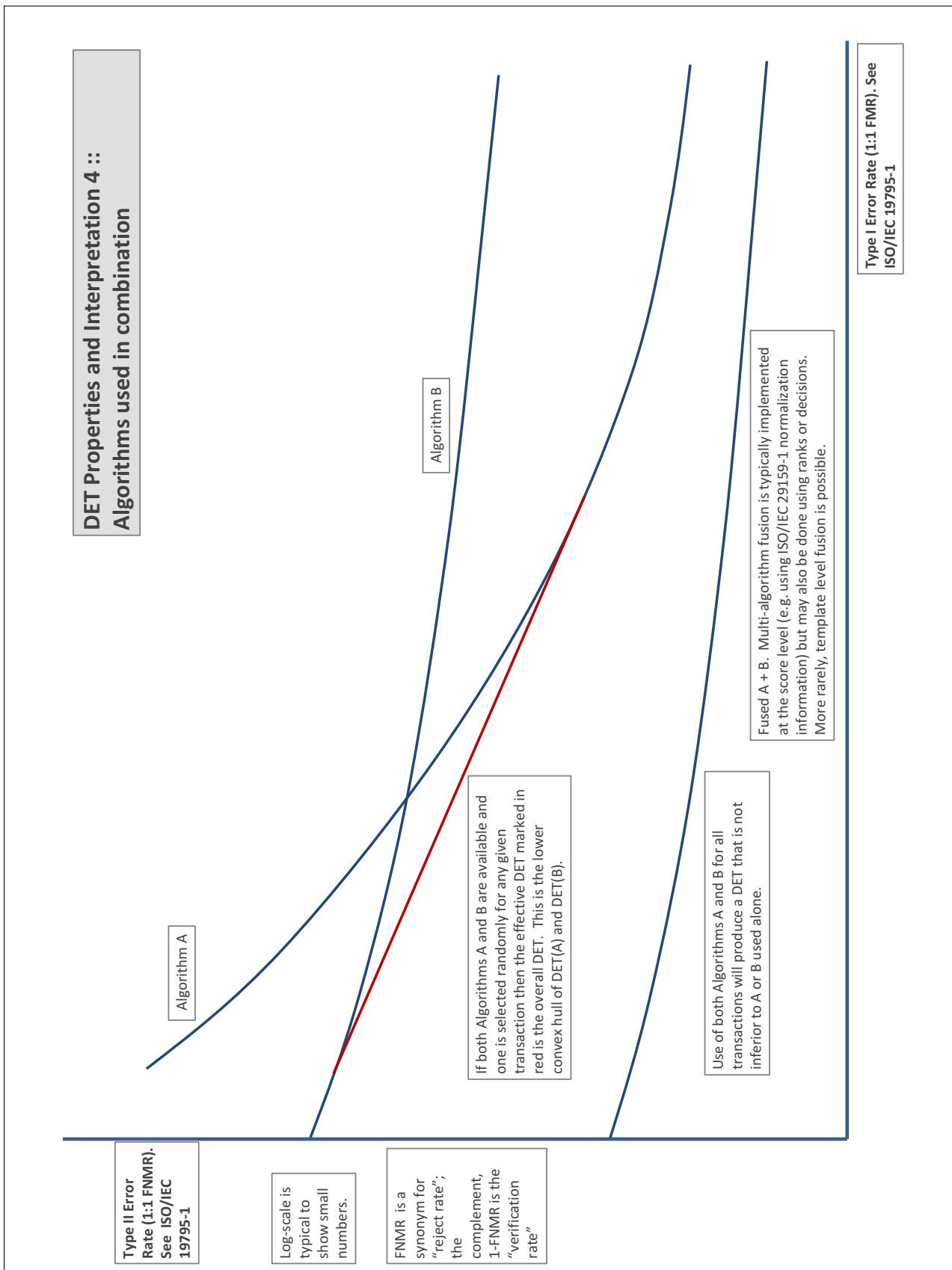
The error tradeoff plots are often called **detection error tradeoff (DET)** characteristics or **receiver operating characteristic (ROC)**. These serve the same function but differ, for example, in plotting the complement of an error rate (e.g., $TMR = 1 - FNMR$) and in transforming the axes most commonly using logarithms, to show multiple decades of FMR. More rarely, the function might be the inverse Gaussian function.

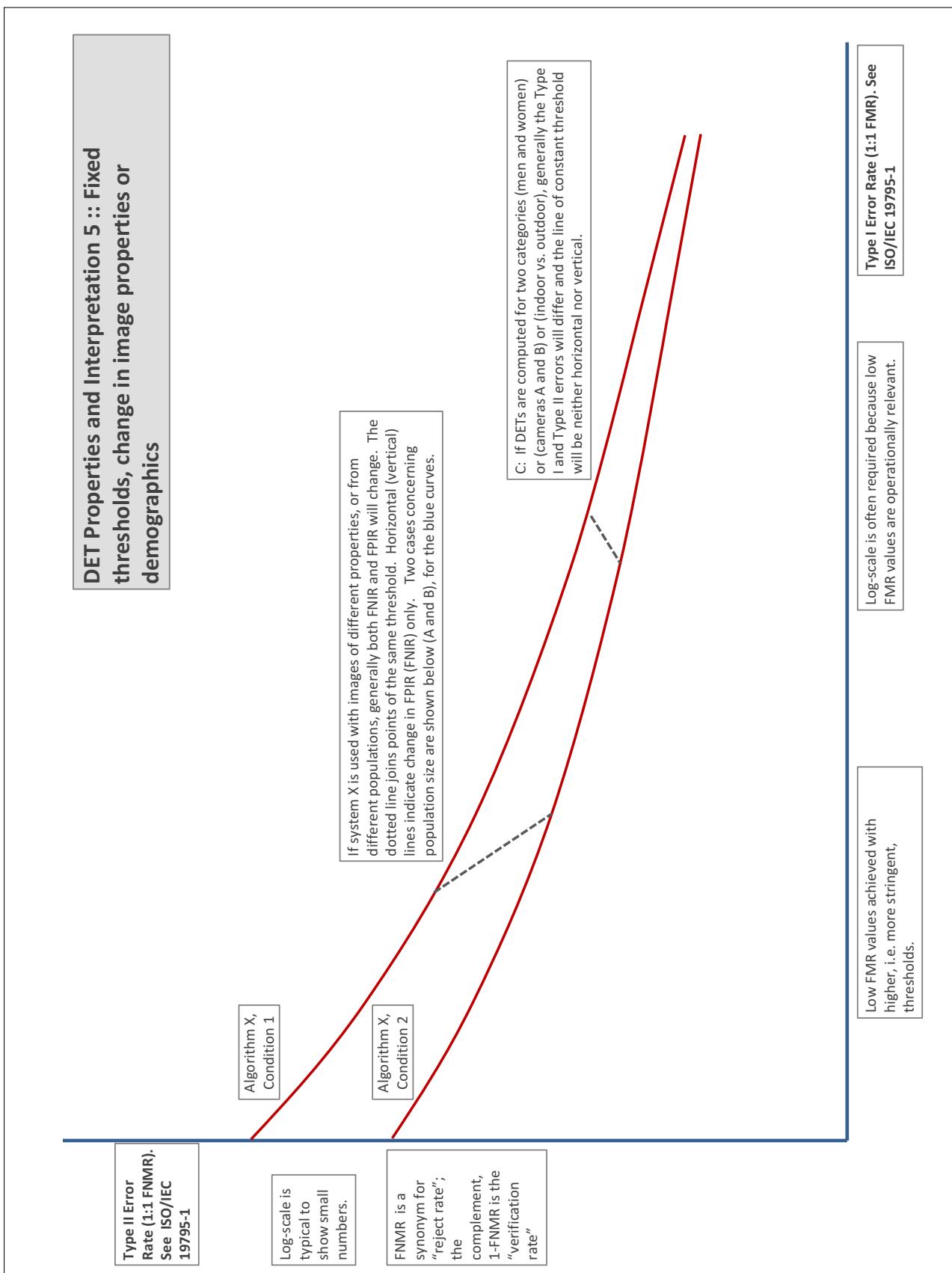
More detail and generality is provided in formal biometrics testing standards, see the various parts of [ISO/IEC 19795 Biometrics Testing and Reporting](#). More terms, including and beyond those to do with accuracy, see [ISO/IEC 2382-37 Information technology -- Vocabulary -- Part 37: Harmonized biometric vocabulary](#)











References

- [1] P. Jonathon Phillips, Amy N. Yates, Ying Hu, Carina A. Hahn, Eilidh Noyes, Kelsey Jackson, Jacqueline G. Cavazos, Géraldine Jeckeln, Rajeev Ranjan, Swami Sankaranarayanan, Jun-Cheng Chen, Carlos D. Castillo, Rama Chellappa, David White, and Alice J. O'Toole. Face recognition accuracy of forensic examiners, superrecognizers, and face recognition algorithms. *Proceedings of the National Academy of Sciences*, 115(24):6171–6176, 2018.